NUCLEAR PHYSICS

JOURNAL DEVOTED TO THE EXPERIMENTAL AND THEORETICAL STUDY OF THE FUNDAMENTAL CONSTITUENTS OF MATTER AND THEIR INTERACTIONS

EDITOR: L. ROSENFELD - COPENHAGEN
ASSOCIATE EDITOR: O. NATHAN - COPENHAGEN

VOLUME IV

NORTH-HOLLAND PUBLISHING COMPANY - AMSTERDAM

NUCLEAR PHYSICS

EDITORIAL BOARD

AUSTRIA:	B. Karlik (Vienna), H. Thirring (Vienna)
BELGIUM:	M. de Hemptinne (Louvain), J. Verhaeghe (Ghent)
CANADA:	G. Volkoff (Vancouver)
DENMARK:	C. Møller (Copenhagen), S. Rozental (Copenhagen)
EGYPT & ARAB COUNTRIES:	F. El Bedewi (Alexandria), M. G. Nooh (Cairo)
FINLAND:	L. Simons (Helsinki)
FRANCE	A. Berthelot (Saclay), S. Gorodetzky (Strasbourg), F. Joliot (Paris)
GERMANY (FED. REP.):	W. Gentner (Freiburg i. B.), J. H. D. Jensen (Heidelberg)
GERMANY (DEM. REP.):	G. Hertz (Leipzig)
GREAT BRITAIN:	S. Devons (Manchester)
HUNGARY:	L. Janossy (Budapest)
INDIA:	H. Bhabha (Bombay), B. Peters (Bombay), R. Ramanna (Trombay)
IRISH REPUBLIC:	J. McConnell (Maynooth)
ISRAEL:	G. Racah (Jerusalem)
ITALY:	E. Amaldi (Rome)
JAPAN:	S. Kikuchi (Tokyo), S. Tomonaga (Tokyo)
NETHERLANDS:	H. Brinkman (Groningen), S. R. de Groot (Leiden)
NORWAY:	E. Hylleraas (Oslo), A. Lundby (Oslo), H. Wergeland (Trondheim)
POLAND:	L. Infeld (Warsaw)
PORTUGAL:	J. M. Araújo (Porto), J. R. de Almeida Santos (Coimbra)
SOUTH AMERICA:	G. Beck (Saõ Paulo), J. Leite Lopes (Rio de Janeiro)
SPAIN:	J. M. Otero (Madrid), C. Sanchez del Rio (Madrid)
SWEDEN:	O. Klein (Stockholm), K. Siegbahn (Uppsala), I. Waller (Uppsala)
SWITZERLAND:	P. Huber (Basel), P. Scherrer (Zürich)
U.S.S.R.:	M. A. Markov (Moscow), I. S. Shapiro (Moscow), D. V. Skobeltzyn (Moscow)
YUGOSLAVIA:	I. Supek (Zagreb)
U.S.A. & MEXICO:	V. Weisskopf (Cambridge, Mass.)
AUSTRALIA & NEW ZEALAND:	H. Messel (Sydney), M. L. Oliphant (Canberra)

NUCLEAR PHYSICS

MONTHLY JOURNAL DEVOTED TO THE EXPERIMENTAL AND THEORETICAL STUDY OF ATOMIC NUCLEI, NUCLEAR FIELDS AND THE FUNDAMENTAL ASPECTS OF COSMIC RADIATION

EDITOR: L. ROSENFELD - MANCHESTER

VOLUME IV

AUGUST 1957—NOVEMBER 1957

NORTH-HOLLAND PUBLISHING COMPANY - AMSTERDAM

PRINTED IN THE NETHERLANDS BY
DRUKKERIJ VOORHEEN GEBROEDERS HOITSEMA, GRONINGEN

Nuclear Physics **4** (1957) 1—20; © *North-Holland Publishing Co., Amsterdam*

Not to be reproduced by photoprint or microfilm without written permission from the publisher

UNE MÉTHODE D'ÉTUDE DES CORRÉLATIONS DANS LES FLUIDES QUANTIQUES EN ÉQUILIBRE

J. YVON

Centre d'Etudes Nucléaires de Saclay, Gif-sur-Yvette (S. et O.)

Reçu le 7 février 1957.

Abstract: The first section recalls the essence of a method for studying correlations in a classical fluid in equilibrium. The following sections attempt to enlarge the method and to apply it to quantic fluids. The state of the system is no longer represented by wave functions but by density operators. The properties of the perfect gases are first of all coordinated with the aid of these operators. Next the problem of systems with interactions is attacked. A series of recurrent equations defines a method of successive approximations. If one is prepared to admit that, in spite of the interactions, the correlations are those of perfect gases, the formulae are identical with those of the self-consistent field. For the case of short-range forces another method is proposed. It is developed from the classical method of Ursell for obtaining the equation of state of a fluid. The results seem to point to the possibility of a kind of Bose Einstein condensation in a system of interacting fermions. The appearance of this phenomenon is due, on the one hand, to the importance, in all dense fluids, of correlations between the particles taken in pairs, and on the other hand to the fact that a pair of fermions constitute a boson.

1. Avantages de la Méthode des Grands Ensembles en Statistique Classique

Nous considérons un système de N particules identiques enfermées dans un thermostat. Les propriétés du système sont entièrement définies par sa densité en phase. Celle-ci s'exprime très simplement en fonction de l'énergie et de la température: c'est la formule de Boltzmann-Gibbs.

Si l'expression est simple, elle n'en est pas moins difficile à exploiter, du moins dans l'espace de configuration, dès que les interactions entre les particules constituantes sont importantes; autrement dit, dès que le système ne se comporte pas comme un gaz parfait.

C'est pourquoi il est commode, en général, d'introduire les quantités moins riches en arguments que la densité en phase et qui expriment le comportement d'une seule particule prise au hasard, c'est la densité simple, le comportement de deux particules prises au hasard, c'est la densité double, et ainsi de suite.

Ces densités se déduisent de la densité dans l'espace de configuration D_c par des intégrations:

$$n_1 = N \int D_c \, \mathrm{d}r_2 \mathrm{d}r_3 \ldots \mathrm{d}r_N ,$$

$$n_{12} = N(N-1) \int D_c \, \mathrm{d}r_3 \mathrm{d}r_4 \ldots \mathrm{d}r_N .$$

On peut aussi les déduire les unes des autres, en allant du compliqué au simple par une succession d'intégrations, de régressions dirons-nous aussi, pour employer le langage expressif de I. Prigogine:

$$(N-2)n_{12} = \int n_{123}\,dr_3, \tag{1}$$

$$(N-1)n_1 = \int n_{12}\,dr_2, \tag{2}$$

avec la condition finale

$$N = \int n_1\,dr_1. \tag{3}$$

Lorsque, supposant le système suffisamment vaste, les points 1 et 2 sont éloignés l'un de l'autre, les corrélations entre les particules sont très faibles, ce qui se traduit par la relation asymptotique

$$n_{12} \approx n_1 n_2. \tag{4}$$

On est tenté de dire que dans un gaz parfait il n'y a aucune corrélation, quelle que soit la distance. On écrirait donc volontiers dans ce cas

$$n_{12} = n_1 n_2. \tag{5}$$

Si on introduit cette expression de la densité double dans la relation (2), il vient, compte tenu de (3),

$$(N-1)n_1 = Nn_1,$$

soit

$$n_1 = 0.$$

Conclusion: dans un gaz parfait la densité est nulle. Ce résultat absurde tient à l'inexactitude de la relation (5). Dans un gaz parfait, il y a une certaine corrélation, la densité double n'est pas le produit des densités simples. La formule exacte est en réalité

$$n_{12} = \left(1 - \frac{1}{N}\right) n_1 n_2. \tag{6}$$

De même, que le système constitue ou non un gaz parfait, la formule (4) n'est jamais rigoureusement satisfaite même à grande distance.

Cette réserve à la rigueur des formules (4) et (5) est extrêmement gênante. On s'en tire une fois pour toutes en passant à la méthode des grands ensembles. Le système est toujours plongé dans un thermostat, mais il n'est plus fermé. Il communique par une étroite ouverture avec un réservoir à particules qui contient un nombre considérable de ces objets en réserve, et beaucoup plus qu'il n'est capable lui-même d'en contenir en aucune circonstance.

Dans ces conditions, les formules (6) et (5) se confondent parce que le nombre de particules qui figure dans (6) n'est plus le nombre de particules contenu dans le système, mais le nombre total de particules disponibles,

qui est quasi infini. De même la formule asymptotique (4) peut désormais être appliqué sans restriction.

D'une manière générale, les formules établies pour un système fermé se transposent aisément à un système ouvert pourvu qu'elles soient linéaires. C'est ainsi que (3), où l'intégration est limitée bien entendu au volume du système et ne pénètre pas dans le réservoir, conserve toute sa valeur à condition de considérer ici N comme le nombre moyen de particules contenues dans le système. Par contre, les formules (1) et (2), fondamentales dans les systèmes fermés, perdent beaucoup de leur intérêt. On peut les oublier pour commencer.

Les équations de récurrence †

$$kT\frac{\partial}{\partial x_1}n_1 = X_1 n_1 + \int X_{12} n_{12}\,\mathrm{d}r_2\,, \tag{7}$$

$$kT\frac{\partial}{\partial x_1}n_{12} = (X_1+X_{12})n_{12} + \int X_{13} n_{123}\,\mathrm{d}r_3\,, \tag{8}$$

$$kT\frac{\partial}{\partial x_2}n_{12} = (X_2+X_{21})n_{12} + \int X_{23} n_{123}\,\mathrm{d}r_3\,, \tag{9}$$

. . . . ,

où X_1 représente le champ appliqué et X_{12} la force intermoléculaire, se transposent sans modification aux systèmes ouverts. Dans une certaine mesure, la méthode des grands ensembles n'est qu'un artifice mathématique. Mais cet artifice est un guide sûr, il évite beaucoup de circonlocutions et je soutiens, par expérience, qu'il faut profiter de ses avantages. C'est en définitive accorder à la méthode une véritable valeur physique.

Je n'ai pas eu la prétention de faire découvrir des mérites au lecteur, mais seulement de les faire paraître sur des exemples très simples où dominent les formules (4) et (5). Les développements des paragraphes suivants ne feront que soutenir les mérites qui viennent d'être signalés.

On notera que nous avons évité toute considération qui suppose le volume du récipient infini. On y parviendrait par des passages à la limite: considérer le volume comme infini présente quelques commodités apparentes, mais les avantages qu'on y peut trouver sont très inférieurs à ceux de la méthode des grands ensembles.

2. Le Principe de „Localisation"

Pour simplifier, nous raisonnons sur le cas de forces à très courte portée. En suivant la méthode régressive à laquelle correspondent les équations (1), (2) et (3) du paragraphe précédent, on a l'impression qu'il faut d'abord

† Il existe d'autres suites d'équations de récurrence. L'une est due à Kirkwood. Consulter le mémoire récent de L. Sarolea et J. E. Mayer [1]).

évaleur les densités d'ordre supérieur avant les densités simple et double et que le problème, par exemple, d'estimer les corrélations des particules deux à deux, est un problème d'intégrations qui font intervenir le système tout entier.

Mais, dans la méthode, recommandée, des grands ensembles, les équations régressives passent au second plan †; on ne dispose plus que des équations de récurrence complétées par les relations asymptotiques.

Le problème fondamental est le suivant: on se donne arbitrairement la répartition en densité n_1 ou $n(x_1, y_1, z_1)$ et on cherche à déterminer quel est le champ de forces qui est susceptible de réaliser cette densité. On procède par approximations successives en déterminant de mieux en mieux les densités multiples en fonction de la densité simple et du potentiel d'interaction. La hiérarchie des équations va du simple au compliqué, contrairement au cas de la méthode régressive. Je n'insisterai pas ici sur l'étude détaillée de ce problème fondamental: il y a certainement des progrès à faire à ce sujet. Ce qu'il faut retenir est le caractère local des estimations. Les propriétés du milieu, du fluide si l'on veut — mais les raisonnements sont également valables pour des systèmes discrets quant à la répartition spatiale — en un point sont définis uniquement par le voisinage.

Pour comprendre ensuite comment le fluide se loge dans le récipient qui lui est offert, il faut procéder à une intégration de point en point qui soude progressivement les petits éléments de volume les uns aux autres.

On a exprimé le champ appliqué en fonction de la densité et non la densité en fonction du champ. Comme la relation entre le champ et la densité n'est, évidemment, pas linéaire, à un champ donné correspondent plusieurs répartitions possibles de la densité. Le formalisme permet ainsi de traiter à la fois de l'état stable et des états métastables. Cette conclusion pratique est en contradiction apparente avec la déduction qui a été utilisée. On comprend néanmoins l'apparition de solutions mathématiquement parasites, mais physiquement intéressantes: une situation locale n'a pas en soi de critère de stabilité, elle est imposée par les forces exercées par le champ appliqué et les tensions dues au voisinage. C'est seulement en examinant l'architecture d'une répartition, et donc seulement après coup, qu'il est possible d'expliciter un critère de stabilité.

De notre point de vue, cette primauté du maillon sur la chaîne, de la maille sur le tissu, des éléments maçonnés sur l'édifice constitue ce que nous appelons le principe — terme ambitieux mais destiné à frapper l'imagination — de localisation. Comprendre les propriétés d'un système macroscopique, c'est consacrer d'abord beaucoup d'efforts à pénétrer les subtilités de ses liaisons internes.

† La transformation des équations régressives dans le cas des grands ensembles sera examinée à propos des équations quantiques qui les généralisent.

Un mot en passant sur les gaz hors d'équilibre: quoique la théorie de ces milieux déséquilibrés soit moins claire que celle des systèmes en équilibre, il n'est pas mauvais de rappeler que dans leur cas aussi la méthode régressive permet de déduire le formalisme fondamental, mais que, dans la déduction de l'équation de Boltzmann: 1° on maltraite le contenu mathématique du formalisme, 2° on donne la primauté à la répartition — ici à la fois en vitesse et dans l'espace — d'une particule prise isolément sur la densité en phase, grandeur globale, 3° on détermine les corrélations par l'hypothèse du chaos moléculaire en fonction de la répartition précédente. Il y a là un nouvel aspect de l'idée de „localisation".

3. Systèmes Quantiques - Notations - Gaz de Bosons ou de Fermions

Nous considérons à nouveau un système fermé de N particules identiques en équilibre de température. Mais le système est maintenant un système quantique.

Il n'est plus question de séparer les problèmes de répartition dans l'espace et les problèmes de répartition en vitesse — mieux dit en quantité de mouvement.

Plus exactement la situation du système n'est plus représentée, dans le formalisme fondamental, par des fonctions de l'espace et de la quantité de mouvement, mais par des matrices densités. La méthode régressive s'applique ici aussi, copiée sur le procédé classique, et définit la matrice densité relative à une seule particule, à deux particules considérées simultanément et ainsi de suite.

Désignons par x_1 l'ensemble des coordonnées d'une particule, coordonnées d'espace et de spin par exemple. La matrice densité à une particule dépend de deux systèmes de valeur des coordonnées, que nous désignerons respectivement par x_1 et par x_1'. Nous écrivons cette matrice $\mathscr{M}_1(x_1, x_1')$. Elle est hermitique. Envisagée comme une matrice continue, $\mathscr{M}_1$ définit une transformation linéaire qui se représente comme une transformation intégrale:

$$g(x_1) = \int \mathscr{M}_1(x_1, x_1')f(x_1')\mathrm{d}r_1 . \tag{1}$$

Il est très commode, et nous ne nous en priverons pas, de symboliser la même transformation avec une notation opératorielle:

$$g_1 = \mu_1 f_1 . \tag{2}$$

Les indices et l'écriture sont réduits au minimum.

La matrice densité qui décrit la situation du système en équilibre à la température

$$T = 1/k\beta,$$

s'explicite

$$\mathscr{D} = \frac{1}{Z} \sum_i \phi_i^*(x_1', x_2', \ldots, x_N') \exp(-\beta H) \phi_i(x_1, x_2, \ldots, x_N). \quad (3)$$

H est l'hamiltonien du système. Z assure la normalisation. Les ϕ_i forment une suite orthonormée complète de fonctions. Les fonctions sont totalement symétriques dans le cas des bosons, totalement antisymétriques dans le cas des fermions. La matrice $\mathscr{D}$ remplace ici la densité en phase des systèmes classiques.

Nous désignerons par D l'opérateur linéaire correspondant, au sens de (1 et (2). On écrira donc

$$D = \frac{1}{Z} \exp(-\beta H). \quad (4)$$

Cet opérateur permet de définir l'opérateur densité à une particule par un un calcul de trace partielle:

$$\mu_1 = N \, \mathrm{T}_{23\ldots N} D.$$

On définira de même des opérateurs densités à 2, 3 particules considérées simultanément:

$$\mu_{12} = N(N-1)\mathrm{T}_{3\ldots N} D,$$

$$\mu_{123} = N(N-1)(N-2)\mathrm{T}_{4\ldots N} D.$$

Ces relations successives peuvent être présentées sous une forme régressive:

. . . .

$$(N-2)\mu_{12} = \mathrm{T}_3 \mu_{123}, \quad (5)$$

$$(N-1)\mu_1 = \mathrm{T}_2 \mu_{12}. \quad (6)$$

Elles sont suivies par la dernière relation exprimant la normalisation:

$$N = \mathrm{T}_1 \mu_1, \quad (7)$$

et sont évidemment copiées sur les relations classiques § 1 (1), (2), (3).

L'opérateur μ_1 a des fonctions propres. Les valeurs propres correspondantes, la preuve en est aisée, sont positives. Ce sont des probabilités. Le système des fonctions propres n'est pas nécessairement complet. Les fonctions propres que nous venons de définir sont les fonctions relatives à une seule particule qu'il est naturel de rencontrer dans l'étude de tout système complexe — ici dans le cas d'un système en équilibre de température, ailleurs pour un système à l'état fondamental, en état excité ou même en régime variable. On comprend ainsi l'intervention de fonctions à une particule seulement dans la théorie nucléaire des couches, laquelle s'applique à des noyaux complexes. Il resterait à prouver l'essentiel, c'est que les fonctions définies ici de manière rationnelle se confondent avec les fonctions empiriques de la théorie des couches. Un de nos objectifs est, sinon de résoudre ce problème, du moins d'amorcer un effort dans ce sens. L'opérateur densité

double définit de même des fonctions orthogonales qu'il associe de manière rationnelle au système étudié.

La formule (4) ne reflète pas le caractère de symétrie des particules. Elle ne permet pas de calculs régressifs sans revenir à la formule explicite (3).

On se débarrasse de cette complication en introduisant dans (7), à la place des fonctions correctement symétrisées des produits ϕ_{0i} de fonction d'une seule particule à la fois, mais en complétant l'expression par un opérateur de symétrisation approprié. La matrice densité s'écrit maintenant

$$\mathscr{D} = \frac{1}{Z} \sum_i \phi_{0i}'^* \frac{B_{12\ldots N}}{N!} \exp(-\beta H) \phi_{0i}. \tag{8}$$

L'opérateur B peut se déduire des permutations simples par récurrence:

$$\begin{aligned} B_1 &= 1, \\ B_{12} &= 1 + \varepsilon P_{12}, \\ &\cdots, \\ B_{12\ldots N} &= [1 + \varepsilon(P_{12} + P_{13} + P_{14} + \cdots + P_{1N})] B_{23\ldots N}. \end{aligned} \tag{9}$$

ε est égal à $+1$ pour les bosons, à -1 pour les fermions. Ceci dit, au lieu de (4) il faut retenir pour l'opérateur densité l'expression

$$D = \frac{1}{Z} \frac{B_{12\ldots N}}{N!} \exp(-\beta H). \tag{10}$$

Appliquons cette formule à un système de particules indépendantes, à un gaz. L'hamiltonien est une somme, où les H_j sont tels que le système est clos:

$$H = H_1 + H_2 + \cdots + H_N. \tag{11}$$

Nous posons pour abréger

$$A_j = \exp(-\beta H_j). \tag{12}$$

Nous aurons à envisager des systèmes contenant des particules en nombre variable, aussi ajouterons-nous en indice aux grandeurs évaluées le nombre N approprié.

Calculons l'opérateur densité à une particule, soit maintenant $\mu_{N,1}$. Par définition

$$Z_N \mu_{N,1} = \mathrm{T}_{23\ldots N} \frac{B_{12\ldots N}}{(N-1)!} A_1 A_2 \ldots A_N. \tag{13}$$

Exprimons B à l'aide de (9). Il vient, compte tenu de l'équivalence des indices muets,

$$\begin{aligned} Z_N \mu_{N,1} = A_1 \mathrm{T}_{23\ldots N} \frac{B_{23\ldots N}}{(N-1)!} A_2 A_3 \ldots A_N + \\ + \varepsilon \mathrm{T}_{23\ldots N} P_{12} A_1 \frac{B_{23\ldots N}}{(N-2)!} A_2 A_3 \ldots A_N. \end{aligned} \tag{14}$$

Les traces du second membre ont une valeur simple dans un système a $N-1$ particules. A l'aide de cette remarque on obtient le résultat suivant:

$$Z_N \mu_{N,1} = Z_{N-1}(A_1 + \varepsilon \mathrm{T}_2 P_{12} A_1 \mu_{N-1,2}). \tag{15}$$

En vertu du lemme suivant relatif au calcul des traces:

$$\mathrm{T}_2 P_{12} A_1 B_2 = B_1 A_1, \tag{16}$$

ceci s'écrit encore

$$Z_N \mu_{N,1} = Z_{N-1}(1 + \varepsilon \mu_{N-1,1}) A_1. \tag{17}$$

Cette formule paraît décevante parce qu'elle associe des grandeurs qui ne correspondent pas à un même remplissage du système. La difficulté est levée en passant aux grands ensembles. La probabilité pour le système de contenir N particules est

$$\pi_N = \frac{Z_N z^N}{\Xi}. \tag{18}$$

Ξ est un coefficient de normalisation. Multiplions membre à membre l'équation (17) par z_N et ajoutons les équations relatives aux différentes valeurs de N. Il vient, les grandeurs étant maintenant exprimées pour un système ouvert,

$$\frac{\mu_1}{1+\varepsilon\mu_1} = z A_1. \tag{19}$$

L'originalité n'est certes pas dans ce classique résultat, ni dans l'emploi de la méthode des grands ensembles, mais un certain intérêt résulte des possibilités de généralisation pour des systèmes pourvus d'interactions.

Par une procédure analogue on évalue les opérateurs multiples. Les formules obtenues ne sont valables rigoureusement que pour les systèmes ouverts. On pourrait à volonté exprimer les opérateurs multiples en fonction des A_j — c'est-à-dire aussi bien en fonction des H_j — ou en fonction des μ_j. L'expérience de la statistique classique montre que la seconde alternative est la meilleure. De même qu'en statistique classique on s'efforce d'éliminer des corrélations le champ appliqué, on s'efforcera d'éliminer dans les problèmes quantiques analogues l'hamiltonien individuel H_j. En définitive,

$$\begin{aligned} \mu_{12} &= (1+\varepsilon P_{12})\mu_1 \mu_2 = \mu_1 \mu_2 (1+\varepsilon P_{12}), \\ \mu_{123} &= (1+\varepsilon P_{12}+\varepsilon P_{13})(1+\varepsilon P_{23})\mu_1 \mu_2 \mu_3, \\ &\cdots\cdots \end{aligned} \tag{20}$$

Ces élégantes formules généralisent la relation classique

$$n_{12} = n_1 n_2.$$

Comme elles ne sont rigoureuses que pour des systèmes ouverts, ce serait une faute de les associer à (5) ou à (6). Par contre (7) conserve une utilité

pratique, à condition que N y représente le nombre moyen de particules contenues dans le système.

Revenons à la matrice qui correspond à l'opérateur μ_1, $\mathcal{M}_1(x_1, x_1')$. A propos des électrons libres Wigner a mis en évidence que cette matrice tend rapidement vers zéro quand la distance d'espace entre les configurations x_1 en x_1' augmente. Il faut que le système soit assez grand et que la densité en électrons soit assez élevée. Le même phénomène se produit pour un gaz de bosons, du moins tant que celui-ci n'a pas subi la condensation de Bose Einstein.

Négligeons, seulement pour simplifier l'écriture, les éventuelles variables de spin. En changeant de variables indépendantes la matrice peut s'écrire

$$\mathcal{M}_1\left(\frac{x_1+x_1'}{2}, x_1'-x_1\right).$$

On peut ainsi lui attribuer, en quelque sorte, une „valeur" en chaque point de l'espace, repéré ici par $\frac{1}{2}(x_1+x_1')$. Il en est de même de μ_1. On peut noter encore à propos de la transformation (1) que $g(x_1)$ ne dépend des valeurs de f que dans le voisinage de x_1. Il y a là un effet de „localisation".

Dans l'opérateur μ_{12} de la formule (20) l'effet de localisation est atténué par la présence du facteur $1+\varepsilon P_{12}$. Mais il se manifeste dans le facteur $\mu_1\mu_2$. Il porte maintenant, bien entendu, sur le voisinage immédiat des points 1 et 2.

Venons-en aux systèmes liés. Notons d'abord les formules suivantes, qui sont absolument générales, que le système soit ouvert ou fermé ou même hors d'équilibre, parce qu'elles résultent uniquement de questions de symétrie:

$$\begin{aligned} &\mu_{12} = \mu_{21} \quad \text{ou} \quad P_{12}\mu_{12} = \mu_{12}P_{12}, \\ &P_{12}\mu_{12} = \varepsilon\mu_{12}. \end{aligned} \tag{21}$$

Des formules analogues existent pour les opérateurs d'ordre supérieur.

Les lignes qui suivent sont intuitives.

Nous admettrons que la localisation étend ses effets même aux systèmes liés, dans les mêmes circonstances générales que pour les systèmes sans interaction. La localisation agit dans les systèmes d'électrons, dans le fluide nucléaire, dans l'hélium liquide, sauf peut-être à basse température, au-dessous du point λ. Nous dirons que la localisation est un phénomène „assez général".

Soulignons que les énoncés de localisation ne sont précis que dans la théorie des grands ensembles. Il n'est guère d'usage de considérer le fluide nucléaire du point de vue thermodynamique, mais cette position n'est pas absurde. Nous y reviendrons.

Nous admettrons donc que l'opérateur μ_1 a le même comportement dans le cas des systèmes liés que dans le cas des gaz.

A propos de l'opérateur double, nous admettrons qu'il peut se mettre sous la forme

$$\mu_{12} = (1+\varepsilon P_{12})C_{12}, \tag{22}$$

l'opérateur C_{12} étant localisé sur 1 et 2. De plus, nous admettrons la propriété asymptotique suivante. Lorsque 1 et 2 sont éloignés l'un de l'autre, on peut poser

$$C_{12} \approx \mu_1\mu_2. \tag{23}$$

Les opérateurs d'ordre supérieur appellent des remarques particulières. A propos de μ_{123}, imaginons que 1 se trouve dans une région de l'espace et 23 dans une région éloignée. On est tenté de poser alors, à l'image de ce qui se passe pour un gaz parfait,

$$\mu_{123} \approx (1+\varepsilon P_{12}+\varepsilon P_{13})\mu_1\mu_{23}.$$

Mais la matrice qui correspond au second membre n'est pas hermitique, en général. Il faut donc corriger cette expression et poser

$$\mu_{123} \approx \mu_1\mu_{23}+\tfrac{1}{2}\varepsilon(P_{12}+P_{13})\mu_1\mu_{23}+\tfrac{1}{2}\varepsilon\mu_1\mu_{23}(P_{12}+P_{13}).$$

De même, à propos de μ_{1234}, on peut être amené à considérer que les cas 1 et 2 sont dans une région de l'espace et 3 et 4 dans une autre. Dans ce cas, la formule asymptotique suivante, déduite qualitativement de ce qui se passe dans un gaz parfait, sera retenue:

$$\mu_{1234} \approx (1+P_{13}P_{24})\mu_{12}\mu_{34}+\tfrac{1}{2}\varepsilon(P_{13}+P_{14}+P_{23}+P_{24})\mu_{12}\mu_{34} + \tfrac{1}{2}\varepsilon\mu_{12}\mu_{34}(P_{13}+P_{14}+P_{23}+P_{24}).$$

Explicitons maintenant les interactions que nous entendons introduire dans les systèmes liés. Ecrivons l'hamitonien

$$H = H_1+H_2+\cdots+H_N+W_{12}+W_{13}+\cdots+W_{N-1,N}.$$

Nous admettons donc que les interactions, représentées par les opérateurs W_{ij}, ne lient les particules que deux à deux.

Les operateurs H_i, W_{ij}, par hypothèse, sont essentiellement des opérateurs locaux.

4. Equations de Récurrence Quantiques

Le calcul des opérateurs densités s'effectue sans approximation lorsque les particules sont libres. Lorsque des forces agissent entre les particules, une solution rigoureuse est impossible. Il est intéressant d'obtenir des relations qui se prêtent à des approximations. Ce sont les équations de récurrence.

Considérons d'abord un système fermé. L'hamiltonien commute avec

l'opérateur D. Par des régressions plus ou moins poussées sur l'équation qui exprime cette propriété, on parvient à la première série de relations, dues à Boon et Green [2]),

$$H_1\mu_1+\mathrm{T}_2W_{12}\mu_{12}=\mu_1H_1+\mathrm{T}_2\mu_{12}W_{12}, \tag{1}$$

$$(H_1+H_2+W_{12})\mu_{12}+\mathrm{T}_3(W_{13}+W_{23})\mu_{123} = \mu_{12}(H_1+H_2+W_{12})+\mathrm{T}_3\mu_{123}(W_{13}+W_{23}), \tag{2}$$

. . . .

Ces importantes relations ne sont suffisantes pour permettre la détermination des opérateurs étudiés. On s'en rend compte aisément dans le cas des interactions nulles.

Nous en obtiendrons d'autres en suivant une méthode due à Félix Bloch [3]). Récrivons l'opérateur D — en négligeant ici d'écrire l'opérateur de permutation que nous avons introduit au paragraphe précédent, seulement pour alléger les formules, car le résultat n'en serait pas changé:

$$D=\frac{1}{Z}\exp(-\beta H). \tag{3}$$

Z est défini par la condition

$$Z=\mathrm{T}\exp(-\beta H). \tag{4}$$

En suivant F. Bloch, dérivons membre à membre par rapport à β. Il vient la valeur de l'énergie moyenne

$$\langle H\rangle=-\frac{\partial}{\partial\beta}\log Z. \tag{5}$$

Dérivons de même l'opérateur densité, puis éliminons Z. Il vient:

$$\frac{\partial}{\partial\beta}D=(\langle H\rangle-H)D=D(\langle H\rangle-H). \tag{6}$$

Nous laisserons de côté pour le moment la dernière égalité qui fait double emploi avec la relation de commutation déjà utilisée.

La trace totale membre à membre de (6) donne

$$\langle H\rangle=\mathrm{T}_1H_1\mu_1+\tfrac{1}{2}\mathrm{T}_{12}W_{12}\mu_{12}. \tag{7}$$

Des calculs de traces partielles donnent de même

$$-\frac{\partial}{\partial\beta}\mu_1=-\langle H\rangle\mu_1+H_1\mu_1+\mathrm{T}_2(H_2+W_{12})\mu_{12}+\tfrac{1}{2}\mathrm{T}_{23}W_{23}\mu_{123}, \tag{8}$$

$$-\frac{\partial}{\partial\beta}\mu_{12}=-\langle H\rangle\mu_{12}+(H_1+H_2+W_{12})\mu_{12}+\mathrm{T}_3(H_3+W_{12}+W_{23})\mu_{123} +\tfrac{1}{2}\mathrm{T}_{34}W_{34}\mu_{1234}, \tag{9}$$

. . . . .

Il convient maintenant de passer aux grands ensembles, afin de pouvoir profiter en toute rigueur des effets de la localisation, au moins dans les cas favorables. Les formules (1), (2) et (7) ne subissent aucune modification. Il n'en est pas de même a priori pour (8) et (9) qui ne sont pas des formules linéaires en raison de la présence du facteur $\langle H \rangle$.

Notons que

$$\mu_1 = \sum \pi_N \mu_{N,1}, \tag{10}$$

avec

$$\pi_N = \frac{Z_N z^N}{\Xi}.$$

On dérive par rapport à β, z restant constant:

$$\frac{\partial}{\partial \beta} \mu_1 = \sum \left(\mu_{N,1} \frac{\partial}{\partial \beta} \pi_N + \pi_N \frac{\partial}{\partial \beta} \mu_{N,1} \right), \tag{11}$$

$$\frac{\partial}{\partial \beta} \log \pi_N = - \frac{\partial}{\partial \beta} \log \Xi + \frac{\partial}{\partial \beta} \log Z_N, \tag{12}$$

$$\frac{\partial}{\partial \beta} \Xi = \sum z^N \frac{\partial}{\partial \beta} Z_N. \tag{13}$$

Soit, d'abord, d'après (5),

$$\frac{\partial}{\partial \beta} \log \Xi = - \sum \pi_N \langle H_N \rangle = - \langle H \rangle. \tag{14}$$

La relation précédente devient

$$\frac{\partial}{\partial \beta} \pi_N = \pi_N (\langle H \rangle - \langle H_N \rangle). \tag{15}$$

Ainsi,

$$\left(\frac{\partial}{\partial \beta} - \langle H \rangle \right) \mu_1 = \sum \pi_N \left(\frac{\partial}{\partial \beta} - \langle H_N \rangle \right) \mu_{N,1}. \tag{16}$$

On s'aperçoit alors que les équations (8) et (9) sont encore valables pour un grand ensemble. Il y a avantage à éliminer l'énergie moyenne de ces formules. On obtient les équations suivantes:

$$- \frac{\partial}{\partial \beta} \mu_1 = H_1 \mu_1 + \mathrm{T}_2 H_2 (\mu_{12} - \mu_1 \mu_2) + \mathrm{T}_2 W_{12} \mu_{12} + \tfrac{1}{2} \mathrm{T}_{23} (\mu_{123} - \mu_1 \mu_{23}), \tag{17}$$

$$- \frac{\partial}{\partial \beta} \mu_{12} = H_{12} \mu_{12} + \mathrm{T}_3 H_3 (\mu_{123} - \mu_{12} \mu_3) + \mathrm{T}_3 (W_{13} + W_{23}) \mu_{123} + \tfrac{1}{2} \mathrm{T}_{34} W_{34} (\mu_{1234} - \mu_{12} \mu_{34}), \tag{18}$$

. . . . .

On a posé

$$H_1 + H_2 + W_{12} = H_{12}.$$

Pour rendre les équations plus symétriques on peut utiliser les formules (1) et (2). De cette manière, les termes se rassemblent en groupes évidemment hermitiques. Il vient

$$-\frac{\partial}{\partial\beta}\mu_1 = \tfrac{1}{2}(H_1\mu_1+\mu_1 H_1)+\mathrm{T}_2 H_2(\mu_{12}-\mu_1\mu_2)+\tfrac{1}{2}\mathrm{T}_2(W_{12}\mu_{12}+\mu_{12}W_{12}) \\ +\tfrac{1}{2}\mathrm{T}_{23}W_{23}(\mu_{123}-\mu_1\mu_{23}), \quad (19)$$

$$-\frac{\partial}{\partial\beta}\mu_{12} = \tfrac{1}{2}(H_{12}\mu_{12}+\mu_{12}H_{12})+\mathrm{T}_3 H_3(\mu_{123}-\mu_{12}\mu_3) \\ +\tfrac{1}{2}\mathrm{T}_3[(W_{13}+W_{23})\mu_{123}+\mu_{123}(W_{13}+W_{23})]+\tfrac{1}{2}\mathrm{T}_{34}W_{34}(\mu_{1234}-\mu_{12}\mu_{34}), \quad (20)$$

. . . . .

Ces équations (17, (18) ou (19), (20) sont plus lourdes que les équations classiques de récurrence, elles font intervenir plus vite des grandeurs d'ordre supérieur. Elles se prêteront moins commodément à des approximations: je crois néanmoins que les principes de celles-ci ne s'en trouveront pas modifiés, les complications qui apparaissent ici sont inévitables et inhérentes aux problèmes quantiques.

Complétons ce paragraphe par d'autres formules rigoureuses, déduites des relations régressives § 3(5) et (6). Avant de passer aux systèmes ouverts, nous récrivons l'équation § 3 (6) pour un système fermé:

$$(N-1)\mu_{N,1} = \mathrm{T}_2\mu_{N,12}. \quad (21)$$

Introduisons les probabilités π_N relatives aux systèmes ouverts. Il vient

$$\sum \pi_N N\mu_{N,1}-\sum \pi_N\mu_{N,1} = \mathrm{T}_2\sum \pi_N\mu_{N,12}, \quad (22)$$

ou

$$\sum \pi_N N\mu_{N,1}-\mu_1 = \mathrm{T}_2\mu_{12}. \quad (23)$$

Mais dérivons par rapport à z la formule (10.) Il vient

$$\frac{\partial}{\partial \log z}\mu_1 = \sum \pi_N N\mu_{N,1}-\mu_1\frac{\partial}{\partial \log z}\log \Xi. \quad (24)$$

En dérivant Ξ lui-même on montre que

$$\frac{\partial}{\partial \log z}\log \Xi = \langle N\rangle. \quad (25)$$

Ainsi,

$$\frac{\partial}{\partial \log z}\mu_1+(\langle N\rangle-1)\mu_1 = \mathrm{T}_2\mu_{12}. \quad (26)$$

Un jeu d'écriture fait disparaître le nombre moyen de particules:

$$\frac{\partial}{\partial \log z}\mu_1-\mu_1 = \mathrm{T}_2(\mu_{12}-\mu_1\mu_2). \quad (27)$$

Nous pourrions montrer de même que

$$\frac{\partial}{\partial \log z}\mu_{12}-2\mu_{12} = T_3(\mu_{123}-\mu_{12}\mu_3), \tag{28}$$

$$\frac{\partial}{\partial \log z}\mu_{123}-3\mu_{12} = T_4(\mu_{1234}-\mu_{123}\mu_4), \tag{29}$$

. . . . .

Ces équations sont la généralisation la plus large d'équations classiques analogues qui interviennent dans la théorie des fluctuations en densité †. Lorsque le fluide est homogène, des raisonnements thermodynamiques permettent de substituer à la dérivation par rapport à z une dérivation par rapport à $\langle N\rangle$, à température constante.
Alors, en effet,

$$\frac{\partial \log z}{\partial \log \langle N\rangle} = \frac{\beta v}{n\chi},$$

n étant la densité et χ le coefficient de compressibilité isotherme.

5. Première Méthode d'Approximation

Le formalisme qui vient d'être exposé ne servirait pas à grand chose s'il ne suggérait pas des méthodes d'approximation. Il s'agit de trouver autre chose que la méthode de perturbation dont on peut penser qu'elle a rendu tous les services qu'on pouvait en attendre.

Dans ce paragraphe nous supposerons que les forces sont faibles, que la densité des particules est modérée. Il est alors naturel de traiter de manière simpliste les corrélations des particules trois à trois, quatre à quatre, etc. Nous ne précisons pas si les forces sont à courte portée. L'étude couvre donc le cas des forces coulombiennes, qui sont des forces faibles à longue portée.

Nous essayons l'approximation de Kirkwood linéarisée — non linéarisée elle serait difficile à transposer des problèmes classiques aux problèmes quantiques pour des raisons de commutation ††. Rappelons que cette approximation, linéarisée, donne de bons résultats dans le cas coulombien et classique des électrolytes [10]).

Posons

$$d_{12} = C_{12}-\mu_1\mu_2, \tag{1}$$

$$\nu_{12} = (1+\varepsilon P_{12})(C_{12}-\mu_1\mu_2). \tag{2}$$

† Depuis Prins et Zernike, ces problèmes ont été repris plusieurs fois. Du point de vue classique, l'auteur y a insisté longuement [4]) sans utiliser malheureusement la méthode des grands ensembles. Le problème quantique a été traité, densités seulement, par P. J. Price [5]). La question reste d'actualité, comme le montre un mémoire récent de R. P. Feynmann et M. Cohen [6]). Citons également réf. [7, 8]).

†† Cette difficulté ne se rencontre pas dans le travail de R. M. Mazo et J. G. Kirkwood [9]), parce que dans ce mémoire la méthode est appliquée à des densités et non à des opérateurs.

Lorsque le principe de localisation s'applique, d_{12} tend rapidement vers zéro quand la distance 12 augmente.

L'approximation de Kirkwood linéarisée se traduit par les formules approchées suivantes:

$$C_{123} = \mu_1\mu_2\mu_3+\mu_2 d_{23}+\mu_2 d_{13}+\mu_3 d_{12}, \tag{3}$$

$$C_{1234} = \mu_1\mu_2\mu_3\mu_4+\mu_1\mu_2 d_{34}+\mu_1\mu_3 d_{21}+\mu_1\mu_4 d_{23}+\mu_2\mu_3 d_{14}+\mu_2\mu_1 d_{13} +\mu_3\mu_1 d_{12}. \tag{4}$$

Ces expressions, introduites dans les équations de récurrences, conduisent au système suivant:

$$\mathrm{T}_2(\mu_{12}-\mu_1\mu_2) = \frac{\partial}{\partial \log z}\mu_1-\mu_1, \tag{5}$$

$$[1+\varepsilon(\mu_1+\mu_2)]\nu_{12}+\nu_{12}[1+\varepsilon(\mu_1+\mu_2)] = \frac{\partial}{\partial \log z}\nu_{12}, \tag{6}$$

$$K_1\mu_1+\mathrm{T}_2 W_{12}\nu_{12} = \mu_1 K_1+\mathrm{T}_2\nu_{12}W_{12}, \tag{7}$$

$$\begin{aligned}(K_1+K_2)\nu_{12}&+[1+\varepsilon(\mu_1+\mu_2)]W_{12}\mu_{12}+(1+\varepsilon P_{12})(\mathrm{T}_3 W_{23}\nu_{13}\mu_2+\mathrm{T}_3 W_{13}\nu_{23}\mu_1)\\ &+\varepsilon\mathrm{T}_3 P_{13}(W_{12}+W_{13})\nu_{23}\mu_1+\varepsilon\mathrm{T}_3 P_{23}(W_{12}+W_{23})\nu_{13}\mu_2\\ =\nu_{12}(K_1+K_2)&+\mu_{12}W_{12}[1+\varepsilon(\mu_1+\mu_2)]+(1+\varepsilon P_{12})(\mu_2\mathrm{T}_3\nu_{13}W_{23}+\mu_1\mathrm{T}_3\nu_{23}W_{13})\\ &+\varepsilon\mathrm{T}_3\mu_1\nu_{23}(W_{12}+W_{13})P_{13}+\varepsilon\mathrm{T}_3\mu_2\nu_{13}(W_{12}+W_{23})P_{23},\end{aligned} \tag{8}$$

$$-\frac{\partial}{\partial\beta}\mu_1 = (1+\varepsilon\mu_1)K_1\mu_1+\mathrm{T}_2 K_2\nu_{12}+(1+\varepsilon\mu_1)\mathrm{T}_2 W_{12}\nu_{12}+\varepsilon T_2\,\nu_{12}W_{12}\mu_1), \tag{9}$$

$$\begin{aligned}-\frac{\partial}{\partial\beta}\mu_{12} = {}&[(1+\varepsilon\mu_1)K_1+(1+\varepsilon\mu_2)K_2]\nu_{12}\\ &+[1+\varepsilon(\mu_1+\mu_2)+\tfrac{1}{2}(1+\varepsilon P_{12})\mu_1\mu_2]W_{12}\mu_{12}\\ &+\nu_{12}[\varepsilon K_1\mu_1+\varepsilon K_2\mu_2+\tfrac{1}{2}W_{12}(1+\varepsilon P_{12})\mu_1\mu_2]\\ &+(1+\varepsilon P_{12})[\tfrac{3}{2}(1+\varepsilon\mu_2)\mathrm{T}_3 W_{23}\nu_{13}\mu_2+\tfrac{3}{2}(1+\varepsilon\mu_1)\mathrm{T}_3 W_{13}\nu_{23}\mu_1]\\ &+\tfrac{1}{2}\varepsilon(1+\varepsilon\mu_2)\mathrm{T}_3 P_{13}W_{12}\nu_{23}\mu_1+\tfrac{1}{2}\varepsilon(1+\varepsilon\mu_1)\mathrm{T}_3 P_{23}W_{12}\nu_{13}\mu_2.\end{aligned} \tag{10}$$

L'opérateur K est l'hamiltonien auquel on a ajouté le champ selfconsistant:

$$K_1 = H_1+\mathrm{T}_2 W_{12}(1+\varepsilon P_{12})\mu_2. \tag{11}$$

Dans les formules (8) et (10) certaines traces comprennent en facteur l'opérateur P_{13} ou l'opérateur P_{23}: il en résulte que, malgré l'écriture, ces traces correspondent à des interactions binaires et non pas à des interactions triangulaires.

6. Forces à Courte Portée

Nous ne posons maintenant aucune restriction à l'intensité des forces qui s'exercent entre les particules, mais nous supposons essentiellement

qu'elles sont à courte portée. La généralisation de la méthode d'Ursell peut s'essayer ici.

Posons, H étant l'hamiltonien du système fermé de N particules,

$$A_{12\ldots N} = \exp(-\beta H). \tag{1}$$

L'identité suivante est fondamentale:

$$A_{12\ldots N} = A_1 A_{23\ldots N} + \sum (A_{12} - A_1 A_2) A_{34\ldots N}$$

somme à $N-2$ termes: 3, 4, ..., N jouent successivement le rôle de 2

$$+ \sum\sum (A_{123} - A_1 A_{23} - A_2 A_{13} - A_3 A_{12}) A_{45\ldots N} + \cdots$$

somme à $\frac{1}{2}(N-2)(N-3)$ termes: tous les couples 2–4, 3–4, ..., 5–9, etc. jouent successivement le rôle du couple 2–3

Pour comprendre ce résultat, on traite momentanément les composantes de l'hamiltonien comme des grandeurs classiques. On pose

$$g_{12} = \exp(-\beta W_{12}) - 1. \tag{3}$$

Alors

$$A_{12\ldots N} = A_1 A_2 \cdots A_N (1+g_{13}) \cdots (1+g_{23}) \cdots (1+g_{N-1,N}). \tag{4}$$

Ensuite on effectue les produits et on ordonne les termes d'après le nombre de particules qui sont liées à la particule 1 par un g. Ceci fait on peut revenir aux notations en A_{12}, A_{123}, ... etc. La formule obtenue a un sens même quand on traite les composantes de l'hamiltonien comme des opérateurs. De plus elle est correcte parce qu'elle ne comprend de produits que d'opérateurs qui commutent.

La suite des calculs ressemble à celui qui a été poursuivi précédemment en l'absence d'interactions. On calcule d'abord l'opérateur densité à une particule pour le système fermé:

$$\begin{aligned} Z_N \mu_{N,1} = {} & \frac{1}{(N-1)!} \mathrm{T}_{23\ldots N} B_{12\ldots N} [A_1 A_{2\ldots N} + (N-1)(A_{12} - A_1 A_2) A_{3\ldots N} \\ & + \tfrac{1}{2}(N-2)(N-3)(A_{123} - A_1 A_{23} - A_2 A_{13} - A_3 A_{12} + 2A_1 A_2 A_3) A_{4\ldots N} + \cdots] \end{aligned} \tag{5}$$

Pour aller plus loin on développe $B_{12\ldots N}$ avec un luxe plus ou moins grand suivant la nature du terme en A qui le multiplie.

$$\begin{aligned} Z_N \mu_{N,1} = {} & \frac{1}{(N-1)!} \mathrm{T}_{23\ldots N} \Big\{ (1 + \sum_{j \neq 1} \varepsilon P_{1j}) A_1 B_{2\ldots N} A_{2\ldots N} \\ & + (1 + \sum_{j \neq 1} \varepsilon P_{1j})(1 + \sum_{\substack{k \neq 1 \\ k \neq 2}} \varepsilon P_{2k})(N-1)(A_{12} - A_1 A_2) B_{3\ldots N} A_{3\ldots N} + \cdots \Big\}. \end{aligned} \tag{6}$$

Les sommes de permutations peuvent être simplifiées par suite de l'équivalence des indices muets. Il vient

$$Z_N \mu_{N,1} = \frac{1}{(N-1)!} \mathrm{T}_{23\ldots N}\{[1+(N-1)\varepsilon P_{12}]A_1 B_{2\ldots N} A_{2\ldots N} + [1+\varepsilon P_{12}+\varepsilon(N-2)(P_{13}+P_{23})+(N-2)P_{12}(P_{13}+P_{23}) + (N-2)(N-3)P_{13}P_{24}](N-1)(A_{12}-A_1 A_2)B_{3\ldots N} A_{3\ldots N}+\cdots\}. \tag{7}$$

La formule associe des systèmes qui n'ont pas le même nombre de particules. On peut en effet la récrire

$$Z_N \mu_{N,1} = Z_{N-1}(1+\varepsilon\mu_{N-1,1})A_1 + Z_{N-2}[1+\varepsilon P_{12}+\varepsilon(\mu_{N-2,1}+\mu_{N-2,2})+P_{12}(\mu_{N-2,1}+\mu_{N-2,2})+\mu_{N-2,12}] (A_{12}-A_1 A_2)+\cdots. \tag{8}$$

On passe ensuite aux systèmes ouverts en posant

$$j_1 = zA_1, \quad j_{12} = z^2 A_{12}. \tag{9}$$

Il vient

$$\mu_1 = (1+\varepsilon\mu_1)j_1+\mathrm{T}_2\{1+\varepsilon P_{12}+\varepsilon(\mu_1+\mu_2)+P_{12}(\mu_1+\mu_2)+\mu_{12}\}(j_{12}-j_1 j_2)+\cdots, \tag{10}$$

ou, en groupant les termes du crochet:

$$\mu_1 = (1+\varepsilon\mu_1)j_1+\mathrm{T}_2\{(1+\varepsilon P_{12})[1+\varepsilon(\mu_1+\mu_2)]+\mu_{12}\}(j_{12}-j_1 j_2)+\cdots. \tag{11}$$

Les termes sont groupés d'après le nombre de „points" qu'ils font intervenir. Jusqu'à la formule (8) comprise, la question de la convergence des expressions ne se pose pas parce que le nombre des termes, même éventuellement très élevé, est fini. La question est d'importance au contraire pour la formule (11): d'une part le nombre des termes est infini, d'autre part la série qui en résulte est inutilisable si elle n'est pas très convergente. C'est ici que l'hypothèse des forces à courte portée, qui a pour effect de limiter le „rayon" de quantités telles que $j_{12}-j_1 j_2$ est essentielle. De plus, une convergence rapide n'est à espérer que si la densité est modérée. Le résultat est plus compliqué que le résultat classique analogue. C'est l'effet des opérateurs de permutation. Entre autres choses, on voit intervenir ici les opérateurs densités d'ordre supérieur, μ_{12} explicitement, μ_{123}, μ_{1234} etc. dans les termes non écrits. Il est au moins indispensable, pour utiliser la formule (11) réduite à ses deux premiers termes, d'avoir une expression approchée de μ_{12}.

La même procédure permet d'y parvenir. On utilise un autre développement de

$$A_{12\ldots N} = A_{12}A_{34\ldots N}+\cdots. \tag{12}$$

Il vient, pour un système fermé,

$$Z_N \mu_{N,12} = \mathrm{T}_{34\ldots N}\frac{1}{(N-2)!}[1+\varepsilon P_{12}+\varepsilon(N-2)(P_{13}+P_{23}) + (N-2)P_{12}(P_{13}+P_{23})+(N-2)(N-3)P_{13}P_{24}]\times A_{12}B_{34\ldots N}A_{34\ldots N}+\cdots, \tag{13}$$

ou

$$Z_N \mu_{N,12} = Z_{N-2}[1+\varepsilon P_{12}+\varepsilon(\mu_{N-2,1}+\mu_{N-2,2})+P_{12}(\mu_{N-2,1}+\mu_{N-2,2}) + \mu_{N-2,12}] A_{12}. \quad (14)$$

On passe aux grands ensembles:

$$\mu_{12}(1-j_{12}) = (1+\varepsilon P_{12})[1+\varepsilon(\mu_1+\mu_2)]j_{12}+\cdots. \quad (15)$$

On arrêtera l'approximation au premier terme sans dissimuler les difficultés qu'entraîneraient l'intervention des termes d'ordre supérieur — c'est-à-dire des interactions triangulaires, quadrangulaires, etc. (15) peut se résoudre par rapport à μ_{12}:

$$\mu_{12} = (1+\varepsilon P_{12})[1+\varepsilon(\mu_1+\mu_2)] \frac{j_{12}}{1-j_{12}}. \quad (16)$$

Les expressions (11) de μ_1 et (16) de μ_{12} ne sont pas hermitiques, ou, du moins, ne le sont pas avec évidence. Il y a là une difficulté que je ne prétends pas éliminer ici de manière tout à fait satisfaisante. Toutefois il est clair que le manque d'hermiticité des expressions (11) et (16) est lié à l'ordre dans lequel ont été placés, avant leur développement, les opérateurs $B_{12\ldots N}$ et $A_{12\ldots N}$. On aurait pu tout aussi bien les placer en ordre inverse. Cette disposition aurait conduit aux expressions adjointes

$$\mu_1 = j_1(1+\varepsilon\mu_1)+\mathrm{T}_2(j_{12}-j_1 j_2)\{(1+\varepsilon P_{12})[1+\varepsilon(\mu_1+\mu_2)]+\mu_{12}\}, \quad (17)$$

$$\mu_{12} = (1+\varepsilon P_{12}) \frac{j_{12}}{1-j_{12}} [1+\varepsilon(\mu_1+\mu_2)]. \quad (18)$$

D'une part la demi-somme des expressions (11) et (17) ou (16) et (18) est satisfaisante au point de vue de l'hermiticité. D'autre part la demi-différence doit être nulle, au moins de manière approchée — c'est là l'embarras. Du moins dans le cas où on néglige les interactions, la seule condition qui en résulte est

$$j_1 \mu_1 = \mu_1 j_1. \quad (19)$$

Elle est équivalente à la relation § 4 (1) lorsqu'on élimine de celle-ci les interactions. Ce cas très particulier se traite harmonieusement dans la méthode du présent paragraphe.

Il est possible également de développer complètement le cas où les forces sont assez faibles — toujours à courte portée — pour qu'on puisse développer linéairement les expressions par rapport à W_{12}. Ensuite on élimine μ_{12} et on prend j_1 — ou H_1 — comme inconnue, au lieu de μ_1. Cette manière de faire est analogue à la méthode classique qui considère que l'inconnue n'est pas la répartition en densité, mais le champ appliqué.

Je donnerai seulement ici le résultat. Il vient

$$\log \frac{\mu_1}{1+\varepsilon\mu_1} = \log Z - \beta[H_1+\mathrm{T}_2(1+\varepsilon P_{12})W_{12}\mu_2]. \quad (20)$$

Le résultat est mis sous forme logarithmique parce que l'expérience m'a prouvé que c'est sous cette forme que les développements sont les plus simples et les plus convergents en théorie non quantique. Il y a donc une présomption qu'il en soit de même en théorie quantique. L'équation (20) n'est pas autre chose qu'une forme élaborée de la théorie du champ self-consistant.

Pour utiliser nos équations dans le cas des forces intenses, il conviendra, avant d'aborder le problème général, d'étudier les situations où le fluide est homogène, ce qui apporte de grosses simplifications. Le fil directeur sera aussi de prendre l'hamiltonien appliqué comme inconnue primaire.

Un fait est notoire, c'est l'apparition dans l'expression de μ_{12} d'un dénominateur qui risque de devenir infini si z est trop élevé. Dans le cas d'un gaz sans interactions, ce phénomène survient à propos de μ_1: il est caractéristique des bosons et il a pour conséquence la condensation de Bose-Einstein. Ici il est indépendant de la nature des particules. C'est une conséquence, si l'on veut, de l'équation

$$\varepsilon^2 = (\pm 1)^2 = 1, \tag{21}$$

ou encore du fait qu'une paire de particules constitue de toute manière un boson. Il faut donc prévoir qu'une espèce de condensation de Bose-Einstein puisse se produire, même avec des fermions. Toutefois le dénominateur responsable de cette possibilité disparait lorsqu'il n'y a pas d'interaction, il n'est pas question d'imaginer une condensation de Bose-Einstein de fermions libres.

7. Conclusion

L'auteur regrette de ne présenter encore que les principes d'une méthode. Il espère toutefois avoir montré que, dans un problème à multiples particules, le problème n'est pas la recherche des fonctions d'onde mais de grandeurs régressives plus simples et plus „locales". Leur détermination fait appel à une méthode d'approximation différente de la méthode de perturbation, la méthode de perturbation s'appliquant bien aux forces faibles et celle proposée ici — surtout au paragraphe 6 — aux forces à courte portée. Si bien qu'elle peut apporter des lumières dans des problèmes différents. Le fait que le système est en équilibre de température et que c'est un système ouvert — au sens thermodynamique — n'exclut pas la possibilité d'extrapoler les résultats au zéro absolu, donc à un système à l'état fondamental et même à un système excité, puisque la méthode couvre — ou du moins espère couvrir — les états métastables, au sens thermodynamique et donc à la limite les états stationnaires autres que l'état fondamental.

L'exploitation, comme point de départ d'une méthode d'approximation, du fait que les forces sont à courte portée, a déjà été, avec une attaque

assez différente, et non thermodynamique, par Brueckner et Levinson [11]). Bethe [12]), en utilisant dans son exposé de la méthode de Brueckner les fonctions propres à une particule dans le champ self-consistant, utilise une approximation des fonctions propres de l'opérateur μ_1, fonctions dont le rôle fondamental a été signalé au paragraphe 3.

Bibliographie

1) L. Sarolea et J. E. Mayer, Phys. Rev. **101** (1956) 1627
2) H. S. Green, The molecular theory of fluids (New York, 1952)
3) F. Bloch, Z. Physik **74** (1932) 295
4) J. Yvon, Recherches sur la théorie cinétique des liquides (Actualités Scient. et Industr. no. 542, 543, Hermann, Paris 1937)
5) P. J. Price, Phys. Rev. **94** (1954) 257
6) R. P. Feynmann et M. Cohen, Phys. Rev. **102** (1956) 1189
7) F. P. Buff et R. Brout, Journal Chem. Phys. **23** (1955) 464
8) G. Fournet, Journal de Physique **17** (1956) 940
9) R. M. Mazo et J. G. Kirkwood, Proc. Nat. Acad. **41** (1955) 204
10) J. Yvon, J. de Physique **7** (1936) 93
11) K. A. Brueckner et C. A. Levinson, Phys. Rev. **97** (1955) 1344; K. A. Brueckner, Phys. Rev. **100** (1955) 36
12) H. A. Bethe, Phys. Rev. **103** (1956) 1353

Nuclear Physics **4** (1957) 21—28; © *North-Holland Publishing Co., Amsterdam*
Not to be reproduced by photoprint or microfilm without written permission from the publisher

A POSSIBLE TEST OF THE PRIMARITY OF THE WEAK INTERACTIONS COMPRISING LEPTONS

S. ONEDA
Theoretical Physics Department, University of Manchester †

Received 4 April 1957

Abstract: A careful analysis of the charge properties of the secondary particles in the K-meson decays comprising leptons is proposed. The occurrence of the modes $K^+ \to \pi^+ + \pi^+ + \mu^-(e^-) + \nu$ and $K^0 \to \pi^+ + \mu^-(e^-) + \nu$ should give good information on the character of the primary weak interactions. Also the importance of the investigation of the alternative decays of hyperons into leptons is stressed.

1. Introduction

It is well known that all the weak interactions observed so far have coupling strengths of the same order of magnitude. So it would be quite attractive to explain the various kinds of weak interactions in terms of the simplest primary weak interactions which have certain universal characters[1]). The following interactions could be chosen as the most suitable elementary interactions:

(a) Weak Fermi interactions (f-int.) — the so-called universal Fermi interactions;

(b) Weak boson-fermion interactions (g-int.) — the $\pi \to \mu + \nu$, $K \to \mu + \nu$ and $\Lambda^0 \to P + \pi^-$ etc..

It is clear that all the weak interactions cannot be explained in terms of only the g-int., because we cannot derive the $\mu \to e + 2\nu$ decay as the combined effects of the strong interactions and the weak g-int. So the following two standpoints remain to be investigated.

(I) The weak Fermi interaction (universal Fermi interaction) is the *sole* source of all weak interactions.

(II) Both interactions do exist as primary interactions.

It is known that from standpoint (I) the asymmetry between the $\pi \to \mu + \nu$ and $\pi \to e + \nu$ modes and the coupling types of β-decay require that the interaction types of f-int. must be dependent on the processes [2]). If standpoint (I) is true, it will be one of the tasks of theoretical physicists to look for regularities among the process-dependent f-int.

From standpoint (II), for example, the asymmetry between the μ, ν and e, ν modes leads Schwinger [3]) to make the following speculations. The μ, ν and e, ν fields are associated with different types of interactions, the muon

† On leave of absence from the Institute of Theoretical Physics, Kanazawa University.

being coupled to bosons (g-int. such as the $\pi \to \mu+\nu$ and $K \to \mu+\nu$ interaction) and the electron to fermions (f-int.).

As our knowledge about the systematisation and the ordering of the weak interactions within the baryon-meson-lepton system is as yet of a preliminary nature, many experiments, especially on the *unwanted processes* — processes which do not occur in nature and require the introduction of selection rules — are desired to clarify the situation. As a matter of fact, it is, in general, difficult to tell which of the two interactions (g-int. and f-int.) are contributing to the processes under consideration, because both interactions have nearly the same coupling strengths. In this paper, as is remarked in ref. [4]), it is pointed out that the primary f-int. and the g-int. reveal remarkable differences in some K-meson phenomena and they may give us a clue to the choice between standpoints (I) and (II).

2. K-meson Decays Comprising Pions and Leptons

In addition to the mode $K^+ \to \mu^+ + \nu$ we have also the $K^+ \to \pi^0 + \mu^+ + \nu$ and $K^+ \to \pi^0 + e^+ + \nu$. We may also have the mode $K^+ \to \pi^+ + 2\nu$ which was discussed in detail in the preceding paper [4]). These processes would be realised by the combined intermediations of the strong baryon-meson interactions and either the g-int. or f-int. For example, the simplest intermediation would be, for the g-int. [3]):

$$K^+ \to \pi^0 + K'^+ \to \pi^0 + (\mu^+(e^+) + \nu), \tag{1}$$

for the f-int. [1, 2]):

$$K^+ \to P + \bar{\Lambda}^0 \to (\pi^0 + P') + \bar{\Lambda}^0 \to \pi^0 + \mu^+(e^+) + \nu. \tag{2}$$

However, the g-int. and f-int. disclose very different results in higher-order processes. Let us investigate the following processes †:

$$K^+ \to \pi^+ + \pi^- + \mu^+(e^+) + \nu, \tag{3}$$

$$K^+ \to \pi^+ + \pi^+ + \mu^-(e^-) + \nu. \tag{4}$$

Our following arguments depend only on two assumptions which are, at present, believed to be true:

(i) Strong baryon-meson interactions are charge-independent and they (as well as electromagnetic interactions) conserve the strangeness quantum number [5]).

(ii) The strengths of the weak interactions, g-int. and f-int., are so weak that their appearance once is just enough to make the instability of the K-mesons compatible with the observed life-times.

It follows from (ii) that in the main mechanism of the processes (3) and (4) shown in fig. 1 the vertex which comprises leptons is the only weak

† Throughout this paper (unless it is necessary) we do not specify neutrino and antineutrino because it does not affect the essential nature of our arguments.

vertex. Other vertices must be all strong interactions and electromagnetic interactions (if the inclusion of internal photon lines is necessary for the leading diagrams, otherwise the radiative corrections due to the electromagnetic field will be neglected completely) which conserve the strangeness quantum number.

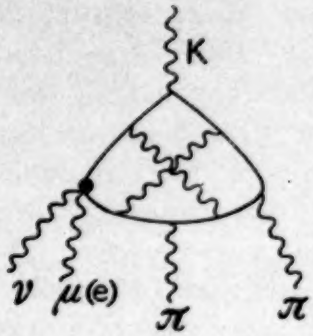

Fig. 1

From these considerations we can infer the character of the *baryon-meson* part of the weak vertex, from which the $\mu^{\pm}$-meson ($e^{\pm}$) and the neutrino are emitted simultaneously. The pion has strangeness quantum number zero. Thus in the processes (3) and (4) the sum of the strangeness quantum numbers of the *baryon-meson* part of the weak vertex (*g*- or *f*-int.) must be equal to that of the initial K^+-meson. By this argument, in the intermediation due to the *g*-int., the process (4), $K^+ \to \pi^+ + \pi^+ + \mu^-(e^-) + \nu$, will not occur since the primary *g*-int., $K^- \to \mu^-(e^-) + \nu$, cannot contribute to the above processes. On the contrary, the *g*-int., $K^+ \to \mu^+(e^+) + \nu$, will be able to intermediate the mode (3), $K^+ \to \pi^+ + \pi^- + \mu^+(e^+) + \nu$.

In contrast to the case of *g*-int., the *f*-int. would, in principle, be able to have the following Fermi interactions, the left-hand side of which has the same strangeness quantum number as the initial K^+-meson:

$$\begin{aligned}
&P + \bar{\Lambda}^0 \to \mu^+(e^+) + \nu \\
&N + \bar{\Sigma}^- \to \mu^+(e^+) + \nu \\
&P + \bar{\Sigma}^0 \to \mu^+(e^+) + \nu \qquad (5) \\
&\Lambda^0 + \bar{\Xi}^- \to \mu^+(e^+) + \nu \\
&\Sigma^+ + \bar{\Xi}^0 \to \mu^+(e^+) + \nu \\
&\Sigma^0 + \bar{\Xi}^- \to \mu^+(e^+) + \nu,
\end{aligned}$$

$$\begin{aligned}
&N + \bar{\Sigma}^+ \to \mu^-(e^-) + \nu \qquad (6) \\
&\Sigma^- + \bar{\Xi}^0 \to \mu^-(e^-) + \nu.
\end{aligned}$$

Then it is possible that we have the $(\pi^+\pi^+\mu^-(e^-)\nu)$ mode as well as the $(\pi^+\pi^-\mu^+(e^+)\nu)$ mode unless there is a selection rule which forbids the reaction (6) from the outset. This is due to the fact that the Σ-particle has three different charge states for the same strangeness quantum number. The Λ^0 cannot be responsible for the mode $(\pi^+\pi^+\mu^-(e^-)\nu)$.

It seems that from (5) and (6) more channels exist for the $\mu^+(e^+) + \nu$

mode than the $\mu^-(e^-)+\nu$ mode. However, *so long as the interactions* (6) *are not forbidden*, the frequency of the mode of $(\pi^+\pi^+\mu^-(e^-)\nu)$ would not be so small compared with that of $(\pi^+\pi^-\mu^+(e^+)\nu)$. So the detection of the mode $(\pi^+\pi^+\mu^-(e^-)\nu)$ would give convincing positive evidence that the f-int. is responsible for the processes under consideration. Then standpoint (I), that the $K\to\mu+\nu$ and $K\to\mu(e)+\nu+\pi$ are also due to the sole intermediation of the f-int. of form (5) and (6), would acquire a firmer basis. It should be noted that our present arguments are free from the detailed properties fo the K-meson and of the interaction types of the intervening couplings, and also are free from the difficulties of the treatment of the strong couplings.

Schwinger's conjecture [3]) mentioned in § 1 should also be examined, since it predicts an asymmetry between the muon mode and the electron mode. That is, we would not have the $(\pi^+\pi^+\mu^-\nu)$ mode, whereas the $(\pi^+\pi^+e^-\nu)$ would appear. It should be remarked that, although the occurrence of the $(\pi^+\pi^+\mu^-(e^-)\nu)$ will give clear proof that f-int. is contributing, the non-occurrence of the above processes does not necessarily mean that f-int. is not playing a part, since there might exist a selection rule which allows the coupling (5) but forbids the (6). Sachs' attribute [6]), e.g., would give such a selection rule. So if existence of the mode $(\pi^+\pi^-\mu^+(e^+)\nu)$ and non-existence of the mode $(\pi^+\pi^+\mu^-(e^-)\nu)$ are confirmed, we need, at least, one more experiment in order to conclude that the g-int. is the sole mechanism of the K-meson decays comprising leptons. That is, we must be sure that all f-int. of the type (5) do not exist. This can be checked by examining the predictions of (5) on the decays such as $\Lambda^0\to P+e^-(\mu^-)+\nu$ and $\Sigma^-\to N+e^-(\mu^-)+\nu$ etc. For instance, the coupling constant of f-int. ($f\approx 10^{-49}$ erg cm^3) predicts that the $\Lambda^0\to P+e^-+\nu$ is less frequent than the $\Lambda^0\to P+\pi^-$ by a factor [1]) 1/60—1/200 except for the pseudoscalar coupling. Only the latter coupling gives a smaller frequency for the $\Lambda^0\to P+e^-+\nu$.

The same phenomena would also be expected in the K^0-meson decays. Let us consider the $K^0\to\mu^\pm(e^\pm)+\nu+\pi^\mp$ modes. By the same reasoning as in the case of the $K\to\pi+\pi+\mu(e)+\nu$ decay, we can easily see that for the intermediation due to the g-int., the $K^0\to\mu^-(e^-)+\nu+\pi^+$ would be negligibly small compared with the $K^0\to\mu^+(e^+)+\nu+\pi^-$, whereas for the f-int. both processes would be of comparable order. (The $K^0\to\mu^+(e^+)+\nu+\pi^-$ might be slightly more probable because there are more channels into $\mu^+(e^+)+\nu$.)

Experimentally, however, it is not so straightforward to check the above possibility, though we may have more experimental data of the $K\to\pi+\mu(e)+\nu$ than of the $K\to\pi+\pi+\mu(e)+\nu$. (The frequency of the latter mode will be discussed in § 3.) This is because the K^0-decays are

best discussed, not in terms of K^0 and $\overline{K}^0$ but rather in terms of K_1^0 and K_2^0, where

$$K^0 = 2^{-1/2}\ (K_1^0 + iK_2^0),$$
$$\overline{K}^0 = 2^{-1/2}\ (K_1^0 - iK_2^0).$$

This was first proposed [7]) under the assumption of the invariance of the theory under charge conjugation and under space reflection. Recently, it has been proved that both invariances are not valid in the weak interactions comprising neutrinos [8]). However, even if the same situation happens for the interactions under consideration, the description in terms of K_1^0 and K_2^0 would be still most adequate [9]), provided the theory is still invariant under the combined inversion (CP), simultaneous inversion under parity and particle-anti-particle conjugation. As the K_1^0 and the K_2^0 are a mixture of the K^0 and the $\overline{K}^0$ meson, the possible asymmetry between the $K^0 \to \pi^+ + \mu^-(e^-) + \nu$ and the $K^0 \to \pi^- + \mu^+(e^+) + \nu$ will be masked in the K_1^0 and K_2^0 description. This problem is discussed in detail by Treiman and Sachs [10]). At the time of production the K^0 (not $\overline{K}^0$) is produced in association with Λ^0 or Σ. So the initial value of the ratio R of the two rates of decays, $W(\pi^+\mu^-(e^-)\nu)$ and $W(\pi^-\mu^+(e^+)\nu)$,

$$R \equiv \left[\frac{W(\pi^+\mu^-(e^-)\nu)}{W(\pi^-\mu^+(e^+)\nu)}\right]_{t=0}$$

would be zero for the g-int. model and would be *nearly equal to unity* for the f-int. model. The time variation of the ratio R would be given† by taking $a_1 = a_2$ and $a_2 \approx 0$ for the g-int. model and the f-int. model, respectively, in equations (8) and (9) of ref. [10]). For the f-int. model ($a_2 \approx 0$) the value of R is nearly constant (≈ 1), but for the g-int. model ($a_1 = a_2$) the value of R changes rather remarkably. That is, in this case, the rate $W(\pi^-\mu^+(e^+)\nu)$ decreases with time but the rate $W(\pi^+\mu^-(e^-)\nu)$ would, on the contrary, increase with time starting from the value zero. This arises from the interference between the K_1- and K_2-decay. The detail can be seen in the results given in ref. [10]).

Thus we may also be able to draw some conclusions about the rôles of the f-int. and the g-int. in the $K^0 \to \pi + \mu(e) + \nu$ decay by a careful analysis of the ratio R of the two alternative processes.

3. Relative Frequency of the Modes $K \to \pi + \pi + \mu(e) + \nu$

The observed branching ratios for various modes of the K^+-mesons, $\mu^+ + \nu$, $\pi^+ + \pi^0$, $\pi^+ + \pi^- + \pi^+$, $\pi^0 + e^+ + \nu$, $\pi^0 + \mu^+ + \nu$ are reported to be, for

† Here a_1 and a_2 denote the transition amplitudes for the modes consisting of $(\pi^-\mu^+(e^+)\bar{\nu})$ and $(\pi^+\mu^-(e^-)\nu)$ which have even and odd parity under CP transformation respectively. In the two-component theory of the neutrino this may be achieved [4]) by just replacing ν and $\bar{\nu}$ by $\frac{1}{2}(1-\gamma_5)\nu$ and $\frac{1}{2}(1+\gamma_5)\bar{\nu}$ respectively.

example, 59 %, 21 %, 5.2 %, 6 % and 5 % respectively. (See ref. [11]) and other data cited there.) Moreover, there are already some examples of non-coplanar τ-meson decays [12]) which are interpreted as the radiative decay of the τ-meson, $\tau^+ \to \pi^+ + \pi^+ + \pi^- + \gamma$. We could imagine that the $K \to \pi + \pi + \mu(e) + \nu$ modes would take place by such a mechanism as substituting a weak vertex (g-int. or f-int.) comprising the $\mu(e)$, ν for a weak vertex responsible for the $K \to \pi + \pi + \pi$ decay, because all weak interactions have coupling strengths of the same order of magnitude. If the above conjecture is true, the $K \to \pi + \pi + \mu(e) + \nu$ would be more favourable than the $K \to \pi + \pi + \pi + \gamma$, since the latter needs to involve the electromagnetic interaction. So we must not be too optimistic about the occurrence of the modes $K \to \pi + \pi + \mu(e) + \nu$. Some experimental evidence on τ-meson-like phenomena in which two charged pions and a μ-meson appear has been reported [13]). They might be examples of $K \to \pi + \pi + \mu + \nu$ mode.

Here we briefly compare the phase space volumes of the processes $K \to \pi + e + \nu$ and $K \to \pi + \pi + e + \nu$.

The probability W of the process

$$K(p) \to \pi(q_1) + \pi(q_2) + e(q_e) + \nu(q_\nu)$$

(the K being at rest) is given by

$$W = |\mathfrak{M}|^2 (2\pi)^4 \delta^4(q_1 + q_2 + q_e + q_\nu - p) \left(\frac{1}{2\pi}\right)^3 \left(\frac{d^3 q_1}{2\omega_1}\right) \times \left(\frac{1}{2\pi}\right)^3 \left(\frac{d^3 q_2}{2\omega_2}\right) \left(\frac{1}{2\pi}\right)^3 \left(\frac{d^3 q_e}{\omega_e}\right) \left(\frac{1}{2\pi}\right)^3 \left(\frac{d^3 q_\nu}{\omega_\nu}\right) \left(\frac{1}{2M_K}\right) \tag{7}$$

where, for instance, p is the four-momentum of the K-meson (with mass M_K) and ω_1 is the energy of the π-meson, $\omega_1 = \sqrt{q_1^2 + m_\pi^2}$. $|\mathfrak{M}|^2$ is the square of the *invariant* matrix-element $\mathfrak{M}$ averaged over the spin states of leptons. We simplify the results by assuming that $|\mathfrak{M}|^2$ is constant. The computation of (7) can be performed in a completely relativistic way by using an analogous method to the procedure used by Dalitz [14]) in the discussion of the $\tau^+ \to \pi^+ + \pi^+ + \pi^- + \gamma$ decay. Compared with the mode $K \to \pi + e + \nu$, we have one extra pion which must be emitted from the strong vertex. We extract this strong-coupling constant G as $\mathfrak{M} = \mathfrak{M}_0 G$. The computation of (7) yields

$$W = 2^{-5}(2\pi)^{-4} \cdot \frac{G^2}{4\pi} \cdot |\mathfrak{M}_0|^2 \cdot \frac{m_\pi^6}{M_K^3} \times 16.8. \tag{8}$$

In the same way the probability of W' of the $K \to \pi + e + \nu$ can be calculated. From dimensional reasoning we assume that the invariant matrix-element $\mathfrak{M}'$ is equal to $\lambda \mathfrak{M}_0$, where λ is a quantity which has the dimension of a mass.

$$W' = 2^{-1}(2\pi)^{-3}|\mathfrak{M}_0|^2 \cdot \frac{m_\pi^2}{M_K} \cdot \lambda^2 \cdot \left\{\frac{1}{8}\frac{(M_K^2+m_\pi^2)(M_K^2-m_\pi^2)}{M_K^2 m_\pi^2} - \tfrac{1}{2}\log\frac{M_K}{m_\pi}\right\}$$

$$= 2^{-1}(2\pi)^{-3}|\mathfrak{M}_0|^2 \cdot \frac{m_\pi^2}{M_K} \cdot \lambda^2 \times 0.92. \qquad (9)$$

Thus

$$\frac{W}{W'} = \frac{G^2}{4\pi} \cdot 2^{-4}(2\pi)^{-1}\left(\frac{m_\pi}{\lambda}\right)^2 \times 1.5.$$

Taking $G^2/4\pi \approx 1$, the frequency ratio $W/W' \approx 1.45 \times 10^{-2}$ for $\lambda = m_\pi$ and $\approx 1.16 \times 10^{-3}$ for $\lambda = M_K$. Thus the frequency of the $K \to \pi+\pi+e+\nu$ would be expected to be of the order a few percent † compared with the $K \to \pi+e+\nu$, mode. The same conclusion would also hold for the muon mode. As the detection of the events having three charged secondary particles is not so difficult, we would have a good chance to observe the processes under consideration in the course of the analysis of the τ-meson-like phenomena.

4. Discussion of Alternative Method

As is discussed in the preceding sections, the accumulation of enough K-meson events would make it possible to draw some conclusion from the investigation proposed here. Another way to clarify the primarity of the weak interactions is as follows. If the K-meson has spin *zero*, we cannot expect the *vector*, *pseudovector* or *tensor* g-type couplings (in such an intermediation as (1)) for the weak vertex comprising $\mu(e), \nu$ because they will be reduced to the scalar or pseudoscalar forms. Thus, if these couplings confirmed in the spin *zero* K-meson decays, such as $K \to \pi+\mu(e)+\nu$, they must be ascribed to the couplings due to the f-int. The preliminary analysis [15]) of the electron spectra in the $K^+ \to \pi^0+e^++\nu$ decays seems to suggest the existence of the *tensor* and *scalar* interactions. This would imply the existence of the β-decay interactions of hyperons such as $\Lambda^0 \to P+e^-+\nu$ which have the same coupling types as the ordinary nucleon β-decay. The polarisation measurements of the electron and μ-meson in the $K \to \pi+\mu(e)+\nu$ decays will also be powerful in determining the coupling types [16]). It should be remembered that, if the standpoint of the primary f-int. is true, we must have the alternative decays of hyperons into leptons. Frequencies of such decays as $\Lambda^0 \to P+e^-(\mu^-)+\nu$ are estimated to be of the order of a few percent when compared with the normal decays of the hyperons [1]). An especially interesting problem arises in ascertaining whether both the

† Note that if G represents the usual pseudoscalar pion-nucleon coupling, $G^2/4\pi \approx 15$. This will be the case for the f-int. intermediation such as (2). In the g-int. model such as (1), G would represent the interaction [3]) $K \to K'+\pi$. It seems that in this case also $G^2/4\pi$ must be large ($\gtrsim 1$) because the $K \to \pi+\mu+\nu$ is quite appreciable compared with the $K \to \mu+\nu$ mode.

$\Sigma^+ \to N+e^+(\mu^+)+\nu$ and the $\Sigma^- \to N+e^-(\mu^-)+\nu$ do exist or one of them is forbidden. If such alternative decays of hyperons into leptons turn out to be much *less frequent*, we would be forced to have recourse to the primary g-int. to explain the occurrence of various modes of K-meson decays comprising leptons. So the simultaneous investigation of the lepton modes of K-meson and hyperon decays is desired because they are of *complementary* nature.

Note added in proof: The test whether the lepton vertices in the $K \to \mu(e)+\nu+\pi$ consist of only scalars with respect to rotation would be powerful in determining the primarity of the $K \to \mu(e)+\nu$ interactions. The angular correlation [17]) between the $\mu^{\pm}(e^{\pm})$ and the $\pi^{\mp}$ in the $K^0 \to \mu^{\pm}(e^{\pm})+\nu+\pi^{\mp}$ could also be useful for this purpose. The possibility that the $\pi \to \mu+\nu$ is the cause of the $\mu^- + P \to N+\nu$ could also be tested by examining whether the lepton covariance in the $\mu^- + P \to N+\nu$ is scalar with respect to rotation.

I shcuild like to express my thanks to Professor L. Rosenfeld for his interest in this work. I am indebted to Dr. S. Ogawa and Dr. A. Wakasa for sending their papers before publication. Thanks are also due to the University of Manchester for the award of an ICI Fellowship.

References

1) K. Iwata, S. Ogawa, H. Okonogi and S. Oneda, Prog. Theor. Phys. **13** (1955) 19;
S. Ogawa, Prog. Theor. Phys. **13** (1955) 367;
N. Dallaporta, Nuovo Cimento **1** (1955) 962;
G. Costa and N. Dallaporta, Nuovo Cimento **2** (1955) 519
2) S. Oneda and A. Wakasa, Nuclear Physics **1** (1956) 125;
F. Duimio, Nuovo Cimento **2** (1955) 1308;
M. Gell-Mann, Proceedings of the Sixth Rochester Conference (1956)
3) J. Schwinger, Phys. Rev. **144** (1956) 1164
4) S. Oneda, Nuclear Physics **3** (1957) 598
5) K. Nishijima, Prog. Theor. Phys. **12** (1954) 107
M. Gell-Mann and A. Pais, Proceedings of the Glasgow Conference on nuclear and meson physics (Pergamon Press, London, 1955)
6) R. G. Sachs, Phys. Rev. **99** (1955) 1573
7) M. Gell-Mann and A. Pais, Phys. Rev. **97** (1955) 1387
8) T. D. Lee and C. N. Yang, Phys. Rev. **103** (1956) 254
9) L. Landau, Nuclear Physics **3** (1957) 127;
T. D. Lee, R. Oehme and C. N. Yang, Phys. Rev. **106** (1957) 340;
R. Gatto, Phys. Rev. in the press
10) S. B. Treiman and R. G. Sachs, Phys. Rev. **104** (1956) 1545
11) T. F. Hoang, M. F. Kaplon and G. Yekutieli, Phys. Rev. **102** (1956) 1187
12) R. R. Daniels and Y. Pal, Proc. Ind. Acad. Sci. **40** (1954) 114
13) K. R. Dixit, Z. Naturf. **9a** (1954) 355
14) R. H. Dalitz, Phys. Rev. **99** (1955) 915
15) S. Furuichi, T. Kodama, S. Ogawa, Y. Sugawara, A. Wakasa and M. Yonezawa, Prog. Theor. Phys. **17** (1957) 89
S. Furuichi, Y. Sugawara, A. Wakasa and M. Yonezawa, Nuovo Cimento **5** (1957) 285
16) J. Werle, Nuclear Physics **4** (1957) 171
17) A. Pais and S. B. Treiman, Phys. Rev. **105** (1957) 1616

Nuclear Physics **4** (1957) 29—38; © *North-Holland Publishing Co., Amsterdam*
Not to be reproduced by photoprint or microfilm without written permission from the publisher

INTERPRETATION OF COSMIC RAY JETS OBSERVED IN PHOTOGRAPHIC EMULSIONS

I. A. IVANOVSKAYA AND D. S. CHERNAVSKY
P. N. Lebedev Physical Institute, USSR Academy of Sciences, Moscow

Received 18 February 1957

Abstract: Showers produced in photographic emulsions by high energy nucleons ($10^{10}-10^{12}$ eV) — the so-called "jets" — are analysed in the present paper.

The analysis is based on Fermi's statistical theory extended to the case of interaction between a nucleon and nucleus.

It is shown that the main features of these showers can be explained without assuming the existence of two different classes of interactions as hitherto has been done.

Numerous investigations of so-called "jets" have been reported recently[1–12]). According to the classification proposed by Daniel *et al.* [13]), showers which are produced in photographic emulsions by high energy cosmic ray particles and which contain only a few grey and black tracks ($n_g+h \leqq 4$) are termed jets. The usual interpretation of these showers is that they arise in the interaction between the primary particle and a hydrogen nucleus or one of the peripheral nucleons of a heavy nucleus. The velocity of the c.m.s., v_c (more precisely the quantity $\gamma_c = (1-v_c^2/c^2)^{-\frac{1}{2}}$) was derived by the authors from the angular distribution of the secondary particles and, by proceeding from the assumption of a nucleon-nucleon interaction, they determined the primary particle energy. It was found that with respect to dependence of the multiplicity (n_s) on primary energy all jets could be divided into two classes: class A jets possess a large multiplicity and small γ_c and class B jets have a small multiplicity and large γ_c. These two classes of jets can moreover be characterized by different values of the so-called inelasticity coefficient K which is defined as the ratio of the total meson energy to the kinetic energy of the nucleons prior to collision in the c.m.s. For nucleon-nucleon interaction the inelasticity coefficient can be expressed by the formula

$$K = \frac{1.5 n_{\pm} \gamma'}{2\mu(\gamma_c - 1)} \tag{1}$$

where $n^{\pm}$ is the number of charged π-mesons in the shower, μ is the ratio between the nucleon and π-meson masses and γ' is the energy of π-mesons in the c.m.s. The authors estimated γ' by using the formula

$$\gamma' = \gamma_c \sin \vartheta_L \qquad (2)$$

where ϑ_L is the maximum angle in the laboratory system.

The value of K calculated from formulae (1) and (2) were found to be close to unity for jets of class A whereas for jets of class B the mean value of K, according to the data of various authors, varied between 1/3 and 1/2.

On basis of these data it was concluded that the kinetic energy of the nucleons was completely spent in the creation of π-mesons in the first case whereas in the second case only part of it was spent.

Various hypotheses have been proposed to explain the existence of two classes of jets:

1) Different types of jets are initiated by different types of particles. Jets of one of the classes are produced by nucleons while those of the second class are created by mesons [5, 10]).

2) π-mesons are predominantly produced in high multiplicity jets whereas in low multiplicity jets heavy mesons are dominant [5]).

3) High multiplicity jets are produced in head-on collisions, low multiplicity jets in peripheral collisions between two nucleons [4, 5]).

All these hypotheses are based on an assumption, which does not appear to be sufficiently grounded, namely, that the primary particle collides with a single nucleon of the nucleus.

Heitler and Terreoux [2]) and, somewhat later, Cocconi [14]), showed that the presence of a small number of grey and black tracks in a shower or even the absence of such tracks is not sufficient proof that only a single nuclear nucleon is involved in the collision since even if the primary particle collides with a nucleon "tunnel" only a small fraction of the excitation energy may be transferred to the nucleus.

The model of a "tube" or "tunnel" cut out by a primary nucleon in the nucleus was first invoked by Roesler and McCusker [1]) and Heitler and Terreoux [2]) to analyse jets. They showed that the experimental data on jets do not contradict the conclusions which follow from the tunnel model. However, the aforementioned authors could not give a thorough analysis since they were unable to determine the dimensions of the tunnel or the energy of the primary particle for each jet.

In the present paper we have attempted to analyse jets on the basis of Fermi's statistical theory and the tunnel model.

A method for determining the energy of the primary particle and dimensions of the tunnel from a knowledge of the number of secondary particles and their angular distribution has been developed.

The idea of this method is the following. The number of particles created in a nuclear interaction depends on the energy of the primary particle and on the number of nucleons involved in the collision, $N = N(E, n)$. The velocity of the c.m.s., which we shall characterize by the quantity γ_c, is

also a function of these quantities $\gamma_c = \gamma_c(E, n)$. Experimentally one can measure the number of created particles N and from their angular distribution determine γ_c. From the two known quantities N and γ_c the two unknown quantities E and n can be determined.

The function $\gamma_c(E, n)$ can easily be deduced from the laws of conservation of energy and momentum:

$$\gamma_c = \frac{E_0^2 + (n-1)^2 - 1}{2E_0(n-1)} \tag{3}$$

where E_0 is the total energy in the c.m.s. expressed in units of rest energy of the nucleon and n is the number of nucleons involved in the collision, including the primary nucleon.

In order to determine $N(E, n)$ we compute for various primary energies the statistical weights of the final states in which n nucleons and m π-mesons are present. It will moreover be assumed that only π-mesons are created in the collision, nucleon-antinucleon pair production being neglected.

The statistical weight of a state involving n nucleons and m π-mesons is given by the relation

$$S = \left(\frac{V}{8\pi^3\hbar^3}\right)^{n+m-1} \frac{\mathrm{d}Q_{n,m}(E_0)}{\mathrm{d}E_0} \frac{1}{m^+!\, m^-!\, m^0!\, n_p!\, n_n!} \tag{4}$$

where V is the volume in coordinate and Q the volume in momentum spaces; the last factor accounts for the existence of three types of mesons and two types of nucleons:

$$m^+ + m^- + m^0 = m; \quad n_p + n_n = n.$$

Volume V is equal to the volume of n nucleons with account of Lorentz contraction

$$V = \frac{4}{3}\pi \left(\frac{\hbar}{\mu}\right)^3 \frac{n}{\gamma_c}, \tag{5}$$

where μ is the π-meson mass.

Following Fermi, in the low energy region where $(E_0 - n)/n < 1$, the factor $\mathrm{d}Q_{n,m}(E_0)/\mathrm{d}E_0 = W_{n,m}(E_0)$ is taken to equal

$$W_{n,m}(E_0) = \frac{(2\pi)^{3m+\frac{3}{2}(n-1)}}{\pi^{2m} n^{\frac{3}{2}}} \cdot \frac{(E_0 - n)^{3m+\frac{3}{2}(n-1)-1}}{[3m + \frac{3}{2}(n-1) - 1]!}. \tag{6}$$

This formula has been obtained by approximately taking into account the law of conservation of momentum and assuming that the nucleons are non-relativistic and the mesons are extremely relativistic.

In the high energy domain (> 50 GeV in the c.m.s.) we use the formula derived by V. M. Maximenko and I. L. Rosental [16]) which exactly takes into account the law of conservation of momentum. In this formula $W_{n,m}(E_0)$

is represented as a series expansion; we shall take the first five terms of the expansion.

In the low energy region the series converges poorly and we therefore determine the statistical weights for intermediate energies by graphical

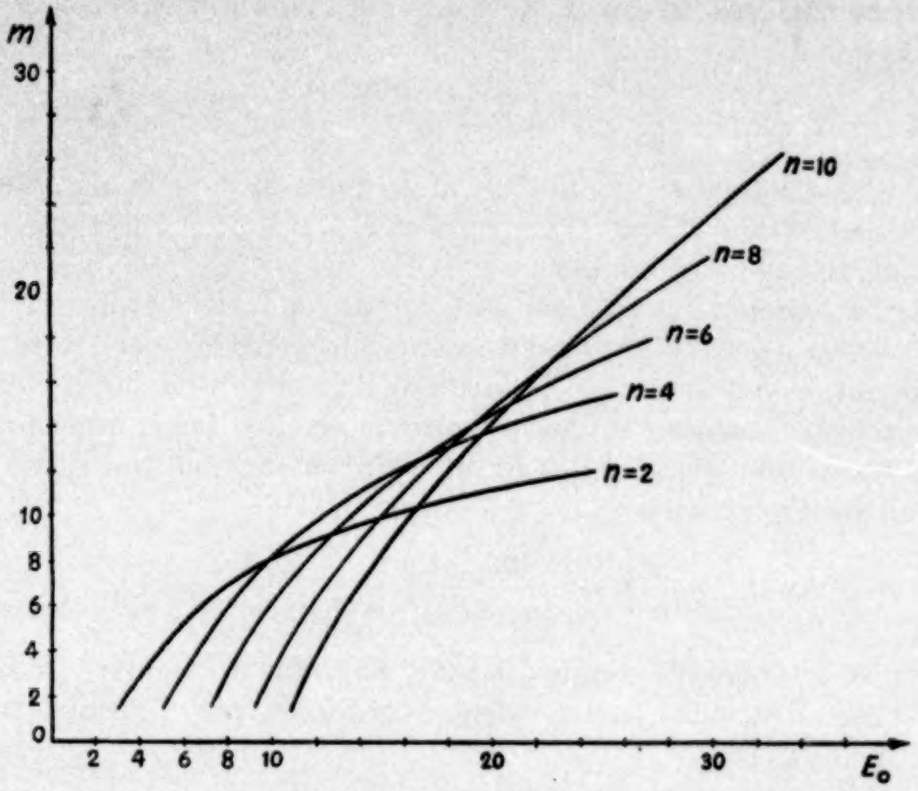

Fig. 1. Dependence of mean number of created π-mesons, on the total energy in the c.m.s., E_0, and on the number of nucleons, n, participating in the collision.

interpolation between the values which the Fermi formula yields and the values which the Rosental-Maximenko formula yields.

The statistical weights of the various states evaluated in this fashion are used to determine the mean number of π-mesons created in a collision between the primary nucleon and a tunnel of nuclear matter consisting of a definite number of nucleons. The results are presented in fig. 1. The total energy in the c.m.s. is plotted along the abscissa axis and the average number of produced π-mesons along the ordinate axis. The numbers on the curves denote the number of nucleons involved in the collision.

This graph was used to determine the dependence of the number of charged shower particles in a jet, n_s, on the quantity γ_c and on the number of nucleons involved in the collision, n (fig. 2).

It has been assumed that a) in the laboratory system all of the nucleons are relativistic, half of them being protons and b) 2/3 of the total number (m) of mesons are charged, that is

$$n_s = \tfrac{2}{3}m + \tfrac{1}{2}n.$$

Fig. 2 can be used to find for each jet the most probable number of nucleons which are struck in a collision, $(n-1)$, and to find from formula (3) the total energy in the c.m.s.

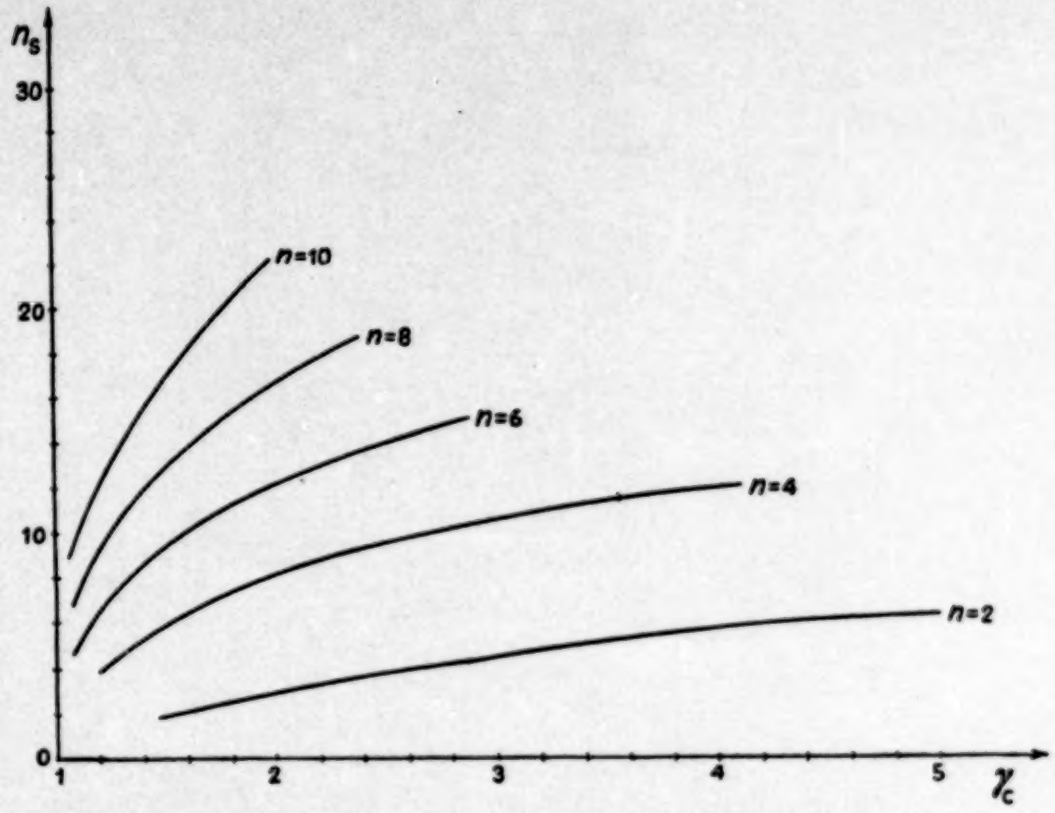

Fig. 2. Dependence of number of charged shower particles n_s on γ_c and on the number of nucleons n, participating in the collision.

These quantities are determined for the jets reported in ref. [4, 5, 6, 9, 10]). The results are presented in table 1. Following Bertolino and Pescetti [10]), we have divided the jets described in ref. [5, 6]) into two classes.

It can be seen from the table that almost all events which these authors consider as class B events were initiated in nucleon-nucleon encounters. Part of these events for which γ_c is very great and the number of particles is small can be interpreted as a peripheral nucleon-nucleon collision. (These cases are denoted by an asterisk in the table).

Almost all class A events were found to be collisions between the primary nucleon and several nucleons of the nucleus (nucleon tunnel). The number of nucleons in a tunnel $n_T = n-1$. is shown in column 4. On the average $n_T = 3$. The values of the total energy, E_0, in the c.m.s. for class A jets are presented in column 5. The authors thought that these events were nucleon-nucleon encounters and therefore assumed $E_0 = 2\gamma_c$. However, as can be seen from the table, E_0 is in fact approximately n_T times larger. Consequently the values of K computed from formula (1) by the authors for

TABLE 1

n_T-number of nucleons in the tunnel, $n_T = n-1$

Author, year	class A				class B		
	n_s†	γ_c	n_T	E_0	n_s†	γ_c	n_T
1	2	3	4	5	6	7	8
Hoang [4]) (1953)	9	3.2	2	13	5	3.2	1
	11	3.8	3	19	8	5.0	1
	11	4.0	3	19	3	6.0	1*
	12	4.3	3	24	8	6.5	1
	15	4.8	4	37	7	8.5	1
	18	7.1	4	≈ 50	8	11.5	1
	22	7.4	5	≈ 65	15	12.2	2
Dilworth *et al.*[5]) (1953)	4	1.1	3–4	6	4	2.6	1
	4	1.1	3–4	6	4	3.3	1
	6	1.8	2	8.5	4	4.2	1*
	6	2.3	2	8.5	4	5.1	1*
	7	1.2	5	10	4	11.0	1*
	7	3.0	2	9.5	4	12.8	1*
	7	3.8	1–2	9.5	4	14.3	1*
	8	3.0	2	13.5	4	18.0	1*
	8	3.3	2	15.5	4	31.5	1*
	8	5.0	1–2	13.5	4	33.0	1*
	9	1.6	4	13.0	5	5.1	1
	9	3.8	2	15.5	5	6.7	1*
	9	4.2	2	15.5	5	7.0	1*
	9	5.1	1–2	15.5	5	15.0	1*
	9	6.0	1–2	15.5	6	3.4	1
	10	2.8	3	15.7	6	3.6	1
	10	4.0	2	19	6	4.1	1
	11	5.1	2	27	6	5.1	1
	11	8.0	1–2	27	6	6.0	1
	12	11.5	1–2	38	6	11.6	1*
	12	11.7	1–2	38	6	16.0	1*
	13	4.1	3–4	26	6	28.0	1*
	15	5.1	4	37	7	4.3	1
	15	12.3	2	≈ 58	7	4.5	1
	17	5.6	4	≈ 48	7	5.8	1
	18	10.0	3–4	≈ 67	7	8.7	1
	20	8.0	4	≈ 70	7	12.2	1*
	21	17.0	3	≈ 90	7	14.3	1*
	24	14.5	4	≈100	7	33.2	1*
	28	32	2–3	≈150	8	5.6	1
	36	10	5–6	≈100	8	6.2	1
					8	10.5	1
					8	11.5	1
					8	18.0	1
					9	25.7	1*

TABLE 1 (continued)

Author, year	class A				class B		
	n_s†	γ_c	n_T	E_θ	n_s†	γ_c	n_T
1	2	3	4	5	6	7	8
Castagnoli *et al.*[6]) (1953)	5	2.1	1–2	6.5	5	5.8	1*
	5	2.4	1–2	6.5	5	5.0	1
	6	1.5	3	8.0	5	4.0	1
	6	2.3	2	8.5	5	4.4	1
	6	1.9	2	8.5	5	9.7	1*
	6	2.4	2	8.5	6	8.6	1*
	6	1.2	4	8.0	7	6.5	1
	6	2.2	2	8.5	7	4.6	1
	7	3.4	1–2	9.5	8	5.0	1
	7	1.4	4	10.0	5	3.1	1
	8	1.4	5	11.0	9	5.6	1–2
	9	2.1	3	13	11	7.1	1–2
	9	3.1	2	13			
	10	5.8	2	22			
	10	4.3	2	19			
	13	4.3	3	30			
	14	5.9	3	37			
	16	3.0	5	36			
	23	5.5	6	≳ 50			
	7	3.1	2	9.5			
	9	1.6	4	13			
	9	3.2	2	13			
Hoang[9]) (1954)	5	1.5	2	6.5	5	2.7	1
	6	2.0	2	8.5	5	3.0	1
	6	2.0	2	8.5	5	3.2	1
	6	2.2	2	8.5	5	3.4	1
	6	2.5	2	8.5	5	4.0	1
	6	2.5	2	8.5	5	4.3	1
	6	3.0	1–2	8.5	5	5.0	1
	7	2.4	2	9.5	5	6.0	1*
	7	3.2	2	9.5	5	6.6	1*
	7	3.4	1–2	9.5	5	19	1*
	7	3.6	1–2	9.5	6	3.4	1
	7	3.9	1–2	9.5	6	5.5	1
	8	3.0	2	13.5	6	21	1*
	9	2.5	3	13.0	7	4.0	1
	9	3.3	2	13.0	7	5.0	1
	9	3.7	2	15.5	7	5.7	1
	10	3.0	3	15.7	7	6.5	1
	11	3.6	3	19.0	7	8.5	1
	11	3.9	3	19.0	7	9.5	1
	12	4.3	3	24	8	5.0	1
	12	4.6	3	24	8	6.5	1
	12	5.9	2–3	28	8	11.5	1

TABLE 1 (continued)

Author, year	class A				class B		
	n_s†	γ_c	n_T	E_0	n_s†	γ_c	n_T
1	2	3	4	5	6	7	8
	13	7.8	2–3	38			
	15	5.0	4	37			
	18	6.0	4	≈ 50			
	18	7.5	4	≈ 50			
	22	7.6	5	≈ 65			
Bertolino and Pescetti [10]) (1954)	6	2.0	2	8.5	5	3.6	1
	6	2.2	2	8.5	5	4.9	1
	6	2.4	2	8.5	5	5.8	1*
	7	1.6	3	9.5	5	10.4	1*
	7	2.0	2–3	9.5	6	2.8	1–2
	7	2.3	2	9.5	6	7.6	1
	7	3,0	2	9.5	6	10.7	1*
	8	1.7	4	10.5	6	18	1*
	8	1.8	3–4	10.5	7	4.4	1
	8	2.0	3	11.0	9	5.8	1–2
	8	2.9	2	13.5	13	15.3	1–2
	9	2.6	3	13.0			
	9	4.0	2	15.5			
	11	2.0	4	17			
	11	2.8	4	17			
	13	2.3	5	21			

† In those cases in which the number of relativistic particles is small ($n_s = 4$) and γ_c is close to 1 ($\gamma_c \approx 1.1$) the experimental errors are so large that it seems unreasonable to analyse the corresponding events. These events have been included only for the sake of completeness of presentation of the experimental material of the respective authors. The number of such cases is not large.

* The energy spectrum of the primary particles deduced from these data in the $10^{11}-10^{12}$ eV energy range is consistent with the spectrum deduced from other experiments.

class A jets are too large †. With account of this circumstance K becomes on the average three times smaller than the previous value and coincides in order of magnitude with the value of K for class B jets.

It should be noted, however, that the absolute values of K deduced from formulae (1) and (2) are systematically found to be too small, both classes being identical in this respect.

Indeed, relation (2) can be applied only if the number of shower particles is sufficiently large. Relation (2) was obtained on the assumption that all particles in the c.m.s. possess the same velocity v' [17]). In this case it can easily be verified from the formula for relativistic transformation of angles

† This is apparently the main reason that in some cases K was found to exceed unity which is, generally speaking, absurd.

that if a particle moves in the c.m.s. at an angle φ_m (such that $\cos\varphi_m = -v'/v_c$) its angle in the laboratory system ϑ_m will be maximum. All other particles moving in the c.m.s. at angles smaller or larger than φ_m will move in the laboratory system at angles which are smaller than ϑ_m.

If the number of particles moving in the c.m.s. at angles close to φ_m is sufficiently large the maximum angle ϑ_m in the laboratory system will then be close to ϑ_m.

However if the number of shower particles $n_s \approx 10-20$ and their angular distribution in the c.m.s. is isotropic it will be found that in the range $\varphi_m - 180°$ not more than one (and frequently even much less than one) particle will be emitted. Therefore, owing to statistical fluctuations $\Delta\varphi_m \approx \varphi_m$.

The quantity γ' is related to the angle φ_m as follows [17]):

$$\gamma' = \frac{1}{\sqrt{1 - v'^2/c^2}} = \frac{1}{\sqrt{1 - \frac{v_c^2}{c^2}\cos^2\varphi_m}} \approx \frac{1}{\sin\varphi_m}. \tag{7}$$

The relative error in γ' produced by a fluctuation $\Delta\varphi_m$ is

$$\frac{\Delta\gamma'}{\gamma'} = \frac{\Delta\varphi_m}{\operatorname{tg}\varphi_m} \approx 1. \tag{8}$$

Thus the error in γ' is of the same order of magnitude as γ' itself. This error, moreover, always leads to a decrease in γ' since any fluctuation of angle φ_m in the c.m.s. leads to a decrease of angle ϑ_L in the laboratory system. The result of this is that K turns out to be much smaller.

Other methods must be used to determine with greater accuracy the fraction of energy spent in the formation of π-mesons.

In the case considered here we purported to show that although the value of K is too low it is the same for jets of various classes.

In conclusion it may be asserted that the main features of the various types of showers can satisfactorily be explained on basis of the tunnel model in conjunction with Fermi's theory of multiple production. It therefore seems unreasonable to divide the jets into different classes.

The authors take the opportunity to express their appreciation to G. T. Zatsepin for a number of valuable remarks, and to V. M. Maximenko and I. L. Rosental for acquainting us with their paper prior to publication.

References

1) F. C. Roesler and C. B. A. McCusker, Nuovo Cimento **10** (1953) 127
2) W. Heitler and Ch. Terreoux, Proc. Phys. Soc. A **66** (1953) 929
3) C. B. A. McCusker and F. C. Roesler, Phys. Rev. **91** (1953) 769
4) T. F. Hoang, Journ. de Phys. **14** (1953) 395
5) C. C. Dilworth, S. J. Goldsack, T. F. Hoang and L. Scarsi, Nuovo Cimento **10** (1953) 1261

6) C. Castagnoli, G. Cortini, C. Franzinetti, A. Manfredini and D. Moreno, Nuovo Cimento **10** (1953) 1539
7) C. B. A. McCusker and F. C. Roesler, Nuovo Cimento **11** (1954) 98
8) C. C. Dilworth, S. J. Goldsack, T. F. Hoang and L. Scarsi, Nuovo Cimento **11** (1954) 424
9) T. F. Hoang, Journ. de Phys. **15** (1954) 337
10) G. Bertolino and D. Pescetti, Nuovo Cimento **12** (1954) 630
11) G. Bertolino and D. Pescetti, Nuovo Cimento **3** (1956) 141
12) A. Watagin, Nuovo Cimento **4** (1956) 154
13) R. R. Daniel, J. H. Davies, J. H. Mulvey and D. H. Perkins, Phil. Mag. **342** (1952) 753
14) G. Cocconi, Phys. Rev. **93** (1954) 1107
15) E. Fermi, Prog. Theor. Phys. **5** (1950) 570
16) V. M. Maximenko and I. L. Rosental, JETP (1956) (in press)
17) Peyrou, d'Espagnat et Leprince-Ringuet Comptes Rendus Acad. Sc. **228** (1949) 1777

Nuclear Physics **4** (1957) 39—43; © *North-Holland Publishing Co., Amsterdam*
Not to be reproduced by photoprint or microfilm without written permission from the publisher

TWO CLOSELY SPACED RESONANCES IN THE REACTION Al^{27} (p, γ) Si^{28}

S. L. ANDERSEN, T. HOLTEBEKK, O. LÖNSJÖ AND R. TANGEN
Institute of Physics, University of Oslo, Blindern

Received 18 March 1957

Abstract: An already known resonance is shown to consist of two separate resonances with $E_p = 504.5 \pm 0.2$ keV and $E_p = 506.5 \pm 0.2$ keV. Gamma transitions from the lower of the two levels proceed mostly to the ground state, while the upper level decays predominantly to the first excited state.

1. Introduction

This investigation originated during a study of the influence of target surface effects on the measured widths of (p, γ) resonances. During measurements on the low lying resonances of the reaction Al^{27} (p, γ) Si^{28}, we noted that the 503 keV resonance came out with a width much larger than expected from our energy resolution and also from earlier measurements of resonance widths in this region [1–4]). After careful studies the resonance turned out to be a closely spaced doublet.

2. Experimental Methods

2.1. THE PROTON BEAM

The new Van de Graaff generator at the University of Oslo was used to produce fast protons. The proton beam was analyzed by a 90° electrostatic analyzer with a mean radius of curvature of 1 000 mm. The voltage across the analyzer plates was stabilized to 1 part in 10 000. The slit widths used in the experiment was 0.5 mm, corresponding to a half width of the energy spread of 0.05 percent [2]). In most of the runs, including those reproduced in fig. 1, we used the H_2^+ beam. The beam current was about 1 μA and the bombarded area of the target about 5 mm^2. As energy standard we adopted the value of 990.8 ± 0.2 keV given by Bumiller, Staub and Weaver [5]) for the strong Al^{27} (p, γ) resonance, formerly known as 993.3 keV from measurements by Herb *et al.* [2]). The same resonance was used when checking the resolution of the analyzer. Within the statistical error the half width obtained was the same as expected due to the finite slit widths.

2.2. TARGETS

All targets were made on copper backings by evaporation in vacuum from a tungsten boat. Pure aluminium targets which had been exposed to

air could not be used for measurements of resonance widths, as the oxide film which quickly forms on the surface in a thickness of a few hundred eV [6]) results in a broadening of the measured resonances. Lacking a target chamber in which targets could be evaporated without being exposed to air, targets of Al_2O_3 were used.

In our experience a dependable measurement of the width of a narrow resonance can only be made on a thick target, where the width can be taken from the slope of the step corresponding to the resonance. A target of 10 keV thickness is a thick target for measurements of the narrow resonances in Al^{27} (p, γ) reactions. On the other hand it is a thin target in the respect that only radiation from the resonances under consideration will be registered. Our yield measurements, therefore, were made on targets of about 10 keV thickness. To avoid the effect of carbon deposits broadening the measured widths, a liquid air trap was placed near to the target. Irradiation over a period of time showed that this was not fully effective. We therefore made the targets in the shape of large circular discs which could be rotated. After each observation the disc was turned a bit so that every observation point could be taken on a fresh area of the target. In this way the highest degree of reproducibility was obtained.

To obtain the individual gamma spectra of the two resonances, the spectra were taken on targets of 1 keV thickness. In order to get maximum intensity, targets of metallic aluminium were used for the purpose, and the proton current was increased by increasing the slit widths to 1 mm. Here also the target was rotated regularly during the bombardment.

2.3. GAMMA RAY DETECTOR

Gamma rays were detected with a 1.5″ NaI crystal mounted on a Du Mont 6292 photomultiplier tube. Yield curves were taken with an integral discriminator usually biased around 2 MeV to suppress background. The gamma ray energy spectra were recorded with a Hutchinson-Scarrott type 80 channel pulse height analyzer.

3. Experimental Results

3.1. GAMMA RAY YIELD CURVES

Yield curves are given in fig. 1. For the 10 keV target only the rise of the curve is given, representing a thick target yield curve of the two resonances. Each point represents an average of several observations taken while running back and forth over the resonances. A comparison between the two curves clearly shows the superiority of the semi-thick target method in giving a true picture of a resonance, the two resonances being completely resolved in the 10 keV target curve.

Uncertainties in the energy scale and in our readings of the 991 and the

505 keV resonances taken into account, we get for the two resonance energies the values 504.5±0.2 keV and 506.5±0.2 keV. The half widths taken from

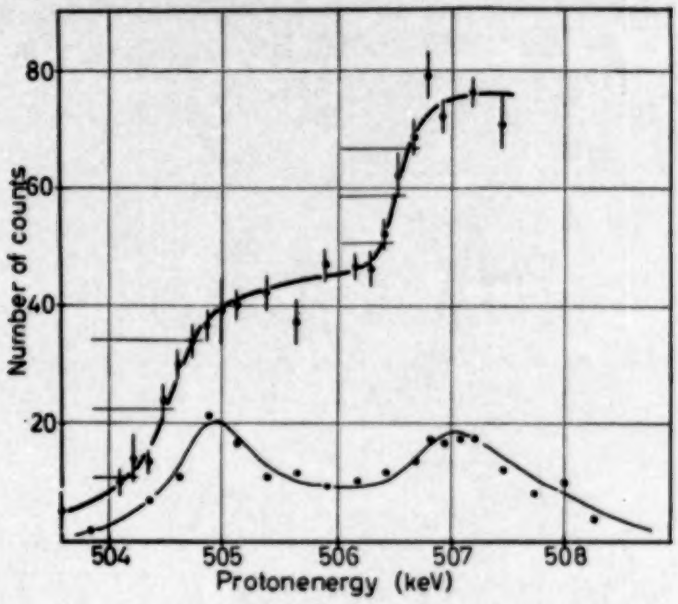

Fig. 1. Yield of gamma rays.
Upper curve: 10 keV target of Al_2O_3.
Lower curve: 0.5 keV target of Al.

the curves are 0.5±0.25 keV for the 504.5 keV resonance and 0.25±0.13 keV for the 506.5 keV resonance. As the half widths due to the analyzer resolution is 0.25 keV, however, the observed half widths give upper limits only for the true half widths of the resonances.

3.2. GAMMA RAY ENERGY SPECTRA

The spectra shown in fig. 2 a and b are each the sum of four separate runs. The energies and an estimate of the relative intensities of the gamma

TABLE 1

Gamma rays observed in the spectra of the two resonances, with the approximate intensities relative to the strongest line of each resonance.

E_p	E_γ	Rel. intensity	Transition
504.5	12.0±0.1	1.00	12.1 → 0
	10.3±0.1	0.25	12.1 → 1.8
506.5	12.0±0.1	0.25	12.1 → 0
	10.3±0.1	1.00	12.1 → 1.8
	7.5±0.1		
	5.2±0.1		

rays corresponding to the most prominent peaks are collected in table 1. The results agree with those of Rutherglen *et al.* [7]), who measured the

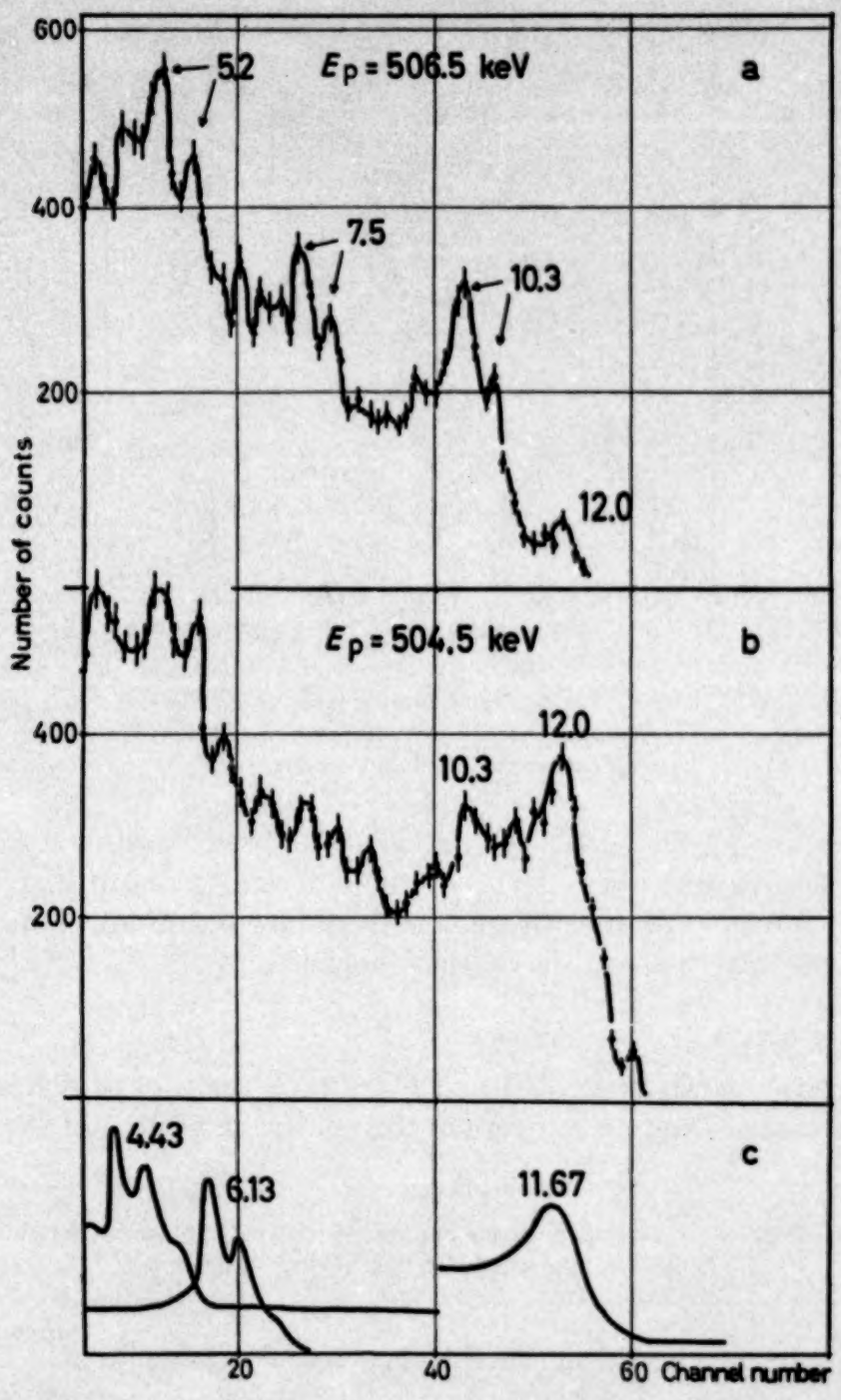

Fig. 2. Gamma ray energy spectra. The numbers given on the curves are gamma ray energies in MeV. For comparison, gamma ray spectra of the reactions B^{11} (p, γ)C^{12} and F^{19} (p, α, γ)O^{16} are given in c.

spectrum from the two resonances combined. We observed that the lower of the resonant states decays chiefly to the ground state. The 10.3 MeV

line has a much lower intensity, and a great part of it, possibly all, may be due to the 506.5 keV resonance since the thin target resolution was not complete. A number of other peaks are visible, but no particular gamma rays can be identified with certainty.

The upper resonant state is seen to decay predominantly to the 1.78 MeV level, the ground state transition being less than 25 percent. Two more lines of energies 7.5 MeV and 5.2 MeV are identified from the peaks.

This work was supported by the Royal Norwegian Council for Scientific and Industrial Research.

References

1) R. Tangen, Kgl. Norske Vid. Selsk. Skrifter (1946) no. 1
2) Herb, Snowdon and Sala, Phys. Rev. **75** (1949) 246
3) S. E. Hunt and W. M. Jones, Phys. Rev. **89** (1953) 1283
4) Bumiller, Müller und Staub, Helv. Phys. Acta **29** (1956) 234
5) Bumiller, Staub und Weaver, Helv. Phys. Acta **29** (1956) 83
6) A. B. Winterbottom, Kgl. Norske Vid. Selsk. Skrifter (1955) no. 1
7) Rutherglen, Grant, Flack and Deuchars, Proc. Phys. Soc. A **67** (1954) 101

Nuclear Physics **4** (1957) 44—60; © *North-Holland Publishing Co., Amsterdam*
Not to be reproduced by photoprint or microfim without written permission from the publisher

STUDIES ON THE LONG-LIVED ACTIVITIES OF EUROPIUM

S. K. BHATTACHERJEE AND SHREE RAMAN
Tata Institute of Fundamental Research, Bombay

Received 25 January 1957

Abstract: Long-lived activities of europium, Eu^{152} (13y) and Eu^{154} (16y), were studied by a coincidence scintillation spectrometer. The measured gamma ray energies (keV) and their relative intensities are $80\pm4(0.52)$, $124\pm4(1.85)$, $244\pm7(1.00)$, $340\pm10(2.16)$, $410\pm20(0.15)$, $710\pm25(0.34)$, $770\pm22(1.27)$, $870\pm30(0.57)$. $970\pm20(1.93)$, $1090\pm21(1.88)$, $1260\pm40(0.5)$, $1410\pm25(1.99)$. X-gamma and gamma-gamma coincidence experiments were carried out by employing pulse-height selection; beta-gamma coincidence were recorded by using an anthracene crystal spectrometer. Decay schemes for the two isotopes are proposed on the basis of our experimental results. The first two excited states of Sm^{152} reached by the capture decay of E^{-}. ^{2} at 121 and 365 keV are identified as rotational levels belonging to the ground stat. configuration; higher excited states in Sm^{152} ($N = 90$) were also reached by capture decay of Eu^{152}. On the other hand the first two excited states of Gd^{152} ($N = 88$) reached by β^--decay of Eu^{152} at 340 and 750 keV are probably vibrational in origin. The ground state spin of Eu^{152} is assigned as 4. The newly found gamma ray of energy 80 keV is identified as the one arising from de-excitation of the first rotational level of Sm^{154}, a state which has also been observed in Coulomb excitation experiments. Decay schemes are discussed in the light of the unified nuclear model.

1. Introduction

Natural europium is a di-isotopic element, Eu^{151} and Eu^{153}, present in almost equal proportions. Thermal neutron bombardment yields two long-lived activities [1]): Eu^{152} (13y), and Eu^{154} (16y) both having dual modes of decay, electron capture and β^--emission. Besides, Eu^{152} exists in an isomeric form of 9.2 h. half-life, the decay character of which is fairly well established [2]).

Magnetic spectrometer studies of these long-lived activities were made by many workers [2, 3, 4, 5]). Slattery *et al.* [5]) made coincidence studies of the X-rays and gamma rays by the NaI-crystal summing technique. Recently Grodzins [6]) has made coincidence studies on Eu^{152} and in its decay he finds a 1410 keV gamma ray. This gamma ray was assigned to Eu^{154} decay by previous workers. Grodzins' data show that a 344 keV gamma ray seems to be in coincidence with two β^--groups of end-point energies 662 keV and 1440 keV; Slattery *et al.* [5]), however, find that a 700 keV β^--group is in coincidence with the K-conversion electrons of the 344 keV gamma ray. As a consequence the energy difference between the ground states of Eu^{152} and Gd^{152} in the decay scheme proposed by Slattery and others is too low in comparison with Grodzins' result. Furthermore the above-mentioned decay scheme does not show coincidences of 123 keV and 344

keV gamma rays as observed in the magnetic coincidence spectrometer work of Fowler and Shreffler [7]).

In the present work the mixed activity of europium has been investigated by means of a coincidence scintillation spectrometer. Studies of these two isotopes lead one to deal with the levels of four even nuclei (Sm^{152} and Gd^{152} from capture and β^--decay of Eu^{152}; Sm^{154} and Gd^{154} from capture and β^--emission of Eu^{154}) in the region of the periodic table where the "strong coupling approximation" of the Bohr and Mottelson [8]) unified nuclear model holds.

2. Experimental Arrangement

Long lived activities of $Eu^{152, 154}$ were obtained from the Atomic Energy Establishment, Harwell, by bombarding natural europium (oxide) by thermal

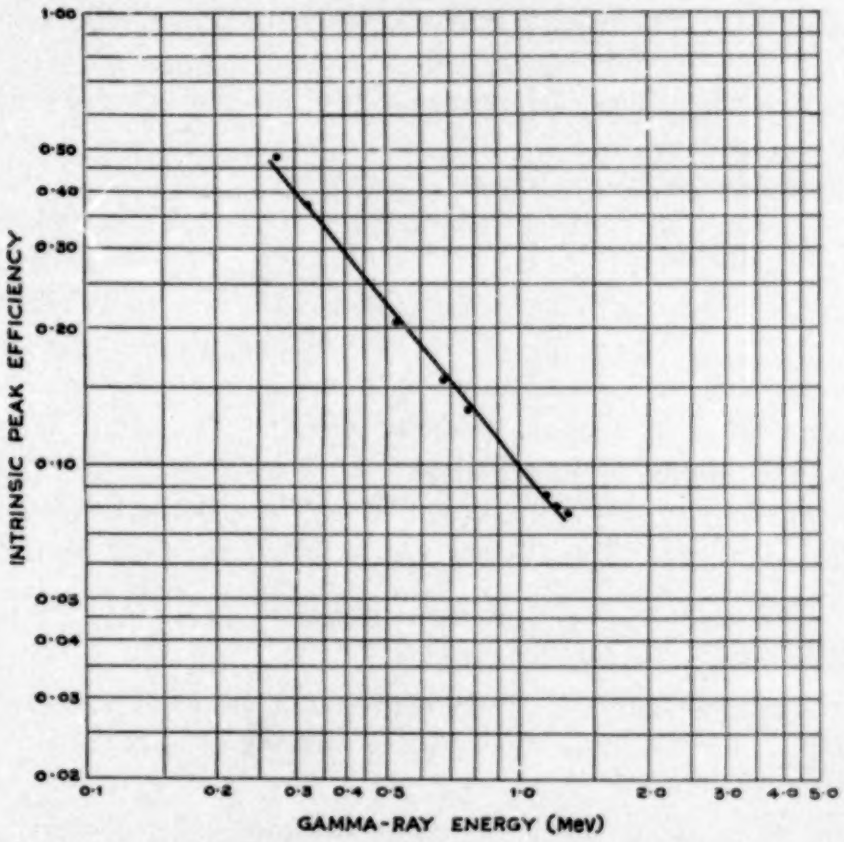

Fig. 1. Intrinsic peak efficiency curve for 2″ thick × 1¾″ diameter NaI(Tl) crystal, at a source to crystal distance 1″.

neutrons. The experiments were started 1½ years after the bombardment.

A coincidence scintillation spectrometer [9]) employing "fast-slow" technique was used for all experimental observations. A NaI(Tl) crystal (1¾″ diam. × 2″) was calibrated from 279 keV to 1330 keV for a source to crystal distance of 1″. This was done by observing the pulse height distributions

of several monoenergetic sources in the crystal, measuring the peak to total ratio R and calculating the total intrinsic efficiency ε_t entirely from the geometry and the linear absorption coefficient of NaI. Then the intrinsic peak efficiency is given by $\varepsilon_p = R\varepsilon_t$. The experimental peak efficiency curve is shown in fig. 1. All γ-ray energies and intensities were measured with this crystal. The resolution for the 662 keV γ-ray of Cs^{137} was about 9 %.

For fast coincidence selection the photomultiplier pulses were fed to two high band-width amplifiers, each with gain ≈ 150 and rise time nearly 0.02 μsec. These pulses were then shaped by EFP-60 shapers to a width of 0.03 μsec and were mixed in a 6BN6 mixer. The resolving time as determined by change coincidence method was 0.06 μsec. The two outer channels with the scintillation detectors represent the usual scintillation spectrometers equipped with non-overload linear amplifiers and single channel analysers.

A NaI(Tl) crystal ($1\frac{3}{4}''$ diam. $\times$ 1″) was used for gating in all coincidence experiments. All high energy coincidences were recorded with two counters oriented at 180°; for low energy coincidences the counters were oriented at 90° to avoid spurious back scattered peaks of high energy γ-rays being detected in either of the counters. Anti-scattering shields were used in both cases in the conventional way.

For $\beta-\gamma$ coincidences the 1″ thick NaI(Tl) crystal was replaced by an anthracene crystal ($1\frac{1}{2}''$ diam. $\times \frac{1}{4}''$). The source for this purpose was mounted on a thin zapon film and was placed at $\approx$ 5 mm from the anthracene crystal with no absorbers in between. 1/8″ thick perspex absorbers were used to determine the γ-background in the anthracene crystal. The resolution for the 624 keV K-conversion line of Cs^{137} was about 17 %.

A multigrid tube EQ80 was used as a triple coincidence mixer, the three inputs to which were shaped by three univibrators giving flat top pulses of appropriate amplitudes. The resolving time of this circuit was nearly 2.5 μsec.

3. Results

3.1. SINGLE GAMMA-SPECTRUM

The gamma spectrum of $Eu^{152, 154}$ is presented in fig. 2. The energies and observed unconverted intensities of the various radiations are given in

TABLE 1

Gamma ray energies and their observed unconverted relative intensities

Energy (keV)	84†	124	244	340	410††	710††	770	870††	970	1090	1260††	1410
Intensity	0.52	1.85	1.0	2.16	0.15	0.34	1.27	0.57	1.93	1.88	0.55	1.99

† That the line 84 keV is not entirely due to summation of capture and conversion X-rays was established by absorption technique. It was found using 600 mg/cm² brass absorber that it did not follow the absorption coefficient of the 40 keV X-radiation. However, this summation might be responsible for a considerable part of the total intensity; the exact correction could not be very well determined.

†† Errors in these cases are somewhat larger than those mentioned above.

table 1. The analysis of the γ-spectrum was performed in the conventional way starting from the highest energy γ-ray and extrapolating the Compton distribution. Energies are measured to within 3 % and intensities to within 10 % except where mentioned otherwise.

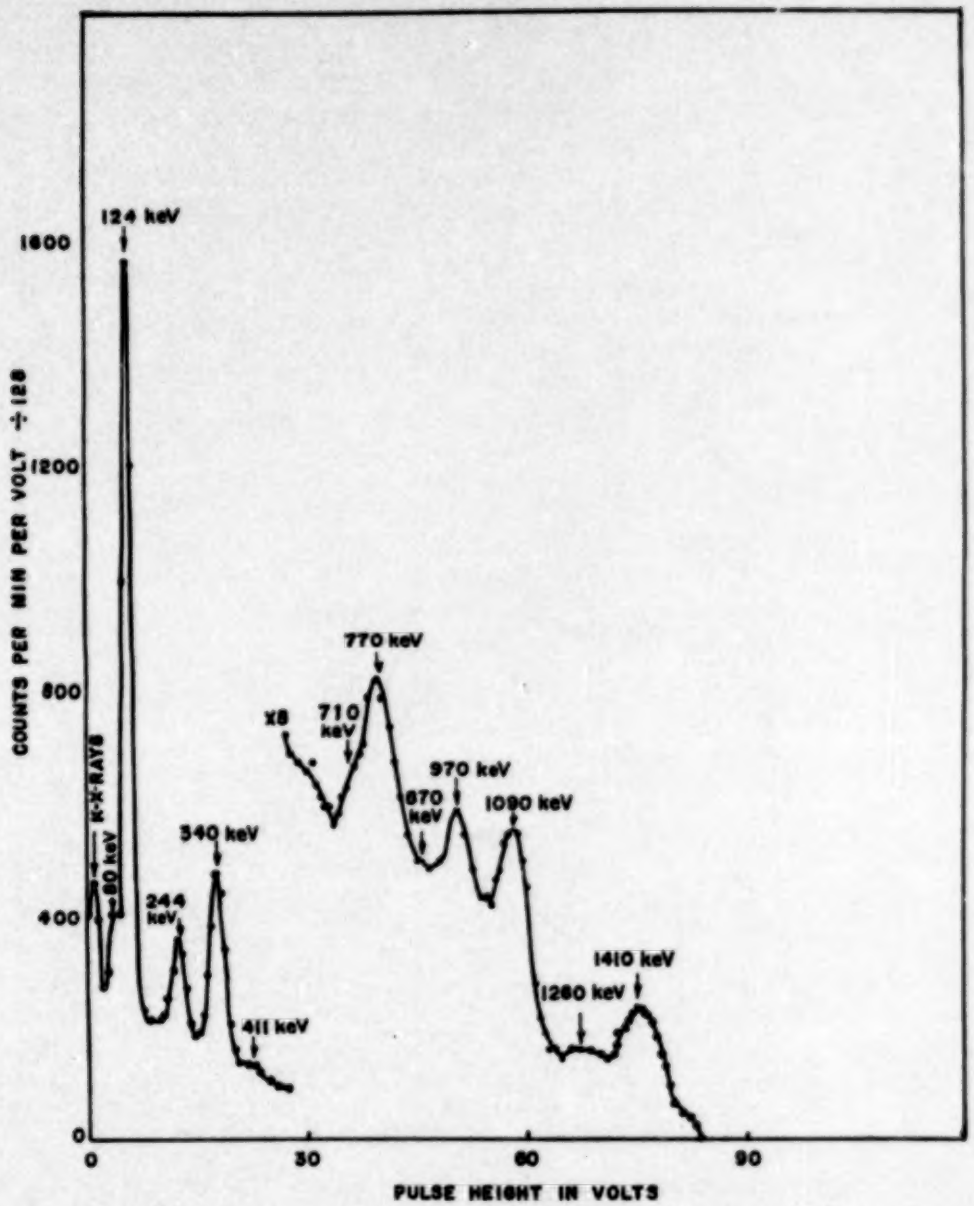

Fig. 2. Gamma spectrum of $Eu^{152, 154}$. A 600 mg/cm² brass absorber was put on top of the crystal in order to suppress intense X-rays.

3.2. X-γ AND $\gamma-\gamma$ COINCIDENCE EXPERIMENTS

Coincident γ-spectra were observed by gating the photopeaks of the 40 keV X-rays and the 124 keV, 244 keV and 340 keV radiations respectively.

The results are presented in figs. 3, 4, 5 and 6 respectively. Table 2 gives a brief summary of these results.

The following information is readily obtained from these spectra:

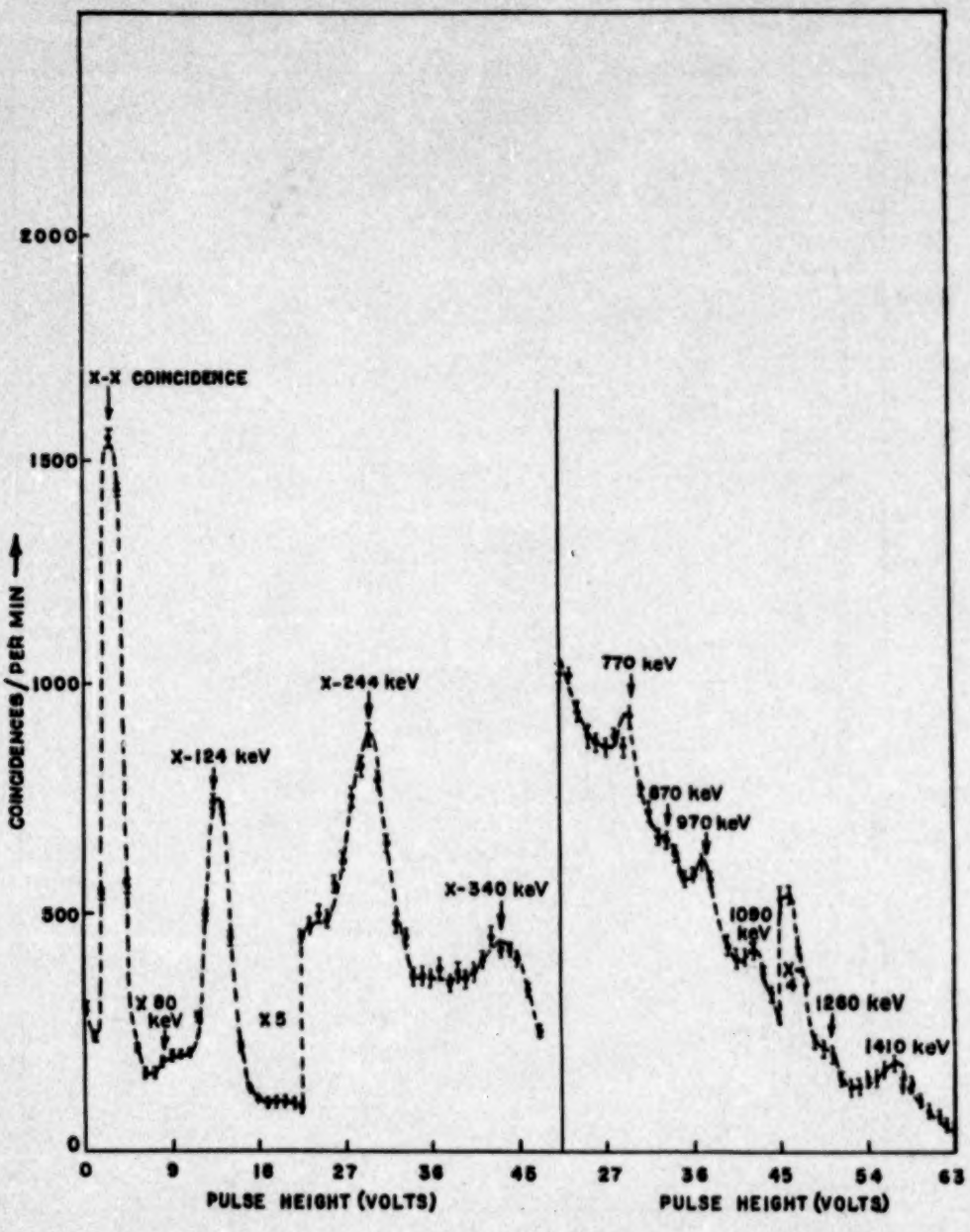

Fig. 3. Total Eu-gamma spectrum in coincidence with X-rays. The low energy portion of the spectrum (up to 340 keV) was taken with the counter axes oriented at 90°; the high energy portion was taken with the counter axes oriented at 180°.

The presence of intense X-ray—X-ray coincidences shows that some of the low energy gamma rays in the capture branch are highly converted.

The 124—124 keV coincidences show that the 124 keV radiation, in at least one of the modes of decay, is composed of two radiations whose energies cannot be distinguished in our set-up.

A similar conclusion is drawn from the 340—340 keV coincidences. The 340 keV coincidences with X-rays and the 124 keV γ-ray are positive evidence that this gamma ray is present in the capture branch.

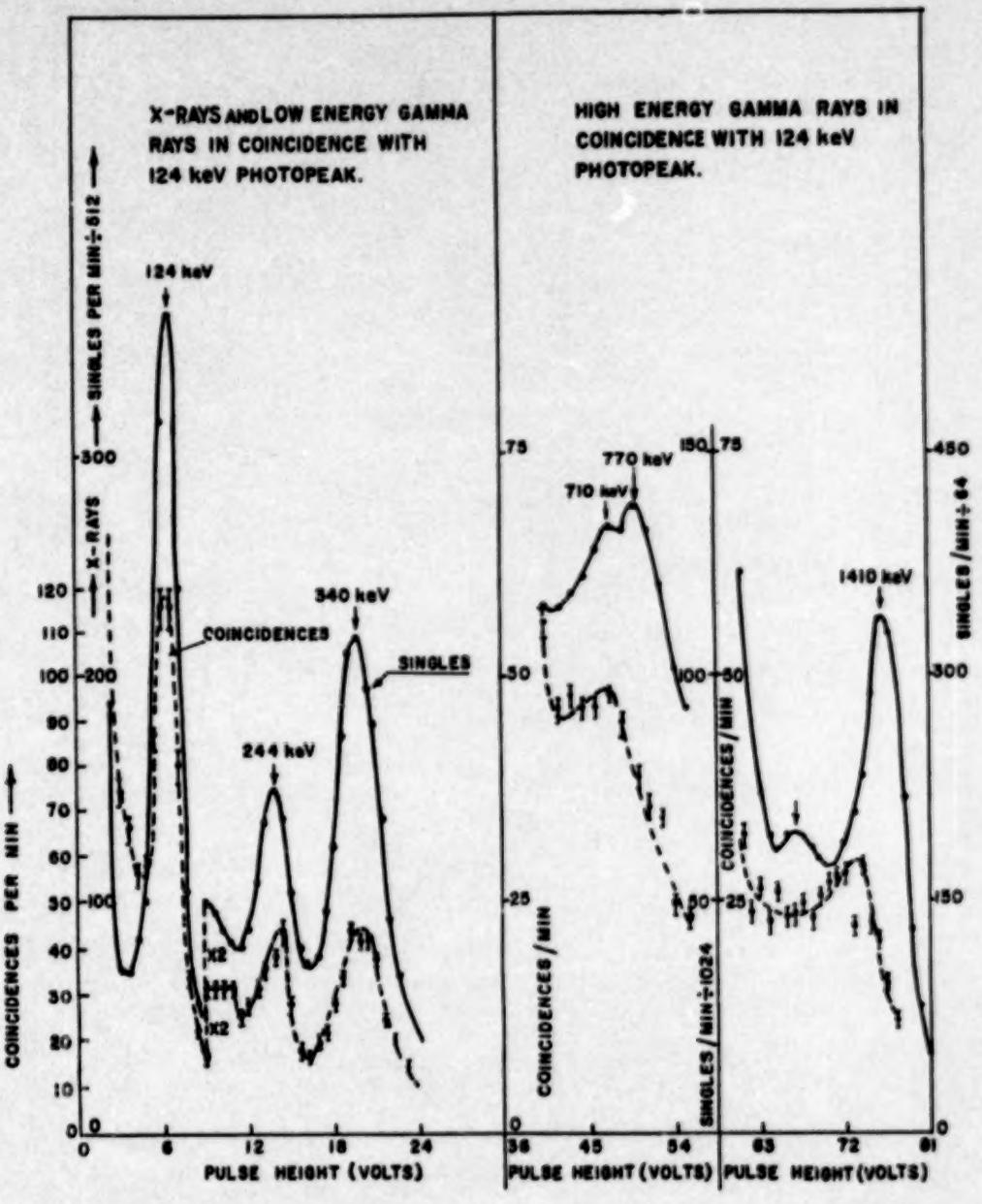

Fig. 4. Eu-gamma spectrum in coincidence with 124 keV photopeak.

The lines 710 and 770 keV which very much overlap in single spectrum separate out clearly in coincidences. The former is in coincidence with the 124 and 244 keV rays while the later is in coincidence with the 340 keV ray only. This fact is of importance and is made use of while investigating $\beta-\gamma$ coincidences.

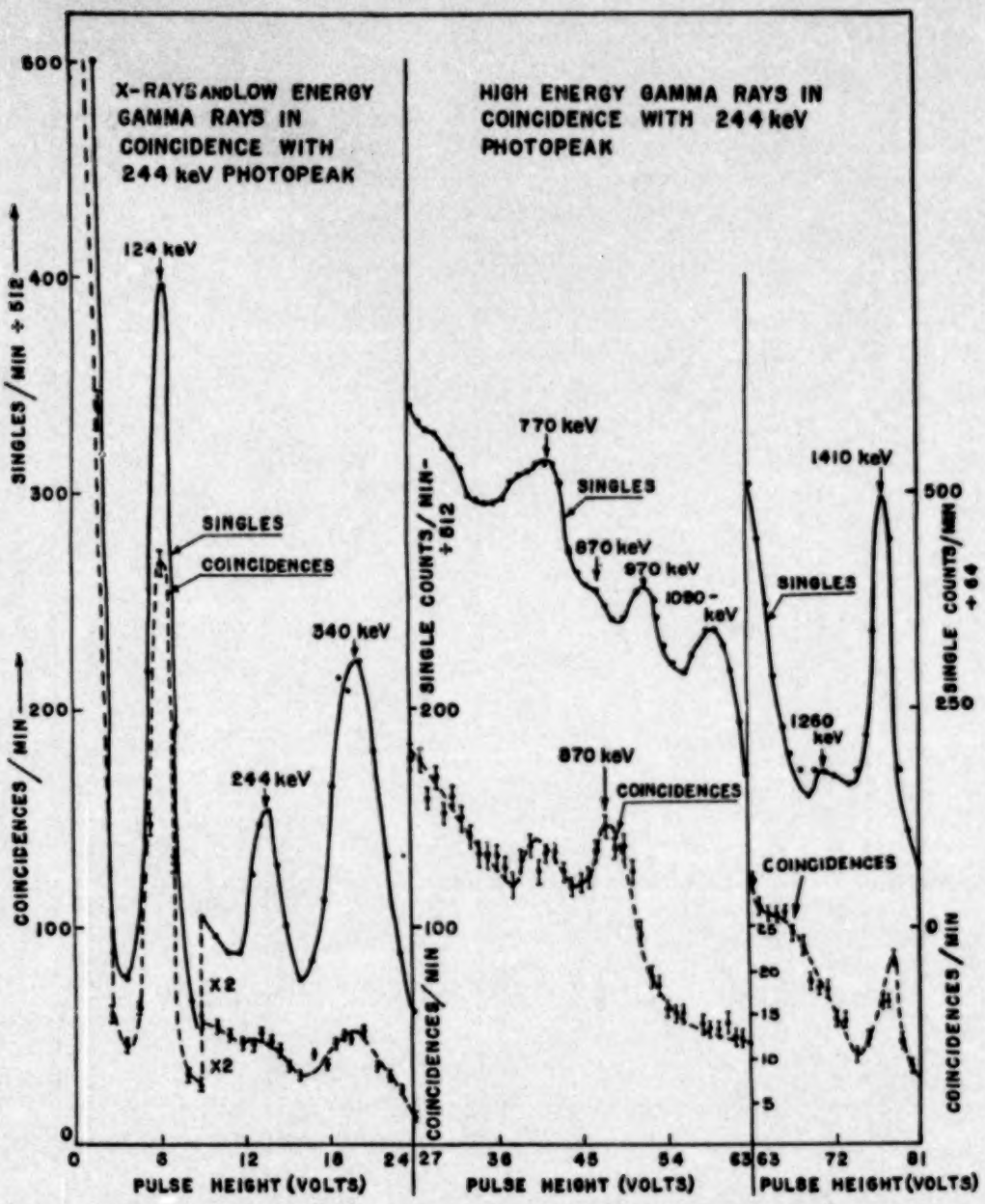

Fig. 5. Eu-gamma spectrum in coincidence with 244 keV photopeak.

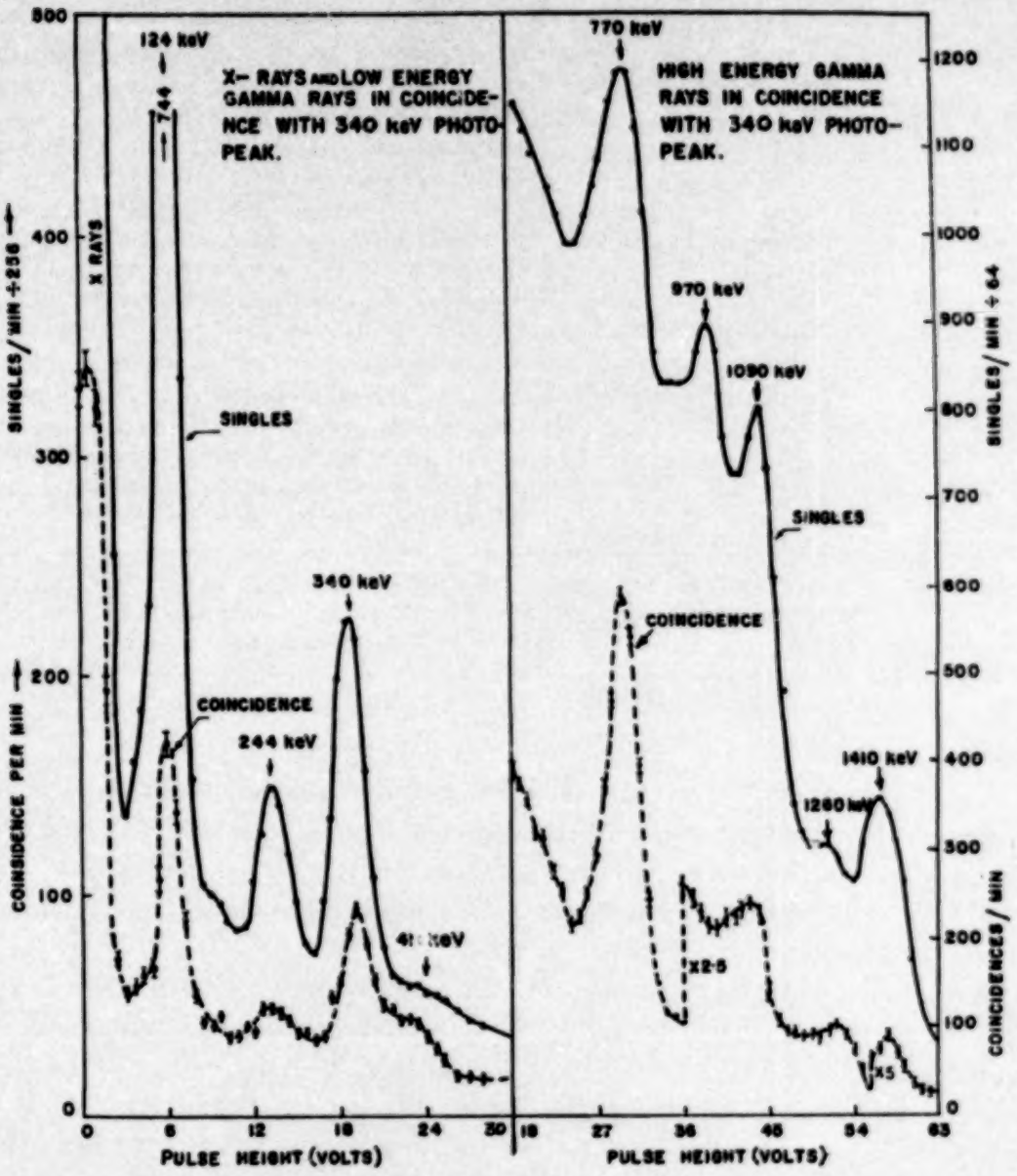

Fig. 6. Eu-gamma spectrum in coincidence with 340 keV photopeak.

TABLE 2

Summary of X–γ and γ–γ coincidences

Gating Radiation	Coincident Radiations (keV)	Remarks
K–X rays	K–X rays, 84, 124, 244, 340, 770, 870, 970, 1090, 1260, 1410	Coincidences with 340 keV show that 340 keV γ-ray must be present partly in capture branch (vide decay scheme fig. 10). The coincidences appearing at 770 keV (see decay scheme) are due to 710 keV γ-ray.
124 keV	K–X rays, 124, 244, 340, 710, 1410	Coincidences with 340 keV again point out that 340 keV γ-ray at least in part should be present in the capture branch of Eu^{152}.
244 keV	K–X rays, 124, 340, 710, 870, 1410	Coincidences with 1410 keV indicate that this line must also be present in capture branch in some fraction since 244 keV γ-ray is known to be exclusively in the capture branch of Eu^{152}. Note the prominance of coincidence peak at 870 keV as compared to single spectrum.
340 keV	K–X rays, 124, 244, 340, 410, 770, 1090, 1260, 1410	The large coincidences with X-rays clearly show (vide decay scheme) that 340 keV ray must be present in part in capture branch.

3.3. β–γ COINCIDENCE EXPERIMENTS

The β^--spectrum [2, 4]) of this activity is fairly well-known; however, we observed the β^--spectrum in the anthracene crystal spectrometer and the Fermi plot showed two strong components with endpoints at 770 and 1450 keV. In addition to this there was a weak high energy group ending at about 1850 keV.

The β^--spectrum was scanned in coincidence with the 340 keV γ-ray. The Fermi plot of these data (fig. 7) showed two distinct components of energies 1460 and 750 keV. In view of the fact that the 340 keV and 770 keV γ-rays are in coincidence (fig. 6) it was expected that the 770 keV γ-rays would show coincidences with the low energy β^--group only. The β^--spectrum was therefore recorded in coincidence with the 770 keV photo-peak. The results (fig. 8) clearly showed that the 770 keV γ-ray is in coincidence with a β-group with end point at $\approx$ 830 keV; the errors in the β^--energy determination are, of course, large ($\approx$ 10 %).

A band of β^--particles of energies from 470 keV to 550 keV was then selected in gate and the low energy portion of the γ-spectrum was recorded in coincidence under sufficiently high amplification. The results (fig. 9) showed very strong coincidences with the 340 keV ray, appreciable coincidences with the 124 keV ray and no significant coincidences with K–X

rays. The 124 keV coincidences may be attributed to the high energy β^--group from Eu^{154} feeding the 123 keV level in Gd^{154} (vide decay scheme). An inspection of the coincidences in the X-ray region reveals that the

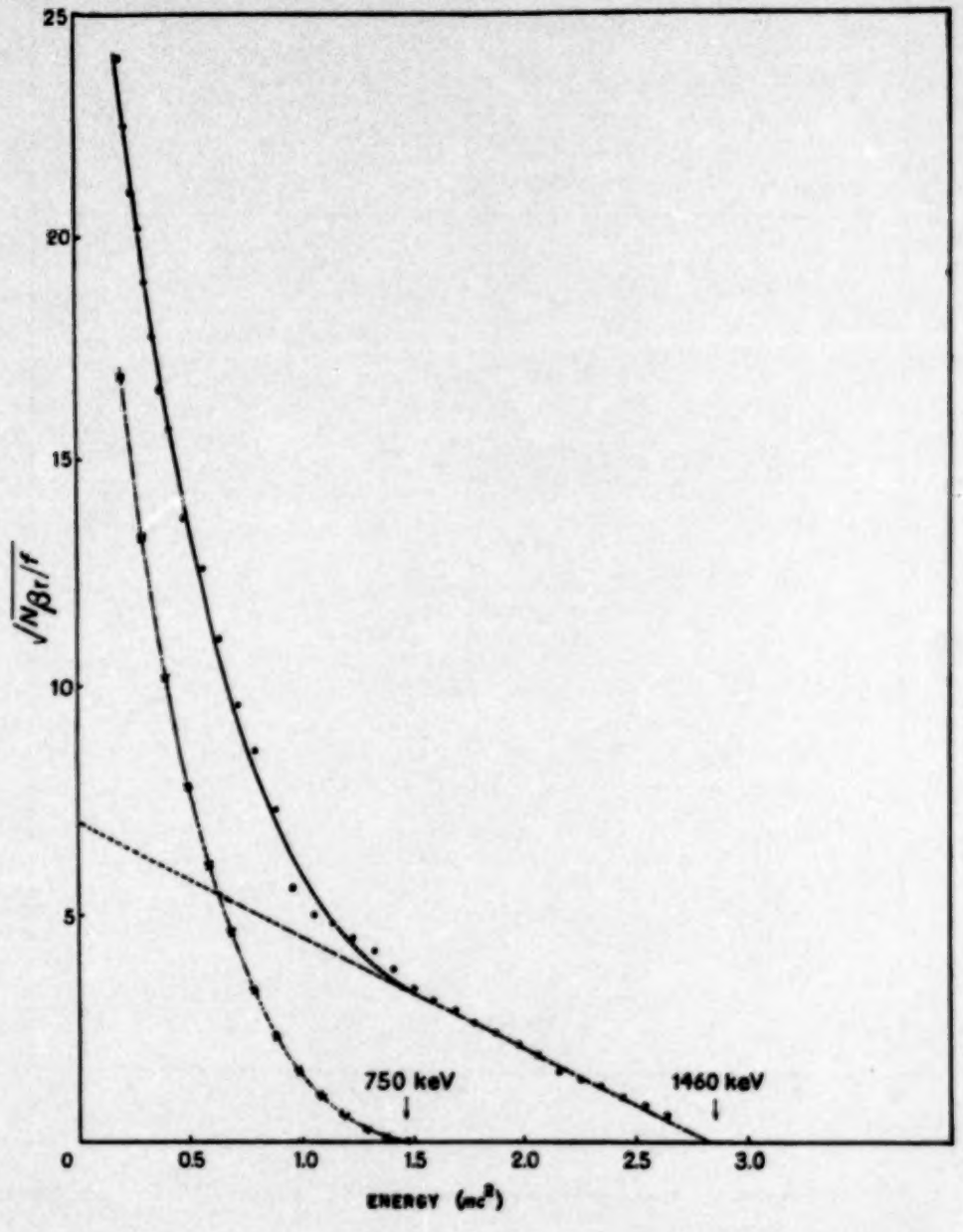

Fig. 7. Fermi plot of the β^--spectrum of Eu in coincidence with 340 keV photopeak. Gamma-gamma coincidence background was determined by interposing perspex absorbers to stop electrons from being detected in the anthracene crystal.

K-conversion coefficient of the 340 keV gamma ray in the β^--decay of Eu^{152} is not very high.

Certain quantitative estimates regarding the composite radiations (124

340 and 1410 keV) could be easily made from our data and the proposed decay scheme (fig. 10).

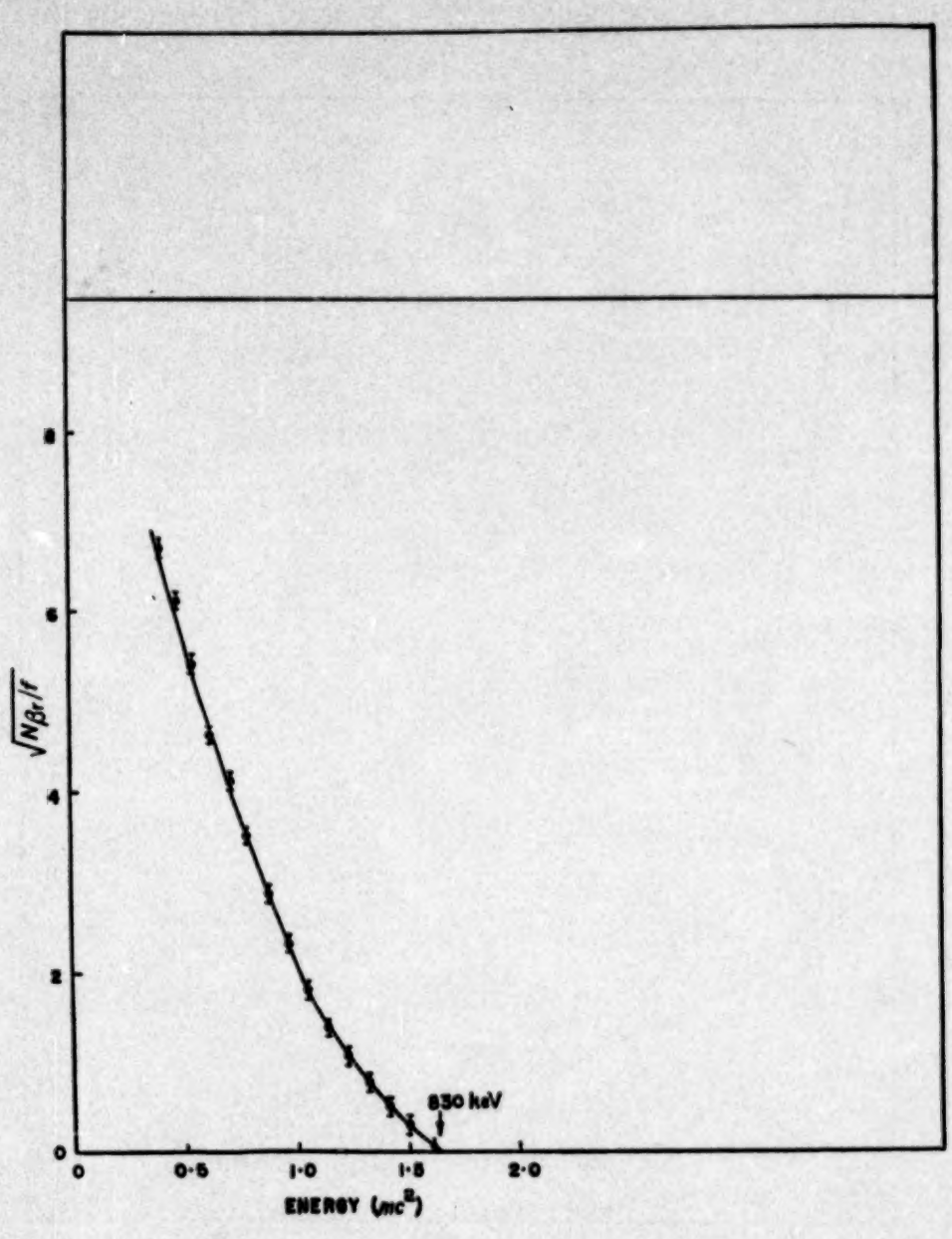

Fig. 8. Fermi plot of the β^--spectrum of Eu in coincidence with 770 keV photopeak.

From the 244 keV coincidences we get the ratio of intensities of the 870 and 1410 keV radiations in the capture branch of Eu^{152},

$$\left(\frac{I_{1410}}{I_{870}}\right)^{244} = \left(\frac{I_{1410}}{I_{870}}\right)^{\text{capture}}$$

since the 870 keV ray is wholly in the capture branch. From the single spectrum we have

$$\frac{I_{1410}}{I_{870}} = \left(\frac{I_{1410}}{I_{870}}\right)^{\text{capture}} + \left(\frac{I_{1410}}{I_{870}}\right)^{\beta^-}.$$

The above relations give I_{1410} (capture) = 5 % of total I_{1410} (from the observed intensity ratios in singles and in coincidences).

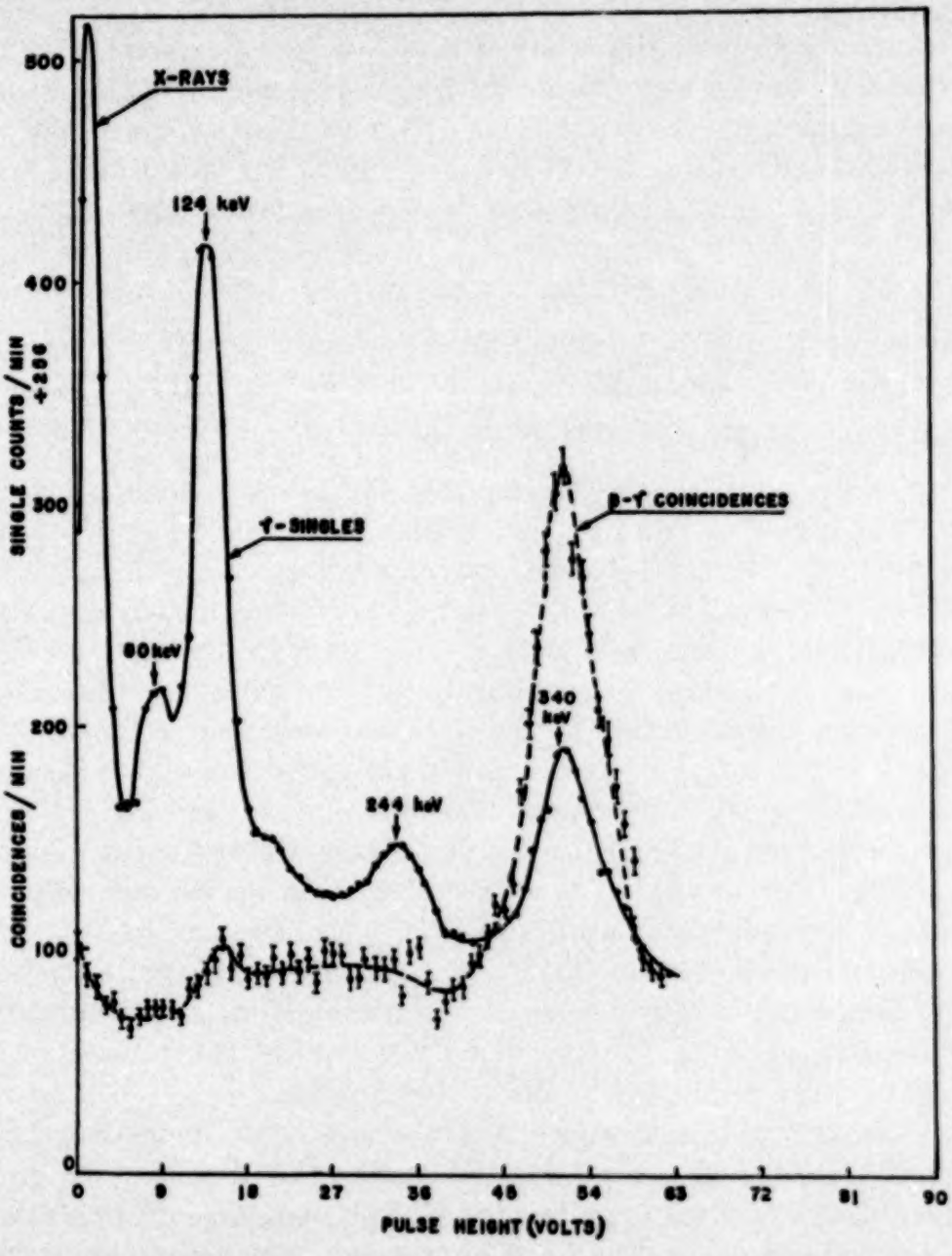

Fig. 9. X-rays and low energy γ-rays in coincidence with β^--particles of energies between 470 and 550 keV. $\gamma-\gamma$ coincidences were usually determined.

In an identical way it can be shown that the 124 keV γ-ray is present in about 75 % of the observed intensity in the capture branch of Eu^{152} and the rest must be due to the decay of Eu^{154}. This ratio is, however,

low as compared to that of curved crystal spectrometer measurements [10]).

Assuming the magnetic spectrometer results [4]) for the intensity-ratio of the 750 and 1460 keV β^--groups as 4 : 1 and using the observed intensities of the 770 and 410 keV γ-rays, it can be shown that the 340 keV ray is present in about 10 % of the total observed intensity in the capture branch of Eu^{152}.

The calculated intensities of the 1410 and 124 keV γ-rays in the decay of Eu^{154} and a rough estimation of the intensity of the 1850 keV β^--group in the anthracence crystal spectrometer enable us to determine the total conversion coefficient of the 124 keV γ-ray (in Gd^{154}), which comes out to be ≈ 3.5. This result is rather high as compared to Sunyar's estimate [11]).

4. Discussion

The decay schemes of Eu^{152} and Eu^{154} are shown in fig. 10. The isotopic assignments are made mostly on the basis of Katz and Lees' [12]) findings.

4.1. DECAY SCHEME OF Eu^{152}

Our results establish conclusively that the 340 keV gamma-radiation, which was known to be exclusively in the β^--branch of Eu^{152}, is present in about 10 % of its total observed intensity in the electron capture branch of the Eu^{152} decay. This radiation in the β^--branch is in coincidence with two β^--groups: the 1110 keV level in Gd^{152} being fed by the 750 keV β^--group, this level then de-excites mostly by 770 keV gamma radiation to the first excited state of Gd^{152} at 340 keV, which is also directly fed by the energetic β^--group of 1460 keV. The 410 keV gamma ray appears in coincidence with the 340 keV gamma ray as also observed by Grodzins [6]); the assignments of the 410 keV gamma ray as the one arising from de-excitation of a level in Gd^{152} at 750 keV is in accordance with the internal conversion electron spectrum measurement of Shull [4]), since he ascribes this line to be converted in the K-shell of Gd. Further, our observed gamma intensities in this branch are in close agreement with the observed β^--branching ratio of Shull; this, of course, assumes that the second excited state at 750 keV in Gd^{152} is very feebly fed by direct β^--transition.

The attempt to assign branching ratios and hence finding the log *ft*-values of the different electron capture transitions of Eu^{152} is handicapped for two reasons: (i) lack of knowledge of the conversion coefficients of the different soft gamma rays and (ii) the presence of composite gamma rays renders their branching evaluation extremely difficult.

The fact that the 244 and 870 keV gamma rays [6]) are exclusively present in the capture branch of Eu^{152} is taken as the guiding point in constructing the decay scheme. We find about 5 % of the total number of 1410 keV gamma rays present in the capture decay of Eu^{152} as also observed by

Grodzins, but our results show the 244 and 121 keV γ-rays both in coincidence with the 1410 keV gamma rays; so the 1410 keV gamma ray arises from de-excitation of the 1775 keV level to the second excited state at 365 keV in Sm^{152}. The newly found gamma ray of 1260 ± 40 keV fits well in the decay scheme as the direct transition to the ground state of Sm^{152} from the 1235 keV level.

Eu^{152} is known to have a 9.2 h half-life isomeric state whose principal mode of decay is by the emission of a β^--group of end-point energy 1880

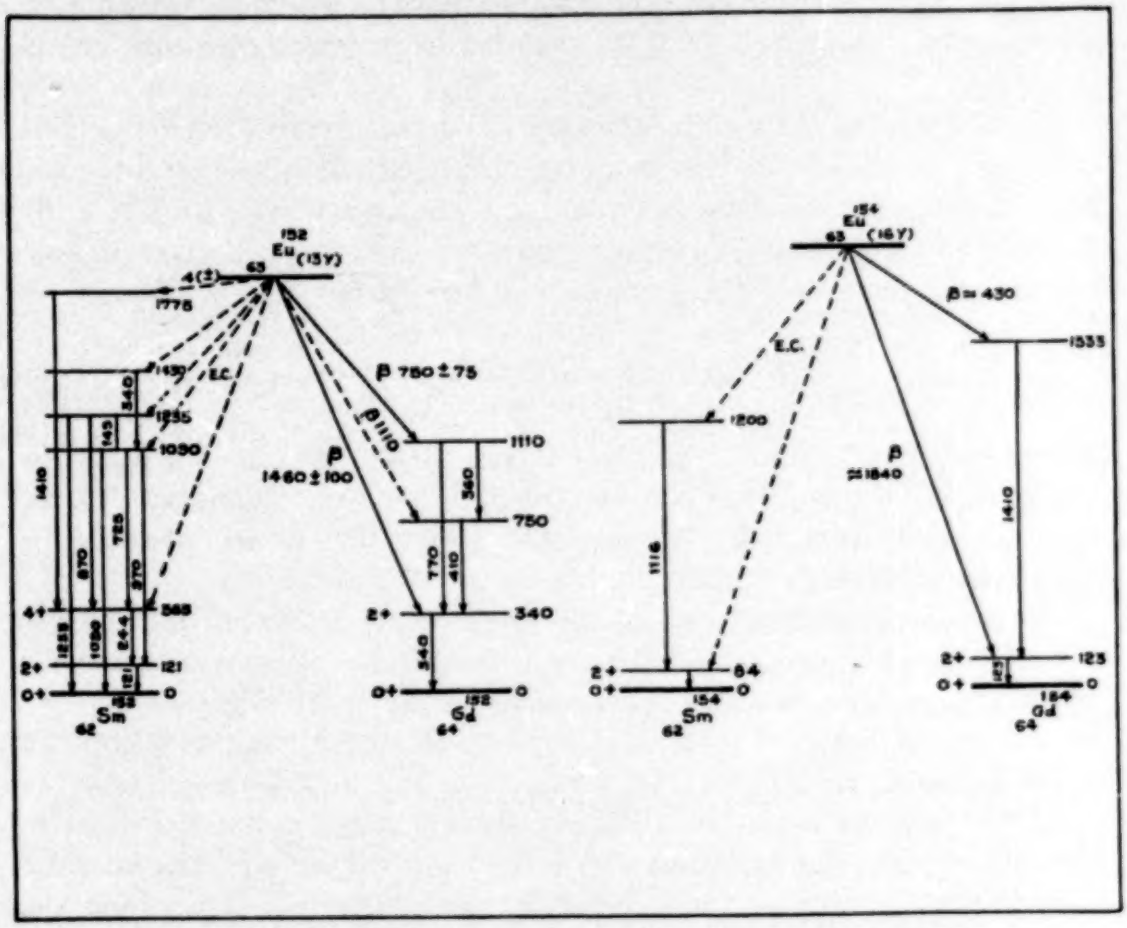

Fig. 10. Proposed decay schemes of Eu^{152} and Eu^{154}.

keV, and since no $\beta-\gamma$ coincidences were observed [2]) one concludes that this β^--group leads to the ground state of Gd^{152}. The Fermi plot shows allowed shape, the calculated log ft — value is about 6.8, which corresponds most probably to a transition involving spin change of at the most $\Delta I = 1$. Since the even nucleus Gd^{152} ground state has configuration $0+$, the isomeric state must have configuration $1(\pm)$. The calculated log ft-value of the 1460 keV β^--group leading to the first excited state in Gd^{152} is about 11, and that of the 750 keV β^--group about 8.8. Log $ft = 11$ means a spin change of at least 2 units. Studies on the systematics of even nuclei [13])

reveal that the first excited state is always of 2+ character. It then follows that the ground state spin of Eu^{152} must be 4 or 0. Grodzins [6]) determines the energy differences between the Eu^{152m} and the ground state to be about 80 ± 25 keV. To explain the existence of the 9.2 h half-life isomeric state one needs at least a spin change of 3 units for the transition energy of $\approx$ 100 keV. This fact suggests that the spin of the ground state of Eu^{152} must be 4. For the single particle shell model Nordheim's coupling rule predicts 2— for the spin and parity of the odd Eu^{152} nucleus. However, assuming Nilsson's [14]) orbitals for the deformed nucleus one can possibly predict the ground state spin of Eu^{152} if the deformation parameter for this nucleus is known.

The first excited state of Sm^{152} at 121 keV has been observed in Coulomb excitation experiments [15, 16]). So one can characterize it as the first rotational level (2+) corresponding to the ground state configuration [17]) ($\Omega = K = 0$). As Bohr and Mottelson [8]) point out, the rotational energy-levels of an even nucleus, far removed from a closed-shell, are given by

$$E_I = \frac{\hbar^2}{2\mathscr{I}} I(I+1), \qquad I = 0, 2, 4, 6, \ldots \text{ (even parity)},$$

where $\mathscr{I}$ is the intrinsic moment of inertia of the deformed nucleus. The de-excitation of these levels is connected by fast E2 transitions with transition probabilities two orders of magnitude greater than encompassed by the transition of a single particle.

The second rotational state of the same family is expected to be 4+ and will have an energy $E_4 = (10/3)E_2$. The 365 keV level connecting the 244 keV gamma ray to the 2+ first excited state in Sm^{152} is characterized as the second rotational state purely on the basis of the energy fit $(E_4/E_2)_{exp} \approx 3$. Hence the 244 keV gamma ray is of pure E2 type. In order to know the nature of the higher excited states in Sm^{152} one has to know the spins of these levels as well as the multipole orders of the energetic gamma rays de-exciting these levels. However, one may guess from the nature of the competing transitions to 0+, 2+ and 4+ states that the spins of the 1090 and 1235 keV levels must be $0 < I < 4$.

The total decay energy for the electron capture transition of Eu^{152} must be higher than 1775 keV according to our decay scheme. Grodzins [6]) finds this difference to be 1740 ± 100 keV. This is in agreement with our result provided one assumes that the 1775 keV level is predominantly fed by L-capture. The decay energy allows positon emission, but no positons were found by Hill and Shephard [2]). This fact is also consistent with our spin assignment of 4 for the Eu^{152} ground state, since it makes the positon transition to the ground state of Sm^{152} highly forbidden; also the transition to the 2+ first excited state is probably a first forbidden transition, for

which case the probability of K-capture is very much higher than that of β^+-emission [18]).

The decay energy for the β^--emission of Eu^{152} is about 1800 keV, in excellent agreement with Grodzins' value of 1790 keV. The spin of the first excited state of Gd^{152} at 340 keV is assigned as 2+ in accordance with the study of the systematics [13]) of even nuclei. Here we find a sharp rise in the energy of the first excited state from 121 keV to 340 keV as we go from $N = 90$ (Sm^{152}) to $N = 88$ (Gd^{152}); this fact is also observed in the Coulomb excitation experiments [15, 16]) with the isotopes of Sm^{150} and Nd^{148}. This apparently sharp break at $N = 88$ amounts to a transition from "strong coupling regions" to the "weak coupling region" in the sense of Bohr—Mottelson's theory. Goldhaber and Weneser [13]) characterize these states as vibrational in origin, arising from core excitations. The first and second excited states are $\hbar\omega$, $2\hbar\omega$, above the ground state, where ω is a measure of the vibrational frequencies: thus $E_2/E_1 = 2$. At $2\hbar\omega$ lies a degenerate triplet, of characters 0+, 2+, 4+. The second excited state in Gd [152] lies at 750 keV and fits rather well in this sort of scheme, $(E_2/E_1)_{exp} \approx 2.2$. If a spin of 2+ is assigned to this state then an E2 transition of 750 keV to the ground state is retarded [13]) or absent as compared to the 410 keV radiation. The 410 keV gamma ray, however, will then be of E2 character (2+ → 2+) with a small M1 admixture. Assignment of 2+ to this level at 750 keV envisages a probable β^--group of endpoint energy ≈ 1110 keV (shown as a dotted line in the decay scheme, fig. 10), which has not been observed by any of the magnetic spectrometer measurements [2, 4, 5]). A 4+ character to this level is also unacceptable for identical reasons. So it seems that the most probable assignment to this level is 0+, in which case the 410 keV gamma ray will be of a pure E2 type: a cross-over transition of 750 keV to the ground state (0+ → 0+) is, however, strictly forbidden; the β^--transition to this level will also be highly forbidden in agreement with experimental findings. By measuring the angular correlation of the 340 keV and 770 keV cascade gamma rays Grodzins assigned 3— as the spin and parity of the 1110 keV level. Log $ft \approx 9$ for the 750 keV β^--group populating this level, which is rather high for a first forbidden transition involving a spin change of unity.

4.2. DECAY SCHEME OF Eu^{154}

The newly reported gamma ray of 84 keV can be readily identified as arising from de-excitation of the first rotational level in Sm^{154}, as this level has been observed recently [15, 16]) in the Coulomb excitation of enriched Sm^{154}. This justifies our assignment of 2+ as the spin and parity of this level. In our singles spectrum (fig. 2) the 1090 keV line is presumably composed of the 1090 keV gamma ray due to Sm^{152} and the 1116 keV gamma ray

assigned to Sm^{154} by electron energy measurements of Cork *et al.* [3]) and also by Katz and Lee [12]). The low intensity β^--group of end point $\approx$ 1840 keV is in coincidence with the 123 keV gamma ray (fig. 9); this level at 123 keV of Gd^{154} is, however, principally fed by the 1410 keV γ-rays. This level can also be identified as rotational in origin since it has been observed in Coulomb excitation experiments [15, 16]). The second excited state of Gd^{154} lies high up at 1533 keV; this level is probably fed by the β^--group of energy 0.330 ± 0.100 keV which Stattery *et al.* [5]) find in their magnetic spectrometer measurements. Recently Hartmann and Wielding [19]) have assigned a spin 6 to this level at 1533 keV in Gd^{154} by observing angular correlation of the 1410—123 keV cascade. The possibility that this level is delayed needs to be further investigated. Our experimental results do not allow us to assign any spin or parity to the ground state of Eu^{154}; also the existence of weakly populated higher states in Gd^{154} is not excluded by this work.

Our sincere thanks are due to Mr. B. Sahai, Mr. S. K. Mitra and Mr. S. V. Godbole for helping us in the various stages of the experiments.

Note added in the proof: After this work was sent for publication, O. Nathan and M. A. Waggoner [20]) have reported the results of their work on Eu^{152} decay. Our results and conclusions are, in essence, in agreement with theirs.

References

1) D. G. Karraker, R. J. Hayden and M. G. Inghram, Phys. Rev. **87** (1952) 901
2) J. M. Hill and L. R. Shepherd, Proc. Phys. Soc. A **63** (1950) 126
3) H. B. Keller and J. M. Cork, Phys. Rev. **84** (1951) 1079
4) F. B. Shull, Phys. Rev. **74** (1948) 917
5) R. E. Slattery, D. C. Lu and M. L. Wiedenbeck, Phys. Rev. **96** (1954) 465
6) I. L. Grodzins, Bull. Am. Phys. Soc. Vol. I No. 4 (1956) 163
7) C. M. Fowler and R. G. Shreffler, Rev. Sci. Instr. **21** (1950) 740
8) A. Bohr and B. R. Mottelson, Mat. Fys. Medd. Dan. Vid. Selsk. **27** (1953) no. 16
9) S. K. Bhattacherjee and Shree Raman, Nuclear Physics **1** (1956) 486
10) B. Andersson, Proc. Phys. Soc. A **69** (1956) 415
11) A. W. Sunyar. Phys. Rev. **98** (1955) 653
12) R. Katz and M. R. Lee, Phys. Rev. **85** (1952) 1038
13) Gertrude Scharaff-Goldhaber and J. Weneser, Phys. Rev. **98** (1955) 212
14) S. G. Nilsson, Mat. Fys. Medd. Dan. Vid. Selsk. **29** (1955) no. 16
15) N. P. Heydenburg and G. M. Temmer, Phys. Rev. **100** (1955) 150
16) H. Mark and G. T. Paulissen, Phys. Rev. **100** (1955) 813
17) Aage Bohr, Rotational States of atomic nuclei (Ejnar Munksgaards Forlag, Copenhagen, 1954)
18) R. Nataf and R. Bouchez, J. Phys. Radium **13** (1952) 190
19) B. Hartmann and T. Wielding, Arkiv f. Fysik **10** (1956) no. 24
20) O. Nathan and M. A. Waggoner, Nuclear Physics **2** (1956/57) 548

Nuclear Physics **4** (1957) 61—87; © *North-Holland Publishing Co., Amsterdam*

Not to be reproduced by photoprint or microfilm without written permission from the publisher

PRODUCTION OF NEUTRAL π-MESONS BY HIGH ENERGY PROTONS

YU. D. BAYUKOV, M. S. KOZODAYEV, YU. D. PROKOSHKIN AND A. A. TYAPKIN

Joint Institute of Nuclear Research

Dubna, U.S.S.R.

Received 18 February 1957

Abstract: The paper contains the results of some investigations carried out by the authors on the synchrocyclotron of the Institute for Nuclear Problems in 1950—1955.

1. Introduction

In an investigation carried out in the first half of 1950 [1]) it was shown that hard γ-rays are emitted by a copper target bombarded by 560 MeV α-particles. The hard γ-radiation was investigated in this work by aid of a 12-channel hodoscope pair spectrometer. In spite of the fact that the background in these measurement was rather considerable a maximum was discovered in the 70—80 MeV region of the γ-spectrum.

The nature of the energy spectrum and the measured yield of hard quanta indicated that a considerable part of the observed hard γ-radiation could not be ascribed to nuclear excitation or bremsstrahlung from α-particles. It seemed probable that the recorded hard α-radiation was connected with the production of neutral π-mesons which subsequently decayed into two γ-quanta. Thus, the results of these investigations were in good agreement with the previously discovered fact [2, 3]) of neutral meson production resulting from collisions between high energy particles and atomic nuclei.

The experiments on π^0-meson production by 470 MeV protons on hydrogen and complex nuclei were carried out in 1951—1952 [4, 5]). For detailed study of the energy spectrum and angular distribution of the high energy γ-quanta and measurement of the cross section for π^0-meson production new measuring equipment was designed. The 12-channel pair spectrometer used in the 1950 experiments was considerably improved [5]). In the new spectrometer the energy region of measured γ-quanta was almost five times larger, the efficiency of γ-quanta registration was higher, and the electron system as well as selection and registration systems were perfected.

2. Investigation of the Energy Spectra of γ-Rays Emitted in the Decay of π^0-Mesons Produced by 470 MeV Protons

2.1. APPARATUS

Gamma quanta energies, lying between 20 and 460 MeV could be measured on the spectrometer. For measurements in the interval from 60 to 460 MeV

pole pieces were used with an angle of opening of 60° (fig. 1ª). The gap between the pole pieces was equal to 3 cm. The range of registered energies

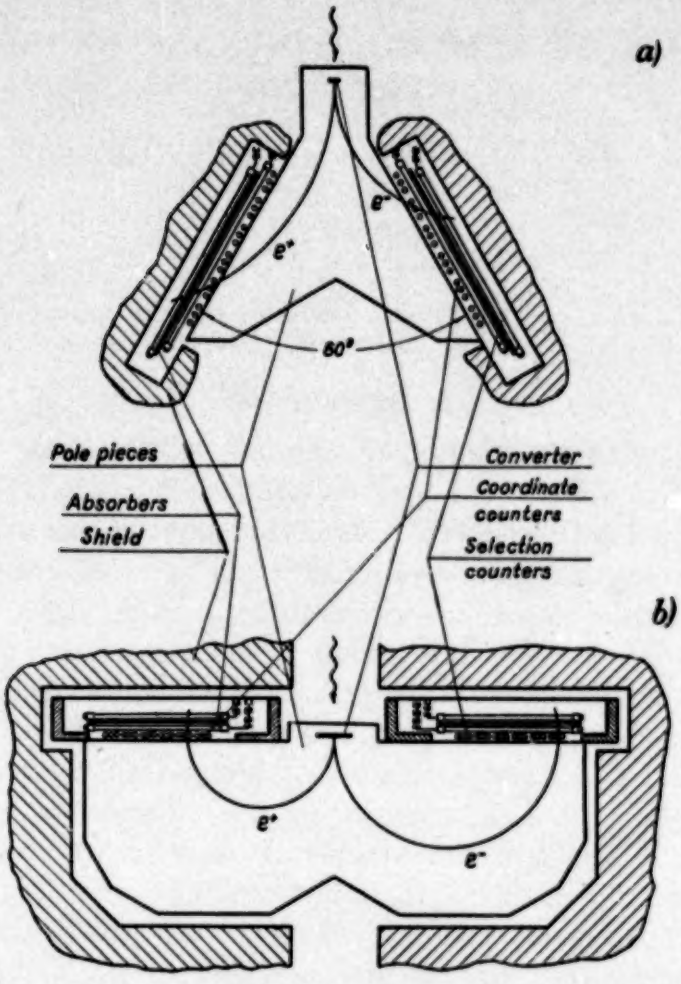

Fig. 1. Magnet pole pieces and arrangement of the counters in the spectrometer.

depended on the strength of the magnetic field in the gap. The maximum magnitude of the magnetic field was 16 000 Oersted. Depending on the energy range various tantalum converters were used, their dimensions being 2×2.5 cm and thicknesses from 0.01 to 0.035 cm.

Owing to the necessity of using thin converters in the low energy measurements, the efficiency of the spectrometer was correspondingly small. Therefore to measure spectra in the 20—110 MeV energy range pole pieces with opening angles of 180° were used (fig. 1ᵇ). The gap between these pole pieces was equal to 4 cm. In these measurements the size of tantalum converters was 3×6 cm.

Coordinate proportional counters which recorded conversion positons and negatons were arranged in a row along the edges of the pole pieces. Each row of proportional counters consisted of 6 groups (channels), each group

having three counters. Behind these counters there were two rows of long "selection counters". The proportional counters used in the spectrometer were filled with pure methylal $CH_2(OCH_3)_2$. The diameter of the copper cathode of the counter was 8 mm.

The pulses from each group of coordinate proportional counters and from the four rows of selection counters were amplified and properly shaped. After being shaped the pulses from the selection counters were fed to a fourfold coincidence circuit. The fourfold coincidence pulse in turn was sent to a triple-coincidence circuit which simultaneously recorded pulses from the proportional counters used to record the negatons and positons. Thus a master pulse was obtained from a sixfold coincidence circuit. The resolving time of the coincidence circuit was $5 \cdot 10^{-7}$ sec.

In the presence of the master pulse a six contact relay was actuated by the amplified proportional counter pulses. Electromechanical counters were switched on by means of these relay contacts; each counter operated by closing of the contacts of various pairs of relays corresponding to γ-quanta of a certain energy interval. The number of pairs (which were also recorded by the proportional counters) was likewise recorded by a corresponding electromechanical counter. From the readings of these 12 counters the relative efficiency of the proportional counters could be computed.

2.2. THE γ-SPECTRA

In the work [4]) devoted to the investigations of the γ-quanta energy spectra the Be, C, Cu, Pb targets were placed in the proton beam inside the accelerator vacuum chamber. The gamma spectrometer was located in a castle constructed of concrete plates at a disctance of 11 m from the target along a tangent to the circular proton orbit (see fig. 2). Measurements of

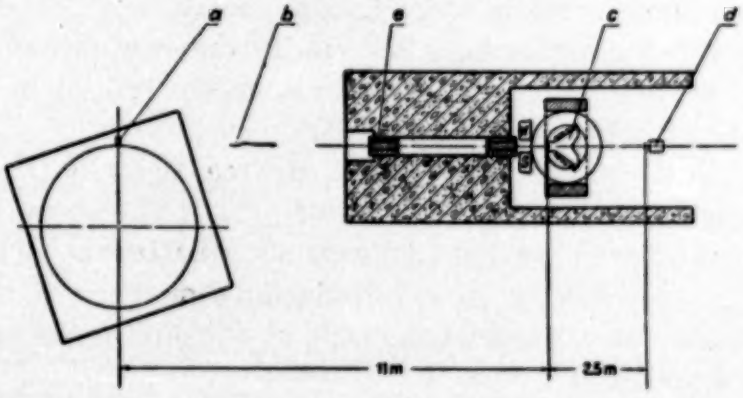

Fig. 2. Experimental arrangement.
a. target, b. γ-ray beam, c. spectrometer, d. monitor, e. collimator

γ-quanta were carried on at 0^0 and 180^0 with respect to the direction of proton motion. A monitor, which recorded the Čerenkov radiation produced by electron pairs from the quanta was used to control the intensity of the

latter. Such a counter successfully registered γ-quanta whose energy exceeded 10 MeV.

Energy spectra of γ-quanta from a beryllium target at angles of 0^0 and 180^0 are shown in fig. 3. About 60 thousand electron pairs were registered

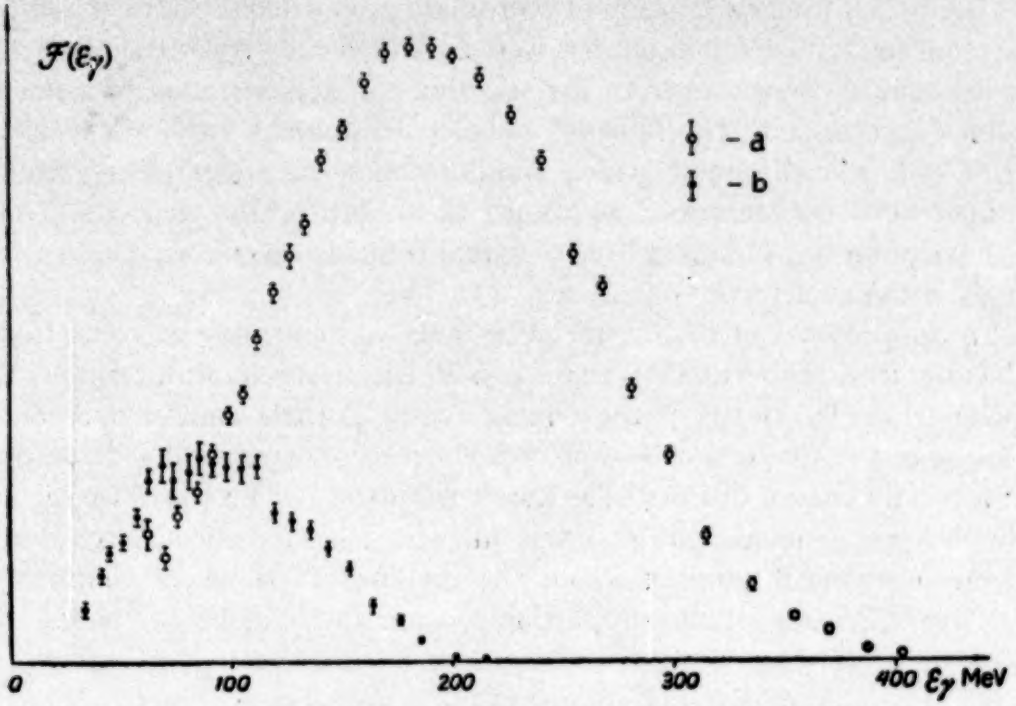

Fig. 3. Energy spectra of γ-quanta from decaying π^0-mesons produced by 470 MeV protons on beryllium nuclei; a. observation angle 0°; b. observation angle 180°.

at an angle of 0^0. Energy measurements of 5 thousand pairs were used to determine the spectrum for 180^0. The ratio of γ-quanta yields at 0^0 and 180^0 was measured by means of a telescope containing a Čerenkov radiation counter. In these measurements the relative values of proton fluxes which had passed through a beryllium target were determined by the induced radioactivity of copper foils.

The ratio of the number of electron pairs registered by the telescope for equal proton fluxes was found to be 6.4 ± 0.4. The average efficiencies of γ-quanta registration at 0^0 and 180^0 were not equal because of the difference in γ-quanta energy spectra. After introducing some corrections to account for the difference in efficiencies the ratio of γ-quanta fluxes at 0^0 and 180^0 was found equal to 5.3 ± 0.5.

2.3. TRANSFORMATION TO C.M.S.

No substantial difference was found in the spectra obtained at 0^0 and 180^0 after transformation to the centre of mass system of the colliding nucleons. This signifies that π^0-mesons are produced as a result of collisions of the impinging protons with separate nucleons but not with the nucleus

as a whole. The insignificant difference in the transformed spectra may be explained by the influence of intranuclear nucleon motion. Owing to this motion no single centre of mass system exists in which the transformed spectra from proton-nucleon impacts would totally coincide. One may only point out the effective value of velocity of the centre of mass system $\beta_c \approx 0.4$ in which the transformed spectra best of all coincide. From the measured high energy end points one may determine the value for the case when the energy of nucleon collision is maximum. The velocity β_c found in this manner was found to be 0.36. Thus the maximum energy of nucleon motion in a nucleus in these collisions is ≈ 20 MeV.

2.4. DERIVATION OF π^0-MESON SPECTRUM

The energy spectrum of γ-quanta, $F(\varepsilon_\gamma)$, for angles of 0^0 and 180^0 in the c.m.s of colliding nucleons is related to the function $\psi(\varepsilon_\pi, \vartheta)$ defining the energy and angular distribution of π^0-mesons by the following relation:

$$F(\varepsilon_\gamma) = \int_{\varepsilon_\pi^*}^{\infty} \frac{\psi(\varepsilon_\pi, \vartheta)}{\sqrt{\varepsilon_\pi^2 - \varepsilon_0^2}} \mathrm{d}\varepsilon_\pi. \tag{1}$$

Here the lower limit of integration is $\varepsilon_\pi^* = \varepsilon_\gamma + (\varepsilon_0^2/4\varepsilon_\gamma)$; ε_0 is the rest energy of the π^0-meson and

$$\vartheta = \arccos \frac{\left(\varepsilon_\pi - \dfrac{\varepsilon_0^2}{2\varepsilon_\gamma}\right)}{\sqrt{\varepsilon_\pi^2 - \varepsilon_0^2}}$$

is the angle between the directions of movement of the π^0-meson and the recorded γ-quantum.

There is no single c.m.s. for colliding nucleons when mesons are produced on complex nuclei because of the intranuclear movement of nucleons. An effective c.m.s. found by means of the impulse approximation with account of the energy dependence of the meson production cross section can, however, be used. As the momenta of the protons bombarding the nucleus considerably exceed those of the intranuclear nucleons, we may use relation (1) to analyse the γ-spectra recalculated for an averaged system of coordinates. Apart from this, in analysing the spectra, we shall consider the angular and energy distributions as independent, i.e., suppose

$$\psi(\varepsilon_\gamma, \vartheta) = f(\varepsilon_\pi)\varphi(\vartheta) \tag{2}$$

where $f(\varepsilon_\pi)$ and $\varphi(\vartheta)$ are the energy spectrum and angular distributions of the π^0-mesons.

In a first approximation the π^0-meson energy spectrum, $f(\varepsilon_\pi)$, can be found by solving the integral equation (1) in the high energy region of the spectrum $F(\varepsilon_\gamma)$ by means of the method of successive extrapolation from large values of ε_π to smaller ones, using the approximate expression $\varphi(\vartheta)$

for the angular distribution. By employing the π^0-meson spectrum found in this manner, a more accurate expression for the angular distribution function $\varphi(\vartheta) = a + b\cos^2\vartheta$ can be found by comparing the experimental γ-spectrum in the region of smaller energies with the spectra calculated for different values of constants a and b.

Fig. 4 shows the energy distributions of π^0-mesons in an effective c.m.s.

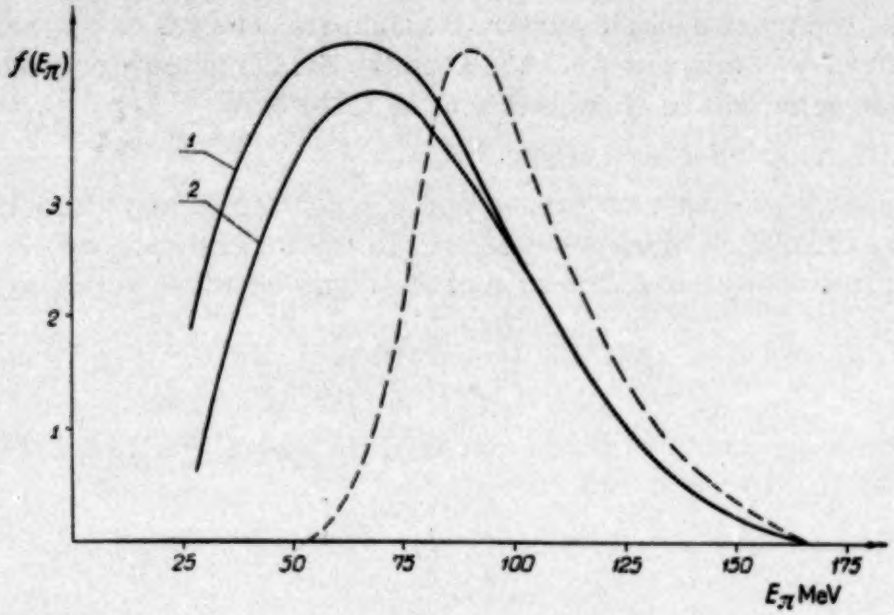

Fig. 4. Energy spectra in an effective c.m.s. of π^0-mesons produced by 470 MeV protons on carbon nuclei. The full lines represent the spectra calculated on basis of the hard part of the experimental γ-spectrum. The dotted curve refers to the spectrum calculated in the impulse approximation on the assumption that the maximal amount of energy in transferred to the produced mesons

for mesons produced on carbon nuclei by 470 MeV protons. These distributions were calculated using the hard part of the γ-spectrum measured at an angle of 0^0 on the assumption of an isotropic (curve 1) and $\cos^2\vartheta$ (curve 2) angular distribution of π^0 mesons. Curves 1 and 2 thus show that the influence of the angular ditribution $\varphi(\vartheta)$ on the shape of spectrum $f(\varepsilon_\pi)$ calculated from the hard part of the γ-spectrum $F(\varepsilon_\gamma)$, is insignificant. A dotted line on the same figure shows the spectrum of π^0 mesons calculated in the impulse approximation on the assumption that the maximum available energy is transferred to the produced mesons. The calculation was made on the assumption that the momentum distribution of nucleons in the nucleus is Gaussian with a mean square momentum of 120 MeV/c.

Comparison of the π^0 meson spectrum (curve 2) with the spectrum thus calculated shows that when a carbon target is bombarded by protons with an energy of 470 MeV, mesons are produced with energies approximating the maximum available one. As a matter of fact, the difference between

curve 2 and the dotted curve is even less if account is taken of the proton energy loss in passage through the carbon nucleus.

In the energy region $\varepsilon_\gamma \leqq \frac{1}{2}\varepsilon_0$ the shape of the γ-spectrum greatly depends on the angular distribution of the π^0 mesons. This circumstance may be used to determine with greater accuracy the angular distribution by comparing the γ-spectrum so measured with the spectra calculated on various assumptions regarding the angular distribution. The calculation of spectra is performed by using the π^0 meson energy distribution previously obtained from the high energy part of the measured γ-spectrum.

Fig. 5 shows the measured and calculated spectra of γ-quanta for a proton

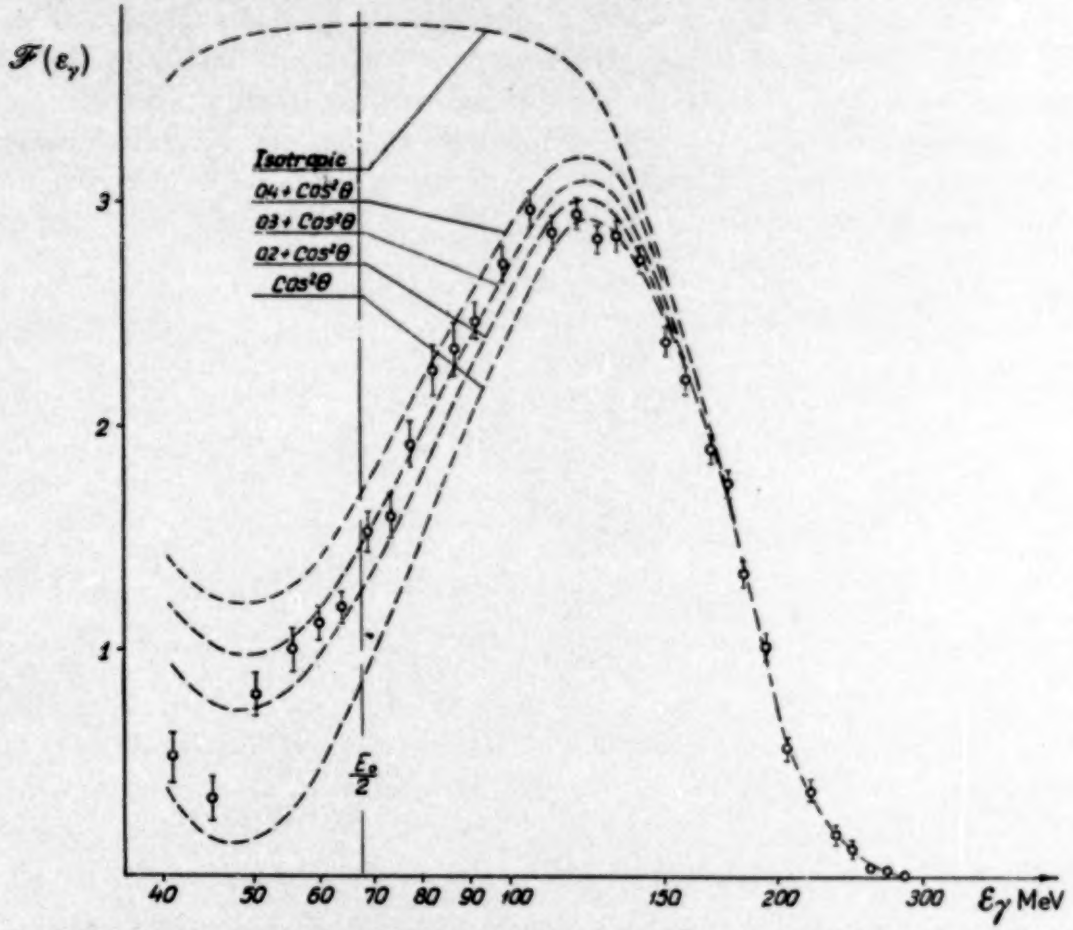

Fig. 5. Energy spectrum in the effective c.m.s. of γ-quanta from decaying π-mesons produced by 470 MeV protons on carbon nuclei. The dotted curves represent spectra computed on various assumptions regarding the magnitude of constant a in the angular distribution formula $\varphi(\vartheta) = a + \cos^2\vartheta$.

energy of 470 MeV and observation angle of 0^0. A comparison of these curves shows that the best agreement is obtained for an angular distribution $\varphi(\vartheta) = 0.3 + \cos^2\vartheta$. Taking into account the errors of the measured spectrum, one may consider that the constant is $a = 0.3 \pm 0.1$.

The energy and angular distributions of π^0-mesons found from the

spectrum of γ-quanta show that neutral mesons produced in nucleon collisions acquire the greater part of the free energy of a collision as well as a large angular momentum and are formed in a p-state.

2.5. INFLUENCE OF π^0 MESON SCATTERING

The scattering of π^0-mesons in nuclei in which they are produced has the effect of flattening out of angular distribution, that is, of making it more isotropic in the laboratory system. To study the influence of π^0-meson scattering on their angular distribution we have measured spectra of γ-rays both for targets made of light elements (Be, C), and heavy ones (Cu, Pb). If the scattering of π^0-mesons considerably changes the angular distribution, the maximum of the spectrum for heavy elements should be shifted towards 70 MeV, that is, to the peak of the isotropic distribution spectrum. Measurements have shown that within the experimental errors the upper limits of the γ-spectra on light (Be, C) and heavy (Cu, Pb)elements are the same (see fig. 3 and 6).

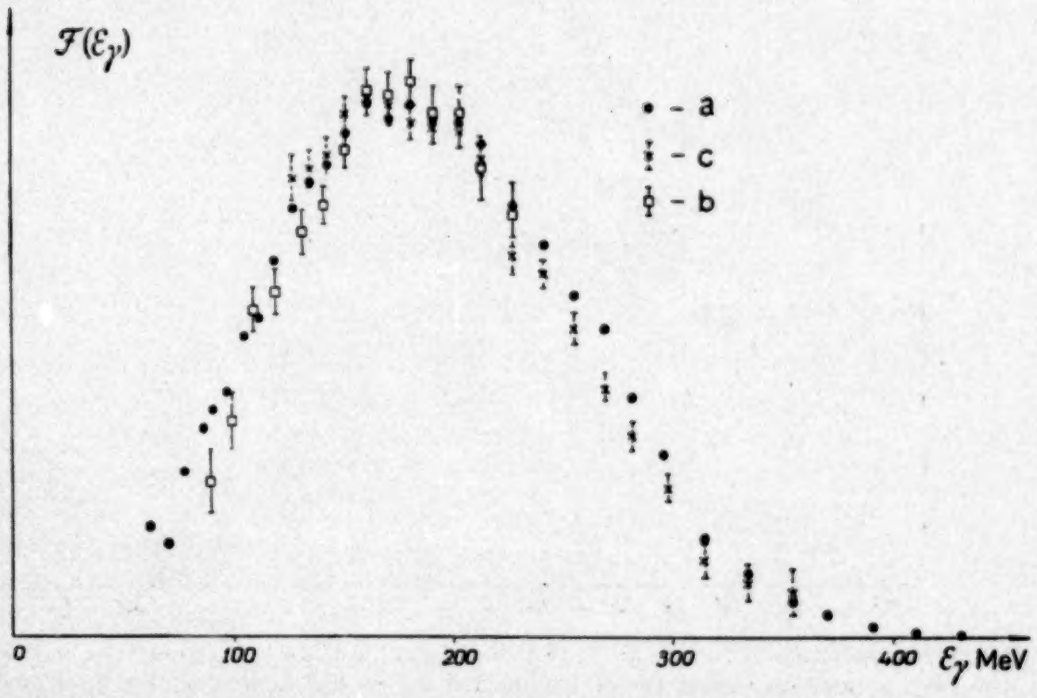

Fig. 6. Energy spectra of γ-quanta from decaying mesons produced by 470 MeV protons on carbon, copper and lead nuclei. a. carbon, b. copper, c. lead.

The peaks of the heavy element spectra cannot be shifted to the low energy region by more than 20 MeV. The experimental evidence permits one to conclude that under the given experimental conditions scattering of π^0-mesons in nuclear matter displays itself but weakly. A possible explanation of this is that the effect of meson absorption predominates.

A paper by W. Crandall and B. Moyer [6]) was published in 1953 in which they described γ-spectra from the decay of neutral mesons produced in the bombardment of a carbon target by 340 MeV protons. The authors of this work also arrived at the conclusion that the angular distribution of neutral mesons produced on complex nuclei is not isotropic, since the peak of the spectrum measured by Crandall and Moyer was considerably shifted to a region of energies higher than those for which an isotropic angular distribution would hold. In the work of Marshall and others [7]) the energy spectra of γ-quanta produced in the bombardment of a beryllium target by 430 MeV protons are given. The spectra obtained in this work are in good agreement with our measurements.

3. Production of π^0-Mesons by 470 MeV Protons on Various Nuclei

3.1. APPARATUS

Simultaneously with the investigation of the energy spectra and angular distribution of γ-quanta [4, 8]) the measurements of the cross sections for production of neutral mesons by 470 MeV protons on various elements were carried out in 1951—1952.

In these experiments the γ-quanta fluxes were measured by two different types of apparatus: by a 12-channel pair spectrometer and by a telescope registering Čerenkov radiation. The flux of protons traversing the target was determined by activation of polystyrene films and also from the γ-activity of copper foils calibrated by a calorimetric method. The positon activity of these films was measured by means of equipment registering $\gamma-\gamma$ coincidences.

3.2. RELATIVE QUANTUM YIELDS

Results of the measurements of relative quantum yields at 0^0 on various elements are shown in fig. 7. For Be, B, C, Al, Cu the relative cross sections for γ-quanta production measured by the spectrometer and Čerenkov counter are, within the statistical errors of measurement, in good agreement with each other. The relative yields of γ-quanta of heavy elements obtained by means of the telescope are somewhat higher in comparison with the spectrometer data. This fact is due to counting losses resulting from heavy loading of the telescope counters when measuring the γ-rays from light elements (the telescope consisted of two rows of proportional counters and a Čerenkov counter).

3.3. PRODUCTION CROSS SECTIONS

As seen from the plot in fig. 7 the cross section for quanta production on complex nuclei rises much more slowly than the number of nucleons in a nucleus. This fact indicates the presence of strong absorption of π^0-mesons in nuclear matter.

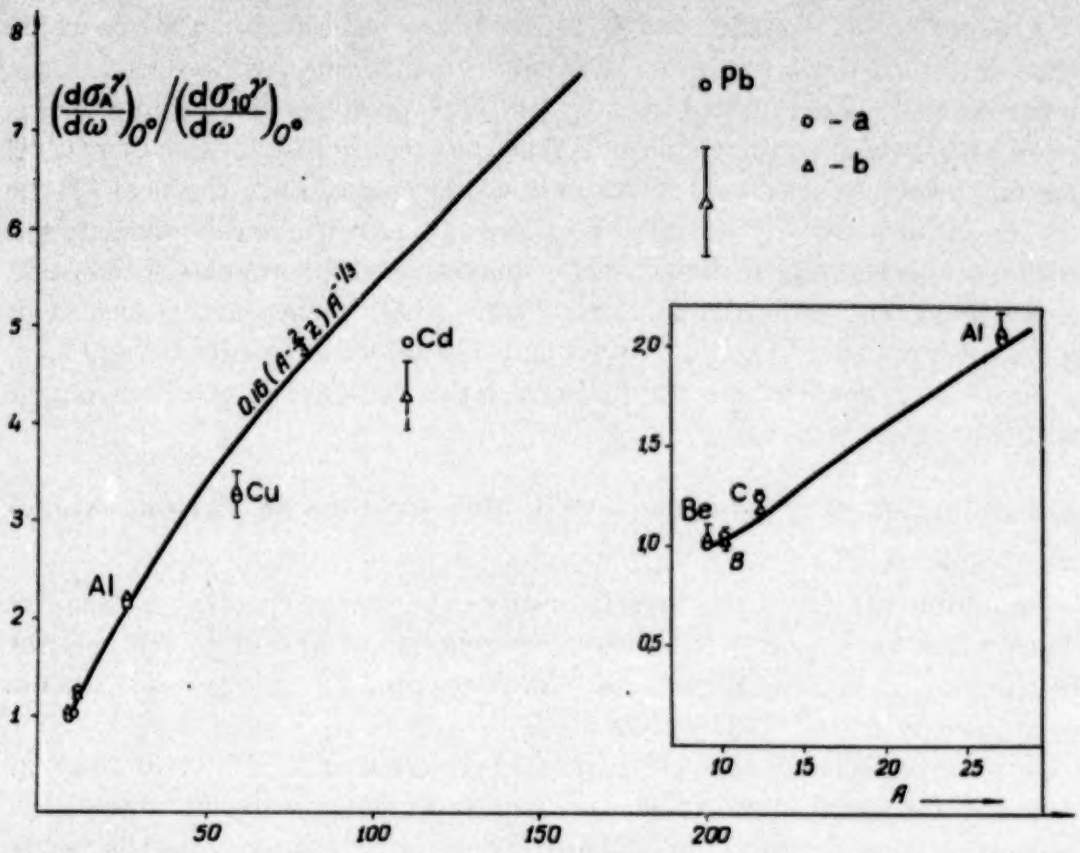

Fig. 7. Relative cross sections for the production of γ-rays at an angle of 0° by 470 MeV protons on nuclei of various elements.
a. Čerenkov counter data
b. γ-spectrometer data.

If we assume that meson production occurs on all the nucleons of a nucleus then the total cross section for meson production in a nucleus with mass number A can be expressed as

$$\sigma_A = f_A\,[\bar{\sigma}_{pn}(A-Z)+\bar{\sigma}_{pp}\,Z]$$

where $\bar{\sigma}_{pn}$ and $\bar{\sigma}_{pp}$ are average cross sections for π^0-meson production on an intranuclear neutron and proton, and the factor f_A accounts for meson absorption within the nucleus. According to calculations [9]) for the case when the cross section of meson absorption is much higher than that of scattering, the factor f_A is expressed by the following function:

$$f_A = 3\left[\frac{1}{2x}-\frac{1}{x^3}+\frac{1}{x^3}(x+1)e^{-x}\right]$$

where $x = r_0 A^{1/3}/\lambda_\pi$ and λ_π is the mean free path of mesons in nuclear matter. Employing this equation for f_A we can find from the experimentally obtained yields of γ-quanta on Be, C, and Al the upper limit for the mean free path of neutral mesons for absorption within the nucleus,

$$\lambda_\pi \leqq 1.5\, r_0$$

where

$$r_0 = 1.3 \times 10^{-13} \text{ cm.}$$

Experiments that will be described in the following sections permit us to draw the conclusion that at a proton energy of 470 MeV the cross section $\sigma_{pn}^{\pi^0}$ is approximately three times the cross section $\sigma_{pp}^{\pi^0}$. If meson production occurs only on surface nucleons ($x \gg 1$) the total cross section for production of π^0-mesons on the compound nucleus will be proportional to $(A - \frac{2}{3}Z)A^{-1/3}$. For heavy nuclei as seen from fig. 7, the differential cross section of γ-quanta production increases more slowly than it would according to the law which corresponds to strong meson absorption ($\lambda_\pi \approx 0$). This fact indicates that there exist other processes which lower the probability of π^0-meson production in complex nuclei. This problem will be considered again in connection with a discussion of the results of the experiments of 1954.

4. Absolute Cross Section for π^0-Meson Production by 470 MeV Protons

4.1. DIFFERENTIAL CROSS SECTION OF CARBON

The absolute differential cross section for γ-ray production on carbon was determined by means of γ-spectrometer and Čerenkov detector. The differential cross section for 0^0 in units of 10^{-27} cm^2/sterad is equal to 6.7 ± 2.0 according to the spectrometer measurements and 5.8 ± 2.0 according to the telescope measurements. The mean value of the cross section is equal to $(6.2 \pm 1.6) \times 10^{-27}$ cm^2/sterad.

4.2. DIFFERENTIAL CROSS SECTION FOR p-p COLLISIONS

The determination of the differential cross section $d\sigma_{pp}^{\gamma}/d\omega$ for p—p collisions was performed by a subtraction method, namely, by measuring yields of γ-quanta from polythene $(CH_2)_n$ and carbon targets bombarded by protons. These measurements yielded the result that the differential cross section for production of γ-quanta in 470 MeV p—p collisions is

$$(d\sigma_{pp}^{\gamma}/d\omega)_{0^0} = (0.26 \pm 0.17) \times 10^{-27} \text{ cm}^2/\text{sterad}$$

according to the telescope measurements and

$$(d\sigma_{pp}^{\gamma}/d\omega)_{0^0} = (0.30 \pm 0.20) \times 10^{-27} \text{ cm}^2/\text{sterad}$$

according to the spectrometer measurements.

4.3. TOTAL PRODUCTION CROSS SECTION

The differential cross sections thus obtained permit one to determine the total cross section for production of neutral mesons. For this purpose it is necessary to know either the angular and energy distributions of mesons in the centre of mass system of the colliding nucleons or the angular distribution of γ-quanta in the laboratory system. The total cross section

for production of neutral mesons is related to the differential cross section in the following way:

$$\sigma^{\pi^0} = \tfrac{1}{2}\alpha\Omega(\mathrm{d}\sigma^{\gamma}/\mathrm{d}\omega)_{0^\circ}$$

where the coefficient $\alpha = (1-\beta_c)/(1+\beta_c)$ accounts for the transformation of solid angles for γ-rays and Ω is a factor which depends on the angular and energy distribution of the π^0-mesons. In the case of collisions of 470 MeV protons with hydrogen nuclei $\alpha = 0.38$.

Calculations carried out in the impulse approximation show that for compound nuclei the most correct value under the conditions of our experiment is $\bar{\alpha} = 0.42$ which corresponds to $\bar{\beta}_c = 0.41$. This calculation was performed on the assumption that the momentum distribution of nucleons in the nucleus is described by a Gaussian law with a mean square momentum of 120 MeV/c, and that the cross sections for π^0 meson production in p—p and p—n collisions are described by the functions $\sigma_{pp}^{\pi^0} \propto p_{max}^6$ and $\sigma_{pn}^{\pi^0} \propto p_{max}^3$ where p_{max} is the maximum possible meson momentum; the ratio of the cross sections $\sigma_{pp}^{\pi^0}/\sigma_{pn}^{\pi^0}$ at a proton energy of 470 MeV has been assumed to be equal to 1/3.

The coefficient Ω may have various values depending on meson energy and angular distributions, and in the case of isotropic distribution, it is equal to 4π. The value of this coefficient can be found by the formula

$$\Omega = \frac{2\pi\int_0^{\pi}\varphi(\vartheta)\sin\vartheta\mathrm{d}\vartheta}{\int_0^{\infty} f(\varepsilon)W(\varepsilon)\mathrm{d}\varepsilon}.$$

Here $\varphi(\vartheta)$ is the angular distribution of mesons in the centre of mass system, ε the total meson energy in units of μc^2, $W(\varepsilon)$ the meson energy spectrum and

$$f(\varepsilon) = \int_{\varepsilon_{\gamma\min}}^{\varepsilon_{\gamma\max}} F(\varepsilon_\gamma, \varepsilon)\mathrm{d}\varepsilon_\gamma$$

where $F(\varepsilon_\gamma, \varepsilon)$ is the energy spectrum of γ-quanta which corresponds to a given angular distribution of mesons possessing an energy ε. In the case of a $\cos^2\vartheta$ angular distribution of π^0 mesons

$$f(\varepsilon) = \frac{\varepsilon^2+1}{\varepsilon^2-1} - \frac{\varepsilon}{(\varepsilon^2-1)^{3/2}}\ln\frac{\varepsilon+\sqrt{\varepsilon^2-1}}{\varepsilon-\sqrt{\varepsilon^2-1}}.$$

The energy spectrum $W(\varepsilon)$ was approximately calculated from the measured γ-ray spectrum and assuming that the angular distribution was proportional to $\cos^2\vartheta$, the coefficient Ω was found to be equal to 2.5π. As a matter of fact a better expression for the angular distribution of neutral mesons is $a+\cos^2\vartheta$ and the coefficient should therefore somewhat exceed 2.5π. The exact value of Ω may be found if we measure the angular distribution of γ-quanta in the laboratory system.

Employing the mean value of the differential cross section $(d\sigma_c^{\gamma}/d\omega)_{0^\circ} = (6.2\pm1.6)\times10^{-27}$ cm²/sterad we find, on the assumption that the angular meson distribution is proportional to $\cos^2\vartheta$, a total cross section for production of π^0-mesons by 470 MeV protons on carbon

$$\sigma_c^{\pi^0} = (10.2\pm2.6)\times10^{-27} \text{ cm}^2.$$

Making use of the mean value

$$(d\sigma_{pp}^{\gamma}/d\omega)_{0^\circ} = (0.28\pm0.18)\times10^{-27} \text{ cm}^2/\text{steradian},$$

obtained from the results of the γ-spectrometer and telescope measurements, we find that the total cross section for production of π^0-mesons in p—p collisions is $\sigma_{pp}^{\pi^0} = (0.7\pm0.4)\times10^{-27}$ cm² in the case of isotropic meson distribution, and $\sigma_{pp}^{\pi^0} = (0.5\pm0.3)\times10^{-27}$ cm² when the angular meson distribution is proportional to $\cos^2\vartheta$. This result is in good agreement with similar data obtained in ref. [10]).

5. π^0-Meson Production by 660 MeV Protons on Various Nuclei

5.1. APPARATUS

π^0-meson production of 660 MeV protons on nuclei of various elements was investigated in 1954 [11]).

The gamma quanta produced on the internal accelerator target were registered by means of a gamma telescope consisting of a scintillation counter and Čerenkov counter. The telescope consisted of two separate blocks. A tolane crystal $50\times50\times9$ mm of size and two photomultipliers connected to it were placed in the first block. A radiator made of plexiglass $105\times115\times40$ mm of size and two photomultipliers connected to it symmetrically were arranged in the second block. The energy threshold for γ-quanta registration could be increased by separating the telescope blocks and inserting between them copper absorbers, and in this way a rough investigation of the γ-quanta spectrum could be made. The mean energies of the γ-spectra were determined from measurements of the γ-ray absorption coefficient in lead on the basis of theoretical data obtained in the work of Davis, Bethe and Maximon [12]).

To determine the total γ-ray flux it was necessary to know the efficiency of the Čerenkov radiation counter. An experimental determination of the telescope efficiency was carried out by successively switching off separate parts of the telescope. For this purpose an electronic four-fold coincidence circuit was employed which could easily be changed to a triple coincidence circuit containing any three photomultipliers of the four being used in the telescope. In switching over from one type of circuit to the other the circuit sensitivity remained unchanged. The inefficiency of the disconnected photomultiplier could be determined from the increase of the counting

rate observed when triple coincidences were substituted for fourfold ones. To check this method it was applied to multipliers connected to a scintillation crystal, whose efficiency was known to be practically 100 %. The experimental efficiency value turned out to be equal to $(99\pm1)\%$.

5.2. RELATIVE YIELDS OF γ-QUANTA

The relative yields of γ-quanta produced from the decay of π^0-mesons created in the bombardment of H, D, Li_6, Li_7, Be, B, C, Al, Cu, Sn, Pb and U nuclei with 670 MeV protons were measured by means of the telescope described above. Measurements of γ-quanta fluxes were carried out at 0 and 180° to the direction of proton motion. The results of these measurements are given in fig. 8. The γ-quanta yield at 0° increases much more

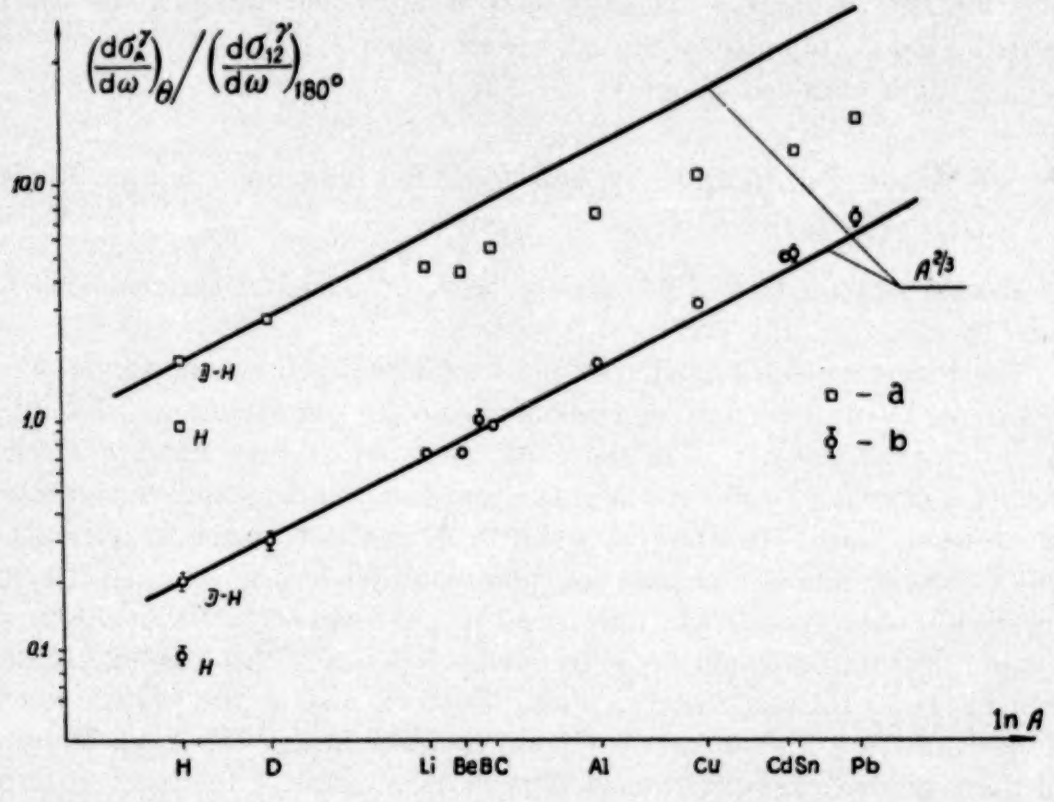

Fig. 8. Relative cross sections for the production of γ-rays by 670 MeV protons on nuclei of various elements.
a. angle of emission 0°
b. angle of emission 180°

slowly than it should do according to the $A^{2/3}$ law. This result is in good agreement with the data obtained at 470 MeV. However the flux measurements at 180° and a proton energy of 660 MeV show that in this case the dependence of the γ-quanta yields on the atomic weight is in good agreement with the $A^{2/3}$ law. The small systematic deviation from this law which sometimes occurs can be explained by the differences in the cross section values for π^0-meson production in p—p and p—n collisions. If this difference is

taken into consideration then the yield at 180° of γ-quanta created in the decay of mesons on the surface of the nucleus should be proportional to

$$\left(\frac{A-Z}{A}\,\bar{\sigma}^{\pi^0}_{pn}+\frac{Z}{A}\,\bar{\sigma}^{\pi^0}_{pp}\right)A^{2/3}.$$

The best agreement with the experimental results occurs for

$$\sigma^{\pi^0}_{pn}/\sigma^{\pi^0}_{pp}=2.0\pm0.5.$$

5.3. PRODUCTION CROSS SECTION

The increase of the γ-ray differential cross section at 180° exactly follows the $A^{2/3}$ law even in the case of light nuclei. This result can hardly be explained by invoking only absorption of mesons and protons in nuclei since, as a rule, only comparatively slow mesons move at an angle of 180° with respect to the direction of proton motion and for such mesons, according to ref. [13, 14]) $\lambda_\pi \approx 7r_0$. To explain the observed variation of the relative cross sections at 180°, besides account of proton and meson absorption one should probably also assume the presence of an additional mechanism which considerably decreases the cross section of meson production on strongly bound nucleons located within nuclei.

The conclusion of a considerable decrease of the probability of π-meson production within a nucleus had been previously made [15, 16]) in respect to π-meson photoproduction by comparing the results of measurements of the dependence of the photomeson yield on atomic weight [17]) with the data on absorption of π-mesons in nuclei. It is difficult to draw an adequate conclusion in the case of meson production by protons because of the large value of the cross section for interaction of protons with nucleons of the nucleus. The reduction of the probability of meson production on inner nucleons of a nucleus can then only affect the course of the relative cross sections of light nuclei. In this connection the existence of an additional mechanism which reduces the probability of meson production by protons on strongly bound nucleons within a nucleus can be proved only if computations which correctly take into account proton and meson absorption in light nuclei are performed.

It should be noted that in ref.[18]) a linear dependence of the cross section on the number of neutrons in a nucleus was observed for light nuclei ($A<27$); and this signifies equal probability of meson production throughout the nuclear volume. The reasons for such a variation of meson production in changing from high to low energy collisions remain unclear. This variation cannot be explained by the difference in absorption of protons and mesons. In both cases the registered γ-radiation is chiefly due to π^0-mesons emitted at a direction opposite to that of the proton beam ($\vartheta \approx 180^0$). In both cases the mesons possess a low energy and are only insignificantly absorbed in the

nucleus. The cross section of interaction of protons with nucleons of the nucleus on the other hand only slightly varies with the energy.

5.4. SCREENING EFFECT

We measured the ratio of the γ-quanta yields at 0^0 and 180^0:

$$\eta_A = \frac{d\sigma_A^\gamma}{d\omega}(0^0) \Big/ \frac{d\sigma_A^\gamma}{d\omega}(180^0).$$

The results of the measurements are presented in fig. 9; it can be seen that even in the region of light nuclei one may observe a fast decrease of the quantity η_A. The reduction of the ratio η_A can be explained by partial opacity of a nucleus for the bombarding protons in the presence of a strong absorption of π^0-mesons.

The screening effect of nucleons of the nucleus due to star-production processes and to scattering of incident protons leads to a considerable reduction in the number of protons which, after passing through the nucleus, possess energy sufficient for effective π^0-meson production. The scattering of π^0-mesons in nuclei at a proton energy of 660 MeV seems to have no considerable influence on the value of η_A since the experimental cross sections at 180^0 increase as $A^{2/3}$, while in the case of strong scattering of π^0-mesons at this angle one should observe an increase in the cross section which should be more rapid than expected from the $A^{2/3}$ law. The departure of the γ-quanta yield dependence at 0^0 from the $A^{2/3}$ law can be satisfactorily explained by means of a nuclear model which depicts the nucleus as being partially opaque for protons. Most of the recorded γ-radiation originates from the decay of π^0-mesons moving from the target towards the γ-detector (this is connected with the transformation of solid angles). In the measurements at 180^0 the chief part of such mesons is emitted from the nucleus surface which is freely irradiated by protons. In this case it is quite natural to expect, if one assumes that mesons are mostly produced on nucleons at the surface of a nucleus, that the $A^{2/3}$ law will hold. In the γ-ray measurements at 0^0 the nuclear surface from which the effectively registered π^0-mesons are emitted is shielded from the incident protons by nuclear nucleons. The screening effect increases with the mass number A and this results in reduction of the ratio η_A.

The screening phenomena mentioned above and the processes of meson absorption in a nucleus should, along with a change in the angular distribution of the γ-quanta, result in a softening of the γ-quanta spectrum at 0^0 with increase of the atomic weight. To detect this effect we measured the γ-quanta yields and the ratio η_A for various elements. The measurements were performed with a detector possessing a high energy threshold (points b in fig. 9) [11]). Only hard γ-quanta were registered in the experiment, these comprising approximately 1/5 of the total flux of γ-rays.

Table 1 shows the ratio $M(A)/M(12)$ for angles 0^0 and 180^0, where the value $M(A)$ denotes the ratio of the number of hard γ-quanta to the total flux of γ-quanta for an element of mass number A.

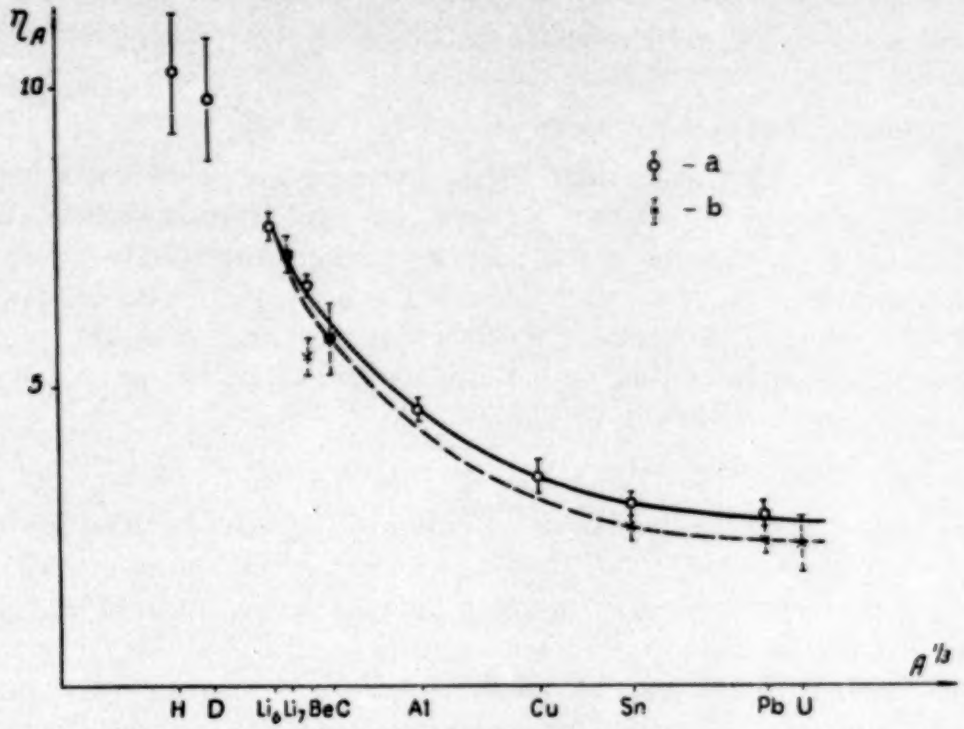

Fig. 9. Dependence on mass number A of the ratio of the γ-quanta yields at 0° and 180°.
a. from measurements on the total flux
b. from "hard" detector measurements.

TABLE 1

Element angle	H	D	Li_6	Li_7	Be	C	Sn	Pb	U
0^0	0.5±0.2	0.8±0.2	0.91±0.04	1.00±0.05	0.8±0.1	1.00±0.04	0.92±0.05	0.95±0.04	0.92±0.04
180°	0.5±0.3	0.9±0.2	1.06±0.04	1.00±0.03	1.0±0.1	1.00±0.03	–	–	–

From the data presented above the conclusion may be drawn that the spectrum of γ-quanta produced in hydrogen is much softer than that of γ-rays produced in complex nuclei. This is quite natural because in the case of complex nuclei hard γ-quanta are due to intranuclear motion which is absent in the hydrogen experiments. At the same time it has been found that the γ-spectrum of beryllium is considerably poorer in hard rays than the spectra obtained from the neighbouring light elements. This can be explained partly by the fact that one of the neutrons in the beryllium nucleus is weakly bound and therefore the π^0-mesons revolving on it have

a relatively low energy and do not appreciably contribute to the hard part of the spectrum.

Only a small difference can be noted in the spectra of light and heavy elements measured at 0^0. This will apparently be difficult to reconcile with the sharp difference in the angular distributions of γ-quanta produced on light and heavy elements detected by us.

5.5. "FORWARD-BACKWARD" RATIO

If in the c.m. system of the colliding nucleons the process of π^0-meson production is symmetric in the "forward-backward" directions (and this is fulfilled for p—p impacts as the particles are indistinguishable) then the ratio is defined only by the Doppler effect and is equal to 9.6 for protons of 660 MeV energy. Owing to intranuclear motion of nucleons in the complex nucleus this value, according to impulse approximation computations, will be slightly smaller. Thus if we assume that

$$\sigma_{pp} \propto p^6_{max}, \ \sigma_{pn} \propto p^3_{max} \text{ and } \sigma_{pp}/\sigma_{pn} \ (660) = \tfrac{1}{2},$$

then in the case of a Gaussian distribution of the nucleon momenta with a mean square impulse of 120 MeV/c and a cut-off at 200 MeV/c, we find that $\bar{\eta} = 9.0$. The smallest value of $\bar{\eta}$ obtains on the assumption that a Fermi distribution with an end-point energy of 22 MeV holds for nucleons in the nucleus. In this case $\bar{\eta} = 8.2$.

The production cross section for γ-quanta on hydrogen by 660 MeV protons was measured by the subtraction method by means of irradiation of targets made of graphite and polythene $(CH_2)_n$. Since the employed targets did not contain any heavy impurities the proton flux was controlled by measuring the annihilation radiation due to the γ-activity of the targets themselves. This procedure, like the calorimetric method, permits one to exclude the effect of the shape and density of the targets. The cross section values (in % with respect to carbon) were found to equal $(18\pm1)\%$ at 0^0 and $(9.5\pm0.8)\%$ at 180^0. Thus, η_H was equal to 11 ± 2. The quantity η_H was also measured by a subtraction method with targets made of LiH and Li and it was found to equal 10 ± 1. The values of η_H found experimentally coincide within the limits of the errors with the theoretical value $\eta = 9.6$. This is an additional proof that the value obtained by us, $\eta_C = 5.8\pm0.2$, is correct and that even for the very light nuclei Li, Be, C the ratio η_A is considerably less than $\bar{\eta}$.

6. Absolute Cross Sections for Production of π^0 Mesons on Hydrogen and Deuterium by 660 MeV Protons

In the measurements of the absolute π^0-meson cross section, absorption of γ-quanta in the target and air was taken into account; errors connected with the presence of an energy threshold in the γ-detector

were measured by special experiments. The telescope efficiency was experimentally determined by the method mentioned above of successively disconnecting separate multipliers. The differential cross section for production of γ-quanta in p—p collisions at 0^0 (or 180^0) in the c.m. system has been found to equal

$$(d\sigma^{\gamma}_{pp}/d\omega)_{0^0} = (0.59 \pm 0.13) \times 10^{-27} \text{ cm}^2/\text{sterad}.$$

Under the assumption of isotropic distribution of π^0-mesons we find for the total cross section for the production of π^0-mesons at a proton energy of 660 MeV:

$$\sigma^{\pi^0}_{pp} = (3.7 \pm 0.8) \times 10^{-27} \text{ cm}^2.$$

The cross section for the production of γ-quanta on deuterium has been measured by a subtraction method (LiD—Li) and found to be equal to

$$(d\sigma^{\gamma}_{pd}/d\omega)_{0^0} = (1.8 \pm 0.3) \times 10^{-27} \text{ cm}^2/\text{sterad}.$$

Hence, neglecting the coupling of nucleons in the deuterium nucleus we find that

$$\sigma^{\pi^0}_{pn} = (7.8 \pm 1.6) \times 10^{-27} \text{ cm}^2.$$

7. Excitation Functions for π^0-Meson Production by Protons

The dependence of the meson production cross section on the bombarding energy of the incident nucleons appears to be extremely significant for the meson production process. Some information on this problem can be obtained by investigation of meson production on a complex nucleus. However there is no possibility in this case for a rigorous interpretation of the obtained results since some assumptions have to be made regarding the momentum distribution of nucleons inside the nucleus, the Pauli exclusion principle, etc.

7.1. PROTON ENERGIES 190—465 MeV

We measured the energy dependence of the cross section for production of neutral mesons on carbon by using protons with energies of 190, 270, 365 and 465 MeV [19]). The proton energy in these measurements was varied by changing the distance between the carbon target inside the accelerator vacuum chamber and the centre of the circular proton orbit. The gamma-quanta were observed at 180^0 with respect to the proton motion. The results of these measurements are shown in fig. 10. The proton energy is plotted along the abscissa axis and the differential cross section for production of γ-quanta along the ordinate axis. A calculation carried out in the impulse approximation with account of Pauli's principle showed that the cross section for production of π^0-mesons in p—n collisions in this region of proton energy depends on the value of the maximum π^0-meson momentum in the following manner:

$$\sigma_{pn} \propto p^{3.5 \pm 0.5}_{max}.$$

7.2. PROTON ENERGIES 470—660 MeV

If the cross section values obtained at the proton energy of 470 and 660 MeV:

$$\sigma_{pp}^{\pi^0}(660) = (3.7 \pm 0.8) \times 10^{-27} \text{ cm}^2, \quad \sigma_{pp}^{\pi^0}(470) = (0.5 \pm 0.3) \times 10^{-27} \text{ cm}^2$$

are compared with the results of measurements obtained by J. Mather and E. Martinelli [20]:

$$\sigma_{pp}^{\pi^0}(340) = (0.010 \pm 0.003) \times 10^{-27} \text{ cm}^2,$$

it can be concluded that the rise of the cross section $\sigma_{pp}^{\pi^0}$ slows down with increase of the bombarding proton energy. On changing from the energy

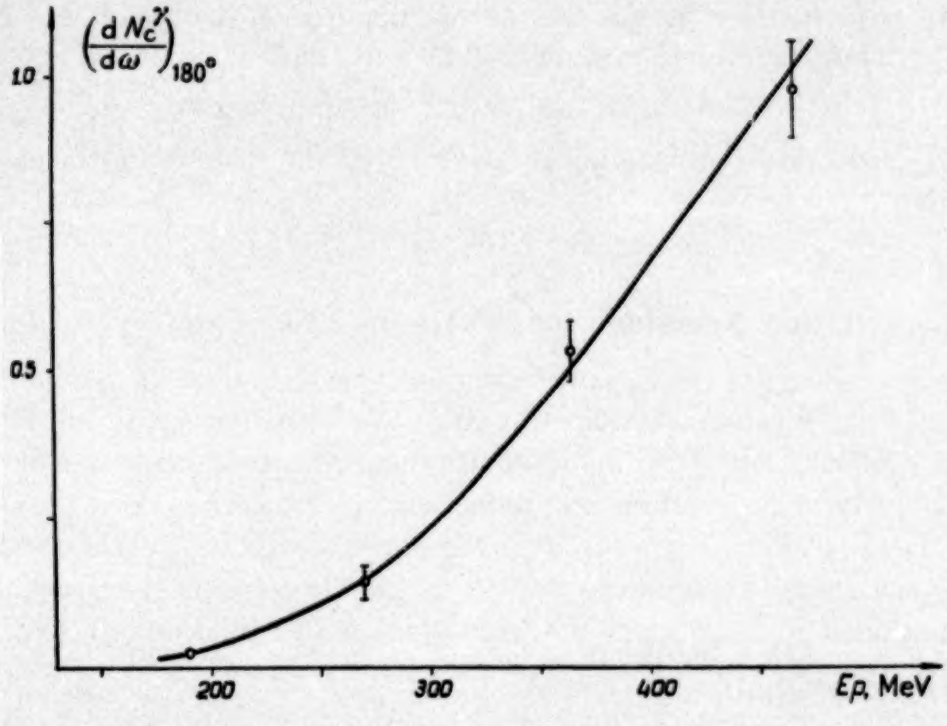

Fig. 10. Dependence of the yield of γ-quanta emitted from carbon nuclei at an angle of 180° on the proton energy.

340 MeV to 470 MeV the cross section is found to increase by fifty times. This increase corresponds to the dependence $\sigma_{pp}^{\pi^0} \propto p_{max}^{6\pm1}$. This type of momentum dependence of the cross sections can be explained by the prohibition of the most "intensive" transition which involves nucleons in the S final state and mesons in the p final state. On the other hand, transitions to other final states (for example P and p) correspond to a very strong momentum dependence of the cross section and to a small value of the cross section near the threshold. From our measurements performed at 470 and 660 MeV it can be seen that in the region of proton energies of 470—660 MeV the dependence on p_{max} can be represented in the following form

$$\sigma_{pp}^{\pi^0} \propto p_{max}^{4.5\pm0.5}.$$

7.3. p—n AND p—d CROSS SECTIONS

Comparison of our cross section value $\sigma_{pn}^{\pi^0}$ (660 MeV) with that for a proton energy of 340 MeV [18, 20], equal to $\sigma_{pn}^{\pi^0} = (0.23 \pm 0.08) \cdot 10^{-27}$ cm^2, shows that the cross section varies as follows

$$\frac{\sigma_{pn}^{\pi^0}\ (660)}{\sigma_{pn}^{\pi^0}\ (340)} = \left[\frac{p_{max}\ (660)}{p_{max}\ (340)}\right]^{3.2 \pm 0.4}.$$

(The cross section σ_{pn} presented here was obtained as the difference $\sigma_{pd} - \sigma_{pp}$.) This is consistent with the assumption that π^0-mesons are created in the p state, while the nucleons remain in the S state.

Measurements of the relative cross sections at 660 MeV yielded

$$\sigma_{pd}^{\pi^0}/\sigma_{pp}^{\pi^0} = (3.1 \pm 0.3).$$

If the coupling of nucleons in the deuteron is neglected

$$\sigma_{pn}^{\pi^0}/\sigma_{pp}^{\pi^0} = (2.1 \pm 0.3).$$

This value is in good agreement with the results obtained in ref. [21]).

8. Investigation of the Energy Spectra of γ-Quanta from the Decay of π^0-Mesons Produced by 660 MeV Protons

8.1. APPARATUS AND RESULTS

Measurements of γ-spectra from the decay of neutral mesons produced by 660 MeV protons on a graphite target at 0^0 and 180^0 were carried out in 1954—55 [22]). The measurements were performed by means of a 12 channel pair spectrometer. The construction of the spectrometer was similar to that described above. The only difference worth mentioning was a magnet with large pole pieces. This improvement broadened the measured energy range and increased the efficiency of the spectrometer. Thus, with pole pieces possessing an opening angle of 180^0 γ-quanta with an energy up to 200 MeV could be recorded, whereas with an opening angle of 90^0 quanta with an energy ranging from 100 to 600 MeV could be recorded. About $6 \cdot 10^4$ electron pairs were recorded in the spectrum measured at an angle of 0^0. The spectrum for 180^0 was constructed on the basis of energy measurements of $4 \cdot 10^4$ pairs. Fig. 11 presents the results of measurement of the γ-spectra at angles of 0^0 and 180^0 obtained by averaging the results of individual measurements in accord with their statistical weights.

The differential cross section for production of γ-quanta at an angle of 180^0 on a carbon nucleus by 660 MeV protons was found to equal in the laboratory system

$$\frac{d\sigma_C^{\gamma}}{d\omega}(180^0) = (1.5 \pm 0.2) \cdot 10^{-27}\ \text{cm}^2/\text{steradian}.$$

The ratio of the total γ-quanta fluxes at 0^0 and 180^0 amounts to 5.1 ± 0.3.

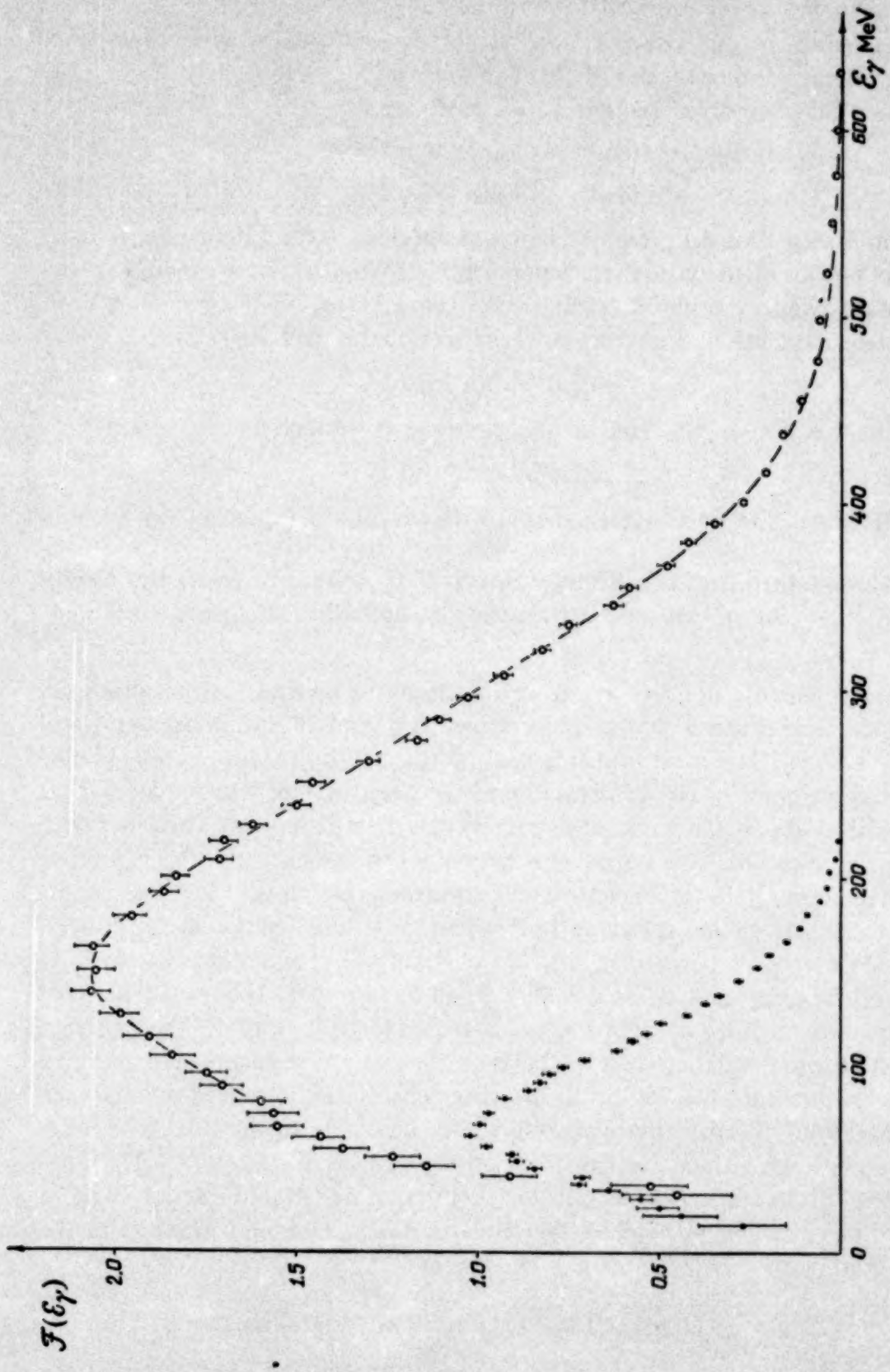

Fig. 11. Energy spectra of γ-quanta from decaying mesons produced by 660 MeV protons on carbon nuclei.
a. at an angle 0°; b. at an angle 180°.

8.2. DISCUSSION

The energy spectrum of π^0-mesons in an effective c.m.s. for a proton energy of 660 MeV is shown in fig. 12. The spectrum was calculated on the

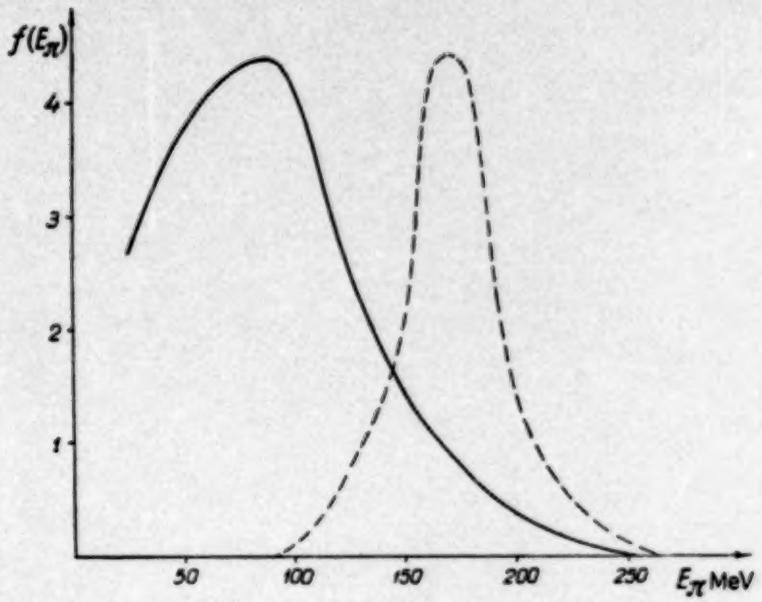

Fig. 12. Energy spectrum in the effective c.m.s. of π^0-mesons produced by 660 MeV protons on carbon nuclei. The dotted curve refers to the spectrum calculated in the impulse approximation on the assumption that the maximal possible energy is transferred to the mesons.

assumption of isotropic distribution of π^0 mesons in the hard part of the γ-spectrum ($\varepsilon_\gamma > \frac{1}{2}\varepsilon_0$), measured at 0^0 (represented by the smooth curve on fig. 11). The dotted curve represents the π^0-meson spectrum calculated in the impulse approximation. The calculation was performed on the assumption that the maximum available energy is transferred to the mesons thus produced.

A comparison of the calculated γ-spectra with the spectrum measured at an angle of 0^0 for 660 MeV protons (fig. 13) indicates that a satisfactory agreement is obtained if the angular distribution is $\varphi(\vartheta) = 1+0.4\cos^2\vartheta$. With account of the errors in measurment of γ-quanta spectrum, the constant b can be considered to equal 0.4 ± 0.2.

Whereas the spectrum of π^0-mesons produced by 470 MeV protons on a complex nucleus does not differ greatly from the spectrum calculated on the assumption that the mesons are always created with the maximum possible energy, there is a considerable difference between the experimental spectrum and the one calculated on the same assumptions for 660 MeV protons. In most cases π^0-mesons produced by 660 MeV protons possess energies which are considerably less than the maximum value. From this it follows that when π^0-mesons are formed by 660 MeV protons, the nucleons acquire a large kinetic energy in the final state, and consequently a large

relative momentum. This occurs, for example, if the final nucleons are in a P-state.

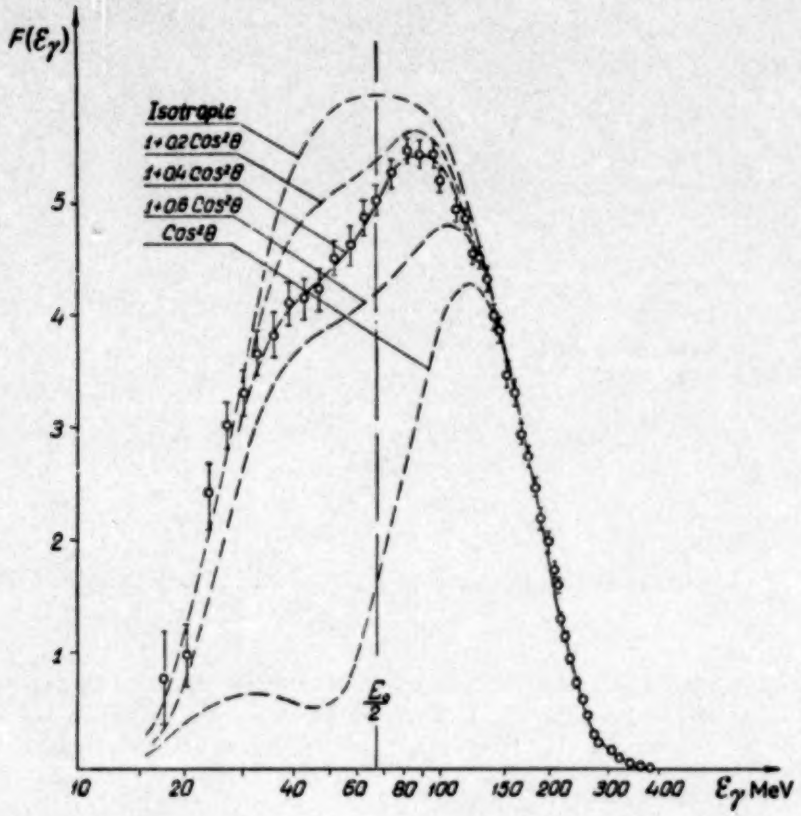

Fig. 13. Energy spectrum in the effective c.m.s. of γ-quanta from decaying π^0-mesons produced by 660 MeV protons on carbon nuclei. The dotted curves represent spectra computed on various assumptions regarding the magnitude of constant b in the angular distribution formula $\varphi(\vartheta) = 1 + b\cos^2\vartheta$.

8.3. DEPENDENCE ON MASS-NUMBER OF TARGET NUCLEUS

An appreciable difference in the γ-spectra produced on nuclei of light and heavy elements has not been found in experiments performed up to the present time. Thus in ref. [23]) it was reported that γ-spectra produced on carbon and tungsten nuclei by 340 MeV protons are practically identical. Also, no considerable difference in the γ-spectra was observed in our measurements in which carbon, copper, and lead targets were bombarded by 470 MeV protons (fig. 6). Likewise no difference was found between 150—450 MeV in the γ-spectra produced on carbon and copper nuclei by 660 MeV protons (these measurements were carried out in 1955).

The energy and angular distribution of γ-quanta are interconnected. Therefore in ref. [18]) the conclusion was drawn that since the energy spectra were identical the angular distribution of γ-quanta produced on light and heavy elements should also be identical. However, as already mentioned above, a sharp dependence of the angular distribution of γ-quanta on the

mass number of nuclei bombarded by 660 MeV protons was observed in ref. [11]). If the observed γ-radiation is considered to be the result of neutral meson decay, this difference in the γ-quanta angular distribution can be attributed to a change in the angular distribution of π^0-mesons produced on complex nuclei. On the other hand a sharp change in the π^0-meson angular distribution with increasing atomic weight of nuclear targets should result in a considerable difference in γ-quanta spectra produced on light and hevy nuclei. The difference in the angular distribution detected here is so considerable that its existence leaves no room for doubt. This fact seems difficult to reconcile with current views according to which the spectra of γ-rays produced on light and heavy nuclei are identical.

The variation of the angular distribution of γ-quanta with increase in the mass number of the bombarded nuclei can be satisfactorily explained by assuming that the nuclei are relatively opaque for protons and by taking into account meson absorption in the nuclei. Calculations conducted for this case show that γ-quanta spectra produced on light and heavy elements substantially differ only in the low energy region ($\varepsilon_\gamma < 70$ MeV). However, it is exactly in this energy region that the spectrometer has a relative low efficiency, while the random coincidences background due to negatons and positons from γ-quanta of higher energies is large. Therefore the absence of a difference in the γ-spectra in the low energy region cannot be considered a reliably established experimental fact †.

9. Summary

The results obtained in our series of papers discussed above permit us to draw the following conclusions regarding the process of π^0-meson production by high energy nucleons.

1. Neutral π-mesons are created on complex nuclei in collisions of incident proton with separate nucleons in the nucleus but not with the nucleus as a whole.

2. At a proton energy of 470 MeV the π^0-mesons produced on a complex nucleus are mainly emitted at small angles with respect to the direction of collision of the nucleons.

A term proportional to $\cos^2\vartheta$ plays a significant role in the angular distribution of π^0-mesons.

3. No difference in the energy spectra of γ-quanta created on light and heavy elements was found. Identity of the spectra can be considered established only for high energy γ-quanta.

4. With the rise of the proton energy to 660 MeV the increase of the cross section for π^0-meson production in collisions of two protons substantially

† *Note added in the proof:* A difference of this kind can be observed in ref. [24]).

slows down in comparison with the rapid increase of this cross section observed in the energy region lying below 470 MeV.

5. π^0-mesons are mostly produced on the surface of complex nuclei bombarded by 660 MeV protons. This effect for heavy and average nuclei can be explained by meson absorption and proton scattering in the nucleus.

6. The angular distribution of γ-quanta produced in π^0-meson decay greatly depends on the mass number of the incident nucleus. With increase of mass number the angular distribution of γ-quanta becomes more isotropic in the c.m. system. For protons this effect can be partly explained by nuclear screening in the presence of strong meson absorption and, to a less extent, by meson scattering in the nuclei.

7. From the dependence of the angular distribution of γ-quanta on mass number found by us it can be inferred that the energy spectra of γ-quanta from the decay of π^0-mesons produced on light and heavy elements should considerably differ in the low energy region of γ-quanta. This difference in the spectra had not been discovered in previous work perhaps because of lack of precise measurements of γ-spectra in the low energy region.

8. The γ-spectrum for 660 MeV protons is only slightly shifted towards high energies with respect to the spectrum from 470 MeV protons. This can be explained by a decrease in the number of π^0-mesons which are produced with energies near to the maximum possible value.

9. The anisotropy if the π^0-meson angular distribution in the centre of mass system of the colliding nucleons is lower at 660 MeV than at 470 MeV.

We wish to express our deep gratitude to A. M. Sinayev and M. M. Kulyukin for their considerable assistance in the development of the equipment.

References

1) M. S. Kozodayev and A. A. Markov, Report of the Institute for Nuclear Problems (Academy of Sciences of the USSR) for the first half of 1950
2) R. Bjorklund, W. Crandall, B. Moyer and R. York, Phys. Rev. **77** (1950) 213
3) J. Steinberger, W. Panofsky and J. Steller, Phys. Rev. **78** (1950) 802
4) M. S. Kozodayev, A. A. Tyapkin, A. A. Markov and Yu. D. Bayukov, Report of the Institute for Nuclear Problems (Academy of Sciences of the USSR) for 1952
5) Yu. D. Bayukov, M. S. Kozodayev, A. A. Markov, A. N. Sinayev and A. A. Tyapkin, Report of the Institute for Nuclear Problems (Academy of Sciences of the USSR) for 1955
6) W. Crandall and B. Moyer, Phys. Rev. **92** (1953) 749
7) J. Marshall, L. Marshall, V. Nedzel and S. Warshaw, Phys. Rev. **88** (1952) 632
8) M. S. Kozodayev, A. A. Tyapkin and R. A. Wanezian, Report of the Institute for Nuclear Problems (Academy of Sciences of the USSR) for 1952
9) K. Brueckner, R. Serber and K. Watson, Phys. Rev. **84** (1951) 258
10) B. Pontecorvo, G. I. Selivanov and B. A. Zukov, Report of the Institute for Nuclear Problems (Academy of Sciences of the USSR) for 1952
11) A. A. Tyapkin, M. S. Kozodayev and Yu. D. Prokoshkin, Dokl. Akad. Nauk SSSR, **100** (1955) 689

12) H. Davis, H. Bethe and L. Maximon, Phys. Rev. **93** (1954) 788
13) J. Perry and C. Angell, Phys. Rev. **91** (1953) 1289
14) D. Bodansky, A. Sachs and J. Steinberger, Phys. Rev. **90** (1953) 997
15) R. Littauer and D. Walker, Phys. Rev. **86** (1952) 838
16) S. Butler, Phys. Rev. **87** (1952) 1117
17) R. Littauer and D. Walker, Bull. Am. Phys. Soc. **26** (1951) 15
18) R. Hales and B. Moyer, Phys. Rev. **89** (1953) 1047
19) M. S. Kozodayev, Yu. D. Prokoshkin and A. A. Tyapkin, Report of the Institute for Nuclear Problems (Academy of Sciences of the USSR) for 1954
20) J. Mather and E. Martinelli, Phys. Rev. **92** (1953) 780
21) B. D. Balashov, V. A. Zukov, B. Pontecorvo and G. I. Selivanov, Report of the Institute for Nuclear Problems (Academy of Sciences of the USSR) for 1954
22) Yu. D. Bayukov, M. S. Kozodayev and A. A. Tyapkin, Report of the Institute for Nuclear Problems (Academy of Sciences of the USSR) for 1954
23) K. Crowe, W. Panofsky, R. Phillips and D. Walker, Phys. Rev. **83** (1951) 893
24) Yu. D. Bayukov, A. N. Sinayev and A. A. Tyapkin, JETP **32** (1957) 385

Nuclear Physics **4** (1957) 88—90; © *North-Holland Publishing Co., Amsterdam*
Not to be reproduced by photoprint or microfilm without written permission from the publisher

OPTICAL MODEL ANALYSIS OF PROTON SCATTERING ON SOME LIGHT NUCLEI

ANWAR HOSSAIN AND SYEDUZZAMAN†
Physics Department, Dacca University, Pakistan

Received 1 March 1957

The scattering of 9.5 MeV protons by He^4, N^{14} and A^{40} has been studied by Freemantle *et al.* [1]). The angular distribution has been discussed from

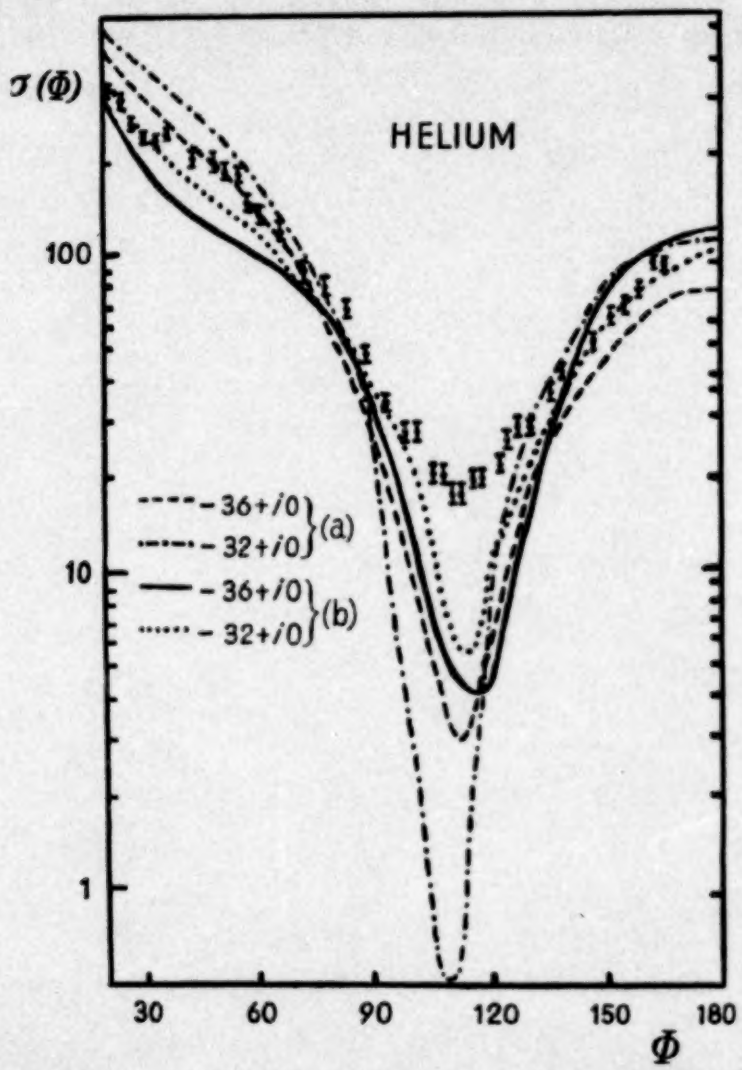

Fig. 1. Experimental and theoretical cross-section for 9.5 MeV protons elastically scattered by He^4. The differential cross-section is given in millibarns/steradian; ϕ is the scattering angle in the c.m. system. The potentials used are
(a) $-(32+i0)$ and $-(36+i0)$ MeV with $R = 1.45\ A^{1/3} \times 10^{-13}$ cm,
(b) $-(32+i0)$ and $-(36+i0)$ MeV with $R = (0.6+1.26A^{1/3}) \times 10^{-13}$ cm.

† Abstract by the Editor of a paper submitted by the authors.

the point of view of the optical model by Burge, Fujimoto and Hossain [2]), using a square well of radius $R = r_0 A^{1/3}$ with values of r_0 of the order 1.45×10^{-13} cm. The details of the assumptions about the depths of the real and imaginary part of the potentials and the exact value of r_0 are given in the captions of fig. 1, 2, 3, which reproduce the empirical data and the theoretical curves.

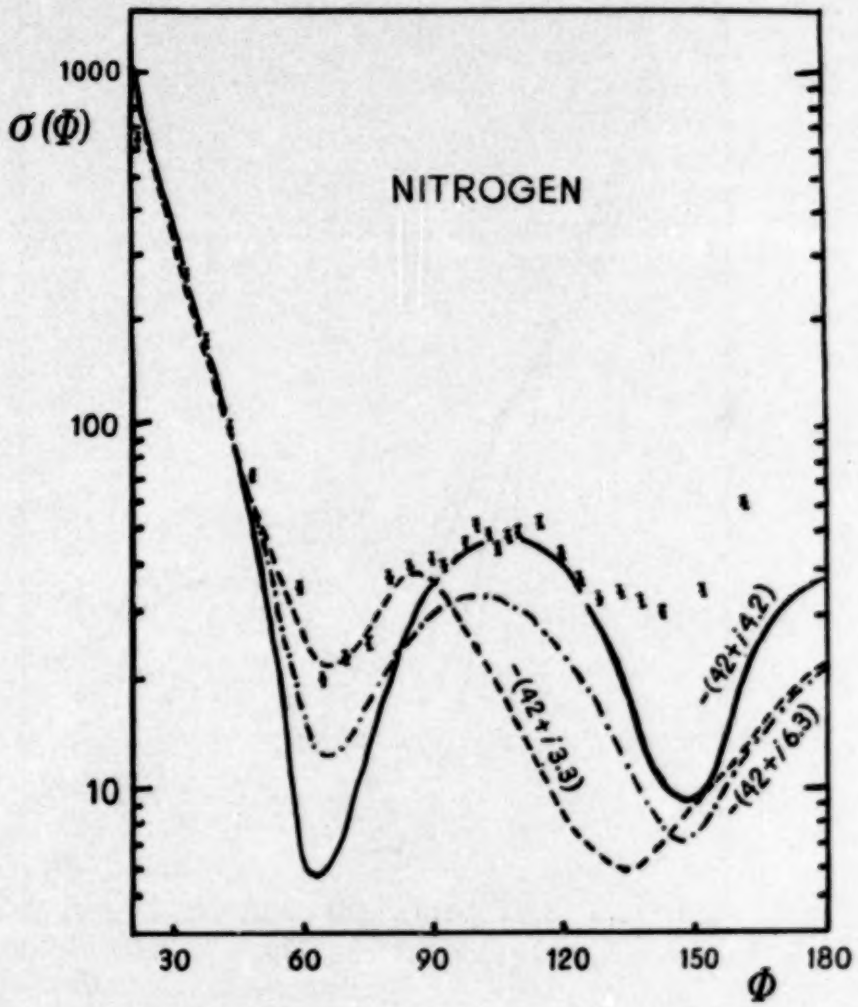

Fig. 2. Experimental and theoretical cross-section for 9.5 MeV protons elastically scattered protons by N^{14}. The potentials used are
$-(42+i6.3)$ and $-(42+i4.2)$ MeV with $R = 1.47A^{1/3} \times 10^{-13}$ cm,
$-(42+i3.3)$ MeV with $R = (0.6+1.26A^{1/3}) \times 10^{-13}$ cm.

Following a suggestion of Professor Weisskopf, new calculations were carried out with a view to ascertaining in how far the fit could be improved by taking for the nuclear radius a value of the form $R = a+r_1 A^{1/3}$. More specifically, the formula $R = (0.6+1.26A^{1/3}) \times 10^{-13}$ cm was used. The figures (the captions of which indicate the assumption about potential depths) show that (1) in the case of He^4 a slight improvement is obtained;

(2) for N^{14} the new value of the radius leads to a poorer fit than the previous one; (3) for A^{40} on the other hand, a much better fit is obtained.

These results suggest that a further amelioration of the fit will necessitate taking into account the shape of the well at the nuclear boundary and including a spin-orbit coupling term in the nuclear potential.

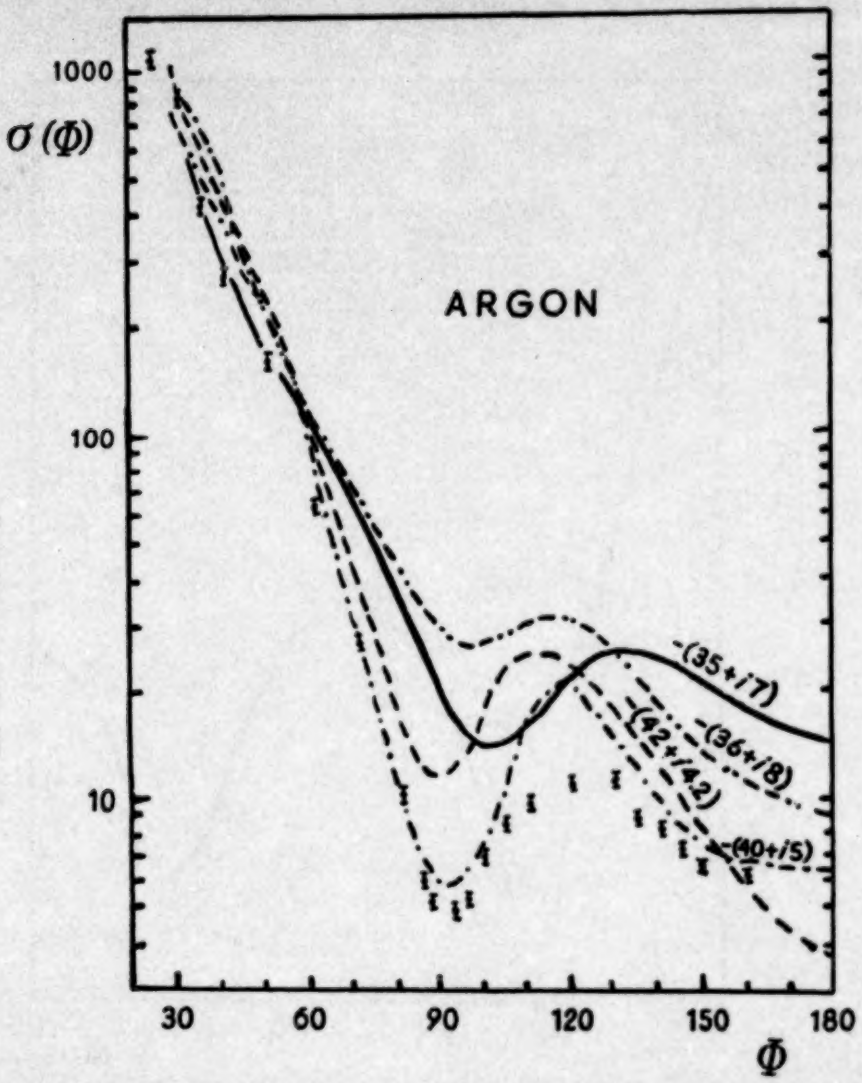

Fig. 3. Experimental and theoretical cross-section for 9.5 MeV protons elastically scattered by A^{40}. The potentials used are
$-(35+i7)$ and $-(42+i4.2)$ MeV with $R = 1.4A^{1/3}\times 10^{-13}$ cm,
$-(36+i8)$ and $-(40+i5)$ MeV with $R = (0.6+1.26\ A^{1/3})\times 10^{-13}$ cm.

We are thankful to Dr. M. Innas Ali for helpful discussion and to Mrs. R. Hossain for making the drawings.

References

1) Freemantle, Grotdal, Gibson, McKeague, Prowse and Rotblat, Phil. Mag. **45** (1954) 1090
Freemantle, Prowse and Rotblat, Phys. Rev. **96** (1954) 1268
Freemantle, Prowse, Hossain and Rotblat, Phys. Rev. **96** (1954) 1270
2) Burge, Fujimoto and Hossain, Phil. Mag. **1** (1956) 19

Nuclear Physics **4** (1957) 91—111; © *North-Holland Publishing Co., Amsterdam*
Not to be reproduced by photoprint or microfilm without written permission from the publisher

SOFT γ-RAYS FROM THE CAPTURE OF THERMAL NEUTRONS BY NUCLEI

I. V. ESTULIN, L. F. KALINKIN AND A. S. MELIORANSKY
Moscow State University

Received 21 February 1957

Abstract: A luminescent spectrometer was used to measure the energies and absolute intensities of the γ-quanta emitted by Co^{59}, Rh^{103}, I^{127}, Sm^{149}, Au^{197} and Hg^{199} nuclei following the capture of thermal neutrons. It is shown that the γ-lines in the 50—500 keV energy range detected in the present work can be ascribed to transition from the lower excited states of the investigated nuclei. A description of the apparatus and method of measurement is presented.

1. Introduction

In recent years the γ-radiation from the (n, γ) reaction has been investigated quite intensively. The most valuable results have been obtained with magnetic spectrometers. High energy ($E_\gamma > 3$MeV) γ-rays have been successfully investigated with a pair spectrometer [1]). By employing a magnetic spectrometer which analyzes Compton electrons it has been possible to extend the range of reliable γ-ray energy measurements down to 250 keV [2]). Softer radiations have been studied less extensively. The soft γ-line energy values cited in ref. [3, 4, 5]) should be checked; the intensities of these lines have not been determined up to the present.

A single crystal luminescent spectrometer was employed in the present work to measure the energies and absolute yields of γ-quanta (in the 50—500 keV energy range) emitted by nuclei after capture of thermal neutrons. Some preliminary results have been reported in an earlier communication [6]).

2. Geometrical Conditions of the Experiment and the Luminescent Spectrometer

The neutron source was an experimental heavy water physical reactor [7]). The neutron collimator which consisted of thick B_4C and Pb layers was mounted inside a horizontal channel in the reactor shield. A Bi layer 12 cm thick in immediate contact with the reactor reservoir shielded the neutron collimator channel from γ-rays of the reactor. The intensity of the collimated thermal neutron beam from the reactor incident on the target was approximately 10^7 neutrons/cm^2 sec.

The geometrical conditions of the experiment are shown in fig. 1. Target 1

which in most experiments had the shape of an ellipse with semi axes $a = 18$ mm and $b = 10$ mm was mounted on an aluminium support at an

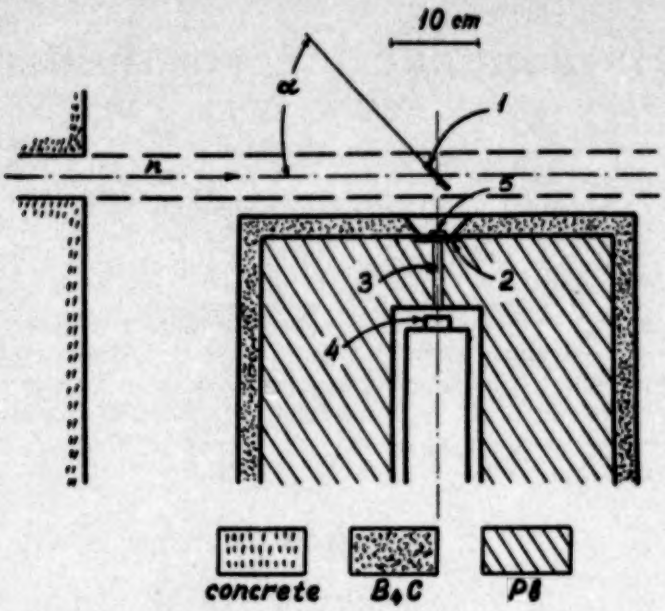

Fig. 1. Geometry of the measurements
1. target 2. B_4C shield 3. channel of γ-ray collimator 4. NaI(Tl) crystal 5. lead filter

angle α with respect to the neutron beam. The target was situated above channel (3) in lead which served as the γ-ray collimator (channel length 75 mm, diameter 10—15 mm). The entrance slit of the γ-ray collimator was covered with B_4C (2), 0.3 g/cm^2 thick which shielded the NaI(Tl) crystal, (4), from the thermal neutrons. In the Co, Rh and Au investigations metallic targets were employed. Powdered substances were enclosed in a thin, 0.07 mm thick, aluminium envelope which did not emit gamma rays of appreciable intensity under the action of the neutrons.

A cylindrical NaI(Tl) crystal 9 mm long and 28 mm in diameter enclosed in a MgO reflector was used in the luminescent spectrometer. Pulses up to 0.5 volt from the photomultiplier were amplified to 100 volt and analyzed in a single-channel pulse height analyzer with a dead time of 3μ sec.

The resolving power, line shape and absolute efficiency of the spectrometer as a function of γ-quantum energy were studied in experiments with Mo^{99}, Hg^{203}, B^{10} (n, α), Li^{7*}, Cu^{64}, Cs^{137} and Zn^{65}. The geometry in these experiments was similar to that which was employed in measurements of the energy and intensity of γ-rays from the (n, γ) reaction. The dependence of the resolving power of the spectrometer (η) on the γ-quantum energy (E_γ) can be expressed by the relation

$$\eta = \frac{186}{\sqrt{E_\gamma}} + 2.5 \qquad (1)$$

where E_γ is in keV and η in %. The pulse height spectrum produced by γ-rays from the B^{10} (n, α) Li^{7*} reaction (B_4C target in neutron beam) is shown in fig. 2. The photo peak from 482 keV γ-quanta, the peak (3) due

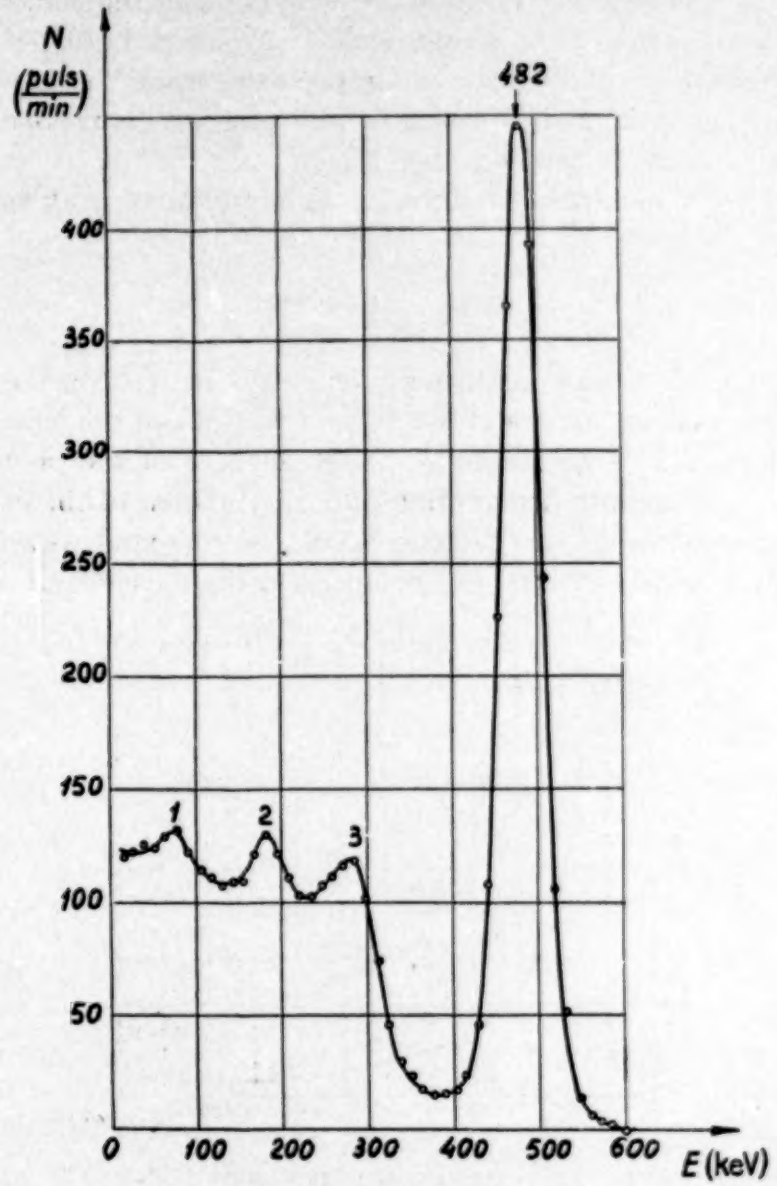

Fig. 2. Pulse height spectrum due to γ-rays from the B^{10} (n, α) Li^{7*} reaction.

to the maximum in the Compton electron energy distribution and also apparatus peaks (1) and (2) due to the characteristic radiations from lead and to γ-rays which passed through the NaI(Tl) crystal and were scattered back into the apparatus, can all be distinctly seen. Similar spectra were obtained with other γ-ray sources but the positions and relative heights of peaks 1, 2, 3 and the photo peak were found to appreciably depend on the γ-ray energy. Graphs plotted on basis of the experimental data permit

one, if the position and height of the photo peak are known, to reconstruct the remaining part of the pulse spectra produced by a monochromatic beam of γ-quanta. It was thus possible to analyze the pulse spectra produced by γ-rays of complex composition by singling out the individual lines. In this case the area of the photo peak (S_{ph}) could be determined with greatest precision, a "photo peak" in the pulse spectrum from monochromatic γ-quanta being defined as a peak whose position corresponds to pulses of maximal amplitude (see e.g. fig. 2).

It will be convenient to introduce the absolute photo peak spectrometer efficiency

$$\varepsilon = \frac{S_{ph}}{S_{tot}} (1 - e^{-\mu x}) \qquad (2)$$

where μ is the absorption coefficient for γ-rays in the NaI(Tl) crystal, x is the thickness of the latter and S_{tot} is the total area of the pulse spectrum. The total area $S_{tot} = S_{ph} + S_c + S_{es}$. S_{ph} is the area of the photo peak, S_c the area of the Compton distribution and S_{es} the area of the escape peak. The experimental values of the ratio S_{ph}/S_{tot} were found as a function of γ-ray energy (curve 2, fig. 3). For comparison the dependence of the ratio

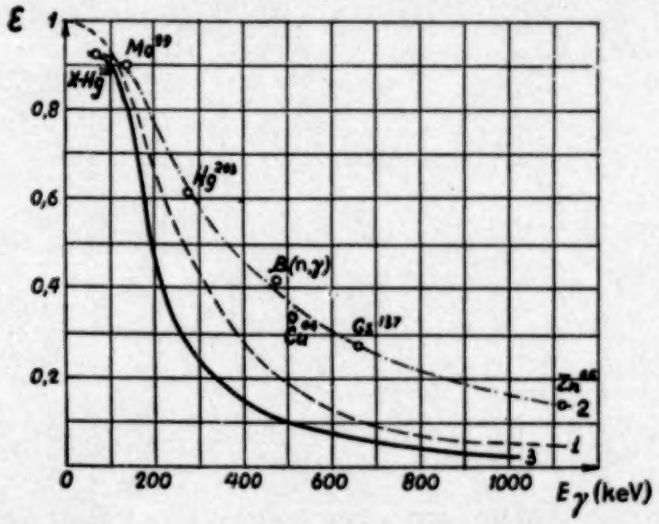

Fig. 3. Spectrometer efficiency ε as function of γ-ray energy, E_γ (curve 3).
Curve 2 — experimental values of the ratio S_{ph}/S_{tot}.
Curve 1 — dependence of $\sigma_{ph}/\sigma_{ph}+\sigma_c$ on E_γ.

$\sigma_{ph}/\sigma_{ph}+\sigma_c$ on energy for the NaI crystal is shown in curve 1 (σ_{ph} and σ_c are the cross sections for photoelectric absorption and Compton scattering of γ-quanta). The discrepancy between curves 1 and 2 results from absorption in the NaI crystal of secondary γ-rays produced as a result of Compton scattering in the crystal. For γ-quanta with-energies $E_\gamma < 100$ keV the effect produced by escape X-rays from the crystal becomes important. The spectrometer efficiency ε (curve 3, fig. 3) was determined from

relation (2) with account of experimental curve 2. The spectrometer is not very effective for hard γ-radiation and can therefore be employed to measure soft γ-radiation with $E_\gamma < 500$ keV even in the presence of more energetic γ-rays.

3. Method of Measurement of γ-Spectra

The pulse height spectrum observed with the target in the neutron beam was measured for a freely propagating neutron beam (N_0) and for a beam with a boron carbide layer 0.3 g/cm² thick placed across the exit of the neutron collimator (N_1); this layer absorbed thermal neutrons but did not change the fast neutron or γ-quanta flux. N_1 did not practically depend on the presence of the target in the beam. The thermal neutron effect is given by the difference of the counting rate $N = N_0 - N_1$. In the absence of the target N was very small. For most of the targets the integral counting rate did not exceed 2500 c.p.s. when N_1 was $\approx$ 700 c.p.s. If a thick B_4C layer which absorbed thermal and fast neutrons was placed across the neutron beam the counting rate decreased to 300 c.p.s.

Compton scattering of γ-quanta led to a certain broadening of the photopeaks if thick targets were used and therefore only thin targets were employed. Even then, however, the photopeaks were sometimes found to be broad due to some instability of the spectrometer. Results of measurements with a Co_2O_3 target are shown in fig. 4 to illustrate the pulse height distri-

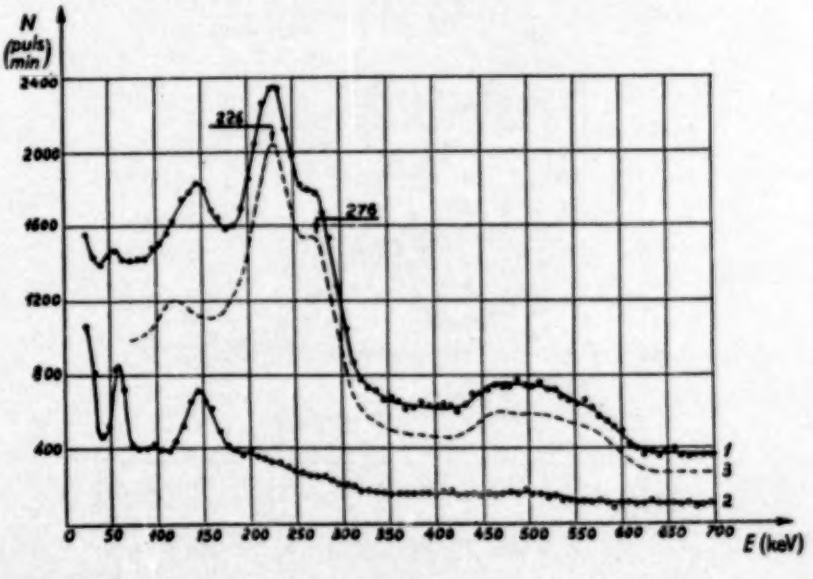

Fig. 4. Pulse height spectrum for Co_2O_3

1. neutron beam open (N_0) 2. B_4C across neutron beam (N_1) 3. effect $N = N_0 - N_1$.

bution obtained by measuring N_0 and N_1. The upper curve, (1), is the pulse spectrum for a free neutron beam (N_0) and curve 2 is the same for a neutron

beam with B_4C interposed (N_1); dotted line (3) is the thermal neutron effect (N). Peaks at energies of about 40—60 keV and 140 keV and a small rise at 480 keV due to radiation from the boron spectrometer shield were observed in the pulse spectrum from the neutron beam with B_4C interposed (curve 2). Because of the peaks in curve 2 it is somewhat more difficult to identify the low intensity γ-lines located near these peaks. The maximum at 140 keV is due to neutron absorption in the NaI(Tl) crystal (γ-rays from the I (n, γ) reaction [6]). A diffuse maximum at 450—550 keV (fig. 4) mainly due to γ-radiation from the boron shield and to annihilation radiation can be seen in the pulse spectrum produced by γ-rays following the capture of neutrons by the target nuclei. The target not only absorbed thermal neutrons but scattered them as well. It was shown in a control experiment that when γ-rays were measured with B_4C in the collimator (2 in fig. 1) the correction to account for the effect from neutrons scattered in the thin targets employed in the investigation was insignificant compared with the effect produced by neutrons captured in the target.

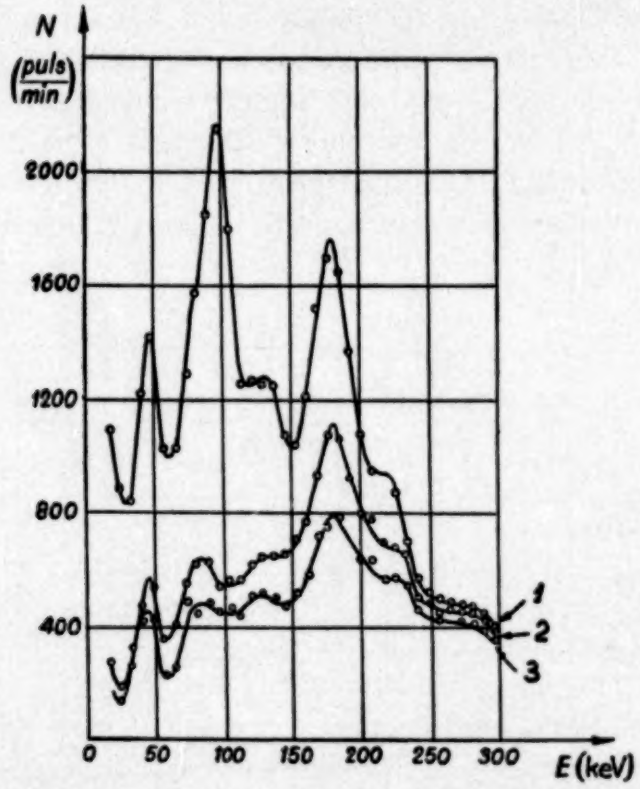

Fig. 5. Pulse height spectrum for Rh
1. without lead filter 2. 0.5 mm Pb 3. 1.0 mm Pb.

Photopeaks from soft γ-rays can be discerned on the pulse "pedestal" produced by penetrating γ-quanta and this circumstance reduces the precision of determination of photopeak areas performed with the purpose

of measurement of the absolute γ-ray intensity. In order to reduce the aforementioned "pedestal" and also in order to separate with greater reliability the apparatus peaks from photopeaks due to γ-quanta emitted by the target we carried out measurements with 0.532—2.55 g/cm² lead filters placed in the γ-ray collimator. For illustration we present in fig. 5 the results of measurements carried out with Rh. Upper curve (1) is the pulse spectrum obtained in experiments without a lead filter, curve 2 with a 0.532 g/cm² Pb filter and curve 3 with a 1.01 g/cm² Pb filter. The peaks at 45, 70 and 135 keV remain in the lead filter measurements and are thus produced by the apparatus. The pulse spectrum of γ-quanta absorbed in the lead filters was used to treat the results of the measurements. In order to determine the number of γ-quanta per captured neutron solid angle of the target relative to the NaI(Tl) crystal and also the neutron flux must be known. An independent determination of these quantities would be a source of new errors. In order to exclude such errors we compared the area of the unknown photopeak $(S_{ph})_\gamma$ with the area of the photopeak from 482 keV γ-quanta $(S_{ph})_B$; the latter quantity was found in measurements with a B_4C target whose shape was identical with that of the investigated substance. The target of the investigated isotope was replaced by a B_4C target which was thus bombarded by the thermal neutrons; the thickness of this target was sufficient to ensure practically total absorption of the thermal neutrons.

Thus

$$\frac{(S_{ph})_\gamma}{(S_{ph})_B} = \frac{n_\gamma}{n_B} \cdot \frac{\varepsilon_\gamma}{\varepsilon_B} \cdot \frac{k_\gamma}{k_B} \cdot \sigma_{cap} \frac{pL}{A} \cdot \varkappa. \tag{3}$$

In relation (3) n_γ is the unknown number of γ-quanta emitted per captured neutron, n_B is the same quantity for the $B^{10}(n, \alpha)\,Li^{7*}$ reaction ($n_B = 0.93$) and k_γ and k_B are corrections which account for absorption of the γ-quanta between the target and NaI(Tl) crystal. The quantity $\sigma_{cap}\, pL/A$ is the probability of neutron capture by target nuclei (σ_{cap} is the neutron capture cross scetion, p the target weight, L the Avogadro number and A the molecular weight). The factor $\varkappa$ accounts for absorption of neutrons and γ-quanta in a target of thickness l:

$$\varkappa = \frac{1 - e^{-(\mu_n + \mu_\gamma \cdot \operatorname{tg}\alpha) \cdot l/\sin\alpha}}{(\mu_n + \mu_\gamma \cdot \operatorname{tg}\alpha) \cdot l/\sin\alpha} \tag{4}$$

where μ_n and μ_γ are the absorption coefficients for neutrons and γ-quanta and α is the angle of inclination of the target relative to the direction of the neutron beam (fig. 1).

4. Results of the Measurements

4.1. COBALT

In the cobalt experiments targets made of powdered cobalt oxide (6.94 g-weight) and metallic cobalt (2.21 g-weight) were used. The cobalt oxide powder was packed in an aluminium foil envelope of cylindrical shape. The metallic target had the shape of an ellipse. A knowledge of the impurities in the targets permitted us to draw the conclusion that practically all neutron capture γ-rays from the target were due to capture by the Co^{59} nuclei. Two peaks at 226 ± 4 and 276 ± 4 keV which were not completely resolved could be discerned in the target pulse spectrum and were interpreted as photopeaks due to γ-quanta of the respective energies. It is possible that cobalt γ-ray peaks with an energy of several per cent exist in the 450—550 keV energy range. Auxiliary absorption experiments of γ-rays in lead filters revealed a small peak at 120 keV which was not related to the cobalt radiation and was of an apparatus origin. Four independent sets of spectrum measurements for cobalt γ-rays absorbed by a 2.02 g/cm^2 lead filter were performed — two with a colbalt oxide target and two with a metallic target. These measurements were carried out in conjunction with measurements on the area of the photopeak for a boron carbide target. The intensities of the γ-lines were ascertained in this way and found to equal $n_{226}=(23\pm4)\%$ and $n_{276}=(23\pm4)\%$. The capture cross section of cobalt was assumed to be 35.4 barns.

The γ-transition energies found in the present investigation are close to those quoted in ref. [3]) (220 keV) and agree with those in ref. [4]) (237 keV and 289 keV) obtained by luminescent spectrometer measurements of γ-rays from the Co (n, γ) reaction. Energies of excited Co^{60} nuclear levels were obtained by measuring the high energy γ-rays from the Co (n, γ) reaction [8]) and the energy of proton groups from the Co (d, p) reaction [9]); the respective excitation energy values were found to be in good agreement and the lowest values are shown in fig. 6. Gamma transition energies close to the γ-line energies found by us, are shown in fig. 6. Various combinations of transitions can explain the observed γ-lines. The only improbable case is that of cascade transitions containing only one of the two γ-rays of approximately 280 keV or 220—230 keV energy. Indeed, for $n_{226}=n_{276}$ one would be compelled, for no other special reason of doing so, to assume that transitions to intermediate cascade levels are prohibited. In view of the comparatively high intensity of the γ-lines detected by us it seems more probable that the corresponding transitions take place between the two lowest levels of Co^{60}, i.e., from the 280 keV level to the ground or isomeric levels, whereas the remaining possible transitions of the same energies weakly contribute to the intensities n_{226} and n_{276} (this assumption is not inconsistent with the

activation cross sections for the ground and isomeric states of Co^{60}). In this case some assumptions concerning the spin and parity of the 280 keV level can be made. Since the probabilities of transition from the 280 keV

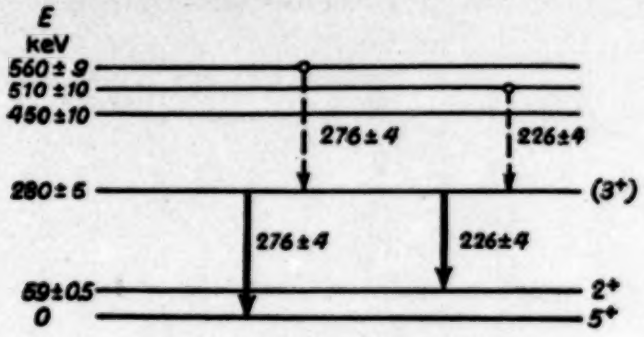

Fig. 6. Lower energy levels of Co^{60}.

level to the isomeric level or ground state are equal one may assume the spin of the 280 keV level equal either to 3 or 4, since the ground and isomeric states are respectively 5^+ and 2^+ [10]). Comparison of the results obtained in ref. [8]) and [9]) leads one to the conclusion that no transition of detectable intensity takes place from the capturing state of Co^{60} to the isomeric state. This fact indicates that the capturing state of Co^{60} is 4^- but not 3^- (the ground state of Co^{59} is $7/2^-$). The intensities of transition from the capturing state Co^{60} to the ground state or to the 280 keV level are approximately the same and equal to 3 % and 4 % respectively [8]). Since the ground state transition is of the E1 type the transition to the 280 keV level would also be expected to be of the E1 type that is, the parity of this level should be positive. The value $I = 3$ seems to be the more preferable of the two possible values for the angular momentum of the 280 keV level. In this case transition to an isomeric level of lower energy should be M1, whereas a higher energy transition to the ground state would be E2.

4.2. RHODIUM

The rhodium target was an ellipse-shaped plate 0.1 mm thick and 0.669g in weight. Rhodium has only one stable isotope, Rh^{103}, and therefore γ-rays from the radiative capture of neutrons should be ascribed to Rh^{104}. The energy range up to 300 keV was investigated in detail in the present work. The pulse height distributions due to Rh^{104} γ-rays in the absence of a lead filter and in the presence of 0.532 g/cm^2 and 1.01 g/cm^2 filters are shown in fig. 5. The pulse spectrum produced by γ-rays absorbed in a 1.01 g/cm^2 filter is shown in fig. 7. By resolving this spectrum into its components it was possible to determine the area of those photopeaks which, according to γ-ray absorption experiments, could be identified with the radiation from the target. The same procedure was applied to the pulse spectrum from

rays absorbed in a 0.532 g/cm² filter. The energies and absolute intensities of the γ-lines were found to be $E_1 = 96 \pm 4$ keV, $E_2 = 133 \pm 3$ keV, $E_3 = 176 \pm 3$ keV, $E_4 = 217 \pm 4$ keV and correspondingly $n_1 = 17$ %, $n_2 \leqq 8$ %, $n_3 = 19$ %, $n_4 = 9$ %. The capture cross section of rhodium was assumed to be 150 barns.

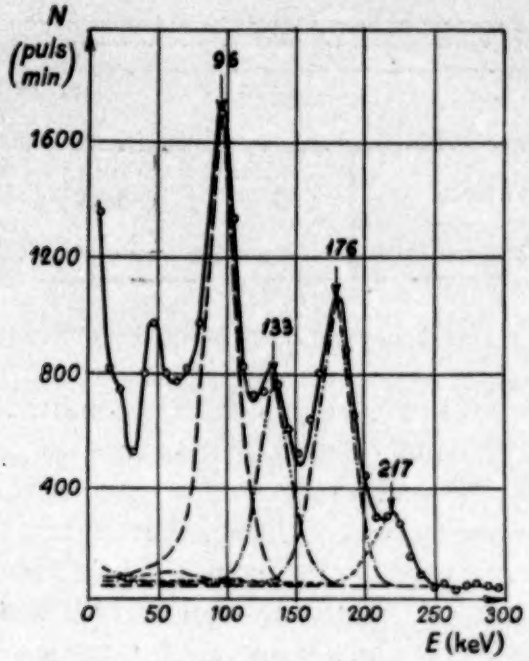

Fig. 7. Pulse height spectrum of γ-rays from Rh (n, γ) absorbed in 1.01 g/cm² lead filter.

The relative error in determination of $n_1 - n_4$ was 15—20 %. Only the upper intensity limit is shown for the 133 keV γ-line as in this energy region a peak occurs in the background (fig. 4) which is not fully excluded if the difference between the readings obtained with and without the B_4C layer in the neutron beam is taken.

γ-rays of 80 and 160 keV energy detected in the study of γ-rays from radiative capture of neutrons in Rh nuclei [3]) were mistakenly interpreted as indicating activation of the target since no such radiation had been observed in the disintegration of Rh^{104} isomers [11]). Apparently the most intense of the γ-rays recorded by us were observed in ref. [3]). From measurements of high energy γ-rays from the Rh (n, γ) reaction performed in ref. [12]) one can determine the energies of the lower levels of the Rh^{104} nucleus. The character of the ground and first two excited levels has been deduced from β-disintegration data for Rh^{104} [11]). It should be noted that the absence of γ-transitions from the capturing state to the first excited level [12]) can be explained only if the capturing state of Rh^{104} is 0^- and the first excited state 2^+. The arguments on basis of which $I = 1$ was assigned to the capturing state in ref. [12]) seem to require reexamination.

The γ-line energies obtained in the present investigation do not seem to be

consistent with the level scheme deduced in ref. [11, 12]) (fig. 8, solid lines). If an additional level at ≈ 230 keV is assumed to exist these γ-lines can be fitted into the scheme as shown by the dotted lines in fig. 8. However, in this case a discrepancy arises which exceeds the experimental errors,

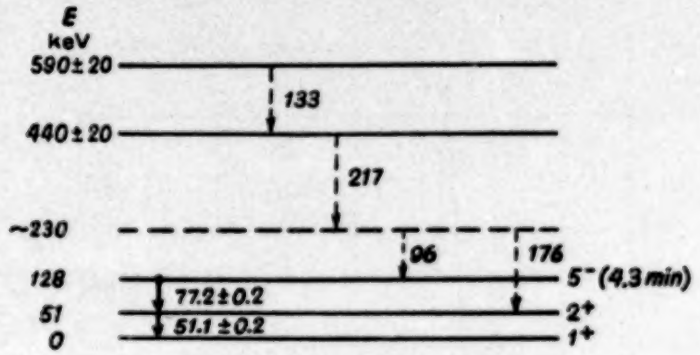

Fig. 8. Lower energy levels of Rh^{104}.

namely, the intensity of the 96 keV isomeric γ-transition (17±3) % does not agree with the probability of activation of the 4.3 minute Rh^{104} isomer (8±3) %. Moreover, it seems difficult to reconcile the approximately equal intensities of the 96 keV and 176 keV γ-lines with the probabilities of the radiative transitions if the values of the angular momenta and parities of the first and second excited levels of Rh^{104} indicated in fig. 8 are accepted. When the most suitable character (3^-) is assigned to the introduced level, transitions involving the aforementioned energies will be respectively of the E2 and M2 types. The ratio of the probabilities for these transitions computed from the Weisskopf formula is ≈ 5. The energies of the observed γ-lines can be satisfactorily fitted into the Rh^{104} level scheme if two additional levels are introduced. However the possible energies of these levels cannot be prescribed uniquely.

4.3. IODINE

A target of pure iodine powder was used (weight 3.96 g.). An intense γ-line of 135±3 keV energy [6]) which hitherto had not been observed in investigations of other authors [3, 4]) could be discerned in the pulse spectrum of γ-rays from the I^{127} (n, γ) I^{128} reaction. The photopeak from the 135 keV γ-line can be distinctly seen in fig. 9 which represents the results of one of the experiments with an I target. Low intensity γ-lines in the vicinity of 255 keV may exist [4]). The disagreement with the data of ref. [4]) evidently can be explained by the fact that in the latter investigation no measures were taken to shield the crystal of the luminescent spectrometer from neutrons scattered from the target whereas the neutron scattering cross section in iodine is comparable with that of the capture cross section. In experiments

carried out with any type of target and without B_4C in the γ-ray collimator (2 on fig. 1) only peaks at 85, 135 and 255 keV were observed in the pulse spectrum. It is probably that just because of this the author of ref. [4]) attributed the 135 keV γ-quanta to the background.

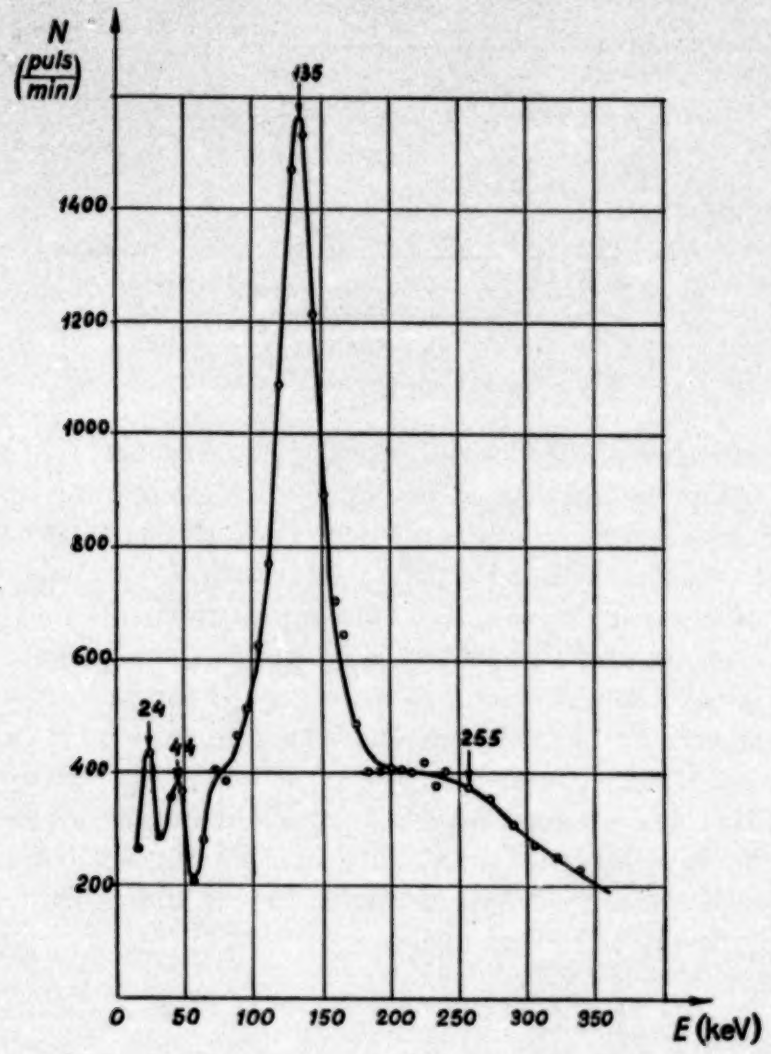

Fig. 9. Pulse height spectrum of γ-rays from I (n, γ).

The intensity of the 135 keV γ-lines, $n = 32$ % per captured neutron, was determined with an accuracy of 15 % from 12 different sets of measurements, including 6 measurements of the spectrum of γ-rays absorbed in the lead filter. The neutron capture cross section was assumed to equal 6.7 barns. The absence of other intense γ-lines in the energy range up to 600 keV and the large intensity of the 135 keV line seem to indicate that these γ-quanta are due to transitions between the first excited level and ground state of I^{128}.

4.4. SAMARIUM

The target was made of 76.5 mg of powdered Sm_2O_3 enclosed in an aluminium foil, it was disc-shaped with a diameter of 10 mm. The pulse height distribution for the samarium target is shown in fig. 10. Two well

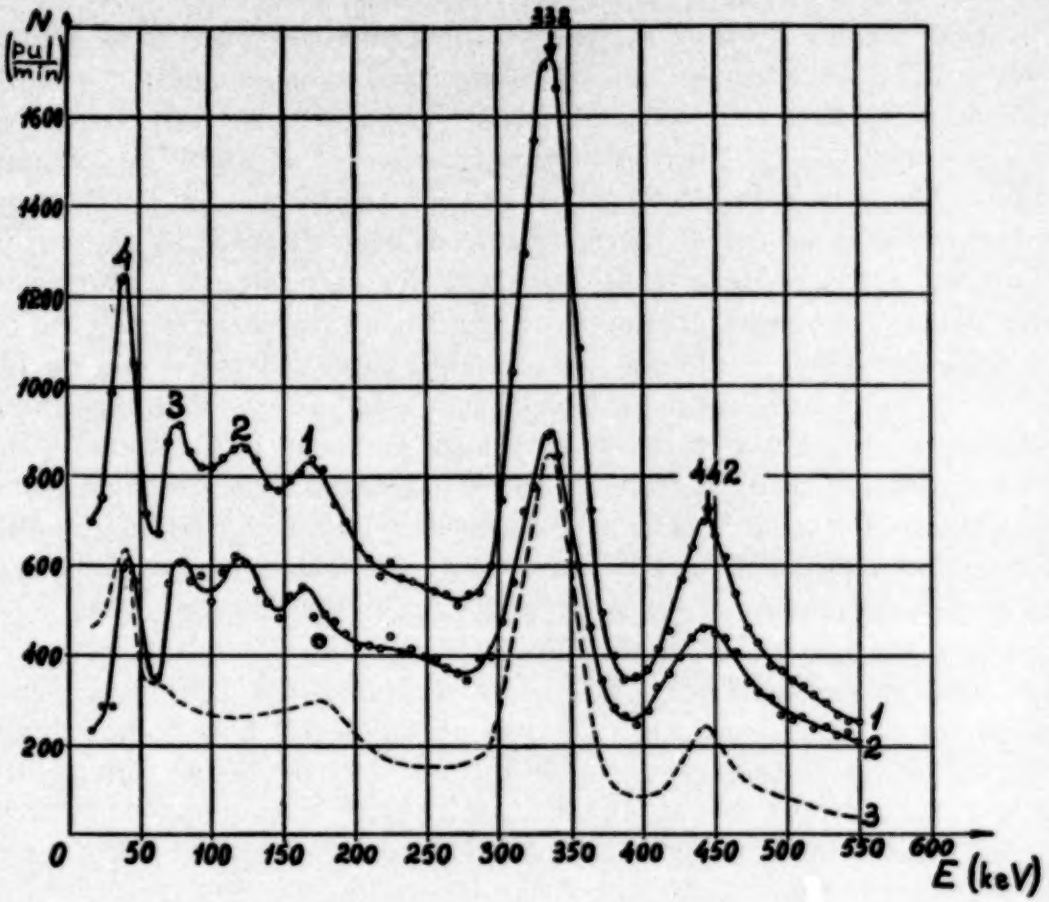

Fig. 10. Pulse height spectrum of γ-rays from Sm (n, γ)
1. without filter 2. with 2.02 g/cm² lead filter
3. pulse spectrum of γ-rays absorbed in the lead filter.

resolved peaks from 442±5 keV and 338±4 keV γ-rays can be seen in the pulse distribution curve (measured without a lead filter); in the low energy region peaks 1, 2, 3 and 4 can be discerned. Absorption of 338 and 442 keV quanta is appreciable in the measurements with a 2.02 g/cm² in thick lead filter (curve 2); moreover a decrease of peak 1 is also noticeable and this peak was correspondingly identified as a maximum in the Compton electron distribution from the 338 keV γ-line (dotted line 3). If peaks 2, 3 and 4 were produced by γ-quanta emitted by the target they would certainly have disappeared in the lead filter measurements. These peaks should thus be attributed to the apparatus. Peak 2 should evidently be ascribed to γ-rays from the I (n, γ) reaction in the NaI(Tl) crystal and peak

3 to X-radiation from the lead spectrometer shield. Within the limits of the experimental errors the energy of peak 4 corresponds to that of the Sm X-rays. However, an intense apparatus peak of the same energy is present in the pulse spectrum and its presence does not permit one to measure the Sm X-rays if their intensity is lower than 10 %. Thus one arrives at the conclusion that no γ-rays of energy below 300 keV were present. The intensities of the detected lines were determined experimentally and found to equal $(34\pm5)\%$ ($E_\gamma = 442$ keV) and $(70\pm10)\%$ ($E_\gamma = 338$ keV) per captured neutron. The neutron capture cross section in Sm^{149} was assumed to be 66200 barns [13]); the final result does not depend critically on the cross section value as almost all thermal neutrons were absorbed by the target. The γ-line energies satisfactorily agree with the data of other authors [5, 14]) who studied the γ-ray spectrum of the Sm (n, γ) reaction whereas the intensity of the 338 keV γ-line is approximately twice as large as that quoted in ref. [14]). The γ-lines under consideration should be ascribed to transitions between the two lower levels of Sm^{150} since the main contribution to the thermal neutron capture cross section for a natural isotopic mixture of samarium is from Sm^{149}. This is confirmed by the fact that these levels also exhibit themselves in the Pm^{150} decay [15]). Comparison of the γ-line intensities indicates that the first excited level in Sm^{150} is the 338 ± 4 keV level. This conclusion agrees with the data presented in ref. [15]). The energy of the second excited level is 777 keV [5]). The low intensity of the hard γ-lines in the Sm (n, γ) spectrum [14, 16]) proves that de-excitation of Sm^{150} from a capturing state occurs via cascade γ-transitions with equal probability to the ground state or to one of the two excited Sm^{150} levels considered above. In this respect the disintegration scheme for Sm^{150} proposed in ref. [14]) is not complete.

4.5. GOLD

The measurements were performed with two pure gold targets: I was 0.277 g/cm² thick (weight 1.56 g) and II was 0.554 g/cm² thick. The pulse height distribution due to γ-quanta absorbed in a 2.02 g/cm² lead filter is shown in fig. 11. Three partially resolved peaks which can be identified with the photopeaks from 252, 210 and 174 keV γ-quanta can be discerned (target II). The accuracy of the energy determinations is ±3 or ±2 keV. After the spectrum was resolved into its components (dotted line in fig. 11) a small residual peak in the energy region $\approx$ 140 keV remained which should apparently be assigned to the background (fig. 4). The intensities of the detected γ-lines are listed in table 1 (accuracy of the measurements ±20 %). The thermal neutron capture cross section was taken to equal 98 barns [17]). Besides the photo peaks mentioned above a maximum at 66 ± 3 keV can be distinguished in fig. 11 which is also associated with the capture of

neutrons in gold. A thin target (I) was used in the measurements of this radiation. Absorption of γ-quanta in the target was determined experimentally. For this purpose the lead filters (5 in fig. 1) were replaced by gold plates and absorption was estimated from the decrease in the area of the

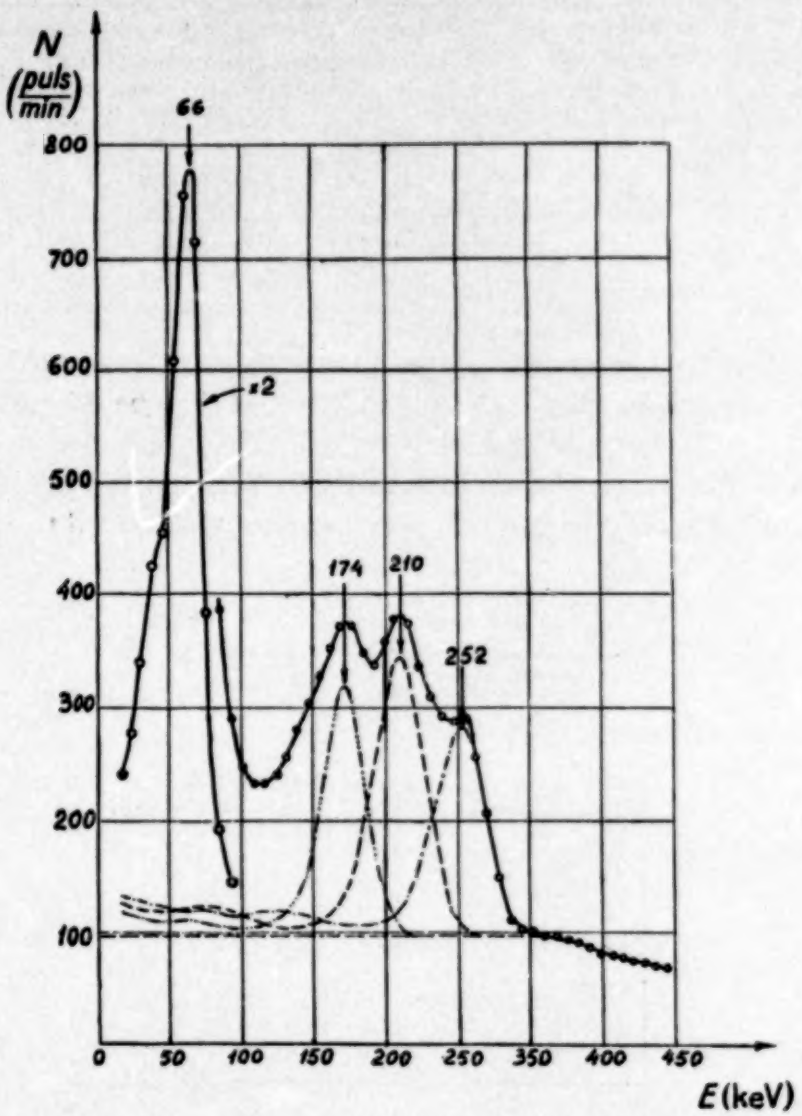

Fig. 11. Pulse height spectrum for Au (n, γ) γ-rays absorbed in 2.02 g/cm^2 lead filter.

peak. The absorption coefficient for 66 ± 3 keV rays in Au found in this way was $\mu = 2.9\pm0.2$ cm^2/g. The intensity of the radiation under consideration is shown in table 1.

A γ-line of 248 keV energy was detected in ref. [4]) in the spectrum from Au (n, γ); this line can evidently be identified as the overall peak of the three γ-lines discovered in the present investigation. The conclusion of the authors of ref. [12]) that the neutron binding energy in Au^{198} $E_b > 6.5$ MeV does not seem to be very convincing. This conclusion was also questioned in

ref. [4]). It would appear to be more correct to assume, in accordance with ref. [18]), that the 6.494±0.008 MeV γ-quanta are due to direct transition

TABLE 1

Soft gamma quanta from the Au (n, γ) reaction

E_γ energy in keV	Number of γ-quanta per captured neutron in %	Theoretical values of the coefficients of internal conversion in the K-shell (α_K)		
		E2	M1	M2
252	22	0.0955	0.447	1.66
210	19	0.152	0.775	3.47
174	11	0.278	1.47	7.42
66	40	—	—	—

of the nucleus to the ground state. From the data presented in ref. [12]) the energies of the excited states of Au^{198} would then be 32±20, 184±16, 245±17, 348±20, 518±20 and 792±20 keV. The γ-lines discovered in the present work can be attributed to transitions between the lowest levels in Au^{198} (fig. 12). In this case 210 keV γ-rays cannot be ascribed to a transition

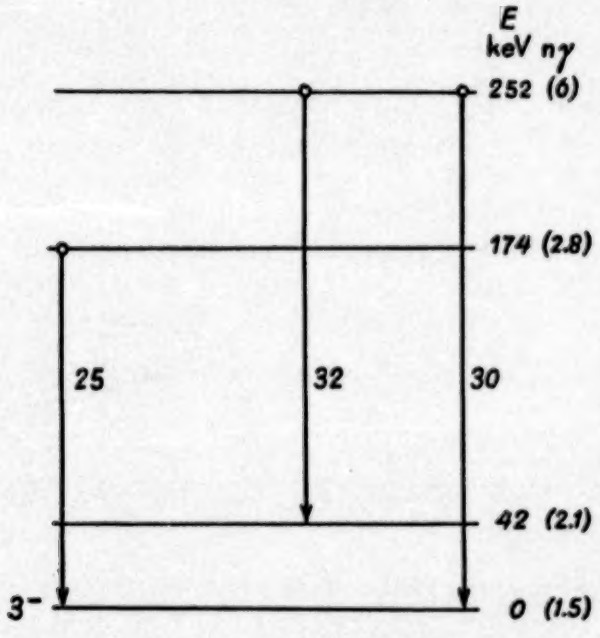

Fig. 12. Transition scheme for Au^{198}.

between any other of the excited levels mentioned above, whereas the other two γ-rays can correspond to transitions between higher levels. A scheme, which in our opinion seems to be more probable, is presented in fig. 12. Gamma radiation of 42 keV energy was not observed in our measurements because of strong absorption in the target and of the background peak which has an approximately equal energy (fig. 4).

The 66 ± 3 keV γ-quanta cannot be attributed to any of the transitions between the lower excited levels. This radiation was interpreted as X-rays from Au resulting from K-conversion. With account of the yield of K-fluorescence from the Au atom, $f = 0.94$ [19]), once can find the number of conversion events in the K-shell, $k = (42\pm6)\%$ per captured neutron. The X-rays cannot be explained by assuming conversion of a single soft line which, because of its low intensity, was not observed in our experiments, as in this case one would be compelled to assume almost total conversion of this hypothetic line; no metastable states, however, have been observed in the Au^{198} nucleus. The conversion is more probably related to the γ-quanta detected in the present work: $k = k_{252}+k_{210}+k_{174}$. The theoretical values of the K-conversion coefficients of Au, (α_K), for dipole and quadrupole transitions have been taken from ref. [20]) are presented in table 1. Because of the large lifetime higher multipoles cannot be invoked. The γ-quanta intensities (n_γ) found in the present investigation permit one to determine the rate of conversion in the K-shell (k) if the values of α_K are known; this rate will depend on the multipolarity of all three γ-lines. The multipolarities of the γ-transitions were chosen in such a way as to satisfy the experimental value of k.

The experimental result is not consistent with the assumption that all three transitions are of the E2 $(k = 7.6\pm1.5)$ or M2 type $(k = 161\pm30)$. Satisfactory agreement with the experiments can be attained if the 252 keV γ-transition is assumed to be M2 and the other two transitions, M1 and E2. This possibility does not seem to be very probable as in the transition scheme under consideration (fig. 12) M2 transitions could not compete with M1 and E2 transitions. Good agreement with the experimental data can be obtained if all three transitions are M1 $(k = 33\pm8)$. Let us consider the case of two M1 transitions (one of these should be a 174 MeV transition) and a single E2 transition. The total number of transitions from excited states is represented in fig. 12 in % per captured neutron. Assuming the transitions are M1 this number is found to equal the sum of the probability of transition by radiation of a γ-quantum (table 1) and the probability of the transition involving k-conversion.

The Au^{198} nucleus in the ground state has negative parity and a spin $I = 3$ [21]). The parity of the excited states shown in fig. 12 should also be negative since only M1 and E2 transitions are possible between them. According to data presented in ref. [12]) the capturing state of Au^{198} possesses a spin 1^+. It has been demonstrated [14]) that the probability of transition from the capturing state to the Au^{198} nuclear states under consideration are the same in order of magnitude (the number of γ-transitions from the capturing state to a state corresponding to a given energy level is expressed in % per captured neutron in fig. 12). The foregoing facts can be fitted into a

consistent scheme if it be assumed that the lower excited states have identical spins 3^- although this type of degeneracy seems to us to be improbable. Moreover, transitions from the capturing state to the states under consideration, including the ground state, should be M2 which would be suppressed by E1 and M2 transitions. In this connection it seems advisable to reconsider the conclusion drawn in ref. [22]) concerning the spin of the initial state. It should also be added that some later results [17]) disprove some of the data used in ref. [22]) to support the assumption that the character of the capturing state is 1^+. If the capturing state in Au^{198} is 2^+ the transitions to the states under consideration will be E1 and the characters of the corresponding states of the Au^{198} nucleus at low excitation energies will be 1^-, 2^- and 3^-.

4.6. MERCURY

The measurements were carried out with a target made of 1.2 g of HgO powder enclosed in an aluminium envelope; the target was disc-shaped with a diameter of 20 mm. A photopeak from 372 ± 5 keV γ-rays and peaks corresponding to softer rays can be distinctly seen in the pulse spectrum obtained in the measurements performed with the target (curve 1, fig. 13). Curve 2 in fig. 13 refers to measurements with a lead filter 2.02 g/cm^2 thick. The area of the photopeak was determined from the spectrum of the radiation absorbed in the lead filter (difference between curves 1 and 2); subsequently, the intensity of the 372 keV radiation was determined and found to be $n_\gamma = (45\pm7)\%$ per captured neutron (the neutron capture cross section was assumed to equal 380 barns). By comparing curves 1 and 3 (the pulse spectrum due to γ-rays transmitted by a 0.5 mm lead filter) it can be seen that the 68 ± 3 keV rays are emitted from the target whereas the 45 keV peak is due to the apparatus. The spectrum due to the radiation absorbed in 0.5 mm of lead (curve 4) is shown in the lower left hand corner of fig. 13. The intensity of the 68 ± 3 keV rays was determined from this spectrum and found to lie in the interval $1.4\ \% < n_\gamma < 4\ \%$ per captured neutron. A more precise determination of the intensity of this radiation is difficult because of the presence of the apparatus peak.

The γ-quanta detected in the present investigation should be ascribed to the Hg^{200} nucleus inasmuch as the Hg^{199} isotope has the largest cross section for thermal neutron capture. In this case the 372 keV γ-rays correspond to a transition of the Hg^{200} nucleus from the first excited level (familiar from the radioactive disintegration of Au^{200} and Tl^{200} [23])) to the ground state. Gamma quanta of close energy were detected in an investigation of the γ-rays following the capture of neutrons in Hg [14]). The only discrepancy is in the intensity of the 372 keV line (our values are approximately 2 times higher than those obtained in ref. [14]).) A similar discrepancy between our

data and those in ref. [14]) was previously detected in measurements of the intensity of the soft line from the Sm (n, γ) reaction.

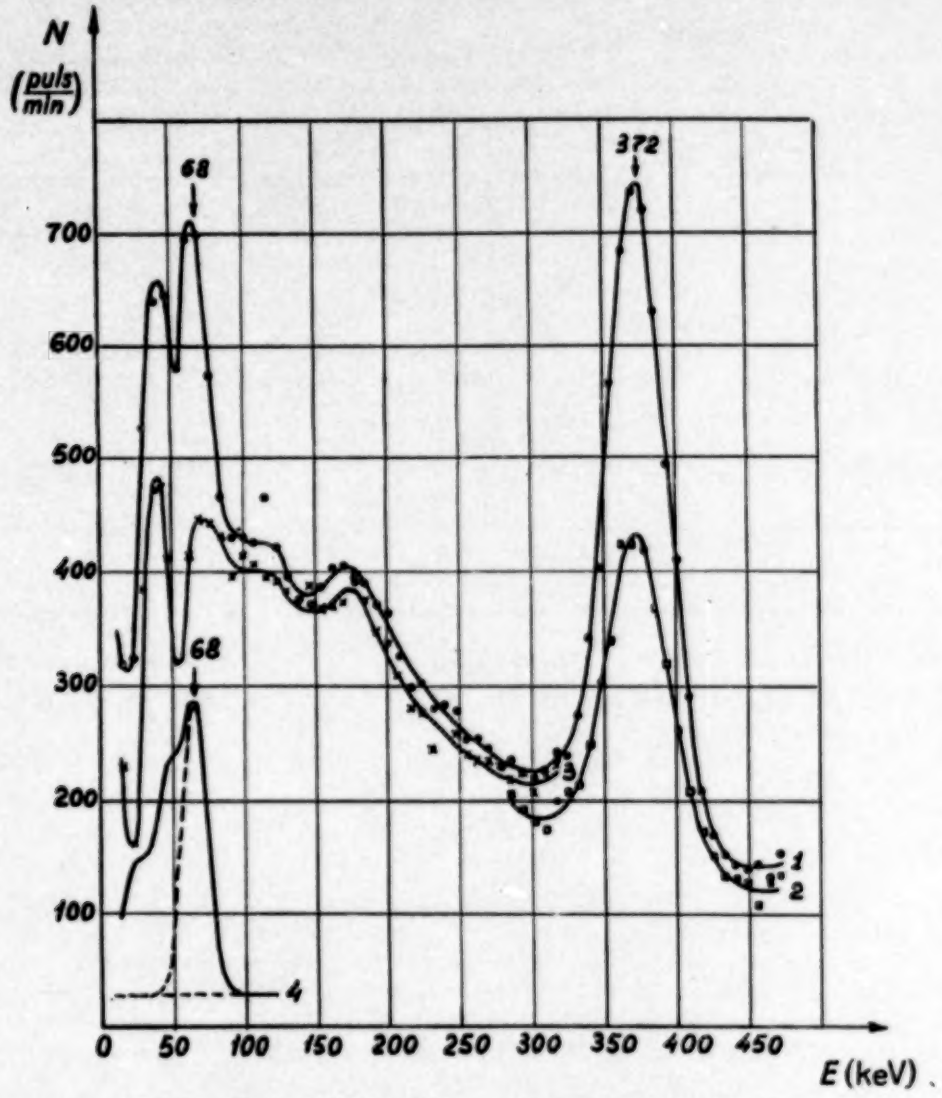

Fig. 13. Pulse height spectrum of γ-rays from mercury
1. without filter 2. with 2.02 g/cm² Pb filter 3. with 0.5 mm of Pb
4. spectrum of radiation absorbed in 0.5 mm of Pb.

It seems natural to identify the 68±3 keV radiation as X-rays from Hg produced by K-conversion of 372 keV γ-quanta. The experimental value of the K-conversion coefficient, α_K, lies in the interval $0.03 < \alpha_K < 0.09$. The only theoretical value which lies within this interval is that corresponding to a E2 transition ($\alpha_K \approx 0.04$ [20])). Thus, in accord with ref. [23]) a spin 2 and positive parity should be assigned to the first excited state of Hg^{200}.

5. Summary of Results

The value of the energies, E_γ, in keV and γ-line intensities n_γ expressed in number of γ-quanta per captured neutron (in %) are presented in table 2.

The absolute intensities have been determined with an accuracy of 15—20%.

TABLE 2

Radiating nucleus	Energy (E_γ) and intensity (n_γ) of gamma rays				
Co^{60}	E_γ (keV)	226±4	276±4		
	n_γ (%)	23	23		
Rh^{104}	E_γ (keV)	96±3	133±3	176±3	217±4
	n_γ (%)	17	≦8	19	9
I^{128}	E_γ (keV)	135±3			
	n_γ (%)	32			
Sm^{150}	E_γ (keV)	338±4	442±5		
	n_γ (%)	70	34		
Au^{198}	E_γ (keV)	66±3	174±3	210±4	252±4
	n_γ (%)	40	11	19	22
Hg^{200}	E_γ (keV)	68±3	372±5		
	n_γ (%)	1.4—4	45		

In conclusion the authors wish to thank Prof. I. M. Frank for interest in this work, Dr. I. S. Shapiro for discussion of the results and the Physical reactor crew for help in the work.

References

1) B. B. Kinsey and G. A. Bartholomew, Can. Journ. Phys. **31** (1953) 537
2) L. V. Groshev, B. P. Adyasevich and A. M. Demidov, Reports of Soviet Delegation at the International Conference on the Peaceful Uses of Atomic Energy (Publ. House of Academy of Sciences of USSR, 1955) Physical Investigations, p. 252
3) B. Hamermesh and V. Hummel, Phys. Rev. **88** (1952) 916
4) M. Reier and M. H. Shames, Phys. Rev. **100** (1955) 1302
5) C. T. Hibdon and C. D. Muehlhause, Phys. Rev. **88** (1952) 943
6) I. V. Estulin, L. F. Kalinkin and A. S. Melioransky, JETP **31** (1956) 886
7) A. I. Alikhanov, V. V. Vladimirsky, S. J. Nikitin, A. D. Galanin, S. A. Gavrilov and N. A. Bugrov, Reports of Soviet Delegation at the International Conference on the Peaceful Uses of Atomic Energy (Publ. House of Academy of Sciences of USSR, 1955) Nuclear Reactor Engineering and Reactor Theory, p. 105
8) G. A. Bartholomew and B. B. Kinsey, Phys. Rev. **89** (1953) 368
9) G. M. Foglesong and D. G. Foxwell, Phys. Rev. **96** (1954) 1001
10) M. Deutsch and G. Scharff-Goldhaber, Phys. Rev. **83** (1951) 1059
11) W. C. Jordan, J. M. Cork and S. B. Burson, Phys. Rev. **90** (1953) 862
12) G. A. Bartholomew and B. B. Kinsey, Can. Journ. Phys. **31** (1953) 1025
13) E. A. Melaike, M. J. Parker, J. R. Petruske and R. H. Tomlinson, Can. Journ. Chem. **33** (1955) 830
14) B. M. Adyasevich, L. V. Groshev and A. M. Demidov. Session of USSR Academy of Sciences on Peaceful Uses of Atomic Energy (1955) p. 270
15) V. Kistiakowsky-Fischer, Phys. Rev. **96** (1956) 1549
16) B. B. Kinsey and G. A. Bartholomew, Can. Journ. Phys. **31** (1953) 1051
17) H. H. London and V. L. Sailor, Phys. Rev. **93** (1954) 1030

18) A. Harvey, Phys. Rev. **81** (1951) 353
19) C. D. Broglies, D. A. Thomas and S. K. Haynes, Phys. Rev. **89** (1953) 715
20) L. A. Sliv and N. M. Band, Tables of Internal Conversion Coefficients of Gamma Rays (1956)
21) L. G. Elliot, A. A. Preston and J. L. Wolfson, Can. Journ. Phys. **32** (1954) 153
22) J. Titman and C. Sheer, Phys. Rev. **83** (1953) 747
23) J. Berostrom, R. D. Hill and G. de Pasquali, Phys. Rev. **92** (1953) 918

Nuclear Physics 4 (1957) 112—119; © *North-Holland Publishing Co., Amsterdam*
Not to be reproduced by photoprint or microfilm without written permission from the publisher

DISTRIBUTION ANGULAIRE DU RAYONNEMENT GAMMA DE 8.34 MeV DE LA RÉACTION $^{14}N(p,\gamma)^{15}O$

S. GORODETZKY, A. GALLMANN, M. CROISSIAUX
ET R. ARMBRUSTER
Institut de Recherches Nucléaires de Strasbourg

Reçu le 18 mars 1957

Abstract: The resonance at 1060 keV in the reaction ^{14}N (p, γ) ^{15}O has been investigated. The angular distribution of the 8.34 MeV radiation has been found to be $W(\theta) = 1 + 0.05\ P_2(\cos\theta)$. It is concluded that the angular momentum of the level at 8.34 MeV in ^{15}O is $J = 3/2$.

1. Introduction

La résonance à 1060 keV dans la réaction ^{14}N (p, γ) ^{15}O aboutit au niveau excité de 8.34 MeV dans ^{15}O. Ce niveau peut se désexciter par rayonnements gamma soit directement vers le niveau fondamental soit par l'intermédiaire des niveaux de 6.82 MeV ou de 5.27 MeV [1]. Nous avons mesuré la distribution angulaire du rayonnement gamma de 8.34 MeV allant directement vers le niveau fondamental.

2. Dispositif Expérimental

Préalablement, afin d'établir le spectre des rayonnements gamma d'une façon précise, nous avons construit un spectromètre à paires externes [2]. Deux cristaux de NaI de $1\frac{1}{2}''$ de diamètre et de hauteur sont placés de part et d'autre d'un 3ème cristal de NaI de mêmes dimensions. Les deux photomultiplicateurs latéraux sont suivis d'amplificateurs linéaires et d'analyseurs d'impulsions à un canal qui sont réglés sur le photopic de 511 keV des rayonnements gamma d'annihilation. Les trois canaux attaquent le circuit de coïncidences triples de l'appareillage décrit précédemment [3]. Chaque coïncidence triple ouvre la porte d'un analyseur à vingt canaux branché sur le canal du milieu. On ne détecte ainsi les rayonnements gamma que par leur seul pic de paires d'énergie $E - 2mc^2$ avec une efficacité environ 300 fois plus faible qu'en spectrographie directe.

La cible a été obtenue en chauffant une feuille de tantale de 0.2 mm d'épaisseur à 1500° C, dans une atmosphère d'azote naturel pendant quelques minutes [4].

La figure 1 montre le spectre obtenu en bombardant la cible de NTa par un faisceau de protons à une énergie de 1060 keV sans déflection

magnétique. Le rayonnement gamma de 4.43 MeV provient de la réaction ^{15}N (p, α, γ) ^{12}C, qui a un rendement environ 1000 fois plus grand que la

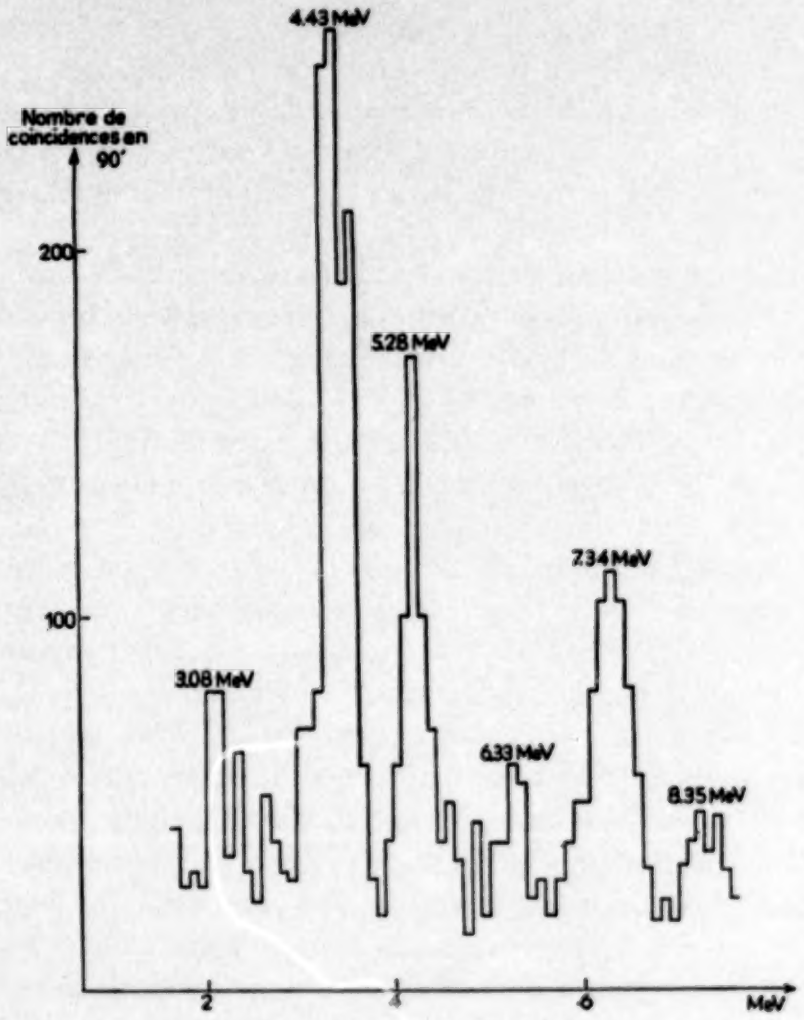

Fig. 1.

réaction ^{14}N (p, γ) ^{15}O. Les 0.156 $^0/_{00}$ de deutérium qui se trouvent dans l'hydrogène natural donnent lieu à la réaction ^{14}N (d, p) ^{15}N. Cette réaction à très grand rendement est gênante, puisqu'en dehors des rayonnements gamma de 7.31 et 6.33 MeV [5]) (fig. 1), elle donne également un rayonnement gamma de 8.32 MeV qui se superposerait, lors de la distribution angulaire, exactement au gamma étudié.

Nous avons ainsi dû nous servir d'une déflection magnétique à 30°, pour éviter cette réaction parasite. Dans le spectre obtenu avec la déflection, les pics correspondants aux rayonnements gamma de 6.33 et de 7.31 MeV ont complètement disparu.

La distribution angulaire a été faite avec déflection du faisceau. Nous avons utilisé un photomultiplicateur 6342 blindé par un cylindre en mumétal

et monté d'un cristal de NaI de 2″×2″. Un toit de Pb de 10 cm d'épaisseur placé au-dessus du bâti de distribution protégeait le cristal des rayonnements gamma de la réaction ^{27}Al (p, γ) ^{28}Si qui pouvait se faire sur les pièces en aluminium de la déflection magnétique.

Malgré cette protection, il restait cependant un comptage lorsque l'on remplaçait la cible de NTa par une feuille de Ta pur. L'intensité de ce comptage parasite a été mesurée aux différents angles dans les conditions mêmes de l'expérience et retranchée de la distribution mesurée sur la cible de N Ta.

Les mesures ont été faites en spectrographie directe, de façon que les trois pics (paires, paires plus un, paires plus deux) du rayonnement gamma étudié se placent dans la bande des 20 canaux de l'analyseur.

Les rayonnements gamma de 511 keV et 1280 keV du ^{22}Na ainsi que le pic d'addition de ces deux gamma ont, avec le pic de paires du rayonnement gamma de 4.43 MeV, constamment servi de points d'étalonnage.

Le porte-cible était constitué par une feuille de cuivre de 0.1 mm d'épaisseur, scellé à chaud par de l'acétate de polyvinyle (Gelva) sur l'extrémité d'un tube de verre dont les parois avaient une épaisseur de 1.5 mm. Un courant continu d'eau traversait une petite cuvette en aluminium soudée sur la face inférieure de la feuille de cuivre.

Du fait des dimensions réduites de ce porte-cible, l'absorption des rayonnements gamma de 8.34 MeV ne variait que de 3 % entre la position ou l'absorption était minimum (105°) et la position où elle était maximum (75°).

Le bâti de corrélation angulaire que nous avions utilisé précédemment [6]) n'a pu servir cette fois-ci, étant donné qu'il ne permettait que des rotations autour d'un axe vertical. Nous avons construit un nouveau bâti de distribution et corrélation angulaire, avec lequel le compteur mobile peut faire une rotation complète autour d'un axe dirigé dans n'importe quelle direction. Un système de visée optique grâce auquel on peut voir l'impact du faisceau sur la cible permet de centrer l'appareil à 0.5 mm près.

3. Résultats Expérimentaux

La mesure de la distribution angulaire isotrope [7]) du rayonnement gamma de 6.14 MeV de la réaction ^{19}F (p, α, γ) ^{16}O à une énergie $E_p = 340$ keV, nous a permis d'obtenir un centrage excellent. Les valeurs trouvées dans 11 positions différentes de part et d'autre de la direction du faisceau étaient égales entre elles aux erreurs statistiques près (1 %).

Nous avons également mesuré la distribution angulaire du rayonnement gamma de 4.43 MeV de la réaction ^{15}N (p, α, γ) ^{12}C à une énergie $E_p = 900$ keV. En accord avec d'autres auteurs (8) nos points expérimentaux se sont placés sur la courbe théorique

$$W(\theta) = 1 - 0.89 \cos^2\theta + 1.58 \cos^4\theta$$

mettant ainsi en évidence une anisotropie de

$$\frac{W(0°) - W(90°)}{W(90°)} = 69\ \%.$$

Sans apporter aucune modification à l'ensemble du dispositif expérimental, cible comprise, nous avons alors mesuré la distribution angulaire du rayonnement gamma de 8.34 MeV de la réaction ^{14}N (p,γ) ^{15}O.

La figure 2 montre la courbe

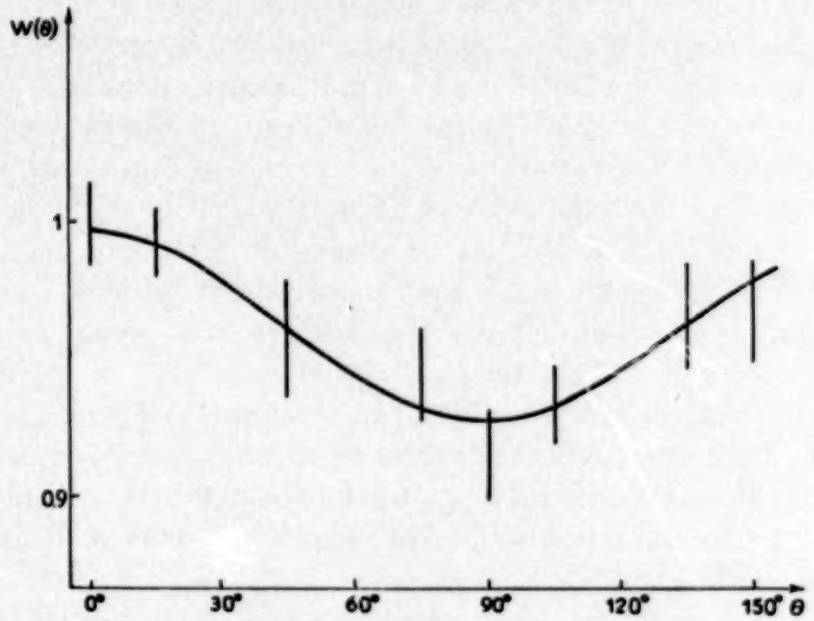

Fig. 2.

$$W(\theta) = (0.9515 \pm 0.0036) + (0.0455 \pm 0.009)\, P_2 + (0.0013 \pm 0.017)\, P_4$$

obtenue à partir des points expérimentaux par la méthode des moindres carrés [9]) après avoir fait les corrections d'absorption ($< 3\ \%$). A noter, que le comptage du moniteur fixe de référence était rigoureusement constant, aux erreurs statistiques près, pendant toute la durée des mesures, ce qui nous a évité de faire des corrections d'activité.

La courbe de distribution était symétrique par rapport à la direction des protons incidents.

La symétrie autour de 90° permet de dire qu'il n'y a pas d'interférence du niveau de 8.34 MeV avec d'autres niveaux de résonances voisines.

Le fait que la cible voit le cristal de NaI sous un angle solide fini, nécessite une correction de la fonction expérimentale trouvée. L'application des formules de Rose [9]) donne

$$W(\theta) = 0.95 + (0.048 \pm 0.0095)\ P_2 + (0.0017 \pm 0.020)\ P_4.$$

On peut admettre que le terme en P_4 est nul. Nous considérons donc que la distribution angulaire est donnée par la relation

$$W(\theta) = 1+(0.050\pm0.010)\ P_2. \qquad (1)$$

4. Interprétation

Nous partons des données suivantes:

moment angulaire du niveau fondamental de ^{14}N: $I = 1^+$,

moment angulaire du niveau fondamental de ^{15}O: $I_0 = 1/2^-$

(déduit de celui du noyau miroir ^{15}N).

En ce qui concerne le niveau de 8.34 MeV de ^{15}O, Evans et ses collaborateurs [10]) ont analysé les distributions angulaires des neutrons de la réaction ^{14}N (d, n) ^{15}O. Ils proposent, sous réserve, pour le moment angulaire J du niveau de 8.34 MeV la limite supérieure de $5/2^-$. Tautfest et Rubin, en accord avec d'autres auteurs [11]) indiquent, par l'étude de la diffusion élastique des protons de ^{14}N, que le niveau de 8.34 MeV est formé par onde s d'où ils concluent que le spin de ce niveau est $J = 1/2^+$ ou $3/2^+$.

Afin d'envisager ces différentes hypothèses, nous avons pris en considération toutes les valeurs de $J \leqq 7/2^+$ et $J \leqq 7/2^-$.

Les calculs ont été faits en utilisant la notation du "channel spin" et en tenant compte d'interférences possibles de diverses ondes de protons et de mélanges possibles de différentes multipolarités du rayonnement gamma de 8.34 MeV. La formule de distribution angulaire la plus générale contient ainsi trois paramètres:

a) t, la proportion de "channel spin" $s = \frac{1}{2}$, celle du "channel spin" $s = \frac{3}{2}$ étant alors $(1-t)$. On a $0 \leqq t \leqq 1$.

b) ε, le coefficient de mélange d'ondes de protons. ε se rapporte à l'onde la moins probable. On normalise alors à $1+\varepsilon^2$.

c) δ, le coefficient de mélange de différentes multipolarités du rayonnement gamma de 8.34 MeV.

A) Nous éliminons les valeurs $J = \frac{1}{2}^+$ et $J = \frac{1}{2}^-$ par l'anisotropie de la distribution angulaire.

B) Pour la valeur $J = \frac{3}{2}$ pour le moment angulaire du niveau de 8.34 MeV, les calculs ont été faits dans les deux cas de parités impaire et paire.

(1°) $J = \frac{3}{2}^-$

Nous avons fait les calculs pour une interférence d'ondes de protons p (amplitude 1) et f (amplitude ε) et pour un mélange de rayonnements gamma M1 (amplitude 1) et E2 (amplitude δ). Dans ces conditions les fonctions de distribution angulaire relatives aux deux "channel spin" s'expriment par

$$w_1 = 4(1+\delta^2)\left[1+\frac{\delta^2+2\sqrt{3}\,\delta-1}{2(1+\delta^2)}\,P_2(\cos\theta)\right] \qquad \text{pour } s=\tfrac{1}{2},$$

$$w_2 = 4(1+\delta^2)(1+\varepsilon^2)\left[1+\frac{\delta^2+2\sqrt{3}\,\delta-1}{2(1+\delta^2)}\cdot\frac{2}{5}\cdot\frac{2\varepsilon^2-3\varepsilon-2}{1+\varepsilon^2}\,P_2(\cos\theta)\right] \qquad \text{pour } s=\tfrac{3}{2},$$

et la fonction de distribution angulaire totale par

$$W(\theta) = tw_1+(1-t)w_2,$$

à comparer avec la distribution angulaire expérimentale (1).

On obtient ainsi une relation entre les trois paramètres t, ε et $\delta : f(t,\varepsilon,\delta)=0.05$.

Les solutions mathématiques de cette relation correspondent à des cas physiques si $0 \leqq t \leqq 1$ et si ε et δ sont réels.

Dans le cas $J=\frac{3}{2}^-$ il existe une infinité de ces solutions. Chaque fois qu'on se fixe les proportions relatives d'ondes p et f on obtient une relation entre t et δ, qui peut donner le mélange de rayonnements gamma de 8.34 MeV pour un couplage déterminé.

On sait qu'une onde p est plus probable qu'une onde f. En prenant le cas extrême $\varepsilon = 0$ (onde p pure) on obtient la relation

$$\frac{\delta^2+2\sqrt{3}\,\delta-1}{2(1+\delta^2)}\cdot\frac{9t-4}{5} = 0.05$$

entre le facteur de couplage t et le coefficient de mélange δ des rayonnements gamma. On voit alors notamment que pour $\delta = 0$ (M1 pur) un couplage correspondant à la valeur $t=\frac{7}{18}$ s'accorde avec le résultat expérimental.

(2°) $J=\frac{3}{2}^+$

On suppose ici que le rayonnement gamma de 8.34 MeV est un rayonnement E1 pur. Pour les protons incidents, on prendra un mélange d'ondes s (amplitude 1) et d (amplitude ε). Les fonctions w deviennent ainsi

$$w_1 = 4\varepsilon^2\left[1-\tfrac{1}{2}P_2(\cos\theta)\right] \qquad \text{pour } s=\tfrac{1}{2},$$

$$w_2 = 4(1+\varepsilon^2)\left[1-\frac{\varepsilon}{1+\varepsilon^2}\,P_2(\cos\theta)\right] \qquad \text{pour } s=\tfrac{3}{2}.$$

La fonction de distribution totale angulaire est encore

$$W(\theta) = tw_1+(1-t)w_2.$$

Pour que $W(\theta)$ puisse correspondre au résultat expérimental, il faut alors que

$$t = \frac{0.05\varepsilon^2+\varepsilon+0.05}{-0.5\varepsilon^2+\varepsilon-0.05}$$

c'est à dire que

$$-20 \leqq \varepsilon \leqq -0.05.$$

A chacune de ces valeurs de ε correspond alors un certain couplage t tel que la distribution angulaire théorique soit égale à $1+0.05\, P_2(\cos\theta)$.

On trouve en particulier qu'une contribution égale ou supérieure à 0.25 % d'onde d à l'onde s prédominante est compatible avec le résultat expérimental.

C) Des calculs ont été faits d'une façon analogue dans les cas $J = \frac{5}{2}^{\pm}$ et $J = \frac{7}{2}^{\pm}$. On obtient une fonction de distribution de la forme

$$W(\theta) = 1+g(t,\ \varepsilon,\ \delta)P_2(\cos\theta)+h\ (t,\ \varepsilon,\ \delta)\ P_4(\cos\theta).$$

Comme expérimentalement on trouve que le terme en $P_4(\cos\theta)$ est nul, on a donc la relation supplémentaire

$$h(t,\ \varepsilon,\ \delta) = 0$$

en plus de la relation

$$g(t,\ \varepsilon,\ \delta) = 0.05.$$

Là encore il existe une infinité de solutions mathématiques. Pour aucune de ces solutions pourtant, on n'a à la fois $0 \leqq t \leqq 1$ et ε et δ réels, ce qui veut dire qu'elles ne correspondent pas à des cas physiques.

5. Conclusion

Nous pensons donc que le niveau de 8.34 MeV de ^{15}O a un moment angulaire $J = \frac{3}{2}$. La seule mesure de la distribution angulaire ne permet pas de préciser la parité du niveau, car les deux valeurs $J = \frac{3}{2}^{+}$ ou $J = \frac{3}{2}^{-}$ conduisent au résultat expérimental.

Hagedorn et ses collaborateurs [12]) par l'étude de la diffusion élastique des protons sur ^{14}N indiquent que le niveau de 8.34 MeV de ^{15}O est formé par onde s et proposent pour le moment angulaire de ce niveau la valeur $J = \frac{3}{2}^{+}$. Nous pensons que la très faible contribution d'onde d indiquée dans la discussion n'est pas en désaccord avec ce résultat.

Bibliographie

1) C. W. Li, Phys. Rev. **92** (1953) 1084A
2) S. A. E. Johansson, Nature **166** (1950) 794; Phil. Mag. **43** (1952) 249
J. K. Bair et F. S. Maienschein, Rev. Sci. Instr. **22** (1951) 343
3) S. Gorodetzky, A. Gallmann, M. Croissiaux et R. Armbruster, Comptes Rendus **241** (1955) 1743
4) J. B. Marion, R. M. Brugger et T. W. Bonner, Phys. Rev. **100** (1955) 46
5) R. D. Bent, T. W. Bonner,. J. H. Mc. Gary, W. A. Ranken, R. F. Sippel, Phys. Rev. **99** (1955) 710

6) S. Gorodetzky, A. Gallmann, M. Croissiaux et R. Armbruster, Comptes Rendus **244** (1957) 62
7) S. Devons, Ph. D. et M. G. N. Hine, Proc. Roy. Soc. A **199** (1949) 56
8) A. A. Kraus Jr., A. P. French, W. A. Fowler et C. C. Lauritsen, Phys. Rev. **89** (1953) 299
9) M. E. Rose, Phys. Rev. **91** (1953) 610
10) W. H. Evans, T. S. Green et R. Middleton, Proc. Phys. Soc. A **66** (1953) 108
11) G. W. Tautfest et S. Rubin, Phys. Rev. **103** (1956) 196
12) F. B. Hagedorn, S. S. Mozer, T. S. Webb, W. A. Fowler et C. C. Lauritsen, Phys. Rev. **105** (1957) 219

Nuclear Physics 4 (1957) 120—124; © *North-Holland Publishing Co., Amsterdam*
Not to be reproduced by photoprint or microfilm wilhout written permission from the publisher

THE LONGITUDINAL ANGULAR DEPENDENCE OF THE PHOTOELECTRIC EFFECT AND ITS INFLUENCE ON THE DETERMINATION OF GAMMA RAY INTENSITIES

SÖLVE HULTBERG AND TIHOMIR NOVAKOV†
Nobel Institute of Physics, Stockholm

Received 25 March 1957

Abstract: The longitudinal angular distribution of photoelectrons has been measured over the whole angular range ($-\pi \leq \vartheta \leq \pi$) for three different gamma ray energies. A 4 mg/cm² U foil was used as converter. From the experimental curves it is possible to obtain relative photoelectric cross-sections by integration from $\vartheta = 0$ to $\vartheta = \vartheta_0$, where ϑ_0 is a limiting angle defined by the geometry of the experimental set-up. A comparison of the measured angular distributions has been made with theory showing for certain characteristic quantities an essential agreement. Also, some interesting deviations have been observed. The study of photoelectron lines as a precise method for determining relative gamma ray intensities is discussed. The method has been applied to the decay of Bi^{206} where relative intensities of about 20 gamma rays have been determined with an instrumental resolution of 0.4 % at high energies.

1. Introduction

The most frequently used method for the precise experimental study of the properties of low-lying nuclear levels is the beta spectrometric measurement of carrier-free activities prepared on thin backings. The technique essentially consists of a magnetic analysis of electrons which arise from the internal conversion of the nuclear gamma rays. The data so obtained lead, however, to no direct conclusion about the number of unconverted gamma rays, a quantity which is often of great interest. When such information is required it is a common practice to use scintillation spectroscopy, external conversion and, to a smaller extent, analysis of Compton electrons. Each method has obvious merits and disadvantages. The scintillation crystal can be used with weak activities but gives a poor energy resolution. In a beta spectrometer the photoelectron lines from external conversion can, at least in principle, be measured with a resolution as high as that of internal conversion lines but large activities are required, giving high background. In addition, the angular dependence of the photo-electric effect must be known as a function of energy. Finally, an analysis of Compton electrons has been used to some advantage in cases of complex spectra, especially where many high energy gamma rays are present, the best resolution possible being intermediate between those of the other two cases. Disadvantages arise from rather com-

† On leave of absence from Institute for Nuclear Sciences "B. Kidrič" Belgrade, Yugoslavia.

plicated experimental set-ups, the enormous source strengths required (of the order of 100 times that necessary for photo conversion) and the lack of well established standard methods of analysis.

Considering the ever increasing need for higher precision in the desired data, a closer inspection of the powers of the external conversion method seemed worthwhile. The lack of full experimental verification of corrections for the well-known phenomenon of the directional dependence of photoelectrons is probably mainly responsible for the very infrequent use of external conversion for the purpose of evaluating accurate gamma ray intensities. The present paper is intended to show that the photoelectron method can be conveniently used in many cases and that the two principal difficulties can be overcome to a large extent. In the following only K-shell photoelectrons will be considered.

2. Experiments

In earlier experiments [1]) it has been demonstrated that the longitudinal angular distribution of photoelectrons is accessible to experiments in a double-focusing beta ray spectrometer. At a sufficiently high angular resolution the distribution curves so obtained should give the variation of the differential photoelectric cross-section per unit solid angle. It should perhaps be pointed out that the terminology and symbols used in this paper are similar to those used in ref. [1]); no definitions will be repeated here for the sake of brevity. The angular distribution curves obtained earlier were, however, incomplete and were measured under varying conditions. Because of the obvious possibilities of obtaining direct experimental values of relative photoelectric cross-sections, all angular distributions of ref. 1) were remeasured under constant conditions. The experimental technique was similar to that used earlier except for the mechanical construction which had been improved in order to permit of an easier and more extensive operation than before. The distance between the gamma ray source and the U converter was in all cases 35 mm. A typical result of such an experiment is shown in fig. 1.

The essentially new feature of the curve of fig. 1 with respect to the earlier measurements is that the distribution is now complete, i.e. photolines could be recorded for any ϑ. Owing to this fact it will be possible to make rather complete and interesting comparisons with the theory [2, 3, 4]).

Multiplication of the ordinates in fig. 1 with $\sin\vartheta$ gives the dotted curve, representing the total photoelectric emission from the converter. By integrating the latter curve from $\vartheta = 0$ to $\vartheta = \vartheta_0$, where ϑ_0 is a limiting angle, and dividing by the source strength in mC it should be possible to obtain experimental values of relative photoelectric cross-sections, applicable to any type of source-converter arrangement for which ϑ_0 can be defined. In this way full experimental allowance can be made for the angular dependence

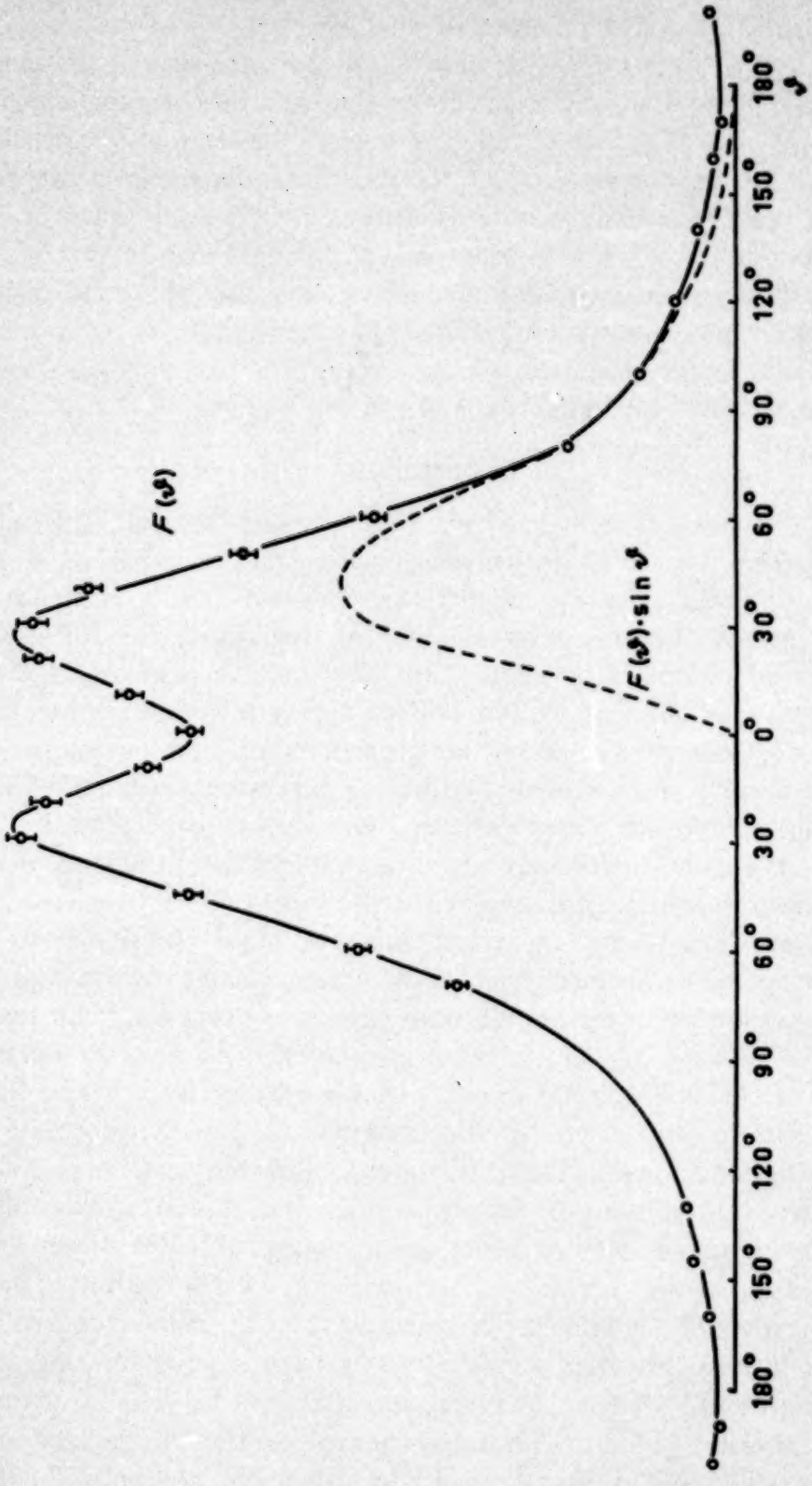

Fig. 1. Angular distribution of K-shell photoelectrons per unit solid angle produced by external conversion of the Au^{198} 411 keV gamma rays in a 4 mg/cm² U foil. The circles represent measured photo-line peak heights.

of the photoelectric effect. Tests were made with certain set-ups, each one defining an angle ϑ_0, and, by the above integration procedure, an agreement, to within 10 %, with the distribution curves of the type of fig. 1 was obtained. Further details will be given in a later and more complete description of these experiments. In all cases uranium converters were used. By employing gamma-ray sources with activities of the order of 10—20 mC and small spectrometer apertures photo-lines can be recorded with a resolution of 0.3 — 0.4 % at intermediate and high gamma ray energies. The strong Compton background is then considerably reduced and many photo-lines become readily measurable. Thus it might be mentioned that, very recently, it has been possible to measure relative intensities of about 20 gamma rays following the decay of Bi^{206} with a resolution of 0.4 % at high energies.

3. Comparison with theory

In order to make a direct comparison with theory the distribution of fig. 1 would have to be corrected for distorting effects such as the limited angular resolution, the limitation arising from the geometry of the experimental set-up, and the multiple scattering of the photoelectrons inside the converter material. These questions are now being studied in more detail than at the time of the earlier experiments [1]) when only a rough estimate was considered necessary because of the incomplete measurements. Here it might be mentioned that the corrections to be applied will cause significant deviations from the curve shown in fig. 1 only around the maxima and in the region between them. It is interesting to notice that, for large angles ϑ, the experimental intensities are far greater than those predicted by theory. It should be mentioned that relative values of the theoretical photoelectric cross-sections for the total absorption in the K-shell ar obtained by integration from 0° to 180° and here an agreement to within 10 % was found.

For a quantitative comparison it is convenient to evaluate integrated quantities from the experimental and theoretical distributions such as the bi-partition angle, the forward to back ratio and the ratio R between the average forward momentum of the photoelectron and the total momentum of the incident photon [3]). Essential agreement between theory and experiment was obtained for the first two quantities. The ratio R, however, was found to deviate significantly from the theoretical curve shown in fig. 23 of ref. 3). From their diagram it is seen that $R \to 1$ for large energies (of the order of some MeV) while for small energies R becomes increasingly larger than 1. Here the electron binding energy E_K has been neglected in comparison to $h\nu$. For uranium as converter material, however, E_K cannot be neglected. An inclusion of E_K in the derivation of the expression for R gives

$$R = \frac{h\nu - E_K}{h\nu} \cdot \sqrt{\frac{2m_0c^2}{h\nu - E_K} + 1} \cdot \overline{\cos\vartheta} \qquad (1)$$

which reduces to eq. (44) of ref. 3) if E_K is neglected. Our eq. (1) shows that $R = 0$ for $h\nu = E_K$. This is in agreement with our experiments so far, as can be seen from fig. 2.

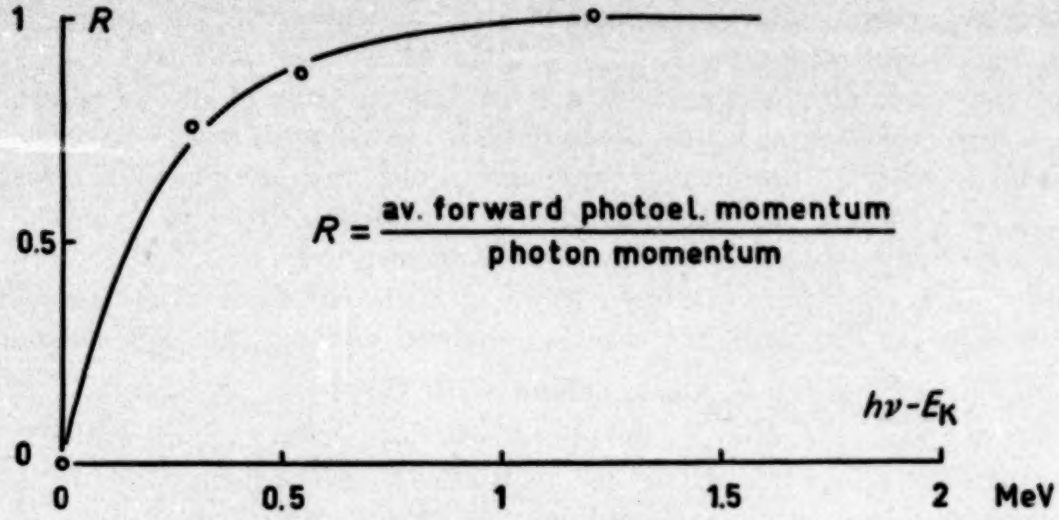

Fig. 2. The ratio R as a function of the energy difference $h\nu - E_K$. $E_K = 0.115$ MeV. A 4 mg/cm² U foil was used as converter for the Au^{198} (0.411 MeV), Cs^{137} (0.662 MeV) and Co^{60} (1.33 MeV) gamma rays.

Our experiments on the uranium atom thus seem to indicate that, as soon as the gamma ray energy becomes large compared with E_K, the photoelectron is ejected in such a way that its average forward momentum equals the total linear momentum of the incident photon.

As this report is a preliminary one, no further details will be given here. The intention is to point out that the present lack of a satisfactory and easily applicable theoretical correction for the angular dependence of the photoelectrons can be compensated for by direct experimental investigations, the results of which are believed to be adaptable to any source-converter arrangement with known geometry. Also it is interesting to observe that the theory of the photoelectric emission can be experimentally tested in a fairly complete way.

The experiments outlined above will later be presented in greater detail. The study of the gamma rays following the decay of Bi^{206} will appear separately.

One of the authors (T.N.) would like to express his gratitude to Prof. Manne Siegbahn, Head of the Nobel Institute, for the hospitality shown to him during his stay at the institute.

References

1) S. Hultberg, Arkiv f. Fysik **9** (1955) 245
2) F. Sauter, Ann. Phys. **11** (1931) 454
3) C. M. Davisson and R. D. Evans, Revs. Mod. Phys. **24** (1952) 79
4) F. Sauter und H. O. Wüster, Zeits. f. Physik **141** (1955) 83

Nuclear Physics **4** (1957) 125—144; © *North-Holland Publishing Co., Amsterdam*
Not to be reproduced by photoprint or microfilm without written permission from the publisher

POSSIBLE VIBRATIONAL LEVELS IN Dy^{160}

OVE NATHAN
Institute for Theoretical Physics, University of Copenhagen

Received 12 May 1957

Abstract: The radiations of Tb^{160} have been studied by means of magnetic and scintillation spectrometers and various coincidence techniques. A decay scheme has been proposed which includes the following excited states in Dy^{160}: 87 keV (2+), 283 keV (4+), 964 keV (2+), 1047 keV (3+), 1262 keV (2−), and 1359 keV (3−). The level scheme is discussed in the light of the unified model and it is suggested that the states at 964 keV and 1047 keV may possibly belong to a rotational band associated with electric quadrupole vibrations (gamma vibrations) and that the states at 1262 keV and 1359 keV similarly may belong to a rotational band associated with electric octupole vibrations.

1. Introduction

Recent studies of the level structure of a number of even nuclei with spheroidal equilibrium shape have given increasing experimental support for the existence of collective vibrational states in such nuclei as predicted by the unified model [1]). The evidence consists mainly in the systematic occurrence in radioactive decays of excited states with energies, spins, parities and decay properties, which in most cases agree with the predictions of the theory. A more crucial test for the collective nature of these states would consist in life-time measurements and in determinations of cross-sections for Coulomb excitation. Up to now, however, such experiments have been attempted only in a few cases [2–5]).

The present study of the level structure of Dy^{160} has been undertaken to extend the systematic picture of vibrational states further in the region of the rare earths where the experimental material in support of such states is still meager. Dy^{160} is formed in the beta decay of 72 day Tb^{160} and sufficient energy is available for the decay to excite states in the daughter nucleus up to about 1800 keV. In view of the fact that several mutually conflicting decay schemes for Tb^{160} have been put forward by previous workers [6–8]) it was felt profitable to reexamine the decay in as many details as possible with available techniques. Hence, the decay scheme proposed in section 7 of this paper is based entirely on experimental data obtained in the course of this investigation.

2. Spectrometers and Sources

The main features of the magnetic and scintillation spectrometers utilized have been described in a previous paper [9]). The relative gamma ray inten-

sities were measured both with a $1\frac{1}{2}'' \times 1\frac{1}{2}''$ and a $3'' \times 3''$ NaI crystal in order to provide an extra check on these quantities. For calibration of the large crystal the intrinsic peak efficiency curve given by Lazar *et al.* [10]) was used, while the efficiency curve for the small crystal was obtained by independent measurements of a number of known activities. The gamma-gamma coincidences were performed mainly with a two microsecond circuit and a kicksorter, employing two crystals facing each at 180° with a few mm spacing. In some cases, however, where it was particularly important to avoid false coincidences due to Compton scattering, a newly completed fast-slow coincidence circuit of conventional design with a resolving time of $4 \cdot 10^{-8}$ second was utilized. In this setup two single channels were used for energy selection and the counters were placed at 90° with a 20 mm lead plate in between to reduce scattering between the counters.

Sources were prepared from Tb_2O_3 irradiated for two months in the Harwell pile. Four weeks after irradiation the amount of Tb^{161} formed in double neutron capture was found to be very small. The source material was purchased from Johnson, Mattey and Co., Ltd., London, and from spectrophotometric analysis the main impurities were given as Gd_2O_3 (≈ 1 %) and Dy_2O_3 (< 0.5 %). The only long-lived activities that could be caused by these impurities are Gd^{153} and Dy^{159} but owing to the low abundances of Gd^{152} and Dy^{158}, only negligible amounts of interfering radiations from these nuclei were expected. No radiations that could be ascribed to contaminations were, indeed, observed.

Simple scotch tape sources were used for most of the gamma ray measurements, while the sources for the beta ray spectrometer were produced by vacuum evaporation on to backings of aluminum foils. The continuous beta spectrum and the internal conversion lines at low energy were studied with sources 20—50 $\mu g/cm^2$ thick on 150 $\mu g/cm^2$ backing, whereas thicker layers (up to 1 mg/cm^2) on 2.5 mg/cm^2 backing were used for the investigation of the more energetic internal conversion lines.

3. Internal Conversion and Beta Ray Spectra

With the spectrometer set for 0.7 % resolution the entire region from 15 keV to 1400 keV was searched for electron lines. Some nineteen conversion lines were found and their energies and intensities measured as shown in table 1. The interpretation of these lines yielded eleven gamma ray energies, and indication for a gamma ray at $\approx$ 960 keV was, moreover, found in the broadening of the 964 keV K-line (fig. 1). This conclusion was confirmed by the gamma-gamma coincidences. The most comprehensive previous measurements on the internal conversion spectrum of Tb^{160} are those reported by Cork *et al.* [11]) and by Keshishian *et al.* [7]). Using

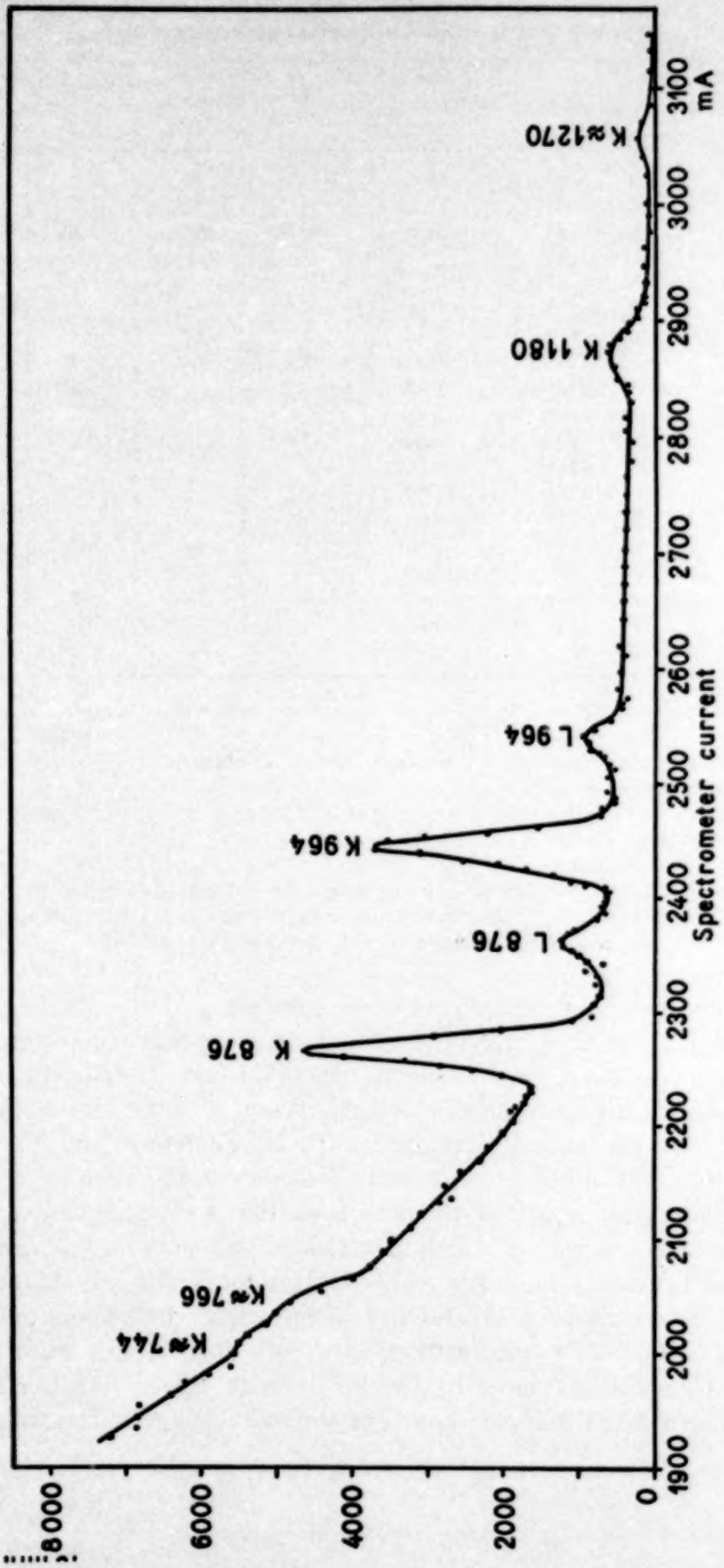

Fig. 1. The Tb^{160} high-energy internal conversion spectrum.

TABLE 1

Energies and intensities of internal conversion lines [a]

Electron energy keV	Assignment		Abs. intensity [b] %	K/L ratio	Theoretical K/L ratio		
					E1	E2	M1
33.7	K	87	16.4				
38.0	K	92[c]	0.18				
78.9	L	87	31.2	0.53	6.4	0.65	5.6
85.0	M	87	9.80[d]				
86.8	N	87					
142	K	196	0.90				
163	K	216	0.14	>6	6.5	2.8	6.1
188	L	196	0.37	2.4	6.5	2.5	6.0
194	M, N	196	0.09				
244	K	298	0.42				
289	L	298	0.054	7.8	7.2	3.7	6.2
≈690	K	≈744[e]	≈0.007				
≈712	K	≈766	≈0.011				
822	K	876	0.11				
870	L, M	876	0.016	≈7	7.3	6.3	6.3
910	K	964[f]	0.10				
957	L, M	964	0.013	≈8	7.3	6.3	6.3
1126	K	1180	0.012				
1218	K	1272	≈0.004				

[a] The energies are believed to be correct to within ±1 % and the intensities to within ±10 %.

[b] The observed relative intensities are converted to absolute values by comparison with the continuous beta spectrum.

[c] Part of this line may be due to the strong 48 keV L-line occurring in the decay of Tb^{161}.

[d] M- and N-lines were not completely resolved.

[e] Assignment uncertain.

[f] This line is slightly broader than the neighbouring 876 keV K-line (fig. 1). A weaker component corresponding to a transition energy of ≈ 960 keV is probably present, but its energy and intensity cannot be determined with the resolution available.

photographic detection techniques these groups reported eighteen gamma rays in addition to those given in table 1. In the present investigation it has not been possible to verify the existence of the corresponding conversion lines in the beta ray spectrometer and no estimates of their strengths have been given by the above mentioned authors. Therefore, the lines have not been included in the present decay scheme considerations.

Some information regarding the multipolarities of the gamma ray transitions may be furnished by the K/L ratios. Along with the experimental ratios, table 1 presents the theoretical K/L ratios for E1, E2 and M1 radiation calculated on the basis of the K- and L-conversion coefficients published by Rose *et al.* [13]). The two transitions at 87 keV and 196 keV must clearly be mainly E2, while the large K/L ratios indicate dipole character for the radiations at 216 keV and 298 keV. For the more energetic transitions the

small theoretical difference in K/L ratios does not allow any reliable choice among E1, E2, and M1.

The continuous beta spectrum was investigated at a resolution of 2 % with all six gaps of the spectrometer in operation and care was taken not to measure in the immediate vicinity of the internal conversion lines. Assuming allowed shape for all groups, a Fermi plot of the data was constructed (fig. 2), revealing the presence of at least four components. Table 2 presents

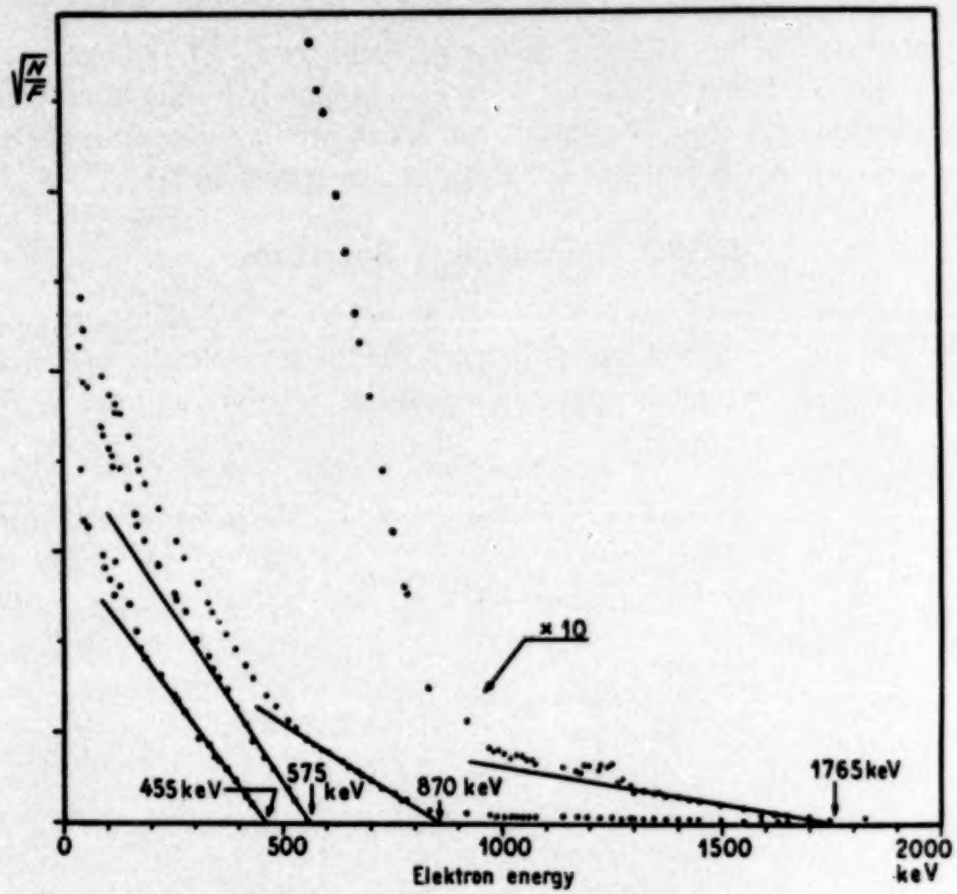

Fig. 2. Fermi plot of the beta spectrum of Tb^{160}.

TABLE 2

Beta groups, intensities and log *ft* values [a]

Group	E_{max} (keV)	Intensity %	log *ft*
β_1	455±20	22	8.1
β_2	575±10	42	8.1
β_3	870±10	36	8.8
β_4	1765±30	0.4	11.9

[a] Maximum energies and branching ratios are calculated by Fermi analysis assuming allowed shape for all components. This procedure makes the energy and intensity determinations of groups β_1 and β_2 somewhat uncertain.

a summary of the analysis, including the log ft values for the different branches. These results are in substantial agreement with previous workers [7, 8, 12, 14]) with the exception of the low-energy branch β_1 for which the figures from the various investigators scatter considerably. This is not surprising, however, since the data for this group were obtained by successive subtractions of the two intense components β_2 and β_3 and, consequently, not too much weight can be given to the values for the maximum energy and the intensity determined in this way.

The origin of the broad hump in the spectrum at about 1200 keV is not fully understood, but it is believed to be caused mainly by the intense high-energy gamma rays from the source which can produce Compton electrons in the surfaces of the walls and baffles of the spectrometer.

4. The Gamma Ray Spectrum

Measurements of the gamma ray spectrum with a 3″×3″ and a 1½″×1½″ NaI crystal and a single channel analyser (fig. 3) revealed the presence of eight photo-peaks whose energies and intensities are given in table 3. With

TABLE 3

Energies and intensities of gamma rays measured with the 3″×3″ and the 1½″×1½″ crystal [a]

Gamma ray energy keV	Abs. intensity [b] %
87	10.3
205 [c]	8.1
300	30
395	2.6
875	33
960 [d]	35
1180 [e]	16
1270 [e]	7.7

[a] The energies are believed to be correct to within ±1 % and the intensities to within ±30 %. The intensities quoted are average values for the two crystals.

[b] The observed relative intensities are converted to absolute values by use of the absolute intensity of the 876 keV K-line (table 1) and the K-conversion coefficient for this transition. The latter quantity was determined experimentally to be $3.4 \cdot 10^{-3}$ by comparison with a Cs^{137} source in identical geometry.

[c] The line width indicates this as double line.

[d] The coincidence data indicates this as a double line.

[e] The presence of additional gamma rays in this energy region cannot be excluded.

the exception of the 395 keV photon all observed gamma rays can be identified with the corresponding lines in the internal conversion spectrum. The 205 keV peak appears wide in the gamma spectrum and it is concluded, therefore, that it is constituted by the 196 keV and 216 keV radiations

observed in the beta spectrometer. The 30 % uncertainty quoted for the gamma ray intensities is based on an estimate of the maximum systematic errors that could be introduced by the following procedures: analysis of unresolved lines, subtraction of the Compton background, and use of

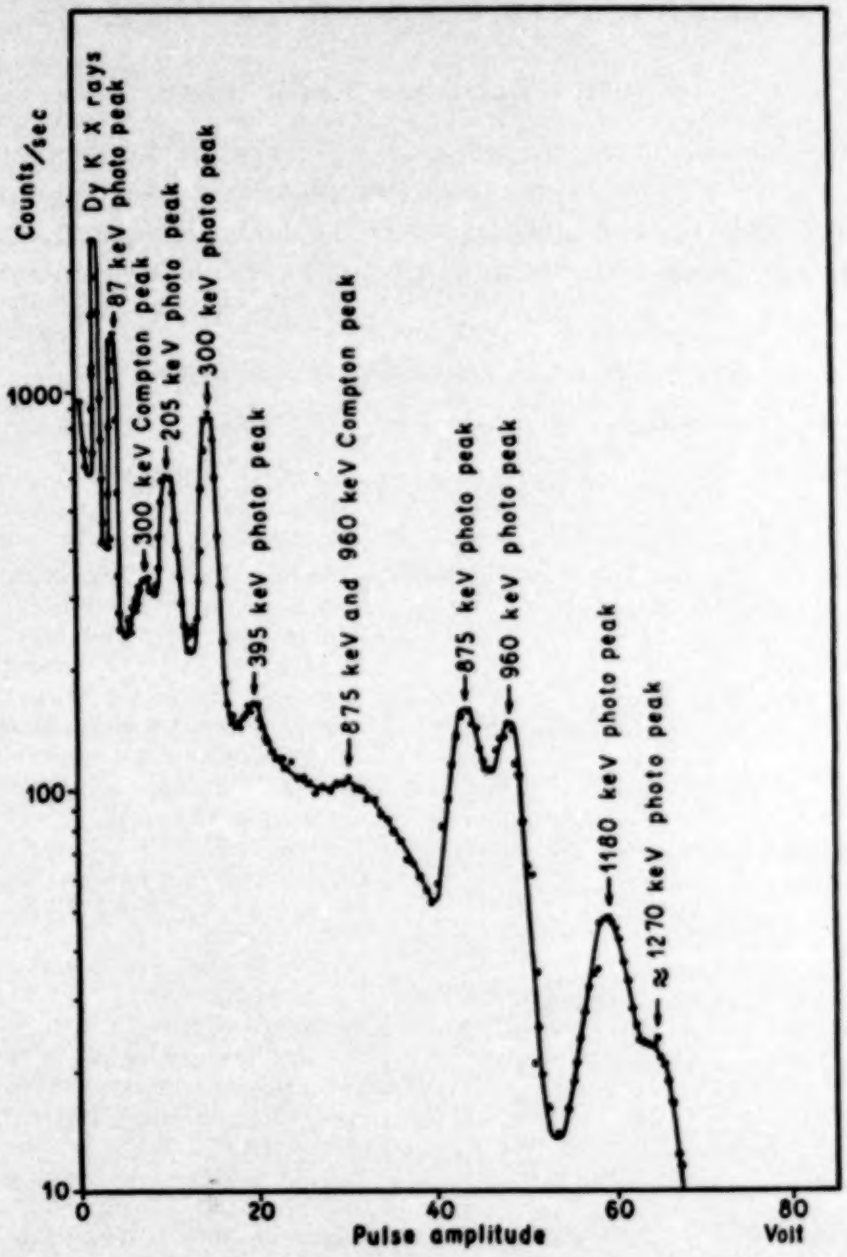

Fig. 3. The gamma ray spectrum of Tb^{160} obtained with a $1\frac{1}{2}'' \times 1\frac{1}{2}''$ NaI crystal. Source to crystal distance 15 cm.

empirical calibration curves for the intrinsic peak efficiencies. The two crystals, for which the efficiencies were independently determined, gave for all gamma rays results which checked within the quoted limit of error.

The gamma ray energies tabulated in table 3 agree well with previous

determinations but this is not quite so for the intensities. Jaffe [15]), working with a NaI crystal, quotes intensities which only in the case of the 300 keV line are seriously at variance with our results, whereas Bertolini *et al.* [8]), using photoelectric conversion, report intensities which disagree by large factors with the values given in table 3.

5. The Coincidence Experiments

Gamma-gamma coincidence work on Tb^{160} has previously been carried out be Burson *et al.* [6]) but, owing to the comparatively low energy resolution obtained by these workers, it was considered valuable to repeat the measurements in some detail. The results of these experiments are contained in

TABLE 4

Results of the gamma-gamma experiments

Selected energy region keV	Gamma rays observed in coincidence with the selected events keV	Remarks
87	205, 300, 395, 875, 960, 1180, 1270	The intensity of the 205 keV gamma line is enhanced with respect to the 300 keV line. Among the high-energy photons, the 875 keV, 1180 keV and 1270 keV lines seem to appear with the same relative intensities as in the singles distribution while the intensity of the 960 keV peak is considerably reduced (fig. 4). $I_{\gamma 960}/I_{\gamma 875} = 0.36 \pm 0.10$.
190–220	87, 205, 300, ≈780, 960 ≈1080	The 205 keV, 300 keV and 780 keV gamma rays are very weak. Compton background from the 875 keV and 960 keV radiations is probably responsible for the 300 keV coincidences.
180–200	87, 215, 300, ≈780, ≈1080	See foregoing note.
210–230	87, 195, 300, ≈780, 960	See foregoing note.
300	87, ≈200, 875, 960	The 200 keV gamma ray is very weak. The intensity ratio between the 875 keV and 960 keV photons is $I_{\gamma 960}/I_{\gamma 875} = 0.68 \pm 0.10$ (fig. 5).
780	87, ≈200, 300	The 200 keV line is wide and must be a double line but its energy appears somewhat lower than in the singles. The 300 keV coincidences are probably due to Compton background.
875	87, 300, ≈400	The intensity of the 400 keV gamma ray is 5–10 % of the 300 keV gamma ray.
960	87, 215, 300, ≈400	See foregoing note.
1080	87, 195	
1180–1300	87	

table 4 and a few typical coincidence spectra are presented in fig. 4 and fig. 5. For the majority of the cases, the findings of Burson and coworkers were confirmed, but a number of additional coincidence relations not reported by this group are also included in table 4. In the following paragraphs the main results of the experiments will be taken up for discussion.

With the single channel set on the 87 keV peak and the kicksorter set to cover the region 500—1400 keV the coincidence spectrum of fig. 4 was recorded. The 87—875 keV and 87—1180 keV coincidences were both found by Burson *et al.*, but these workers were unable to draw any firm conclusions

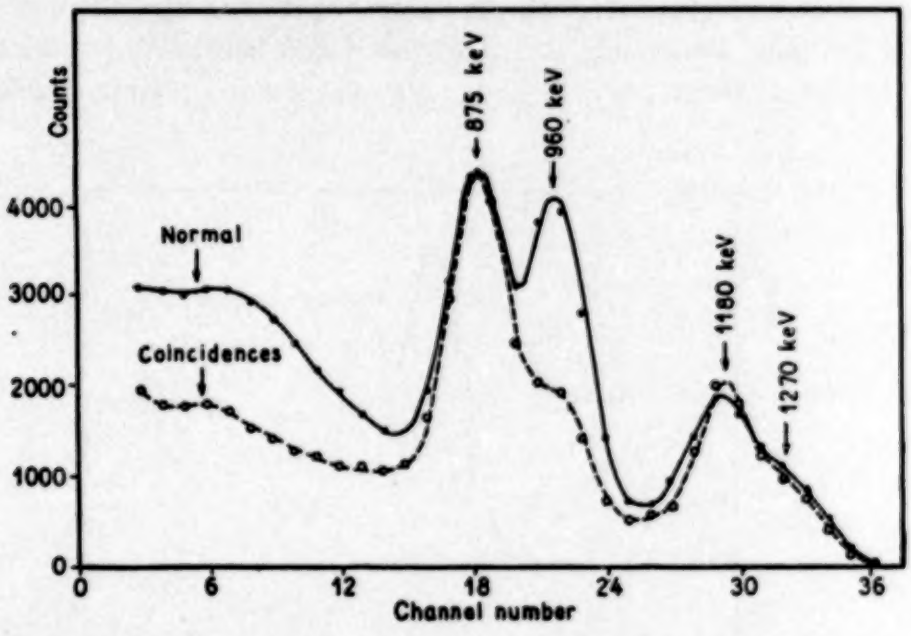

Fig. 4. High-energy gamma rays of Tb^{160}. Normal distribution and coincidences with the 87 keV gamma ray obtained with the 2 microsec circuit and the kicksorter. For convenience, the two curves are normalized at the 875 keV peak.

about the coincidence behaviour of the 960 keV and 1270 keV transitions. However, it appears from fig. 4 that a considerable part of the 960 keV gamma rays is coincident with the 87 keV radiation, and that most likely all of the 1270 keV gamma rays are also coincident. The experiment thus indicates that the 960 keV line has a composite structure, in accordance with the suggestion put forward in section 3 on the basis of the internal conversion data.

A series of coincidence measurements were carried out involving the 196 keV and 216 keV radiations which in common contribute to the 205 keV peak observed in the NaI crystal. By setting the fixed channel on each side of the double line, the coincidence relations of the two rays could to some extent be studied separately. It appeared that the two radiations are weakly in coincidence with each other and that both are coincident with the 87 keV transition and with a gamma ray at about 780 keV. More-

over, a gamma ray near 1080 keV was observed in coincidence with the 196 keV photon, while a 960 keV line appeared in coincidence with the 216 keV radiation. These results were confirmed by setting the channel on the appropriate high-energy lines and observing coincidences in the 200 keV region. Single lines at 195 keV and 215 keV were recorded for the 1080 keV and 960 keV settings of the channel, while a double line was observed for the 780 keV setting. However, the 200 keV coincident line in this case contained relatively more of the low-energy component than in the normal distribution.

Fig. 5 shows a coincidence spectrum recorded with the channel set on the 300 keV line. Peaks due to the 875 keV and 960 keV photons can be seen, whereas no gamma rays at higher energies are observed in coincidence.

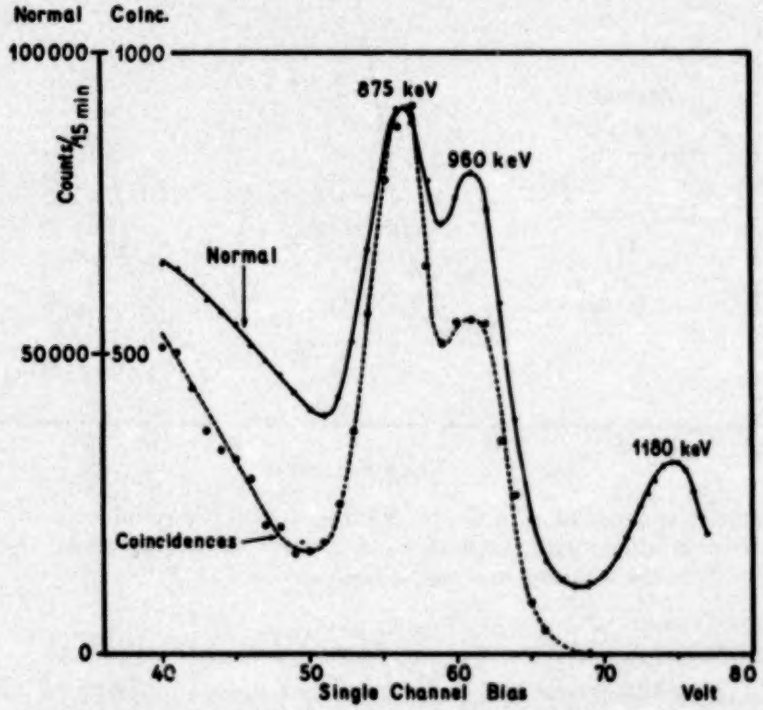

Fig. 5. High-energy gamma rays of Tb^{160}. Normal distribution and coincidences with the 300 keV gamma ray obtained with the fast-slow circuit.

The intensity of the 960 keV gamma ray relative to the 875 keV line is somewhat lower than in the singles spectrum, and a closer analysis of the intensities (see table 4) makes it very likely that the 960 keV gamma ray seen in this coincidence experiment corresponds to that part of the composite 960 keV photopeak which was not observed in the coincidence measurements involving the 87 keV transition.

Owing to the large Compton background under the 395 keV photo-peak, coincidence experiments with this gamma ray were in many cases somewhat inconclusive. A 87—395 keV coincidence relation was definitely established

and a weak gamma ray at about 400 keV was furthermore observed when the single channel was set on the 875 keV and 960 keV peaks.

In order to study the relationship between the various beta ray groups and the gamma transitions occurring in Dy^{160}, a number of beta-gamma coincidence measurements were performed with the beta spectrometer, using a NaI crystal immediately behind the source and recording the coincident gamma spectra on the kicksorter for different settings of the spectrometer on the continuous beta spectrum. In this way it was possible to estimate the maximum beta energy at which a certain gamma ray occurred although in some cases poor statistics and insufficient energy resolution in the crystal limited the accuracy in the end-point determination considerably. A summary of the measurements is given in table 5, and it

TABLE 5

Results of the beta-gamma coincidence experiments

Selected coinc. gamma ray keV	Max. beta energy at which coinc. with the selected gamma ray was observed keV	Beta group	Remarks
87	850±30	β_3	Due to the low intensity of the β_4 group, no coincidence measurements were performed at settings above 900 keV.
≈205 (composite peak)	550±50	β_2	At spectrometer settings below about 500 keV, the 205 keV peak appears in the coincidence spectrum with the the same line width and the same intensity relative to the 300 keV peak as in the singles spectrum.
195	>700	β_3	The 195 keV peak is present only with very low intensity between 500 and 800 keV beta ray energy.
300	550±50	β_2	
395	400±100	β_1	
875,960	850±30	β_3	
1180	550±50	β_2	
1270	400±100	β_1	

can be seen that the observed end-points are consistent with the results of the Fermi analysis (see table 2) within the experimental limits of error. Previous beta-gamma coincidence work has been carried out by Burson *et al.* [6]) working with an anthracene crystal and by Bertolini *et al.* [8]) who used a lens spectrometer. In most cases the data of these workers agree with those presented here.

Electron-gamma coincidences often provide a useful supplement to the

gamma-gamma coincidence data, particularly in cases where the gamma-gamma work is impeded by insufficient resolution. In order to check the gamma-gamma results involving the unresolved 205 keV peak, electron-gamma coincidences were searched for with the beta-spectrometer focused on the 196 keV K-line. No conclusive results were, however, obtained due to the large coincident beta background under the line.

6. Internal Conversion Coefficients and Multipolarities

The intensities of the internal conversion lines obtained with the beta spectrometer and the relative gamma ray intensities measured with the NaI crystal determine the internal conversion coefficients apart from an arbitrary constant. This constant was fixed by means of a Cs^{137} source, by measuring the intensity of the 661 keV gamma line and the corresponding K-conversion line in the same geometry as used for the Tb^{160} experiments. Assuming the K-conversion coefficients for the 661 keV transition in

TABLE 6

K-conversion coefficients and multipolarity assignments

Transition	Energy keV	Meas. abs. intensity of K-conv. lines (I_K %)	Meas. abs. intensity of gamma rays (%)	Exp. K-conv. coeff.	Theor. K-conv. coeff. α_K			Assigned multipole	Calc. abs. int. of gamma rays [a] (I_K/α_K %)
					E1	E2	M1		
BA	87	16.4	10.3	1.6(0)	3.7(−1)	1.6(0)	2.9(0)	E2 [b]	10.3
CB	196	0.90	8.1		4.3(−2)	1.8(−1)	2.8(−1)	E2 [b]	5.0
FE	216	0.14			3.4(−2)	1.3(−1)	2.2(−1)	E1 [c]	4.1
FD	298	0.42	30	1.4(−2)	1.5(−2)	4.7(−2)	8.8(−2)	E1 [c]	28
GD	395	<0.02 [d]	2.6	<8 (−3)	7.5(−3)	2.3(−2)	4.5(−2)	(E1)	
DB	876	0.11	33	3.4(−3)	1.3(−3)	3.3(−3)	5.9(−3)	E2 [c, h]	34
EB+DA	960+964	0.10	12+23 [f]	2.9(−3)	1.1(−3)	2.6(−3)	4.7(−3)	(E2) [g, h]	
FB	1180	0.012	16	7.5(−4)	7.4(−4)	1.8(−3)	2.9(−3)	E1 [h]	16
GB	1270	≈ 0.004	7.7	≈5.2(−4)	6.5(−4)	1.5(−3)	2.3(−3)	E1 [h]	6.2

[a] Calculated on the assumption of pure multipoles.

[b] K/L ratio indicates E2 radiation (table 1).

[c] K/L ratio indicates dipole radiation (table 1). The measured gamma intensity precludes M1.

[d] No line was observed, thus only upper limit can be given.

[e] The conversion coefficient for this transition was determined by direct comparison with a Cs^{137} source in identical geometry. The K-conversion coefficient for the 661 keV transition occurring in Ba^{137} was taken as 0.094 ± 0.004 [16, 17]).

[f] The relative intensities of the 960 keV and the 964 keV gamma rays were taken from the gamma-gamma coincidence measurements.

[g] Since the K-conversion lines were not resolved in the beta spectrometer, the separate conversion coefficients could not be determined. From the theoretical values it seems, however, that both transitions are mainly E2 or that DA is E2 and EB is M1.

[h] These multipole orders can be assigned only on the basis of the conversion coefficients, the K/L ratios being almost similar for E1, E2 and M1 in this energy region (table 1).

Ba^{137} to be 0.094 ± 0.004 [16, 17]), the K-conversion coefficient for the 876 keV transition in Dy^{160} was determined to be $3.4 \cdot 10^{-3}$. Table 6 presents the experimental K-conversion coefficients together with Sliv and Band's [18]) theoretical values for E1, E2 and M1 radiation and, moreover, the multipolarities assigned by comparing these two sets of values. Only the dominant multipole order is indicated in the table, since the experimental uncertainties on the conversion coefficients preclude a more precise determination of the multipole mixtures.

In the case of the 87 keV and 298 keV transitions, the multipole orders assigned by means of the conversion coefficients agree satisfactorily with the K/L ratios previously discussed. The 196 keV and 216 keV radiations were not resolved in the gamma spectrometer, so that only the sum of the gamma ray intensities is known. From K/L ratios, however, the 196 keV radiation is known to be E2 while the 216 keV gamma ray is characterized as dipole. These data together fix the 216 keV transition as E1. The conversion line corresponding to the 395 keV gamma ray was not observed in the internal conversion spectrum, but the upper limit which was estimated for its strength seems to indicate that this transition is also E1. The two transitions near 960 keV were unresolved in the beta spectrometer but the ratio between the corresponding gamma rays could be obtained from the gamma-gamma coincidences. By considering the different possible assignments it seems most likely that both radiations are predominantly E2, although M1 admixtures cannot be excluded.

The last column of table 6 gives the absolute gamma ray intensities calculated from the absolute strengths of the observed K-conversion lines and the theoretical K-conversion coefficients, assuming pure multipoles. These quantities are considered more accurate than the directly measured gamma intensities and have been used in fig 6. for the determinations of the total transition intensities.

7. Energy Levels and Transition Intensities

The foregoing results can be summarized in a consistent way in the decay scheme given in fig. 6. The only gamma ray not accounted for is the very weak 744 keV transition found in the internal conversion spectrum. A 681 keV gamma ray has been proposed in the decay scheme between the states D and C, but it has actually not been observed. Its existence is inferred from the beta-gamma coincidences in which the transition CB was shown to be coincident with the β_3 beta group. A weak gamma ray at 681 keV would be very hard to detect in the gamma spectra due to the Compton background from the strong transitions around 900 keV. The upper limit of 0.5 % given for its intensity is based on an estimate of the

sensitivity which could be obtained for gamma rays of this energy in the various coincidence experiments.

The weak 92 keV radiation observed in the beta spectrometer has been placed tentatively between levels F and G, but this position could not be

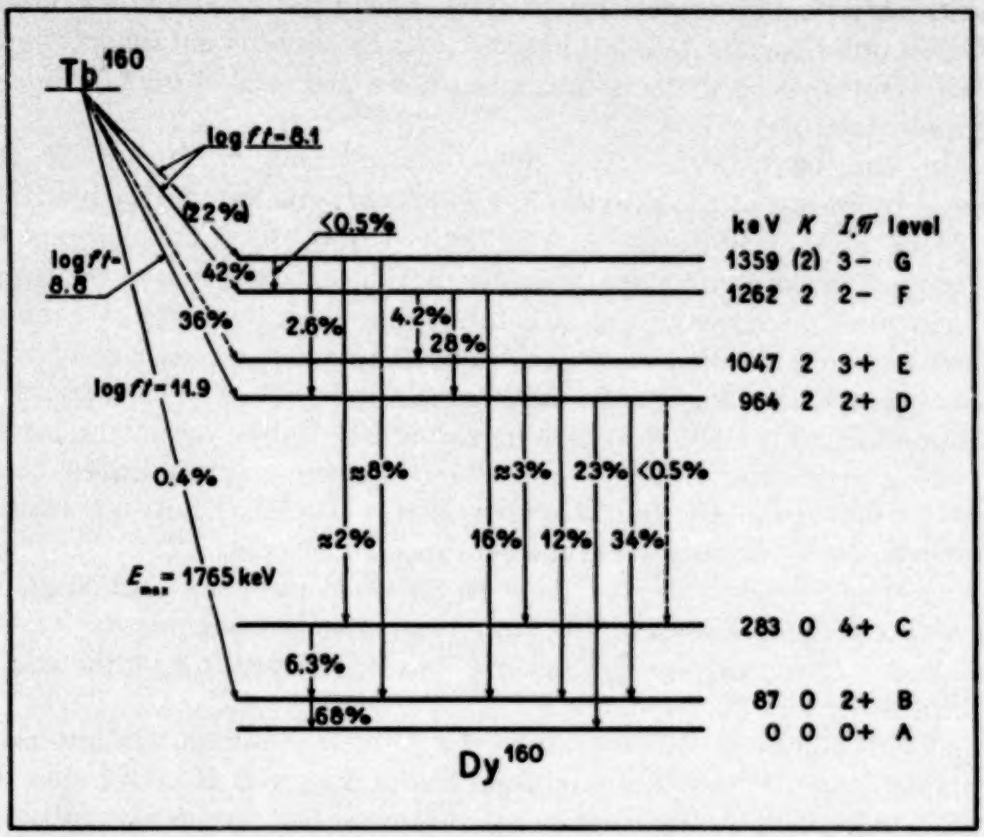

Fig. 6. Decay scheme of Tb^{160}. The beta ray groups are deduced from the Fermi analysis with the exception of the group leading to level E which is indicated with a dotted line. The intensities of the transitions in Dy^{160} are total gamma and internal conversion intensities given as percentage of all disintegrations.

supported by coincidence measurements. The only other possibility for fitting it into the decay scheme is between levels D and E but this alternative seems very unlikely from a consideration of the spacing of these two levels as derived from the conversion data.

The level energies given in fig. 6 are all based on internal conversion and gamma ray measurements. From a comparison of these energies with the maximum energies of the beta ray components obtained by Fermi analysis (table 2) it can be seen that a satisfactory agreement is obtained if one assumes that the β_4 transition leads to level B. This is the only beta ray whose position could not be ascertained by the beta-gamma coincidences.

If one considers the total intensity of the gamma and internal conversion radiation into and out of the various levels shown in fig. 6 and compares

with the intensities of the beta groups as derived in the Fermi analysis, some discrepancies appear. In the case of level B, however, a subtraction analysis of the six transitions going into and out of the level is very questionable, considering the uncertainties involved and the small net intensity. The disagreement in the case of levels D and E is apparently more serious. Level E is fed by the 216 keV gamma ray of 4 % intensity, but it is deexcited by two gamma rays of total intensity 15 %. The Fermi plot showed no beta component to this level. The data for level D, on the other hand, show a 26 % net intensity of gamma rays out of the level, while the Fermi analysis indicates a 36 % beta group to this state. From the gamma ray data it thus seems likely that two beta rays exist which lead to levels E and D, respectively, and with a total intensity equal to that of the observed β_3 group. The assumption that this group is a doublet is, however, not incompatible with the data presented in fig. 2, if the uncertainties involved in the Fermi analysis of a complex beta spectrum are taken into account. The strong beta group β_2 was shown to excite level F and in this case the agreement between the beta ray data and the gamma ray intensities is satisfactory. If, finally, one considers the low-energy group β_1, the intensity as given by Fermi analysis comes out somewhat high but, as previously stressed, the figures for this transition can be only of approximate nature.

The information obtained in part 6 on the multipole orders of the various transitions allow us to give rather definite spin and parity assignments to the energy levels in Dy^{160}. The spin and parity 2+ assigned to the first excited state is strongly suggested by the conversion data, if one assumes that the ground state has spin 0 and even parity. The character of level C was not directly proved in this investigation but energy considerations make it very likely that states B and C can be classified as the second and third members of a rotational band associated with the ground state, in which case state C has spin 4, even parity. This assumption is supported by the E2 character of transition CB and the absence of a 283 keV crossover to the ground state.

The ground state transition DA must be a pure multipole and from table 6 it must then be assigned as E2. This means that the spin and parity of level D is 2+ which is consistent with the E2 character of gamma ray DB and with the existence of the transition DC. Level E must have the same parity as level D since both are excited by E1 transitions from level F.
Furthermore, two gamma rays have been observed from level E to levels B and C, of which transition EB is M1 or E2, whereas no ground state transition was found. From this information its seems most likely that level E has spin 3 or 4, even parity. A 2− assignment to level F is strongly suggested by the intense E1 transition to level B and the absence of other radiations

leading to the ground state rotational band. Having fixed the characters of level F one can now make a choice between the alternatives 3 and 4 for the spin of level E since only spin 2 is compatible with the E1 multipolarity of transition FE.

Odd parity and spin 1, 2, or 3 is suggested for level G by the E1 transition that takes place from this state to the 2+ member of the ground state rotational band. Spins 1 and 2, however, would demand E3 and M2 multipolarity, respectively, for the transition GC and, in either case, the corresponding K-conversion line would probably have been detected. The exclusion of these alternatives is also suggested by lifetime arguments, and, in the case of the 1− assignment, furthermore by the absence of a transition to the ground state. Hence, we conclude that level G is most likely to have the characters 3−.

This assignment was moreover supported by the angular correlation of the 196 keV and 1080 keV gamma rays which was measured with the fast-slow circuit and a source of Tb_2O_3 dissolved in HCl. A 3 mm lead absorber was inserted in front of the high-energy crystal to prevent low-energy gamma rays produced by scattering in this counter from reaching the low-energy detector. After correction for the finite size of the detectors[19]) the anisotropy was found to be -0.25 ± 0.05 in fair agreement with the theoretical value -0.20 for the spin sequence 3-4-2, assuming pure dipole and pure quadrupole radiations. No significant P_4 term was observed in the correlation.

8. Discussion

Dy^{160} is situated in a region of strongly deformed nuclei and is therefore, on the basis of the unified model, expected to exhibit a ground state rotational spectrum of characters 0+, 2+, 4+, . . . Moreover, electric quadrupole and electric octupole vibrational states are likely to occur at higher excitation energies, and associated with these states one expects to find rotational sequences of states in which the separation between the first and second member is of the same order of magnitude as in the ground state band [1]). Each rotational band is characterized by the quantum number K which represents the projection of the total angular momentum along the nuclear symmetry axis. Quadrupole vibrations may either have $K = 0$ (beta vibrations) and the associated band will then contain the members 0+, 2+, 4+, . . . or they will have $K = 2$ (gamma vibrations), the band in that case comprising the states 2+, 3+, 4+, . . . The octupole vibrations are expected to have odd parity and $K = 0$, 1, 2 and 3, and the associated band will consist of the levels $I = K, K+1, K+2, \ldots$ with the exception of the $K = 0$ case where the sequence is expected to be 1, 3, 5, . . .

If one considers the energies, spins and parities of the high-lying excited

states proposed in fig. 6, it appears very likely that these states form two rotational bands of the nature described above. The two even parity states D and E may possibly be interpreted as the two first members of a band associated with gamma vibrations and the odd parity levels G and F similarly as the first two members of a band connected with octupole vibrations and having $K = 2$. The occurrence of these types of vibrations is in good agreement with observations made on neighbouring even nuclei such as Sm^{152} [9]), Gd^{154} [20, 21]) Gd^{156} [21]) and W^{182} [22]), but a more crucial test on the validity and internal consistency of the interpretation consists in a consideration of the branching ratios in the gamma decays of the states involved. The gamma branching ratios in the emission of various multipole radiations which are not K-forbidden, from a given state to different members of a rotational sequence, have been treated theoretically by Alaga *et al.* [23]) and it has been shown that the ratios of the reduced transition probabilities can be expressed in terms of vector addition coefficients involving only the multipole order and the spins and K-values of the states in question. In table 7 a number of branching ratios have been

TABLE 7

Theoretical ratios of reduced transition probabilities [23]) in the decay of states D, E, F and G.

State D (2+):	
$K = \begin{cases} 0 \\ 1 \\ 2 \end{cases}$ implies B(E2, D → A) : B(E2, D → B) : B(E2, D → C) =	$\begin{cases} 0.7 : 1.0 : 1.8 \\ 2.8 : 1.0 : 2.3 \\ 0.7 : 1.0 : 0.05 \end{cases}$
Experimental ratio assuming pure E2 radiation:	$0.42 : 1.0 : < 0.05$
State E (3+):	
$K = 2$ implies B(E2, E → B) : B(E2, E → C)	$= 2.5$
Experimental ratio assuming pure E2 radiation:	≈ 1.3
State F (2−):	
$K = \begin{cases} 1 \\ 2 \end{cases}$ implies B(E1, F → D) : B(E1, F → E)	$= \begin{cases} 0.5 \\ 2.0 \end{cases}$
Experimental ratio assuming pure E1 radiation:	2.6
State G (3−):	
$K = \begin{cases} 2 \\ 3 \end{cases}$ implies B(E1, G → D) : B(E1, G → E)	$= \begin{cases} 0.71 \\ 2.8 \end{cases}$
Experiments inconclusive since transition G → E was not observed.	

calculated from the theory for different K-assignments and are compared with the experimental data.

State D has the characters 2+ and decays by two E2 radiations to the 0+ and 2+ members of the ground state rotational band. A third radiation has been assumed in the decay scheme going to the 4+ state but nothing

is known experimentally about its multipole order. Spin 2 allows the possibilities $K = 0, 1, 2$, and in all these cases E2 transitions to the ground state band are K-allowed. The theoretical E2 branching ratios for the three values of K are given in table 7 together with the measured branching ratios corrected for the fifth power energy dependence. It can be seen that the $K = 2$ assignment gives a satisfactory fit, whereas the data definitely preclude $K = 0$ and 1 even if one admits large M1 admixtures in the transitions DB and DC.

The information on the radiations from level E is less clear, since the M1—E2 mixture ratios in the transitions to the 2+ and 4+ members of the ground state rotational band cannot be estimated from the measurements. Assuming $K = 2$ and both radiations to be pure E2 it appears that the theoretical and experimental branching ratios differ by a factor of two. This discrepancy, however, is of the order of magnitude expected from the uncertainties in the experimental data in this particular case.

Two E1 radiations are indicated on fig. 6 going from the 2— level F to the 2+, 3+ rotational family having $K = 2$. A third electric dipole transition takes place from level F to the 0, 2+ member of the ground state band and this transition is considerably slower than the 216 keV and 298 keV radiations. This fact seems to rule out a $K = 0$ assignment for level F, since in that case the opposite situation would be expected due to K-forbiddenness. Hence, one is left with the alternatives $K = 1$ and 2, and for these cases the theoretical branching ratios are given in table 7 together with the experimental value obtained after correction for the third power energy dependence. It can be seen that the data strongly suggest $K = 2$ for level F in accordance with the observed slowness of transition FB.

Level G has spin 3, odd parity and has been found to decay by E1 radiations to the $K = 0+$ and $K = 2+$ bands. From similar arguments as used in the case of level F the assignments $K = 2$ or 3 appear as the most likely but the data do not allow us to decide unambiguously between these alternatives since only the 395 keV transition GD has been observed to the $K = 2$ band. Using the theoretical E1 branching ratios given in table 7 for $K = 2$ and 3 and the observed intensity of the 395 keV gamma ray, the strength of a 310 keV E1 transition between levels G and E turns out to be so small that the transition would have remained undetected both in the electron and gamma ray spectra. However, the 97 keV energy difference between levels F and G is so near the spacing between the first two members of the ground state band that it appears probable that the two states belong to the same family having $K = 2$.

One might speculate why no $K = 0$ bands associated with quadrupole and octupole vibrations are observed in the decay of Tb^{160}. Particularly striking is the absence of an analogous state to the 0, 1— state occurring

at 960 keV excitation energy in Sm^{152} [24, 9]). It is probable that this feature can be accounted for by the action of K-forbiddenness: From the proposed decay scheme it seems reasonable to assign $I = K = 2$ or 3 to the ground state of Tb^{160} in which case the high ft-value for the group β_4 leading to the 0, 2+ state would be explained from the K-selection rules. Higher lying states with low spin and $K = 0$ would also be populated very weakly by beta transitions, so that radiations from such states probably would have been too weak for detection in this investigation. Similar arguments apply when one considers the possible population of high-lying $K = 0$ states by gamma radiation from the $K = 2$ bands. For instance, a hypothetical 0, 1− state around 1 MeV excitation energy might be fed by M1 or E2 gamma rays from level F but the M1 transition would be very weak due to K-forbiddenness and the E2 transition rate would be reduced owing to the competition of the E1 radiations to the 2+ rotational band. The absence of other $K = 0$ levels in the decay scheme of fig. 6 can be accounted for in a similar way. More profitable approaches to the problem of finding such states in Dy^{160} may, therefore, be Coulomb excitation experiments or a more detailed investigation of the decay of Ho^{160} [25, 26]).

The author is very indebted to Professor Niels Bohr for the excellent working conditions at his Institute and to Professor A. Bohr and Dr. B. Mottelson for their continued interest and helpful suggestions concerning this work. Thanks are also due to Mr. O. B. Nielsen for the use of the six-gap beta ray spectrometer, to Mr. B. S. Madsen for the loan of the kicksorter, and to Mr. C. Andreassen for assistance in constructing part of the electronic equipment. It is a pleasure to acknowledge a special indebtedness to Professor S. Frankel for his generous assistance in the design of the fast-slow coincidence circuit.

References

1) K. Alder, A. Bohr, T. Huus, B. Mottelson and A. Winther, Revs. Mod. Phys. **28** (1956) 432
2) P. H. Stelson and F. K. McGowan, Phys. Rev. **99** (1955) 112
3) M. S. Moore, C. M. Class, F. W. Prosser Jr. and J. P. Schiffer, Bull. Am. Phys. Soc. **1** (1956) 88
4) T. Huus, private communication
5) L. Grodzins, Bull. Am. Phys. Soc. **1** (1956) 329
6) S. B. Burson, W. C. Jordan and J. M. LeBlanc, Phys. Rev. **94** (1954) 103
7) V. Keshishian, H. W. Kruse, R. J. Klotz and C. M. Fowler, Phys. Rev. **96** (1954) 1050
8) G. Bertolini, M. Bettoni and E. Lazzarini, Nuovo Cimento **3** (1956) 754
9) O. Nathan and M. A. Waggonner, Nuclear Physics **2** (1956/57) 548
10) N. H. Lazar, R. C. Davis and P. R. Bell, Nucleonics **14** no. 4 (1956) 52
11) J. M. Cork, C. E. Branyan, W. C. Rutledge, A. E. Stoddard and J. M. LeBlanc, Phys. Rev. **78** (1950) 304
12) S. B. Burson, K. W. Blair and D. Saxon, Phys. Rev. **77** (1950) 403

13) M. E. Rose in Beta- and Gamma-Ray Spectroscopy, edited by K. Siegbahn (North Holland Publishing Company, Amsterdam, 1955) and M. E. Rose, G. H. Goertzel and C. J. Swift, privately circulated tables of L-conversion coefficients
14) L. J. Shavtvalov, Izv. Akad. Nauk. SSSR Ser. Fiz. **17** (1953) 503
15) Harold Jaffe, Thesis (1954) UCRL-2537 (unpublished)
16) M. A. Waggoner, Phys. Rev. **80** (1950) 489
17) A. H. Wapstra, Ark. f. Fysik **7** (1954) 275
18) L. A. Sliv and J. M. Band, Tables of Gamma-Ray Internal Conversion Coefficients, Part 1 (Isdatelstvo Akademia Nauk SSSR, Moskow and Leningrad, 1956)
19) A. M. Feingold and S. Frankel, Phys. Rev. **97** (1955) 1025
20) F. S. Stephens Jr., Thesis (1955) UCRL-2970
21) R. Sheline, P. Gregers Hansen and O. B. Nielsen, to be published
22) F. Boehm, P. Marmier and J. W. M. DuMond, Phys. Rev. **95** (1954) 864
23) G. Alaga, K. Alder, A. Bohr and B. R. Mottelson, Mat. Fys. Medd. Dan. Vid. Selsk. **29** (1955) no. 6
24) L. Grodzins, Bull. Am. Phys. Soc. **1** (1956) 163
H. Kendall and L. Grodzins, Bull. Am. Phys. Soc. **1** (1956) 164
25) W. E. Nervik and G. T. Seaborg, Phys. Rev. **97** (1955) 1092
26) J. W. Mihelich, B. Harmatz, T. H. Handley and J. J. Pinajian, Bull. Am. Phys. Soc. **1** (1956) 330

Nuclear Physics **4** (1957) 145—156; © *North-Holland Publishing Co., Amsterdam*
Not to be reproduced by photoprint or microfilm without written permission from the publisher

TIME REVERSAL AND POLARIZATION PHENOMENA IN $N+N \rightleftarrows d+\pi$ REACTIONS

L. I. LAPIDUS

Joint Institute of Nuclear Research, Laboratory of Theoretical Physics
Dubna, U.S.S.R.

Received 26 February 1957

Abstract: An analysis of polarization phenomena in $N+N \rightleftarrows d+\pi$ reactions reveals how time-reversal invariance leads to connections between polarization phenomena in direct and inverse reactions. The Wolfenstein theorem has been extended to the case of a binary reaction. Expressions are given for various observable quantities in $N+N \rightleftarrows d+\pi$ reactions for the case when only s, p and d waves with $J \leq 2$ are considered as well as for the general case.

1. Introduction

It is well known [1, 2, 3]), that the condition of invariance under change of the sign of time leads to symmetry of the S-matrix (notations of ref. [2]) with correction introduced in ref. [3])):

$$S^J_{\alpha' s' l'; \alpha s l} = S^J_{\alpha s l; \alpha' s' l'}. \tag{1}$$

A consequence of this condition is, that for interacting spinless particles, the differential cross-sections for direct and inverse reactions are equal (to an accuracy of the square of the ratio of the relative momenta in the direct and inverse reactions). For non-zero spin particles, for which the inverse process noticeably differs from the time-reversed process, this same condition leads to equality of the direct and inverse reaction cross-sections averaged over the spins. However, for non-zero spin interacting particles not only the interaction cross-section for unpolarized particles but also the mean values of the spin operators of the direct and inverse processes can be expressed through the S-matrix elements. In view of the existence of condition (1) it would seem of interest to examine its consequences for polarization phenomena in the direct and inverse reactions and to attempt to find some relations which would be similar to those which connect the cross-sections for interaction of an unpolarized beam with an unpolarized target. A relation of this type has been discussed in the literature in connection with work pertaining to polarization processes in elastic scattering. It has been shown in ref. [4, 5]) that in the case of spin $\frac{1}{2}$ particles elastically scattered on a target of arbitrary spin (the principle of detailed balance brings an identity) the requirement of invariance under time reversal leads to a relation between the particle polarization $\langle \hat{\sigma} \rangle_t$ due to

interaction of unpolarized particles and the azimuthal asymmetry I_p of the cross-section for polarized particles scattered on an unpolarized target. This relation has the form

$$I_p = I_0(\theta)\,\langle\hat{\sigma}\rangle_t \cdot \mathbf{N} \tag{2}$$

where $I_0(\theta)$ is the scattering cross-section for unpolarized particles and $\mathbf{N}$ is the direction of polarization of the incident beam.

According to Lakin [6]) a similar relation is also valid for elastic scattering of spin 1 particles.

In the present work we have carried out a phenomenological analysis of polarization phenomena in the reactions

$$\mathrm{p+p} \to \mathrm{d}+\pi^+ \quad \text{(A)} \qquad \mathrm{n+p} \to \mathrm{d}+\pi^0 \quad \text{(C)}$$

$$\mathrm{d}+\pi^+ \to \mathrm{p+p} \quad \text{(B)} \qquad \mathrm{d}+\pi^0 \to \mathrm{n+p} \quad \text{(D)}$$

with the purpose of ascertaining on the basis of this special case just what are the consequences of condition (1) for the more general case of binary reactions (nuclear reactions involving two particles in the initial and final states).

The chief result obtained by us is an extension of Wolfenstein's theorem [2]) to the reaction under consideration. As by-products we have obtained some general expressions for various observable quantities in reactions (A) and (B) in terms of the interaction amplitude; these expressions may be useful in reconstructing the amplitude for experimental data.

2. S-Matrix

Let l' and l denote the relative angular momenta of the initial and final states of reaction (B) and choose axis z along the direction of the incident π-mesons. Furthermore, let $C^{j_1 j_2 j}_{m_1 m_2}$ denote the Clebsch coefficients, ψ_M the four spin functions of the N—N system ($M = +1, 0, -1$ for a triplet and $M \equiv \mathrm{C}$ for a singlet) and φ_m the deuteron spin functions. The S-matrix for reaction (B) can be represented as

$$S_B = \sum_{m,\,M} \psi_M \Big\{ \sum_{Jll'}{}' \,(2l'+1)^{\frac{1}{2}} (l|S^B_J|l') C^{lsJ}_{m-M,\,M} C^{l'1J}_{0m} Y^{m-M}_l(\theta,\varphi) \Big\} \varphi^+_m \tag{3}$$

(s is the spin of the nucleon system). The S-matrix for reaction (A) will then have the form

$$S_A = \sum_{m,\,M} \varphi_m \Big\{ \sum_{Jll'}{}' \,(2l+1)^{\frac{1}{2}} (l'|S^A_J|l) C^{l'1J}_{M-m,\,m} C^{lsJ}_{0M} Y^{M-m}_{l'}(\theta,\varphi) \Big\} \psi^+_M . \tag{4}$$

Condition (1) implies that $(l|S^B_J|l') = (l'|S^A_J|l) = (l'|S_J|l)$. (It is important here that the S-matrix elements are defined as in ref. [3])).

If we consider only the interaction of mesons in the s, p and d states we find that the transitions allowed by the law of conservation of total angular

momentum and parity are $^3P_0 \to {}^1S_0$ (amplitude $(0|S_0|1) \equiv a_0$), $^3S_1 \to {}^3P_1$ (amplitude a_1), $^3P_2 \to {}^1D_2$ (a_2), $^3D_1 \to {}^3P_1(a_3)$, $^3D_2 \to {}^3P_2(a_4)$, $^3D_2 \to {}^3F_2(a_5)$, $^3D_3 \to {}^3F_3(a_6)$. In the following analysis we shall neglect the transition $^3D_3 \to {}^3F_3$ with $J = 3$ and retain transitions with $J \leqq 2$.†

The S-matrices for reactions (A) and (B) can be represented in the form

$$\begin{aligned}
&4\sqrt{4\pi}\,S_B = \psi_C\{-\sqrt{2}\,a_0(\mathbf{k}_0\cdot\boldsymbol{\varphi}^+)+\sqrt{10}\,a_2[3t(\mathbf{k}\cdot\boldsymbol{\varphi}^+)-(\mathbf{k}_0\cdot\boldsymbol{\varphi}^+)]\}+i\sqrt{6}\,a_1(\mathbf{k}\cdot[\boldsymbol{\psi}\wedge\boldsymbol{\varphi}^+])\\
&+i\sqrt{3}\,a_3\{3t(\mathbf{k}_0\cdot[\boldsymbol{\psi}\wedge\boldsymbol{\varphi}^+])-(\mathbf{k}\cdot[\boldsymbol{\psi}\wedge\boldsymbol{\varphi}^+])-2[(\boldsymbol{\psi}\cdot\mathbf{n})(\mathbf{k}_0\cdot\boldsymbol{\varphi}^+)+(\boldsymbol{\psi}\cdot\mathbf{k}_0)(\mathbf{n}\cdot\boldsymbol{\varphi}^+)]\}\\
&+i\sqrt{5}\,a_4\{3t(\mathbf{k}_0\cdot[\boldsymbol{\psi}\wedge\boldsymbol{\varphi}^+])-(\mathbf{k}\cdot[\boldsymbol{\psi}\wedge\boldsymbol{\varphi}^+])+[(\boldsymbol{\psi}\cdot\mathbf{n})(\mathbf{k}_0\cdot\boldsymbol{\varphi}^+)+(\boldsymbol{\psi}\cdot\mathbf{k}_0)(\mathbf{n}\cdot\boldsymbol{\varphi}^+)]\} \qquad (3')\\
&+i\sqrt{10}\,a_5\{(5t^2-1)(\mathbf{k}\cdot[\boldsymbol{\psi}\wedge\boldsymbol{\varphi}^+])-2t(\mathbf{k}_0\cdot[\boldsymbol{\psi}\wedge\boldsymbol{\varphi}^+])+[(\boldsymbol{\psi}\cdot\mathbf{n})(\mathbf{k}_0\cdot\boldsymbol{\varphi}^+)\\
&+(\boldsymbol{\psi}\cdot\mathbf{k}_0)(\mathbf{n}\cdot\boldsymbol{\varphi}^+)]-5t[(\boldsymbol{\psi}\cdot\mathbf{n})(\mathbf{k}\cdot\boldsymbol{\varphi}^+)+(\mathbf{k}\cdot\boldsymbol{\psi})(\mathbf{n}\cdot\boldsymbol{\varphi}^+)]\}
\end{aligned}$$

and

$$\begin{aligned}
&4\sqrt{4\pi}\,S_A = \{-\sqrt{2}\,a_0(\mathbf{k}\cdot\boldsymbol{\varphi})+\sqrt{10}\,a_2[3t(\mathbf{k}_0\cdot\boldsymbol{\varphi})-(\mathbf{k}\cdot\boldsymbol{\varphi})]\}\psi_C^+ + i\sqrt{6}\,a_1(\mathbf{k}_0\cdot[\boldsymbol{\varphi}\wedge\boldsymbol{\psi}^+])\\
&+i\sqrt{3}\,a_3\{3t(\mathbf{k}\cdot[\boldsymbol{\varphi}\wedge\boldsymbol{\psi}^+])-(\mathbf{k}_0\cdot[\boldsymbol{\varphi}\wedge\boldsymbol{\psi}^+])-2[(\boldsymbol{\varphi}\cdot\mathbf{n})(\mathbf{k}\cdot\boldsymbol{\psi}^+)+(\boldsymbol{\varphi}\cdot\mathbf{k})(\mathbf{n}\cdot\boldsymbol{\psi}^+)]\}\\
&+i\sqrt{5}\,a_4\{3t(\mathbf{k}\cdot[\boldsymbol{\varphi}\wedge\boldsymbol{\psi}^+])-(\mathbf{k}_0\cdot[\boldsymbol{\varphi}\wedge\boldsymbol{\psi}^+])+[(\boldsymbol{\varphi}\cdot\mathbf{n})(\mathbf{k}\cdot\boldsymbol{\psi}^+)+(\boldsymbol{\varphi}\cdot\mathbf{k})(\mathbf{n}\cdot\boldsymbol{\psi}^+)]\} \qquad (4')\\
&+i\sqrt{10}\,a_5\{(5t^2-1)(\mathbf{k}_0\cdot[\boldsymbol{\varphi}\wedge\boldsymbol{\psi}^+])-2t(\mathbf{k}\cdot[\boldsymbol{\varphi}\wedge\boldsymbol{\psi}^+])+[(\mathbf{k}\cdot\boldsymbol{\varphi})(\mathbf{n}\cdot\boldsymbol{\psi}^+)\\
&+(\mathbf{n}\cdot\boldsymbol{\varphi})(\mathbf{k}\cdot\boldsymbol{\psi}^+)]-5t[(\mathbf{k}_0\cdot\boldsymbol{\varphi})(\mathbf{n}\cdot\boldsymbol{\psi}^+)+(\mathbf{n}\cdot\boldsymbol{\varphi})(\mathbf{k}_0\cdot\boldsymbol{\psi}^+)]\}
\end{aligned}$$

where $\mathbf{k}_0$ and $\mathbf{k}$ are unit vectors of the relative momenta in the initial and final states, $t = (\mathbf{k}_0\cdot\mathbf{k}) = \cos\theta$, $\mathbf{n} = \mathbf{k}_0 \wedge \mathbf{k}$. (The quantities a_1, a_2, a_3, ... in (3) and (4) differ by the factor $(2l+1)^{\frac{1}{2}}$ from the respective quantities in ref. [8]).

In the general case, the S-matrix for reaction (A) can be represented in the form

$$\begin{aligned}
&\sqrt{4\pi}\,S_A = [A(\mathbf{k}\cdot\boldsymbol{\varphi})+B(\mathbf{k}_0\cdot\boldsymbol{\varphi})]\psi_C^+ + i\{C[(\boldsymbol{\varphi}\cdot\mathbf{n})(\mathbf{k}\cdot\boldsymbol{\psi}^+)+(\boldsymbol{\varphi}\cdot\mathbf{k})(\mathbf{n}\cdot\boldsymbol{\psi}^+)]\\
&+D[(\boldsymbol{\varphi}\cdot\mathbf{n})(\mathbf{k}_0\cdot\boldsymbol{\psi}^+)+(\boldsymbol{\varphi}\cdot\mathbf{k}_0)(\mathbf{n}\cdot\boldsymbol{\psi}^+)]+E(\mathbf{k}\cdot[\boldsymbol{\varphi}\wedge\boldsymbol{\psi}^+])+F(\mathbf{k}_0\cdot[\boldsymbol{\varphi}\wedge\boldsymbol{\psi}^+])\} \qquad (5)
\end{aligned}$$

($\sqrt{4\pi}$ and the multiplier i have been retained for better conformity with (4').) In virtue of condition (1), for reaction (B) we analogously obtain

$$\begin{aligned}
&\sqrt{4\pi}\,S_B = \psi_C[A(\mathbf{k}_0\cdot\boldsymbol{\varphi}^+)+B(\mathbf{k}\cdot\boldsymbol{\varphi}^+)]+i\{C[(\mathbf{k}_0\cdot\boldsymbol{\psi})(\mathbf{n}\cdot\boldsymbol{\varphi}^+)+(\mathbf{n}\cdot\boldsymbol{\psi})(\mathbf{k}_0\cdot\boldsymbol{\varphi}^+)]\\
&+D[(\mathbf{k}\cdot\boldsymbol{\psi})(\mathbf{n}\cdot\boldsymbol{\varphi}^+)+(\mathbf{n}\cdot\boldsymbol{\psi})(\mathbf{k}\cdot\boldsymbol{\varphi}^+)]+E(\mathbf{k}_0\cdot[\boldsymbol{\psi}\wedge\boldsymbol{\varphi}^+])+F(\mathbf{k}\cdot[\boldsymbol{\psi}\wedge\boldsymbol{\varphi}^+]). \qquad (6)
\end{aligned}$$

Restricting our consideration to s, p and d waves with $J \leqq 2$ we get

† Expansion in the conservative quantity J seems to be more rational than expansion in terms of l. Use of the latter may sometimes lead to misunderstandings. Thus, for example, expansion in l for analysis of p−p scattering led to the result [7]) (which is wrong [2])) that mixing coefficients enter into the expression for the integrated cross-section; this mistake was due to incomplete account of states with various l for a given J.

$$2A = -(2a_0+\sqrt{10}\,a_2);\ 2B = 3\sqrt{10}\,a_2 t;\ 4C = -2\sqrt{3}a_3+\sqrt{5}\,a_4+\sqrt{10}\,a_5$$
$$4D = -5\sqrt{10}\,a_5 t;\ 4E = (3\sqrt{3}\,a_3+3\sqrt{5}\,a_4-2\sqrt{10}\,a_5)t; \qquad (7)$$
$$4F = \sqrt{6}\,a_1-\sqrt{3}\,a_3-\sqrt{5}\,a_4+\sqrt{10}\,a_5(5t^2-1).$$

In the general case

$$A(-t) = A(t);\quad B(-t) = -B(t);\quad C(-t) = C(t)$$
$$D(-t) = -D(t);\quad E(-t) = -E(t);\quad F(-t) = F(t). \qquad (7')$$

3. Interaction Cross-Section for Unpolarized Particles

Equality of the interaction cross-sections for unpolarized particles immediately follows from (5) and (6): $4I_0^{(A)}(\theta) = 3I_0^{(B)}(\theta)$; in this case the following equation holds (the ratio of the squares of the relative momenta being omitted)

$$16\pi I_0^{(A)}(\theta) = 12\pi I_0^{(B)}(\theta) = |A|^2+|B|^2+2\,\mathrm{Re}\,[(A^+B)+2(E^+F)]\cos\theta$$
$$+2|E|^2+2|F|^2+2\sin^2\theta\,[|C|^2+|D|^2+2\,\mathrm{Re}\,(C^+D)\cos\theta]. \qquad (8)$$

Considering only s, p and d waves with $J \leqq 2$ we obtain from (7) and (8)

$$64\pi I_0^{(A)}(\theta) = 48\pi I_0^{(B)}(\theta) = 4\varrho_0^2+12\varrho_1^2+10\varrho_2^2(1+3\cos^2\theta)$$
$$+[6(\sqrt{2}\,\omega_{13}+\sqrt{10}\,\omega_{14}+\sqrt{5}\,\omega_{34})-4\sqrt{10}\,\omega_{02}+4\sqrt{15}\,\omega_{15}+2\sqrt{30}\,\omega_{35}](3\cos^2\theta-1)$$
$$+3[\varrho_3^2(5-3\cos^2\theta)+5\varrho_4^2(1+\cos^2\theta)]+10\varrho_5^2(1+6\cos^2\theta-5\cos^4\theta) \qquad (8')$$
$$+10\sqrt{6}\,\omega_{45}(10\cos^4\theta-9\cos^2\theta+1)$$

$$(a_m = \varrho_m e^{i\alpha_m};\quad \omega_{mn} = \varrho_m\varrho_n\cos(\alpha_m-\alpha_n))$$

which is identical with previously obtained results [8,9]).

Before passing over to a comparison of the polarization phenomena in reactions (A) and (B) it should be noted that a study of reaction (B) for a total meson energy, E_π, should enable one to obtain information concerning reaction (A) for a proton (kinetic) energy W defined by

$$W = \frac{M_d}{M}E_\pi + \frac{\mu}{M}\mu c^2 - \varepsilon\left(\frac{M_d}{M}+1\right) \approx 2E_\pi \qquad (9)$$

(M_d, M, μ are respectively the deuteron, nucleon and π-meson masses, ε is the deuteron binding energy).

From (9) it follows, for example, that by using a π^+-meson beam of energy $E_\pi = 320+140 = 460$ MeV to study reaction (B) (such beams can be obtained from the 680 MeV accelerator of the Joint Institute of Nuclear Research) one may obtain information on meson formation in reaction (A) for proton energies of approximately 920 MeV, an energy which is appreciably greater than that of the accelerator particles. This "energy gain" is due to

the fact that in reaction (A) a considerable fraction of the energy is spent on the motion of the centre of mass of the system whereas in the inverse reaction the energy in the c.m.s. does not appreciably differ from that in the laboratory system.

4. Polarization Phenomena in Direct and Inverse Reactions

4.1. CROSS-SECTIONS

We shall now compare the data obtained by studying polarization phenomena. In view of isobaric invariance we may directly consider the general process $N+N \rightleftarrows d+\pi$ where N denotes a nucleon and π a $\pi^{+,0}$ meson. The cross-section for meson production in reaction (A) by polarized protons can be expressed by the formulae

$$I(\theta, \varphi) = I_0(\theta)+p \cos\varphi\, P(\theta) = I_0(\theta)+pI_y \tag{10}$$

(**p** is the nucleon beam polarization; the y-axis is chosen along the direction of polarization).

Using the formula $(\hat{\boldsymbol{\sigma}}_1 \cdot \mathbf{p})S = S_C(\boldsymbol{\psi} \cdot \mathbf{p})+(\mathbf{S} \cdot \mathbf{p})\psi_C+i([\mathbf{p} \wedge \boldsymbol{\psi}] \cdot \mathbf{S})$ we obtain $(S = S_C\psi_C+(\mathbf{S} \cdot \boldsymbol{\psi}))$

$$\begin{aligned} &16\pi I_{p_1}(\theta) \cos\varphi = 4\pi \operatorname{tr} S_A(\hat{\boldsymbol{\sigma}}_1 \cdot \mathbf{p})S_A^+ = (\mathbf{n} \cdot \mathbf{p})P_1(\theta), \\ &P_1(\theta) = 2 \operatorname{Im}\{[C^+(A+B\cos\theta)+D^+(A\cos\theta+B)+B^+E+AF^+] \\ &\quad +[\sin^2\theta(CD^+)+F^+E+C(E+F\cos\theta)^+ +D(E\cos\theta+F)^+]\}. \end{aligned} \tag{10'}$$

The first four terms in the expression for $P_1(\theta)$ which reflect the contribution of singlet-triplet transitions in reaction (A) do not change their sign when $\theta \to \pi-\theta$ that is, they are symmetric with respect to 90°; the remaining terms which reflect the contribution from triplet-triplet transitions change sign when $\theta \to \pi-\theta$ that is, they vanish for $\theta = 90°$.

Comparing the formulae

$$(\hat{\boldsymbol{\sigma}}_2 \cdot \mathbf{p})S = -[S_C(\boldsymbol{\psi} \cdot \mathbf{p})+(\mathbf{S} \cdot \mathbf{p})\psi_C]+i([\mathbf{p} \wedge \boldsymbol{\psi}] \cdot \mathbf{S})$$

with the previous expression for $(\hat{\boldsymbol{\sigma}}_1 \cdot \mathbf{p})\, S$ it can be seen that for a polarized target the azimuthal asymmetry expression differs from (10′) by the signs of the first four terms:

$$\begin{aligned} &16\pi\, I_{p_2}(\theta) \cos\varphi = 4\pi \operatorname{tr} S_A(\hat{\boldsymbol{\sigma}}_2 \cdot \mathbf{p})S_A^+ = (\mathbf{n} \cdot \mathbf{p})P_1'(\theta), \\ &P_1'(\theta) = 2 \operatorname{Im}\{-[C^+(A+B\cos\theta)+D^+(A\cos\theta+B)+B^+E+AF^+] \\ &\quad +[\sin^2\theta(CD^+)+F^+E+C(E+F\cos\theta)^+ +D(E\cos\theta+F)^+]\}. \end{aligned} \tag{10''}$$

On the other hand when the deuteron target is unpolarized we obtain from (6) the following expression for the nucleon polarization in reaction (B):

$$12\pi I_0^{(B)}(\theta)\langle\hat{\boldsymbol{\sigma}}_1\rangle_f = 4\pi \operatorname{tr} S_B^+ \hat{\boldsymbol{\sigma}}_1 S_B = \mathbf{n}P_1(\theta); \tag{11}$$

$P_1(\theta)$ is defined in (10′). For the polarization of the other nucleon we get

$$12\pi I_0^{(B)}(\theta)\,\langle\hat{\boldsymbol{\sigma}}_2\rangle_f = \mathbf{n}P_1'(\theta), \tag{11'}$$

where $P_1'(\theta)$ is defined in (10''). From (7'), (10'), (10''), (11') and (8),

$$\langle\hat{\boldsymbol{\sigma}}_1(\theta,\varphi)\rangle = \langle\hat{\boldsymbol{\sigma}}_2(\pi-\theta,\ \pi+\varphi)\rangle.$$

From (10) and (11) we get the following equation

$$4I_p^{(A)} = 3I_0^{(B)}(\theta)\langle\hat{\boldsymbol{\sigma}}\rangle\cdot\mathbf{N} \tag{12}$$

(the ratio of the momenta has been omitted).

Thus a knowledge of the nucleon polarization in reaction (B) yields the same information as the cross-section for meson production by polarized nucleons in reaction (A).

Additional information can be obtained by investigating the polarization of deuterons created in reaction (A). Considering only the polarization vector in our analysis of interaction of unpolarized particles, we find from the formula $\hat{\mathbf{S}}(S_m\varphi_m) = i[\mathbf{S}\wedge\boldsymbol{\varphi}]$ and (4') the following relation for this vector:

$$\begin{aligned} 16\pi I_0^{(A)}(\theta)\langle\hat{\mathbf{S}}\rangle_f &= \mathbf{n}P_2(\theta), \\ P_2(\theta) &= 2\,\mathrm{Im}\,\{(AB^+)+\sin^2\theta(CD^+)+(C+F)^+E \\ &\quad +(D^+F)+(C^+F+D^+E)\cos\theta\}. \end{aligned} \tag{13}$$

If only waves with $J\leqq 2$ are considered the angular dependence will have the form

$$\begin{aligned} &2\sin\theta\,P_2(\theta) \\ &= \sin\theta\cos\theta\,\{6\sqrt{10}\,\varepsilon_{02}+9\sqrt{2}\,\varepsilon_{13}+3\sqrt{10}\,\varepsilon_{14}+2\sqrt{15}\,\varepsilon_{15}-6\sqrt{5}\,\varepsilon_{34}-2\sqrt{30}\varepsilon_{35}\} \end{aligned}$$

where $\varepsilon_{mn} = \varrho_m\varrho_n\sin(\alpha_m-\alpha_n)$. As can be seen from (7'), in the general case proportionality to the product of $\sin 2\theta$ with an even function of $\cos\theta$ also remains.

Consider now the expression for the cross-section of reaction (B) on a polarized target. If the polarization of the target is assumed to be such that only the mean value of the deuteron spin vector differs from zero we find that the cross-section may be represented by an expression similar to (10). Formula (6) then yields

$$3I_p^{(B)} = 12\pi\,\mathrm{tr}\,S_B(\mathbf{S}\cdot\mathbf{p})S_B^+ = (\mathbf{n}\cdot\mathbf{p})P_2(\theta). \tag{14}$$

By comparing (13) and (14) we obtain another corollary of time-reversal invariance:

$$3I_p^{(B)} = 4I_0^{(A)}(\theta)\langle\hat{\mathbf{S}}\rangle_f\cdot\mathbf{N}. \tag{15}$$

Equations (12) and (15) are generalizations of relation (2) for the case of the binary reaction under consideration.

4.2. DEUTERON POLARIZATION TENSOR

The deuteron polarization state, as is well known [4, 6]), is characterized not only by the mean value of the deuteron spin vector $\hat{\mathbf{S}}$ but also by a second rank tensor which can be constructed from the spin vector. A tensor familiar from the literature is $\hat{D}_{ik}=\frac{1}{2}(\hat{S}_i\hat{S}_k+\hat{S}_k\hat{S}_i)-\frac{2}{3}\delta_{ik}=\hat{T}_{ik}-\frac{2}{3}\delta_{ik}$ introduced by Dalitz and also the tensor $T_{2,m}$ with components

$$\begin{aligned} 2T_{2,\pm 2} &= \sqrt{3}\{(\hat{S}_x^2-\hat{S}_y^2)\pm i(\hat{S}_x\hat{S}_y+\hat{S}_y\hat{S}_x)\} \\ 2T_{2,\pm 1} &= \mp\sqrt{3}\{(\hat{S}_x\hat{S}_z+\hat{S}_z\hat{S}_x)\pm i(\hat{S}_z\hat{S}_y+\hat{S}_y\hat{S}_z)\} \\ \sqrt{2}\,T_{2,0} &= 3\hat{S}_z^2-2. \end{aligned} \tag{16}$$

From the results of ref. [10]) it can be deduced and, in fact, it has already been mentioned in ref. [6]), that a relation of type (2) not only holds for the mean value of the polarization vector and the corresponding term in the cross-section but for the tensor terms as well. Correspondence between the vector terms for reactions (A) and (B) has been previously established. Compare now for the binary reaction under consideration the expression for the deuteron polarization tensor of reaction (A) involving unpolarized interacting protons and the cross-section of reaction (B) for a randomly polarized deuterium target.

Performing the calculations and using the formula

$$[\hat{S}_i\hat{S}_k+\hat{S}_k\hat{S}_i](S_m\varphi_m)=2\delta_{ik}(S_m\varphi_m)-[S_i\varphi_k+S_k\varphi_i]$$

for the mean values of the tensor $\langle\hat{D}_{ik}\rangle$ we obtain

$$\begin{aligned} &16\pi I_0^{(A)}(\theta)\left\{\tfrac{1}{3}\delta_{ik}-\langle\hat{D}_{ik}\rangle\right\}=\delta_{ik}\{|E|^2+|F|^2+2\,\mathrm{Re}\,(E^+F)\cos\theta\} \\ &+k_ik_k\{|A|^2+|C|^2\sin^2\theta-|E|^2+2\,\mathrm{Re}\,[C^+(E\cos\theta+F)]\} \\ &+k_{0i}k_{0k}\{|B|^2+|D|^2\sin^2\theta-|F|^2-2\,\mathrm{Re}\,[D^+(E+F\cos\theta)]\} \\ &+n_in_k\{|C|^2+|D|^2+2\,\mathrm{Re}\,[C^+(D\cos\theta-F)+D^+E]\} \\ &+(k_{0i}k_k+k_{0k}k_i)\,\mathrm{Re}\,\{(AB^+)+\sin^2\theta(C^+D)-(EF^+)-[C^+(E+F\cos\theta)] \\ &+[D^+(E\cos\theta+F)]\}=D_1(\theta)\delta_{ik}+D_2(\theta)k_ik_k+D_3(\theta)k_{0i}k_{0k} \\ &+D_4(\theta)n_i\,n_k+D_5(\theta)(k_{0i}k_k+k_{0k}k_i). \end{aligned} \tag{17}$$

For $D_1, D_2 \ldots$ as functions of $t=\cos\theta$ the following symmetry properties result from (17) and (7′):

$$\begin{aligned} &D_1(-t)=D_1(t);\quad D_2(-t)=D_2(t);\quad D_3(-t)=D_3(t); \\ &D_4(-t)=D_4(t);\quad D_5(-t)=-D_5(t). \end{aligned} \tag{17′}$$

As can readily be verified, condition (1) yields the result that the expression for the corresponding term in the cross-section differs from (17) by the interchange $D_2 \rightleftarrows D_3$. Thus, investigation of all the polarization tensor components in reaction (A) yields the same information as does a study of the cross-section of reaction (B) on a polarized deuterium target.

It can be seen from (17) that relations (12) and (15) will hold for some

contractions of the polarization tensor (such as $\langle \hat{D}_{ik} \rangle n_i n_k$) this being a consequence of the requirement of symmetry under time-reversal. If the relations between $T_{2,m}$ and $\hat{T}_{ik} = \hat{D}_{ik} + \frac{2}{3}\delta_{ik}$, which follow from (16), are used one can obtain from (17) expressions for $\langle T_{2,m} \rangle$:

$$\begin{aligned} 2T_{2,\pm 2} &= \sqrt{3}\,\{(\hat{T}_{xx} - \hat{T}_{yy}) \pm 2i\hat{T}_{xy}\} = \sqrt{3}\,\{(\hat{D}_{xx} - \hat{D}_{yy}) \pm 2i\hat{D}_{xy}\} \\ T_{2,\pm 1} &= \mp\sqrt{3}\,(\hat{T}_{xy} \pm i\hat{T}_{yz}) = \pm\sqrt{3}\,(\hat{D}_{xy} \pm i\hat{D}_{yz}) \\ \sqrt{2}\hat{T}_{2,0} &= 3\hat{T}_{zz} - 2 = \hat{D}_{zz}. \end{aligned} \tag{16'}$$

Availability of polarized proton beams permits one to study deuteron polarization in reaction (A) produced by polarized protons. The expression for the mean values of tensor D_{ik} assumes the form

$$\langle \hat{D}_{ik} \rangle = \frac{\frac{1}{4}\,\mathrm{tr}\,[S_A(1 + \mathbf{p}\cdot\hat{\boldsymbol{\sigma}}_1)S_A^+\,\hat{D}_{ik}]}{\frac{1}{4}\,\mathrm{tr}\,[S_A(1 + \mathbf{p}\cdot\hat{\boldsymbol{\sigma}}_1)S_A^+]}, \tag{18}$$

the expression derived from (8) and (10) for the cross-section of reaction (A), $I^{(A)}(\theta, \varphi)$, appearing in the denominator. The polarization of the incident protons is denoted by p. The expression for interaction of unpolarized particles can be obtained from (18) by putting $p = 0$. Thus, for polarized protons one should consider only the additional values due to the second term in the numerator; $I_0(\theta)$ should be replaced by $I(\theta, \varphi)$ in the previous expressions.

For the additional term in the deuteron polarization vector we obtain the expression ($\mathbf{m} = \mathbf{k} \wedge \mathbf{n}$; $\mathbf{l} = \mathbf{k}_0 \wedge \mathbf{n}$)

$$\begin{aligned} 4\pi\,\mathrm{tr}\,(\hat{\boldsymbol{\sigma}}_1 \cdot \mathbf{p})S_A^+\hat{\mathbf{S}}S_A &= \mathbf{n}(\mathbf{n}\cdot\mathbf{p})\,2\mathrm{Re}[(BC^+) - (AD^+)] \\ &+ [\mathbf{n} \wedge \mathbf{p}]\,2\,\mathrm{Re}\,\{C^+(E + F\cos\theta) + D^+(F + \cos\theta \cdot E)\} \\ &+ \mathbf{p}\,2\,\mathrm{Re}\,\{A^+(E + F\cos\theta) + B^+(E\cos\theta + F)\} \\ &- \mathbf{k}\,2\,\mathrm{Re}\,\{[(\mathbf{p}\cdot\mathbf{k})(A + E) + (\mathbf{p}\cdot\mathbf{k}_0)(B + F)]E^+\} \\ &- \mathbf{k}_0\,2\,\mathrm{Re}\,\{[(\mathbf{p}\cdot\mathbf{k})(A + E) + (\mathbf{p}\cdot\mathbf{k}_0)(B + F)]F^+\} \\ &+ \mathbf{l}\,2\,\mathrm{Re}\,\{(\mathbf{p}\cdot\mathbf{k})(BC^+) + (\mathbf{p}\cdot\mathbf{k}_0)(BD^+) + (\mathbf{p}\cdot\mathbf{l})|D|^2 + (\mathbf{p}\cdot\mathbf{m})(C^+D)\} \\ &+ \mathbf{m}\,2\,\mathrm{Re}\,\{(\mathbf{p}\cdot\mathbf{k})(AC^+) + (\mathbf{p}\cdot\mathbf{k}_0)(AD^+) + (\mathbf{p}\cdot\mathbf{m})|C|^2 + (\mathbf{p}\cdot\mathbf{l})(C^+D)\}. \end{aligned} \tag{19}$$

Similarly, for the polarization of protons on a polarized deuterium target in reaction (B) (only $\langle \hat{\mathbf{S}} \rangle \neq 0$), we get

$$\begin{aligned} 4\pi\,\mathrm{tr}\,\hat{\mathbf{S}}S_B^+(\hat{\boldsymbol{\sigma}}_1 \cdot \mathbf{p})S_B &= \mathbf{n}(\mathbf{n}\cdot\mathbf{p})2\,\mathrm{Re}\,[(BC^+) - (A^+D)] \\ &+ \mathbf{p}\,2\,\mathrm{Re}\,\{[A^+(E + F\cos\theta)] + [B^+(F + E\cos\theta)]\} \\ &- [\mathbf{n} \wedge \mathbf{p}]2\,\mathrm{Re}\,\{[C^+(E + F\cos\theta)] + [D^+(F + E\cos\theta)]\} \\ &+ \mathbf{l}\,2\,\mathrm{Re}\,\{(\mathbf{p}\cdot\mathbf{m})(C^+D) + |C|^2(\mathbf{p}\cdot\mathbf{l}) - (\mathbf{p}\cdot\mathbf{k})(A^+D) - (\mathbf{p}\cdot\mathbf{k}_0)(A^+C)\} \\ &+ \mathbf{m}\,2\,\mathrm{Re}\,\{(\mathbf{p}\cdot\mathbf{l})(C^+D) + |D|^2(\mathbf{p}\cdot\mathbf{m}) - (\mathbf{p}\cdot\mathbf{k}_0)(B^+C) - (\mathbf{p}\cdot\mathbf{k})(B^+D)\} \\ &- \mathbf{k}\,2\,\mathrm{Re}\,\{F^+[(\mathbf{p}\cdot\mathbf{k}_0)(A + E) + (\mathbf{p}\cdot\mathbf{k})(B + F)]\} \\ &- \mathbf{k}_0\,2\,\mathrm{Re}\,\{E^+[(\mathbf{p}\cdot\mathbf{k}_0)(A + E) + (\mathbf{p}\cdot\mathbf{k})(B + F)]\} \end{aligned} \tag{20}$$

from which the correspondence to (19) can readily be seen. A similar correspondence also holds for the tensor terms. We shall therefore give only the expressions for the additional deuteron polarization terms in reaction (A). From (5) and (18) we get ($\mathbf{q}_0 = \mathbf{p} \wedge \mathbf{k}_0$, $\mathbf{q} = \mathbf{p} \wedge \mathbf{k}$)

$$
\begin{aligned}
&4\pi \left\{\tfrac{1}{3}\delta_{ik} \operatorname{tr} (\hat{\boldsymbol{\sigma}}_1 \cdot \mathbf{p}) S_A^+ S_A - \operatorname{tr} (\hat{\boldsymbol{\sigma}}_1 \cdot \mathbf{p}) S_A^+ \hat{D}_{ik} S_A\right\} \\
&= (\mathbf{n}\cdot\mathbf{p}) \operatorname{Im} \{2[(CD^+) n_i n_k + k_i k_k (AC^+) + k_{0i} k_{0k} (BD^+)] + (k_{0i} k_k + k_{0k} k_i)[(AD^+) + (BC^+)]\} \\
&+ (n_i k_k + n_k k_i) \operatorname{Im} \{(\mathbf{p}\cdot\mathbf{k})[C^+(A+2E)] + (\mathbf{p}\cdot\mathbf{k}_0)[(AD^+) + 2(C^+F)] + (\mathbf{p}\cdot\mathbf{l})(C^+D)\} \\
&+ (n_i k_{0k} + n_k k_{0i}) \operatorname{Im} \{(\mathbf{p}\cdot\mathbf{k})[(BC^+) + 2(D^+E)] + (\mathbf{p}\cdot\mathbf{k}_0)[D^+(B+2F)] + (\mathbf{p}\cdot\mathbf{m})(C^+D)\} \\
&+ (p_k n_i + p_i n_k) \operatorname{Im} \{[C(E + F\cos\theta)^+] + [D(E\cos\theta + F)^+] + (EF^+)\} \qquad (21) \\
&+ (q_i k_k + q_k k_i) \operatorname{Im} (AE^+) + (q_{0i} k_k + k_i q_{0k}) \operatorname{Im} (AF^+) \\
&+ (q_i k_{0k} + q_k k_{0i}) \operatorname{Im} (BE^+) + (q_{0i} k_{0k} + q_{0k} k_{0i}) \operatorname{Im} (BF^+).
\end{aligned}
$$

The expression for the term proportional to δ_{ik} is identical to (10′).

4.3. CORRELATION OF NUCLEON POLARIZATIONS

As a last example we shall compare the expressions for the correlation of proton (nucleon) polarizations in reaction (B) when an unpolarized target is employed, with the additional terms in the meson production cross-section in reaction (A) when the beam as well as the target are polarized. With help of the formulae

$$(\hat{\boldsymbol{\sigma}}_2 \cdot \mathbf{b})\psi_C = -(\mathbf{b}\cdot\boldsymbol{\psi}); \qquad (\hat{\boldsymbol{\sigma}}_2 \cdot \mathbf{b})(\boldsymbol{\psi}\cdot\mathbf{p}) = -(\mathbf{p}\cdot\mathbf{b})\psi_C + i(\boldsymbol{\psi}\cdot[\mathbf{p}\wedge\mathbf{b}])$$

it is not difficult to obtain for the polarization correlation ($S_B = S_C \psi_C + \mathbf{S}\cdot\boldsymbol{\psi}$)

$$
\begin{aligned}
&4\pi \operatorname{tr} S_B^+ (\hat{\boldsymbol{\sigma}}_2 \cdot \mathbf{b})(\hat{\boldsymbol{\sigma}}_1 \cdot \mathbf{p}) S_B = 12\pi I_0^{(B)}(\theta) \langle (\hat{\boldsymbol{\sigma}}_2 \cdot \mathbf{b})(\hat{\boldsymbol{\sigma}}_1 \cdot \mathbf{p})\rangle \\
&= (\mathbf{b}\cdot\mathbf{p}) \{12\pi I_0^{(B)}(\theta) - 2[|A|^2 + |B|^2 + |E|^2 + |F|^2 + 2\operatorname{Re}(A^+B)\cos\theta - 2\operatorname{Re}(E^+F)\cos\theta]\} \\
&+ (\mathbf{n}\cdot[\mathbf{p}\wedge\mathbf{b}]) 2\operatorname{Re}\{[A^+(C+F+D\cos\theta)] + [B^+(C\cos\theta + D - E)]\} \\
&- (\mathbf{n}\cdot\mathbf{p})(\mathbf{n}\cdot\mathbf{b}) \{|C|^2 + |D|^2 + 4\operatorname{Re}[C^+(D+F) - (D^+E)]\} \\
&- 2(\mathbf{k}_0\cdot\mathbf{b})(\mathbf{k}_0\cdot\mathbf{p}) \{|C|^2 \sin^2\theta - |E|^2\} - 2(\mathbf{k}\cdot\mathbf{b})(\mathbf{k}\cdot\mathbf{p}) \{|D|^2 \sin^2\theta - |F|^2\} \\
&+ [(\mathbf{k}\cdot\mathbf{b})(\mathbf{k}_0\cdot\mathbf{p}) + (\mathbf{k}\cdot\mathbf{p})(\mathbf{k}_0\cdot\mathbf{b})]\, 2\operatorname{Re}[(E^+F) - (C^+D)\sin^2\theta] \qquad (22) \\
&+ [(\mathbf{p}\cdot\mathbf{k}_0)(\mathbf{b}\cdot\mathbf{l}) + (\mathbf{b}\cdot\mathbf{k}_0)(\mathbf{p}\cdot\mathbf{l})]\, 2\operatorname{Re}(C^+E) \\
&+ [(\mathbf{p}\cdot\mathbf{k}_0)(\mathbf{b}\cdot\mathbf{m}) + (\mathbf{b}\cdot\mathbf{k}_0)(\mathbf{p}\cdot\mathbf{m})]\, 2\operatorname{Re}(C^+F) \\
&+ [(\mathbf{p}\cdot\mathbf{k})(\mathbf{b}\cdot\mathbf{l}) + (\mathbf{b}\cdot\mathbf{k})(\mathbf{p}\cdot\mathbf{l})]\, 2\operatorname{Re}(D^+E) \\
&+ [(\mathbf{p}\cdot\mathbf{k})(\mathbf{b}\cdot\mathbf{m}) + (\mathbf{b}\cdot\mathbf{k})(\mathbf{p}\cdot\mathbf{m})]\, 2\operatorname{Re}(D^+F).
\end{aligned}
$$

The expression for $I_{pp}(\theta, \varphi)$ can be obtained from (22) by performing the substitution $\mathbf{k}_0 \rightleftarrows \mathbf{k}$. Thus, just as for other tensor quantities, condition (1) yields the result that identical information can be obtained by investigating the components of the two quantities and, for some contractions such as $\langle (\hat{\boldsymbol{\sigma}}_2 \cdot \mathbf{n})(\hat{\boldsymbol{\sigma}}_1 \cdot \mathbf{n})\rangle$, a relation of the same type as (12) is valid.

Comparison of (22) and (17) shows that a study of the correlation of

proton polarization in reaction (B) yields more abundant information than a study of deuteron polarization in reaction (A).

All the results obtained hitherto for reactions (A), (B) can be directly applied to the reaction

$$\mathrm{n+p} \rightleftarrows \mathrm{d}+\pi^0. \qquad \text{(C–D)}$$

Isobaric invariance moreover enables one to find the relation between the properties of the cross-sections for reaction (A–B) and (C–D); in this case, as is well known

$$I(\mathrm{p+p} \rightleftarrows \mathrm{d}+\pi^+) = 2I(\mathrm{n+p} \rightleftarrows \mathrm{d}+\pi^0). \qquad (23)$$

This relation is valid for the interaction cross-section of unpolarized [11]) as well as of polarized particles [10]). For the interaction between polarized particles some additional relations can be obtained. The first relation that should be mentioned is

$$\langle\hat{\boldsymbol{\sigma}}\rangle_f I_0^{(\mathrm{A})}(\theta) = 2\langle\hat{\boldsymbol{\sigma}}\rangle I_0^{(\mathrm{D})}(\theta) \qquad (24)$$

whose existence follows from (23), (10) and (1). Since (23) is valid for the interaction between unpolarized particles it follows from (24) that the polarizations of the corresponding nucleons in the reactions $\mathrm{d}+\pi^0 \to \mathrm{n}+\mathrm{p}$ and $\mathrm{d}+\pi^+ \to \mathrm{p}+\mathrm{p}$ are equal. Similar equalities hold for deuteron polarization and for correlation of nucleon polarization.

5. Discussion

From the very existence of condition (1) it is evident that the overall information which can be obtained from a study of the direct reaction is the same as that which can be derived from a study of the inverse reaction. The results of the present work show that for the binary reaction considered a consequence of condition (1) is the appearance of relations between the azimuthal asymmetry and the polarization which are of the same type as (12) and (15) and which are similar to the relation between the unpolarized cross-sections. An inspection of the tensor terms reveals that for some contractions, such as $\langle\hat{D}_{ik}\rangle n_i n_k$, relations of type (12) remain valid. As a whole a study of the components of the corresponding tensor quantities in reactions (A) and (B) yields the same information.

If we put $C = D = E = F = 0$ in expressions (5) and (6) and assume only A and B to be different from zero the resulting formulae will refer to a process in which the interaction of two spinless particles entails the formation of a spinless particle of opposite parity and a particle of spin 1. As can be seen from (13) a relation of the same type as (15) also remains valid in this case. The expression for the tensor $\langle\hat{D}_{ik}\rangle$ takes the form

$$4\pi\left\{\tfrac{1}{3}\delta_{ik} - \langle\hat{D}_{ik}\rangle\right\} I_0(\theta) = |A|^2 k_i k_k + |B|^2 k_{0i} k_{0k} + \mathrm{Re}\,(AB^+)(k_{0i} k_k + k_{0k} k_i).$$

The opposite case, when $A = B = 0$ and C, D, E and F are not zero, corresponds to the transformation of a scalar particle interacting with a spin 1 particle into a pseudoscalar one. In these cases symmetry properties (7′) do not hold.

The considered case of a binary reaction in which the particle spins in the initial and final states are different is quite a general case. It is not difficult to extend Wolfenstein's theorem to the case of binary reactions in which the particle spins do not change (and the intrinsic particle parities are constant). For the simplest case when the spins in the initial and final states are 0 and $\frac{1}{2}$ this immediately follows from the fact that the transition amplitude can be represented as

$$M = a(\theta)+b(\theta)(\hat{\boldsymbol{\sigma}} \cdot \mathbf{n})$$

if the intrinsic parities of the spinless particles are identical in the initial and final states and

$$M = b_1(\theta)(\hat{\boldsymbol{\sigma}} \cdot \mathbf{k}_0)+b_2(\theta)(\hat{\boldsymbol{\sigma}} \cdot \mathbf{k})$$

($\mathbf{k}_0$ and $\mathbf{k}$ are the relative momenta) if, for example, a scalar particle interacting with a nucleon transforms into a pseudo-scalar particle.

For the case when the particle spins $s_1 = s_2 = \frac{1}{2}$ such as in the reaction

$$\mathrm{p}+\mathrm{H}^3 \rightleftarrows \mathrm{n}+\mathrm{He}_2^3, \qquad \text{(E)}$$

validity of the consequences of invariance under time reversal which were established for elastic nucleon-nucleon scattering should be apparent if it is shown that in this case also amplitude M does not differ from that for elastic scattering. The latter statement can be proved by requiring that MM^+ be invariant instead of M, or, following Wright [13]), by analyzing the various transitions in reaction (E). Each of these procedures permits one to apply the results of time-reversal obtained for elastic scattering to the case of binary reactions in which the particle spins (and parities) do not change. In binary reactions which differ from elastic scattering and in which the particles in the final state are not the same as those in the initial state a peculiar "doubling" of relations of type (2) occurs.

The author is indebted to J. A. Smorodinsky, S. M. Bilenky and R. M. Ryndin for helpful discussions.

References

1) E. P. Wigner and L. Eisenbud, Phys. Rev. **72** (1949) 29
F. Coester, Phys. Rev. **89** (1953) 619; **84** (1951) 1259
2) J. M. Blatt and L. C. Biedenharn, Rev. Mod. Phys. **24** (1952) 258
3) R. Huby, Proc. Phys. Soc. A **67** (1954) 1103
4) R. H. Dalitz, Proc. Phys. Soc. A **65** (1952) 175
5) L. Wolfenstein and J. Ashkin, Phys. Rev. **85** (1952) 947

6) W. Lakin, Phys. Rev. **98** (1955) 139
7) E. Clementel and C. Villi, Nuovo Cimento **2** (1955) 1165
8) F. Mandl and T. Regge, Phys. Rev. **99** (1955) 1479
9) S. M. Bilenky and L. I. Lapidus, Report Institute Nucl. Probl. Acad. Sci. USSR (1955)
10) O. D. Cheyshvili, JETP **30** (1956) 1147
11) R. L. Garwin, Phys. Rev. **85** (1952) 1045
12) V. B. Berestetsky, Doklady, USSR, **94** (1954) 421
13) S. C. Wright, Phys. Rev. **99** (1955) 996

Nuclear Physics **4** (1957) 157—170; © *North-Holland Publishing Co., Amsterdam*
Not to be reproduced by photoprint or microfilm without written permission from the publisher

THE ENERGY LEVELS OF Pb^{206}

M. J. KEARSLEY
Department of Mathematics, University of Manchester

Received 12 March 1957

Abstract: The energy levels of Pb^{206} are calculated on the shell model, regarding Pb^{206} as two holes in the double closed shell nucleus Pb^{208}. The single hole energies are derived from data on Pb^{207} and interaction energies are calculated using harmonic oscillator wave functions and a Yukawa potential. The lowest seven excited states with energies up to 3 MeV are in good agreement with experiment.

1. Introduction

The shell model of the nucleus has been very successful in predicting properties such as ground state spins and magnetic moments, but in its original form is less successful for the excited states. Although it has been found necessary to introduce forms of collective motion in the nucleus, it is probable that the shell model gives a good first approximation for those nuclei in the neighbourhood of closed shells and also that the collective effects may be partly described in terms of configurational mixing. In order to test these assumptions a detailed calculation has been made of the excited energy levels of the nucleus Pb^{206}.

The nucleus Pb^{208} is a double closed shell of 126 neutrons and 82 protons and is particularly stable in its ground state configuration, its first excited state lying at 2.62 MeV and due most probably, to the excitation of a proton as it is not observed in the reaction Pb^{207} (d p) Pb^{208}. Its great stability suggests that one could treat those nuclei differing by only a few nucleons from Pb^{208} by the independent particle model [1]), regarding the additional nucleons or nucleon holes as if they moved in a potential due to the Pb^{208} core, the core itself remaining undisturbed by the extra particles or holes. Each extra nucleon or nucleon hole could then be ascribed a definite energy state, the degeneracy of the states arising from the configuration being split by the specific nucleon-nucleon interaction and the resultant states classified by their total angular momenta.

Pb^{206} which has 124 neutrons and 82 protons, thus has two neutron holes in the double closed shell. To first order the energies of the two holes will consist of (1) the energies of the separate holes moving in the effective field of the core and (2) the interaction between them. An estimate of the energies (1) can be obtained from the experimental data of Alburger and

Sunyar [2]) on the energy levels of Pb^{207}, which possesses one hole in the double closed shell.

TABLE 1

Energy levels of Pb^{207}

	(MeV)
$p_{1/2}$	0
$f_{5/2}$	0.569
$p_{3/2}$	0.894
$i_{13/2}$	1.633
$f_{7/2}$	2.338

The level at 2.338 MeV in Pb^{207} was at one time thought to be an $h_{9/2}$ state [3]) but the evidence is now more in favour of an $f_{7/2}$ state [2]). The level scheme for Pb^{206} has in fact been calculated for both cases, but as it is found that the differences in the resultant schemes are negligible, in the following calculation only configurations built up from the five states in table 1 will be described and the relevant changes for the $h_{9/2}$ state indicated at the end of the calculation. Higher states of Pb^{207} have been found by Harvey [4]) at approximately 2.75 MeV and 3.6 MeV and assigned spins $g_{9/2}$ and $i_{11/2}$ respectively, as these are available on the basis of shell model theory, but as these levels are so high, they will not greatly affect the relative positions of the lowest states. They, together with core excited states which may be expected to occur in the same energy region, have not been included in the calculation.

The states of the individual neutron holes couple together to give a state of given resultant total angular momentum J and z component M,

$$\Phi(j_1 j_2 JM) = \sum_{m_1+m_2=M} C^{JM}_{j_1 m_1 j_2 m_2} \psi^{m_1}_{j_1}(r_1\theta_1\phi_1)\,\psi^{m_2}_{j_2}(r_2\theta_2\phi_2)$$

where $\psi^{m_1}_{j_1}$, $\psi^{m_2}_{j_2}$ are two of the single hole states $p_{1/2}$, $f_{5/2}$, $p_{3/2}$, $i_{13/2}$, $f_{7/2}$. A totally antisymmetric wave function $(1/\sqrt{2})[\Phi(j_1 j_2 JM)-\Phi(j_2 j_1 JM)]$ for $j_1 \neq j_2$ will be denoted by $|j_1 j_2 JM\rangle$.

The potential energy function in the Hamiltonian for the model consists of a term corresponding to the effective central field of the core together with a term representing the central interaction between the holes, here treated as a perturbation. The possible tensor forces in the interaction are neglected.

For convenience in calculating, the effect of the core will be represented by a potential well of harmonic oscillator form, so that the central core Hamiltonian H_c is

$$H_c = \frac{1}{2m}(p^2+m^2\omega^2 r^2).$$

The eigenfunctions are then harmonic oscillator wave functions of the form

$$\psi_{nlm}(r\theta\phi) = R_{nl}(r)/rY_l^m(\theta\phi),$$

$$R_{nl}(r) = N(nl)e^{-\frac{\nu}{2}r^2} r^{l+1} \mathscr{V}(nl;\ r), \qquad \nu = \frac{\omega m}{\hbar},$$

where $\mathscr{V}(nl;\ r)$ is the associated Laguerre polynomial $L_{n+l+\frac{1}{2}}^{l+\frac{1}{2}}(\nu r^2)$ and $N(nl)$ is a normalising constant chosen so that

$$\int\{R_{nl}(r)\}^2\,dr = 1,$$

i.e.

$$[N(nl)]^2 = \frac{2^{l-n+2}(2l+2n+1)!!\nu^{l+3/2}}{\sqrt{\pi}\ n![(2l+1)!!]^2}.$$

For the nucleus Pb^{206} on the basis of the shell model, the p, f and i states taken as possible single hole states are the third p state, the second f state and the first i state respectively, so that the factors $\mathscr{V}(nl;\ r)$ occurring in the wave functions are

p state: $\mathscr{V}(21;\ r) = (1-\frac{4}{5}\nu r^2+\frac{4}{35}\nu^2 r^4)$,

f state: $\mathscr{V}(13;\ r) = (1-\frac{2}{9}\nu r^2)$,

i state: $\mathscr{V}(06;\ r) = 1$.

The interaction between the holes in a given state to first order is

$$\langle j_1 j_2 JM\,|V|\,j_1 j_2 JM\rangle$$

where V is the potential energy operator of the hole-hole interaction. In general there are other states of angular momenta j_3, j_4, which can also couple together to give a state with resultant angular momentum J and z component M. For Pb^{206} these states lie well within 1 MeV of each other, so that configuration interaction must be taken into account. Therefore states of the form

$$|JM\rangle = \sum \alpha(j_1 j_2 JM)|j_1 j_2 JM\rangle$$

are considered, the summation running over all combinations of single hole states which couple to angular momentum J, M. The $\alpha(j_1 j_2 JM)$ are then found in the usual way, by minimising the total energy of the system with respect to them, the $|JM\rangle$ and corresponding energy values being the eigenvectors and eigenvalues of the matrices

$$[\langle j_1 j_2 JM\,|H|\,j_3 j_4 JM\rangle]$$

where

$$H = \sum_{i=1,2} \frac{1}{2m}(p_i^2+m^2\omega^2 r_i^2)+V(r_{12});$$

approximately, as stated above,

$$\langle j_1 j_2 JM|H|j_3 j_4 JM\rangle = E_n(j_1 j_2)\delta_{j_1 j_2, j_3 j_4} + E_{nn}(j_1 j_2 : j_3 j_4 JM)$$

where E_n represents the sum of the energies of single holes in states j_1 and j_2, and

$$E_{nn}(j_1 j_2 : j_3 j_4 JM) = \langle j_1 j_2 JM|V|j_3 j_4 JM\rangle.$$

As there are so many terms of the form $\langle j_1 j_2 JM|V|j_3 j_4 JM\rangle$ almost any experimental energy level scheme could be fitted, were they all to be regarded as adjustable parameters. It is thus more interesting to make an assumption as to the form of V, fixing all parameters except one, beforehand, and proceed to calculate the necessary interaction energies, choosing the one variable parameter at the end of the calculation by comparison with the experimental data on Pb^{206}.

The interaction between the neutron holes will be assumed to be central and of the form suggested by Rosenfeld [5]):

$$V_{12} = V_c \boldsymbol{\tau}_1 \cdot \boldsymbol{\tau}_2 \,(0.1 + 0.23\, \boldsymbol{\sigma}_1 \cdot \boldsymbol{\sigma}_2)\, \frac{e^{-r_{12}/a}}{r_{12}/a}$$

where $\boldsymbol{\tau}_1$ = isobaric spin vector for nucleon 1,
$\boldsymbol{\sigma}_1$ = spin vector for nucleon 1.
This is equivalent to

$$V_{12} = V_c \frac{e^{-r_{12}/a}}{r_{12}/a}[0.13W - 0.46B - 0.93M + 0.26H]$$

where W, B, M, H are the Wigner, Bartlett, Majorana and Heisenberg operators respectively. The particular exchange character of V causes it to be charge symmetric, sufficient to cause saturation and for $V_c \approx 50$ MeV gives the singlet triplet separation for the deuteron in the absence of tensor forces. However V is to be regarded only as a suitable effective potential acting between the neutron holes and not necessarily that acting in the deuteron (in any case the tensor forces have been neglected in estimating the form of V and the saturation requirements for holes and particles in the presence of the core may well be different).
The Yukawa potential is chosen to have a range $a = 1.37 \times 10^{-13}$ cm corresponding to a meson mass of $276m$ and the strength of the interaction V_c is treated as the variable parameter.

It is convenient to work in the LS coupling scheme, expressing a state $|j_1 j_2 JM\rangle$ as a superposition of states $|J;\, L,\, S\rangle_{LS}$ of given orbital angular momentum L and spin S;

$$|j_1 j_2 JM\rangle$$
$$= \sqrt{\alpha}\,|J;\, J,\, 0\rangle_{LS} + \sqrt{\beta}\,|J;\, J,\, 1\rangle_{LS} + \sqrt{\gamma}\,|J;\, J+1,\, 1\rangle_{LS} + \sqrt{\delta}\,|J;\, J-1,\, 1\rangle_{LS}$$

where the coefficients α, β, γ, δ have been given by Pryce [1]) and their phases by Blin Stoyle [6]).

Then

$$V_{12}\,|j_1 j_2 JM\rangle = V_0 \frac{e^{-r_{12}/a}}{r_{12}/a}\,[-0.6\sqrt{\alpha}\,|J;J,0\rangle + 0.34(\sqrt{\beta}\,|J;J,1\rangle + \sqrt{\gamma}\,|J;J+1,1\rangle + \sqrt{\delta}\,|J;J-1,1\rangle)].$$

The calculation thus involves evaluating terms such as $\langle l_1 l_2 LM|V(r_{12})|l_3 l_4 LM\rangle$ where $|l_1 l_2 LM\rangle$ represents the orbital part of the wave function and is either symmetric or antisymmetric in the coordinates of the two neutron holes.

2. Calculation of the Matrix Elements

As the usual Slater method for calculating the matrix elements is somewhat inconvenient for the Yukawa potential, the following method, which is simple in practice, has been employed.

Since $V(r_{12})$ is central and spherically symmetric, the value of $\langle l_1 l_2 LM|V(r_{12})|l_3 l_4 LM\rangle$ is independent of the azimuthal quantum number M and so the integral may be replaced by

$$E(l_1 l_2;\ l_3 l_4 : L) = \frac{1}{2L+1} \sum_{M=-L}^{L} \langle l_1 l_2 LM\,|V|\,l_3 l_4 LM\rangle.$$

Let $\varrho(r_1 r_2)$ denote the density function

$$\varrho(r_1 r_2) = \frac{1}{2L+1} \sum_{M=-L}^{L} |l_3 l_4 LM\rangle\langle l_1 l_2 LM|$$

so that

$$E(l_1 l_2;\ l_3 l_4 : L) = \iint V(r_{12})\,\varrho(r_1 r_2)\,d\tau_1\,d\tau_2.$$

Put

$$\varrho(l_1 l_3 r_1;\ l_2 l_4 r_2) = \frac{1}{2L+1} \sum_{M=-L}^{L} \Phi(l_3 l_4 LM)\Phi^*(l_1 l_2 LM).$$

In full

$$\Phi(l_1 l_2 LM) = N(n_1 l_1)N(n_2 l_2)\,e^{-\frac{\nu}{2}(r_1^2+r_2^2)}\,\mathcal{Y}(n_1 l_1;\ r_1)\,\mathcal{Y}(n_2 l_2;\ r_2) \times \sum r_1^{l_1} r_2^{l_2} C^{LM}_{l_1 m_1 l_2 m_2} Y^{m_1}_{l_1}(\theta_1\varphi_1) Y^{m_2}_{l_2}(\theta_2\varphi_2).$$

Put

$$F(l_1 l_3 r_1;\ l_2 l_4 r_2) = N(n_1 l_1)N(n_2 l_2)N(n_3 l_3)N(n_4 l_4)e^{-\nu(r_1^2+r_2^2)}\mathcal{Y}(n_1 l_1; r_1)\mathcal{Y}(n_2 l_2; r_2)\mathcal{Y}(n_3 l_3; r_1)\mathcal{Y}(n_4 l_4; r_2)$$

so that

$$\varrho(l_1 l_3 r_1;\ l_2 l_4 r_2) = \frac{1}{2L+1} F(l_1 l_3 r_1;\ l_2 l_4 r_2) \sum r_1^{l_1+l_3} r_2^{l_2+l_4} \phi^*(l_1 l_2 LM)\phi(l_3 l_4 LM)$$

where

$$\phi(l_1 l_2 LM) = \sum_{M=m_1+m_2} C^{LM}_{l_1 m_1 l_2 m_2} Y^{m_1}_{l_1}(\theta_1\varphi_1) Y^{m_2}_{l_2}(\theta_2\varphi_2).$$

In the expression for $\varrho(l_1 l_3 r_1;\ l_2 l_4 r_2)$ the spherical harmonics of like argument can now be coupled together and the resultant expression simplified to the form

$$\varrho(l_1 l_3 r_1;\ l_2 l_4 r_2) = \frac{1}{2L+1} F(l_1 l_3 r_1;\ l_2 l_4 r_2) \times \sum_{b=-s}^{s} A(b,\ l_1 l_2 l_3 l_4 L) P_b(\cos\theta_{12}) r_1^{l_1+l_3} r_2^{l_2+l_4}$$

where θ_{12} is the angle between the radii vectores $\mathbf{r}_1 = (r_1\theta_1\varphi_1)$ and $\mathbf{r}_2 = (r_2\theta_2\varphi_2)$, $P_b(\cos\theta_{12})$ is a Legendre polynomial of order b; $s = \text{Min}\,(l_1+l_3,\cdot l_2+l_4)$, and $A(b,\ l_1 l_2 l_3 l_4 L)$ are coefficients containing sums of Racah coefficients.

Expanding the terms $P_b(\cos\theta_{12})$ as power series in $\cos\theta_{12}$ and replacing $r_1^b r_2^b\,(\cos\theta_{12})^b$ by $(\mathbf{r}_1\cdot\mathbf{r}_2)^b$ gives

$$\varrho(l_1 l_3 r_1;\ l_2 l_4 r_2) = \frac{1}{2L+1} F(l_1 l_3 r_1;\ l_2 l_4 r_2) \times \sum_{b=0\text{ or }1}^{s} B(b,\ l_1 l_2 l_3 l_4 L)(\mathbf{r}_1\cdot\mathbf{r}_2)^b r_a^t r_1^{s-b} r_2^{s-b}$$

where the $B(b,\ l_1 l_2 l_3 l_4 L)$ are numerical coefficients, $t = |(l_1+l_3)-(l_2+l_4)|$, and

$$r_a = r_1 \text{ or } r_2 \text{ as } s = l_2+l_4 \text{ or } l_1+l_3;$$

the summation over b runs from 0 or 1 according as s is even or odd. For non vanishing matrix elements, occurring only between states of like parity, t is always even.

In practice the simplest way to determine the coefficients $B,\ (b, l_1 l_2 l_3 l_4 L)$ in the expression

$$\sum \phi^*(l_1 l_2 LM)\phi(l_3 l_4 LM)\, r_1^{l_1+l_3} r_2^{l_2+l_4} = \sum_{b=0,1}^{s} B(b, l_1 l_2 l_3 l_4 L)(\mathbf{r}_1\cdot\mathbf{r}_2)^b r_a^t r_1^{s-b} r_2^{s-b}$$

is to express both sides in terms of

$$p_1 = x_1+iy_1, \qquad q_1 = x_1-iy_1, \qquad z_1;$$
$$p_2 = x_2+iy_2, \qquad q_2 = x_2-iy_2, \qquad z_2;$$

using

$$r_1^2 = p_1 q_1 + z_1^2, \qquad \mathbf{r}_1\cdot\mathbf{r}_2 = \tfrac{1}{2}\,[p_1 q_2 + p_2 q_1 + 2z_1 z_2].$$

On comparing suitable terms in the highest powers of p, q, and z, a set of simultaneous equations of triangular form can be obtained in the B's and solved immediately by a chain process. It is easy to check the calculation as there are many more equations than unknowns available and tables of the B functions can be constructed rapidly in practice for all required combinations of the p, f and i states, the results holding for any shell, since the expression is independent of the term $F(l_1 l_3 r_1;\ l_2 l_4 r_2)$.

Before expanding the $F(l_1 l_3 r_1;\ l_2 l_4 r_2)$ it is convenient to change to variables ξ_1, ξ_2 where

$$\xi_{21} = \sqrt{\nu}\,\mathbf{r}_1, \qquad \xi_{22} = \sqrt{\nu}\,\mathbf{r}_2.$$

The complete expansion of $\varrho(l_1 l_3 r_1;\ l_2 l_4 r_2)$ is then of the form

$$\varrho(l_1 l_3 r_1;\ l_2 l_4 r_2) = \mathrm{e}^{-(\xi_1^2+\xi_2^2)} \sum_{\substack{pqt \\ p+t=l_1+l_3 \\ q+t=l_2+l_4}} A(pqt)\xi_1^{\,p}\,\xi_2^{\,q}(\xi_{21}\cdot\xi_{22})^t$$

where the $A(pqt)$ are the resultant expansion coefficients.

Since the wave functions $|l_1 l_2 LM\rangle$ are either antisymmetric or symmetric in the coordinates of the two neutron holes, $\varrho(r_1 r_2)$ contains the combinations

$$[\varrho(l_1 l_3 r_1;\ l_2 l_4 r_2)+\varrho(l_2 l_4 r_1;\ l_1 l_3 r_2)]$$

and

$$[\varrho(l_1 l_4 r_1;\ l_2 l_3 r_2)+\varrho(l_2 l_3 r_1;\ l_1 l_4 r_2)].$$

Put

$$E'(l_1 l_2;\ l_3 l_4 : L) = \int [\varrho(l_1 l_3 r_1;\ l_2 l_4 r_2)+\varrho(l_2 l_4 r_1;\ l_1 l_3 r_2)]V(r_{12})\mathrm{d}\tau_1\,\mathrm{d}\tau_2.$$

Then

$$E'(l_1 l_2;\ l_3 l_4 : L) = \sum_{\substack{pqt \\ p+t=l_1+l_2 \\ q+t=l_3+l_4}} A(pqt)\,I(pqt)$$

where

$$I(pqt) =$$

$$\int \mathrm{e}^{-(\xi_1^2+\xi_2^2)} V(|\xi_{21}-\xi_{22}|)(\xi_1^{\,p}\xi_2^{\,q}+\xi_1^{\,q}\xi_2^{\,p})(\xi_{21}\cdot\xi_{22})^t \sin\theta_1 \sin\theta_2\, \xi_1^{\,2}\xi_2^{\,2}\,\mathrm{d}\xi_1\,\mathrm{d}\xi_2\,\mathrm{d}\theta_1\,\mathrm{d}\theta_2\,\mathrm{d}\varphi_1\,\mathrm{d}\varphi_2.$$

For potential functions such as the Yukawa potential which involve $|\xi_{21}-\xi_{22}|$ and harmonic oscillator wave functions, the next step is to transform to

$$\xi_{21} = \frac{\mathbf{R}-\mathbf{r}}{\sqrt{2}}, \quad \xi_{22} = \frac{\mathbf{R}+\mathbf{r}}{\sqrt{2}},$$

so that

$$\xi_1^{\,2} + \xi_2^{\,2} = R^2+r^2, \quad \xi_{21}\cdot\xi_{22} = \tfrac{1}{2}\ (R^2-r^2).$$

Expanding

$$(\xi_1^{\,p}\xi_2^{\,q}+\xi_1^{\,q}\xi_2^{\,p}) = \sum_{abd} A_{abd}\,R^a r^b c^d$$

where

$$c = \frac{\mathbf{R}\cdot\mathbf{r}}{Rr}, \quad \mathbf{R} = (R\Theta\Phi), \quad \mathbf{r} = (r\theta\phi),$$

one gets

$$I(pq0) = \int \mathrm{e}^{-(R^2+r^2)} V(r) \sum_{abd} A_{abd}\,R^a r^b c^d\, R^2 r^2 \sin\Theta \sin\theta\,\mathrm{d}\theta\,\mathrm{d}\Theta\,\mathrm{d}\phi\,\mathrm{d}\Phi\,\mathrm{d}r\,\mathrm{d}R.$$

This can be integrated immediately to give

$$I(pq0) = 16\pi^2 \sum_{abd} \frac{A_{abd}}{(d+1)}\,K_{a+2}\,J_{b+2}$$

where

$$K_{2n} = \int_0^\infty e^{-R^2} R^{2n}\, dR = \frac{\sqrt{\pi}\,(2n-1)!}{2^{2n}(n-1)!}$$

$$J_m = \int_0^\infty e^{-r^2} V(r) r^m\, dr.$$

Similarly the $I(pqt)$ are given simply from the $I(pq0)$ expansion by

$$I(pqt) = \frac{16\pi^2}{2^t} \sum_{p=0}^{t} \sum_{abd} (-1)^p \binom{t}{p} \frac{A_{abd}}{(d+1)} K_{a+2+2(t-p)}\, J_{b+2+2p}$$

where $\binom{t}{p}$ is a binomial coefficient.
For the Yukawa potential

$$V(r_{12}) = \frac{V_c\, e^{-|\mathbf{r}_1-\mathbf{r}_2|/a}}{|\mathbf{r}_1-\mathbf{r}_2|/a}$$

one has

$$J_m = \frac{V_c}{b} \frac{\sqrt{\pi}}{2} e^{\mu^2} Q_{m-1},$$

where

$$Q_m = \frac{2}{\sqrt{\pi}} \int_\mu^\infty e^{-x^2} (x-\mu)^m\, dx, \quad \mu = \frac{1}{a\sqrt{2\nu}}, \quad Q_m = \frac{(m-1)}{2} Q_{m-2} - \mu Q_{m-1}.$$

Once a value of μ is determined the J's can be tabulated, whence the $I(pqt)$'s, the $E(l_1 l_2; l_3 l_4: L)$'s and finally the matrix elements of the energy matrices.

The quantity ν is a measure of the linear extension of the harmonic oscillator wave functions and in principle could be determined by a variational calculation in which the total energy of the system is minimised. As this is not practicable the criterion proposed by Swiatecki [7]) and employed by Elliott and Flowers [8]) in their calculations on the level spectra of nuclei of mass 18 and 19 is used here. The value of ν is determined by associating the nuclear radius $1.42A^{1/3} \times 10^{-13}$ cm with the point at which the probability density $[R_{nl}(r)/r]^2$ falls to a quarter of its maximum value. For $A = 206$ this gives

$$\sqrt{\nu} = 3.70 \times 10^{12}\ \text{cm}^{-1} \text{ and } \mu = 1.4.$$

The calculations of Elliott and Flowers [8]) suggest that the energy levels are not highly sensitive to the value of μ.

Since the particular form of the nucleon-nucleon interaction is to be regarded as no more than an effective interaction, it is of interest to see how the energy levels vary with the strength V_c. The energy matrices for each value of the total angular momentum J were therefore calculated for $V_c = 0$ to 100 MeV in steps of 10 MeV and their eigenvalues and corresponding eigenvectors determined.

3. Singlet and Triplet Interactions

It should be mentioned at this point that though in the zero range approximation and other approximate methods, the interaction between nucleons in their triplet spin states has been assumed to be negligible compared to the singlet interaction, the present calculations using the Rosenfeld central force mixture with a Yukawa potential suggest that this is a poor approximation, especially for states of low spin. In magnitude the triplet matrix elements are rarely less than a quarter and sometimes greater than a half of the corresponding singlet matrix element. In transforming to the *jj*-coupling scheme, the triplet matrix elements frequently have greater weight than the singlets, so that as the central force mixture is attractive for singlets and repulsive for triplets (for like nucleons), the attraction between two nucleons in a given state is considerably altered if the triplet matrix elements are neglected. This effect is particularly noticeable in the diagonal matrix elements, where the triplet repulsion cancels much of the singlet attraction. Though these conclusions are based on a particular form of interaction, it is probable that they are broadly correct for most of the usual finite range forces.

4. Results

The pairs of states chosen from $p_{1/2}$, $f_{5/2}$, $p_{3/2}$, $i_{13/2}$ and $f_{7/2}$, which can couple to give a state of resultant angular momentum J ($J = 0$ to 7) and given parity are shown in table 2.

TABLE 2

J									
0+	$p^2_{1/2}$	$f^2_{5/2}$	$p^2_{3/2}$	$i^2_{13/2}$	$f^2_{7/2}$				
1+	$p_{3/2}\,p_{1/2}$	$f_{5/2}\,p_{3/2}$	$f_{7/2}\,f_{5/2}$						
2+	$p_{1/2}\,f_{5/2}$	$p_{3/2}\,p_{1/2}$	$f^2_{5/2}$	$p_{3/2}\,f_{5/2}$	$p^2_{3/2}$	$f_{7/2}\,f_{5/2}$	$i^2_{13/2}$	$p_{3/2}\,f_{7/2}$	$f^2_{7/2}$
3+	$p_{1/2}\,f_{5/2}$	$p_{3/2}\,f_{5/2}$	$p_{1/2}\,f_{7/2}$	$f_{7/2}\,f_{5/2}$	$p_{3/2}\,f_{7/2}$				
4+	$f^2_{5/2}$	$p_{3/2}\,f_{5/2}$	$f_{7/2}\,p_{1/2}$	$f_{7/2}\,f_{5/2}$	$i^2_{13/2}$	$f_{7/2}\,p_{3/2}$	$f^2_{7/2}$		
5—	$i_{13/2}\,f_{5/2}$	$i_{13/2}\,p_{3/2}$	$f_{7/2}\,i_{13/2}$						
6—	$i_{13/2}\,p_{1/2}$	$i_{13/2}\,f_{5/2}$	$i_{13/2}\,p_{3/2}$	$f_{7/2}\,i_{13/2}$					
7—	$i_{13/2}\,p_{1/2}$	$i_{13/2}\,f_{5/2}$	$i_{13/2}\,p_{3/2}$	$f_{7/2}\,i_{13/2}$					

The energy matrices are thus of order 5, 3, 9, 5, 7, 3, 4, 4, respectively.

Figure 1 shows the variation of the energy levels with increase in the

strength of the effective central force mixture, when configuration interaction is taken into account.

In the figure, for clarity, only the lowest states for each J, together

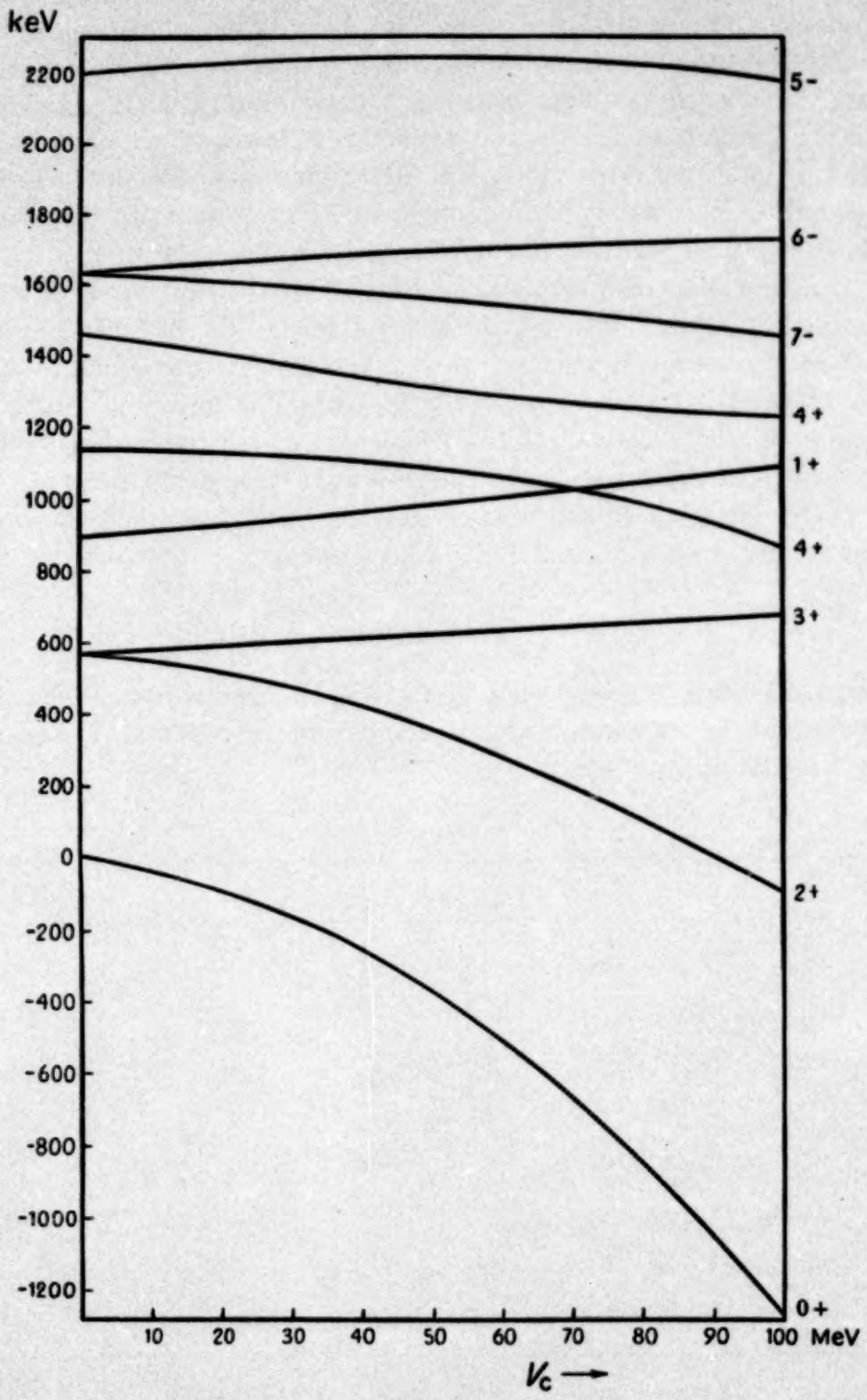

Fig. 1. Calculated energy levels for Pb^{206} including configuration interaction and showing the dependence of the levels on the strength V_c of the nucleon-nucleon interaction.

with the second 4+ state, have been plotted. The 1+ state has been included for completeness though a state of this spin and parity is not observed experimentally.

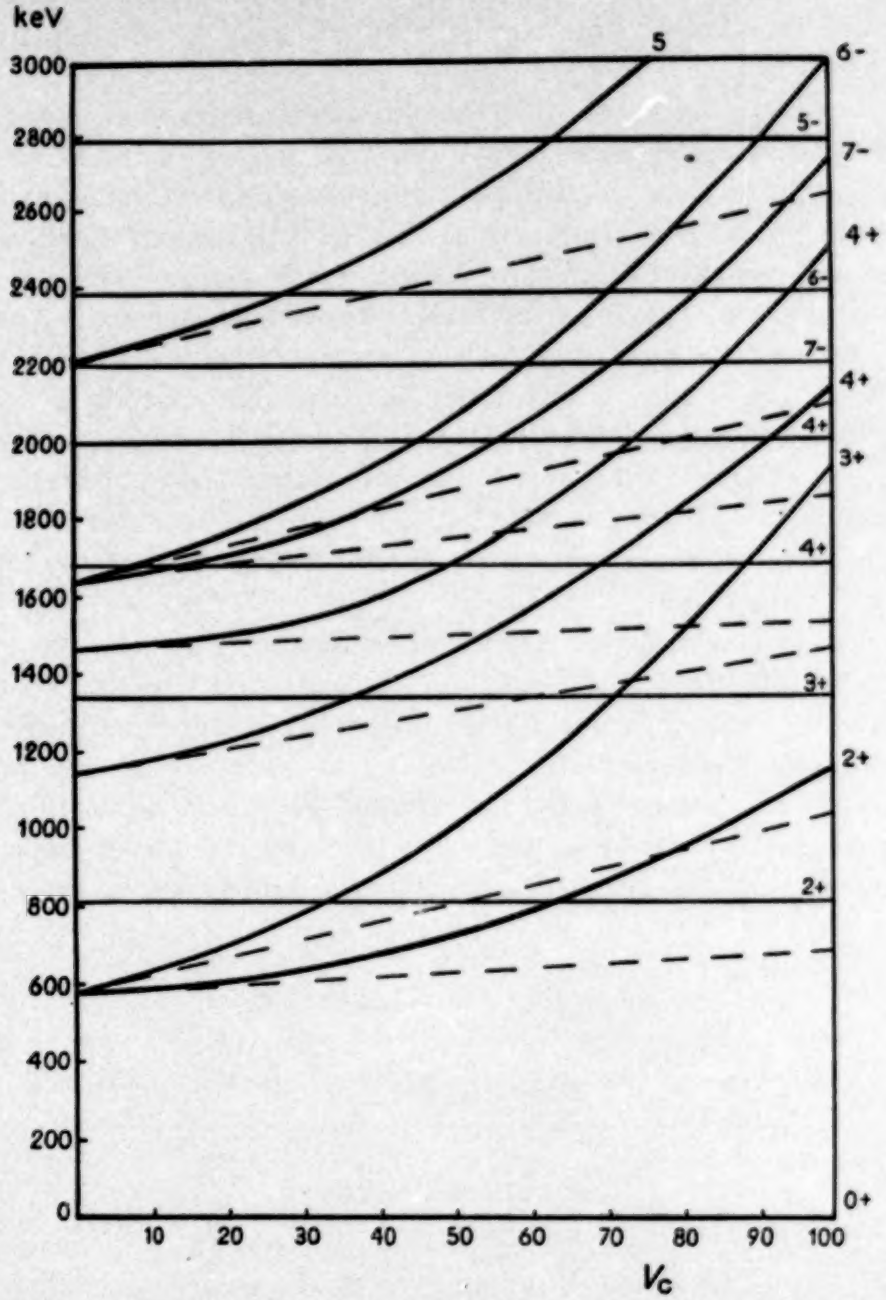

Fig. 2. Calculated energy levels for Pb^{206} plotted relative to the ground state. The curves are a plot of $E(J)-E(0)$ against V_c the strength of the nucleon-nucleon interaction, where $E(J)$ = energy of level of spin J, including the effect of configuration interaction. The dashed lines plot $E'(J) - E'(0)$ against V_c, where $E'(J)$ = energy of level of spin J including the nucleon-nucleon interaction but neglecting configuration interaction. The straight continuous lines are the experimental energy levels.

In figure 2, the values of $E(J)-E(0)$ are plotted against V_c, where

$E(J)$ is the energy of the state of total spin J. When configuration interaction is allowed the continuous curves result.
For comparison, the dashed straight lines are a plot of $E'(J)-E'(0)$, where $E'(J)$ is the energy of the state of spin J without configuration interaction. The straight lines parallel to the V_c axis are the experimental energy levels [3]).

It is clear from the figures that the effect of configuration interaction is important and depresses the states of given J by markedly different amounts. The levels obtained including the nucleon-nucleon interaction but excluding configuration interaction are in poor agreement with the experimental levels for reasonable values of V_c. With configuration interaction and a strength $V_c \approx 70$ MeV there is excellent agreement between theory and experiment for the lowest seven excited states [3]) observed in the decay of Bi^{206}. As expected the configuration interaction is particularly strong in the 0+ ground state, causing a depression below the energy of two $p_{1/2}$ state holes of 0.66 MeV. The 2+ level is also considerably depressed (0.36 MeV) whilst the remaining levels are less affected.

In table 3 are listed all the theoretical and experimental energy levels of energy less than 3 MeV.

The position of the higher levels is less certain, since the presence of higher energy single hole states ($g_{9/2}$, $i_{11/2}$) in Pb^{207} and core excited states, which have been excluded in the present calculation will affect these levels through configuration interaction. These excluded levels will also interact with the lowest states and cause the required Pb^{206} level separations for a lower value of V_c, so that $V_c \approx 70$ MeV is to be regarded as an upper limit to the strength of the interaction (within the limitations of the model).

TABLE 3

Energy levels of Pb^{206} less than 3 MeV.

Spin and parity	Experimental (MeV)		Theoretical (MeV), $V_c = 70$ MeV				
0+	0		0	1.124	2.123		
1+			1.699	2.324			
2+	0.803		0.868	1.219	1.685	2.197	2.453
3+	1.341		1.312	2.180			
4+	1.683	1.998	1.692	1.937	2.861		
5−	2.783		2.875				
6−	2.385		2.373	2.910			
7−	2.200		2.189				

It can be seen from table 3, that the lowest energy levels for $J = 0+$, $2+, 3+, 5-, 6-, 7-$ and the two lowest levels for $J = 4+$ are all predicted within 0.1 MeV of the experimental levels with these spin and parities.

The remaining theoretical levels are unexcited and are not observed. No predicted levels lie near the uncertain level at 2.5255 MeV believed to be 3− and probably due to core excitation.

The changes in the predicted level scheme if the single hole state at 2.338 MeV in Pb^{207} is assumed to be $h_{9/2}$ instead of $f_{7/2}$ are very slight. The states involving $f_{7/2}$ cause a slightly greater depression after configuration interaction than similar states with $h_{9/2}$ (as expected) amounting to 45 keV in the ground state and less for higher states. This is satisfying as it shows that such calculations are relatively insentitive to the spin values attached to the higher single hole states.

The extent of configurational mixing is demonstrated in table 4, which gives the normalised wave functions for the lowest seven excited states with $V_c = 70$ MeV. The symbol $(i\ j)$ signifies the totally antisymmetric state of given total angular momentum J formed from the single hole states i and j.

TABLE 4

Normalised eigenfunctions $(J\pm)$ for the lowest levels of Pb^{206}

$(0+) =$	$0.840(p_{1/2})^2$	$+0.332(f_{5/2})^2$	$+0.379(p_{3/2})^2$	$-0.139(i_{13/2})^2$	$+0.142(f_{7/2})^2$
$(1+) =$	$0.9999(p_{3/2}p_{1/2})$	$-0.016(f_{7/2}f_{5/2})$			
$(2+) =$	$0.766(f_{5/2}p_{1/2})$	$+0.530(p_{3/2}p_{1/2})$	$+0.233(f_{5/2})^2$	$+0.123(f_{5/2}p_{3/2})$	
	$+0.182(p_{3/2})^2$	$+0.052(f_{7/2}f_{5/2})$	$-0.068(i_{13/2})^2$	$+0.135(f_{7/2}p_{3/2})$	
	$+0.068(f_{7/2})^2$				
$(3+) =$	$0.997(f_{5/2}p_{1/2})$	$+0.078(f_{5/2}p_{3/2})$	$+0.003(f_{7/2}p_{1/2})$	$-0.004(f_{7/2}f_{5/2})$	
	$+0.020(f_{7/2}p_{3/2})$				
$(4+) =$	$0.828(f_{5/2})^2$	$+0.516(f_{5/2}p_{3/2})$	$+0.147(f_{7/2}p_{1/2})$	$+0.111(f_{7/2}f_{5/2})$	
	$-0.053(i_{13/2})^2$	$+0.091(f_{7/2}p_{3/2})$	$+0.059(f_{7/2})^2$		
$(4-) =$	$0.548(f_{5/2})^2$	$-0.823(f_{5/2}p_{3/2})$	$-0.124(f_{7/2}p_{1/2})$	$-0.018(f_{7/2}f_{5/2})$	
	$+0.023(i_{13/2})^2$	$-0.081(f_{7/2}p_{3/2})$	$-0.009(f_{7/2})^2$		
$(5-) =$	$0.889(i_{13/2}f_{5/2})$	$-0.447(i_{13/2}p_{3/2})$	$+0.101(i_{13/2}f_{7/2})$		
$(6-) =$	$0.994(i_{13/2}p_{1/2})$	$+0.067(i_{13/2}f_{5/2})$	$+0.084(i_{13/2}p_{3/2})$	$-0.017(i_{13/2}f_{7/2})$	
$(7-) =$	$0.987(i_{13/2}p_{1/2})$	$-0.104(i_{13/2}f_{5/2})$	$+0.115(i_{13/2}p_{3/2})$	$-0.049(i_{13/2}f_{7/2})$	

From the magnitude of the coefficients it is clear that the admixtures are considerable, especially for the 0+ and 2+ levels, so that calculations based on pure independent particle states are poor approximations.

5. Conclusion

The present detailed application of shell model theory to the nucleus Pb^{206}, treating it as a system of two holes moving in the presence of the Pb^{208} core, has shown that it is very successful in predicting quantitatively, the energies, spins and parities of the excited states, provided configuration interaction is taken into account.

The writer would like to thank Professor M. H. L. Pryce, Drs. B. H. Flowers and J. P. Elliott for helpful discussions and Manchester University for the use of the Mark 1 electronic computor to diagonalise the energy matrices.

References

1) M. H. L. Pryce, Proc. Phys. Soc. A **65** (1952) 773
2) D. E. Alburger and A. W. Sunyar, Phys. Rev. **99** (1955) 695
3) D. E. Alburger and M. H. L. Pryce, Phys. Rev. **95** (1954) 1482
4) J. A. Harvey, Canad. J. Phys. **31** (1953) 278
5) L. Rosenfeld, Nuclear Forces (North-Holland Publishing Company, Amsterdam, 1948) p. 234
6) R. J. Blin-Stoyle, Proc. Phys. Soc. A **66** (1953) 729
7) W. J. Swiatecki, Proc. Roy. Soc. A **205** (1951) 238
8) J. P. Elliott and B. H. Flowers, The structure of the nuclei of mass 18 and 19 (A.E.R.E. preprint 1954)

Nuclear Physics **4** (1957) 171—182; — *North-Holland Publishing Co., Amsterdam*
Not to be reproduced by photoprint or microfilm without written permission from the publisher

POLARISATION OF μ-MESONS AND ELECTRONS IN K-MESON DECAYS

J. WERLE

Department of Theoretical Physics, University of Manchester†

Received 25 March 1957

Abstract: The longitudinal polarisation of the μ-mesons and electrons emitted in $K \to \pi + \nu + \mu$ (or e) is investigated under the assumption that the neutrino is completely polarised in the direction parallel to its direction of motion. The general form of the S-matrix containing four coupling types is taken into account. It turns out that the polarisation as a function of the energy depends in a very sensitive way on the type of coupling. This may provide a new powerful tool for the investigation of the form of coupling.

1. Introduction

It has been pointed out by T. D. Lee and C. N. Yang [1]) that the parity may not be conserved in weak interactions. With respect to the interactions involving a neutrino, violation of parity conservation implies at least a partial longitudinal polarisation of the neutrino. Several theoretical considerations [2]) suggest that the polarisation of the neutrino may be complete and parallel to its direction of motion. Polarisation of the anti-neutrino would then always be antiparallel. Recent experiments [3, 4]) seem already to support strongly these theoretical ideas. Longitudinal polarisation of the neutrino implies the possibility of partial or even total polarisation of other particles appearing together with the neutrino.

The aim of this paper is to show, using the K-meson decays as an example, that the measurements of polarisation can be used with a somewhat wider purpose than a mere proof of violation of parity conservation. Polarisation measurements can in fact provide a powerful new tool for the investigation of the types of coupling in various processes involving neutrinos. Some of these polarisation experiments may be comparatively simple. For example, μ-meson polarisation can be measured by checking the asymmetry in the angular distribution of the electrons emitted in the subsequent decay of the μ-meson [2, 4]). In other cases the measurements of the polarisation may be more difficult, e.g. in the case of electrons, when a scattering experiment is needed [5]). However, it should be pointed out that the degree of polarisation often depends on the type of coupling in a much more sensitive way than, say, the energy distributions. This is due to the fact that in the expression for the probability of finding the particle in an energy interval dE, a rather

† On leave of absence from the Physical Institute of the University of Warsaw.

troublesome energy-dependent phase-density factor appears which suppresses the differences between different coupling types [7]). This fact makes the analysis of the experimental energy distributions rather difficult and not always very convincing. On the other hand, in the polarisation measurements we are interested in the ratio of probabilities of finding parallel or antiparallel polarisation of the particle. It can easily be seen that the rather disturbing energy-dependent phase-space factor will be cancelled. The expression for the degree of polarisation depends therefore much more strongly on the type of coupling.

We shall discuss in this paper only longitudinal polarisation of μ-mesons or electrons emitted in the processes $K \to \pi+\nu+\mu$ (or e). This means that we shall confine our attention to the simplest possible case when the correlation between π-meson and μ-meson (or electron) momenta is not measured.

2. General Formulae for Longitudinal Polarisation of μ-meson or Electron

Let us assume that the K-mesons observed in the decays

$$K \to \pi+\mu+\nu \tag{1}$$

$$K \to \pi+e+\nu \tag{2}$$

have spin zero. The transition matrix-elements corresponding to these processes will then have the following general form which describes (1) as well as (2):

$$S'_{fi} = \langle f|S'|i\rangle = i\delta_4(P'-P-p-q)\langle f|S|i\rangle \tag{3}$$

with

$$S = g\phi(P')\varphi^*(P)\psi^*(p)\left\{c_S\gamma_4 + \frac{1}{M}(c_V P_\alpha + c'_V P'_\alpha)\gamma_4\gamma_\alpha + c_T\frac{1}{4M^2}(P'_\alpha P_\beta - P'_\beta P_\alpha)\gamma_4(\gamma_\alpha\gamma_\beta - \gamma_\beta\gamma_\alpha)\right\}\psi_\nu(q) + \text{h.c.}, \tag{4}$$

where P', P, p, q and $\phi(P')$, $\varphi(P)$, $\psi(p)$, $\psi_\nu(q)$ denote the four-momenta and the corresponding quantised wave functions of the K-meson, π-meson, μ-meson (or electron) and neutrino respectively. M, m, μ will denote the rest-masses of the K-meson, π-meson and μ-meson (or electron) respectively. We are using here a representation in which all γ_α's are real. The c's may satisfy the normalisation equation $|c_S|^2+|c_V|^2+|c'_V|^2+|c_T|^2 = 1$. The values of g and c's will be of course different for (1) and (2).

Because of the vanishing mass of the neutrino we cannot distinguish between scalar and pseudoscalar K-mesons merely by studying decays (1) or (2). The same form (4) for the matrix S can, therefore, be used for scalar as well as for pseudoscalar K-mesons.

In general the c's and g can depend on the scalar product $P'_\alpha \cdot P_\alpha$, i.e. essentially on the energy of the emitted π-meson. After having made this allowance we can derive the form (4) of the matrix S from general invariance principles under the only simplifying assumption that the fermions μ, ν (or e, ν) are created simultaneously and do not interact afterwards with any real or virtual particle. This assumption, however, can easily be justified as the result of the universal Fermi interaction (acting e.g. through a virtual nucleon-hyperon pair) and the fact that none of the fermions μ, e, ν interacts strongly with any hitherto known particle [6, 7]). Therefore, the terms in S differing in form from (4) can only be very small corrections. The assumption made above is just sufficient to ensure that the fermion momenta $\not{p}_\alpha$ and q_α appear in (4) only in the combination $(\not{p}_\alpha + q_\alpha)$ which can be replaced by the boson momenta owing to the conservation equation $q_\alpha + p_\alpha = P'_\alpha - P_\alpha$. Thus we see that only two independent momenta P'_α, P_α are left for the construction of the covariant forms as is shown by the structure of (4).

In the coordinate system in which the K-meson is at rest $P'_\alpha = (0, 0, 0, iM)$ and the matrix S can be put into the following, more convenient, form:

$$S = g\phi\varphi^* \sum_{i=1}^{2} \sum_{\alpha=1}^{4} A^i_\alpha \psi^* \Omega^i_\alpha \psi_\nu + \text{h.c.} \tag{5}$$

with

$$A^1_k = i\frac{c_T}{M} P_k, \quad A^1_4 = c_S, \quad A^2_k = \frac{c_V}{M} P_k, \quad A^2_4 = i\left(c'_V + c_V \frac{\varepsilon}{M}\right), \quad k = 1, 2, 3;$$

$$\Omega^1_\alpha = \gamma_\alpha, \quad \Omega^2_\alpha = \gamma_4 \gamma_\alpha. \tag{6}$$

ε and E denote correspondingly the energies of the π-meson and μ-meson (or electron) in the rest system of the K-meson.

Let us calculate the polarisation of the μ-meson (or electron) under the assumption that the neutrino (or anti-neutrino) emitted in (1) or (2) is completely polarised. We are interested in the case when the momentum of the π-meson is not measured. Since this means that we must average over all the possible π-meson momenta, the only remaining polarisation is the longitudinal one. In order to make the following discussion more specific let us confine our attention to the process

$$K^- \to \pi^0 + \tilde{\nu} + \mu^- \text{ (or } e^-). \tag{7}$$

This does not imply any serious restriction since simple symmetry relations can be found between (7) and other decays of the type (1) or (2). We assume that $\tilde{\nu}$ emitted simultaneously with μ^- or e^- is completely polarised in the direction antiparallel to its direction of motion $\mathbf{q}$. This seems to be strongly suggested by recent experiments [3]).

The probabilities of finding μ^- (or e^-) in (7) in a state of momentum $\mathbf{p}$

and parallel (+) or antiparallel (−) polarisation will be denoted by $R_+(p)$ and $R_-(p)$ respectively. The degree of polarisation $\Pi(p)$ of μ^- (or e^-) is then defined by

$$\Pi(p) = \frac{R_+(p) - R_-(p)}{R_+(p) + R_-(p)}. \tag{8}$$

$\Pi = +1$ means complete parallel polarisation; $\Pi = -1$ means complete antiparallel polarisation of the μ-meson (or electron). Because of the structure of (8) we are interested only in the relative probabilities defined by the ratio

$$\frac{R_+(p)}{R_-(p)} = \frac{\int \delta(M-\varepsilon-E-q)\delta_3(\mathbf{P}+\mathbf{p}+\mathbf{q})|S_{+-}(\mathbf{P},\ \mathbf{p},\ \mathbf{q})|^2 \mathrm{d}_3 P \mathrm{d}_3 q}{\int \delta(M-\varepsilon-E-q)\delta_3(\mathbf{P}+\mathbf{p}+\mathbf{q})|S_{--}(\mathbf{P},\ \mathbf{p},\ \mathbf{q})|^2 \mathrm{d}_3 P \mathrm{d}_3 q} \tag{9}$$

with

$$|S_{+-}(\mathbf{P}, \mathbf{p}, \mathbf{q})|^2 = \frac{b}{\varepsilon} T_{+-}(\mathbf{P}, \mathbf{p}, \mathbf{q}),\ |S_{--}(\mathbf{P}, \mathbf{p}, \mathbf{q})|^2 = \frac{b}{\varepsilon} T_{--}(\mathbf{P}, \mathbf{p}, \mathbf{q}), \tag{10}$$

$$T_{\pm,-}(\mathbf{P}, \mathbf{p}, \mathbf{q}) = gg^* \sum_{i,j=1}^{2} \sum_{\alpha,\beta=1}^{4} A_\alpha^i(\mathbf{P}) A_\beta^{j*}(\mathbf{P}) \operatorname{tr}\{\lambda_\pm(\mathbf{p}) \Lambda(\mathbf{p}) \Omega_\alpha^i \lambda_-(\mathbf{q}) \Lambda^0(\mathbf{q}) \Omega_\beta^{j*}\}.$$

b is a normalisation constant which is irrelevant for the present calculations; Λ, Λ^0 are the usual energy projection operators for μ-meson (or electron) and neutrino respectively; $\lambda_\pm$ are spin projection operators (see appendix).

Performing the $\mathrm{d}_3 P$ and $\mathrm{d}_3 q$ integrations, we obtain the following general formula describing the polarisation of μ^- (or e^-) in (7):

$$\frac{R_+(p)}{R_-(p)} = \frac{\int_{-1}^{+1} T_{+-}(\mathbf{P}', \mathbf{p}, \mathbf{q}')\, q'^3\, \mathrm{d}z}{\int_{-1}^{+1} T_{--}(\mathbf{P}', \mathbf{p}, \mathbf{q}')\, q'^3\, \mathrm{d}z}, \tag{11}$$

with

$$\mathbf{P}' = -(\mathbf{p}+\mathbf{q}'),\quad q' = \frac{M^2 - m^2 + \mu^2 - 2ME}{2(M - E + pz)},\quad z = \cos\theta = \frac{\mathbf{p}\cdot\mathbf{q}}{pq}. \tag{12}$$

The expressions under the integral signs in (11) are functions of p and z only. Let us introduce the notations

$$\begin{aligned} T_{+-}(\mathbf{P}',\ \mathbf{p},\ \mathbf{q}')q'^3 &= f(p,\ z) \\ T_{--}(\mathbf{P}',\ \mathbf{p},\ \mathbf{q}')q'^3 &= h(p,\ z) \end{aligned}. \tag{13}$$

Simple relations between the traces involved in (10) can be established (see appendix) which show that

$$h(p,\ z) = f(-p,\ -z). \tag{14}$$

Since

$$\int_{-1}^{+1} h(p,\ z)\mathrm{d}z = \int_{-1}^{+1} f(-p,\ -z)\mathrm{d}z = \int_{-1}^{+1} f(-p,\ z)\mathrm{d}z \tag{15}$$

we obtain the simple relation

$$\frac{R_+(p)}{R_-(p)} = \frac{F(p)}{F(-p)}, \tag{16}$$

where

$$F(p) = \int_{-1}^{+1} f(p, z)\mathrm{d}z. \tag{17}$$

Therefore

$$\Pi(p) = \frac{F(p)-F(-p)}{F(p)+F(-p)}. \tag{18}$$

If it turns out that ν and not $\tilde{\nu}$ is emitted in (7) we must calculate T_{++} and T_{-+} instead of T_{+-} and T_{--}. We find however that

$$T_{++} = T_{--},\ T_{+-} = T_{-+}, \tag{19}$$

which means that in this case the ratio R_+/R_- will be just inverse to that given by (11).

Evaluation of $T_{+-}(\mathbf{P}', \mathbf{p}, \mathbf{q}')q'^3 = f(p, z)$ gives the following result:

$$f(p, z) = \frac{g^* g}{4E}\{(q'-p)^2 B_1 + (q'-p)B_2 + B_3\}q'^3(1-z) \tag{20}$$

with

$$B_1(p, z) = \frac{1}{M^2}\{(E+p)c_T c_T^* + (E-p)c_V c_V^* + i\mu(c_T c_V^* - c_T^* c_V)\}$$

$$B_2(p, z) = \frac{1}{M}\left\{-(E+p)(c_T c_S^* + c_T^* c_S) + (E-p)\left(c_V c_V'^* + c_V^* c_V' + 2c_V c_V^* \frac{\varepsilon'}{M}\right)\right.$$
$$\left. + i\mu\left[(c_T c_V'^* - c_T^* c_V') + (c_T c_S^* - c_V^* c_S) + (c_T c_V^* - c_T^* c_V)\frac{\varepsilon'}{M}\right]\right\} \tag{21}$$

$$B_3(p, z) = \left\{(E+p)c_S c_S^* + (E-p)\left[c_V' c_V'^* + (c_V c_V'^* + c_V^* c_V')\frac{\varepsilon'}{M} + c_V c_V^* \frac{\varepsilon'^2}{M^2}\right]\right.$$
$$\left. + i\mu\left[(c_V' c_S^* - c_V'^* c_S) + (c_V c_S^* - c_V^* c_S)\frac{\varepsilon'}{M}\right]\right\}$$

and

$$\varepsilon' = M - E - q'. \tag{22}$$

3. Invariance under Combined Inversion

So far we did not specify whether the quantities g and c's are real or complex. We shall now simplify the expressions (21) by imposing some additional invariance condition on the transition matrix S.

We know that the hypothesis of a complete parallel polarisation of the neutrino is equivalent to a two component neutrino theory or to a replacement of ψ_ν by $\frac{1}{2}(1+\gamma_5)\psi_\nu$ [2]). Such a theory is not invariant under the usual space inversion I and charge conjugation C separately but is still invariant

under so called combined inversion defined by the product CI. If we now demand that S should also be invariant under CI transformation then we find that this can be satisfied only if $gc_j = g^* c_j^*$. This relation simplifies (21) considerably. In fact all the interference terms between S or T and V or V′(i.e. all the terms in (21) which are proportional to $i\mu$) vanish. Only (S, T) and (V, V′) interference terms remain.

The invariance under CI transformation guarantees also complete symmetry between $K^- \to \pi^0 + \bar{\nu} + \mu^-$ (or e^-) and $K^+ \to \pi^0 + \nu + \mu^+$ (or e^+). With respect to polarisation this means that μ^+ has just the opposite polarisation to μ^- at the same energy. The same symmetry obtains in neutral K-meson decays $K^0 \to \pi^- + \nu + \mu^+$ (or e^+) and $K^0 \to \pi^+ + \bar{\nu} + \mu^-$ (or e^-). Therefore if we neglect electromagnetic interaction between charged π-mesons and μ-mesons (or electrons) we can use the same formulae for neutral K-meson decay.

It can easily be seen that without any further restriction we can assume that the quantities c_j are all real. Then g must of course also be real.

4. First-Order Approximation

In order to be able to perform the last integration over z explicitly we must know the dependence of g and c's on ε. Since g and c's vary rather slowly with the π-meson energy ε, we can assume in the first approximation that all c's and g are constants. In this case the integration over z can be carried out in a straightforward way and we obtain the following expression for the polarisation:

$$\Pi(p) = \frac{\sum_{i=1}^{6} a_i J_i(p)}{\sum_{i=1}^{6} a_i K_i(p)} \tag{23}$$

where

$$a_1 = c_T^2, \quad a_2 = c_S^2, \quad a_3 = c_V^2, \quad a_4 = c_V'^2, \quad a_5 = 2c_T c_S, \quad a_6 = 2c_V c_V', \tag{24}$$

and

$$J_i(p) = \tfrac{1}{2}(L_i(p) - L_i(-p)), \quad K_i(p) = \tfrac{1}{2}(L_i(p) + L_i(-p)) \tag{25}$$

with

$$L_1(p) = (M(E+p) - \mu^2)\left\{\frac{p^2}{M^2} - \frac{p}{M}\frac{W-E}{W'-E}\left(1 + \frac{\frac{1}{3}p - E}{M}\right) + \frac{(W-E)^2}{4(W'-E)^2}\left[\left(1 + \frac{\frac{1}{3}p - E}{M}\right)^2 + \frac{2}{9}\frac{p^2}{M^2}\right]\right\}, \tag{26}$$

$$L_2(p) = (E+p)M - \mu^2,$$

$$L_3(p) = [M(E-p)-\mu^2]\frac{2(W'-E)}{M},$$

$$L_4(p) = [M(E-p)-(E-p)^2],$$

$$L_5(p) = [M(E+p)-\mu^2]\left\{\frac{p}{M} - \frac{W-E}{2(W'-E)}\left(1+\frac{\frac{1}{3}p-E}{M}\right)\right\}, \qquad (26)$$

$$L_6(p) = 2(E-p)(W'-E)$$

$$W = E_{\max} = \frac{M^2-m^2+\mu^2}{2M}, \quad W' = W+\frac{m^2}{2M} = \frac{M^2+\mu^2}{2M}.$$

In all these expressions we have omitted a factor common to all L's which depends on E only and is therefore cancelled in (23) (see appendix).

If it turns out that for some reasons the first approximation is not sufficient one can calculate the second approximation which consists in retaining in g and c's the terms linear in ε. The number of arbitrary constants will of course be double of that in the first approximation.

5. Discussion

It can be seen already from the general relation (18) that there is no polarisation in the nonrelativistic limit $p \to 0$ because $\lim_{p\to 0} F(p)-F(-p)=0$. Very slow μ-mesons or electrons emitted in (7) will therefore show no appreciable polarisation. This conclusion is completely independent of any particular assumption about the relative magnitudes or energy-dependence of the c's and g.

With increasing energy the polarisation becomes more and more appreciable. Its sign and absolute magnitude depends however not only on the energy, but also on the type of coupling. Fig. 1 gives the polarisation of μ^- emitted in (7) in four cases of pure couplings S, V, V' ,T. We see that pure scalar coupling gives a positive (i.e. parallel) polarisation of μ^- which increases quite rapidly, reaching practically complete polarisation already at about $0.6\,p_{\max}$. It should be pointed out that in this case the polarisation is always greater than the value $p/E = v/c$. The curve for pure V coupling is just an exact counterpart of that for pure S coupling. Pure V coupling gives therefore negative (antiparallel) polarisation of the same absolute magnitude as pure S coupling. Pure V' coupling gives also a negative polarisation which, however, reaches a maximum absolute value of $\approx 55\,\%$ and then decreases again. The pure tensor coupling gives rise to the most peculiar form of the polarisation curve. Starting from very low momenta the polarisation is positive, but remains very small till $p \approx 0.7\mu c$ when it becomes quite rapidly negative, reaching the minimum negative value of $\approx 64\,\%$ at $p \approx 1.3\mu c$. Then the polarisation increasing very

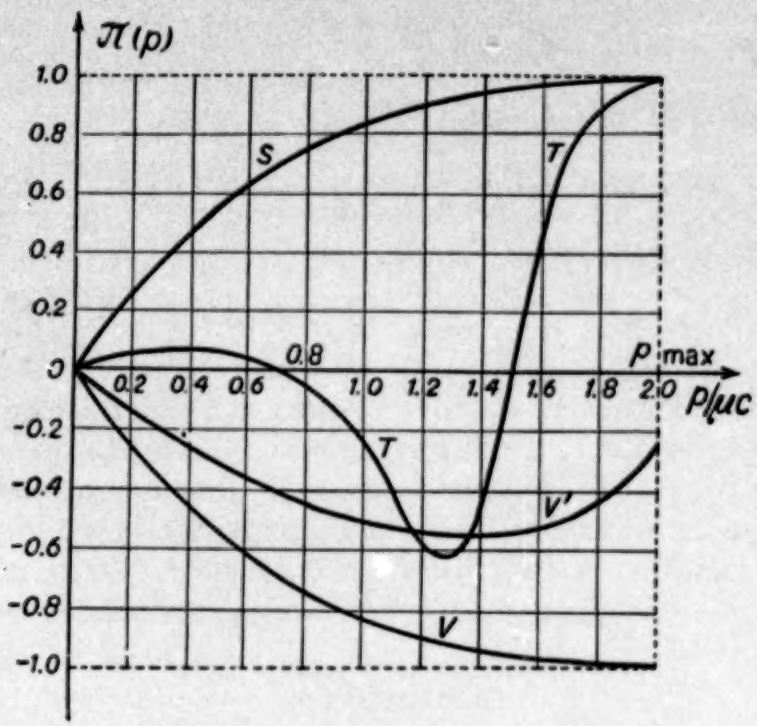
π(p)
1.0
0.8
0.6
0.4
0.2
0
-0.2
-0.4
-0.6
-0.8
-1.0
S
T
0.8
p max
0.2 0.4 0.6 1.0 1.2 1.4 1.6 1.8 2.0
p/μc
T
V'
V

Fig. 1

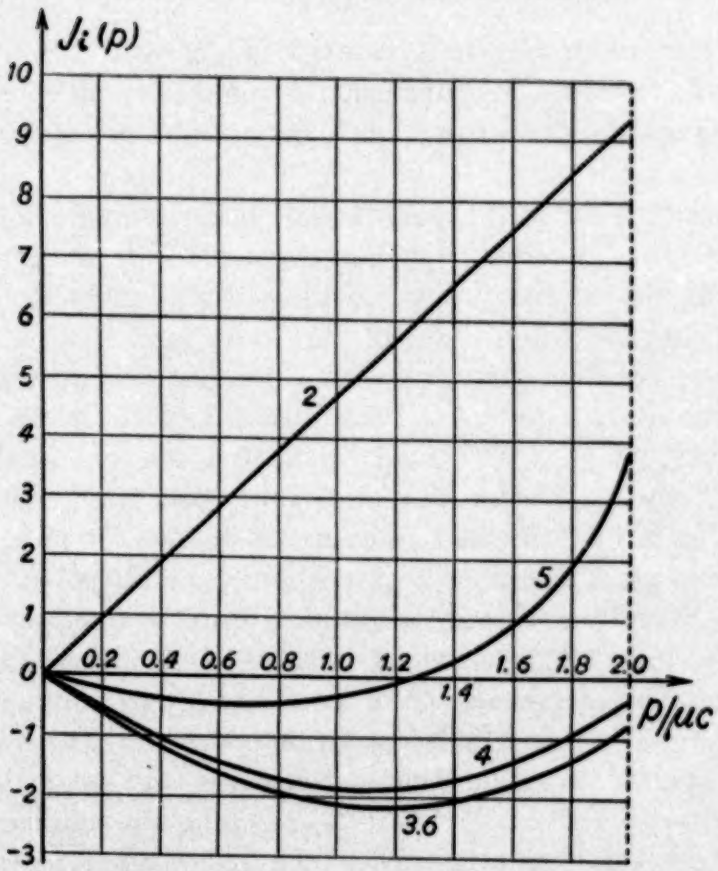
Ji(p)
10
9
8
7
6
5
4
3
2
1
0
-1
-2
-3
2
5
0.2 0.4 0.6 0.8 1.0 1.2 1.6 1.8 2.0
1.4
p/μc
4
3.6

Fig. 2

rapidly, becomes again positive at $p \approx 1.5\mu c$ reaching practically complete positive polarisation at the end of the curve. The large differences between different couplings make it possible to use the polarisation measurements as a new tool for the investigation of the coupling form. The possibility of a mixed type of coupling is however not excluded. In order to make a general

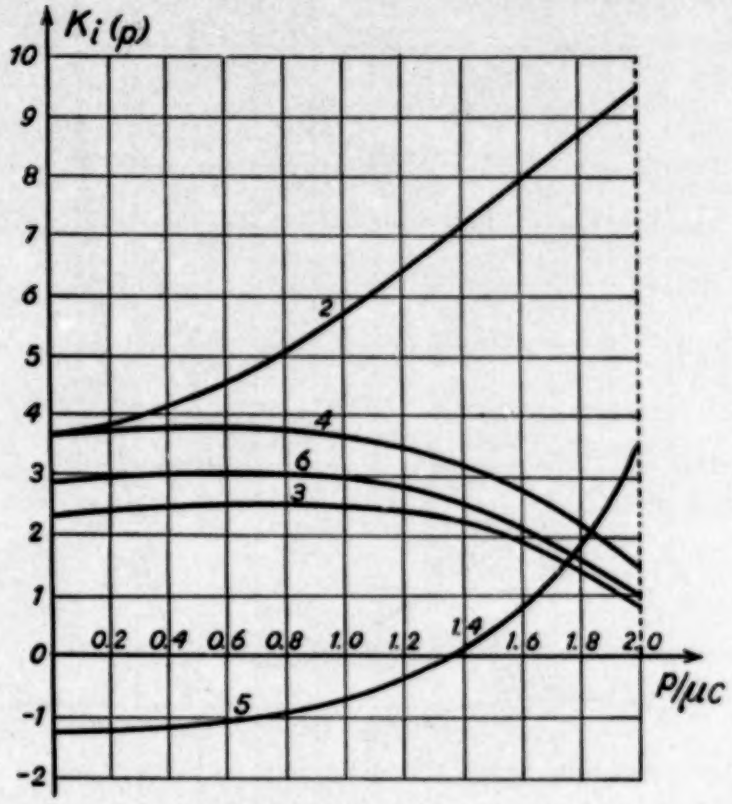

Fig. 3

analysis possible, the figures 2, 3, 4 show the plots of the functions $J_i(p)$ and $K_i(p)$ for μ^-.

In the case of electron decay the situation is much simpler. Because of the smallness of the electron mass most of the electrons emitted in (7) have highly relativistic energies. We can always neglect μ^2 in comparison with ME, $(M-E)E$ or even $(M-2E)E$. It can easily be seen from eqs. (25, 26) that for pure couplings S, T the polarisation of e^- is always positive and complete apart from a very small region of low energies. The polarisation in the case of pure V or V′ coupling is always negative and also complete apart from the region of low energies, where v/c is appreciably smaller than unity. Thus we see that in the case of the electron the situation is much simpler, because of the relativistic energies and the smallness of the electron mass. The measurement of the polarisation of a high-energy electron may be a rather difficult task [5]). On the other hand, the analysis of the data

will be rather simpler than in the case of μ-mesons. For instance: (i) if we find complete parallel polarisation of e^-, we know that only S and T can occur; (ii) if we find complete and antiparallel polarisation then only V

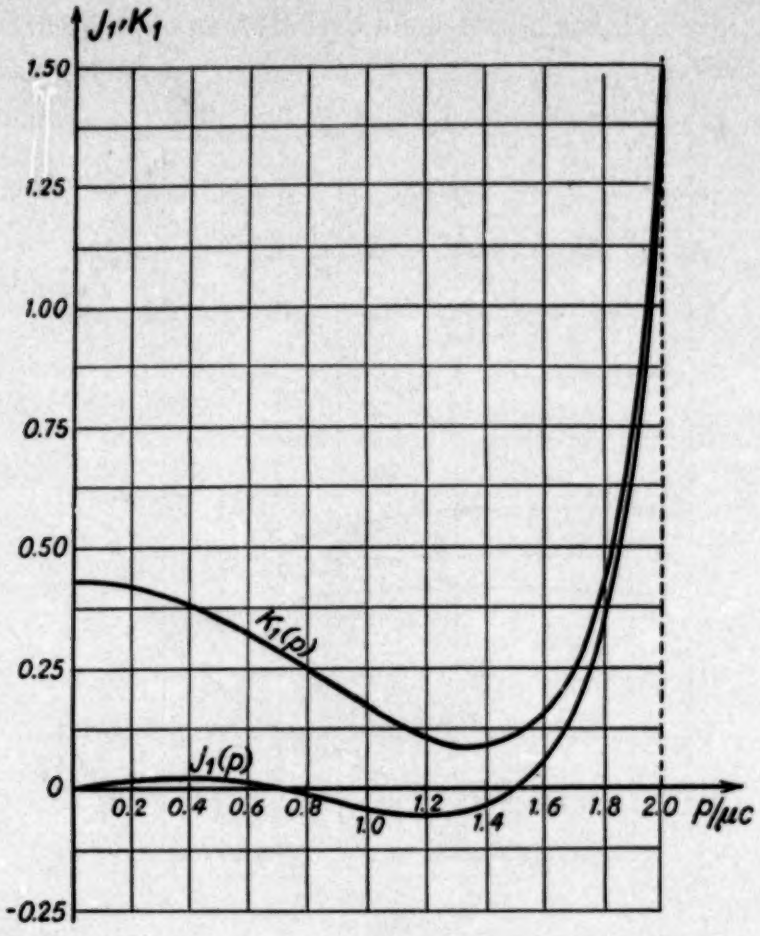

Fig. 4

and V′ can be present; (iii) if the polarisation is only partial, both groups of couplings, S, T and V, V′ must be represented, etc.

I should like to express my gratitude to Professor L. Rosenfeld for making it possible for me to carry out this work at Manchester University. I wish also to thank him and Dr. S. Oneda for helpful discussions.

Appendix

(I) The traces occurring in the calculation of $\Pi(p)$ for negative K-meson decay have the following form:

$$T^{ij}_{\pm,\,\pm\alpha\beta}(\mathbf{p},\,\mathbf{q}) = \mathrm{tr}\,\{\lambda_\pm(\mathbf{p})\Lambda(\mathbf{p})\Omega^i_\alpha\lambda_\pm(\mathbf{q})\Lambda^0(\mathbf{q})\Omega^{j*}_\beta\} \tag{A1}$$

with

$$\Lambda(\mathbf{p}) = \frac{E+i\gamma_4\gamma_k p_k+\gamma_4\mu}{2E}, \quad \Lambda^0(\mathbf{q}) = \frac{q+i\gamma_4\gamma_k q_k}{2q}, \quad \lambda_\pm(\mathbf{k}) = \frac{k\pm\sigma_j k_j}{2k}. \tag{A2}$$

With respect to the neutrino we can use another more convenient form of the spin-projection operator $\lambda^0_\pm = \frac{1}{2}(1\pm\gamma_5)$ which follows from the relation

$$\frac{q\pm\boldsymbol{\sigma}\cdot\mathbf{q}}{2q}\,\frac{q+i\gamma_4\boldsymbol{\gamma}\cdot\mathbf{q}}{2q}=\frac{1\pm\gamma_5}{2}\,\frac{q+i\gamma_4\boldsymbol{\gamma}\cdot\mathbf{q}}{2q}. \tag{A3}$$

All the traces (A1) can be reduced to the following form:

$$\begin{aligned} T^{ij}_{+-\alpha\beta}(\mathbf{p},\,\mathbf{q}) &= B^{ij}(p)t_{\alpha\beta}(\mathbf{p},\,\mathbf{q}), \quad T^{ij}_{++\alpha\beta}(\mathbf{p},\,\mathbf{q}) = B^{ij}(-p)t_{\alpha\beta}(-\mathbf{p},\,\mathbf{q}),\\ T^{ij}_{-+\alpha\beta}(\mathbf{p},\,\mathbf{q}) &= B^{ij}(p)t_{\alpha\beta}(\mathbf{p},\,\mathbf{q}), \quad T^{ij}_{--\alpha\beta}(\mathbf{p},\,\mathbf{q}) = B^{ij}(-p)t_{\alpha\beta}(-\mathbf{p},\,\mathbf{q}) \end{aligned} \tag{A4}$$

where

$$t_{\alpha\beta}(\mathbf{p},\,\mathbf{q}) = \mathrm{tr}\left\{\frac{1+\gamma_5}{2}\,\frac{p+i\gamma_4\gamma_k p_k}{2p}\,\gamma_\alpha\,\frac{q+i\gamma_4\gamma_k q_k}{2q}\,\gamma_\beta\right\} \tag{A5}$$

and

$$B^{11}(p)=\frac{E+p}{2E}, \quad B^{12}(p)=B^{21}(p)=\frac{\mu}{2E}, \quad B^{22}(p)=\frac{E-p}{2E}. \tag{A6}$$

Evaluation of $t_{\alpha\beta}(\mathbf{p},\,\mathbf{q})$ and contraction of the resulting $T^{ij}_{\pm,-\alpha\beta}(\mathbf{p},\,\mathbf{q})$ with $A^i_\alpha(\mathbf{P})A^{j*}_\beta(\mathbf{P})$ gives

$$\begin{aligned} T_{+-}(\mathbf{P},\,\mathbf{p},\,\mathbf{q}) = \frac{gg^*}{4E}\Big\{&B_1(p,\,P)\left[(1+z)\mathbf{P}^2-2\,\frac{(\mathbf{P}\cdot\mathbf{p})(\mathbf{P}\cdot\mathbf{q})}{pq}\right]\\ &+B_2(p,P)\left[\frac{\mathbf{p}}{p}-\frac{\mathbf{q}}{q}\right]\cdot\mathbf{P}+B_3(p,\,P)\,(1-z)\Big\} \end{aligned} \tag{A7}$$

$$\begin{aligned} T_{--}(\mathbf{P},\,\mathbf{p},\,\mathbf{q}) = \frac{gg^*}{4E}\Big\{&B_1(-p,P)\left[(1-z)\mathbf{P}^2+2\,\frac{(\mathbf{P}\cdot\mathbf{p})(\mathbf{P}\cdot\mathbf{q})}{pq}\right]\\ &+B_2(-p,\,P)\left[-\frac{\mathbf{p}}{p}-\frac{\mathbf{q}}{q}\right]\cdot\mathbf{P}+B_3(-p\;\;P)(1+z)\Big\}. \end{aligned} \tag{A8}$$

Replacing now $\mathbf{P}$ by $\mathbf{P}'=-\mathbf{p}-\mathbf{q}'$, and $\mathbf{q}$ by $\mathbf{q}'$ we obtain

$$\begin{aligned} T_{+-}(p,z)q'^3 &= f(p,z)\\ &= \{B_1(p,z)(q'--p)^2+B_2(p,z)(q'-p)+B_3(p,z)\}\,\frac{q'^3g^*g}{4E}\,(1-z) \end{aligned} \tag{A9}$$

$$\begin{aligned} T_{--}(p,z)q'^3 &= h(p,z)\\ &= \{B_1(-p,-z)(q'+p)^2+B_2(-p,-z)(q'+p)+B_3(-p,-z)\}\,\frac{q'^3g^*g}{4E}\,(1+z) \end{aligned} \tag{A10}$$

with $B_i(p,\,z)$ defined by (21). Comparing eq. (A9) with eq. (A10), and remembering that q' and ε' do not change under the replacement $p\to -p$, $z\to -z$ we find the relation (14).

(II) It can easily be seen from (20) and (21) that the functions $L_i(p)$ have originally the form

$$L'_1(p) = \frac{E+p}{M^2}(p^2N_3 - 2pN_4 + N_5), \qquad L'_2(p) = (E+p)N_3,$$

$$L'_3(p) = \frac{E-p}{M^2}(E+p-M)^2N_3, \qquad L'_4(p) = (E-p)N_3, \qquad \text{(A11)}$$

$$L'_5(p) = \frac{E+p}{M}(pN_3 - N_4), \qquad L'_6(p) = \frac{E-p}{M}(M-E-p)N_3,$$

with

$$N_n(p) = \frac{b}{E}\int_{-1}^{+1} q'^n(1-z)\mathrm{d}z, \qquad b = \text{constant}. \qquad \text{(A12)}$$

However, in the formula (23) the energy-dependent factor

$$\frac{bM}{2E}\,\frac{(W-E)^3}{(W'-E)^2} \qquad \text{(A13)}$$

which appears in all L_j is cancelled. Thus we are left with the somewhat simpler expressions (26).

References

1) T. D. Lee and C. N. Yang, Phys. Rev. **104** (1956) 254
2) L. D. Landau, Nuclear Physics **3** (1957) 127
   A. Salam, Nuovo Cimento **5** (1957) 229
   T. D. Lee and C. N. Yang, Phys. Rev. **105** (1957) 1671
3) C. S. Wu *et al.* Phys. Rev. **105** (1957) 1413
4) L. Garvin, L. M. Lederman and M. Weinrich **105** (1957) 1415
5) H. A. Tolhoek, On the theory of beta radioactivity (the Hague, 1951); Rev. Mod. Phys. **28** (1956) 277
6) K. Iwata, S. Ogawa, H. Okongi, B. Sakita and S. Oneda, Progress Theor. Phys. **13** (1955) 19
7) S. Furuichi, T. Kodama, Y. Suguhara, A. Wakasa and T. Yonezawa, Progress Theor. Phys. **16** (1956) 64

Nuclear Physics **4** (1957) 183—187; © *North-Holland Publishing Co., Amsterdam*
Not to be reproduced by photoprint or microfilm without written permission from the publisher

REMARKS ON PARITY CONSERVATION AND THE TWO-COMPONENT THEORY OF THE NEUTRINO

J. SERPE
Department of Mathematical Physics,
University of Liege, Belgium †

Received 26 April 1957

Abstract: Attention is drawn to a property of the two-component neutrino theory which was established a few years ago by the author; namely, that this theory is equivalent to Majorana's abbreviated theory. Some comments are made on the particle-antiparticle concept and on the formulation of the β-interaction with the help of the two-component neutrino-field.

1. Introduction

Recently a two-component theory of the neutrino has been proposed [1]) in connection with the discovery of parity non-conservation [2]) in weak interactions. However, some incorrect statements have been made concerning this theory. In a paper [3]) published in 1952 we investigated some properties of the two-component theory and obtained, among other results, the following: the two-component neutrino theory is equivalent to the so-called abbreviated or Majorana theory [4]). Since, as is well known, this abbreviated theory is, in its usual form, invariant separately for time and space reflections, the same property is valid for the corresponding two-component formulation. Of course, the possibility exists of modifying the original form of the Majorana theory by introducing coupling terms which do not conserve parity. In the present note we first recall briefly (section 2) some of the results obtained in our previous work [3]). In section 3 we give an additional remark on the particle-antiparticle concept, in order to clarify the fact that the neutrino and the antineutrino (in the sense of the ref. [1,3]) mentioned above) might be described by the abbreviated theory. In section 4 we make some comments on the formulation of the β-decay interaction with the help of the two-component neutrino field.

2. Two-component and Majorana Theories

The usual Dirac theory of fermions involve a four-component "complex" ψ satisfying the equations

$$\{\psi_K^*(\mathbf{x}, t), \psi_L(\mathbf{x}', t)\}_+ = \delta_{KL}\,\delta(\mathbf{x}-\mathbf{x}'), \qquad (1)$$

† On leave of absence at the Institute for Theoretical Physics, Copenhagen, Denmark.

$$\{\psi_K(\mathbf{x}, t), \psi_L(\mathbf{x}', t)\}_+ = \{\psi_K^*(\mathbf{x}, t), \psi_L^*(\mathbf{x}', t)\}_+ = 0, \tag{2}$$

$$\dot{\psi} + \boldsymbol{\alpha} \cdot \operatorname{grad} \psi + im\beta\psi + \sum_{s = V,T,S,P,A} g_s \mathscr{A}_s \mathscr{F}_s \psi = 0, \tag{3}$$

where $\boldsymbol{\alpha}$, β, $\mathscr{A}_s$ are the usual matrices, $\mathscr{F}_s$ denotes an external field which is supposed to be real, and g_s is the corresponding (real) interaction constant. As is well known, the hermitian matrices $\mathscr{A}_s$ are real (thus symmetric) for the interactions S, P, A and imaginary (thus skew-symmetric) for the interactions V, T. The sources (bilinear functions of the ψ_K and ψ_L^*) to be associated with the different types of interactions are †

$$\mathscr{S}_s = \tfrac{1}{2} g_s (\psi^* \mathscr{A}_s \psi - \tilde{\psi} \tilde{\mathscr{A}}_s \bar{\psi}). \tag{4}$$

In order to simplify the discussion we shall use the following particular representation of the Dirac matrices:

$$\alpha_1 = \begin{vmatrix} \sigma_1 & \cdot \\ \cdot & \sigma_1 \end{vmatrix}, \alpha_2 = \begin{vmatrix} \cdot & i\sigma_2 \\ -i\sigma_2 & \cdot \end{vmatrix}, \alpha_3 = \begin{vmatrix} \sigma_3 & \cdot \\ \cdot & \sigma_3 \end{vmatrix}, \beta = \begin{vmatrix} \sigma_2 & \cdot \\ \cdot & -\sigma_2 \end{vmatrix}. \tag{5}$$

If $g_V = g_T = 0$, we may abbreviate the theory by substituting for ψ a "real" four-component Φ $(= \bar{\Phi})$ satisfying the equations

$$\dot{\Phi} + \boldsymbol{\alpha} \cdot \operatorname{grad} \Phi + im\beta\Phi + \sum_{s = P,S,A} g_s \mathscr{A}_s \mathscr{F}_s \Phi = 0, \tag{6}$$

$$\{\Phi_K(\mathbf{x}, t), \Phi_L(\mathbf{x}', t)\}_+ = \delta_{KL}\, \delta(\mathbf{x} - \mathbf{x}'). \tag{7}$$

Now, if we introduce the two-component spinors φ_R and φ_I by putting

$$\Phi = \begin{vmatrix} \varphi_R \\ \varphi_I \end{vmatrix}, \tag{8}$$

and if we define the two-component complex φ by

$$\varphi = \varphi_R + i\varphi_I, \tag{9}$$

φ satisfies the equations

$$\{\varphi_K^*(\mathbf{x}, t), \varphi_L(\mathbf{x}', t)\}_+ = \delta_{KL}\, \delta(\mathbf{x} - \mathbf{x}'), \tag{10}$$

$$\{\varphi_K(\mathbf{x}, t), \varphi_L(\mathbf{x}', t)\}_+ = \{\varphi_K^*(\mathbf{x}, t), \varphi_L^*(\mathbf{x}', t)\}_+ = 0, \tag{11}$$

$$\dot{\varphi} + \boldsymbol{\sigma} \cdot \operatorname{grad} \varphi + im\sigma_2 \bar{\varphi} - ig_A[(\mathbf{A} \cdot \boldsymbol{\sigma}) - A_0]\varphi + ig_S \mathscr{F}_S \sigma_2 \bar{\varphi} + g_P \mathscr{F}_P \sigma_2 \bar{\varphi} = 0, \tag{12}$$

where $(\mathbf{A}, A_0)$ is the pseudovector external field called $(\mathbf{A}, V)$ in our previous paper [3]). The two-component equation (12) is linear if $m = 0$ and if the scalar and pseudoscalar interactions are missing. In that case, the pseudovector source

† *Notations*: If M denotes a matrix, $\overline{M}$ is its complex conjugate, M^* its hermitian conjugate, and $\tilde{M} = \overline{M}^*$ is the transposed matrix. In the case of a quantized spinor ψ, these definitions must be understood in the following way:

$$\psi = \begin{vmatrix} \psi_1 \\ \psi_2 \\ \psi_3 \\ \psi_4 \end{vmatrix}, \quad \tilde{\psi} = |\psi_1\, \psi_2\, \psi_3\, \psi_4|, \quad \bar{\psi} = \begin{vmatrix} \psi_1^* \\ \psi_2^* \\ \psi_3^* \\ \psi_4^* \end{vmatrix}, \quad \psi^* = |\psi_1^* \psi_2^* \psi_3^* \psi_4^*|,$$

where ψ_K^* is the hermitian conjugate of ψ_K.

$$\begin{aligned} \mathbf{s} &= \tfrac{1}{2} g_A (\varphi^* \boldsymbol{\sigma} \varphi - \tilde{\bar{\varphi}} \tilde{\boldsymbol{\sigma}} \bar{\varphi}), \\ s_0 &= \tfrac{1}{2} g_A (\varphi^* \varphi - \tilde{\bar{\varphi}} \bar{\varphi}), \end{aligned} \tag{13}$$

satisfies a continuity equation.

The theory described by the equations (10), (11), (12) is invariant, not only for the proper Lorentz group but also for space and time reflections, if the following transformation laws are adopted †:

$$\begin{aligned} \varphi &\to \pm i\sigma_2 \bar{\varphi}, \quad \text{for} \quad \mathbf{x}' = -\mathbf{x}, \quad t' = t, \\ \varphi &\to \pm \sigma_2 \bar{\varphi}, \quad \text{for} \quad \mathbf{x}' = \mathbf{x}, \quad t' = -t. \end{aligned} \tag{14}$$

It was also shown in our paper [3]), in the case of the free Majorana particles of zero rest mass, that the particle and the antiparticle states correspond to different (unquantized) wave equations in configuration space; each of these equations is associated with one of the spin states.

We may conclude from this section that the possibility of distinguishing between particles and antiparticles in the abbreviated theory is a matter of definition. The differentiation appears (does not appear) in the complex two-component (abbreviated four-component) formulation. We shall see in the next section that an analogous situation can be found in the case of electron theory ††.

3. Distinction between Particles and Antiparticles

The usual electron theory (with particles and antiparticles distinct from each other) is built with the help of a four-component complex field $\psi = \psi_R + i\psi_I$, where ψ_R and ψ_I are "real". This theory could equivalently be written with the help of an eight-component real

$$\Xi = \begin{vmatrix} \psi_R \\ \psi_I \end{vmatrix}.$$

In this form, it can be considered as the result of the abbreviation of a theory involving an eight-component complex field ††† Ψ. To each interaction of the field Ψ with an external field we shall again associate a corresponding

† The considerations on time reflection given in the appendix of our previous work [3]) must be cancelled; actually, the formulas (22), (22'), (23) and (25) need no change, when time reflection is considered, provided the order reversal of the operators is properly taken into account.

†† The content of section 3 is essentially part of a communication presented at a Colloquium on the Theory of particles in Brussels (April 1953).

††† The wave equation satisfied by Ψ is

$$\dot{\Psi} + \begin{vmatrix} \boldsymbol{\alpha} & \cdot \\ \cdot & \boldsymbol{\alpha} \end{vmatrix} \cdot \operatorname{grad} \Psi + \begin{vmatrix} i\beta & \cdot \\ \cdot & i\beta \end{vmatrix} m\Psi + i\Sigma_k g_k \mathscr{A}_k \mathscr{F}_k \Psi = 0,$$

where the $\mathscr{F}_k$ are external fields and the $\mathscr{A}_k$ some eight-dimensional matrices. Of course, this equation is reducible in the free case, but it allows new interactions in comparison with the usual formalism (cf. Biedenharn [5])). The Dirac theory of the neutrino is also reducible, in the free case, for $m = 0$.

source which will be a bilinear expression in the Ψ_K and Ψ_L^*. The sources may be written

$$\mathscr{S} = \tfrac{1}{2}g(\Psi^* \mathscr{A} \Psi - \tilde{\Psi} \tilde{\mathscr{A}} \overline{\Psi}), \tag{15}$$

and are of the following types (a_r denotes a real hermitian matrix and a_i an imaginary hermitian matrix):

type $\mathrm{I_r}$, $\mathscr{A} = \begin{vmatrix} \cdot & ia_r \\ -ia_r & \cdot \end{vmatrix}$, tensor character V, T;

$\mathrm{I_i}$, $\mathscr{A} = \begin{vmatrix} \cdot & ia_i \\ -ia_i & \cdot \end{vmatrix}$, S, P, A;

$\mathrm{II_r}$, $\mathscr{A} = \begin{vmatrix} a_r & \cdot \\ \cdot & a_r \end{vmatrix}$, V, T;

$\mathrm{II_i}$, $\mathscr{A} = \begin{vmatrix} a_i & \cdot \\ \cdot & a_i \end{vmatrix}$, S, P, A;

$\mathrm{III_r}$, $\mathscr{A} = \begin{vmatrix} a_r & \cdot \\ \cdot & -a_r \end{vmatrix}$, V, T;

$\mathrm{III_i}$, $\mathscr{A} = \begin{vmatrix} a_i & \cdot \\ \cdot & -a_i \end{vmatrix}$, S, P, A;

$\mathrm{IV_r}$, $\mathscr{A} = \begin{vmatrix} \cdot & a_r \\ a_r & \cdot \end{vmatrix}$, V, T;

$\mathrm{IV_i}$, $\mathscr{A} = \begin{vmatrix} \cdot & a_i \\ a_i & \cdot \end{vmatrix}$, S, P, A.

If we define the particle-antiparticle transformation in the usual way, i.e. $\Psi \to \overline{\Psi}$, the interactions which *do not* change sign are $\mathrm{I_r}$, $\mathrm{II_i}$, $\mathrm{III_i}$, $\mathrm{IV_i}$. If these are the only interactions present, we may build up an abbreviated theory and use a real eight-component Ξ, identifying in this way particles and antiparticles. Now, writing

$$\Xi = \begin{vmatrix} \psi_R \\ \psi_I \end{vmatrix},$$

and introducing the complex four-component field $\psi = \psi_R + i\psi_I$, we can rewrite the wave equation in the usual Dirac form, except that if interactions $\mathrm{III_i}$ or $\mathrm{IV_i}$ are present, the equation involves $\bar{\psi}$ besides ψ, and this is incompatible with charge conservation. In the usual theory, involving only the interactions $\mathrm{I_r}$ and $\mathrm{II_i}$, we may again classify the states into particle and antiparticle states associated with opposite signs of g_V and g_T in the configuration space representation.

4. β-Decay Interactions

The fact that Lee and Yang [1]) obtain a violation of parity conservation in β-decay is not a direct consequence of their using the two-component neutrino theory; this violation follows from the fact that they use coupling terms of the type C' (in their notation) besides coupling terms of the type C. It is true that, by imposing the condition $C = \pm C'$, one is automatically led to the two-component description of the neutrino field for the particular representation of the α-matrices used by Lee and Yang, but this two-component theory, being equivalent to Majorana's theory, could also be used without violating parity conservation. For instance, the scalar † parity-conserving interaction of β-decay, in the representation (5) would be, in terms of the two-component neutrino field φ_ν,

$$(\psi_p^* \gamma_4 \psi_n) \cdot \psi_e^* \begin{vmatrix} 1 & 1 \\ i & -i \end{vmatrix} \begin{vmatrix} \sigma_2 \varphi_\nu \\ \sigma_2 \bar{\varphi}_\nu \end{vmatrix}, \tag{16}$$

while the corresponding coupling used by Lee and Yang (with $C = -C'$) is

$$(\psi_p^* \gamma_4 \psi_n) \cdot \psi_e^* \begin{vmatrix} 1 & \cdot \\ \cdot & i \end{vmatrix} \begin{vmatrix} \sigma_2 \varphi_\nu \\ \sigma_2 \varphi_\nu \end{vmatrix}. \tag{17}$$

In contrast to the parity-conserving interaction (16), the coupling term (17) does not involve †† $\bar{\varphi}_\nu$ besides φ_ν. This explains why the phenomenon of double β-decay, with no neutrino emitted, cannot occur with the interaction (17). We also see that parity conservation *must* be violated (interaction (17)) if we assume both the two-component neutrino theory and the conservation law of fermions †††. The conservation law for the number of fermions is clearly equivalent (see the form of the mass-term in equation (12)) to the condition that no self-mass effects appear for the neutrino (cf. Salam [6])).

It is a pleasure to thank the members of the Institute for Theoretical Physics in Copenhagen for their gracious hospitality. I am indebted to the Fondation Franqui (Belgium) for its financial support.

† The vector, tensor, pseudovector and pseudoscalar β-decay interactions can be written in a similar way.

†† Of course, $\bar{\varphi}_\nu$ appears in the hermitian conjugate expression of (17), which is also contained in the interaction.

††† This remark has been stressed by W. Pauli (Copenhagen colloquium, April 1957). See also a paper by Touschek [7]).

References

1) T. D. Lee and C. N. Yang, Phys. Rev. **105** (1957) 1671; L. C. Landau, Nuclear Physics **3** (1957) 127
2) C. S. Wu, E. Ambler, R. W. Hayward, D. D. Hoppes and R. P. Hudson, Phys. Rev. **105** (1957) 1413; R. L. Garwin, L. M. Ledermann and M. Weinrich, Phys. Rev. **105** (1957) 1415
3) J. Serpe, Physica **18** (1952) 295
4) E. Majorana, Nuovo Cimento **14** (1937) 171
5) L. Biedenharn, Phys. Rev. **82** (1951) 100
6) A. Salam, Nuovo Cimento **5** (1957) 299
7) B. F. Touschek, Nuovo Cimento **5** (1957) 754

Nuclear Physics **4** (1957) 188; © *North-Holland Publishing Co., Amsterdam*
Not to be reproduced by photoprint or microfilm without written permission from the publisher

BOOK REVIEW

CERN *Symposium on high-energy accelerators and pion physics* (*Geneva* 11—23 *June* 1956) *Proceedings* (CERN, Geneva, 1956. Vol. 1: xiii-567 pages. Vol. 2: xii-443 pages. 40 Sw. Fr. each)

Those physicists (if such there be) who may have watched with some misgivings the expansion of the administrative machinery of CERN, and may even have had on their lips the word 'bureaucracy' in alluding to it, ought to pay amends to all concerned in presence of the stately volumes we are reviewing and the achievement which their production represents. Within four months the CERN people have managed, not only to collect some 150 papers and reports and to edit them in an orderly fashion, together with substantial accounts of the discussions and a very readable summary (by J. B. Adams) of the first week's proceedings, but also to get all this material neatly printed, with figures and plates, and elegantly bound in two large, but handy volumes.

The first volume is devoted to the problems raised by the construction of large accelerators; it contains not only descriptions of the existing machines (including the Russian ones), but breath-taking speculations about novel means of attaining still higher energies. The second volume opens with a discussion of more modest, but no less ingenious and beautiful instruments aiming at the detection and identification of particles and nuclear processes: bubble chambers, large cloud chambers, Čerenkov and other counters.

The larger part of the volume, however, is taken up by theoretical discussions and communications of new experimental data about all the main aspects of high-energy nuclear physics: the detection and properties of the anti-proton, the nucleon-nucleon scattering, the various reactions of π-mesons with nucleons and nuclei, and the more abstract aspects of quantum field theory. This part is perhaps less satisfactory than the others, because of the relative paucity of synthetic considerations: the few articles of this character are excellent, but one would have wished more of them. The very important work of Hofstadter and his group on the structure of the proton has been classified under 'Photoproduction of pions': this is not unlogical, but a bit forced; the subject would have deserved a special heading.

Should not an organisation like CERN, invested with such prestige and authority, give the good example in respecting the recommendations of the IUPAP on symbols and units? In the present case, they may be excused for inconsistencies in this respect by pressure of time: let us hope, however, that they will in the future pay more attention to this question.

L. R.

Nuclear Physics **4** (1957) 189—205; © *North-Holland Publishing Co., Amsterdam*

Not to be reproduced by photoprint or microfilm without written permission from the publisher

MIXING RATIOS OF $2^+ \rightarrow 2^+$ TRANSITIONS IN SOME EVEN NUCLEI

TORSTEN LINDQVIST AND INGVAR MARKLUND

Institute of Physics, Uppsala, Sweden

Received 20 April 1957

Abstract: Mixing ratios of $2^+ \rightarrow 2^+$ transitions in Se^{76}, Te^{122}, Te^{124} and Os^{186} have been measured by means of directional gamma-gamma correlations. Ten other similar cases in even nuclei have been summarized. The E2 radiation is dominating, although the amount of M1 radiation is measurable. The investigated transitions are examples of transitions between vibrational states, which according to theory should proceed by pure E2. The presence of M1 might indicate that the wave functions involved are not pure. The possibility of emission of E0 conversion electrons has been discussed. In six cases an upper limit has been given for the emission rate.

1. Introduction

Electromagnetic transitions between nuclear states a and b of characters (spin and parity) (I_a, π_a) and (I_b, π_b), respectively, may proceed by a multipole order L determined by

$$|I_a+I_b| \geqq L \geqq |I_a-I_b|. \tag{1}$$

If $\Delta I = 0, \pm 1$ and no change of parity takes place, the transition can occur by emission of a mixture of magnetic dipole and electric quadrupole radiation. Since there does not exist any multipole radiation with $L = 0$, relation (1) implies that electromagnetic transitions between two states with angular momentum $I_a = I_b = 0$ are absolutely forbidden.

According to the single particle shell model, the magnetic dipole transition will usually be much stronger than the electric quadrupole transition. However, it is found from empirical transition rates that the two multipolarities M1 and E2 may be of comparable intensities. Sometimes the E2 character is even dominating. As long as $E_\gamma < 1$ MeV, higher multipole transitions than quadrupole need not be considered.

It is of great importance to investigate the mixing ratios of M1 and E2 transitions, because they reflect the types of excitation involved.

When $I_a = I_b = 2$ and $\pi_a = \pi_b =$ even parity, we have a case where the transition is an admixture of M1 and E2. Such states occur frequently in even nuclei as first and second excited states. The ground state of these nuclei is always of spin zero and even parity. Scharff-Goldhaber and Weneser [1]) have reported a large class of even nuclei exhibiting regularities, which can be summarized as follows:

a. The ratio of the energies of the second excited state (E_2) to that of the first excited state (E_1) ranges between 2 and 2.5.
b. The spins of the low-lying states are commonly in the sequence (from the ground state) 0^+, 2^+, 2^+.
c. The first and second excited states decay predominantly by E2 radiation. The E2 matrix elements are enhanced over the single-particle matrix elements.
d. The E2 crossover transition (from second excited to ground state) occurs with much smaller probability than the upper transition (from second to first excited state).

The type of excitation of these 2^+ states may be of particle character or collective character, depending on the number of nucleons in the nucleus. In the case of collective motions Wilets and Jean [2]) have recently treated the 2^+ states in the spin sequence $2^+ \rightarrow 2^+ \rightarrow 0^+$ as surface oscillations. The upper transition proceeds solely be E2 radiation according to theory. An investigation of the mixing ratio of the upper transition is thus a test of the purity of the wave functions for the excited states involved.

The mixing ratio of M1 and E2 in the upper transition can be determined very accurately be means of directional correlation experiments. The fact that the lower transition (first excited to ground state) is pure E2 ($2^+ \rightarrow 0^+$) makes the determination unique. The method of directional correlation has the advantage over the method of conversion coefficient determination that it is independent of the theoretical conversion coefficients.

2. Method of Measurements

Four cases were investigated, namely

$$As^{76} \rightarrow Se^{76}$$
$$Sb^{122} \rightarrow Te^{122}$$
$$Sb^{124} \rightarrow Te^{124}$$
$$Re^{186} \rightarrow Os^{186}.$$

In all four cases the decay scheme seems to be well established and simple, with the exception of Sb^{124}.

The directional correlation between the two gamma radiations in the $2^+ \rightarrow 2^+ \rightarrow 0^+$ cascade was measured. The correlation is described by the correlation function

$$W(\theta) = 1 + A_2 P_2(\cos\theta) + A_4 P_4(\cos\theta) \qquad (2)$$

where $P_2(\cos\theta)$ and $P_4(\cos\theta)$ are the Legendre polynomials. A_2 and A_4 depend on spins and radiation multipolarities. In this case, when the spin sequence is fixed, A_2 and A_4 are functions only of the mixing parameter δ of the upper transition.

The parameter δ is defined as the ratio of the reduced matrix element of the electric quadrupole to that of the magnetic dipole. It can be either positive or negative. A more significant figure from the physical point of view is obtained in δ^2 which is equal to the ratio between the quadrupole and the dipole intensities.

For the spin sequence $2^+ \rightarrow 2^+ \rightarrow 0^+$ the theoretical coefficients [3]) in eq. (2) are

$$A_2 = \frac{1}{1+\delta^2}(0.250+0.732\delta-0.077\delta^2) \tag{3}$$

$$A_4 = \frac{0.326\delta^2}{1+\delta^2} \tag{4}$$

where δ is the mixing ratio of the upper transition. One sees immediately that the amount of quadrupole radiation is reflected in the size of the A_4 coefficient. For pure dipole radiation $A_4 = 0$. A_2 and A_4 as functions of the mixing parameter δ are shown in fig. 1. A_2 has two branches, one for $\delta > 0$ and one for $\delta < 0$. Therefore, a measured A_2 coefficient may fit two different

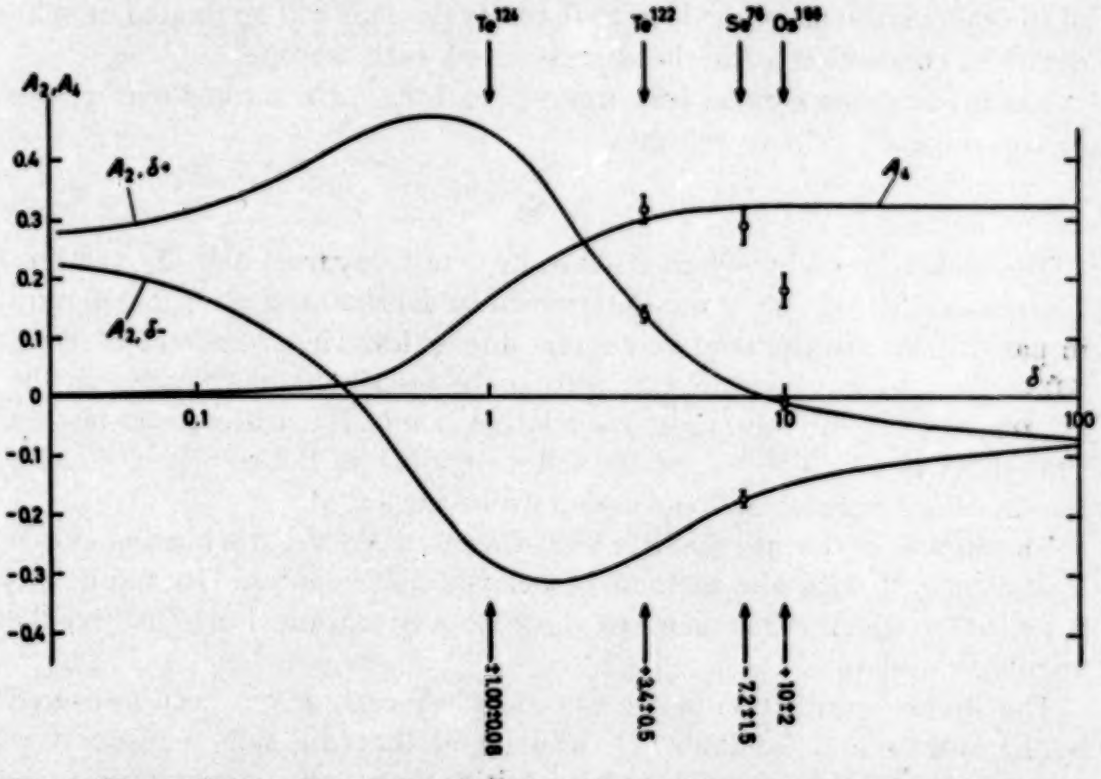

Fig. 1. The coefficients A_2 and A_4 as functions of the mixing parameter δ for the cascade $2^+ \rightarrow 2^+ \rightarrow 0^+$. Experimental values for Se^{76}, Te^{122} and Os^{186} are given.

values of δ. The A_4 coefficient, though not measured with the same accuracy as A_2, then determines uniquely the right value of δ. The measured value of

A_2 has been given preference in the determination of δ. The value of A_4 is then considered in the limits of error.

The angular correlation experiments were performed with a scintillation coincidence spectrometer with an effective resolving time of 10^{-7}s. The detectors were $1\frac{1}{2}$ in.$\times 1\frac{1}{2}$ in. NaI(Tl) crystals with RCA 6342 photomultipliers. The distance between source and crystal was 50 mm.

The data were recorded automatically. The number of coincidences at 225°, 180°, 135° and 90° between the counters were recorded by a camera. The single counting rates of each counter at corresponding position were recorded simultaneously. The recording time at each position was 30 min or 60 min. The cycle of angles was repeated continously until good statistics were obtained. After correcting for accidental coincidences the coefficients A_2 and A_4 in the correlation function $W(\theta)$ were calculated according to Gimmi *et al.* [4]). The coefficients thus obtained have to be corrected for the counter solid angles.

The radioactive sources for the correlation experiments were of such dimensions that no correction for the source size was necessary.

No extranuclear effects on the angular correlation were present, because of the short lifetimes of the intermediate levels. This will be treated in more detail in connection with the discussion of each isotope.

The investigated gamma transitions in each case are marked with circles in the respective decay schemes.

3. Se^{76}

The excited states in Se^{76} are reached by beta decay from As^{76} ($T_{\frac{1}{2}} = 26$ h). The decay scheme in fig. 2 was determined by Kurbatov *et al.* [5]). The figures in parentheses are the relative gamma intensities. The cascade considered, 643—560 keV, was measured by setting the discriminator channels on the photopeaks, respectively. From the relative gamma intensities it can be seen that the 1.40—1.20 MeV cascade will contribute to the coincidences with less than one percent and can therefore be neglected.

The lifetime of the intermediate level, the 560 keV level, has been measured by Coleman [6]) with the method of delayed coincidences. His result was 2.3×10^{-11}s, which is too short to allow for any extranuclear effect on the angular correlation.

The angular correlation of the 643—560 keV cascade has been measured by Kraushaar and Goldhaber [7]), who found that the spin sequence was $2 \rightarrow 2 \rightarrow 0$ and that the 643 keV transition was a dipole-quadrupole admixture with 34—80 % E2 radiation. The same correlation has also been measured by Metzger and Todd [8]), who found the same spin sequence and $\delta > 2.4$, i.e. > 85 % E2 in the 643 keV transition.

An upper limit of the K conversion coefficient of the 643 keV transition

has been determined by Bäckström [9]), $\alpha_k < 3\times10^{-3}$. From this information nothing can be said about the mixing ratio.

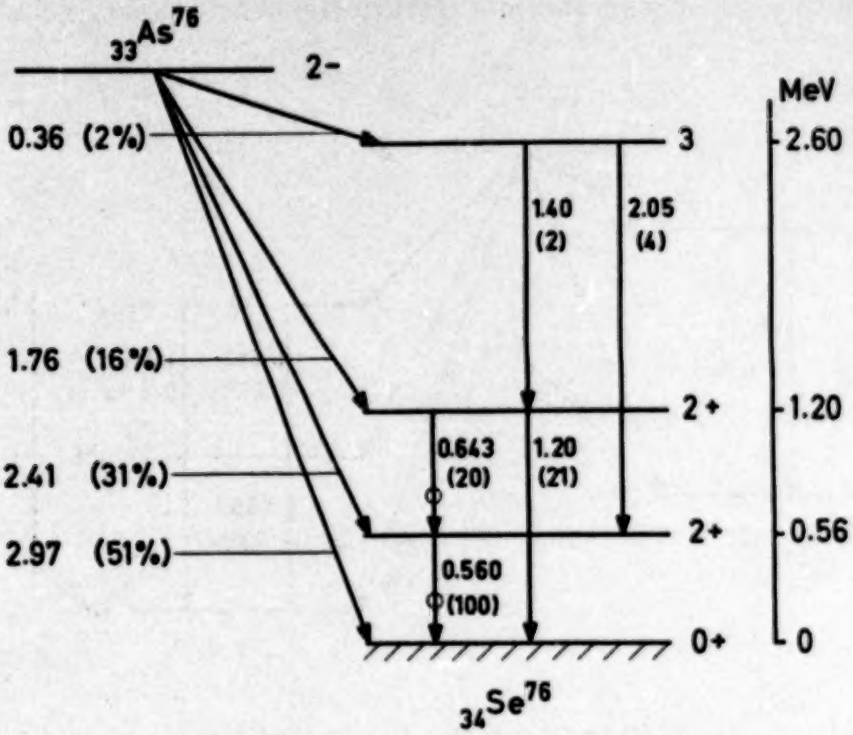

Fig. 2. Decay scheme of As^{76} according to ref. [5]).

In our experiment metal powder of „specpure" arsenic from Johnson, Matthey and Co, London, was bombarded with thermal neutrons in the reactor of AB Atomenergi, Stockholm †. The powder was then used as a source for the correlation experiment. Absorbers were used in front of the NaI crystals in order to stop the beta rays. After a correction for counter solid angles the correlation function was

$$W(\theta) = 1-(0.169\pm0.015)P_2(\cos\theta)+(0.293\pm0.030)P_4(\cos\theta).$$

According to fig. 1 the mixing parameter for the $2^+ \rightarrow 2^+$ transition in Se^{76} is

$$\delta = -7.2\pm1.5.$$

The A_4 coefficient is slightly too small which is probably due to some systematic error. It is concluded that the 643 keV transition is

$$(98\pm1)\%\ \text{E2}+(2\pm1)\%\ \text{M1}.$$

4. Te^{122}

The excited states in Te^{122} are reached by beta decay from Sb^{122} ($T_{\frac{1}{2}} = 65$ h). The decay scheme of Sb^{122} in fig. 3 is determined by Glaubman [10]). The

† The authors are indebted to AB Atomenergi, Stockholm, for all irradations mentioned in this paper.

693—563 keV cascade in Te^{122} represents the spin sequence $2^+ \rightarrow 2^+ \rightarrow 0^+$. Sb^{122} decays also by electron capture and positon emission to levels in Sn^{122}. This branch of the decay does not disturb the 693—563 keV coincidences.

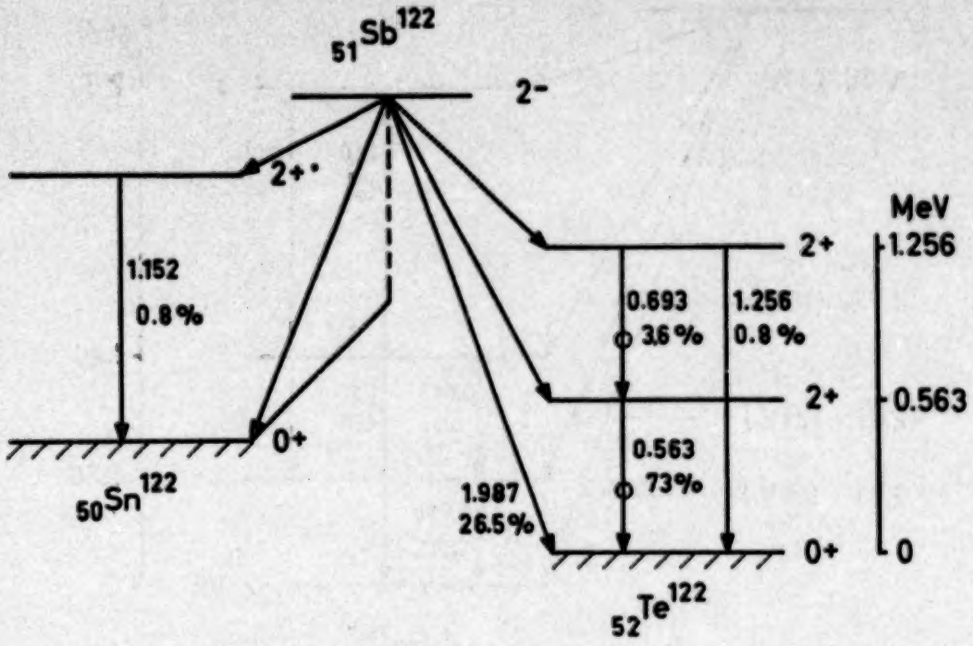

Fig. 3. Decay scheme of Sb^{122} according to ref. [10]).

The lifetime of the 563 keV level has been measured by Temmer and Heydenburg [11]) by means of Coulomb excitation to be 1.4×10^{-11}s. Coleman [6]) has measured the same lifetime by means of delayed coincidences and found the value 1.5×10^{-10}s. Although the two lifetimes disagree they are both too short to give any observable extranuclear effect on the angular correlation.

The angular correlation of the 693—563 keV cascade has been measured by Glaubman [10]), who found that the spin sequence was $2 \rightarrow 2 \rightarrow 0$ and that the 693 keV transition was 91 % E2+9 % M1.

The conversion coefficient of the 693 keV transition has not so far been measured.

In our correlation experiments we have used two kinds of sources. In the first run natural antimony in the form of metal powder was irradiated by thermal neutrons. Natural antimony consists of 57 % Sb^{121} and 43 % Sb^{123}. Thus Sb^{124} ($T_{\frac{1}{2}} = 60$ d) was produced simultaneously. After a short irradiation, one hour, the Sb^{122} activity dominates by far over Sb^{124}. However, the presence of some unidentified material in the commercial antimony gave some activity, that made the anisotropy decrease during the measurements. Therefore, as a second source we used irradiated enriched Sb^{121} (97.7 %, from Oak Ridge, U.S.A.). The metal powder was used in the ex-

periment. Absorbers were used in front of the crystals to stop the beta rays. After corrections for counter solid angles the correlation function was

$$W(\theta) = 1+(0.140\pm0.015)P_2(\cos\theta)+(0.032\pm0.025)P_4(\cos\theta).$$

According to fig. 1 the mixing parameter for the $2^+ \rightarrow 2^+$ transition in Te^{122} is

$$\delta = +3.4\pm0.5,$$

i.e. the 693 keV transition is

$$(92\pm4)\ \%\ E2+(8\pm4)\ \%\ M1,$$

which is in excellent agreement with Glaubman.

5. Te^{124}

The excited states in Te^{124} are reached by beta decay from Sb^{124} ($T_{\frac{1}{2}} = 60$ d.) The decay scheme in fig. 4 is determined by Lazar [12]). Recent work by B. S. Dzhelepov *et al.* [13]) and Tomlinson [14]) on the gamma spectrum of Sb^{124}

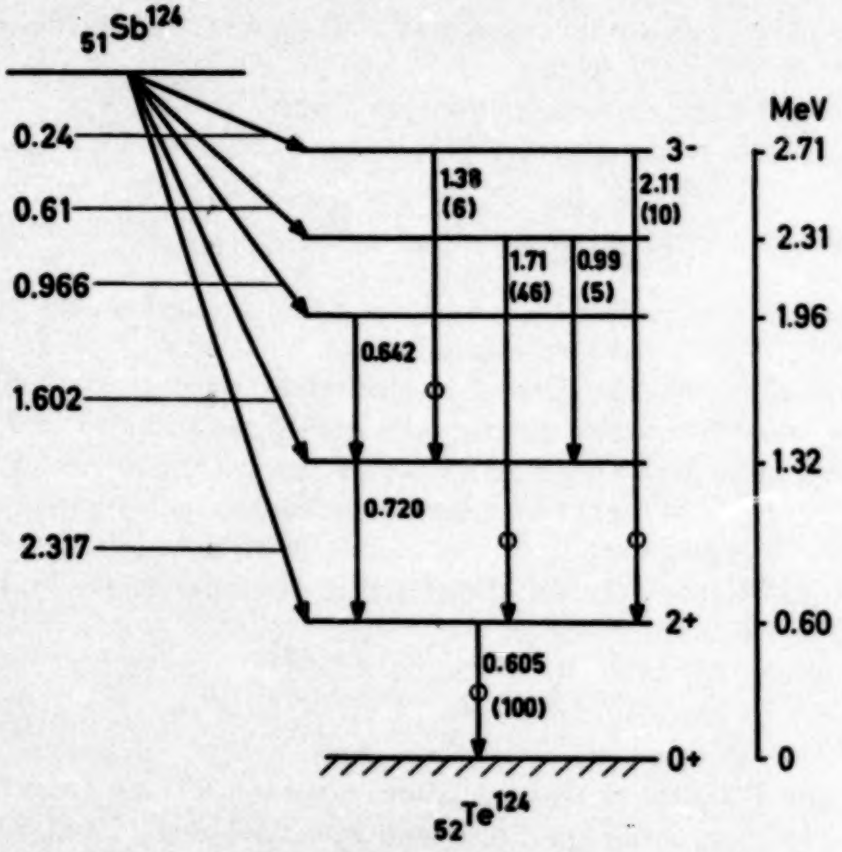

Fig. 4. Decay scheme of Sb^{124} according to ref. [12]).

indicates that there are a few other gamma lines than those given by Lazar. However, they are of low intensity and they do not change the level scheme.

The spins of all levels are not known. The first excited level was given spin 2^+ on the basis of conversion data [15]). The spin of the 2.71 MeV level was determined with gamma-gamma angular correlation between the 1.71 MeV and 0.60 MeV lines by Kloepper *et al.* [16]), who found the spin to be 3^-. Thus there was no given $2^+ \rightarrow 2^+ \rightarrow 0^+$ cascade in this nucleus. However, it is very reasonable to assume that the spin of the 1.32 MeV level is either 2^+ or 4^+. This assumption is based on a comparison with other even nuclei. It is very difficult to carry out an angular correlation measurement of the 0.72—0.605 MeV cascade in order to determine the spin of the 1.32 MeV level. Contributions from four other cascades, namely the 2.11—0.605, 1.71—0.605, 1.38—0.605 and 0.99—0.605 MeV cascades, will make an analysis of the data nearly impossible. In the 1.38—(0.72)—0.605 MeV cascade, however, one gets measurable contributions only from the 1.71—0.605 MeV cascade, for which one can make a correction from knowing the relative intensities of the gamma rays concerned.

The lifetime of the 0.605 MeV level has been measured by Temmer and Heydenburg [11]), who gave the value 1.3×10^{-11}s. Thus no extra-nuclear effects are expected. No determination of the conversion coefficient of the 0.72 MeV line is made so far.

The following angular correlations were investigated:

$W_1(\theta)$ for 2.11—0.605 MeV
$W_2(\theta)$ for 1.71—0.605 MeV
$W_3(\theta)$ for 1.38—(0.72)—0.605 MeV;

$W_1(\theta)$ can be measured directly by setting the channels on the respective photopeaks. $W_2(\theta)$ must be measured in combination with $W_1(\theta)$ owing to the Compton distribution of the 2.11 MeV under the 1.71 MeV photopeak. However, from the relative gamma intensities it is concluded that the 2.11 MeV contribution can be neglected. $W_3(\theta)$, which is a triple correlation of the „first-third" type [17]), cannot be measured without the contribution of $W_2(\theta)$. In this case it is necessary to correct for the contribution, with the relative intensities as weighting factors. If the measured correlation is called $W_{3,\,\mathrm{exp.}}(\theta)$ the following relation holds:

$$W_{3,\,\mathrm{exp.}} = \frac{1}{A+B}\left[A \cdot W_2 + B \cdot W_3\right] \qquad (5)$$

where A and B are the relative contributions of the 1.71 MeV and 1.38 MeV lines, respectively, within the discriminator channel used. A and B were determined graphically from the single gamma ray spectrum.

Natural antimony in the form of metal powder was irradiated by thermal neutrons for one month. The activity was then allowed to decay for one month in order to let shortlived activities disappear. The metal powder was

used in the experiment. Absorbers were put in front of the detectors to prevent the beta rays to be detected. After corrections for counter solid angles the following correlations were obtained:

$$W_1(\theta) = 1-(0.034\pm0.006)P_2(\cos\theta)+(0.007\pm0.012)P_4(\cos\theta)$$
$$W_2(\theta) = 1-(0.063\pm0.003)P_2(\cos\theta)+(0.002\pm0.008)P_4(\cos\theta)$$
$$W(\theta)_{3,\,\mathrm{exp.}} = 1-(0.049\pm0.004)P_2(\cos\theta)+(0\pm0.007)P_4(\cos\theta).$$

Within the limits of error all A_4 coefficients are zero, therefore they will be neglected in this case. According to eq. (5) one gets

$$W_3(\theta) = 1-(0.027\pm0.008)P_2(\cos\theta).$$

The correlation function $W_1(\theta)$ for the 2.11—0.605 MeV cascade, where $A_2 = -0.034\pm0.006$, fits the spin sequence $3 \to 2 \to 0$. The theoretical value is $A_2 = -0.071$ for pure multipoles. An admixture of less than one percent of quadrupole radiation in the 2.11 MeV transition gives the experimental value of A_2. Thus it is concluded that the 2.11 MeV transition is practically pure dipole and the spin of the 2.71 MeV level is 3.

The correlation function $W_2(\theta)$ for the 1.71—0.605 MeV cascade, where $A_2 = -0.063\pm0.003$, is very similar to $W_1(\theta)$. In this case the admixture of quadrupole radiation is still less. It is therefore concluded that the 1.71 MeV transition is pure dipole and the spin of the 2.31 MeV level is 3. Nothing can be said about the parities of the 2.71 MeV and 2.31 MeV levels.

A first-third triple correlation function for the spin sequence $j_0(L_1)j_1(L_2)j_2(L_3)j_3$ (see fig. 5) has the form [17])

$$W(\theta) = N\sum_\nu F_\nu(L_0L_0j_0j_1)F_\nu(L_2L_2j_2j_3)\times W(j_1j_1j_2j_2;\nu L_1)P_\nu(\cos\theta) \quad (6)$$

where

$$N = (-1)^{L_1-j_1-j_2}[(2j_1+1)(2j_2+1)]^{\frac{1}{2}}.$$

The coefficients F_ν and the quantities W (the Racah coefficients) are tabulated.

When the unobserved radiation between j_1 and j_2 is mixed, the final correlation function is [18])

$$W_{\mathrm{mix}}(\theta) = \frac{1}{1+\delta^2}[W(L_1)+\delta^2\cdot W(L'_1)] \quad (7)$$

where δ is the mixing parameter, L_1 and L'_1 are the multipolarities of the mixed radiation. $W(L_1)$ and $W(L'_1)$ are given by eq. (6).

$W_3(\theta)$ is the triple correlation for the 1.38—(0.72)—0.605 MeV cascade. The spin sequence is $3(L_0)j_1(L_1)2(\mathrm{E2})0$, where j_1 is the spin of the 1.32 MeV level. The spin j_1 is 4^+ or 2^+, as explained above.

Let us first consider the case $j_1 = 4^+$. Then the 0.72 MeV transition (L_1) is pure E2 and the 1.38 MeV transition (L_0) is dipole, or possibly a dipole-quadrupole mixture. The fact that $A_{4,\,\mathrm{exp.}} = 0$ excludes the possibility of an

admixture in the 1.38 MeV radiation. For pure multipoles one gets $A_{2,\,\mathrm{theor}} = -0.140$, which is far from the experimental value $A_{2,\,\mathrm{exp.}} = -0.027 \pm 0.008$ The case $j_1 = 4^+$ is therefore excluded and it is concluded that $j_1 = 2^+$.

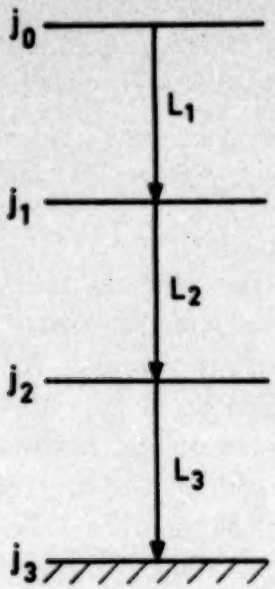

Fig. 5. Triple cascade.

Thus the 0.72 MeV transitions is a $2^+ \rightarrow 2^+$ transition, which usually is an M1+E2 mixture. According to eq. (7) the correlation function is a linear combination of the correlations for the respective pure multipoles. According to eqs. (2) and (6) one obtains

$$A_2(\mathrm{M1}) = -0.094 \text{ and } A_2(\mathrm{E2}) = +0.040.$$

Eq. (7) then gives

$$A_{2,\,\mathrm{exp.}} = \frac{1}{1+\delta^2}\left[A_2(\mathrm{M1}) + \delta^2 \cdot A_2(\mathrm{E2})\right]. \tag{8}$$

With the experimental values inserted one obtains

$$-0.027 \pm 0.008 = \frac{1}{1+\delta^2}\left[-0.094 + \delta^2 \cdot 0.040\right],$$

hence

$$\delta^2 = 1.00 \pm 0.17 \text{ and } \delta = \pm 1.00 \pm 0.08.$$

With this method it is impossible to determine the sign of δ.

The final conclusion is that the spin of the 1.32 MeV level in Te^{124} is 2^+ and that the 0.72 MeV radiation is an admixture of

$$(50 \pm 10)\ \%\ \mathrm{E2} + (50 \pm 10)\ \%\ \mathrm{M1}.$$

6. Os^{186}

The main features of the level scheme of Os^{186} have been established by Metzger and Hill [19]). They determined the decay scheme of Re^{186} ($T_{\frac{1}{2}} = 89$ h), which partly decays to levels in Os^{186} (fig. 6). The spin of the 764 keV level has been determined with gamma-gamma angular correlation by Hurley and Jastram [20]). Their measured correlation of the 627—137 keV cascade indicated the spin sequence $2 \rightarrow 2 \rightarrow 0$. However, nothing was said about a possible admixture of multipoles in the 627 keV transition.

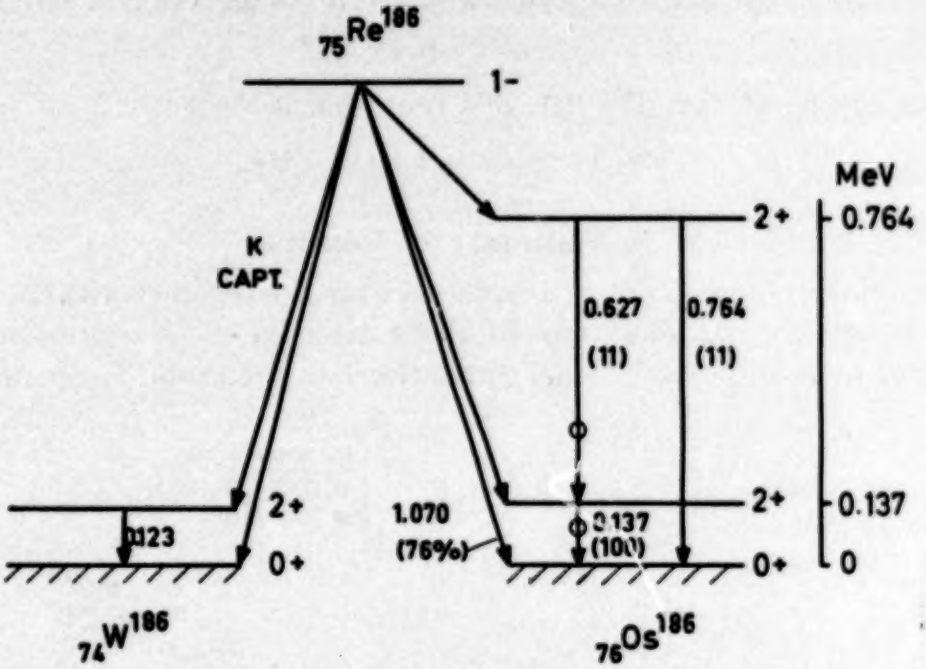

Fig. 6. Decay scheme of Re^{186} according to ref. [19]).

The lifetime of the 137 keV level has been measured with delayed coincidences by McGowan [21]) to be 8×10^{-10}s. It is therefore assumed that the extranuclear effects are small. The conversion coefficient of the 627 keV transition is not determined.

Natural rhenium (37 % Re^{185} and 63 % Re^{187}) as well as enriched rhenium (85.4 % Re^{185}, from Oak Ridge, U.S.A.) were used for the isotope production. When bombarding with thermal neutrons in the case of natural rhenium one obtains besides Re^{186} also Re^{188} ($T_{\frac{1}{2}} = 16.9$ h). Because this half life is much shorter than that of Re^{186}, it is necessary to wait some time before starting the measurement. When using enriched rhenium the measurement can start earlier after the bombardment.

The radioactive source was in the form of metal powder. The discriminator channels accepted the 627 keV and 137 keV photopeaks, respectively. The beta rays were absorbed. The two sources, natural rhenium and enriched

rhenium, gave the same results. After corrections for counter solid angles the following mean value was obtained:

$$W(\theta) = 1-(0.02\pm0.01)P_2(\cos\theta)+(0.18\pm0.03)P_4(\cos\theta).$$

According to fig. 1 the A_2 coefficient defines $\delta = +10$. The A_4 coefficient, however, does not fit on its curve. It is possible that in spite of the short lifetime of the 137 keV level, 8×10^{-10}s, some extra nuclear attenuation is present. In such a case the small A_2 coefficient should not be very much changed. The region $\delta < 0$ is hardly possible, because then A_4 would be smaller than the measured value. Therefore the following value is adopted:

$$\delta = +10\pm2.$$

It is concluded that the 627 keV transition is

$$(99\pm1)\ \%\ \text{E2}+(1\pm1)\ \%\ \text{M1}.$$

7. Summary of Results

The results obtained are summarized in table 1 together with 10 other cases reported in the literature. In all 14 cases the mixing ratios are determined by means of directional correlation measurements. The parameter

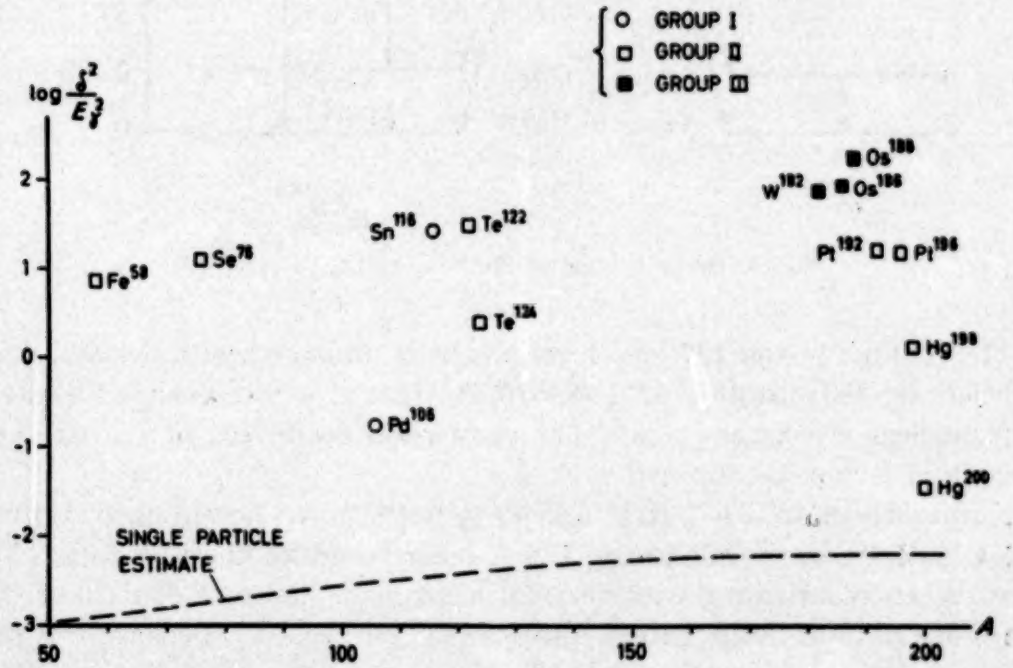

Fig. 7. Reduced mixing ratios, δ^2/E_γ^2, as functions of the mass number A. Group I = open circles, group II = open squares, group III = filled squares (see text for the group definitions). Dashed line is single particle estimate according to Moszkowski [22]).

δ, which is the primary figure coming out of the experiment, as well as the percentage of E2 are tabulated. It is obvious that the

$$\text{percentage of E2} = \frac{100\delta^2}{1+\delta^2}. \qquad (9)$$

It is rather surprising to find such large percentages of E2 radiation in the mixed transitions. The single particle estimate by Moszkowski [22]) cannot account for this fact. The reduced mixing ratios, δ^2/E_γ^2, where E_γ is the transition energy in MeV, are plotted as a function of the mass number A in fig. 7. The dashed line represents the single particle estimate. The experimental values scatter very much, but they are all much larger than the single particle estimate.

8. Discussion

Alder *et al.* [23]) have recently discussed the various types of excitation in even nuclei with the spin sequence (from the ground state) 0^+, 2^+, 2^+. In general it is possible to distinguish between two different modes of excitation, the first associated with the motion of the individual nucleons and the second with collective types of nuclear motion. In the adiabatic approximation, i.e. when the frequencies of the collective excitations are small compared with those characterizing the intrinsic nucleon motion, one may separate the two types of motion. This is certainly justified when moving away from closed shells.

The collective excitations can be of rotational or vibrational type. In the vicinity of closed shells, where the spherical shape represents a stable equilibrium, the collective excitations correspond to vibrations about this shape. The frequencies of these vibrations are expected to decrease with the addition of particles.

For deformed nuclei the collective spectrum can be of vibrational as well as of rotational type. The first corresponds to oscillations about the equilibrium shape for a fixed orientation of the nucleus, while the second represents a motion which rotates the nuclear orientation while preserving the shape. The rotational spectra in even nuclei give the well known spin sequence (from the ground state) 0^+, 2^+, 4^+, 6^+, ...

The properties of the vibrational modes of excitation, in spherical and deformed nuclei, are at present less well established. For an even spherical nucleus one usually has a quadrupole vibrational spectrum, in which the excited states have energies $\hbar\nu$, $2\hbar\nu$, $3\hbar\nu$ . . . (ν is the vibration frequency). Accordingly, the ratio $E_2/E_1 = 2$. The fact that the crossover is much weaker than the upper transition follows from the favored nature of one phonon jump.

In strongly deformed nuclei the lowest collective excitations correspond to rotations with preservation of shape. One may also expect these nuclei to exhibit collective excitations corresponding to vibrations about the equili-

brium shape. The energy of the vibrational levels in even non-spherical nuclei is usually of the order of 1 MeV.

Accordingly one can divide the 2^+ states in even nuclei into three groups:

I. particle excitation,
II. vibrational excitation of spherical nuclei,
III. vibrational excitation of non-spherical nuclei.

In the classification column of table 1 it is shown which type of excitation the various nuclei represent.

TABLE 1

The occurence of E2 radiation in $2^+ - 2^+$ transitions of even nuclei.

Nucleus	E_γ keV	δ^2	Percent E2 radiation	Phase	E_2/E_1	Classification	References
$_{26}Fe^{58}$	810	4.9	83 ± 4	0	2.0	II	a
$_{34}Se^{76}$	643	52	98 ± 1	π	2.2	II	Present work
$_{46}Pd^{106}$	1045	0.04	4.1 ± 0.2	—	—	I or II	b
$_{50}Sn^{116}$	800	9	≈ 90	0	1.65	I or II	c
$_{52}Te^{122}$	693	11.5	92 ± 4	0	2.2	II	Present work
$_{52}Te^{124}$	720	1	50 ± 10	—	2.2	II	Present work
$_{74}W^{182}$	1122	9	≈ 90	π	—	III	d
$_{76}Os^{186}$	627	100	99 ± 1	0	5.6	III	Present work
$_{76}Os^{188}$	480	200	99.6	π	4.2	III	e
$_{78}Pt^{192}$	296	19	≈ 95	π	1.94	II	f
$_{78}Pt^{194}$	295	∞	≈ 100	—	1.91	II	g
$_{78}Pt^{196}$	332	19	95 ± 1	π	1.94	II	h
$_{80}Hg^{198}$	676	1.5	60 ± 5	π	2.7	II	i
$_{80}Hg^{200}$	1207	0.05	≈ 5	π	—	II	j

Phase = 0 means $\delta > 0$ and phase = π means $\delta < 0$. E_2/E_1 is the ratio of the energies of second to first excited states. When no figure is given, the $2^+ \rightarrow 2^+$ transition does not take place between second and first excited state. Classification: I = particle excitation, II = vibrational excitation in spherical nuclei, III = vibrational excitation in non-spherical nuclei.

a) H. Frauenfelder, N. Levine, A. Rossi and S. Singer, Phys. Rev. **103** (1956) 352
b) E. D. Klema and F. K. McGowan, Phys. Rev. **92** (1953) 1469
c) R. P. Scharenberg, M. G. Stewart and M. L. Wiedenbeck, Phys. Rev. **101** (1956) 689
d) R. C. Williams and K. I. Roulston, Can. J. Phys. **34** (1956) 1087
e) V. R. Potnis, V. S. Dubey and C. E. Mandeville, Phys. Rev. **102** (1956) 459
f) V. H. Kelly and M. L. Wiedenbeck, Phys. Rev. **102** (1956) 1130
g) C. E. Mandeville, J. Varma and B. Saraf, Phys. Rev. **98** (1955) 94
h) R. M. Steffen, Phys. Rev. **89** (1953) 665
i) C. D. Schrader, Phys. Rev. **92** (1953) 928
j) T. Lindqvist, Arkiv för Fysik (to be published)

In group I no systematic trend is expected. In groups II and III, according to theory, the transition between vibrational states should proceed solely by E2 radiation. The results show that in groups II and III the E2 radiation is dominating, although the amount of M1 radiation is measurable. The presence of M1 radiation indicates that the wave functions are not quite pure.

One explanation for this is that the adiabatic approximation is not correct. With more data accumulated it might be possible to estimate the finer details of this model.

9. Electric Monopole Transitions

The emission of a single electric monopole gamma ray is strictly forbidden by the transverse nature of the electro-magnetic field. An E0 transition proceeds solely by internal conversion, when the energy is smaller than $2mc^2$. No angular momentum is transferred to the ejected electron. Church and Weneser [24]) have recently treated this problem and pointed out that nuclei with spin sequence $2^+ \rightarrow 2^+ \rightarrow 0^+$ are very interesting from this point of view.

The absolute transition probability for E0 conversion, $W(\mathrm{E0})$, may be written as the product of an electronic factor Ω and the square of the nuclear „strength parameter", ϱ, which contains the nuclear matrix elements:

$$W(\mathrm{E0}) = \Omega \cdot \varrho^2. \tag{10}$$

The electronic factor, Ω, is independent of the spin of the nuclear states involved. The strength parameter ϱ, would be of the order of unity in the „Weisskopf" approximation. It would be of great interest to measure the value of ϱ, because theoretical estimates are available for certain nuclear models.

In a transition between two 2^+ states, only E0, M1 and E2 transitions need to be considered. A convenient measure of the intensity of the monopole transition is

$$\varepsilon^2 = \frac{\text{rate of E0 conversion}}{\text{rate of E2 gamma emission.}} \tag{11}$$

the relation between ε, the mixing ratio δ and the conversion coefficients is

$$\alpha_{\mathrm{K,\,exp.}} = \frac{\alpha_{\mathrm{K}}(\mathrm{M1}) + \delta^2[\alpha_{\mathrm{K}}(\mathrm{E2}) + \varepsilon^2]}{1+\delta^2} \tag{12}$$

or

$$\varepsilon^2 = \alpha_{\mathrm{K,\,exp.}} \left(1 + \frac{1}{\delta^2}\right) - \frac{1}{\delta^2}\alpha_{\mathrm{K}}(\mathrm{M1}) - \alpha_{\mathrm{K}}(\mathrm{E2}) \tag{13}$$

where $\alpha_{\mathrm{K,\,exp.}}$ is the experimentally observed conversion coefficient and $\alpha_{\mathrm{K}}(\mathrm{M1})$ and $\alpha_{\mathrm{K}}(\mathrm{E2})$ are the theoretical conversion coefficients. The mixing ratio δ is the same as defined in eq. (3). It is perhaps worth noting that the gamma-gamma directional correlations are unaffected by an E0 component in one of the transitions.

To obtain a quantitative estimate of the absolute transition probability

of the E0 component, the E2 gamma transition probability, $T(E2)$, must be known. From eq. (10) we find

$$W(E0) = \Omega \cdot \varrho^2 = \varepsilon^2 \cdot T(E2). \qquad (14)$$

Ω is tabulated by Church and Weneser [24]).

Thus one must measure three quantities, namely $\alpha_{K,\,exp.}$, δ and $T(E2)$ in order to calculate the strength parameter ϱ. The mixing ratio δ is available in

TABLE 2

Upper limit for the emission rate ε^2 of electric monopole conversion electrons and for the strength parameter ϱ^2.

Nucleus	$\frac{E_\gamma}{mc^2}$	$\alpha_{k,\,exp.}$	$\alpha_{k,\,theor}$(Sliv)		δ^2	ε^2	$T(E2)$ sec^{-1}	$W_{exp.}(E0)$	W(E0) Ω^2	ϱ^2
			M1	E2						
$_{34}Se^{76}$	1.26	<0.003[a])	8.8×10^{-4}	1.2×10^{-3}	52	$<5\times10^{-3}$	1.7×10^{11}[g])	$<8\times10^{8}$	2×10^{8}	<4
$_{74}W^{182}$	2.20	0.003[b])	6.4×10^{-3}	3.0×10^{-3}	9	$<5\times10^{-4}$	—	—	—	—
$_{78}Pt^{192}$	0.58	0.065[c])	0.269	0.064	19	$<10^{-3}$	1.6×10^{11}[h])	$<1.6\times10^{8}$	10^{11}	<0.002
$_{78}Pt^{194}$	0.58	≈0.2[d])	0.269	0.064	∞	<0.14	1.6×10^{11}[h])	$<2.2\times10^{10}$	10^{11}	<0.22
$_{78}Pt^{196}$	0.65	0.059[e])	0.198	0.048	19	$<5\times10^{-3}$	2×10^{11}[h])	$<10^{9}$	10^{11}	<0.01
$_{80}Hg^{198}$	1.32	0.0224[f])	0.031	0.010	1.5	$<8\times10^{-3}$	1.1×10^{11}[h])	$<8.8\times10^{9}$	2×10^{11}	<0.04

The gamma transition probability, $T(E2)$, for the upper transition has been estimated according to ref. [24]). *Note*: Church and Weneser [24]) have treated the cases Pt^{192}, Pt^{196} and Hg^{198}.

a) see ref. [9])
b) J. J. Murray, F. Boehm, P. Marmier and J. W. M. DuMond, Phys. Rev. **97** (1955) 1007
c) L. L. Baggerly, P. Marmier, F. Boehm and J. W. M. DuMond, Phys. Rev. **100** (1955) 1364
d) M. W. Johns and S. V. Nablo, Phys. Rev. **96** (1954) 1599
e) M. T. Thieme and E. Bleuler, Phys. Rev. **101** (1956) 1031
f) L. G. Elliot, M. A. Preston and J. L. Wolfson, Can. J. Phys. **32** (1954) 153
g) see ref. [6])
h) see ref. [24])

14 cases (table 1). Among these 14 cases only six conversion coefficients and no gamma transition probabilities are measured. The transition probability can be estimated semi-empirically [24]). In table 2 the six cases are given. Three of them have been treated by Church and Weneser [24]) but are taken up here for the sake of completeness. Since all cases include the value zero for both ε^2 and ϱ^2 one can only give upper limits. The difficulty of conversion coefficient measurements as well as lifetime measurements of these weak $2^+ \rightarrow 2^+$ transitions makes it almost impossible to get anything else than upper limits for ε^2 and ϱ^2. Directional correlations between conversion electrons and gamma rays seem to be more promising [24]).

The authors are indebted to Professor Kai Siegbahn for his interest in this work. Theoretical discussions with Professor Aage Bohr and Dr. Ben Mottelson are acknowledged. The work has been supported by the Swedish Atomic Committee and by the U.S. Air Research and Development Command.

References

1) G. Scharff-Goldhaber and J. Weneser, Phys. Rev. **98** (1955) 212
2) L. Wilets and M. Jean, Phys. Rev. **102** (1956) 788
3) M. Ferentz and N. Rosenzweig, ANL-5324 (not published)
4) F. Gimmi, E. Heer and P. Scherrer, Helv. Phys. Acta **29** (1956) 147
5) J. D. Kurbatov, B. B. Murray and M. Sakai, Phys. Rev. **98** (1955) 674
6) C. F. Coleman, Phil. Mag. **46** (1955) 1135
7) J. J. Kraushaar and M. Goldhaber, Phys. Rev. **89** (1953) 1081
8) F. R. Metzger and W. B. Todd, J. Franklin Inst. **256** (1953) 277
9) G. Bäckström, Arkiv för Fysik **11** (1956) 357
10) M. J. Glaubman, Phys. Rev. **98** (1955) 645
11) G. M. Temmer and N. P. Heydenburg, Phys. Rev. **104** (1956) 967
12) N. H. Lazar, Phys. Rev. **95** (1954) 292
13) B. S. Dzhelepov, N. N. Zhukovsky, V. G. Nedovesov, I. F. Uchevatkin and V. G. Chumin, Nuclear Physics **2** (1956/57) 408
14) E. P. Tomlinson, Bull. Amer. Phys. Soc. **1** (1956) 329
15) L. M. Langer, N. H. Lazar and R. J. D. Moffat, Phys. Rev. **91** (1953) 338
16) R. M. Kloepper, E. S. Lennox and M. L. Wiedenbeck, Phys. Rev. **88** (1952) 695
17) L. C. Biedenharn and M. E. Rose, Rev. Mod. Phys. **25** (1953) 720
18) M. E. Rose, ORNL 1555 (not published)
19) F. R. Metzger and R. D. Hill, Phys.Rev. **82** (1951) 646
20) J. P. Hurley and P. S. Jastram, Phys. Rev. **95** (1954) 627A
21) F. K. McGowan, Phys. Rev. **81** (1951) 1066
22) S. A. Moszkowski, Beta and Gamma Ray Spectroscopy, Ed. K. Siegbahn (North Holland Publ. Co., Amsterdam, 1955) Ch. XIII, p. 373
23) K. Alder, A. Bohr, T. Huus, B. Mottelson and A. Winther, Rev. Mod. Phys. **28** (1956) 432
24) E. L. Church and J. Weneser, Phys. Rev. **103** (1956) 1035

Nuclear Physics **4** (1957) 206—212; © *North-Holland Publishing Co., Amsterdam*
Not to be reproduced by photoprint or microfilm without written permission from the publisher

COULOMB CORRECTIONS IN ALLOWED BETA TRANSITIONS†

J. D. JACKSON,†† S. B. TREIMAN and H. W. WYLD JR.
Palmer Physical Laboratory, Princeton University Princeton, New Jersey

Received 8 April 1957

Abstract: Complete expressions, with all Coulomb effects taken into account, are given for the distribution functions for allowed beta decay, including recoil, nuclear orientation, and electron polarization effects. The expressions are general in that no assumptions are made as to invariance with respect to space inversion, charge conjugation, or time reversal. Simple arguments based on the behaviour of the various momenta and angular momenta under space inversion and time reversal are used to elucidate which combinations of vectors will appear when the different symmetry laws are violated, and the modifications of these arguments necessary because of the Coulomb interaction in the final state are pointed out. Various tests of time reversal invariance, previously suggested, are re-evaluated in view of the results for the Coulomb corrections.

1. Introduction

In a recent report by the present authors [1]) general distribution functions, including recoil, nuclear orientation, and electron polarization effects, were given for allowed beta transitions. These calculations were quite general in that no assumptions as to invariance with respect to space inversion, charge conjugation, or time reversal invariance were made. However, Coulomb corrections were ignored in this work. We wish here to give complete results, including all Coulomb corrections, for allowed transitions †††.

2. Rate formulae

The rate formulae are similar in form to those given previously [1]). For completeness we repeat them here using the same notation as in ref. [1])*.

For the distribution in electron and neutrino directions and electron energy for an allowed transition from oriented nuclei we find

† This work was supported in part by the Office of Naval Research and the U.S. Atomic Energy Commission.

†† Visiting Guggenheim Fellow, on leave of absence from McGill University, Montreal, Canada.

††† The completely general distribution for an experiment including recoil, nuclear orientation, and electron polarization simultaneously contains terms in addition to those present in equations (1), (2), and (3). See the following paper by Ebel and Feldman.

* The indices e and ν refer to electron and neutrino, respectively. The symbols E, p, Ω denote energy, momentum and angular coordinates of the leptons; m is the electron mass. The initial nucleus, of charge $Z \mp 1$, has an angular momentum $\mathbf{J}$; $\mathbf{j}$ is a unit vector in the direction of $\mathbf{J}$.

$$\omega(\langle \mathbf{J}\rangle | E_e,\ \Omega_e,\ \Omega_\nu)\mathrm{d}E_e\,\mathrm{d}\Omega_e\,\mathrm{d}\Omega_\nu = \frac{F(\pm Z,\ E_e)}{(2\pi)^5}\, p_e E_e (E^0 - E_e)^2\,\mathrm{d}E_e\,\mathrm{d}\Omega_e\,\mathrm{d}\Omega_\nu$$

$$\times\xi\left\{1 + a\frac{\mathbf{p}_e\cdot\mathbf{p}_\nu}{E_e E_\nu} + b\frac{m}{E_e} + c\left[\frac{\mathbf{p}_e\cdot\mathbf{p}_\nu}{3E_e E_\nu} - \frac{(\mathbf{p}_e\cdot\mathbf{j})(\mathbf{p}_\nu\cdot\mathbf{j})}{E_e E_\nu}\right]\left[\frac{J(J+1) - 3\langle(\mathbf{J}\cdot\mathbf{j})^2\rangle}{J(2J-1)}\right]\right. \quad (1)$$

$$\left. + \frac{\mathbf{J}}{J}\cdot\left[A\frac{\mathbf{p}_e}{E_e} + B\frac{\mathbf{p}_\nu}{E_\nu} + D\frac{\mathbf{p}_e\times\mathbf{p}_\nu}{E_e E_\nu}\right]\right\}.$$

Here $F(\pm Z,\ E_e)$ is the usual Fermi function for negatons and positons respectively [2]).

The distribution in electron and neutrino direction and electron polarization for allowed beta decay from non-oriented nuclei is

$$\omega(\boldsymbol{\sigma}|E_e,\ \Omega_e,\ \Omega_\nu)\mathrm{d}E_e\,\mathrm{d}\Omega_e\,\mathrm{d}\Omega_\nu = \frac{F(\pm Z,\ E_e)}{(2\pi)^5}\, p_e E_e (E^0 - E_e)^2\,\mathrm{d}E_e\,\mathrm{d}\Omega_e\,\mathrm{d}\Omega_\nu$$

$$\times\tfrac{1}{2}\xi\left\{1 + a\frac{\mathbf{p}_e\cdot\mathbf{p}_\nu}{E_e E_\nu} + b\frac{m}{E_e}\right. \quad (2)$$

$$\left. + \boldsymbol{\sigma}\cdot\left[G\frac{\mathbf{p}_e}{E_e} + H\frac{\mathbf{p}_\nu}{E_\nu} + K\frac{\mathbf{p}_e}{E_e + m}\left(\frac{\mathbf{p}_e\cdot\mathbf{p}_\nu}{E_e E_\nu}\right) + L\frac{\mathbf{p}_e\times\mathbf{p}_\nu}{E_e E_\nu}\right]\right\}.$$

The distribution in electron energy and angle and electron polarization for allowed beta decay from oriented nuclei is

$$\omega(\langle \mathbf{J}\rangle,\ \boldsymbol{\sigma}|E_e,\ \Omega_e)\mathrm{d}E_e\,\mathrm{d}\Omega_e = \frac{F(\pm Z,\ E_e)}{(2\pi)^4}\, p_e E_e (E^0 - E_e)^2\,\mathrm{d}E_e\,\mathrm{d}\Omega_e$$

$$\times\,\xi\left\{1 + b\frac{m}{E_e} + \frac{\mathbf{p}_e}{E_e}\cdot\left(A\frac{\langle \mathbf{J}\rangle}{J} + G\boldsymbol{\sigma}\right)\right. \quad (3)$$

$$\left. + \boldsymbol{\sigma}\cdot\left[N\frac{\langle \mathbf{J}\rangle}{J} + Q\frac{\mathbf{p}_e}{E_e + m}\left(\frac{\langle \mathbf{J}\rangle}{J}\cdot\frac{\mathbf{p}_e}{E_e}\right) + R\frac{\langle \mathbf{J}\rangle}{J}\times\frac{\mathbf{p}_e}{E_e}\right]\right\}.$$

The coefficients $a,\ b, \ldots$ including all Coulomb corrections are listed in the appendix. In order to obtain results for the two component neutrino theory [3, 4]) one must set $C'_S = -C_S$, $C'_V = -C_V, \ldots$ in these formulae.

As can be seen from eq. (2) or eq. (3) the longitudinal polarization of electrons emitted in ordinary beta decay is

$$P = \frac{G\dfrac{v_e}{c}}{1 + b\dfrac{m}{E_e}}. \quad (4)$$

This effect has been found experimentally by Frauenfelder *et al.* [5]) for negatons in the decay of Co^{60} and by Page and Heinberg [6]) for positons in the decay of Na^{22}.

3. Discussion

The expressions given above and in the appendix are perfectly general in that no assumptions concerning invariance with respect to space inversion, charge conjugation, or time reversal have been made. Invariance with respect to space inversion implies that the coupling constants C' vanish (or alternatively the C vanish). Invariance with respect to charge conjugation implies that the constants C are real and the constants C' pure imaginary, up to an overall phase. Invariance under time reversal would imply that all coupling constants C, C' are real, again up to an overall phase.

A more physical statement of what is involved in these criteria can be given: The terms which violate space inversion invariance in eqs. (1), (2), and (3) are those which change sign under inversion (momentum vectors $\mathbf{p}$ change sign under inversion, spin vectors $\boldsymbol{\sigma}$, $\mathbf{J}$ do not). If Coulomb corrections are ignored, the terms which violate time reversal invariance are those which change sign under time reversal (all vectors, $\mathbf{p}$, $\boldsymbol{\sigma}$, $\mathbf{J}$ change sign under time reversal). If $\mathbf{p}$ represents a linear momentum (either $\mathbf{p}_e$ or $\mathbf{p}_\nu$) and $\mathbf{S}$ represents an angular momentum (either $\mathbf{J}$ or $\boldsymbol{\sigma}$), the combinations of vectors which appear in the angular distributions are of the following types: $\mathbf{p}_1 \cdot \mathbf{p}_2$, $\mathbf{S}_1 \cdot \mathbf{S}_2$, $\mathbf{S} \cdot \mathbf{p}$, $\mathbf{S} \cdot (\mathbf{p}_1 \times \mathbf{p}_2)$, $\mathbf{S}_1 \cdot (\mathbf{S}_2 \times \mathbf{p})$, as well as the bilinear forms $(\mathbf{S}_1 \cdot \mathbf{p}_1)(\mathbf{p}_1 \cdot \mathbf{p}_2)$ and $(\mathbf{S}_1 \cdot \mathbf{p})(\mathbf{S}_2 \cdot \mathbf{p})$. In the absence of the Coulomb field, it is clear that the first and second types violate neither space inversion (P) nor time reversal invariance (T). By the Schwinger-Lüders-Pauli theorem [7]), they therefore do not violate charge conjugation invariance (C). Consequently such terms can appear in the beta spectrum even if all symmetry properties are valid, as is well known from "old" beta decay theory. This can be explicitly verified by inspection of the $Z = 0$ part of their coefficients, a and N, in the appendix. The third type $(\mathbf{S} \cdot \mathbf{p})$ violates space inversion invariance, but not time reversal invariance, and so will appear in the beta spectrum only if P and C are violated. Again this can be explicitly seen from the form of the coefficients A, B, G, and H. By similar arguments, it can be shown that terms of the form $\mathbf{S} \cdot (\mathbf{p}_1 \times \mathbf{p}_2)$ will appear only if T and C are violated, while $\mathbf{S}_1 \cdot (\mathbf{S}_2 \times \mathbf{p})$ occurs only if P and T are not conserved. The coefficients D, L and R, respectively, contain these requirements.

The presence of the Coulomb field alters these arguments. The effect of interaction in the final state is to cause a breakdown of the arguments about time reversal based on the properties of the various vectors. The space inversion arguments with vectors are, of course, still valid. Inspection of the coefficients in the appendix shows that if a given combination of vectors behaved in a certain way under time reversal and charge con-

jugation, the Coulomb correction linear in αZ will behave in the opposite way. Thus, for example, for the $\mathbf{J} \cdot \mathbf{p}_e$ term, with coefficient A, the $Z = 0$ part is present if P and C are not conserved, while the Coulomb correction is present only if P and T are violated. Similarly, for $\mathbf{J} \cdot (\mathbf{p}_e \times \mathbf{p}_\nu)$, the $Z = 0$ part tests T and C, while the Coulomb correction is present even if P, C, and T are separately conserved.

Before the discovery of parity violations in beta decay [8]) it was generally thought that the vector and axial vector coupling constants were small compared to the scalar and tensor coupling constants [9–13]). However, the most precise experiment of this sort, that of Sherr and Miller [13]), shows only that the Gamow-Teller part of b is zero, and according to the appendix (eq. (A.5)) this proves only that

$$\mathrm{Re}\,(C_T C_A^* + C'_T C'^*_A) = 0.$$

If $|C_A|$, $|C'_A|$ should turn out to be comparable to $|C_T|$, $|C'_T|$, while at the same time $b = 0$, there would seem to be a clear indication of violation of time reversal invariance, barring of course a fortuitous cancellation of terms in $\mathrm{Re}\,(C_T C_A^* + C'_T C'^*_A)$. Whether or not $|C_A|$, $|C'_A|$, $|C_V|$, $|C'_V|$ are really small compared to $|C_S|$, $|C'_S|$, $|C_T|$, $|C'_T|$ can in principle be tested by further refinement of the standard electron neutrino angular correlation experiments [10–12]).

On the other hand if $|C_A|$, $|C'_A|$, $|C_V|$, $|C'_V|$ are negligibly small compared to $|C_S|$, $|C'_S|$, $|C_T|$, $|C'_T|$ the Coulomb corrections to A and G (eqs. (A.7) and (A.10)) will be small. This may make it difficult to detect possible violations of time reversal invariance by observation of the momentum dependence of A and G [14, 15]).

Consider now the terms involving D, L, and R. It has been suggested [1]) that a search for any one of these three terms in beta decay experiments would provide a test for the violation of time reversal invariance. It must be noted, however, that the Coulomb corrections to D, L, and R do not violate time reversal invariance. Thus if the test is to be definitive (in the absence of measurement of the energy dependence of the coefficient) the Coulomb corrections must be small. If the vector and axial vector coupling constants are small relative to the scalar and tensor coupling constants, this is indeed the case for D, but not for L and R. Thus the recoil experiment on oriented nuclei as described by eq. (1) and discussed in ref. [1]) is very likely a much more sensitive test for violation of time reversal invariance than the experiments described by eqs. (2) and (3).

Appendix

In the following formulae the upper signs refer to negaton decay and the lower signs to positon decay. $|M_F|^2$ is the conventional Fermi nuclear

matrix element with selection rule $\Delta J = 0$, no nuclear parity change; and $|M_{GT}|^2$ is the Gamow-Teller matrix element with selection rule $\Delta J = 0, \pm 1$, no nuclear parity change, $J = 0 \to J' = 0$ forbidden. J and J' are the angular momenta of the original and final nuclei, $\delta_{J'J}$ is the Kronecker delta symbol and

$$\lambda_{J'J} = \begin{cases} 1 & J \to J' = J-1 \\ \dfrac{1}{J+1} & J \to J' = J \\ -\dfrac{J}{J+1} & J \to J' = J+1 \end{cases} \tag{A.1}$$

$$\Lambda_{J'J} = \begin{cases} 1 & J \to J' = J-1 \\ -\dfrac{(2J-1)}{J+1} & J \to J' = J \\ \dfrac{J(2J-1)}{(J+1)(2J+3)} & J \to J' = J+1. \end{cases} \tag{A.2}$$

Z is the atomic number of the final nucleus, α is the fine structure constant, and $\gamma = (1-\alpha^2 Z^2)^{\frac{1}{2}}$.

$$\xi = |M_F|^2(|C_S|^2+|C_V|^2+|C'_S|^2+|C'_V|^2) + |M_{GT}|^2(|C_T|^2+|C_A|^2+|C'_T|^2+|C'_A|^2) \tag{A.3}$$

$$a\xi = |M_F|^2 \left\{[-|C_S|^2+|C_V|^2-|C'_S|^2+|C_V|^2] \mp \frac{\alpha Zm}{p_e} 2 \text{ Im } (C_S C_V^* + C'_S C'^*_V)\right\}$$

$$+\frac{|M_{GT}|^2}{3}\left\{[|C_T|^2-|C_A|^2+|C'_T|^2-|C'_A|^2] \pm \frac{\alpha Zm}{p_e} 2\text{Im}\,(C_T C_A^* + C'_T C'^*_A)\right\} \tag{A.4}$$

$$b\xi = \pm 2\gamma \text{ Re}[|M_F|^2(C_S C_V^* + C'_S C'^*_V) + |M_{GT}|^2(C_T C_A^* + C'_T C'^*_A)] \tag{A.5}$$

$$c\xi = |M_{GT}|^2 \Lambda_{J'J}\left[|C_T|^2-|C_A|^2+|C'_T|^2-|C'_A|^2 \pm \frac{\alpha Zm}{p_e} 2\text{Im}\,(C_T C_A^* + C'_T C'^*_A)\right] \tag{A.6}$$

$$A\xi = |M_{GT}|^2 \lambda_{J'J}\left[\pm 2 \text{ Re}(C_T C'^*_T - C_A C'^*_A) + \frac{\alpha Zm}{p_e} 2 \text{ Im } (C_T C'^*_A + C'_T C_A^*)\right]$$

$$+\delta_{J'J} M_F M_{GT} \sqrt{\frac{J}{J+1}}\left[2 \text{ Re } (C_S C'^*_T + C'_S C_T^* - C_V C'^*_A - C'_V C_A^*)\right.$$

$$\left. \pm \frac{\alpha Zm}{p_e} 2 \text{ Im } (C_S C'^*_A + C'_S C_A^* - C_V C'^*_T - C'_V C_T^*)\right] \tag{A.7}$$

$$B\xi = 2\,\mathrm{Re}\left\{|M_{GT}|^2\lambda_{J'J}\left[\frac{\gamma m}{E_e}(C_T C'_A{}^* + C'_T C_A{}^*) \pm (C_T C'_T{}^* + C_A C'_A{}^*)\right]\right.$$
$$-\delta_{J'J} M_F M_{GT}\sqrt{\frac{J}{J+1}}\left[(C_S C'_T{}^* + C'_S C_T{}^* + C_V C'_A{}^* + C'_V C_A{}^*)\right. \quad \text{(A.8)}$$
$$\left.\left. \pm \frac{\gamma m}{E_e}(C_S C'_A{}^* + C'_S C_A{}^* + C_V C'_T{}^* + C'_V C_T{}^*)\right]\right\}$$

$$D\xi = \delta_{J'J} M_F M_{GT}\sqrt{\frac{J}{J+1}}\left[2\,\mathrm{Im}\,(C_S C_T{}^* - C_V C_A{}^* + C'_S C'_T{}^* - C'_V C'_A{}^*)\right.$$
$$\left. \mp \frac{\alpha Z m}{p_e}\,2\,\mathrm{Re}\,(C_S C_A{}^* - C_V C_T{}^* + C'_S C'_A{}^* - C'_V C'_T{}^*)\right] \quad \text{(A.9)}$$

$$G\xi = |M_F|^2\left[\pm 2\,\mathrm{Re}\,(C_S C'_S{}^* - C_V C'_V{}^*) + \frac{\alpha Z m}{p_e}\,2\,\mathrm{Im}\,(C_S C'_V{}^* + C'_S C_V{}^*)\right]$$
$$+|M_{GT}|^2\left[\pm 2\,\mathrm{Re}\,(C_T C'_T{}^* - C_A C'_A{}^*) + \frac{\alpha Z m}{p_e}2\,\mathrm{Im}\,\langle C_T C'_A{}^* + C'_T C_A{}^*)\right] \quad \text{(A.10)}$$

$$H\xi = 2\,\mathrm{Re}\left\{|M_F|^2\left[-(C_S C'_V{}^* + C'_S C_V{}^*) \mp \frac{\gamma m}{E_e}(C_S C'_S{}^* + C_V C'_V{}^*)\right]\right.$$
$$\left. + \frac{|M_{GT}|^2}{3}\left[C_T C'_A{}^* + C'_T C_A{}^* \pm \frac{\gamma m}{E_e}(C_T C'_T{}^* + C_A C'_A{}^*)\right]\right\} \quad \text{(A.11)}$$

$$K\xi = 2\left(\frac{E_e - \gamma m}{E_e - m}\right)\mathrm{Re}\left\{|M_F|^2(\mp C_S C'_S{}^* \mp C_V C'_V{}^* + C_S C'_V{}^* + C'_S C_V{}^*)\right.$$
$$\left. + \frac{|M_{GT}|^2}{3}(\pm C_T C'_T{}^* \pm C_A C'_A{}^* - C_T C'_A{}^* - C'_T C_A{}^*)\right\} \quad \text{(A.12)}$$

$$L\xi = |M_F|^2\left[2\,\mathrm{Im}\,(C_S C_V{}^* + C'_S C'_V{}^*) \mp \frac{\alpha Z m}{p_e}(|C_S|^2 - |C_V|^2 + |C'_S|^2 - |C'_V|^2)\right]$$
$$+\frac{|M_{GT}|^2}{3}\left[-2\,\mathrm{Im}\,(C_T C_A{}^* + C'_T C'_A{}^*) \pm \frac{\alpha Z m}{p_e}(|C_T|^2 - |C_A|^2 + |C'_T|^2 - |C'_A|^2)\right] \quad \text{(A.13)}$$

$$N\xi = 2\,\mathrm{Re}\left\{|M_{GT}|^2\lambda_{J'J}\left[\frac{1}{2}\frac{\gamma m}{E_e}(|C_T|^2 + |C_A|^2 + |C'_T|^2 + |C'_A|^2) \pm (C_T C_A^* + C'_T C'_A{}^*)\right]\right.$$
$$+\delta_{J'J} M_F M_{GT}\sqrt{\frac{J}{J+1}}\left[(C_S C_A{}^* + C_V C_T{}^* + C'_S C'_A{}^* + C'_V C'_T{}^*)\right. \quad \text{(A.14)}$$
$$\left.\left. \pm \frac{\gamma m}{E_e}(C_S C_T{}^* + C_V C_A{}^* + C'_S C'_T{}^* + C'_V C'_A{}^*)\right]\right\}$$

$$Q\xi = 2\left(\frac{E_e-\gamma m}{E_e-m}\right)\mathrm{Re}\,\{|M_{GT}|^2\lambda_{J'J}[\tfrac{1}{2}(|C_T|^2+|C_A|^2+|C'_T|^2+|C'_A|^2)\mp(C_TC_A^*+C'_TC'^*_A)]$$
$$-\delta_{J'J}M_FM_{GT}\sqrt{\frac{J}{J+1}}\,[(C_SC_A^*+C_VC_T^*+C'_SC'^*_A+C'_VC'^*_T) \qquad \text{(A.15)}$$
$$\mp(C_SC_T^*+C_VC_A^*+C'_SC'^*_T+C'_VC'^*_A)]\}$$

$$R\xi = |M_{GT}|^2\lambda_{J'J}\left[\pm 2\,\mathrm{Im}\,(C_TC'^*_A+C'_TC_A^*)-\frac{\alpha Zm}{p_e}\,2\,\mathrm{Re}(C_TC'^*_T-C_AC'^*_A)\right]$$
$$+\delta_{J'J}M_FM_{GT}\sqrt{\frac{J}{J+1}}\,[2\,\mathrm{Im}\,(C_SC'^*_A+C'_SC_A^*-C_VC'^*_T-C'_VC_T^*) \qquad \text{(A.16)}$$
$$\mp\frac{\alpha Zm}{p_e}\,2\,\mathrm{Re}\,(C_SC'^*_T+C'_SC_T^*-C_VC'^*_A-C'_VC_A^*)].$$

The product M_FM_{GT} which appears in some of the formulae above is defined by

$$(\Psi(J',M'),\Psi(J,M))(\Psi(J,M),\sigma_3\Psi(J',M'))=\delta_{MM'}\delta_{JJ'}\frac{M}{\sqrt{J(J+1)}}M_FM_{GT} \qquad \text{(A.17)}$$

where $\Psi(J, M)$ and $\Psi(J', M')$ are the initial and final nuclear wave functions. If the nuclear Hamiltonian is invariant with respect to time reversal, M_FM_{GT} is real. Furthermore $|M_FM_{GT}| = |M_F||M_{GT}|$. The sign of M_FM_{GT} must, however, be determined by explicit calculation of the left hand side of eq. (A.17).

References

1) J. D. Jackson, S. B. Treiman and H. W. Wyld Jr., Phys. Rev. **106** (1957) 517
2) See, e.g., J. M. Blatt and V. F. Weisskopf, Theoretical Nuclear Physics (John Wiley and Sons, New York, 1952) p. 682
3) T. D. Lee and C. N. Yang, Phys. Rev. **105** (1957) 1671
4) L. Landau, Nuclear Physics **3** (1957) 127
5) H. Frauenfelder, R. Bobone, E. von Goeler, N. Levine, H. R. Lewis, R. N. Peacock, A. Rossi and G. DePasquali, Phys. Rev. **106** (1957) 386
6) L. A. Page and M. Heinberg, Phys. Rev. (to be published)
7) G. Lüders, Mat. Fys. Medd. Dan. Vid. Selsk. **28** (1954) no. 5; W. Pauli, Niels Bohr and the development of physics (Pergamon Press, London, 1955) (See also ref. [14]).
8) C. S. Wu, E. Ambler, R. W. Hayward, D. D. Hoppes and R. P. Hudson, Phys. Rev. **105** (1957) 1413
9) E. J. Konopinski, Beta- and Gamma-Ray Spectroscopy, ed. K. Siegbahn (North Holland, Amsterdam, 1955) p. 311
10) J. M. Robson, Phys. Rev. **100** (1955) 933
11) B. M. Rustad and S. L. Ruby, Phys. Rev. **97** (1955) 991
12) W. P. Alford and D. R. Hamilton, Phys. Rev. **105** (1957) 673
13) R. Sherr and R. H. Miller, Phys. Rev. **93** (1954) 1076
14) T. D. Lee, R. Oehme and C. N. Yang, Phys. Rev. **106** (1957) 340
15) R. B. Curtis and R. R. Lewis, Phys. Rev. (to be published)

Nuclear Physics **4** (1957) 213—214; © *North-Holland Publishing Co., Amsterdam*
Not to be reproduced by photoprint or microfilm without written permission from the publisher

FURTHER REMARKS ON COULOMB CORRECTIONS IN ALLOWED BETA TRANSITIONS†

M. E. EBEL and G. FELDMAN
Department of Physics, University of Wisconsin, Madison, Wisconsin

Received 8 April 1957

Abstract: The terms which have not been included in the previous paper by Jackson, Treiman and Wyld [1]) are added here for completeness.

We have carried out an independent calculation similar to the one given in the previous paper [1]). Rather than list the results twice, we add here for the sake of completeness the terms which have not been included in that paper. These terms are those which require the simultaneous measurement of nuclear orientation, recoil and electron polarization and/or its momentum.

The complete distribution function is written

$$\omega(\langle\mathbf{J}\rangle,\boldsymbol{\sigma}|E_e,\Omega_e,\Omega_\nu)\mathrm{d}E_e\mathrm{d}\Omega_e\mathrm{d}\Omega_\nu=\tfrac{1}{2}\frac{F(\pm Z,E_e)}{(2\pi)^5}p_e E_e(E^0-E_e)^2\mathrm{d}E_e\,\mathrm{d}\Omega_e\,\mathrm{d}\Omega_\nu X$$

in the notation of JTW. The normalization of X is such that the first term is ξ. The extra terms in X are to lowest order in $Z\alpha$:

$$\begin{aligned}\xi\Bigg\{ & I\left[\frac{1}{3}\frac{\boldsymbol{\sigma}\cdot\mathbf{p}_\nu}{E_\nu}-\frac{(\mathbf{j}\cdot\boldsymbol{\sigma})(\mathbf{j}\cdot\mathbf{p}_\nu)}{E_\nu}\right]\left[\frac{J(J+1)-3\langle(\mathbf{J}\cdot\mathbf{j})^2\rangle}{J(2J-1)}\right]\\ & +K'\frac{\boldsymbol{\sigma}\cdot\mathbf{p}_e}{E_e+m}\left[\frac{1}{3}\frac{(\mathbf{p}_e\cdot\mathbf{p}_\nu)}{E_eE_\nu}-\frac{(\mathbf{j}\cdot\mathbf{p}_e)(\mathbf{j}\cdot\mathbf{p}_\nu)}{E_eE_\nu}\right]\left[\frac{J(J+1)-3\langle(\mathbf{J}\cdot\mathbf{j})^2\rangle}{J(2J-1)}\right]\\ & +M\left[\frac{1}{3}\frac{\boldsymbol{\sigma}\cdot\mathbf{p}_e\times\mathbf{p}_\nu}{E_eE_\nu}-\frac{(\mathbf{j}\cdot\boldsymbol{\sigma})(\mathbf{j}\cdot\mathbf{p}_e\times\mathbf{p}_\nu)}{E_eE_\nu}\right]\left[\frac{J(J+1)-3\langle(\mathbf{J}\cdot\mathbf{j})^2\rangle}{J(2J-1)}\right]\\ & +S\frac{(\langle\mathbf{J}\rangle\cdot\boldsymbol{\sigma})}{J}\frac{\mathbf{p}_e\cdot\mathbf{p}_\nu}{E_eE_\nu}+T\frac{(\boldsymbol{\sigma}\cdot\mathbf{p}_e)}{E_e}\frac{\langle\mathbf{J}\rangle}{J}\cdot\frac{\mathbf{p}_\nu}{E_\nu}\\ & +U\frac{(\boldsymbol{\sigma}\cdot\mathbf{p}_\nu)}{E_\nu}\frac{\langle\mathbf{J}\rangle}{J}\cdot\frac{\mathbf{p}_e}{E_e}+V\frac{\langle\mathbf{J}\rangle}{J}\cdot\frac{\boldsymbol{\sigma}\times\mathbf{p}_\nu}{E_\nu}\\ & +W\frac{(\boldsymbol{\sigma}\cdot\mathbf{p}_e)}{E_e+m}\frac{\langle\mathbf{J}\rangle}{J}\cdot\frac{\mathbf{p}_e\times\mathbf{p}_\nu}{E_eE_\nu}\Bigg\},\end{aligned}$$

where

† Supported in part by the U.S. Atomic Energy Commission.

$$I\xi = |M_{GT}|^2 \Lambda_{J'J}\, 2\,\mathrm{Re}\left\{(C_T C_{A'}^* + C_{T'} C_A^*) \pm \frac{m}{E_e}(C_T C_{T'}^* + C_A C_{A'}^*)\right\},$$

$$K'\xi = |M_{GT}|^2 \Lambda_{J'J}\, 2\,\mathrm{Re}\,\{\pm(C_T C_{T'}^* + C_A C_{A'}^*) - (C_T C_{A'}^* + C_{T'} C_A^*)\},$$

$$M\xi = |M_{GT}|^2 \Lambda_{J'J}\{-2\,\mathrm{Im}\,(C_T C_A^* + C_{T'} C_{A'}^*) \pm \eta(|C_T|^2 + |C_{T'}|^2 - |C_A|^2 - |C_{A'}|^2)\},$$

$$S\xi = \delta_{J'J}|M_F||M_{GT}|\sqrt{\frac{J}{J+1}}\{2\,\mathrm{Re}[-(C_S C_A^* + C_{S'} C_{A'}^*) + (C_V C_T^* + C_{V'} C_{T'}^*)]$$
$$\mp\eta\, 2\,\mathrm{Im}\,(C_S C_{T'}^* + C_{S'} C_{T'}^* - C_V C_A^* - C_{V'} C_{A'}^*)\}.$$

$$T\xi = \delta_{J'J}|M_F||M_{GT}|\sqrt{\frac{J}{J+1}}\{2\,\mathrm{Re}[\mp(C_S C_T^* + C_{S'} C_{T'}^*) \pm (C_V C_A^* + C_{V'} C_{A'}^*)]$$
$$-\eta\, 2\,\mathrm{Im}\,(C_S C_{A'}^* + C_{S'} C_{A'}^* - C_V C_T^* - C_{V'} C_{T'}^*)\}$$
$$+|M_{GT}|^2 \lambda_{J'J}\{(|C_T|^2 + |C_{T'}|^2 - |C_A|^2 - |C_{A'}|^2) \pm \eta\ 2\,\mathrm{Im}\,(C_T C_A^* + C_{T'} C_{A'}^*)\},$$

$$U\xi = \delta_{J'J}|M_F||M_{GT}|\sqrt{\frac{J}{J+1}}\{2\,\mathrm{Re}[(C_S C_A^* + C_{S'} C_{A'}^*) - (C_V C_T^* + C_{V'} C_{T'}^*)]$$
$$\pm\eta\, 2\,\mathrm{Im}\,[(C_S C_{T'}^* + C_{S'} C_{T'}^* - (C_V C_A^* + C_{V'} C_{A'}^*)]\},$$

$$V\xi = \delta_{J'J}|M_F||M_{GT}|\sqrt{\frac{J}{J+1}}\, 2\,\mathrm{Im}\,\left[\pm\frac{m}{E_e}(C_S C_{T'}^* + C_{S'} C_T^* + C_V C_{A'}^* + C_{V'} C_A^*)\right.$$
$$\left.+(C_S C_{A'}^* + C_{S'} C_A^* + C_V C_{T'}^* + C_{V'} C_T^*)\right],$$

$$W\xi = \delta_{J'J}|M_F||M_{GT}|\sqrt{\frac{J}{J+1}}\, 2\,\mathrm{Im}\,[\pm(C_S C_{T'}^* + C_{S'} C_T^* + C_V C_{A'}^* + C_{V'} C_A^*)$$
$$-(C_S C_{A'}^* + C_{S'} C_A^* + C_V C_{T'}^* + C_{V'} C_T^*)],$$

$$\eta = \frac{Z\alpha m}{p_e}.$$

Reference

1) Jackson, Treiman and Wyld, Nuclear Physics 4 (1957) 206

Nuclear Physics **4** (1957) 215—220; © *North-Holland Publishing Co., Amsterdam*
Not to be reproduced by photoprint ro microfilm without written permission from the publisher

INDIVIDUAL PARTICLE AND COLLECTIVE ASPECTS OF THE NUCLEAR PHOTOEFFECT †

D. M. BRINK

Department of Physics and Laboratory for Nuclear Science, Massachusetts Institute of Technology, Cambridge, Massachusetts

Received 16 April 1957

Abstract: The coordinate corresponding to the dipole photon absorption operator is exactly separable in the oscillator shell model. It is shown that in an electric dipole absorption a mode of the shell model is excited in which the protons vibrate against the neutrons. In shell models other than the oscillator model this collective mode is damped; in heavy nuclei this damping gives a line width of $\approx$ 4 MeV.

1. Introduction

The cross section for absorption of photons in nuclei shows a giant resonance whose position varies slowly and uniformly with atomic weight from about 20 MeV in light nuclei to 14 MeV in heavy nuclei; and whose width is almost constant at about 5 MeV over the entire periodic table(see, e.g., Montalbetti, Goldemberg and Katz [1])). It is recognized that the major part of the cross section is due to photon absorption in electric dipole transitions, and two apparently different models, one a collective model and the other an individual particle model, have been proposed to describe the absorption process.

The collective model, proposed in two forms by Goldhaber and Teller [2]), says the giant resonance corresponds to a collective mode of the nucleus in which the protons vibrate against the neutrons. In the first variation, developed by Gallone and Businaro [3]) and Fujita [4]), the proton cloud and the neutron cloud pass back and forth through one another without distortion in the collective vibration; while in the second, developed by Steinwedel and Jensen [5]), the total nuclear density remains unaltered and only the relative proton-neutron density changes when the collective mode is excited. The width of the giant resonance reflects the damping of the collective mode due to viscous effects arising from the relative motion of the proton and neutron clouds.

The individual particle model has been developed particularly by Wilkinson [6]) and Rand [7]) and is based on the shell model. An individual proton or neutron in the nucleus absorbs the incoming photon and, for an electric

† This work was supported in part by the Joint Program of the U.S. Office of Naval Research and the U.S. Atomic Energy Commission.

dipole transition, is excited to the next shell of opposite parity. Since for all reasonable shell model potentials, all possible transitions have approximately the same energy there should be a peak in the absorption cross section at this energy. The finite width of the peak arises partly because of the slight spread in single particle absorption energies and partly because the single particle states decay by making inelastic collisions in the nucleus (cloudy crystal ball effect).

2. The Electric Dipole Transition Operator

Because of centre-of-mass recoil the dipole operator $\mathbf{Q}_1$ is not $e\sum_Z \mathbf{r}_i$, but $e\sum_Z(\mathbf{r}_i-\mathbf{R})$ summed over all protons, where $\mathbf{R}$ is the nuclear centre-of-mass radius vector

$$\mathbf{R}=\frac{1}{A}[\sum_i \mathbf{r}_i+\sum_j \mathbf{r}_j]$$

(suffices i indicate proton coordinates and suffices j neutron coordinates). Now

$$\mathbf{Q}_1=e\sum_i(\mathbf{r}_i-\mathbf{R})=\frac{eN}{A}\sum_i \mathbf{r}_i-\frac{eZ}{A}\sum_j \mathbf{r}_j=\frac{eNZ}{A}(\mathbf{R}_Z-\mathbf{R}_N) \tag{1}$$

or

$$\mathbf{Q}_1=\frac{NZ}{A}\mathbf{r}, \tag{2}$$

where $\mathbf{R}_Z$ and $\mathbf{R}_N$ are the position vectors of the centres of mass of protons and neutrons respectively and $\mathbf{r}=\mathbf{R}_Z-\mathbf{R}_N$ is a neutron-proton relative coordinate.

Written in the form (1) $\mathbf{Q}_1$ is a sum of one particle operators and connects nuclear wave functions differing at most by the state of one particle. The protons have an effective charge eN/A and the neutrons $-eZ/A$. Written in the form (2), however, the dipole operator is expressed in terms of a collective coordinate, the position of the centre of mass of the protons relative to the centre of mass of the neutrons. Already the form (2) of the operator $\mathbf{Q}_1$ contains symptoms of collective motion.

3. The Oscillator Shell Model

In the following section we will analyze the oscillator shell model, for which the coordinate $\mathbf{r}$ is separable. In this particular case it turns out that the Goldhaber collective mode is contained already within the shell model description.

The oscillator Hamiltonian is

$$H = T_Z + T_N + \tfrac{1}{2}k\left[\sum_i \mathbf{r}_i^2 + \sum_j \mathbf{r}_j^2\right], \tag{3}$$

where T_Z and T_N are the proton and neutron kinetic energies. Introducing the centre of mass and relative coordinates with their conjugate momenta

$$\mathbf{R} = \frac{1}{A}(Z\mathbf{R}_Z + N\mathbf{R}_N), \qquad \mathbf{P} = \mathbf{P}_N + \mathbf{P}_Z,$$

$$\mathbf{r} = \mathbf{R}_Z - \mathbf{R}_N, \qquad \mathbf{p} = \frac{1}{A}(N\mathbf{P}_Z - Z\mathbf{P}_N),$$

the Hamiltonian (3) separates as follows:

$$\begin{aligned} H &= H_{Z\text{int}} + H_{N\text{int}} + \frac{1}{2AM}\mathbf{P}^2 + \tfrac{1}{2}kA\mathbf{R}^2 + \frac{A}{2NZM}\mathbf{p}^2 + \tfrac{1}{2}k\frac{NZ}{A}\mathbf{r}^2 \\ &= H_{Z\text{int}} + H_{N\text{int}} + H_{\text{cm}} + H_{\text{r}}. \end{aligned} \tag{4}$$

In this form $H_{Z\text{int}}$ and $H_{N\text{int}}$ contain only proton-proton and neutron-neutron relative coordinates respectively, hence are quite independent of the centre of mass, and proton-neutron relative coordinates. An almost identical separation to (4) has been used by Elliot and Skyrme [8]) in the study of centre of mass effects in shell models.

Since the shell model Hamiltonian can be expressed as a sum of four independent (i.e., commuting) parts, we can find a complete set of eigenvectors of the shell model Hamiltonian (3) which are simultaneous eigenvectors of $H_{Z\text{int}}$, $H_{N\text{int}}$, H_{cm} and H_{r}. The energy corresponding to the shell model eigenvector is the sum of the energies corresponding to the internal, centre of mass and relative motion eigenvectors. If Φ is one of the lowest energy eigenvectors of the shell model Hamiltonian, (only those states satisfying the exclusion principle are admitted) then

$$\Phi = \psi_{Z\text{int}}\,\chi_{N\text{int}}\,\alpha_0(\mathbf{R})\,\beta_0(\mathbf{r}). \tag{5}$$

Here $\psi_{Z\text{int}}$ and $\chi_{N\text{int}}$ contain respectively only proton-proton and neutron-neutron relative coordinates, while $\alpha_0(\mathbf{R})$ and $\beta_0(\mathbf{r})$ are the lowest S state wave functions for the centre of mass motion and proton-neutron relative motion.

Suppose the shell model state Φ absorbs a photon in an electric dipole transition. The electric dipole operator is $eNZ\mathbf{r}/A$ and the only part of the wave function depending on $\mathbf{r}$ is the factor $\beta_0(\mathbf{r})$ representing a relative motion of protons and neutrons in an S state. The dipole absorption will excite this mode into its first P state $\beta_1(\mathbf{r})$ and the total wave function for the excited state will be

$$\Phi_1 = \psi_{Z\text{int}}\,\chi_{N\text{int}}\,\alpha_0(\mathbf{R})\,\beta_1(\mathbf{r}). \tag{6}$$

The wave function (6) represents a collective motion of all the protons against

all the neutrons in which the proton-proton and neutron-neutron relative motions remain undisturbed, i.e., it is a Goldhaber-Teller collective oscillation of the first kind.

From the point of view of the shell model, the form (1) of the dipole operator tells us that only single particle transitions are possible on dipole absorption. The above analysis demonstrates that when light is absorbed by a nucleus in a dipole transition a particular linear combination of single particle excitations is produced, just that linear combination which correspond to a Goldhaber-Teller collective excitation.

4. Deviations from the Oscillator Model

Because of its high degeneracy the oscillator model represents a idealized case in the general class of shell models. In the present section we make one step towards reality by removing this degeneracy. Changing the shape of the shell model potential splits the oscillator states into levels classified by particle orbital angular momentum $\mathbf{l}_i^2$ and to the first order the splitting is quite well represented by adding a term $H' = \beta \sum_A \mathbf{l}_i^2$ to the oscillator Hamiltonian. With this new Hamiltonian the ground state wave function can still be separated in the form (5) (provided β is not so great that neighbouring shells overlap) and we expect that the collective mode represented by the wave function (6) would be excited in a dipole photon absorption. Now, however, the collective state is not a solution of the modified shell model equations and is, in fact, a superposition of single particle excitations which now have slightly different energies. Thus even though the collective state (6) may be excited at the instant of photon absorption, the relative phases of the single particle states making up the collective mode will not be preserved. The single particle excitations will get out of step in a time of the order of $\hbar/\Gamma$, where Γ is a measure of the spread in energy of the single particle excitations, and the collective oscillation will be dissipated into incoherent single particle modes.

The energy spread Γ defined as a half width, has no exact meaning in a shell model because of its small number of states and high degeneracies. In order to have something definite to calculate we have used the estimate of $\Gamma = \sqrt{M_2}$, where M_2 is the second moment of the energy spread of the collective state taken about its mean energy. In problems for which a half width can be defined, $\Gamma < \sqrt{M_2}$ so at least our estimate should provide an upper limit to Γ. The calculation is elementary in the modified oscillator model and for closed shells yields the result

$$M_2 = \beta^2 N(N+4),$$

where N is the number of the last oscillator shell to be filled ($N = 0$ for the lowest shell). The parameter β is undetermined in the modified oscillator

model and in order to get some quantitative estimate of M_2 we make a comparison with the infinite square well shell model. Within a shell in an infinite square well the splitting of the orbits with different l can be represented well by a term of the form $\beta l(l+1)$ in the energy with

$$\beta = -\frac{4E_0}{(2N+1)\pi^2},$$

where E_0 is the energy gap between shells at the top of the Fermi sea. E_0 depends upon the well parameters and the possibility of the occurrence of an effective mass for the nucleon and should be approximately equal to the energy of the giant resonance for photon absorption. Using these estimates we find that

$$\Gamma/E_0 \approx \sqrt{M_2}/E_0 = \frac{4\sqrt{N(N+4)}}{\pi^2(2N+1)},$$

giving values of $\Gamma \approx 4$ MeV in agreement with results of Gallone and Businaro [3]).

5. Summary

As a result of this investigation it is seen that the wave function of the state reached in the dipole photoeffect should not be thought of as a mixture of shell model and collective model wave functions. We have shown that the shell model description already contains the collective vibration predicted by Goldhaber and Teller [2]). The collective and single particle description is contained in the same wave function and the information the wave function gives depends upon the questions asked of it. If for instance we want to know the cross section for direct emission of a neutron in an S state we select that particular component of the collective wave function which contains the excitation of a single neutron in an S state. The Wilkinson picture gives directly the amplitude of such a component in the excited state wave function, thus is particularly suited to discussing direct emission; but we have shown that the complementary collective description has exactly the same wave function, hence it contains the same information.

In the Goldhaber-Teller and Steinwedel-Jensen collective models the width of the giant resonance was ascribed to damping due to viscous effects arising in the relative motion of the proton and neutron fluids. On the other hand, we have seen that the Goldhaber-Teller collective mode excited in a shell model is damped because the various components of the collective motion get out of phase on reflection at the nuclear surface. In a more realistic model with interparticle forces it is to be expected that the width of the giant resonance is due partly to this shell model damping arising from the coherent part of the nuclear interactions and partly to inelastic collisions

between individual particles in the neutron proton clouds, i.e., the incoherent part of the nuclear interaction. Comparison of the width calculated in § 4 with the experimental value of 5 MeV may indicate that the damping arising from the coherent part may be an appreciable fraction of the total damping.

I would like to express my thanks to Prof. V. Weisskopf for his continued interest in this work and for many stimulating discussions, and to Prof. A. Kerman for helpful criticism of the manuscript.

References

1) R. Montalbetti, L. Katz and J. Goldemberg, Phys. Rev. **91** (1953) 659
2) M. Goldhaber and E. Teller, Phys. Rev. **74** (1948) 1046
3) S. Gallone and U. L. Businaro, Nuovo Cimento **1** (1955) 1285
4) J. Fujita, Prog. Theor. Phys. **16** (1956) 112
5) H. Steinwedel and J. H. D. Jensen, Z. Naturforschung **5a** (1950) 413
6) D. H. Wilkinson, Physica **22** (1956) 1039
7) Rand (to be published)
8) J. P. Elliot and T. H. R. Skyrme, Proc. Roy. Soc. A **232** (1955) 561

Nuclear Physics **4** (1957) 221—223; © *North-Holland Publishing Co., Amsterdam*
Not to be reproduced by photoprint or microfilm without written permission from the publisher

ON FOUR-DIMENSIONAL ISOBARIC SPIN FORMALISMS

P. W. HIGGS
Department of Physics, University College, London

Received 14 April 1957

Abstract: It is shown that the use of a four-dimensional isobaric spin space with an indefinite metric is inconsistent with the probability definitions of quantum mechanics.

Since the original work of Pais [1]), various four-dimensional isobaric spin formalisms have been proposed by several authors [2,3,4]). Meanwhile, the Gell-Mann [5]) classification of baryons and mesons has been interpreted in terms of the better established three-dimensional formalism by d'Espagnat and Prentki [6]). In the course of a discussion of how the number of independent interactions allowed by three-dimensional invariance may be reduced by imposing higher symmetries on the theory, d'Espagnat, Prentki and Salam [7]) have reviewed the various four-dimensional formalisms, including those which use a Lorentz metric as well as those based on Euclidian geometry. The purpose of this note is to point out that it is impossible to introduce a Lorentz metric without running into difficulties arising from the probability definitions of quantum mechanics. This fact appears to have been noticed already by Pais [8]), but it seems worth while to treat the matter in more detail.

Let us first consider isobaric space transformations at the level of single-particle wave functions; unless the theory is consistent here it is unlikely to be satisfactory at the level of quantum field theory. If the wave functions ψ_j ($j = 1$ to n) carry an irreducible representation (of dimension n) of the group of isobaric space transformations, then we require the Hilbert space scalar product of two such wave functions to be of the form

$$(\psi^{(1)}, \psi^{(2)}) = \sum_{j=1}^{n} \psi_j^{*(1)} \psi_j^{(2)}, \tag{1}$$

in order that the Hilbert space metric be positive definite. (In (1) summations and integrations over space-time variables have been omitted for the sake of clarity.) Now the bilinear form (1) is an isobaric space invariant only if the representation carried by ψ_j is unitary, and this can occur for finite values of n (apart from the trivial case, $n = 1$) only if the group is an orthogonal group, not a Lorentz group.

To take a particular example, let us suppose that we want to treat $(\boldsymbol{\Sigma}, \Lambda)$ as a four-vector, that is, to regard Λ as Σ_4. Then, if the four-space is Euclid-

ian, the invariant normalization integral for the particle whose different isobaric spin states are (Σ, Λ) is

$$(\psi, \psi) = \int d\sigma_\mu \sum_{j=1}^{4} \bar{\psi}_j \gamma^\mu \psi_j. \tag{2}$$

The right-hand side of (2) is positive definite, as it should be. On the other hand, if the four-space has a Lorentz metric, the only normalization integral which we can construct to be an isobaric invariant is

$$(\psi, \psi) = \int d\sigma_\mu \{ \sum_{j=1}^{3} \bar{\psi}_j \gamma^\mu \psi_j - \bar{\psi}_4 \gamma^\mu \psi_4 \}. \tag{3}$$

The right-hand side of (3) is indefinite; if the wave-function of Σ is normalized to $+1$, that of Λ is normalized to -1, and vice versa. Such a situation is difficult to reconcile with the definition of the wave functions as probability amplitudes.

The analogous difficulty which arises from the Lorentz metric of space-time when we consider vector wave functions (e.g. photon theory) is of course resolved by imposing the Lorentz condition ($\partial_\mu A^\mu = 0$), which ensures that only wave functions of positive norm correspond to observable (spin 1) particles. This way out of the difficulty exists in space-time because there we are really concerned with the unitary representations of the *inhomogeneous* Lorentz group (see, for example, Wigner [9])): the Lorentz condition, which reduces the representation of this group by vector wave functions, involves the infinitesimal generators of displacements, $p_\mu = i\partial_\mu$. No such way out exists in isobaric space, where only homogeneous transformations are admitted, so the Lorentz metric must be rejected.

At the level of quantum field theory, the difficulty manifests itself in the commutation rules for the field operators. Consider the interaction-free part of the Lagrangian for the system (Σ, Λ). If we write the Lagrangian for a single free spin $\frac{1}{2}$ field in the form

$$\bar{\psi}\lambda\psi \equiv \bar{\psi}(i\gamma^\mu \partial_\mu - M)\psi,$$

then the Lagrangian for (Σ, Λ) is

$$L = \sum_{j=1}^{4} \bar{\psi}_j \lambda \psi_j \tag{4}$$

or

$$L = \sum_{j=1}^{3} \bar{\psi}_j \lambda \psi_j - \bar{\psi}_4 \lambda \psi_4 \tag{5}$$

according as we postulate Euclidian or Lorentz invariance. (We assume here that the observed mass differences arise from interactions of lower symmetry.) The anticommutation rules which follow in the usual way from (4) and (5) are respectively

$$\{\psi_j(x), \bar{\psi}_k(x')\} = i\delta_{jk} S(x-x') \tag{6}$$

and

$$\{\psi_j(x), \bar{\psi}_k(x')\} = ig_{jk}S(x-x'), \tag{7}$$

where

$$g_{jk} = 0 \ (j \neq k), \qquad g_{jj} = +1 \ (j = 1, 2, 3), \qquad g_{44} = -1.$$

On analysing ψ, $\bar{\psi}$ into annihilation and creation operators we obtain from (6) the usual occupation number representation of the theory, but from (7) we obtain for the Λ-particle operators relations of the form

$$\{a_4, a_4^*\} = -1. \tag{8}$$

Since the left-hand side of (8) is positive definite, the theory is inconsistent. Once again, we cannot save the situation as we do in photon theory, by introducing a Hilbert space metric which is indefinite with respect to a set of unobservable states, identified covariantly by the auxiliary Lorentz condition: all four particles ($\boldsymbol{\Sigma}$, Λ) are observable.

I am happy to acknowledge useful discussions on this topic with Professor Abdus Salam and Dr. J. C. Taylor. The work was carried out during the tenure of an I.C.I. Research Fellowship.

References

1) A. Pais, Proc. Nat. Acad. Sci. **40** (1954) 484
2) A. Salam and J. C. Polkinghorne, Nuovo Cimento **2** (1955) 685
3) J. Schwinger, Phys. Rev. **104** (1956) 1164, and unpublished lecture notes
4) P. T. Matthews and A. Salam, Nuclear Physics **2** (1957) 582
5) M. Gell-Mann, Phys. Rev. **92** (1953) 833
6) B. d'Espagnat and J. Prentki, Nuclear Physics **1** (1956) 33
7) B. d'Espagnat, J. Prentki and A. Salam, Nuclear Physics **3** (1957) 446
8) A. Pais, ref. [1]), bottom of p. 491
9) E. P. Wigner, Ann. Math. **40** (1939) 149

Nuclear Physics **4** (1957) 224—233; © *North-Holland Publishing Co., Amsterdam*
Not to be reproduced by photoprint or microfilm without written permission from the publisher

THE ISOMERISM OF ELEMENTARY PARTICLES

HIROOMI UMEZAWA † AND ANTOINE VISCONTI ††
University of Maryland, College Park, Maryland

Received 7 May 1957

Abstract: Weak interactions are discussed from the point of view of the isomerism of elementary particles. A generalized gauge transformation is introduced to discuss the isomerism of the neutrino. A possible formulation for the isomerism of particles with finite masses is also pointed out.

1. Introduction

It has been recently suggested that some weak interactions involving neutrinos are not invariant under space inversion. This leads us to the question of how nature behaves under space inversion. To study the invariance properties of the theory, we usually start by considering the class of all the commutable transformations which leave the *free* field equations invariant. It may happen that the field equations of the *interacting* fields remain invariant under the product of two transformations of this class, although the interactions are not invariant with respect to each of them separately.

Contrary to the situation of the point particle in classical mechanics, where a particle at rest has only one state, the particle at rest in relativistic quantum theory seems to have various states, e.g. particle-antiparticle states, isobaric states, etc. If the different states of a particle at rest would be characterized by some internal property, the space inversion could introduce a shift of these states. Then, the space-inversion would be the product of the "classical" space inversion (or the S-transformation which keeps the rest states of the particles invariant under space inversion) with another transformation [1]). The latter transformation could be the exchange of particle and antiparticle ††† [2]) (C-transformation) or the exchange of proton-neutron or something else.

The interactions between four fermions (ψ_a, ψ_b, ψ_c, ψ_d) can be invariant under the SC-transformation when it has the form

$$\sum_A g_A(\bar{\psi}_a \gamma_A \psi_b)(\bar{\psi}_c \gamma_A(1+a\gamma_5)\psi_d).$$

† On leave from University of Tokyo, Department of Physics.

†† On leave from Institut H. Poincaré, Paris.

††† We would like to express our deep appreciation to Professor L. Rosenfeld for informing us of Landau's work before its publication and for his inspiring discussion on the problem of non-conservation of parity.

Here A signifies the well-known five types (S, V, T, P, A) of interactions and a is a real constant. As is well-known, this form of the β-interaction is not inconsistent with the experiments and has an intimate relation with the d- (dextrorotatory or right handed) and l- (laevorotatory or left handed) states of the neutrino. In § 2, we shall study this interaction by introducing a generalized gauge-transformation.

Since the interactions concerning the neutrino are extremely weak, it seems difficult to explain the mysterious situation of the τ- and θ-particles by means of the special property of the neutrino. The aim of § 3 is to show that the d- and l-states can be reasonably introduced for a particle of mass $m \neq 0$.

2. The Generalized Gauge Transformation

Consider the neutrino wave equation:

$$\gamma_\mu \partial_\mu \psi = 0 \tag{1}$$

and the two projection operators

$$\Lambda_1 = \frac{1+\gamma_5}{2}, \qquad \Lambda_2 = \frac{1-\gamma_5}{2}. \tag{2}$$

The positive $u^+(k)$, and negative frequency $u^-(k)$ parts of $\psi(x)$ satisfy the following equation:

$$(\boldsymbol{\sigma} \cdot \mathbf{k}) u^\pm(k) = -\gamma_5 \omega u^\pm(k), \tag{3}$$

where ω is the energy of the neutrino ($\geqq 0$) and $\boldsymbol{\sigma}$ is the 4×4 spin matrix:

$$\sigma_1 = -i\gamma_2\gamma_3, \qquad \text{etc.}$$

Defining the operators

$$u_1^\pm(k) = \Lambda_1 u^\pm(k), \qquad u_2^\pm(k) = \Lambda_2 u^\pm(k) \tag{4}$$

and the corresponding charge conjugate operators

$$u_1^{(C)} \equiv C\bar{u}_1^{\mathrm{T}}, \qquad \text{etc,}$$

we obtain the following equations:

$$\begin{aligned} (\boldsymbol{\sigma} \cdot \mathbf{k}) u_1^\pm(k) &= -\omega u_1^\pm(k) \\ (\boldsymbol{\sigma} \cdot \mathbf{k}) u_2^\pm(k) &= +\omega u_2^\pm(k), \end{aligned} \tag{5}$$

$$\begin{aligned} (\boldsymbol{\sigma} \cdot \mathbf{k}) u_1^{(C)\pm}(k) &= +\omega u_1^{(C)\pm}(k) \\ (\boldsymbol{\sigma} \cdot \mathbf{k}) u_2^{(C)\pm}(k) &= -\omega u_2^{(C)\pm}(k). \end{aligned} \tag{6}$$

One can therefore build up the following table †:

l-state particle	l-state antiparticle	d-state particle	d-state antiparticle
u_1^-	u_1^+	u_2^-	u_2^+
$u_2^{(C)+}$	$u_2^{(C)-}$	$u_1^{(C)+}$	$u_1^{(C)-}$
u_2^{*+}	u_2^{*-}	u_1^{*+}	u_1^{*-}

† (−)-superscript — creation operator, (+)-superscript — annihilation operator.

This shows that $u_1^{*\pm}$ correspond respectively to annihilation and creation operator for particle and antiparticle 2 and $u_2^{*\pm}$ correspond to annihilation and creation operators of particle 1.

This is the special case of the general theorem [3]) which says that any massless field (with spin > 0) has only two states provided that its interactions are invariant under gauge transformations. The two states are those where the spin is parallel or antiparallel to the momentum (or right and left circular waves).

In the case of spin $\frac{1}{2}$, the gauge-transformation is the trivial identity transformation ($\psi \to \psi' = \psi$). The gauge-transformation is invariant under the S-transformation. However, we can restrict further the types of interactions of the massless particles by introducing a generalized gauge-transformation, when these interactions are not invariant under the S-transformation. We shall first study the generalized gauge-transformation in the case of the neutrino and, later, discuss its relation with the ordinary gauge-transformation of the electromagnetic field.

One may easily check that the neutrino equation is invariant under the following transformation:

$$\psi \to \psi' = (\alpha \Lambda_1 + \alpha^* \Lambda_2)\psi \tag{7}$$

where $\alpha = \exp(ia)$ with a real parameter a. We shall call this the generalized gauge-transformation for the neutrino. It is apparent that the self-energy of the neutrino is zero as far as its interactions are invariant under the transformation (7).

The interactions between fermions are built up of products of terms of the form

$$\psi_{(a)} \gamma_A f(\gamma_5) \psi \tag{8}$$

where $f(\gamma_5)$ is a function of γ_5 and $\psi_{(a)}(x)$ is the wave function of a fermion with a given mass m. Writing $f(\gamma_5)$ in the form

$$f(\gamma_5) = A\Lambda_1 + B\Lambda_2, \tag{9}$$

we see that (7) transforms (8) into

$$\bar{\psi}'_{(a)} \gamma_A \{A e^{ia} \Lambda_1 + B e^{-ia} \Lambda_2\} \psi.$$

The term (8) can be invariant under the transformation (7), when

$$B = 0: \qquad f(\gamma_5) = \frac{A}{2}(1+\gamma_5), \qquad \psi_{(a)} \to \psi'_{(a)} = \psi_{(a)} e^{ia}, \tag{10}$$

or

$$A = 0: \qquad f(\gamma_5) = \frac{B}{2}(1-\gamma_5), \qquad \psi_{(a)} \to \psi'_{(a)} = \psi_{(a)} e^{-ia}. \tag{11}$$

The particle $\psi_{(a)}$ interacts with the neutrino described either by ψ_1 (for (10)) or by ψ_2 (for (11)). It is furthermore useful to introduce a "neutrino charge" for the particle $\psi_{(a)}$: it has a positive (or negative) "neutrino charge" if (11) (or (10)) holds. A particle has a 0 "neutrino charge" if its wave function does not change under the generalized gauge transformation.

This analysis applies immediately to β-decay processes; one may see that this sort of interaction can be represented as follows:

$$\sum_{S,V,T,P,A} G_A(\bar{\psi}_P \gamma_A \psi_N)(\bar{\psi}_e \gamma_A(1\pm\gamma_5)\psi_\nu) + \sum_{S,V,T,P,A} G'_A(\bar{\psi}_P \gamma_A \psi_N)(\bar{\psi}_e \gamma_A(1\pm\gamma_5)\psi_\nu^{(c)}) \tag{12}$$

The same sign of γ_5 should be taken in the above two terms. The experiments tend to support the positive sign of γ_5.

Let us assume that the nucleons have zero neutrino charge, the neutrino charge of the leptons is then determined by the gauge invariance requirement. The electron has negative neutrino charge.

The interaction for the μ-meson decay is

$$\sum_{(S,T,P,A,V)} G_A(\bar{\psi}_\mu \gamma_A(1\pm\gamma_5)\psi_\nu)(\bar{\psi}_e \gamma_A(1\pm\gamma_5)\psi_\nu) + (G_A \to G'_A, \quad \psi_\nu \to \psi_\nu^{(C)}) \tag{13}$$

for the decay scheme $\mu \to e+\nu+\nu$. The signs of γ_5 in two brackets should be different for a positive neutrino charge of the μ-meson, and all the γ_5 should have positive sign for a negative neutrino charge of the μ-meson.

Assuming the decay scheme $\mu \to e+\nu+\bar{\nu}$, we obtain

$$\sum_{(V,A)} G_A(\bar{\psi}_\mu \gamma_A \psi_e)(\bar{\psi}_\nu \gamma_A(1+a'\gamma_5)\psi_\nu) \tag{14}$$

or

$$\sum_{(S,T,P)} G_A(\bar{\psi}_\mu \gamma_A \psi_e)(\bar{\psi}_\nu \gamma_A(1+a'\gamma_5)\psi_\nu). \tag{15}$$

Here a' is a real constant. The case (14) ((15)) corresponds to the case where the μ-meson and electron have equal (opposite) neutrino charges.

The two-component theory of the neutrino [4]) is the special case

$$\psi_1 = \psi_1^* = \psi_1^{(C)} = 0. \tag{16}$$

Under this assumption, the $(1+\gamma_5)$ type of interaction leads to the process

$$N \to P+e+\bar{\nu}.$$

It must be noted that only (14) (with $a' = 1$) is possible for the case $\mu \to e+\nu+\bar{\nu}$ in the two-component theory.

A better understanding of the nature of the transformation (7) can be obtained by investigating its connection with the gauge transformation in electrodynamics.

The wave function φ of a massless particle of spin 1 like the photon be-

haves, under a Lorentz transformation, as the tensorial product of two spinors. Calling Λ_i and Λ'_i the projection operators (defined in (2)) in each spinor space, we shall prove that the transformation

$$\varphi \to \varphi' = \varphi + (\Lambda_1 \times \Lambda'_2 + \Lambda_2 \times \Lambda'_1)\lambda \tag{17}$$

is equivalent to the ordinary gauge transformation. Here, λ satisfies the following equations:

$$\partial_\mu \beta_\mu \lambda = 0, \tag{18}$$

$$\Box \lambda = 0, \tag{19}$$

and the β_μ are defined as follows:

$$\beta_\nu = \frac{\gamma_\nu \times I' + I \times \gamma'_\nu}{2}, \quad \nu = 1, \cdots, 5. \tag{20a}$$

We shall consider a representation for the γ'_μ such that

$$\gamma'_\mu = \gamma_\mu^{\mathrm{T}}, \quad \mu = 1, \cdots, 4. \tag{20b}$$

It is useful to introduce the following operators:

$$\eta_\nu = \gamma_\nu \times \gamma'_\nu; \tag{21a}$$

$$\eta_+ = \frac{1+\eta_5}{2} = \Lambda_1 \times \Lambda'_1 + \Lambda_2 \times \Lambda'_2,$$

$$\eta_- = \frac{1-\eta_5}{2} = \Lambda_1 \times \Lambda'_2 + \Lambda_2 \times \Lambda'_1; \tag{21b}$$

η_+ (η_-) is the projection operator which picks up the components corresponding to the same (or different) eigenvalues of γ_5 and γ'_5. We shall now prove that the Maxwell equations can be written as follows:

$$\begin{aligned} &\beta_\mu \partial_\mu \eta_+ \varphi = 0, \\ &\beta_\mu \beta_5 \partial_\mu \eta_+ \varphi = 0. \end{aligned} \tag{22}$$

Using the formulae (20) and (21), the former equations take the form

$$\gamma_\mu \partial_\mu \varphi + \partial_\mu \varphi \gamma_\mu + \gamma_\mu \gamma_5 \partial_\mu \varphi \gamma_5 + \gamma_5 \partial_\mu \varphi \gamma_5 \gamma_\mu = 0, \tag{23a}$$

$$\gamma_\mu \gamma_5 \partial_\mu \varphi + \gamma_5 \partial_\mu \varphi \gamma_\mu + \gamma_\mu \partial_\mu \varphi \gamma_5 + \partial_\mu \varphi \gamma_5 \gamma_\mu = 0. \tag{23b}$$

Since we consider a particle of spin 1, its wave function φ can be written as follows[5]):

$$\varphi = \gamma_\mu A_\mu + \gamma_\mu \gamma_\nu F_{\mu\nu}. \tag{24}$$

The quantities A_μ, $F_{\mu\nu}$ are respectively a vector and an antisymmetric tensor. One verifies that η_+ and η_- pick up the tensor and vector components respectively:

$$\begin{aligned} &\varphi^+ = \eta_+ \varphi = \gamma_\mu \gamma_\nu F_{\mu\nu}, \\ &\varphi^- = \eta_- \varphi = \gamma_\mu A_\mu. \end{aligned} \tag{25}$$

Introducing (24) into (23) and using the trace method, one obtains the Maxwell equations

$$\varepsilon_{\mu\nu\sigma\varrho}\partial_\nu F_{\sigma\varrho} = 0,$$
$$\partial_\mu F_{\mu\nu} = 0.$$

The formula (17) may be written by using η_-:

$$\varphi \to \varphi' = \varphi + \eta_-\lambda.$$

Since the Maxwell equations are expressed by means of φ^+ only, they are invariant under the transformation (17). We can furthermore show that the term $\eta_-\lambda$ contributes to the vector potential A_μ by the gauge term $\partial_\mu\Lambda$, where Λ is a scalar function. It has to be noted that the transformation (17) is invariant under the S-transformation.

If now we add and substract the equations (22), we may also write the Maxwell equation in the following form:

$$\begin{aligned}\beta_\mu\partial_\mu(1+\beta_5)\eta_+\varphi &= 0,\\ \beta_\mu\partial_\mu(1-\beta_5)\eta_+\varphi &= 0.\end{aligned} \tag{26}$$

Let us now consider the wave functions $\varphi_\pm = (1\pm\beta_5)\eta_+\varphi$. They are orthogonal to each other and one has

$$\begin{aligned}\varphi_\pm &= \gamma_\mu\gamma_\nu(F_{\mu\nu}\pm\tfrac{1}{2}\varepsilon_{\mu\nu\sigma\varrho}F_{\sigma\varrho})\\ &\equiv \gamma_\mu\gamma_\nu F^\pm_{\mu\nu}.\end{aligned} \tag{27}$$

The quantities $\varphi_\pm$ therefore correspond to left and right circular waves as shown by the expression of $F^\pm_{\mu\nu}$:

$$F^\pm_{12} = H_3 + iE_3, \quad \text{etc.}, \tag{28}$$

where **H** and **E** are the magnetic and electric field strengths. It must also be noted that $F^-_{\mu\nu}$ describes the antiparticle of $F^+_{\mu\nu}$ since it is hermitian conjugate to the latter. Since the equations (27) are independent of each other, the theory is invariant under the relative change of the phases of two components

$$\begin{aligned}\eta_+\varphi &\to \left(\alpha\frac{1+\beta_5}{2} + \alpha^*\frac{1-\beta_5}{2}\right)\eta_+\varphi\\ &= (\alpha\varphi_+ + \alpha^*\varphi_-),\end{aligned} \tag{29}$$

which is the generalized gauge transformation for a massless particle of spin 1. The electromagnetic interactions are not invariant under the generalized gauge transformation, since the electromagnetic interaction implies a sum $(F^+_{\mu\nu}+F^-_{\mu\nu})$ because of its invariance under the S-transformation. However, the weak interactions — not invariant under the S-transformation — could be invariant under the generalized gauge transformation. The preceding considerations on the neutrino can be given as an example of the generalized gauge transformation. Similar considerations could be extended to the gravitational field.

3. Particle with Non-Zero Mass

In the preceding sections we have discussed the theory of the d- and l-states of massless particles. It is not easy to introduce these states of charged particles in the case of spin $\frac{1}{2}$ and mass $m \neq 0$. This is because the projection operators Λ_1, Λ_2 are not commutable with the Hamiltonian of the Dirac particle with non-zero mass. A possible formulation of the spin $\frac{1}{2}$ particle with finite mass will be discussed later. We first introduce the isomerism (d- or l- states) † for particles with spin 0 and mass $m \neq 0$. This would give one of the possibilities for clarifying the mysterious behavior of the τ, θ particles.

A straightforward generalization of the equations in § 2 leads us to consider the equation

$$\{\tfrac{1}{2}(\gamma_\mu \times I' + \gamma_\mu \times \gamma_5')\partial_\mu + m\}\psi = 0. \tag{30}$$

Since we consider a field of spin 0 we shall write ψ in terms of scalar, pseudoscalar, vector, and pseudovector quantities[5]):

$$\psi = \phi + \gamma_5\phi' + \gamma_\mu\phi_\mu + \gamma_5\gamma_\mu\phi_\mu'. \tag{31}$$

Note first that

$$\frac{1-\gamma_5'}{2}\psi = 0. \tag{32}$$

We have therefore

$$\begin{aligned} \phi &= \phi', \\ \phi_\mu &= -\phi_\mu', \end{aligned} \tag{33}$$

and finally

$$\psi = (1+\gamma_5)\phi + (1-\gamma_5)\gamma_\mu\phi_\mu. \tag{34}$$

We note moreover that

$$\begin{aligned} \eta_+\psi &= (1+\gamma_5)\phi, \\ \eta_-\psi &= (1-\gamma_5)\gamma_\mu\phi_\mu. \end{aligned} \tag{35}$$

In other words, the projection operator η_+ introduces the scalar part without any definite parity. ϕ and ϕ_μ satisfy the following equations:

$$\begin{aligned} \partial_\mu\phi_\mu + m\phi &= 0, \\ \partial_\mu\phi + m\phi_\mu &= 0. \end{aligned} \tag{36}$$

These are the well-known equations for the particle of spin 0. The S-transformation has to be defined by the matrix η_4:

$$\psi \to \psi' = \eta_4\psi.$$

The lagrangian and the wave equation are not invariant under this transformation. The C-transformation is given by

† After this work was finished, we were informed that a similar discussion has been independently carried out by Professor S. Watanabe (private communication).

$$\psi^{(C)} = C \times C' \overline{\psi}^{T} \tag{37}$$

where C and C' are the charge conjugation operators in the two spinor spaces, and $\overline{\psi} = \psi^* \eta_4$. We can then derive the relation †

$$\psi^{(C)} = (1-\gamma_5)\phi^* + (1+\gamma_5)\gamma_\mu \phi_\mu{}^*. \tag{38}$$

If we call the state of the particle the l- state when its scalar part is an eigenvector of $\frac{1}{2}(1+\gamma_5)$, then we find that the antiparticle appears in the d- state. The operators ψ^- (negative frequency part of ψ) and ψ^{*-} (negative frequency part of ψ^*) create the particle in the l- state and the antiparticle in the d- state. The equation (30) can be written in a form symmetric with respect to the two spinor spaces as follows:

$$\left\{\frac{1}{\sqrt{2}}(\gamma_\mu \times A'_1 + A_1 \times \gamma'_\mu)\partial_\mu + m\right\}\psi = 0$$

or

$$\left\{\frac{1}{\sqrt{2}}(\beta_\mu + [\beta_\mu, \beta_5]_+)\partial_\mu + m\right\}\psi = 0. \tag{39}$$

There exists, however, another possibility that τ and θ would be the different states of an isomerism. Such a doublet theory can be formulated in the following way: The equation for the d- state particle can be shown to be

$$\left\{\frac{1}{\sqrt{2}}(\beta_\mu - [\beta_\mu, \beta_5]_+)\partial_\mu + m\right\}\psi = 0. \tag{40}$$

Introducing the two dimensional matrices

$$\tau_1 = \begin{pmatrix} 0 & 1 \\ 1 & 0 \end{pmatrix}, \quad \tau_2 = \begin{pmatrix} 0 & -i \\ i & 0 \end{pmatrix}, \quad \tau_3 = \begin{pmatrix} 1 & 0 \\ 0 & -1 \end{pmatrix},$$

the equation of the doublet particle can be derived by combining (39) and (40) in the following way:

$$\left\{\frac{1}{\sqrt{2}}(\beta_\mu + \tau_3[\beta_\mu, \beta_5]_+)\partial_\mu + m\right\}\psi = 0. \tag{41}$$

The eigenstates of τ_3 with the eigenvalues $+1$ and -1 describe l- and d- particles states respectively. This theory is invariant under the S-transformation together with the transformation $\psi \to \tau_1 \psi$. The latter is the transformation which exchanges the two states of the isomerism.

Thus, we have introduced an intrinsic isomerism for the spin zero particle. It seems difficult, however, to make the electromagnetic and strong interactions invariant under the S-transformation because of the intrinsic isomerism of the particle††. This difficulty can be solved by assuming the free

† Note that $\phi_4{}^* \equiv -i\phi_0{}^*$ where ϕ_0 is the $i\phi_4$.

†† The authors are indebted to Professor Coester and Dr. Takahashi for critical discussions on this point.

field equation invariant under the S-transformation and by introducing the weak interactions picking up the d- or l- state of the particle. This can be done in the following way: Assuming the field equation (cf. (30)):

$$(\gamma_\mu \partial_\mu + mI) \times I' \psi = 0, \tag{42}$$

we obtain the solution for the spin zero field

$$\psi = \phi + \gamma_5 \phi' - \frac{1}{m} \gamma_\mu \partial_\mu \phi + \frac{1}{m} \gamma_5 \gamma_\mu \partial_\mu \phi'$$

with

$$(\Box - m^2)\phi = (\Box - m^2)\phi' = 0.$$

The field equation (42) is invariant under the S-transformation.

We shall now introduce the fields ϕ_1, ϕ_2 by means of the following unitary transformation:

$$\begin{aligned} \phi_1 &= \frac{1}{\sqrt{2}} (\phi - \phi'), \\ \phi_2 &= \frac{1}{\sqrt{2}} (\phi + \phi'). \end{aligned} \tag{43}$$

Then we obtain (cf. (34))

$$\begin{aligned} \frac{1+\gamma'_5}{2} \psi &= \frac{1}{\sqrt{2}} \left\{ (1+\gamma_5)\phi_2 - \frac{1}{m} (1-\gamma_5)\gamma_\mu \partial_\mu \phi_2 \right\}, \\ \frac{1-\gamma'_5}{2} \psi &= \frac{1}{\sqrt{2}} \left\{ (1-\gamma_5)\phi_1 - \frac{1}{m} (1+\gamma_5)\gamma_\mu \partial_\mu \phi_1 \right\}. \end{aligned} \tag{44}$$

This shows that ϕ_2 and ϕ_1 refer to the d- and l- states of the spin zero particles. It can be shown that the d- and l- states $\frac{1}{2}(1 \pm \gamma_5)'\psi$ are the eigenstates of the Hamiltonian

$$H = \gamma_4 (\gamma_k \partial_k + mI) \times I'.$$

Since the electromagnetic interaction and the strong interactions are invariant under the S-transformation, they contain ψ as a whole. Assuming that the weak interactions contain $\frac{1}{2}(1+\gamma'_5)\psi$ and $\frac{1}{2}(1-\gamma'_5)\psi$ separately, they pick up d- or l- states of the particles (i.e. ϕ_1, ϕ_2). In other words, the particles are produced in the states ϕ or ϕ' and only ϕ_1- or ϕ_2- components of these states can decay through weak interactions.

It is impossible to introduce the d- and l- states of the spin $\frac{1}{2}$ field (with mass $m \neq 0$) by means of the projection operator $\frac{1}{2}(1 \pm \gamma_5)$. To solve this difficulty, it is instructive to remember that we have used in effect the two spinor spaces to represent the Bose field. We shall now introduce a product of the two-dimensional τ-space and the four-dimensional spinor space to represent the spin $\frac{1}{2}$ field. In this representation the wave function of the spin $\frac{1}{2}$ field is built up of eight components.

Assuming the field equation of the spin $\frac{1}{2}$ field

$$(\gamma_\mu \partial_\mu + m\tau_1)\psi = 0, \tag{45}$$

we see that the operators

$$\frac{1 \pm \tau_3 \gamma_5}{2} \tag{46}$$

are commutable with the Hamiltonian

$$H = \gamma_4 (\gamma_k \partial_k + m\tau_1).$$

We shall call the states

$$\frac{1+\tau_3\gamma_5}{2}\psi \qquad \frac{1-\tau_3\gamma_5}{2}\psi \tag{47}$$

the l- and d- states of the Fermion field ψ respectively. Applying this theory to the problem of the hyperons, we see that some of the weak interactions may pick up any one of two components (47), although the strong interactions and electromagnetic interaction should contain ψ as a whole.

The authors would like to express their gratitude to Professor J. S. Toll for his inspiring discussions and kind hospitality. One of the authors (H. U.) is indebted to Professor J. M. Jauch for enabling him to complete this work during his stay at the State University of Iowa.

References

1) H. Umezawa, S. Kamefuchi and S. Tanaka, Prog. Theor. Phys. **12** (1954) 383
2) L. Landau, Nuclear Physics **3** (1957) 127
3) M. Fierz and W. Pauli, Proc. Roy. Soc. A **173** (1939) 211
4) T. D. Lee and C. N. Yang, Phys. Rev. **105** (1957)
5) L. de Broglie, Théorie générale des particules à spin (Gauthier-Villars, Paris 1943)

Nuclear Physics **4** (1957) 234—239; © *North-Holland Publishing Co., Amsterdam*
Not to be reproduced by photoprint or microfilm without written permission from the publisher

AN ALPHA-PARTICLE MODEL FOR THE NUCLEAR PHOTODISINTEGRATION OF O^{16}

HANS WILHELMSSON AND MARGITA NILSSON

Institute for Theoretical Physics, University of Lund

Received 11 April 1957

Abstract: The photonuclear effect in O^{16} is studied theoretically for the case of one emitted nucleon. The giant resonance is described with the aid of a simple model, which assumes that in the O^{16} nucleus only four nucleons, forming an α-particle, are affected by the γ-ray. The α-particle is assumed to be moving in a static collective potential from the other nucleons, these being undisturbed during the photodisintegration process. Gaussian wave functions are used. The results obtained are not in disagreement with recent experimental information.

1. Introduction

In recent years the photonuclear disintegration of the α-particle has been the subject of several investigations. Theoretically this problem has been treated by Flowers and Mandl [1]) and at the same time independently by Gunn and Irving [2]). Experimental studies have been performed by Fuller [3]).

It has been suggested [4]) that a modified α-particle model of nuclei might possibly be consistent with experimental data on the dipole resonances of the reactions (γ, n) and (γ, p). At present the nucleus for which the photodisintegration is most thoroughly known by experiment is O^{16}. This nucleus has recently been studied extensively by Johansson and Forkman [5]). It is also well suited for considerations on α-particle structure of nuclear matter.

We want to investigate, in the case of O^{16}, whether or not a model in which a single α-particle is assumed to be bound in a central potential, describing the interaction with the remaining nucleons, is able to account for the main data obtained from experiment. Our calculations apply only to the giant resonance of the cross section for nuclear emission, which seems well established to be an electric dipole effect. It is assumed that the emitted nucleon originates from the bound α-particle and that the remaining nucleons are left undisturbed by the γ-ray. This might be justified by the fact that the mutual motions of the α-particles are not influenced by dipole effects because they have the same charge to mass ratio. During the photodisintegration process the emitted nucleon is assumed to be coupled to the other nucleons in the α-particle, which in turn is bound to the centre of a static collective potential from the rest of the nucleons in O^{16}.

The value obtained from experiment for the maximum cross section of the reaction $O^{16}(\gamma, p)N^{15}$ is 23 millibarns at a photon energy of 23 MeV [5], whereas for the reaction $He^4(\gamma, p)H^3$ the corresponding quantities are 1.8 millibarns and 26 MeV [6]†.

For a dipole transition there exist the following possibilities for the photodisintegration of an α-particle [3]:

Reaction	Threshold energy
$He^4(\gamma, p)H^3$	20 MeV
$He^4(\gamma, n)He^3$	20 MeV
$He^4(\gamma, p\,n)D$	26 MeV
$He^4(\gamma, 2p\,2n)$	28 MeV.

The threshold energy of the giant resonance in O^{16} lies at about 20 MeV [5]) It is apparent that at this energy only two-particle disintegrations are possible. We therefore consider only the former two processes. Electrostatic effects are neglected, so the same cross section is obtained for either of them. For the sake of definiteness $He^4(\gamma, n)He^3$ is chosen.

2. Wave Functions and Matrix Elements

According to the model assumed the initial and final wave functions are of the form

$$\begin{aligned} \Psi_i &= \psi_{3\alpha} \cdot \psi_{CM\,(\alpha)} \cdot \psi_{intr\,(\alpha)}, \\ \Psi_f &= \psi_{3\alpha} \cdot \psi_{CM\,(He^3)} \cdot \psi_{intr\,(He^3)} \cdot R_{n,\,He^3}. \end{aligned} \tag{1}$$

Here $\psi_{3\alpha}$ describes the motion of the nucleons that remain undisturbed during the process. $\psi_{CM\,(\alpha)}$ and $\psi_{CM\,(He^3)}$ are the wave functions for the centres of mass of the α-particle and the He^3-nucleus respectively, while $\psi_{intr\,(\alpha)}$ and $\psi_{intr\,(He^3)}$ are the intrinsic wave functions. R describes the relative motion of the emitted neutron and the rest of the α-particle.

As the true wave functions are not known we have to use some approximation. The procedure of calculation is now essentially that used by Flowers and Mandl [1]). Thus our wave functions $\psi_{intr\,(\alpha)}$ and $\psi_{intr\,(He^3)} \cdot R$ are equal to the initial and final wave functions used by these authors in the case of a free α-particle disintegration. The wave functions ψ are assumed to be of the Gaussian form, e.g.

$$\psi_{intr\,(\alpha)} = \exp\left[-b \sum_{i,j} (\mathbf{r}_i - \mathbf{r}_j)^2\right],$$

$\mathbf{r}_i$ being the position vector of the ith nucleon in the α-particle and b a constant determined from the spatial extension of the bound α-particle. R is assumed to be a free particle wave function.

† These values correspond to smooth curves approximating experimental data.

Similarly, we assume for the unnormalized functions $\psi_{CM(\alpha)}$, $\psi_{CM(He^3)}$

$$\psi_{CM(\alpha)} = e^{-\delta\rho_\alpha^2} \qquad \psi_{CM(He^3)} = e^{-\beta\rho^2}, \tag{2}$$

where $\boldsymbol{\rho}_\alpha$ and $\boldsymbol{\rho}$ are the position vectors of the centres of mass of the α-particle and the He^3-nucleus respectively. The explicit forms of Ψ_i and Ψ_f are given in the appendix. δ and β are determined from the radius of O^{16}.

We use first order perturbation theory and calculate the matrix element for the $^1S \rightarrow {}^1P$ transition

$$M_{E1} = 2\sqrt{2}\int \Psi_i M \Psi_f, \tag{3}$$

where M is the electric dipole operator (see appendix). The factor $\sqrt{2}$ takes into account the possibility of emission of either of the two neutrons and the factor 2 allows this emission to be made from any of the four α-particles. The cross section is then determined from the formula [7])

$$\sigma_{E1} = \frac{8\pi^3\nu}{c} \sum_{m=-1}^{1} |M_{E1}|^2, \tag{4}$$

where ν is the frequency of the γ-ray.

The value for the cross section found from eq. (4) is sensitive to the approximations made for the wave functions. It is obvious that if we express the cross section for O^{16} as

$$\sigma_{O^{16}}(E) = F(E) \cdot \sigma_\alpha(E), \tag{5}$$

where

$$F(E) = \frac{|\langle \Psi_i | M | \Psi_f \rangle|^2 \cdot N}{|\langle \psi_{intr(\alpha)} | M | \psi_{intr(He^3)} \cdot R \rangle|^2}, \qquad N \equiv \int \psi^2_{intr(\alpha)} \int \psi^2_{intr(He^3)} \cdot R^2,$$

and E is the energy of the incident photon, and if we further use experimental values for $\sigma_\alpha(E)$, we obtain a result for $\sigma_{O^{16}}(E)$ less dependent upon the approximations. We are here mainly interested in the question whether or not the described model for the photodisintegration of O^{16} has any validity. The best way seems then to take $\sigma_\alpha(E)$ from experiment [6]).

3. Results of Calculation

We take into account the possibility that the size of the α-particle bound in O^{16} differs somewhat from the size of a free α-particle and introduce the constant λ for the bound α-particle different from the corresponding constant λ' for the free α-particle (see appendix). Similarly the μ for the bound He^3-particle is assumed to be different from the corresponding free particle value μ'.

The factor $F(E)$ is found to be

$$F(E) = 4 \cdot \frac{\delta^{3/2}\beta^{3/2}}{\left(\frac{\delta+\beta}{2}\right)^3} \cdot \left(\frac{\lambda'}{\lambda}\right)^{3/2} \cdot \left(\frac{\mu}{\mu'}\right)^3 \cdot \left(\frac{2\lambda'+3\mu'}{2\lambda+3\mu}\right)^6 \cdot \frac{1}{\left(1+\frac{1}{12}\cdot\frac{1}{\lambda}\cdot\frac{\delta\beta}{\delta+\beta}\right)^5}$$

$$\cdot \exp\left\{-(E-E_0)\cdot\left[\frac{1}{\varepsilon+\frac{\delta\beta}{12(\delta+\beta)}\cdot\frac{\hbar^2}{M}} - \frac{1}{\varepsilon'}\right]\right\}, \qquad (5)$$

where $\varepsilon = \lambda \cdot \hbar^2/M$ and $\varepsilon' = \lambda' \cdot \hbar^2/M$. Here M is the nucleon mass and E_0

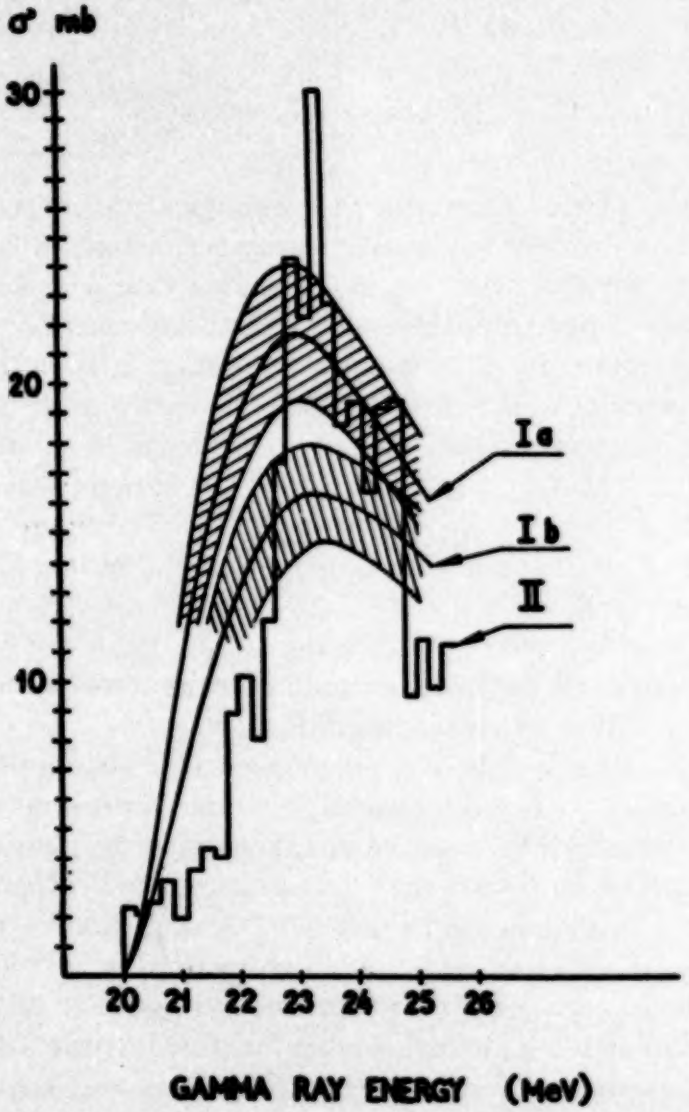

Fig. 1. Cross section for the reaction $O^{16}(\gamma, p)N^{15}$.

I. Theoretical curves with $1/\sqrt{\mu'} = 1/\sqrt{\lambda'} = 3.4 \cdot 10^{-13}$ cm and a) $1/\sqrt{\delta} = 1/\sqrt{\beta} = 1/\sqrt{\lambda} = 1/\sqrt{\mu} = 4.7 \cdot 10^{-13}$ cm ($R^{\text{bound}} = 1.4 \cdot R^{\text{free}}$), b) $1/\sqrt{\delta} = 1/\sqrt{\beta} = 1/\sqrt{\lambda} = 1/\sqrt{\mu} = 4.4 \cdot 10^{-13}$ cm ($R^{\text{bound}} = 1.3 \cdot R^{\text{free}}$). Shaded regions correspond to uncertainties in the experimental values of the cross section for the reaction $He^4(\gamma, p)H^3$ used in the calculations.

II. Experimental cross section obtained by Johansson and Forkman[5]).

is the threshold for nucleon emission in the photoeffect for the free α-particle. In view of the approximations made for the wave functions we may take $\delta = \beta$, $\lambda = \mu$ and $\lambda' = \mu'$. The constants δ and λ are also chosen equal, being of the same order of magnitude from considerations on the size of the α- and O^{16}-nuclei. The effect of the binding in the static collective potential amounts in $F(E)$, according to eq. (5), to about 4% in the exponential function and to 20 % in all factors in front of the exponential function. $F(E)$ is comparatively insensitive to the values of δ and β, so it is not possible to determine these constants accurately from experiment.

For $\delta = \beta = \lambda = \mu$ and $\lambda' = \mu'$ we obtain

$$F(E) = 4 \cdot \left(\frac{24}{25}\right)^5 \cdot \left(\frac{\lambda'}{\lambda}\right)^{7/2} \cdot \exp\left\{-(E-E_0)\left(\frac{24}{25}\cdot\frac{1}{\varepsilon} - \frac{1}{\varepsilon'}\right]\right\}. \qquad (5a)$$

In figure 1 is plotted the result of a numerical calculation. The shaded regions correspond to uncertainties in the experimental values for the cross section of the photodisintegration of a free α-particle which are used in this calculation. For comparison the experimental cross section of the reaction $O^{16}(\gamma, p)N^{15}$ obtained by Johansson and Forkman [5]) is shown in the same figure. It appears that the result of the calculation is in agreement with experiment if it is assumed that the radius of the bound α-particle is 1.3—1.4 times larger than that of a free α-particle. The experimental value for the O^{16}-radius is 1.9 times the free α-particle radius. The figure shows that the theoretical cross section becomes larger when the radius of the bound α-particle is increased.

It should be emphasized that for reasonable values of the parameters satisfactory results are obtained for the maximum cross section and for the energy corresponding to maximum cross section.

The concept of the radius of a bound α-particle should of course not be taken too literally. It is only a measure of the dimensions of the subunit configuration which we here assume to take part in the photodisintegration.

The authors want to express their deep gratitude to Professor T. Gustafson for his interest in their work in this field. Sincere thanks are also due to Dr S. Johansson, who suggested an investigation of O^{16}, for stimulating advice and for information on his experimental results in advance of publication. We also wish to thank members of the Institutes for Theoretical Physics in Copenhagen and Lund for discussions and criticism.

Appendix

For explicit calculation it is convenient to use a coordinate system in which the wave functions can be most simply written. We introduce

$$\begin{aligned} 3\mathbf{t}_1 &= \mathbf{r}_1+\mathbf{r}_2+\mathbf{r}_3-3\mathbf{r}_4 \\ 2\mathbf{t}_2 &= \mathbf{r}_1+\mathbf{r}_2-2\mathbf{r}_3 \\ \mathbf{t}_3 &= (\mathbf{r}_1-\mathbf{r}_2)\sqrt{3/2} \\ 3\boldsymbol{\rho} &= \mathbf{r}_1+\mathbf{r}_2+\mathbf{r}_3, \end{aligned} \tag{6}$$

where $\mathbf{r}_1$ and $\mathbf{r}_2$ are the position vectors of the two protons in the α-particle and $\mathbf{r}_3$ and $\mathbf{r}_4$ the position vectors of the two neutrons.

In terms of these coordinates the initial wave function can be expressed as

$$\Psi_1 = N_1 \cdot \psi_{3\alpha} \cdot e^{-\delta\left(\rho^2+\frac{t_1^2}{16}-\frac{1}{2}\boldsymbol{\rho}\cdot\mathbf{t}_1\right)} \cdot e^{-\lambda(\frac{3}{4}t_1^2+\frac{2}{3}t_2^2+\frac{2}{3}t_3^2)}; \tag{7}$$

N_1 is a normalization constant and the constants δ and λ are determined from the condition that $\delta^{-\frac{1}{2}}$ and $\lambda^{-\frac{1}{2}}$ should be of the order of magnitude of the radius of O^{16} and of the bound α-particle. The final wave function is

$$\Psi_f = N_2 \cdot \psi_{3\alpha} \cdot e^{-\beta\rho^2} \cdot e^{-\mu(t_2^2+t_3^2)} \cdot R(t_1), \tag{8}$$

where

$$R(t_1) = \left(\frac{\pi}{2kt_1}\right)^{\frac{1}{2}} \cdot J_{\frac{3}{2}}(kt_1) \cdot Y_1^m(\theta, \varphi),$$

$\hbar k$ being the momentum of the emitted particle. The free particle wave function R is not strictly orthogonal to the initial wave function, but this should not give rise to more serious errors than other approximations made in these calculations.

The dipole moment operator is

$$M = e(z_1+z_2),$$

where e is the electronic charge and z_1 and z_2 the z-components of $\mathbf{r}_1$ and $\mathbf{r}_2$. We assume the direction of polarization of the γ-ray to be the z-axis and further neglect the momentum of the γ-ray.

References

1) B. H. Flowers and F. Mandl, Proc. Roy. Soc. A **206** (1951) 131
2) J. C. Gunn and J. Irving, Phil. Mag. **42** (1951) 1353
3) E. G. Fuller, Phys. Rev. **96** (1954) 1306
4) J. S. Levinger and H. A. Bethe, Phys. Rev. **78** (1950) 115
5) S. A. E. Johansson and B. Forkman, (to be published)
6) J. E. Perry Jr. and S. J. Bame Jr., Phys. Rev. **99** (1955) 1368
7) H. A. Bethe and R. F. Bacher, Rev. Mod. Phys. **8** (1936) 126

Nuclear Physics **4** (1957) 240—247; © *North-Holland Publishing Co., Amsterdam*

Not to be reproduced by photoprint or microfilm without written permission from the publisher

INVESTIGATION OF CONVERSION LINES IN THE β-SPECTRUM OF Ir^{192}

V. M. KELMAN, R. YA. METSKHVARISHVILI, V. A. ROMANOV and V. V. TUCHKEVICH

Physical-Technical Institute, USSR Academy of Sciences, Leningrad

Received March 21, 1957

Abstract: A prism β-spectrometer with a resolving power of 0.04 % was employed to study the conversion electron spectrum of excited Pt^{192} and Os^{192} produced in the disintegration of Ir^{192}. The conversion coefficient ratios K/L and $L_I : L_{II} : L_{III}$ have been determined for transition energies 136.3, 201.3, 205.8, 295.9, 308.5, 316.5, 468.0 and 604.5 keV; for the most intense transitions the ratios K/M, $M_I : M_{II} : M_{III}$, K/N and K/O have also been determined. All investigated transitions were found to be of the E2 or E2+M1 type. The contribution of the M1 admixture has been determined.

The radioactive isotope Ir^{192} has been investigated by a number of authors [1, 2, 3]). It decays in two ways: by emission of electrons it transforms into Pt^{192} and by K-capture into Os^{192}. The γ-radiation from excited Pt^{192} and Os^{192} is due to E2 and E2+M1 transitions [3]). These isotopes are thus convenient for investigation of internal conversion associated with the indicated transitions. It would seem of interest to investigate the conversion electron spectra by using a high resolution β-spectrometer with the aim of separating conversion in the L-subshells and, where possible, in the M-subshells. For completeness it would also be desirable to determine the ratios of the total conversion coefficients in the K, L, M, N and O shells.

Such investigations have been performed on a prism β-spectrometer [4, 5]). The resolution of the instrument corresponded to a relative line half-width of 0.04 % (on a momentum scale); the transmission was 0.02 %. The source was a thin layer of natural iridium deposited by cathode evaporation on a strip of aluminium foil irradiated with neutrons. The thickness of the aluminium foil was 5μ. The following procedure was employed to determine the thickness of the iridium film. The aluminium strip 1 (fig. 1) on which the iridium was deposited was placed on a glass plate 2 and covered by a thin metallic plate 3 with a slit 4, which defined the source area and also with several circular holes 5 which left the glass uncovered near the slit. The iridium vapour simultaneously deposited on the aluminium foil and on the glass. The thickness of the iridium layer on the glass was measured by the interferometer method [6]). It was assumed to be the same as that of the iridium layer deposited on the aluminium. Even if this were not exactly the case, this procedure, nevertheless, would permit one to determine the

relative thicknesses of the iridium films and it thus significantly facilitates selection of a suitable source. In this way a set of samples was prepared

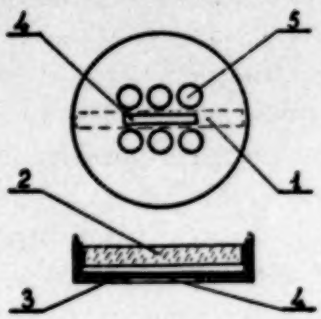

Fig. 1. (explanation in text).

from which a source with a 0.48 mg/cm² thick iridium film was selected; this source yielded sufficiently strong conversion lines with half-widths which did not significantly differ from that of the instrument. The area of the iridium film was 1.6×11 mm².

Measurement of the spectrum within the limits of a set of lines was performed by applying a voltage to the source. Since in this method monoenergetic electrons passed through the spectrometer it was not necessary to introduce a correction to account for the width of the energy interval within the limits of a single group. It should be necessary to apply such a correction when changing from one set of lines to another in which case it would be required to modify the magnetic system of the spectrometer. The formula for the correction is

$$n_{\mathrm{tr.}} = k \frac{n_{\mathrm{m}}}{\varepsilon\left(1+\dfrac{1}{1+\dfrac{\varepsilon}{m_0 c^2}}\right)},$$

where $n_{\mathrm{tr.}}$ is the number of electrons corresponding to the true line intensity and n_{m} is the measured counting rate, k is a coefficient which depends on the transmission of the instrument and ε is the electron energy. ε is usually expressed in keV and hence the rest mass should be expressed in the same units: $m_0 c^2 = 511$ keV.

The β-rays entered the counter chamber through a window covered by a mica sheet 0.87 mg/cm² thick. The electrons then traversed two aluminium foils which covered the two neighbouring counter windows, their total thickness being 1.1 mg/cm². A correction for absorption in the mica was applied in accord with the data presented in ref [7]). The correction for absorption in the aluminium foil was determined experimentally by comparing the counting rates in the first and second counters. For transition

energies above 300 keV these corrections did not appreciably alter the results even in the K/L measurements.

Conversion lines were measured which corresponded to transitions of 136.3, 295.9, 308.5, 316.5, 468.0 and 604.5 keV in Pt and 201.3 and 205.8 keV in Os. The transition energies cited above are taken from ref. [3]). Measurements of the distances between the L-sublevel lines enabled us to confirm the indicated transition assignments. Separate regions of the β-spectrum are depicted in figs. 2, 3, 4 and 5 (the counter background is subtracted). As can be seen, the resolution of the instrument is sufficient for complete separation of the L-subshell conversion lines even when the γ-quantum energy is 604.5 keV. The ratios of the M-subshell conversion

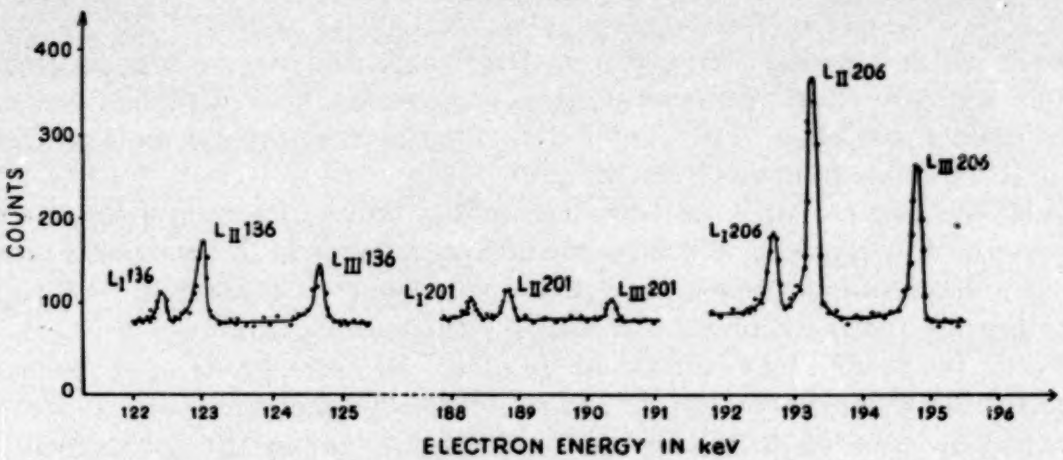

Fig. 2. Electron lines from 136.3, 201.3 and 205.8 keV γ-rays converted in L-subshells.

coefficients can be determined for the most intense transitions. In this case, since the M-subshell conversion lines could not be completely resolved, it was necessary to separate them graphically. Conversion lines from intense γ-rays in the N and O-shells are distinctly visible. In order to resolve the two coinciding lines due to conversion of 308.5 keV γ-quanta in the L_{II} subshell and conversion of 296 keV γ-quanta on the N-shell the ratio N/L_{II} for the 296 keV transition was assumed to equal the measured ratio N/L_{II} for the 316.5 keV transition. Knowing the area of the L_{II} peak for the 296 keV transition one can then determine the area corresponding to the N-conversion line for this transition and hence separate it from the L_{II} line associated with the 308.5 keV transition. Separation of the electrons due to conversion of 308.5 keV γ-quanta in the M_I subshell from electrons due to conversion of 316.5 keV γ-rays in the L_{III} subshell was performed graphically. To determine the ratios of the conversion coefficients each set of lines was measured 5 times and the mean values of the ratios of their areas and the probable errors were then determined. Results of measure-

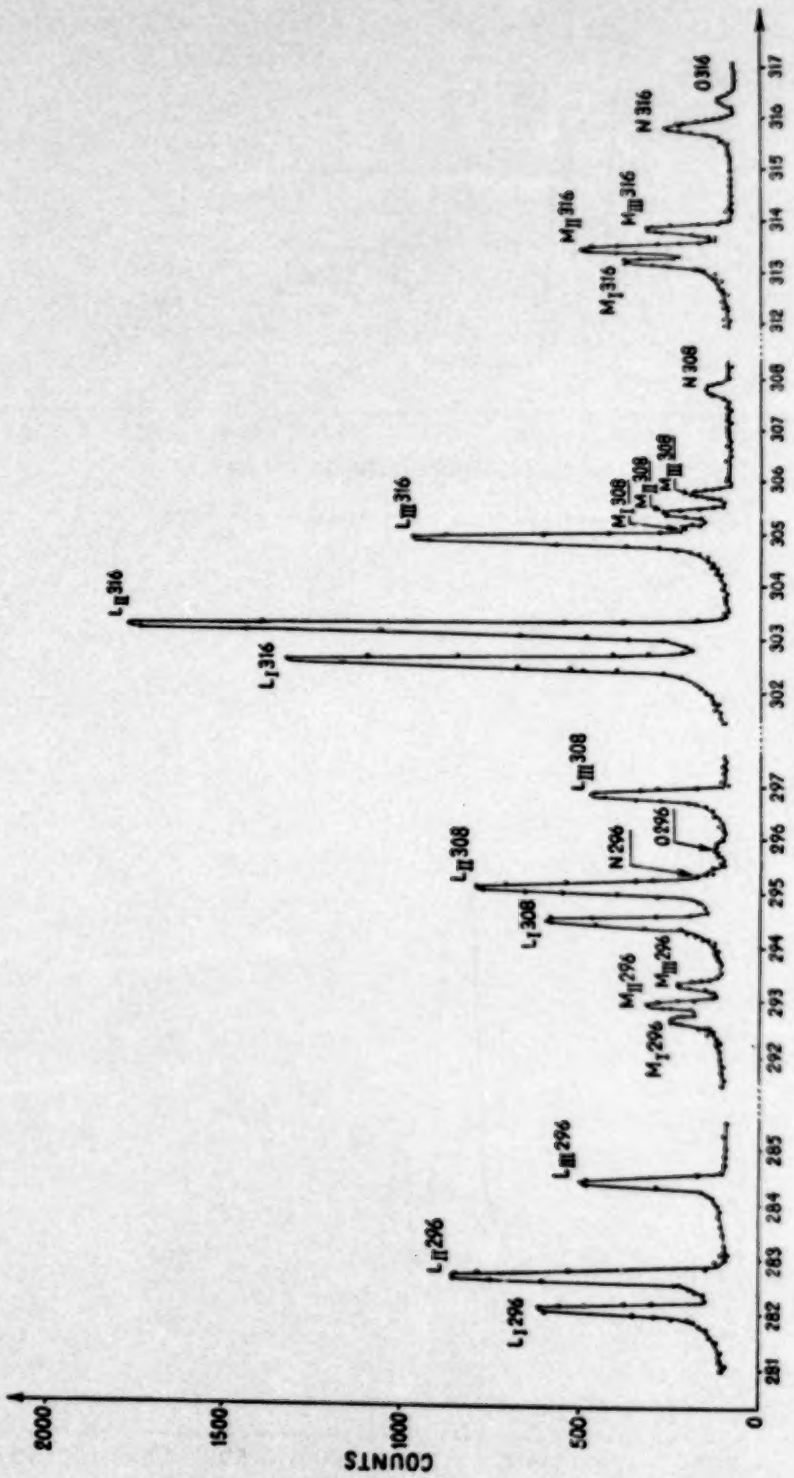

Fig. 3. Conversion lines from 295.9, 308.5 and 316.5 keV γ-rays.

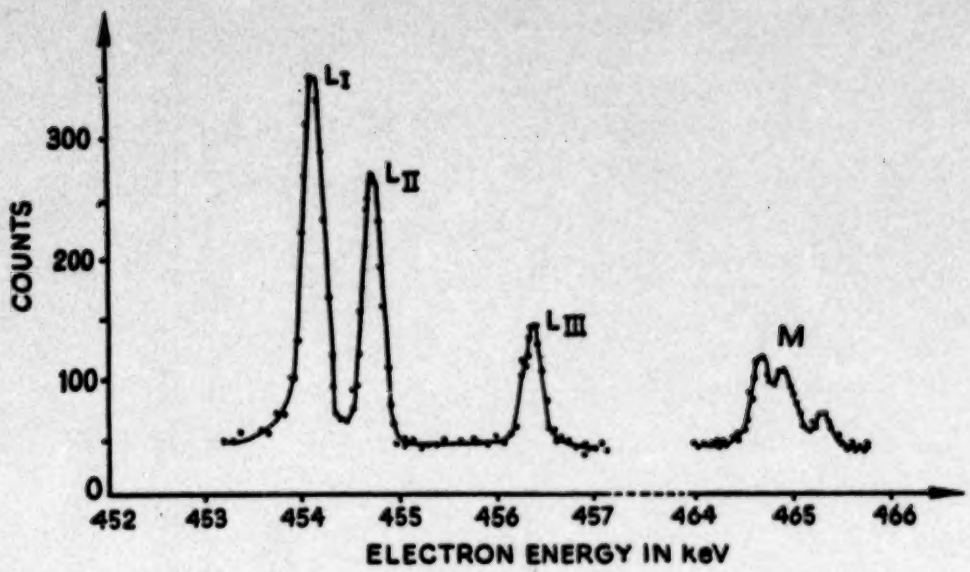

Fig. 4. Conversion lines from 468.0 keV γ-rays.

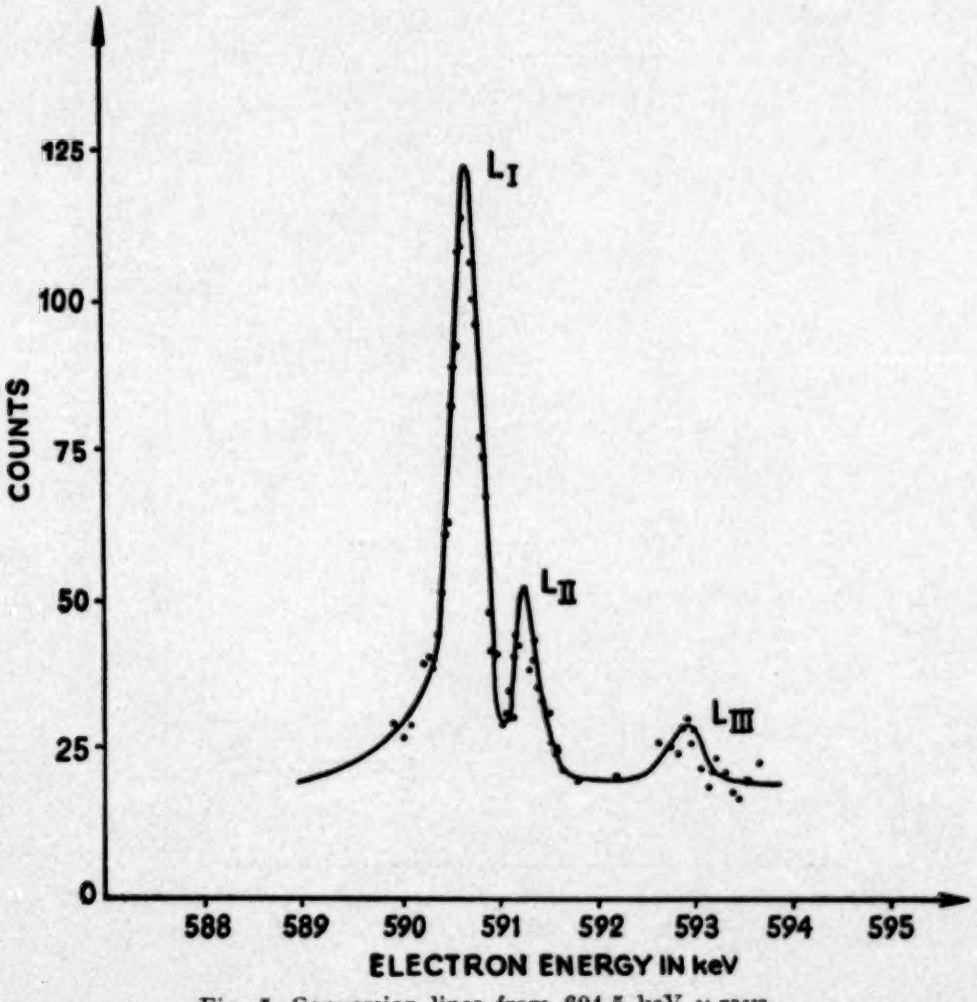

Fig. 5. Conversion lines from 604.5 keV γ-rays.

ments of the ratios K/L and $L_I : L_{II} : L_{III}$ after application of the relevant corrections are presented in table 1.

TABLE 1

Transition energy in keV	Experimental ratio of conversion coefficients		Theoretical conversion coefficient ratios for E2 transitions		Type of transition	Fraction of M1 admixture determined from		Type of transition according to data in ref. [3])
	K/L	$L_I : L_{II} : L_{III}$	K/L	$L_I : L_{II} : L_{III}$		L_{II}/L_I	L_{III}/L_I	
136.3	–	1:(2.1 ±0.1):(1.7 ±0.1)	0.62	1:6.7 :5.0	E2+M1	21 %	19 %	E2
201.3	1.85±0.04	1:(1.42±0.06):(0.89±0.07)	1.5	1:2.9 :1.7	E2+M1	16 %	13 %	E2+M1
205.8	1.83±0.04	1:(2.32±0.02):(1.41±0.02)	1.5	1:2.8 :1.7	E2	–	–	E2
295.9	2.35±0.04	1:(1.39±0.03):(0.74±0.02)	2.0	1:1.7 :0.8	E2	–	–	E2
308.5	2.38±0.02	1:(1.18±0.02):(0.67±0.01)	2.2	1:1.5 :0.7	E2+M1	5 %	1 %	E2
316.5	2.22±0.02	1:(1.38±0.01):(0.73±0.01)	2.3	1:1.5 :0.7	E2	–	–	E2
468.0	3.0 ±0.1	1:(0.68±0.01):(0.29±0.01)	3.1	1:0.77:0.30	E2	–	–	E2
604.5	4.7 ±0.1	1:(0.33±0.01):(0.13±0.01)	4.0	1:0.50:0.19	E2+M1	14 %	10 %	E2+(M1)

In order to determine the multipole order of the transitions the measured ratios of the L-subshell conversion coefficients and the K to L shell coefficients were compared with the respective theoretical ratios for different multipole orders. The theoretical ratios of the L-subshell conversion coefficients and values of the total L-shell conversion coefficients were derived from the tables of M. E. Rose [8]) and the theoretical K-shell conversion coefficients from the very detailed and exact tables of L. A. Sliv and I. M. Band [9]). In accord with ref. [3]) it was found that all of the investigated transitions were either E2 or E2+M1. The theoretical K/L and $L_I : L_{II} : L_{III}$ ratios for E2 transitions are also presented in table 1. For magnetic dipole transitions the theoretical ratio $L_I : L_{II} : L_{III}$ only weakly depends on the energy and for the considered transitions has practically a constant value of 1:0.088:0.006.

The percentage of magnetic dipole admixture p in mixed transitions is

$$p = \frac{\gamma_1}{\gamma_1+\gamma_2} \cdot 100 = \frac{\delta_{12}^2}{1+\delta_{12}^2} \cdot 100,$$

where γ_1 and γ_2 are respectively the magnetic dipole and electrical quadrupole transition intensities and $\delta_{12}^2 = \gamma_1/\gamma_2$ is the mixture ratio. The latter can be determined if the conversion coefficients in any two shells or subshells are known for the mixed transition under consideration and the conversion coefficients for pure transitions in the same shells are known [10]):

$$\delta_{12}^2 = \frac{\alpha_{2k}}{\alpha_{1k}} \frac{R_0-R_2}{R_1-R_0}, \quad \text{where} \quad R_i = \frac{\alpha_{ij}}{\alpha_{ik}}.$$

Here α_{ij} and α_{ik} are the absolute coefficients for i type γ-ray conversion

in j or k-shells or subshells. They have been determined from the tables of theoretical values mentioned above. $R_0 \equiv \alpha_{0j}/\alpha_{0i}$ is the experimental ratio of the conversion coefficients. To determine the mixture ratio we used the ratios L_{II}/L_I and L_{III}/L_I. The ratio K/L is less sensitive to the presence of a M1 admixture and was therefore not used to determine the admixture ratio. The admixture values thus found are given in the last two columns but one of table 1; the ratio L_{II}/L_I or L_{III}/L_I used to obtain the corresponding data is also indicated. It should be mentioned that due to the small number of theoretically computed L-subshell conversion coefficients (L_{II} has been evaluated for $Z = 25$, 55 and 85, L_{III} for $Z = 55$ and 85) it is not possible to carry out with sufficient precision the interpolation required to find the necessary values. The errors in the admixture fractions given in table 1 may be of the order of several per cent. In particular, an admixture value of 5 % does not necessarily signify the presence of a real admixture since it may be due to an error in interpolation. For this reason we have given in table 1 only those admixtures which exceed 5 %; otherwise the transition is assumed to be a pure one. The only exception is the 308.5 keV transition for which a M1 admixture can be deduced by comparing the ratio of the L-subshell conversion coefficients with the ratio for the neighbouring 296 and 316.5 keV transitions. Smaller admixture values can be established only by using more complete tables of the theoretical values. The presence of an M1 admixture in the 604.5 keV transition signifies that in the Pt^{192} level scheme proposed in ref. [3]) a spin of 3^+ should be assigned to the 920.9 keV level.

Results of determination of multipole order presented in ref. [3]), are given in the last column of table 1.

The ratios K/M, $M_I : M_{II} : M_{III}$, K/N and K/O for the most intense transitions are presented in table 2.

TABLE 2

Experimental conversion coefficient ratios				
Transition energy in keV	K/M	$M_I : M_{II} : M_{III}$	K/N	K/O
295.9	8.9±0.2	1:(1.59±0.05):(0.87±0.03)	–	(28±3)·10
308.5	9.5±0.2	1:(1.69±0.05):(0.87±0.04)	44±2	–
316.5	9.3±0.2	1:(1.90±0.07):(1.06±0.03)	38±1	255±7
468.0	10.2±0.2			

Not in a single case has conversion in the M_{IV} or M_V subshells been observed. The approximate equality of the ratios $M_I : M_{II} : M_{III}$ and $L_I : L_{II} : L_{III}$ is noteworthy. This fact has also been established for M1 transitions [11]).

Measurement of the energy intervals between the conversion peaks denoted by N and O in fig. 3 and the respective M_{III} peaks and comparison with X-ray data show that the N peaks correspond to conversion in the N_I, N_{II} and N_{III} subshells. No conversion electrons from the N_{IV} or N_V subshells located between the N and O peaks were observed in the present work. Electrons from the N_{VI} and N_{VII} subshells merge with those from the O shell and form common peaks denoted as O in the fig.

Assuming, as we have done in the case of M shell conversion, that conversion in the N shell primarily proceeds in the first three subshells it may be considered that O peaks are mainly due to O shell electrons. The conversion coefficient ratios K/N and K/O given in table 2 were derived on the aforementioned assumption.

References

1) J. M. Cork, J. M. LeBlanc, A. E. Stoddard, W. J. Child, C. E. Branjan and D. W. Martin, Phys. Rev. **82** (1951) 258
2) A. A. Bashilov, N. M. Antonyeva and B. S. Dzhelepov, Izv. Akad. Nauk SSSR, Ser. Fyz. **16** (1952) 264
3) L. L. Baggerly, P. Marmier, F. Boehm and J. W. M. DuMond, Phys. Rev. **100** (1955) 1364
4) V. M. Kelman, D. L. Kaminsky and V. A. Romanov, Izv. Akad. Nauk SSSR, Ser. Fyz. **18** (1954) 209
5) V. M. Kelman, V. A. Romanov, R. Ya. Metskhvarishvili and V. A. Kolyunov, Nuclear Physics **2** (1956) 395
6) S. Tolansky, Multiple-Beam Interferometry (Oxford, 1948) p. 147
7) L. H. Martin and A. A. Towsend, Proc. Roy. Soc. A **170** (1939) 190
8) K. Siegbahn, Beta and Gamma Ray Spectroscopy (Amsterdam, 1955) p. 905
9) L. A. Sliv and I. M. Band, Tables of Gamma Ray Internal Conversion Coefficients (Moscow-Leningrad 1956)
10) E. L. Church and J. E. Monahan, Phys. Rev. **98** (1955) 718
11) V. M. Kelman, V. A. Romanov and R. Ya. Metskhvarishvili, Doklady **103** (1955) 577

Nuclear Physics **4** (1957) 248—256; © *North-Holland Publishing Co., Amsterdam*

Not to be reproduced by photoprint or microfilm without written permission from the publisher

NOTE ON THE (γ, d) REACTIONS

J. SAWICKI

Institute of Theoretical Physics, University of Warsaw, Warsaw

W. CZYŻ

Institute of Nuclear Research, Polish Academy of Sciences Dept. of Cracow, Cracow

Received 8 April 1957

Abstract: The large observed ratios of (γ, d) to (γ, p) cross-sections are explained in terms of a two — stage mechanism of the (γ, d) process from the point of view of the nuclear shell model. The incident photon is assumed to be absorbed by a single nucleon which in its turn picks up another nucleon within the nucleus with the right momentum to form an outgoing deuteron. The method of calculation of $\sigma(\gamma, d)/\sigma(\gamma, p)$ in a general case is presented. The example of the $^{32}S(\gamma, d)\,^{30}P$ reaction is discussed. The importance of investigating (γ, d) angular distributions is indicated.

1. Introduction

The investigations of (γ, n), (γ, p) and (γ, d) reactions within the last few years established the failure of the statistical theory explanation of these reactions (see e.g. ref. [1–13])). The main bulk of the evidence are the angular distributions of (γ, n) and (γ, p) reactions and the ratios of (γ, d) to (γ, p) or (γ, n) reaction yields. The particularly drastic departure from the statistical model are the magnitudes of the (γ, d) yields being about thousand times larger than those predicted from the model. It is the subject of this paper to present some remarks on this problem.

Similarly as Byerly and Stephens [2]) and Toms and Stephens [9]) the photodeuterons are assumed in the present treatment to be formed in pick-up process within the nucleus. I.e. the two — stage mechanism of the reaction is supposed to be valid: the incident photon is absorbed by a single nucleon which, subsequently, on its way out picks up a second nucleon with the right momentum to form a deuteron which emerges from the nucleus. It is easy to present several arguments showing why the probability of pickup process for a sufficiently energetic nucleon *within a nucleus* is sufficiently large to explain the observed $\sigma(\gamma, d)/\sigma(\gamma, p)$ ratios.

It is possible to estimate this probability by assuming that the cross-section for a pickup process σ_p can be written as $\sigma_p = \sigma_g \not{p}$, σ_g being the geometrical cross - section for hitting the nucleus by the incident nucleon, $\not{p}$ the probability of pickup. On substituting the observed cross-sections for σ_p and the geometrical cross-section for σ_g one obtains $\not{p}$ of the order 0.1. In our simple picture $\not{p} = \sigma(\gamma, d)/\sigma(\gamma, p)$. The observed ratios $\sigma(\gamma, d)/\sigma(\gamma, p)$ are in fact of the same order of magnitude.

We wish now to present another estimation of p. An oversimplified one-dimensional pickup process as indicated in fig. 1 can also give the feeling of the order of magnitude of $\sigma(\gamma, d)/\sigma(\gamma, p)$. A plane shield with a thickness of the order of nuclear dimensions and containing bound nucleons is irradiated

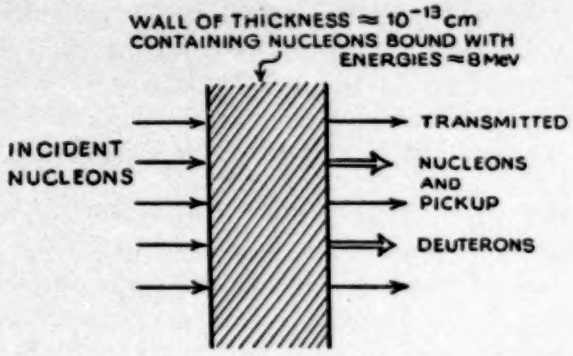

Fig. 1

by a proton beam of sufficiently high energy. On the back side of the wall appear outgoing deuterons and transmitted protons. The ratio of the intensity of the outgoing deuteron beam to the intensity of the proton beam equals p. In this one-dimensional picture every incident proton has to hit the target and hence the σ_g factor is eliminated. On using the standard Born approximation one obtains

$$p = \frac{v_d}{v_p}\left|\frac{2\alpha\sqrt{2\alpha}}{iK}\int_{-\infty}^{+\infty} dx \exp\left[-i(K-k)x\right]\psi(x)\right|^2$$

where $-\alpha^2\hbar^2/M$ is the binding energy of the deuteron ($= -2.23$ MeV), K and v_d are the wave number and the velocity of the deuteron, k and v_p-the wave number and the velocity of the incident proton, $\psi(x)$ is the wave function of bound neutrons. For the sake of the further estimates we assume $\psi(x) = \sqrt{q}\sqrt[4]{2\pi}\exp(-\frac{1}{2}q^2x^2)$ where $q = 1.18\times10^{13}$ cm^{-1} ($\psi(x)$ is practically zero beyond the region larger than 2×10^{-13} cm). The integration gives $p = (4\alpha^3\sqrt{2\pi}/kKq)\exp[-(k-K/q)^2]$. On assuming the binding energy of neutrons in the target equal 8 MeV we get for $\hbar^2k^2/2M = 10$ MeV, 15 MeV, 20 MeV respectively $p = 0{,}24$, 0.13, 0.09. One may therefore suspect that considerable values of p are largely independent of the mechanism of the absorption of the photon.

A number of recent papers indicate that the Independent Particle Model (I.P.M.) of the nucleus gives satisfactory explanation of photonuclear reactions (see e.g. ref. [14–17])). Also the survey of the observed $\sigma(\gamma, d)/\sigma(\gamma, p)$ ratios (see e.g. ref. [11])) for various elements at intermediate energies exhibits considerable fluctuations which seem to indicate that the emission of photo-

deuterons is sensitive to the details of the nuclear shell structure rather than to the general type of the momentum distribution of nucleons in the nucleus. †

Unfortunately, the existing data give very scarce information concerning angular distributions of photodeuterons which seem to be able to give much information regarding the mechanism of the (γ, d) reaction. These facts encourage to consider $\sigma(\gamma, \mathrm{d})/\sigma(\gamma, \mathrm{p})$ in a simplified case which would, however, present a picture of the reaction based on I.P.M.

2. Theory of the Two-Stage Mechanism

We shall calculate $\sigma(\gamma, \mathrm{d})/\sigma(\gamma, \mathrm{p})$ for a simplified system of two bound nucleons: the neutron and the proton (we shall first neglect the spins of the nucleons) are bound via the potentials $V_{\mathrm{n}}(\mathbf{r}_{\mathrm{n}})$ and $V_{\mathrm{p}}(\mathbf{r}_{\mathrm{p}})$ their mutual interaction being $V_{\mathrm{np}}(\mathbf{r}_{\mathrm{n}}-\mathbf{r}_{\mathrm{p}})$ and the interaction with the electromagnetic field is $H_{\mathrm{e.m.}}$. The total hamiltonian of the system $H = H_{\mathrm{n}}+H_{\mathrm{p}}+V_{\mathrm{np}}+H_{\mathrm{e.m.}}$ where $H_{\mathrm{n(p)}} = -(\hbar^2/2M)\Delta_{\mathrm{n(p)}}+V_{\mathrm{n(p)}}$, M being the nucleon mass. Let us assume (it is not essential here) that $H_{\mathrm{e.m.}}$ interacts with only one nucleon proton, say). If there were no V_{np} the motions of both the nucleons would be independent. We might then write the wave function of the system in the form

$$\psi_0(\mathbf{r}_{\mathrm{n}}, \mathbf{r}_{\mathrm{p}}, t) = f(\mathbf{r}_{\mathrm{n}}) \exp\left(-\frac{i}{\hbar}\varepsilon_{\mathrm{n}} t\right)\left[u(\mathbf{r}_{\mathrm{p}}) \exp\left(-\frac{i}{\hbar}\varepsilon_{\mathrm{p}} t\right)\right.$$

$$\left. + w(\mathbf{r}_{\mathrm{p}}) \exp\left[-\frac{i}{\hbar}(\varepsilon_{\mathrm{p}}+\hbar\omega)t\right] + v(\mathbf{r}_{\mathrm{p}}) \exp\left[-\frac{i}{\hbar}(\varepsilon_{\mathrm{p}}-\hbar\omega)t\right]\right], \qquad (1)$$

$\varepsilon_{\mathrm{p(n)}}$ being the binding energies of the proton (neutron), $\hbar\omega$ the photon energy, $f(\mathbf{r}_{\mathrm{n}})$-the wave function of the bound neutron and the bracket term represents the wave function of the photoproton obtained in analogy to Sommerfeld and Schur [21]). From the three functions u, w, v only w has a wave zone and contributes in our case; $u(\mathbf{r}_{\mathrm{p}})$ represents the wave function of the bound proton. The function w satisfies the differential equation (see ref. [21]))

$$\Delta w + (k_{\mathrm{f}}^2 - U)w = \Lambda u \qquad (2)$$

where

$$k_{\mathrm{f}}^2 = \frac{2M}{\hbar^2}(\varepsilon_{\mathrm{p}}+\hbar w),\ U = \frac{2M}{\hbar^2}V_{\mathrm{p}},\ \Lambda = \frac{2M}{\hbar^2}E_0 e' \sqrt{\frac{\pi}{3}} r Y_{1,0}(\theta, \phi),$$

provided the incident photon wave is polarized along the z-axis and only

† On the other hand the correlations in the nuclear ground state wave function (in the spirit of e.g. Chew and Goldberger [18]), Brueckner, Eden, Francis [19]), Levinger [20]) and many others) i.e. the high energy components in the momentum distributions of the nucleons in the nucleus may be important at high energies.

electric dipole transitions are taken into consideration†; E_0 denotes the amplitude of the electric field, e' is the effective charge of nucleon.

Let us consider now the wave equation of the system $i\hbar\,\partial\psi/\partial t = H\psi$. We seek the solution in the form $\Psi = \Psi_0 + \Psi_1$. After simple transformations we obtain for Ψ_1 the equation

$$\left(H - i\hbar\frac{\partial}{\partial t}\right)\Psi_1 = -V_{np}\,fu\exp\left(-\frac{i}{\hbar}\varepsilon_0 t\right) - V_{np}\,fw\exp\left(-\frac{i}{\hbar}Et\right) - V_{np}\,fv\exp\left(-\frac{i}{\hbar}\varepsilon_1 t\right) \tag{3}$$

where

$$\varepsilon_0 = \varepsilon_p + \varepsilon_n < 0,\ \varepsilon_1 = \varepsilon_p + \varepsilon_n - \hbar\omega < 0,\ E = \varepsilon_p + \varepsilon_n + \hbar\omega > 0.$$

We search Ψ_1 in the form

$$\Psi_1 = \zeta\exp\left(-\frac{i}{\hbar}\varepsilon_0 t\right) + \xi\exp\left(-\frac{i}{\hbar}\varepsilon_1 t\right) + \chi\exp\left(-\frac{i}{\hbar}Et\right).$$

We obtain

$$(H-\varepsilon_0)\zeta = -V_{np}\,fu,\ (H-\varepsilon_1)\xi = -V_{np}\,fv$$

and

$$(H-E)\chi = -V_{np}\,fw. \tag{4}$$

Only the last equation has a wave zone and can represent the emission of photodeuterons. After changing the variables, viz. $\frac{1}{2}(\mathbf{r}_n+\mathbf{r}_p) = \mathbf{R}$, $\mathbf{r}_n - \mathbf{r}_p = \boldsymbol{\rho}$ and neglecting $H_{e.m.}$ as compared with other terms, eq. (4) takes on the form

$$(H_d + T_R - E)\chi(\mathbf{R}, \boldsymbol{\rho}) = -(V_n + V_p)\chi(\mathbf{R}, \boldsymbol{\rho}) - V_{np}\,fw \tag{5}$$

where H_d is the hamiltonian of the n−p system and T_R the kinetic energy operator of the centre of mass of the deuteron. Let us expend χ in terms of n−p system eigenfunctions:

$$\chi(\mathbf{R}, \boldsymbol{\rho}) = D(\mathbf{R})\eta(\boldsymbol{\rho}) + \text{orthogonal terms}, \tag{6}$$

$\eta(\boldsymbol{\rho})$ being the deuteron ground state wave function. On substituting (6) into (5) we have for $D(\mathbf{R})$

$$(\Delta + K^2)D(\mathbf{R}) = \frac{4M}{\hbar^2}\int \mathrm{d}^3\boldsymbol{\rho}\,\eta^*(\boldsymbol{\rho})[V_n(\mathbf{R}+\tfrac{1}{2}\boldsymbol{\rho}) + V_p(\mathbf{R}-\tfrac{1}{2}\boldsymbol{\rho})]\chi(\mathbf{R},\boldsymbol{\rho}) + \frac{4M}{\hbar^2}\int \mathrm{d}^3\boldsymbol{\rho}\,\eta^*(\boldsymbol{\rho})\,V_{np}(\boldsymbol{\rho})f(\mathbf{R}+\tfrac{1}{2}\boldsymbol{\rho})w(\mathbf{R}-\tfrac{1}{2}\boldsymbol{\rho}) \tag{7}$$

where $K^2 = (4M/\hbar^2)(E-\varepsilon_d)$ (ε_d = the binding energy of the deuteron). As $D(\mathbf{R})$ is the wave function of the outgoing deuteron, the crudest ap-

† These transitions are strongly dominant for nuclei according to recent papers (see e.g. ref. [18]).

proximation for it is to set $\chi(\mathbf{R}, \boldsymbol{\rho}) = 0$ on the right hand side of eq. (7) and assume the zero -range n-p interaction i.e.

$$\eta(\boldsymbol{\rho})V_{\mathrm{np}}(\boldsymbol{\rho}) = -\frac{4\pi\hbar^2}{M}\sqrt{\frac{\alpha}{2\pi}}\delta(\boldsymbol{\rho}).$$

Then

$$(\Delta+K^2)D^{(0)}(\mathbf{R}) = -16\pi\sqrt{\frac{\alpha}{2\pi}}f(\mathbf{R})w(\mathbf{R}). \tag{8}$$

Eq. (8) determines the Born approximation reaction amplitude. Since the pickup process occurs inside the nucleus where both V_{n} and V_{p} are most important, the approximation of eq. (8) is a very poor approximation only. On expanding $V_{\mathrm{n}}+V_{\mathrm{p}}$ in powers of $\boldsymbol{\rho}$ one can show, assuming $\chi(\mathbf{R}, \boldsymbol{\rho}) \approx D(\mathbf{R})\eta(\boldsymbol{\rho})$, that the first essential correction to the effective interaction $(V_{\mathrm{n}}+V_{\mathrm{p}})_{\varrho=0} = V_{\mathrm{eff}}(\mathbf{R})$ being proportional to ϱ^2 is small. One is led, therefore, to the "distorted" wave" approximation for eq. (7):

$$\left(\Delta+K^2-\frac{4M}{\hbar^2}V_{\mathrm{eff}}\right)D(\mathbf{R}) = -16\pi\sqrt{\frac{\alpha}{2\pi}}f(\mathbf{R})w(\mathbf{R}). \tag{9}$$

Eq. (9) neglects, of course, the effects of the deuteron dissociation in the process within the nucleus.

One can easily obtain the angular distributions of the photodeuterons from eq. (9) if one knows the angular dependence of $w(\mathbf{R})$ and assumes specific bound states wave functions f and u. For the sake of illustration let us assume f and u to represent S-states. Let us expand $w(\mathbf{R})$ of eq. (2) in spherical harmonics:

$$w(\mathbf{R}) = \sum_{l,m} w_l(R)Y_{l,m}(\theta, \phi).$$

Substitution into eq. (2) and comparison of the coefficients of the spherical harmonics gives a series of differential equations for $w_l(R)$. Only the equation for w_1 is inhomogeneous since the expansion of the right hand side contains one spherical harmonic $Y_{1,0}$ only. Only this equation has, therefore, the solution satisfying the proper required boundary conditions: to be regular at $R = 0$ and to produce a spherical divergent wave in infinity. All the remaining w_l satisfying homogeneous equations are to be set equal to zero, since they cannot satisfy the boundary conditions. The angular dependence of $w(\mathbf{R})$ is therefore $Y_{1,0}(\theta, \phi)$. The angular dependence of $D(\mathbf{R})$ can be determined similarly from eq. (9) after expanding $D(\mathbf{R})$ in spherical harmonics. Since f is in our simple example a spherically symmetric S-state, $D(\mathbf{R})$ has the angular dependence $Y_{1,0}(\theta, \phi)$ also. Thus if the "photo-pickup" process is of the type (S, S) i.e. both the photoeffect and pickup come from S-states, then (γ, p) and (γ, d) processes have the same

angular distributions. It follows that the ratio $\sigma(\gamma, \mathrm{d})/\sigma(\gamma, \mathrm{p})$ is isotropic. The matter gets complicated when the (γ, d) process if of the type (S, D), (P, S), (D, S) etc. We can then expand the right hand side of eq. (2) in spherical harmonics, making use of the formula

$$Y_{l,m}Y_{1,0} = \sum_L \left[\frac{(2l+1)3}{4\pi(2L+1)}\right]^{\frac{1}{2}} C_{l1}(L,\ 0;\ 0,\ 0)C_{l1}(L,\ m;\ m,\ 0)\,Y_{L,m}, \qquad (10)$$

where C_{ll} are the usual Clebsh-Gordon coefficients. We can now solve the inhomogeneous equations for w_l and find $w(\mathbf{R})$. $D(\mathbf{R})$ can be then found by eq. (10), but the ratio $\sigma(\gamma, \mathrm{d})/\sigma(\gamma, \mathrm{p})$ will, in general, no longer be isotropic.

Let us now pass over to the construction of the photonucleon wave function $w(\mathbf{R}) = \sum_{l,m} w_l(\mathrm{R})Y_{l,m}$. From eq. (2) it is seen that w_l satisfies the equation

$$\frac{1}{R^2}\frac{\mathrm{d}}{\mathrm{d}R}\left(R^2\frac{\mathrm{d}w_l}{\mathrm{d}R}\right) + \left(k_l^2 - U - \frac{l(l+1)}{R^2}\right)w_l(R) = (\Lambda u)_l. \qquad (11)$$

The solution can be written in the form

$$w_l(R) = \int_0^\infty G_l(R/R')(\Lambda u)_l R'^2\,\mathrm{d}R', \qquad (12)$$

the Green's function being

$$G_l(R/R') = k_l\,\mathrm{e}^{-i\eta_l}\begin{cases} F_l(k_l R')I_l^{(+)}(k_l R) & \text{for } R' < R \\ F_l(k_l R)I_l^{(+)}(k_l R') & \text{for } R' > R, \end{cases} \qquad (13)$$

where F_l and $I_l^{(+)}$ are, respectively, the properly normalized regular and irregular (outgoing) solutions of the homogeneous equation (see e.g. ref. [22]) for neutrons). If the Coulomb potential (for protons) is included in U, we have to replace the respective expressions occurring in eqs. (29)—(34) of ref. [22]) by their Coulomb analogous, viz.

$$j_l(x) \text{ by } \mathrm{e}^{i\sigma_l(n)}F_l^c(n, x)/x$$
$$n_l(x) \text{ by } \mathrm{e}^{i\sigma_l(n)}G_l^c(n, x)/x$$

where $\sigma_l(n) = \arg\Gamma(l+1+in)$, n being the Gamow parameter of the proton. The phase-shift η_l being δ_l for neutrons is $\delta_l^c + \sigma_l(n)$ for protons. In view of eq. (13), eq. (12) can be rewritten in the form

$$w_l(R) = k_l\,\mathrm{e}^{-i\eta_l}\{I_l^{(+)}(k_l R)\int_0^R F_l(k_l R')(\Lambda u)_l R'^2\,\mathrm{d}R' + F_l(k_l R)\int_R^\infty I_l^{(+)}(k_l R')(\Lambda u)_l R'^2\,\mathrm{d}R'\}. \qquad (14)$$

Eq. (14) represents the photonucleon wave over all space (including the interior of the nucleus).

The same procedure can be applied to the photodeuteron wave function $D_l(R)$. The asymptotic form of $D_l(R)$ following from eq. (9) is

$$D_l(R) \sim -16\pi\sqrt{\frac{\alpha}{2\pi}}R^{-1}\exp\left[i(KR-n_d\ln 2KR+\eta_l^d+\sigma_l(n_d))\right] \times \int_0^\infty \mathscr{F}_l(KR)[f(\mathbf{R})w(\mathbf{R})]_l R^2\,dR, \qquad (15)$$

$\mathscr{F}_l(KR)$ being the properly normalized regular solution of the homogeneous equation

$$\left[\frac{1}{R^2}\frac{d}{dR}R^2\frac{d}{dR}+K^2+\frac{4M}{\hbar^2}V_{eff}-\frac{l(l+1)}{R^2}\right]\mathscr{F}_l(KR)=0. \qquad (16)$$

3. The Example of the ^{32}S (γ, d) ^{30}P Reaction

The theory presented above can be applied, for instance, to the $^{32}S(\gamma, d)$ ^{30}P reaction. According to the nuclear shell model the most loosely bound nucleons are the four 2s-shell nucleons (2 protons+2 neutrons). One may assume, therefore, that near the threshold of the reaction (19.15 MeV, see ref. [3]) deuterons are produced mainly by the (S, S) process and hence, after averaging over the directions of the photon polarization, the photodeuterons will have an angular distribution of the form $\sin^2\theta$, θ being the angle between the direction of the incident γ-rays and the direction of the outgoing deuterons in the c.m. system. One can calculate the ratio $\sigma(\gamma, d)/\sigma(\gamma, p)$ the (γ, p) process being assumed to come mainly from S-states†:

$$\frac{\sigma(\gamma, d)}{\sigma(\gamma, p)} = \left(16\pi\sqrt{\frac{\alpha}{2\pi}}\right)^2 \tfrac{1}{2}Kk_f\left|\int_0^\infty \mathscr{F}_1(KR)[f(\mathbf{R})w(\mathbf{R})]_1 R^2\,dR\right|^2 \times \left|\int_0^\infty \mathscr{F}_1(k_f R)(Au)_1 R^2\,dR\right|^{-2}. \qquad (17)$$

Taking into account of the particle spins introduces in the case of eq. (17) simply the factor 3/4. Since we have the same number of neutrons and protons in the 2S-shell the taking into account of their average effective charges does not affect eq. (17) (assuming that either a proton or a neutron can be the initial photonucleon). One has also to improve eq. (17) by taking into account the finiteness of the mass of the nucleus. This gives a constant factor < 1.

The computation in the crudest case of Born approximation was improved by taking into account the effects of the Coulomb and nuclear interactions (of V_{eff} and V_p) by the barrier penetrabilities calculated on

† Eq. (17) does not represent the experimental $\sigma(\gamma, d)/\sigma(\gamma, p)$ since it takes into account only the photoprotons from the S-shell while the incident photon energy, being > 19.15 MeV, is sufficient to produce photoprotons form lower lying shells.

the method given by Dedrick (see ref. [23])). For $\hbar\omega = 25$ MeV the ratio of the penetrability factors is 0.53. The final result in the (S, S) case is $\sigma(\gamma, d)/\sigma(\gamma, p) = 0.9$. If one improved $\sigma(\gamma, p)$ by the consideration of other proton shells this ratio might be reduced. In any case it is seen, however, that the number obtained may be viewed only as one more very crude estimation indicating large values for the ratio $\sigma(\gamma, d)/\sigma(\gamma, p)$ †. For the energy $\hbar\omega = 25$ MeV the (S, D) and (D, S) processes are already possible. They modify the angular distribution of photodeuterons from the $\sin^2\theta$ type to the type $a+b\sin^2\theta$. The constants a and b can be calculated by the methods outlined in the preceding sections.

4. Conclusions

The estimations obtained indicate that the pickup mechanism can, in fact, explain the large observed $\sigma(\gamma, d)/\sigma(\gamma, p)$ values. The best way of checking this conclusion seems to be the measurement of angular distributions of photodeuterons, e.g. for the $^{32}S(\gamma, d)^{30}P$ reaction. Near the threshold of this reaction the pickup mechanism should produce the angular distribution $\sin^2\theta$ according to the nuclear shell model. The outlined method of calculation may be applied, in principle, to nuclei of more complicated shell structure. It seems that in such nuclei the correlation effects between nucleons due to the antisymmetrization of the wave function of particular shells are important. This should introduce the fractional parentage overlaps (see e.g. ref. [17])). The fluctuations of the observed ratios $\sigma(\gamma, d)/\sigma(\gamma, p)$ (see ref. [11])) might be explained with the help of coefficients of fractional parentage. The I.P.M. is probably not suitable at high energies to describe (γ,d) reactions (the two-body correlations are then important, see e.g. ref. [18,19])) On the other hand, it seems that at intermediate energies these correlations are of no great importance. Apparently considerable values of the cross-sections for (γ, np) reactions (of the same order of magnitude as those for (γ, d) reactions: e.g. in ref. [3]) for $\hbar\omega = 28$ MeV on ^{32}S $\sigma(\gamma, d)$ is equal to 2.8 mb while $\sigma(\gamma, np) = 6$ mb) might indicate the importance of these correlations. On the other hand, however, it is possible to explain this fact from the point of view of I.P.M.. From this point of view the (γ, np) process would be due to the knock-out mechanism of the secondary nucleon by the photonucleon. The relative probabilities of these two processes (pickup and knockout) are of the same order of magnitude. It would be, therefore, interesting to measure the n-p coincidences with discrimination of energy. Such measurements might cast light on the mechanism of (γ, np) reaction

† $\sigma(\gamma, p)$ in the (S, S) case was also calculated taking into account U (with no Coulomb effect) in the final state and found very sensitive to the choice of U. One can obtain a reasonable $\sigma(\gamma, d)/\sigma(\gamma, p)$ ratio by properly adjusting U.

i.e. might discern whether n-p pairs are produced via photodisintegration of "quasideuterons" within the nucleus or due to the knock-out mechanism.

Our sincere thanks are due to Dr. J. Dąbrowski, by whom our attention has been called to the importance of the problem of large $\sigma(\gamma, d)/\sigma(\gamma, p)$ values. We would like to thank Professors O. A. Hanson and L. Katz for a helpful correspondence on the problem and Professor W. C. Parkinson for kindly sending us a microfilm of Dedrick's unpublished thesis.

REFERENCES

1) F. Heinrich, H. Wäffler and M. Walter, Helv. Phys. Acta **29** (1956) 3
2) P. R. Byerly and W. E. Stephens, Phys. Rev. **81** (1951) 473; **83** (1951) 54
3) L. Katz and A. S. Penfold, Phys. Rev. **81** (1951) 815; **83** (1951) 169
4) W. H. Smith and L. J. Laslett, Phys. Rev. **86** (1952) 523
5) L. S. Ring, Phys. Rev. **99** (1955) 137
6) J. F. De Wire, A. Silverman and B. Wolfe, Phys. Rev. **92** (1953) 519
7) D. A. Edwards, B. Wolfe, A. Silverman and F. W. De Wire, Phys. Rev. **95** (1954) 629
8) M. E. Toms and W. E. Stephens, Phys. Rev. **92** (1953) 362
9) M. E. Toms and W. E. Stephens, Phys. Rev. **95** (1954) 1209
10) F. Ferrere, L. Gonella, R. Malvano, C. Tribuno and A. O. Hanson, Nuovo Cimento **5** (1957) 242
11) B. Forkman, Arkiv f. Fysik **11** (1956) 265
12) A. G. W. Cameron, Phys. Rev. **86** (1952) 435
13) A. K. Mann *et al.*, Phys. Rev. **87** (1952) 146
14) A. M. Lane and L. A. Radicati, Proc. Phys. Soc. A **67** (1954) 167
15) D. H. Wilkinson, Phil. Mag. **1** (1956) 127
16) D. H. Wilkinson, Proc. Int. Conf. Nucl. Reactions, Amsterdam (July 2—7, 1956) p. 1039
17) A. M. Lane and D. H. Wilkinson, Phys. Rev. **97** (1955) 1199
18) G. Chew and M. L. Goldberger, Phys. Rev. **77** (1950) 470
19) K. A. Brueckner *et al.*, Phys. Rev. **98** (1955) 1445
20) J. S. Levinger, Phys. Rev. **84** (1951) 43
21) A. Sommerfeld and G. Schur, Ann. der Physik **4** (1930) 409
22) J. R. Lamarsh and H. Feshbach, Phys. Rev. **104** (1956) 1632
23) K. G. Dedrick, Phys. Rev. **100** (1955) 58; Thesis, University Microfilms, 313 N 1st St., Ann Arbor, Michigan, Cat. No. 11171 (unpublished)

Nuclear Physics **4** (1957) 257—270; © *North-Holland Publishing Co., Amsterdam*
Not to be reproduced by photoprint or microfilm without written permission from the publisher

THE ENERGY LOSS OF FAST CHARGED PARTICLES PART III

D. A. TIDMAN
The F. B. S. Falkiner Nuclear Research Laboratory,† *School of Physics, The University of Sydney*

Received 1 March 1957

Abstract: Formulae for a quantum treatment of the energy loss of a fast charged particle and the density effect have previously been obtained. The present paper investigates these numerically, comparing their predictions with experiment for the case of oxygen. Good agreement is obtained.

1. Introduction

We discussed in a previous paper [1]) the use of a canonical transformation of the radiation field in a medium to calculate quantally the energy loss of a charged particle in the region where polarisation of the medium is important. The transformed oscillators of the radiation field were called 'physical photons'. The present paper has two purposes. The first is a numerical investigation of the quantal formulae aimed at showing that the usual classical treatment of the density effect is sufficiently accurate for most purposes. Sternheimer [2]) has evaluated these classical formulae using simplified equivalent oscillator models for the atoms. The second is to consider in detail the particular case of the formation of a cloud chamber track in oxygen. The energy loss involved in the production of such a track is separated into its components, with the hope that this treatment will be useful in understanding other cases, particularly when the existing less detailed calculations are not adequate.

The energy loss of fast charged particle depends on two distinct effects of the medium. The first is the scattering property of the medium for radiation. Here the propagation properties of the radiation field of the particle are modified without change of state of the medium. This is described by the quantum refractive index [1, 3]), and in some circumstances leads to the emission of Čerenkov radiation by the particle. The second effect is due to the ability of the medium to change its state, for example by absorbing a quantum of the radiation field. Here, line breadths for absorption and other processes determined by the structure of the medium are important for calculating the collision excitation or ionization probability of an individual atom.

† Also supported by the Nuclear Research Foundation within the University of Sydney.

2. Ionization

We distinguish between primary ionization and the secondary ionization caused by the reabsorption in the medium of Čerenkov photons and photons from the decay of excited atoms. In this section we consider only primary ionization, leaving secondary ionization till later.

The general expression for the distant collision energy loss to ionization was shown to be

$$\left(\frac{\mathrm{d}E}{\mathrm{d}x}\right)_{\mathrm{d}}^{\mathrm{ion}} = \frac{4\pi Z^2 e^4 N}{\beta^2 mc^2} \sum_e n_e \int_{\tilde{\nu}_e}^{\frac{\beta c}{R_e}} \mathrm{d}E_i f_{ie} \varrho(E_i)(L_e+T) \tag{2.1}$$

where n_e is the number of eth shell electrons, $\tilde{\nu}_e$ the threshold frequency for ionization, E_i the kinetic energy of the electron produced, f_{ie} the oscillator strength for the transition $\psi_e \to \psi_i$ and $\varrho(E_i)$ the density of states ψ_i; L_e and T represent the contributions to the integrand from the longitudinal and transverse components of the electromagnetic field of the particle. They are given by

$$L_e = \log \frac{\beta c}{R_e \tilde{\nu}} \tag{2.2}$$

and

$$T = \mathrm{SS}' \int_{\frac{\hbar\tilde{\nu}}{\beta c}}^{\infty} \frac{\mathrm{d}P_\lambda c^2 \tilde{\nu}^2 P_\lambda}{\hbar^2 \mu^2(\tilde{\nu}_\lambda)\mu^2(\tilde{\nu}'_\lambda)} \left(\beta^2 - \frac{\hbar^2 \tilde{\nu}^2}{c^2 P_\lambda^2}\right) A(\tilde{\nu}_\lambda, \tilde{\nu}'_\lambda) \tag{2.3}$$

with

$$A = \frac{(\tilde{\nu}^2-\tilde{\nu}_\lambda^2)(\tilde{\nu}^2-\tilde{\nu}_\lambda'^2)+\tilde{\nu}^2\tilde{\gamma}_\lambda(\tilde{\nu}_\lambda)\tilde{\gamma}_\lambda(\tilde{\nu}'_\lambda)}{[(\tilde{\nu}^2-\tilde{\nu}_\lambda^2)^2+\tilde{\nu}^2\tilde{\gamma}_\lambda^2(\tilde{\nu}_\lambda)][(\tilde{\nu}^2-\tilde{\nu}_\lambda'^2)^2+\tilde{\nu}^2\tilde{\gamma}_\lambda^2(\tilde{\nu}'_\lambda)]}.$$

The frequency $\tilde{\nu}$ corresponds to the excitation energy required in the transition, i.e.;

$$\hbar\tilde{\nu} = E_i + \hbar\tilde{\nu}_e$$

and P_λ to the momentum of the physical photon in the intermediate state of the collision process. The frequency of a physical photon of momentum P_λ is not unique and the sums S and S′ extend over all possible frequencies for a given momentum P_λ. They are determined by roots of the energy-momentum relation for physical photons, namely

$$\hbar\tilde{\nu}_\lambda = c\mu^{-1}(\tilde{\nu}_\lambda)P_\lambda. \tag{2.4}$$

In the expression (2.3) we have resonance functions A in which line breadths $\tilde{\gamma}_\lambda(\tilde{\nu}_\lambda)$ occur. These line breadths result because the intermediate state of a collision process involving an individual atom can be robbed by other real processes occurring in the medium. Formally $\tilde{\gamma}_\lambda(\tilde{\nu}_\lambda)$ is the total transition probability from the state in which a fast charged particle is passing through a medium with one physical photon oscillator of frequency

$\tilde{\nu}_i$ excited. This is the most important intermediate state in the ionization process.

3. Photo-Ionization Cross-Sections

The oscillator strength f_{ie} for the transition $e \to i$ can be related to the photo-ionization cross-section $\phi_e(\tilde{\nu})$ for the eth shell electron by

$$f_{ie}\,\varrho(E_i)\mathrm{d}E_i = \frac{mc}{2\pi^2 e^2}\,\phi_e(\tilde{\nu})\mathrm{d}\tilde{\nu}$$

so that equation (2.1) becomes

$$\left(\frac{\mathrm{d}E}{\mathrm{d}x}\right)_{\mathrm{d}}^{\mathrm{ion}} = \frac{2Z^2}{\pi\beta^2}\cdot\frac{e^2}{\hbar c}\cdot N\hbar\sum_e n_e\int_{\tilde{\nu}_e}^{\frac{\beta c}{R_e}}\phi_e(\tilde{\nu})\mathrm{d}\tilde{\nu}(L_e+T). \tag{3.1}$$

Exact expressions for the photo-ionization cross-sections for most materials are lacking. However we use in this discussion the following cross-sections calculated and fitted to experimental data by Stobbe [4]) for the K and L shell electrons:

$$\phi(1\mathrm{s}) = \phi_0 2^6\pi\,\frac{137^3}{Z_1^{\,2}}\left(\frac{\tilde{\nu}_1}{\tilde{\nu}}\right)^4\frac{\exp\left[-4\left(\frac{\tilde{\nu}_1}{\tilde{\nu}-\tilde{\nu}_1}\right)^{\frac{1}{2}}\cot^{-1}\left(\frac{\tilde{\nu}_1}{\tilde{\nu}-\tilde{\nu}_1}\right)^{\frac{1}{2}}\right]}{1-\exp\left[-2\pi\left(\frac{\tilde{\nu}_1}{\tilde{\nu}-\tilde{\nu}_1}\right)^{\frac{1}{2}}\right]} \tag{3.2}$$

$$\phi(2\mathrm{s}) = \phi_0 2^{11}\pi\,\frac{137^3}{Z_2^{\,2}}\left(\frac{\tilde{\nu}_2}{\tilde{\nu}}\right)^4\left(1+\frac{3\tilde{\nu}_2}{\tilde{\nu}}\right)\frac{\exp\left[-8\left(\frac{\tilde{\nu}_2}{\tilde{\nu}-\tilde{\nu}_2}\right)^{\frac{1}{2}}\cot^{-1}\left(\frac{\tilde{\nu}_2}{\tilde{\nu}-\tilde{\nu}_2}\right)^{\frac{1}{2}}\right]}{1-\exp\left[-4\pi\left(\frac{\tilde{\nu}_2}{\tilde{\nu}-\tilde{\nu}_2}\right)^{\frac{1}{2}}\right]} \tag{3.3}$$

$$\phi(2\mathrm{p}) = \phi_0 2^{12}\pi\,\frac{137^3}{Z_2^{\,2}}\left(\frac{\tilde{\nu}_2}{\tilde{\nu}}\right)^5\left(1+\frac{8\tilde{\nu}_2}{3\tilde{\nu}}\right)\frac{\exp\left[-8\left(\frac{\tilde{\nu}_2}{\tilde{\nu}-\tilde{\nu}_2}\right)^{\frac{1}{2}}\cot^{-1}\left(\frac{\tilde{\nu}_2}{\tilde{\nu}-\tilde{\nu}_2}\right)^{\frac{1}{2}}\right]}{1-\exp\left[-4\pi\left(\frac{\tilde{\nu}_2}{\tilde{\nu}-\tilde{\nu}_2}\right)^{\frac{1}{2}}\right]} \tag{3.4}$$

where $\tilde{\nu}_1$ and $\tilde{\nu}_2$ are the threshold frequencies for the K and L shells, and Z_1 and Z_2 are the effective nuclear charges experienced by these electrons taking account of inner screening. The following values of Z_1 and Z_2 were used by Stobbe:

$$Z_1 = Z-0.3,$$
$$Z_2 = Z-0.85\,n_1-(n_2-1)0.35;$$

n_1 and n_2 are the number of K and L shell electrons respectively. The absorption edge frequencies are those measured experimentally, and depend both on inner screening and also the outer electron shells.

Using the above cross-sections in the integrand of (3.1) we can obtain exactly the energy loss to ionization for the first ten elements of the periodic table. Exact calculations for heavier elements would require knowledge of the appropriate photo-ionization cross-sections for these elements.

4. Simplification of the Transverse Contribution T

Equation (2.3) for the transverse term is complicated as it stands. It can however be considerably simplified as we show by considering in numerical detail the particular case of oxygen. In order to do this we first require explicit expressions for the refractive index and line breadths.

The exact refractive index is given by

$$\mu(\bar{\nu}_\lambda)-1 = 2\pi \frac{Ne^2}{m} \sum_e n_e \sum_n \frac{f_{en}(\bar{\nu}_{en}^2-\bar{\nu}_\lambda^2)}{(\bar{\nu}_{en}^2-\bar{\nu}_\lambda^2)^2+\gamma_n^2\bar{\nu}_{en}^2} \tag{4.1}$$

where Σ_e sums over the eth shell electrons and Σ_n is to be understood as a sum over all excited states and an integral over all continuous states. The expression (4.1) is frequently replaced by a single sum over lumped oscillators for the electron shells, namely

$$\mu(\bar{\nu}_\lambda)-1 = \frac{2\pi Ne^2}{m} \sum_e \frac{n_e(\bar{\nu}_e^2-\bar{\nu}_\lambda^2)}{(\bar{\nu}_e^2-\bar{\nu}_\lambda^2)^2+\gamma_e^2\bar{\nu}_e^2} \tag{4.2}$$

where $\bar{\nu}_e$ is the absorption edge for the eth shell electrons. This expression reproduces the refractive index to sufficient accuracy for frequencies displaced from the various excitation frequencies of the atom. The line breadth γ_e is the collision breadth for which we use an expression given by Weisskopf [5]).

We previously showed [1]) that the line breadth $\bar{\gamma}_\lambda$ was made up of three contributions:

$$\bar{\gamma}_\lambda(\bar{\nu}_\lambda) = \gamma_i + \frac{\pi Ne^2}{\mu^2 m} \sum_e \frac{\bar{\gamma} f_e}{(\bar{\nu}_e^2-\bar{\nu}_\lambda^2)+\frac{1}{4}\bar{\gamma}^2} + \bar{\gamma} \tag{4.3}$$

where the first term is the photo-ionization contribution, the second the photo-excitation and $\bar{\gamma}$ is the line breadth representing the reaction of the medium on the particle.

We have plotted in fig. 1 the following photo-ionization probabilities as a function of freuqency for oxygen:

$$\gamma_i = \gamma_i(1s)+\gamma_i(2s)+\gamma_i(2p) \tag{4.4}$$

where

$$\begin{aligned} \gamma_i(1s) &= 2Nc\phi(1s) \\ \gamma_i(2s) &= 2Nc\,\phi(2s) \\ \gamma_i(2p) &= 4Nc\,\phi(2p) \end{aligned} \tag{4.5}$$

using the data given in table 1. An average value for the $2p^4$ and $2s^2$ ioniza-

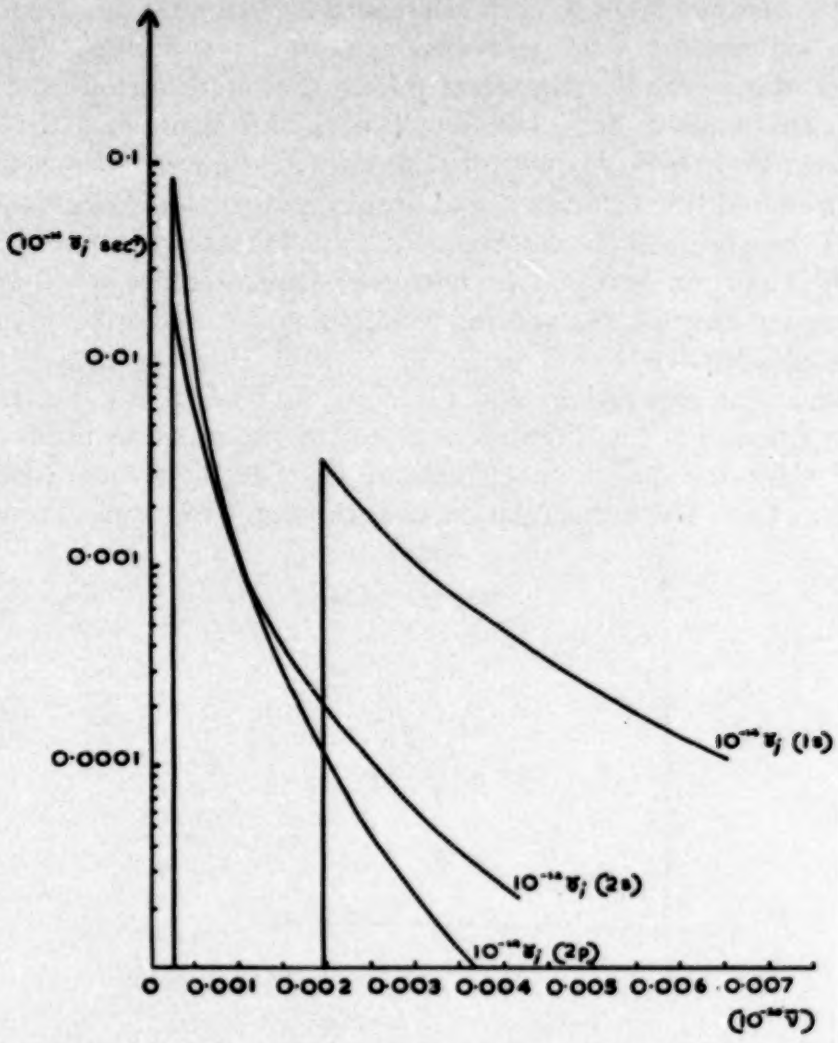

Fig. 1.

tion thresholds of $\bar{\nu}_2 = 0.0276 \times 10^{18}$ sec^{-1} was taken using the values given by Bacher and Goudsmit [6]).

TABLE 1

Electron configuration (oxygen)	$\frac{c}{R_s}$ sec^{-1}	$\bar{\nu}_s$ sec^{-1}	Effective Z_s (screening)	Collision line breadth γ_s sec^{-1}	Density at N.T.P.
$1s^2$	0.4374×10^{20}	0.1956×10^{18}	7.70	2.2×10^{11}	0.5378×10^{20}
$2s^2\ 2p^2$	0.2585×10^{20}	0.0276×10^{18}	4.55	26.2×10^{11}	atoms/cm^3

In order to calculate the excitation contribution to $\bar{\gamma}_\lambda$, i.e. the second term of equation (4.3), we require the line breadth $\bar{\gamma}$. Now the plateau

value for the energy loss in oxygen is about 2 keV/cm and the mean energy transfer in ionizing and exciting collisions is of order of 90 eV. This gives us an order of magnitude estimate of $\bar{\gamma}$ from the intercollision-time for the particle in the medium of $\approx 10^{12}$ sec^{-1}. With this value of $\bar{\gamma}$ the rapidly varying excitation term of equation (4.3) rises at the resonance frequencies to several hundred times that of γ_i and drops rapidly below γ_i for frequencies displaced from the resonances. The fact that the excitation contribution to $\bar{\gamma}_\lambda$ is only important at resonance frequencies and is completely dominated by the comparitively slowly varying function $(\gamma_i+\bar{\gamma})$ for other frequencies enables us to simplify T.

To evaluate the expression (2.3) for T we first have to understand the relative importance of the different roots of the energy-momentum relation (2.4) over which the sums S and S′ extend. Consider how these roots arise. In figure 2 we have drawn the relation (2.4) through a few typical resonances

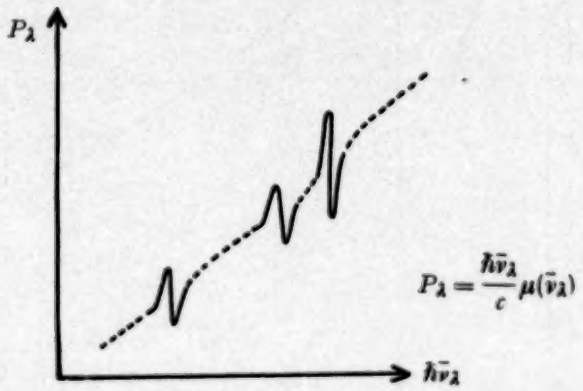

Fig. 2. Energy-momentum relation for physical photons.
Region A - - - - - - - -
Region B ————————

corresponding to excitation frequencies for the atomic electrons. In the regions between resonances the momentum is a steadily increasing function of $\bar{\nu}_\lambda$. However at the resonance frequencies $\mu(\bar{\nu}_n)$ varies rapidly with $\bar{\nu}_\lambda$ and a line P_λ = constant may cut several of these regions of high dispersion. If we consider first only the diagonal terms of the double summation S′S we have a contribution to T of

$$T'(\bar{\nu},\beta) = \frac{c^2\bar{\nu}^2}{\hbar^2}\,\mathrm{S}\int_{\frac{\hbar\bar{\nu}}{\beta c}}^{\infty}\frac{P_\lambda\,\mathrm{d}P_\lambda}{\mu^4(\bar{\nu}_\lambda)}\left(\beta^2-\frac{\hbar^2\bar{\nu}^2}{c^2P_\lambda^2}\right)[(\bar{\nu}^2-\bar{\nu}_\lambda^2)^2+\bar{\nu}^2\bar{\gamma}_\lambda^2(\bar{\nu}_\lambda)]^{-1}. \quad (4.6)$$

The integrand has resonances when $\bar{\nu}=\bar{\nu}_\lambda$. The corresponding value of P_λ at the centre of such a resonance will be $\hbar\bar{\nu}c^{-1}\mu(\bar{\nu})$, and a necessary condition that this lies inside the range of integration for T is that

$$1 \leqq \beta\mu(\bar{\nu}) \leqq \infty.$$

Note that in the regions between excitation frequencies $\mu(\tilde{\nu}) \approx 1$ so that as $\beta \to 1$ the integrand of (4.6) approaches a resonance — though it may not approach close enough for $\tilde{\gamma}_\lambda$ to become important. We divide the integral for T' into two parts as follows:

Region A

This is the range of frequencies displaced at least several $\tilde{\gamma}$ from the resonance frequencies $\tilde{\nu}_e$. Now $\tilde{\gamma}_\lambda(\tilde{\nu}_\lambda)$ is only important in the integral (4.6) for $|\tilde{\nu}_\lambda - \tilde{\nu}| \lessapprox \tilde{\gamma}_\lambda$. Thus since for region A, $\tilde{\gamma}_\lambda \approx \tilde{\gamma}_i + \tilde{\gamma}$ which is a slowly varying function of $\tilde{\nu}_\lambda$ we can use $\tilde{\gamma}_\lambda(\tilde{\nu})$ in place of $\tilde{\gamma}_\lambda(\tilde{\nu}_\lambda)$ in the integration for this region of frequencies.

Next consider $\mu(\tilde{\nu}_\lambda)$. We are displaced from the most highly dispersive region of frequencies so that the quantity $(\tilde{\nu}^2 - \tilde{\nu}_\lambda^2)$ can be written as

$$(\tilde{\nu}^2 - \tilde{\nu}_\lambda^2) \approx \left(\tilde{\nu}^2 - \frac{c^2 P_\lambda^2}{\hbar^2 \mu^2(\tilde{\nu})}\right)$$

since again only for $\tilde{\nu}_\lambda$ close to $\tilde{\nu}$ does the exact value of $\mu(\tilde{\nu}_\lambda) - 1$ become important for the integral (4.6).

Making the above approximations for region A we find

$$T'(\tilde{\nu}, \beta) = \frac{(\beta^2\mu^2 - 1)}{2\mu^4} \cdot \frac{\tilde{\nu}}{\tilde{\gamma}_\lambda} \cdot \left(\frac{\pi}{2} - \tan^{-1} \frac{2\tilde{\nu}}{\tilde{\gamma}_\lambda}\left(\frac{1}{\beta\mu} - 1\right)\right) - \frac{(1+\beta\mu)}{8\mu^4} \log \frac{\mu^2\beta^2\tilde{\gamma}_\lambda^2}{4\tilde{\nu}^2}\left[1 + \frac{4\tilde{\nu}^2}{\tilde{\gamma}_\lambda^2}\left(\frac{1}{\beta\mu} - 1\right)^2\right]. \quad (4.7)$$

Region B

Suppose $\tilde{\nu}$ lies within a few $\tilde{\gamma}$ of a resonance frequency $\tilde{\nu}_e$. Then over a fairly large range of P_λ there will be two local roots ν_1 and ν_2 of the energy-momentum relation (2.4) in the dispersive region for which $\tilde{\nu} \approx \nu_1 \approx \nu_2$. For both of these roots the resonance denominator can be written approximately

$$A(\nu_1, \nu_1) = A(\nu_2, \nu_2) \approx \tilde{\nu}^{-2}\tilde{\gamma}_\lambda^{-2}(\tilde{\nu}_e)$$

for $\tilde{\nu} \approx \tilde{\nu}_e$ since $\tilde{\gamma}_\lambda$ has an extremely large resonance of breadth $\tilde{\gamma}$ in this region due to the excitation term of equation (4.3). In general the roots of the energy-momentum relation which give frequencies close to the excitation frequencies will contribute little to the integral T' due to the resonance in $\tilde{\gamma}_\lambda$ in this region. Thus since cross terms of the double summation in equation (2.3) are always such that at least one of the frequencies lies in the highly dispersive regions we shall neglect them. The expression (4.6) for T' will therefore be used for all values of $\tilde{\nu}$ since the error in using this expression for the small frequency ranges $\tilde{\nu}_e \pm \tilde{\gamma}$ is negligible. Our final expression for the primary ionization energy loss then becomes

$$\left(\frac{dE}{dx}\right)_d^{ion} = \frac{2}{\pi\beta^2}\cdot\frac{e^2}{\hbar c}\cdot Z^2 N\hbar \sum_e n_e \int_{\bar{\nu}_e}^{\frac{\beta e}{R_e}} d\bar{\nu}\,\phi_e(\bar{\nu})\left[\log\frac{\beta c}{R_e\bar{\nu}}\right. \tag{4.8}$$

$$\left. + \frac{(\beta^2\mu^2-1)}{2\mu^4}\cdot\frac{\bar{\nu}}{\bar{\gamma}_\lambda}\cdot\cot^{-1}\frac{2\bar{\nu}}{\bar{\gamma}_\lambda}\left(\frac{1}{\beta\mu}-1\right) - \frac{(1+\beta\mu)}{8\mu^4}\log\frac{\mu^2\beta^2\bar{\gamma}_\lambda^2}{4\bar{\nu}^2}\left(1+\frac{4\bar{\nu}^2}{\bar{\gamma}_\lambda^2}\left(\frac{1}{\beta\mu}-1\right)^2\right)\right].$$

We have to specify the photo-ionization cross-sections $\phi_e(\bar{\nu})$, the refractive index $\mu(\bar{\nu})$ and the line breadth $\bar{\gamma}_\lambda(\bar{\nu})$ in order to evaluate this.

It is interesting to note at this stage that the energy loss depends primarily on the value of the refractive index for frequencies displaced from excitation frequencies, and for these frequencies the refractive index is fairly close to unity. We require this for the perturbation treatment we used in deriving these formulae to give a good approximation.

4.1. NUMERICAL VALUE OF T

The transverse term T was first examined using (4.3), (4.4) and (3.2) to (3.4) for $\bar{\gamma}_\lambda$ and the expression (4.2) for the refractive index with the appropriate constants taken from table 1. We write $\mu^4 T$ as a function of $\beta\mu$ and $(\bar{\gamma}_\lambda/\bar{\nu})$ where $\bar{\gamma}_\lambda$ and μ are functions of $\bar{\nu}$. Then the larger of the two quantities $|1-\beta\mu|$ and $(\bar{\gamma}_\lambda/\bar{\nu})$ is most important for determining the magnitude of T. We note that at the threshold for production of Čerenkov frequencies, i.e. when $\beta\mu = 1$, the expression for T simplifies to $0.5\ \mu^{-4}$ $\log(4\bar{\nu})\bar{\gamma}_\lambda)$.

In figure 3 we have plotted $2^{-5}T$ as a function of $\bar{\nu}$ for $\beta = 1$ for two values of the reaction of the medium on the particle equal to 0 and 4×10^{12}

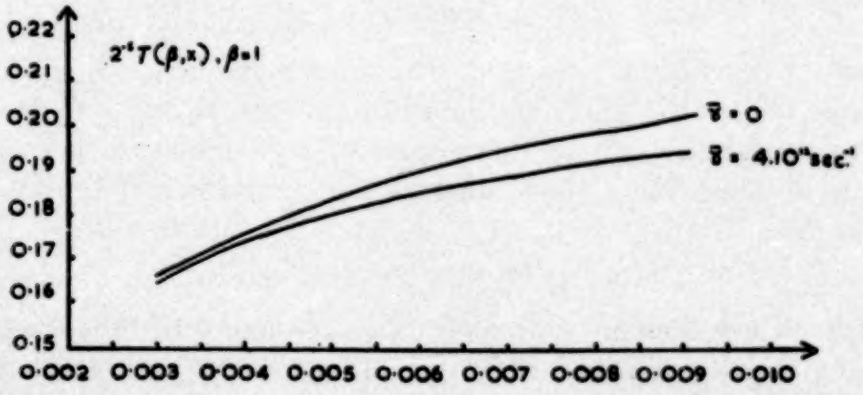

Fig. 3.

sec^{-1} to test the sensitivity of T to this quantity. In the case $\bar{\gamma} = 0$, $\bar{\gamma}_\lambda$ is made up of the three contributions $\gamma_i(1s)$, $\gamma_i(2s)$ and $\gamma_i(2p)$ of equation (4.5). For the plausible value of $\bar{\gamma} = 4\times10^{12}$ sec^{-1}, $\bar{\gamma}_\lambda$ is made up mainly of $\bar{\gamma}$ for frequencies a little above the absorption edge frequencies. Table 2 gives the values of the quantities $|1-\beta\mu|$, $(\bar{\gamma}_\lambda/\bar{\nu})$ and T for the above values of $\bar{\gamma}$. From these figures we see that for $\bar{\gamma} = 0$, $|1-\beta\mu|$ dominates over

$(\bar{\gamma}_\lambda/\bar{\nu})$ for the entire frequency range considered, whereas for $\bar{\gamma} = 4\times10^{12}$ $\sec^{-1}$, it dominates only for the region of smaller frequencies close to the absorption edges. Further, irrespective of this, T is very insensitive to the ratio $(\bar{\gamma}_\lambda/\bar{\nu})$ and thus to $\bar{\gamma}$. Even for $\bar{\nu}$ as large as 9.1×10^{17} $\sec^{-1}$, the two values of T differ only by 4 %. Thus since $\phi_e(\bar{\nu})$ also decreases rapidly with increasing $\bar{\nu}$ the value of $\bar{\gamma}$ can be neglected in the expression (4.8).

In figure 4 we have also plotted the longitudinal and transverse contributions L_e and T to the integrand of (4.8) as a function of β for the particular

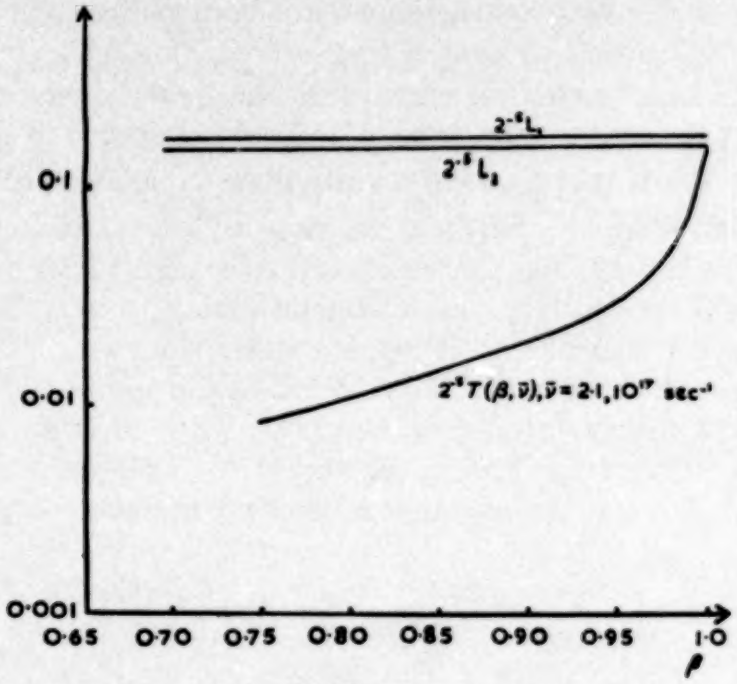

Fig. 4.

frequency $\bar{\nu} = 2.1\times10^{17}$ $\sec^{-1}$. The transverse contribution is seen to give us the relativistic rise, to a plateau value, for the primary ionization distant collision energy loss. This rise is not due to the reabsorption of Čerenkov radiation which would be a secondary process contributing a further rise.

TABLE 2

$10^{-17}\ \bar{\nu}$ $\sec^{-1}$	$10^7\lvert1-\beta\mu\rvert$	$\bar{\gamma}=0,\ \beta=1$		$\bar{\gamma}=4\times10^{12}\sec^{-1},\ \beta=1$	
		$10^8(\bar{\gamma}_\lambda/\bar{\nu})$	$2^{-5}T$		
9.1	8.365	0.47	0.2032	440.0	0.1953
8.1	10.59	0.75	0.1995	494.5	0.1925
7.1	13.86	1.27	0.1953	564.6	0.1894
6.1	18.93	2.32	0.1903	658.0	0.1855
5.1	27.47	4.69	0.1844	789.0	0.1808
4.1	43.73	10.95	0.1771	986.5	0.1746
3.1	83.08	31.95	0.1671	1322	0.1657
2.1	410.7	137.9	0.1422	2042	0.1420

5. Evaluation of $(\mathrm{d}E/\mathrm{d}x)_{\mathrm{d}}^{\mathrm{ion}}$

The expression (4.8) for the distant collision energy loss to ionization has been integrated numerically by the Silliac electronic computor using equations (3.2) to (4.3) We write (4.8) as the sum of two terms, namely

$$\left(\frac{\mathrm{d}E}{\mathrm{d}x}\right)_{\mathrm{d}}^{\mathrm{ion}} = \frac{64}{\pi}\cdot\frac{e^2}{\hbar c}\cdot 10^7 Z^2 \hbar c (F_{\mathrm{K}}+F_{\mathrm{L}})$$

where F_{K} and F_{L} are the integrals deriving from the K and L shell electrons respectively. These two contributions have been plotted as a function of E/Mc^2 for the ionizing particle in figure 6.

In order to make a comparison with the ionization observed experimentally we have to consider the Čerenkov radiation absorbed in the region of the track of the particle; and also reabsorbed radiation arising from the decay of excited atoms. Further, the close collision loss (for which the electrons are treated as free) has in general to be added if we are interested in energy transfers less than some maximum value $\varepsilon_{\mathrm{M}} > (\hbar\beta c/R_e)$. However, these close collisions make no contribution here since we confine ourselves to energy transfers <1 keV. (Note "close" as used here means "with impact parameter less than an atomic radius".) We write down for reference all the *primary* energy losses which, together with (4.8), are relevant to the formation of a track, for example in a cloud chamber or photographic emulsion:

$$\left(\frac{\mathrm{d}E}{\mathrm{d}x}\right)_{\mathrm{close}} = \frac{2\pi Z^2 e^4 N}{mc^2\beta^2}\sum_e n_e \log\frac{2\varepsilon_M m R_e^{\,2}}{\hbar^2} \tag{5.2}$$

$$\left(\frac{\mathrm{d}E}{\mathrm{d}x}\right)_{\text{Čerenkov}} = \int \mathrm{d}\tilde{\nu}\; v\;\tilde{\nu}\,\frac{Z^2e^2}{c^2}\left(1-\frac{c^2}{v^2\mu^2(\tilde{\nu})}\right) \tag{5.3}$$

$$\left(\frac{\mathrm{d}E}{\mathrm{d}x}\right)_{\mathrm{d}}^{\mathrm{ext}} = \frac{4\pi Z^2 e^4 N}{mc^2\beta^2} f_{ee'}\left(\log\frac{\beta c}{R_e\tilde{\nu}_{ee'}(1-\beta^2\mu^2)^{\frac{1}{2}}} - \frac{\beta^2}{2}\right). \tag{5.4}$$

The expression $(\mathrm{d}E/\mathrm{d}x)_{\mathrm{d}}^{\mathrm{ext}}$ is for excitation of an electron in state ψ_e to an excited state $\psi_{e'}$ for the case in which $\mu(\tilde{\nu}_{ee'}) < 1$. This condition is usually true for the frequencies required to excite the inner shell electrons, and further only radiation from the *inner* shell electrons is capable of ionizing the outer electron shells.

It should also be stated here that if $|\mu(\tilde{\nu})-1| \gg (\tilde{\nu}_\lambda/\tilde{\nu})$ we can simplify the expression (4.8) for the primary ionization to one which is closely related to that given by Budini [7]), namely,

$$\left(\frac{\mathrm{d}E}{\mathrm{d}x}\right)_{\mathrm{d}}^{\mathrm{ion}} \approx \frac{2}{\pi\beta^2}\cdot\frac{e^2}{\hbar c}\cdot N\hbar Z^2\sum_e n_e\int_{\tilde{\nu}_e}^{\frac{\beta c}{R_e}}\mathrm{d}\tilde{\nu}\phi_e(\tilde{\nu})\left[\log\frac{\beta c}{R_e\,\tilde{\nu}|1-\beta\mu|^{\frac{1}{2}}} - \frac{\beta^2}{2}\right]. \tag{5.5}$$

In the expression (5.3) we have omitted the factor

$$\frac{u_\lambda(\bar{\nu}_\lambda)}{U_\lambda(\bar{\nu}_\lambda)}, \tag{5.6}$$

i.e. the ratio of the phase to the group velocity, which occurred in the expressions (3.31), (3.14) and (3.29) for the Čerenkov emission as calculated in the previous paper [1]). This is because we can only sensibly use the expression for the group velocity,

$$U_\lambda(\bar{\nu}_\lambda) = c\frac{\mathrm{d}\bar{\nu}_\lambda}{\mathrm{d}\nu_\lambda}, \tag{5.7}$$

for the range of frequencies $\bar{\nu}_\lambda$ displaced from the regions of anomalous dispersion. This is because a frequency $\bar{\nu}_\lambda$ cannot be defined to within an uncertainty $\Delta\bar{\nu}_\lambda$ which is the absorption probability for this frequency, and so we must take $\mathrm{d}\bar{\nu} > \Delta\bar{\nu}_\lambda$. The breadth $\Delta\bar{\nu}_\lambda$ is in turn considerably greater than the atomic line breadths $\bar{\gamma}_s$ over which the regions of anomalous dispersion extend. For the range that (5.7) can be used (5.6) is reasonably close to unity.

The above energy losses are those from the primary quantal processes of ionization, excitation and Čerenkov radiation occurring in the neighbourhood, d, of the path of the particle over which its electromagnetic field

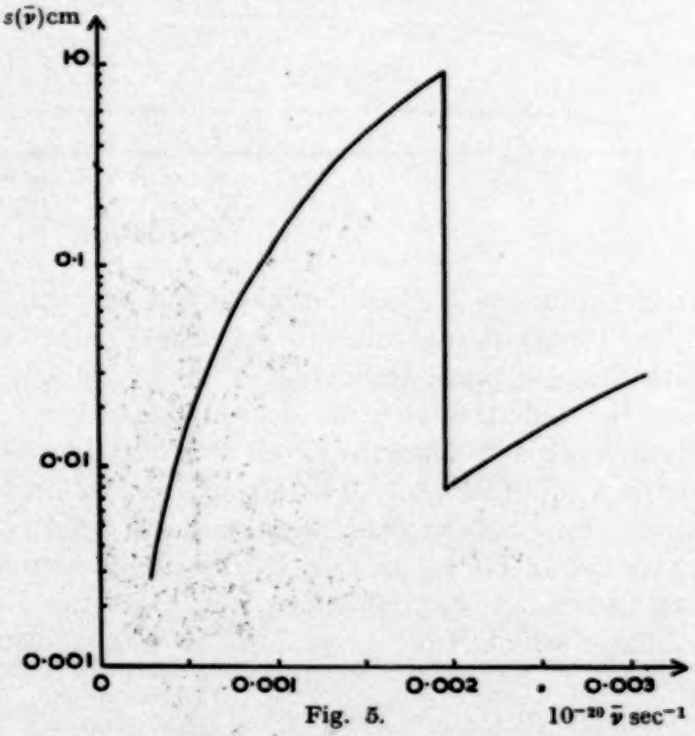

Fig. 5.

extends. In the case of Čerenkov radiation, until a physical photon has emerged from this region we cannot identify it as a real quantum. The value

of d depends on the energy transfers one is considering, being greater than an interatomic distance and less than approximately 10^{-4} cm.

In order to obtain the energy loss which for example gives rise to a trail of drops in a cloud chamber, we require the ionization occurring in a cylinder of radius approximately 1 mm around the path of the particle — considerably larger than the radius d inside which primary quantum processes

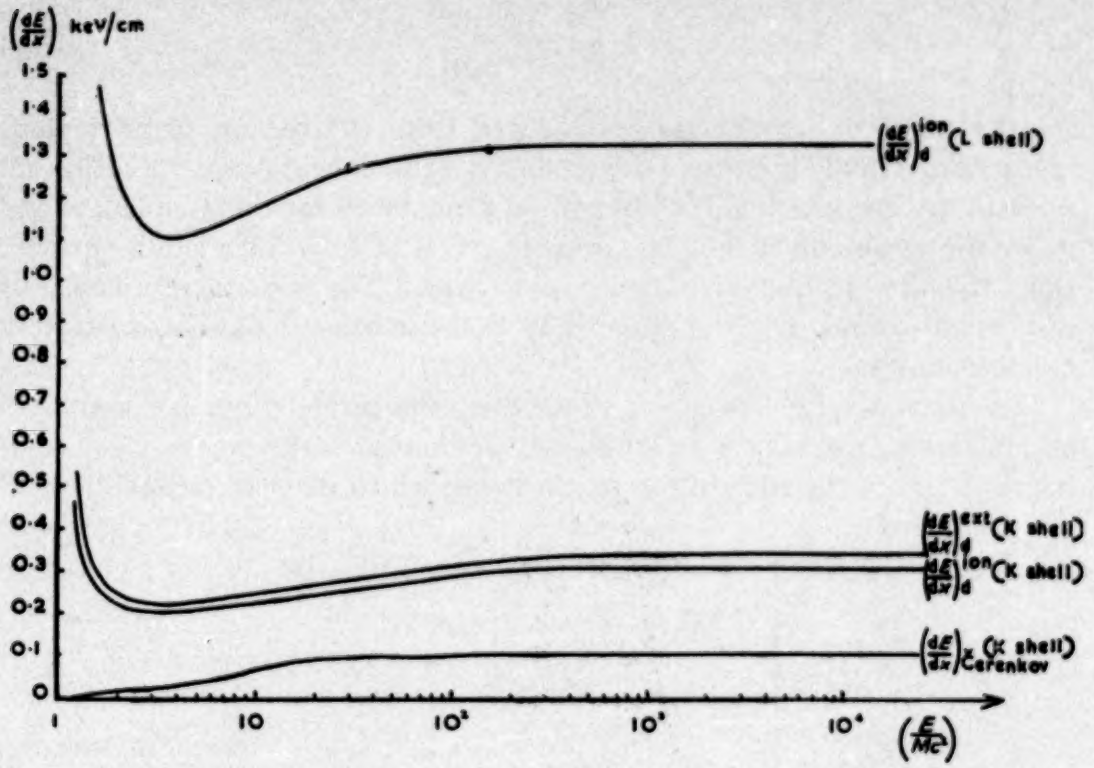

Fig. 6.

occur. Practically all of the K shell Čerenkov and excitation radiation will give rise to L shell ionization inside this cylinder despite the fact that the mean free path $s(\bar{\nu})$ for photo-ionization is about 0.4 cm (see figure 5). This is because the radiation is centred around resonance excitation frequencies and undergoes a large number of excitation absorptions and emissions with a mean free path λ before giving rise to ionization. The result of these 'scatters' is to increase the total path length of the radiation emerging from the cylinder along a radius R to approximately $R^2\lambda^{-1} \gg 0.4$ cm.

We estimate the secondary ionization from (5.3) and (5.4) as follows. Firstly the oscillator strength per electron for K shell transitions to excited states is

$$0.723 - \frac{mc}{2\pi^2 e^2}\int_{\bar{\nu}_1}^{\infty} \phi(\bar{\nu})\mathrm{d}\bar{\nu}$$

where the oscillator strength of 0.723 is that given by Bethe [8]). Secondly

a K shell electron once having been excited by absorbing a photon will not necessarily decay by producing a *single* photon capable of ionizing the L shell. Rather, in general, alternative decays will occur in which some low energy photons will be emitted together with a transition which fills the K shell. Only when radiation has a frequency corresponding to an $L \rightarrow K$

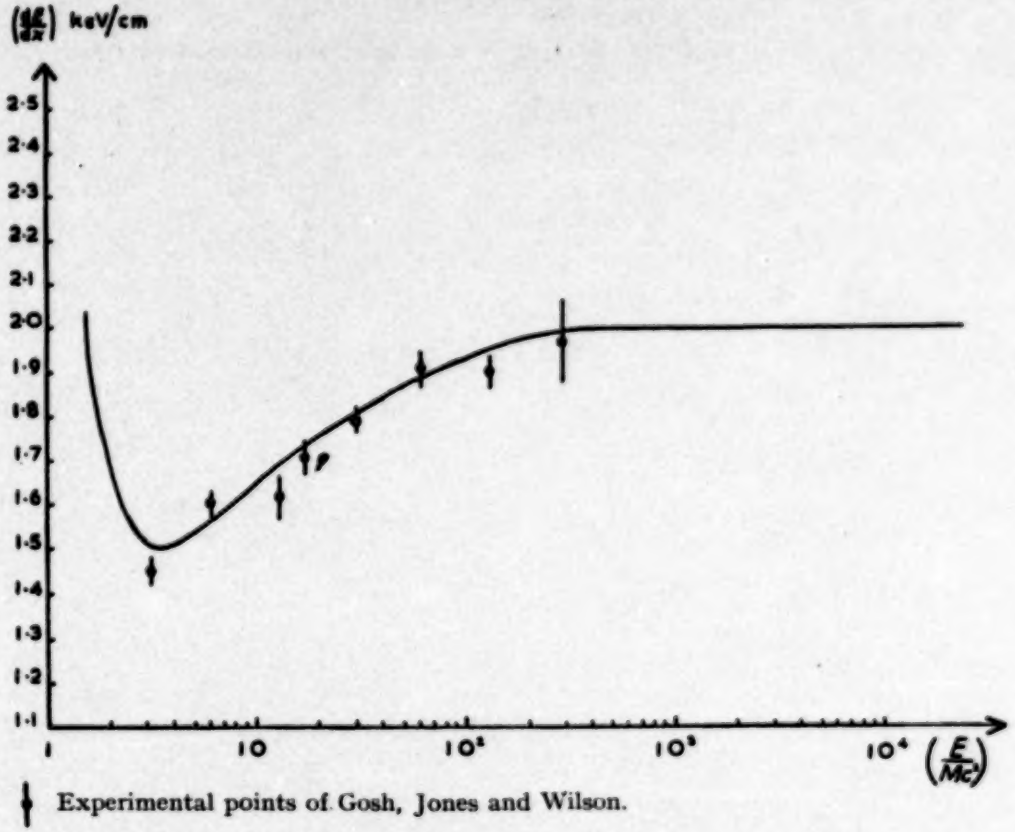

Fig. 7.

transition will the emitted photon have the same frequency as the absorbed photon. We estimate that approximately 20 % of the radiation will be lost in this way to low energy photons incapable of ionizing the L shell.

In figures 6 and 7 the detailed distribution of the relevant energy losses are given and the total ionization which contributes to formation of a trail of drops in a cloud chamber is compared with the experimental results of Gosh, Jones and Wilson [9]). These results were obtained by evaluating the expressions (4.8) to (5.5) using the Silliac electronic computor.

I would like to thank Professor Messel for the excellent research facilities provided in the School of Physics and also the Silliac computor group for help in using the machine.

References

1) D. A. Tidman, Nuclear Physics **2** (1956) 289
2) R. M. Sternheimer, Phys. Rev. **88** (1952) 851; **91** (1953) 256; **103** (1956) 511
3) S. M. Neamtan, Phys. Rev. **92** (1953) 1362
4) M. Stobbe, Ann. d. Phys. **7** (1930) 661
5) V. Weisskopf, Z. Physik **34** (1933) 1
6) R. F. Bacher and S. Goudsmit, Atomic Energy States (McGraw-Hill Book Co., 1932)
7) P. Budini, Nuovo Cimento **10** (1953) 236
8) H. Bethe, Ann. d. Phys. **5** (1930) 325
9) S. G. Gosh, G. M. D. B. Jones and J. G. Wilson, Proc. Phys. Soc. A **65** (1952) 58

Nuclear Physics **4** (1957) 271—272; © *North-Holland Publishing Co., Amsterdam*
Not to be reproduced by photoprint or microfilm without written permission from the publisher

8 A ON THE POLARIZATION OF ELECTRONS IN β-DECAY

M. E. VISHNEVSKY, V. K. GRIGORIEV, V. A. ERGAKOV, S. J. NIKITIN, E. V. PUSHKIN AND YU. V. TREBUKHOVSKY
U.S.S.R. Academy of Sciences, Moscow

Received 9 April 1957

Extending the concept of non-conservation of parity in weak interactions, introduced by Lee and Yang [2]), Landau has recently suggested [1]) that a so-called two-component or longitudinal neutrino may exist. According to this idea the neutrino is polarized along its momentum.

One of the possibilities of proving this hypothesis would be to study the polarization of β-electrons since the electrons emitted in allowed transitions should be longitudinally polarized, the polarization being equal to v/c.

We accordingly performed experiments with electrons emitted by Cu^{64} ($\Delta J = 1$, no). In order to observe longitudinal polarization, the electrons emitted by Cu^{64} were deflected in an electric field of a cylindrical condenser and the azimuthal asymmetry in the number of electrons scattered by a thin foil was studied. The angle between the spin and momentum of the electrons deflected within the condenser was 90°.

A deflected beam of 145 keV electrons ($v/c = 0.63$) was scattered by a thin gold foil, the direction of the beam making an angle of 45° with the plane of the scatterer.

The scattered electrons were counted by means of two telescopes, each containing two G-M counters. The axis of the telescopes formed an angle equal to 180°.

In order to determine the azimuthal asymmetry the telescopes and scattering target were rotated about the beam axis and the number of scattered electrons at various azimuthal angles were counted; one of the telescopes thus counted electrons reflected by the foil and the other electrons transmitted by the foil.

The source consisted of a thin layer of CuO ($\leqq 2$ mg/cm²) deposited on a 0.5 mg/cm² Al foil. The electrons were scattered by a thin gold layer, evaporated on a 0.04 mg/cm² cellophane film. Gold layers of 0.120 mg/cm² and 0.240 mg/cm² were used. An azimuthal asymmetry in the number of scattered electrons, corresponding to an electron polarization opposite to the direction of momentum (right-left asymmetry) was observed.

The value of the observed asymmetry $A = (2I_{\rightarrow} - I_{\leftarrow})/(I_{\rightarrow} + I_{\leftarrow})$ averaged over several runs for electrons penetrating the scatterer, measured with two slightly different arrangements, was found equal to 0.35 ± 0.05 and 0.27 ± 0.05 respectively. The asymmetry obtained with electrons reflected by the scatterer was considerably less than the results given above owing to a larger multiple-scattering effect within the scatterer. The errors given correspond to the statistical errors only and do not take into account depolarization effects within the source, multiple scattering within the target or possible small apparatus errors. No up-down asymmetry exceeding the statistical errors was observed.

The theoretical value for the asymmetry in the case of the two-component neutrino is equal to 0.34 [3]; our result is in qualitative agreement with this value.

At present a more refined experimental study of the polarization of β-electrons is being carried out with the aim of quantitatively checking Landau's theory.

A similar investigation has recently been performed by A. I. Alikhanov, G. P. Yeliseyev, V. A. Liubimov and B. V. Ershler [4] with Sr^{90} and Y^{90}. Some time before completion of our experiments we were informed about the experiments performed by the Illinois University group [5]. The data obtained by both of the aforementioned groups of investigators closely agree with our results.

The authors wish to thank V. V. Vladimirsky for numerous helpful discussions.

The apparatus used was constructed by N. I. Afanasiev, E. G. Savinov, V. M. Berezin and I. I. Yermakov. The high specific activity Cu^{64} sources were prepared by the cyclotron crew headed by B. M. Stasevich.

The authors wish to express their thanks to all of them.

References

1) L. D. Landau, Nuclear Physics **3** (1957) 127
2) T. D. Lee and C. N. Yang, Phys. Rev. **104** (1956) 254
3) N. Sherman, Phys. Rev. **103** (1956) 1601
4) A. I. Alikhanov, G. P. Yeliseyev, V. A. Liubimov and B. V. Ershler, Nuclear Physics (in press)
5) H. Frauenfelder, R. Bobone, E. von Goeler, N. Levine, H. R. Lewis, R. N. Peacock, A. Rossi and G. de Pasquali, Phys. Rev. **106** (1957) 386

Nuclear Physics **4** (1957) 273—276; © *North-Holland Publishing Co., Amsterdam*
Not to be reproduced by photoprint or microfilm without written permission from the publisher

ON THE INTERACTION BETWEEN μ-MESONS AND NUCLEONS

I. S. SHAPIRO, E. I. DOLINSKY AND L. D. BLOKHINTSEV
Moscow State University, U.S.S.R.

Received 5 May 1957

Abstract: The angular distribution and longitudinal polarization of neutrons produced in the capture of μ^--mesons by μ-mesohydrogen are computed.

At present, experimental data relating to non-electromagnetic interaction between μ-mesons and nucleons are quite sparse; the only important fact which emerges from the currently available data is that the interaction is of the "weak" type. However, a more detailed study of μ-meson-nucleon interaction would be of great interest from the viewpoint of elucidating the nature of the μ-meson — one of the most puzzling of the known fundamental particles (both the μ-meson and electron are characterized by the same type of interaction — weak and electromagnetic — and by equal spins, but the μ-meson mass exceeds that of the electron by a factor 206.7). In particular, a determination of the nature of the μ-meson-nucleon interaction could be a decisive step in finding out why π- and K-mesons decay into μ and ν † but not into e and ν. Indeed, if π- and K-meson decay occurs via a baryon vacuum it should be easy to show that if the mesons are considered to be pseudoscalar the decay should be prohibited for scalar, vector and tensor coupling of the four-fermion interaction, but allowed for pseudoscalar and pseudovector coupling. Since (as β-decay seems to indicate) only scalar and tensor coupling is involved in the electron-nucleon interaction one would expect decay of π- and K-mesons into e and ν to be prohibited. Decay into μ and ν would signify the presence of pseudoscalar and/or pseudovector coupling in the μ-meson-nucleon interaction.

If, on the other hand, π- and K-meson decay occurs, at least partially, as a result of direct interaction between the π- or K-meson and μ-meson and neutrino, the μ-meson-nucleon interaction Hamiltonian should contain pseudoscalar coupling.

It is well known that slowed down negative μ-mesons suffer nuclear absorption in matter, an intermediate stage in this process being the formation of a mesic atom. μ^--meson absorption is usually considered to proceed according to the reaction

$$\mu^- + \mathrm{p} \rightarrow \mathrm{n} + \nu. \qquad (1)$$

† ν denotes a neutrino.

The angular distribution of neutrons emitted as a result of capture of μ^--mesons by protons in μ-mesohydrogen is considered in the present paper. The μ^--meson is assumed to be polarized †. In this case, in virtue of parity non-conservation in weak interactions the neutron angular distribution will, generally speaking, be anisotropic, the sign and magnitude of the anisotropy depending on the type of interaction.

Taking account of parity non-conservation the interaction energy between μ-meson and nucleon may be written in the following form

$$H = \sum_{k}(\bar{\psi}_n O_k \psi_p)(\bar{\psi}_\nu[g_k - g'_k \gamma_5]O_k \psi_\mu) + \text{comp. conj.} \tag{2}$$

where O_k are the operators in the familiar β-decay theory and consist of Dirac matrices γ_μ, k = s, p, v, a, t where s, p, v, a, t denote respectively scalar, pseudoscalar, vector, pseudovector and tensor coupling. If $g'_k = -g_k$ we arrive at the longitudinally polarized neutrino theory proposed by L. D. Landau [1]).

The neutron angular distribution is described by the formula

$$W(\theta) = 1 + \alpha \cos\theta \tag{3}$$

where θ is the angle between the direction of neutron emission and the direction of μ^--meson polarization. In the general case (all types of coupling being present in (2)) α has the following form:

$$\alpha = A/B \tag{4}$$

where

$$\begin{aligned} A = {} & (E+M)h_{ss} + (E-M)h_{pp} + 2(M+\varepsilon)h_{vv} - 2(M-\varepsilon)h_{aa} \\ & - 8(E+2\varepsilon)h_{tt} + 2(E+M+\varepsilon)\,\mathrm{Re}\,h_{sv} + 4\varepsilon\,\mathrm{Re}\,h_{st} \\ & + 2(E-M+\varepsilon)\,\mathrm{Re}\,h_{ap} + 4\varepsilon\,\mathrm{Re}\,h_{tp} - 4\varepsilon\,\mathrm{Re}\,h_{va} \\ & - 4(E-M+\varepsilon)\mathrm{Re}\,h_{vt} - 4(E+M+\varepsilon)\,\mathrm{Re}\,h_{at}, \end{aligned} \tag{4a}$$

$$\begin{aligned} B = {} & (E+M)f_{ss} + (E-M)f_{pp} + 2(2E-M+\varepsilon)f_{vv} \\ & + 2(2E+M+\varepsilon)f_{aa} + 8(3E+2\varepsilon)f_{tt} + 2(E+M+\varepsilon)\,\mathrm{Re}\,f_{sv} \\ & + 4\varepsilon\,\mathrm{Re}\,f_{st} + 2(E-M+\varepsilon)\,\mathrm{Re}\,f_{ap} + 4\varepsilon\,\mathrm{Re}\,f_{tp} + 4\varepsilon\,\mathrm{Re}\,f_{va} \\ & + 12(E-M+\varepsilon)\,\mathrm{Re}\,f_{vt} + 12(E+M+\varepsilon)\,\mathrm{Re}\,f_{at}. \end{aligned} \tag{4b}$$

Here

$$f_{ik} = g_i^* g_k + g_i'^* g'_k, \quad h_{ik} = g_i^* g'_k + g_i'^* g_k, \tag{5}$$

E and M are the total energy and rest energy of the neutron, and ε is the neutrino energy ($E = 944.7$ MeV, $M = 939.5$ MeV, $\varepsilon = 99.1$ MeV). The

† μ^--mesons emitted from decaying π-mesons are polarized in a direction parallel to that of their motion [1]). Slowing down and formation of a μ-mesic atom may cause depolarization which, however, may not be complete [2]). Of course, measurement of μ^--meson polarization in a mesic atom (e.g. by measuring the anisotropy in the decay electron angular distribution) should precede the study of the angular distribution in reaction (1).

values of the coefficient α for various types of coupling in (2), on the assumption of a longitudinal neutrino, are presented in table 1 †.

TABLE 1

Type of coupling	s	p	v	a	t
α	−1	−1	−0.99	+0.29	0.38

In view of the special significance of the s+t and p+a combinations, the values of α for these cases will be given separately. If, in accord with the hypothesis of conservation of combined parity, the scalar and tensor interaction constants are considered to be real and their values derived from nucleon β-decay are used (see e.g. ref. [4])), that is,

$$g_s = (+1.4 \text{ or } -1.4)\times 10^{-49} \text{ erg}\cdot\text{cm}^3, \quad g_t = +1.8\times 10^{-49} \text{ erg}\cdot\text{cm}^3,$$

we obtain in the case of a longitudinal neutrino $\alpha^{s+t} = 0.30$ or 0.32. Similarly, in the case of a longitudinal neutrino and p+a combination we obtain

$$\alpha^{p+a} = (1.78|g_a|^2 - 0.0055|g_p|^2 - 0.22 \text{ Re } g_a^* g_p)/(6.20|g_a|^2 + 0.0055|g_p|^2 + 0.22 \text{ Re } g_a^* g_p). \tag{6}$$

The dependence of α^{p+a} on $x = g_a/g_p$ in the case when the latter ratio is real, is plotted in fig. 1.

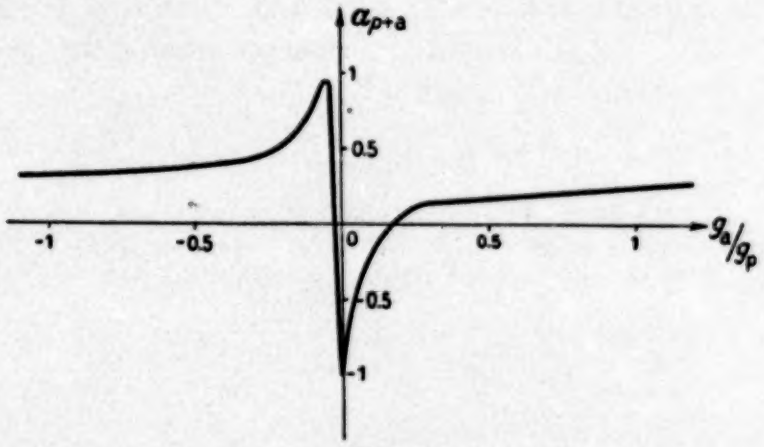

Fig. 1

It should be noted that for comparable values of the constants g_p and g_a, the values of the coefficient α^{p+a} will be very close to α^a, since a small factor v/c (v = neutron velocity) always accompanies the pseudoscalar constant. Conversely, if the experimental value of α is close to α^p, one may be sure that the pseudovector and tensor admixture is insignificant.

It might be mentioned that similar types of formulae can be obtained for

† In accord with experimental data [3]) the antineutrino emitted in β^--decay of nucleons is polarized against its direction of motion. If an antineutrino is emitted as a result of μ^--meson capture the sign of α will be reversed.

μ^--mesons captured by protons bound in a nucleus. Generally speaking, the coefficient α in this case will depend on the nuclear matrix elements, a circumstance which should make the interpretation of the experimental data more difficult. For some light nuclei these matrix elements can be estimated if the final state of the residual nucleus formed as a result of process (1) is known.

Besides anisotropy of the neutron angular distribution another way of determining the type of interaction would be to make use of the fact that neutrons from process (1) are, in general, polarized. This polarization may be transverse as well as longitudinal, part of the latter being due to parity non-conservation, and it should occur even if the captured μ^--mesons are not polarized. The values for the longitudinal polarization P of neutrons produced by capture of unpolarized μ^--mesons by free protons are given in table 2 for the case of a longitudinal neutrino.

TABLE 2

Type of coupling	s	p	v	a	t
P	0	0	0.005	0.64	0.72

The same results also approximately hold for capture of μ^--mesons by nuclei, inasmuch as the nuclear spin-orbit interaction does not change the longitudinal neutron polarization and its depolarization in the Coulomb field of the residual nucleus is insignificant.

References

1) L. Landau, JETP **32** (1957) 405, 407; Nuclear Physics **3** (1957) 127
2) R. L. Garwin, L. M. Lederman and M. Weinrich, Phys. Rev. **105** (1957)
3) C. S. Wu, E. Ambler, R. W. Hayward, D. D. Hoppes and R. P. Hudson, Phys. Rev. **105** (1957) 1413
4) J. Smorodinsky, Uspekhi Fiz. Nauk **56** (1955) 201

Nuclear Physics **4** (1957) 277—281; © *North-Holland Publishing Co., Amsterdam*

Not to be reproduced by photoprint or microfilm without written permission from the publisher

THE SCATTERING OF 181 MeV PROTONS OFF HELIUM

H. TYRÉN, G. TIBELL AND TH. A. J. MARIS

The Gustaf Werner Institute for Nuclear Chemistry, University of Uppsala

Received 17 May 1957

Abstract: The energy spectra of 181 MeV protons scattered off helium have been recorded with a magnetic analyser. Gaseous helium was used as a target, and four angles were studied: 10°.2, 14°.2, 18°.2, and 23°.2.

1. Experimental Arrangements and Procedure

This is a preliminary report of a study of the scattering of 181 MeV protons from helium performed at this Institute.

The energy spectra of the protons scattered from a 150 atm gaseous He^4 target have been measured at four angles with a magnetic analyser [1]). The essentials of the experimental technique have been described earlier [2]).

The high pressure chamber used for the gas was made of duralumin, and a section of it is shown in fig. 1. The alignment of the chamber was checked photographically, and care was taken to avoid that any part of the beam struck the top or the bottom of the chamber volume. The proton beam entered and left the chamber through oval-shaped 2.5 mm thick windows in the wall (marked b and c in the figure). The scattered beam left the chamber through windows of the same thickness. These were designed for each of the scattering angle intervals 15°—30°, 30°—45° etc. For angles smaller than 15° the scattered beam passed through the same window as the main beam. The target thickness was defined by a collimator fixed to the outer rim of the chamber and the entrance slit of the magnetic analyser.

For the purpose of calibration the gas chamber was filled with hydrogen and the experiment repeated. From the known p—p cross sections differential cross sections for the protons scattered off helium could be calculated taking the known energy dependence of the transmission of the analyser into account.

2. Results

The results are presented in fig. 2, where the cross sections are given as a function of the excitation energy of the helium nucleus for each of the four angles studied. Representative statistical errors are shown. The cross section scale is thought to be good to 15 %.

The peak in the cross section at about 23 MeV excitation energy is caused by inelastic scattering on He^4 nuclei. The evidence for this comes both from

the various background tests made with the chamber and from the fact that the corresponding energy after the centre of mass transformation is constant for the four angles.

The elastic peaks of the spectra have half widths of about 2 MeV. Because of this limited resolution it was quite possible to miss a fine structure of the

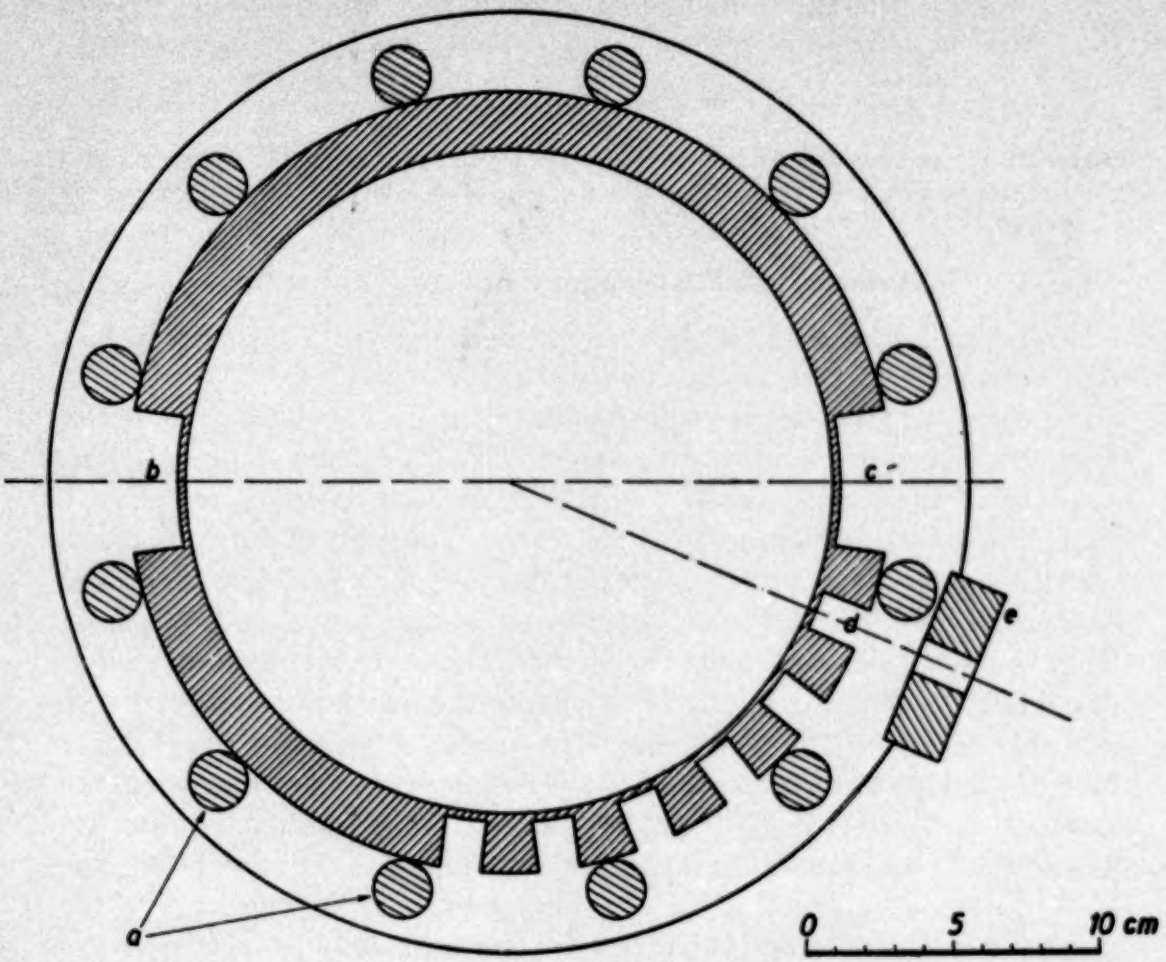

Fig. 1. Section of the high pressure chamber.

a: Steel screws. *b*: Main beam entrance. *c*: Exit of unscattered beam. *d*: Exit for 15°—30° scattering angle. *e*: Collimator.

observed peak at 22.7 ± 0.4 MeV. The maxima shown in the figures are too broad to correspond to an ordinary level. On the other hand a calculation with the impulse approximation would probably show that they are too narrow to be accounted for by a simple break-up of the nucleus. For the moment it seems to be a matter of taste whether the maximum should be said to be due to one or more virtual levels of very small life time or to a break-up of the nucleus by a knock-on collision in which the wave function of the slow knocked-out nucleon is strongly distorted by the residual nucleus.

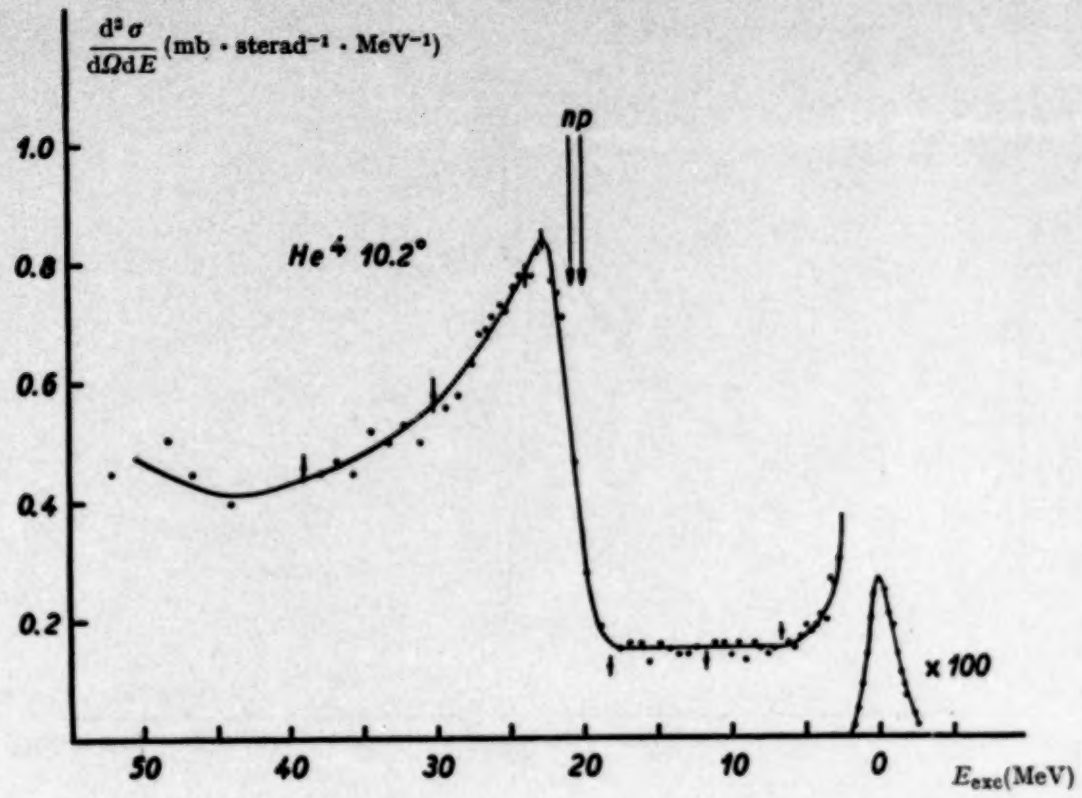
$\frac{d^2\sigma}{d\Omega dE}$ (mb · sterad^{-1} · MeV^{-1})
np
He^4 10.2°
1.0
0.8
0.6
0.4
0.2
x 100
50
40
30
20
10
0
E_{exc}(MeV)

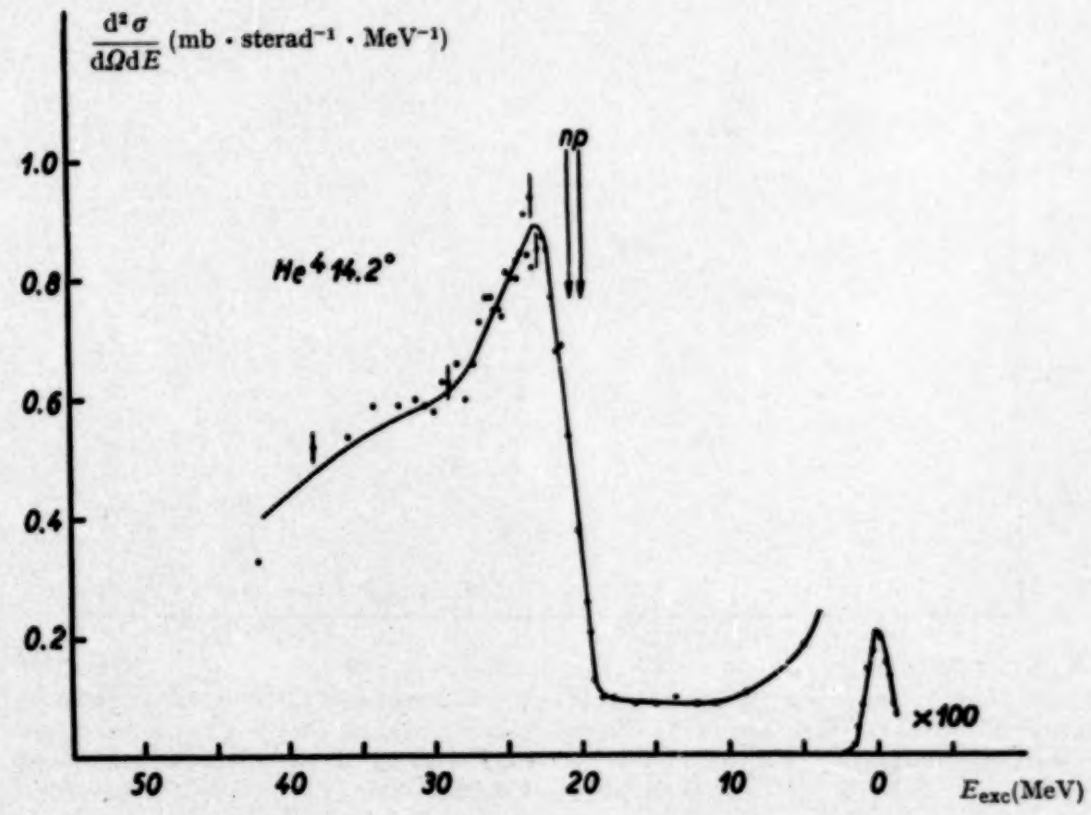
$\frac{d^2\sigma}{d\Omega dE}$ (mb · sterad^{-1} · MeV^{-1})
np
He^4 14.2°
1.0
0.8
0.6
0.4
0.2
x100
50
40
30
20
10
0
E_{exc}(MeV)

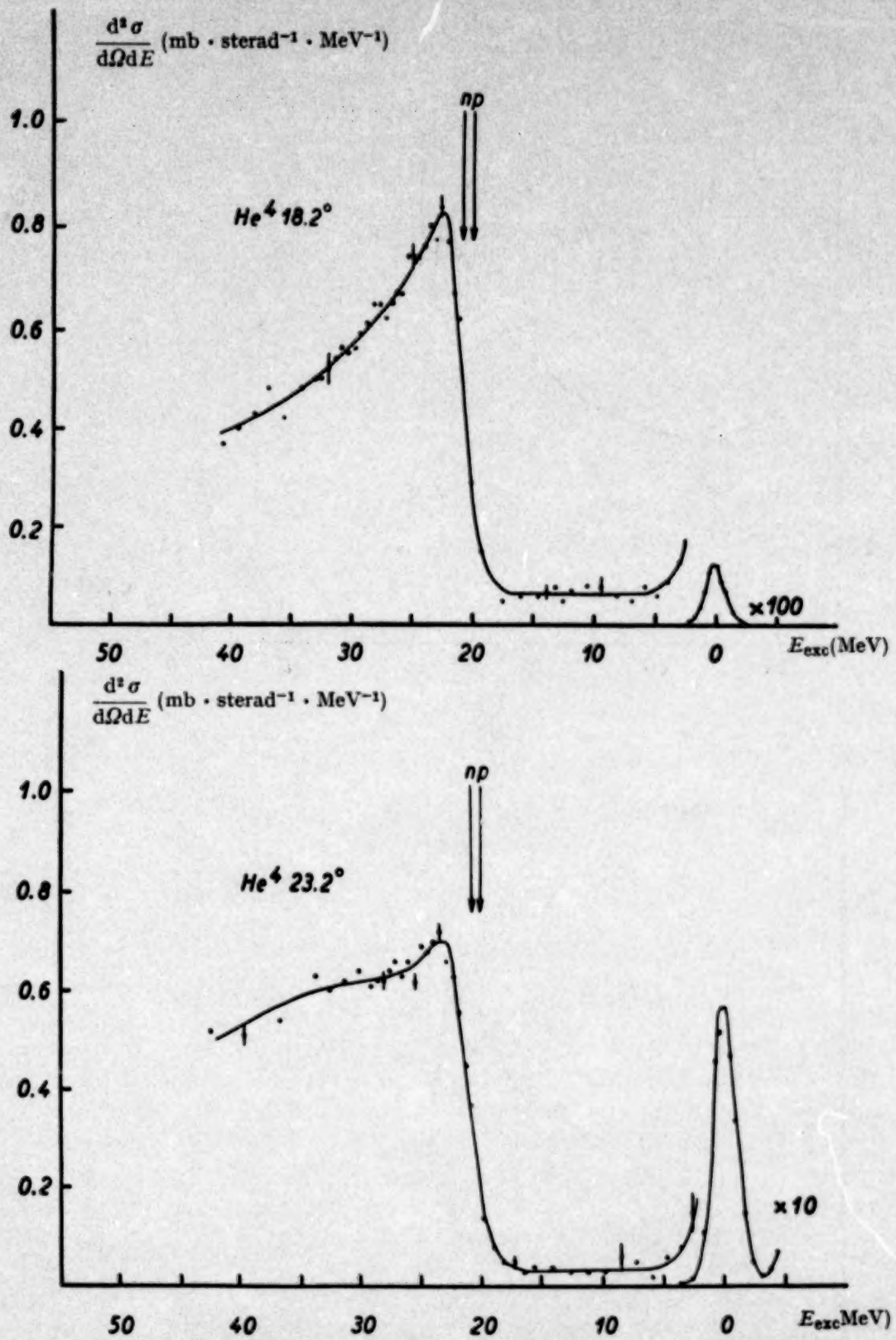

Fig. 2. The differential cross section of 181 MeV protons scattered off He^4 versus energy loss in the centre of mass system. The cross section and scattering angle are given in the laboratory system. Representative statistical errors are shown. The separation energies for a neutron and a proton are indicated.

We hope to come back to this question after having improved and extended the measurements with a liquid helium target.

The authors wish to thank Professor The Svedberg for his interest in this work. Thanks are also due to Mr K. Ståhl who constructed the high pressure chamber and to the cyclotron crew headed by Mr. Å. Svanheden for assistance during the runs. The work has been supported by the Swedish Atomic Energy Commission.

References

1) A. Lovati and H. Tyrén, Journ. Sci. Instr. **33** (1956) 151
2) H. Tyrén and Th. A. J. Maris, Nuclear Physics **3** (1957) 52

Nuclear Physics 4 (1957) 282—286; © *North-Holland Publishing Co., Amsterdam*
Not to be reproduced by photoprint or microfilm without written permission from the publisher

I.D.1
I.E.1

SHELL MODEL INTERPRETATION OF ENERGY LEVELS IN Li^7 AND Be^7

JERRY B. MARION†
Department of Physics, University of Rochester, Rochester, New York ††

Received 15 May 1957

Abstract: The experimental evidence regarding the energy levels in Li^7 and Be^7 is reviewed and compared with the predictions of the shell model near the *LS* limit. It is found that the nucleon and α-particle reduced widths strongly favor the 7.45-MeV state in Li^7 and the 7.13-MeV state in Be^7 being the $J = 5/2$ members of the ^4P multiplets rather than of the ^2F multiplets as previously assumed. None of the available experimental results is inconsistent with this identification. The location and a possible method for detecting the $^2F_{5/2}$ level is discussed. It is also suggested that the broad level structure near 6.5 MeV in Li^7 and Be^7 is not adequately described by the simple model proposed by Lane, and an alternative explanation is presented.

1. Introduction

The ordering of levels in the $A = 7$ polyad has been calculated in intermediate coupling approximately by Inglis [1]) and more completely by Kurath [2]). These results show the following ordering for the odd parity states (in *LS* notation): $^2P_{3/2}$, $^2P_{1/2}$, $^2F_{7/2}$, $^2F_{5/2}$, $^4P_{5/2}$, etc. The only established $J = 5/2^-$ levels are found at 7.45 MeV in Li^7 and 7.13 MeV in Be^7. These states have long been thought to be the upper members of the ^2F doublets, and the lowest level of the ^4P multiplet has been supposed to lie at a somewhat higher energy. The lower levels of the ^2F multiplets have been considered to be the states near 4.6 MeV which are known in both members of the polyad. If the states near 7.3 MeV and 4.6 MeV comprise the ^2F doublets, the splitting is approximately 6 times ††† the splitting of the ^2P doublets which are well established as the ground and first excited states. Difficulties in reconciling this result with the splitting ratio in the *LS* limit * led Meskhov and Ufford[3]) to suggest that the 7.3-MeV levels were actually members of the ^4P multiplet and that the $^2F_{5/2}$ levels were at lower energies. Consideration of the nucleon

†Now at the University of Maryland, College Park, Maryland.

†† Supported in part by the U.S. Atomic Energy Commission.

††† Actually, the energies of the states should be corrected for the level shifts Δ_λ before the splitting ratios are calculated. With this correction, the 7.3-MeV states are shifted upwards by about 0.4 MeV while te 4.6-MeV states undergo lesser shifts, thereby increasing the splitting ratio to about 7.

* If the states involved are all of the pure $[\alpha] = [3]$ space symmetry type, then the splitting ratio is 7/3 (see ref. [16]); however, if an admixture of $[\alpha] = [21]$ is allowed in the ^2P states, then the ratio can reasonably be made as large as 4, but certainly not as large as 6 (see ref. [4])).

and α-particle reduced widths of the 7.3- and 4.6-MeV levels led French and Fujii [4]) to a similar hypothesis. Additional experimental evidence which has recently become available now practically insures that the interpretation of the 7.3-MeV states as being $^4P_{5/2}$ levels is indeed correct.

2. Interpretation of Experimental Results

2.1. NUCLEON REDUCED WIDTHS

An analysis of the scattering of neutrons by Li^6 has established [5]) that the 7.45-MeV state in Li^7 is formed by p-wave neutrons and has $J = 5/2^-$. The $Li^6(n\alpha)$ and $Li^6(p\alpha)$ reactions have been extensively investigated in the region of the 7.3-MeV levels, and the situation with regard to both reactions has recently been discussed by Marion, Weber, and Mozer [6]) who extracted the resonance parameters for the 7.45-MeV state in Li^7 and the 7.13-MeV state in Be^7. On the basis of the $J = 5/2^-$ identification from the neutron scattering experiment, the dimensionless reduced nucleon widths † of these levels were found to be $\theta_n^2(Li^{7*}, 7.45\ MeV) = 0.26$ and $\theta_p^2(Be^{7*}, 7.13\ MeV) = 0.24$. The close agreement between these reduced widths confirms the expectation that these are mirror levels and fixes the J-value of the Be^7 level as $5/2^-$.

The fact that these states are formed by p-wave nucleons and have rather large reduced widths immediately casts doubt on the interpretation that these are $^2F_{5/2}$ levels, since in this case the widths should be vanishingly small near the LS limit. The ratio of the reduced width θ^2 to the single-particle reduced width θ_0^2 should be $S = \theta^2/\theta_0^2 = 2/3$ for the $^4P_{5/2}$ states in the LS limit [4]). Under the assumption that the 7.3-MeV states are pure $^4P_{5/2}$ states and using the measured values for θ^2, one finds $\theta_0^2 = 0.38$, a value quite close to that predicted by Lane [7]) on the basis of a modified harmonic oscillator potential.

2.2. α-PARTICLE REDUCED WIDTHS

Values of the α-particle reduced widths of the 7.3-MeV levels have also been obtained [6]) from the $Li^6(n\alpha)$ and $Li^6(p\alpha)$ experiments. In both cases the values are quite small: $\theta_\alpha^2(Li^{7*}, 7.45\ MeV) = 0.0085$ and $\theta_\alpha^2(Be^{7*}, 7.13\ MeV) = 0.048$. The corresponding reduced width of the 4.58-MeV level in Be^7 has been obtained by Phillips and Miller [8]) from a study of the He^4+He^3 scattering: $\theta_\alpha^2(Be^{7*}, 4.58\ MeV) = 0.31$. This level is certainly the $^2F_{7/2}$ state predicted [1,2]) to lie near this energy. If it is assumed that the 4.61-MeV state in Li^7 is the analogue state and also has $J = 7/2^-$, then the α-particle reduced width may be deduced from the 0.3 ± 0.1 MeV width of this level observed [9]) in the $Li^6(dp)Li^7$ reaction: $\theta_\alpha^2(Li^{7*}, 4.61\ MeV) = 0.5\pm0.2$. Due to the

† Notation $\theta^2 = \gamma^2 \times (2MR/3\hbar^2)$; R is taken to be $1.45 \times (A_1^{1/3}+A_2^{1/3}) \times 10^{-13}$ cm throughout.

limited accuracy of this measurement, the value of $\theta_\alpha^2(Li^{7*}, 4.61\ MeV)$ cannot be considered significantly different from $\theta_\alpha^2(Be^{7*}, 4.58\ MeV)$.

If the 4.6- and 7.3-MeV states were the components of the ^2F doublets, the α-particle reduced widths of these levels should be equal. The experimental results indicate discrepancies of a factor of about 60 in Li^7 and of 6.5 in Be^7. However, if the 7.3-MeV states are actually to be identified as $^4P_{5/2}$, then α-particle emission would be forbidden in the LS limit since $l_\alpha = 3$ uniquely, whereas $\Delta L = 1$. Any admixture of $^2F_{5/2}$ in these levels † or of D states in the α-particle and He^3 or H^3 would of course allow α-particle emission, but such admixtures are expected to be small, thereby yielding only small values of the α-particle reduced widths. As a result, the large ratio of $\theta_\alpha^2(Be^{7*}, 7.13\ MeV)$ to $\theta_\alpha^2(Li^{7*}, 7.45\ MeV)$, which previously was disturbing if the states were to be identified as mirror levels [6]), can now be understood. Since the α-particle widths of these states should vanish except for the admixtures noted above, and since the Coulomb effects can be quite different in the two cases because of the low Z, there is no reason to expect the perturbations to be identical, and a difference of a factor of 6 in the θ_α^2 is not at all unreasonable.

2.3. THE BROAD LEVELS

Broad level structure near 6.6 MeV in Li^7 has been observed in the $Li^6(dp)Li^7$ reaction [9,10]) and in the $Be^9(d\alpha)Li^7$ reaction [11]). Similar structure has been found in Be^7 near 6.4 MeV in the $Li^6(p\alpha)He^3$ reaction [6,12]), in the $B^{10}(p\alpha)Be^7$ reaction [13]), and in the $Li^6(p\gamma)Be^7$ reaction [14]). Lane [7]) interprets these results together with the large thermal neutron cross section of Li^6 as indicating $J = 1/2^+$ and $J = 3/2^+$ levels arising from the coupling of an s-nucleon to a Li^6 core, i.e., configurations of $[^3S \times s]_{J=\frac{1}{2}}$ and $[^3S \times s]_{J=\frac{3}{2}}$, where the letters specify the states of the Li- core and the extra nucleon respectively, and the cross means "coupled to."

The large effect that the broad levels have on the $Li^6(p\alpha)$ reaction near $E_p = 1$ MeV and on the $Li^6(n\alpha)$ reaction at thermal energies indicates s-wave formation with large reduced widths for both the nucleons and the α-particles. Also, the angular distributions of the α-particles from the $Li^6(p\alpha)$ reaction show marked asymmetries even at low bombarding energies [6,12]). This indicates interference between states of opposite parity formed by the same channel spin. Since one of these levels is the $J = 5/2^-$ state at 7.13 MeV which is formed by channel spin 3/2, the other level must have $J = 3/2^+$ if it is formed by s-waves. Under the assumption that only these two levels contribute to the cross section, the low energy angular distributions can be qualitatively explained. However, the distributions cannot be fitted in

† The ^2F and ^4P multiplets can be coupled directly by a tensor force; coupling is also possible through the spin-orbit part of the interaction, but only through D states and hence in second order.

detail by this simple assumption [6]), and seem to indicate the presence of at least one additional level. This state cannot be the $[^{13}S \times s]_{J=\frac{1}{2}}$ level alone, since it would be formed by channel spin $\frac{1}{2}$ and therefore would be incoherent with the formation of the other two states. This would only add an isotropic background to the cross section and could not bring the distributions calculated on the two-level assumption into agreement with experiment regardless of the magnitude of the isotropic term. A further difficulty is that a state of the configuration $[^{13}S \times s]_{J=3/2}$ could not, by orbital angular momentum conservation, be expected to contribute any appreciable α-particle width as is required by experiment. Thus it appears that Lane's simple model is inadequate to explain the broad levels near 6.5 MeV.

A possible and reasonable explanation is that these states are both single $J = 3/2^+$ levels arising naturally from the first excited configurations of 7 nucleons: s^4p^2s, s^4p^2d, and s^3p^4. The large nucleon widths required would then be the result of the s-component, $[^{13}S \times s]_{J=3/2}$, and the large α-particle widths would be allowed by any of the d-components, $[^{13}S \times d]_{J=3/2}$, $[^{13}D \times s]_{J=3/2}$, etc. It should be noted that the occurrence of the $^2F_{5/2}$ states in the neighbourhood of the 6.5-MeV levels would not be inconsistent with the above model since the formation of an F state by low energy particles is greatly inhibited by the large angular momentum transfer.

It is not yet clear whether the broad level in Be^7 plays an appreciable role in the $Li^6(p\gamma)Be^7$ reaction at low energies since conflicting results have been obtained [14,15]). Perhaps the more plausible of the possible explanations is that of Warren *et al.* [15]), who suggest that a direct capture process is involved. In such a case, the $Li^6(p\gamma)Be^7$ reaction cannot furnish information regarding the character of the levels in this region.

3. Location of the $^2F_{5/2}$ Levels

If we are now to identify the 7.3-MeV levels in Li^7 and Be^7 as belonging to the ^4P multiplet †, we must ask where the $^2F_{5/2}$ levels are located and how they can be detected. Intermediate coupling calculations [2,4]) indicate that the spacing between the $^2F_{5/2}$ and $^4P_{5/2}$ levels should be about 2 MeV. On this basis the $^2F_{5/2}$ levels would be expected to lie near an excitation of 6 MeV in both Li^7 and Be^7. This would also yield a reasonable value for the $^2F-{}^2P$ splitting ratio.

Under the assumption that both members of the ^2F doublet have the same α-particle reduced widths and negligible nucleon reduced widths, it is pos-

† After this report was prepared it came to the attention of the author that the Princeton group had reached the same conclusion regarding the identification of the 7.45-MeV level in Li^7 based on entirely independent evidence, viz., the comparison of the cross section ratios to the ^2F and $^4P_{5/2}$ states in the Li^7 (pp′) reaction to those calculated from direct-interaction distorted-wave theory [17]).

sible to estimate the centre-of-mass width of the $^2F_{5/2}$ levels to be approximately 1 MeV. Since other states of about this width are also located near the same energy in both nuclei, the firm experimental identification of the $^2F_{5/2}$ levels would appear to be difficult. The most promising line of approach is probably a continuation to higher energies of the He^4+He^3 scattering, since the Rice experiment [8]) was limited by the available bombarding energy to an investigation of the region in Be^7 below about 5 MeV. In order to study the region up to 7 MeV, bombarding energies of 9.5 MeV will be required for the He^3 particles or up to 12 MeV if α-particles are accelerated. The behavior of the f-wave phase shifts in this energy region will probably be the most satisfactory method of identifying the $^2F_{5/2}$ level. Even though s- and d-states will also be expected to contribute to the scattering, the f-wave contribution should be detectable since the penetrabilities for $l = 0$, 1, 2, and 3 are in the ratio 1 : 0.85 : 0.57 : 0.25 in this energy region and α-particle emission from the $^2F_{5/2}$ level should be strong.

The author is indebted to Professor J. B. French for several helpful discussions of this problem.

References

1) D. R. Inglis, Revs. Mod. Phys. **25** (1953) 390
2) D. Kurath, Phys. Rev. **101** (1956) 216
3) S. Meshkov and C. W. Ufford, Phys. Rev. **101** (1956) 734
4) J. B. French and A. Fujii, Phys. Rev. **105** (1957) 652
5) Johnson, Willard, and Bair, Phys. Rev. **96** (1954) 985; Williard, Bair, and Kington, Phys. Rev. **101** (1956) 765
6) Marion, Weber, and Mozer, Phys. Rev. **104** (1956) 1402
7) A. M. Lane, Atomic Energy Research Establishment Report T/R 1289 (1954)
8) G. C. Phillips and P. Miller, Bull. Am. Phys. Soc. **2** (1957) 28
9) Levine, Bender, and McGruer, Phys. Rev. **97** (1955) 1249
10) L. M. Khromchenko and V. A. Blinov, Soviet Phys. JETP **1** (1955) 596; Zhur. Eksp. i Teoret. Fiz. **28** (1955) 741
11) J. J. Jung and P. Cuer, J. Phys. Radium **17** (1956) 555
12) S. Bashkin and H. T. Richards, Phys. Rev. **84** (1951) 1124
13) J. B. Reynolds, Phys. Rev. **98** (1955) 1289
14) S. Bashkin and R. R. Carlson, Phys. Rev. **97** (1955) 1245
15) Warren, Alexander, and Chadwick, Phys. Rev. **101** (1956) 242
16) E. Feenberg and E. Wigner, Phys. Rev. **51** (1937) 597
17) D. R. Maxon and E. F. Bennett, Bull. Am. Phys. Soc. **2** (1957) 180 and verbal report; C. A. Levinson and M. K. Banerjee, NYO-8010 (1957) (unpublished)

NEWS ITEMS

NORTHWESTERN UNIVERSITY CONFERENCE ON LIQUID SCINTILLATION COUNTING

(EVANSTON, 20–22 AUGUST 1957)

The National Science Foundation has made an award of $ 4000 to Northwestern University to support in part the Northwestern University Conference on Liquid Scintillation Counting to be held on August 20–22, 1957, at the Technological Institute, Evanston, Illinois. The grant will be used to bring five specialists to the conference from England, France, Germany, and the Sarre.

The Conference will be the first devoted exclusively to Liquid Scintillation Counting and will cover most phases of the field in theory and applications: coincidence counters, single channel counters, chemistry of liquid scintillators, and applications in biology and medicine, industry, archaeology, physics, chemistry and engineering.

Persons interested in giving short papers at the conference are invited to submit abstracts to Dr. F. N. Hayes, Los Alamos, New Mexico. Other information can be supplied by C. G. Bell, Northwestern University, Evanston, Illinois.

There will be no commercial sponsors of the conference and it will not be conducted for profit.

PRELIMINARY PROGRAM

20 August (morning)

Chairman: C. G. Bell

Welcoming Remarks:
Opening Address: H. Kallman, New York University
Limits of Sensitivity of Liquid Scintillation Counters: R. K. Swank, Argonne National Laboratory

20 August (afternoon)
Instrumentation Session

Chairman: E. C. Anderson

R. D. Hiebert, Los Alamos Scientific Laboratory
L. F. Slattery, Remington-Rand Corporation
L. E. Packard, Packard Instrument Company
G. R. Utting, Technical Measurement Corporation
R. Steele, Brookhaven National Laboratory
T. S. Hodgson, Shell Oil Company

21 August (morning)
Round-Table Discussion on Chemistry of the Counting Solution

Chairman: F. N. Hayes

J. D. Davidson, National Institutes of Health
S. Helf, Picatinny Arsenal
D. G. Ott, Los Alamos Scientific Laboratory
N. S. Radin, Veterans Research Hospital, Chicago
H. H. Seliger, National Bureau of Standards

21 August (afternoon)
General Applications

Chairman: D. G. Ott

Archaelogy and Chemistry: J. R. Arnold, Princeton University
Biology and Medicine: W. H. Langham, Los Alamos Scientific Laboratory
Engineering: C. G. Bell, Northwestern University
Industry: V. P. Guinn, Shell Development Company
Physics: F. B. Harrison, Los Alamos Scientific Laboratory

22 August
Specific Applications (short contributed papers)

CONFERENCE ON EXTRA-ATMOSPHERIC COSMIC RADIATION RESEARCH (BALTIMORE, MARCH 29, 1957)

On March 29, 1957 a conference of a group of cosmic ray physicists interested in the application of emulsion techniques and a number of engineers and government scientists interested in the scientific application of rockets was held in Baltimore under RIAS sponsorship. The main business of the conference was the consideration of the possibility of studying by the use of nuclear emulsions cosmic ray primaries outside the atmosphere, and in particular, of detecting the presence of any hitherto unobserved component of a low penetrating power.

Mr. R. Patterson and Mr. W. J. Benckert, engineers of the Advanced Design Department of the Martin Company of Baltimore, presented a preliminary design of a vehicle which would allow an oriented stack of 50 pounds of emulsions to be exposed for 40 minutes with a total shielding of less than 0.1 g/cm^2 while outside the atmosphere. This vehicle, which is to be launched in a vertical shot, would be capable of preserving the emulsion during re-entry into the earth's atmosphere and the eventual fall to earth. During the subsequent discussion, it became evident that such a vehicle could also be used to great advantage for a number of other experiments without interfering with the emulsion studies.

In view of the great scientific potentialities of such a cosmic ray experiment, the physicists formed a committee to consider it in more detail and to arrange a program of cooperative research of all interested scientists at such time as the vehicle is launched. The membership of the committee is: G. Groetzinger (chairman), M. F. Kaplon, S. A. Korff, E. P. Ney, W. J. Otting, A. Pevsner, M. Pomerantz, B. Rossi, M. Schein, M. M. Shapiro, S. Silverman, and H. Yagoda. In a subsequent meeting the committee chose to designate itself as "National Committee for Extra-Atmospheric Cosmic Ray Research" and to consider also the possibility of other new extra-atmospheric cosmic ray experiments. At this meeting, J. A. Simpson joined the committee and W. A. Benckert was designated a consultant.

ELECTRON MICROSCOPE SOCIETY OF AMERICA

The Annual Meeting of the Electron Microscope Society of America will be held at the Massachusetts Institute of Technology, Boston, Mass. on September 9, 10 and 11, 1957. The address of the Society is: Chrysler Corporation, P.O.Box 1118, Detroit 31, Michigan (D. Maxwell Teague, Secretary).

Nuclear Physics **4** (1957) 289—294; © *North-Holland Publishing Co., Amsterdam*
Not to be reproduced by photoprint or microfilm without written permission from the publisher

THE CLASSIFICATION OF STATES OF SURFACE VIBRATIONS

G. RAKAVY

CERN *Theoretical Study Division at the Institute for Theoretical Physics, University of Copenhagen* †

Received 13 April 1957

Abstract: The classification of surface oscillations is improved by introducing an additional quantum number which is specially suitable for the treatment of "γ-unstable oscillations". A selection rule implied by this quantum number is discussed.

1. Introduction

In the theory of surface vibrations of order λ [1]) the problem arises of the classification of the states of a $(2\lambda+1)$-dimensional oscillator according to angular momenta. In the most interesting case of surface oscillations of order two the first few low-lying states may be uniquely classified by means of the total excitation N, the angular momentum I, and its z-component M. For an excitation $N = 4$ or higher several states with the same I and M appear, and additional quantum numbers are needed to distinguish among them. In this note elementary group theory is used to construct an additional quantum number, which turns out to be suitable for the classification of the states also in the general case of "γ-unstable oscillations" [2]).

2. The Multidimensional Oscillator

We define a $(2\lambda+1)$-dimensional space with coordinates x_m $(m = \lambda, \lambda-1, \ldots, 0, \ldots, -\lambda)$. A set of coordinates x_m corresponds to a given set of coordinates XYZ in ordinary 3-dimensional space; if we rotate the XYZ system by Eulerian angles $\alpha\beta\gamma$, the coordinates x_m transform to new coordinates x'_m by means of the matrix $D^{\lambda}(\alpha\beta\gamma)$. We furthermore impose on the (complex) coordinates x_m the conditions

$$x_m^* = (-)^m x_{-m}. \tag{1}$$

It may sometimes be convenient, instead of the complex coordinates x_m, to use real coordinates q_i defined by

† Permanent address: Hebrew University, Jerusalem, Israel.

$$x_m = \frac{1}{\sqrt{2}}(q_m + iq_{\lambda+m})$$
$$x_0 = q_0 \qquad (m > 0) \tag{2}$$
$$x_{-m} = \frac{(-1)^m}{\sqrt{2}}(q_m - iq_{\lambda+m}).$$

The Hamiltonian of the system is defined as follows:

$$\begin{aligned} H &= -\tfrac{1}{2}\sum_{m=-\lambda}^{+\lambda}(-)^m \frac{\partial^2}{\partial x_m\,\partial x_{-m}} + \tfrac{1}{2}\sum_{m=-\lambda}^{+\lambda}(-)^m x_m x_{-m} \\ &= -\tfrac{1}{2}\sum_{i=0}^{2\lambda}\frac{\partial^2}{\partial q_i^2} + \tfrac{1}{2}\sum_{i=0}^{2\lambda} q_i^2 \equiv \sum H_i \end{aligned} \tag{3}$$

and the scalar product of states $\psi_1(x)$ and $\psi_2(x)$ is defined to be

$$(\psi_1(x), \psi_2(x)) = \int_{-\infty}^{+\infty}\int_{-\infty}^{+\infty}\cdots\int_{-\infty}^{+\infty}\psi_1^*(x)\psi_2(x)\prod_0^{2\lambda} dq_i. \tag{4}$$

We now proceed to write down the eigenstates of the Hamiltonian (3) with the aid of the creation and annihilation operators defined as follows:

$$\begin{aligned} \bar{a}_m &= \frac{1}{\sqrt{2}}\left\{(-)^m x_m - \frac{\partial}{\partial x_{-m}}\right\} \\ a_m &= \frac{1}{\sqrt{2}}\left\{x_{-m} + (-)^m\frac{\partial}{\partial x_m}\right\}. \end{aligned} \tag{5}$$

These operators satisfy the usual commutation rules

$$\begin{aligned} [a_k, a_{k'}] = [\bar{a}_k, \bar{a}_{k'}] &= 0, \\ [a_k, \bar{a}_{k'}] &= \delta_{kk'} \end{aligned} \tag{6}$$

and transform with the matrices $D^{\lambda}(R_3)$ and $D^{-1} = D^{*\lambda}(R_3)$, respectively.

The "reality conditions" (1) are satisfied if $\bar{a}_m$ is represented by the hermitian conjugate matrix of a_m, and consequently we may use the usual representation of these operators. The set of orthonormal states

$$C\,\bar{a}_{m_1}\bar{a}_{m_2}\ldots\bar{a}_{m_N}|0\rangle, \tag{7}$$

where

$$|0\rangle = \pi^{-\lambda-\frac{1}{2}}\exp\{-\tfrac{1}{2}\textstyle\sum(-)^m x_m x_{-m}\} = \pi^{-\lambda-\frac{1}{2}}\exp\textstyle\sum -\tfrac{1}{2}q_i^2$$

and

$$C = [\prod_m (N_m!)]^{-\frac{1}{2}}$$

(N_k = number of times the index k appears in the row $m_1 m_2 \cdots m_n$), span the space of eigenstates of excitation N.

3. Classification of the States

To linear transformations of the operators $\tilde{a}_m$:

$$\tilde{a}'_m = \sum C_{mn} \tilde{a}_n, \tag{8}$$

correspond linear transformations of the states (7), in fact, they transform like symmetrical tensors of rank N. The space of symmetrical tensors is irreducible under the linear group †, but if we restrict the transformations (5) to orthogonal transformations, the tensor space may be reduced into subspaces by the process of contraction [3]). The space of symmetrical tensors of rank N breaks up into a traceless space and trace spaces of orders $v = (N-2); v = (N-4)$ etc. A trace space of order v transforms like the traceless part of the space of symmetrical tensors of rank v (occasionally we shall refer to v as "seniority").

We define our orthogonal group $R_{2\lambda+1}$ as the group of all transformations (8) leaving invariant the quadratic form

$$\sum (-)^m \tilde{a}_m \tilde{a}_{-m}. \tag{9}$$

This form is kept invariant by the transformations $D^{\lambda}(\mathrm{R}_3)$, and consequently the group $D^{\lambda}(\mathrm{R}_3)$ is contained in $\mathrm{R}_{2\lambda+1}$. It should also be remarked that the transformations belonging to the orthogonal group $R_{2\lambda+1}$ are in fact simple coordinate transformations in the x_m space while the general linear transformations (8) are not. Consequently the transformations of $\mathrm{R}_{2\lambda+1}$ leave invariant also the form

$$r^2 = \sum (-)^m x_m x_{-m}. \tag{10}$$

Finally we reduce each subspace (v) into its irreducible invariant parts with respect to the group of transformations $D^{\lambda}(\mathrm{R}_3)$. Each is a basis for some representation $D^{I}(\mathrm{R}_3)$ and will be designated by I. We may now classify the states by the row of quantum numbers N, V, I, M describing the row of subspaces with respect to $\mathrm{R}_{2\lambda+1}$, R_3, and R_2 in which the state lies. This classification is not complete because a certain I may appear more than once in a given subspace (v), however, this does not occur for small values of the seniority (for example: for $\lambda = 2$ the first case occurs at $v = 6$ when $I = 6$ appears twice).

The reduction of the space (v) into its subspaces I may be achieved directly by using methods of group theory, but it is also possible to achieve it by an elementary procedure: First one breaks up the total space of states of a given excitation into the subspaces I. This is achieved simply by counting

† The state of a group of particles in an oscillator well may be written in a way similar to eq. (7). In this case some of the creation operators refer to particle no. 1, some to particle no. 2 etc. The states are not completely symmetrical, and the tensor space may be split up into invariant subspaces under the linear group. This procedure may provide useful quantum numbers.

the M values: let k_m be the number of times the factor a_m occurs in (7), then, corresponding to a rotation φ around the Z-axis the state (7) is multiplied by $\exp iM\varphi$, where

$$M = \sum_{m=-\lambda}^{+\lambda} mk_m \quad (\sum_{m=-\lambda}^{+\lambda} k_m = N). \tag{11}$$

Let us denote the number of solutions of equations (11) (i.e. the number of states with the given M) by $b_N(M)$. The number of times a subspace of given I occurs in the space of symmetrical tensors of rank N is

$$c_N(I) = b_N(M = I) - b_N(M = I+1), \tag{12}$$

and finally we obtain the number of times I appears in (v):

$$d_v(I) = c_v(I) - c_{v-2}(I). \tag{13}$$

In the following table the reduction of the first few subspaces of lowest seniority is given for vibrations of order $\lambda = 2$:

TABLE 1

$d_v(I)$ $(\lambda = 2)$

v \ I	0	1	2	3	4	5	6	7	8	9	10	11	12
0	1												
1			1										
2			1		1								
3	1			1	1		1						
4			1		1	1	1		1				
5			1		1	1	1	1	1		1		
6	1			1	1		2	1	1	1	1		1

If we can find a subgroup of $R_{2\lambda+1}$ which contains $D^\lambda(R_3)$, we may perform the reduction of the spaces (v) into I in two steps. First we reduce (v) into invariant irreducible subspaces with respect to this additional group (let us classify them by some symbol (u)), and then proceed to reduce each space (u) into the subspaces I. This procedure yields an additional quantum number (u), which may serve to distinguish among states with the same I appearing in the same space (v). An example of such an additional group occurs for vibrations of order $\lambda = 3$. The group R_7 has a special subgroup denoted G_2 which in turn contains $D^3(R_3)$ as subgroup.

There exists an alternative starting point for our discussion: Instead of using the fact that the space of states (7) is invariant (and irreducible) under the general linear transformations (8), we could base our discussion on the fact that the Hamiltonian (3), which can also be written in the form: $\sum \{a_m \bar{a}_m\}$, is invariant under the linear transformations (8), provided we *define* the transformations of the a_m's to be contragredient to those of the $\bar{a}_m$'s.

4. Modification of the Hamiltonian by Terms Depending on r^2 ("γ-Unstable Oscillations")

If the Hamiltonian (3) is modified by a function of r^2 only, the eigenstates of the modified Hamiltonian can no longer, generally, be written in the form (7), and N is no longer a good quantum number. Yet, as r^2 is invariant under the orthogonal transformations ($R_{2\lambda+1}$), the seniority (v) remains a good quantum number (the same applies obviously to I and M). This means that the degeneracy between states lying in the same irreducible space (v) is not lifted when such a modification is introduced into the Hamiltonian, and that selection rules implied by the seniority quantum number remain valid. A simple example of a selection rule is the one for electric 2^λ-pole radiation: The operator in question is proportional to x_m [4]). The coordinate x_m has matrix elements only between states with a seniority difference of ± 1. This is easily seen in the following way: By multiplying traceless tensors of the rank v by x's, we get tensors of rank $v+1$. These tensors may be split into traceless parts (i.e. states of seniority $v+1$) and trace parts which are obtained by a single contraction. Further contractions are impossible as these will include two indices of the original traceless tensors. Thus the trace space is irreducible and is equivalent to the space of traceless tensors of rank $(v-1)$ (i.e. contains only states of seniority $v-1$). The selection rule discussed in ref. [2]) is a special case of our result.

Finally we remark that the Hamiltonian may be separated into a part depending on r^2 only, and another part depending on other (2λ) coordinates, and that the separation constant is simply related to our seniority quantum number v. Introducing, besides r, 2λ coordinates ξ_i, which are homogeneous functions of order zero of the x_m's, the Hamiltonian (3) can be written in the form

$$H = -\tfrac{1}{2}\left\{\frac{1}{r^\lambda}\frac{\partial^2}{\partial r^2}r^\lambda - \frac{\Lambda+\lambda(\lambda-1)}{r^2}\right\}+\tfrac{1}{2}r^2 \qquad (14)$$

(with possibly some function of r added to it), where

$$-\Lambda = \sum P_k \frac{\partial}{\partial \xi_k} + \sum Q_{ij}\frac{\partial^2}{\partial \xi_i \partial \xi_j},$$

$$P_k = r^2 \sum_m (-)^m \frac{\partial^2 \xi_k}{\partial x_m \partial x_{-m}}, \qquad Q_{ij} = r^2 \sum_m (-)^m \frac{\partial \xi_i}{\partial x_m}\frac{\partial \xi_j}{\partial x_{-m}};$$

P_k and Q_{ij} are homogeneous functions of order zero in the x's and consequently depend only on the ξ's. The wave functions may be factored in the form $\psi = r^{-\lambda}\varphi(r)\chi(\xi)$. The equation for $\varphi(r)$ is independent of the number of dimensions; hence we may use the known results from the 3-dimensional case and determine for a given energy the possible values of Λ. We also know that the states of excitation N have seniorities $v = N; N-2 \ldots$; hence we

may easily determine the following connection between Λ and v:

$$\Lambda = v(v+2\lambda-1). \tag{15}$$

References

1) A. Bohr, Mat. Fys. Medd. Dan. Vid. Selsk. **26** (1952) no. 14
2) L. Wilets and M. Jean, Phys. Rev. **102** (1956) 788
3) H. Weyl, The Classical Groups (Princeton U. P., 1939) pp. 150–151
4) A. Bohr and B. Mottelson, Mat. Fys. Medd. Dan. Vid. Selsk. **27** (1953) no. 16

Nuclear Physics 4 (1957) 295—312; © *North-Holland Publishing Co., Amsterdam*
Not to be reproduced by photoprint or microfilm without written permission from the publisher

NUCLEAR MAGNETIC MOMENTS AND THE MANY BODY PROBLEM

J. S. BELL
Atomic Energy Research Establishment, Harwell, Berks.

Received 29 March 1957

Abstract: The Brueckner theory predicts corrections to the shell model moments of even such simple nuclei as N^{15}, O^{17}, and K^{39}. Calculation is difficult because of the many states excited by the model operator. To obtain some notion of orders of magnitude a simple model is examined in which the core is represented by a uniform Fermi gas; the summations then become integrals in momentum space. It is assumed, as is usual in shell model work, that the effective two-body potential can be crudely represented by a static central potential with exchange. The second order corrections are found to be of the same order of magnitude as, but somewhat smaller than, the effect in first order of the usual space-exchange current.

1. Introduction

An attempt is made here to estimate the implications of the Brueckner theory [1]) for nuclear dipole magnetic moments. This work was started in an earlier paper [2]) which was concerned mainly to show that the effective moment operator is not simply related to the effective mass; however some more positive proposals were also made, and these are re-evaluated in the light of the present work in section 7.

We consider only the simplest nuclei, such as N^{15}, O^{17}, and K^{39}, which consist of doubly closed shells in the *LS* sense plus or minus an odd nucleon. For these nuclei the shell model wave function Φ is just a product of two determinants, one for the protons and one for the neutrons. The real wave function Ψ is given by $\Psi = F\Phi$, where F is the "model operator". What we have to compute is the expectation value

$$(F\Phi, \mathbf{M}F\Phi)/(F\Phi, F\Phi) \tag{1.1}$$

of the magnetic moment operator **M**.

To begin with the two-body interaction is assumed to be of the non-singular type usually considered in shell model work. Then we determine F by perturbation theory; this is rather bad for the collision of free nucleons but might be hoped to converge reasonably for the nuclear problem because of the action of the exclusion principle [1]). A difficulty in applying this programme to a finite nucleus is that the expression (1.1) becomes a sum over infinitely many intermediate states. In practice only a finite number of these

would be considered, and the truncation error is not easily estimated. Another difficulty is that of handling self-consistently the fictitious single-body shell model potential. Now, as has been much exploited in the nuclear saturation problem, these difficulties are greatly reduced in an infinite nucleus with essentially plane rather than spherical geometry; the summations over intermediate states become integrals in momentum space, and the single-body potential becomes diagonal in this space. It is our object here to try to extract information on the magnetic moment problem from such an infinite nuclear model.

We consider therefore a system comprising a uniform Fermi gas with all levels filled up to some given energy and with an odd particle in one of the next lowest plane wave states (or with a hole in the topmost level). The odd particle — say a neutron — collides with the particles in the core and in particular shares its momentum to some extent with the protons. Thus a current is induced, and the neutron may be said to develop an effective charge. In a finite nucleus this process gives rise to modification of the orbital magnetic moment. It is felt, although a formal proof cannot be given, that the effective charge calculated from our plane wave model would indeed be that relevant to the magnetic moment of a large nucleus. The nuclei mentioned above are of course not large, and indeed there are no heavy nuclei of this type. Nevertheless it has been thought worthwhile to work out the simplified problem in the hope of obtaining at least some notion of the orders of magnitude involved. The straightforward perturbation theory is developed in section 2—section 5. In section 6 is given the modified formalism associated with an expansion in terms of the Brueckner effective potential t rather than the real potential v, as is required when the latter is singular.

It should be said that our approach is relevant only to the orbital part of the magnetic moment, for it will be seen below that effects depending on spin do not arise naturally in the present model.

2. Formalism

In the simplified problem we have to evaluate

$$\ll \mathbf{J} \gg = \langle F^+ \mathbf{J} F \rangle / \langle F^+ F \rangle \tag{2.1}$$

where $\mathbf{J}$ is the operator of current density; double and single angular brackets denote expectation values in the states Ψ and Φ respectively.

The Schrödinger equation is

$$\mathscr{H}\Psi = E\Psi \tag{2.2}$$

with

$$\mathscr{H} = T + \sum_{i>j} v_{ij} = \sum_i p_i^2/2m + \sum_{i>j} v_{ij} \tag{2.3}$$

where v_{ij}, the two body interaction, is the same for all pairs. This is to be

compared with the model equation

$$\mathscr{H}_0\Phi = E_0\Phi \tag{2.4}$$

where

$$\mathscr{H}_0 = T + \sum_i V_i \tag{2.5}$$

and V_i denotes the effective single-body potential. Treating as a perturbation the difference in the two Hamiltonians,

$$\mathscr{H} - \mathscr{H}_0 = \sum_{i>j} v_{ij} - \sum_i V_i,$$

we have, with $\varepsilon = E_0 - \mathscr{H}_0$,

$$F = 1 + \frac{Q}{\varepsilon}\left\{\sum_{i>j} v_{ij} - \sum_j V_i + \ldots\right\} \tag{2.6}$$

where the omitted terms are of second and higher order. The projection operator Q is defined, in the plane wave representation that we always assume, to eliminate states with $\mathscr{H}_0 = E_0$ and states in which the Pauli principle is violated; the latter requirement is convenient rather than necessary, for contributions from such states would automatically cancel in the calculation as a whole because of the antisymmetry of the wave-functions. Because of the properties of Q, and because F always acts on Φ, we may omit the ΣV that appears explicitly in (2.6) ,for this operator is diagonal in momentum space and so does not excite the model state; of course ΣV still appears implicitly in ε.

The explicit form for $\mathbf{J}$ is determined by the requirement that the interaction energy density with a weak external vector potential $\mathbf{A}$ should be $-\mathbf{A}\cdot\mathbf{J}$. The current in our model will be uniform over space and we need therefore consider only a uniform $\mathbf{A}$. For this reason the ambiguities usually associated with exchange currents do not appear, and it is also for this reason that spin dependent effects are absent. The interaction energy is obtained by the usual rule $\mathbf{p}_j \to \mathbf{p}_j - e_j\mathbf{A}$ (note that we use units with $\hbar = c = 1$). The result may be expressed as

$$\mathbf{J} = \sum e_j \partial\mathscr{H}/\partial\mathbf{p}_j = [\mathscr{H}, i\sum e_j\mathbf{r}_j] \tag{2.7}$$

where e_j is the charge on particle j and $\mathbf{r}_j$ its position. More explicitly

$$\mathbf{J} = \frac{1}{m}\sum_i e_i\mathbf{p}_i + \sum_{i>j}\mathbf{j}_{ij} \tag{2.8}$$

with

$$\mathbf{j}_{ij} = [v_{ij}, i(e_i\mathbf{r}_i + e_j\mathbf{r}_j)]. \tag{2.9}$$

We will refer to $\mathbf{j}_{ij}$ as the exchange current. In a non-relativistic theory v_{ij} commutes with the centre of mass of the two particles, $\mathbf{r}_i + \mathbf{r}_j$, so that $\mathbf{j}_{ij}$ is zero when the nucleons concerned have the same charge; it vanishes com-

pletely of course when v is a static potential without exchange. If we reserve the indices p and n for protons and neutrons respectively, then (2.7) may be written

$$\mathbf{J} = \frac{e}{m} \sum_{\mathrm{p}} \mathbf{p}_{\mathrm{p}} + \sum_{\mathrm{p,n}} \mathbf{j}_{\mathrm{pn}} \tag{2.10}$$

with

$$\mathbf{j}_{\mathrm{pn}} = [v_{\mathrm{pn}}, ie\mathbf{r}_{\mathrm{p}}]. \tag{2.11}$$

To second order in v the perturbation expansion of (2.1), using (2.6) and (2.10), is

$$\ll \mathbf{J} \gg = \frac{e}{m} \sum_{\mathrm{p}} \left\{ \langle \mathbf{p}_{\mathrm{p}} \rangle + \langle \sum v \frac{Q}{\varepsilon} (\mathbf{p}_{\mathrm{p}} - \langle \mathbf{p}_{\mathrm{p}} \rangle) \frac{Q}{\varepsilon} \sum v \right\}$$
$$+ \sum_{\mathrm{p,n}} \left\{ \langle \mathbf{j}_{\mathrm{pn}} \rangle + \langle \sum v \frac{Q}{\varepsilon} \mathbf{j}_{\mathrm{pn}} \rangle + \langle \mathbf{j}_{\mathrm{pn}} \frac{Q}{\varepsilon} \sum v \rangle \right\} \tag{2.12}$$

where Σv means $\Sigma_{i>j} v_{ij}$. The two groups of terms represent respectively the ordinary and exchange current. It will be noted that the first correction to the former is of second order. This is because the operator $\mathbf{p}$ does not excite the model state and because the quantity $(F-1)$ has Q for leading factor. Not only the first order terms, but the complete expressions

$$\langle \mathbf{p}_{\mathrm{p}}(F-1) \rangle, \quad \langle (F^{+}-1)\mathbf{p}_{\mathrm{p}} \rangle$$

are zero; it is for this reason that second order terms in (2.6) are not required.

It is readily seen from (2.12) and (2.9), using the conservation of total momentum $\Sigma_i \mathbf{p}_i$, that on going to the mirror nucleus (interchanging protons and neutrons) the perturbation corrections just change sign. This is in fact accurately true to all orders. So for definiteness we will generally suppose the odd particle to be a neutron.

In what follows the interaction is taken to be a static central potential with exchange,

$$v_{ij} = u(|\mathbf{r}_i - \mathbf{r}_j|)[W + MP^{r}_{ij} + BP^{\sigma}_{ij} + HP^{r}_{ij}P^{\sigma}_{ij}] \tag{2.13}$$

where P^{r} and P^{σ} are space and spin exchange operators; the sum of the constants W, M, B, H is unity. In the numerical work u is supposed to have the Yukawa shape, with conventional range and a strength suggested by shell model studies:

$$u = -U \frac{\mathrm{e}^{-|\mathbf{r}_i - \mathbf{r}_j|/\alpha}}{|\mathbf{r}_i - \mathbf{r}_j|/\alpha}, \tag{2.14}$$
$$\alpha = 1.4 \times 10^{-13} \text{ cm}, \quad U = 40 \text{ MeV}.$$

The Fourier transform of this is needed:

$$\tilde{u}(k) = \int u(r) \mathrm{e}^{-i\mathbf{k}\cdot\mathbf{r}} \, \mathrm{d}\mathbf{r} = -4\pi\alpha^3 U/(1+k^2\alpha^2). \tag{2.15}$$

The Fermi gas which represents the core in this work has equally many protons and neutrons, and we have used the numbers

$$r_0 = 1.2\times10^{-13}\,\text{cm}, \quad k_F = 1.5/r_0, \quad k_F^2/2m = 33\,\text{MeV},$$

for the nuclear radius constant, the Fermi momentum, and the Fermi kinetic energy. We employ the usual technique of first supposing the plane waves to be normalised in, and to satisfy periodic boundary conditions on the surface of, a cube of unit volume; subsequently the rule

$$\sum_{\mathbf{k}} \to \int \frac{d\mathbf{k}}{(2\pi)^3} \tag{2.16}$$

is used to pass to the infinite system.

3. The Single Body Potential

Let us consider for the moment the core alone, in the absence of odd particles and holes. The definition of V in the Brueckner theory is then

$$V(k) = \sum_{|\mathbf{l}|<k_F} 4(\mathbf{lk}|\overline{t(1-P^\sigma P^\tau)}|\mathbf{lk}) \tag{3.1}$$

where the bar denotes averaging over ordinary and isobaric spin, and t is the reaction operator for which (until section 6) an adequate approximation is

$$t = v. \tag{3.2}$$

Because of the symmetry of the core V is spherically symmetric and spin and charge independent. In the presence of an odd particle or hole we might modify (3.1) by an appropriate contribution. This we choose *not* to do, for it would spoil the afore mentioned symmetry properties; it would do so only through a term which would vanish as the system became infinite, but even such a term could in suitable combination with others make a finite contribution. Of course whatever choice we make here is ultimately compensated when (and if) higher order terms in the perturbation series are calculated.

Using (3.1) and (2.13), performing the averaging, and converting the sum into an integral, one finds

$$\begin{aligned} V(k) = {} & (4W-M+2B-2H)(2\pi)^{-3}\int_{l<k_F} d\mathbf{l}\,\tilde{u}(0) \\ & +(4M-W-2B+2H)(2\pi)^{-3}\int_{l<k_F} d\mathbf{l}\,\tilde{u}(|\mathbf{k}-\mathbf{l}|). \end{aligned} \tag{3.3}$$

It would be difficult to perform the integrals met in this work incorporating V accurately; following Brueckner we use an approximation linear in k^2. It turns out that the most important momenta here are those near k_F, so we take

$$V(k)-V(k_F) \approx \frac{k^2-k_F^2}{2k_F^2}\left\{\mathbf{k}\cdot\frac{\mathrm{d}}{\mathrm{d}\mathbf{k}}V(k)\right\}_{\mathbf{k}=\mathbf{k}_0} \tag{3.4}$$

where $\mathbf{k}_0$ is some vector of magnitude k_F. In the energy denominator $\varepsilon = E_0-\mathscr{H}_0$ we are concerned only with the difference in V between the ground and excited state. So the use of (3.4) amounts to replacing the kinetic energy $k^2/2m$ by $k^2/2m^*$, where the effective mass is given by

$$\frac{1}{m^*}-\frac{1}{m} = \frac{1}{k_F^2}\left\{\mathbf{k}\cdot\frac{\mathrm{d}}{\mathrm{d}\mathbf{k}}V(k)\right\}_{\mathbf{k}=\mathbf{k}_0} \tag{3.5}$$

or from (3.3)

$$\frac{m}{m^*}-1 = (4M-W-2B+2H)\frac{2m}{k_F^2}\int\frac{\mathrm{d}\mathbf{l}}{(2\pi)^3}\mathbf{k}_0\cdot(\mathbf{k}_0-\mathbf{l})\tilde{u}'(|\mathbf{k}_0-\mathbf{l}|) \tag{3.6}$$

where

$$\tilde{u}'(k) = (\mathrm{d}/\mathrm{d}k^2)\tilde{u}(k). \tag{3.7}$$

This reduces to

$$(4M-W-2B+2H)\frac{mk_F}{2\pi^2}\int_0^1 \mathrm{d}x(4x^3-2x)\tilde{u}(2k_F x) \tag{3.8}$$

and finally, with the Yukawa shape,

$$\frac{m}{m^*}-1 = (4M-W-2B+2H)\frac{\gamma}{4\pi}\frac{mU}{k_F^2}\{(1+2\gamma^{-2})\log(1+\gamma^2)-2\} \tag{3.9}$$

where $\gamma = 2k_F\alpha$. With the potentials used here the numerical results are:

Majorana	$m^*/m = 0.60$
Rosenfeld	$m^*/m = 0.71$
Serber	$m^*/m = 0.79$
Wigner	$m^*/m = 1.20.$

The Rosenfeld potential is defined by $W = -0.13$, $M = 0.93$, $B = 0.46$, $H = -0.26$; the Serber potential is $W = M = 0.5$, $B = H = 0$.

It should be noted that our m^*, associated with momenta near k_F, is not the usual effective mass; the latter is an average over momenta from 0 to k_F, and is therefore more different from m. With the above Majorana force, for example, one finds at zero momentum $m^*/m = 0.50$ rather than 0.60.

The idea that the effective mass m^* might imply an effective gyromagnetic ratio e/m^* has been disposed of already [2]). Two additional arguments may be mentioned briefly. Firstly, this would imply corrections to the moment only when the odd particle were a proton, in violation of the mirror theorem of section 2. Secondly, it would imply first order corrections even for Wigner forces, for which, because they give no exchange current, the real corrections are of second order and higher.

4. Ordinary Current

We now consider the first two terms in (2.12) which will be denoted by $\ll \mathbf{J} \gg_0$ and $\ll \mathbf{J} \gg_1$. When the odd particle is a neutron $\ll \mathbf{J} \gg_0$ is of course zero. In the second term, because $\mathbf{p}$ is a diagonal operator for plane waves, and because states excited by different Qv_{ij} are orthogonal, the double summation reduces to a single one:

$$\ll \mathbf{J} \gg_1 = \frac{e}{m} \sum_{\mathrm{p}} \sum_{i>j} \langle v_{ij} \frac{Q}{\varepsilon} (\mathbf{p}_\mathrm{p} - \langle \mathbf{p}_\mathrm{p} \rangle) \frac{Q}{\varepsilon} v_{ij} \rangle. \tag{4.1}$$

Secondly, because of conservation of momentum, intermediate states in which the excited pair of particles have the same charge do not contribute; we have therefore

$$\ll \mathbf{J} \gg_1 = \frac{e}{m} \sum_{\mathrm{p,n}} \langle v_{\mathrm{pn}} \frac{Q}{\varepsilon} (\mathbf{p}_\mathrm{p} - \langle \mathbf{p}_\mathrm{p} \rangle \frac{Q}{\varepsilon} v_{\mathrm{pn}} \rangle. \tag{4.2}$$

At this point we can forget about antisymmetrising the state Φ and talk as if each nucleon had a definite momentum and spin; for the expectation value is that of an essentially two-body operator involving non-identical particles, so that exchange contributions do not occur.

Now in the absence of the odd particle, for obvious symmetry reasons, the quantity $\ll \mathbf{J} \gg_1$ would have to be zero. The addition of the odd particle causes two changes in (4.2). First there are the new terms involving v_{po} where O denotes the odd particle; if for the moment we ignore spin, setting $B = H = 0$, then the corresponding contribution is

$$\frac{e}{m} \sum_{l'>k_F,\ k'>k_F,\ l\le k_F} \frac{(\mathbf{l}\mathbf{k}_0|v|\mathbf{l}'\mathbf{k}')(\mathbf{l}'-\mathbf{l})(\mathbf{l}'\mathbf{k}'|v|\mathbf{l}\mathbf{k}_0)}{\{(l^2+k_0^2-l'^2-k'^2)/2m^*\}^2} \tag{4.3}$$

where $\mathbf{k}_0$ is the initial momentum of the odd neutron, $\mathbf{l}$ that of a proton in the core, and

$$(\mathbf{l}'\mathbf{k}'|v|\mathbf{l}\mathbf{k}) = \int \mathrm{d}\mathbf{r}_1 \mathrm{d}\mathbf{r}_2 \mathrm{e}^{-i(\mathbf{l}'\cdot\mathbf{r}_1+\mathbf{k}'\cdot\mathbf{r}_2)} v \mathrm{e}^{i(\mathbf{l}\cdot\mathbf{r}_1+\mathbf{k}\cdot\mathbf{r}_2)}$$

$$= \delta(\mathbf{l}'+\mathbf{k}', \mathbf{l}+\mathbf{k})\{W\tilde{u}(|\mathbf{l}'-\mathbf{l}|)+M\tilde{u}(|\mathbf{l}'-\mathbf{k}|)\} \tag{4.4}$$

With

$$\begin{aligned} \mathbf{a} &= \mathbf{l}'-\mathbf{l} = \mathbf{k}_0-\mathbf{k}' \\ -\mathbf{b} &= \mathbf{l}'-\mathbf{k}_0 = \mathbf{l}-\mathbf{k}' \end{aligned} \tag{4.5}$$

and using (2.16), (4.3) becomes

$$(m^*/m)^2(2\pi)^{-6} me \int_{\substack{|\mathbf{k}_0-\mathbf{a}|>k_F \\ |\mathbf{k}_0-\mathbf{b}|>k_F \\ |\mathbf{k}_0-\mathbf{a}-\mathbf{b}|<k_F}} \mathrm{d}\mathbf{a}\,\mathrm{d}\mathbf{b}\,\mathbf{a}\{W\tilde{u}(a)+M\tilde{u}(b)\}^2(\mathbf{a}\cdot\mathbf{b})^{-2}. \tag{4.6}$$

The second change caused by the odd particle is through the exclusion operator Q, for the state occupied by this particle is no longer available as an inter-

mediate state to a neutron excited from the core; so we have a contribution

$$-\frac{e}{m}\sum_{l\leq k_F,\ l'\leq k_F,\ l'>k_F}\frac{(\mathbf{lk}'|v|\mathbf{l}'\mathbf{k}_0)(\mathbf{l}'-\mathbf{l})(\mathbf{l}'\mathbf{k}_0|v|\mathbf{lk}')}{\{(l^2+k'^2-l'^2-k_0^2)/2m^*\}^2}. \tag{4.7}$$

With

$$\begin{aligned}-\mathbf{a}&=\mathbf{l}'-\mathbf{l}=\mathbf{k}'-\mathbf{k}_0\\ -\mathbf{b}&=\mathbf{l}'-\mathbf{k}'=\mathbf{l}-\mathbf{k}_0\end{aligned} \tag{4.8}$$

this becomes

$$+(m^*/m)^2(2\pi)^{-6}me\int_{\substack{|\mathbf{k}_0-\mathbf{a}|<k_F\\ |\mathbf{k}_0-\mathbf{b}|<k_F\\ |\mathbf{k}_0-\mathbf{a}-\mathbf{b}|>k_F}}\mathrm{d}\mathbf{a}\,\mathrm{d}\mathbf{b}\,\mathbf{a}\{W\tilde{u}(a)+M\tilde{u}(b)\}^2(\mathbf{a}\cdot\mathbf{b})^{-2}. \tag{4.9}$$

The total $\ll\mathbf{J}\gg_1$ is the sum of (4.6) and (4.9). On restoring spin we obtain first a factor 2 from density of states, and secondly contributions from B and H; the expressions corresponding to (4.3) and (4.7) then contain P_σ which can be brought together and eliminated using

$$P_\sigma^2=1,\quad \bar{P}_\sigma=\tfrac{1}{2}, \tag{4.10}$$

where the bar denotes averaging over the spin of one of the particles. Clearly $\ll\mathbf{J}\gg_1$ will be proportional to $\mathbf{k}_0$,

$$\ll\mathbf{J}\gg_1=(e/m)q_1\mathbf{k}_0,$$

where q_1 is the contribution to the effective charge of the odd neutron in units of e; thus

$$q_1=(m/ek_0^2)\mathbf{k}_0\cdot\ll\mathbf{J}\gg_1. \tag{4.11}$$

We obtain finally

$$\begin{aligned}q_1=\left(\frac{m^*}{m}\right)^2&(W^2+WB+B^2)I_{11}+(M^2+MH+H^2)I_{12}\\ &+(2WM+2BH+WH+MB)I_{13}\}\end{aligned}$$

where

$$I_{11}=\frac{2m^2}{(2\pi)^6}\left\{\int_{\substack{|\mathbf{k}_0-\mathbf{a}|>k_F\\ |\mathbf{k}_0-\mathbf{b}|>k_F\\ |\mathbf{k}_0-\mathbf{a}-\mathbf{b}|<k_F}}\mathrm{d}\mathbf{a}\,\mathrm{d}\mathbf{b}+\int_{\substack{|\mathbf{k}_0-\mathbf{a}|<k_F\\ |\mathbf{k}_0-\mathbf{b}|<k_F\\ |\mathbf{k}_0-\mathbf{a}-\mathbf{b}|>k_F}}\mathrm{d}\mathbf{a}\,\mathrm{d}\mathbf{b}\right\}\frac{\mathbf{a}\cdot\mathbf{k}_0}{k_0^2}\frac{\tilde{u}(a)\tilde{u}(a)}{(\mathbf{a}\cdot\mathbf{b})^2} \tag{4.12}$$

and the remaining integrals are obtained by replacing $\tilde{u}(a)\tilde{u}(a)$ by $\tilde{u}(b)\tilde{u}(b)$ for I_{12}, and by $\tilde{u}(a)\tilde{u}(b)$ for I_{13}.

The evaluation of I_{11} and I_{12} is tedious and straightforward; the procedure is sketched in Appendix B, and leads to

$$(I_{11},I_{12})=\pi^{-4}m^2k_F^2\int_{-1}^{\infty}\mathrm{d}x\{\tilde{u}(2k_Fx)\}^2|x|\,(F_{11},F_{12}) \tag{4.13}$$

with †, for $|x|<1$,

† Contributions from $|x|>1$ are found to be negligible for all the integrals I of this paper.

$$F_{11}=\frac{1}{3}(x^2+x^3)-\frac{1}{3}(3x-2x^3)\log 2-\frac{1}{6}(1+x^3)\log(1+x)-\frac{1}{6}(1-x^3)\log(1-x)$$
$$F_{12}=-\frac{1}{48}(1+12x+9x^2-2x^3)+\frac{1}{6}(2+3x-x^3)\log 2+\frac{3}{32x}(1-x^2)^2\log\frac{1+x}{1-x}. \tag{4.14}$$

Using (2.15) we arrive at combinations of simple integrals; most of these are elementary but those with logarithms were done numerically; we find

$$I_{11}=0.07, \qquad I_{12}=0.43. \tag{4.15}$$

The third integral is rather more difficult; however if it is assumed that $\tilde{u}$ has always the same sign, the inequality

$$0<I_{13}<\tfrac{1}{2}(I_{11}+I_{12}) \tag{4.16}$$

can be established (Appendix A); this is quite sufficient for our purposes. From (4.15),

$$0<I_{13}<0.25. \tag{4.17}$$

The numerical results for q_1 are given in the first column of the table. The error associated with the Serber force comes from the use of (4.17). There is no corresponding error for the Rosenfeld force, because the coefficient of I_{13} happens to be nearly zero — it is about (-0.02).

5. Space Exchange Current

The matrix element of the exchange current (2.11) corresponding to the potential (2.13) is readily found to be

$$(\mathbf{l}'\mathbf{k}'|\mathbf{j}|\mathbf{l}\mathbf{k})=e(M+HP^\sigma)2\mathbf{b}\tilde{u}'(b)\delta(\mathbf{l}'+\mathbf{k}',\mathbf{l}+\mathbf{k}) \tag{5.1}$$

where $\mathbf{l}$ is the proton momentum, $\mathbf{k}$ the neutron momentum,

$$\mathbf{b}=\mathbf{l}'-\mathbf{k}', \qquad \tilde{u}'(b)=(\mathrm{d}/\mathrm{d}b^2)\tilde{u}(b), \tag{5.2}$$

and the expression of course remains an operator in spin space.

Consider now the first order contribution, which will be called $\ll\mathbf{J}\gg_2$. The terms involving two core particles must cancel, and we are left with those involving the odd neutron and some proton; one finds

$$\ll\mathbf{J}\gg_2=(M+\tfrac{1}{2}H)2e(2\pi)^{-3}\int_{l<k_F}\mathrm{d}\mathbf{l}\,2(\mathbf{l}-\mathbf{k}_0)\tilde{u}'(|\mathbf{l}-\mathbf{k}_0|). \tag{5.3}$$

The integral here occurred previously in (3.6). The effective charge q_2 is obtained in analogy with (4.11), and the result is

$$q_2=-(M+\tfrac{1}{2}H)\frac{\gamma}{\pi}\frac{mU}{2k_F^2}\{(1+2\gamma^{-2})\log(1+\gamma^2)-2\}. \tag{5.4}$$

This is equivalent to a formula derived before by Miyazawa [3]). Numerical results are given in the table.

The last two terms in (2.12) may be taken together; they are Hermitian conjugates, and as they turn out to be real we have to compute

$$\ll \mathbf{J} \gg_3 = 2 \sum_{\mathrm{pn}} \langle \mathbf{j}_{\mathrm{pn}} \frac{Q}{\varepsilon} \sum v \rangle . \tag{5.5}$$

The evaluation of this is closely similar to that of $\ll \mathbf{J} \gg_1$, and results in

$$q_3 = \frac{m^*}{m} \{(M^2+MH+H^2)I_{32}+(MW+HB+\tfrac{1}{2}HW+\tfrac{1}{2}MB)I_{33}\} \tag{5.6}$$

where

$$I_{32} = -\frac{8m^2}{(2\pi)^6} \left\{ \int \mathrm{da}\, \mathrm{db} + \int \mathrm{da}\, \mathrm{db} \right\} \frac{\mathbf{b}\cdot\mathbf{k}_0}{{k_{\mathrm{F}}}^2} \frac{\tilde{u}'(b)\tilde{u}(b)}{\mathbf{a}\cdot\mathbf{b}} \tag{5.7}$$

and the limits on the two integrals are as in (4.12); I_{33} is obtained on replacing $\tilde{u}'(b)\tilde{u}(b)$ by $\tilde{u}'(b)\tilde{u}(a)$.

We find

$$I_{32} = -\pi^{-4} m^2 {k_{\mathrm{F}}}^2 \int_{-1}^{\infty} \mathrm{d}x\, x^2 \frac{\mathrm{d}}{\mathrm{d}x^2} \{\tilde{u}(2k_{\mathrm{F}}x)\}^2 |x| F_{32}(x) \tag{5.8}$$

where, for $|x| < 1$,

$$F_{32} = \frac{1}{24}(13+12x-3x^2-2x^3)+\frac{1}{3}(x^3-3x-2)\log 2+\frac{1}{16x}(1-x^2)^2 \log\frac{1+x}{1-x}. \tag{5.9}$$

With the Yukawa force (2.14),

$$I_{32} = +0.16.$$

The cross term I_{33} is again more difficult and has not been evaluated. For this reason there is in the table no entry under q_3 against the Serber force; the entry against the Rosenfeld force assumes that I_{33} is not more than an order of magnitude greater than I_{32}.

6. The Brueckner Expansion

The perturbation expansion breaks down if, for example, v has an infinite repulsive core, for then the matrix elements of v are infinite. The Brueckner theory then prescribes the rearrangement of the series for F in terms of the finite reactance operator t:

$$t = v + v\frac{Q}{\varepsilon} t. \tag{6.1}$$

The first few terms of the new series are quickly obtained by substituting the expansion

$$v = t - t\frac{Q}{\varepsilon} t + \ldots \tag{6.2}$$

in the old. We must also eliminate v where it appears in the definition (2.11)

of $\mathbf{j}$: there also we tentatively make the substitution (6.2). We then obtain to second order in t:

$$\ll \mathbf{J} \gg = \sum_{0}^{4} \ll \mathbf{J} \gg_i \tag{6.3}$$

where the first four terms are obtained from (2.12) simply by replacing v by t everywhere, including the definition of $\mathbf{j}$, and

$$\ll \mathbf{J} \gg_4 = -\sum_{pn} \langle [t_{pn} \frac{Q}{\varepsilon} t_{pn}, \quad ie\mathbf{r}_p] \rangle. \tag{6.4}$$

The new term is a correction arising because $\ll \mathbf{J}_2 \gg$ is now written linear in t rather than v.

These expressions are again reduced by considering how they change on adding an odd particle to the core. A new point which arises is that the operator t is changed, through the Q appearing in its definition, by the presence of the odd particle. The new quantity t' is given by

$$t' = v + v \frac{Q'}{\varepsilon} v + \ldots. \tag{6.5}$$

Substituting (6.2) in this we obtain t' in terms of t:

$$t' = t + t \left(\frac{Q'}{\varepsilon} - \frac{Q}{\varepsilon} \right) t + \ldots. \tag{6.6}$$

Thus $t' - t$ is of second and higher order in t and so can consistently be ignored in $\ll \mathbf{J} \gg_1$ and $\ll \mathbf{J} \gg_3$ which are already of second order. We must be more careful with $\ll \mathbf{J} \gg_2$. However if $\ll \mathbf{J} \gg_2$ and $\ll \mathbf{J} \gg_4$ are taken together the result of a systematic expansion in t is quite simple, as can be seen as follows. To this order we have of course

$$\ll \mathbf{J} \gg_2 + \ll \mathbf{J} \gg_4 = \sum_{pn} \langle [v_{pn}, \quad ie\mathbf{r}_p] \rangle, \tag{6.7}$$

and in this expression we can immediately discard, by the symmetry of the core, those terms not involving the odd neutron. Thus

$$\ll \mathbf{J} \gg_2 + \ll \mathbf{J} \gg_4 = \sum_{p} \langle [v_{po}, ie\mathbf{r}_p] \rangle.$$

Restoring in this expression the expansion (6.2), the combined contribution to the effective charge is $q_3 + q_4$ with

$$(e/m)\mathbf{k}_0 q_3 = \sum_{p} \langle [t_{po}, \quad ie\mathbf{r}_p] \rangle \tag{6.8}$$

$$(e/m)\mathbf{k}_0 q_4 = -\sum_{p} \left\langle \left[t_{po} \frac{Q}{\varepsilon} t_{po}, \; ie\mathbf{r}_p \right] \right\rangle. \tag{6.9}$$

To obtain numerical results from these formulae in a realistic way would require information about the operator t that is not yet available. However

in the usual shell model it is in effect assumed that it is t, rather than v, that can be represented at least crudely by a non-singular static potential with exchange. Such an assumption is qualitatively wrong in a number of ways; if we constructed v from such a t using (5.2) we would find that it did not commute with the centre of mass of the two particles and that it behaved peculiarly on the Fermi surface. Moreover it is likely that the second order effects considered here are more sensitive to such approximations than the simple first order energy integrals usually required in shell model work. Nevertheless, for want of something better, let us set t equal to the right hand side of (2.13). Then the quantities q_1, q_2, q_3 are exactly what they were before, and the numerical results are those tabulated.

It remains to compute q_4. In the momentum space $\mathbf{r}$ becomes a differential operator, and we find

$$q_4 = -2mk_F^{-2} \sum_{l<k_F} \mathbf{k}_0 \cdot \frac{\partial}{\partial \mathbf{l}} \left(\mathbf{l}\mathbf{k}_0 \left| \overline{t \frac{Q}{\varepsilon} t} \right| \mathbf{l}\mathbf{k}_0 \right) \tag{6.10}$$

where the bar denotes averaging over spin. The corresponding integral may be replaced by a surface integral:

$$q_4 = -2mk_F^{-3}(2\pi)^{-3} \int_{l<k_F} d\mathbf{l}\, \delta(l-k_F)\mathbf{k}_0 \cdot \mathbf{l} (\mathbf{l}\mathbf{k}_0 \left| \overline{t \frac{Q}{\varepsilon} t} \right| \mathbf{l}\mathbf{k}_0). \tag{6.11}$$

Now

$$\left(\mathbf{l}\mathbf{k}_0 \left| t \frac{Q}{\varepsilon} t \right| \mathbf{l}\mathbf{k}_0 \right) = \sum_{l'>k_F,\ k'>k_F} \frac{(\mathbf{l}\mathbf{k}_0|t|\mathbf{l}'\mathbf{k}')(\mathbf{l}'\mathbf{k}'|t|\mathbf{l}\mathbf{k}_0)}{(k_0^2+l^2-k'^2-l'^2)/2m^*}. \tag{6.12}$$

Using for t the right hand side of (2.13), averaging over spins, and introducing (4.5), we have the result.

$$q_4 = \frac{m^*}{m} \{(W^2+WB+B^2)I_{41}+(M^2+MH+H^2)I_{42} + (2WM+2BH+WH+MB)I_{43} \tag{6.13}$$

where

$$I_{41} = \frac{2m^2}{(2\pi)^6} \int_{\substack{|\mathbf{k}_0-\mathbf{a}|>k_F \\ |\mathbf{k}_0-\mathbf{b}|>k_F}} d\mathbf{a}\, d\mathbf{l}\, \delta(l-k_F) \frac{\mathbf{k}_0 \cdot \mathbf{l}}{k_F^3} \frac{\tilde{u}(a)\tilde{u}(a)}{-\mathbf{a}\cdot\mathbf{b}} \tag{6.14}$$

and the other integrals are obtained by replacing $\tilde{u}(a)\tilde{u}(a)$ by $\tilde{u}(b)\tilde{u}(b)$ for I_{42} and by $\tilde{u}(a)\tilde{u}(b)$ for I_{43}. One finds

$$I_{41} = I_{42} = -\pi^{-4} m^2 k_F^2 \int_0^\infty dx \{\tilde{u}(2k_F x)\}^2 x F_{41}(x) \tag{6.15}$$

with, for $x < 1$,

$$F_{41} = \tfrac{1}{6}(2+3x-x^3) - \tfrac{1}{3}(1+3x-2x^2)\log 2. \tag{6.16}$$

With the potential (2.14),

$$I_{41} = I_{42} = -0.04.$$

The cross term I_{43} has again not been evaluated, and the result quoted in the table for the Rosenfeld force assumes that I_{43} does not exceed I_{41} by more than an order of magnitude.

It is seen that q_4 turns out to be very small. Whether it will remain small when t is treated more realistically, and whether indeed the expansion (6.2) is then a sensible way to handle the exchange current, are questions needing investigation.

7. Another Approach

In the Brueckner theory the first approximation to the total energy is

$$E = \langle T + \sum_{i>j} t_{ij} \rangle. \tag{7.1}$$

The change in this due to the application of a uniform vector potential **A** is

$$\delta E = \langle \delta T + \sum \delta t \rangle, \tag{7.2}$$

for the model wave function is unchanged, being entirely fixed by symmetry considerations. The first term of (7.2) is of course

$$\delta T = -(e/m) \sum_{\mathbf{p}} \mathbf{p}_{\mathbf{p}} \cdot \mathbf{A}. \tag{7.3}$$

We have to compute the second term from

$$\delta v = e[v, -ie \sum_{\mathbf{p}} \mathbf{r}_{\mathbf{p}} \cdot \mathbf{A}]. \tag{7.4}$$

From (6.1),

$$\delta t = \delta v \left(1 + \frac{Q}{\varepsilon} t\right) - v \frac{Q}{\varepsilon} \delta e \frac{Q}{\varepsilon} t + v \frac{Q}{\varepsilon} \delta t$$

or

$$\delta t = \left(1 - v \frac{Q}{\varepsilon}\right)^{-1} \left\{\delta v \left(1 + \frac{Q}{\varepsilon} t\right) - v \frac{Q}{\varepsilon} \delta \varepsilon \frac{Q}{\varepsilon} t\right\}.$$

Now

$$\left(1 - v \frac{Q}{\varepsilon}\right)^{-1} = 1 + v \frac{Q}{\varepsilon} + v \frac{Q}{\varepsilon} v \frac{Q}{\varepsilon} + \ldots$$

$$= \left(1 + t \frac{Q}{\varepsilon}\right)$$

and similarly

$$\left(1 - v \frac{Q}{\varepsilon}\right)^{-1} v = t.$$

Thus, to second order in t,

$$\delta t = \left(1 + t \frac{Q}{\varepsilon}\right) \left[t - t \frac{Q}{\varepsilon} t, -ie \sum \mathbf{r} \cdot \mathbf{A}\right] \left(1 + \frac{Q}{\varepsilon} t\right) - t \frac{Q}{\varepsilon} \delta t \frac{Q}{\varepsilon} t \tag{7.5}$$

where (6.2) has been used. The principal part of $\delta\varepsilon$ comes from δT, (7.3),

$$\delta\varepsilon = (e/m)(\sum_{\mathbf{p}} \mathbf{p}_{\mathbf{p}} \cdot \mathbf{A} - \langle \sum_{\mathbf{p}} \mathbf{p}_{\mathbf{p}} \cdot \mathbf{A} \rangle). \tag{7.6}$$

There is also a contribution from the change δV in the single body potential, but this we ignore, for it would be proportional to δt and on iterating (7.5) would give rise to terms only of third order and higher. Substituting (7.6) into (7.5), and (7.5) with (7.3) into (7.2), we obtain an explicit expression for δE; the coefficient of $-\mathbf{A}$ in this gives $\ll \mathbf{J} \gg$. How it is readily shown that (7.1) and (7.2) are in fact accurate to second order in t. To this order the corresponding expression for $\ll \mathbf{J} \gg$ should agree with (2.12). This is indeed found to be so.

The point of view of this section was adopted in a previous paper [2]). There however δt was tentatively determined from the momentum dependence of t by the gauge invariance rule $\mathbf{p}_{\mathbf{p}} \to \mathbf{p}_{\mathbf{p}} - e\mathbf{A}$, or equivalently

$$\delta t = [t, -ie \sum_{\mathbf{p}} \mathbf{r}_{\mathbf{p}} \cdot \mathbf{A}]. \tag{7.7}$$

It is seen now that this gives only the first order term of a power series in t for $\ll \mathbf{J} \gg$, and the method of our previous paper gives only the contribution q_2 to the effective charge. As it happens we have found this contribution to be the largest, but the others are not at all negligible.

It is interesting to consider why, even in this simple case of determining the reaction of the system to a uniform vector potential, gauge invariance arguments must be used with some caution. The answer is that while it is of course possible to introduce such a potential merely by a gauge transformation, this does not lead to the state of the system which is of interest. If we consider the adiabatic growth of what we may call a "real" uniform vector potential from zero, then while it grows there is an electric field which induces the current that in a finite nucleus would be associated with the Larmor precession; this comes about not by a change in the momenta of the particles, which in the model state are unaltered, but by a change in the relation of velocity to momentum:

$$m\mathbf{v}_i = \mathbf{p}_i - e_i \mathbf{A}.$$

In the state obtained merely by gauge transformation the momenta are altered in such a way that this current is cancelled. Now the potential v was assumed to be a definite function of the vector $\mathbf{A}$ in no way dependent on the state on which it acts. But this assumption cannot consistently be made of t. This operator is constructed with reference (through Q, which depends on the momenta of all particles) to a definite state of the system as a whole. It is because the states for which they are designed differ that (7.5) differs from (7.7). The latter is appropriate to the new description of the old state

obtained by gauge transformation; the former is appropriate to the new state obtained by application of a real field.

TABLE

Effective charge on an odd neutron due to (1) collision with the core, (2) space-exchange current in first order, (3) space-exchange current in second order, and (4) difference between real and effective potential.

	q_1	q_2	q_3	q_4
Majorana	0.15	−0.34	0.10	−0.03
Rosenfeld	0.16	−0.27	0.08	−0.02
Serber	0.12 ± 0.04	−0.17		
Wigner	0.10	0	0	−0.05

8. Conclusion

In the above we have for definiteness considered the case of an odd neutron above the Fermi sea; this is found to have an effective charge $q = \sum_1^4 q_i$. If instead of adding a neutron we removed one from the top level then we would simply be removing from the current contributions equal to those formerly added; at the same time we would be removing momentum, and since the effective charge is the ratio of total current to total momentum it is the same (in this model) for a hole and a particle. With an odd proton the effective charge, according to the mirror theorem of section 2, would be $(1-q)$.

This work is limited by a much simplified nuclear model and by a probably unrealistic treatment of the effective two body potential t. Within these limitations it has been found that the largest correction to the effective current, and therefore to the magnetic moment, is the usual space exchange current in first order. But there are additional corrections which (even after allowing for the considerations of Appendix B) are of the same order of magnitude. Let us take for example the first order space-exchange effective charge q_2 for the Serber force. Using this in the single particle magnetic moment formulae [4]) it predicts for N^{15}, O^{17}, and K^{39}, deviations from the Schmidt lines of 0.11, −0.34, and 0.31 nuclear magnetons. The experimental values are 0.0, 0.0, and 0.3. We would guess that the other contributions to q, allowing for the considerations of Appendix B, would reduce the theoretical values by about half, spoiling the agreement for K^{39} but reducing the disagreement for the others.

Clearly no model can reproduce the experimental results without paying more attention than ours to the details of individual nuclei. However we believe the qualitative conclusions of this paper will be valid for finite nuclei; then in attempting to predict accurately the moments of even the simplest it will be necessary to consider not only the first order space exchange current

(and the spin exchange current which did not appear here) but also the perturbation corrections.

I am indebted for valuable discussion of this work to Dr. J. P. Elliott, Dr. J. Hubbard, Dr. E. J. Squires, and especially to Dr. T. H. R. Skyrme. I thank Mrs. M. Bell and Dr. Squires for checking parts of the algebra.

Appendix A

AN INEQUALITY

It will be shown that when each of the three integrals I_{11}, I_{12}, I_{13} is written in the form ${}^1I+{}^2I$ where the two parts correspond to the two integrals in (4.12), then the result (4.16) holds for ${}^1I$ and ${}^2I$ separately.

The second part, ${}^2I$, is simplest. Because $k_0 = k_F$, the restriction $|\mathbf{k}_0-\mathbf{a}| < k_F$ requires that $\mathbf{a}\cdot\mathbf{k}_0$ be positive (and in fact exceed $\frac{1}{2}a^2$). Since we assume $\tilde{u}$ always to have the same sign the whole integrand is then positive. From

$$0 \leqq \tilde{u}(a)\tilde{u}(b) \leqq \tfrac{1}{2}\{\tilde{u}(a)\}^2+\tfrac{1}{2}\{\tilde{u}(b)\}^2 \tag{A1}$$

it follows that

$$0 < {}^2I_{13} < \tfrac{1}{2}\{{}^2I_{11}+{}^2I_{12}\}. \tag{A2}$$

For ${}^1I$, note that the restriction $|\mathbf{k}_0-\mathbf{a}-\mathbf{b}| < k_F$ requires $(\mathbf{a}+\mathbf{b})\cdot\mathbf{k}_0$ to be positive. Thus, using (A1),

$$0 < \int d\mathbf{a}\, d\mathbf{b}\, \frac{(\mathbf{a}+\mathbf{b})\cdot\mathbf{k}_0}{(\mathbf{a}\cdot\mathbf{b})^2}\,\tilde{u}(a)\tilde{u}(b) \tag{A3}$$

$$< \int d\mathbf{a}\, d\mathbf{b}\, \frac{(\mathbf{a}+\mathbf{b})\cdot\mathbf{k}_0}{(\mathbf{a}\cdot\mathbf{b})^2}\,\tfrac{1}{2}(\{\tilde{u}(a)\}^2+\{\tilde{u}(b)\}^2)$$

where the integration is restricted as in the first term of (4.12). Because the other factors are symmetric in $\mathbf{a}$ and $\mathbf{b}$ we may here replace $(\mathbf{a}+\mathbf{b})\cdot\mathbf{k}_0$ by $2\mathbf{a}\cdot\mathbf{k}_0$, so obtaining

$$0 < {}^1I_{13} < \tfrac{1}{2}\{{}^1I_{11}+{}^1I_{12}\}. \tag{A4}$$

The result (4.16) follows on adding (A2) and (A4).

Appendix B

THE EFFECT OF AN ENERGY GAP

The Fermi gas which represented the core in this work has excited states of infinitesimal excitation energy. Experimentally the first excited states of the closed shell nuclei Ca^{40} and O^{16} are at 3 and 6 MeV respectively. We will try to estimate roughly the importance of this. Previously we have taken for the energies of the single particle states

$$E(k) = k^2/2m^*. \tag{B1}$$

This is retained for $k \leqq k_F$ but for $k > k_F$ we now take

$$E(k) = k^2/2m^* + \Delta E. \tag{B2}$$

With this energy gap ΔE in the spectrum it is hoped to simulate crudely the difficulty of exciting the real core.

We will consider only the integral I_{12} which gives the effective charge q_1 for a simple Majorana force. Suppose for definiteness there is an additional odd particle (rather than a hole) occupying now a state with energy $\Delta E + k_F^2/2m^*$. The new integral, I'_{12}, is obtained from the old by augmenting the energy denominators. Specifically, the substitution

$$-\mathbf{a}\cdot\mathbf{b} \to m^*\Delta E - \mathbf{a}\cdot\mathbf{b} \tag{B3}$$

is made in the first term of (4.12), which involves the excitation of one core particle, and

$$\mathbf{a}\cdot\mathbf{b} \to 2m^*\Delta E + \mathbf{a}\cdot\mathbf{b} \tag{B4}$$

in the second, which involves the excitation of two particles through the energy gap. Despite appearances the left hand sides of both (B3) and (B4) are positive in the appropriate regions of integration.

In performing the integrals it is convenient to replace $\mathbf{a}$ as integration variable by $\mathbf{l} = \mathbf{k}_0 - \mathbf{a}$. The integration over $\mathbf{l}$ is then performed first, using cylindrical polar co-ordinates with $\mathbf{b}$ as axis and $\mu = \mathbf{b}\cdot\mathbf{l}/bk_F$. The $\mathbf{b}$ integration is done using spherical polar co-ordinates with $\mathbf{k}_0$ as axis, $\nu = \mathbf{b}\cdot\mathbf{k}_0/bk_F$, and $x = \frac{1}{2}b/k_F$. The result is

$$I_{12} - I'_{12} = \frac{m^2 k_F^2}{\pi^4}\begin{cases} \int_0^\infty \mathrm{d}x\{\tilde{u}(2k_F x)\}^2\{F(x,0) - F(x,\xi)\} \\ -\int_0^1 \mathrm{d}x\{\tilde{u}(2k_F x)\}^2\{F(-x,0) - F(-x,2\xi)\} \end{cases} \tag{B5}$$

where

$$8F(x,\xi) = \begin{cases} \int_{-x}^1 \mathrm{d}\nu \int_{-x}^1 \mathrm{d}\mu (1-\mu^2)(1+\overline{\mu+2x\nu})(\xi+\mu+2x+\nu)^{-2} \\ -\int_{-x}^1 \mathrm{d}\nu \int_{x}^1 \mathrm{d}\mu (1-\mu^2)(1+\mu\nu)(\xi+\mu+\nu)^{-2} \end{cases} \tag{B6}$$

and

$$\xi = m^*\Delta E/2xk_F^2. \tag{B7}$$

The relation between this F and that used in (4.13) is

$$xF_{12} = F(x,0). \tag{B8}$$

Now the introduction of ξ, because of its implicit dependence on x in (B7), will be most important for small x. Moreover the quantity $\tilde{u}(2k_F x)$ is largest for small x; with the assumptions (2.14),

$$\{\tilde{u}(2k_F x)\}^2 \propto \{1 + 12.25\,x^2\}^{-2}.$$

These remarks suggest that an adequate approximation to (B5) is obtained

by expanding the F's in powers of x and discarding powers higher than the first. The result is

$$F(x,\xi) = \frac{x}{2}\int_0^1 d\nu \int_0^1 d\mu\, \mu(1+\mu\nu)(\mu+\nu+\xi)^{-2}$$

$$= \frac{x}{6}\{(2+\xi^3)\log(1+2/\xi) - (2+3\xi+2\xi^3)\log(1+1/\xi) + (1+\xi)\} \quad . \quad \text{(B9)}$$

Finally the integrations in (B5) are performed numerically. This method gives for I_{12} (i.e. with $\xi = 0$) the value 0.51 instead of the correct 0.43. Using the approximation only to compute the difference $I_{12} - I'_{12}$ for which it should be somewhat better, we obtain for a simple Majorana force the following results:

ΔE (MeV)	0	3	6	12
q_1	0.15	0.11	0.09	0.06

The effect of ΔE on other integrals has not been calculated. However we would guess that the behaviour of I_{12} is reasonably typical of at least those integrals which are important when the force has a large space-exchange component. We would say then that with an energy gap of a few MeV the second order corrections are probably not reduced by more than half.

References

1) H. A. Bethe, Phys. Rev. **103** (1956) 1353, and references therein to the work of Brueckner and his collaborators
2) J. S. Bell, R. J. Eden and T. H. R. Skyrme, Nuclear Physics **2** (1956/57) 586
3) H. Miyazawa, Progr. Theor. Phys. **6** (1951) 801
4) R. J. Blin-Stoyle, Rev. Mod. Phys. **28** (1956) 75

Nuclear Physics 4 (1957) 313—324; © *North-Holland Publishing Co., Amsterdam*
Not to be reproduced by photoprint or microfilm without written permission from the publisher

LOW LYING LEVELS IN Th^{228}

S. BJØRNHOLM, O. NATHAN, O. B. NIELSEN AND R. K. SHELINE †
Institute for Theoretical Physics, University of Copenhagen

Received 18 May 1957

Abstract: The decay scheme $Ac^{228} \rightarrow Th^{228}$ has been reinvestigated. The observation of new conversion lines and coincidence relations establish a revised decay scheme. An analysis of the level scheme in the light of the unified model classifies the levels as members of two rotational bands above the ground state band. Two states of energies 328 and 396 keV with $K = 0$ and $I = 1^-$ and 3^- are interpreted as an octupole vibrational band, and states at 966 and 1018 keV with $K = 2$ and $I = 2^+$ and 3^+ as a γ-vibrational band. The presence of a second octupole vibrational band with $K = 2$ and $I = 2^-, 3^-, \ldots$ is suggested. The close similarity with the level schemes of other strongly deformed nuclei in the actinide as well as in the lanthanide regions is emphasized.

1. Introduction

Great interest is attached to the study of the low energy states of deformed even nuclei, since these states probably represent pure collective excitations. A considerable amount of information on the level schemes of heavy even nuclei has already been accumulated, mainly from the study of α-decays [1, 2]). An important observation is the systematic occurrence of rotational bands, which are believed to be associated with collective vibrations of different types. One of the bands has odd parity and is possibly connected with an asymmetric oscillation of the nucleus.

The lowest levels in Th^{228} excited in the α-decay of U^{232} are easily recognized as the ground state rotational band of this strongly deformed nucleus [3, 4]). Moreover, a level excited in this decay has tentatively been identified as the first member of an odd parity band.

In the transitions $Ac^{228} \rightarrow Th^{228}$ and $Pa^{228} \rightarrow Th^{228}$, numerous levels are excited [5, 6, 7, 8]), but so far no definite decay scheme has been established. The complicated nature of the decay $Ac^{228} \rightarrow Th^{228}$ (Mesothorium 2 → Radiothorium) suggests that this decay offers a favourable opportunity for the study of the Th^{228} level scheme. In particular, measurements of the branching ratios in β- and γ-transitions to different members of a rotational band provide an important tool for the interpretation of the levels involved, as these ratios depend in a simple way on the quantum numbers K and I of the initial and final states [9]).

This paper is a preliminary report of a reinvestigation of the decay scheme,

† Guggenheim and Fulbright research scholar during the years 1955—56 and 1956—57.

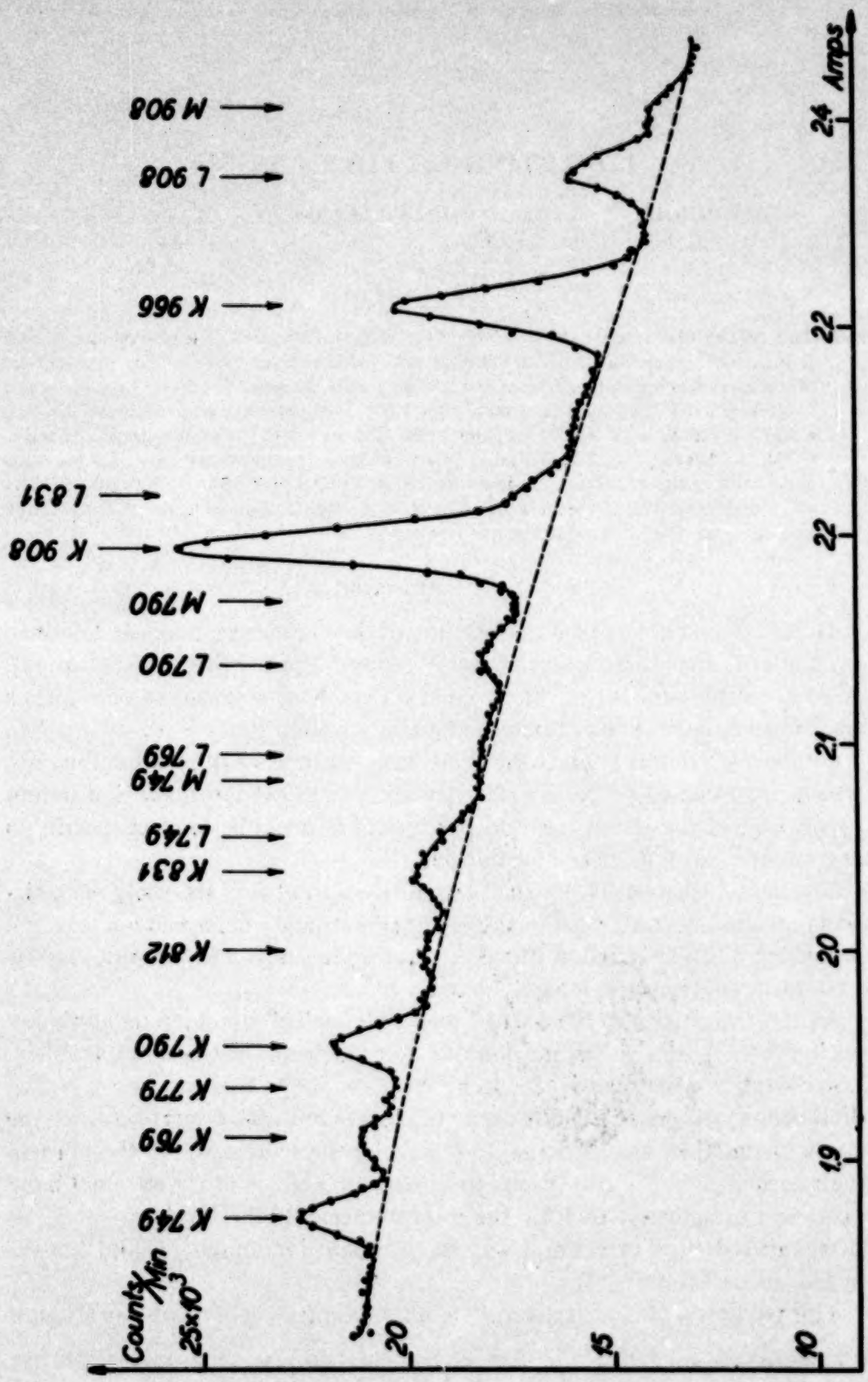

Fig. 1. Part of the conversion line spectrum. Resolution ≈ 1 %.

dealing with the lower excited levels, which can be discussed in the light of the unified model.

2. Experimental

The sources of Ac^{228} were separated from the long lived mother activity Ra^{228} by ion-exchange. Ra^{228} was stored on a small column of Dowex-50

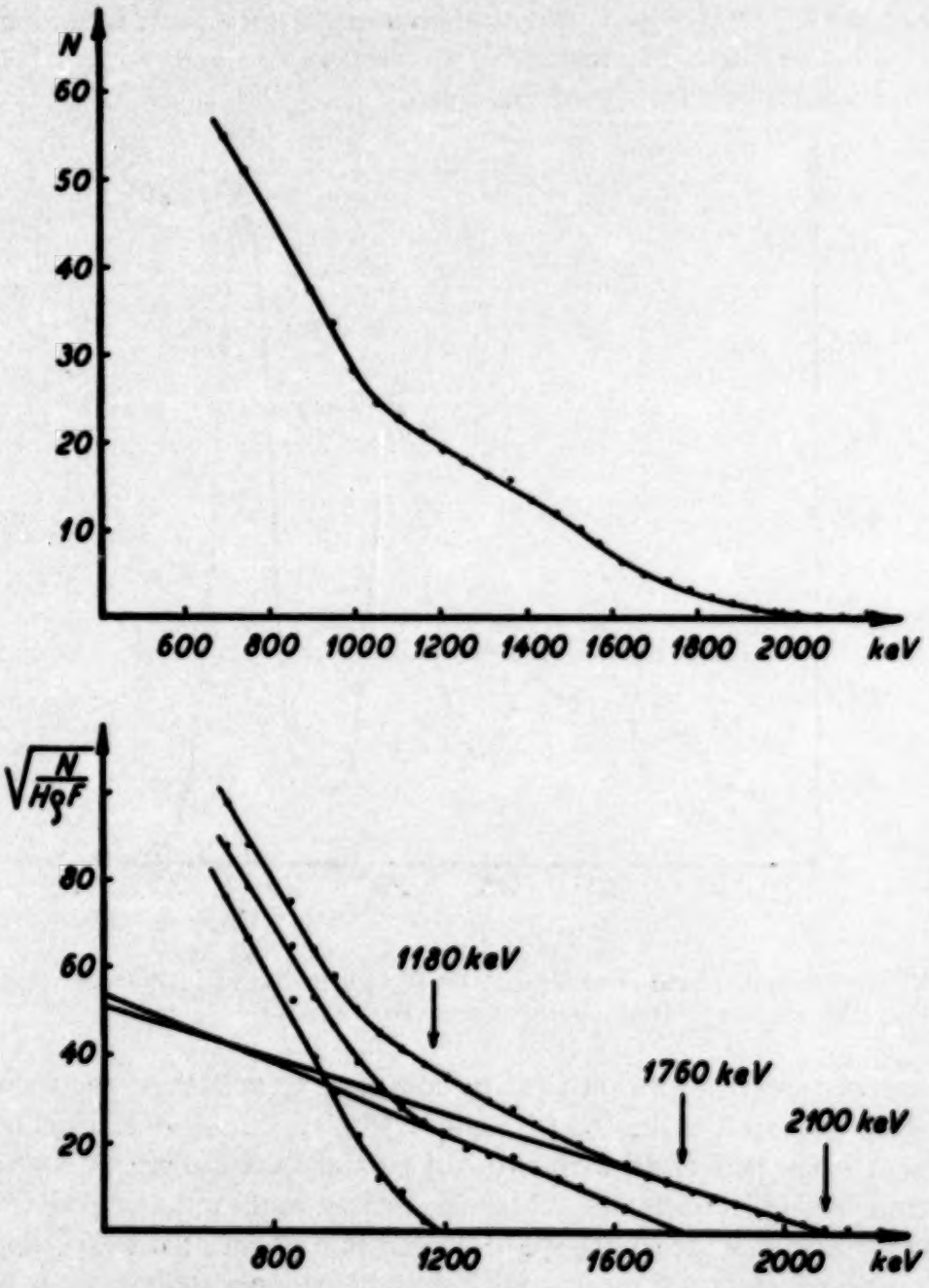

Fig. 2. Above: High energy end of the continuous β-ray spectrum.
Below: Fermi analysis.

resin, where it sticks at low pH-values. The Ac^{228}, which is formed continuously, could be milked out daily by elution with a 5 % ammonium citrate solution (pH = 4.3). The preparation of sources for the β-ray spectrometer was performed by a microchemical method, which has been described already [10]. β-ray sources with a strength up to about 0.5 mC were available.

β-rays and conversion lines were investigated in a six gap β-ray spectrometer [11]. The stronger sources made it possible to scan the spectrum at a resolution 0.7—1.0 % with a statistical accuracy of a few parts in a thousand (fig. 1). Under these circumstances, a considerable number of earlier unreported conversion lines were observed.

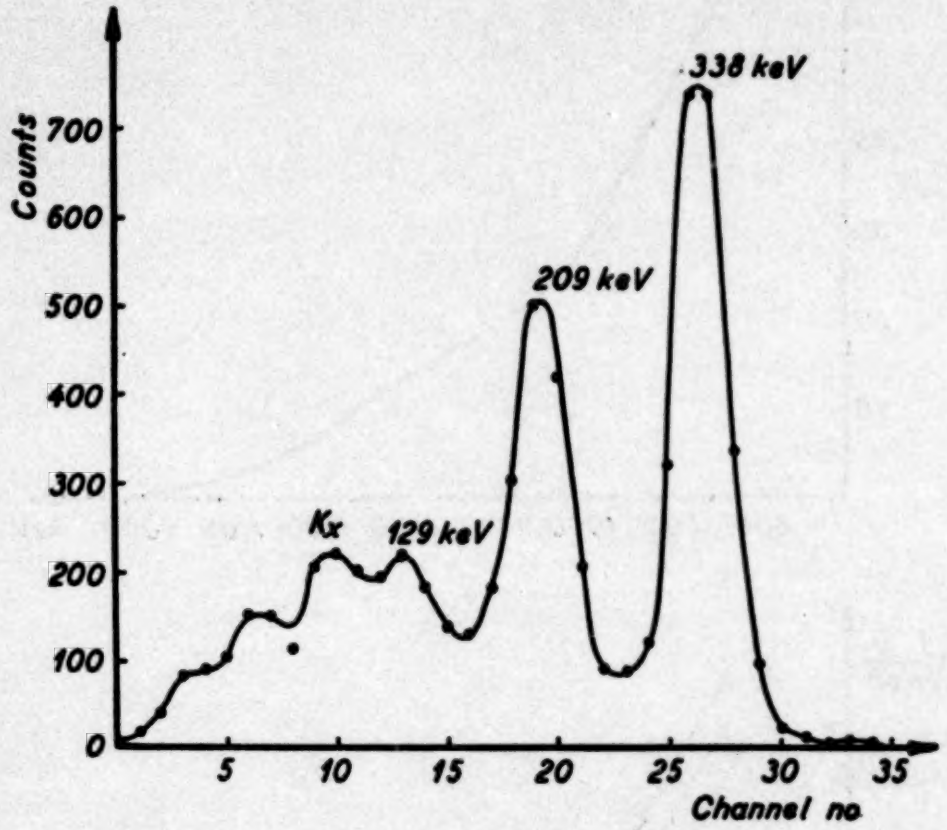

Fig. 3. γ-ray spectrum coincident with the 1760 keV β-group. The energies are as obtained in the conversion line measurement.

The γ-ray spectrum was studied by means of scintillation spectrometers with NaI-crystals 1.5″ dia × 1.5″ and 3″ dia × 3″. $\gamma-\gamma$ coincidence experiments were performed with two NaI crystals. Coincidences with β-rays and conversion electrons were obtained with an anthracene or NaI crystal placed behind the source in the spectrometer. In the coincidence experiments, the coincident spectrum was recorded on a 36 channel analyzer. The β-ray spectrum of Ac^{228} contains a number of extremely strong conversion lines corresponding to transition energies of 58, 100, 129 and 184 keV. These high-

ly converted transitions could be utilized very efficiently for coincidence experiments in the six gap spectrometer.

In many cases, more accurate measurements of absolute and relative γ-ray intensities were obtained in coincident spectra, which had a much simpler structure than the total γ-ray spectrum (see e. g. fig. 3).

For the measurement of the life time of the 58 keV level, a conventional fast slow coincidence set-up with plastic phosphors was used.

3. The Decay Scheme

Fig. 2 shows the high energy part of the continuous β-ray spectrum. Fermi analysis reveals two components with endpoints about 2100 and 1760 keV. The 2100 keV branch was strongly coincident with low energy electrons, but

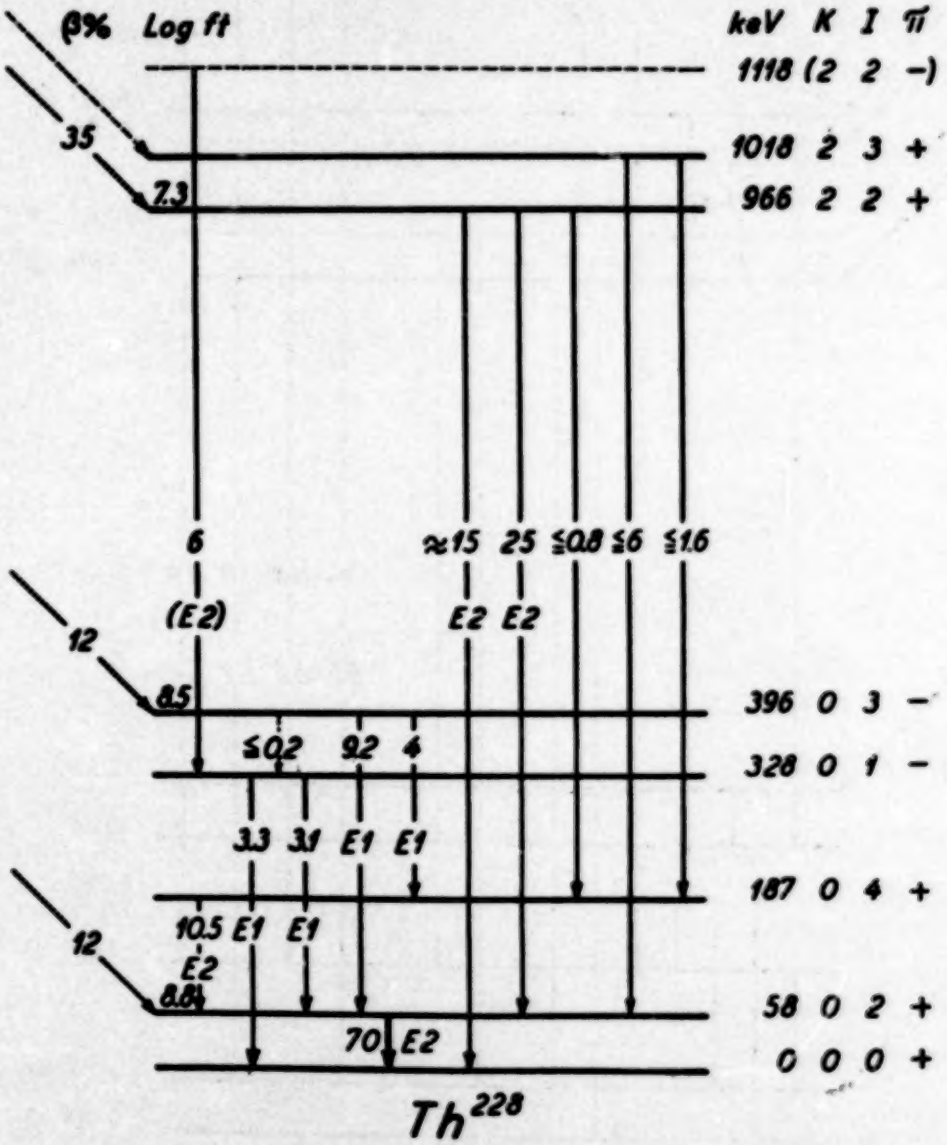

Fig. 4. Low lying levels in Th^{228}.

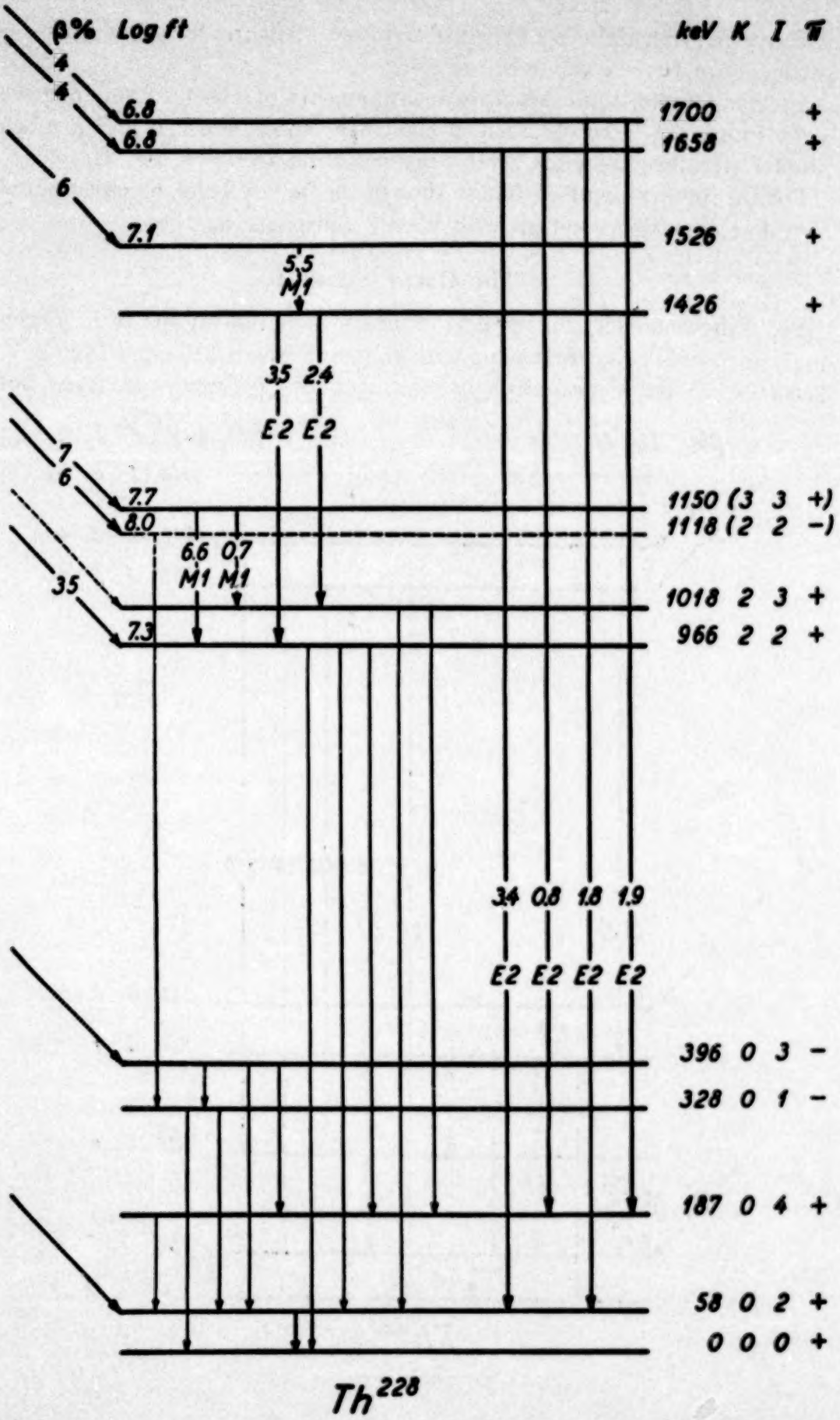

Fig. 5. Tentative decay scheme. In addition, weak conversion lines corresponding to γ-rays of 178 (M1), 282, 321, 443, 473, 484, 510, 555, 573, 619, 749 and 769 keV have been observed.

with no γ-ray. It is thus confirmed, as suggested by Kyles *et al.* [6]), that it excites the 58 keV level (fig. 4), which decays predominantly by internal conversion in the L and M shells.

With the spectrometer placed between 1180 and 1760 keV, the γ-ray spectrum fig. 3 appeared on the kicksorter. Coincidences between the 129 and 209 keV transitions were established with the spectrometer on the conversion lines L_{129}. In addition, it could be demonstrated, that all three lines were coincident with the conversion lines L_{58}.

Levels at 58 and 187 keV are known from the α-decay of U^{232}. The coincidence relations clearly establish a level at 396 keV and places the above transitions in the decay scheme as shown in fig. 4.

The 328 keV level, which is known from the α-decay, is excited by a γ-ray of about 800 keV, which was observed in coincidence with γ-rays of 328 and 270 keV. The conversion line K_{790}(fig. 1) most likely represents this transition, although the γ-ray energy was not measured accurately enough to exclude the line K_{769}. The conversion lines for the transitions from the 328 keV level were observed, and it was confirmed, that the line K_{328} was not coincident with conversion electrons from the 58 keV transition.

The two γ-rays of 966 and 908 keV appeared in coincidence with β-rays of energy below 1180 keV. Both were coincident with the conversion lines of the 100 and 184 keV transitions (fig. 5), whereas only the 908 keV line was coincident with 58 keV.

These relations establish a level at 966 keV, which deexcites to the ground state and to 58 keV. The E2 character of these transitions (see next section) assigns the level as 2^+, and thus a 779 keV transition to the 187 keV level could also proceed by E2 radiation. The γ-ray spectrum coincident with the 129 keV conversion lines contains a broad peak of unresolved lines about 800 keV, and a weak conversion line of the right energy was also found, but the position in the decay scheme could not be clearly confirmed by coincidence experiments.

A level at 1018 keV, which is naturally identified as the 3^+ state in the rotational band of 966 keV, is established by the coincidence relations of the 408 keV γ-ray. This line appears together with the 460 keV line in the spectrum coincident with the conversion lines of the 100 keV transition (fig. 5). The 460 keV ray is coincident with γ-rays of about 910 and 960 keV, whereas the 408 keV ray is coincident with γ-rays of about 830 and 960 keV. These γ-rays thus represent the deexcitations from 1018 keV to the 187 and 58 keV levels, which would be expected from a 3^+ level.

The conversion line K_{831} has been observed (fig. 1), but the intensity of the γ-ray is not known accurately enough for a multipole assignment. The line K_{960} is not resolved from K_{966} with our present resolution.

We have not completed the investigation of transitions involving higher

excited states, but the levels of fig. 5 are established by the measurements. In addition, we have observed a considerable number of weaker transitions (fig. 5), which are still not placed into the scheme.

4. Multipole Order of the Transitions

Tables 1 and 2 contain conversion line ratios pertinent to the assignment of multipole orders. Table 3 shows intensities of conversion lines and of γ-rays. Column 6 gives γ-ray intensities calculated from the observed conversion lines by dividing with the theoretical conversion coefficients. Comparison between these values and the measured γ-ray intensities in column 7 checks the consistency of the multipole assignments. In cases when the multipole assignment is unambiguous, the intensities in column 6 are believed to give more accurate results than γ-ray intensities obtained in a complicated scintillation spectrum.

TABLE 1

$(L_I+L_{II})/L_{III}$ ratios

E_γ keV	Assignment	Experimental	Theoretical		
			E1	E2	M1
58	E2	1.15±0.15	2.0	1.25	180
129	E2	1.7 ±0.2	3.7	1.8	200

The conversion ratios are obtained from the tables of Rose *et al.* [13]).

TABLE 2

K/L ratios

E_γ keV	Assignment	Experimental	Theoretical			
			E1	E2	M1	M2
129	E2	0.12±0.03	≈5	≲0.15	≈5	≈2
209	E1	≈5	5.4	0.5	5.3	3.1
270	E1	≈4	5.6	0.9	5.3	3.6
328	E1	≈5	5.7	1.3	5.3	3.9
338	E1	5±1	5.7	1.3	5.3	3.9

The conversion ratios are obtained from the tables of Rose *et al.* [13]).

The E2 nature of the transitions from the two lowest excited states is apparent from the $(L_I+L_{II})/L_{III}$ ratio, for the 129 keV transition from the K/L ratio as well.

The E1 assignment for the four transitions from 328 and 395 keV are based on K conversion coefficients and K/L ratios. The assignments are quite unambiguous, even though the γ-ray intensities are not known very

TABLE 3

Transition intensities

E_γ keV	Assignment	Shell	$I_{line} \times 10^4$	Conversion Coefficient Theor.	I_γ calc. %	I_γ obs. %	Transition Intensity %
58	E2	L	5300	144	0.3	—	70 ±7
129	E2	L	520	1.55	3.4	4	10.5±1.0
209	E1	L	5	1.2×10^{-2}	4	4.5	4
270	E1	K	12	3.8×10^{-2}	3.0	3	3.1
328	E1	K	8	2.5×10^{-2}	3.2	4	3.3
338	E1	K	22	2.4×10^{-2}	9.2	11	9.5
779	(E2)	K	$\lesssim 1$	1.2×10^{-2}	(0.8)	—	(0.8)
790	(E2)	K	5.5	1.2×10^{-2}	(4.5)	6 †	(4.5)
831	(E2)	K	≈ 1.7	1.1×10^{-2}	(1.6)	—	(1.6)
908	E2	K	24	9.5×10^{-3}	25	25	25
960 +966	E2	K	16	8.3×10^{-3}	19	20	19

† $I_{270}+I_{328}$

The intensity of conversion lines and the conversion coefficients refer to the shell indicated in column 3. The L conversion coefficients are from the tables of Rose *et al.* [12]), the K coefficients from those of Sliv and Band [13]). The transition intensities in column 8 include γ-rays and conversion lines.

accurately, since the K/L ratios exclude E2 radiation, and the K conversion coefficients for all other multipoles are at least a factor of 10 higher. Also a very low limit can be set on M2 admixtures.

The assignments on the higher energy transitions are based mainly on the K conversion coefficients. In these cases, considerable multipole admixtures cannot be excluded.

5. The Level Structure

Except for 1018 and 1118 keV, angular momenta and parities for the excited levels on fig. 4 can be inferred from the multipole nature of the γ-rays with the only assumption of 4^+ for the 187 keV level, which decays by E2 radiation to the 58 keV 2^+ level, with no cross-over to the ground state †.

The life-time of the 58 keV level was found to be $\lesssim 5\times10^{-10}$ sec. The corresponding E2 transition probability, which is more than 200 times the single particle value, thus confirms the collective nature of the state.

The branching ratio for the γ-rays from the 329 keV level has already been given by Asaro and Perlman [3]) and by Scharff-Goldhaber *et al.* [4]), who found $(\gamma_{270}/\gamma_{328})(328/270)^3 = 1.8$ and 2.4, respectively, in good agreement with our value 1.7. The theoretical ratio is 2, assuming the K quantum number 0 for the 1^- state.

† The 184 keV transition, which earlier was believed to be a cross-over [5, 6]), is about 100 % coincident with the γ-rays from the 966 keV level, and not with any other strong γ-ray, and can be placed definitely between the 1050 and 966 keV levels.

Similarly, we have obtained $(\gamma_{208}/\gamma_{338})(338/208)^3 = 1.8 \pm 0.3$, to be compared with the theoretical value 1.33, assuming $K = 0$ for the 3^- state. For $K = 1$, these ratios should be 0.5 and 0.75 for the 1^- and 3^- levels, respectively. The $K = 0$ assignment for this odd parity band is thus further confirmed.

We have observed a weak conversion line with an energy corresponding to the L_{II} conversion line of a 68 keV transition from 396 to 328 keV. This position in the decay scheme could not be confirmed by any coincidence experiment due to the low intensity. Assuming E2 character, the transition accounts for less than 0.2 % of all transitions, or about 1 % of all decays from the 396 keV level. This figure thus represents an upper limit for the intensity of the transition from the 3^- to the 1^- level.

The branching ratio based on conversion lines for the transitions from the 966 keV level to the 0^+, 2^+ and 4^+ levels of the ground state band is $0.45 : 1 : \lessapprox 0.07$. The intensity of K_{966} is corrected by the most probable contribution from the line K_{960}. For $K = 2$, this ratio is calculated to $0.7 : 1 : 0.05$, whereas other assignments of K give a poor fit.

The two γ-rays from the 1018 keV level was observed separately in the coincident spectrum of the 408 keV transition. The ratio, corrected for the energy dependence, between the transitions to 2^+ and 4^+ is ≈ 2. The theoretical value is 2.5, assuming $(K, I) = (2, 3)$ for 1018 keV, and E2 nature for the γ-rays.

The intensity of the line K_{790}, which probably represents the transition populating the 328 keV 1^- level, indicate E2 nature. An assignment $K = 2$ is then suggested for the 1118 keV level, which decays to a $(0, 1^-)$ level with E2 radiation, whereas no E1 radiation to the ground state band is observed. The angular momentum is then most probable 2^-, in which case a ratio of $5 : 1$ for the γ-rays to the 1^- and 3^- states would be expected, when the energy dependence is taken into account. The weakness of the unobserved transition to the 3^- state is then explained. $I = 3^-$ is less probable, as a 3^- level would decay mainly to the $(0, 3^-)$ state.

6. Discussion

Our experimental results are not essentially in disagreement with earlier investigations, but the observation of new conversion lines and coincidence relations establishes a revised decay scheme.

The low lying levels in Th^{228} above the ground state band belong to two rotational families, which occur regularly in even nuclei in this region.

The odd parity band with $K = 0$ and $I = 1^-, 3^-, \ldots$ has been observed in a number of cases in the actinide region [1,2]). There are indications too, of the occurrence of similar states in deformed nuclei in the lanthanide region[14]).

The states are tentatively interpreted as representing an octupole vibration of the nuclear shape [2]).

The moment of inertia $\mathcal{J}$ for a nuclear state is related to the energy differences in the rotational band by

$$\Delta E = \frac{\hbar}{2\mathcal{J}} I(I+1).$$

The energy difference of 68 keV between the 1^- and 3^- states indicates that the moment of inertia is about 40% higher than for the ground state. This result is in accord with the trend in neighbouring nuclei [1]).

The transition probability for E2 radiation between rotational levels in neighbouring even nuclei is systematically more than 10^2 times the single particle value. Assuming a similar enhancement of the 68 keV transition from 396 to 328 keV, its probable partial life time is about 10^{-9} sec. The limit set on the intensity of the 68 keV line corresponds to an upper limit for the partial life time of the 338 keV E1 transition of 10^{-11} sec or 10^3 times the single particle value †.

The rotational band with $K = 2$ and $I = 2^+, 3^+, \ldots$ is interpreted as a γ-vibrational band [2]). There is evidence for a similar band occurring at about 1 MeV in other strongly deformed even nuclei in the rare earth as well as in the actinide region [1,2,9,14,18,19]).

Although the arguments for the assignment of $(2, 2^-)$ to the 1118 keV level are in no way conclusive, the situation deserves some attention. At present, evidence is accumulating for the systematic occurrence of states, interpreted as a second octupole vibrational band, with $K = 2$ and $I = 2^-, 3^-, \ldots$ in deformed even rare earth isotopes [14,18,19]). The position of the band is a few hundreds of keV above the γ-vibrational band.

The β-decay to levels in Th^{228} with angular momentum 2 and 3 suggests $K = I = 2$ or 3 for Ac^{228}. The low intensity for the β-decay to the two lowest rotational bands relative to the transitions to high energy levels is thus probably due to K-forbiddenness. This effect can also explain the fact that an excited band with $K = 0$ and $I = 0^+, 2^+, 4^+, \ldots$ has not been observed. Members of such a band, which is believed to represent a β-vibration [2]), have been observed in Pu^{238}, U^{234} [1]) and Th^{232} [2]), and the position of the $I = 0$ level in Th^{228} can be extrapolated to about 650 keV.

We are indebted to Professor N. Bohr for ideal working conditions in his Institute. This investigation was strongly stimulated by Professor A. Bohr

† A 960 keV level in Sm^{152} with $(K, I) = (0, 1^-)$ is probably of similar nature [14]). In this case, Grodzyns [16]) has found a lower limit for the life time 130 times the single particle value. E1 transitions from these assumed octupole vibrational states thus seem to be $10^2 - 10^3$ times slower than single particle transitions. Theoretical estimates [16,17]) give an E1 transition probability of the same order.

and Dr. B. R. Mottelson. Their continuous interest and advice has been of decisive importance.

One of us (R. K. S.) wishes to thank the Institute, the Fulbright Foundation and the Guggenheim Memorial Foundation for a visiting professorship and grants which made possible his participation in this work.

The multichannel analyzer has been placed at our disposal by Mr. B. Madsen. The majority of the sources used in the investigation have been prepared by Mr. J. Brix-Petersen.

References

1) I. Perlman and J. Rasmussen, α-Radioactivity in Handbuch der Physik
2) K. Alder, A. Bohr, T. Huus, B. R. Mottelson and Å. Winther, Rev. Mod. Phys. **28** (1956) 432
3) F. Asaro and I. Perlman, Phys. Rev. **99** (1955) 38
4) G. Scharff-Goldhaber, E. der Mateossian, G. Harbottle and M. McKeown, Phys. Rev. **99** (1955) 180
5) O. H. Black, Proc. Roy. Soc. A **106** (1924) 632
6) J. Kyles, C. G. Campbell and W. J. Henderson, Proc. Phys. Soc. A **66** (1953) 519
7) H. C. Box and G. S. Klaiber, Phys. Rev. **95** (1954) 1247
8) Ong Ping Hok and E. Arbman, Ark. f. Fys. **11** (1956) 193
9) G. Alaga, K. Alder, A. Bohr and B. R. Mottelson, Mat. Fys. Medd. Dan. Vid. Selsk. **29** (1955) no. 9
10) S. Bjørnholm, O. B. Nielsen and R. K. Sheline, Nature **178** (1956) 1110
11) O. B. Nielsen and O. Kofoed Hansen, Mat. Fys. Medd. Dan. Vid. Selsk. **29** (1955) no. 6
12) M. E. Rose, G. H. Goertzel and C. L. Perry, ORNL-1923 (1953); M. E. Rose, G. H. Goertzel and C. Swift, L-she'l internal conversion coefficients, privately distributed
13) L. Sliv and J. Band, K conversion coefficients
14) O. Nathan and M. A. Waggoner, Nuclear Physics **2** (1956/57) 548
15) L. Grodzyns, BAPS **1** (1956) 329
16) V. M. Strutinsky, Physica **22** (1956) 1166
17) A. Bohr and B. R. Mottelson, Nuclear Physics, in print
18) O. Nathan, Nuclear Physics **4**(1957)124
19) P. Gregers Hansen, O. B. Nielsen and R. K. Sheline, to be published

Nuclear Physics **4** (1957) 325—329; © *North-Holland Publishing Co., Amsterdam*
Not to be reproduced by photoprint or microfilm without written permission from the publisher

THE DECAY OF ^{109}Cd, ^{109}Ag AND ^{109}Pd

A. H. WAPSTRA AND W. VAN DER EIJK
Instituut voor Kernphysisch Onderzoek, Amsterdam

Received 6 May 1957

Abstract: The K conversion coefficient of the 88 keV E3 gamma ray in ^{109}Ag* is found to be 10.3 ± 0.5. The theoretical value is 11.6. The electron capture decay energy of ^{109}Cd to this level of 75^{+15}_{-10} keV is obtained from the ratio of K and L capture. Gamma rays of 305 and 410 keV which could originate from known levels at these energies in ^{109}Ag occur for 0.07 % and < 0.03 % per decay of ^{109}Pd.

1. Introduction

^{109}Cd and ^{109}Pd decay both to the isomeric level ($T_{\frac{1}{2}} = 39$ sec) at 87.7 keV [5]) in ^{109}Ag (see fig. 1). Table 1 summarizes several results about the conversion properties of the transition between this level and the ground state of ^{109}Ag. ^{109}Pd decays by emission of an allowed β-spectrum of 1020 ± 5 keV [5]). It may also decay to levels at 305 and 410 keV in ^{109}Ag found by Coulomb excitation experiments [7,8]). The latter transitions have not yet been reported. The ratio of electron captures in the L and K electron shells has been found to be 0.32 ± 0.04 [9]) and 0.28 ± 0.03 [10]); the reported decay energies derived from these ratios are 67^{+8}_{-3} and 73^{+12}_{-6} keV.

TABLE 1

Conversion data of isomeric γ-rays in ^{109}Ag*
(87.7 ± 0.2 keV [5])

α_K	K/L	$K/(M+N)$	$K/(L+M)$	References
9.5 ± 1.5 †	1.01 ± 0.06	6.1 ± 1.0	(0.86 ± 0.07)	1)
6.6				2)
8.6 ± 1				3)
9.5 ± 1			0.80 ± 0.04	4)
	0.97	(6.2)	0.84	5)
12.4 ± 1			0.85 ± 0.02	6)
10.3 ± 0.5				This work
11.6	0.96			Theory [14,15])

† This is the result as corrected by ref. [4]); the original value is 8.8 ± 1.5.

2. Measurements

We determined the ratio of the intensities of the X_K-rays and the 88 keV gamma rays in ^{109}Pd and ^{109}Cd with a scintillation spectrometer. ^{109}Cd was obtained carrier free from Messrs. Philips-Roxane. ^{109}Pd was prepared by

bombarding mass separated ^{108}Pd with deuterons. After dissolving the target and adding hold back carriers, silver was repeatedly precipitated as the chloride; thereafter Pd was precipitated with dimethylglyoxim.

The ratio of the numbers of K Röntgen rays and gamma quanta in ^{109}Cd was measured with a 1" NaI(Tl) scintillation crystal. The crystal was mounted in a holder with a thin beryllium window, in which the absorption

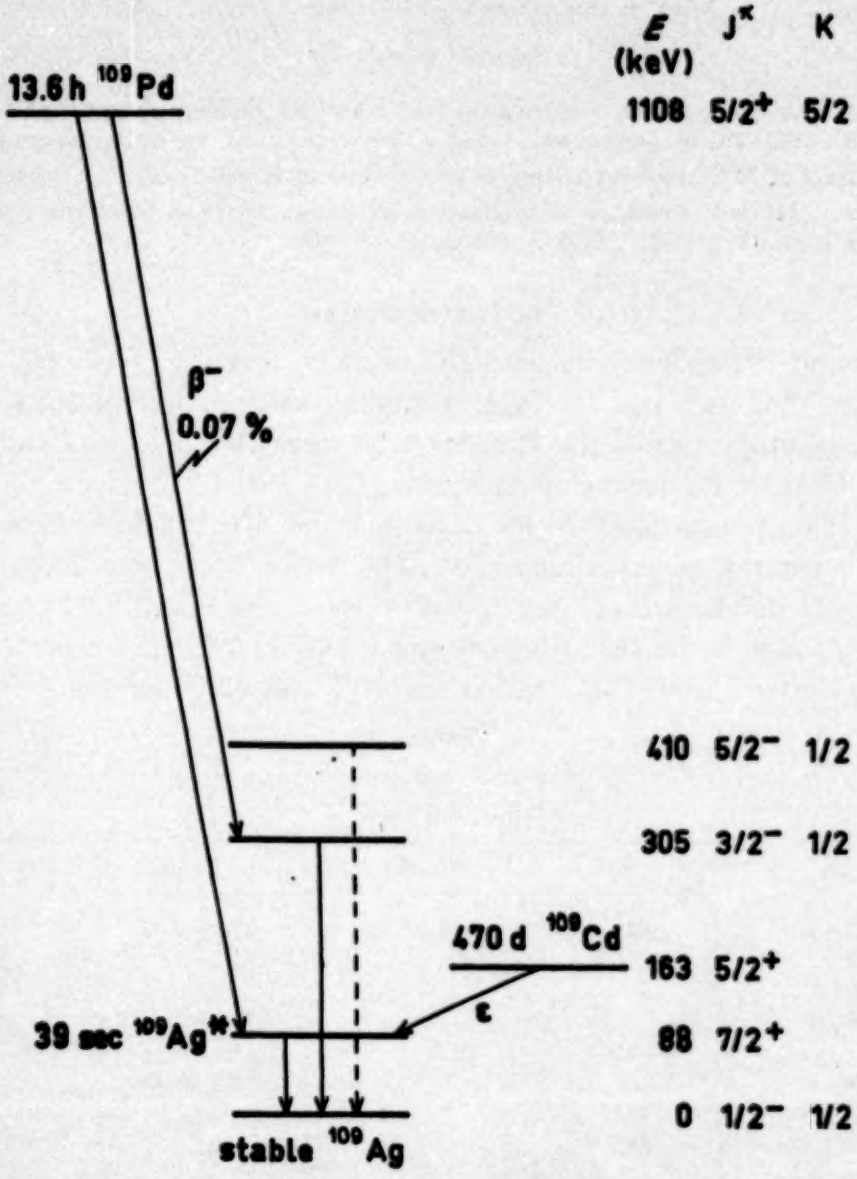

Fig. 1 Decay scheme of ^{109}Pd, ^{109}Ag* and ^{109}Cd.

even of the 22 keV X_K-rays could be neglected. The computed efficiency for measuring both radiations was in all cases over 90 % of the solid angle divided by 4π; the errors in these efficiencies can therefore be assumed to be small. The average result of several runs was $x = (X_K/\gamma)_{Cd} = 33.8 \pm 0.7$. This

value agrees well with other results [9, 12, 4]). (The value $x = 33.8 \pm 2.5$ given in ref. [4]) is an error, it should be 21.7 ± 1.7. The conclusions in that paper were based on the correct figure.)

Results for the ratio $y = (X_K/\gamma)_{Cd}/(X_K/\gamma)_{Pd}$ obtained with use of two ^{109}Pd sources, of which one was nearly three times as thick as the other one, agreed well; consequently no corrections for self-absorption were necessary. Several measurements yielded an average value of $y = 2.85 \pm 0.05$.

A 305 keV gamma ray with an intensity 1.8 % of that of the 89 keV gamma ray was found in the ^{109}Pd sample. The estimated intensity of a 410 keV gamma ray is less than 0.8 %.

3. The Conversion Coefficients

The K conversion coefficient of the 88 keV transition is

$$\alpha_K = x/yW_K$$

in which W_K is the fluorescent yield. Experimental values for W_K are 0.795 (Arends [13]), 0.838 (Backhurst [13]), 0.81 (Stephenson [13]) and 0.83 (Bradt *et al.* [1]). We estimated $W_K = 0.815 \pm 0.015$ by taking into account values W_K for neighbouring nucleides. Knowing x and y one obtains $\alpha_K = 10.3 \pm 0.5$. This result agrees with the average value $\alpha_K = 10.0 \pm 0.9$ of the earlier results collected in table 1. If the value found by Brunner *et al.* [5]) (the only one deviating considerably from the other results) is excluded, the average experimental value for α_K becomes 9.8 ± 0.4. These results therefore indicate that the theoretical K conversion coefficient for an E3 transition $\alpha_K = 11.6$ as derived from the tables of Rose and Goertzel [14]) and those of Sliv and Band [15]) may be significantly too large.

Large deviations in the same direction from the tables of Rose and Goertzel were found for M1 and E2 transitions in nucleides with mass numbers around 200 [17]). These deviations are at least partly explained by the fact that Rose and Goertzel's computations did not take into account the effects of the finite nuclear size. This effect should be almost negligible for E3 transitions in nucleides with masses around 100: Rose and Goertzel's value in this case is equal to that of Sliv and Band which is corrected for this effect. It should be mentioned that the experimental values of the M1 and E2 conversion coefficients in the heavy nucleides discussed above are still about 10 % lower than the values obtained from Sliv and Band's tables. These measurements were made in a probably more dependable way than those reported in this paper; nevertheless we are inclined to believe that the present deviation too is outside the limits of the possible errors. All these deviations may be due to the effect that the conversion coefficients may depend upon nuclear matrix elements, as discussed by Church and Weneser [18]).

The ratio of K and L conversion electrons agrees well with the theoretical value computed by Rose and Goertzel, as can be seen from table 1.

4. Other Decay Data in ^{109}Pd and ^{109}Cd

Using the experimental conversion coefficient of the 88 keV gamma-ray we find that the possible transitions of ^{109}Pd to the 305 and 410 keV states in ^{109}Ag have intensities of 0.07 % and $\geqq$ 0.03 % respectively. The log ft values for these transitions are 9.2 and $\geqq$ 9.3 respectively as compared with a value 6.1 for the allowed transition to the 88 keV level. These large values may be explained by an assumed K-forbiddenness of these transitions. The decay scheme is presented in fig. 1.

The percentage K captures per decay of ^{109}Cd is

$$\varepsilon_K/\varepsilon_{tot} = \frac{y-1}{(W_K y/x)+1+[(L+M)/K]}$$

The data discussed above yield $\varepsilon_K/\varepsilon_{tot} = 0.805\pm0.027$. The ratio of capture in higher shells to K capture is then $0.24_3\pm0.04$. This result agrees with the value 0.28 ± 0.03 found by der Mateosian. The result of Bertolini *et al.* 0.32 ± 0.04 is computed using now obsolete values for the conversion coefficient; after a correction it becomes 0.30 ± 0.04 which value is still somewhat higher than the results discussed above. Since this difference may be due to uncertainties in the L shell fluorescent yields used in their work, we will assume an average value

$$(\varepsilon_L+\varepsilon_M+\ldots)/\varepsilon_K = 0.26_5\pm0.03.$$

The ratio of capture in the Y shell (Y = L, M, N ...) to that in the K shell is in allowed transitions

$$\varepsilon_Y/\varepsilon_K = A_Y\{(Q-B_Y)/(Q-B_K)\}^2$$

in which approximately

$$A_Y = \frac{1}{n^3}\left(\frac{Z-Z_Y}{Z-Z_K}\right)^3;$$

n is the principal quantum number, Z_Y the Slater screening constant and B_Y the binding energy of the Y shell (the differences in binding energies between subshells are neglected); Z is the nuclear charge number, and Q the transition energy. From this formula it follows that for $Z = 47$ $A_L = 0.0965$, $A_M = 0.0166$, $A_N = 0.0012$, and therefore $(A_L+A_M+A_N+\ldots)/A_L = 1.19$. A more exact computation by Rose and Jackson yields a rather higher value 0.110 for A_L; it may, however, be assumed that a more exact computation would not affect $(A_L+A_M+\ldots)/A_L$ seriously.

We thus find in our case

$$(\varepsilon_L+\varepsilon_M+\ldots)/\varepsilon_K = 0.13\{(Q-3.8\text{ keV})/(Q-25.5\text{ keV})\}^2.$$

This formula differs from that used by der Mateosian and by Bertolini *et al.* in two respects: 1) we used experimental binding energies instead of values derived from a theoretical formula, and 2) we have not neglected capture in M, N . . . shells. We find in this way a disintegration energy 75^{+15}_{-10} keV. This result agrees reasonably well with the value 95 keV derived from beta decay systematics.

We thank Professor Dr. P. C. Gugelot and Dr. R. van Lieshout for their interest in this work, which is part of a program of the Foundation for Fundamental Research of Matter (F.O.M.) and financially supported by the Netherlands Foundation for Pure Scientific Research (Z.W.O.).

References

1) H. Bradt, P. C. Gugelot, O. Huber, H. Medicus, P. Preiswerk, P. Scherrer and R. Steffen, Helv. phys. Acta **20** (1947) 153; O. Huber, F. Humbel, H. Schneider and A. de Shalit, Helv. phys. Acta **25** (1952) 1
2) K. Siegbahn, E. Kondaiah and S. Johansson, Nature **164** (1949) 405
3) P. Avignon, J. Phys. Radium **14** (1953) 636
4) A. H. Wapstra, Ark f. Fys. **7** (1953) 265
5) J. Moreau, J. Phys. Radium **15** (1954) 380
6) J. Brunner, O. Huber, R. Joly and D. Maeder, Helv. phys. Acta **26** (1953) 588
7) N. P. Heydenburg and G. M. Temmer, Phys. Rev. **95** (1954) 861
8) L. W. Fagg, E. A. Wolicki, R. O. Bondelid, K. L. Dunning and S. Snijder, Phys. Rev. **100** (1955) 1299
9) G. Bertolini, A. Bisi, E. Lazzarini and L. Zappa, Nuovo Cimento, **11** (1954) 539
10) E. der Mateosian, Phys. Rev. **92** (1953) 938
11) L. Th. M. Ornstein, R. E. W. Kropveld and A. H. Wapstra, Physica **19** (1953) 915
12) D. Maeder *et al.*, private communication
13) E. H. S. Burhop, The Auger Effect (Cambridge University Press, London, 1952)
14) M. E. Rose and G. H. Goertzel, privately circulated tables
15) L. A. Sliv and I. M. Band, Akad. Nauk. SSSR (Moscow-Leningrad, 1956)
16) F. A. Johnson, Can. J. Phys. **31** (1953) 1136
17) A. H. Wapstra and G. J. Nijgh, Nuclear Physics **1** (1956) 245; to be published
18) E. L. Church and J. Weneser, Bull. Amer. Phys. Soc. **1** (1956) 331
19) M. E. Rose and J. L. Jackson, Phys. Rev. **76** (1949) 1540

Nuclear Physics **4** (1957) 330—336; © *North-Holland Publishing Co., Amsterdam*
Not to be reproduced by photoprint or microfilm without written permission from the publisher

ON THE RADIUS OF THE ALPHA-PARTICLE

I. I. LEVINTOV
USSR Academy of Sciences, Moscow

Received 25 March 1957

Abstract: The parameters of the alpha particle potential are estimated from data relating to the polarization and cross section for scattering of 315 MeV protons on He^4. Comparison with low energy data indicates that the p—He^4 interaction range decreases by 30 % when E_p increases from $\approx$ 10 MeV to $\approx$ 300 MeV.

1. Introduction

The amount of data available at present on scattering of protons on He^4 is sufficient for a phenomenological description of p—He^4 interaction. Comparison of the low ($\approx$ 10 MeV) and high ($\approx$ 300 MeV) energy data leads to some interesting conclusions regarding the dependence of the range of nuclear forces on nucleon velocity.

By analyzing proton cross section and electron scattering data Drell [1]) was able to show that a difference of about 20 % exists between the range of nuclear forces and the radius of nuclear matter distribution, the latter being close to that for the charge distribution. This difference is especially appreciable for alpha particles. Thus from the angular distribution of 150 MeV electrons scattered on He^4 a charge radius of $1.6 \cdot 10^{-13}$ cm [2]) can be inferred whereas the range for nucleon-He^4 interaction at low energies is deduced to be $2.3 \cdot 10^{-13}$ cm (see below). It might therefore be expected that α particle effects associated with the existence of a virtual meson cloud should be particularly pronounced and easily observable.

On the other hand the α particle possesses some peculiar features which greatly facilitate determination and comparison of the interaction parameters at low and high nucleon energies. First of all, due to the zero spin, the number of experiments required to obtain complete information on the scattering amplitude is restricted to those which yield data on the cross section $\sigma(\theta)$ and polarization $\mathbf{P}(\theta)$. In this respect N—α collisions favourably differ from nucleon-nucleon collisions; up to the present high energy nucleon-nucleon collisions have not been adequately described due to the complexity of the scattering amplitude.

The fact that He^4 is a very closed system leads to the result that up to energies of $E_p \approx 10-15$ MeV the p—He^4 scattering phase shifts are real and their energy dependence corresponds to the motion of a body in a real central potential field containing an additional spin-orbit term [3,4])

$$U(r) = V_1 \varrho_1(r) + V_2 \frac{1}{r} \frac{d\varrho_2}{dr} (\mathbf{l} \cdot \boldsymbol{\sigma}) \qquad (1)$$

where ϱ_1, ϱ_2 are functions which are similar to the nucleon density distribution. In other words, at the energies considered one may neglect the contribution from the narrow many-particle levels in Li^5 (He^5) occurring at $E \gtrsim 20$ MeV (e.g. the $3/2^+$ level in the H^3 (d, p)He^4 reaction).

At high energies the V_1 and V_2 in potential (1) become complex and the number of parameters increases. However, because of the small radius of the system the Born approximation is valid for scattering on He^4 (in contrast to the other nuclei), and thus the radius may be determined from the angular dependence of the cross section even when the potential well depth is unknown.

Applicability of this approximation is explained by the fact that the density, mean absorption and refractive coefficients of nuclear matter are approximately the same for all nuclei. Thus nuclear matter layers of a thickness of the same order as the α particle radius are transparent and the shifts in the real part of the phases are small.

Moreover, the high excitation energy of the α-particle permits one to obtain information on purely elastic scattering into comparatively large angles [6]). These circumstances greatly ease the determination of the potential parameters from experimental data obtained at high energies.

2. Discussion of Experiments

Let us now consider the experimental facts.

2.1. NUCLEON-α SCATTERING AT LOW ENERGIES

At energies up to 10 MeV the S, $P_{1/2}$ and $P_{3/2}$ waves are considerably perturbed. Sack, Biedenharn and Breit [3]) have shown that the $P_{1/2}$, $P_{3/2}$ phase shifts correspond to scattering from a potential of the same type as (1) which possesses the following parameters:

$V_1 = 47$ MeV; $\quad V_2/V_1 = 3.3 \cdot 10^{-27}$ cm^2; $\quad \varrho_1 = \varrho_2 = \exp(-r^2/r_0^2)$

where $r_0 = 2.3 \cdot 10^{-13}$ cm.

The most up-to-date experimental values for the P phase shifts are shown in fig. 1 [5]). The solid lines denote P phase shifts corresponding to scattering of protons on potential (1). In these calculations the Coulomb field of the α particle was assumed to be produced by a charge uniformly distributed over a volume of radius $r_c = 2.31 \cdot 10^{-13}$ cm †. The P phase shift is sensitive to the choice of the effective radius of $\varrho(r)$ in (1). This can be demonstrated as follows. In the energy range under consideration the $P_{1/2}$ phase shift is $< \frac{1}{2}\pi$. Thus for rough estimations the following formula can be used:

† The values of the potential parameters derived from the phase shifts do not appreciably depend on the magnitude of r_c. Use of a point charge changes the potential parameter by less than 0.5 % [3]).

$$\delta_l = \frac{\pi m}{\hbar^2}\int U(r)[J_{l+\frac{1}{2}}(kr)]^2 r\,dr. \qquad (2)$$

For the $P_{1/2}$ phase shift and at $kr \lesssim 1$ eq. (2) yields $\delta_{P\frac{1}{2}} \propto V_{1/2} r_0^2 (kr_0)^3$ where $V_{1/2}$ is the effective well depth in the $P_{1/2}$ state.

On the other hand, at $E_p \approx 2$ MeV the $P_{3/2}$ phase shift passes through $\frac{1}{2}\pi$. This fact implies the extistence of a single-particle $P_{3/2}$ level in Li^5 (He^5) whose position is determined by $V_{3/2} r_0^2$. In virtue of (1) the depths $V_{1/2}$ and $V_{3/2}$ are related as follows: $V_{3/2} - V_{1/2} = c/r_0^2$, where c is proportional to the spin-orbit interaction constant. From the relations presented above it follows that small changes in r_0 sharply change in the course of the $P_{1/2}$ and $P_{3/2}$ phase shifts.

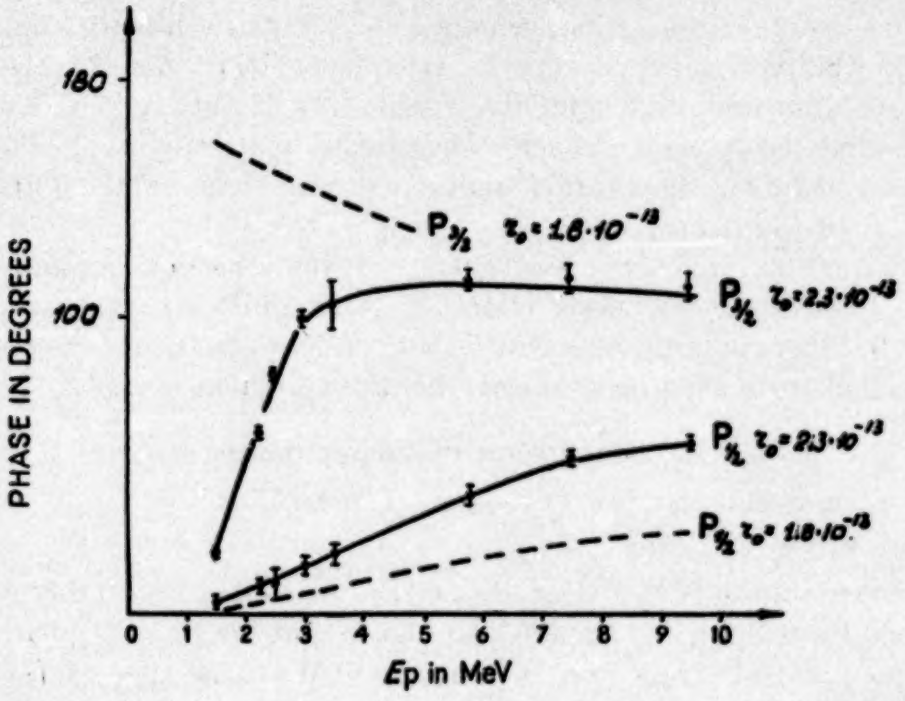

Fig. 1

If the position of the $P_{3/2}$ level remains constant ($V_{3/2} r_0^2 = \text{const.}$) when r_0 varies, the $P_{1/2}$ phase shift will be $\propto r_0^3$. If, however, we require that the course of the $P_{1/2}$ phase shift does not change when r_0 is varied we find that $V_{3/2} \cdot r_0^2$, and hence the level position, will vary inversely proportional to r_0^3. Thus, decrease of r_0 by 30 % (down to $1.8 \cdot 10^{-13}$ cm) leads either to a decrease of the $P_{1/2}$ phase by 2.2 times or to a shift of the $P_{3/2}$ level to the region $E < 0$. According to the general theory the latter circumstance signifies that for $E_p \to 0$ the $P_{3/2}$ phase shift will tend to π but not to zero and its magnitude will decrease with increase of E_p. The approximate course of the $P_{1/2}$ or $P_{3/2}$ phase shifts for $r_0 = 1.8 \cdot 10^{-13}$ cm is shown in fig. 1 by the dotted line and, evidently, contradicts the experimental data.

2.2. p–α SCATTERING AT HIGH ENERGIES

Data on p–He^4 elastic scattering and polarization at an energy of 315 MeV and angle interval between 10^0 and 42^0 in the c.m.s. have been obtained by Chamberlain, Segré *et al.* [6]).

For spin $\frac{1}{2}$ particles scattered by zero spin particles we have

$$P(\theta) \cdot \sigma(\theta) = g^* h + h^* g; \qquad \sigma(\theta) = |g|^2 + |h|^2. \tag{3}$$

It can be shown that in the Born approximation the amplitudes g and h

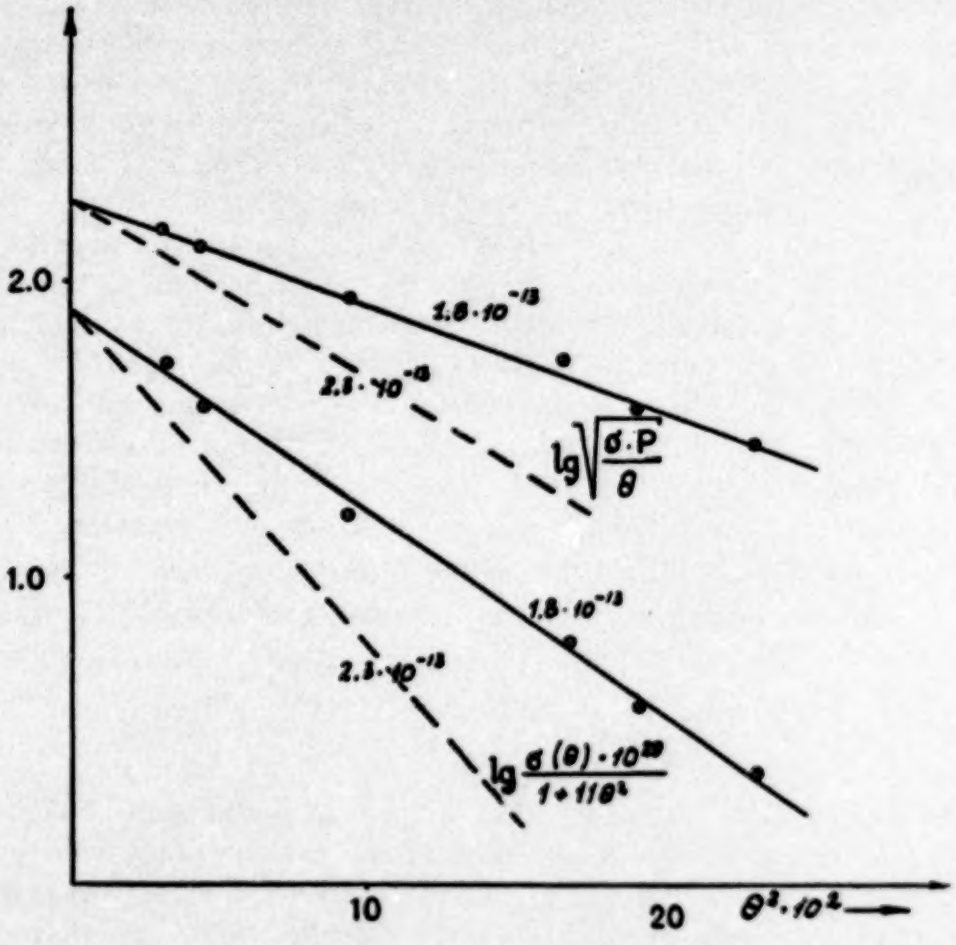

Fig. 2

can be expressed in terms of form factors F_1, F_2, which correspond to the distributions ϱ_1 and ϱ_2 in potential (1):

$$g = V_1 \cdot \frac{2m}{\hbar^2} \int j_0 \left(2kr \sin \frac{\theta}{2}\right) \varrho_1(r) r^2 \mathrm{d}r \equiv V_1 \cdot F_1, \tag{4a}$$

$$h = iV_2 \cdot k^2 \cdot \sin\theta \frac{2m}{\hbar^2} \int j_0 \left(2kr \sin \frac{\theta}{2}\right) \varrho_2(r) r^2 \mathrm{d}r \equiv iV_2 k^2 \cdot \sin\theta \cdot F_2. \tag{4b}$$

If we set $\varrho_1 = \varrho_2$, we get $h = g\,(V_2/V_1)ik^2 \sin\theta$. In general, $P(\theta)$ does not depend on the shape of ϱ and is defined by a formula yielding a single maximum; for small angles

$$P(\theta) = i\left|\frac{V_2}{V_1} - \frac{V_2^*}{V_1^*}\right|\theta \Big/ \left(1 + k^4\left|\frac{V_2}{V_1}\right|^2\theta^2\right). \tag{5}$$

Hence

$$\left|\frac{V_2}{V_1}\right| = \frac{1}{k^2\theta_m}$$

where θ_m is the angle of maximal polarization. The peak in the Chamberlain Segré curve yields $|V_2/V_1| = 3.3 \cdot 10^{-27}\,\mathrm{cm}^2$ in accord with the value of V_2/V_1 at $E_p \lesssim 10$ MeV. However, the course of the polarization at $\theta \gtrsim 27°$ in the c.m.s. appreciably differs from that predicted by (5). The polarization passes through zero and changes sign at $\theta = 33°30'$ (c.m.s.). This means that h is not exactly proportional to $g \sin\theta$ and that g or h goes through zero at $\theta = 33°30'$ (c.m.s.). It is probably h which goes through zero but for final elucidation of this point a triple scattering experiment would be required [7]). Passage of the polarization through zero thus signifies that the radial dependence of central potential ϱ_1 differs from that of the spin-orbit potential ϱ_2. Since $\sigma(\theta)$ and $P(\theta)$ have been determined for a comparatively small angle interval it would not seem reasonable to attempt the construction of h and g separately; however comparison of the angular dependences of h and g shows that the difference in ϱ_1 and ϱ_2 is not great. Therefore to determine the effective radius of interaction in terms consistent with the low energy data we introduce the mean form-factor $\bar{F} = \sqrt{F_1 \cdot F_2}$ which we determine by the expression

$$\bar{F} = \frac{2m}{\hbar^2}\int j_0\left(2kr\sin\frac{\theta}{2}\right)\varrho(r)r^2\,\mathrm{d}r \propto \sqrt{\frac{P\cdot\sigma}{\sin\theta}}. \tag{6}$$

The angular half-width of the form-factor is, as is well known, determined by the effective radius and weakly depends on the shape of the density function. Thus the half-width of the mean form factor introduced by us will be determined by the density function $\varrho(r)$ whose dimensions are intermediate between ϱ_1 and ϱ_2 in (1). Approximating $\varrho(r)$ in $\bar{F}$ by a Gaussian function we obtain for small angles

$$\ln\left(\frac{P\cdot\sigma}{\theta}\right)^{1/2} = C - \left(\frac{kr_0}{2}\right)^2 \cdot \theta^2. \tag{7}$$

The actual dependence of $\ln\,(\sigma \cdot P/\theta)^{1/2}$ on θ^2 is shown in fig. 2; for angles up to $\approx 27^0$ in the c.m.s. the dependence is in fact a straight line. The curve cannot be extended for $\theta > 27^0$ as one of the amplitudes changes sign and introduction of a mean form factor would have no meaning. The angle

interval in which dependence (7) is a straight line contains about 97 % of the scattered particles and therefore neglection of the remaining angular interval should not yield an appreciable error in the estimation of r_0.

A value $r_0 = 1.8 \cdot 10^{-13}$ cm can be deduced from the slope of the line in fig. 2 and this sharply contrasts with $r_0 = 2.3 \cdot 10^{-13}$ cm derived from low energy data. The course of $\ln (\sigma P/\theta)^{1/2}$ for $r_0 = 2.3 \cdot 10^{-13}$ cm is shown in fig. 2 by the dotted line and evidently is absolutely inconsistent with the experimental results of Chamberlain *et al.*.

To estimate the absolute value of potential V_1 in (1) we put $\varrho_1 = \varrho_2 = \exp[-(r/r_0)^2]$, $|V_2/V_1| = 3.3 \cdot 10^{-27}$ cm^2. For $\sigma(\theta)$ this gives

$$\ln \frac{\sigma(\theta)}{1+11\theta^2} = C_1 - \tfrac{1}{2}(kr_0)^2 \cdot \theta^2 \qquad (8)$$

where

$$C_1 = \ln |V_1|^2 \cdot \left(\frac{2m}{\hbar^2}\right)^2 \cdot \frac{\pi r_0^6}{16}.$$

The dependence of $\ln [\sigma(\theta)/(1+11\theta^2)]$ on θ^2 is plotted in fig. 2. The slope of the straight line again agrees with the value $r_0 = 1.8 \cdot 10^{-13}$ cm (the dotted line corresponds to $r_0 = 2.3 \cdot 10^{-13}$ cm).

The absolute value $|V_1|$ which we obtain is $|V_1| = 24$ MeV. We can now estimate the error due to application of the Born approximation. Validity of the Born approximation depends on smallness of the parameter

$$a = \frac{|V_1| r_0}{k} \cdot \frac{m}{\hbar^2}.$$

The values for r_0 and $|V_1|$ obtained above yield $a \approx 0.25$. It follows that the errors in estimation of the parameters due to neglect of the higher terms in the amplitude expansion are of the order of $(0.25)^2$ or 6 %. The magnitude of the modulus is $|V_1| = \sqrt{v^2+w^2}$ where v and w are respectively the depths of the real and imaginary parts of the potential. At present, owing to the absence of data on σ_{p-He^4}, it is not possible to determine v and w separately.

3. Results

A summary of α particle parameters obtained by various methods is presented in the following table:

Method	Shape of distribution	$r_0 \cdot 10^{13}$ cm	$\lvert V_1 \rvert$	$\left\lvert \frac{V_2}{V_1} \right\rvert$ cm^2
Phase shifts 1–10 MeV	Gaussian	2.3	47 MeV	$3.3 \cdot 10^{-27}$
Cross sections and polarization 315 MeV	Gaussian	1.8	24 MeV	$3.3 \cdot 10^{-27}$
Electron scattering 185 MeV	Uniform	1.6	–	–

The analysis carried out here thus points to an appreciable depression in the nuclear force radius already at $v/c \approx 0.7$. Apparently this same phenomenon is related to the correspondence observed in ref. [8]) and [9]) between the nuclear radii for inelastically scattered 1.4 GeV neutrons and the nuclear charge distribution radii. It is possible that this radius depression explains the "inhibition" of high angular momenta in p—p scattering in the hundred MeV range.

The author would like to thank K. A. Ter-Martirosyan for helpful discussions.

References

1) S. D. Drell, Phys. Rev. **100** (1955) 97
2) R. W. McAllister and R. Hofstadter, Phys. Rev. **102** (1956) 851
3) S. Sack, L. C. Biedenharn and G. Breit, Phys. Rev. **98** (1954) 321
4) E. v. d. Spuy, Nuclear Physics **1** (1956) 381
5) T. M. Putman, J. E. Brolley and Ir. L. Rosen, Phys. Rev. **104** (1956) 1303
6) O. Chamberlain, E. Segré, C. Wiegand and T. Ypsilantis, Phys. Rev. **102** (1956) 1659
7) L. Wolfenstein, Phys. Rev. **96** (1954) 1654
8) T. Coor, D. Hill, W. Hornyak, L. Smith and G. Snow, Phys. Rev. **98** (1955) 1369
9) W. Williams, Phys. Rev. **98** (1955) 1387

Nuclear Physics **4** (1957) 337—362; © *North-Holland Publishing Co., Amsterdam*
Not to be reproduced by photoprint or microfilm without written permission from the publisher

ON THE THEORY OF SCATTERING MEASUREMENTS IN NUCLEAR EMULSION

I. THE DISTRIBUTION FUNCTIONS OF THE COORDINATE DIFFERENCES

N. SOLNTSEFF

The F.B.S. Falkiner Nuclear Research and Adolph Basser Computing Laboratories, School of Physics,† The University of Sydney, Sydney, N.S.W.

Received 4 April 1957

Abstract: Molière's theory of multiple scattering measurements in nuclear emulsion is here treated in a mathematically simpler way. The distribution functions of the second, third and fourth differences of coordinates arising from true scattering and noise are derived for the constant-cell method.

In the derivation, the parameters B_r (eq. (4.17)) are not assumed to be all equal as was assumed by Molière. As a consequence the scattering constant (eq. (6.5)) agrees better with experimental results than the scattering constant calculated by Gottstein *et al* [11]).

It is shown that the relation between the mean noise ε_r for the rth differences and the error σ_N of a coordinate measurement is $\varepsilon_2 = 1.96\sigma_N$, $\varepsilon_3 = 3.56\sigma_N$ and $\varepsilon_4 = 6.68\sigma_N$. Therefore, to obtain a noise level of 0.15 μ for second differences the error σ_N should be less than 0.075 μ. In this case $\varepsilon_2 = 0.28$ μ and $\varepsilon_4 = 0.50$ μ.

The effect of the finite size of the nucleus on the distribution functions of the coordinate differences is evaluated in an approximate way.

CONTENTS

1. Introduction 338
1.1. THE PROBLEM
1.2. OUTLINE OF THE PRESENT METHOD

2. The Correlation between the x_i 242

3. The Joint Probability Function of the x_i due to Noise . . . 345

4. The Distribution of the x_i due to Scattering 347
4.1. THE JOINT PROBABILITY FUNCTION
4.2. THE FREQUENCY FUNCTION
4.3. THE NORMAL APPROXIMATION TO THE JOINT PROBABILITY FUNCTION
4.4. THE CALCULATION OF THE PARAMETER B_r

† Also supported by the Nuclear Research Foundation within the University of Sydney.

5. The Distribution Functions of the Observed x_i. 355
5.1. THE JOINT PROBABILITY FUNCTION
5.2. THE FREQUENCY FUNCTION
6. Discussion 356
6.1. THE FREQUENCY FUNCTIONS
6.2. THE SCATTERING CONSTANT
6.3. CONCLUSIONS

1. Introduction

1.1. THE PROBLEM

The measurement of multiple scattering is extensively used in nuclear emulsion work for the identification of particles. The techniques which are commonly used have been, for the most part, developed empirically and the aim of this review is to give an account of the theory underlying the methods of measurement.

When we make a scattering measurement we want to obtain the momentum of the particle from the amount of the scattering suffered by the particle. In this review we will only consider particles which do not lose an appreciable amount of energy as they traverse the emulsion. In this case, the usual method [1]) is to divide the track into equal cells of length s microns, and then to measure the coordinates of the track at each point of division with respect to a straight reference line, the axis of motion of the microscope stage. The second or higher-order differences of the coordinates then provide a measure of the scattering in a section of track of length s.

The estimation of the momentum from the set of the observed coordinate differences is complicated by the presence of fluctuations in the track coordinates which are not due to true multiple scattering. These fluctuations arise from experimental errors and this makes $|\overline{D_i}|$, the mean of the coordinate differences irrespective of sign, not equal to zero when scattering is zero. In the following we shall call $|\overline{D_i}|$ the arithmetic mean to distinguish it from the ordinary, or algebraic, mean.

True scattering gives a contribution to $|\overline{D_i}|$ which is proportional to $s^{3/2}$ and it is convenient to classify errors into those that give a contribution to $|\overline{D_i}|$ that is independent of s and those that give a cell-dependent contribution. We distinguish two types of errors:

1) Random Errors. Errors which are independent of the cell length or of position along the track and do not affect the algebraic mean of the D_i but increase the spread of the distribution of the D_i will be called Random Errors. The contribution of such errors to $|\overline{D_i}|$ we will call "Noise". This definition is slightly different from that used by some other authors, but it is a more useful one since the second type of error gives cell-dependent contribution.

2) Systematic Errors. Errors which affect the algebraic mean of the D_i will be called Systematic Errors.

Random errors arise from a number of causes. They may be distinguished as follows:

a) When we make a coordinate measurement, the ideal situation is one where we can measure the position of the actual trajectory of the particle. Since we have to infer the position of the trajectory from a series of grains forming the track, and the centres of the grains do not all lie along the trajectory but are distributed about it, there will be an error in the coordinate y_i. This error will be called 'grain error' and the contribution to $|\overline{D_i}|$ because of this error will be called 'grain noise'.

b) Even in the ideal case, there will be a personal error due to the observer when measuring the coordinate y_i. This type of error will be called 'reading error' and its contribution to $|\overline{D_i}|$ 'reading noise'.

c) Ideally the reference line is a straight line defined by the stage motion of the microscope. In practice there will be sidewise displacements when the stage is moved. If these displacements are small and are equally likely to increase as to decrease the measured value of y_i, this departure of the stage motion from a smooth curve will give rise to an error which we shall call 'stage error'. It will give rise to 'stage noise'.

The contribution of the systematic errors can be subdivided into 'distortion' and 'spurious scattering'. The former arises if there is a shear stress in the emulsion which results in C- or S-shaped distortion of tracks. If the stage motion of the microscope is not linear but curved there will be a contribution $|\overline{D_i}|$ which we will call 'stage distortion'. Distortion can also arise through the thermal expansion of microscope parts which causes the microscope objective to move relative to the emulsion while the measurements are in progress. This effect will be called 'temperature distortion'. We use the term 'distortion' to denote the combination of stage, emulsion or temperature distortion because all three have similar effects on $|\overline{D_i}|$.

Small-scale dislocations in the emulsion give rise to spurious scattering. It has been investigated by a number of authors [2]), and although there has been some disagreement as to the magnitude of the contribution and the exact way in which it depends on the cell length, it has been shown that spurious scattering is present in all emulsions and that it seriously affects the measurements in the very-high-energy region.

The dislocations in the emulsion responsible for spurious scattering occur in regions whose extent is comparable to the cell length used, in contrast to emulsion distortion where the emulsion fault occurs over a region large compared to the cell length. If there are irregularities or jumps in the stage motion these will also produce spurious scattering. In the following we will not consider spurious scattering further because the only way of estimating its magnitude is by measuring the scattering of particles of known energy.

A theory of multiple-scattering measurements that is to be applicable to

nuclear-emulsion measurements has to take into account the effects of distortion and noise and allow unbiassed estimation of the mean coordinate difference due to true multiple scattering.

The first theoretical investigation of the problem of estimating true scattering from the results of scattering measurements was made by Moyal [3]. Molière [4] derived the distribution functions of the second differences and also extended the theory of estimation. D'Espagnat [5] used Molière's theory to derive expressions to be used to eliminate noise from the mean of the observed second differences. An investigation of the theory of estimation has been made by Huybrechts [6].

The elimination of C-shaped distortion has been discussed by Fowler [1] and by D'Espagnat [5] who suggested the use of third differences. A considerable amount of experimental work on the use of third differences has been reported [7]. The problem of scattering measurements in the presence of distortion is discussed in Part 2 of this paper.

In Part 1 we derive the distribution functions of any quantity that can be used as a measure of the scattering. The treatment given is essentially that of Molière [4]. It differs from Molière's, however, in three ways. Firstly, we have used the Transport Equation in deriving the distribution functions. Secondly, we have treated the experimental errors in a simpler way that allows a better understanding of the physical principles involved. Finally, we have not assumed that the parameters B_r, defined in subsection 4.2, are all equal as was done by Molière. One of the consequences of this is the evaluation of the scattering constant in better agreement with experiment.

Molière and d'Espagnat in their work only considered the distribution functions of the second differences of coordinates. We have extended the theory to third and fourth differences.

1.2. OUTLINE OF THE PRESENT TREATMENT

The aim of the treatment given is the derivation of the expressions to be used to estimate, in the presence of experimental errors, the contribution of true scattering to a quantity which is a measure of the scattering of the particle. Any such quantity that we can use we will call a "scattering characteristic" or simply "characteristic". The characteristic can be the angle between tangents drawn to the track, the angle between chords or any order difference of coordinates.

The track of the particle is divided into a number of equal cells of length s and we will denote the characteristic measured for the ith cell by x_i. When we wish to distinguish the contribution of true scattering, noise and distortion to the observed value of a characteristic, we will denote the latter by x_i and use the symbol x_{si} for true scattering, x_{ei} for noise and x_{di} for distortion. We will use the symbol $f(x_i)$ to denote any distribution function. If

two distribution functions have to be distinguished, this will be done by using different symbols for the argument of the functions or by bracketed superscripts. The statistical expectation or the theoretical average of a quantity x_i will be denoted by $E(x_i)$ to distinguish it from $\bar{x}_i$, the average experimentally observed.

The problem that we have to deal with is one of sampling. The result of a measurement on a track is a set of characteristics x_i obtained for a number of cells. This set can be considered to be a sample of n values of the x_i and from this sample we have to estimate the amount of scattering suffered by the particle. A convenient quantity to estimate is the arithmetic mean $E(|x_{si}|)$. The relation between $E(|x_{si}|)$ and the momentum p of a particle can be written as

$$E(|x_{si}|) = \frac{Ks^{3/2}}{pv} \tag{1.1}$$

where v is the velocity of the particle and K is called the scattering constant. Once we have found $E(|x_{si}|)$ we can determine pv.

The theory of sampling has been extensively studied in statistics and with little trouble we can adapt it to the problem of scattering measurements. We can make use of the general theory of sampling [8]) to determine what distribution functions we have to derive in order to obtain the required information from a sample of coordinate differences. In sampling theory the important distribution is the "Joint Probability Function" of the sample elements $x_1, x_2, \ldots, x_n$, which can be defined as the probability that, given a value of pv, the value of x_i lies between x_i and x_i+dx_i, $i = 1, \ldots, n$. We will denote the Joint Probability Function (JPF) by the symbol

$$f(x_1, x_2, \ldots, x_n; pv)\mathrm{d}x_1\,\mathrm{d}x_2 \ldots \mathrm{d}x_n = f(\mathbf{x})\mathrm{d}^n\mathbf{x}.$$

The JPF is an n-dimensional frequency function and it is convenient to employ the matrix notation for the set x_i to simplify the expressions used.

As we shall see in the next section, the x_i are not all independent but those obtained from neighbouring cells are correlated. The importance of the JPF is that we derive the function for the correlated x_i and then use the fact that the x_{si} are correlated differently from the x_{ei} as a means of estimating the true scattering of the particle in the presence of noise, as described in Part 2 of this paper.

From the set of n values of the sample of the x_i we can also obtain the frequency function of the x_i, i.e. the probability that any one of the x_i has a magnitude between x_i and $x_i+\mathrm{d}x_i$. Since we have limited our treatment to particles that do not lose energy, the frequency function (FF) is independent of position on the track and we can denote the FF by $f(x)dx$. Mathematically, the FF can be obtained from the JPF by integrating $f(\mathbf{x})\mathrm{d}^n\mathbf{x}$ with respect to all but one of the x_i.

In Part 1 of this paper we derive the JPF and FF of the coordinate differences including true scattering and noise. The consideration of distortion is left to Part 2, so that in the following we assume $x_{di} = 0$. The JPF of the x_i is derived first in section 3. The JPF and the FF of the x_{si} are derived in section 4. The method involves solving the Transport Equation using the approximate cross section obtained by Molière [9]).

There is experimental evidence [10]) that the scattering constant, as calculated by Gottstein *et al.* [11]) from the Molière theory, is two to four per cent lower than observed. In subsection 6.2 it is shown that this discrepancy can be understood if we take into account the fact that the parameters B_r are not equal. Because of this, Molière and Gottstein *et al.* have underestimated the ratio of $E(|\alpha|)$, the mean angle between chords drawn through the cells, to $E(|\varphi|)$, the mean angle between tangents, and a better approximation to this ratio is given in subsection 6.2.

2. The Correlation between the x_i

In this section we will describe an important property of the x_i, namely the way in which the characteristics obtained from two adjacent cells are correlated. Let m be the number of cells of length s into which the track is divided. We number the cells 0, 1, 2, . . ., m. Let y_i be the coordinate reading at the beginning of the ith cell. We then form the characteristics x_i by differencing the coordinates y_i:

$$x_i = \sum_{j=i-1}^{i-1+r} c_{i,j} y_j \tag{2.1}$$

where r is the order of differencing and $c_{i,j}$ are coefficients that depend on the order of differencing. In the case of second differences, for example, we have $c_{i,i-1} = 1$, $c_{i,i} = -2$, $c_{i,i+1} = 1$ and all the other $c_{i,j}$ are zero.

Because each y_i will contribute to several of the x_i, the x_i, even in the absence of scattering, will not all be independent. In the absence of true scattering, spurious scattering and distortion, i.e. if the only errors present are those that give rise to noise, the rth differences x_i and x_{i+k} with $k = 1, 2, \ldots, r$ will be correlated. In other words, the covariance $E(x_i x_{i+k})$ will not be zero. We can assume that the y_i are independent normal variates with mean zero and standard deviation σ_N. Then the variances and the covariances of x_{si} are given by the theorem of the addition of statistical variables [7]):

$$\lambda_{ii} = E(x_{si}^2) = \sum_j c_{i,j}^2 \sigma_N^2 \tag{2.2}$$

$$\lambda_{ik} = E(x_{si} x_{sk}) = \sum_j c_{i,j} c_{k,j} \sigma_N^2 . \tag{2.3}$$

$\mathbf{\Lambda} = \lambda_{ij}$, the matrix of the variances and the covariances, is known in statistical literature as the moment matrix.

We will adopt Molière's notation and denote the matrix whose elements are $\sum_j c_{i,j} c_{k,j}$ by the symbol $\mathbf{A}^{(s)}$,

$$A_{ij}^{(s)} = \sum_j c_{i,j} c_{k,j} = \lambda_{ij}/\sigma_N^2. \tag{2.4}$$

By definition the coefficient of correlation between x_i and x_j is given by

$$a_{ij}^{(s)} = \lambda_{ij}/\lambda_{ii} = \sum_j c_{i,j} c_{k,j} / \sum c_{i,j}^2 \tag{2.5}$$

since all the y_i have the same normal distribution. The matrix of the $a_{ij}^{(s)}$ will be denoted by $\mathbf{a}^{(s)}$. Note that

$$\mathbf{a}^{(s)} = \mathbf{A}^{(s)}/A_{11}^{(s)}. \tag{2.6}$$

The above correlation arises from the errors of measurement only and we can call it the correlation due to noise. When scattering is present there will be an additional correlation between the x_i. This correlation arises because the y_i are no longer independent since any scattering prior to the ith point affects the magnitude of both y_i and y_k if $k > i$. We can see this by considering a simple example. Assume that the particle is initially travelling parallel to the reference line RR′ (fig. 1) without scattering. At the point O it has a

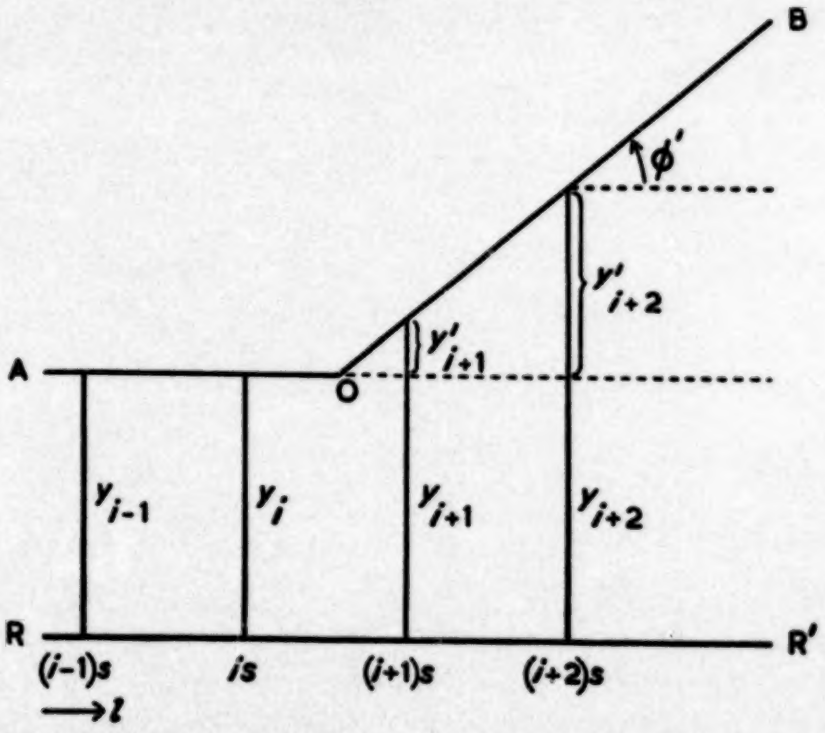

Fig. 1. The contribution to the coordinates y_j from one scattering collision in the ith cell. The angular deviation is equal to φ'.

collision after which it moves in the direction OB without further scattering. Let φ' be the deflection at O and let the contribution to y from this collision

by y'_j. Then if l denotes the position of O from the point at which the measurements were started, in the small angle approximation,

$$y'_j = \begin{cases} (js-l)\varphi' & \text{if } l < js, \\ 0 & \text{if } l > js. \end{cases} \tag{2.7}$$

This relation may be written as

$$y'_j = \gamma'_j(l)\varphi'. \tag{2.7a}$$

In general, for any characteristic that is a linear combination of the y_i, we can express the contribution x'_i to x_i arising from the collision at O as

$$x'_i = \gamma_i(l)\varphi'. \tag{2.8}$$

The $\gamma_i(l)$ will be called "coupling factors".

The coupling factors for the x_i can be found directly from the $\gamma'_i(l)$ defined by equation (2.7). The x_i are a linear combination of the y_i, so that from equation (3.1) we have

$$\gamma_i(l) = \sum_j c_{i,j}\gamma(l). \tag{2.9}$$

Using equation (2.8), the coupling factors for second, third and fourth differences can be easily calculated. The $\gamma_i(l)$ are given below, where the abbreviation $\xi = (l-is)/s$ has been used.

Second Differences

$$\gamma_i(\xi) = \begin{cases} (\xi+1)s & \text{if } -1 < \xi < 0 \\ (1-\xi)s & \text{if } 0 < \xi < 1 \end{cases} \tag{2.10}$$

and is zero otherwise.

Third Differences

$$\gamma_i(\xi) = \begin{cases} (1+\xi)s & \text{if } -1 < \xi < 0 \\ (1-2\xi)s & \text{if } 0 < \xi > 1 \\ (\xi-2)s & \text{if } 1 < \xi < 2. \end{cases} \tag{2.11}$$

Fourth Differences

$$\gamma_i(\xi) = \begin{cases} (1+\xi)s & \text{if } -1 < \xi < 0 \\ (1-3\xi)s & \text{if } 0 < \xi < 1 \\ (3\xi-5)s & \text{if } 1 < \xi < 2 \\ (3-\xi)s & \text{if } 2 < \xi < 3. \end{cases} \tag{2.12}$$

Because of equation (2.8) there will be equations connecting some of the x_i. For an actual track the number of collisions is very large and the deflections φ' are very small so that there will be a statistical correlation between the x_i. We can express this correlation by means of a matrix of correlation coefficients. The element $a_{ij}^{(s)}$ of the correlation matrix $\mathbf{a}^{(s)}$ is defined by

$$a_{ij}^{(s)} = E(x_{si}x_{sj})/E(x_{si}^2). \tag{2.13}$$

3.1. THE JOINT PROBABILITY FUNCTION OF THE x_{si}

In this section we derive the JPF of the x_{si} and we shall assume that we are considering a track left by a particle of very high energy, so that $x_{si} = 0$, and that there is no distortion or spurious scattering present.

The errors accompanying a measurement of the coordinate y_i can be treated statistically by saying that the y_i are distributed normally with mean zero and standard deviation σ_N:

$$\sigma_N^2 = \sigma_R^2 + \sigma_G^2 + \sigma_S^2, \tag{3.1}$$

where σ_R is the reading error, σ_G is the grain error and σ_S is the stage error. It is convenient to treat the resultant error as a whole. We thus avoid having to analyse in detail the act of taking a coordinate reading and the exact way in which the errors arise.

We assume that there are m cells and that there are $n = m+1-r$ r^{th} differences x_{si}. Without loss of generality we can assume that the track is parallel to the reference line. The FF of the y_i can thus be written as

$$f(y_k)\mathrm{d}y_k = \frac{\mathrm{d}y_k}{\sqrt{2\pi}\,\sigma_N} \exp\{-y_k^2/2\sigma_N^2\}. \tag{3.2}$$

Since we have assumed that the y_i are normally distributed, any linear combination of these quantities will also be normally distributed. The x_{si}, therefore, will be normally distributed correlated variables. The JPF of n such variables can be written as [7])

$$f(\mathbf{x}_s)\mathrm{d}\mathbf{x}_s = \mathrm{d}\mathbf{x}_s[(2\pi)^n|\Lambda|]^{-\frac{1}{2}} \exp -\{\sum_{j,k}[\mathbf{\Lambda}^{-1}]_{jk} x_j x_k\} \tag{3.3}$$

where $\mathbf{\Lambda}$ is the moment matrix and $|\Lambda|$ is its determinant. Using the correlation matrix $\mathbf{A}^{(s)}$ equation (3.3) can also be written

$$f(\mathbf{x}_s)\mathrm{d}\mathbf{x}_s = \mathrm{d}\mathbf{x}_s[(2\pi\sigma_N^2)^n|A^{(s)}|]^{-\frac{1}{2}} \exp -\{\sum_{j,k}[\mathbf{A}^{(s)-1}]_{jk} x_j x_k/2\sigma_N^2\} \tag{3.4}$$

where $|A^{(s)}|$ is the determinant of $\mathbf{A}^{(s)}$.

In section 5 we will need $f(\mathbf{x}_s)\mathrm{d}\mathbf{x}$ expressed as a Fourier Integral. This expression is given by Cramér as

$$f(\mathbf{x}_s)\mathrm{d}\mathbf{x}_s = (2\pi)^{-n}\mathrm{d}\mathbf{x}_s \int_{-\infty}^{\infty}\cdots\int_{-\infty}^{\infty} \mathrm{d}\boldsymbol{\eta} \exp\{-i\boldsymbol{\eta}^{\mathrm{T}}\mathbf{x} - \tfrac{1}{2}\sigma_N^2 \boldsymbol{\eta}^{\mathrm{T}}\mathbf{A}^{(s)}\boldsymbol{\eta}\} \tag{3.5}$$

where $\boldsymbol{\eta}^{\mathrm{T}}$ is the transpose of the single-column matrix $\boldsymbol{\eta}$.

The elements of the matrix $\mathbf{A}^{(s)}$ can be easily found from equation (2.4). They are given in table 1. $\mathbf{A}^{(s)}$ is a symmetric matrix with only $r+1$ independent elements.

The variances and the covariances of the x_{si} can be found by making use of the following property of the Fourier Transforms. Let $g(\boldsymbol{\eta})$ be the FT of $f(\mathbf{x}_s)$, i.e.

TABLE 1

	Second Differences	Third Differences	Fourth Differences
$A^{(s)}_{ii}$	6	20	70
$A^{(s)}_{i,i+1}$	−4	−15	−56
$A^{(s)}_{i,i+2}$	1	6	28
$A^{(s)}_{i,i+3}$	0	−1	−8
$A^{(s)}_{i,i+4}$	0	0	1

$$g(\boldsymbol{\eta}) = \int_{-\infty}^{\infty} \cdots \int_{-\infty}^{\infty} d\mathbf{x}_s \exp\{i\boldsymbol{\eta}^T \mathbf{x}_s\} f(\mathbf{x}). \tag{3.6}$$

With $f(\mathbf{x}_s)$ given by equation (3.4) we have

$$g(\boldsymbol{\eta}) = \exp\{-\tfrac{1}{2}\sigma_N{}^2 \boldsymbol{\eta}^T \mathbf{A}^{(s)} \boldsymbol{\eta}\}. \tag{3.7}$$

Then, $E(x_{si}x_{sj})$ is given by [7])

$$E(x_{si}x_{sj}) = -\left[\frac{\partial}{\partial\eta_1}\frac{\partial}{\partial\eta_j} g(\boldsymbol{\eta}).\right]_{\eta=0}. \tag{3.8}$$

From equations (3.7) and (3.8) we get

$$E(x_{s1}^2) = A_{11}^{(s)} \sigma_N{}^2 = \sigma_s{}^2 \tag{3.9a}$$

$$E(x_{si}x_{sj}) = A_{ij}^{(s)} \sigma_N{}^2 = a_{ij}^{(s)} \sigma_s{}^2 \tag{3.9b}$$

where σ_s is the standard deviation of the FF of the x_{si}. We shall denote $E(|x_{si}|)$, the mean value of x_{si} irrespective of sign, by ε_r, i.e. $\varepsilon_r = \sqrt{(2/\pi)}\sigma_s$.

From table 1 and equation (3.9a) we can obtain ε_r in terms of the error σ_N:

$$\begin{aligned} \varepsilon_2 &= 1.96\, \sigma_N, \\ \varepsilon_3 &= 3.56\, \sigma_N, \\ \varepsilon_4 &= 6.68\, \sigma_N. \end{aligned} \tag{3.10}$$

From these relations we see that the noise ε_r increases with the order of differencing r. Further, they enable us to determine to what accuracy the y_i should be measured to give a required noise level. For example, to obtain a noise level of 0.15 microns the errors of measurement should be less than 0.075 microns. The ratios $\varepsilon_3/\varepsilon_2$ and $\varepsilon_4/\varepsilon_2$ can be found from (3.10). These are

$$\varepsilon_3/\varepsilon_2 = 1.826 \text{ and } \varepsilon_4/\varepsilon_2 = 3.4161. \tag{3.11}$$

The same values for these ratios were previously given by Biswas *et al.* [12]).

4. The Distribution Functions of the x_i due to Scattering

4.1. THE JOINT PROBABILITY FUNCTION

In this section we derive the JPF of x_{si}. We assume that there is no noise or distortion present. The set of the quantities x_{si}, with $i = 1, 2, \ldots, n$, can be considered as a vector in n-dimensional space. The JPF $f(\mathbf{x}_s)d\mathbf{x}_s$ is then the probability that the end point of the vector $\mathbf{x}_s$ falls into an element of hypervolume dx_s^n around the point $\mathbf{x}_s$.

To derive $f(\mathbf{x}_s)$ we introduce an additional characteristic φ, the projected angle between end tangents to the track. Let $f(\mathbf{z})$ be the JPF of the z_i, where $\mathbf{z}$ is the $(n+1)$—dimensional vector $(x_{s1}, x_{s2}, \ldots, x_{sn}, \varphi)$.

We define $w(\mathbf{z}', l)d\mathbf{z}'dl$ to be the probability of a collision occurring in the element of track length dl at l such that the contribution of the scattering to the z_i lie between z_1 and z_2+dz_1, z_2 and z_2+dz_2, and so n. $f(\mathbf{z})$ satisfies the Transport Equation

$$\frac{\partial f(\mathbf{z})}{\partial l} = -f(\mathbf{z})\int_{-\infty}^{\infty}\cdots\int_{-\infty}^{\infty} d\mathbf{z}'\,\mathbf{w}(\mathbf{z}', l)+\int_{-\infty}^{\infty}\cdots\int_{-\infty}^{\infty} d\mathbf{z}'\,f(\mathbf{z}-\mathbf{z}')\mathbf{w}(\mathbf{z}', l) \quad (4.1)$$

where $f(\mathbf{z}-\mathbf{z}')$ is the probability that before the collision at l the magnitude of the vector $\mathbf{z}$ was $\mathbf{z}-\mathbf{z}'$.

Expanding $f(\mathbf{z})$ as an $(n+1)$-dimensional Fourier Integral:

$$f(\mathbf{z}) = (2\pi)^{-n-1}\int_{-\infty}^{\infty}\cdots\int_{-\infty}^{\infty} d\boldsymbol{\eta}\,\exp\{-i\boldsymbol{\eta}^{\mathrm{T}}z\}g(\boldsymbol{\eta}) \quad (4.2)$$

where

$$g(\boldsymbol{\eta}) = \int_{-\infty}^{\infty}\cdots\int_{-\infty}^{\infty} d\mathbf{z}\,\exp\{i\mathbf{z}^{\mathrm{T}}\boldsymbol{\eta}\}f(\mathbf{z}) \quad (4.3)$$

and applying the theorem of the Folding Product of Fourier Integrals, equation (4.1) reduces to

$$\frac{\partial}{\partial l}g(\boldsymbol{\eta}) = -g(\boldsymbol{\eta})\int_{-\infty}^{\infty}\cdots\int_{-\infty}^{\infty} d\mathbf{z}'\,w(\mathbf{z}', l)[1-\exp(i\boldsymbol{\eta}^{\mathrm{T}}z')] \quad (4.4)$$

which can be integrated with respect to l to give

$$g(\boldsymbol{\eta}) = \exp\left\{-\int_0^{l_{\mathrm{T}}} dl\int_{-\infty}^{\infty}\cdots\int_{-\infty}^{\infty} d\mathbf{z}'\,w(\mathbf{z}', l)[1-\exp(i\boldsymbol{\eta}^{\mathrm{T}}\mathbf{z}')]\right\} \quad (4.5)$$

where l_{T} is the total length of track measured.

$w(\mathbf{z}', l)$ can be expressed in terms of the projected angular cross section $\sigma(\varphi')d\varphi'$, since the contributions $\mathbf{z}'$ to $\mathbf{z}$ can be completely expressed in terms of the contributions φ' to φ, with the help of the coupling factors $\gamma_i(l)$ (equation 2.8). Hence we can write

$$w(\mathbf{z}', l) = N\sigma(\varphi')\delta[x'_1-\gamma_1(l)\varphi']\,\delta[x'_2-\gamma_2(l)\varphi']\ldots\delta[x'_n-\gamma_n(l)\varphi'] \quad (4.6)$$

where N is the density of scattering centres cm^{-3}, and $\delta[x'_i-\gamma_i(l)\varphi']$ is the delta function, defined by [8]

$$\int_{-\infty}^{\infty} \mathrm{d}x'_i \delta\,[x'_i - \gamma_i(l)\varphi'] = \begin{cases} 1 \text{ if } x'_i = \gamma_i(l)\varphi' \\ 0 \text{ otherwise.} \end{cases} \tag{4.7}$$

Using equation (4.7) the integration with respect to the x'_i can be easily performed and we get

$$g(\boldsymbol{\eta}) = \exp\left\{-N\int_0^{l_\tau} \mathrm{d}l \int_{-\infty}^{\infty} \mathrm{d}\varphi'[1 - \exp\,(iv\varphi' + \eta_{n+1}\varphi')] \times \sigma(\varphi')\right\} \tag{4.8}$$

where we have used the abbreviation $v = \sum_k \eta_k \gamma_k\,(l)$.

We are thus left with the evaluation of only the integral with respect to φ'. We can now obtain the Fourier Transform of $f(\mathbf{x}_s)$ from $g(\boldsymbol{\eta})$ given by equation (4.8) by setting η_{n+1} equal to zero.

The cross section $\sigma(\varphi')$ that we have to use is the one for scattering of charged particles by atoms. In this case the screening of the nuclear charge by the atomic electrons is important for very large impact parameters and small angles of scatter. The actual cross section remains finite for small angles and does not diverge as the classical or Rutherford cross section. Molière [8]) showed that the effect of screening can be taken into account by introducing a single parameter χ_a. This parameter is evaluated by Molière using the Thomas-Fermi distribution of electrons in an atom, but a more accurate expression can be obtained if we use a more accurate electron distribution. The projected angular cross section can be written in Molière's notation as

$$\begin{aligned} N\sigma(\varphi')\mathrm{d}\varphi' &= \tfrac{1}{2}\chi_c'^2(\varphi'^2 + \chi_a^2)^{-3/2}\mathrm{d}\varphi' \\ &= \tfrac{1}{2}\chi_c'^2 q(\varphi')\varphi'^{-3}\mathrm{d}\varphi \end{aligned} \tag{4.9}$$

where $q(\varphi')$ is the ratio of the actual to the Rutherford cross section. χ'_c is defined by

$$\chi'_c = \frac{Zze^2}{pv}(4\pi N)^{\frac{1}{2}} \tag{4.10}$$

where Ze is the charge number of the scattering centres, N their density cm^{-3}, and ze, p, v are the charge, momentum and velocity of the scattered particle.

If s is the cell length, then $\chi'_c\sqrt{s}$, usually denoted by χ_c, is an angle such that the probability of single scattering through an angle χ_c in any direction is exactly one.

From equation (4.9) we see that when $\varphi' \gg \chi_a$, $q(\varphi') \to 1$ and the scattering is classical. As $\varphi' \to 0$, $q(\varphi')$ tends to a constant value χ_a^{-2}, and the scattering is determined purely by the screening parameter. The physical meaning of χ_a thus is the scattering angle for which screening becomes important.

Making use of the behaviour of $q(\varphi')$ for small and large values of φ', we can split the region of integration in equation (4.8) into two parts as was done by Bethe [13]) in the derivation of the angular distribution function. The

two regions are $|\varphi'| > k$ and $|\varphi'| < k$ where k is an angle such that $\chi_a \ll k \ll \chi'_c\sqrt{s}$. The evaluation of the integral is given in appendix A. The final result is

$$g(\boldsymbol{\eta}) = \exp\left\{\int_0^{l_T} \mathrm{d}l\, \tfrac{1}{4}\chi_c'^2 v^2 \ln\left[\frac{\gamma^2}{4e}\chi_a^2 v^2\right]\right\} \tag{4.11}$$

where $\ln e = 1$, $\ln \gamma = C$ is Euler's constant and $v = \sum_k \gamma_k(l)\eta_k$. The JPF $f(\mathbf{x}_s)$ is therefore given by

$$f(\mathbf{x}_s) = (2\pi)^{-n}\int_{-\infty}^{\infty}\cdots\int_{-\infty}^{\infty} \mathrm{d}\boldsymbol{\eta} \exp\{-i\boldsymbol{\eta}^{\mathrm{T}}\mathbf{x}_s\} \times \exp\left\{\int_0^{l_T} \mathrm{d}l\, \tfrac{1}{4}\chi_c'^2 v^2 \ln\left[\frac{\gamma^2}{4e}\chi_a^2 v^2\right]\right\}. \tag{4.12}$$

4.2. THE FREQUENCY FUNCTION

The FF $f(x_s)\mathrm{d}x_s$ can be obtained from equation (4.12) by integrating it with respect to all but one component of $\mathbf{x}_s$. This is equivalent to putting all but one of the η_k equal to zero and writing $(2\pi)^{-1}$ instead of $(2\pi)^{-n}$. We get

$$f(x_s)\mathrm{d}x_s = \mathrm{d}x_s(2\pi)^{-1}\int_{-\infty}^{\infty}\mathrm{d}\eta_k \exp(-ix_s\eta_k) \exp\left\{\int_0^{l_T}\mathrm{d}l\, \tfrac{1}{4}\chi_c'^2\gamma_k^2(l)\eta_k^2 \ln\left[\frac{\gamma^2}{4e}\chi_a^2\gamma_k^2(l)\eta_k^2\right]\right\}. \tag{4.13}$$

It must be noted that equation (4.13) has the same value whatever the value of the subscript k, because $\gamma_k(l)$ has the same value when l changes by an integral number of cell lengths, i.e. $\gamma_i(l) = \gamma_{i+k}(l+ks)$, and no other function of l appears in the equation provided that χ'_c and χ_a are independent of l. The latter condition holds in the case of a particle that does not lose energy, in which case all the x_{si} have the same FF.

If we now introduce the abbreviations

$$x_c^2 = \chi_c'^2\int_0^{l_T}\mathrm{d}l\gamma_k^2(l) \tag{4.14}$$

and

$$\ln x_a^2 = \frac{1}{x_c^2}\int_0^{l_T}\mathrm{d}l\chi_c'^2\gamma_k^2(l)\ln[\chi_a^2\gamma_k^2(l)], \tag{4.15}$$

the Fourier Transform of $f(\mathbf{x}_s)$ becomes

$$g(\eta) = \exp\left\{\frac{x_c^2\eta^2}{4}\ln\left(\frac{\gamma^2}{4e}x_a^2\eta^2\right)\right\}. \tag{4.16}$$

Following Molière we introduce a parameter B_r defined by

$$B_r - \ln B_r = \ln\frac{e}{\gamma^2}\frac{x_c^2}{x_a^2}. \tag{4.17}$$

The FF of the x_{si} irrespective of sign can be obtained from equation (4.16). After making a change of variables given by

$$\xi = x_c \sqrt{B_r}\,\eta \tag{4.18}$$

and

$$u = |x_s|/x_c\sqrt{B_r} \tag{4.19}$$

the FF $f(u)\mathrm{d}u$ can be put into the form

$$f(u)\mathrm{d}u = \frac{2\mathrm{d}u}{\pi}\int_0^\infty \mathrm{d}\xi \cos(u\xi)\exp\left(-\frac{\xi^2}{4}+\frac{\xi^2}{4B_r}\ln\frac{\xi^2}{4}\right). \tag{4.20}$$

Equation (4.20) is of the same form as equation (20) of Bethe [13]) and equation (8.3) of Molière [8]). The exponential can now be expanded in a power series in $1/B_r$ to give

$$f(u)\mathrm{d}u = \mathrm{d}u\left\{\frac{2}{\sqrt{\pi}}\exp(-u^2)+\frac{1}{B_r}f^{(1)}(u)+\frac{1}{B_r^2}f^{(2)}(u)+\ldots\right\} \tag{4.21}$$

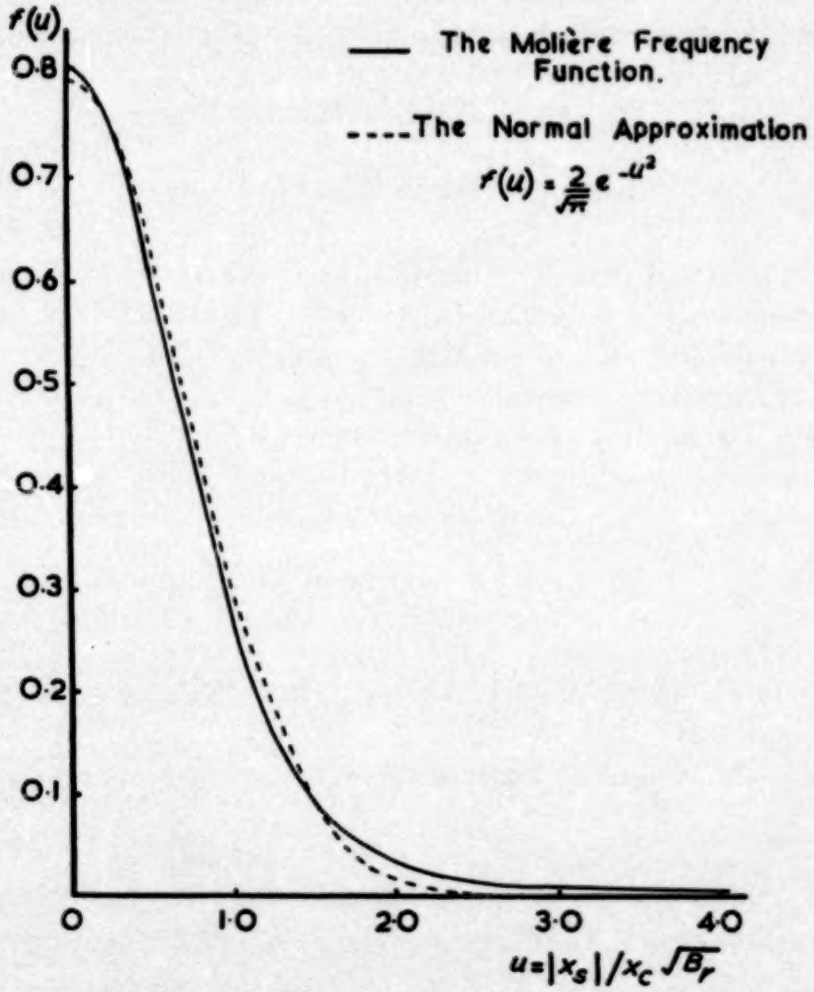

Fig. 2. The comparison of the Molière FF (equation 4.21) and the normal approximation. ———— Molière FF. ------ Normal Approximation.

where $f^{(1)}(u)$ and $f^{(2)}(u)$ are the Molière functions which have been tabulated by Molière [8]).

The mean value of $|x_s|$ can be obtained from equation (4.21). Molière has given the following expression for $E(|x_s|)$:

$$E(|x_s|) = \frac{x_c\sqrt{B_r}}{\sqrt{\pi}}\left\{1+\frac{0.982}{B_r}-\frac{0.117}{B_r^2}+\ldots\right\}. \tag{4.22}$$

In equation (4.2) the term containing exp $(-u^2)$ can be interpreted as the distribution of multiple scattering and is generally called the "normal approximation" to the FF. The Molière FF is given graphically in fig. 2. The dashed curve is the normal approximation $f(u) = 2\exp(-u^2)/\sqrt{\pi}$. It can be seen that for small values of u the FF is nearly a gaussian but for large u it falls off less steeply. The terms $f^{(1)}(u)$, $f^{(2)}(u)$, and so on, arise from single and plural scattering because if the particle suffers one or at most a few collisions which deflect it through a large angle, multiple scattering, before or after the large-angle scatter, will not appreciably affect the resultant distribution. The correction arising from these terms is appreciable even for small u, for u less than 2, i.e. $|x_s|$ less than approximately three times the mean $|x_s|$, it is of the order of $1/B_r$ or about 10 per cent [13]).

4.3. THE NORMAL APPROXIMATION TO THE JOINT PROBABILITY FUNCTION

If we introduce the parameter B_r, defined by equation (4.17), we can rewrite (4.11) as

$$g(\eta) = \exp -\int_0^{l_T} \mathrm{d}l\,\frac{\chi_c'^2 B_r}{4}\sum_{j,k}\gamma_j(l)\gamma_k(l)\eta_j\eta_k \times\left\{1-\frac{1}{B_r}\ln\frac{\chi_a^2 B_r}{4}\frac{x_c^2}{x_a^2}v^2\right\}. \tag{4.23}$$

In (4.23) the logarithmic term gives the contribution of single and plural scattering to $f(x_s)$. This can be seen if we reduce $g(\eta)$ given by (4.23) to the Fourier Transform $g(\eta)$ of a one-dimensional FF. From (4.23) we obtain equation (4.16) by setting all but one of the η_k equal to zero. This justifies the introduction of B_r and not B_0, the parameter of the angular distribution function, as was done by Molière.

The JPF whose Fourier Transform is given by equation (4.23) has infinite second moments $E(x_{si}x_{sj})$ because of the logarithmic term. The physical reason for the divergence of the second moments is that in the derivation of the JPF we neglected to take into account the finite radius of the nucleus which imposes a cut off for large scattering angles. Olbert [14]) has treated the case of scattering from a nucleus of finite radius and derived a correction to the Molière FF (eq. 4.21). A method of correcting $g(\eta)$ for this effect is given in appendix B. The important conclusions that can be drawn from

Olbert's work is that due to this effect the correction to the FF and the expression for $E(|x_s|)$ (eq. 4.22) is negligible provided that the cell length s is shorter than approximately 5 mm.

Another factor, this time an experimental one, which we did not take into account is the rejection of large values of $|x_i|$, usually those greater than four times the mean $|\bar{x}_i|$. The cut off is imposed because $|\bar{x}_i|$ is sensitive to the presence of large x_i, for although the "single-scattering tail" contributes on the average only about 10 % to the value of $|\bar{x}_i|$, the effect of large-angle scatters on individual tracks is very pronounced. The JPF with experimental cut off cannot be derived because of the complexity of equation (4.12).

The inversion of the Fourier Transform (4.23) to obtain $f(\mathbf{x}_s)$ is intractable because of the presence of the logarithmic term. This prevents the separation of the n integrals with respect to η_k into a product of n integrals. Also, as we shall see in Part 2 of this paper a JPF with infinite second moments cannot be used for developing a method of estimation. We thus have to seek some approximation to $f(\mathbf{x}_s)$. The most obvious approximation is to neglect the second term of (4.23). We shall call this approximation the normal approximation to the JPF.

If we use the normal approximation the n-fold integration of $g(\boldsymbol{\eta})$ becomes separable, and $f(\mathbf{x}_s)$ can be easily obtained in integrated form [8]). The variances and the covariances now become

$$\lambda_{ii} = \frac{\chi_c'^2 B_r}{2} \int_0^{l_T} \mathrm{d}l \gamma_i^2(l) = \tfrac{1}{2} B_r x_c^2, \tag{4.24}$$

which is consistent with equation (4.22), and

$$\lambda_{ij} = \frac{\chi_c'^2 B_r}{2} \int_0^{l_T} \mathrm{d}l \gamma_i(l) \gamma_j(l). \tag{4.25}$$

The matrix of correlation coefficients can be found from equations (4.24) and (4.25). The element $a_{ij}^{(s)}$ of this matrix is by definition

$$a_{ij}^{(s)} = \frac{\int_0^{l_T} \mathrm{d}l \gamma_i(l) \gamma_j(l)}{\int_0^{l_T} \mathrm{d}l \gamma_i^2(l)}. \tag{4.26}$$

From equation (4.26), by analogy with equation (2.6), we can call the matrix of the quantities

$$A_{ij}^{(s)} = \int_0^{l_T} \mathrm{d}l \gamma_i(l) \gamma_j(l) \tag{4.27}$$

the correlation matrix $\mathbf{A}^{(s)}$ due to true scattering. It has been shown by Schonland [15]) that provided the mean square angle of single scattering is well defined the value of the correlation matrix $\mathbf{a}^{(s)}$ given by equation (4.26) is independent of the exact form of the distribution of the x_i. Hence, equation (4.26) is valid whatever the exact form of the JPF as long as the second moments are finite.

We can easily calculate the $A_{ij}^{(s)}$ from equation (4.27) and the coupling factors $\gamma_i(l)$ given in section 2. The matrix $\mathbf{A}^{(s)}$ is a symmetrical matrix with only r independent elements. In table 2 the $A_{ij}^{(s)}$ are given for the second, third and fourth differences of the coordinates.

Let

$$\sigma_s^2 = \tfrac{1}{2}\chi_c'^2 A_{11}^{(s)} B_r, \tag{4.28}$$

then σ_s will be the standard deviation, in the normal approximation, of the x_i due to true scattering. Then equations (4.24) and (4.25) can be written as

$$\lambda_{ii} = \sigma_s^2 \tag{4.24a}$$

and

$$\lambda_{ij} = a_{ij}^{(s)} \sigma_s^2. \tag{4.25a}$$

TABLE 2

	$A_{11}^{(s)}/s^3$	$A_{12}^{(s)}/s^3$	$A_{13}^{(s)}/s^3$	$A_{14}^{(s)}/s^3$	$A_{15}^{(s)}/s^3$
Second Differences	2/3	1/6	0	0	0
Third Differences	1	−1/3	−1/6	0	0
Fourth Differences	8/3	−3/2	0	1/6	0

Because of the cut off used, the characteristic x_i is no longer a linear function of the y_i, and we should derive the JPF for a non-linear characteristic x_i and then choose the function $x_i = x_i(y)$ so that large-angle scatters make small contributions to the final estimates. It has been shown by Huybrechts[6]) however, that we can choose the value of the cut off, for any given track, so that the resulting distribution is very nearly normal †. As we shall see in Part 2 of this paper, the non-normal nature of the JPF will only affect the accuracy with which we can estimate true scattering, but will not lead to a biassed estimate because the matrix $\mathbf{a}^{(s)}$ is independent of the exact form of the JPF of the x_i.

4.4. THE CALCULATION OF THE PARAMETER B_r

In section 4.2 we have seen that the arithmetic mean of the x_{si} depends upon the parameter B_r. B_r is defined by equation (4.17). In the case of the distribution of angles between tangents drawn to the track the quantity which plays a similar role is B_0, which is defined by [8])

$$B_0 - \ln B_0 = \ln \frac{e}{\gamma^2} \frac{\chi_c'^2}{\chi_a^2} s. \tag{4.29}$$

B_0 and B_r depend on the particle velocity and the cell length used. Gottstein *et al.* [11]) have published a graph of the quantity $\Omega_0/s = \chi_c'^2/\chi_a^2$ as a function

† *Note added in proof:* Dr. M. Huybrechts has pointed out to me that he only showed that, using a suitable cut off, the standard deviation of the mean x_i with cut off is approximately equal to the standard deviation obtained using the normal approximation for the distribution function of the scattering angles φ.

of the particle velocity $\beta = v/c$. B_0 can then be obtained from fig. 3. Since B_0 can thus be easily obtained, it is convenient to derive the relation between B_r and B_0.

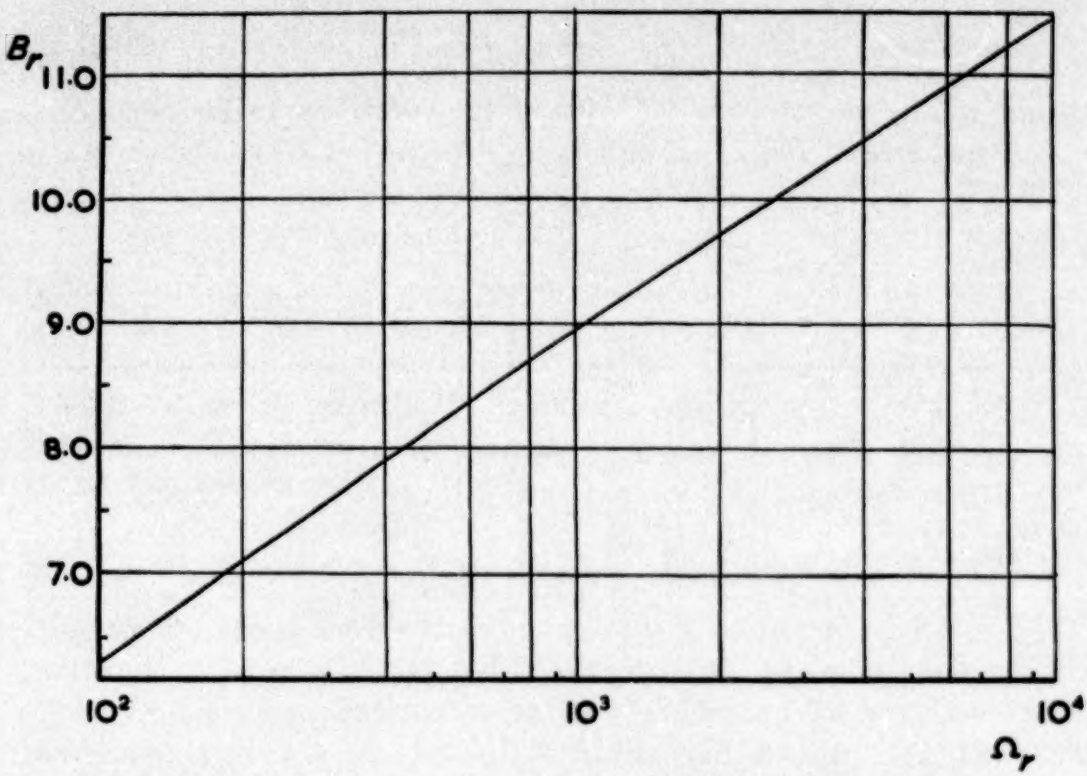

Fig. 3. The parameter B_r as a function of Ω_r ($r = 0, 2, 3, \ldots$).

From fig. 3 it is seen that the graph of B_0 as a function of Ω_0 or of B_r as a function of $\Omega_r = x_c^2/x_a^2$ is almost a straight line. We take for B_r, where $r = 0, 2, 3, \ldots$, the approximate relation

$$B_r = 1.0013 + 2.6426 \log_{10} \Omega_r. \tag{4.30}$$

The magnitude of Ω_r is of the order of the number of collisions suffered by the particle. For a typical case, $\Omega_r \approx 3000$ and the error in B_r introduced through the use of equation (4.30) is approximately 0.3 per cent.

Combining equations (4.17), (4.29) and (4.30) we obtain

$$B_r - \ln B_r = 1.1477 \ln (\Omega_r/\Omega_0). \tag{4.31}$$

An expression for $\ln (\Omega_r/\Omega_0)$ can be easily obtained from equations (4.14) and (4.15)

$$\ln (\Omega_r/\Omega_0) = \ln A_{11}^{(s)} - \frac{1}{A_{11}^{(s)}} \int_0^{l_r} \mathrm{d}l \gamma_1^2(l) \ln \gamma_1^2(l). \tag{4.32}$$

Table 3 gives the values of $\ln (\Omega_r/\Omega_0)$ and $B_r - B_0$ for second, third and fourth differences.

TABLE 3

	$\ln(\Omega_r/\Omega_0)$	$B_r - B_0$
Second Differences	0.2612	0.300
Third Differences	0.6667	0.759
Fourth Differences	0.7223	0.828

5. The Distribution of the Observed Characteristics in the Absence of Distortion

5.1. THE JOINT PROBABILITY FUNCTION

When distortion is absent the observed characteristics x_i can be considered to be the sum of x_{si} and x_{ei}. The case when distortion is not negligible is treated in Part 2 of this paper. The JPF of the x_i is the Folding Product of the JPFs of the x_{si} and x_{ei}. The normal approximation to $f(\mathbf{x}_s)$ can be written as

$$f(\mathbf{x}_s) = (2\pi)^{-n}\int_{-\infty}^{\infty}\cdots\int_{-\infty}^{\infty} d\boldsymbol{\eta}\, \exp\{-i\boldsymbol{\eta}^T\mathbf{x}_s - \tfrac{1}{4}\chi_c'^2 B_r \boldsymbol{\eta}^T\mathbf{A}^{(s)}\boldsymbol{\eta}\} \qquad (5.1)$$

and $f(\mathbf{x}_r)$ is given by equation (3.5):

$$f(\mathbf{x}_e) = (2\pi)^{-n}\int_{-\infty}^{\infty}\cdots\int_{-\infty}^{\infty} d\boldsymbol{\eta}\, \exp\{-i\boldsymbol{\eta}^T\mathbf{x} - \tfrac{1}{2}\sigma^{N2}\boldsymbol{\eta}^T\mathbf{A}^{(e)}\boldsymbol{\eta}\}; \qquad (5.2)$$

the JPF of the x_i can now be written as

$$f(\mathbf{x}) = (2\pi)^{-n}\int_{-\infty}^{\infty}\cdots\int_{-\infty}^{\infty} d\boldsymbol{\eta}\, \exp\{-i\boldsymbol{\eta}^T\mathbf{x} - \tfrac{1}{2}\sigma_0^2\boldsymbol{\eta}^T\mathbf{a}\boldsymbol{\eta}\} \qquad (5.3)$$

where $\mathbf{a}$ is the matrix of the correlation coefficients of the observed x_i. $\mathbf{a}$ is given by

$$\mathbf{a} = (\chi_c'^2 B_r\mathbf{A}^{(s)} + \sigma_N^2\mathbf{A}^{(e)})/\sigma_0^2 \qquad (5.4)$$

where σ_0 is the standard deviation of the x_i in the normal approximation:

$$\sigma_0^2 = \sigma_s^2 + \sigma_e^2 = \tfrac{1}{2}\chi_c'^2 B_r A_{11}^{(s)} + \sigma_N^2 A_{11}^{(e)}. \qquad (5.5)$$

The matrix $\mathbf{a}$ can also be expressed as

$$\mathbf{a} = \sigma_s^2\mathbf{a}^{(s)} + \sigma_e^2\mathbf{a}^{(e)}/(\sigma_s^2 + \sigma_e^2). \qquad (5.6)$$

Integrating (5.3) with respect to $\boldsymbol{\eta}$, we get [8])

$$f(\mathbf{x})d\mathbf{x} = d\mathbf{x}[(2\pi\sigma_0^2)^n|a|]^{-\frac{1}{2}}\exp\{-\mathbf{x}^T\mathbf{a}^{-1}\mathbf{x}/2\sigma_0^2\} \qquad (5.7)$$

where $\mathbf{a}^{-1}$ is the inverse of the matrix $\mathbf{a}$ and $|a|$ its determinant.

5.2. THE FREQUENCY FUNCTION

The FF of the observed characteristics x_i can be found from the Folding Product of the FFs $f(x_s)$ and $f(x_e)$. $f(x_e)$ can be obtained from equation (3.5) and $f(x_s)$ from (4.16). The method shown below was first given by Menon *et al.* [1]). The FF of the $|x_i|$ can be written as

$$f(|x|)\mathrm{d}|x| = \frac{\mathrm{d}|x|}{\pi}\int_0^\infty \mathrm{d}\eta \exp\left\{-i\eta x + \tfrac{1}{4}\eta^2 x_c^2 \ln\left(\frac{\gamma^2}{4e}\, x_a^2\, \eta^2\right) - \tfrac{1}{2}\sigma_N\, A_{11}^{(e)}\, \eta^2\right\}. \quad (5.8)$$

Let

$$\mu' = 2\sigma_N^2 A_{11}^{(e)}/x_c^2; \quad (5.9)$$

then we int oduce the parameter B_r^* defined by

$$B_r^* - \ln B_r^* = \ln \frac{e}{\gamma^2}\Omega_r^* = \ln\left[\frac{e}{\gamma^2}\,(x_c^2/x_a^2)e^{\mu'}\right]. \quad (5.10)$$

B_r^* is introduced so that after a change of variables $\xi = x_c\sqrt{B_r^*}\,\eta$ and $u = |x|/x_c\sqrt{B_s^*}$, equation (5.10) can be put into the standard form:

$$f(u)\mathrm{d}u = \frac{2\mathrm{d}u}{\pi}\int_0^\infty \mathrm{d}\xi \cos(u\xi) \exp\left(-\frac{\xi^2}{4} + \frac{\xi^2}{4B_r}\ln\frac{\xi^2}{4}\right). \quad (5.11)$$

After an expansion of the exponential in a power series in $1/B_r^*$ we get the Molière equation (4.21) but with B_r replaced by B_r^*. As before $E(|x|)$ is given by the expression

$$E(|x|) = \frac{x_c\sqrt{B_r^*}}{\sqrt{\pi}}\left\{1 + \frac{0.982}{B_r^*} - \frac{0.117}{B_r^{*2}} + \ldots\right\}. \quad (5.12)$$

Let μ_r be the square of the noise-to-signal ratio in the normal approximation: $\mu_r = \sigma_e^2/\sigma_s^2$, then with the help of equation (4.30), equations (4.17) and (5.10) can be combined to give B_r^* in terms of B_r:

$$B_r^* = (1 + 1.1477\,\mu_r)\,B_r, \quad (5.13)$$

which determines B_r^* once B_r and μ_r are known.

6. Discussion

6.1. THE FREQUENCY FUNCTION

The FF of any characteristic has the same form as equation (4.21) but with different values of the parameter B_r and the correlation matrix A. The values of B_r for second, third or fourth differences can be found as described in section 4.4, and the elements of the correlation matrix **A** are given in table 2.

The FF of the x_i is given in fig. 2. The Molière FF, given by equation (4.21), is plotted as a full curve. The dashed curve is the normal approximation, $f(u) = 2\exp(-u^2)/\sqrt{\pi}$. It can be seen that the Molière FF departs from normality for values of u as small as the mean. Quantitatively, the degree of departure from normality can be obtained from the values of the ratios $|\bar{D}_r|/|\bar{D}_{r'}|$, where $|\bar{D}_r|$ is the arithmetic mean of the rth differences due to true scattering only. If the FF of the x_{si} were strictly normal then the FF of the third and fourth differences would also be normal, and we would have

$$|\bar{D}_3|/|\bar{D}_2| = \sqrt{3/2} \tag{6.1}$$

and

$$|\bar{D}^4|/|\bar{D}_2| = 2. \tag{6.2}$$

To estimate the value of $|\bar{D}_3|/|\bar{D}_2|$ and $|\bar{D}_4|/|\bar{D}_2|$ that is given by the present theory we consider, as an example, the case of a fast μ-meson measured with a cell length of 250 μ. Then $B_0 = 8.83$, $B_2 = 9.13$, $B_3 = 9.59$ and $B_4 = 9.66$. From equation (4.22) we have

$$\frac{|\bar{D}_r|}{|\bar{D}_{r'}|} = \frac{[A_{11}^{(r)} B_r]^{\frac{1}{2}} M_r}{[A_{11}^{(r')} B_{r'}]^{\frac{1}{2}} M_{r'}} \tag{6.2}$$

where

$$M_r = 1 + (0.982/B_r) - (0.117/B_r^2). \tag{6.3}$$

Substituting the values of B_2, B_3 and B_4 into equation (6.2) we obtain $|\bar{D}_3|/|\bar{D}_2| = 1.020\sqrt{3/2}$ and $|\bar{D}_4|/|\bar{D}_2| = 1.023 \times 2$. Hence, the Molière FF gives a ratio $|\bar{D}_r|/|\bar{D}_{r'}|$ that is about two per cent higher than that given by the normal approximation. The experimental value of $|\bar{D}_3|/|\bar{D}_2|$ is between $1.06\sqrt{3/2}$ and $1.09\sqrt{3/2}$, i.e. 4 to 7 per cent higher than that given by equation (6.2). It seems therefore that the observed distribution is less normal than predicted by the theory. The reason for the discrepancy could be connected with the cut off procedure used. The cut off is imposed on the observed differences D_i which include the contribution of true scattering and noise.

The observed ratio $|\bar{D}_r|/|\bar{D}_{r'}|$ will depend on the exact procedure used for cut off. In order that the results obtained by different groups can be compared it is advisable to standardize the cut off procedures. When using r^{th} differences it is preferable to apply the cut off to the sets of rth differences individually. Since it seems that cut off with replacement, i.e. replacing large r^{th} differences by four times the mean D_r, leads to better internal consistency of the results [16,17]), the two values of D_r obtained with and without replacement should be given.

6.2. THE SCATTERING CONSTANT

Since the principal use of the scattering theory is the estimation of pv from a measurement of rth differences we can write equation (4.22) in the form

$$E(|D_r|) = K_r s^{\frac{3}{2}}/pv \tag{6.4}$$

where K_r is called the scattering constant and is given by

$$K_r = 2Zze^2[(A_{11}^{(s)}/s^3)\, NB_r]^{\frac{1}{2}} M_r. \tag{6.5}$$

Gottstein *et al.* [11]) have calculated the scattering constant in the case where the characteristic used is α, the angle between chords. They assumed that B_r was equal to B_0. In other words, they assumed that the ratio of

$E(|\alpha|)/E(|\varphi|)$, where φ is the angle between tangents, was equal to $\sqrt{2/3}$, and not

$$\frac{E(|\alpha|)}{E(|\varphi|)} = \left[\frac{2B_2}{3B_0}\right]^{\frac{1}{2}} \frac{M_r}{M_0}, \tag{6.6}$$

the expression obtained from equation (4.22).

If we denote the Gottstein scattering constant by K_G, from equation (6.5) we see that

$$K_2 = 1.02\, K_G. \tag{6.7}$$

Therefore, the present treatment, which takes into account the fact that the B_r are all different, gives a value of the scattering constant in better agreement with experiment than K_G, since recent experimental evidence [10]) indicates that the observed value of K_2 is 2—4 % higher than calculated by Gottstein *et al.*

6.3. CONCLUSIONS

The conclusions that can be drawn from the above are:

(1) The relation between ε_r, the arithmetic mean noise, and σ_N, the error of a coordinate measurement, is

$$\varepsilon_r = [2A_{11}^{(e)}/\pi]^{\frac{1}{2}} \sigma_N$$

and this equation determines the accuracy with which coordinate readings should be made so as to give a required value of ε_r. For example, to obtain a noise level of 0.15 microns for second differences the error σ_N should be less than 0.075 microns.

(2) The FF and the JPF of the x_i are not strictly normal. However, the departure from normality, seen from the value of the ratio $|\bar{D}_r|/|\bar{D}_{r'}|$, is small. There is a discrepancy between the theoretical and experimental values of $|\bar{D}_r|/|\bar{D}_{r'}|$ of the order of 5 per cent.

(3) The scattering constant, given by equation (6.5), agrees better with experimental determination than the scattering constant calculated by Gottstein *et al.*

I wish to acknowledge the helpful discussions I have had with Dr. A. J. Herz and B. A. Chartres. I should like to express my appreciation to Professor Messel for making it possible for me to work under excellent conditions. I am also indebted to the Research Committee of the University of Sydney for a Research Studentship.

Appendix A

We have to evaluate the integral

$$I = \tfrac{1}{2}\chi_c'^2 \int_{-\infty}^{\infty} \mathrm{d}\varphi'\, q(\varphi')[1-\mathrm{e}^{i\omega\varphi'}]\varphi'^{-3} \tag{A.1}$$

where $v = \sum_k \gamma_k(l)\eta_k$, and

$$q(\varphi') = \varphi'^3(\varphi'^2+\chi_a^2)^{-3/2}.$$

We split the region of integration into two parts:
(1) $|\varphi'| > k$, in which $q(\varphi') \approx 1$, and
(2) $|\varphi'| < k$, in which we can use the approximation

$$1-e^{iv\varphi'} = -iv\varphi'+v^2\varphi'^2.$$

The value of k is chosen so that

$$\chi_a \ll k \ll \chi_c, \tag{A.2}$$

where $\chi_c = \chi'_c\sqrt{s}$.

For the second region we have

$$I_1 = \tfrac{1}{2}\chi_c'^2 v^2 \int_0^k d\varphi' \frac{\varphi'^2}{(\varphi'^2+\chi_a^2)^{3/2}} = \tfrac{1}{2}\chi_c'^2 v^2(-1 + \ln 2 + \ln k - \ln \chi_a). \tag{A.3}$$

For the first region of integration the integral is a standard form

$$I_2 = \chi_c'^2 v^2 \int_{vk}^{\infty} dx \frac{(1-\cos x)}{x^3}$$

where $x = v\varphi'$. Hence,

$$I_2 = \tfrac{1}{2}\chi_c'^2 v^2 \left(\frac{1}{v^2k^2} - \frac{\cos vk}{v^2k^2} + \frac{\sin vk}{vk} - \mathrm{Ci}\, vk\right) \tag{A.4}$$

where Ci vk is the Cosine Integral [18]). $vk \ll 1$ so that (A.3) becomes

$$I_2 = \tfrac{1}{2}\chi_c'^2 v^2(\tfrac{3}{2} - \ln \gamma v - \ln k) \tag{A.5}$$

where $\ln \gamma = C = 0.577\ldots$ is Euler's Constant.

Combining (A.3) and (A.5) we get

$$I = -\tfrac{1}{4}\chi_c'^2 v^2 \left(\ln \frac{\gamma^2}{4e} \chi_a^2 v^2\right) \tag{A.6}$$

where $\ln e = 1$. $g(\eta)$ is now given by

$$g(\eta) = \exp\left(-\int_0^{l_T} dl\right) \tag{A.7}$$

and $f(\mathbf{x}_0)$ by equation (4.12).

The validity of equation (A.6) can be studied as follows. If we introduce the parameter B_r, defined by equation (4.17), we get

$$g(\eta) = \exp\left\{-\tfrac{1}{4}\int_0^{l_T} dl\, \chi_c'^2 v^2 B_r \left(1 - \frac{1}{B_r} \ln \frac{B_r x_c^2}{4x_a^2} \chi_a^2 v^2\right)\right. \tag{A.8}$$

Since the $\gamma_k(l) < 1$, the magnitude of v^2 is of the order of $n\eta^2 s^3$, where n is the number of the x_i. Therefore, $g(\eta) \approx \exp(-\frac{1}{4}\chi_c'^2 B_r n\eta^2 s^3)$, and will be small if $ns^2\chi_c^2\,\eta^2 \gg 1$. The important values of η will be $\approx 1/\sqrt{n}\,\chi_c s$ or less. If we take $\eta \approx 1/\sqrt{n}\,\chi_c s$, condition (A.2) can be written as

$$\sqrt{n}\, s\chi_a \ll \sqrt{n}\, sk\eta \ll 1.$$

Therefore, the derivation will be in error if $\eta > 1/\sqrt{n}\, s\chi_a$, in which case $g(\eta) \approx \exp(-\frac{1}{4}\chi_c^2/\chi_a^2)$. Now χ_c^2/χ_a^2 is of the order of the number of collisions suffered by the particle [9,13]). For nuclear emulsion work χ_c^2/χ_a^2 is usually about 10^3, so that the error is very small of the order of e^{-250}.

Appendix B

SCATTERING BY A NUCLEUS OF RADIUS r_n

An approximate method of taking into account the finite radius of the nucleus can be developed if we assume that the cross section is given by equation (4.9) for angles of scatter φ' less than φ_m, and is zero for $\varphi' > \varphi_m$, where φ_m depends on the nuclear radius r_n. We take for φ_m the expression used by Olbert [14]):

$$\varphi_m = \chi_a \frac{a}{r_n} \tag{B.1}$$

where χ_a is the characteristic screening angle, $a = 1.67\times10^4\, e^2/m_e c^2\, Z^{-1/3}$ is the Thomas-Fermi radius of the atom, and

$$r_n = \frac{e^2}{m_e c^2} A^{1/3}$$

is the nuclear radius.

φ_m is defined by Olbert in this way so that when the classical approximation is valid $\varphi_m \approx (2Zze^2/pv)1/r_n$, i.e. (B.1) gives the angle of scatter with impact parameter r_n, and when the Born approximation is valid $\varphi_m \approx \lambda\!\!\!^{-}/r_n$, where $\lambda\!\!\!^{-}$ is the de Broglie wave length of the scattered particle. If we calculate φ_m for emulsion using Molière's method of averaging [9]), we get $\varphi_m \approx 2\times10^3\chi_a$, so that $\varphi_m \approx 50\,\chi_c$.

$g(\eta)$ is still given by equation (A.7) but I is now

$$I = \tfrac{1}{2}\chi_c'^2 \left\{\int_{-\infty}^{\infty} d\varphi'\, q(\varphi')[1-e^{iv\varphi'}]\varphi'^{-3} - 2\int_{\varphi_m}^{\infty} d\varphi'[1-e^{iv\varphi'}]\varphi'^{-3}. \right. \tag{B.2}$$

The FF $f(x_s)$ obtained using equation (B.2) is given by Olbert (equation 15).

The first term of (B2) is given by equation (A.6), while the correction term can be written as

$$I_c = -\tfrac{1}{2}\chi_c'^2 v^2 \left\{\frac{1-\cos v\varphi_m}{v^2\varphi_m^2} + \frac{\sin v\varphi_m}{v\varphi_m} - \mathrm{Ci}\, v\varphi_m\right\}. \tag{B.3}$$

We can express $\mathrm{Ci}\, v\varphi_m$ as [18])

$$\mathrm{Ci}\, v\varphi_m = \ln \gamma v + \ln \varphi_m - \int_0^{\varphi_m} dx\, \frac{1-\cos vx}{x}. \tag{B.4}$$

If we now combine equations (A.6), (B.3) and (B.4) we get

$$I = \tfrac{1}{2}\chi_c'^2 \left\{ B' v^2 - \frac{1}{\varphi_m^2}(1 - \cos v\varphi_m) - \frac{v}{\varphi_m}\sin v\varphi_m - v^2 S(v\varphi_m) \right\} \quad \text{(B.5)}$$

where we have put $B' = \ln 2\sqrt{e'}\,\varphi_m/\chi_a \approx 8.80$ and

$$S(v\varphi_m) = \int_0^{\varphi_m} dx\, \frac{1 - \cos vx}{x} = \frac{1}{2}\frac{v^2\varphi_m^2}{2!} - \frac{1}{4}\frac{v^4\varphi_m^4}{4!} + \frac{1}{6}\frac{v^6\varphi_m^6}{6!} - \ldots \quad \text{(B.6)}$$

The series $S(v\varphi_m)$ is finite for all values of v [19]) and tends to zero as $v \to \infty$. We have thus eliminated the term $\ln v$ which was responsible for the divergence of the second moments. We have also obtained another 'normal approximation':

$$g(\eta) = \exp\{-\tfrac{1}{2}\chi_c'^2 B' \sum_{j,k} A_{jk}\eta_j\eta_k\}. \quad \text{(B.7)}$$

Making use of equation (3.8) we can calculate $E(x_i^2)$ and $E(x_i x_j)$. We get

$$E(x_i^2) = (B' - \tfrac{3}{2})\chi_c'^2 A_{ii}^{(s)} \quad \text{(B.8)}$$

and

$$E(x_i x_j) = (B' - \tfrac{3}{2})\chi_c'^2 A_{ij}^{(s)}, \quad \text{(B.9)}$$

where the elements of the correlation matrix $\mathbf{A}^{(s)}$ are the same as found previously (4.27). This is in agreement with Schonland's proof [15]) that the matrix of correlation coefficients is independent of the exact shape of the distribution function provided that the second moments are finite.

The fourth moment $E(x_i^4)$ is given by

$$E(x_i^4) = 3[E(x_i^2)]^2 + \tfrac{1}{2}\chi_c'^2\varphi_m^2 \int_0^{l_T} dl\, \gamma_k^4(l). \quad \text{(B.10)}$$

For a normal distribution $E(x_i^4) = 3[E(x_i^2)]^2$ so that the second term of equation (B.10) is due to the non-normal character of the JPF.

If we compare the variance of the x_i obtained on the basis of the normal approximation given in section 4.3 with that given by equation (B.8) we obtain, in the case of a relativistic particle measured with a cell length of 500 μ so that $B_r = 9.75$,

$$E(x_i^2) \approx 1.5 E_M(x_i^2)$$

where $E_M(x_i^2)$ is the variance given by equation (4.28). Therefore, the standard deviation of the x_i is about 20 % bigger than the standard deviation given by the normal approximation to the Molière JPF.

References

1) P. H. Fowler, Phil. Mag. **41** (1950) 169; M. G. K. Menon, C. O'Ceaillaigh and M. Rochat, Phil. Mag. **42** (1951) 932; A. Beiser, Rev. Mod. Phys. **24** (1952) 273; Y. Goldschmidt-Clermont, Ann. Rev. of Nucl. Sci. **3** (1953) 141; L. Voyvodic, Prog. Cosmic Ray Phys. **2** (1954) 219

2) S. Biswas, B. Peters and Rama, Proc. Ind. Acad. Sci. **41** (1951) 154; H. Fay, Zeits. für

Naturf. **10a** (1955) 572; E. Lohrman and M. Teucher, Nuovo Cimento **3** (1956) 59; F. A. Brisbout, C. Dahanayake, A. Engler, P. H. Fowler and P. B. Jones, Nuovo Cimento **3** (1956) 1400; A. J. Apostolakis, J. O. Clarke and J. V. Major (1956) (to be published)
3) J. E. Moyal, Phil. Mag. **41** (1950) 1058
4) G. Molière, privately circulated preprint (1950); Zeits. für Naturf. **10a** (1955) 177
5) B. D'Espagnat, Comptes Rendus **232** (1951) 800; Jour. de Phys. **13** (1952) 74; Rep. Bagnères Conf. (1953) 78
6) M. Huybrechts, Ph.D. Thesis (Université Libre de Bruxelles 1956, Bulletin No. 41)
7) S. Biswas, E. C. George, B. Peters and M. S. Swamy, Nuovo Cimento **12** (1954) 369; A. Bonetti, R. Levi Setti, B. Locatelli and G. Tomasini, Nuovo Cimento **1** (1955) 904; L. Jauneau and J. Trembley, Nuovo Cimento Suppl. **1** (1955) 236; R. H. W. Johnston and C. O'Ceallaigh, Phil. Mag. **46** (1955) 393; G-Stack Collaboration, Nuovo Cimento **2** (1956) 1064
8) H. Cramér, Mathematical Methods of Statistics (Princeton University Press, 1954)
9) G. Molière, Zeits. für Naturf. **2a** (1947) 133; **3a** (1948) 78
10) G-Stack Collaboration, Nuovo Cimento **2** (1955) 1064
11) K. Gottstein, M. G. K. Menon, J. H. Mulvey, C. O'Ceallaigh and O. Rochat, Phil. Mag. **42** (1951) 708
12) S. Biswas, E. C. George, B. Peters and M. S. Swamy, Nuovo Cimento Supp. **12** (1954) 369
13) H. A. Bethe, Phys. Rev. **89** (1953) 1256
14) S. Olbert, Phys. Rev. **87** (1952) 319
15) D. S. Schonland, Proc. Phys. Soc. A **65** (1952) 640
16) D. M. Ritson, Communication CERN-BS3 of the CERN Bureau of Standards (1954)
17) A. J. Herz, R. M. May and N. Solntseff, Nuovo Cimento **4** (1956) 1623
18) E. Jahnke and F. Emde, Tables of Functions, Fourth Ed. (Dover, 1945)
19) E. Madelung, Die mathematischen Hilfsmittel des Physikers (Dover, 1943)

Nuclear Physics **4** (1957) 363—374; © *North-Holland Publishing Co., Amsterdam*
Not to be reproduced by photoprint or microfilm without written permission from the publisher

ZWEITEILCHENNÄHERUNGEN DES MEHRKÖRPERPROBLEMS I

W. BRENIG
Max Planck-Institut für Physik, Göttingen

Received 17 May 1957

Abstract: The Schroedinger equation for the many body problem is replaced by a system of coupled equations between 1-particle, 2-particle, ... n-particle functions. The energy may be expressed in terms of only 1- and 2-particle functions. Arguments are given that it should be possible to approximate three and four particle functions by products of one and two particle functions. The resulting equations are essentially those given by Brueckner, Eden and Bethe. The results are derived without using perturbation theory.

1. Einleitung

Seit den Anwendungen der Brueckner-Methode zur Energieberechnung bei unendlich ausgedehnten Systemen [1]) sind eine Reihe von Versuchen unternommen worden, Verfahren für endliche Systeme zu entwickeln [2,3,4,5]).

Auf grund der engen Verwandtschaft der bei Wechselwirkungen mit einem „hard core" auftretenden Probleme mit denen in der Theorie der realen Gase und Flüssigkeiten, liegt es nahe, dort entwickelte Methoden auszunutzen. Die in Ref. [2,3,4]) zitierten Verfahren haben in der Tat gewisse Ähnlichkeit mit den verallgemeinerten Clusterentwicklungen der Flüssigkeitstheorie [6]).

Wir wollen im folgenden versuchen, eine Näherungsmethode analog zur Born-Greenschen bzw. Kirkwoodschen Theorie der Flüssigkeiten zu entwickeln. Es zeigt sich, dass auf diesem Wege ein besonders einfacher und direkter Zugang zu einem Verfahren gegeben ist, das im Wesentlichen eine Verallgemeinerung der Brueckner-Methode auf endliche Systeme bedeutet.

2. Mittleres Potential und Vorwärtsstreuung

Wir beginnen mit einer Plausibilitätsbetrachtung für den Zusammenhang zwischen Energieverschiebung und Vorwärtsstreuamplitude für die Bewegung eines Teilchens in einem mit Streuzentren angefüllten Periodizitätskasten vom Volumen W (vgl. auch Ref. [7])).

Für die freie Bewegung gilt

$$-\frac{\hbar^2}{2m}\Delta\varphi_{\mathbf{k}} = T\varphi_{\mathbf{k}} = \varepsilon_{\mathbf{k}}\varphi_{\mathbf{k}};\quad \varphi_{\mathbf{k}} = \mathrm{e}^{\mathrm{i}\mathbf{k}\mathbf{r}}/\sqrt{W};\quad \varepsilon_{\mathbf{k}} = \hbar^2 k^2/2m. \tag{1}$$

Beim langsamen Einschalten eines Streupotentials v wird sich $\varepsilon_{\mathbf{k}}$ im allgemeinen verschieben:

$$(T+v)\psi_{\mathbf{k}} = (\varepsilon_{\mathbf{k}}+V(\mathbf{k}))\psi_{\mathbf{k}} = E_{\mathbf{k}}\psi_{\mathbf{k}}. \tag{2}$$

Für die Energieverschiebung $V(\mathbf{k})$ bekommt man bei der Normierung $(\varphi|\psi) = 1$

$$V(\mathbf{k}) = (\varphi_{\mathbf{k}}|v|\psi_{\mathbf{k}}). \tag{3}$$

Lässt man W gegen unendlich gehen, so geht $\psi_{\mathbf{k}} \cdot \sqrt{W}$ gegen die Lösung $\chi_{\mathbf{k}}$ des Streuproblems im unendlichen Raum mit der Randbedingung stehender Streuwellen und

$$V(\mathbf{k}) \to (e^{i\mathbf{kr}}|v|\chi_{\mathbf{k}})/W.$$

Füllt man jedoch das Volumen bei seiner Vergrößerung mit Streuzentren auf, so daß deren Dichte $n = N/W$ konstant bleibt, dann wird bei Vernachlässigung von Mehrfachstreuungen

$$V(\mathbf{k}) = n(e^{i\mathbf{kr}}|v|\chi_{\mathbf{k}}). \tag{4}$$

Für hinreichend kleine $\mathbf{k}$ bekommt man daraus nach Standardmethoden [8])

$$V(\mathbf{k}) = -n\frac{2\pi\hbar^2}{m}a_k, \tag{5}$$

wobei a_k die Vorwärtsstreuamplitude ist. Dieses Resultat ist schon bei W. Lenz [6]) zu finden.

Falls die Bornsche Näherung ausreicht, ist $\chi_{\mathbf{k}} \approx \exp(i\mathbf{k}\cdot\mathbf{r})$. Für das mittlere Potential bekommt man dann die bekannte Beziehung

$$V = n\int v(\mathbf{r})d\mathbf{r}. \tag{6}$$

Die Mehrfachstreuungen kann man pauschal berücksichtigen, indem man nicht die Streuung im freien Raum, sondern im Medium der übrigen Streuzentren berechnet, $\psi_{\mathbf{k}}$ also nicht als Lösung von (2) sondern von

$$\{T+V(-i\,\mathrm{grad})+v\}\psi_{\mathbf{k}} = E_{\mathbf{k}}\psi_{\mathbf{k}} \tag{7}$$

bestimmt.

Zur Lösung dieser Gleichung kann man ein selfconsistent field Verfahren benutzen: Man nimmt zunächst ein geeignetes $V(\mathbf{k})$ an, bestimmt damit nach (7) $\psi_{\mathbf{k}}$ und setzt dieses in (4) ein. Mit dem so ermittelten $V(\mathbf{k})$ geht man wieder in (7) ein usw. bis sich V nicht mehr ändert.

3. Mittleres Potential und Zweiteilchennäherung beim Mehrteilchenproblem

Wir wollen nun versuchen, die Gl. (4) und (7) für das mittlere Potential und das Streuproblem auf das N-Teilchenproblem zu verallgemeinern. Da sich herausstellen wird, daß das mittlere Potential im allgemeinen ein nichthermitescher Operator ist, erweist es sich als zweckmäßig, von vornherein

mit nichtorthogonalen Systemen von Einteilchenfunktionen zu rechnen. Dies bringt nur eine unbedeutende Erschwerung des allgemeinen Verfahrens mit sich und dürfte auch bei praktischen Rechnungen keine großen Schwierigkeiten machen, da zu erwarten ist, daß die antihermiteschen Anteile bei größeren Teilchenzahlen klein sind (vgl. dazu Abschn. 5) und als Störung behandelt werden können. Wie man nichthermitesche Potentiale völlig vermeiden kann, wollen wir in einer späteren Arbeit untersuchen.

Wir setzen für die mittlere Wellenfunktion eine Determinante aus N linear unabhängigen Einteilchenfunktionen $\varphi^1(1), \ldots, \varphi^N(N)$ an. Die genauere Form der φ^ν wird erst im weiteren Verlauf der Rechnung festgelegt werden, (vgl. dazu Abschn. 4). Fürs erste denke man etwa an die üblichen Funktionen des Schalenmodells bzw. Fermigasmodells. Die richtige Wellenfunktion des N-Teilchensproblems sei $\psi(1 \ldots N)$. Dann gilt wegen der Antisymmetrie in den Variablen $1 \ldots N$ für jeden in $1 \ldots N$ symmetrischen Operator A

$$(D|A|\psi) = N!\,(\prod|A|\psi)$$

wobei D die Determinante aus den $\varphi^\mu(\nu)$ ist und

$$\prod = \prod_{\varrho=1}^{N} \varphi^\varrho(\varrho)$$

das Produkt der Diagonalglieder †. Die Normierung von ψ und Π wollen wir im weiteren so wählen, daß $(\Pi|\psi) = 1$ ist. Wir definieren weiterhin die Funktionen

$$\Pi^\mu = \prod_{\varrho \neq \mu} \varphi^\varrho(\varrho), \quad \Pi^{\mu\nu} = \prod_{\varrho \neq \mu,\nu} \varphi^\varrho(\varrho) \quad \text{für } \mu < \nu, \tag{8}$$

$\Pi^{\mu\nu\varrho}$ entsprechend; sowie

$$\begin{aligned} \varphi_\mu &= \int \Pi^{\mu *} \psi \mathrm{d}' 1 \ldots N, \\ \psi_{\mu\nu} &= \int \Pi^{\mu\nu *} \psi \mathrm{d}' 1 \ldots N, \end{aligned} \tag{9}$$

$\psi_{\mu\nu\varrho}$ entsprechend (der Strich am Integralzeichen bedeutet Auslassung der an Π als oberer Index stehenden Variablen). Die zunächst nur für $\mu < \nu$ definierten Funktionen $\psi_{\mu\nu}(1, 2)$ sind antisymmetrisch in den Variablen und wir wollen die Definition auf beliebige Quantenzahlen durch die Festsetzungen

$$\psi_{\mu\nu} = -\psi_{\nu\mu}; \quad \psi_{\mu\nu\varrho} = -\psi_{\mu\varrho\nu} = -\psi_{\nu\mu\varrho} \text{ etc.} \tag{10}$$

erweitern. Auf Grund der Antisymmetrie von $\psi(1 \ldots N)$ genügen dann die φ^μ und φ_ν den Orthogonalitätsrelationen

$$(\varphi^\mu|\varphi_\nu) = (\Pi|\psi)\delta_{\mu\nu} = \delta_{\mu\nu}. \tag{11}$$

† Die Diagonalglieder liefern eine eindeutige Zuordnung zwischen den Quantenzahlen μ und den Variablen $1 \ldots N$, so dass wir im Folgenden beide oft in gleicher Weise bezeichnen können.

Ebenso gilt entsprechend

$$\int \varphi^{\lambda *}(2)\psi_{\mu\nu}(1,2)\mathrm{d}2 = \varphi_\mu(1)\delta_{\lambda\nu} - \varphi_\nu(1)\delta_{\lambda\mu}. \tag{12}$$

Den Inhalt der Gl. (12) kann man noch etwas anschaulicher ausdrücken. Wir denken uns dazu die φ^ν und φ_ν zu je einer vollständigen Basis des Hilbertraums fortgesetzt, derart, daß die Relationen (11) allgemein gelten. Dann kann man $\psi_{\mu\nu}$ nach den antisymmetrischen Zweiteilchenfunktionen

$$\varphi_{\varkappa\lambda}(1,2) = \varphi_\varkappa(1)\varphi_\lambda(2) - \varphi_\lambda(1)\varphi_\varkappa(2) \tag{13}$$

entwickeln:

$$\psi_{\mu\nu}(1,2) = \varphi_{\mu\nu}(1,2) + \sum_{\varkappa\lambda \neq \mu\nu} \Omega^{\varkappa\lambda}{}_{\mu\nu}\varphi_{\varkappa\lambda}(1,2) \equiv \Omega_{12}\varphi_{\mu\nu} \tag{14}$$

und (12) besagt jetzt, daß in der $\varkappa\lambda$-Summe nicht nur das schon vor die Summe gestellte Glied $\varphi_{\mu\nu}$ fehlt, sondern alle Funktionen $\varphi_{\varkappa\lambda}$, bei denen $\varkappa$ oder λ kleiner als N ist. Liest man die Gl. (14) so, daß man sagt, die $\varkappa\lambda$-Summe beschreibt die „Streuwelle" für die Streuung der Teilchen aneinander im Zustand $\varphi_{\mu\nu}$ und bezeichnet noch die Gesamtheit der Quantenzahlen $\mu < N$ als „Fermikugel", so bedeutet (12): Bei der Streuung zweier Teilchen in der Fermikugel treten nur solche Zwischenzustände auf, bei denen sich beide Teilchen außerhalb der Fermikugel befinden.

Die Gl. (14) legt weiterhin nahe, für die Fälle, bei denen es auf das genaue Verhalten von $\psi_{\mu\nu}(1,2)$ bei $\mathbf{r}_1 \approx \mathbf{r}_2$ nicht ankommt, $\psi_{\mu\nu}$ näherungsweise durch $\varphi_{\mu\nu}$ zu ersetzen.

Nach diesen Vorbereitungen fällt es nicht schwer, die Grundgleichungen des Verfahrens aufzustellen. Zur Berechnung der Energie multiplizieren wir

$$\mathscr{H}\psi(1\ldots N) = \{\sum_\mu T_\mu + \tfrac{1}{2}\sum_{\mu\neq\nu} v_{\mu\nu}\}\psi = E\psi \tag{15}$$

skalar von links mit Π und bekommen nach unseren Festsetzungen

$$E = (\Pi|\mathscr{H}|\psi) = \sum_{\mu=1}^{N} (\varphi^\mu|T|\varphi_\mu) + \tfrac{1}{2}\sum_{\mu,\nu}^{N} (\varphi^\mu\varphi^\nu|v|\psi_{\mu\nu}). \tag{16}$$

Die μ,ν-Summe kann über alle μ und ν erstreckt werden, da $\psi_{\mu\nu}$ für $\mu = \nu$ automatisch verschwindet. Zur Bestimmung von E benötigt man also nur die Funktionen φ^μ, φ_μ und $\psi_{\mu\nu}$, für die wir jetzt Gleichungen aufstellen wollen. Dazu multiplizieren wir (15) zunächst mit $\Pi^{\mu *}$ und integrieren. Dann ergibt sich nach Trennung der Summen in Terme, die μ enthalten, und solche, die μ nicht enthalten,

$$T_\mu\varphi_\mu + \sum_\nu (\varphi^\nu|v_{\mu\nu}|\psi_{\mu\nu}) + \sum_\nu (\varphi^\nu|T_\nu|\psi_{\mu\nu}) + \tfrac{1}{2}\sum_{\nu,\varrho} (\varphi^\nu\varphi^\varrho|v_{\nu\varrho}|\psi_{\mu\nu\varrho}) = E\varphi_\mu. \tag{17}$$

Die Summen können wieder wegen der Antisymmetrie der $\psi_{\mu\nu}$ und $\psi_{\mu\nu\varrho}$ in den Quantenzahlen über alle ν und ϱ erstreckt werden.

Gl. (17) bedeutet eine Gleichung für φ_μ in der jedoch außer den Zwei-

teilchenfunktionen $\psi_{\mu\nu}$ auch noch Dreiteilchenfunktionen $\psi_{\mu\nu\varrho}$ vorkommen. Die Gleichung für $\psi_{\mu\nu}$, $\psi_{\mu\nu\varrho}$ usw. bekommt man entsprechend aus (15) durch Multiplikation mit $\Pi^{\mu\nu}$, $\Pi^{\mu\nu\varrho}$ usw. Auf diesem Wege bekommt man ein System von gekoppelten Gleichungen für die Ein- Zwei- und Dreiteilchenfunktionen etc. Das erste Glied der zweiten Teile von (17) lautet nun etwas ausführlicher

$$\int \varphi^{\nu *}(2) T_2 \psi_{\mu\nu}(1, 2) \mathrm{d}2.$$

Bei der Integration über 2 ist 1 meistens weit von 2 entfernt, so daß man für $\psi_{\mu\nu}$ den asymptotischen Wert $\varphi_{\mu\nu}$ einsetzen kann. Entsprechend ist beim zweiten Glied der zweiten Zeile μ meistens weit von ν und ϱ entfernt. Wir schreiben deshalb hier entsprechend

$$\psi_{\mu\nu} = \varphi_{\mu\nu} \tag{18a}$$

$$\psi_{\mu\nu\varrho}(1, 2, 3) = \varphi_\mu(1)\psi_{\nu\varrho}(2, 3) - \varphi_\nu(1)\psi_{\mu\varrho}(2, 3) - \varphi_\varrho(1)\psi_{\nu\mu}(2, 3). \tag{18b}$$

Bei der Näherung (18b) bleibt die Antisymmetrie in $\mu\nu\varrho$ streng erhalten, die Antisymmetrie in 123 nur noch in dem Bereich des Konfigurationsraumes, wo die Näherung gut ist. Es hat jedoch keinen Sinn, die Wellenfunktion (18b) zu antisymmetrisieren, weil dadurch die Näherung gerade an den Stellen, wo 2 und 3 sich nahe sind, in unzulässiger Weise verschlechtert wird.

Wir führen nun den Einteilchenoperator „mittleres Potential" ein mit den Matrixelementen

$$V^\lambda{}_\mu = \sum_{\nu=1}^{N} (\varphi^\lambda \varphi^\nu | v | \psi_{\mu\nu}) = \sum (\varphi^\lambda \varphi^\nu | K | \varphi_{\mu\nu}) \tag{19}$$

mit $K = v\Omega$.

Hier ist zunächst noch $\mu \leqq N$. Wir wollen jedoch diese Definition auf alle μ ausdehnen. Zu diesem Zwecke müssen wir auch die Definition (9) der $\psi_{\mu\nu}$ auf $\mu > N$ ausdehnen. Dies geschieht am einfachsten durch Ausdehnung der Gl. (24) (s. u.) auf $\mu > N$.

Dann wird aus (17)

$$(T+V)\varphi_\mu = \sum_{\lambda=1}^{N} (T+V)^\lambda{}_\mu \varphi_\lambda. \tag{20}$$

Diese Gleichung stimmt umso besser, je besser die Näherungen (18a, b) sind, was davon abhängt, wie groß der Bereich ist, in dem die Funktionen $\psi_{\mu\nu}$ bzw. $\psi_{\mu\nu\varrho}$ von der mittleren Welle $\varphi_{\mu\nu}$ bezw. (18b) merklich abweichen. Gl. (18) wird z.B. bei Vorhandensein harter, abstoßender Kerne nur dann gut sein, wenn der Radius des harten Kerns klein gegenüber dem mittleren Abstand der Teilchen ist.

Führt man nun mit den φ^ν eine sonst beliebige lineare Transformation durch mit der Determinante 1:

$$\varphi'^\mu = \sum_{\nu=1}^{N} A^\mu{}_\nu \varphi_\nu, \quad \mathrm{Det}\,(A^\mu{}_\nu) = 1,$$

so ändert sich an der Slaterdeterminante D nichts. Die φ_μ erfahren jedoch ebenfalls eine lineare Transformation (die zu $A^\mu{}_\nu$ kontragrediente $(A^{-1})^{\nu^*}_{\mu^*}$), und $(T+V)^\lambda{}_\mu$ transformiert sich in

$$\sum_{\lambda',\,\mu'} A^{\mu^*}_{\lambda'}(T+V)^{\lambda'}{}_{\mu'}(A^{-1})^{\mu'^*}_{\lambda} = (T'+V')^\mu{}_\lambda.$$

Wir nehmen an, daß A so wählbar ist, daß $(T'+V')^\lambda{}_\mu$ diagonal wird †, und setzen jetzt voraus, daß die φ^ν von Anfang an so gewählt sind, daß dies der Fall ist. Dann hat man für φ_μ die Gleichung

$$\begin{aligned}(T+V)\varphi_\mu &= \varepsilon_\mu \varphi_\mu \\ \varepsilon_\mu &= (\varphi^\mu|T+V|\varphi_\mu) = T^\mu{}_\mu + \sum_\nu (\varphi^\mu \varphi^\nu|v|\psi_{\mu\nu}).\end{aligned} \tag{21}$$

Dies ist ein System von Einteilchengleichungen vom Typ der Hartree-Fockschen Gleichungen. Sie enthalten dieselben direkt als Grenzfall, wenn man überall in (16), (19) und (21) die Einteilchennäherung $\psi_{\mu\nu} = \varphi_{\mu\nu}$ und $\varphi^\mu = \varphi_\mu$ einsetzt (vgl. dazu Abschn. 4). In den obigen Gleichungen treten jedoch noch als Unbekannte die $\psi_{\mu\nu}$ auf, für die man weitere Gleichungen benötigt. Wir multiplizieren dazu (15) mit $\Pi^{\mu\nu*}$ und integrieren. Dann bekommt man wie bei (17)

$$\begin{aligned}&(T_\mu+T_\nu)\psi_{\mu\nu} + \sum_\varrho (\varphi^\varrho|v_{\mu\varrho}+v_{\nu\varrho}|\psi_{\mu\nu\varrho}) + v_{\mu\nu}\psi_{\mu\nu} \\ &+ \sum_\varrho (\varphi^\varrho|T_\varrho|\psi_{\mu\nu\varrho}) + \tfrac{1}{2}\sum_{\varrho,\sigma}(\varphi^\varrho\varphi^\sigma|v_{\varrho\sigma}|\psi_{\mu\nu\varrho\sigma}) = E\psi_{\mu\nu}.\end{aligned} \tag{22}$$

Wir wollen auch hier die Zweiteilchennäherung einführen. Es ist jedoch nicht angebracht, in der ersten Zeile für $\psi_{\mu\nu\varrho}$ eine Näherung der Art (18b) zu machen, denn μ und ν bleiben freie Variable. Auf Grund der Vermutung, daß die erste Zeile von (22) den Term $(V_\mu+V_\nu)\psi_{\mu\nu}$ enthält, beginnen wir mit einer Umformung von $V_1\psi_{\mu\nu}(1, 2)$. Man bekommt zunächst nach (14) und (19)

$$V_1\psi_{\mu\nu}(1, 2) = \sum_\varrho (\varphi^\varrho(3)|v_{13}|\Omega_{13}\{\psi_{\mu\nu}(1, 2)\varphi_\varrho(3) - \psi_{\mu\nu}(3, 2)\varphi_\varrho(1)\}).$$

Man addiere und subtrahiere in der geschweiften Klammer den Term $\psi_{\mu\nu}(1, 3)\varphi_\varrho(2)$; dann kann man in etwas besserer Näherung † als (18b) setzen:

$$\psi_{\mu\nu\varrho}(123) = \Omega_{13}\{\psi_{\mu\nu}(1, 2)\varphi_\varrho(3) - \psi_{\mu\mu}(3, 2)\varphi_\varrho(1)\} - \psi_{\mu\nu}(1, 3)\varphi_\varrho(2) \tag{23a}$$

und bekommt damit

$$V_1\psi_{\mu\nu}(1, 2) = \sum_\varrho (\varphi^\varrho(3)|v_{13}|\psi_{\mu\nu\varrho}(123)) + \sum_{\substack{\varrho<N \\ \varkappa}} (\varphi^\varkappa\varphi^\varrho|v|\psi_{\mu\nu})\varphi_\varkappa(1)\varphi_\varrho(2). \tag{23b}$$

Bei einfacher Übernahme von (18b) bekäme man statt dessen

† Dies wird dann möglich sein, wenn die antihermiteschen Anteile von V nicht zu gross sind.

† Diese Näherung ist ähnlich der „superposition approximation" für die Dreierkorrelation in der Flüssigkeitstheorie. Ihre genauere Übertragung würde etwa lauten: $\psi_{\mu\nu\varrho} = \Omega_{12}\Omega_{23}\Omega_{31}\varphi_{\mu\nu\varrho}$.

$$\sum_{\varrho}(\varphi^{\varrho}(3)|v_{13}|\psi_{\mu\nu\varrho}(123)) = V_1\varphi_{\mu\nu}(12) - \sum_{\substack{\varrho<N\\ \varkappa}}(\varphi^{\varkappa}\varphi^{\varrho}|v|\psi_{\mu\nu})\varphi_{\varkappa}(1)\varphi_{\varrho}(2).$$

In der zweiten Zeile von (22) benutzen wir wieder (18b) und schreiben außerdem für $\psi_{\mu\nu\varrho\sigma}$ analog

$$\psi_{\mu\nu\varrho\sigma}(1234) = \psi_{\mu\nu}(12)\psi_{\varrho\sigma}(34) + \text{ antisymmetrische Permutationen von } \mu\nu\varrho\sigma. \tag{23c}$$

Dann bekommt man nach einigen Zwischenrechnungen

$$\{\mathcal{H}_1+\mathcal{H}_2+(1-\tilde{Q}_{12})v_{12}\}\psi_{\mu\nu}(1,2) = \varepsilon_{\mu\nu}\psi_{\mu\nu}(1,2) \tag{24}$$

mit

$$\mathcal{H}_{\nu} = T_{\nu}+V_{\nu}, \quad \varepsilon_{\mu\nu} = \varepsilon_{\mu}+\varepsilon_{\nu}$$

und

$$\tilde{Q} = \tfrac{1}{2}\sum_{\substack{\varkappa<N\\ \lambda}}|\varphi_{\varkappa\lambda})(\varphi^{\varkappa\lambda}| - \tfrac{1}{4}\sum_{\substack{\varkappa,\lambda\\ <N}}|\psi_{\varkappa\lambda})(\varphi^{\varkappa\lambda}|. \tag{25}$$

Dies ist eine Differentialgleichung zur Bestimmung von $\psi_{\mu\nu}$, welche bis auf das Auftreten des Operators $\tilde{Q}$ der Brueckner'schen Integralgleichung [1]) zur Bestimmung der Reaktionsmatrix K völlig äquivalent ist. Die ursprüngliche Brueckner'sche Form

$$\{\mathcal{H}_1+\mathcal{H}_2+v_{12}\}\psi_{\mu\nu} = \varepsilon_{\mu\nu}\psi_{\mu\nu} \tag{26}$$

anstelle von (24) enthält jedoch einen Widerspruch zu (21). Bildet man nämlich die Projektion von (24) auf die „Fermikugel", so bekommt man wegen (14) und (21)

$$(\mathcal{H}_1+\mathcal{H}_2)\varphi_{\mu\nu} = \varepsilon_{\mu\nu}\varphi_{\mu\nu}, \tag{27}$$

aus (26) jedoch

$$(\mathcal{H}_1+\mathcal{H}_2)\varphi_{\mu\nu}+Q_{12}v_{12}\psi_{\mu\nu} = \varepsilon_{\mu\nu}\varphi_{\mu\nu}, \tag{28}$$

wobei Q, der Operator der Projektion auf die Fermikugel, dadurch aus $\tilde{Q}$ entsteht, daß man in (25) $\psi_{\varkappa\lambda}$ durch $\varphi_{\varkappa\lambda}$ ersetzt †.

Da (28) im allgemeinen falsch ist und (14) eine unmittelbare Folge des Pauliprinzips ist, kann man auch sagen, daß die Gleichung (26) dem Pauliprinzip nicht genügt. Bethes Gleichungen (vgl. auch Ref. [1])) sind statt (24) äquivalent

$$\{\mathcal{H}_1+\mathcal{H}_2+(1-Q_{12})v_{12}\}\psi_{\mu\nu} = \varepsilon_{\mu\nu}\psi_{\mu\nu}; \tag{29}$$

wie man sofort sieht, entsteht hieraus durch Projektion auf die Fermikugel wegen $QQ = Q$ die Gl. (27). Das gleiche gilt wegen $Q\tilde{Q} = QQ = Q$ auch für Gl. (24).

Bethe hat schon darauf hingewiesen, daß diese Konsequenz des Pauliprinzips bei einigermaßen glattem Verlauf der Funktionen v_{12} nicht eine Erschwerung, sondern eine Erleichterung der Rechnungen bedeutet. Da

† Wir bemerken an dieser Stelle, daß man mit Hilfe des Projektionsoperators Q Gl. (14) abkürzen kann als

$$\psi_{\mu\nu} = \varphi_{\mu\nu}+(1-Q)\psi_{\mu\nu}.$$

nämlich $(1-Q_{12})v_{12}$ im allgemeinen merklich kleiner ist als v_{12}, kann es als Störung behandelt werden, selbst, wenn v_{12} nicht klein ist. Da Q etwa den langwelligen Anteil des Einheitsoperators darstellt, bedeutet $(1-Q_{12})v_{12}$ nur den kurzwelligen Anteil von v_{12}.

Man kann den gleichen Sachverhalt noch von einer anderen Seite beleuchten, wenn man (29) als Integralgleichung schreibt:

$$\psi_{\mu\nu} = \varphi_{\mu\nu} + \frac{\mathrm{P}(1-Q)}{\varepsilon_{\mu\nu}-\mathscr{H}} v\psi_{\mu\nu} = \varphi_{\mu\nu} + \sum_{\varkappa>\lambda>N} \frac{\mathrm{P}}{\varepsilon_{\mu\nu}-\varepsilon_{\varkappa\lambda}} (\varphi^{\varkappa}\varphi^{\lambda}|v|\psi_{\mu\nu})\varphi_{\varkappa\lambda}. \tag{29a}$$

Das Zeichen P soll für Ausschließung der Singularität $\varepsilon_{\mu\nu} = \varepsilon_{\varkappa\lambda}$ aus der Summation sorgen; es ist im Grundzustande überflüssig, da der Operator $1-Q$ automatisch dafür sorgt. Entscheidend in (29) ist die Tatsache, daß $1-Q$ nicht nur die Singularität selbst, sondern auch alle Zwischenzustände von der Summation ausschließt, welche zur Fermikugel gehören. Dies bedeutet im Grundzustande für alle Zustände $\mu\nu$, bei denen nicht gerade ε_μ und ε_ν gleichzeitig nahe am Rande der Fermikugel liegen, das Auftreten großer Energienenner in (29), so daß bei nicht zu stark singulären Potentialen v in guter Näherung $\psi_{\mu\nu} \approx \varphi_{\mu\nu}$ gesetzt werden darf. Nur die Zustände am Rande der Fermi-Kugel werden durch die Wechselwirkung stärker beeinflußt. Dies ist der Grund dafür, daß die Hartree-Fockschen Gleichungen in vielen Fällen eine so gute Näherung darstellen.

4. Ein Variationsprinzip

Bisher waren die Ausgangsfunktionen ziemlich willkürlich und es erhebt sich die Frage, welche φ^μ die günstigsten sind. Insbesondere tritt diese Frage auf beim Grenzübergang zur Hartree-Fockschen Näherung. Diese ergibt sich als Einteilchennäherung der obigen Gleichungen nur unter der Annahme $\varphi^\mu = \varphi_\mu$ und es ist noch zu klären, was diese Annahme bedeutet. Daß die Hartree-Fockschen Gleichungen sich nicht für beliebige φ^μ als Grenzfall der Gleichungen (21) einstellen können, ist schon deshalb klar, weil die Hartree-Fockschen Einteilchenfunktionen nicht beliebige sind, sondern solche, welche den Erwartungswert der Energie minimal machen. Die Minimalforderung $\delta(D|\mathscr{H}|D)/(D|D)$ ist jedoch im allgemeinen nicht zu gebrauchen, da bei stark singulären Potentialen der Erwartungswert $(D|v|D)$ der potentiellen Energie divergiert.

Eine Möglichkeit, günstige Näherungsfunktionen zu definieren, besteht darin, daß man verlangt, der Abstand (oder Winkel) im Hilbertraum zwischen der Näherungsfunktion D und der exakten Funktion ψ soll minimal sein †, d.h., mit einem Lagrangeschen Parameter $(1-\lambda)$,

$$\delta\{(D-\psi|D-\psi)-(1-\lambda)(D|D)\} = 0 \tag{30}$$

woraus folgt

$$(\delta D|\psi-\lambda D) = 0$$

oder, wenn man in D die einzelnen φ^μ variiert

† Die Bedeutung dieser Minimalbedingung für die Energieberechnung ist vermutlich nicht gross. Will, man darauf verzichten, daß das Verfahren im Grenzfall schwacher Wechselwirkung in die Hartree-Fockgleichungen übergeht, so kann man sich auf die Lösungsmethode 1. von Abschn. 5 beschränken, und auf (31) völlig verzichten.

$$\varphi_\mu = \sum_1^N \lambda_{\nu\mu}\varphi^\nu \tag{31}$$

Die $\lambda_{\nu\mu}$ in (31) bestimmen sich aus $(\varphi^\mu|\varphi_\nu) = \delta_{\mu\nu}$ zu $\lambda_{\nu\mu} = (\varphi_\nu|\varphi_\mu)$. Ist insbesondere das mittlere Potential hermitesch, so stehen die φ_μ orthogonal aufeinander, und es folgt

$$\varphi_\mu = \varphi^\mu.$$

Im Allgemeinen liegt jedoch φ_μ nur in dem aus den φ^ν aufgespannten Unterraum des Hilbertraumes.

Bildet man Skalarprodukte $(D'|\psi)$ zwischen Determinanten aus den so bestimmten günstigsten Einteilchenfunktionen φ^μ mit der richtigen Funktion ψ, so verschwinden diese immer dann, wenn D' sich von D nur in einer Funktion φ^μ unterscheidet, welche auf den φ^ν $(\nu = 1 \ldots N)$ orthogonal steht. Den Inhalt der Gleichungen (31) kann man also auch so ausdrücken daß man sagt, bei der Entwicklung von ψ nach den Einteilchenfunktionen, welche dem Variationsprinzip (30) bzw. den Gl. (31) genügen, treten außer D nur höhere als Einteilchenanregungen auf (bei denen also mindestens 2 der φ^μ aus D' auf den φ^ν $(\nu = 1 \ldots N)$ orthogonal stehen).

Die Festlegung (30) der günstigsten Einteilchenfunktion ist noch nicht vernünftig, falls die Teilchen nur untereinander und nicht mit äußeren Kräften wechselwirken. Dann ist der Gesamtimpuls mit $\mathfrak{H}$ vertauschbar, und die stationären Zustände ψ sind nicht lokalisiert. Nehmen wir z.B. an, ψ sei Eigenfunktion zu $\mathbf{P}$ mit dem Eigenwert 0. dann bekommt man aus (30) durch Entwicklung nach Eigenfunktionen von $\mathbf{P}$ (unter Vernachlässigung der Spinkoordinaten):

$$\delta \frac{\int \varphi_0^*(\mathbf{r})\psi_0(\mathbf{r})d\mathbf{r} + \text{conj. compl.}}{\int \sum_{\mathbf{k}} \varphi_{\mathbf{k}}^*(\mathbf{r})\varphi_{\mathbf{k}}(\mathbf{r})d\mathbf{r}} = 0, \tag{32}$$

$$\varphi_{\mathbf{k}}(\mathbf{r}) = \int \frac{e^{-i\mathbf{kR}}}{\sqrt{W}} D d\mathbf{R}.$$

Dabei bedeutet W ein hinreichend großes Periodizitätsvolumen, $\mathbf{R}$ die Schwerpunktskoordinate, $\mathbf{r}$ die Gesamtheit der Relativkoordinaten. Da nun im Zähler von (32) nur die Komponente von D in Richtung $\mathbf{P} = 0$ vorkommt, kann man den Bruch stets dadurch extremal machen, daß man alle $\varphi_{\mathbf{k}}$ mit $\mathbf{k} \neq 0$ Null setzt. Determinanten D, welche zu $\mathbf{P} = 0$ gehören, sind jedoch aus φ^μ aufgebaut, welche ebenen Wellen entsprechen. Möglicherweise hat (32) noch andere Extremalen, welche lokalisierten Zuständen entsprechen. Da es uns bisher nicht gelungen ist, dieses allgemein einzusehen, wollen wir (30) durch eine etwas abgeänderte Forderung ersetzen, welche lokalisierte Lösungen liefert und bei großen Teilchenzahlen näherungsweise zu den Gln. (31) führt.

Es liegt nahe an Stelle von (32) einfach zu verlangen

$$\delta \frac{\int \varphi_0^*(\mathbf{r})\psi_0(\mathbf{r})d\mathbf{r} + \text{conj. compl.}}{\int \varphi_0^*(\mathbf{r})\varphi_0(\mathbf{r})d\mathbf{r}} = 0. \tag{33}$$

Diese Forderung liefert bei gebundenen Zuständen ψ sicher lokalisierte Funktionen φ als Lösung, nur macht die Variation des Normierungsintegrales im Nenner Schwierigkeiten. (Am Zähler hat sich gegenüber (30) nichts geändert). Bei hinreichend großen Teilchenzahlen kann man jedoch erwarten, daß der Unterschied zwischen (32) und (33) nicht viel ausmacht, so daß die Gln. (31) doch näherungsweise gültig sind. Man sieht dies am einfachsten, wenn man das Normierungsintegral im $\mathbf{k}$-raum ausführt:

$$(\varphi_0|\varphi_0) = \sum_P (-1)^P \sum (\varphi^1(\mathbf{k}_1)|\varphi^{P_1}(\mathbf{k}_1) \ldots (\varphi^N(\mathbf{k}_N)|\varphi^{P_N}(\mathbf{k}_N))\delta_{\mathbf{k}_1 + \ldots + \mathbf{k}_N, 0}.$$

Bei der Variation von $\varphi^1(\mathbf{k}_1)$ bekommt man also

$$\sum_P (-1)^P \sum (\delta\varphi^1(\mathbf{k}_1)|\varphi^{P_1}(\mathbf{k}_1)) \sum_{\mathbf{k}_2 \ldots} \overbrace{(\varphi^2(\mathbf{k}_2)|\varphi^{P_2}(\mathbf{k}_2) \ldots \delta_{\mathbf{k}_1+\ldots\mathbf{k}_N,0}}^{w_1(\mathbf{k}_1)} + \text{conj. compl.}$$

Die Funktion $w_1(\mathbf{k}_1)$ gibt im wesentlichen die Verteilung von $\mathbf{k}_1 = -(\mathbf{k}_2 + \ldots + \mathbf{k}_N)$ wieder, ihre Abhängigkeit von $\mathbf{k}_1$ kann also bei großen N gegenüber der von $\varphi^1(\mathbf{k}_1)$ vernachlässigt werden. Also wird näherungsweise wieder

$$\delta(\varphi_0|\varphi_0) = (\delta\varphi^1|\Sigma\lambda_{1\mu}\varphi^\mu) + \text{conj. compl.}$$

und man kommt zu den Gln. (31) zurück. Die Abweichungen davon beginnen dann merklich zu werden, wenn die Zeit für das Auseinanderfließen des Schwerpunktes vergleichbar wird mit den Umlaufzeiten der Teilchen, d.h. bei kleinen Teilchenzahlen.

5. Grundsätzliches zu den Lösungsmethoden

Zur Lösung der Gln. (21) und (24) kann man Erweiterungen des self-consistent-field-Verfahrens benutzen: Man nimmt in nullter Näherung ein mittleres Potential V an und bestimmt dazu die Eigenfunktionen φ^μ und Eigenwerte, welche in nullter Näherung mit den φ_μ bzw. ε_μ von (21) identifiziert werden. In manchen Fällen wird es sogar einfacher sein, gar nicht erst ein Potential anzunehmen, sondern direkt gleich ein vollständiges Orthogonalsystem φ^μ und dazugehörige ε_μ. Das dazugehörige V ist dann im allgemeinen geschwindigkeitsabhängig und kann als Integraloperator geschrieben werden mit dem Kern

$$V(\mathbf{r}, \mathbf{r}') = \sum_\mu \varepsilon_\mu \varphi^{\mu*}(\mathbf{r})\varphi_\mu(\mathbf{r}') - \frac{\hbar^2}{2m}.$$

Mit den φ^μ, φ_μ und ε_μ geht man in (24) ein und bestimmt die $\psi_{\mu\nu}$. Von hier ab gibt es zwei Möglichkeiten, fortzufahren:

1. Man bestimmt die neue Potentialmatrix $V^\mu{}_\lambda$ bzw. $V(\mathbf{r}, \mathbf{r}')$ nach (19) mit den alten φ^μ und den neuen $\psi_{\mu\nu}$. Wie man sieht, braucht man nur solche $\psi_{\mu\nu}$, bei denen mindestens eine der Quantenzahlen μ oder $\nu < N$ ist. Mit dem neuen V ist die gleiche Prozedur zu wiederholen usw.

2. Man sucht den Operator Ω für den nach (24) $\Omega\varphi_{\mu\nu} = \psi_{\mu\nu}$ ist. Dann kann man für dieses bestimmte Ω (21) zusammen mit (31) als Gleichungssystem vom Hartree-Fockschen Typ mit den „effektiven Zweiteilchenkräften" $v\Omega$ lesen und nach dem gewöhnlichen Verfahren des self-consistent-field lösen. Hat man jedoch die für diese Zweiteilchenkräfte selbstkonsistenten Einteilchenfunktionen gefunden, so muß man im dazugehörigen Potential V nach (24) das neue Ω bestimmen und wieder von vorne anfangen.

Das Potential erster Näherung wird im Gegensatz zur Hartree-Fock-Näherung im allgemeinen nicht hermitesch sein, auch wenn man es in nullter Näherung als hermitesch angenommen hatte. Eine Ausnahme bildet der Fall des Grundzustandes für $N = \infty$. In diesem Falle kann wegen der Gleichberechtigung aller Raumpunkte V nur eine Funktion des Impulses $\mathbf{p}$ sein, welche, wie Brueckner gezeigt hat, reell ist.

Dies soll zunächst an Bemerkungen zu den Grundlagen der Methode genügen. Als weitere Punkte wären zu klären:

1. Die Güte der Vernachlässigung von cluster-Termen bei der Ableitung der Gleichungen (21) und (24), d.h. der Benutzung der Näherungen (18a, b), (23a, c). Abschätzungen hierzu sind von Brueckner und Bethe gemacht worden, allerdings unter der Voraussetzung, daß die Zweiteilchenwechselwirkung nur zu Streuungen und nicht zu Bindungen zweier herausgegriffener Teilchen Anlaß gibt. Das trifft vermutlich im allgemeinen zu (auch bei gebundenen Einteilchenzuständen haben die Wellenfunktionen innerhalb des mittleren Potentialtopfes oszillierenden Charakter), wird jedoch z.B. in der Kernphysik bedenklich, wenn merkliche Beimischungen des a-Teilchenmodells zum Schalenmodell vorliegen; dies würde nämlich heißen, daß (23c) vermutlich eine schlechte Näherung ist.

2. Zur Berechnung anderer Größen als der Energie, z.B. magnetischer Momente, Impulsverteilungen u.a. benötigt man eine Darstellung der Wellenfunktion ψ. Der Brueckersche Näherungsansatz, welcher in unserer Bezeichnungsweise bis auf kleine Korrekturen lautet:

$$\psi = \{1 + \sum_{\mu<\nu} (\Omega_{\mu\nu} - 1)\} \operatorname{Det} (\varphi_\varrho),$$

ist hierfür nicht zu gebrauchen. Er reicht nicht einmal zur Berechnung des Skalarproduktes $(\psi|\psi)$, da ψ in dieser Näherung z.B. bei stark abstossenden Kräften nicht genügend stark verschwindet, falls zwei Teilchen sich nahe kommen. Bedeutend besser in dieser Hinsicht ist der Ausdruck von Bethe, welcher im wesentlichen lautet:

$$\psi = \prod_{\mu<\nu} \Omega_{\mu\nu} \operatorname{Det} (\varphi_\varrho).$$

Erwartungswerte in dieser Näherung für ψ können möglicherweise mit Hilfe der Cluster-Entwicklungen aus der Theorie der realen Gase berechnet werden. (Vgl. etwa Ref. [6]), indem man das dortige W auf Seite 138 bzw. 145 durch den Operator $\Omega = \Pi\Omega_{\mu\nu}$ ersetzt.)

3. Wir haben den Fall, daß die ε_μ entartet sind, nicht genauer betrachtet. Es macht keine prinzipiellen Schwierigkeiten, die Theorie in dieser Hinsicht zu erweitern. Die rechnerischen Schwierigkeiten steigen natürlich sehr bei höheren Anregungszuständen wegen der ständig zunehmenden Entartung. Wir werden darauf in einer späteren Arbeit genauer eingehen.

Herrn Prof. W. Heisenberg danke ich für sein Interesse am Entstehen dieser Arbeit. Den Herren Dr. G. Lüders und Dr. G. Süssmann verdanke ich mehrere kritische Bemerkungen.

Anhang

EINIGE EIGENSCHAFTEN NICHTHERMITESCHER OPERATOREN

Die Eigenfunktionen von $\mathscr{H}$ und $\mathscr{H}^\dagger$,

$$\mathscr{H}\varphi_\mu = \varepsilon_\mu \varphi_\mu$$
$$\mathscr{H}^\dagger \varphi^\mu = \varepsilon_\mu^* \varphi^\mu,$$

genügen bei geeigneter Normierung den Orthogonalitätsrelationen

$$(\varphi^\mu|\varphi_\nu) = \delta_{\mu\nu}; \quad \varepsilon_\mu \text{ nicht entartet.}$$

Die lineare Unabhängigkeit der Eigenfunktionen bei $\varepsilon_\mu = \varepsilon_\nu$, sowie die Vollständigkeit der φ_μ läßt sich nicht wie bei hermiteschen Operatoren allgemein beweisen. Im Falle der Vollständigkeit läßt sich der Einheitsoperator zerlegen in

$$1 = \sum |\varphi^\mu)(\varphi_\mu| = \sum |\varphi_\mu)(\varphi^\mu|.$$

Der Operator g, welcher zwischen den φ_μ und φ^μ vermittelt:

$$\varphi_\mu = g\varphi^\mu,$$

ist hermitesch und positiv definit. Die Eigenwerte ε_μ sind genau dann reell, wenn $\mathscr{H}^\dagger = g^{-1}\mathscr{H}g$ ist.

In diesem Falle kann man durch

$$\tilde{\mathscr{H}} = g^{-1/2}\mathscr{H}g^{1/2},$$
$$\chi_\nu = g^{1/2}\varphi^\nu = g^{-1/2}\varphi_\nu$$

einen hermiteschen Operator $\tilde{\mathscr{H}}$ mit dem vollständigen Orthogonalsystem χ_ν als Eigenfunktionen einführen.

References

1) K. A. Brueckner und W. Wada, Phys. Rev. **103** (1956) 1010 und die dort zitierten Arbeiten
2) R. J. Eden, Proc. Roy. Soc. A **235** (1956) 408
3) H. A. Bethe, Phys. Rev. **103** (1956) 1353
4) W. B. Riesenfeld und K. M. Watson, Phys. Rev. **104** (1956) 492
5) J. Goldstone, Proc. Roy. Soc. A **239** (1957) 267
6) G. Hirschfelder, Curtiss und Bird, Molecular Theory of Gases and Liquids (London, 1954) S. 138.
7) Reifman, De Witt und Newton, Phys. Rev. **101** (1956) 877
8) B. Lippmann und J. Schwinger, Phys. Rev. **79** (1950)469
9) W. Lenz, Z. Phys. **56** (1929) 778

Nuclear Physics **4** (1957) 375—394; © *North-Holland Publishing Co., Amsterdam*
Not to be reproduced by photoprint or microfilm without written permission from the publisher

ROTATIONAL SPECTRA OF NUCLEI FOLLOWING O^{16}

G. RAKAVY

Institute for Theoretical Physics, University of Copenhagen

and CERN *Theoretical Study Division, Copenhagen*

Received 12 March 1957

Abstract: The possibility of the application of the strong coupling collective model (rotational model) to nuclei in the region following O^{16} (s—d shells) is discussed. A calculation shows that nuclei with big deformations may be expected in the considered region. In the light of this result the experimental data on nuclei up to $A = 25$ are reviewed, and it is shown that they are consistent with the general implications of the model.

CONTENTS

1. Introduction 376

2. The Asymptotic Wave Functions 376

3. The Equilibrium Deformation and Zero Point Oscillations 378

4. Analysis of Experimental Data. 383

4.1. NUCLEI OF MASS 19

a. *Ground state spins* 383
b. *Energy levels of* F^{19} 385
c. *γ-transitions* 387
d. *β-transitions* 387

4.2. DATA ON OTHER NUCLEI

a. *Spins and parities* 388
I. *Even nuclei* 388
II. *Odd mass nuclei* 388
III. *Odd nuclei* 389
b. *Magnetic moments* 390
c. *Quadrupole moments* 391
d. *β- and γ-transitions* 391

5. Concluding Remarks 393

1. Introduction

The possibility of interpreting the spectra of some light nuclei according to the rotational model has recently been suggested. Specially striking are the rotational spectra in Al^{25} and Mg^{25} † where all the levels up to 4 MeV could be ascribed to four rotational bands. E. B. Paul also suggested that the spectra of F^{19} could be described by the same model.

The very simple calculation of equilibrium deformations of nuclei described below shows that the deformations in nuclei following O^{16} increase very rapidly. Already in nuclei of mass 18 the deformation attains a value characteristic of heavy nuclei revealing rotational spectra (i.e. nuclei in the region $A = 160$ to $A = 180$). The deformation is fully developed when we reach Ne^{20} and afterwards stays almost constant until we reach $A = 25$ when it begins to decrease again (cf. table 1). This result suggests that rotational spectra should be found systematically throughout the whole region between $A = 18$ and $A = 28$.

The discussion below makes use of S. G. Nilsson's model of independent particle description of the internal motion [2]). It begins with some remarks on the use of asymptotic wave functions for big deformations, and a simple formula is given for the equilibrium deformation. This is followed by a discussion of the possible effect of the "residual interactions" on the equilibrium deformations, and also the problem of zero point oscillations is mentioned. The general discussion is followed by a survey of the experimental data on nuclei from $A = 18$ to $A = 24$.

2. The Asymptotic Wave Functions

In nuclei considered in this work, the calculated equilibrium deformations are rather big so that the anisotropy of the field in which the nucleons move must be treated exactly. On the other hand, the effect of the spin orbit coupling is relatively small. We are therefore led to use the "asymptotic wave functions" (cf. ref. [2]), p. 44). These asymptotic functions are expected to be accurate enough to describe all properties which are not very sensitive functions of the deformation. In particular the equilibrium deformation itself may be calculated by using the asymptotic functions, the error being of the order of 10 %. Also the selection rules [3]) implied by these functions are expected to be very effective in the nuclei considered here.

The energy of a nucleon in the asymptotic case is given by eqs. (2), (B1), (B2) and (B3) of ref. [2]). In fig. 1 are shown the energies of those states which are relevant to our discussion as functions of the deformation. Each level is designated by its asymptotic quantum numbers.

† Litherland, Paul, Bartholomew and Gove, ref. [1]). A more detailed theoretical discussion is to be published by B. Mottelson and S. G. Nilsson.

Neglecting the spin-orbit coupling, which does not influence the equilibrium deformations provided they are big enough, the total energy of the particles

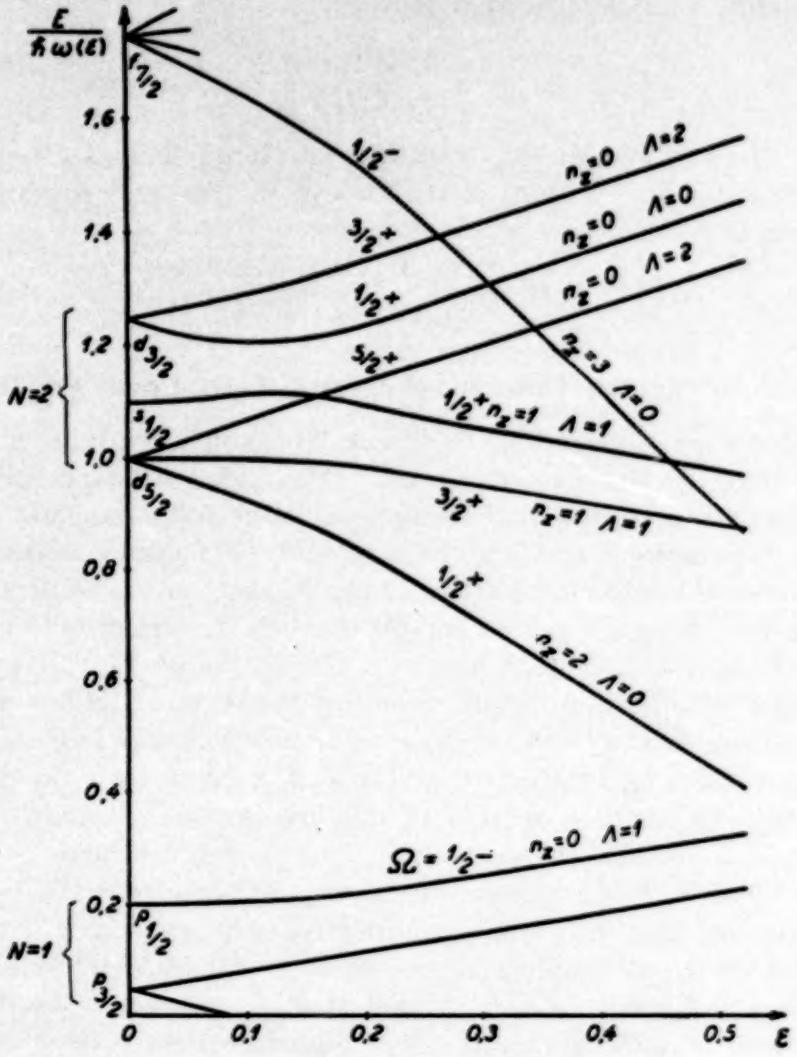

Fig. 1. Energy Levels in Deformed Nuclei.

in the deformed field is

$$W = \tfrac{3}{4}\sum_p [\hbar\omega_{xy}(n_x+n_y+1)+\hbar\omega_z(n_z+\tfrac{1}{2})]$$
$$= \tfrac{3}{4}\hbar\omega(\varepsilon)\sum_p [(1+\tfrac{1}{3}\varepsilon)(n_x+n_y+1)+(1-\tfrac{2}{3}\varepsilon)(n_z+\tfrac{1}{2})]$$

where $\omega(\varepsilon)$, which is determined from the assumption of volume conservation, is given by

$$\omega(\varepsilon) \approx \omega_0(1+\tfrac{1}{9}\varepsilon^2).$$

Neglecting terms of third order in ε and leaving out terms independent, of ε, we get

$$W = \tfrac{1}{12}\sum_p (N+\tfrac{3}{2})\varepsilon^2 + \tfrac{1}{4}\sum_p (N-3n_z)\varepsilon \qquad (1)$$

and the equilibrium deformation is

$$\varepsilon_{eq} = -\frac{3}{2}\frac{\Sigma(N-3n_z)}{\Sigma(N+\frac{3}{2})}. \qquad (2)$$

Obviously the sum of $(N-3n_z)$ vanishes for closed shells so that only the particles outside the O^{16} core contribute to it. The energy gain through deformation is

$$\Delta W = -W_{\min} = \frac{3}{16}\frac{[\Sigma(N-3n_z)]^2}{\Sigma(N+\frac{3}{2})}\hbar\omega_0. \qquad (3)$$

3. The Equilibrium Deformation and Zero Point Oscillations

The assumption underlying the primitive considerations in the last section is that the main effect of the interactions between the nucleons in a nucleus can be represented by some average potential field (including spin orbit interaction) and the requirement of volume conservation of nuclear matter. An additional effect of the interactions is to depolarize the nucleus by producing a "loss of energy through deformation". This "loss" originates from the fact that the expectation value of the (attractive) interactions is smaller in absolute value for the wave functions adapted to the deformed field. The "loss" is expected to be approximately equal to half the maximal splitting between the states of a given isobaric spin in the spherical case. In the case of $A = 19$ this loss is not expected to be bigger than 2—3 MeV † while the calculated energy gain through deformation (eq. (3)) is 8.7 MeV. In the general case it may be hoped that the depolarizing effect of the interactions will be ineffective whenever the "energy gain through deformation", ΔW, is bigger than 5—10 MeV (cf. table 1).

A rotating, deformed field is a good starting point for the description of the state of a nucleus only if the equilibrium deformation sufficiently exceeds the amplitude of zero point oscillations. It is clear that the general trend of the amplitude of the zero point oscillations is to decrease with the mass. (For example the hydrodynamical model predicts a $A^{-7/15}$ dependence; cf. ref. [5]), eqs. (71), (4) and (6).) But in fact we have no reliable estimate for the zero point oscillations, and therefore it is impossible to predict how big the calculated equilibrium deformation of a nucleus must be in order to secure the appearance of a rotational spectrum.

A calculation shows that regions of big equilibrium deformations appear around Ne^{20} (cf. table 1) and around Be^8. The following analysis of the experimental data for nuclei following O^{16} indicates that rotational spectra

† Consider for example the energy levels given by I. P. Elliot and B. H. Flowers, ref. [4]), fig. 6.

TABLE 1

Configurations, expected and measured ground st ate spins, equilibrium deformations ε and energy gain through deformation of nuclei in the region $A = 18$ to $A = 28$.

A	Nucleus	configuration (a)		g.s. spin (b)		ε_{eq}	Energy gain (c) MeV	
		protons	neutrons	theor.	exp.			
18	O^{18}		$(1/2)^2$	0	even nucleus	0.28	4.2	
	F^{18}	1/2	1/2	1 (0)	1	0.28	4.2	
	Ne^{18}	$(1/2)^2$		0	even nucleus	0.28	4.2	
19	O^{19}		$(1/2)^2$ 3/2	3/2	5/2 (or 3/2)	0.29	4.8	
	F^{19}	1/2	$(1/2)^2$	1/2	1/2	0.39	8.7	
	Ne^{19}	$(1/2)^2$	1/2	1/2	1/2 (Mir)	0.39	8.7	
20	F^{20}	1/2	$(1/2)^2$ 3/2	2 (1)	2 or 3	0.42	9.5	
	Ne^{20}	$(1/2)^2$	$(1/2)^2$	0	even nucleus	0.48	14.4	
21	F^{21}	1/2	$(1/2)^2(3/2)^2$	1/2	?	0.39	11.5	
	Ne^{21}	$(1/2)^2$	$(1/2)^2$ 3/2	3/2	3/2	0.48	15.2	
	Na^{21}	$(1/2)^2$ 3/2	$(1/2)^2$	3/2	(3/2) (Mir)	0.48	15.2	
22	Ne^{22}	$(1/2)^2$	$(1/2)^2(3/2)^2$	0	even nucleus	0.47	16.0	
	Na^{22}	$(1/2)^2$ 3/2	$(1/2)^2$ 3/2	3 (0)	3	0.47	16.0	
23	Ne^{23}	$(1/2)^2$	$(1/2)^2(3/2)^2$ 5/2	5/2	5/2 (or 3/2)	0.40	8.6	
	Na^{23}	$(1/2)^2$ 3/2	$(1/2)^2(3/2)^2$	3/2	3/2	0.47	17	
	Mg^{23}	$(1/2)^2(1/2)^2$	$(1/2)^2$ 3/2	3/2	3/2 (Mir)	0.47	17	
24	Ne^{24}	$(1/2)^2$	$(1/2)^2(3/2)^2(5/2)^2$	0	even nucleus	0.33	8.6	
	Na^{24}	$(1/2)^2$ 3/2	$(1/2)^2(3/2)^2$ 5/2	4 (1)	4	0.39	12.6	
	Mg^{24}	$(1/2)^2(1/2)^2$	$(1/2)^2(3/2)^2$	0	even nucleus	0.47	17.6	
25	Na^{25}	$(1/2)^2$ 3/2	$(1/2)^2(3/2)^2(5/2)^2$	3/2	5/2	0.33	9.4	
	Mg^{25}	$(1/2)^2(3/2)^2$	$(1/2)^2(3/2)^2$ 5/2	5/2	5/2	0.4	13.5	
	Al^{25}	$(1/2)^2(3/2)^2$ 5/2	$(1/2)^2(3/2)^2$	5/2	5/2	0.4	13.5	
26	Mg^{26}	$(1/2)^2(3/2)^2$	$(1/2)^2(3/2)^2(5/2)^2$	0	even nucleus	0.34	10.1	
	Al^{26}	$(1/2)^2(3/2)^2$ 5/2	$(1/2)^2(3/2)^2$ 5/2	5 (0)	5	0.34	10.1	
27	Mg^{27}	$(1/2)^2(3/2)^2$	$(1/2)^2(3/2)^2(5/2)^2 1/2$	1/2	1/2	0.34	11	
	Al^{27}	$(1/2)^2(3/2)^2$ 5/2	$(1/2)^2(3/2)^2(5/2)^2$	5/2	5/2	0.28	7.3	
	Si^{27}	$(1/2)^2(3/2)^2(5/2)^2$	$(1/2)^2(3/2)^2$ 5/2	5/2	5/2 (Mir)	0.28	7.3	
28	Al^{28}	$(1/2)^2(3/2)^2$ 5/2	$(1/2)^2(3/2)^2(5/2)^2 1/2$	3 (2)	3	0.29	8.1	
	Si^{28}	$(1/2)^2(3/2)^2(5/2)^2$	$(1/2)^2(3/2)^2(5/2)^2$	0	even nucleus	0.23	5.2	
		Configurations of odd parity bands						
19	F^{19}	$(1/2^-)^{-1}(1/2)^2$	$(1/2)^2$	$1/2^-$	$1/2^-$	0.546	17	hole in O^{16} core and $1/2^+$ orbital completely filled.
25	Al^{25}	$(1/2)^2(3/2)^2(1/2)^-$	$(1/2)^2(3/2)^2$					
	Mg^{25}	$(1/2)^2(3/2)^2$	$(1/2)^2(3/2)^2$ $1/2^-$	$3/2^-$(d)	$3/2^-$	0.57	28	$1/2^-$ orbital originating from the $N = 3$ shell.

(a) Particles external to the O^{16} core are listed by their Ω's.

(b) All spin assignments are taken from Aizenberg and Lauritsen, Rev. Mod. Phys. **29** (1952) 321; Endt and Kluyver, Rev. Mod. Phys. **26** (1954) 95; Nuclear Data Cards ed. by K. Way *et al.*
Underlined spins are directly measured. Spin assignments made on ground of a superallowed mirror transition are marked by „Mir". Even nuclei are assumed to have spin 0.

(c) In eq. (3) $\hbar\omega_0$ is chosen to be 15 MeV in accordance with the calculations of Carlson and Talmi, Phys. Rev. **96** (1954) 436.

(d) The lowest spin of the $K = 1/2^-$ band in Mg^{25} and Al^{25} calculated with a decoupling constant $a = -3.2$ is 3/2.

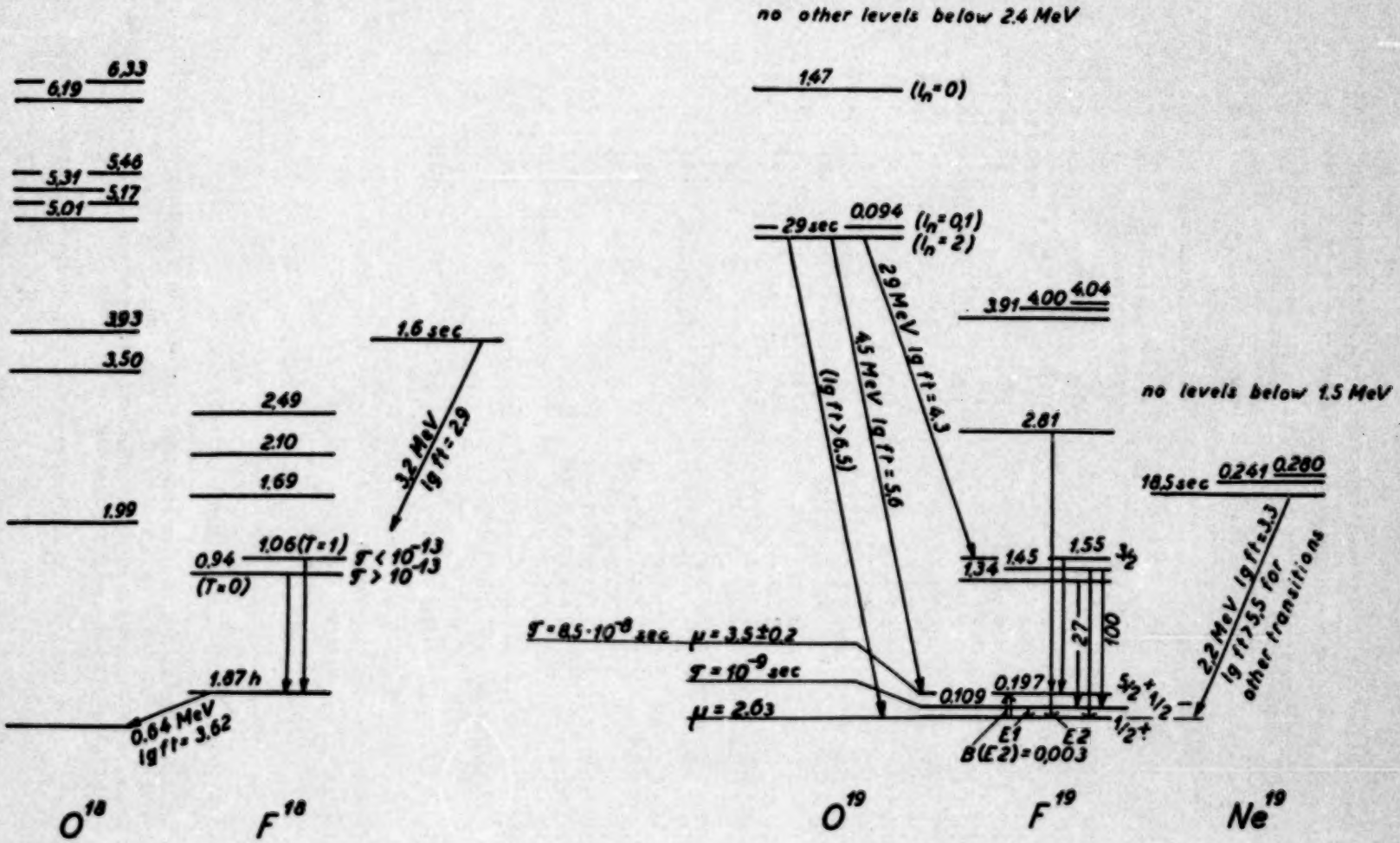
no other levels below 2.4 MeV
1.47
(l_n=0)
6.33
6.19
5.46
5.31
5.17
5.01
3.93
3.50
1.99
2.49
2.10
1.69
1.6 sec
3.2 MeV lg ft=2.9
0.94
1.06(T=1)
(T=0)
τ < 10^-13
τ > 10^-13
1.87 h
0.64 MeV lg ft=3.62
O^18
F^18
29 sec
0.094
(l_n=0,1)
(l_n=2)
(lg ft>6.5)
4.5 MeV lg ft=5.6
2.9 MeV lg ft=4.3
3.91
4.00
4.04
no levels below 1.5 MeV
2.81
18.5 sec
0.241
0.280
1.34
1.45
1.55
3/2
27
100
τ=8.5·10^-8 sec
μ=3.5±0.2
τ=10^-9 sec
μ=2.63
0.109
0.197
5/2+
1/2-
1/2+
E1
E2
B(E2)=0.003
2.2 MeV lg ft=3.3
lg ft>5.5 for other transitions
O^19
F^19
Ne^19

Fig. 2a

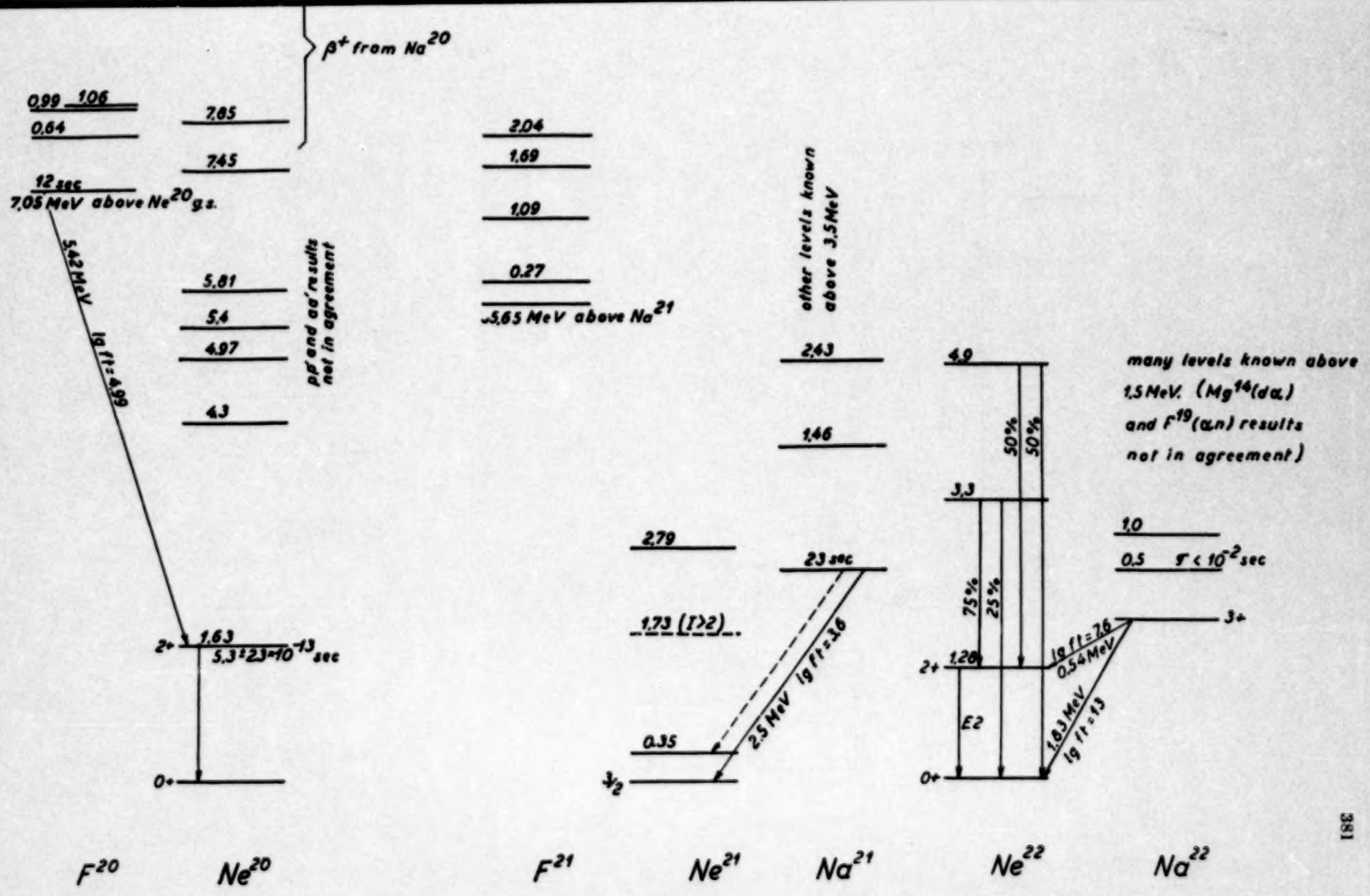
β+ from Na20
0.99 1.06
0.64
7.85
7.45
12 sec
7.05 MeV above Ne20 g.s.
5.42 MeV
lg ft=4.99
5.81
5.4
4.97
4.3
pr and αr results not in agreement
2+
1.63
5.3±2.3×10-13 sec
0+
2.04
1.69
1.09
0.27
-5.65 MeV above Na21
other levels known above 3.5 MeV
2.43
1.46
2.79
23 sec
1.73 (I>2)
0.35
2.5 MeV lg ft=3.6
3/2
4.9
50%
50%
3.3
75%
25%
1.28
2+
E2
0+
lg ft=7.6
0.54 MeV
1.63 MeV
lg ft=13
3+
1.0
0.5 T < 10-2 sec
many levels known above 1.5 MeV. (Mg24(dα) and F19(α,n) results not in agreement)
F20
Ne20
F21
Ne21
Na21
Ne22
Na22

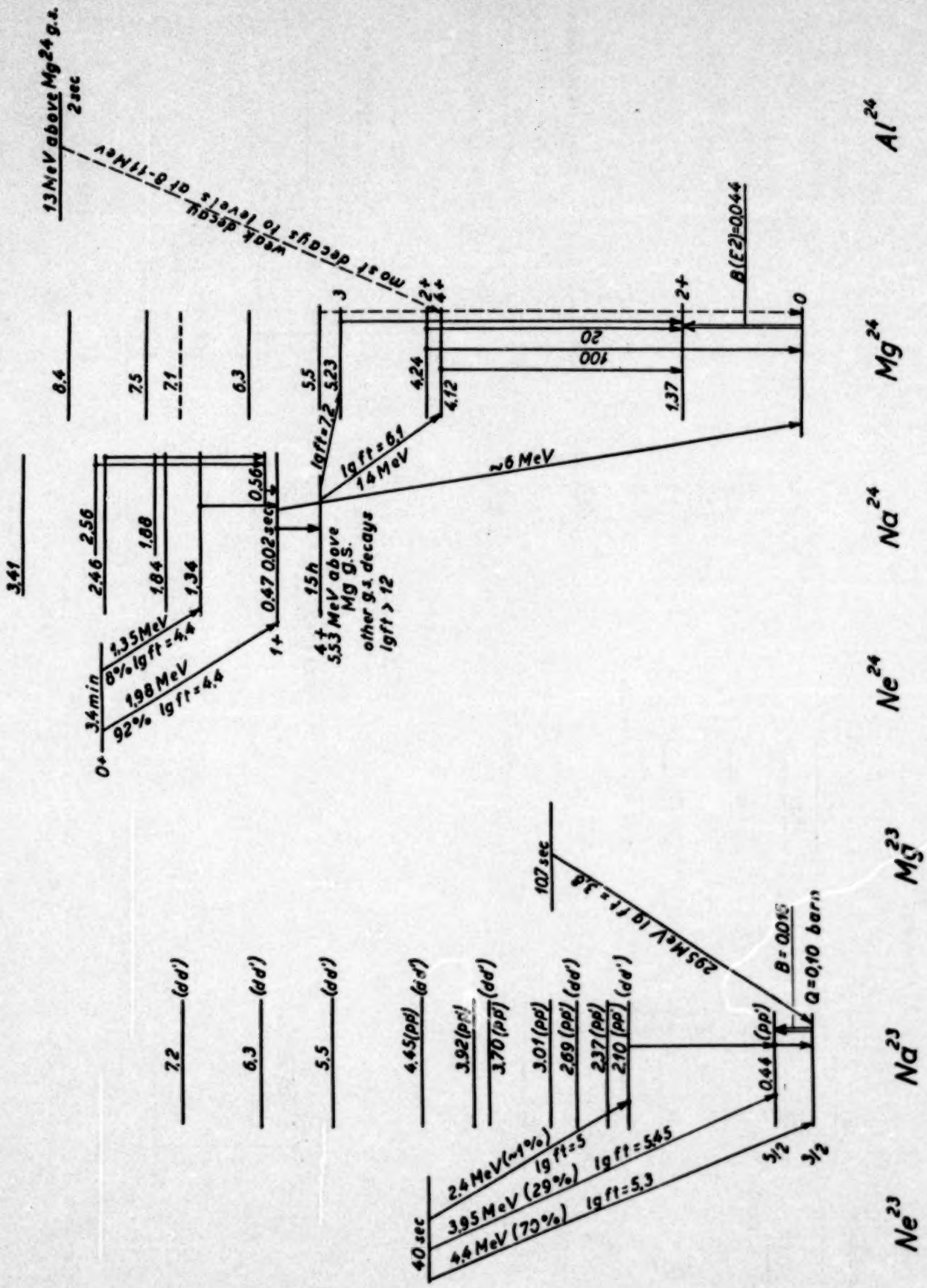
13 MeV above Mg24 g.s.
2 sec
weak decay
most decays to levels at 8-11 MeV
B(E2)=0,044
3,41
2,46
2,56
1,84
1,88
1,34
0,47
0,02 sec
0,56
1,35 MeV
8% lg ft = 4,4
1,98 MeV
92% lg ft = 4,4
3,4 min
0+
1+
15 h
4+
5,53 MeV above Mg g.s.
other g.s. decays
lg ft > 12
lg ft = 7,2
lg ft = 6,1
14 MeV
~6 MeV
8,4
7,5
7,1
6,3
5,5
5,23
4,24
4,12
1,37
3
2+
4+
2+
0
20
100
7,2 (dd')
6,3 (dd')
5,5 (dd')
4,45 (pp') (dd')
3,92 (pp')
3,70 (pp') (dd')
3,01 (pp')
2,69 (pp') (dd')
2,37 (pp')
2,10 (pp') (dd')
0,44 (pp')
295 MeV lg ft = 3,8
10,7 sec
B = 0,016
Q = 0,10 barn
40 sec
2,4 MeV (~1%) lg ft = 5
3,95 MeV (29%) lg ft = 5,45
4,4 MeV (70%) lg ft = 5,3
5/2
3/2
Ne23
Na23
Mg23
Ne24
Na24
Mg24
Al24

Fig. 2c

really appear throughout the whole region of big deformations which occurs there. The situation in the p shell nuclei which may have big deformations is much less definite.

4. Analysis of Experimental Data

As the most extensive data in the region of interest concern nuclei of mass 19, we start with a somewhat more detailed discussion of these nuclei, and the discussion of all the other nuclei is given later. The relevant experimental data are presented in fig. 2.

4.1. NUCLEI OF MASS 19

An analysis of the spectra of F^{19} in terms of the rotational model has been attempted by E. B. Paul †. The discussion which follows differs in some details from Paul's and especially emphasizes the general selection rules which are in operation in the various cases.

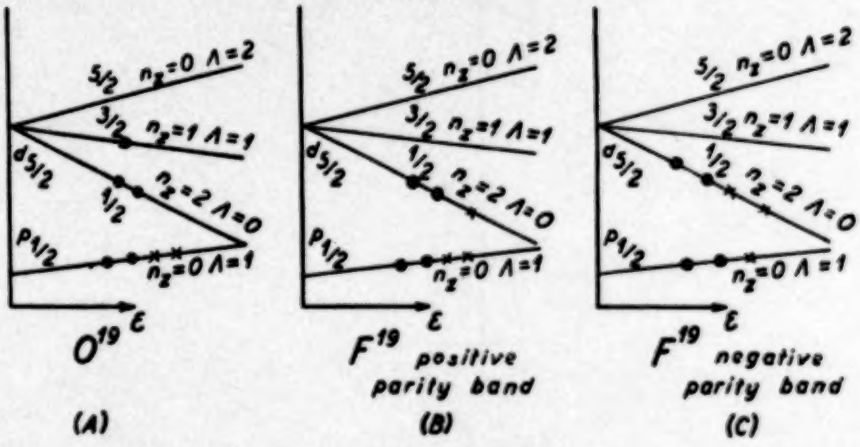

Fig. 3.

a. *Ground state spins*

The expected internal configurations are shown in fig. 3. It is seen that the g.s. of O^{19} is expected to have a spin of 3/2. The decoupling constant of the $\Omega = 1/2$ orbit may vary between 1 to 3, and consequently the ground states of F^{19} and Ne^{19} are expected to be $I = \Omega = 1/2$ states. In fact the measured spins of F^{19} and Ne^{19} are 1/2 as expected. The assignment of the g.s. spin of O^{19} is usually assumed to be 5/2+ since no β-decay has been found to the 1/2+ g.s. of F^{19}. A few possibilities arise here:

(i) The deformation ($\varepsilon = 0.29$) and the energy gain (4.8 MeV) of O^{19} are too small to facilitate the appearance of rotational spectra. In this case a weak coupling model or the usual shell model description may be more adequate. Both models predict a 5/2+ ground state.

(ii) Assuming the rotational model to be a good starting point for the description of the spectra of O^{19}, a $K = 3/2$ rotational band is predicted

† Private communication.

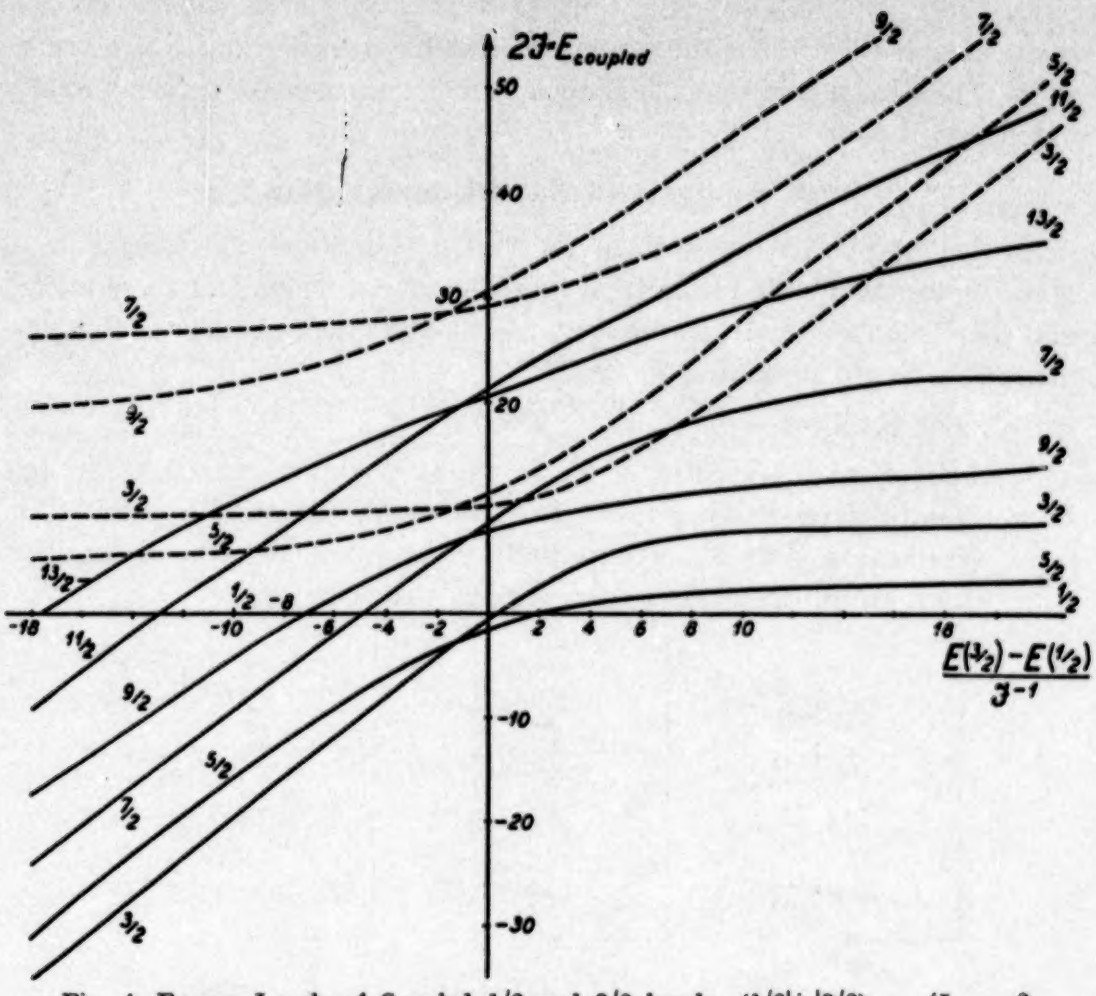

Fig. 4. Energy Levels of Coupled 1/2 and 3/2 bands. $\langle 1/2|j_-|3/2\rangle = \sqrt{5}$ $a=2$

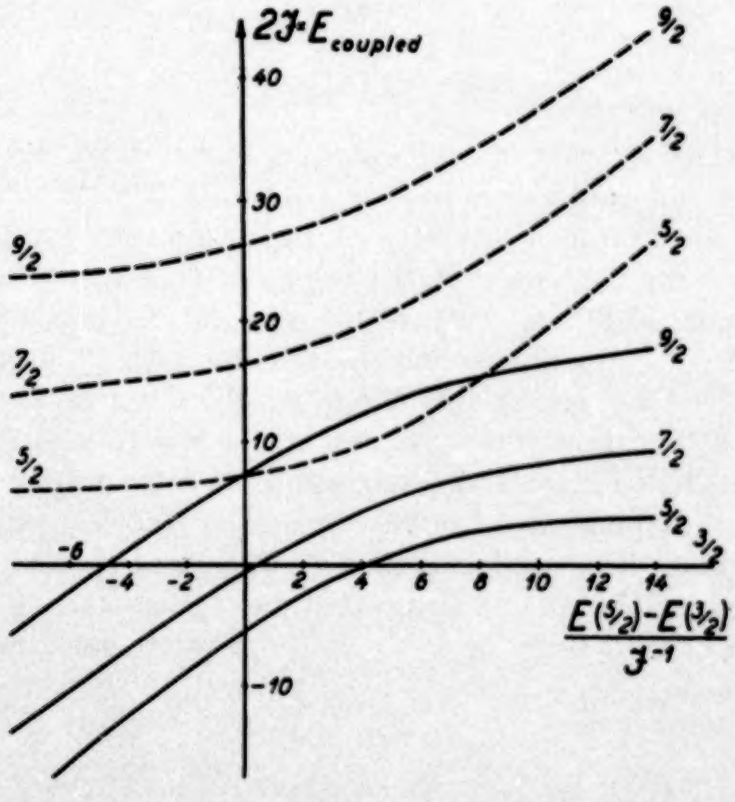

Fig. 5. Energy Levels of Coupled 3/2 and 5/2 bands $\langle 3/2|j_-|5/2\rangle = \sqrt{5}$

to lie lowest. Yet, this band may interact strongly with a $K = 1/2$ band arising from the configuration $1/2\ (3/2)^2$ or with a $K = 5/2$ band arising from the configuration $(1/2)^2\ 5/2$ or with both, so that a $5/2$ member of the mixed bands is pushed down lowest (cf. figs. 4 and 5).

Another possibility is that the g.s. of O^{19} is really a $I = 3/2$ level as predicted by the rotational model (when rotational interactions play only a minor role) and that a special selection rule prevents the decay to the g.s. of F^{19}.

b. *Energy levels of* F^{19}

There appear to exist two rotational bands both having $K = 1/2$. The g.s. band has positive parity, and the band starting at 0.1 MeV has negative parity. The g.s., 0.2 MeV, 1.57, and 2.81 MeV levels constitute the $1/2^+$, $5/2^+$, $3/2^+$, and $9/2^+$ memebers of the positive parity band and the remaining level, i.e. the 0.1, 1.35, and 1.45 MeV levels, are the $1/2^-$, $5/2^-$, and $3/2^-$ members of the negative parity band. It is shown below that this assignment is consistent with the available data.

The internal configuration of the negative parity band is shown in fig. 3c. At the big equilibrium deformation corresponding to this configuration the large energy gain through deformation compensates for the energy required to produce the hole in the (deformed) p shell. Similar low lying negative parity bands are expected to occur in Ne^{19} and in the other F isotopes.

The parameters of both bands can be roughly determined theoretically. The moments of inertia are expected to be almost equal to that of a rigid body i.e. $\mathscr{I}^{-1} \approx 0.55$ MeV †. The decoupling constants may be determined from S. G. Nilsson's wave functions. The decoupling constant of the positive parity band is rather sensitive to the deformation, it ranges from $+1$ for the asymptotic function to $+3$ for very small deformations. For the calculated deformation of F^{19} it should lie rather near to $+2$. The decoupling constant for the negative parity band is $+1$ for both the asymptotic case and for very small deformations, and it is insensitive to the exact deformation. Therefore also for the actual case the value $+1$ should be rather accurate.

Using the above parameters we do not get a good fit between the calculated and experimental levels of the positive parity band. It is clear that a rather strong rotational interaction with a $K = 3/2^+$ band is required to improve the fit. In fig. 4 we see the levels of the coupled system as a function of the internal energy difference. A reasonable fit to the experimental data may be obtained by choosing

$$E_{3/2} - E_{\frac{1}{2}} = 4\mathscr{I}^{-1}; \qquad \mathscr{I}^{-1} = 0.6 \text{ MeV and } a = 2.$$

† $\mathscr{I}^{-1}$ stands for $\hbar^2/\mathscr{I}$ and is measured in MeV.

For the negative parity band a very good fit is obtained by using the parameters $\mathcal{I}^{-1} = 0.43$ MeV, $a = 1.2$.

Qualitative predictions can be made for higher levels. Levels below 7 MeV belonging to the $1/2^+$ (mixed with the $3/2^+$ band) and the $1/2^-$ band are drawn in fig. 6. Three levels belonging to the positive bands with spins $3/2^+$, $7/2^+$, and $5/2^+$ and two negative parity levels with spins $7/2^-$ and $9/2^-$ are expected to appear between 4 and 5 MeV.

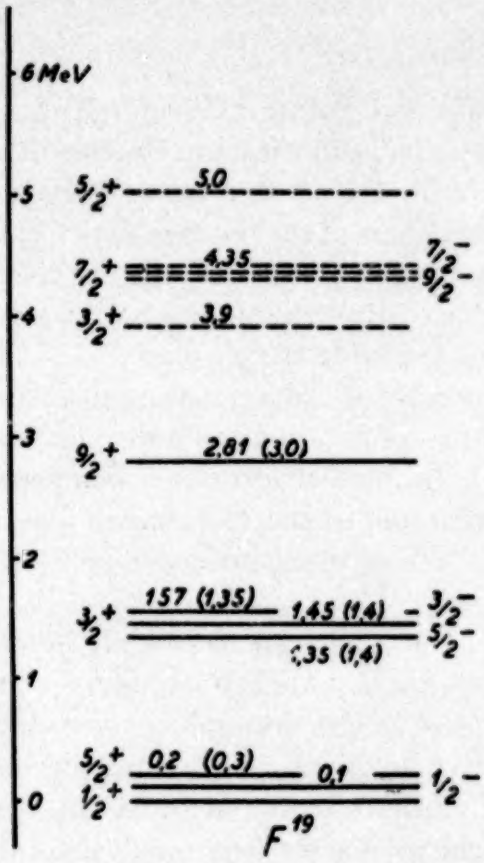

Fig. 6. Levels of F^{19}.

It is assumed implicitly in the present model that a considerable energy is needed to break up a pair of identical nucleons moving in the same orbit. The low lying states should therefore be accounted for by considering only the collective degrees of freedom and the motion of the last odd particle, but at excitations higher than the "pairing energy" many other, more complex, states may also appear. The pairing energy is estimated to be roughly 4 MeV by considering the excitation energy of the lowest "non collective" state in the neighbouring even-even nuclei. It is therefore expected that besides the levels belonging to the various rotational bands built on the s.p. intrinsic states other, more complex, states may appear above 4 MeV.

c. *γ-transitions*

The outstanding fact about the γ transitions within the $K = 1/2^+$ band is that the transition from the $3/2^+$ to the $1/2^+$ level is very weak. The ratios of the M1 transition probabilities within a $K = 1/2$ band depend on the internal wave-function. In fact if, for the internal wave-function, we use a single particle asymptotic function, the M1 transition probability from the $3/2^+$ to the $1/2^+$ level vanishes, while the 3/2 to 5/2 transition has its normal strength. This result is very insensitive to the deformation, and is also almost unaffected by a rotational admixture of the $K = 3/2$ function into the $I = 3/2$ state, because, the M1 transition from this admixture to the $I = K = 1/2$ state is very weak.

E2 transitions within a rotational band are expected to be enhanced. In fact both the lifetime and the Coulomb excitation data of the $5/2^+$ state show that the $5/2^+ \rightleftarrows 1/2^+$ E2 transition is appreciably faster than the s.p. estimate (cf. table 3).

All E1 transitions between levels belonging to the $K = 1/2^+$ band and levels of the $K = 1/2^-$ band are asymptotically hindered, and for the actual deformation ($\varepsilon \approx 0.4$) hindrance factors of 10 to 20 are estimated. This estimate is unchanged by the big $K = 3/2^+$ rotational admixture because the transition from this component to the $K = 1/2^-$ states is also hindered. A further reduction of the transition probability results from a Franck-Condon effect due to the big difference in equilibrium deformations of the two bands. In fact, the lifetime of the $1/2^-$ level is measured to be 10^{-9} sec which is 200 times longer than the s.p. estimate. Also all the measured branching ratios indicate that all the E1 transitions are highly hindered:

(i) The E1 transition from the $3/2^+$ to the $1/2^-$ level is at least 14 times weaker than the competing M1 transition to the $5/2^+$ level, which means a hindrance factor > 100 for the E1 transition.

(ii) The E2 transition from the $5/2^-$ to $1/2^-$ level is at least 10 times stronger than the $5/2^-$ to $5/2^+$ E1 transition, which means a reduction in the E1 transition probability by a factor of about $10^4 - 10^5$.

(iii) The $3/2^-$ level decays mainly by a M1 transition to the $1/2^-$ state, the competing E1 transitions to the $1/2^+$ and $5/2^+$ levels are weaker, which again gives rather high hindrance factors for the E1 transitions.

d. *β-transitions*

The $Ne^{19}(\beta^+)F^{19}$ g.s. to g.s. decay is a superallowed transition between mirror nuclei with a $\log ft = 3.29$. Using the rotational model with asymptotic wave functions one predicts $\log ft = 3.11$ for the g.s. decay, and the decay to the $3/2^+$ level at 1.57 MeV is completely forbidden. This result is insensitive to the deformation: for $\varepsilon = 0.3$ one gets $\log ft(1/2 \to 1/2) = 3.18$, $\log ft(1/2 \to 3/2) > 6$.

O^{19} decays to the $3/2^+$ and $5/2^+$ members of the $K = 1/2$ rotational band of F^{19} with log ft values of 4.3 and 5.6, respectively. The decay to the $1/2^+$ g.s. is hindered by at least another factor of 10.

If O^{19} has a g.s. spin of $5/2^+$ either because the rotational model is invalid for this nucleus of relatively small deformation or because of excessive rotational interactions, the absence of g.s. to g.s. decay is naturally understood and no other predictions for the β-decay can be done. It should however be remarked that the absence of g.s. to g.s. transition can be understood also in the frame of the simple rotational model: The $\Omega = 3/2$ to $\Omega = 1/2$ decay is asymptotically hindered, and there can be no $\Omega = 3/2$ rotational admixture in the $1/2^+$ g.s. through which the decay could proceed. (Such admixtures exist in the 3/2 and 5/2 members of the band and consequently the transition to these states is possible.)

4.2. DATA ON OTHER NUCLEI

a. *Spins and Parities*

Spins and parities are known mainly for the ground states, these are summarized in table 1. In all known cases, with the exception of Na^{25} and possibly also O^{19}, they fit the theoretical predictions.

I. *Even nuclei*

The even nuclei in the region considered here are Ne^{20}, Ne^{22}, and Mg^{24}. In Ne^{20} and Ne^{22} only the spins of the first excited states are known, they are 2^+. In Mg^{24} also the second excited 4^+ state is known. The energy ratio between the 4^+ and 2^+ states is 3, while the model predicts 10/3. In Mg^{24} also two higher levels (at 4.24 and 5.23 MeV) have been identified to have spins 2^+ and 3^+. These levels may belong to a second rotational band with $K = 2$. The moments of inertia in all these cases are rather near to the rigid body value.

II. *Odd mass nuclei*

Among the odd mass nuclei significant data are available only on Na^{23}. Two excited states of this nucleus have been observed at 0.436 and 2.084 MeV. These states may very well be the 5/2 and 7/2 members of a $K = 3/2$ rotational band built on the $3/2^+$ g.s.. This conjecture is specially suggested by the big Coulomb excitation cross-section for the first excited state (cf. table 3). In order to fit the levels one must assume rather strong rotational interactions. From the analysis of the data of F^{19} we know that the $\Omega = 1/2$ state interacts strongly with the $\Omega = 3/2$ state, therefore we must assume also in Na^{23} a strong rotational interaction between the proton configurations $(1/2)^2$ 3/2 and 1/2 $(3/2)^2$. Furthermore the $(1/2)^2$ 5/2 configuration should lie at about the same height as the 1/2 $(3/2)^2$ configuration,

and a rotational interaction with it should also modify the spectrum. With such a number of configurations interacting, there is much freedom to fit the 3 known levels (with reasonable moments of inertia and interaction parameters), but even so qualitative predictions can be made for the expected higher levels. The levels of the interacting configurations $(1/2)^2\ 3/2$ and $1/2\ (3/2)^2$ are drawn in the left part of fig. 4 ($E(1/2) > E(3/2)$). It is seen that for a resaonable separation of the intrinsic energies, say $-6 < \mathscr{I}(E(3/2)-E(1/2)) < -2$, a $1/2^+$ level comes within 1 MeV above the 7/2 level. After this $5/2^+$ and $3/2^+$ levels are predicted at excitations of 3 to 4 MeV. At these energies the $(1/2)^2\ 5/2$ configuration may show up, and therefore the level picture as given in fig. 4 may be distorted: in particular levels of spin 5/2 and greater will be pushed down relative to 1/2 and 3/2 levels. At energies above 4 MeV again more complex states, originating from "broken pairs", may appear.

A rather unique prediction of the rotational model is that different odd mass nuclei with the odd particle in the same orbit should have similar spectra. The addition of a pair of nucleons to the even group may alter somewhat the equilibrium deformation or the strength and shape of the deformed field, and thereby the relative position of the intrinsic states and the parameters of the collective motion may change. The changes in the moment of inertia and the coupling and decoupling parameters are expected to be small provided the latter parameters are not very sensitive to the deformation. The change in the relative position of some intrinsic states may be rather big because the relevant unit of energy $\hbar\omega_0$ is quite big ($\approx$ 15 MeV).

Groups of nuclei with the odd particle in the same orbit are (1) $Ne^{19}\ F^{19}\ F^{21}$ (2) $(O^{19})\ Ne^{21}\ Na^{21}\ Na^{23}(Na^{25})$ (3) $Ne^{23}\ Mg^{25}\ Al^{25}$ $(Al^{27}\ Si^{27})$. The nuclei in brackets may have too small deformations to be described by the model. In no case enough data is available to check the prediction.

III. *Odd nuclei*

Somewhat more data are available about odd nuclei. In the case that the two odd particles lie in different orbitals we expect low lying bands in which the Ω's combine to give $K = \Omega_1+\Omega_2$ and others in which $K = |\Omega_1-\Omega_2|$. If the two odd particles are in the same orbital, we expect three low lying bands: one band with $K = 2\Omega$ and isobaric spin of the odd pair $T_{\text{pair}} = 0$) and two bands with $K = 0$, one of them having $T_{\text{pair}} = 0$ and the other $T_{\text{pair}} = 1$. The first band has only levels with odd spins, while the second has only levels with even spins. We therefore expect three low lying states with spins $I = 2\Omega$, $I = 1$, and $I = 0$. If we take into account the residual interparticle forces, then the order of the levels depends on the special form of the forces, but for a rather wide variety of interactions the $I = 2\Omega$

state is pressed down so that it becomes the ground state. A detailed investigation is necessary in order to determine whether the $I = 0$ or $I = 1$ state comes lower.

All the g.s. spins of odd nuclei which could be determined experimentally (F^{18} Na^{22} Na^{24} Al^{26} Al^{28}) fit the theoretical predictions (cf. table 1). The β-decays of F^{20} and Al^{24} are also consistent with the predictions.

In the cases of Na^{24} and Al^{28} the theory predicts uniquely low lying states of spins 1^+ and 2^+, respectively. In fact the first excited states in both cases have the predicted spins. In the cases of Na^{22} and Al^{26}, where the theoretical predictions are not unique, we find first excited states of spin 0^+, which is compatible with the theory.

No low lying levels of negative parity are expected in nuclei with more than 10 protons and neutrons. In such nuclei it should be rather hard to produce a hole in the O^{16} (deformed) core, and on the other hand, the negative parity orbitals coming down from the $N = 3$ shell are not yet easily available. Only in Mg^{25} and Al^{25} a rather high lying negative parity rotational band built on a $N = 3, \Lambda = 0, n_z = 3, \Omega = 1/2$ orbital is observed.

b. *Magnetic moments*

In table 2 the measured magnetic moments of F^{19}, Na^{22}, and Na^{23} are compared with the values calculated by means of the rotational model and Schmidt's extreme s.p. model. The magnetic moments are rather insensitive to the deformations so that asymptotic functions could be used in the calculations. The fit of the rotational model values with experiment is in all cases satisfactory.

TABLE 2.

Magnetic moments

Nucleus	spin I	μ experimental	μ rotational model	μ Schmidt's model	assumed state N	n_z	Λ	Ω	K	I	Remarks
F^{19} g.s. F^{19*}	1/2	2.63	2.76	2.79	2	2	0	1/2	1/2	1/2	(a)
200 keV	5/2	3.5 ± 0.2	3.8	4.8	2	2	0	1/2	1/2	5/2	(b)
Na^{22}	3	1.75	1.78	1.73	2	1	1	3/2	3	3	(c)
Na^{23}	3/2	2.22	2.50	3.70	2	1	1	3/2	3/2	3/2	(d)

(a) Extensive shell model calculations give for the g.s. moment some value between 2.80 and 2.87 (cf. ref. [4]).

(b) The rotational model value is insensitive to the most important $K = 3/2$ rotational admixture. An approximate calculation of the magnetic moment with the shell model functions given in ref. [4]) yields $\mu = 3.46$.

(c) The moment calculated by the shell model (with jj coupling) depends only on the assumption of charge symmetry of nuclear forces and the configuration $(j = 5/2)^4$, but is otherwise independent of the exact state.

c. *Quadrupole moments*

Information about intrinsic quadrupole moments can be obtained from spectroscopic measurement of static quadrupole moments or from quadrupole transition probabilities within a rotational band (cf. ref. [6]), pp. 54—57 and 109). The latter may be obtained from Coulomb excitation cross-sections (cf. ref. [6]), App. VI) or from direct lifetime measurements. The data are collected in table 3. Columns 1—3 list the nucleus and the measurement performed ($\tau_{\frac{1}{2}}$ = measured half life, $B_{\text{C.E.}}$ = reduced transition

TABLE 3

Intrinsic Quadrupole Moments

(1) Nucleus	(2) Transition	(3) Measurement	(4) B $e^2\times10^{-48}$ cm^4	(5) Q_0 barn	(6) ε	(7) $F=\left(\frac{G_0}{\frac{3}{5}R^2}\right)^2$	(8) ref.
F^{19}	g.s.$(1/2^+)\rightarrow 0.2(5/2^+)$	$B_{\text{C.E.}}=0.003$	0.003	0.22	0.31	12	(a)
F^{19}	$0.2(5/2^+)\rightarrow$ g.s.$(1/2^+)$	$\tau_{1/2}=(0.85\pm0.05)\times10^{-7}$ sec	0.0063	0.32	0.45	25	(b)
Ne^{20}	$1.63(2^+)\rightarrow$ g.s. (0^+)	$\tau_{1/2}=(5.3\pm2.3)\times10^{-13}$ sec	0.045	0.67	0.85	110	(c)
Na^{23}	g.s.	$Q_{\text{spect.}}=0.10$	—	0.50	0.5	60	(d)
Na^{23}	g.s.$(3/2^+)\rightarrow 0.44(5/2^+)$	$B_{\text{C.E.}}=0.016$	0.016	0.33	0.33	25	(e)
Mg^{24}	g.s.$(0^+)\rightarrow 1.37(2^+)$	$B_{\text{C.E.}}=0.044$ †	0.044	0.66	0.6	100	(f)

† Value obtained from inelastic electron scattering.

References:

(a) Sherr, Li and Christy, Phys. Rev. **94** (1954) 1076
(b) M. Fiehrer *et al.*, Com. Rend. Acad. Sci. **241** (1955) 1746
(c) Devons *et al.*, Proc. Phys. Soc. **A69** (1956) 173
(d) Perl, Rabi and Senitzky, Phys. Rev. **98** (1955) 611; **97** (1955) 838
(e) Temmer and Heydenburg, Phys. Rev. **104** (1956) 967
(f) R. H. Helm, Ph.D. thesis, Stanford University (1956)

probability deduced from Coulomb excitation cross-section, Q_{spect} = spectroscopically measured quadrupole moment). In column (4) are given the reduced transition probabilities for the g.s. to excited state transitions. Columns (5) and (6) give the intrinsic quadrupole moments and the corresponding deformation (calculated under the assumption $R=0.12\times10^{-12}A^{1/3}$ cm). The F factors listed in column (7) are some measure for the ratio of the observed transition probability to the s.p. estimate. On account of the lower charge one expects smaller F factors for the light nuclei than for heavy nuclei revealing rotational spectra. A value $F=20$ should be characteristic of the former ones. The F factors found strongly support the rotational interpretation of the spectra.

d. *β- and γ-transitions*

The selection rules implied by the rotational model [7, 8]) explain in a qualitative way most facts known about β-transitions in the region con-

sidered. It is impossible to make quantitative predictions without a complete analysis of rotational admixture, which cannot be done now because of lack of data. The asymptotic selection rules seem to slow down the transitions by a factor of 10 to 100. The effect of K forbiddenness is crucially dependent on the rotational admixtures. The experimental data on β-decays is presented in fig. 2, and some remarks on the various decays follow below.

1) The decays of Na^{25} [9]), and probably also that of O^{19}, show that these nuclei have a g.s. spin 5/2 and not 3/2 as predicted by the model. Both nuclei have relatively small (calculated) equilibrium deformations, and therefore it is probable that the model does not apply to them.

2) F^{20}—Ne^{20}. Assuming the g.s. of F^{20} to be a $(O^{16})(1/2)^3\,3/2$, $K = 2$, $I = 2$ state and the 1.63 MeV level of Ne^{20} a $(O^{16})(1/2)^4$, $K = 0$, $I = 2$ state, the β-transition is both K forbidden and asymptotically hindered. The high $\log ft$ (≈ 5) of the decay is thus readily explained by the model.

3) Na^{21}—Ne^{21}. The calculated $\log ft (= 3.5)$ for the g.s. to g.s. decay agrees exactly with the experimental value. Assuming the 0.35 MeV level of Ne^{21} to belong to a pure rotational band built on the g.s., a decay to this level is expected to proceed with a $\log ft = 4.1$. Rotational admixtures cannot affect the decay rate very much. There is no experimental data on this decay. The Mg^{23}—Na^{23} decay is expected to be very similar to the Na^{21}—Ne^{21} decay.

4) Na^{22}—Ne^{22}. Here we have again an allowed transition with a very high $\log ft (= 7.6)$ which is readily explained by K forbiddenness. The g.s. of Na^{22} is probably a $K = I = 3$ state while the 1.28 MeV level of Ne^{22} is assumed to be a $K = 0$, $I = 2$ state belonging to the g.s. rotational band. The decay involves $\Delta K = 3$ and is therefore highly hindered.

5) Ne^{23}—Na^{23}. Assuming the g.s. of Ne^{23} to belong to the configuration $(Ne^{20})(3/2)^2\,5/2$ and the states of Na^{23} to be members of a rotational band with the internal configuration $(Ne^{20})(3/2)^3$, the transitions are asymptotically hindered. This selection rule may account for the rather high $\log ft$ (≈ 5) of the transitions, but detailed quantitative check cannot be done without accurate knowledge of the rotational admixtures.

6) Ne^{24}—Na^{24}. Not having a detailed analysis of the states of Na^{24}, very little can be said on these transitions. Assuming the 0.47 MeV level of Na^{24} to belong to the lowest configuration $(Ne^{20})(3/2)^3 5/2$, the transition to this level should be asymptotically hindered. The observed $\log ft$ ($= 4.4$) is consistent with such an assumption.

7) Na^{24}—Mg^{24}. The decay from a $K = I = 4$ g.s. of Na^{24} to the $K = 0$, $I = 4$ and $K = 2$, $I = 3$ states of Mg^{24} should be highly hindered. In fact the $\log ft$'s are very high for allowed transitions ($\log ft = 6.1$ and $\log ft = 7.2$, respectively).

The only case where the relative γ-intensities implied by the model may

be checked is the decay of the third excited state of Mg^{24}. Assuming this level to be a $K = I = 2$ state, it can decay to the members of the g.s. rotational band (having $K = 0$) only by E2 transitions. In practice only the transitions to the 0^+ and 2^+ states are observed, the former being 5 times stronger than the latter. This fits exactly to the theoretical prediction.

5. Concluding Remarks

It is difficult to state the exact region of validity of the rotational model. The experimental evidence seems to show that the model fails for Na^{25} and possibly also for O^{19}. The calculated equilibrium deformation is in both cases around 0.3, and therefore one may tentatively set $\varepsilon = 0.35$ to be a rough lower limit for the validity of the model in this region of light nuclei. The model seems to fail also for nuclei of mass $A = 27$. According to the model Al^{27} should have a similar spectrum to that of Al^{25}, i.e. a $5/2^+$ g.s. and above it 1/2 and 3/2 levels belonging to a $K = 1/2^+$ rotational band. The g.s. of Mg^{27} should be a $1/2^+$ state corresponding to the first excited $1/2^+$ state in Al^{27}. Mg^{27} should therefore have superallowed decays to the 1/2 and 3/2 levels of Al^{27}. In fact the spins fit the predictions, but neither the spacing between the 3/2 and 1/2 levels in Al^{27} nor the high log ft values of the decay of Mg^{27} are compatible with the model. On the other hand R. K. Sheline [10]) has been able to correlate a number of facts in the spectrum of Al^{28} in the framework of the model.

The analysis of rotational spectra in light nuclei is complicated by the fact that the rotational energies ($\mathscr{I}^{-1}$) are not small compared to the s.p. states spacings. Therefore a rather complete analysis of the rotational interactions may be necessary in order to give a detailed description of the spectra. In view of the relatively simple configurations expected in the nuclei considered here an analysis of the effect of the residual forces and a rather complete treatment of the rotational admixtures should be possible.

I want to thank cordially Prof. A Bohr and Dr. B. Mottelson for the active interest which they took in this work. I am grateful to them for many stimulating discussions and fruitful suggestions.

I wish also to express my appreciation to the Danish Committee for the Weizmann Institute of Science and CERN for grants which have made this work possible, and to Prof. Niels Bohr for extending to me the hospitality of the Institute for Theoretical Physics in Copenhagen.

References

1) Litherland *et al.*, Phys. Rev. **102** (1956) 208
2) S. G. Nilsson, Mat. Fys. Medd. Dan. Vid. Selsk. **29** (1955) no. 16
3) Alaga, Phys. Rev. **100** (1955) 432

4) Elliot and Flowers, Proc. Roy. Soc. A **229** (1955) 536
5) A. Bohr, Mat. Fys. Medd. Dan. Vid. Selsk. **26** (1952) no. 14
6) A. Bohr and B. Mottelson, Mat. Fys. Medd. Dan. Vid. Selsk. **27** (1953) no. 16
7) Alaga, Alder, Bohr and Mottelson, Mat. Fys. Medd. Dan. Vid. Selsk. **29** (1955) no. 9
8) Alaga, Phys. Rev. **100** (1955) 432
9) Gove *et al.*, Bul. Am. Phys. Soc. **1**, no. 1 (1956) 29
10) R. K. Sheline, Nuclear Physics **2** (1956/57) 382

References to figure 2

O^{18} levels (tα): Jarmie, Bull. Amer. Phys. Soc. **1**, no. 1 (1956) 28 GA4
F^{18} levels ($He^4p\gamma$): Butler *et al.*, Bull. Amer. Phys. Soc. **1**, no. 1 (1956) 29 GA5
γ's: Roclawski *et al.*, Compt. Rend. **242** (1956) 1443
Ne^{18} β^+: Gow and Alvarez, Phys. Rev. **94** (1954) 365
F^{19} levels: Squires *et al.*, Phys. Rev. **104** (1956) 414
γ's: Toppel *et al.*, Phys. Rev. **100** (1955) 1254
J. M. Freeman, Phil. Mag. **1** (1956) 591
τ_γ (0.2 MeV): Compt. Rend. **241** (1955) 1746
τ_γ (0.1 MeV): Thirion *et al.*, Phys. Rev. **94** (1954) 1076
μ(0.2 MeV): Fiehrer *et al.*, Compt. Rend. **241** (1955) 700, 1746
γ(109 keV) = E1, $\alpha_K = 0.00210$ (± 45) } Mills Jr. *et al.*, Phys.
γ (197 keV) = E2, $\alpha_K = 0.00190$ (± 60), K/L = 8 } Rev. **100** (1955) 1794
spins: (109 and 297 keV levels), Sherr *et al.*,
Phys. Rev. **96** (1954) 1258; **94** (1954) 1076 ($\alpha\alpha'\gamma$)
Petersen *et al.*, Phys. Rev. **94** (1954) 1075; **94** (1954) 951 ($pp'\gamma$)
1.56 MeV level (3/2): Jones *et al.*, Phys. Rev. **96** (1954) 547 ($\gamma\gamma$)
N^{19} levels: Marion *et al.*, Phys. Rev. **100** (1955) 91
β^+: Jones *et al.*, Phys. Rev. **96** (1954) 547
O^{19} l_n of levels: Stratton *et al.*, Phys. Rev. **98** (1955) 629; Popič, Nuovo Cimento **6** (1956) 1597
Ne^{20} τ_γ (1.63 MeV): Devons *et al.*, Proc. Phys. Soc. A **69** (1956) 173
levels: Schrank, O'Neill, Bull. Amer. Phys. Soc. **1**, no. 1 (1956) 29 GA7 (pp')
spin (1.63 MeV): Clegg *et al.*, Proc. Phys. Soc. A **68** (1955) 538 (γ, γ)
F^{20} β: Wong, Phys. Rev. **95** (1954) 761
levels: Takemoto *et al.*, Phys. Rev. **101** (1956) 772
Ne^{21} levels: Ahnlund, Arkiv f. Fysik **9** (1955) 39
g. s. spin: J. B. Hubbs and G. M. Grosof, Phys. Rev. **104** (1956) 715
F^{21} Jarmie, Phys. Rev. **99** (1955) 1043
Ne^{22} levels and γ: Foster *et al.*, Phys. Rev. **94** (1955) 804
Seidlitz, Bull. Amer. Phys. Soc. **1**, no. 1 (1956) 29
γ (1.28 MeV) = E2, $\alpha = 6.7 \times 10^{-6}$: Leamer and Hinman, Phys. Rev. **96** (1954) 1607
Na^{22} levels: Mg^{24} (dα) ($T = 0$ levels): Browne *et al.*, Phys. Rev. **99** (1955) 644
F^{19} (αn): Quinton and Doyle, Phys. Rev. **101** (1956) 669
Na^{23} decay of Ne^{23} and γ's: Penning and Schmidt, Nuclear Data cards ed. by K. Way *et al.*
spin of 440 keV level = $5/2^+$(?) from pγ (θ): Krone and Read, Phys. Rev. **104** (1956) 1018
q: Perl, Rabi, Senitzky, Phys. Rev. **98** (1955) 611
μ: Walchli, ORNL 1775 (1954)
B(E2): Temmer and Heydenburg, Phys. Rev. **104** (1956) 967
Mg^{23} β^+: Hunt *et al.*, Phys. Rev. **95** (1954) 611
Mg^{24} levels up to 5.23 MeV and γ's: Newton, Phys. Rev. **96** (1954) 241
levels: Calvert *et al.*, Proc. Phys. Soc. A **68** (1955) 1008
B(E2) from inelastic electron scattering: Helm, Phys. Rev. **104** (1956) 1466
Ne^{24} and Na^{24} β-decays: Dropsky and Schardt, Phys. Rev. **102** (1956) 426
Na^{24} levels from n capture γ's: H. Motz, Brookhaven N. L. report
Al^{24} decay: Glass and Richardson, Phys. Rev. **98** (1955) 1251

Nuclear Physics **4** (1957) 395—407; © *North-Holland Publishing Co., Amsterdam*

Not to be reproduced by photoprint or microfilm without written permission from the publisher

3 A
3 B

CONVERSION-ELECTRON AND PHOTON SPECTRA OF Gd^{147} AND Gd^{149}

VIRGINIA S. SHIRLEY, WARREN G. SMITH † AND JOHN O. RASMUSSEN

Radiation Laboratory and Department of Chemistry
University of California, Berkeley, California ††

Received 23 April 1957

Abstract: A new gadolinium isotope decaying by electron capture with a 29-hour half-life was found. Its mass number was determined to be 147 by examination of its excitation function for production by alpha particle bombardment of $Sm_2^{147}O_3$. The electron-capture isotope Gd^{149} was also studied, and its half-life was redetermined to be 9.3 ± 0.3 days. The conversion-electron and photon spectra of Gd^{147} and Gd^{149} were studied. Relative photon and electron intensities were determined for some of the transitions, and some coincidence measurements were made. From the data a few multipolarities are assigned and partial decay schemes are suggested.

1. Introduction

No previous electron or gamma spectroscopic work on any gadolinium isotopes lighter than Gd^{151} has been reported up to this time. The region around the light gadolinium isotopes is of special interest because of the many sudden changes in nuclear properties observed in passing between 88 and 90 neutrons. From optical spectroscopic results, Brix and Kopfermann [1]) have called attention to sharp breaks in isotope shifts occurring between isotopes having 88 and 90 neutrons. They have also noted [2]) the large difference in the quadrupole moments of the stable europium isotopes, which have 88 and 90 neutrons. The first excited states of even nuclei drop sharply at 90 neutrons, and well-developed nuclear rotational bands appear. The large deformation approximation of the Bohr-Mottelson model [3]) has been successful in describing nuclei in this region of $N \geqq 90$ but not in the region of $N \leqq 88$.

In this work information on the excited levels in Eu^{147} and Eu^{149} was obtained by studying the conversion-electron and photon spectra of gadolinium activities produced by alpha-particle bombardments on samarium oxide and deuteron bombardments on europium oxide.

† Present address: Department of Physics, Indiana University, Bloomington, Indiana.

†† This work was performed under the auspices of the U.S. Atomic Energy Commission.

2. Experimental Procedures

2.1. BOMBARDMENTS

Activities were produced in the Berkeley 60-inch cyclotron by 48-MeV helium ions and 17-MeV deuterons. The samarium and europium target materials were bombarded in the oxide form in "boats" stamped from 10-mil platinum foil and covered with 1/4-mil platinum foil covers. The boats fit into standard target assemblies and were cooled by water directed at the back of the targets.

2.2. CHEMISTRY

The platinum boats containing the irradiated rare earth oxides were placed in hot 8 *M* hydrochloric acid until the oxides dissolved. The platinum was then removed and ammonia was passed into the acid solution until the rare earths precipitated as hydroxides. The precipitate was washed and dissolved in a minimum amount of 8 *M* hydrochloric acid. The gadolinium produced was separated from the remaining rare earths by an ion-exchange method identical to that described by Thompson, Harvey, Choppin, and Seaborg [4]). The column (3 mm in diameter, 5 cm in length) was heated to 87°C by a trichloroethylene vapor jacket. The eluting agent was 0.4 *M* alpha-hydroxyisobutyric acid buffered to a *p*H of 3.93 with ammonium hydroxide, and the resin was Dowex-50 spherical resin, 200—400 mesh size, 12 % cross-linked. Since the maximum capacity of the column was ≈ 10 mg of rare earths, it was necessary to remove the bulk of the target material by another method. A sodium amalgam reduction method was used for this purpose. Sodium amalgam is capable of reducing tripositive rare earth ions to the metal and amalgamating them; and since both samarium and europium have dipositive states to act as intermediate states, the reduction of Sm^{+3} and Eu^{+3} is much faster than that of Gd^{+3}. The rare earths, dissolved in a minimum amount of 8 *M* hydrochloric acid, were transferred to a separatory funnel, and 10 ml of water and ≈ 1/3 ml of glacial acetic acid (to maintain the hydrogen ion concentration) were added. 0.3% sodium amalgam (15 ml for 150 mg rare earths) was added and the mixture shaken for 10 seconds. After the amalgam layer was removed the remaining aqueous layer seemed to retain about 10 % of the original target material. The procedure was repeated three times in order to be sure that the total rare earth mass retained was under 10 mg. Ammonia was passed into the final aqueous layer until the rare earths precipitated as hydroxides. The precipitate was washed, dissolved in a minimum amount of 1 *M* hydrochloric acid, and finally concentrated into 2 drops of 0.05 *M* hydrochloric acid for adsorption on the column. After completing the ion-exchange separation of the remaining rare earth mass, the alpha-hydroxyisobutyric acid solution containing the gadolinium activity was made 0.5—1 *M* in hydrochloric acid. This solution was placed

on a Dowex-50, 4 % cross-linked, 3 mm × 5 cm column at room temperature. 0.5 *M* hydrochloric acid was passed through until all of the alpha-hydroxy-isobutyric acid was removed, and the activity was then eluted with 8 *M* hydrochloric acid.

2.3. INSTRUMENTS

An argon-flow-type ionization chamber was used for alpha counting. The instruments used for measuring the conversion-electron spectra of the gadolinium activities were four permanent-magnet 180° spectrographs described by Smith and Hollander [5]). They have fields of approximately 50, 100, 200 and 350 gauss and operate at resolutions of about 0.15 %. Gadolinium sources for them were plated onto 10-mil platinum wires from a solution of 0.1 *M* ammonium bisulfate at a *p*H of 3.6. The procedure used was that suggested by Harvey *et al.*[6]) in which the wire is made the cathode of an electrolysis cell. Since the hydroxide ion concentration around the cathode is relatively high, the rare earths are deposited onto the wire as hydroxides. The wire is heated to a red color in a bunsen burner flame for a few seconds before placing it in the spectrograph. Electrons from the source are recorded on a photographic plate. By previous calibration of the instruments with electrons of known energies the conversion electron energies may be determined quite accurately. Densitometer traces of the spectrograph plates were made to measure the relative intensities of the electrons. Relative intensities of the strong conversion electrons were also measured with more accuracy with a double-focusing spectrometer [7]). This is a shaped-field, 256°, prismatic spectrometer operating at about 0.3 % resolution. A 100-channel gamma analyzer † with about 8.5 % resolution was used to measure gamma-ray energies and intensities. This instrument is a gamma pulse-height analyzer used with a $1\frac{1}{2}'' \times 1''$ sodium iodide crystal and photomultiplier tube. It records data by means of a magnetic-core matrix memory, and is able to record at relatively high counting rates.

3. Conversion-Electron Spectra of Gd^{147} and Gd^{149}

From bombardments of natural samarium (3.16 % Sm^{144}, 15.07 % Sm^{147}, 11.27 % Sm^{148}, 13.84 % Sm^{149}, 7.47 % Sm^{150}, 26.63 % Sm^{152}, and 22.53 % Sm^{154}) [8]) with alpha particles, one would expect to make a variety of gadolinium isotopes. Among the unstable of these are Gd^{148} (140-year alpha) [9]), Gd^{149} (9-day electron-capture alpha) [8]), Gd^{150} (long-lived alpha) [8]), Gd^{151} (150-day electron capture) [8]), and Gd^{153} (236-day electron capture) [8]). In addition, one might expect to produce the unreported isotope, Gd^{147}, by the reactions Sm^{144} (α, n) Gd^{147} and Sm^{147} (α, 4n) Gd^{147}.

It was determined from scintillation analysis that Gd^{149}, with a 9 ± 1 day

† 100-Channel Gamma Analyzer; Manufactured by: Pacific Electro-Nuclear Company, Culver City, California.

half-life [10]), emits a 150-keV gamma ray. The decay rates of the conversion lines observed in the permanent magnet spectrograms were compared to the decay rate of the 150-keV lines. We have redetermined the half-life of Gd^{149} to be 9.3 ± 0.3 days by following the decay of the conversion electrons of the 150-keV transition. All lines whose energy differences corresponded to europium binding-energy differences were assigned to gadolinium activities. All lines which decayed at the same rate as the lines of the 150-keV transition were assigned to Gd^{149}. A second group of gadolinium lines with a half-life of approximately $1\frac{1}{2}$ days (later redetermined as 29 hours) was tentatively assigned to Gd^{147}. The rest of the gadolinium lines were longer-lived. Those resulting from the decay of Gd^{151} and/or Gd^{153} could be positively identified by observing them in a deuteron bombardment designed to produce only Gd^{151} and heavier gadolinium isotopes. In this experiment natural europium, which is composed entirely of Eu^{151} and Eu^{153}, was bombarded with 17-MeV deuterons. A few remaining long-lived gadolinium lines, which were seen in the alpha-particle bombardments of Sm_2O_3 but not in the deuteron bombardments of Eu_2O_3, could not be assigned to the decay of any isotope. These lines may belong to an isomer of one of the gadolinium isotopes, but further study is needed. Lines which grew in intensity were assigned to $Eu^{147-149}$ if the energy differences among the lines corresponded to samarium binding-energy differences. Eu^{147} has a half-life of 24 days [8]), Eu^{149} one of about 120 days †. Eu^{151} and Eu^{153} are stable.

Table 1 lists the transitions assigned to the various isotopes. The intensities given are visual estimates obtained from the permanent-magnet spectrograph plates. Energies are given to the nearest 0.1 keV if five or more different energy determinations were made and to the nearest keV if less than five were made.

4. Excitation Functions for Alpha-Induced Reactions on Sm^{147}

Samarium oxide enriched† to 85 atomic percent in Sm^{147}, with the other 15 percent being mainly Sm^{148} and Sm^{149}, was bombarded with helium ions in a Faraday cup assembly. A stacked-foil technique was used so that excitation functions could be determined. The function for the Sm^{147} $(\alpha, 3n)Gd^{148}$ reaction was obtained by alpha-counting the eight target samples, and the function for the Sm^{147} $(\alpha, 2n)$ Gd^{149} reaction was determined by counting the samples in the 100-channel gamma pulse-height analyzer and integrating the 9-day, 150-keV peak in each plate. A function for the 29-hour activity was determined in the latter manner using the 229-keV peak; its shape and peak energy are clearly those expected of an $(\alpha, 4n)$ reaction. Thus, we have assigned the 29-hour activity to Gd^{147}.

† Electromagnetically enriched stable isotope, purchased from Oak Ridge Research and Development Division.

TABLE 1
Conversion Electron Data

	Transition Energy (keV)	Lines seen	Visual Relative Intensities †					
			K	L_I	L_{II}	L_{III}	M_I	N_I
Gd^{147}	136	K	VVW					
	142	K	W-M					
	147	K	W					
	217	K	VVW					
	226	K	VVW					
	229.5	K L_I	VVS	W				
		M_I N_I					VW	VVW
	241	K	VW					
	261.0	K L_I	VW	VVW				
	310	K	VW					
	348	K	VVW					
	370	K L_I	W	VVVW				
	374	K	VVW					
	391	K	VVW					
	396.2	K L_I M_I	M-S	W			VVW	
	485	K	VVW					
	502	K	VVW					
Gd^{149}	107	K	VVW					
	120	K	VW					
	126.1	K L_I	W-M	W				
	132	K	W-M					
	149.9	K L_I L_{II}	VVS	VVS	VW			
		L_{III} M_I N_I				VVW	W-M	W
	244	K L_I	VVVW	VVVW				
	253	K	VVVW					
	272.7	K L_{I-II}	W	VVW				
		M_I					VVW	
	298.8	K L_I	W-M	W				
	346.7	K L_I	VS	W				
		M_I N_I					VW	VVVW
	461	K	VVVW					
	496	K L_{I-II}	VVW	VVVW				
	517	K	VVW					
	534	K	VVW					
	750	K L_I	VVVW	VVVW				
	790	K	VVVW					
Gd?	22.9	L_I L_{II} L_{III}		M	W	W		
		M_I N_I					M	VVW
	77.7	K	VVW					
	114.7	K L_I L_{II}	VS	M	VVVW			
		L_{III} M_I N_I				masked	VVW	VVW
	115.5	K L_I L_{II}	VS	M	VVW			
		M_I N_I					VVW	VVW
	154.8	K L_I	M-S	W				
		M_I N_I					VW	VVVW
	198.8	K L_I	W	VVW				
	329	K	VVW					
$Eu^{147-149}$	38	L_I L_{III} N_I		VVW		VVW		VVVW
	53	L_I L_{III}		VVW		VVW		
	66	K	VW					
	68	K	M					
	69	K	VW					
	121.3	K L_I	M-S	VW				
		M_I N_I					VVW	VVVW
	219.8	K L_I	VVW	VVVW				
	277	K L_I	W	VVVW				

† S = strong, M = moderate, W = weak, V = very.

The best half-life determined for Gd^{147} was obtained by following the decay of the 229-keV photopeak. The half-life observed in this manner, 29 hours, is consistent with half-lives of 30 hours found by resolving K X-ray and Geiger-Mueller decay curves into their Gd^{147} and Gd^{149} components.

Fig. 1 gives the excitation functions for alpha-induced reactions on Sm^{147}. It was not possible to calculate absolute cross sections with any confidence because of lack of knowledge of the detailed decay schemes of Gd^{147} and Gd^{149} and of the half-life of Gd^{148}.

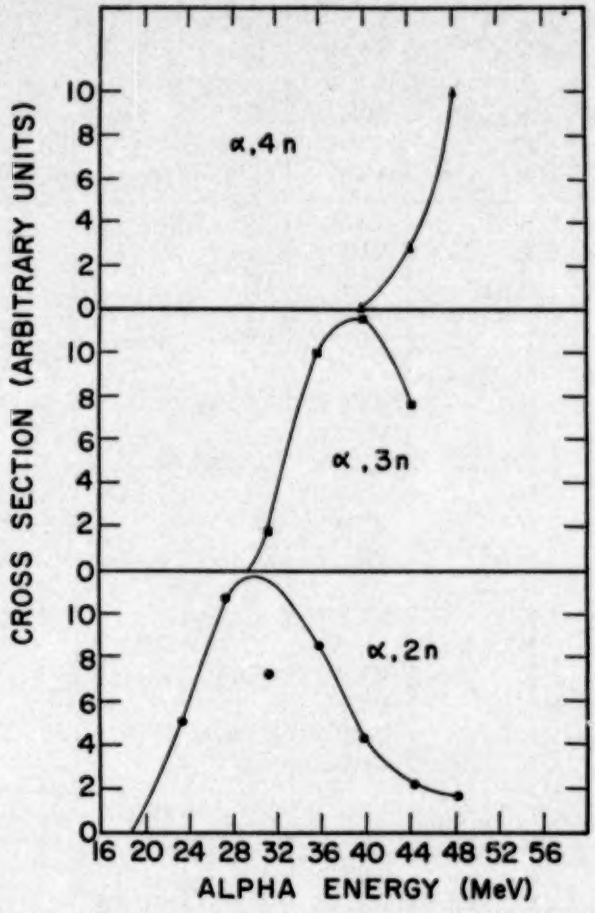

Fig. 1. Excitation function for alpha-induced reactions on Sm^{147}. Ordinates are in arbitrary units.

5. Relative Photon and Electron Intensities of Gd^{147} and Gd^{149} Gamma Rays

Fig. 2 shows the gamma ray spectrum of Gd^{147}, and fig. 3 gives the spectrum of Gd^{149}. Since energies were accurately known from permanent-magnet spectrograph work, complex peaks could be resolved with some confidence, and where peaks were small and indefinite, upper limits for photon intensities could be set. The values of Davisson and Evans [11]) were used in correcting for absorption through lead absorbers. Curves from Kalkstein and

Hollander [12]) were used to obtain NaI crystal counting efficiencies. No photopeaks were seen for any of those transitions not assigned to the decay of a particular gadolinium isotope. In later runs on the 100-channel gamma analyzer the 120- and 210-keV transitions from the decay of Eu^{147} [8]) were observed. Relative electron intensities were measured with the double-focusing spectrometer and also from the permanent-magnet films by the use of a photodensitometer. Because of the many corrections necessary in obtaining

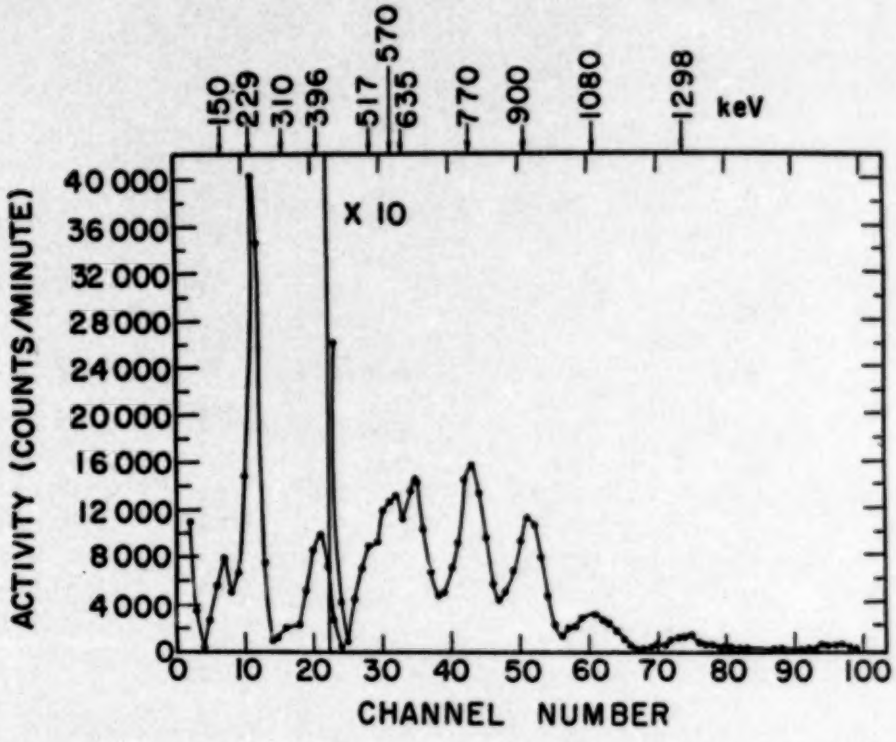

Fig. 2. Sodium iodide scintillation gamma spectrum of Gd^{147} (background subtracted). The 150-keV peak is the strongest photopeak of Gd^{149}, present in small abundance in the Gd^{147} sample.

intensities from the spectrograms the intensities obtained from the double-focusing spectrometer are probably more accurate.

Table 2 gives the intensity values for some of the gammas of Gd^{147} and Gd^{149}. In the case of Gd^{149} the electron intensities are given relative to an intensity of 1.00 for the K-line of the 346.7-keV transition, and in the case of Gd^{147} the intensities are given relative to the K-line of the 396.2-keV transition. To convert the relative photon intensities to the same scale as the electron intensities, multipolarities of the 149.9-keV transition of Gd^{149} and the 229.5-keV transition of Gd^{147} were considered. L-subshell conversion coefficients calculated by Rose [13]) and K-shell conversion coefficients calculated by Sliv [14]) were used in assigning multipolarities to these transitions. Theoretical K/L ratios from Rose's conversion coefficients were used.

TABLE 2

Relative Intensities of Gd^{147} and Gd^{149} Gammas

Gamma energy (keV)	Line	Electron intensity from double-focusing spectrometer	Electron intensity from densitometer	Photon intensity	Total transition intensity
		Gd^{147}			
229.5				12.4	15.1
	K	1.93	1.57		
	L_I	0.56	0.29		
	M_I		0.11		
	N_I		0.06		
241					0.04
	K		0.04		
261.0					0.09
	K		0.09		
310				< 0.75	< 0.88
	K		0.13		
370				2.1	2.3
	K	0.25	0.16		
396.2				5.2	6.3
	K	1.00	1.00		
	L_I	0.14	0.31		
(517)				1.1	1.1
(570)				1.2	1.2
(635)				2.6	2.6
(770)				4.6	4.6
(900)				4.9	4.9
(1080)				1.5	1.5
(1298)				0.72	0.72
		Gd^{149}			
107				< 0.32	< 0.32
126.1				< 0.26	< 0.26
149.9				8.6	13.7
	K		4.30		
	L_I	0.55	0.46		
	M_I	0.19	0.18		
	N_I		0.06		
244				< 0.33	< 0.33
272.7				< 1.0	< 1.2
	K	0.09	0.08		
	L_I-L_{II}		0.05		
	M_I		0.06		
298.8				5.9	6.5
	K	0.49	0.44		
	L_I	0.09	0.08		
346.7				3.6	4.9
	K	1.00	1.00		
	L_I	0.23	0.20		
461				< 0.32	< 0.32
496				0.32	0.32
517				0.84	0.84
534				0.76	0.76
(650)				0.55	0.55
750				< 1.4	< 1.4
790				< 1.4	< 1.4
(937)				0.67	0.67

From K/L ratios, L subshell ratios, and K/M ratios, both the 149.9- and 229.5-keV transitions appear to be magnetic dipole (or possibly M2) transitions. Electric multipolarity assignment for either transition is ruled out because of the small amount of conversion in the L_{II} subshell, and higher magnetic multipole orders were not considered because of their long lifetimes and the lack of conversion in the L_{III} subshell. In doing coincidence work on these transitions neither was found to be delayed (i.e., both life-

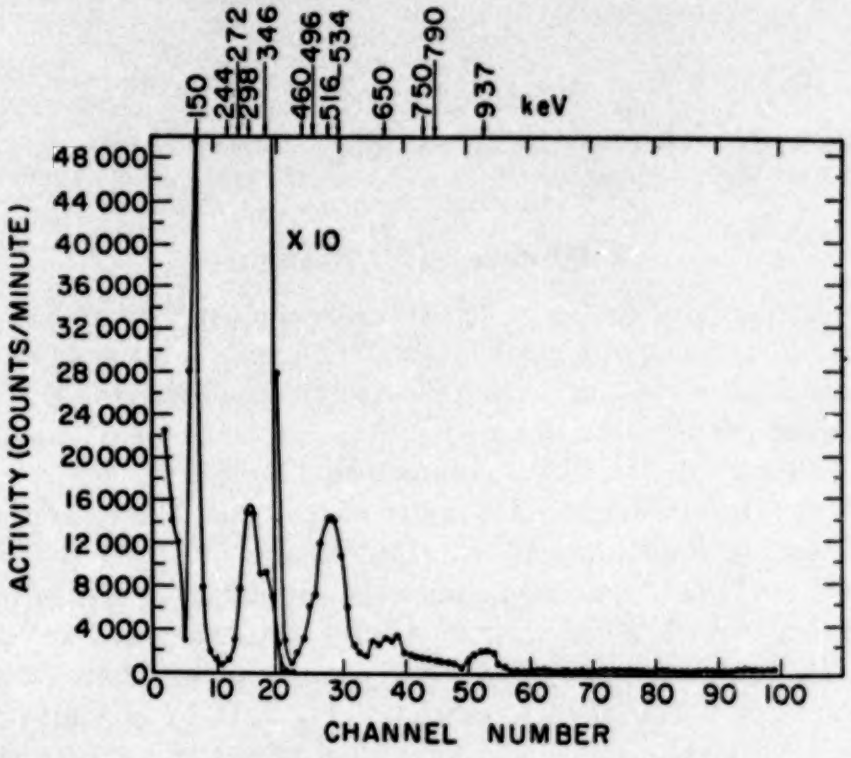

Fig. 3. Sodium iodide scintillation gamma spectrum of Gd^{149} (background subtracted).

times less than a millimicrosecond). Assuming that both of these transitions were magnetic dipole, the relative photon intensities were normalized to give these transitions the proper K-shell conversion coefficients. Gamma rays for which photons but no conversion electrons were seen are placed in parentheses. Their energies are uncertain by several kilovolts.

6. Coincidence Measurements

Table 3 gives the results of coincidence measurements made on a mixed sample of Gd^{147} and Gd^{149} by Strominger [15]). At the same time he looked for positons and was able to set limits on the positon emission to K-capture decay ratios. The limit for positon emission by Gd^{149} was determined to be $\beta^+/K < 0.4\,\%$ and that for Gd^{147} to be $< 1.2\,\%$.

TABLE 3

Gamma-Gamma Coincidence Data

Isotope	Gate gamma energy (keV)	Energy of gammas in coincidence (keV)
Gd^{149}	150	350
		500
		760
Gd^{147}	229	390
		760
		930
Gd^{149}	630	750
Gd^{149}	750	150
		630

7. Discussion of Results

The multipolarity of the 149.9-keV transition in Gd^{149} decay has already been discussed as being either M1 or M2. Although the M1 assignment has already been assumed in normalizing the photon intensities, the M2 possibility was considered to check this assumption. If the 149.9-keV gamma were an M1 transition, the 346.7-keV gamma would have a K-shell conversion coefficient of 0.18 ± 0.02 and a K/L ratio of 5.0 ± 0.6. These agree reasonably with an M2 transition ($\alpha_K = 0.190$; K/L = 5.8). M1, E1 and E2 assignments could be ruled out because they would have K-shell conversion coefficients lower by a factor of 4 or more. If the 149.9-keV gamma were an M2 transition, the 346.7-keV gamma would have a K-shell conversion coefficient of 1.7 ± 0.2, which is at least a factor of 9 greater than the theoretical values for transitions of multipolarity less than three. It therefore seems likely that the M1 assignment to the 149.9-keV gamma and subsequent M2 assignment to the 346.7-keV gamma are correct. In addition, an assignment could be made to the 298.8-keV gamma. This transition has a K-shell conversion coefficient of 0.08 ± 0.01 and a K/L ratio of 5.5 ± 0.7, in reasonable agreement with an M1 ($\alpha_K = 0.077$; K/L = 7.2). E2 was ruled out as a possible assignment because a fairly strong L_I line was seen but no L_{II} or L_{III}. If the transition were an E2, the L_{II} line would definitely be seen. M2 was ruled out because of its high α_K, E1 because of its low α_K, and higher multipole orders because of their long lifetimes. Nothing may be said about the multipole orders of the other transitions, except that of the 272.7-keV gamma. E1 may be ruled out as a multipolarity for this transition because the theoretical value of α_K for an E1 transition is 0.017 and the 272.7-keV gamma has a minimum $\alpha_K \geqq 0.064\pm0.008$. No definite multipolarity assignments can be made to any of the Gd^{147} transitions.

Fig. 4 shows partial decay schemes for Gd^{147} and Gd^{149}. These schemes are

uniquely consistent with the available energy, intensity, and coincidence data, but are far from complete. Their complexity is evidently such that, without further information about each transition, the gammas may be placed into several different schemes. An IBM 650 computer program † was

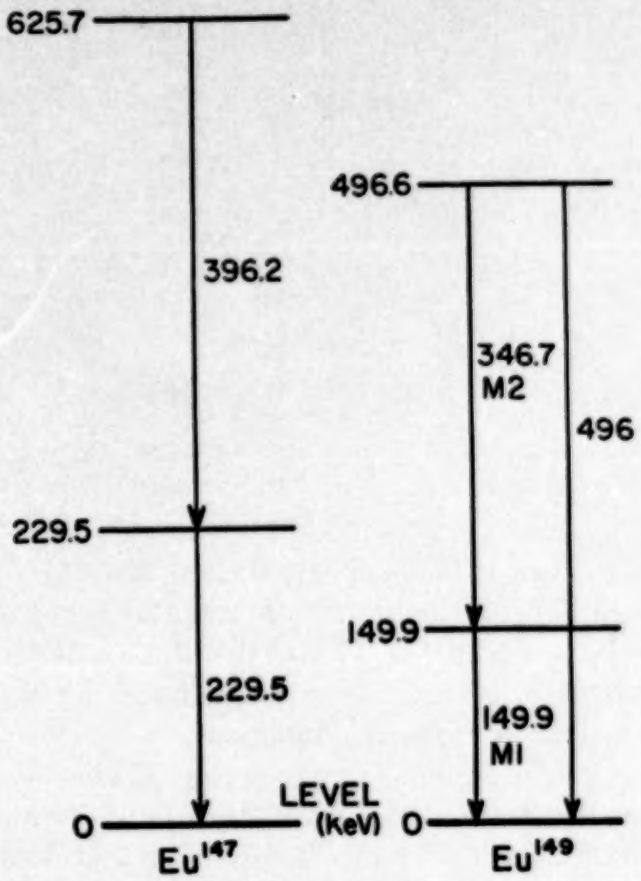

Fig. 4. Partial decay scheme for Gd^{147} and Gd^{149}.

used to determine all cases where the sums of two transition energies agree within 0.1 % with another energy or with the sum of two other energies. Table 4 tabulates the results of this comparison. The transition-energy values are reported to a greater number of significant figures in this table than they are elsewhere in the paper; although the absolute values of the energies are not known to better than 0.5 %, the relative energy values are probably somewhat better.

The number of sums of two transition energies agreeing with the energy of a third transition expected by chance is 1.4 and the number of sums of two with two expected by chance is 8.2. For this reason one may attach some statistical significance to the sums of two with one, but probably not to those of two with two.

The 496.6-keV state in the levels of Eu^{149} is of special interest because of

† Program devised by Mr. Kent Curtis of the UCRL theoretical physics group.

TABLE 4

Energy Sums for Gd^{149} Transitions

Transition Energy	Code Letter	Transition Energy	Code Letter
$106._4$	A	298.8	J
$119._8$	B	346.7	K
126.1	C	$460._8$	L
$132._9$	D	$496._3$	M
149.9	E	$516._7$	N
$244._3$	F	$534._2$	O
$252._7$	G	$749._5$	P
272.7	H	$789._8$	Q

Sums Found

E + K = M	D + O = E + N
F + G = M	D + P = K + O
F + H = N	E + K = F + G
G + M = P	F + P = L + O
H + N = Q	G + N = H + M
	H + O = K + L

possible isomerism, since it is depopulated by a 346.7-keV M2 transition. The theoretical mean life for this transition, using Moszkowski's [16]) formula was calculated to be $\approx 6\times10^{-8}$ sec. Thus, the lifetime of this state is probably measurable by delayed-coincidence techniques, but we have not had the opportunity to attempt the measurement.

No rotational structure is immediately obvious in the levels of Eu^{147} and Eu^{149}. In Coulomb excitation work Heydenburg and Temmer [17]) found a definite ground-state rotational band in Eu^{153} (90 neutrons) and distorted rotational structure in Eu^{151} (88 neutrons). The present work indicates that Eu^{147} and Eu^{149} have very complex level schemes without apparent rotational band structure. Their proximity to the closed 82-neutron shell probably favors a spherical rather than spheroidal nuclear equilibrium shape. Some theoretical treatments [18, 19]) have correlated levels and properties of even nuclei in this intermediate region between the closed shells and onset of stable spheroidal deformation. Theoretical work on odd-mass nuclei of the intermediate region would be of the greatest interest.

We wish to acknowledge the assistance of Dr. Jack M. Hollander in interpreting results obtained from the permanent-magnet spectrographs and of Dr. Donald Strominger in making coincidence measurements. We also wish to thank W. B. Jones and the crew of the Berkeley 60-inch cyclotron for help with bombardments and Health Chemistry for monitor service and target transportation. This work was performed under the auspices of the U.S. Atomic Energy Commission.

References

1) P. Brix and H. Kopfermann, Phys. Rev. **85** (1952) 1050
2) P. Brix and H. Kopfermann, Z. Physik **126** (1949) 344
3) A. Bohr and B. R. Mottelson, Mat. Fys. Medd. Dan. Vid. Selsk. **27** (1953) no. 16
4) Thompson, Harvey, Choppin and Seaborg, J. Am. Chem. Soc. **76** (1954) 6229
5) W. G. Smith and J. M. Hollander, Phys. Rev. **101** (1956) 746
6) Harvey, Chetham-Strode, Ghiorso, Choppin and Thompson, Phys. Rev. **104** (1956) 1315
7) G. D. O'Kelley, Ph.D. Thesis, University of California (1951) (Radiation Laboratory Unclassified Report UCRL-1243) unpublished
8) Original references listed in Table of Isotopes in Hollander, Perlman and Seaborg, Revs. Modern Phys. **25** (1953) 469
9) Rasmussen, Thompson and Ghiorso, Phys. Rev. **88** (1953) 33
10) Hoff, Rasmussen and Thompson, Phys. Rev. **83** (1951) 1068
11) C. M. Davisson and R. D. Evans, Revs. Modern Phys. **24** (1952) 79
12) M. I. Kalkstein and J. M. Hollander, University of California Radiation Laboratory Report UCRL-2764 (October 1954) (unpublished)
13) M. E. Rose, privately circulated tables of relativistic L-shell conversion coefficients with screening.
14) L. A. Sliv, privately circulated tables of relativistic K-shell conversion coefficients with screening; corrections for finite nuclear size are made.
15) D. Strominger, Ph.D. Thesis, University of California (1956) (Radiation Laboratory Unclassified Report UCRL-3374) unpublished
16) S. A. Moszkowski, in Beta- and Gamma-Ray Spectroscopy, edited by Kai Siegbahn (North-Holland Publishing Co., Amsterdam, 1955) XIII p. 373
17) N. P. Heydenburg and G. M. Temmer, Phys. Rev. **100** (1955) 156
18) G. Scharff-Goldhaber and J. Weneser, Phys. Rev. **98** (1955) 212
19) L. Wilets and M. Jean, Phys. Rev. **102** (1956) 788

Nuclear Physics **4** (1957) 408—426; © *North-Holland Publishing Co., Amsterdam*
Not to be reproduced by photoprint or microfilm without written permission from the publisher

MÉTHODE DES CHAMPS ADHÉRENTS

A. HOURIET
Université de Fribourg, Suisse

Reçu le 10 avril 1957

Abstract: A new method of calculation of the nucleon-meson interaction is proposed. It is developed for the case of a pseudoscalar meson field coupled with nucleons by pseudoscalar coupling. The nucleon possesses isobars similar to those of the strong coupling theory, associated to a nuclear core.

1. Introduction

L'expérience établit avec une netteté de plus en plus grande la structure complexe du nucléon: diffusion de résonance des mésons π, coeur nucléonique introduit par Jastrow [1]), extension électromagnétique révélée par la diffusion d'électrons [2]). Du côté théorique, les succès obtenus par l'usage d'un "cut-off" sont appréciables [3]) et les travaux de Lévy [4]) montrent que les descriptions théoriques actuelles conduisent à un coeur nucléonique. Ce travail se propose d'expliciter la structure du nucléon résultant d'une interaction déterminée, à l'aide d'une méthode mathématique nouvelle.

Si l'on examine l'interaction pion-nucléon dans le cadre habituel de la théorie des champs, la reconstitution du nucléon réel ("dressed"), associé à son champ mésonique propre, n'est pas satisfaisante. Sa décomposition en nucléon "nu" et champ mésonique découplé traduit un schéma mathématique et non physique. La méthode présentée sera exempte de ce défaut. Tout calcul touchant un ou plusieurs nucléons sera précédé de la détermination de champs mésonique et nucléonique non-séparables (d'où le terme de champs "adhérents"), dont l'association décrit le nucléon réel et dont la forme dépend de l'interaction choisie.

Sur le plan mathématique, la méthode considère que deux champs classiques en interaction obéissent à des équations non-linéaires. La quantification ne change rien à ce fait, même si elle le masque partiellement. Les solutions d'équations non-linéaires diffèrent essentiellement des solutions d'équations linéaires. Elles n'obéissent pas au principe de superposition, possèdent des normes privilégiées. Leur décomposition légitime suivant des systèmes complets le fait parfois oublier. Il était indispensable d'examiner leurs propriétés en relation avec l'interaction choisie. Les résultats furent inattendus: dans un tel système non-linéaire, les solutions des deux champs sont liées entre elles (et non séparables en ondes planes lorsque la constante de couplage G tend vers 0). Ces solutions liées, adhérentes, décrivent l'asso-

ciation du nucléon "nu" à son champ mésonique propre. La méthode conduit à des fonctions de forme et légitime à postériori l'usage de sources étendues et de "cut-off". Mais son avantage principal est de faire apparaître la structure interne du nucléon comme conséquence directe de l'interaction choisie. Puisque la méthode explicite des fonctions de forme, elle utilisera soit les procédés de calcul habituels au couplage fort, soit le "cut-off". On trouvera dans ce travail les traits caractéristiques d'un calcul à couplage fort, dont la technique a été simplifiée (cf. § 5).

Les résultats obtenus sont satisfaisants. Ils ne prétendent cependant pas établir que la théorie mésonique utilisée ici donne une description correcte de l'interaction pion-nucléon. Ils montrent plutôt que cette théorie attribue au nucléon une structure interne que la méthode permet d'expliciter. Le contenu des théories du type de Yukawa est beaucoup plus riche que les analyses habituelles le laissent supposer. La méthode développée a d'ailleurs un champ d'applications plus étendu que l'étude des champs nucléaires.

2. Notion de Champs Adhérents †

Soit un nucléon "nu", isolé, de masse M, décrit par la fonction ψ à deux composantes isobariques. Supposons qu'il interagisse avec un champ mésonique mixte pseudoscalaire φ_ϱ (interaction pseudoscalaire, μ = masse du méson, $\hbar = c = 1$). Les équations covariantes classiques des champs non-quantifiés sont

$$i\frac{\partial\psi}{\partial t} = \{(\alpha\cdot p)+\beta M+iG\beta\gamma_5(\tau\cdot\varphi)\}\psi, \tag{2.1}$$

$$(\mu^2-\Box)\varphi_\varrho+iG(\psi^*\beta\gamma_5\tau_\varrho\psi) = 0. \tag{2.2}$$

Ces équations décrivent le mouvement d'un nucléon isolé, associé à son champ mésonique propre. On suppose habituellement que le terme d'interaction est une perturbation $\propto G$, ce qui permet de construire les solutions à partir d'ondes planes (pour ψ et pour φ_ϱ). Mais il est évident que si cette hypothèse est inexacte, les équations (2.1,2) ont des solutions beaucoup plus complexes que la simple équation de Dirac du nucléon "nu".

L'hamiltonien non quantifié H correspondant à (2.1,2), avec π_ϱ et $i\psi^*$ canoniquement conjugués à φ_ϱ et ψ, est

$$H=\int dV\psi^*\{(\alpha\cdot p)+\beta M+iG\beta\gamma_5(\tau\cdot\varphi)\}\psi+\sum_{\varrho=1}^{3}\tfrac{1}{2}\int dV\{\pi_\varrho^2+\varphi_\varrho(\mu^2-\Delta)\varphi_\varrho\} \tag{2.3}$$

et les équations canoniques

† Formellement, la méthode peut être considérée comme une exploration des solutions fermées d'une théorie superquantifiée et renormalisée des champs ψ et φ_ϱ, dont on a écrit les équations de mouvement en représentation de Heisenberg. (- et où on a négligé $\delta\mu^2$ et δM devant μ^2 et M, ainsi que le terme en $\lambda\varphi^3$ -)

$$\dot{\pi}_\varrho = -\frac{\delta H}{\delta \varphi_\varrho}, \qquad \dot{\varphi}_\varrho = \frac{\delta H}{\delta \pi_\varrho}, \qquad \dot{\psi}_\varrho = -\frac{\delta H}{\delta (i\psi^*)}, \qquad \dot{\psi}_\varrho^* = \frac{\delta H}{\delta (i\psi)}. \quad (2.4)$$

La limite non quantifiée (2.1,2) reste obligatoirement sous-jacente à toute quantification du champ φ_ϱ (ψ décrivant un seul nucléon), puisque le théorème des moyennes la restitue. Cette limite peut être proche de la solution quantifiée et en garder les traits essentiels. La quantification (cf. § 5) montrera que c'est le cas ici. Une étude des solutions de (2.1,2) est donc utile et doit guider la recherche des solutions quantifiées.

Examinons les traits caractéristiques des solutions de (2.1,2):

a) Toute onde plane ψ jointe au champ $\varphi_\varrho = 0$ est solution de (2.1,2), et cela indépendamment de G. C'est donc un système singulier de solutions de (2.1,2) qui sert de départ au calcul habituel du champ propre.

b) Le développement des solutions suivant une série de puissances croissantes de G suppose que la limite $G = 0$ a un sens pour toutes les solutions de (2.1,2). Or la transformation $\Psi = \psi/G$, $\Phi_\varrho = \varphi_\varrho/G$ qui conduit à des équations indépendantes de G pour Ψ et pour Φ_ϱ montre qu'il n'en est rien. (On remarquera en passant que la norme N de ψ est proportionnelle à $1/G^2$.) Le paramètre G introduit une singularité des solutions pour $G = 0$. La quantification de φ_ϱ n'élimine pas cette difficulté puisque les relations de commutation

$$i[\pi_\sigma(\mathbf{x}),\ \varphi_\varrho(\mathbf{x}')] = \delta_{\sigma,\varrho}\delta(\mathbf{x}-\mathbf{x}') \quad (2.5)$$

pourront être remplies par des champs φ_ϱ quasistatiques, à la limite $G \to 0$.

c) L'idée de normer ψ, à 1 p. ex., pour éviter le point singulier $G = 0$, est une échappatoire discutable, puisque les équations admises (2.1,2) sont en soi non-linéaires, et que les solutions à normes déterminées en constituent une sélection arbitraire.

Ces remarques et notamment b) montrent que le découplage préalable des solutions pour $G = 0$ est mathématiquement discutable. Les solutions ψ et φ_ϱ de (2.1,2) sont liées entre elles, et la limite $G = 0$ n'y change rien.

Deux positions sont alors concevables. On peut ignorer ces solutions, ce qui revient à en nier le contenu physique. Mais, outre la difficulté considérable que cette élimination présente sur le plan mathématique, cette échappatoire n'est pas acceptable puisqu'elle élimine justement les solutions caractéristiques de l'interaction choisie. Il faut accepter ces solutions, en assurer l'univocité, et s'en servir pour définir la structure interne du nucléon physique ("dressed") résultant d'une interaction déterminée. C'est le point de vue adopté dans ce travail. Formellement, la méthode peut être considérée comme une exploration des solutions fermées d'une théorie quantifiée et renormalisée des champs ψ et φ_ϱ, dont on a écrit les équations de mouvement en représentation de Heisenberg, et où on a négligé les renormalisations $\delta\mu^2$ et δM devant μ^2 et M, ainsi que le terme en φ^3.

3. Définition des Champs Adhérents du Nucléon au Repos Système Propre du Nucléon

Parmi les solutions de (2.1,2), sélectionnons celles, ψ et φ_ϱ, qui sont susceptibles de décrire le nucléon au repos associé à son champ mésonique propre. Puisque le système choisi est celui où le nucléon est au repos, le temps t s'identifiera au temps propre τ du nucléon.

Soit d'abord un nucléon (ou éventuellement un antinucléon) isolé, de masse M, au repos. La mécanique ondulatoire de Dirac associe au point masse M une onde monochromatique d'amplitude constante en chaque point du système propre du nucléon:

$$\psi_D = C\, e^{(\mp) iM\tau} \tag{3.1}$$

solution de l'équation du nucléon (antinucléon) nu

$$i \frac{\partial}{\partial t} \psi = \{(\alpha \cdot p) + \beta M\} \psi \tag{3.2}$$

dans le système propre. L'opérateur invariant $\partial/\partial\tau$ fixe l'énergie au repos M du nucléon.

L'interaction entraîne le passage de (3.2) à (2.1,2). Du point de vue purement mathématique, une solution ψ de (2.1,2) au temps t dépend de la connaissance, à l'instant initial $t = 0$, des fonctions φ_ϱ, $\partial\varphi_\varrho/\partial t$ et ψ. Elle n'est donc pas univoque comme l'est pratiquement (3.1). Notre but principal sera de la définir univoquement.

Caractérisons d'abord φ_ϱ dans le système propre du nucléon. Puisque le champ φ_ϱ n'est pas quantifié, postulons un champ φ_ϱ statique:

$$\frac{\partial \varphi_\varrho}{\partial \tau} = 0 \text{ pour tout } \tau. \tag{3.3}$$

La forme des équations (2.1,2) ne permet pas de retrouver exactement la solution ψ_D (3.1). On peut cependant supposer qu'il existe des solutions ψ de (2.1,2) qui s'identifient à ψ_D dans tout le système propre, à l'exception d'une région spatiale très petite, d'extension linéaire $\approx M^{-1}$ (coeur). Postulons alors le principe de correspondance suivant: parmi les solutions de (2.1,2), seules les solutions ψ telles que $\psi \approx \psi_D$ à l'extérieur du "coeur" du nucléon sont à retenir:

$$\psi \approx \psi_D \qquad \text{à l'extérieur du coeur.} \tag{3.4}$$

A l'intérieur du coeur, on admettra par contre que ψ peut différer totalement de ψ_D. Cette partie interne, désignée par ψ_C, absente de (3.1), est introduite par l'interaction, et doit être déterminée. Dans ce but posons comme solution de (2.1,2)

$$\psi \approx \psi_C + \psi_D \tag{3.5}$$

où ψ_C désigne une fonction d'extension linéaire $\approx M^{-1}$ et telle que ψ_D soit négligeable devant ψ_C dans et aux environs du coeur. Mathématiquement,

c'est un développement de ψ autour de ψ_C avec la condition

$$|\psi_D| \ll |\psi_C| \quad \text{dans le coeur,} \tag{3.6}$$

remplaçant le développement autour de $\psi = \psi_D$ utilisé jusqu'ici. Dans cette perspective, cela signifie que nous admettons que les équations (2.1,2) fixent essentiellement ψ_C. Recherchons-en les solutions stationnaires dans le système propre:

$$\psi_C = e^{-iEt} u(x), \tag{3.7}$$

ce qui donne pour $u(x)$

$$\{(\alpha \cdot p) + \beta M + iG\beta\gamma_5 (\tau \cdot \varphi)\} u = Eu, \tag{3.8}$$

$$(\mu^2 - \Delta)\varphi_\varrho + iG(u^* \beta\gamma_5 \tau_\varrho u) = 0. \tag{3.9}$$

Il reste à fixer E. Si l'on exige que la masse M soit la masse observée du nucléon (champs non-quantifiés), le choix $E \approx 0$ est, selon nos connaissances actuelles, le seul qui soit cohérent, pour décrire le proton et le neutron.

4. Calcul des Champs Adhérents d'un Nucléon au Repos

4.1. MÉTHODE UTILISÉE ET SIMPLIFICATIONS ADOPTÉES

Il s'agit de trouver, dans le système propre du nucléon, les solutions $u(x)$ et $\varphi_\varrho(x)$ satisfaisant

$$\{(\alpha \cdot p) + \beta M + iG\beta\gamma_5 (\tau \cdot \varphi)\} u = 0, \tag{4.1}$$

$$(\mu^2 - \Delta)\varphi_\varrho + iG(u^* \beta\gamma_5 \tau_\varrho u) = 0. \tag{4.2}$$

L'opérateur $\{(\alpha \cdot p) - \beta M + iG\beta\gamma_5 (\tau \cdot \varphi)\}$ appliqué à (4.1) donne

$$\{M^2 - \Delta + G^2 \boldsymbol{\varphi}^2 + G\beta(\boldsymbol{\sigma} \cdot \operatorname{grad} (\tau \cdot \varphi))\} u = 0 \tag{4.3}$$

et la substitution de u et u^* (4.1) dans (4.2)

$$(\mu^2 - \Delta)\varphi_\varrho + \frac{G^2}{M}(u^* \beta u)\varphi_\varrho - \frac{G}{2M} \operatorname{div} (u^* \boldsymbol{\sigma} \tau_\varrho u) = 0, \quad \varrho = 1, 2, 3. \tag{4.4}$$

(4.3,4) sont les équations de variation de H_0 donné par

$$H_0 = \int dV \left\{ \frac{u^* \beta (M^2 - \Delta) u}{2M} + \frac{G^2}{2M} \varphi_\varrho u^* \beta u \varphi_\varrho + \frac{G}{2M} \sum_{j,\varrho=1}^{3} (u^* \sigma_j \tau_\varrho u) \frac{\partial \varphi_\varrho}{\partial x_j} + \sum_{\varrho=1}^{3} \frac{1}{2} \varphi_\varrho (\mu^2 - \Delta)\varphi_\varrho \right\}. \tag{4.5}$$

Pour u vérifiant (4.1), H de (2.3) est lié à H_0 (4.5) par

$$H = H_0 + \tfrac{1}{2} \sum_{\varrho=1}^{3} \pi_\varrho^2 = H_0 + H_C; \tag{4.6}$$

H_0 représente l'énergie des champs u et φ_ϱ à l'exception du terme "cinétique" H_C du champ φ_ϱ:

$$H_C = \tfrac{1}{2} \sum_{\varrho=1}^{3} \pi_\varrho^2. \tag{4.7}$$

Si le champ φ_ϱ n'est pas quantifié, les solutions telles que $\pi_\varrho = 0$ sont

admissibles, et représentent des solutions statiques. Quantifié, H_c introduit des isobares (cf. § 5).

Les solutions du système (4.3,4) se séparent en deux spectres distincts correspondant à $\beta = \pm 1$. Le spectre $\beta = 1$ sera seul discuté ici. Les solutions u ont alors deux composantes de spin et deux composantes de spin isobarique. Parmi la multiplicité de ces solutions, nous sélectionnons celles de symétrie sphérique autour d'une origine arbitraire 0, choisie dans le système propre du nucléon: $u(x) = u(r)$. L'étude du système (4.3,4) conduit à l'hypothèse suivante qui se révèle judicieuse (cf. § 4.4): chacune des quatre fonctions de double spineur sera choisie proportionnelle à une même fonction de r désignée par $v(r)$:

$$u(x) = Av(r) \tag{4.8}$$

où A est un spineur constant normé, $A^*A = 1$, décrivant le spin et le spin isobarique. On trouve que $v(r)$ est une fonction d'extension linéaire $a \approx 1/M$ (cf. § 4.4). Soit N sa norme:

$$N = \int \mathrm{dV}\, v^*(r)\, v(r). \tag{4.9}$$

$v(r)$ introduit la fonction de forme normée $\delta_a(r)$ définie par

$$\delta_a(r) = \frac{1}{N} v^* v. \tag{4.10}$$

Rappelons que la norme N sera $\propto$ à $1/G^2$.

Dans ce cas particulier, la recherche des champs u et φ_ϱ revient à trouver $v(r)$, A et le champ mésonique φ_ϱ tels que (4.5) soit un extrémum. De (4.5) définissons H_1 tel que

$$H_0 = A^* H_1 A. \tag{4.11}$$

Introduisons dans H_1 les hypothèses faites ci-dessus. Il vient ($\beta = 1$)

$$H_1 = \int \mathrm{dV} \left\{ \frac{N}{2M} \delta_a^{\frac{1}{2}} (M^2 - \Delta) \delta_a^{\frac{1}{2}} + \frac{G^2 N}{2M} \boldsymbol{\varphi}^2 \delta_a \right.$$
$$\left. + \frac{GN}{2M} \sum_{j,\varrho=1}^{3} \sigma_j \tau_\varrho \frac{\partial \varphi_\varrho}{\partial x_j} \cdot \delta_a + \tfrac{1}{2} \sum_{\varrho=1}^{3} \varphi_\varrho (\mu^2 - \Delta) \varphi_\varrho \right\}. \tag{4.12}$$

Dégageons d'abord le sens de A dans notre calcul: pour un couple de champs u et φ_ϱ donnés, le choix de A est le choix d'un état ou d'une combinaison des 4 états de spin et spin isobarique de (4.12). Nous résolvons le problème en déterminant non pas simultanément, mais successivement A, $v(r)$ et φ_ϱ. Dans ce but, nous calculons d'abord A et φ_ϱ pour $v(r)$ donnée et d'extension $a \approx 1/M$, puis nous montrons que l'on peut déterminer $v(r)$ répondant aux hypothèses faites à son sujet.

Lorsque $v(r)$ est donné, et que les valeurs attribuées à $|GN/2M|$ sont

suffisamment grandes, la recherche de A et φ_ϱ conduit à un calcul du type couplage fort. C'est le cas ici: cf. § 7. De plus l'analyse du terme en G^2 de (4.12) montre que sans être négligeable, son influence n'est pas essentielle. Pour faciliter l'exposé et recourir à des méthodes déjà connues, le terme en G^2 sera supprimé. Les modifications apportées aux résultats par ce terme seront discutées au § 7. Cette simplification remplace H_1 (4.12) par H_2:

$$H_2 = E_2 + \frac{GN}{2M} \sum_{j,\varrho=1}^{3} \sigma_j \tau_\varrho \int \mathrm{dV}\, \delta_a(r) \frac{\partial \varphi_\varrho}{\partial x_j} + \tfrac{1}{2} \sum_{\varrho=1}^{3} \int \mathrm{dV}\, \varphi_\varrho (\mu^2 - \Delta) \varphi_\varrho \quad (4.13)$$

avec

$$E_2 = \frac{N}{2M} \int \mathrm{dV}\, \delta_a^{\frac{1}{2}} (M^2 - \Delta) \delta_a^{\frac{1}{2}}. \quad (4.14)$$

Rechercher l'extrémum de H_2 à $v(r)$ donné, c'est trouver A et φ_ϱ tels que H_2 soit ici minimum. Dans ce but décomposons $H_2 - E_2$ en deux parties:

$$H_2 - E_2 = H(\varphi^2) + H_{\mathrm{int}}, \quad (4.15)$$

$$H(\varphi^2) = \tfrac{1}{2} \sum_{\varrho=1}^{3} \int \mathrm{dV}\, \varphi_\varrho (\mu^2 - \Delta) \varphi_\varrho, \quad (4.16)$$

$$H_{\mathrm{int}} = \frac{GN}{2M} \sum_{j,\varrho=1}^{3} \sigma_j \tau_\varrho \int \mathrm{dV}\, \delta_a(r) \frac{\partial \varphi_\varrho}{\partial x_j}. \quad (4.17)$$

4.2. CHOIX DU SPINEUR A ET MINIMUM DE H_{int}

La recherche de A et de φ_ϱ qui rendent (4.15) minimum est un problème bien connu de la théorie du couplage fort. Rappelons-en brièvement la solution. Définissons

$$\varphi_{j,\varrho} = \int \mathrm{dV} \frac{\partial \delta_a}{\partial x_j} \varphi_\varrho = - \int \mathrm{dV}\, \delta_a(x) \frac{\partial \varphi_\varrho}{\partial x_j}. \quad (4.18)$$

Du point de vue tensoriel, $\varphi_{j,\varrho}$ est un vecteur de l'espace x (indices $_j$) et un vecteur de l'espace isobarique (indice $_\varrho$). L'opérateur (4.16) est diagonal relativement au spin et au spin isobarique, tandis que H_{int} ne l'est pas. Trouver le spineur A associé au minimum de $H_2 - E_2$ donné par (4.15) revient à déterminer une transformation unitaire U telle que

$$U^* H_{\mathrm{int}} U = \text{diagonale}. \quad (4.19)$$

On démontre aisément que U existe pour tout champ φ_ϱ c'est à dire pour des $\varphi_{j,\varrho}$ quelconques.

La construction de U s'appuie sur les théorèmes suivants [5]): Soient les deux tenseurs symétriques

$$Q_{j,k} = Q_{k,j} = \sum_{\varrho=1}^{3} \varphi_{j,\varrho} \varphi_{k,\varrho} \text{ de l'espace } x, \quad (4.20)$$

$$Q'_{\varrho,\sigma} = Q'_{\sigma,\varrho} = \sum_{j=1}^{3} \varphi_{j,\varrho} \varphi_{j,\sigma} \text{ de l'espace isobarique.} \quad (4.21)$$

Ils possèdent les mêmes valeurs propres positives désignées par r_n^2 ($n = 1, 2, 3$). Soient $s'(\vartheta', \varphi', \psi')$ et $s''(\vartheta'', \varphi'', \psi'')$ deux transformations orthogonales construites sur les angles d'Euler ϑ' φ', ψ' et ϑ'', φ'', ψ'', et $r_n = +\sqrt{r_n^2}$. On démontre [5]) que l'on peut écrire $\varphi_{j,\varrho}$ sous la forme

$$\varphi_{j,\varrho} = \sum_{n=1}^{3} r_n s'_{j,n} s'_{\varrho,n}. \tag{4.22}$$

Définissons

$$g = -\frac{GN}{2M} > 0 \tag{4.23}$$

et d'après (4.17) et (4.19)

$$H_{\text{int}} = g \sum_{j,\varrho=1}^{3} \sigma_j \tau_\varrho \varphi_{j,\varrho} = g \sum_{n=1}^{3} r_n \Big(\sum_{j=1}^{3} \sigma_j s'_{jn} \Big) \Big(\sum_{\varrho=1}^{3} \tau_\varrho s''_{\varrho n} \Big). \tag{4.24}$$

H_{int} est transformée en

$$U_0^* H_{\text{int}} U_0 = g \sum_{n=1}^{3} \sigma_n \tau_n r_n \tag{4.25}$$

si l'on choisit pour U_0 le produit de deux rotations construites sur les angles d'Euler ϑ', φ' ψ' et ϑ'', φ'', ψ'' dans l'espace x et dans l'espace isobarique:

$$U_0 = U' \cdot U'' \tag{4.26}$$

avec

$$U' = e^{i\sigma_3 \frac{\varphi'}{2}} \cdot e^{i\sigma_2 \frac{\vartheta'}{2}} \cdot e^{i\sigma_3 \frac{\psi'}{2}} \tag{4.27}$$

$$U'' = e^{i\tau_3 \frac{\varphi''}{2}} \cdot e^{i\tau_2 \frac{\vartheta''}{2}} \cdot e^{i\tau_3 \frac{\psi''}{2}}. \tag{4.27}$$

Complétée par Z:

$$Z = \frac{1}{\sqrt{2}} (\sigma_1 + i\tau_2), \tag{4.28}$$

$$U = U_0 Z, \tag{4.29}$$

on trouve

$$U^* H_{\text{int}} U = -g(r_1\tau_3 + r_2\sigma_3 + r_3\sigma_3\tau_3) \tag{4.30}$$

qui est diagonale et dont les 4 valeurs propres sont

$$\begin{aligned} E^{\text{I}} &= -g(r_1 + r_2 + r_3) \\ E^{\text{II}} &= g(r_1 + r_2 - r_3) \\ E^{\text{III}} &= g(r_2 + r_3 - r_1) \\ E^{\text{IV}} &= g(r_3 + r_1 - r_2). \end{aligned} \tag{4.31}$$

Lorsque G tend vers 0, la norme N (4.9) de $u(r)$ tendra vers ∞ comme $1/G^2$ et g (4.23) tendra vers ∞ comme $1/G$. Le point $G = 0$ n'étant pas régulier, faire tendre $G \to 0$ n'implique pas du tout le découplage des solutions en ondes planes. Les 4 valeurs E (4.31) se séparent et la distance de E^{I}

aux autres valeurs E de (4.31) devient infinie pour $G = 0$. On se trouve devant un problème dont les prémisses sont celles du couplage fort. La valeur E^{I} étant la plus basse, le choix du spineur A actualise simplement le choix de E^{I} parmi les 4 valeurs possibles (4.31).

E^{I} étant choisi, nous déterminons successivement $\varphi_\varrho = \mathring{\varphi}_\varrho$ et $v(r)$ telles que (4.5) soit extrémal. La détermination de $\mathring{\varphi}_\varrho(x)$ entraînant une simplification importante, nous l'exposons ici. (4.15) est invariant par rapport aux rotations de l'espace isobarique ainsi que les champs $\mathring{\varphi}_\varrho(x)$ qui le rendent minimal. Par conséquent,

$$r_1 = r_2 = r_3 = r_0 \quad \text{pour} \quad \varphi_\varrho(x) = \mathring{\varphi}_\varrho(x). \tag{4.32}$$

Imaginons le développement de φ_ϱ voisin de $\mathring{\varphi}_\varrho$ suivant

$$\varphi_\varrho(x) = \mathring{\varphi}_\varrho(x) + \varphi'_\varrho(x) \tag{4.33}$$

avec, selon (4.18),

$$\varphi_{j,\varrho} = \mathring{\varphi}_{j,\varrho} + \varphi'_{j,\varrho} \tag{4.34}$$

$$\mathring{\varphi}_{j,\varrho} = -\int \mathrm{dV}\, \delta_a(x) \frac{\partial \mathring{\varphi}_\varrho}{\partial x_j} = \int \mathrm{dV}\, \frac{\partial \delta_a(x)}{\partial x_j} \mathring{\varphi}_\varrho(x) \tag{4.35}$$

$$\varphi'_{j,\varrho} = -\int \mathrm{dV}\, \delta_a(x) \frac{\partial \varphi'_\varrho}{\partial x_j} = \int \mathrm{dV}\, \frac{\partial \delta_a(x)}{\partial x_j} \varphi'_\varrho(x). \tag{4.36}$$

D'après (4.22) et (4.32)

$$\mathring{\varphi}_{j,\varrho} = \sum_{n=1}^{3} r_n s'_{j,n} s''_{\varrho,n} = r_0 \sum_{n=1}^{3} s'_{jn} s''_{\varrho n}; \tag{4.37}$$

$\mathring{\varphi}_{j,\varrho}$ ne dépend que du produit des deux rotations s' et s''. Mais ce produit de deux rotations est lui-même une rotation à laquelle sont attribués les angles d'Euler Θ, Φ, Ψ:

$$\sum_{n=1}^{3} s'_{jn} s''_{\varrho n} = S_{j,\varrho}(\Theta, \Phi, \Psi), \tag{4.38}$$

et $\mathring{\varphi}_{j,\varrho}$ ne dépend que des 3 variables Θ, Φ, Ψ. Les $\varphi_{j,\varrho}$ sont en principe des variables représentatives du champ $\varphi_\varrho(x)$ correspondant au développement suivant un certain système complet. La formule (4.22) est un changement des variables $\varphi_{j,\varrho}$ en r_n, ϑ', φ', ψ', ϑ'', φ'', ψ''. La position du minimum ne fait intervenir que les 3 variables Θ, Φ, Ψ, il est naturel de les introduire explicitement et de les compléter par 6 autres. Soient $\xi_{\varrho,\sigma} = \xi_{\sigma,\varrho}$ telles que

$$\varphi'_{j,\varrho} = \sum_{\sigma=1}^{3} \xi_{\varrho,\sigma} S_{j,\sigma}; \tag{4.39}$$

avec (4.37) et (4.36),

$$\mathring{\varphi}_{j,\varrho} = r_0 S_{j,\varrho} \tag{4.40}$$

et

$$\varphi_{j,\varrho} = r_0 S_{j,\varrho} + \sum_{\sigma=1}^{3} \xi_{\varrho,\sigma} S_{j,\sigma}. \tag{4.41}$$

D'après ce qui précède, $\xi_{\varrho,\sigma}$ mesure l'élongation de l'amplitude du champ à partir de la valeur r_0. Dans la perspective de ce travail $|\xi_{\varrho,\sigma}|$ sera considéré comme négligeable devant r_0 (cf. § 5).

Le fait que $\overset{\circ}{\varphi}_{j,\varrho}$ dépend des 3 variables Θ, Φ, Ψ (4.38) entraîne les simplifications complémentaires suivantes. De (4.24, 40)

$$H_{\text{int}} = -g r_0 \sum_{j,\varrho=1}^{3} \sigma_j \tau_\varrho S_{j,\varrho}. \tag{4.42}$$

On peut remplacer U_0 (4.26) par

$$U'_0 = e^{i\sigma_3 \frac{\Phi}{2}} \cdot e^{i\sigma_2 \frac{\Theta}{2}} \cdot e^{i\sigma_3 \frac{\Psi}{2}} \tag{4.43}$$

et

$$(U'_0 Z)^* H_{\text{int}} (U'_0 Z) = -g r_0 (\tau_3 + \sigma_3 + \sigma_3 \tau_3) \tag{4.44}$$

est diagonal. Ses 4 valeurs propres se séparent en un singulet $E^{\text{I}} = E^{\text{s}} = -3gr_0$ et un triplet $E^{\text{II}} = E^{\text{III}} = E^{\text{IV}} = E^{\text{t}} = -gr_0$. Le choix du spineur A actualise le choix de E^{s}.

4.3. CALCUL DU CHAMP $\overset{\circ}{\varphi}_\varrho(x)$

Après avoir choisi E^{I}, il s'agit de déterminer $\overset{\circ}{\varphi}_\varrho(x)$ tel que (4.13) soit extrémum, ici minimum. Le plus simple est de postuler le résultat et de le vérifier. Soit [cf. (4.23,10)]

$$\varphi_\varrho(x) = g \sum_{k=1}^{3} S_{k,\varrho} \frac{\partial}{\partial x_k} \left\{ \frac{1}{\mu^2 - \Delta} \cdot \delta_a(x) \right\} \tag{4.45}$$

avec

$$\frac{1}{\mu_2 - \Delta} \cdot \delta_a(x) = \frac{1}{4\pi} \int \mathrm{d}V' \frac{e^{-\mu|\mathbf{x}-\mathbf{x}'|}}{|\mathbf{x}-\mathbf{x}'|} \delta_a(\mathbf{x}'). \tag{4.46}$$

On trouve, avec U'_0 donné par (4.43) et $U = U'_0 Z$,

$$U^*(H_2 - E_2)U = \frac{g^2}{2} I_0 - U^* \left\{ \frac{g^2}{3} \sum_{j,\varrho} \sigma_j \tau_\varrho S_{j,\varrho} I_0 \right\} U \tag{4.47}$$

avec

$$I_0 = \int \mathrm{d}V \, \delta_a(x) \left\{ \frac{-\Delta}{\mu^2 - \Delta} \, \delta_a(x) \right\}. \tag{4.48}$$

Le choix du singulet E^{s} donne

$$[U^*(H_2 - E_2)U]_{\text{s}} = -\frac{g^2 I_0}{2}. \tag{4.49}$$

Montrons que (4.45) est bien l'extrémale cherchée. Dans ce but, développons $\varphi_\varrho(x)$ à partir de $\overset{\circ}{\varphi}_\varrho(x)$ suivant (4.33), et remplaçons dans

$$[U^*(H_2-E_2)U]_s \tag{4.50}$$

avec $U'_0 Z$ donné par (4.43, 28). On doit vérifier que les termes linéaires en g disparaissent pour le singulet E^s. Il s'agit simplement d'effectuer la transformation U; il vient:

$$U^*(H_2-E_2)U = -\frac{g^2 I_0}{2} + \tfrac{1}{2}\sum_{\varrho=1}^{3}\int \mathrm{dV}\,\varphi'_\varrho\,(\mu^2-\Delta)\varphi'_\varrho$$

$$+g\sum_{k,\varrho=1}^{3} S_{k,\varrho}\int \mathrm{dV}\,\varphi'_\varrho\,\frac{\partial\delta_a(x)}{\partial x_k} + g\sum_{k,\varrho=1}^{3}(U^*\sigma_k\tau_\varrho U)\int \mathrm{dV}\,\varphi'_\varrho\,\frac{\partial\delta_a(x)}{\partial x_k}\,. \tag{4.51}$$

Les éléments $(U^*\sigma_k\tau_\varrho U)$ qui apparaissent dans le dernier terme de (4.51) sont, les uns diagonaux relativement aux états diagonaux (4.31), les autres non-diagonaux. Pour les distinguer, écrivons explicitement d'après (4.43)

$$(U^*\sigma_k\tau_\varrho U) = Z^*\,(\sum_{n=1}^{3}\sigma_n S_{kn}\tau_\varrho)Z. \tag{4.52}$$

On vérifie sans grande difficulté que

$$Z^*\sigma_n\tau_\varrho Z \tag{4.53}$$

possède des valeurs diagonales valant ± 1 lorsque $n=\varrho$. Pour le singulet $E^s = -3gr_0$, on a

$$Z^*\sigma_n\tau_n Z = -1 \tag{4.54}$$

tandis que

$$Z^*\sigma_n\tau_\varrho Z = 0 \text{ si } n\neq\varrho. \tag{4.54a}$$

Par contre (4.54a) possède des valeurs hors diagonale différentes de 0. Mais on démontre (cf. G. Wentzel, ref. [5]), § 8) que les termes perturbateurs $\propto \xi_{\varrho,\sigma}$ y relatifs peuvent être négligés. Dans cette approximation, on voit que le troisième terme de (4.51) compense exactement le quatrième pour l'état singulet E^s de (4.44). $\overset{\circ}{\varphi}_\varrho(x)$ donné par (4.45) est donc bien l'extrémale cherchée.

4.4. LA FONCTION $v(r)$

Tout ce qui précède repose sur l'existence d'une ou de plusieurs fonctions $u(r)$ du type (4.8,9,10). Il s'agit de démontrer que cette supposition est exacte. La méthode suivie est basée sur la connaissance de A (choix de E^s) et sur la formule (4.45) pour $\overset{\circ}{\varphi}_\varrho(x)$. Trouver $v(r)$, c'est résoudre le problème de variation posé par (4.12) relativement à $\delta_a(x)$ ou à $v(r)$. Le terme en G^2 sera encore une fois ignoré (et son influence analysée au § 7). Pour le singulet E^s, les formules (4.52, 53, 54) montrent que $(U^*\sigma_k\tau_\varrho U)$ doit être remplacé par $-S_{k,\varrho}$. Cette règle de calcul conduit facilement à l'équation de $v(r)$, soit

$$(M^2-\Delta)w = w\left(\frac{\Delta}{\Delta-\mu^2}\,w^2\right), \quad \text{où} \quad w(r) = \frac{G}{(2M)^{\frac{1}{2}}}\cdot v(r); \tag{4.55}$$

lorsque $a\mu \ll 1$ (pour la validité de cette supposition voir § 7), cette équation sera remplacée par

$$(M^2-\Delta)w = w^3. \tag{4.56}$$

Cette équation non linéaire relativement à $v(r)$ possède des solutions en général non intégrables au sens de la mécanique ondulatoire. Si l'on se limite à la recherche des solutions qui ne dépendent que de r (indépendantes des angles), les solutions intégrables forment un spectre dénombrable $v_n(r)$, dont la dimension linéaire (le rayon a_n) va croissant. Nous choisissons la fonction $v_0(r)$ de rayon minimum, telle que $a_0 = \text{min. } \{a_n\}$ pour définir le nucléon. Cette fonction peut être représentée approximativement par les formules

$$\begin{aligned} v_0(y) &= \frac{2^{1/3}M^{2/3}}{G}\{3.04-1.74\,y\} \quad \text{pour } 0 \leqq y \leqq 1.2 \\ v_0(y) &= \frac{1.14\,e^{-(y-1.2)}}{G} \qquad\qquad \text{pour } 1.2 \leqq y \leqq \infty \end{aligned} \tag{4.57}$$

avec $y = rM$. La norme de $v_0(r)$ vaut [cf. éq. (4.9)]

$$N = \frac{20\pi}{G^2}. \tag{4.58}$$

Nous reviendrons dans un prochain travail sur les autres fonctions de forme solutions de (4.12).

5. Quantification du Champ $\varphi_\rho(x)$

5.1. ISOBARES DU NUCLÉON

Bien que la quantification du champ $\varphi_\varrho(x)$ puisse être effectuée selon des méthodes déjà connues (cf. ref. [5])), nous développerons ici une technique simplifiée qui conduit rapidement aux résultats connus. La fonction $v(r)$, (4.57), sert de point de départ. On utilise l'hamiltonien (4.6) que l'introduction de $u(r) = Av(r)$ transforme ($\beta = +1$) [cf. (4.12, 13, 14)] en

$$H'_2 - E_2 = \tfrac{1}{2}\sum_{\varrho=1}^{3}\int dV\,\{\pi_\varrho^2+\varphi_\varrho(\mu^2-\Delta)\varphi_\varrho\} + \frac{G^2N}{2M}\int dV\,\delta_a(x)\varphi^2 + \frac{GN}{2M}\sum_{j,\varrho=1}^{3}\sigma_j\tau_\varrho\int dV\,\delta_a(x)\frac{\partial\varphi_\varrho}{\partial x_j}. \tag{5.1}$$

Comme jusqu'ici on néglige les termes en G^2.

La quantification (2.5) ne permet plus de poser $\pi_\varrho = 0$. Pour $\delta_a(x)$ déterminée, il s'agit de rendre diagonal, à l'aide de transformations canoniques,

$$H' = \tfrac{1}{2}\sum_{\varrho=1}^{3}\int dV\,\{\pi_\varrho^2+\varphi_\varrho(\mu^2-\Delta)\varphi_\varrho\} + g\sum_{j,\varrho=1}^{3}\sigma_j\tau_\varrho\int dV\,\frac{\partial\delta_a(x)}{\partial x_j}\varphi_\varrho(x). \tag{5.2}$$

Ces opérations seront effectuées en supposant réalisée la condition de couplage fort

$$g = \left|\frac{GN}{2M}\right| \gg a. \tag{5.3}$$

Dans le § 7, on prouvera que c'est bien le cas: voir (7.4).

La quantification repose sur l'introduction d'un système complet de fonctions orthonormées $K_n(x)$, destinées à développer $\varphi_\varrho(x)$ et $\pi_\varrho(x)$. Choisissons, pour $j = 1, 2, 3$,

$$K_j(x) = \alpha \frac{\partial}{\partial x_j}\left\{\frac{1}{\mu^2 - \Delta}\,\delta_a(x)\right\}. \tag{5.4}$$

Pour que

$$\int \mathrm{dV}\, K_j^2(x) = 1 \tag{5.5}$$

il faut que

$$\frac{\alpha^2}{3}\int \mathrm{dV}\left\{\frac{1}{\mu^2-\Delta}\,\delta_a(x)\right\}\left\{\frac{-\Delta}{\mu^2-\Delta}\,\delta_a(x)\right\} = 1. \tag{5.6}$$

Par extension de la définition habituelle du "rayon nucléonique a" posons

$$\frac{1}{4\pi a} = \int \mathrm{dV}\left\{\frac{1}{\mu^2-\Delta}\,\delta_a(x)\right\}\left\{\frac{-\Delta}{\mu^2-\Delta}\,\delta_a(x)\right\}, \tag{5.7}$$

ce qui donne $\alpha^2 = 12\pi a$, ou

$$\alpha = \sqrt{12\pi a}. \tag{5.8}$$

Remarquons que l'on a, selon (4.45) et (5.8),

$$\overset{\circ}{\varphi}_\varrho(x) = \frac{g}{\sqrt{12\pi a}} \sum_{j=1}^{3} S_{j,\varrho} K_j(x)\,. \tag{5.9}$$

Décomposons $\varphi_\varrho(x)$ et $\pi_\varrho(x)$:

$$\varphi_\varrho(x) = \sum_{j=1}^{3} q_{j,\varrho} K_j(x) + \varphi''_\varrho(x), \tag{5.10}$$

$$\pi_\varrho(x) = \sum_{j=1}^{3} p_{j,\varrho} K_j(x) + \pi''_\varrho(x), \tag{5.11}$$

avec

$$\int \mathrm{dV}\, \varphi''_\varrho(x) K_j(x) = \int \mathrm{dV}\, \pi''_\varrho(x) K_j(x) = 0. \tag{5.12}$$

La quantification (2.5) entraîne

$$i[p_{j,\varrho},\, q_{k,\sigma}] = \delta_{j,k}\delta_{\varrho,\sigma}, \tag{5.13}$$

$$i[\pi''_\varrho(x),\, \varphi''_\sigma(x')] = \delta_{\varrho,\sigma}\{\delta(x,x') - \sum_{j=1}^{3} K_j(x)K_j(x')\}. \tag{5.14}$$

Parallèlement à (4.33) décomposons $q_{j,\varrho}$ en

$$q_{j,\varrho} = \overset{\circ}{q}_{j,\varrho} + q'_{j,\varrho} \tag{5.15}$$

tels que

$$\begin{aligned} \overset{\circ}{q}_{j,\varrho} &= \int \mathrm{dV}\, \overset{\circ}{\varphi}_\varrho(x) K_j(x), \\ q'_{j,\varrho} &= \int \mathrm{dV}\, \varphi'_\varrho(x) K_j(x). \end{aligned} \tag{5.16}$$

Par comparaison avec (5.10) et (4.33) on trouve

$$\varphi'_\varrho(x) - \varphi''_\varrho(x) = \sum_{j=1}^{3} q'_{j,\varrho} K_j(x) \tag{5.17}$$

et d'après (5.9)

$$\overset{\circ}{q}_{j,\varrho} = \frac{g}{\sqrt{12\pi a}} S_{j,\varrho}(\Theta, \Phi, \Psi). \tag{5.18}$$

L'application de la transformation $U = U'_0 Z$, (4.43) et (4.28), à H' (5.2) donne

$$U^* H' U = U^* \left\{ \sum_{j,\varrho=1}^{3} \frac{p_{j,\varrho}^2}{2} \right\} U + \tfrac{1}{2} \sum_{\varrho=1}^{3} \int \mathrm{dV}\, \{\pi''^2_\varrho + \varphi'_\varrho(\mu^2 - \Delta)\varphi'_\varrho\} \tag{5.19}$$

en négligeant les termes non-diagonaux du type (4.54a) et le terme constant $-\frac{1}{2}g^2 I_0$. L'influence de la différence (5.17) peut être ignorée dans les problèmes de diffusion pour lesquels, ω étant l'énergie du méson, on a $a\omega \ll 1$ (cf. G. Wentzel, ref. [5]), § 10).

Puisque la différence entre $\varphi'_\varrho(x)$ et $\varphi''_\varrho(x)$ peut être ignorée, il y a donc séparation de variables dans (5.19), $q_{j,\varrho}$ et $p_{j,\varrho}$ étant alors pratiquement séparées des $\pi''_\varrho(x)$ et $\varphi''_\varrho(x)$. Introduisons parallèlement aux $\xi_{\varrho,\sigma} = \xi_{\sigma,\varrho}$ (4.39), les $\eta_{\varrho,\sigma} = \eta_{\sigma,\varrho}$ tels que

$$q_{j,\varrho} = \frac{g}{\sqrt{12\pi a}} S_{j,\varrho}(\Theta, \Phi, \Psi) + \sum_{\sigma=1}^{3} S_{j,\sigma} \eta_{\sigma,\varrho} \tag{5.20}$$

et considérons le passage des 9 variables $q_{j,\varrho}$ aux nouvelles variables Θ, Φ, Ψ, $\eta_{\varrho,\sigma} = \eta_{\sigma,\varrho}$, passage engendré par la fonction génératrice

$$T = \sum_{j,\sigma,\varrho=1}^{3} S_{j,\sigma} \left(\frac{g}{\sqrt{12\pi a}} \delta_{\sigma,\varrho} + \eta_{\sigma,\varrho} \right) p_{j,\varrho}, \tag{5.21}$$

qui permet de définir les moments associés aux nouvelles variables

$$p_\Theta = \frac{\partial T}{\partial \Theta},\ p_\Phi = \frac{\partial T}{\partial \Phi},\ p_\Psi = \frac{\partial T}{\partial \psi},\ \pi_{\sigma,\varrho} = \pi_{\varrho,\sigma} = \frac{\partial T}{\partial \eta_{\varrho,\sigma}}. \tag{5.22}$$

Ces relations permettent de calculer les $p_{j,\varrho}$ en fonction des nouvelles variables et de leurs moments conjugués.

On facilite le calcul en introduisant au lieu de p_Θ, p_Φ, p_Ψ les combinaisons linéaires suivantes:

$$P_1 = \sin\Psi\cdot p_\Theta + \frac{\cos\Psi}{\sin\Theta}(p_\Phi + \cos\Theta\cdot p_\Psi)$$
$$P_2 = \cos\Psi\cdot p_\Theta + \frac{\sin\Psi}{\sin\Theta}(p_\Phi + \cos\Theta\cdot p_\Psi) \tag{5.23}$$
$$P_3 = p_\Psi,$$

qui satisfont les relations de commutation habituelles des moments cinétiques

$$[P_1,\ P_2] = iP_3 \qquad \text{cycliquement} \tag{5.24}$$
$$[P_n,\ S_{j,n}] = 0$$
$$i[P_3,\ S_{j,2}] = S_{j,1} \qquad \text{cycliquement.} \tag{5.25}$$

L'hypothèse de couplage fort (5.3) entraîne

$$|\eta_{\varrho,\sigma}| \ll \frac{g}{\sqrt{12\pi a}} \tag{5.26}$$

(cf. G. Wentzel, ref. [5]), § 5, en particulier (5.13), ainsi que § 6). Dans le calcul des $p_{j,\varrho}$ en fonction des nouvelles variables (5.21), on pourra développer suivant les puissances croissantes de $|\eta_{\varrho,\sigma}(g/\sqrt{12\pi a})^{-1}|$. Si l'on se borne aux termes indépendants de $\eta_{\varrho,\sigma}$, on trouve

$$p_{j,1} = \frac{\sqrt{3\pi a}}{g}(S_{j,3}P_2 - S_{j,2}P_3 + iS_{j,1}) + S_{j,1}\pi_{1,1} + \tfrac{1}{2}(S_{j,2}\pi_{12} + S_{j,3}\pi_{1,3}), \tag{5.27}$$

dont on tire

$$\tfrac{1}{2}\sum_{j,\varrho=1}^{3} p_{j,\varrho}^2 = \frac{3\pi a}{g^2}\{P_1^2 + P_2^2 + P_3^2\} + \tfrac{1}{2}\sum_{\varrho,\sigma=1}^{3}\pi_{\varrho,\sigma}^2. \tag{5.28}$$

On a pour l'état singulet de (4.44)

$$U^*\,(\sum_{n=1}^{3} P_n^2)\,U = \sum_{n=1}^{3} P_n^2 + \tfrac{3}{4}, \tag{5.29}$$

de sorte que (5.27) remplacé dans (5.19) donne

$$U^* H' U = \frac{3\pi a}{g^2}(\sum_{n=1}^{3} P_n^2) + \frac{9\pi a}{4g^2} + \tfrac{1}{2}\sum_{\varrho,\sigma=1}^{3}\pi_{\varrho,\sigma}^2 + \tfrac{1}{2}\sum_{\varrho=1}^{3}\int \mathrm{dV}\,\{\pi_\varrho'^2 + \varphi_\varrho'(\mu^2 - \Delta)\varphi_\varrho'\}. \tag{5.30}$$

Si l'on exprime les P_n en fonction des variables Θ, Φ, Ψ, p_Θ, p_Φ, p_Ψ on trouve

$$P^2 = \sum_{n=1}^{3} P_n^2 = \frac{1}{\sin\Theta}\,p_\Theta \sin\Theta\cdot p_\Theta + \frac{p_\Phi^2 + 2\cos\Theta\cdot p_\Phi p_\Psi + p_\Psi^2}{\sin^2\Theta}. \tag{5.31}$$

L'hamiltonien H' pose un problème de valeurs propres usant d'une fonc-

tionnelle F, à laquelle s'appliquent les arguments habituels d'univocité relativement aux angles Θ, Φ, Ψ. L'hamiltonien transformé $\overline{H}' = U^* H' U$ (5.31) utilise la fonctionnelle $F' = U^* F$. Les variables Φ et Ψ sont cycliques. $F' = (U'_0 Z^*)F$ contient les demi angles $\frac{1}{2}\Theta$, $\frac{1}{2}\Phi$, $\frac{1}{2}\Psi$ [cf. (4.43)]. En conséquence, on a

$$F' \propto e^{i(m\Phi+n\Psi)} f(\Theta) \tag{5.32}$$

où m et n sont demi-entiers. Les valeurs propres de P^2 (5.29) sont

$$P^2 = j(j+1), \qquad j \geqq |n|, \ |m|, \tag{5.33}$$
$$j = \tfrac{1}{2}, \ \tfrac{3}{2}, \ \tfrac{5}{2} \ldots,$$

ce qui donne pour (5.30)

$$U^* H' U = \frac{9\pi a}{4g^2} + \frac{3\pi a}{g^2} j(j+1) + H'',$$

c.à.d.

$$U^* H' U = \frac{9\pi a}{4g^2} + \frac{3\pi a}{g^2} j(j+1) + \tfrac{1}{2} \sum_{\varrho,\sigma=1}^{3} \pi_{\varrho,\sigma}^2 + \tfrac{1}{2} \sum_{\varrho=1}^{3} \int dV \{\pi_\varrho''^2 + \varphi_\varrho'(\mu^2 - \Delta)\varphi_\varrho'\}. \tag{5.34}$$

Les variables Θ, Φ, Ψ étant considérées comme variables internes du nucléon et H'' décrivant les mésons diffusés, l'énergie

$$E_j = \frac{3\pi a}{g^2} j(j+1) \tag{5.35}$$

est une énergie interne du nucléon, correspondant à des états excités, ("isobares"), dont

$$\Delta E_j = \frac{3\pi a}{g^2} (j(j+1) - \tfrac{3}{4}) \tag{5.36}$$

est l'énergie d'excitation, relativement à l'état $j = \frac{1}{2}$ attribué au nucléon.

5.2. INTÉGRALES PREMIÈRES DES ÉTATS ISOBARES

L'attribution d'intégrales premières aux états isobares repose sur le fait que Θ, Φ, Ψ sont considérées comme variables internes tandis que toutes les autres variables du champ $\eta_{\varrho,\sigma}$, φ'_ϱ sont définies comme variables externes. Les champs $\varphi_\varrho(x)$ et $\pi_\varrho(x)$ seront décomposés en leurs parties interne et externe. On obtient aisément la partie interne en posant formellement $\eta_{\varrho,\sigma} = \varphi'_\varrho = \pi_{\varrho,\sigma} = \pi''_\varrho = 0$.

La définition des intégrales premières repose sur l'invariance de la théorie relativement aux rotations spatiales et aux rotations dans l'espace isobarique. Les éléments infinitésimaux générateurs de ces rotations déterminent les intégrales premières.

On trouve d'abord, pour les rotations de l'espace (en utilisant le fait que la fonction $\delta_\varrho(x)$ admise est dépendante de r seul),

$$J_{j,k} = \sum_{\varrho=1}^{3} \int \mathrm{dV}\, \pi_\varrho \left(x_j \frac{\partial}{\partial x_k} - x_k \frac{\partial}{\partial x_j} \right) \varphi_\varrho + \frac{\sigma_{j,k}}{2} \quad (j \neq k), \tag{5.37}$$

et

$$J^2 = J_{1,2}^2 + J_{2,3}^2 + J_{3,1}^2; \tag{5.38}$$

et dans l'espace isobarique

$$T_{\varrho,\sigma} = \int \mathrm{dV}\, (\pi_\varrho \varphi_\sigma - \pi_\sigma \varphi_\varrho) + \frac{\tau_{\varrho,\sigma}}{2} \tag{5.39}$$

et

$$T^2 = T_{1,2}^2 + T_{2,3}^2 + T_{3,1}^2. \tag{5.40}$$

On choisit une représentation diagonale pour J^2, T^2, $J_{12} = J_3$ et $T_{12} = T_3$. En ne retenant que les parties internes de ces observables, on trouve

$$J^2 = T^2 = j(j+1), \tag{5.41}$$

$$J_3 = p_\Phi = m, \tag{5.42}$$

$$T_{1,2} = T_3 = p_\Psi = n \tag{5.43}$$

(cf. ref. [5])).

J^2 représente le spin total du nucléon réel, J_3 est sa composante suivant l'axe z. $T^2 = J^2$ est le carré du spin isobarique et T_3 sa composante suivant l'axe 3 de l'espace isobarique, généralement relié à la charge par

$$L^{(\mathrm{N})} = (n + \tfrac{1}{2})\, e_0 \tag{5.44}$$

où e_0 est la charge élémentaire, pour les nucléons, et

$$L^{(\mathrm{A})} = (n - \tfrac{1}{2}) e_0 \tag{5.45}$$

s'il s'agit d'antinucléons. Dans cette perspective, les antiparticules possèdent un spectre d'excitation analogue à celui des particules, déplacé de $-e_0$ relativement aux charges.

6. Forces Nucléaires

Nous ne soulignons ici qu'un aspect important des forces nucléaires, résultant des théories à couplage fort, aspect qui fut négligé lors du développement de ces théories. Un travail en cours sur le deutéron nous permettra d'y revenir plus longuement.

Dès l'instant où une structure a été adoptée pour le nucléon, le problème des forces nucléaires est déterminé. Si l'on néglige le terme en G^2, le potentiel d'interaction entre deux nucléons se ramène à des formules connues [6]). Si le premier nucléon se trouve en $\mathbf{x}_1$, le second en $\mathbf{x}_2$, avec $\mathbf{R} = \mathbf{x}_2 - \mathbf{x}_1$, et Θ_1, Φ_1, Ψ_1; Θ_2, Φ_2, Ψ_2 désignant les variables internes de chacun des nucléons, on a

$$V_{1,2}(\mathbf{R}) = V_0\left\{\Gamma_1 \frac{e^{-z}}{z} + \Gamma_2 \frac{e^{-z}}{z}\left(1+\frac{3}{z}+\frac{3}{z^2}\right)\right\} \tag{6.1}$$

où $\mathbf{z} = \mu\mathbf{R}$, $V_0 = (g\mu)^2\mu/36\pi$,

$$\Gamma_1 = 3\sum_{\varrho=1}^{3}(\mathbf{e}_{\varrho,1}\cdot\mathbf{e}_{\varrho,2}),\ \Gamma_2 = 9\left\{\frac{3(\mathbf{e}_{\varrho,1}\cdot\mathbf{z})(\mathbf{e}_{\varrho,2}\cdot\mathbf{z})}{z^2} - (\mathbf{e}_{\varrho,1}\cdot\mathbf{e}_{\varrho,2})\right\}, \tag{6.2}$$

$$(\mathbf{e}_{\varrho,1})_j = S_{j,\varrho}(\Theta_1,\ \Phi_1,\ \Psi_1),\ (\mathbf{e}_{\varrho,2})_j = S_{j,\varrho}(\Theta_2,\ \Phi_2,\ \Psi_2). \tag{6.3}$$

Mais la formule (6.1), bien connue en couplage fort, n'est valable que pour des valeurs de R

$$R > r_c \approx a; \tag{6.4}$$

car un calcul élémentaire montre que l'effet de la fonction de forme $\delta_a(x)$ est d'introduire pour $R < r_c \approx a$ un potentiel fortement répulsif:

$$V_{1,2}(\mathbf{R}) \approx \infty \text{ pour } R < r_c \approx a. \tag{6.5}$$

Le potentiel d'interaction de deux nucléons est représenté par les formules (6.1) valable pour $R > r_c$ et (6.5) pour $R < r_c$. Ce fait change appréciablement les résultats obtenus naguère [7]) sur les états ^3S et ^1S du système proton-neutron.

7. Résultats et Conclusions

Dans ce travail, le terme en G^2 a été systématiquement ignoré dans (4.5). Une étude appronfondie de son influence sur les isobares (5.35) et sur les forces nucléaires (6.1) a montré qu'elle se traduit pratiquement par une augmentation de 25 % du rayon nucléonique donné par la formule (5.7) usant de (4.57). C'est cette valeur corrigée de a qui entre dans les résultats qui suivent.

Si l'on utilise la formule (5.7), on trouve pour a corrigé

$$a \approx \frac{2.5}{M},\ \text{donc}\ a\mu \approx \tfrac{1}{3}, \tag{7.1}$$

et pour r_c (6.4,5)

$$r_c \approx a. \tag{7.2}$$

Admettons que l'énergie d'excitation de l'isobare $j = 3/2$ se situe aux environs de 280—300 MeV:

$$\Delta E_{j=3/2} = \frac{9\pi a}{g^2} = 280\text{—}300\ \text{MeV}. \tag{7.3}$$

Cela donne pour V_0 de (6.1)

$$V_0 \approx 6\text{—}6.6\ \text{MeV et}\ g \approx 6a, \tag{7.4}$$

et les calculs en cours sur le deutéron montrent que les résultats sont alors en accord avec l'expérience pour les états ^1S et ^3S.

La méthode appliquée au champ pseudoscalaire mixte, en interaction pseudoscalaire, donne donc des résultats satisfaisants. Mais, comme le titre du travail l'indique, notre but est surtout de montrer que la méthode proposée conduit à une analyse nouvelle des théories du type Yukawa. Le fait de tenir compte de la singularité introduite par la valeur $G = 0$, dans les équations couplées, révèle une richesse insoupçonnée de ces théories et doit permettre dans l'avenir de mieux discerner celle qui correspond à la réalité.

Bibliographie

1) R. Jastrow, Phys. Rev. **81** (1951) 165
2) E. E. Chambers and R. Hofstadter, CERN Symposium (1956)
3) G. F. Chew, Phys. Rev. **89** (1953) 591; **95** (1954) 285
F. J. Dyson *et al.*, Phys. Rev. **95** (1954) 1644
G. F. Chew and F. E. Low, Phys. Rev. **101** (1956) 1570, 1579
4) M. M. Lévy, Phys. Rev. **88** (1952) 72, 725
5) W. Pauli et S. M. Dancoff, Phys. Rev. **62** (1952) 85, § 4
G. Wentzel, Helvet. Phys. Acta **16** (1943) 551, § 4; *ibid.* **13** (1940) 269
R. Serber et S. M. Dancoff, Phys. Rev. **63** (1943) 143
S. Tomonaga, Progr. Th. Phys. **1** (1946) 83, 108; *ibid.* **2** (1947) 6, 22; *ibid.* **3** (1948) 36
6) W. Pauli, Meson theory of nuclear forces (Int. Publ., 1946) Ch. VI; W. Pauli et S. Kusaka, Phys Rev. **63** (1943) 400, en particulier formules (61) et (62)
7) F. Villars, Helvet. Phys. Acta **19** (1946) 323

Nuclear Physics **4** (1957) 427—452; © *North-Holland Publishing Co., Amsterdam*
Not to be reproduced by photoprint or microfilm without written permission from the publisher

PHOTOPRODUCTION PROCESSES AND DISPERSION RELATIONS

A. A. LOGUNOV AND A. N. TAVKHELIDZE

Joint Institute of Nuclear Research, Laboratory of Theoretical Physics, Dubna, U.S.S.R.

and

L. D. SOLOVYOV

Moscow State University, U.S.S.R.

Received 14 February 1957

Abstract: Dispersion relations for photoproduction of π-mesons on nucleons are obtained. The role of "bound states" is discussed in connection with an analysis of the unobservable energy region. The matrix structure of the photoproduction amplitude is considered. The dispersion relations are presented in a form convenient for phase shift analysis.

Introduction

A study of scattering of π-mesons on nucleons or of photoproduction of π-mesons on nucleons is particularly important as this is the simplest way of obtaining data on the interaction between meson and nucleon fields. Investigation of π-meson scattering, photoproduction, etc., have revealed the inadequacy of theoretical calculations based on the current perturbation theory. In this connection a theoretical investigation of meson-nucleon interaction without recourse to perturbation theory seemed to be of particular interest. A work of this type is that of Goldberger *et al.* [1]) on the deduction of the dispersion relations. Comparison of the theoretical and experimental results demonstrated the fruitfulness of the new method and this explains the keen interest recently evoked by work on the deduction of the dispersion relations for various processes.

However, in the work of Goldberger and subsequent authors the dispersion relations were not deduced with sufficient mathematical rigorousness. The attempts made by some authors to provide the required mathematical basis did not meet with success.

A proof of the existence of dispersion relations for an arbitrary scattering angle was obtained by N. N. Bogolyubov on basis of general principles of present-day quantum field theory [2]) †. A proof for the particular case of forward scattering has been presented by Symanzik †.

Dispersion relations for photoproduction of π-mesons on nucleons are derived in the present work. The main results of this work were reported at the All-Union Conference on High Energy Particle Physics in Moscow in May 1956 (see also ref. [3, 4, 5])).

† Reported at the Seattle, USA, conference in September 1956.

An analysis of the photoproduction dispersion relations [3, 4, 5]) shows that the results obtained in ref. [6]) are erroneous. It should be noted that some of the results of ref. [3, 4]) have been recently obtained in another paper [7]).

1. Photoproduction Amplitude

Let $\varphi_\varrho^{(-)}(q)$ denote the absorption operator for a meson of the kind ϱ ($\varrho = 1, 2, 3$) and let $a_\nu^{(+)}(k)$ ($\nu = 1, 2$) denote the photon creation operator. With the aid of the S-matrix formalism the photoproduction matrix element can then be written in the form

$$S(\alpha, k;\ \omega,\ q) = (2\pi)^3 \langle \phi^*_{\nu' s'}\, \varphi_\varrho^{(-)}(q) S\, a_\nu^{(+)}(k) \phi_{ps} \rangle. \tag{1.1}$$

Here ϕ_{ps} denotes the amplitude of the scatterer state and the indices α and ω, which refer respectively to the initial and final states, contain all quantum numbers characterizing the system, excepting the photon and meson momenta.

Since †

$$\begin{aligned} A_\mu(x) &= \frac{1}{(2\pi)^{3/2}} \int \frac{\mathrm{d}\mathbf{k}}{\sqrt{2k^0}} \{a_\lambda^{(+)}(k) \mathrm{e}^{ikx} + a_\lambda^{(-)}(k) \mathrm{e}^{-ikx}\} e_\mu^{\ \lambda} \\ \varphi_\varrho(x) &= \frac{1}{(2\pi)^{3/2}} \int \frac{\mathrm{d}\mathbf{q}}{\sqrt{2q^0}} \{\varphi_\varrho^{(+)}(q) \mathrm{e}^{iqx} + \varphi_\varrho^{(-)}(q) \mathrm{e}^{-iqx}\} \end{aligned} \tag{1.2}$$

one gets

$$\begin{aligned} [\varphi_\varrho^{(-)}(q),\ \varphi_\varrho(x)] &= \frac{(2\pi)^{-3/2}}{\sqrt{2q^0}} \mathrm{e}^{iqx} \\ [A_\mu(x),\ a_\nu^{(+)}(k)] &= \frac{(2\pi)^{-3/2}}{\sqrt{2k^0}} \mathrm{e}^{-ikx} e_\mu^{\ \nu}(k) \end{aligned} \tag{1.3}$$

and hence

$$\begin{aligned} [\varphi_\varrho^{(-)}(q),\ S] &= \frac{(2\pi)^{-3/2}}{\sqrt{2q^0}} \int \mathrm{e}^{iqx} \frac{\delta S}{\delta \varphi_\varrho(x)} \mathrm{d}x \\ [S,\ a_\nu^{(+)}(k)] &= \frac{(2\pi)^{-3/2}}{\sqrt{2k^0}} \int \mathrm{e}^{-iky} \frac{\delta S}{\delta A_\mu(y)} e_\mu^{\ \nu}(k) \mathrm{d}y. \end{aligned} \tag{1.4}$$

Writing in (1.1) all the creation operators to the left and all the annihilation operators to the right we obtain with the help of (1.4)

$$S(\alpha,\ k;\ \omega,\ q) = \sum_\mu e_\mu^{\ \nu}(k) S^{\mu\varrho} \tag{1.5}$$

where

† The following notations have been employed in the present work:

$$kx = k^0 x^0 - \mathbf{k} \cdot \mathbf{x},$$

$$\gamma^\mu \gamma^\nu + \gamma^\nu \gamma^\mu = 2g^{\mu\nu};\ g^{00} = 1,\ g^{11} = g^{22} = g^{33} = -1.$$

$$S^{\mu\varrho} = \frac{1}{\sqrt{4k^0 q^0}} \int e^{i(qx-ky)} \langle \phi^*_{p's'} \frac{\delta^2 S}{\delta\varphi_\varrho(x)\delta A_\mu(y)} \phi_{ps} \rangle \, dx dy.$$

We shall assume that ϕ_{ps} describes a scatterer in the ground energy state. No spontaneous processes will then be able to occur and

$$S\phi_{ps} = \phi_{ps} \tag{1.6}$$

or, in virtue of the unitarity property of the S-matrix

$$S^+ \phi_{ps} = \phi_{ps}. \tag{1.7}$$

In virtue of (1.7) one may rewrite (1.5) as follows:

$$S^{\mu\varrho} = \frac{1}{\sqrt{4k^0 q^0}} \int e^{i(qx-ky)} \langle \phi^*_{p's'} \frac{\delta^2 S}{\delta\varphi_\varrho(x)\delta A_\mu(y)} S^\dagger \phi_{ps} \rangle \, dx dy. \tag{1.8}$$

We introduce the operators

$$\begin{aligned} j^\varrho(x) &= i \frac{\delta S}{\delta\varphi_\varrho(x)} S^\dagger \\ i^\mu(x) &= i \frac{\delta S}{\delta A_\mu(x)} S^\dagger \end{aligned} \tag{1.9}$$

which we shall respectively call the meson current operator and electromagnetic current operator. The operators $j^\varrho(x)$ and $i^\mu(x)$ are hermitian. Indeed,

$$j^{\varrho+}(x) = -iS \frac{\delta S^\dagger}{\delta\varphi_\varrho(x)};$$

but since $S^\dagger S = 1$, it follows that

$$S \frac{\delta S^\dagger}{\delta\varphi_\varrho(x)} = -\frac{\delta S}{\delta\varphi_\varrho(x)} S^\dagger$$

and hence

$$j^{\varrho+}(x) = j^\varrho(x), \tag{1.10}$$

and similarly

$$i^{\mu+}(y) = i^\mu(y). \tag{1.11}$$

By variation of (1.9) the following relations can be obtained:

$$\begin{aligned} \frac{\delta^2 S}{\delta A_\mu(y)\delta\varphi_\varrho(x)} S^\dagger &= -j^\varrho(x) i^\mu(y) - i \frac{\delta j^\varrho(x)}{\delta A_\mu(y)} \\ \frac{\delta^2 S}{\delta A_\mu(y)\delta\varphi_\varrho(x)} S^\dagger &= -i^\mu(y) j^\varrho(x) - i \frac{\delta i^\mu(y)}{\delta\varphi_\varrho(x)}. \end{aligned} \tag{1.12}$$

Subtracting one of these formulae from the other we get

$$\frac{\delta i^\mu(y)}{\delta\varphi_\varrho(x)} - \frac{\delta j^\varrho(x)}{\delta A_\mu(y)} = -i[j^\varrho(x), \, i^\mu(y)]. \tag{1.13}$$

Let us consider the expression $\langle \phi^*_{p's'} j^\varrho(x) i^\mu(y) \phi_{ps} \rangle$. To do this we change to the Heisenberg representation

$$\langle \phi^*_{p's'} j^\varrho(x) i^\mu(y) \phi_{ps} \rangle = \langle \psi^*_{p's'} J^\varrho(x) I^\mu(y) \psi_{ps} \rangle. \tag{1.14}$$

Here J and I are current operators in the real particle representation and ψ_{ps} is the amplitude of the nucleon state in the same representation. Suppose that energy-momentum operator $\hat{P}$ for the system under consideration possesses a complete system of eigenfunctions which we shall denote by $\psi_{n,\mathbf{l}}$. The index $\mathbf{l}$ denotes the momentum of the system and n the remaining quantum numbers defining the state of the system. The energy of the n-th state of the system will be

$$E_n = \sqrt{M_n^2 + \mathbf{l}^2}. \tag{1.15}$$

Since the system was assumed to be complete one may write

$$\langle \psi^*_{p's'} J^\varrho(x) I^\mu(y) \psi_{ps} \rangle = \frac{1}{(2\pi)^3} \sum_n \int d\mathbf{l} \langle \psi^*_{p's'} J^\varrho(x) \psi_{\mathbf{l},n} \rangle \langle \psi^*_{\mathbf{l},n} I^\mu(y) \psi_{ps} \rangle. \tag{1.16}$$

From translational invariance considerations the operators $J^\varrho(x)$ and $I^\mu(y)$ may be written as follows:

$$\begin{aligned} J^\varrho(x) &= e^{i\hat{p}x} J^\varrho(0)\, e^{-i\hat{p}x}, \\ I^\mu(y) &= e^{i\hat{p}y} I^\mu(0)\, e^{-i\hat{p}y} \end{aligned} \tag{1.17}$$

Inserting (1.17) into (1.16) and keeping in mind that $\psi_{\mathbf{l},n}$ are eigenfunctions of the energy-momentum operator $\hat{P}$ we obtain

$$\begin{aligned} \langle \psi^*_{p's'} J^\varrho(x) I^\mu(y) \psi_{ps} \rangle &= \frac{1}{(2\pi)^3} \sum_n \int d\mathbf{l} \langle \psi^*_{p's'} J^\varrho(0) \psi_{\mathbf{l},n} \rangle \langle \psi^*_{\mathbf{l},n} I^\mu(0) \psi_{ps} \rangle \\ &\cdot \exp\left\{ -il_n(x-y) + \frac{i}{2}(p+p')(x-y) + \frac{i}{2}(p'-p)(x+y) \right\}; \end{aligned} \tag{1.18}$$

$$l_n x = \sqrt{M_n^2 + \mathbf{l}^2}\, x^0 - \mathbf{l} \cdot \mathbf{x}:$$

Introducing the notation

$$\begin{aligned} F^{\varrho\mu}_{p's';ps}(x-y) &= \frac{1}{(2\pi)^3} \sum_n \int d\mathbf{l} \langle \psi^*_{p's'} J^\varrho(0) \psi_{\mathbf{l},n} \rangle \langle \psi^*_{\mathbf{l},n} I^\mu(0) \psi_{ps} \rangle \\ &\cdot \exp\left\{ -il_n(x-y) + \frac{i}{2}(p+p')(x-y) \right\} \end{aligned} \tag{1.19}$$

we can write (1.18) in the form

$$\langle \psi^*_{p's'} J^\varrho(x) I^\mu(y) \psi_{ps} \rangle = e^{i\frac{p'-p}{2}(x+y)} F^{\varrho\mu}_{p's';ps}(x-y). \tag{1.20}$$

Similarly, from translation invariance considerations one may write

$$\langle \phi^*_{p's'} \frac{\delta^2 S}{\delta A_\mu(y) \delta \varphi_\varrho(x)} S^\dagger \phi_{ps} \rangle = e^{i\frac{p'-p}{2}(x+y)} V^{\varrho\mu}_{p's';ps}(x-y), \tag{1.21a}$$

$$\langle \phi^*_{p's'} \frac{\delta i^\mu(y)}{\delta \varphi_\varrho(x)} \phi_{ps} \rangle = e^{i\frac{p'-p}{2}(x+y)} W^{\varrho\mu}_{p's';\,ps}(x-y), \tag{1.21b}$$

$$\langle \phi^*_{p's'} i^\mu(y) j^\varrho(x) \phi_{ps} \rangle = e^{i\frac{p'-p}{2}(x+y)} F^{\mu\varrho}_{p's';\,ps}(y-x). \tag{1.21c}$$

We shall now establish some relationships between functions F, V and W. From formulae (1.20) and (1.21) it follows that

$$\overset{*}{F}{}^{\varrho\mu}_{p's';\,ps}(x) = F^{\mu\varrho}_{ps;\,p's'}(-x). \tag{1.22}$$

Using relations (1.12) and (1.13) we find

$$V^{\varrho\mu}_{p's';\,ps}(x) = -iW^{\varrho\mu}_{p's';\,ps}(x) - F^{\mu\varrho}_{p's';\,ps}(-x) \tag{1.23a}$$

$$W^{\varrho\mu}_{p's';\,ps}(x) - W^{\mu\varrho}_{p's';\,ps}(-x) = -i[F^{\varrho\mu}_{p's';\,ps}(x) - F^{\mu\varrho}_{p's';\,ps}(-x)] \tag{1.23b}$$

$$\overset{*}{W}{}^{\varrho\mu}_{p's';\,ps}(x) = W^{\varrho\mu}_{ps;\,p's'}(x). \tag{1.23c}$$

In accord with (1.21a) formula (1.8) can be written in the following form:

$$S^{\mu\varrho} = \frac{1}{\sqrt{4k^0 q^0}} \int e^{\frac{i}{2}(k+q)(x-y)+\frac{i}{2}(q-k)(x+y)+\frac{i}{2}(p'-p)(x+y)} V^{\varrho\mu}_{p's';\,ps}(x-y)\,dx\,dy. \tag{1.24}$$

After integrating over $(x+y)$ we obtain

$$S^{\mu\varrho} = \frac{i(2\pi)^4}{\sqrt{4k^0 q^0}} \delta(p'+q-p-k) T^{\varrho\mu}_{p's';\,ps}\left(\frac{k+q}{2}\right) \tag{1.25}$$

where

$$T^{\varrho\mu}_{p's';\,ps}\left(\frac{k+q}{2}\right) = -i \int e^{i\frac{k+q}{2}x} V^{\varrho\mu}_{p's';\,ps}(x)\,dx.$$

2. Auxiliary Amplitude and Its Properties

Expression (1.25) is somewhat complicated for investigation. We introduce the amplitude

$$\mathcal{M}(\alpha, k; \omega, q) = -\frac{i}{\sqrt{4k^0 q^0}} \sum_\mu e^*_\mu \int e^{i(qx-ky)} \langle \phi^*_{p's'} \frac{\delta i^\mu(y)}{\delta \varphi_\varrho(x)} \phi_{ps} \rangle\,dx\,dy, \tag{2.1}$$

which, in virtue of (1.21b), can be rewritten in the form

$$\mathcal{M}(\alpha, k; \omega, q) = -\frac{i}{\sqrt{4k^0 q^0}} \sum_\mu e^*_\mu \int e^{\frac{i}{2}(k+q)(x-y)+\frac{i}{2}(q-k)(x+y)+\frac{i}{2}(p'-p)(x+y)} W^{\varrho\mu}_{p's';\,ps}(x-y)\,dx\,dy. \tag{2.2}$$

Performing the integrating with respect to $(x+y)$ we obtain

$$\mathcal{M}(\alpha, k; \omega, q) = \frac{i(2\pi)^4}{\sqrt{4k^0 q^0}} \delta(p'+q-p-k) \sum_\mu M^{\varrho\mu}_{p's';\,ps}\left(\frac{k+q}{2}\right) e^*_\mu \tag{2.3}$$

where

$$M^{\alpha\mu}_{p's';ps}\left(\frac{k+q}{2}\right) = -\int e^{i\frac{k+q}{2}x} W^{\alpha\mu}_{p's';ps}(x)dx.$$

We shall show that in the observable region (the momenta are real and the energies positive), the amplitudes T and M are equal. Subtracting (2.3) from (1.25) and taking into account (1.23a) we obtain

$$T^{\alpha\mu}_{p's';ps}\left(\frac{k+q}{2}\right) - M^{\alpha\mu}_{p's';ps}\left(\frac{k+q}{2}\right) = i\int e^{i\frac{k+q}{2}x} F^{\mu\alpha}_{p's';ps}(-x)dx. \quad (2.4)$$

Inserting the expression (1.19) for F into (2.4) and performing elementary calculations we obtain

$$T^{\alpha\mu}_{p's';ps}\left(\frac{k+q}{2}\right) - M^{\alpha\mu}_{p's';ps}\left(\frac{k+q}{2}\right)$$

$$= 2\pi i \sum_n \langle \psi^*_{p's'} I^\mu(0)\psi_{1,n}\rangle\langle \psi^*_{1,n} J^\alpha(0)\psi_{ps}\rangle \delta\left(\sqrt{M_n^2+\mathbf{l}^2} + \frac{k^0+q^0}{2} - \frac{p^0+p'^0}{2}\right). \quad (2.5)$$

It can be shown that in the observable region the argument of the δ-functions is greater than zero. Indeed, from the laws of conservation of energy and momentum

$$k^0 - p'^0 = q^0 - p^0$$

$$\mathbf{p}' - \mathbf{k} = \mathbf{p} - \mathbf{q}$$

we get

$$\sqrt{M_n^2+\mathbf{l}^2} + \frac{k^0+q^0}{2} - \frac{p^0+p'^0}{2} = \sqrt{M_n^2+(\mathbf{p}-\mathbf{q})^2} + \sqrt{\mu^2+\mathbf{q}^2} - \sqrt{M^2+\mathbf{p}^2}.$$

As $M_n \geqq M$, in order to prove the correctness of the statement made above one should show that

$$\sqrt{M^2+(\mathbf{p}-\mathbf{q})^2} > \sqrt{M^2+\mathbf{p}^2} - \sqrt{\mu^2+\mathbf{q}^2}.$$

It is not difficult to prove this inequality by eliminating the root signs. Thus, in a real region, amplitudes T and M are equal.

In the future we shall work in the coordinates system in which

$$\mathbf{p}+\mathbf{p}' = 0. \quad (2.6)$$

Employing the laws of conservation of energy and momentum

$$\mathbf{k}^2 = \mathbf{q}^2+\mu^2$$

$$\mathbf{k}-\mathbf{q} = -2\mathbf{p}$$

we obtain

$$\frac{\mathbf{k}-\mathbf{q}}{2} = -\mathbf{p}$$

$$\frac{\mathbf{k}+\mathbf{q}}{2} = \lambda\mathbf{e} - \frac{\mu^2}{4\mathbf{p}^2}\mathbf{p}. \quad (2.7)$$

Vector **e** is orthogonal to vector **p**. It is easy to obtain from expressions (2.7) that

$$\begin{aligned}\mathbf{k} &= \lambda\mathbf{e}-[1+(\mu^2/4\mathbf{p}^2)]\mathbf{p}\\ \mathbf{q} &= \lambda\mathbf{e}+[1-(\mu^2/4\mathbf{p}^2)]\mathbf{p}.\end{aligned} \tag{2.8}$$

The quantity λ can be expressed in terms of the meson energy E as follows

$$E^2 = \lambda^2+[1+(\mu^2/4\mathbf{p}^2)]^2\mathbf{p}^2. \tag{2.9}$$

After the remarks made above regarding the system of coordinates chosen by us we return to our study of the properties of amplitude M which we write in the form

$$M^{\sigma\mu}_{\sigma'\sigma';\,\rho\rho} = D^{\sigma\mu}_{\sigma'\sigma';\,\rho\rho}+iA^{\sigma\mu}_{\sigma'\sigma';\,\rho\rho} \tag{2.10}$$

where

$$D^{\sigma\mu}_{\sigma'\sigma';\,\rho\rho} = \tfrac{1}{2}(M^{\sigma\mu}_{\sigma'\sigma';\,\rho\rho}+\overset{*}{M}{}^{\mu\sigma}_{\rho\rho;\,\sigma'\sigma'}) \tag{2.10a}$$

$$A^{\sigma\mu}_{\sigma'\sigma';\,\rho\rho} = \frac{1}{2i}(M^{\sigma\mu}_{\sigma'\sigma';\,\rho\rho}-\overset{*}{M}{}^{\mu\sigma}_{\rho\rho;\,\sigma'\sigma'}). \tag{2.10b}$$

Substituting the expression for M (2.3) in (2.10a) and (2.10b) and taking into account properties (1.23), we get

$$A^{\sigma\mu}_{\sigma'\sigma';\,\rho\rho}\left(\frac{k+q}{2}\right) = \frac{1}{2}\int e^{i\frac{k+q}{2}x}\{F^{\sigma\mu}_{\sigma'\sigma';\,\rho\rho}(x)-F^{\mu\sigma}_{\sigma'\sigma';\,\rho\rho}(-x)\}\,dx, \tag{2.11}$$

$$D^{\sigma\mu}_{\sigma'\sigma';\,\rho\rho}\left(\frac{k+q}{2}\right) = -\frac{1}{2}\int e^{i\frac{k+q}{2}x}\{W^{\sigma\mu}_{\sigma'\sigma';\,\rho\rho}(x)+W^{\mu\sigma}_{\sigma'\sigma';\,\rho\rho}(-x)\}\,dx. \tag{2.12}$$

We now introduce functions X and Y as follows:

$$X^{\sigma\nu}_{\sigma'\sigma';\,\rho\rho}\left(\frac{k+q}{2}\right) = \sum_{\mu} e_\mu{}^{\nu} D^{\sigma\mu}_{\sigma'\sigma';\,\rho\rho}\left(\frac{k+q}{2}\right), \tag{2.13}$$

$$Y^{\sigma\nu}_{\sigma'\sigma';\,\rho\rho}\left(\frac{k+q}{2}\right) = \sum_{\mu} e_\mu{}^{\nu} A^{\sigma\mu}_{\sigma'\sigma';\,\rho\rho}\left(\frac{k+q}{2}\right). \tag{2.14}$$

By making use of relations (2.11—2.14) and also the invariance properties of the amplitude $M^{\sigma\mu}_{\sigma'\sigma';\,\rho\rho}$ upon reflection of the momenta we can obtain the following important relations:

$$P_{ss'}\overset{*}{X}{}^{\sigma\nu}_{\sigma'\sigma';\,\rho\rho}\left(\frac{k^0+q^0}{2},\ \frac{\mathbf{k}+\mathbf{q}}{2}\right) = X^{\sigma\nu}_{\sigma'\sigma';\,\rho\rho}\left(-\frac{k^0+q^0}{2},\ \frac{\mathbf{k}+\mathbf{q}}{2}\right). \tag{2.15}$$

$$P_{ss'}\overset{*}{Y}{}^{\sigma\nu}_{\sigma'\sigma';\,\rho\rho}\left(\frac{k^0+q^0}{2},\ \frac{\mathbf{k}+\mathbf{q}}{2}\right) = -Y^{\sigma\nu}_{\sigma'\sigma';\,\rho\rho}\left(-\frac{k^0+q^0}{2},\ \frac{\mathbf{k}+\mathbf{q}}{2}\right) \tag{2.16}$$

$P_{ss'}$ is the spin transposition operator $s \rightleftarrows s'$.

Indeed

$$\overset{*}{Y}{}^{\sigma\nu}_{\sigma'\sigma';\,\rho\rho}\left(\frac{k+q}{2}\right) = \frac{1}{2}\sum_{\mu}\int e^{-i\frac{k+q}{2}x}\{\overset{*}{F}{}^{\sigma\mu}_{\sigma'\sigma';\,\rho\rho}(x)-\overset{*}{F}{}^{\mu\sigma}_{\sigma'\sigma';\,\rho\rho}(-x)\}\,e_\mu{}^{\nu}\,dx.$$

In virtue of (1.22) this expression can be rewritten as follows:

$$\overset{*}{Y}{}^{\varrho\nu}_{p'\sigma';\,p\sigma}\left(\frac{k+q}{2}\right)=-\frac{1}{2}\int e^{-i\frac{k+q}{2}x}\{F^{\varrho\mu}_{p\sigma;\,p'\sigma'}(x)-F^{\mu\varrho}_{p\sigma;\,p'\sigma'}(-x)\}\,e_\mu{}^\nu\,dx. \quad (2.17)$$

Comparing (2.17) and (2.14) and taking into account invariance of the reaction amplitude upon reflection of the momenta

$$\mathbf{k}\to-\mathbf{k},\ \mathbf{q}\to-\mathbf{q},\ \mathbf{p}\to-\mathbf{p},\ \mathbf{p}'\to-\mathbf{p}';\ (\mathbf{p}=-\mathbf{p}')$$

one can verify the validity of (2.16) in the coordinates system chosen by us. In an analogous manner it can be proved that relation (2.15) also holds.

With the help of (2.15) and (2.16) one can construct the combinations

$$(1\pm P)X^{\varrho\nu}_{p'\sigma';\,p\sigma}(E)=X^{\varrho\nu}_{p'\sigma';\,p\sigma}(E)\pm P_{\sigma\sigma'}X^{\varrho\nu}_{p'\sigma';\,p\sigma}(E) \quad (2.18)$$

$$(1\pm P)Y^{\varrho\nu}_{p'\sigma';\,p\sigma}(E)=Y^{\varrho\nu}_{p'\sigma';\,p\sigma}(E)\pm P_{\sigma\sigma'}\overset{*}{Y}{}^{\varrho\nu}_{p'\sigma';\,p\sigma}(E) \quad (2.19)$$

which possess the following parity properties with respect to E:

$$\begin{array}{lll}(1+P)X^{\varrho\nu}_{p'\sigma';\,p\sigma}(E) & & \text{even}\\ (1-P)X^{\varrho\nu}_{p'\sigma';\,p\sigma}(E) & \text{is an} & \text{odd}\\ (1+P)Y^{\varrho\nu}_{p'\sigma';\,p\sigma}(E) & & \text{odd}\\ (1-P)Y^{\varrho\nu}_{p'\sigma';\,p\sigma}(E) & & \text{even}\end{array}\quad \text{function of } E. \quad (2.20)$$

Role of "Bound States" in Photoproduction Processes

A study of the significance of "bound states" in the dispersion relations for photoproduction processes is quite important since this problem involves an analysis of the unobservable energy region in the dispersion formulae. In the coordinates system chosen by us ($\mathbf{p}+\mathbf{p}'=0$) the photoproduction threshold is

$$E_p=\frac{\mathbf{p}^2+\frac{1}{4}\mu^2}{|\mathbf{p}|}.$$

We shall consider the energy region E in which $E<E_p$ and hence formation of a virtual "bound state" is possible. The situation we encounter in this case is similar to that which arises in the scattering of π-mesons on nucleons.

Inserting expression (1.19) into (2.11) and integrating over x we obtain

$$\begin{aligned}Y^{\varrho\nu}_{p'\sigma';\,p\sigma}(E,\ \lambda\mathbf{e})=\pi\sum_n e_\mu{}^\nu\langle\psi^*_{-p,\sigma'}J^\varrho(0)\psi_{n,\,\lambda\mathbf{e}-t\mathbf{p}}\rangle\langle\psi^*_{n,\,\lambda\mathbf{e}-t\mathbf{p}}I^\mu(0)\psi_{p\sigma}\rangle\\ \cdot\delta(\sqrt{M^2+\mathbf{p}^2}+E-\sqrt{M_n{}^2+\lambda^2+t^2\mathbf{p}^2})\\ -\pi\sum_n e_\mu{}^\nu\langle\psi^*_{-p,\sigma'}I^\mu(0)\psi_{n,\,-\lambda\mathbf{e}+t\mathbf{p}}\rangle\langle\psi^*_{n,\,-\lambda\mathbf{e}+t\mathbf{p}}J^\varrho(0)\psi_{p\sigma}\rangle\\ \cdot\delta(\sqrt{M^2+\mathbf{p}^2}-E-\sqrt{M_n{}^2+\lambda^2+t^2\mathbf{p}^2})\end{aligned} \quad (3.1)$$

where $t=\frac{1}{4}\mu^2/\mathbf{p}^2$.

Because of the smallness of the coupling constant e (electric charge) the interaction energy in an electromagnetic field can be considered as a perturbation. A result of this is that the expansion can be carried out in terms of the eigenfunctions of the meson-nucleon system energy-momentum vector. Keeping in mind the approximation made above and the supposition concerning the absence between M and $M+\mu$ of bound states of the meson nucleon system one can show (for small scatterer momenta $\mathbf{p}^2 < \frac{1}{2}M\mu$) that in the energy interval

$$0 < E < \frac{M\mu+\frac{1}{4}\mu^2-\mathbf{p}^2}{\sqrt{M^2+\mathbf{p}^2}} \tag{3.2}$$

the quantity $Y^{\sigma\sigma'}_{\mathbf{p}'s';\,\mathbf{p}s}(E,\,\lambda\mathbf{e})$ can be expressed by the formula

$$Y^{\sigma\sigma'}_{\mathbf{p}'s';\,\mathbf{p}s}(E,\,\lambda\mathbf{e}) = -\pi\,\frac{M^2-\frac{1}{4}\mu^2}{M^2+\mathbf{p}^2}\sum_{s''} e_\mu{}^{\sigma}\langle\psi^*_{-\mathbf{p},s'}I^\mu(0)\psi_{-\lambda\mathbf{e}+t\mathbf{p},s''}\rangle$$
$$\cdot\langle\psi^*_{-\lambda\mathbf{e}+t\mathbf{p},s''}J^\sigma(0)\psi_{\mathbf{p}s}\rangle\delta\left(E-\frac{\mathbf{p}^2+\frac{1}{4}\mu^2}{\sqrt{M^2+\mathbf{p}^2}}\right). \tag{3.3}$$

Indeed, consider the δ-functions of expression (3.1). It can readily be shown that for $M_n = M$ these functions have δ-peculiarities at energies

$$E_1 = -\frac{\mathbf{p}^2+\frac{1}{4}\mu^2}{\sqrt{M^2+\mathbf{p}^2}}$$

for the first δ-function and

$$E_2 = \frac{\mathbf{p}^2+\frac{1}{4}\mu^2}{\sqrt{M^2+\mathbf{p}^2}}$$

for the second δ-function. In the case when $M_n \neq M$ $(M_n \geqq M+\mu)$ δ-peculiarities in these functions occur at energies

$$E_1' \geqq \frac{M\mu+\frac{1}{4}\mu^2-\mathbf{p}^2}{\sqrt{M^2+\mathbf{p}^2}}$$

for the first δ-function and

$$E_2' \leqq -\frac{M\mu+\frac{1}{4}\mu^2-\mathbf{p}^2}{\sqrt{M^2+\mathbf{p}^2}}$$

for the second δ-function.

If $\mathbf{p}^2 \leqq \frac{1}{2}M\mu$ (small scatterer momenta) it can easily be seen that

$$E_2 < E_1'$$

and thus in interval (3.2) the function $Y^{\sigma\sigma'}_{\mathbf{p}'s';\,\mathbf{p}s}$ can be represented by formula (3.3). In deriving (3.3) we took into account that

$$\delta(E+\sqrt{M^2+\lambda^2+t^2\mathbf{p}^2}-\sqrt{M^2+\mathbf{p}^2}) = \frac{M^2-\frac{1}{4}\mu^2}{M^2+\mathbf{p}^2}\,\delta\left(E-\frac{\mathbf{p}^2+\frac{1}{4}\mu^2}{\sqrt{M^2+\mathbf{p}^2}}\right).$$

When separating the unobservable energy range the following circumstance should be kept in mind; if

$$\frac{M\mu}{2} > \mathbf{p}^2 > \tfrac{1}{4}\mu^2 \frac{M}{M+\mu} \tag{3.3a}$$

the lower integration limit will be smaller than the photoproduction threshold and the unobservable energy region will lie in the interval

$$\frac{M\mu+\frac{1}{4}\mu^2-\mathbf{p}^2}{\sqrt{M^2+\mathbf{p}^2}} < E < \frac{\mathbf{p}^2+\frac{1}{4}\mu^2}{|\mathbf{p}|}.$$

If, however,

$$\mathbf{p}^2 = \tfrac{1}{4}\mu^2 \frac{M}{M+\mu} \tag{3.3b}$$

the lower integration limit will coincide with the photoproduction threshold and no unobservable energy region will exist. In conclusion we shall consider in this section the mean current values which enter expression (3.3). As an example we shall compute the mean value of the meson current $J^\varrho(0)$. The mean value of the electromagnetic current can be computed in a similar manner. We have

$$\langle \psi^*_{\mathbf{p}',s'} J^\varrho(x) \psi_{\mathbf{p}s} \rangle = e^{i(p'-p)x} \langle \psi^*_{\mathbf{p}'s'} J^\varrho(0) \psi_{\mathbf{p}s} \rangle$$

and on the other hand

$$\langle \psi^*_{\mathbf{p}'s'} J^\varrho(x) \psi_{\mathbf{p}s} \rangle = i \langle \phi^*_{\mathbf{p}'s'} \frac{\delta S}{\delta \varphi_\varrho(x)} \phi_{\mathbf{p}s} \rangle.$$

Performing the Fourier transformation

$$\varphi_\varrho(x) = \frac{1}{(2\pi)^4} \int e^{iqx} \varphi_\varrho(q) dq$$

and taking into account that

$$\frac{\delta S}{\delta \varphi_\varrho(q)} = \frac{1}{(2\pi)^4} \int e^{iqx} \frac{\delta S}{\delta \varphi_\varrho(x)} dx$$

we get

$$i \langle \phi^*_{\mathbf{p}'s'} \frac{\delta S}{\delta \varphi_\varrho(q)} \phi_{\mathbf{p}s} \rangle = \langle \psi^*_{\mathbf{p}'s'} J^\varrho(0) \psi_{\mathbf{p}s} \rangle \delta(q-p+p').$$

The latter expression may be symbolically represented by the sum of the following graphs:

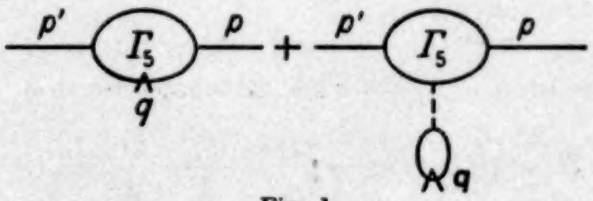

Fig. 1

Here Γ_5 is the strongly bound part. If free meson lines were written in place of the sign Λ the sum under consideration would equal

$$S_5^{\varrho}(p, p', q)\Delta_{\varrho}^{\varrho}(q).$$

As no free meson lines exist in our case the expression obtained by us should be additionally multiplied by $(\mu^2-\mathbf{q}^2)$. Applying the normalization condition of the vertex part operator for the values $p^2 = p'^2 = M^2$, $q^2 = \mu^2$ as well we obtain the following final expression for the mean current value $J^{\varrho}(0)$:

$$\langle \psi^*_{p's'} J^{\varrho}(0)\psi_{ps}\rangle = g\langle \bar{u}_{s'}(p')\gamma_5\tau_{\varrho}u_s(p)\rangle \tag{3.4}$$

where g is the renormalized coupling constant for the meson and nucleon fields. In the case of an electromagnetic current we have

$$\langle \psi^*_{p's'} I^{\mu}(0)\psi_{ps}\rangle = \langle \bar{u}_{s'}(p')\left\{e\frac{1+\tau_3}{2}\gamma^{\mu}+\tfrac{1}{2}\hat{\mu}[(k\cdot\gamma),\gamma^{\mu}]\right\}u_s(p)\rangle. \tag{3.5}$$

Here e is the renormalized proton electric charge and

$$\hat{\mu} = \mu'_{\mathrm{p}}\frac{1+\tau_3}{2}+\mu_{\mathrm{n}}\frac{1-\tau_3}{2} \tag{3.6}$$

where μ'_{p}, μ_{n} are the anomalous proton and neutron magnetic moments. By using (3.4—3.6) expression (3.3) can be rewritten as follows

$$Y^{\varrho\nu}_{p's';ps}(E,\lambda\mathbf{e}) = -\pi\frac{M^2-\frac{1}{4}\mu^2}{M^2+\mathbf{p}^2}g\sum_{\mu,s''}e_{\mu}^{\nu}\langle\bar{u}_{s'}(-\mathbf{p})\left\{e\frac{1+\tau_3}{2}\gamma^{\mu}\right.$$
$$\left.+\tfrac{1}{2}\hat{\mu}[(k\cdot\gamma),\gamma^{\mu}]\right\}u_{s''}(\mathbf{p}'')\rangle\langle\bar{u}_{s''}(\mathbf{p}'')\gamma_5\tau_{\varrho}u_s(\mathbf{p})\rangle\delta(E-E_2) \tag{3.7}$$

where

$$\mathbf{p}'' = -\lambda\mathbf{e}+t\mathbf{p}.$$

Since

$$\sum_{s''}u_{s''}(p'')\bar{u}_{s''}(p'') = \frac{1}{2p''_0}(\gamma\cdot p''+M), \quad k = p'-p'',$$

we get

$$\langle\psi^*_{p's'}I^{\mu}(0)\psi_{p''s''}\rangle\langle\psi^*_{p''s''}J^{\varrho}(0)\psi_{ps}\rangle$$
$$= \frac{1}{2}\frac{\sqrt{M^2+\mathbf{p}^2}}{M^2-\frac{1}{4}\mu^2}\{-eg\bar{u}_{s'}(p')\gamma^{\mu}(\gamma\cdot k)\gamma_5\tau_p\tau_{\varrho}u_s(p)$$
$$+2eg\bar{u}_{s'}(p')p'^{\mu}\gamma_5\tau_p\tau_{\varrho}u_s(p)$$
$$-g\bar{u}_{s'}(p')\gamma^{\mu}\gamma^{\nu}(\gamma\cdot p'-\gamma\cdot k+M)\gamma_5\hat{\mu}\,\tau_{\varrho}u_s(p)k_{\nu}\}.$$

Employing the notations

$$\hat{P}^{\mu\nu}_1 = \gamma_5(p^{\mu}p'^{\nu}-p^{\nu}p'^{\mu})$$
$$\hat{P}^{\mu\nu}_2 = -\gamma_5(\gamma^{\mu}p^{\nu}-\gamma^{\nu}p^{\mu})$$
$$\hat{P}^{\mu\nu}_3 = -\gamma_5(\gamma^{\mu}p'^{\nu}-\gamma^{\nu}p'^{\mu}) \qquad \hat{R}_s = \hat{P}^{\mu\nu}e_{\mu}k_{\nu} \tag{3.8}$$
$$\hat{P}^{\mu\nu}_4 = -\gamma_5(\gamma^{\mu}\gamma^{\nu}-\gamma^{\nu}\gamma^{\mu})$$

expression (3.7) can be represented in the system in which $\mathbf{p}+\mathbf{p}'=0$ as

$$Y^{\varrho\nu}_{s's;\,s\mathfrak{s}}(E,\lambda\mathbf{e})=\frac{\pi}{2p^0}\left\{\bar{u}_{s'}(p')\left(\frac{eg}{p^0k^0}\hat{R}_1\tau_p\tau_\varrho+2g\hat{R}_3\hat{\mu}\,\tau_\varrho\right.\right.$$
$$\left.\left.-\left(\frac{eg}{2}\tau_p\tau_\varrho+Mg\hat{\mu}\,\tau_\varrho\right)\hat{R}^4\right)u_s(p)\right\}\delta(E-E_2). \qquad (3.9)$$

For the following it will be convenient to write $\tau_p\tau_\varrho$ and $\hat{\mu}\tau_\varrho$ in the form

$$\tau_p\tau_\varrho=\tfrac{1}{2}\{\delta_{3\varrho}+\tau_\varrho-\tfrac{1}{2}[\tau_\varrho,\tau_3]\} \qquad (3.10)$$
$$\hat{\mu}\tau_\varrho=\tfrac{1}{2}\{(\mu'_p-\mu_n)\delta_{3\varrho}+(\mu'_p+\mu_n)\tau_\varrho-\tfrac{1}{2}(\mu'_p-\mu_n)[\tau_\varrho,\tau_3]\}.$$

4. Matrix Structure of the Photoproduction Amplitude

From considerations of relativistic and gradient invariance one may write the photoproduction amplitude in the form [8])

$$\hat{R}^{\varrho\nu}=\sum_s\hat{\Omega}_\varrho{}^s\bar{u}(p')\hat{P}^{\alpha\beta}_s(k,p,p',\gamma)u(p)e_\alpha{}^\nu k_\beta \qquad (4.1)$$

where $\hat{R}^{\varrho\nu}=\hat{X}^{\varrho\nu}+i\hat{Y}^{\varrho\nu}$, $\hat{P}^{\alpha\beta}_s$ being an antisymmetric (with respect to α and β) operator.

The following four linearly independent operators can be written in pseudoscalar theory †

$$\hat{P}^{\alpha\beta}_s=\begin{cases}\gamma_5(p^\alpha p'^\beta-p^\beta p'^\alpha), & -\gamma_5(\gamma^\alpha p^\beta-\gamma^\beta p^\alpha)\\ -\gamma_5(\gamma^\alpha p'^\beta-\gamma^\beta p'^\alpha), & -\gamma_5(\gamma^\alpha\gamma^\beta-\gamma^\beta\gamma^\alpha)\end{cases} \qquad (4.2)$$

where $\hat{\Omega}^s$ are the isobaric spin operators. In a system consisting of a nucleon field, π-meson field and electromagnetic field the only matrices involved in a description of the interaction are the τ_ϱ matrices when a nucleon and π-meson field are coupled and the electric charge operator $\frac{1}{2}(1+\tau_3)$ for coupling between a nucleon and electromagnetic fields. Since in photoproduction processes the initial state is that of a nucleon + electromagnetic field and the final state is that of a nucleon + meson field one can then write the most general expression for the amplitude of the reaction in isobaric space in the form

$$\hat{\Omega}_\varrho{}^s=\Omega_1{}^s\delta_{3\varrho}+\Omega_2{}^s\tau_\varrho+\Omega_3{}^s\tfrac{1}{2}[\tau_\varrho,\tau_3]. \qquad (4.3)$$

In the case of transverse polarization in the reference system $(\mathbf{p}+\mathbf{v}'=0)$ chosen by us we can write the photoproduction amplitude as

$$\hat{R}^{\varrho\nu}=(\boldsymbol{\sigma}\cdot\boldsymbol{\pi}^\nu)\hat{R}_\varrho{}^1+(\boldsymbol{\sigma}\cdot\mathbf{p})(\mathbf{p}\cdot\boldsymbol{\pi}^\nu)\hat{R}_\varrho{}^2+\boldsymbol{\sigma}\cdot[\mathbf{p}\wedge(\boldsymbol{\pi}^\nu\wedge\mathbf{k})]\hat{R}_\varrho{}^3+\mathbf{p}\cdot(\boldsymbol{\pi}^\nu\wedge\mathbf{k})\hat{R}_\varrho{}^4 \qquad (4.4)$$

† Other possible operators which involve a third independent vector k make expression (4.1) vanish in virtue of conditions $(k\cdot e^\nu)=0$, $k^2=0$; this can easily be verified by a direct check. It should also be noted that expression (4.1) satisfies the condition of gradient invariance since it vanishes when $e_\mu{}^\nu$ is substituted for k_μ.

where the $\hat{R}_\varrho^i$ have an isobaric structure similar to that of (4.3). Since $\hat{R}^{\sigma\nu} = \hat{X}^{\sigma\nu} + i\hat{Y}^{\sigma\nu}$ we have

$$\begin{aligned} X^{\sigma\nu} &= (\boldsymbol{\sigma}\cdot\boldsymbol{\pi}^\nu)\hat{X}_\varrho^1 + (\boldsymbol{\sigma}\cdot\mathbf{p})(\mathbf{p}\cdot\boldsymbol{\pi}^\nu)\hat{X}_\varrho^2 + \boldsymbol{\sigma}\cdot[\mathbf{p}\wedge(\boldsymbol{\pi}^\nu\wedge\mathbf{k})]\hat{X}_\varrho^3 + \mathbf{p}\cdot(\boldsymbol{\pi}^\nu\wedge\mathbf{k})\hat{X}_\varrho^4 \\ Y^{\sigma\nu} &= (\boldsymbol{\sigma}\cdot\boldsymbol{\pi}^\nu)\hat{Y}_\varrho^1 + (\boldsymbol{\sigma}\cdot\mathbf{p})(\mathbf{p}\cdot\boldsymbol{\pi}^\nu)\hat{Y}_\varrho^2 + \boldsymbol{\sigma}\cdot[\mathbf{p}\wedge(\boldsymbol{\pi}^\nu\wedge\mathbf{k})]\hat{Y}_\varrho^3 + \mathbf{p}\cdot(\boldsymbol{\pi}^\nu\wedge\mathbf{k})\hat{Y}_\varrho^4 \end{aligned} \tag{4.5}$$

where

$$\begin{aligned} \hat{X}_\varrho^i &= X_1^i\delta_{3\varrho} + X_2^i\tau_\varrho + X_3^i\tfrac{1}{2}[\tau_\varrho, \tau_3] \\ Y_\varrho^i &= Y_1^i\delta_{3\varrho} + Y_2^i\tau_\varrho + Y_3^i\tfrac{1}{2}[\tau_\varrho, \tau_3]. \end{aligned} \tag{4.6}$$

On basis of (2.20) the following important relations can easily be derived:

$$\left.\begin{aligned} X_j^i(E,\lambda\mathbf{e}) \pm \overset{*}{X}_j^i(E,\lambda\mathbf{e}) &= \pm(X_j^i(-E,\lambda\mathbf{e}) \pm \overset{*}{X}_j^i(-E,\lambda\mathbf{e})) \\ Y_j^i(E,\lambda\mathbf{e}) \pm \overset{*}{Y}_j^i(E,\lambda\mathbf{e}) &= \mp(Y_j^i(-E,\lambda\mathbf{e}) \pm \overset{*}{Y}_j^i(-E,\lambda\mathbf{e})) \end{aligned}\right\} (j = 1, 2);$$

$$\left.\begin{aligned} X_j^i(E,\lambda\mathbf{e}) \pm \overset{*}{X}_j^i(E,\lambda\mathbf{e}) &= \mp(X_j^i(-E,\lambda\mathbf{e}) \pm \overset{*}{X}_j^i(-E,\lambda\mathbf{e})) \\ Y_j^i(E,\lambda\mathbf{e}) \pm \overset{*}{Y}_j^i(E,\lambda\mathbf{e}) &= \pm(Y_j^i(-E,\lambda\mathbf{e}) \pm \overset{*}{Y}_j^i(-E,\lambda\mathbf{e})) \end{aligned}\right\} (j = 3). \tag{4.7}$$

Taking into account formulae (2.10—2.14) and also that

$$\hat{R}^{\sigma\nu+} = \sum_s \hat{\Omega}_\varrho^{s*}\,\bar{u}(p')\hat{P}_s^{\alpha\beta}u(p)e_\alpha{}^\nu k_\beta \tag{4.8}$$

where

$$\hat{\Omega}_\varrho^{s*} = \overset{*}{\Omega}_1{}^s\delta_{3\varrho} + \overset{*}{\Omega}_2{}^s\tau_\varrho + \overset{*}{\Omega}_3{}^s\tfrac{1}{2}[\tau_\varrho, \tau_3]$$

one can easily obtain

$$\begin{aligned} \hat{X}^{\sigma\nu} &= \sum_s (\operatorname{Re}\hat{\Omega}_\varrho{}^s)\bar{u}(p')\hat{P}_s^{\alpha\beta}u(p)e_\alpha{}^\nu k_\beta \\ \hat{Y}^{\sigma\nu} &= \sum_s (\operatorname{Im}\hat{\Omega}_\varrho{}^s)\bar{u}(p')\hat{P}_s^{\alpha\beta}u(p)e_\alpha{}^\nu k_\beta \end{aligned} \tag{4.9}$$

where

$$\begin{aligned} \operatorname{Re}\hat{\Omega}_\varrho{}^s &= (\operatorname{Re}\Omega_1{}^s)\delta_{3\varrho} + \tau_\varrho \operatorname{Re}\Omega_2{}^s + \tfrac{1}{2}[\tau_\varrho, \tau_3]\operatorname{Re}\Omega_3{}^s \\ \operatorname{Im}\hat{\Omega}_\varrho{}^s &= \delta_{3\varrho}\operatorname{Im}\Omega_1{}^s + \tau_\varrho \operatorname{Im}\Omega_2{}^s + \tfrac{1}{2}[\tau_\varrho, \tau_3]\operatorname{Im}\Omega_3{}^s. \end{aligned}$$

We shall now find the relation between the coefficients Y_ϱ^i and $\operatorname{Im}\Omega_\varrho^s$. Since

$$\begin{aligned} \bar{u}(p')\hat{P}_1^{\alpha\beta}u(p)e_\alpha{}^\nu k_\beta &= 2iE(\boldsymbol{\sigma}\cdot\mathbf{p})(\mathbf{p}\cdot\boldsymbol{\pi}^\nu) \\ \bar{u}(p')\hat{P}_2^{\alpha\beta}u(p)e_\alpha{}^\nu k_\beta &= -i\boldsymbol{\sigma}\cdot[\mathbf{p}\wedge(\boldsymbol{\pi}^\nu\wedge\mathbf{k})] + iEp^0(\boldsymbol{\sigma}\cdot\boldsymbol{\pi}^\nu) - \frac{iE}{p^0+M}(\boldsymbol{\sigma}\cdot\mathbf{p})(\mathbf{p}\cdot\boldsymbol{\pi}^\nu) \\ \bar{u}(p')\hat{P}_3^{\alpha\beta}u(p)e_\alpha{}^\nu k_\beta &= i\boldsymbol{\sigma}\cdot[\mathbf{p}\wedge(\boldsymbol{\pi}^\nu\wedge\mathbf{k})] + iEp^0(\boldsymbol{\sigma}\cdot\boldsymbol{\pi}^\nu) - \frac{iE}{p^0+M}(\boldsymbol{\sigma}\cdot\mathbf{p})(\mathbf{p}\cdot\boldsymbol{\pi}^\nu) \\ \bar{u}(p')\hat{P}_4^{\alpha\beta}u(p)e_\alpha{}^\nu k_\beta &= i\frac{2ME}{p^0}(\boldsymbol{\sigma}\cdot\boldsymbol{\pi}^\nu) + \frac{2}{p^0}\mathbf{p}\cdot(\boldsymbol{\pi}^\nu\wedge\mathbf{k}) + \frac{2iE}{p^0(p^0+M)}(\boldsymbol{\sigma}\cdot\mathbf{p})(\mathbf{p}\cdot\boldsymbol{\pi}^\nu) \end{aligned} \tag{4.10}$$

we find, by substituting (4.10) into (4.9),

$$\hat{Y}_\varrho^1(E, \mathbf{p}^2) = iE\left\{p^0 \operatorname{Im} \hat{\Omega}_\varrho^2 + p^0 \operatorname{Im} \hat{\Omega}_\varrho^3 + \frac{2M}{p^0} \operatorname{Im} \hat{\Omega}_\varrho^4\right\}$$

$$\hat{Y}_\varrho^2(E, \mathbf{p}^2) = iE\left\{2 \operatorname{Im} \hat{\Omega}_\varrho^1 - \frac{1}{p^0+M}(\operatorname{Im} \hat{\Omega}_\varrho^2 + \operatorname{Im} \hat{\Omega}_\varrho^3) + \frac{2}{p^0(p^0+M)} \operatorname{Im} \hat{\Omega}_\varrho^4\right\} \tag{4.11}$$

$$\hat{Y}_\varrho^3(E, \mathbf{p}^2) = -i\{\operatorname{Im} \hat{\Omega}_\varrho^2 - \operatorname{Im} \hat{\Omega}_\varrho^3\}$$

$$\hat{Y}_\varrho^4(E, \mathbf{p}^2) = \frac{2}{p^0} \operatorname{Im} \hat{\Omega}_\varrho^4.$$

The inverse relations can also readily be obtained

$$\operatorname{Im} \hat{\Omega}_\varrho^1(E, \mathbf{p}^2) = -\frac{i}{2E} \hat{Y}_\varrho^2 - \frac{1}{2(p^0+M)}\left\{\frac{i}{p^0 E} \hat{Y}_\varrho^1 + \frac{M}{p^0} \hat{Y}_\varrho^4\right\} - \frac{1}{2(p^0+M)} \hat{Y}_\varrho^4$$

$$\operatorname{Im} \hat{\Omega}_\varrho^2(E, \mathbf{p}^2) = -\frac{i}{2p^0 E} \hat{Y}_\varrho^1 - \frac{M}{2p^0} \hat{Y}_\varrho^4 + \frac{i}{2} \hat{Y}_\varrho^3$$

$$\operatorname{Im} \hat{\Omega}_\varrho^3 = -\frac{i}{2p^0 E} \hat{Y}_\varrho^1 - \frac{M}{2p^0} \hat{Y}_\varrho^4 - \frac{i}{2} \hat{Y}_\varrho^3$$

$$\operatorname{Im} \hat{\Omega}_\varrho^4 = \frac{p^0}{2} Y_\varrho^4.$$

In the following it will be convenient to replace the functions $\Omega_j^i(E, \mathbf{p}^2)$, by the functions $t_j^i(E, \mathbf{p}^2)$ defined as follows:

$$\begin{aligned} t_j^1(E, \mathbf{p}^2) &= \Omega_j^1(E, \mathbf{p}^2) \\ t_j^2(E, \mathbf{p}^2) &= \Omega_j^2(E, \mathbf{p}^2) + \Omega_j^3(E, \mathbf{p}^2) \\ t_j^3(E, \mathbf{p}^2) &= \Omega_j^2(E, \mathbf{p}^2) - \Omega_j^3(E, \mathbf{p}^2) \\ t_j^4(E, \mathbf{p}^2) &= \Omega_j^4(E, \mathbf{p}^2). \end{aligned} \tag{4.13}$$

Taking into account (4.7) the following important relations can easily be established for the imaginary parts of function $t_j^i(E, \mathbf{p}^2)$:

$$\left.\begin{aligned} \operatorname{Im} t_j^1(E, \mathbf{p}^2) &= -\operatorname{Im} t_j^1(-E, \mathbf{p}^2) \\ \operatorname{Im} t_j^2(E, \mathbf{p}^2) &= -\operatorname{Im} t_j^2(-E, \mathbf{p}^2) \\ \operatorname{Im} t_j^3(E, \mathbf{p}^2) &= \operatorname{Im} t_j^3(-E, \mathbf{p}^2) \\ \operatorname{Im} t_j^4(E, \mathbf{p}^2) &= -\operatorname{Im} t_j^4(-E, \mathbf{p}^2) \end{aligned}\right\} (j = 1, 2);$$

$$\begin{aligned} \operatorname{Im} t_3^1(E, \mathbf{p}^2) &= \operatorname{Im} t_3^1(-E, \mathbf{p}^2) \\ \operatorname{Im} t_3^2(E, \mathbf{p}^2) &= \operatorname{Im} t_3^2(-E, \mathbf{p}^2) \\ \operatorname{Im} t_3^3(E, \mathbf{p}^2) &= -\operatorname{Im} t_3^3(-E, \mathbf{p}^2) \\ \operatorname{Im} t_3^4(E, \mathbf{p}^2) &= \operatorname{Im} t_3^4(-E, \mathbf{p}^2) \end{aligned} \tag{4.14}$$

and similarly for the real parts

$$\left.\begin{aligned}
\operatorname{Re} t_j^1(E, \mathbf{p}^2) &= \operatorname{Re} t_j^1(-E, \mathbf{p}^2)\\
\operatorname{Re} t_j^2(E, \mathbf{p}^2) &= \operatorname{Re} t_j^2(-E, \mathbf{p}^2)\\
\operatorname{Re} t_j^3(E, \mathbf{p}^2) &= -\operatorname{Re} t_j^3(-E, \mathbf{p}^2)\\
\operatorname{Re} t_j^4(E, \mathbf{p}^2) &= \operatorname{Re} t_j^4(-E, \mathbf{p}^2)
\end{aligned}\right\} (j = 1, 2);$$

$$\begin{aligned}
\operatorname{Re} t_3^1(E, \mathbf{p}^2) &= -\operatorname{Re} t_3^1(-E, \mathbf{p}^2)\\
\operatorname{Re} t_3^2(E, \mathbf{p}^2) &= -\operatorname{Re} t_3^2(-E, \mathbf{p}^2)\\
\operatorname{Re} t_3^3(E, \mathbf{p}^2) &= \operatorname{Re} t_3^3(-E, \mathbf{p}^2)\\
\operatorname{Re} t_3^4(E, \mathbf{p}^2) &= -\operatorname{Re} t_3^4(-E, \mathbf{p}^2).
\end{aligned} \tag{4.15}$$

The foregoing investigation of the unobservable energy region and also of the matrix structure of the photoproduction amplitude permits one (in conjunction with the analyticity property of the amplitude in the upper half-plane E) to obtain the dispersion relations for the process under consideration.

5. Dispersion Relations

Consider the amplitude for photoproduction of π-mesons on nucleons (4.4) which can be expressed in the variables E, $\mathbf{p}$, $\mathbf{e}$ as follows:

$$\hat{R}^{\varrho\nu} = (\boldsymbol{\sigma}\cdot\boldsymbol{\pi}^\nu)\hat{L}_\varrho^1(E, \mathbf{p}^2) + (\boldsymbol{\sigma}\cdot\mathbf{p})(\mathbf{p}\cdot\boldsymbol{\pi}^\nu)\hat{L}_\varrho^2 + \lambda(\mathbf{e}\cdot\boldsymbol{\sigma})(\mathbf{p}\cdot\boldsymbol{\pi}^\nu)\hat{L}_\varrho^3 + \lambda(\mathbf{p}\wedge\mathbf{e})\pi^\nu\hat{L}_\varrho^4. \tag{5.1}$$

N. N. Bogolyubov has shown that the functions $\hat{L}_\varrho^i(E, \mathbf{p}^2)$ are analytic with respect to E in the upper half-plane E. In order to eliminate the cuts in upper half-plane E due to linear (with respect to λ) terms in expression (5.1) we shall consider the following combinations:

$$\begin{aligned}
\mathfrak{S}_\mathbf{e}\hat{R}^{\varrho\nu}(E, \lambda\mathbf{e}) &= \hat{R}^{\varrho\nu}(E, \lambda\mathbf{e}) + \hat{R}^{\varrho\nu}(E, -\lambda\mathbf{e})\\
\mathfrak{A}_\mathbf{e}\hat{R}^{\varrho\nu}(E, \lambda\mathbf{e}) &= \frac{1}{\lambda}(\hat{R}^{\varrho\nu}(E, \lambda\mathbf{e}) - \hat{R}^{\varrho\nu}(E, -\lambda\mathbf{e}))
\end{aligned} \tag{5.2}$$

which are analytic in the upper half-plane E. Before using the generalized Cauchy theorem and writing the dispersion relations some definite assumptions regarding the rate of increase of the photoproduction amplitude at infinity must be made. Since the rate of increase of the reaction amplitude is a dynamic factor it cannot be obtained from any kinematic considerations. We shall further assume that the rate of increase of the photoproduction amplitude is zero. On basis of this assumption concerning the increase rate and application of the Cauchy theorem we can write the following relations for combinations (5.2):

$$\begin{aligned}
\mathfrak{S}_\mathbf{e}\hat{R}^{\varrho\nu}(E, \lambda\mathbf{e}) &= \frac{1}{\pi i}V_p\int_{-\infty}^{\infty}\frac{\mathfrak{S}_\mathbf{e}\hat{R}^{\varrho\nu}(E', \lambda'\mathbf{e})}{E'-E}\,dE' + \hat{C}^{\varrho\nu}\\
\mathfrak{A}_\mathbf{e}\hat{R}^{\varrho\nu}(E, \lambda\mathbf{e}) &= \frac{1}{\pi i}V_p\int_{-\infty}^{\infty}\frac{\mathfrak{A}_\mathbf{e}\hat{R}^{\varrho\nu}(E', \lambda'\mathbf{e})}{E'-E}\,dE';
\end{aligned} \tag{5.3}$$

or, separating the hermitian part of expression (5.3), we obtain the dispersion relations between the hermitian part of the amplitude, $\hat{X}^{\varrho\nu}$, and the antihermitian part $\hat{Y}^{\varrho\nu}$

$$\begin{aligned}\mathbb{S}_\alpha \hat{X}^{\varrho\nu}(E, \lambda\mathbf{e}) &= \frac{1}{\pi} V_p \int_{-\infty}^{\infty} \frac{\mathbb{S}_\alpha \hat{Y}^{\varrho\nu}(E', \lambda'\mathbf{e})}{E'-E}\, dE' + \hat{b}^{\varrho\nu} \\ \mathfrak{A}_\alpha \hat{X}^{\varrho\nu}(E, \lambda\mathbf{e}) &= \frac{1}{\pi} V_p \int_{-\infty}^{\infty} \frac{\mathfrak{A}_\alpha \hat{Y}^{\varrho\nu}(E', \lambda'\mathbf{e})}{E'-E}\, dE'.\end{aligned} \tag{5.4}$$

Taking into account (2.18—2.19) we can write the dispersion relations in the form

$$\mathbb{S}_\alpha(1\pm P)\hat{X}^{\varrho\nu}(E, \lambda\mathbf{e}) = \frac{1}{\pi} V_p \int_0^{\infty} \left\{\frac{1}{E'-E} \pm \frac{1}{E'+E}\right\} \mathbb{S}_\alpha(1\pm P)\hat{Y}^{\varrho\nu}(E', \lambda'\mathbf{e})dE' + (1\pm P)\hat{b}^{\varrho\nu} \tag{5.5a}$$

$$\mathfrak{A}_\alpha(1\pm P)\hat{X}^{\varrho\nu}(E, \lambda\mathbf{e}) = \frac{1}{\pi} V_p \int_0^{\infty} \left\{\frac{1}{E'-E} \pm \frac{1}{E'+E}\right\} \mathfrak{A}_\alpha(1\pm P)\hat{Y}^{\varrho\nu}(E', \lambda'\mathbf{e})dE'. \tag{5.5b}$$

In order to write the dispersion relations which do not contain spin and isobaric operators we represent $\hat{X}^{\varrho\nu}$ and $\hat{Y}^{\varrho\nu}$ in a form analogous to that of (5.1):

$$\begin{aligned}\hat{X}^{\varrho\nu}(E, \lambda\mathbf{e}) = {} & (\boldsymbol{\sigma}\cdot\boldsymbol{\pi}^\nu)\hat{\mathscr{X}}_\varrho^{\,1}(E, \mathbf{p}^2) + (\boldsymbol{\sigma}\cdot\mathbf{p})(\mathbf{p}\cdot\boldsymbol{\pi}^\nu)\hat{\mathscr{X}}_\varrho^{\,2}(E, \mathbf{p}^2) \\ & + \lambda(\boldsymbol{\sigma}\cdot\mathbf{e})(\mathbf{p}\cdot\boldsymbol{\pi}^\nu)\hat{\mathscr{X}}_\varrho^{\,3}(E, \mathbf{p}^2) + \lambda(\mathbf{p}\wedge\mathbf{e})\cdot\boldsymbol{\pi}^\nu\hat{\mathscr{X}}_\varrho^{\,4}(E, \mathbf{p}^2)\end{aligned} \tag{5.6}$$

$$\begin{aligned}\hat{Y}^{\varrho\nu}(E, \lambda\mathbf{e}) = {} & (\boldsymbol{\sigma}\cdot\boldsymbol{\pi}^\nu)\hat{\mathscr{Y}}_\varrho^{\,1}(E, \mathbf{p}^2) + (\boldsymbol{\sigma}\cdot\mathbf{p})(\mathbf{p}\cdot\boldsymbol{\pi}^\nu)\hat{\mathscr{Y}}_\varrho^{\,2}(E, \mathbf{p}^2) \\ & + \lambda(\boldsymbol{\sigma}\cdot\mathbf{e})(\mathbf{p}\cdot\boldsymbol{\pi}^\nu)\hat{\mathscr{Y}}_\varrho^{\,3}(E, \mathbf{p}^2) + \lambda(\mathbf{p}\wedge\mathbf{e})\cdot\boldsymbol{\pi}^\nu\hat{\mathscr{Y}}_\varrho^{\,4}(E, \mathbf{p}^2).\end{aligned}$$

$\hat{\mathscr{Y}}_\varrho^{\,i}(E, \mathbf{p}^2)$ can easily be expressed through $\operatorname{Im} \hat{t}_\varrho^{\,i}(E, \mathbf{p}^2)$ by using (4.11) and (4.13):

$$\begin{aligned}\hat{\mathscr{Y}}_\varrho^{\,1}(E, \mathbf{p}^2) &= i(1+t)\mathbf{p}^2 \operatorname{Im} \hat{t}_\varrho^{\,3} + iEp^0 \operatorname{Im} \hat{t}_\varrho^{\,2} + i\frac{2ME}{p^0} \operatorname{Im} \hat{t}_\varrho^{\,4} \\ \hat{\mathscr{Y}}_\varrho^{\,2}(E, \mathbf{p}^2) &= 2iE \operatorname{Im} \hat{t}_\varrho^{\,1} - i(1+t) \operatorname{Im} \hat{t}_\varrho^{\,3} - \frac{iE}{p^0+M} \operatorname{Im} \hat{t}_\varrho^{\,2} + \frac{2iE}{p^0(p^0+M)} \operatorname{Im} \hat{t}_\varrho^{\,4} \\ \hat{\mathscr{Y}}_\varrho^{\,3}(E, \mathbf{p}^2) &= -i \operatorname{Im} \hat{t}_\varrho^{\,3} \\ \hat{\mathscr{Y}}_\varrho^{\,4}(E, \mathbf{p}^2) &= -\frac{2}{p^0} \operatorname{Im} \hat{t}_\varrho^{\,4}\end{aligned} \tag{5.7}$$

or, separating the isobaric structure, we obtain

$$\mathscr{Y}_j^1(E, \mathbf{p}^2) = i(1+t)\mathbf{p}^2 \operatorname{Im} t_j^3 + iE\dot{p}^0 \operatorname{Im} t_j^2 + i\frac{2ME}{\dot{p}^0} \operatorname{Im} t_j^4$$

$$\mathscr{Y}_j^2(E, \mathbf{p}^2) = 2iE \operatorname{Im} t_j^1 - i(1+t) \operatorname{Im} t_j^3 - \frac{iE}{\dot{p}^0+M} \operatorname{Im} t_j^2 + \frac{2iE}{\dot{p}^0(\dot{p}^0+M)} \operatorname{Im} t_j^4 \tag{5.8}$$

$$\mathscr{Y}_j^3(E, \mathbf{p}^2) = -i \operatorname{Im} t_j^3$$

$$\mathscr{Y}_j^4(E, \mathbf{p}^2) = -\frac{2}{\dot{p}^0} \operatorname{Im} t_j^4.$$

Applying antisymmetrization of (5.2) to $\hat{Y}^{\varrho\nu}(E, \lambda\mathbf{e})$ and taking into account (5.7) we obtain the following expression for $\mathfrak{A}_e \hat{Y}^{\varrho\nu}(E, \lambda\mathbf{e})$:

$$\mathfrak{A}_e \hat{Y}^{\varrho\nu}(E, \lambda\mathbf{e}) = -(\mathbf{p} \wedge \mathbf{e}) \cdot \boldsymbol{\pi}^\nu \frac{4}{\dot{p}^0} \operatorname{Im} \hat{t}_\varrho^4 - (\boldsymbol{\sigma} \cdot \mathbf{e})(\mathbf{p} \cdot \boldsymbol{\pi}^\nu) 2i \operatorname{Im} \hat{t}_\varrho^3. \tag{5.9}$$

It should be recalled that the operators $\hat{t}_\varrho^i(E, \mathbf{p}^2)$ have an isobaric structure of the following form:

$$\hat{t}_\varrho^i(E, \mathbf{p}^2) = \delta_{3\varrho} t_1^i + \tau_\varrho t_2^i + \tfrac{1}{2}[\tau_\varrho, \tau_3] t_3^i. \tag{5.10}$$

We now construct the combination $\mathfrak{A}_e(1 \pm P)\hat{Y}^{\varrho\nu}$. For this purpose consider the effect of operator P on expression (5.9):

$$\mathfrak{A}_e P \hat{Y}^{\varrho\nu}(E, \lambda\mathbf{e}) = -(\mathbf{p} \wedge \mathbf{e}) \cdot \boldsymbol{\pi}^\nu \frac{4}{\dot{p}^0} \operatorname{Im} \hat{t}_\varrho^{4+}(E, \mathbf{p}^2) + (\boldsymbol{\sigma} \cdot \mathbf{e})(\mathbf{p} \cdot \boldsymbol{\pi}^\nu) 2i \operatorname{Im} \hat{t}_\varrho^{3+}(E, \mathbf{p}^2) \tag{5.11}$$

where

$$\operatorname{Im} \hat{t}_\varrho^{i\dagger}(E, \mathbf{p}^2) = \delta_{3\varrho} \operatorname{Im} t_1^i(E, \mathbf{p}^2) + \tau_\varrho \operatorname{Im} t_2^i(E, \mathbf{p}^2) - \tfrac{1}{2}[\tau_\varrho, \tau_3) \operatorname{Im} t_3^i(E, \mathbf{p}^2).$$

It should be noted that operator P commutes with the operation $\mathfrak{A}_e$. Adding and subtracting expressions (5.9) and (5.11) we obtain

$$\begin{aligned} \mathfrak{A}_e(1+P)\hat{Y}^{\varrho\nu}(E, \lambda\mathbf{e}) &= -(\mathbf{p} \wedge \mathbf{e}) \cdot \boldsymbol{\pi}^\nu \frac{8}{\dot{p}^0} \{\delta_{3\varrho} \operatorname{Im} t_1^4(E, \mathbf{p}^2) + \tau_\varrho \operatorname{Im} t_2^4(E, \mathbf{p}^2)\} \\ &\quad - (\boldsymbol{\sigma} \cdot \mathbf{e})(\mathbf{p} \cdot \boldsymbol{\pi}^\nu) 4i \operatorname{Im} t_3^3(E, \mathbf{p}^2) \tfrac{1}{2}[\tau_\varrho, \tau_3] \\ \mathfrak{A}_e(1-P)\hat{Y}^{\varrho\nu}(E, \lambda\mathbf{e}) &= -(\mathbf{p} \wedge \mathbf{e}) \cdot \boldsymbol{\pi}^\nu \frac{8}{\dot{p}^0} \tfrac{1}{2}[\tau_\varrho, \tau_3] \operatorname{Im} t_3^4(E, \mathbf{p}^2) \\ &\quad - (\boldsymbol{\sigma} \cdot \mathbf{e})(\mathbf{p} \cdot \boldsymbol{\pi}^\nu) 4i \{\delta_{3\varrho} \operatorname{Im} t_1^3(E, \mathbf{p}^2) + \tau_\varrho \operatorname{Im} t_2^3(E, \mathbf{p}^2)\}. \end{aligned} \tag{5.12}$$

Inserting (5.12) into (5.5b) and taking into account the linear independence of the spin and isobaric operators we obtain

$$\mathscr{Y}_j^1(E, \mathbf{p}^2) = i(1+t)\mathbf{p}^2 \operatorname{Im} t_j^3 + iEp^0 \operatorname{Im} t_j^2 + i\frac{2ME}{p^0} \operatorname{Im} t_j^4$$

$$\mathscr{Y}_j^2(E, \mathbf{p}^2) = 2iE \operatorname{Im} t_j^1 - i(1+t) \operatorname{Im} t_j^3 - \frac{iE}{p^0+M} \operatorname{Im} t_j^2 + \frac{2iE}{p^0(p^0+M)} \operatorname{Im} t_j^4 \tag{5.8}$$

$$\mathscr{Y}_j^3(E, \mathbf{p}^2) = -i \operatorname{Im} t_j^3$$

$$\mathscr{Y}_j^4(E, \mathbf{p}^2) = -\frac{2}{p^0} \operatorname{Im} t_j^4.$$

Applying antisymmetrization of (5.2) to $\hat{Y}^{\alpha\nu}(E, \lambda\mathbf{e})$ and taking into account (5.7) we obtain the following expression for $\mathfrak{A}_e \hat{Y}^{\alpha\nu}(E, \lambda\mathbf{e})$:

$$\mathfrak{A}_e \hat{Y}^{\alpha\nu}(E, \lambda\mathbf{e}) = -(\mathbf{p} \wedge \mathbf{e}) \cdot \boldsymbol{\pi}^\nu \frac{4}{p^0} \operatorname{Im} \hat{t}_\varrho^4 - (\boldsymbol{\sigma} \cdot \mathbf{e})(\mathbf{p} \cdot \boldsymbol{\pi}^\nu) 2i \operatorname{Im} \hat{t}_\varrho^3. \tag{5.9}$$

It should be recalled that the operators $\hat{t}_\varrho^{\,i}(E, \mathbf{p}^2)$ have an isobaric structure of the following form:

$$\hat{t}_\varrho^{\,i}(E, \mathbf{p}^2) = \delta_{3\varrho} t_1^i + \tau_\varrho t_2^i + \tfrac{1}{2}[\tau_\varrho, \tau_3] t_3^i. \tag{5.10}$$

We now construct the combination $\mathfrak{A}_e(1 \pm P)\hat{Y}^{\alpha\nu}$. For this purpose consider the effect of operator P on expression (5.9):

$$\mathfrak{A}_e P \hat{Y}^{\alpha\nu}(E, \lambda\mathbf{e}) = -(\mathbf{p} \wedge \mathbf{e}) \cdot \boldsymbol{\pi}^\nu \frac{4}{p^0} \operatorname{Im} \hat{t}_\varrho^{4+}(E, \mathbf{p}^2) + (\boldsymbol{\sigma} \cdot \mathbf{e})(\mathbf{p} \cdot \boldsymbol{\pi}^\nu) 2i \operatorname{Im} \hat{t}_\varrho^{3+}(E, \mathbf{p}^2) \tag{5.11}$$

where

$$\operatorname{Im} \hat{t}_\varrho^{\,i+}(E, \mathbf{p}^2) = \delta_{3\varrho} \operatorname{Im} t_1^i(E, \mathbf{p}^2) + \tau_\varrho \operatorname{Im} t_2^i(E, \mathbf{p}^2) - \tfrac{1}{2}[\tau_\varrho, \tau_3) \operatorname{Im} t_3^i(E, \mathbf{p}^2).$$

It should be noted that operator P commutes with the operation $\mathfrak{A}_e$. Adding and subtracting expressions (5.9) and (5.11) we obtain

$$\begin{aligned}
\mathfrak{A}_e(1+P)\hat{Y}^{\alpha\nu}(E, \lambda\mathbf{e}) &= -(\mathbf{p} \wedge \mathbf{e}) \cdot \boldsymbol{\pi}^\nu \frac{8}{p^0} \{\delta_{3\varrho} \operatorname{Im} t_1^4(E, \mathbf{p}^2) + \tau_\varrho \operatorname{Im} t_2^4(E, \mathbf{p}^2)\} \\
&\quad - (\boldsymbol{\sigma} \cdot \mathbf{e})(\mathbf{p} \cdot \boldsymbol{\pi}^\nu) 4i \operatorname{Im} t_3^3(E, \mathbf{p}^2) \tfrac{1}{2}[\tau_\varrho, \tau_3] \\
\mathfrak{A}_e(1-P)\hat{Y}^{\alpha\nu}(E, \lambda\mathbf{e}) &= -(\mathbf{p} \wedge \mathbf{e}) \cdot \boldsymbol{\pi}^\nu \frac{8}{p^0} \tfrac{1}{2}[\tau_\varrho, \tau_3] \operatorname{Im} t_3^4(E, \mathbf{p}^2) \\
&\quad - (\boldsymbol{\sigma} \cdot \mathbf{e})(\mathbf{p} \cdot \boldsymbol{\pi}^\nu) 4i \{\delta_{3\varrho} \operatorname{Im} t_1^3(E, \mathbf{p}^2) + \tau_\varrho \operatorname{Im} t_2^3(E, \mathbf{p}^2)\}.
\end{aligned} \tag{5.12}$$

Inserting (5.12) into (5.5b) and taking into account the linear independence of the spin and isobaric operators we obtain

Taking into account (4.13) we find from here

$$\operatorname{Im} \overset{\circ}{t}_1^2 = \pi \frac{M}{p^0} \frac{f}{\mu} (\mu'_p - \mu_n), \quad \operatorname{Im} \overset{\circ}{t}_2^2 = \pi \frac{M}{p^0} \frac{f}{\mu} (\mu'_p + \mu_n), \quad \operatorname{Im} \overset{\circ}{t}_3^2 = -\pi \frac{M}{p^0} \frac{f}{\mu} (\mu'_p - \mu_n)$$

$$\operatorname{Im} \overset{\circ}{t}_1^3 = -\pi \frac{M}{p^0} \frac{f}{\mu} (\mu'_p - \mu_n), \quad \operatorname{Im} \overset{\circ}{t}_2^3 = -\pi \frac{M}{p^0} \frac{f}{\mu} (\mu'_p + \mu_n), \quad \operatorname{Im} \overset{\circ}{t}_3^3 = \pi \frac{M}{p^0} \frac{f}{\mu} (\mu'_p - \mu_n)$$

$$\operatorname{Im} \overset{\circ}{t}_1^1 = \pi \frac{M}{p^0} \frac{f}{\mu} \frac{e}{2p^0 E_2}, \quad \operatorname{Im} \overset{\circ}{t}_2^1 = \pi \frac{M}{p^0} \frac{f}{\mu} \frac{e}{2p^0 E_2}, \quad \operatorname{Im} \overset{\circ}{t}_3^1 = -\pi \frac{M}{p^0} \frac{f}{\mu} \frac{e}{2p^0 E_2} \tag{5.16}$$

$$\operatorname{Im} \overset{\circ}{t}_1^4 = -\pi \frac{M}{p^0} \left(\frac{ef}{4\mu} + \frac{Mf}{2\mu} (\mu'_p - \mu_n) \right)$$

$$\operatorname{Im} \overset{\circ}{t}_2^4 = -\pi \frac{M}{p^0} \left(\frac{ef}{4\mu} + \frac{Mf}{2\mu} (\mu'_p + \mu_n) \right)$$

$$\operatorname{Im} \overset{\circ}{t}_3^4 = \pi \frac{M}{p^0} \left(\frac{ef}{4\mu} + \frac{Mf}{2\mu} (\mu'_p - \mu_n) \right).$$

Dispersion relations (5.13) and (5.14) can be rewritten in a more compact form:

$$\operatorname{Re} t_j^s(E, \mathbf{p}^2) = r_j^s \left(\frac{1}{E_1 - E} \pm \frac{1}{E_1 + E} \right) \frac{M}{p^0} + \frac{1}{\pi} V_p \int_{\frac{M_\mu + \frac{1}{2}\mu^2 - \mathbf{p}^2}{\sqrt{M^2 + \mathbf{p}^2}}}^{\infty} \left\{ \frac{1}{E' - E} \pm \frac{1}{E' + E} \right\} \operatorname{Im} t_j^s(E', \mathbf{p}^2) \mathrm{d}E' \tag{5.17}$$

where the r_j^s are constants arising from the unobservable region and given, according to (5.16), by

$$r_1^2 = -\frac{f}{\mu} (\mu'_p - \mu_n), \quad r_2^2 = -\frac{f}{\mu} (\mu'_p + \mu_n), \quad r_3^2 = -\frac{f}{\mu} (\mu'_p - \mu_n)$$

$$r_1^3 = -\frac{f}{\mu} (\mu'_p - \mu_n), \quad r_2^3 = -\frac{f}{\mu} (\mu'_p + \mu_n), \quad r_3^3 = -\frac{f}{\mu} (\mu'_p - \mu_n)$$

$$r_1^1 = -\frac{f}{\mu} \frac{e}{2p^0 E_2}, \quad r_2^1 = -\frac{f}{\mu} \frac{e}{2p^0 E_2}, \quad r_3^1 = -\frac{f}{\mu} \frac{e}{2p^0 E_2} \tag{5.18}$$

$$r_1^4 = \left(\frac{ef}{4\mu} + \frac{Mf}{2\mu} (\mu'_p - \mu_n) \right)$$

$$r_2^4 = \left(\frac{ef}{4\mu} + \frac{Mf}{2\mu} (\mu'_p + \mu_n) \right)$$

$$r_3^4 = \left(\frac{ef}{4\mu} + \frac{Mf}{2\mu} (\mu'_p - \mu_n) \right).$$

The upper sign is taken in dispersion relations (5.17) if $s = 1, 2, 4$;

$j = 1, 2$ or $s = 3; j = 3$. The lower (minus) sign should be taken if $s = 1, 2, 4$; $j = 3$ or $s = 3$; $j = 1, 2$.

In writing dispersion relations (5.17) we took into account that

$$\frac{1}{E_2-E} \pm \frac{1}{E_2+E} = \mp \left\{ \frac{1}{E_1-E} \pm \frac{1}{E_1+E} \right\} \tag{5.19}$$

where

$$E_1 = -E_2.$$

Dispersion relations (5.17) are written in the reference system ($\mathbf{p}+\mathbf{p}^\Lambda = 0$). For purposes of usual phase shift analysis it would be more convenient to have them rewritten in the centre of mass system. In virtue of the laws of conservation of energy and momentum only three of the four vectors k, p, q, p' are independent. Noting that $k^2 = 0$, $p^2 = p'^2 = M^2$, $q^2 = \mu^2$ we can set up only two independent scalar products from the three independent vectors. For example,

$$\nu = \frac{1}{2M} k(p+p'), \quad \nu_1 = \frac{1}{2M} (kq). \tag{5.20}$$

Functions Ω_j^i depend only on the scalar products, that is, they are functions of ν and ν_1. In the coordinate system chosen by us they are functions of E and $\mathbf{p}^2$. Let us express the variables E and $\mathbf{p}^2$ through the invariants ν and ν_1.

Elementary calculation yield

$$\begin{aligned} \mathbf{p}^2 &= M\nu_1 - \tfrac{1}{4}\mu^2 \\ E &= \frac{M\nu}{\sqrt{M^2+\mathbf{p}^2}}. \end{aligned} \tag{5.21}$$

Changing the variables and denoting

$$t_j^s(E, \mathbf{p}^2) = h_j^s(\nu, \nu_1) \tag{5.22}$$

one can easily rewrite dispersion relations (5.17) in a covariant form †:

$$\begin{aligned} \operatorname{Re} h_j^s(\nu, \nu_1) &= r_j^s \left(\frac{1}{\nu_2-\nu} \pm \frac{1}{\nu_2+\nu} \right) \\ &+ \frac{1}{\pi} V_p \int_{\mu\left(1+\frac{\mu}{2M}-\frac{\nu_1}{\mu}\right)}^{\infty} \left\{ \frac{1}{\nu'-\nu} \pm \frac{1}{\nu'+\nu} \right\} \operatorname{Im} h_j^s(\nu', \nu_1) d\nu' \end{aligned} \tag{5.23}$$

† N. N. Bogolyubov has kindly informed us that similar results were reported at the Seattle conference in September 1956 by Goldberger, Low, Nambu and Chew. The authors are thankful to Prof. Low for sending a preprint of this work.

where

$$r_1^1 = -\frac{ef}{\mu}\frac{1}{2Mv_1},\ r_2^1 = -\frac{ef}{\mu}\frac{1}{2Mv_1},\ r_3^1 = -\frac{ef}{\mu}\frac{1}{2Mv_1}$$

$$r_1^2 = -\frac{f}{\mu}(\mu'_p-\mu_n),\ r_2^2 = -\frac{f}{\mu}(\mu'_p+\mu_n),\ r_3^2 = -\frac{f}{\mu}(\mu'_p-\mu_n)$$

$$r_1^3 = -\frac{f}{\mu}(\mu'_p-\mu_n),\ r_2^3 = -\frac{f}{\mu}(\mu'_p+\mu_n),\ r_3^3 = -\frac{f}{\mu}(\mu'_p-\mu_n) \quad (5.24)$$

$$r_1^4 = \frac{ef}{4\mu}+\frac{Mf}{2\mu}(\mu'_p-\mu_n),\ r_2^4 = \frac{ef}{4\mu}+\frac{Mf}{2\mu}(\mu'_p+\mu_n)$$

$$r_3^4 = \frac{ef}{4\mu}+\frac{Mf}{2\mu}(\mu'_p-\mu_n).$$

The upper (plus) sign is to be taken in dispersion relations (5.23) if $s = 1, 2, 4$; $j = 1, 2$ or $s = 3$, $j = 3$. The lower (minus) sign should be taken if $s = 1, 2, 4$; $j = 3$ or $s = 3$; $j = 1, 2$.

6. Dispersion Relations in the Centre of Mass System†

With a view to applications to the usual phase shift analysis we shall carry out all future work in the centre of mass system.

In this system the photoproduction amplitude (4.1) can be written in the following form:

$$\hat{R}^{\varrho\nu} = (\boldsymbol{\sigma}\cdot\boldsymbol{\pi}^\nu)\hat{M}_1+\frac{1}{|\mathbf{k}||\mathbf{q}|}(\boldsymbol{\sigma}\cdot\mathbf{q})\boldsymbol{\sigma}\cdot(\mathbf{k}\wedge\boldsymbol{\pi}^\nu)\hat{M}_2+\frac{1}{|\mathbf{k}||\mathbf{q}|}(\boldsymbol{\sigma}\cdot\mathbf{k})(\mathbf{q}\cdot\boldsymbol{\pi}^\nu)\hat{M}_3$$
$$+\frac{1}{|\mathbf{q}|^2}(\boldsymbol{\sigma}\cdot\mathbf{q})(\mathbf{q}\cdot\boldsymbol{\pi}^\nu)\hat{M}_4 \quad (6.1)$$

where $\mathbf{k}$, $\mathbf{q}$ are particle momenta in the c.m.s.

Taking into account that in the c.m.s.

$$\bar{u}(p')\hat{P}_1^{\alpha\beta}u(p)e_\alpha{}^\nu k_\beta = iN_kN_q\frac{k^0W}{E_q+M}(\boldsymbol{\sigma}\cdot\mathbf{q})(\mathbf{q}\cdot\boldsymbol{\pi}^\nu)-iN_kN_q\frac{k^0W}{E_k+M}(\boldsymbol{\sigma}\cdot\mathbf{k})(\mathbf{q}\cdot\boldsymbol{\pi}^\nu)$$

$$\bar{u}(p')\hat{P}_1^{\alpha\beta}u(p)e_\alpha{}^\nu k_\beta = iN_kN_q(kp)(\boldsymbol{\sigma}\cdot\boldsymbol{\pi}^\nu)+N_kN_q\frac{(kp)}{(E_k+M)(E_q+M)}(\boldsymbol{\sigma}\cdot\mathbf{q})\boldsymbol{\sigma}\cdot(\mathbf{k}\wedge\boldsymbol{\pi}^\nu)$$

$$\bar{u}(p')\hat{P}_3^{\alpha\beta}u(p)e_\alpha{}^\nu k_\beta = iN_kN_q(kp')(\boldsymbol{\sigma}\cdot\boldsymbol{\pi}^\nu)+N_kN_q\frac{(kp')}{(E_k+M)(E_q+M)}(\boldsymbol{\sigma}\cdot\mathbf{q})\boldsymbol{\sigma}\cdot(\mathbf{k}\wedge\boldsymbol{\pi}^\nu) \quad (6.2)$$
$$-iN_kN_q\frac{2W}{W+M}(\boldsymbol{\sigma}\cdot\mathbf{k})(\mathbf{q}\cdot\boldsymbol{\pi})-iN_kN_q\frac{2W}{W+M}\cdot\frac{k^0}{E_q+M}(\boldsymbol{\sigma}\cdot\mathbf{q})(\mathbf{q}\cdot\boldsymbol{\pi})$$

$$\bar{u}(p')\hat{P}_4^{\alpha\beta}u(p)e_\alpha{}^\nu k_\beta = iN_kN_q\frac{2k^0(W+M)}{E_k+M}(\boldsymbol{\sigma}\cdot\boldsymbol{\pi}^\nu)-N_kN_q\frac{2}{E_q+M}\frac{W+M}{E_k+M}(\boldsymbol{\sigma}\cdot\mathbf{q})\boldsymbol{\sigma}\cdot(\mathbf{k}\wedge\boldsymbol{\pi}^\nu)$$

$$N_k = \left(\frac{E_k+M}{2E_k}\right)^{\frac{1}{2}},\ E_k = \sqrt{M^2+\mathbf{k}^2},\ W = k^0+p^0 = q^0+p'^0$$

† In section 6 we assume $\mu = 1$.

$$\begin{aligned}
\operatorname{Re} t_j^4(E, \mathbf{p}^2) &= \frac{1}{\pi} V_p \int_0^\infty \left\{ \frac{1}{E'-E} + \frac{1}{E'+E} \right\} \operatorname{Im} t_j^4(E', \mathbf{p}^2) dE' \\
\operatorname{Re} t_3^3(E, \mathbf{p}^2) &= \frac{1}{\pi} V_p \int_0^\infty \left\{ \frac{1}{E'-E} + \frac{1}{E'+E} \right\} \operatorname{Im} t_3^3(E', \mathbf{p}^2) dE' \\
\operatorname{Re} t_3^4(E', \mathbf{p}^2) &= \frac{1}{\pi} V_p \int_0^\infty \left\{ \frac{1}{E'-E} - \frac{1}{E'+E} \right\} \operatorname{Im} t_3^4(E', \mathbf{p}^2) dE' \\
\operatorname{Re} t_j^3(E, \mathbf{p}^2) &= \frac{1}{\pi} V_p \int_0^\infty \left\{ \frac{1}{E'-E} - \frac{1}{E'+E} \right\} \operatorname{Im} t_j^3(E', \mathbf{p}^2) dE' \\
&(j = 1, 2).
\end{aligned} \tag{5.13}$$

Performing analogous computations for the combinations $\mathfrak{S}_e (1 \pm P) \hat{\gamma}^\nu(E, \lambda e)$ and substituting the obtained expressions into (5.5a) we find

$$\begin{aligned}
\operatorname{Re} t_3^i(E, \mathbf{p}^2) &= \frac{1}{\pi} V_p \int_0^\infty \left\{ \frac{1}{E'-E} - \frac{1}{E'+E} \right\} \operatorname{Im} t_3^i(E', \mathbf{p}^2) dE' \\
\operatorname{Re} t_j^i(E, \mathbf{p}^2) &= \frac{1}{\pi} V_p \int_0^\infty \left\{ \frac{1}{E'-E} + \frac{1}{E'+E} \right\} \operatorname{Im} t_j^i(E', \mathbf{p}^2) dE' \\
&(j, i = 1, 2).
\end{aligned} \tag{5.14}$$

The contribution from the unobservable energy region was calculated in section 3. In order to apply the results obtained there we shall write the inhomogeneous term (3.9) in a form analogous to that of (4.1) and (4.3) and compute the corresponding $\mathring{\Omega}_j^s$. Carrying out these elementary calculations we get

$$\begin{aligned}
&\operatorname{Im} \mathring{\Omega}_1^1 = \frac{\pi}{2p^0} \left(\frac{eg}{2p^0 E_2} \right), \quad \operatorname{Im} \mathring{\Omega}_2^1 = \frac{\pi}{2p^0} \left(\frac{eg}{2p^0 E_2} \right), \quad \operatorname{Im} \mathring{\Omega}_3^1 = -\frac{\pi}{2p^0} \left(\frac{eg}{2p^0 E_2} \right) \\
&\operatorname{Im} \mathring{\Omega}_1^3 = \frac{\pi}{2p^0} g(\mu'_p - \mu_n), \quad \operatorname{Im} \mathring{\Omega}_2^3 = \frac{\pi}{2p^0} g(\mu'_p + \mu_n), \quad \operatorname{Im} \mathring{\Omega}_3^3 = -\frac{\pi}{2p^0} g(\mu_p' - \mu_n) \\
&\operatorname{Im} \mathring{\Omega}_1^4 = -\frac{\pi}{2p^0} \left(\frac{eg}{4} + \frac{Mg}{2} (\mu'_p - \mu_n) \right) \\
&\operatorname{Im} \mathring{\Omega}_2^4 = -\frac{\pi}{2p^0} \left(\frac{eg}{4} + \frac{Mg}{2} (\mu'_p + \mu_n) \right) \\
&\operatorname{Im} \mathring{\Omega}_3^4 = \frac{\pi}{2p^0} \left(\frac{eg}{4} + \frac{Mg}{2} (\mu'_p - \mu_n) \right).
\end{aligned} \tag{5.15}$$

Taking into account (4.13) we find from here

$$\begin{aligned}
&\operatorname{Im} \mathring{t}_1^2 = \pi \frac{M}{p^0} \frac{f}{\mu} (\mu'_p - \mu_n), \ \operatorname{Im} \mathring{t}_2^2 = \pi \frac{M}{p^0} \frac{f}{\mu} (\mu'_p + \mu_n), \ \operatorname{Im} \mathring{t}_3^2 = -\pi \frac{M}{p^0} \frac{f}{\mu} (\mu'_p - \mu_n) \\
&\operatorname{Im} \mathring{t}_1^3 = -\pi \frac{M}{p^0} \frac{f}{\mu} (\mu'_p - \mu_n), \ \operatorname{Im} \mathring{t}_2^3 = -\pi \frac{M}{p^0} \frac{f}{\mu} (\mu'_p + \mu_n), \ \operatorname{Im} \mathring{t}_3^3 = \pi \frac{M}{p^0} \frac{f}{\mu} (\mu'_p - \mu_n) \\
&\operatorname{Im} \mathring{t}_1^1 = \pi \frac{M}{p^0} \frac{f}{\mu} \frac{e}{2p^0 E_2}, \ \operatorname{Im} \mathring{t}_2^1 = \pi \frac{M}{p^0} \frac{f}{\mu} \frac{e}{2p^0 E_2}, \ \operatorname{Im} \mathring{t}_3^1 = -\pi \frac{M}{p^0} \frac{f}{\mu} \frac{e}{2p^0 E_2} \qquad (5.16) \\
&\operatorname{Im} \mathring{t}_1^4 = -\pi \frac{M}{p^0} \left(\frac{ef}{4\mu} + \frac{Mf}{2\mu} (\mu'_p - \mu_n) \right) \\
&\operatorname{Im} \mathring{t}_2^4 = -\pi \frac{M}{p^0} \left(\frac{ef}{4\mu} + \frac{Mf}{2\mu} (\mu'_p + \mu_n) \right) \\
&\operatorname{Im} \mathring{t}_3^4 = \pi \frac{M}{p^0} \left(\frac{ef}{4\mu} + \frac{Mf}{2\mu} (\mu'_p - \mu_n) \right).
\end{aligned}$$

Dispersion relations (5.13) and (5.14) can be rewritten in a more compact form:

$$\begin{aligned}
\operatorname{Re} t_j^s(E, \mathbf{p}^2) = r_j^s &\left(\frac{1}{E_1 - E} \pm \frac{1}{E_1 + E} \right) \frac{M}{p^0} \\
&+ \frac{1}{\pi} V_p \int_{\frac{M_\mu + \frac{1}{2}\mu^2 - \mathbf{p}^2}{\sqrt{M^2 + \mathbf{p}^2}}}^{\infty} \left\{ \frac{1}{E' - E} \pm \frac{1}{E' + E} \right\} \operatorname{Im} t_j^s(E', \mathbf{p}^2) \mathrm{d}E' \qquad (5.17)
\end{aligned}$$

where the r_j^s are constants arising from the unobservable region and given, according to (5.16), by

$$\begin{aligned}
&r_1^2 = -\frac{f}{\mu} (\mu'_p - \mu_n), \ r_2^2 = -\frac{f}{\mu} (\mu'_p + \mu_n), \ r_3^2 = -\frac{f}{\mu} (\mu'_p - \mu_n) \\
&r_1^3 = -\frac{f}{\mu} (\mu'_p - \mu_n), \ r_2^3 = -\frac{f}{\mu} (\mu'_p + \mu_n), \ r_3^3 = -\frac{f}{\mu} (\mu'_p - \mu_n) \\
&r_1^1 = -\frac{f}{\mu} \frac{e}{2p^0 E_2}, \ r_2^1 = -\frac{f}{\mu} \frac{e}{2p^0 E_2}, \ r_3^1 = -\frac{f}{\mu} \frac{e}{2p^0 E_2} \qquad (5.18) \\
&r_1^4 = \left(\frac{ef}{4\mu} + \frac{Mf}{2\mu} (\mu'_p - \mu_n) \right) \\
&r_2^4 = \left(\frac{ef}{4\mu} + \frac{Mf}{2\mu} (\mu'_p + \mu_n) \right) \\
&r_3^4 = \left(\frac{ef}{4\mu} + \frac{Mf}{2\mu} (\mu'_p - \mu_n) \right).
\end{aligned}$$

The upper sign is taken in dispersion relations (5.17) if $s = 1, 2, 4$;

$j = 1, 2$ or $s = 3; j = 3$. The lower (minus) sign should be taken if $s = 1, 2, 4$; $j = 3$ or $s = 3$; $j = 1, 2$.

In writing dispersion relations (5.17) we took into account that

$$\frac{1}{E_2-E} \pm \frac{1}{E_2+E} = \mp \left\{\frac{1}{E_1-E} \pm \frac{1}{E_1+E}\right\} \tag{5.19}$$

where

$$E_1 = -E_2.$$

Dispersion relations (5.17) are written in the reference system $(\mathbf{p}+\mathbf{p}^* = 0)$. For purposes of usual phase shift analysis it would be more convenient to have them rewritten in the centre of mass system. In virtue of the laws of conservation of energy and momentum only three of the four vectors k, p, q, p' are independent. Noting that $k^2 = 0$, $p^2 = p'^2 = M^2$, $q^2 = \mu^2$ we can set up only two independent scalar products from the three independent vectors. For example,

$$\nu = \frac{1}{2M} k(p+p'), \quad \nu_1 = \frac{1}{2M} (kq). \tag{5.20}$$

Functions Ω_j^s depend only on the scalar products, that is, they are functions of ν and ν_1. In the coordinate system chosen by us they are functions of E and $\mathbf{p}^2$. Let us express the variables E and $\mathbf{p}^2$ through the invariants ν and ν_1.

Elementary calculation yield

$$\begin{aligned} \mathbf{p}^2 &= M\nu_1 - \tfrac{1}{4}\mu^2 \\ E &= \frac{M\nu}{\sqrt{M^2+\mathbf{p}^2}}. \end{aligned} \tag{5.21}$$

Changing the variables and denoting

$$t_j^s(E, \mathbf{p}^2) = h_j^s(\nu, \nu_1) \tag{5.22}$$

one can easily rewrite dispersion relations (5.17) in a covariant form †:

$$\begin{aligned} \operatorname{Re} h_j^s(\nu, \nu_1) &= r_j^s \left(\frac{1}{\nu_2-\nu} \pm \frac{1}{\nu_2+\nu}\right) \\ &+ \frac{1}{\pi} V_\nu \int_{\mu\left(1+\frac{\mu}{2M}-\frac{\nu_1}{\mu}\right)}^{\infty} \left\{\frac{1}{\nu'-\nu} \pm \frac{1}{\nu'+\nu}\right\} \operatorname{Im} h_j^s(\nu', \nu_1) d\nu' \end{aligned} \tag{5.23}$$

† N. N. Bogolyubov has kindly informed us that similar results were reported at the Seattle conference in September 1956 by Goldberger, Low, Nambu and Chew. The authors are thankful to Prof. Low for sending a preprint of this work.

where

$$r_1^1 = -\frac{ef}{\mu}\frac{1}{2M\nu_1},\ r_2^1 = -\frac{ef}{\mu}\frac{1}{2M\nu_1},\ r_3^1 = -\frac{ef}{\mu}\frac{1}{2M\nu_1}$$

$$r_1^2 = -\frac{f}{\mu}(\mu'_p-\mu_n),\ r_2^2 = -\frac{f}{\mu}(\mu'_p+\mu_n),\ r_3^2 = -\frac{f}{\mu}(\mu'_p-\mu_n)$$

$$r_1^3 = -\frac{f}{\mu}(\mu'_p-\mu_n),\ r_2^3 = -\frac{f}{\mu}(\mu'_p+\mu_n),\ r_3^3 = -\frac{f}{\mu}(\mu'_p-\mu_n) \quad (5.24)$$

$$r_1^4 = \frac{ef}{4\mu}+\frac{Mf}{2\mu}(\mu'_p-\mu_n),\ r_2^4 = \frac{ef}{4\mu}+\frac{Mf}{2\mu}(\mu'_p+\mu_n)$$

$$r_3^4 = \frac{ef}{4\mu}+\frac{Mf}{2\mu}(\mu'_p-\mu_n).$$

The upper (plus) sign is to be taken in dispersion relations (5.23) if $s = 1, 2, 4$; $j = 1, 2$ or $s = 3$, $j = 3$. The lower (minus) sign should be taken if $s = 1, 2, 4$; $j = 3$ or $s = 3$; $j = 1, 2$.

6. Dispersion Relations in the Centre of Mass System†

With a view to applications to the usual phase shift analysis we shall carry out all future work in the centre of mass system.

In this system the photoproduction amplitude (4.1) can be written in the following form:

$$\hat{R}^{\sigma\nu} = (\boldsymbol{\sigma}\cdot\boldsymbol{\pi}^\nu)\hat{M}_1+\frac{1}{|\mathbf{k}||\mathbf{q}|}(\boldsymbol{\sigma}\cdot\mathbf{q})\boldsymbol{\sigma}\cdot(\mathbf{k}\wedge\boldsymbol{\pi}^\nu)\hat{M}_2+\frac{1}{|\mathbf{k}||\mathbf{q}|}(\boldsymbol{\sigma}\cdot\mathbf{k})(\mathbf{q}\cdot\boldsymbol{\pi}^\nu)\hat{M}_3$$
$$+\frac{1}{|\mathbf{q}|^2}(\boldsymbol{\sigma}\cdot\mathbf{q})(\mathbf{q}\cdot\boldsymbol{\pi}^\nu)\hat{M}_4 \quad (6.1)$$

where $\mathbf{k}$, $\mathbf{q}$ are particle momenta in the c.m.s.

Taking into account that in the c.m.s.

$$\bar{u}(p')\hat{P}_1^{\alpha\beta}u(p)e_\alpha{}^\nu k_\beta = iN_kN_q\frac{k^0W}{E_q+M}(\boldsymbol{\sigma}\cdot\mathbf{q})(\mathbf{q}\cdot\boldsymbol{\pi}^\nu)-iN_kN_q\frac{k^0W}{E_k+M}(\boldsymbol{\sigma}\cdot\mathbf{k})(\mathbf{q}\cdot\boldsymbol{\pi}^\nu)$$

$$\bar{u}(p')\hat{P}_1^{\alpha\beta}u(p)e_\alpha{}^\nu k_\beta = iN_kN_q(kp)(\boldsymbol{\sigma}\cdot\boldsymbol{\pi}^\nu)+N_kN_q\frac{(kp)}{(E_k+M)(E_q+M)}(\boldsymbol{\sigma}\cdot\mathbf{q})\boldsymbol{\sigma}\cdot(\mathbf{k}\wedge\boldsymbol{\pi}^\nu)$$

$$\bar{u}(p')\hat{P}_3^{\alpha\beta}u(p)e_\alpha{}^\nu k_\beta = iN_kN_q(kp')(\boldsymbol{\sigma}\cdot\boldsymbol{\pi}^\nu)+N_kN_q\frac{(kp')}{(E_k+M)(E_q+M)}(\boldsymbol{\sigma}\cdot\mathbf{q})\boldsymbol{\sigma}\cdot(\mathbf{k}\wedge\boldsymbol{\pi}^\nu) \quad (6.2)$$
$$-iN_kN_q\frac{2W}{W+M}(\boldsymbol{\sigma}\cdot\mathbf{k})(\mathbf{q}\cdot\boldsymbol{\pi})-iN_kN_q\frac{2W}{W+M}\cdot\frac{k^0}{E_q+M}(\boldsymbol{\sigma}\cdot\mathbf{q})(\mathbf{q}\cdot\boldsymbol{\pi})$$

$$\bar{u}(p')\hat{P}_4^{\alpha\beta}u(p)e_\alpha{}^\nu k_\beta = iN_kN_q\frac{2k^0(W+M)}{E_k+M}(\boldsymbol{\sigma}\cdot\boldsymbol{\pi}^\nu)-N_kN_q\frac{2}{E_q+M}\frac{W+M}{E_k+M}(\boldsymbol{\sigma}\cdot\mathbf{q})\boldsymbol{\sigma}\cdot(\mathbf{k}\wedge\boldsymbol{\pi}^\nu)$$

$$N_k = \left(\frac{E_k+M}{2E_k}\right)^{\frac{1}{2}},\ E_k = \sqrt{M^2+\mathbf{k}^2},\ W = k^0+p^0 = q^0+p'^0$$

† In section 6 we assume $\mu = 1$.

we obtain

$$\hat{M}_1 = iN_kN_q(W-M)\left[\frac{W+M}{2}(\hat{\Omega}^2+\hat{\Omega}^3)-\frac{2Mv_1}{W-M}\hat{\Omega}^3+2\hat{\Omega}^4\right]$$

$$\hat{M}_2 = N_kN_q\frac{|\mathbf{q}|}{E_q+M}(W-M)\left[\frac{W-M}{2}(\hat{\Omega}^2+\hat{\Omega}^3)-\frac{2Mv_1}{W+M}\hat{\Omega}^3-2\hat{\Omega}^4\right] \tag{6.3}$$

$$\hat{M}_3 = -iN_kN_q|\mathbf{q}|(W-M)\left[\frac{W-M}{2}\hat{\Omega}^1+\hat{\Omega}^3\right]$$

$$\hat{M}_4 = iN_kN_q\frac{\mathbf{q}^2(W-M)}{E_q+M}\left[\frac{W+M}{2}\hat{\Omega}^1-\hat{\Omega}^3\right].$$

The following relations which hold in the c.m.s. were used in obtaining (6.3):

$$E_q = \sqrt{\mathbf{q}^2+\mu^2} = k+\frac{\mu^2}{2W},\quad \frac{k}{M+E_k} = \frac{W-M}{W+M};\ k = \frac{W^2-M^2}{2W}.$$

Taking into account (4.13) we have

$$\hat{M}_1 = iN_kN_q(W-M)\left[\frac{W+M}{2}t_q^2-\frac{Mv_1}{W-M}(t_q^2-t_q^3)+2t_q^4\right]$$

$$\hat{M}_2 = N_kN_q\frac{|\mathbf{q}|}{E_q+M}(W-M)\left[\frac{W-M}{2}t_q^2-\frac{Mv_1}{W+M}(t_q^2-t_q^3)-2t_q^4\right] \tag{6.4}$$

$$\hat{M}_3 = -iN_kN_q|\mathbf{q}|(W-M)\tfrac{1}{2}[(W-M)t_q^1+t_q^2-t_q^3]$$

$$\hat{M}_4 = iN_kN_q\frac{\mathbf{q}^2(W-M)}{E_q+M}\left[\frac{W+M}{2}t_q^1-\tfrac{1}{2}(t_q^2-t_q^3)\right].$$

We shall introduce the following notations:

$$\hat{u}_1 = \frac{i}{W-M}\left(\frac{4E_kE_q}{(E_k+M)(E_q+M)}\right)^{\frac{1}{2}}\hat{M}_1$$

$$\hat{u}_2 = \frac{1}{|\mathbf{q}|(W-M)}\left(\frac{4E_kE_q(E_q+M)}{E_k+M}\right)^{\frac{1}{2}}\hat{M}_2$$

$$\hat{u}_3 = \frac{i}{|\mathbf{q}|(W-M)}\left(\frac{4E_kE_q}{(E_k+M)(E_q+M)}\right)^{\frac{1}{2}}\hat{M}_3 \tag{6.5}$$

$$\hat{u}_4 = \frac{i}{|\mathbf{q}|(W-M)}\left(\frac{4E_kE_q(E_q+M)}{E_k+M}\right)^{\frac{1}{2}}\hat{M}_4.$$

On the basis of formulae (6.4—6.5) we have

$$\begin{aligned}
\hat{\mathfrak{U}}_1 &= \frac{W+M}{2} t_0^2 - \frac{M\nu_1}{W-M}(t_0^2 - t_0^3) + 2t_0^4 \\
\hat{\mathfrak{U}}_2 &= \frac{W-M}{2} t_0^2 - \frac{M\nu_1}{W+M}(t_0^2 - t_0^3) - 2t_0^4 \\
\hat{\mathfrak{U}}_3 &= -\left[\frac{W-M}{2} t_0^1 + \tfrac{1}{2}(t_0^2 - t_0^3)\right] \\
\hat{\mathfrak{U}}_4 &= \frac{W+M}{2} t_0^1 - \tfrac{1}{2}(t_0^2 - t_0^3)
\end{aligned} \tag{6.6}$$

whence the inverse expressions can easily be obtained:

$$\begin{aligned}
t_0^1 &= \frac{1}{W}(\hat{\mathfrak{U}}_4 - \hat{\mathfrak{U}}_3) \\
t_0^2 &= \frac{1}{W}(\hat{\mathfrak{U}}_1 + \hat{\mathfrak{U}}_2) - \frac{2M\nu_1}{W(W-M)}\hat{\mathfrak{U}}_3 - \frac{2M\nu_1}{W(W+M)}\hat{\mathfrak{U}}_4 \\
t_0^3 &= \frac{1}{W}(\hat{\mathfrak{U}}_1 + \hat{\mathfrak{U}}_2) - \frac{1}{W}\left(\frac{2M\nu_1}{W-M} - W - M\right)\hat{\mathfrak{U}}_3 \\
&\qquad - \frac{1}{W}\left(\frac{2M\nu_1}{W+M} - W + M\right)\hat{\mathfrak{U}}_4 \\
t_0^4 &= \frac{1}{4W}[(W-M)\hat{\mathfrak{U}}_1 - (W+M)\hat{\mathfrak{U}}_2].
\end{aligned} \tag{6.7}$$

Introducing the notations

$$\alpha = \frac{1}{\nu' - \nu} = \frac{2M}{W'^2 - W^2}$$

$$\beta = \frac{1}{\nu' + \nu} = \frac{2M}{W'^2 + W^2 - 4M\nu_1 - 2M^2}$$

and employing formulae (6.6) and dispersion relations (5.23) we obtain

$$\begin{aligned}
\operatorname{Re}\mathfrak{U}_j^1(W, \nu_1) = \mathring{\mathfrak{U}}_j^1 + \int_{M+1}^{\infty} dW' \frac{W'}{M}(\alpha \pm \beta)\left\{\left(\frac{W+M}{2} - \frac{M\nu_1}{W-M}\right)\operatorname{Im} t_j^2(W', \nu_1)\right. \\
\left. + 2\operatorname{Im} t_j^4(W', \nu_1)\right\} + \int_{M+1}^{\infty} dW' \frac{W'}{M}(\alpha \pm \beta)\frac{M\nu_1}{W-M}\operatorname{Im} t_j^3(W', \nu_1).
\end{aligned}$$

The upper sign is taken if $j = 1, 2$; the lower sign if $j = 3$.

Replacing $\operatorname{Im} t_j^2$, $\operatorname{Im} t_j^3$, $\operatorname{Im} t_j^4$ in the preceding formula by the respective

expressions obtained from (6.7) after some elementary calculations we obtain

$$\begin{aligned}\operatorname{Re}\mathcal{U}_j^1(W,\nu_1)=\mathring{\mathcal{U}}_j^1+\frac{1}{\pi}\int_{M+1}^{\infty}dW'\Bigg\{&\operatorname{Im}\mathcal{U}_j^1(W',\nu_1)\left[\frac{1}{W'-W}\pm\frac{W'+W-\dfrac{4M\nu_1}{W-M}}{W'^2+W^2-2M^2-4M\nu_1}\right]\\&-\operatorname{Im}\mathcal{U}_j^2(W',\nu_1)\left[\frac{1}{W'+W}\pm\frac{W'-W+\dfrac{4M\nu_1}{W-M}}{W'^2+W^2-2M^2-4M\nu_1}\right]\\&+\begin{pmatrix}0\\1\end{pmatrix}\left[\frac{\operatorname{Im}\mathcal{U}_j^3(W',\nu_1)}{W'-M}+\frac{\operatorname{Im}\mathcal{U}_j^4(W',\nu_1)}{W'+M}\right]\frac{4M\nu_1}{W-M}\Bigg\}.\end{aligned}\tag{6.8}$$

The dispersion relations for the quantities $\mathcal{U}_j^2$, $\mathcal{U}_j^3$, $\mathcal{U}_j^4$ can be written in a similar manner:

$$\begin{aligned}\operatorname{Re}\mathcal{U}_j^2(W,\nu_1)=\mathring{\mathcal{U}}_j^2+\frac{1}{\pi}\int_{M+1}^{\infty}dW'\Bigg\{&\operatorname{Im}\mathcal{U}_j^2(W',\nu_1)\left[\frac{1}{W'-W}\pm\frac{W'+W-\dfrac{4M\nu_1}{W+M}}{W'^2+W-4M\nu_1-2M^2}\right]\\&-\operatorname{Im}\mathcal{U}_j^1(W',\nu_1)\left[\frac{1}{W'+W}\pm\frac{W'-W+\dfrac{4M\nu_1}{W+M}}{W'^2+W^2-4M\nu_1-2M^2}\right]\\&+\begin{pmatrix}0\\1\end{pmatrix}\left[\frac{\operatorname{Im}\mathcal{U}_j^3(W',\nu_1)}{W'-M}+\frac{\operatorname{Im}\mathcal{U}_j^4(W',\nu_1)}{W'+M}\right]\frac{4M\nu_1}{W+M}\Bigg\}\end{aligned}$$

$$\begin{aligned}\operatorname{Re}\mathcal{U}_j^3(W,\nu_1)=\mathring{\mathcal{U}}_j^3+\frac{1}{\pi}\int_{M+1}^{\infty}dW'\Bigg\{&\operatorname{Im}\mathcal{U}_j^3(W',\nu_1)\left[\frac{1}{W'-W}\pm\frac{W-W'-2M+\dfrac{4M\nu_1}{W'-M}}{W'^2+W^2-4M\nu_1-2M^2}\right]\\&+\operatorname{Im}\mathcal{U}_j^4(W',\nu_1)\left[\frac{1}{W'+W}\pm\frac{2M-W'-W+\dfrac{4M\nu_1}{W'+M}}{W'^2+W^2-4M\nu_1-2M^2}\right]\\&\mp2[\operatorname{Im}\mathcal{U}_j^1(W',\nu_1)+\operatorname{Im}\mathcal{U}_j^2(W',\nu_1)]\frac{1}{W'^2+W^2-4M\nu_1-2M^2}\Bigg\}\end{aligned}\tag{6.9}$$

$$\begin{aligned}\operatorname{Re}\mathcal{U}_j^4(W,\nu_1)=\mathring{\mathcal{U}}_j^4+\frac{1}{\pi}\int_{M+1}^{\infty}dW'\Bigg\{&\operatorname{Im}\mathcal{U}_j^4(W',\nu_1)\left[\frac{1}{W'-W}\pm\frac{W-W'+2M+\dfrac{4M\nu_1}{W'+M}}{W'^2+W^2-4M\nu_1-2M^2}\right]\\&+\operatorname{Im}\mathcal{U}_j^3(W',\nu_1)\left[\frac{1}{W'+W}\pm\frac{-W'-W-2M+\dfrac{4M\nu_1}{W'-M}}{W'^2+W^2-4M\nu_1-2M^2}\right]\\&\mp2[\operatorname{Im}\mathcal{U}_j^1(W',\nu_1)+\operatorname{Im}\mathcal{U}_j^2(W',\nu_1)]\frac{1}{W'^2+W^2-4M\nu_1-2M^2}\Bigg\}.\end{aligned}$$

Expressions for the coefficients $\mathring{\mathscr{U}}_j^1$ can easily be obtained by using formulae (6.6). Thus, for example,

$$\mathring{\mathscr{U}}_1^4 = \frac{W+M}{2} r_1^1(\alpha+\beta) - \tfrac{1}{2}(\alpha+\beta) r_1^2 + \tfrac{1}{2}(\alpha-\beta) r_1^3$$

whence, on basis of (5.24), we get

$$\mathring{\mathscr{U}}_1^4 = -\frac{ef}{\mu}\frac{1}{2M\nu_1}\frac{W+M}{2}(\alpha+\beta) + \tfrac{1}{2}(\alpha+\beta)\frac{f}{\mu}(\mu'_p-\mu_n) - \tfrac{1}{2}(\alpha-\beta)\frac{f}{\mu}(\mu'_p-\mu_n)$$

$$= \tfrac{1}{2}ef\frac{1}{M\nu_1}\left[\frac{M}{W-M} - \frac{M(W+M)}{W^2-M^2-4M\nu_1}\right] - f(\mu'_p-\mu_n)\frac{2M}{4M\nu_1-W^2+M^2}. \quad (6.10)$$

The other $\mathring{\mathscr{U}}_j^i$ coefficients can be computed in a similar manner. Summing up the results we obtain:

$$\begin{aligned}
\mathring{\mathscr{U}}_{je}^1 &= -\mathring{\mathscr{U}}_{je}^2 = -\tfrac{1}{2}ef\left[\frac{2M}{W^2-M^2} \mp \frac{2M}{W^2-M^2-4M\nu_1}\right] \\
\mathring{\mathscr{U}}_{je}^3 &= -\frac{ef}{4M\nu_1}\left[\frac{2M}{W+M} \mp \frac{2M(W-M)}{W^2-M^2-4M\nu_1}\right] \\
\mathring{\mathscr{U}}_{je}^4 &= \frac{ef}{4M\nu_1}\left[\frac{2M}{W-M} \mp \frac{2M(W+M)}{W^2-M^2-4M\nu_1}\right].
\end{aligned} \quad (6.11)$$

The upper sign is taken if $j = 1, 2$ and the lower sign if $j = 3$. The other part of $\mathscr{U}_j^i$ which depends on the anomalous neutron and proton magnetic moments can be written in the form

$$\begin{aligned}
\mathring{\mathscr{U}}_{j\mu}^1 &= \tfrac{1}{2}f(\mu'_p \mp \mu_n)\left[\frac{2M}{W+M} + \frac{2M(W-M) - \dfrac{8M^2\nu_1}{W-M}}{M^2-W^2+4M\nu_1}\right] \\
\mathring{\mathscr{U}}_{j\mu}^2 &= \tfrac{1}{2}f(\mu'_p \mp \mu_n)\left[\frac{2M}{W-M} + \frac{2M(W+M) - \dfrac{8M^2\nu_1}{W+M}}{M^2-W^2+4M\nu_1}\right] \\
\mathring{\mathscr{U}}_{3\mu}^j &= \tfrac{1}{2}f(\mu'_p-\mu_n)\left[\frac{2M}{W\pm M} - \frac{2M(W\mp M) - \dfrac{8M^2\nu_1}{W\mp M}}{M^2-W^2+4M\nu_1}\right] \\
&\qquad (j = 1, 2,)
\end{aligned} \quad (6.12)$$

(if $j = 1$, the upper sign is taken and if $j = 2$, the lower sign);

$$\begin{aligned}
\mathring{\mathscr{U}}_{i\mu}^3 &\mp \mp f(\mu'_p-\mu_n)\frac{2M}{4M\nu_1-W^2+M^2} \qquad (i = 1, 3) \\
\mathring{\mathscr{U}}_{i\mu}^4 &= \mathring{\mathscr{U}}_{i\mu}^3
\end{aligned} \quad (6.13)$$

(the upper sign is taken if $i = 1$ and the lower sign if $i = 3$);

$$\mathring{\mathcal{U}}^3_{2\mu} = -f(\mu'_p+\mu_n)\ \frac{2M}{4Mv_1-W^2+M^2}. \qquad (6.14)$$

It should be noted that

$$\mathring{\mathcal{U}}^j_i = \mathring{\mathcal{U}}^j_{ie}+\mathring{\mathcal{U}}^j_{i\mu}. \qquad (615)$$

In order to perform phase shift analysis in dispersion relations (6.8—6.9) one should express the coefficients in terms of the photoproduction amplitudes in the total angular momentum or parity representation or representation of other conservative quantities [9]).

In conclusion the authors express their appreciation to Academician N. N. Bogolyubov whose investigations and attention prompted us to carry out this work and also to B. V. Medvedyev, B. M. Stepanov and D. V. Shirkov for discussions.

References

1) M. Gell-Mann, M. L. Goldberger and W. E. Thirring, Phys. Rev. **95** (1954) 1612
2) N. N. Bogolyubov, B. V. Medvedyev and M. L. Polivanov, Problems related to the theory of dispersion relations (in print)
3) A. A. Logunov and B. M. Stepanov, Doklady Akademii Nauk **110** (1957) 368
4) A. A. Logunov, B. M. Stepanov and A. N. Tavkhelidze, Doklady Akademii Nauk **112** (1957) No. 1
5) A. A. Logunov and A. N. Tavkhelidze, JETP (1957) No. 6
6) B. Ioffe, JETP **31** (1956) 583
7) E. Corinaldesi, Nuovo Cimento **4** (1956) 1384
8) Koba, Katani and Nakai, Progr. Theor. Phys. **6** (1951) 849; Nakano and Nishijima, Progr. Theor. Phys. **6** (1952) 53
9) L. D. Solovyov, Nuclear Physics (in print)

Nuclear Physics **4** (1957) 453—456; © *North-Holland Publishing Co., Amsterdam*
Not to be reproduced by photoprint or microfilm without written permission from the publisher

β-γ-CORRELATION FOR ALLOWED TRANSITIONS INVOLVING NON-CONSERVATION OF PARITY

YU. V. GAPONOV AND V. S. POPOV

Moscow State University, U.S.S.R.

Received 16 April 1957

Abstract: The angular correlation between the directions of emission of electron and circularly-polarized γ-quantum in cascade β-γ-transitions is considered for allowed β-transitions, taking account of parity non-conservation. The effect of the nuclear Coulomb field is neglected.

Lee and Yang [1]) (see also review [2])) have pointed out that non-conservation of parity in β-decay should lead to a correlation between the circularly polarized γ-quantum and the decay electron in a $\beta-\gamma$ cascade process. We have performed calculations relating to this phenomenon for allowed transitions without taking into account the effect due to the nuclear Coulomb field. If a γ-transition takes place after β-decay the probability of emission of a γ-quantum at an angle θ with respect to the direction of emission of the electron will be

$$W(\theta) = 1-\mu\alpha\frac{v}{c}\cos\theta \tag{1}$$

where $\mu = \pm 1$ corresponds to right or left polarization of the γ-quantum; v is the electron velocity and α is a coefficient which depends on the coupling constants, nuclear angular momenta and γ-quantum multipole order:

$$\alpha = \frac{B\cdot 2\sqrt{j_2(j_2+1)}\delta_{j_2 j_1}+D[2+j_2(j_2+1)-j_1(j_1+1)]}{2\sqrt{j_2(j_2+1)}(A\delta_{j_2 j_1}+C)} \times \frac{j_2(j_2+1)+L_1(L_1+1)-j_3(j_3+1)}{2L_1(L_1+1)\sqrt{j_2(j_2+1)}}. \tag{2}$$

Here j_1, j_2 and j_3 are the angular momenta of the initial nucleus and the excited and ground levels of the final nucleus. L_1 is the multipole order of the γ-quantum. The coefficient α does not depend on the type of radiation (electric or magnetic) but only on its multipole order. The constants A, B, C and D in formula (2) are equal to

$$
\begin{aligned}
A &= \left\{|C_S|^2+|C'_S|^2+|C_V|^2+|C'_V|^2+\frac{2mc^2}{E}\,\mathrm{Re}(C_S^* C_V+C_S'^* C'_V)\right\}|a|^2\\
B &= 2\,\mathrm{Re}\,\{(C_S^* C'_T+C_S'^* C_T-C_V^* C'_A-C_V'^* C_A]a^* b\}\\
C &= \left\{|C_T|^2+|C'_T|^2+|C_A|^2+|C'_A|^2+\frac{2mc^2}{E}\,\mathrm{Re}\,(C_T^* C_A+C_T'^* C'_A)\right\}|b|^2\\
D &= 2\,\mathrm{Re}\,\{C_T^* C'_T-C_A^* C'_A\}|b|^2.
\end{aligned}
\tag{3}
$$

The quantities C_S, C'_S, etc., are constants which enter the β-interaction Hamiltonian written in a manner which takes into account non-conservation of parity (see for example ref. [1])). The primed constants refer to terms which arise as a result of non-conservation of parity in β-decay (if parity is conserved all $C' = 0$); m and E are respectively the electron mass and energy; a and b are nuclear matrix elements which are independent of the magnetic quantum numbers:

$$
\begin{aligned}
a &= \langle j_1|1|j_1\rangle\delta_{j_2 j_1}\\
b &= \langle j_2 m_1|\sigma_z|j_1 m_1\rangle\varepsilon^{m_1}_{j_1 j_2}
\end{aligned}
\tag{4}
$$

where

$$
\varepsilon^{m_1}_{j_1 j_2} = \begin{cases}
\sqrt{\dfrac{(2j_1+1)(j_1+1)}{(j_1-m_1+1)(j_1+m_1+1)}} & \text{for } j_2 = j_1+1\\[2ex]
\dfrac{\sqrt{j_1(j_1+1)}}{m_1} & \text{for } j_2 = j_1\\[2ex]
-\sqrt{\dfrac{j_1(2j_1+1)}{(j_1+m_1)(j_1-m_1)}} & \text{for } j_2 = j_1-1.
\end{cases}
$$

A and B enter formula (2) when $j_2 = j_1$. As can be seen from formulae (3) and (2) the angular distribution is anisotropic only if parity is not conserved.

The experiments of Wu and Lederman (see ref. [2])) confirm the longitudinal neutrino hypothesis proposed independently by Landau [3]) and Lee and Yang [4]). In this case $C = \pm C'$ and formulae (3) assume a simpler form. An analysis of the experiments carried out by Wu *et al.* [5]) indicates that $C = -C'$. Thus

$$
\begin{aligned}
A &= 2(|C_S|^2+|C_V|^2+\frac{2mc^2}{E}\,\mathrm{Re}(C_S^* C_V)|a|^2\\
B &= -4\,\mathrm{Re}\,[(C_S^* C_T-C_V^* C_A)a^* b]\\
C &= 2\left(|C_T|^2+|C_A|^2+\frac{2mc^2}{E}\,\mathrm{Re}\,C_T^* C_A\right)|b|^2\\
D &= -2(|C_T|^2-|C_A|^2)|b|^2.
\end{aligned}
\tag{5}
$$

Formula (1) can be extended to the case when the β-decay is followed by several successive γ-transitions. The probability of emission of the nth

($n > 1$) γ-quantum at an angle θ to the direction of emission of the electron is then given by the same formula (1) where now

$$\alpha = \frac{B \cdot 2\sqrt{j_2(j_2+1)}\delta_{j_2 j_1} + D[2 + j_2(j_2+1) - j_1(j_1+1)]}{2\sqrt{j_2(j_2+1)}(A\delta_{j_2 j_1} + C)} \times \frac{j_{n+1}(j_{n+1}+1) + L_n(L_n+1) - j_{n+2}(j_{n+2}+1)}{2L_n(L_n+1)\sqrt{j_{n+1}(j_{n+1}+1)}} \times \prod_{i=1}^{n-1} \frac{j_{i+1}(j_{i+1}+1) + j_{i+2}(j_{i+2}+1) - L_i(L_i+1)}{2\sqrt{j_{i+1}(j_{i+1}+1)j_{i+2}(j_{i+2}+1)}}. \tag{6}$$

Here j_1 is the angular momentum of the initial nucleus which experiences a β-transition to an excited level of the final nucleus of angular momentum j_2; by successive emission of γ-quanta possessing angular momenta $L_1, L_2, \ldots, L_n$, the nucleus goes over to levels with $j_3, \ldots, j_{n+2}$. As in the foregoing A, B, C, D are defined by formulae (3) and for the longitudinal neutrino by formulae (5).

The experimental data indicate that $C_V = C_A = 0$ [6]) and formulae (4) may be considerably simplified. The values of α computed on this assumption for some particular nuclei are given in tables 1 and 2. It should be noted that

TABLE 1

Initial nucleus	j_1	j_2	γ-transition	α	E_γ (keV)
K^{43}_{19}	3/2+	5/2+	5/2+ (E1) 3/2−	−0.70	373
			3/2− (M1) 5/2−	0.42	258
			5/2− (M1) 7/2−	0.42	369
			3/2− (E2) 7/2−	0.28	627
Co^{60}_{27}	5+	4+	4+ (E2) 2+	0.33	1172
			2+ (E2) 0+	0.33	1332
I^{131}_{53}	7/2+	5/2+	5/2+ (E2) 1/2+	0.33	184
			1/2+ (M1) 3/2+	−0.17	180
			5/2+ (M1) 3/2+	0.50	364
			5/2+ (E2) 3/2+	0.26	364
W^{187}_{74}	3/2−	5/2−	5/2− (E1) 5/2+	0.20	686
			5/2− (E1) 7/2+	0.50	552
			7/2+ (M1) 5/2+	−0.64 †	134
			5/2− (E2) 9/2−	0.33	480
			9/2− (M2) 5/2+	0.41	206
			9/2− (E3) 5/2+	−0.26	206
			9/2− (E1) 7/2+	−0.61	72
			7/2+ (M1) 5/2+	−0.61 ††	134

† In this transition the second γ-quantum is in the cascade 3/2− (β^-) 5/2− (E1) 7/2+ (M/1) 5/2+

†† In this transition the third γ-quantum is in the cascade 3/2− (β^-) 5/2− (E2) 9/2− (E1) 7/2+ (M1) 5/2+.

TABLE 2

Initial nucleus	j_1	j_2	γ-transition	$\alpha(A+C)$	E_γ (keV)
Na^{24}_{11}	4^+	4^+	4^+ (E2) 2^+ 2^+ (E2) 0^+	$0.373B+0.083D$ $0.373B+0.083D$	2750 1370
Sc^{46}_{21}	4^+	4^+	4^+ (E2) 0^+ 2^+ (E2) 0^+	 $0.373B+0.083D$	890 1120
Sc^{48}_{21}	6^+	6^+	6^+ (E2) 4^+ 4^+ (E2) 2^+ 2^+ (E2) 0^+	$0.360B+0.056D$ $0.360B+0.056D$ $0.360B+0.056D$	1050 1325 990

for transitions with $j_2 = j_1 \pm 1$ the nuclear matrix elements a and b do not enter at all into the expression for α. If $j_2 = j_1$, α depends explicitly on a and b, whose values are known at present with sufficient accuracy for light and mirror nuclei [7]).

A, B, C and D in tables 1 and 2 are computed from formulae (5) by taking into account that $C_V = C_A = 0$.

The nuclear decay schemes employed in tables 1 and 2 are taken from ref. [8]).

In conclusion it should be mentioned that despite the difficulties involved in the measurement of γ-ray polarization [2]), experimental investigation of the effect considered in the present paper would seem to be desirable especially in the case of transitions with $j_2 = j_1$. The reason for this is that α depends on the phase difference of constants C_S and C_T which, generally speaking, may be complex (it whould be mentioned that the matrix elements a and b which occur in α in this case are real). If, on the other hand, Landau's hypothesis [3]) of conservation of combined parity is correct, C_S and C_T should both be real (or both imaginary). Thus, investigation of the effect discussed here should permit one to ascertain the properties of the β-interaction Hamiltonian, which is important for the solution of the problem of parity non-conservation.

The authors wish to express their appreciation to Dr. I. S. Shapiro for suggesting the problem examined in the present paper and for valuable advice and encouragement.

References

1) T. D. Lee and C. N. Yang, Phys, Rev. **104** (1956) 254
2) I. S. Shapiro, Uspekhi Fiz. Nauk **61** (1957) No. 3
3) L. D. Landau, Nuclear Physics **3** (1957) 127
4) T. D. Lee and C. N. Yang, Phys. Rev. **105** (1957) 1671
5) C. S. Wu *et al.*, Phys. Rev. **105** (1957) 1413
6) Ya. B. Zeldovich, Uspheki Fiz. Nauk **56** (1955) 165
7) J. A. Smorodinsky, Uspekhi Fiz. Nauk **56** (1955) 201
8) B. S. Dzhelepov and L. K. Pekar, Decay Schemes of Radioactive Isotopes (Moscow-Leningrad, 1957)

Nuclear Physics **4** (1957) 457—462; © *North-Holland Publishing Co., Amsterdam*
Not to be reproduced by photoprint or microfilm without written permission from the publisher

A FURTHER STUDY OF THE DECAY OF Ir^{192}

J. MRÁZ
Central Research Institute for Physics, Dept. for Atomic Physics, Budapest

Received 19 June 1957

Abstract: We have measured the angular correlations of 308—316, 308—296 and 296—316 keV gamma cascades in the radiations of Pt^{192} to remove the ambiguities in the spin assigned to the fourth excited level of Pt^{192}. In the discussion we give an interpretation of the excited levels of Pt^{192}.

1. Introduction

Ir^{192} decays by negaton emission into Pt^{192} and by orbital electron capture into Os^{192}. The resulting gamma rays of Pt^{192} and Os^{192} have been extensively

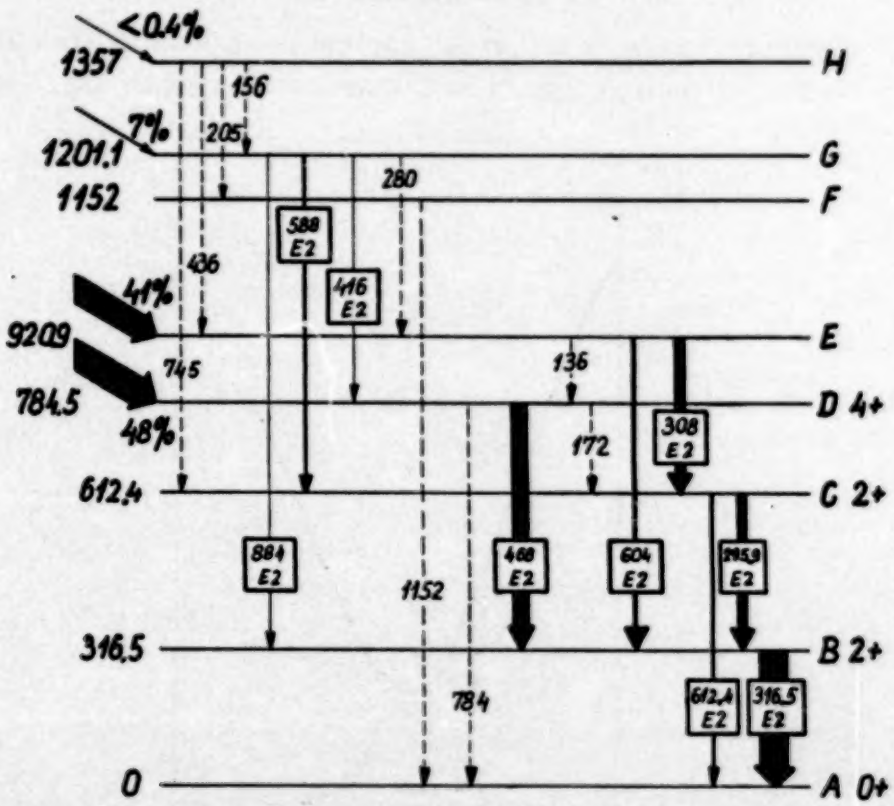

Fig. 1. Pt^{192} level scheme according to Baggerly *et al.* [2]). The thickness of arrows is proportional to the intensity of each transition.

studied[1–5]). The level scheme of Pt^{192} is shown in fig. 1 [2]). Spins and parities of the levels were determined by measurements of internal conversion

coefficients and angular correlations of the different cascades. The values given for the spin assigned to the fourth excited level, however, are uncertain and even contradictory: $j_E = 4$ [1]); $j_E = 3$ or 4 [2]); $j_E = 2$ or 3 or 4 or 5 [3]); $j_E = 3$ [4]). Therefore, it has seemed advisable to carry out further measurements to determine the spin of this level. Consequently the angular correlation of the Pt^{192} gamma radiation was measured.

2. Apparatus

NaI (Tl) scintillation crystals were used as a detector coupled to RCA 6342 photomultipliers. The pulses were fed into a fast-slow coincidence circuit. Differential discriminators were applied in both channels to select the appropriate gamma energies. The resolving time of the fast coincidence system was about 10^{-7} sec. In order to eliminate the scattered gamma rays the NaI (Tl) crystals were surrounded by a Pb layer of 12 mm thickness having a frontal aperture of solid angle of 12°. The actual solid angle was measured by positon annihilation radiation.

3. Experiment

Both discriminators were set on the photopeak at 300 keV. In all, 67 800 coincidences were counted. The ratio of true coincidences to accidental ones

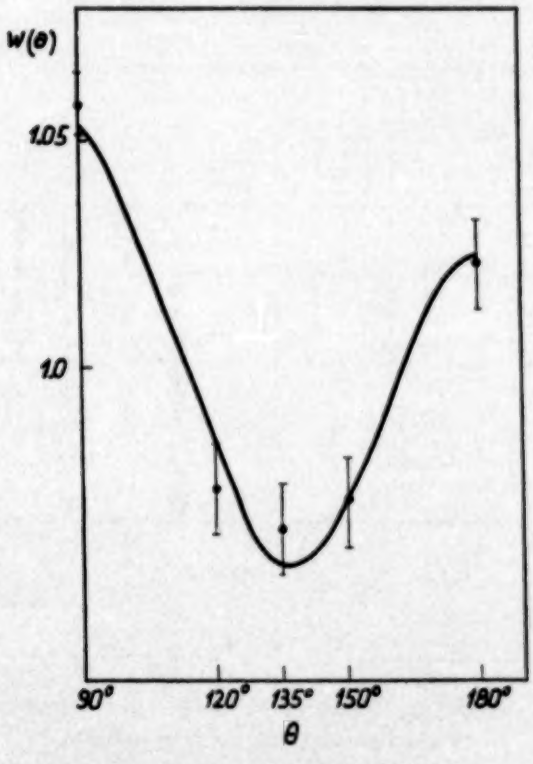

Fig. 2. Measured angular correlation in Pt^{192} gamma radiation.

was ≈ 50. The measured angular correlation is shown in fig. 2. Determining

from this the coefficients of the Legendre polynomials by the least squares method, we obtained $A_2 = -0.051 \pm 0.0077$, $A_4 = 0.076 \pm 0.0092$. Correcting for the finite angular resolution of the detectors, we obtained from this $A_2 = -0.056 \pm 0.0085$, $A_4 = 0.104 \pm 0.013$.

The angular correlation measured in this way is, however, the composite angular correlation of several cascades. Thus the determination of their relative intensities becomes necessary. We examined first the fractional contributions of cascades at about 600 keV (588, 604, 612 keV), at 468 keV and at about 300 keV (296, 308, 316 keV), respectively, to the pulses entering the differential discriminator channel.

The spectrum was analysed in the following way. The gamma spectrum of Cs^{137} ($E_\gamma = 667$ keV) was contracted in such a measure as to make its photopeak coincide with that of the Pt^{192} spectrum at 600 keV. The spectrum thus obtained was then subtracted from the Pt^{192} spectrum. The fractional contribution of the 468 keV gamma radiation was determined in a similar way by means of the Au^{198} spectrum. (The adjustment of the photopeaks was made, of course, after the subtraction of the contribution of the group at about 600 keV.) The contributions of the three gamma cascades at about 300 keV were determined on the basis of the decay scheme and relative intensities [2]). In this way we have obtained for the fractional contributions of the various gamma cascades the data collected in the following table:

Cascade (keV)	%
296–316	33.7
308–296	22.3
308–316	22.3
468–316	20.3
308–612	0.4
604–316	1.0

Subtracting the known 468–316 keV cascade contribution from the correlation coefficients, the following values are obtained:

$$A_2 = -(0.096 \pm 0.011), \quad A_4 = 0.128 \pm 0.016.$$

4. Discussion

The following assumptions have been examined:

1) The 308 and 296 keV gamma radiations are both pure E2.

In this case the experimental data cannot be interpreted either by a $j_E = 3$ or by a $j_E = 4$ spin assignment. Thus both transitions cannot be of a pure E2 type.

2) The 308 keV transition is of a mixed ($M1+\delta_1 E2$) type.

Then it ought to be $j_E = 3$. For this assumption, however, there is no δ_1 value to fit the experimental data.

3) The 308 keV transition is of a pure E2 and the 296 keV transition of a (M1+δ_2 E2) type.

a) For $j_E = 3$ again no δ_2 value can be found to interpret the experimental data.

b) For $j_E = 4$ the admixture ratio $\delta_2 = -6.5 \pm 1.5$ is in agreement with the experimental data. In fig. 3 we have plotted the coefficients A_2 and A_4 as functions of the admixture parameter δ_2. The full line represents the values for $j_E = 4$ and the dotted line those for $j_E = 3$. The shadowed

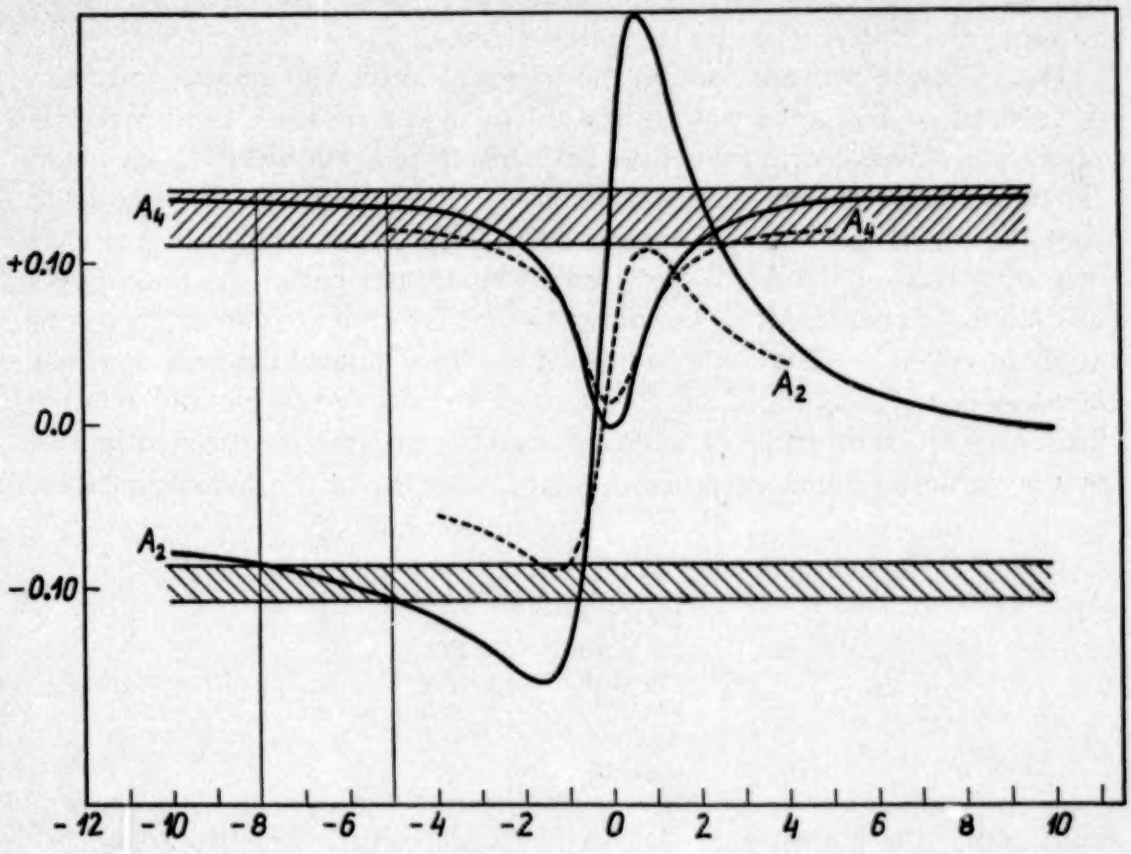

Fig. 3. Coefficients A_2 and A_4 as functions of the admixture parameter $\delta_2 - j_E = 4, \ldots j_E = 3$. The shadowed areas represent the measured values of A_2 and A_4 including errors of measurement.

areas represent the experimental values of A_2 and A_4, errors included. The appropriate value of δ_2 is that for which both curves A_2 and A_4 are in the corresponding measuring interval.

4) $j_E = 3$ and both transitions are mixed. Then only a relation between the admixture parameters δ_1 and δ_2 may be given from the measured angular correlation coefficients. (From the equation for the coefficient A_4 only the $|\delta_2| \geqq 2$ solution may be obtained.) Taking into account, however, the conversion coefficients as measured [2, 5]) including errors, we obtain as a result that there are no pairs of values by which both the angular

correlation coefficients and the internal conversion coefficients may be explained simultaneously.

It follows from the above considerations that the spin of the fourth excited level must be $j_E = 4$, its parity being + (taking into account the internal conversion data). The 308 keV radiation is pure E2. The 296 keV radiation is mixed and its admixture parameter is $\delta = -6.5 \pm 1.5$. This value is consistent with the values of the internal conversion coefficients. Our result confirms that obtained by H. W. Taylor and R. W. Pringle [1]).

On the basis of the Pt^{192} decay scheme and considering the results of our measurements, the following relations could be established:

1) The excitation energies of the first, second and fourth levels may be expressed approximately as

$$E_B \approx \hbar\omega, \quad E_C \approx 2\hbar\omega, \quad E_E \approx 3\hbar\omega.$$

2) The transition between levels C and B (in short the C → B transition) is of a much higher intensity than that of the C → A transition although in fact the decay occurs in both cases by an E2 emission.

The case is similar for the transitions E → C and E → B.

3) Spins and parities of levels A, B, C, E are 0^+, 2^+, 2^+, 4^+, respectively.

4) The E2 emission is of a much higher intensity than the M1 emission in the C → B transition.

Following from the above it seems that levels B, C and E constitute a vibration level series [6, 7]).

5) The relative intensities of the transitions D → C and D → B approach the intensity ratios of single-particle transitions.

6) The E → D transition is of E2 type, although the M1 transition between the two 4^+, 4^+ levels would also be allowed according to the single-particle model.

7) Besides the D → B electrical quadrupole transition the D → A crossover is also to be detected, which can be an E4 transition only.

Points 5, 6 and 7 may be interpreted by assuming D to be a single-particle excitation level and further the transition between single-particle excitation and vibration levels to be forbidden.

Finally I should like to thank Prof. K. Simonyi for his constant interest in my work, Mr. L. Keszthelyi for his valuable advice concerning the experiment and Mr. L. Lakosi and Mrs. I. Cornides for their assistance in the course of the measurements.

References

1) H. W. Taylor and R. W. Pringle, Phys. Rev. **99** (1955) 1345
2) L. L. Baggerly, P. Marmier, F. Boehm and J. W. M. Du Mond, Phys. Rev. **100** (1955) 1364

3) W. H. Kelly and M. L. Wiedenbeck, Phys. Rev. **102** (1956) 1130
4) V. Shiel, L. D. Wyly and C. H. Braden, Phys. Rev. **105** (1957) 1521
5) Bashilov *et al.*, Izvest. Akad. Nauk Ser. Phys. SSSR **16** (1952) 264
6) G. Scharff—Goldhaber and J. Weneser, Phys. Rev. **98** (1955) 212
7) A. Bohr, Suppl. Nuovo Cimento **4** (1956) 1091

Nuclear Physics 4 (1957) 463—468; © *North-Holland Publishing Co., Amsterdam*
Not to be reproduced by photoprint or microfilm without written permission from the publisher

ELASTIC SCATTERING OF ANTIPROTONS BY NUCLEI

I. E. McCARTHY
Cavendish Laboratory, Cambridge †

Received 3 June 1957

Abstract: The large annihilation cross section for antiprotons may be due either to a very strong attraction or to a very small mean free path in nuclear matter and a large nuclear rim of low density. In either case the nucleus must be considered black to antiprotons and the behaviour of the beam in the nuclear boundary is important. It is shown that the anomalously small diffraction cross section observed in early experiments cannot be explained by a boundary effect if the real potential is not very large. Emulsion experiments have shown that the differential cross section near 2° is less than that predicted by Rutherford scattering. A similar discrepancy arises from assuming that the nucleus is a charged totally absorbing sphere.

1. Introduction

Experiments on antiproton annihilation and scattering have been performed with counters and in emulsions. Attenuation experiments with counters have been done with various targets and with antiproton energies from about 200 MeV to 800 MeV. In the first type [1]) the final counter subtended a large angle so that diffraction scattering events would not count as attenuation events. The observed cross section should be that for annihilation.

The cross section in copper and beryllium was found to be about twice the "geometrical" cross section, defined as

$$\sigma_G = \pi(1.4A^{1/3})^2 \times 10^{-26} \text{ cm}^2. \quad (1)$$

In further experiments the absorption cross section in lead was 1 to 1.5 times σ_G, confirming the idea that the excess cross section is due to the effect of a surface whose thickness is roughly independent of the size of the nucleus [2]).

The second type of counter experiment was performed with "good geometry". That is to say scatterings outside 2.5 degrees were counted as attenuation events [2]). In this case the observed cross section should include most of the diffraction cross section and thus should be about four times σ_G, assuming a black nucleus of cross section $2\sigma_G$. In fact, for hydrogen, carbon, beryllium and lead, only about half the expected diffraction cross section was observed.

In an experiment by Stork *et al.* [3]) with 1000 MeV/c antiprotons on a beryllium target in good geometry, the final counter was replaced by an

† Now at the School of Physics, University of Minnesota.

emulsion which was later scanned for annihilation events. Two events were found, indicating that the cross section was probably about 3 to 4.5 times σ_G. For $\sigma_{\bar{p}}/\sigma_G = 2, 3, 4.5$, the expected number of annihilations was 30, 7, 0.7 respectively. These results seem to contradict the counter experiment. The total cross section may be of the order of magnitude expected on the basis of the black nucleus theory.

Experiments with 50 MeV to 200 MeV antiprotons in nuclear emulsion have been reported from Berkeley [4]). From 21 annihilations in flight, the annihilation cross section was observed to be $(2.56 \pm 0.6)\sigma_G$. Nine small angle scattering events were observed. Of these, six were in the range $6^0 < \theta < 14^0$ which is consistent with diffraction scattering, but in the range $2^0 < \theta < 6^0$, where Rutherford scattering predicts 10.7, only three were observed. It is improbable that this is entirely a statistical fluctuation. Preliminary data reported at the 1957 Rochester conference show a peak at angles less than about 2^0 but still less than Rutherford scattering.

Rough calculations [2]) have shown that the antinucleon-nucleon interaction is characterised by a radius roughly equal to the internucleon distance in nuclei, so the nucleus should be opaque to antiprotons.

Previous theoretical work by Duerr and Teller [5, 6]) predicted the large annihilation cross section for antiprotons on the basis of a velocity-dependent potential which, at the present energies, is of the order of 1000 MeV.

Electron scattering experiments [7]) have shown in the case, for example, of copper, that the nuclear density has dropped to 10 % of its internal value at a radial distance of 6×10^{-13} cm. The optical model calculations of Woods and Saxon [8]) have shown that the nucleon-nucleus potential at this distance is not great, and classical calculations of nucleon-nucleus scattering by Elton and Gomes [9]) indicate that the number of nucleons to be found on the average outside the Saxon potential is three, of which about one would be seen by the incident beam. Since the antiproton data require strong absorption at 7×10^{-13} cm in the case of copper, it is not certain that they can be accounted for merely by the presence of nuclear matter, and a strong attraction extending appreciably to such distances seems possible.

The present work is an attempt to account for some of the effects observed in the above experiments. In section 2, the diffraction scattering is considered on the basis of the simple optical model of Fernbach, Serber and Taylor [10]). It is shown for real potentials of known orders of magnitude, that a partially absorbing and refracting rim on a black nucleus cannot reduce the diffraction cross section below that for the black nucleus itself, contrary to what may at first seem possible.

To test the hypothesis of a potential so strong as to extend appreciably beyond the matter distribution, we must first see if the data can be accounted

for merely by assuming a black nucleus. In section 3, the nucleus is represented by a charged totally absorbing sphere whose radius is that which gives the observed absorption cross section. The differential cross section for small angle scattering is calculated. It turns out to be less than that for Rutherford scattering at angles so small that diffraction scattering is unimportant (less than 6^0). The reduction is not as large as that in the first Berkeley experiment, but the data known at present are not good enough for comparison.

2. Effect of an Absorbing and Refracting Rim on Diffraction Scattering

Consider a cylindrically symmetrical potential well, the real and imaginary parts of which are constant up to a radial distance a and then drop to zero in a finite distance in an arbitrary way.

Using an argument similar to that of Fernbach, Serber and Taylor [10]), the total cross section for diffraction scattering from a cylindrically symmetrical system is

$$\sigma_d = 2\pi \int_0^\infty \varrho d\varrho |1-a(\varrho)|^2, \tag{2}$$

where $a(\varrho)$ is the complex amplitude of the wave at a distance ϱ from the axis. In the general case where the potentials vary with z, the coordinate along the axis, we have

$$a_\varrho = \exp\{-\tfrac{1}{2}\int_{-\infty}^{\infty} K(z)dz + i\int_{-\infty}^{\infty} k_1(z)dz\}. \tag{3}$$

$K(z)$ is the absorption constant in the notation of Fernbach *et al.*, and

$$k_1(z) = \{2M[E+V(z)]\}^{\frac{1}{2}}/\hbar - (2ME)^{\frac{1}{2}}/\hbar, \tag{4}$$

where E is the kinetic energy of the incident particle, and V is the real part of the potential. The dependence of the right hand side of eq. (3) on ϱ is not written explicitly. The case of a spherically symmetric nucleus is included in this formula.

For the above system,

$$\sigma_d = 2\pi \int_0^a \varrho d\varrho |1-a_c(\varrho)|^2 + 2\pi \int_a^\infty \varrho d\varrho |1-a_r(\varrho)|^2, \tag{5}$$

where a_c, a_r are the amplitudes in the central part and the rim respectively.

Since the second term in (5) is positive definite, a rim of any shape whatever cannot interfere in such a way as to reduce the total diffraction cross section below that for the central part by itself.

Since the nucleus must be black up to a radius at least "geometrical" in order to produce the large observed annihilation cross section, the lack of observed diffraction scattering in counter attenuation experiments is very difficult to understand in the light of the result of this section.

It must be remembered that the Fernbach approximation neglects refraction at the surface of the nucleus, which is small for real potentials of known orders of magnitude, but may be appreciable for very large potentials. Hence this section applies only if the large cross section for annihilation is really due to the matter distribution and not to a large potential. It is not obvious what the effect of the rim would be in this case.

3. Very Small Angle Scattering

In this section we will consider the scattering of antiprotons at angles small compared to the first minimum of the diffraction pattern. At such energies Coulomb scattering is much more important than diffraction scattering. We will study the Coulomb scattering from a charged black sphere using a model in which the amplitude for the scattering is given by omitting all partial waves of such angular momentum that the classical impact parameter is less than the nuclear radius.

This model has been discussed by Akhieser and Pomeranchuk [11]) and used extensively by Blair [12]) for calculations of α-particle scattering for which the nucleus can also be regarded as black. We will refer to this as the Blair model. It is expected to represent the physical situation when the wavelength of the incident particles is small compared with the nuclear radius and the number of partial waves omitted is quite large. Wegner *et al.* [13]) found that the model fitted the α-particle scattering data quite well at fairly low angles but not at large angles.

A high energy analytical approximation for the Blair model has been given by Clementel and Coen [14]). In their notation the angular momentum of the last partial wave whose classical impact parameter is less than the nuclear radius R is

$$l_c = kR\left(1-\frac{Z'Ze^2}{ER}\right)^{\frac{1}{2}}, \tag{6}$$

where k, E are respectively the momentum and kinetic energy of the incident particle.

The amplitude of the scattered wave in the Blair approximation is

$$f(\theta) = \frac{1}{2ik}\sum_{l=l_c}^{\infty}(2l+1)\exp(2i\eta_l)P_l(\cos\theta), \tag{7}$$

where

$$\eta_l = \arg\Gamma(1+l+in) = \eta_0+\sum_{r=1}^{l}\arctan\frac{n}{r}, \tag{8}$$

$$n = (Z'Ze^2)/\hbar v.$$

In the case $|n| \lesssim 1$, $l_c \gg 1$, and $\sin\theta \approx \theta$,

$$\eta_l \cong n \log l. \tag{10}$$

Replacing the sum in (7) by an integral,

$$f(\theta) = -\frac{1}{k\theta^2}\{2n \exp\left[i\left(-2n \log \frac{\theta}{2} - 2nC\right)\right] + l_c\theta \exp\left[i\left(2n \log l_c - \frac{\pi}{2}\right)\right] J_1(l_c\theta)$$
$$-2n \exp\left[-2in \log \theta\right] \int_0^{l_c\theta} y^{2in} J_1(y)\mathrm{d}y, \tag{11}$$

where C is Euler's constant.

Equation (11) shows that reversing the charge on the incident particle is equivalent to taking the complex conjugate of $f(\theta)$ with the sign reversed, except for the effect on l_c, (which is unimportant at the energies concerned). Thus the cross section $|f(\theta)|^2$ is not affected.

The scattering has been calculated for antiprotons of energy > 50 MeV in emulsion using (11). Graphical methods were used where possible to simplify the calculation. In figure 1, the cross sections for Blair scattering

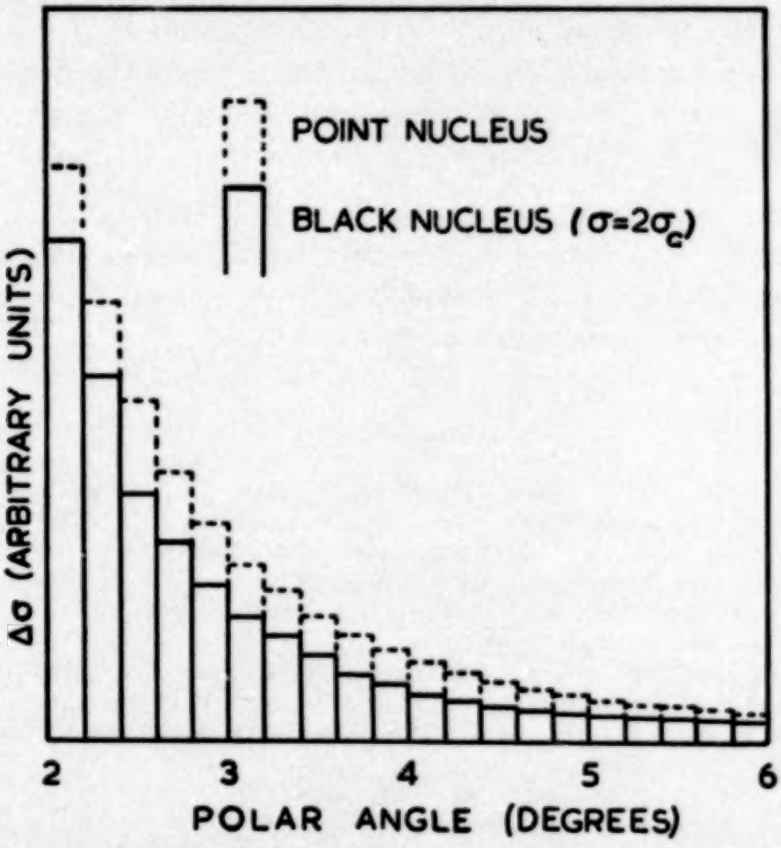

Fig. 1. Blair scattering compared with Rutherford scattering for antiprotons of energy greater than 50 MeV in emulsion.

at angles from 2^0 to 6^0 are plotted and compared with those for Rutherford (point nucleus) scattering. The radii used were $\sqrt{2}$ times the geometrical radii.

For $\theta < 2^0$ the Rutherford scattering term is predominant. For $\theta > 6^0$

the angular distribution begins to look like that for pure diffraction scattering. In the intermediate region, the interference terms are important and the differential cross section is definitely less than that for Rutherford scattering, being not much more than half between 4^0 and 5^0. The total cross section from 2^0 to 6^0 is 75 % of the corresponding Rutherford cross section. The minimum value on this model is 60 %, corresponding to scattering from a black disc of radius about twice geometrical.

Clearly this is not in agreement with the early Berkeley data although the interference appears in the right region. There is reason to believe (from preliminary data quoted at the 1957 Rochester conference) that more precise data will conform more closely to the prediction of the black nucleus theory. If this should not be so, it is clear that there must be a strong attractive potential which is appreciable outside the matter distribution. It is likely that the scattering at small angles is very sensitive to this potential and would provide a good means of investigating it (where it is not blanketed by absorption). Such an investigation has already been made by Costa and Patergnani [15]) for K^+ scattering where the nucleus is almost transparent. It is perhaps worth pointing out that the present analysis would apply to K^- scattering where the absorption is known to be strong.

I would like to thank Drs. R. M. Eisberg, J. Hamilton and D. H. Wilkinson and Mr. P. B. Jones for many valuable discussions, and Dr. Hamilton for suggesting the work. I am indebted to the Royal Dutch Shell Group for a grant under which this work was performed.

References

1) O. Chamberlain, D. V. Keller, E. Segrè, H. M. Steiner, C. Wiegand and T. Ypsilantis, University of California Radiation Laboratory Report No. UCRL-3327 (February 1956)
2) B. Cork, G. R. Lambertson, O. Piccioni and W. A. Wenzel, University of California Radiation Laboratory Report No. UCRL-3650 (1957)
3) D. H. Stork, R. W. Birge, R. P. Haddock, L. T. Kerth, J. Sandweiss and M. N. Whitehead, Phys. Rev. **105** (1957) 729
4) W. H. Barkas, R. W. Birge, W. W. Chupp, A. G. Ekspong, G. Goldhaber, S. Goldhaber, H. H. Heckman, D. H. Perkins, J. Sandweiss, E. Segrè, F. H. Smith, D. H. Stork, L. van Rossum, E. Amaldi, G. Baroni, C. Castagnoli, C. Franzinetti and A. Manfredini, Phys. Rev. **105** (1957) 1037
5) H. Duerr and E. Teller, Phys. Rev. **101** (1956) 494
6) H. Duerr, Phys. Rev. **103** (1956) 469
7) Hahn, Ravenhall and Hofstadter, Phys. Rev. **101** (1956) 1131
8) R. D. Woods and D. S. Saxon, Phys. Rev. **95** (1954) 577
9) L. R. B. Elton and L. C. Gomes, Phys. Rev. **105** (1957) 1027
10) S. Fernbach, R. Serber and T. B. Taylor, Phys. Rev. **75** (1949) 1352
11) A. Akhieser and I. Pomeranchuk, J. Phys. (USSR) **9** (1945) 471
12) J. S. Blair, Phys. Rev. **95** (1954) 1218
13) H. E. Wegner, R. M. Eisberg and G. Igo, Phys. Rev. **99** (1955) 825
14) E. Clementel and A. Coen, Nuovo Cimento **10** (1953) 988
15) G. Costa and G. Patergnani, Nuovo Cimento **2** (1957) 448

Nuclear Physics **4** (1957) 469—471; © *North-Holland Publishing Co., Amsterdam*
Not to be reproduced by photoprint or microfilm without written permission from the publisher

The 3^- LEVEL IN A^{40}

R. THIEBERGER
The Weizmann Institute of Science, Rehovoth
and The Israel Atomic Energy Commission, Tel-Aviv

and

A. DE-SHALIT
The Weizmann Institute of Science, Rehovoth

Received 3 June 1957

Abstract: The calculation of the 3^- level in A^{40} is attempted. The calculation is based on comparing energy levels in neighbouring nuclei. The result obtained is 2.51 MeV.

Recent calculations by Talmi and coworkers[1–3]) have revealed a very good agreement between the results obtained from the shell model and experimental data concerning binding energies of nuclei and the energies of some related configurations in different nuclei. It is not yet clear, however, how general this agreement is and to what sort of data it applies.

It has been pointed out by Glaubman [4]) that lowest excited states of odd parity in even nuclei have odd multiples of $\hbar$ for their total angular momentum. This experimental rule has been explained by Talmi [5]) on the assumption that the odd parity state involves a new configuration, resulting from the breaking up of a nucleon pair. Thus the lowest odd parity state in an even nucleus is, in a sense, a "ground state", and it is interesting to check whether its binding energy could be reproduced by the shell model.

The following is an example of the sort of calculation which may lead to the prediction of the location of odd parity states in even nuclei. We treat the nucleus of A^{40} where some contradictory results have been reported[6–8]). A 3^- state has been reported by Morinaga at an excitation of 4.2 MeV whereas Heitler *et al.* have observed a 2.4 MeV level and van Heerden and Prowse a 2.22 MeV or 2.66 MeV level which might be the 3^- state (see the results of the calculations below). The calculation is based on comparing energy levels in neighbouring nuclei. The levels used and their assumed configurations are given in table 1 †.

A^{40} probably has its last protons in the $d_{3/2}$ shell and its last neutrons

† We wish to thank Prof. P. M. Endt for information concerning the experimental data.

in the $f_{7/2}$ shell. An odd parity state can be produced most easily by transferring a proton from its $d_{3/2}$ state to the $f_{7/2}$ shell; all other possibilities probably involve a much higher excitation. We therefore assume for the lowest 3^- level in A^{40} a configuration $\pi d_{3/2}\ \pi f_{7/2}\ \nu f_{7/2}^2$, where we use π, ν to denote a proton and a neutron respectively. We shall assume that we can work in a scheme where the two protons are coupled to $J = 3$, and the two neutrons to $J = 0$. The assumption that the lowest level of this configuration is 3 (and not 5) is based on comparison with the experimental data of A^{38}. The calculations mentioned above[1-3]) showed that the potential well of the nucleus is constant, to a good approximation, at least in nuclei where the same shell is being filled. Therefore, assuming that the two neutrons are coupled to zero, and assuming that the residual interaction between the two protons does not change, we can expect that if the lowest level of the configuration $\pi d_{3/2}\ \pi f_{7/2}$ is 3 (as is probably the case in A^{38}) then this is also true for A^{40}. The same argument of constant potential well will be used in the treatment of the experimental data of K^{39} and K^{41}, as will be seen later.

In the following calculations it is shown that under the assumption mentioned above, the difference between the excitations of the 3^- level in A^{38} and A^{40} is the same as the diference between the excitations of the 7/2 level in K^{39} and K^{41}. The levels used and their assumed configurations are given in table 1.

TABLE 1

The experimental levels used in the calculation and their assumed configurations

nucleus	level (MeV)	spin and parity	configuration
$_{18}A^{38}_{20}$	g.s.	0+	$d_{3/2}^2$
	3.75	3−	$d_{3/2}\ f_{7/2}$
$_{19}K^{39}_{20}$	g.s.	3/2+	$d_{3/2}^3$
	2.53	7/2+ (assumed)	$d_{3/2}^2\ (0)\ f_{7/2}$
$_{19}K^{41}_{22}$	g.s.	3/2+	$d_{3/2}^3\ f_{7/2}^2(0)$
	1.29	7/2	$d_{3/2}^2\ (0)\ f_{7/2}\ f_{7/2}^2(0)$

Let us write the energy of a given level in the form

$$E(j_1^n(J_1)j_2^m(J_2)J) = E(j_1^n(J_1)) + E(j_2^m(J_2)) + V(j_1^n(J_1)j_2^m(J_2)J),$$

where $j_i^n(J_i)$ stands for n nucleons j_i coupled to a total angular momentum J_i; E is the interaction between the group of nucleons with the closed shells and with one another, plus their kinetic energy; V is the interaction between the two groups of nuclei, when coupled to resultant angular momentum J.

Writing the energy in this form we get for the difference between the excitations of the two 7/2 levels in K^{39} and in K^{41}:

$$[E\pi d^2_{3/2}(0)\pi f_{7/2}(7/2)7/2) - E(\pi d^3_{3/2}(3/2))]$$
$$-[E(\pi d^2_{3/2}(0)\pi f_{7/2}(7/2), \nu f^2_{7/2}(0)7/2) - E(\pi d^3_{3/2}(3/2), \nu f^2_{7/2}(0)3/2)]$$
$$= V(\pi d_{3/2}(3/2), \nu f^2_{7/2}(0)3/2) - V(\pi f_{7/2}(7/2), \nu f^2_{7/2}(0)7/2).$$

In a similar way we get for the difference between the excitations of the two 3^- levels in A^{38} and in A^{40}:

$$[E(\pi d_{3/2}(3/2)\pi f_{7/2}(7/2)3) - E(\pi d^2_{3/2}(0))]$$
$$-[E(\pi d_{3/2}(3/2)\pi f_{7/2}(7/2), \nu f^2_{7/2}(0)3) - E(\pi d^2_{3/2}(0), \nu f^2_{7/2}(0)0)]$$
$$= V(\pi d_{3/2}(3/2), \nu f^2_{7/2}(0)3/2) - V(\pi f_{7/2}(7/2), \nu f^2_{7/2}(0)7/2).$$

In these calculations we used the two relations

$$V(\pi d^2_{3/2}(0), \nu f^2_{7/2}(0)0) = 2V(\pi d_{3/2}(3/2), \nu f^2_{7/2}(0)3/2),$$
$$V(\pi d^3_{3/2}(3/2), \nu f^2_{7/2}(0)3/2) = 3V(\pi d_{3/2}(3/2), \nu f^2_{7/2}(0)3/2).$$

These relations result from the fact that the two $f_{7/2}$ particles are coupled to $J = 0$, and therefore the interaction with them depends only on the number of particles [9]).

Therefore the energy difference between the ground state and the 3— level in A^{40} is

$$E(\pi d_{3/2}(3/2)\pi f_{7/2}(7/2), \nu f^2_{7/2}(0)3) - E(\pi d^2_{3/2}(0), \nu f^2_{7/2}(0)0)$$
$$= [E(\pi d_{3/2}(3/2)\pi f_{7/2}(7/2)3) - E(\pi d^2_{3/2}(0))] + [E(\pi d^2_{3/2}(0)\pi f_{7/2}(7/2), \nu f^2_{7/2}(0)7/2)$$
$$- E(\pi d^3_{3/2}(3/2), \nu f^2_{7/2}(0)3/2)] - [E(\pi d^2_{3/2}(0)\pi f_{7/2}(7/2)7/2) - E(\pi d^3_{3/2}(3/2))]$$
$$= 2.51 \text{ MeV}.$$

The three sets of differences in this expression are the excitation energies of the three nuclei given in table 1. With these values we obtain the result 2.51 MeV.

We would like to stress that no assumptions were made concerning the interactions between nucleons or about the shape of the wave functions; therefore a fair fit with experiment is expected. As the experimental material is not yet conclusive, it would be desirable to obtain more information concerning the experimental levels in the vicinity of our calculated 3^- level.

References

1) S. Goldstein and I. Talmi, Phys. Rev. **102** (1956) 589
2) I. Talmi and R. Thieberger, Phys. Rev. **103** (1956) 718
3) S. Goldstein and I. Talmi, Phys. Rev. **105** (1957) 995
4) M. J. Glaubman, Phys. Rev. **90** (1953) 1000
5) I. Talmi, Phys. Rev. **90** (1953) 1001
6) H. Heitler, A. N. May and C. F. Powell, Proc. Roy. Soc. A **190** (1947) 180
7) H. Morinaga, Phys. Rev. **103** (1956) 504
8) I. J. van Heerden and D. J. Prowse, Phil. Mag. **1** (1956) 967
9) N. Zeldes, Nuclear Physics **2** (1956) 1

Nuclear Physics **4** (1957) 472—476; © *North-Holland Publishing Co., Amsterdam*

Not to be reproduced by photoprint or microfilm without written permission from the publisher

COMPOUND NUCLEUS FORMATION AS AN IRREVERSIBLE THERMODYNAMICAL PROCESS

C. E. PORTER †

Åbo Akademi and University of Turku, Turku, Finland

Received 3 June 1957

Abstract: It is emphasized that in the energy region where the level widths are much smaller than the spacings between levels compound nucleus formation is appropriately characterized as an irreversible thermodynamical process and that therefore there is an analogue of the Nyquist formula in which the strength function plays the rôle of the customary admittance factor.

1. Introduction

The past few years have witnessed developments[1–10]) in the theory of nuclear reactions that led in particular to a successful description of entrance channel phenomena for neutrons. This description involves as its central concept the notion of carrying out an average of the measured cross sections with respect to the energy of the incident neutron and identifying these averaged cross sections with those predicted by complex potential models. The unaveraged cross sections, especially in the neutron energy region from zero to a few hundred electron volts for heavy nuclei, exhibit many closely spaced, "fine-structure" resonances; in the averaging process this fine-structure is washed out leaving the "giant" or "gross-structure" resonances that can be identified with predominantly one individual-particle component of the wave function of the incident neutron. The purpose of this note is to emphasize that in the low energy region (that is to say in the region where the fine-structure widths are much smaller than the spacings between levels) compound nucleus formation is quite appropriately characterized as an irreversible thermodynamical process in the sense of Prigogine [11]) and de Groot [12]).

2. Theory

A fine-structure line is characterized by its energy position, its spin J ($J = \frac{1}{2}$ for S-wave neutrons incident on even target nuclei; for targets with spin $I \neq 0$, J may be either $I + \frac{1}{2}$ or $I - \frac{1}{2}$; to date very few spins have been measured [13])), its parity (that of the ground state of the target nucleus

† Fulbright Lecturer (1956—57) on leave of absence from Brookhaven National Laboratory, Upton, New York, U.S.A.

in the case of S-wave neutrons), and the various partial widths making up the total width $\Gamma = \Gamma_n + \Gamma_\gamma + \Gamma_f$ where Γ_n, Γ_γ, and Γ_f are respectively neutron, radiation, and fission widths. (Except for isotopes that fission with thermal neutrons, $\Gamma_f = 0$ in the energy region covered by the high resolution experiments). The data on these many widths are quite extensive [14]).

Since the discussion in this paper is concerned primarily with the formation of the compound nucleus, our attention will be focussed on the neutron widths and their manifestation in the gross-structure. We will confine our discussion to low energy, i.e. to S-wave neutrons. The analysis of low energy resonances for neutron widths provides the quantity $2g\Gamma_n^{(0)}$ where $2g$, the statistical weight factor, is

$$2g = \begin{cases} 1, & I = 0 \\ 1 \pm \dfrac{1}{2I+1}, & I = J \mp \tfrac{1}{2}. \end{cases} \tag{1}$$

(Note that $2g \to 1$ for $I \gg 1$.) $\Gamma_n^{(0)}$ is the reduced neutron width given by the relation

$$\Gamma_n^{(0)} = (E^{(0)}/E)^{\frac{1}{2}} \Gamma_n. \tag{2}$$

The energy $E^{(0)}$ to which the neutron width is reduced is conventionally taken as one electron volt. E is the energy of the incident neutron at which Γ_n is measured; this is usually the resonance energy.

Now the gross cross section most directly related to the neutron width is the cross section for compound nucleus formation σ_c which is expressed as[1])

$$\sigma_c = \pi \lambda\!\!\!^{-} \lambda\!\!\!^{-(0)} 2\pi \bar{\Gamma}_n^{(0)}/D, \tag{3}$$

where $\lambda\!\!\!^{-}$ is the neutron wavelength divided by 2π, $\lambda\!\!\!^{-(0)}$ is the reduced neutron wavelength corresponding to $E^{(0)}$, and D is the average level spacing. The bar over the neutron width signifies an average of many fine-structure neutron widths taken over an energy interval much greater than the spacing between levels and yet much less than the spacing between single-particle or gross-structure levels. To make contact with the R-matrix formalism we recall that the neutron width $\Gamma_{\lambda c}$ for fine-structure level λ and channel c (in this case a neutron channel) is related to the reduced width $\gamma_{\gamma c}^2$ via the connection $\Gamma_{\lambda c} = 2kR\gamma_{\gamma c}^2$ where k is the wave number of the incident neutron and R is the radius of the spherical surface which defines the R-matrix [2]. We can then write eq. (3) as

$$\sigma_c = 4\pi^2 R \lambda\!\!\!^{-} s(E), \tag{4}$$

in which $s(E) = \langle \gamma^2 \rangle / D$ is the so-called strength function describing the giant resonance behavior mentioned above. The quantities $\gamma_{\lambda c}$ are proportional to the eigenfunctions $\phi_{\lambda c}$ of the compound system evaluated at the nuclear surface [15]):

$$\gamma_{\lambda c} = (2\pi\hbar^2 R/M)^{\frac{1}{2}} \phi_{\lambda c}(R). \tag{5}$$

Thus $\gamma_{\lambda c}^2$ has the simple interpretation of being proportional to the probability that the neutron in normal mode λ is at the nuclear surface, while the factor kR in $\Gamma_{\lambda c}$ is a penetration factor.

Perhaps the most appropriate way of making the connection between compound nucleus formation and the notion of an irreversible thermodynamical process is to appeal to the discussion of noise phenomena given by Callen and Welton [16]). They point out that the notion of electrical Johnson noise [17]) can be generalized to include the fluctuations involved in any dissipative (thermodynamically irreversible) process and that a generalized Nyquist formula[18]) can be obtained. (Large fluctuations of the type that occur near critical points and lead to phenomena such as critical opalscence are excluded from our discussion.)

Since the interpretation of the complex potential models that have been used in neutron scattering calculations involves an energy average over fine-structure resonances and hence, since this implies that the time of observation of the compound nucleus $\hbar/I$ (here I is the energy width of the incoming beam [4]) is much shorter than the recurrence time or period $2\pi\hbar/D$ (here D is the mean level spacing) of the internal motion of the compound nucleus [19]), a gross dissipative effect, the analogy with the electrical Johnson noise accompanying dissipation in a resistor leads one to look for a generalized Nyquist formula to describe the dissipative process of compound nucleus formation. To obtain such a formula we recall that the essential feature of the thermodynamical approach to the derivation for the electrical case was to calculate the average time rate of energy transfer (power transfer) between two resistors at a constant temperature. In a similar way we are led to consider the time rate of energy transfer $\mathrm{d}U/\mathrm{d}t$ from the incident neutron beam to a compound nucleus at temperature T. As long as the total width Γ is much less than the level spacing, it is expected that the notion of temperature will have a well defined meaning since, according to the very old qualitative argument [4]), the lifetime for decay $\hbar/\Gamma$ in such circumstances is much longer than the period $2\pi\hbar/D$ characterizing the internal motion of the compound nucleus. (This is in contrast to the state of affairs in the higher energy range where the direct interaction processes occur.) If we assume the volume of the nucleus to be constant, then

$$\mathrm{d}U/\mathrm{d}t = T(\mathrm{d}S/\mathrm{d}t), \tag{6}$$

where S is the entropy of the compound system.

We can imagine the fine-structure levels of the compound nucleus to constitute a set of oscillators each of which has a mean energy $\bar{\varepsilon}(E_\lambda, T)$ depending upon its natural energy E_λ (level λ) and the temperature T. The

differential probability per unit time dP of a neutron making a transition from the incident beam to those fine-structure levels within dE_λ at E_λ which levels have a density $\varrho(E_\lambda)$ is

$$dP = (\Gamma_n/\hbar)\,\varrho(E_\lambda)dE_\lambda. \tag{7}$$

Here, Γ_λ is the average value of the neutron widths for the levels in dE_λ. Therefore, the differential mean rate of compound nucleus energy production in dE_λ is

$$d(dU/dt) = \bar{\varepsilon}(E_\lambda, T)(\Gamma_n/\hbar)\varrho(E_\lambda)dE_\lambda, \tag{8}$$

or since $E_\lambda = E+B$ where E is the energy of the incident neutron and B is the neutron binding energy,

$$\frac{d}{dE}\left(\frac{dU}{dt}\right) = \bar{\varepsilon}(E+B, T)\frac{1}{\hbar}\frac{\Gamma_n}{D}. \tag{9}$$

The equipartition value of $\bar{\varepsilon}$ is $k_B T$ (k_B is Boltzmann's constant) so that for high temperature T,

$$\frac{d}{d(E/\hbar)}\left(\frac{dU}{dt}\right) = k_B T 2kRs(E). \tag{10}$$

This is the nuclear analogue of the original Nyquist formula in which the strength function $s(E)$ plays a rôle similar to the factor involving the input admittance in the electrical Nyquist formula, i.e. the strength function specifies the gross "tuning" (giant resonance character) of the circuit (compound nucleus).

It is perhaps worth pointing out that there is in some sense a "nuclear Johnson noise" underlying the nuclear Nyquist formula of eq. (10) above. From eq. (5) we see that the amplitudes $\gamma_{\lambda c}$ are essentially the eigenfunctions of the compound nucleus evaluated at the nuclear surface. The fluctuating character from level to level of these functions is similar to that encountered in the Johnson noise for a collection of simple oscillators [20]). Arguments justifying a Gaussian distribution of the $\gamma_{\lambda c}$ from level to level have been given by Thomas [10]).

References

1) Feshbach, Porter, and Weisskopf, Phys. Rev. **96** (1954) 448; see also Paper No. 830, International Conference on the Peaceful Uses of Atomic Energy (1955)
2) R. G. Thomas, Phys. Rev. **97** (1955) 224
3) Lane, Thomas and Wigner, Phys. Rev. **98** (1955) 693
4) F. L. Friedman and V. F. Weisskopf, in Niels Bohr and the Development of Physics (Pergamon Press, London, 1955)
5) E. P. Wigner, Am. J. Phys. **23** (1955) 371
6) E. Vogt, Phys. Rev. **101** (1956) 1792
7) K. A. Brueckner, Phys. Rev. **103** (1956) 172; Phys. Rev. **103** (1956) 1121; A. M. Lane and C. F. Wandel, Phys. Rev. **98** (1955) 1524
8) V. F. Weisskopf, Physica **22** (1956) 952
9) C. Bloch, Nuclear Physics **3** (1957) 137

10) R. G. Thomas and C. E. Porter, Phys. Rev. **104** (1956) 483
11) I. Prigogine, Étude Thermodynamique des Phénomènes Irreversibles (Ed. Desoer, Liège, 1947)
12) S. R. de Groot, Thermodynamics of Irreversible Processes (North Holland Publ. Co., Amsterdam, 1952)
13) V. L. Sailor, Phys. Rev. **104** (1956) 736
14) D. J. Hughes and J. A. Harvey, Neutron Cross Sections (Brookhaven National Laboratory Report 325, 1955). Some more recent references are: H. H. Landon, Phys. Rev. **100** (1955) 1414; G. Igo and H. H. Landon, Phys. Rev. **101** (1956) 726; Simpson, Fluharty and Simpson, Phys. Rev. **103** (1956) 971; Bollinger, Dahlberg, Palmer and Thomas, Phys. Rev. **100** (1955) 126; and Pilcher, Harvey and Hughes, Phys. Rev. **103** (1956) 1342
15) J. M. Blatt and V. F. Weisskopf, Theoretical Nuclear Physics (John Wiley and Sons, Inc., New York, 1952) p. 553
16) H. B. Callen and T. A. Welton, Phys. Rev. **83** (1951) 34. A review article concerned with irreversible processes which contains a comprehensive list of references was published in 1954: E. W. Montroll and M. S. Green, Ann. Rev. Phys. Chem. **5** (1954) 449. Some references available since this review was written are: G. E. Uhlenbeck, Higgins Lectures, (Princeton University, 1954); E. P. Wigner, J. Chem. Phys. **22** (1954) 1912; I. Prigogine, Ann. Rev. Phys. Chem. **6** (1955) 457; L. Van Hove, Physica **21** (1955) 517; R. T. Cox, Statistical Mechanics of Irreversible Change (The Johns Hopkins Press, Baltimore, 1955); G. H. Cole, Repts. on Prog. in Physics **19** (1956) 1; R. O. Davies, Repts on Prog. in Physics **19** (1956) 326; M. S. Green, J. Chem. Phys. **25** (1956) 836; R. K. Wangsness, Phys. Rev. **104** (1956) 857; H. B. Callen, Phys. Rev. **105** (1957) 360; F. Bloch, Phys. Rev. **105** (1957) 1206; U. Fano, Revs. Mod. Physics **29** (1957) 74; H. Nakano, Prog. Theor. Physics **17** (1957) 145
17) J. B. Johnson, Phys. Rev. **32** (1928) 97
18) H. Nyquist, Phys. Rev. **32** (1928) 110
19) S. Chandrasekhar, Revs. Mod. Physics **15** (1943) 1 (see p. 56)
20) M. C. Wang and G. E. Uhlenbeck, Revs. Mod. Physics **17** (1945) 323 (see p. 335)

Nuclear Physics **4** (1957) 477—487; © *North-Holland Publishing Co., Amsterdam*
Not to be reproduced by photoprint or microfilm without written permission from the publisher

ANGULAR CORRELATIONS OF GAMMA RAY CASCADES FOLLOWING THE DECAY OF Eu^{152}

S. OFER

Department of Physics, Hebrew University, Jerusalem

Received 3 June 1957

Abstract: The angular correlations of five γ-ray cascades following the decay of Eu^{152} to Sm^{152} and to Gd^{152} were measured. From these measurements, assignments for the spins of excited levels and multipolarities of the γ-radiations are made. The results strongly support the suggestion that the 1082 keV and 1226 keV levels of Sm^{152} should be interpreted as collective vibrational levels.

1. Introduction

Recently, two articles dealing with the decay scheme of Eu^{152} have been published [1, 2]. In both works, almost identical schemes are proposed. The

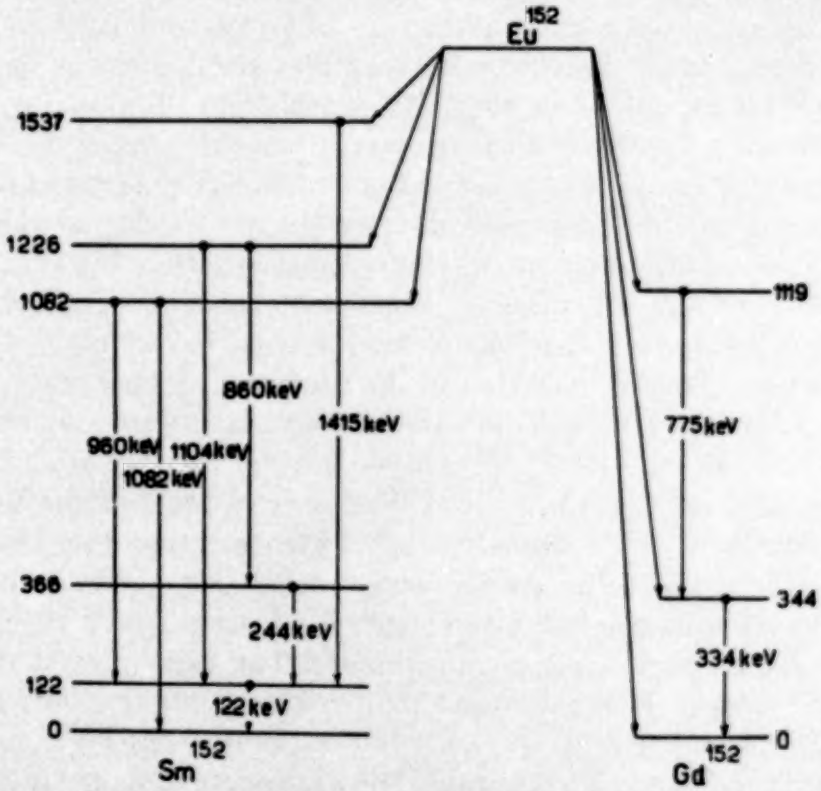

Fig. 1. Decay scheme of Eu^{152} as proposed by Nathan and Waggoner.

decay scheme given in fig. 1 includes all γ-transitions, about which there is agreement between the two works. This scheme does not include some

weak γ-transitions, the existence of which is in doubt and about whose place in the decay scheme there is no agreement.

In the work of O. Nathan and M. A. Waggoner, the K-conversion coefficients of the γ-rays were measured. Taking into account these values and the branching ratios of the radiations from various levels, these authors propose values for the spins and parities of the levels and assign the multipolarities of the γ-rays. The conversion coefficients were estimated in their work by measuring the relative intensities of the γ-lines and comparing these with the relative intensities of the internal conversion lines as obtained in a β-spectrometer, assuming the correctness of the theoretical value of the K-conversion coefficient of the 334 keV γ-line which is of the E2 type. As explained by Nathan and Waggoner, there are experimental difficulties in the determination of the relative intensities of the γ-lines because of the complex shape of the scintillation spectrum obtained. The photo-peaks of the γ-lines contain a high percentage of pulses belonging to the Compton tail of higher energy γ-rays. Similarly, there is a difficulty in estimating the relative intensities of the conversion lines, since the fact that they appear on the background of the continuous β-spectrum limits the accuracy in estimating their relative intensities. Since these authors assume errors of 30 % in the estimated relative intensities of γ-rays and 10 % in these of conversion electrons, it may be concluded that the conversion coefficient, may be in error by at least of 40 %. As the theoretical internal conversion coefficients often do not change by more than 40 percent for different assumed multipolarities of the γ-radiations in the cases of interest, and as the theoretical conversion coefficient may be inexact due to the neglect of the finite size of the nucleus in their calculation, it is clear that in some of the cases, spin and multipolarity assignments which depend only on the experimental conversion coefficients cannot be relied upon.

In particular, the multipolarities of the transitions taking place from the 1226 keV level (i.e. 1104 keV and the 860 keV transitions) and from the 1082 keV level (i.e. the 1082 keV and 960 keV transitions) are interesting, since as pointed out by Nathan and Waggoner, a proof of the E2 nature of these transitions would strongly support the suggestion that these levels can be interpreted as collective vibrational levels for which there is other evidence. On this interpretation the 860 keV, 1104 keV and 960 keV γ-lines should be K-forbidden for M1 transitions [3]). The experimental results of Nathan and Waggoner point to M1 multipolarities for the 1104 keV and 860 keV transitions, E2 for the 1082 keV transition but leave undecided the nature of the 960 keV transition. The examination of the angular correlation of cascades of radiations can, in many cases, supply unambiguous information about the values of spins and the multipolarities of radiations. In this work, the angular correlations of five cascades resulting from the

decay of Eu^{152} were examined. The conclusions drawn from the experimental results are in most cases in agreement with the spin-values and multipolarity assignments suggested by Nathan and Waggoner. But in some cases, mainly in the assignments of multipolarities to the radiations discussed before, the conclusions drawn are different from those obtained from the uncertain conversion coefficients and in fact confirm the suggestion of the vibrational character of the levels.

2. Experimental Details

The source used in this work was a very dilute aqueous solution of $Eu_2(SO_4)_3$. The radioactive material was produced by neutron bombardment in the Harwell pile. The isotopes produced in this way were Eu^{152} (13 years half life) and Eu^{152m} (9 hours half life) which decay by K-capture to Sm^{152} and by β-decay to Gd^{152}, and also, Eu^{154} (10 years half-life) which decays by K-capture to Sm^{154} and by β-decay to Gd^{154}. The experiments were carried about one year after the bombardment with neutrons so that the source was free of Eu^{152m}. It appears that the contribution from Eu^{154} to the observed γ-lines of the isotopic mixture is probably less than 15 % [2]). The radiations were detected by two NaI (Tl) scintillators. The diameter of the crystals used was 1.5 inches and their height was 1 inch. The width of the output pulses from the amplifiers was 1 μsec and the resolution of the detectors was 9.5 % at 661 keV. The coincidences between γ-radiations were recorded using a fast-slow coincidence circuit. The resolving time of the fast circuit was 7×10^{-8} sec. In most of the measurements carried out, the number of random-coincidences was about 10 % of the total number of coincidences. In some of the measurements, lead absorbers were suitably disposed to prevent coincidences arising from Compton scattering of γ-rays from one counter into the other. The distance between source and crystals was 7 cm in all measurements. The angular correlations were measured by adjusting the channels of the pulse analysers in the slow circuit to select the full peaks of the γ-lines which belong to the cascade investigated. In some measurements, the channels situated at the full peak would include pulses belonging to radiations of higher energy, which were absorbed in the crystals by Compton effect. The correlation functions had to be corrected, as described later, for the presence of these Compton pulses. These corrections increased, to some extent, the possible errors for the correlation coefficients beyond the usual statistical errors. The values of the coefficients of the correlation had also to be corrected for the finite solid angle of the detectors. This correction was carried out using the correction tables of Rose [4]) which were calculated for geometrical conditions identical with those of our experiments.

Although the possible errors on the values of the coefficients of Legendre

polynomials in the angular correlation function are in some measurements about 25 %, clear conclusions concerning spins of levels and multipolarities the radiations could be drawn from them.

3. Experimental Results

Fig. 2 shows the "singles" spectrum of γ-rays obtained from the source. This is essentially identical with the spectrum obtained by Nathan and Waggoner [2]), but is given here for the sake of clarity.

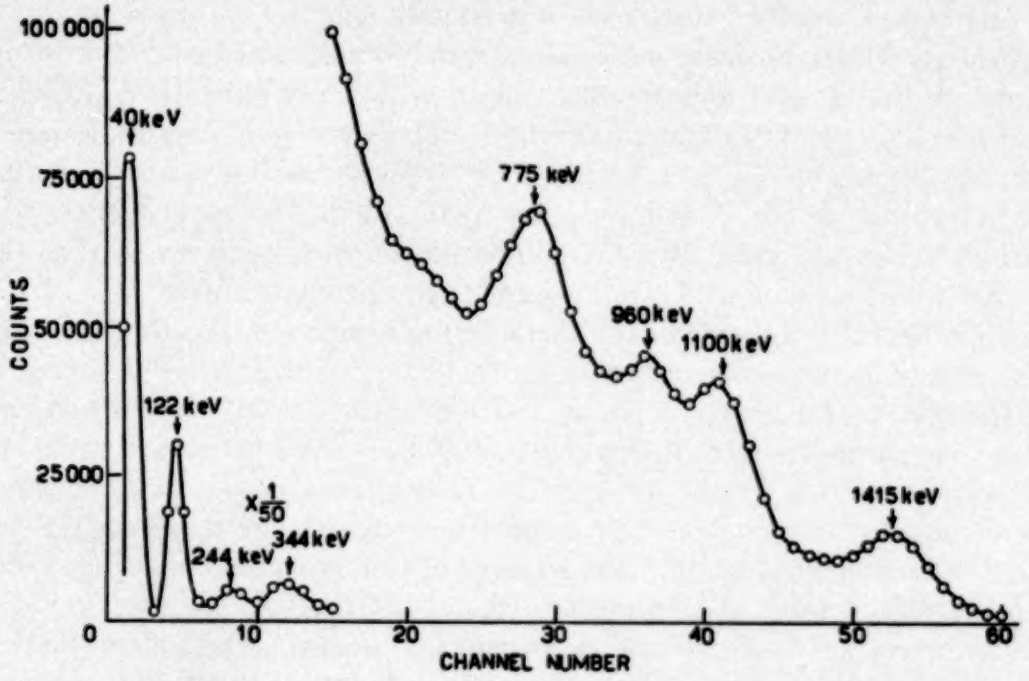

Fig. 2. Differential spectrum of pulse heights from Eu^{152} and Eu^{154} γ-rays.

3.1. ANGULAR CORRELATION OF THE 1415 keV–122 keV CASCADE

The angular correlation function obtained in this case, after correcting for the finite solid angle of the detector, was

$$P(\theta) = A[1+(0.21\pm0.02)P_2(\cos\theta)+(0.02\pm0.03)P_4(\cos\theta)].$$

As the 1415 keV radiation is of the highest energy in the spectrum, false coincidences resulting from Compton scattering from one crystal to the other could not be formed in this case and the coincidences counted are free of coincidences belonging to other cascades. In this case the angular correlation was also measured for a liquid source, of viscosity equal to 5 poise, which was obtained by mixing the aqueous solution of $Eu_2(SO_4)_3$ with glycerine. The correlation function obtained in this case was identical with that obtained for the pure aqueous solution.

3.2. ANGULAR CORRELATION OF THE 1103 keV–122 keV CASCADE

In this case an absorber of 4 mm lead was placed between the source and scintillator which detected the 1103 keV radiations and a 10 mm lead absorber for only scattered radiation was suitably placed between the detectors, to avoid the production of false coincidence pulses. False coincidence pulses could be formed by Compton scattering of 1415 keV γ-rays in one crystal and absorption of the secondary γ-ray emitted from this crystal by the second crystal. A pulse whose height corresponds to about 120 keV γ-radiation can be obtained in the second crystal if the secondary γ-ray is absorbed in the second crystal by the Compton effect. The experimental results were corrected for the existence of true coincidences arising from coincidences of the Compton pulses belonging to the 1415 keV radiation in the photo peak of the 1103 keV γ-rays with the 112 keV γ-rays. By an analysis of the 122 keV γ-rays coincidence spectrum it was found that the number of the Compton coincidences belonging to the 1415 keV radiation were 26 % of the total number of coincidences which entered the channel chosen at 1103 keV, when the angle between the detectors was 90°. In order to correct properly for other angles it was necessary to use the correlation function obtained in the previous section. The correlation function obtained after all the corrections was

$$P(\theta) = A[1-(0.14\pm0.04)P_2(\cos\theta)-(0.08\pm0.02)P_4(\cos\theta)].$$

3.3. ANGULAR CORRELATION OF THE 960 keV–122 keV CASCADE

The experimental arrangements were identical in this case with those of the previous case. As in the previous case it was necessary to correct for the true Compton coincidences arising from the 1415 keV and 1103 keV transitions. The number of the Compton coincidences belonging to the 1415 keV radiations were about 17 % of the total number of coincidences in the channel chosen at 960 keV when the angle between detectors was 90°. The contribution from coincidences resulting from the 1103 keV radiation was less than 2 % of the total number of coincidences, because the channel chosen fell between the photo-peak and the Compton peak of the 1103 keV γ-ray. The angular correlation function obtained in this case was

$$P(\theta) = A[1-(0.02\pm0.02)P_2(\cos\theta)+(0.22\pm0.05)P_4(\cos\theta)].$$

3.4. ANGULAR CORRELATION OF THE 244 keV–122 keV CASCADE

It is clear that the peak at 244 keV contains a high percentage of Compton pulses and back scattering pulses belonging to all the radiations whose energy is higher than 244 keV. In order to find the angular correlation function of the 244 keV–122 keV cascade the following measurements were carried out. The angular correlation was examined with no absorbers between source and detectors (except the thin absorbers of Al and MgO

of the crystal housing which prevented the β-radiation from entering the detectors). The angular correlation function obtained without any corrections was

$$P(\theta) = A[1+0.065P_2(\cos\theta)+0.002\,P_4(\cos\theta)].$$

When the angle between detectors was 180°, the number of coincidences was measured as a function of the number of lead absorbers each of 1 mm thickness, which were placed between the source and the scintillator which detected the 244 keV radiation. In fig. 3 the logarithm of the number of

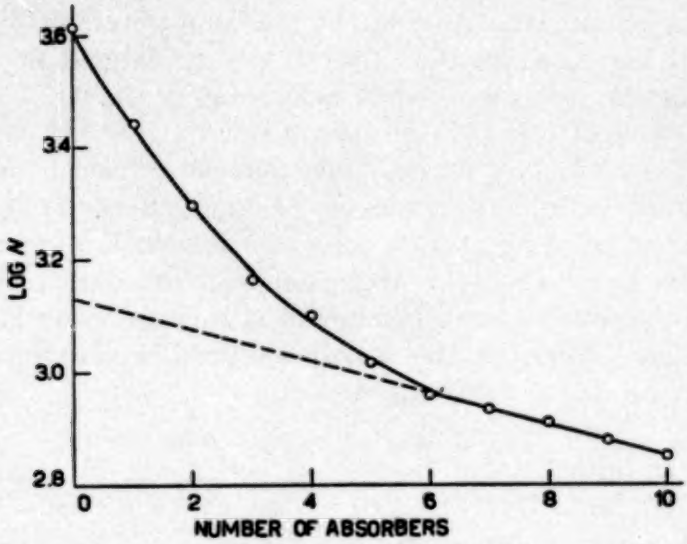

Fig. 3. Plot of logarithm of number of coincidences obtained with the pulse analysers fixed on the 122 keV and 244 keV photo-peaks, as a function of number of 1 mm lead absorbers placed between source and scintillator which detected the 244 keV radiation.

coincidences is shown as a function of the number of absorbers. By extrapolation of the final straight part of the curve, it was found that the number of coincidence pulses which do not belong to the 244 keV—122 keV cascade, obtained without absorbers and when the angle between detectors was 180°, was $(30\pm3)\%$ of the total number of coincidences.

The angular correlation was measured when an absorber of 1 cm lead was placed between the source and scintillator which detected the 244 keV radiation. In this way all the 244 keV γ-rays were absorbed and the coincidences were produced by higher energy radiations. It was found in this case that the correlation was isotropic to within 1 %. (This is not surprising because of the complexity of the γ-ray spectrum coincident with the 122 keV radiation which leads to a superposition of many angular correlations.) The desired angular correlation was then determined by subtracting the isotropic correlation obtaining from the higher energy radiations from the overall angular correlation given above. After correcting for the finite

solid angle of the detectors, the function obtained for the angular correlation of the 244 keV—122 keV cascade was

$$P(\theta) = A[1+(0.11\pm0.01)P_2(\cos\theta)+(0.00\pm0.02)P_4(\cos\theta)].$$

3.5. ANGULAR CORRELATION OF THE 775 keV—344 keV CASCADE

In this case there is almost no possibility that coincidences belonging to other cascades will be counted and the angular correlation function obtained was

$$P(\theta) = A[1-(0.065\pm0.01)P_2(\cos\theta)+(0.01\pm0.01)P_4(\cos\theta)].$$

4. Analysis of the Experimental Results

4.1. The 244 keV—122 keV CASCADE

From the values of the conversion coefficients of the 122 keV γ-line and from the fact that this level is excited by Coulomb excitation of Sm^{152}, it follows that the spin and parity of this level is 2+. The experimental results of the angular correlation measurement of the 244 keV—122 keV cascade approve the assignment of spin and parity 4+ to the 366 keV level and multipolarity E2 to the 244 keV radiation. The theoretical correlation function for a cascade of the type 4(2)2(2)0 is

$$P(\theta) = A[1+0.10P_2(\cos\theta)-0.01\,P_4(\cos\theta)].$$

This function is in full agreement with that obtained experimentally. The value of the K-conversion coefficient found by Nathan and Waggoner for the 244 keV line also shows that this radiation is E2.

4.2. THE 1415 keV—122 keV CASCADE

The fact that there is no transition from the 1537 keV level to the ground state shows that the spin of this level cannot be 1. The experimentally observed angular correlation cannot be reconciled with a spin of 3 or 4 for this level. Agreement between the theoretical and experimental angular correlation functions can be obtained if a spin of 5 or 6 is assumed for the 1537 keV level. On the other hand such a high spin would imply that this level is metastable. Slattery, Lu and Wiedenbeck [5]) and Hartmann and Wiedling [6]) indeed assumed that the 1537 keV level is metastable and that its half life is longer than 1 μsec. That this is not the case is shown by the following.

(1) The spectrum of γ-rays coincident with the 40 keV X-rays was examined, using a resolving time of 2.5×10^{-8} sec. It was found that the ratio of the number of "singles" pulses to the number of coincident pulses, in the region of 1415 keV is equal to the ratio obtained in the regions of 1100 keV, 1000 keV and 244 keV. This fact shows that the half life of the 1537 keV level is shorter than 2×10^{-8} sec, since, otherwise, the coincidence

losses between the K-capture X-rays and the 1415 keV γ-rays would cause a smaller "singles" to coincidences ratio in the 1415 keV region. (The experiment also shows that the 1415 keV radiation follows the decay of Eu^{152} by K-capture and not the β-decay of Eu^{154}, as assumed by Slattery, Lu and Wiedenbeck [5]) and by Hartmann and Wiedling [6]).)

(2) The K-conversion coefficient obtained by Nathan and Waggoner for the 1415 keV γ-ray is in fair agreement with the theoretical value if E1 multipolarity is assigned to the 1415 keV transition, but is at least 10 times smaller than the value expected if the spin were higher than 4.

The only spin and parity assigment for the 1537 keV level which fits all the experimental results is 2−. The theoretical angular correlation function for a cascade of type 2(1,2)2(2)0 is

$$P(\theta) = A\left[1+\frac{0.25+0.72\delta-0.08\delta^2}{1+\delta^2}P_2(\cos\theta)+\frac{0.33\delta^2}{1+\delta^2}P_4(\cos\theta)\right],$$

where δ^2 denotes the ratio between the M2 to E1 transition probabilities in the first component of the cascade. The experimental correlation function fits the theoretical one if $\delta^2 = 1/400$. It is possible that δ^2 is smaller than 1/400 and that the coefficient of $P_2(\cos\theta)$ is attenuated by the magnetic hyperfine interaction associated with the magnetic moment of the 2+ level. (The attenuation factor on the assumption that $\delta = 0$ would be about 0.9. This would not be an unreasonable value taking into account the 1.4×10^{-9} sec life time [7]), a value of Z/A for the gyromagnetic ratio of the 2+ level and the high probability that the samarium ion formed after K-capture would be strongly paramagnetic.) Serious time-dependent quadrupole interactions are excluded by the independence of the correlation on the viscosity of the source. The certain conclusion that can be drawn from the experiments is that the 1415 keV radiation is predominantly E1 and that the M2/E1 mixing ratio is in this case equal to or smaller than 1/400.

4.3. THE 1103 keV−122 keV CASCADE

The existence of transitions from the 1226 keV level to the 122 keV level whose spin is 2 and to the 366 keV level whose spin is 4, shows that the spin of this level is 2, 3 or 4. The negative sign obtained for the coefficient of $P_4(\cos\theta)$ in the angular correlation function of the 1103 keV−122 keV cascade shows that the spin cannot be 2 or 4. It can therefore be concluded that the spin of the 1225 keV level is 3. The theoretical angular correlation function for a cascade of 3(1,2)2(2)0 type is

$$P(\theta) = A\left[1+\frac{-0.07-0.78\delta-0.20\delta^2}{1+\delta^2}P_2(\cos\theta)-\frac{0.08\delta^2}{1+\delta^2}P_4(\cos\theta)\right],$$

where δ^2 denotes the ratio between quadrupole to dipole transition prob-

abilities in the first component of the cascade. The experimental value of (-0.08 ± 0.02) obtained for the coefficient of $P_4(\cos\theta)$ shows that $\delta^2 > 3$. Assuming this latter result, the experimental value (-0.14 ± 0.04) obtained for the coefficient of $P_2(\cos\theta)$ proves that $|\delta| > 8$ or that $\delta^2 > 64$. (A unique value for δ^2 is not obtained from the coefficient of $P_2(\cos\theta)$ if it is not assumed that δ^2 is greater than 3. The two coefficients are necessary in order to obtain the best lowest limit for δ^2). This means that in the 1103 keV γ-line the quadrupole transition probability is more than 64 times larger than the dipole transition probability. Although the assignment of Nathan and Waggoner is M1 for this transition, their experimental results are consistent with the theoretical value for E2 transition, taking into account their experimental error. The theoretical value of the K-conversion coefficient for a M2 transition is about 4 times larger than the experimental value obtained for the 1103 keV radiation. The conclusion is that the spin and parity of the 1225 keV level is 3+ and that the 1103 keV γ-transition is predominantly of the E2 type.

4.4. THE 960 keV–112 keV CASCADE

The existence of transitions from the 1082 keV level to the ground state whose spin is 0 and to the 122 keV level whose spin is 2 proves that the spin of this level is either 1 or 2. The value of 1 must be rejected because of the positive sign obtained for the coefficient of $P_4(\cos\theta)$ in the angular correlation of the 960 keV–112 keV cascade. The value obtained by Nathan and Waggoner [2]) for the K conversion coefficient is near the theoretical value for E2 transition but is 10 times smaller than the theoretical value for M2 transition. The conclusion drawn is that the spin and parity of the 1082 keV level is 2+ and that the 1082 keV γ-radiation is of the E2 type. The theoretical angular correlation function for a cascade of 2(1,2)2(2)0 type is

$$P(\theta) = A\left[1+\frac{0.25+0.72\delta-0.076\delta^2}{1+\delta^2}P_2(\cos\theta)+\frac{0.32\delta^2}{1+\delta^2}P_4(\cos\theta)\right],$$

where δ^2 denotes the ratio between the E2 to M1 transition probabilities in the first component of the cascade. The experimental value of (0.22 ± 0.04) obtained for the coefficient of $P_4(\cos\theta)$ in the correlation function shows that $\delta^2 > 1$. The value of (-0.02 ± 0.02) obtained for the coefficient of $P_2(\cos\theta)$ together with the latter result shows that $|\delta| > 9$ or that $\delta^2 > 80$. One, cannot rely, in this case, too much on the numerical values obtained for δ^2 as not all the coincidences counted in this case belong to the 960 keV–122 keV cascade. Part of the coincidences counted (not more than 25 percent) belongs to a 1000 keV–122 keV cascade. (It is not clear whether all the γ-rays in the neighbourhood of 1000 keV follow the decay of Eu^{154} to Sm^{154} or that part of them follow the decay of Eu^{152} to Sm^{152}.) The

value of the lower limit for δ^2 obtained above is however, probably not in error by more than 25 %. The important conclusion that can be drawn about the 960 keV radiation is that it is mainly of E2 type.

4.5. THE 775 keV–344 keV CASCADE

The information obtained from the angular correlation measurements and from the measurements of the K-conversion coefficient of the second component of the 775 keV–344 keV cascade shows that this cascade is of 3(1)2(2)0 type. The parity of the 1119 keV level is odd and the 775 keV radiation is mainly of the E1 type. Similar conclusions were obtained for this cascade by Kendall and Grodzins [1]), working on this level obtained in the disintegration of Eu^{152m}. The results of the angular correlation measurements show that for the 775 keV radiation, the M2 transition probability is less than 1/2500 of the E1 transition probability.

5. Conclusions

According to the unified model [3]), the lowest modes of collective excitation of deformed nuclei, correspond to rotations in which the shape of the nuclei is not changed. According to the predictions of this model, nuclei can also be excited by collective vibrations around the equilibrium shapes of the nuclei. The lowest order shape vibrations are of quadrupole type. In even nuclei of spheroidal shape, the vibrations give rise to sequences of states of characters 0, 2, 4, . . . (beta vibrations) and 2, 3, 4, . . . (gamma vibrations). For the beta vibrational spectrum $K = 0$, while $K = 2$ for the gamma-vibrations, where K is the quantum number which represents the projection of total angular momentum on the axis of symmetry of the nucleus. M1 radiation is forbidden in the decay of gamma-vibrational excitations, even when $\Delta I = 0$ or 1, because of K-forbiddeness. The empirical data on the spectra of even nuclei indicates that the quadrupole (gamma) vibrational energies for the very strongly deformed nuclei may be of the order of a MeV in the heavy nuclei and that the separation between the two first members of vibrational bands is expected to be nearly the same as the corresponding separation in the ground state rotational band.

It is very reasonable to interpret the 122 keV and 244 keV levels of Sm^{152} as rotational levels. The spins of the 1082 keV and the 1226 keV levels are 2 and 3 respectively, their parity is even, their excitation energies are about 1 MeV and their energy separation is nearly the same as the corresponding separation in the ground-state rotational band. These results together with the rather striking result that they decay predominantly by E2 radiation although $\Delta I = 0$ or 1 support strongly the suggestion to interpret these levels as vibrational excitations with $K = 2$.

The proposed scheme for the spins, parities and K-values of the states

obtained by the decay of Eu^{152} and the proposed multipolarity assignments for the radiations emitted, are given in fig. 4. The main differences between

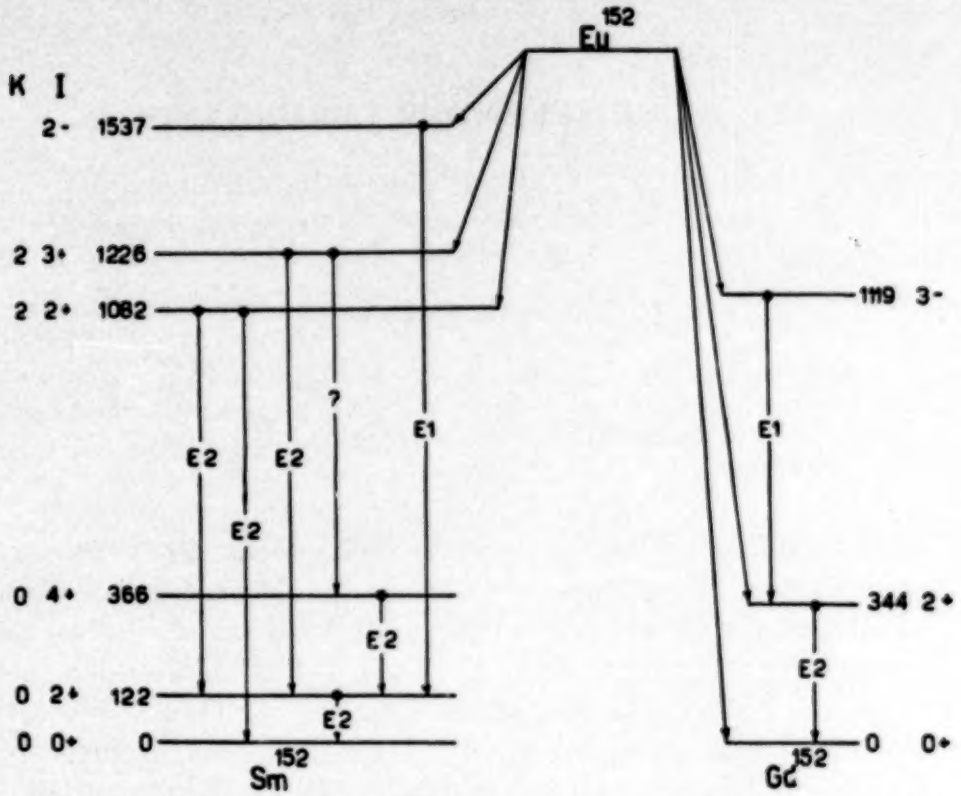

Fig. 4. Spin, parity and multipolarity assignments in Sm^{152} and in Gd^{152}.

this scheme and the one suggested by Nathan and Waggoner [2]) are connected with the multipolarity assignment for the radiations emitted from the 1082 keV and 1226 keV levels. The single γ-radiation whose character is not clear is the 862 keV γ-ray. The experimental internal K— conversion coefficient supports an M1 assignment, whereas, according to the picture drawn in this article, one would guess an electric quadrupole multipolarity. But it is to be pointed that the theoretical conversion coefficient for an E2 transition would be consistent with the experimental conversion coefficient, taking into account the possible errors.

The author would like to thank Dr. S. G. Cohen for his continued interest and guidance.

References

1) L. Grodzins and H. Kendall, Bull. Am. Phys. Soc. **1** (1956) 163, 164
2) O. Nathan and M. A. Waggoner, Nuclear Physics **2** (1956) 548
3) K. Alder, A. Bohr, T. Huus, B. Mottelson and A. Winther, Reviews of modern Physics **28** (1956) 432
4) M. E. Rose, Phys. Rev. **91** (1953) 610
5) R. E. Slattery, C. D. Lu and M. L. Wiedenbeck, Phys. Rev. **96** (1954) 465
6) B. Hartmann and T. Wiedling, Arkiv Fysik **10** (1956) 355
7) A. W. Sunyar, Phys. Rev. **98** (1955)

Nuclear Physics **4** (1957) 488—490; © *North-Holland Publishing Co., Amsterdam*
Not to be reproduced by photoprint or microfilm without written permission from the publisher

ZUR REICHWEITE DER KERNKRÄFTE

P. GOMBÁS, P. SZÉPFALUSY UND E. MÁGORI
Physikalisches Institut der Universität für Technische Wissenschaften, Budapest

Received 3 April 1957

Abstract: Assuming scalar Yukawa interaction between the nucleons, the authors determine the value of the range of the nuclear force which gives the best fit for the energies, the atomic numbers of the most stable isobars and the nuclear radii, as derived from the statistical nuclear model.

In einigen früheren Arbeiten [1]) wurde von einem der Verfasser eine statistische Theorie des Atomkerns im Sinne der Thomas-Fermischen Methode entwickelt, die für die Kernenergien, für die Kernradien sowie für die Ordnungszahl der stabilsten Isobare Resultate liefert, die mit den entsprechenden empirischen Werten gut übereinstimmen. Die Theorie gründet sich auf die Voraussetzung, dass die Bindungskräfte zwischen Neutronen und Protonen Austauschkräfte vom Majoranaschen Typ und weiterhin die Bindungskräfte zwischen Neutronen einerseits und Protonen andererseits spinabhängige Kräfte seien. Zwischen den Nucleonen wurden verschiedene Typen einer reinen skalaren Wechselwirkung in Betracht gezogen. Die ausführlichsten Berechnungen wurden für den Fall einer Yukawaschen Wechselwirkungsenergie zwischen den Nucleonen durchgeführt. Dabei wurde für die Reichweite des Yukawapotentials der feste Wert

$$a = 1.355 \times 10^{-13}\ \text{cm} \tag{1}$$

angenommen, der mit der Compton-Wellenlänge des π-Mesons (für eine Mesonmasse von $285 m_e$) übereinstimmt. Variiert wurde in dem in diesen Arbeiten zur Anwendung gelangten Ritzschen Verfahren die Nucleonendichte und die in der Wechselwirkungsenergie auftretende Potentialstärke V_0.

Durch den zugrunde gelegten Ansatz der Kernkräfte wird die tatsächliche Wechselwirkung zwischen den Nucleonen nur grob erfasst. Es ist daher naheliegend, auch a als einen Variationsparameter zu betrachten und festzustellen, bei welchem a-Wert die Übereinstimmung der berechneten Kernenergien und Kernradien mit den empirischen optimal ist. Dies ist das Ziel der vorliegenden Arbeit.

Die Berechnungen können auf Grund der in I angegebenen Formeln leicht durchgeführt werden. Für a haben wir Werte gewählt, die im Bereich

$$0.5\times10^{-13}\text{ cm} \leqq a \leqq 3.0\times10^{-13}\text{ cm}$$

liegen. Es ergibt sich, dass für a-Werte, die in den Bereich

$$1.6\times10^{-13}\text{ cm} \leqq a \leqq 2.0\times10^{-13}\text{ cm}$$

fallen, tatsächlich eine Verbesserung der berechneten Kernenergien und Ordnungszahlen der stabilsten Isobare erzielt werden kann. Für a-Werte, die ausserhalb dieses Bereiches liegen, tritt durchweg eine Verschlechterung in der Übereinstimmung mit der Erfahrung ein.

Die beste Übereinstimmung mit der Erfahrung erhält man für

$$a \approx 1.7\times10^{-13}\text{ cm}, \tag{2}$$

also für eine Reichweite die um rund 25 % grösser ist als die in I, II und III zugrunde gelegte Reichweite (1). Die Verbesserung, die mit der Reichweite (2) erzielt wird, äussert sich darin, dass sich die Kernenergie bei kleinen Massenzahlen im Verhältnis zu den in I erhaltenen zu hohen Werten etwas vertieft und die Ordnungszahlen der schweren stabilsten Isobare sich im

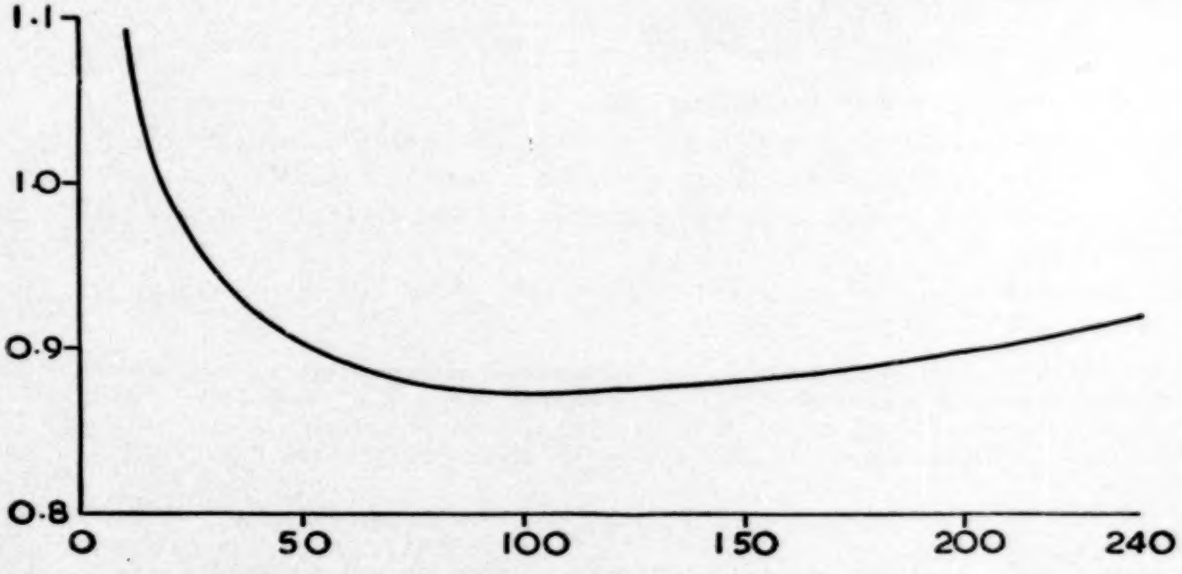

Fig. 1. Berechnete Kernradien.

Verhältnis zu den in I erhaltenen etwas zu grossen Werten ein wenig verkleinern. Die Abweichungen von den empirischen Resultaten werden jedoch in beiden Fällen nur um circa 1/3 verringert.

Für die mit der Reichweite (2) berechneten Kernradien wird die Übereinstimmung mit der Erfahrung im Verhältnis zu den in I erhaltenen Kernradien praktisch nicht geändert. Für den Radius R der äquivalenten homogenen Kugelverteilung der Kernladung (d.h. derjenigen homogenen Ver-

teilung, die für das quadratische Moment denselben Wert ergibt) erhält man † nämlich, mit dem üblichen Ansatz $R = r_0 A^{1/3}$, folgende mittlere Werte des Parameters r_0:

$$\text{mit der Reichweite (2)}, \quad r_0 = 0.895 \times 10^{-13}\ \text{cm},$$

$$\text{mit der Reichweite (1)}, \quad r_0 = 0.848 \times 10^{-13}\ \text{cm}.$$

Der Kernradius erweist sich also in beiden Fällen als zu klein und die Verbesserung mit der neuen Reichweite ist sehr gering.

Interessant sind jedoch die Resultate, die man erhält, wenn man die einzelnen Werte von r_0 für die verschiedenen Kerne einsetzt. Es ergibt sich dann ein Gang mit A, der weitgehend dem experimentell festgestellten [2]) entspricht. Mit der neuen Reichweite erhält man (vgl. fig. 1) ††

A	r_0	A	r_0
10	1.09	80	0.876
16	1.02	120	0.875
28	0.957	160	0.884
40	0.919	200	0.899
60	0.892	240	0.919

(r_0 in 10^{-13} cm-Einheiten)

Abschliessend sei noch erwähnt, dass sich für die im Verhältnis zu (1) grössere Reichweite (2) eine kleinere Potentialstärke ergibt als für die Reichweite (1), wie dies auch zu erwarten ist. Man erhält mit der Reichweite (2) $V_0 = 49.04$ MeV, während sich in I für die Reichweite (1) der Wert $V_0 = 70.42$ MeV ergab.

Die ausführlicheren numerischen Resultate dieser Arbeit erscheinen in den *Acta Physica Hungarica*.

† Die Resultate bezüglich der Kernradien wurden auf Veranlassung des Herausgebers von Prof. Gombás in einem Brief vom 15. Mai 1957 freundlich mitgeteilt. Sie sind in Einvernehmen mit den Verfassern in das ursprüngliche Manuskript eingefügt (L.R.).

†† Der Anstieg der Kurve für grosse A illustriert das in Ref. [2]), S. 452, Gesagte (L.R.).

Literatur

1) P. Gombás, Acta Phys. Hung. **1** (1952) 329 (im folgenden als I zitiert);
P. Gombás, Acta Phys. Hung. **2** (1952) 223 (im folgenden als II zitiert);
P. Gombás, E. Mágori, B. Molnár und É. Szabó, Acta Phys. Hung. **4** (1955) 267 (im folgenden als III zitiert);
man vgl. auch P. Gombás, Ann. d. Phys. **10** (1952) 223; **12** (1953) 155; P. Gombás, E. Mágori, B. Molnar und É. Szabó, Ann. d. Phys. **16** (1955) 93

2) L. Rosenfeld, Nuclear Physics **2** (1956/57) 450

BOOK REVIEWS

R. J. BLIN-STOYLE, *Theories of nuclear moments* (Oxford University Press 1957. 89 pages. 8 s. 6 d. in U.K. only).

This pamphlet inaugurates a new series, called the Oxford Library of the Physical Sciences, and founded at the initiative of the regretted Sir Francis Simon. The idea is to produce monographs on topical problems of physics, sufficiently cheap to be purchased by advanced students and research workers, thus encouraging them to build up their own scientific library. The first item of the series is the reproduction, with only very slight additions, of a survey article recently published in *Reviews of Modern Physics*. As such it is excellent, but it does not seem to me quite to answer the purpose of the new collection: on the one hand it is not enough of an introduction to the subject (the main concepts and formulae are not explained, but taken for granted), on the other the full references to the special papers, while corresponding to the exigencies of a survey of recent progress, tend to be confusing to the reader who wants only a general view of the question. The scope and level of the 'Interscience tracts' (see this journal **2** (1956/57) 109; **3** (1957) 624) would appear better adapted to the requirements of this class of readers.

Dr. Blin-Stoyle's general discussion of the present state of the theory of nuclear moments is undoubtedly the best one can wish for, although there might be a little more to say about quadrupole moments. Coming to details, I should have liked to get from him less summary indications, for each particular nucleus, of the probable cause of the deviation of its magnetic moment from the Schmidt value, and in particular a more precise discussion of the degree of equivalence of the alternative explanations suggested by the individual and the collective models. It is also a pity that a writer of his authority should have shrunk from the admittedly somewhat invidious, but very useful task of giving explicit criticism of the papers quoted: he knows better than anyone else that some at least of the interpretations put forward in papers he mentions without comment are erroneous or doubtful, and it is a bit hard on the reader to leave it to him to find this out by himself.

L. R.

W. H. SULLIVAN, *Trilinear chart of nuclides*, 2nd Edition (U.S. Government Printing Office, Washington 1957, $ 2).

This large chart of nucleides (as purists prefer to say), originating from Oak Ridge, is a familiar view in nuclear laboratories, for which its ingenious honeycomb pattern provides a functionalistic wall decoration. In this new edition, the colouring has been abandoned and the size slightly enlarged, with the result of increased legibility. A circular letter accompanying the review copy gives the following interesting information: 'The design changes will also permit keeping the Chart up to date by periodic issuance of corrections and new data in the form of gummed hexagon stamp sheets. At the present time we are well along in working out the attendant production problems, and should demand for this service warrant we will be in a position to issue the first sheet of stamps within a reasonably short time.'

Considering the amount of absolutely reliable information which the producers have managed to squeeze in these hexagons in an easily legible way, I can heartily endorse the next sentence in the circular: 'We feel that the novel features of this second edition of the Trilinear Chart of Nuclides will make it of real value to researchers, teachers and students in the field of nuclear science and engineering.'

L. R.

B. DAVISON, with the collaboration of J. B. SYKES, *Neutron Transport Theory* (Clarendon Press, O.U.P. 1957. XX+450 pages. 75 s.)

The theory of neutron transport developed rapidly during and just after the war, yet no comprehensive account of the theory has appeared until now. In this book, Dr. Davison provides an authoritative, and in many places an elegant description of nearly all the known methods of solving the transport equation. The basic physical assumptions of the theory and the mathematical properties of the Boltzmann transport equation are first derived, and then the solution of the equation in the constant cross-section approximation is considered. The Wiener-Hopf, spherical harmonics, Serber-Wilson, variational and other methods are described. In many places the author has developed and systematized the war time work. In the second part of the book energy dependent problems are considered, including discussions of the multi-group theory, age theory, and methods useful for considering the slowing down of neutrons emitted by a point source. The work is distinguished throughout by the careful description of all the mathematical methods used, and the detailed examination of any assumptions made. There are some sections on the numerical methods which have recently been used for solving the transport equation. These sections contain the only errors and omissions we found. The numerical method of solving the age equation (page 359) is not always stable, and in most circumstances is inferior to the 'implicit' method of solution, not described by Davison. The method of Spencer and Fano (section 25.5) for finding the penetration of X-rays, has been applied, with a number of important changes, to neutron diffusion †, and the method as described by Dr. Davison has been abandoned.

A. Hassitt

† J. Certaine, A.E.C. unclassified reports N70-3081 (1954), N70-6268 (1955).

F. MÜNZINGER, *Atomkraft: Der Bau von Atomkraftwerke und seine Probleme*, 2. Auflage (Springer-Verlag, Berlin, 1957. xii—224 p. DM 29.40).

The first edition of this book appeared in 1955, and had a reprinting before the appearance of the present edition, which is revised to incorporate material from the conferences at Geneva (1955) and Vienna (1956). The book is written as an introduction for practising engineers, fuel technologists, and economists. It may also serve as a first text for students.

The central section of the book consists of descriptions of about twenty reactors, existing and projected. Possible power cycles and associated turbines are then discussed.

This central material is preceded by a qualitative treatment of the basic nuclear physics required for its appreciation, and a brief survey of relevant properties of reactor materials.

In the final section of the book, economic factors are discussed, and comparisons are made with coal-fired power plants, with special reference to conditions in West Germany.

When material is reported from an original paper, only the authors' names are quoted; a full reference is not given. A bibliography is given, but is highly selective. This may suffice in an elementary book.

Errata are printed on a loose sheet.

To summarise, this book deals with elementary material in a qualitative fashion and may be recommended as first reading to the professional technical man and the student.

P. H. Price

ERRATUM

Shell-model interpretation of energy levels in Li^7 and Be^7, by J. Marion (Nuclear Physics **4** (1957) 282).

The values of $\theta_\alpha^2(Li^{7*}, 7.45\ MeV)$ and $\theta_\alpha^2(Be^{7*}, 7.13\ MeV)$ were calculated incorrectly in ref. [6]) and should be increased by a factor of 2 to 0.017 and 0.095 respectively. As a result the ratios of the θ_α^2 in Li^7 become

$$\theta_\alpha^2(Li^{7*}, 4.61\ MeV)/\theta_\alpha^2(Li^{7*}, 7.45\ MeV) = 29$$

and

$$\theta_\alpha^2(Be^{7*}, 4.58\ MeV)/\theta_\alpha^2(Be^{7*}, 7.13\ MeV) = 3.3.$$

The comments and conclusions in the text are unaltered by this correction.

Nuclear Physics **4** (1957) 493—496; © *North-Holland Publishing Co., Amsterdam*
Not to be reproduced by photoprint or microfilm without written permission from the publisher

NEWS ITEMS

THE SEVENTH ROCHESTER CONFERENCE
(15-19 April 1957)

J. WERLE
Institute for Theoretical Physics, Warsaw

The Seventh Rochester Conference was as usual a highly interesting event in high energy nuclear physics. This year the Conference was attended by nearly 300 physicists from all over the world. The Russian physicists that, according to the preliminary program, were supposed to give several lectures and shorter reports did not come this time. In spite of this fact the Conference was rather overloaded as there was no division into parallel sessions as is usually the case at larger conferences. This arrangement had, however, the advantage of allowing everybody to hear everything of interest.

The Conference was obviously dominated by the parity problem. T. D. Lee gave a very interesting review of the present state of the parity problem in weak interactions. Several experiments proposed last year by Lee and Yang had been carried out already. All the known results confirmed the non-conservation of parity in β-decays and in light-meson decays. The pseudoscalar part of the corresponding transition probabilities was found to be big enough to give a very strong support to the two-component neutrino theory proposed recently by Salam, Landau, and Lee and Yang. Probably we should not wait very long for a more quantitative confirmation of this point. The problem of so called combined inversion (C P) was much more obscure since there were no conclusive experiments done as yet. However, there were some indications that the invariance under CP transformation might not be a general physical law. The problem of parity violation in those weak interactions which do not involve neutrinos was still more obscure. It was proposed to regard the mesons τ and θ as one particle decaying according to different modes without conservation of parity. On the other hand there was rather very little said about the parity conservation (or non-conservation) in heavy meson and hyperon decays.

There was a large group of experimental and theoretical contributions to the parity problem in β and light meson decays. The most beautiful and the most difficult were the experiments with oriented nuclei described by Wu. Other experiments were concerned with longitudinal polarisation of β-electrons emitted from unoriented nuclei and with $\pi-\mu-$e-decays. All these experiments gave quite convincing proofs of non-conservation of parity but were still not accurate enough to give a quantitative proof of the two component theory of the neutrino field.

Case and Feynman pointed out that other theories of the neutrino could give different results with respect to polarisation and other phenomena.

From other new ideas not connected with parity we should note one presented by Gell-Mann. According to his proposal the interaction of the hyperon Λ^0 with the nucleons should be mainly due to an exchange of two π-mesons, the exchange of one K-meson giving much smaller contributions.

Many interesting but so far not very well understood results had been obtained recently with antiprotons. It was confirmed that the cross-section for scattering of antiprotons by nuclei was twice as big as that for protons. A high multiplicity of π-mesons created in antiproton annihilation was found to be rather unexpected.

Numerous reports on various reactions with artificially created hyperons and heavy mesons made us think in a very optimistic mood about the near future of this branch of physics.

So far all the known results were not in disagreement with the simplest possible assumption that the spins of Λ^0 and Σ were $\frac{1}{2}$.

Some progress had been obtained recently in the problem of the nucleon-nucleon interaction. By adding a spin-orbit term to the central and tensor potentials a quite good fit to the experimental data at some energies could be obtained. The results were still not very conclusive since they did not cover all the energies of interest.

The problem of the structure of the nucleons was of course one of the most interesting topics discussed at the conference. The experiments on high energy electron-proton and electron-deuteron scatterings revealed some interesting non-uniformities in the charge distributions, which could possibly throw some light on the problem of internal structure of the nucleons.

INSTITUTE OF NUCLEAR RESEARCH OF THE POLISH ACADEMY OF SCIENCES

After the war physics in Poland found itself facing great difficulties—the laboratories were nearly completely destroyed, there was a lack of funds for research, our scientists were either no longer alive or were scattered all over the world.

Work on nuclear research was taken up at two centres—Warsaw University and the Jagiellonian University in Cracow. The work of the centre in Warsaw was based mainly on the 0.8 MeV accelerator. Nuclear reactions and neutron moderation were studied there. Erection of a Van de Graaff generator and a beta-ray spectrometer has been started. In addition some prototypes of detecting instruments have been designed and constructed, and studies of unstable heavy particles and of high energy collisions have been continued. In the other centre in Cracow studies have been developed of photonuclear reactions, structural investigation by means of non-coherent neutron scattering, gamma radiation, cosmic rays, etc.

In 1955 the U.S.S.R. proposed to sell Poland an experimental reactor and a cyclotron, whereupon preliminary work on our own reactor was interrupted and preparations were made for work on new large instruments.

In the second half of 1955 the Institute of Nuclear Research was established. Professor Andrew Soltan has been appointed general director of the Institute. Various institutes of the Polish Academy of Sciences in Warsaw and Cracow and the Institute of the Physics of Elementary Particles of the Polish Academy of Sciences have been incorporated and their studies continued.

The institute started with a programme comprising a wide range of purely scientific and technical problems, thus becoming an institute of wide scientific scope.

At the same time, the newly created Institute of Nuclear Research has assumed additional duties, such as education, popularization of science etc., connected with the problems of the utilization of nuclear energy in Poland, since at present it is the only institution concerned with nuclear problems.

In July, 1956, Wilhelm Billig was appointed Commissioner for the Utilisation of Nuclear Energy. He heads the Government Council for the Utilization of Nuclear Energy, which has been formed in the wake of a previous Government Commission.

The Institute of Nuclear Research is directly under the Commissioner and, as regards its scientific activity, is under the jurisdiction of the Polish Academy of Sciences through the Academy's Commission for the Peaceful Use of Nuclear Energy.

The scientific activity of the respective sections of the Institute may be outlined as follows:

Division I A, Physics 1 (Z. Wilhelmi, Division Chief; address: ul. Hoża 69, Warsaw). This division is carrying out studies which can be called fundamental studies in the field of the physics of the atomic nucleus.

The main line of research is neutron physics and nuclear reactions of small energies. The basic tool today is the cascade accelerator for 0.8 MeV deuterons which belongs to the Warsaw University. It is expected that within a few months a Van de Graaff generator will start working. Moreover, at the end of the year, erection will be finished of the water moderated

thermal reactor of 2 MW and a mean flux of 10^{13} n cm^{-2} $sec.^{-1}$ Studies on nuclear spectroscopy are also being developed.

Division I B, Physics 2 (B. Buras, address: ul. Panienska, Warsaw). Its field deals mainly with the application of nuclear physics to structural studies and the investigation of solids. The Division is now starting structural studies by neutron diffraction of the influence of nuclear radiation on solids, especially on semi-conductors.

It will be possible, in the near future, for the Division to do some work in the field of neutron spectroscopy, similar to Division I A.

Division II, Physics 3 (H. Niewodniczański, address: ul. Golebia 13, Cracow). The research is of similar character as in Division I A, and activities are concentrated around fundamental studies of nuclear physics. Whereas in Warsaw the main tool of the physicists will be the reactor, in Cracow it will be a cyclotron which will be able to accelerate deuterons to an energy of 12 MeV. The accelerator, imported from the U.S.S.R., will be started up in 1958. Until it is assembled it may be possible to operate a small cyclotron of domestic construction. The main lines of research in Division II are nuclear reactions of medium energy, nuclear spectroscopy, and structural studies by means of thermal neutron scattering. Recently, research has begun on nuclear paramagnetic resonance.

Division III, Electronics and Automation (J. Keller), address: Warsaw-Żerań). This Division has the task of designing and constructing special instruments required by the laboratories of the Institute. In the first period of its existence the division concentrated on research and the technique of design; prototypes of different nuclear instruments were constructed and their manufacture was then taken up within the Institute or on the outside. The other task of Division III is to suggest to other institutes and factories manufacturing programmes including production of elements indispensable for construction of new equipment for nuclear research.

Division IV, Technology of Reactor Materials (T. Adamski, address: Warsaw-Żerań). Its chief task is to develop the most economical methods of extracting uranium from the existing ore, of producing concentrates through mechanical enrichment, and of obtaining nuclear pure uranium compounds and metallic uranium. Within the division's interest are analytic problems connected with the determination of contaminates and studies connected with heat treatment of metallic uranium and the technique of obtaining fuel elements.

Division V, Radiochemistry and Chemistry of Isotopes (I. G. Campbell, address: Warsaw-Żerań). Division V has rather varied activities. Its main activity till now was the distribution of isotopes. In the future, it will concentrate on the production of radio-isotopes by the reactor, synthesis of uranium compounds, consultations on the erection of isotope laboratories, on the use of radioisotopes in different branches of science and technology, and cooperation with users of isotopes. Moreover, the division is developing and improving measuring techniques important for studies of isotopes, designing sets of instruments for handling isotopes, etc.

Division VI, Cosmic Rays (M. Danysz, addresses: ul. Hoża 69, Warsaw; ul. Mickiewicza 30, Cracow; ul. Narutowicza, Łódź). Studies are being continued of unstable particles resulting from high energy collisions in nuclear emulsions, of large cosmic ray showers, of the effect of fast particles on matter, using nuclear emulsions. The division is closely cooperating with several scientific centres abroad.

In addition to its scientific divisions, the Institute of Nuclear Research has several independent sections. Some of them emerged recently from those divisions described above.

The *Analytical Section* (J. Minczewski) develops analytical methods principally for the use of Division IV, from which it emerged. Methods are being developed for determinating uranium contents in ores, products of its treatment and products derived from the recyclization of nuclear fuel, determination of contaminates (such as boron, lithium etc.). Basic studies are being continued of the analysis of reactor materials. It is particularly important in the preparation of the plan for the development of nuclear energetics in Poland.

Health Section (E. Kowalski). Besides the tasks that its name suggests, the section is making scientific studies on the influence of nuclear radiation on metabolism in the human body, and especially on the metabolism of porphyrine and on the coagulation system.

Nuclear Energy Division (W. Frankowski). Studies have begun on the design of a second reactor to be built in Poland.

The *Section of Education* trains the newly accepted employees of the Institute of Nuclear Research and outside scientists and engineers who intend to handle radioactive isotopes. The section also cooperates with the Nuclear Physics Department of the University of Warsaw.

The table illustrates the growth of the institute during the last few years:

Employment

Year	Advanced Scientific Workers	University Graduates	Technicians and Laboratory Assistants
Sept. 1955	18	57	27
Dec. 1955	21	148	62
Dec. 1956	24	293	163

As seen from the above table the rapid increase in employment of university graduates was not accompanied by a corresponding increase of the number of advanced scientific workers. In late 1956, there were 12 graduates for each member of the scientific supervisory staff. It must be stated that the ratio is not favourable and it will hamper the future development of scientific work at the Institute.

In 1956, the employees of the Institute published 25 scientific papers and prepared a further 24 for print. Among them there are papers on cosmic rays, diffuse neutron scattering, nuclear reactions, determination of contaminates in reactor materials, etc.

The greatest effort, however, has been put into work connected with the preparation of future work in the field of fundamental research. It consists of the design and building of a number of instruments. The construction of the 10 MeV linear proton accelerator is started, the erection of a universal neutron spectrometer has begun, as well as design of neutron velocity-selectors. To work in conjunction with the selectors, a 144 channel time analyser and a 14 channel amplitude analyser are being prepared. Construction of several types of spectrometers for beta and gamma rays has been finished or is considerably advanced.

Among the difficulties faced by the Institute during the past period was the already mentioned shortage of scientific personnel. This difficulty can be eliminated by raising the qualifications of the workers through scientific work and practice in the best centres abroad. A first effort in this direction has already been made.

The normal development of the Institute of Nuclear Research is hindered by scarcity of space. The situation will change when big centres of nuclear research are opened in Świerk, outside Warsaw, and in Bronowice near Cracow.

In 1957 the Section of Reactor Exploitation and Divisions I A and I B will move to Świerk. They will be followed by the other Divisions of the Institute of Nuclear Research in Warsaw except for Division IV, which remains in Żerań, and Division VI, which will enjoy the hospitality of the University of Warsaw.

According to the Świerk project the total floor space of all laboratories and offices, together with a small hotel for guests studying the use of the reactor, will amount to about 30 000 m², and the total personnel of the Institute of Nuclear Research will be 1300 in 1960.

At the same time, 350 employees will be working in Żerań. The floor space of the laboratories and other buildings will be approximately 6 000 m².

The Institute of Nuclear Research in Cracow will then have about 220 employees and a total floor space of 10 000 m².

THIS ISSUE OF NUCLEAR PHYSICS IS
DEDICATED TO THE MEMORY OF

IRÈNE JOLIOT-CURIE

Nuclear Physics **4** (1957) 497—502; © *North-Holland Publishing Co., Amsterdam*
Not to be reproduced by photoprint or microfilm without written permission from the publisher

IRÈNE JOLIOT-CURIE
(1897-1956)

J. TEILLAC
Faculté des Sciences, Paris

Reçu le 24 juin 1957

Le 17 Mars 1956, à l'Hôpital Curie, Irène Joliot-Curie s'éteignait; le communiqué médical précisait que sa mort était due à „une leucémie subaiguë consécutive aux travaux sur les corps radioactifs dont elle s'était occupée toute sa vie". La nouvelle de sa disparition a soulevé dans le monde entier une intense émotion, comme en ont témoigné les innombrables marques de sympathie reçues de toutes parts.

Irène Joliot-Curie est née en 1897, un an avant que ses parents Pierre et Marie Curie ne publient la découverte du polonium et du radium. Elle a raconté † comment, dès son enfance, elle voulait faire de la recherche scientifique avec sa mère. L'éducation peu conventionnelle qu'elle reçut d'un petit groupe de savants, la place presque exclusive que le travail scientifique tenait dans la vie de sa mère, ont joué un grand rôle dans l'éveil de cette vocation. Elle prépara ses certificats de licence pendant la première guerre mondiale, tout en travaillant sous la direction de sa mère dans les services de radiologie où étaient soignés les soldats blessés. En 1918, ses études terminées, Irène Joliot-Curie devient préparatrice de Marie Curie à l'Institut du Radium.

Son premier travail, publié en 1921, porte sur la détermination du poids atomique du chlore provenant de divers minéraux, dans le but de déceler une éventuelle différence de composition isotopique entre le chlore contenu dans des roches anciennes et le chlore d'origine marine. Puis elle entreprend une étude sur les propriétés des rayons α émis par le polonium (fluctuation de parcours, vitesse d'émission, pouvoir ionisant) qui fait l'objet de sa thèse de doctorat en 1925.

En 1926, Irène Curie épouse Frédéric Joliot. On sait de combien de remarquables découvertes leur travail commun allait enrichir la science. Seule ou en collaboration avec son mari, Irène Joliot-Curie consacre une grande partie de ses efforts à extraire et à purifier des quantités importantes de radium D et de polonium, accumulés dans le radium, et à préparer des sources de polonium de très grande activité par électrolyse ou par volatilisa-

† I. Joliot-Curie, „Marie Curie, ma mère" (Europe, Déc. 1954)

tion. C'est grâce à ces grandes quantités de polonium qu'Irène et Frédéric Joliot-Curie ont pu entreprendre les travaux qui ont contribué à la mise en évidence du neutron et ceux qui aboutirent à la découverte de la radioactivité artificielle.

Reprenant l'étude des transmutations des éléments légers sous l'action des rayons α, Irène et Frédéric Joliot étudièrent le rayonnement de très faible intensité et de très grande pénétration découvert par Bothe et Becker. Ils montrèrent que ce rayonnement avait la propriété remarquable de projeter des noyaux d'atomes d'hydrogène avec une énergie de plusieurs millions d'électrons-volts. C'est à la suite de ces expériences que Chadwick démontra la généralité du phénomène de projection des noyaux et proposa de l'expliquer par la présence de neutrons. Mais, au cours de ces recherches et sur des clichés obtenus au moyen de l'appareil à détente de Wilson avec un champ magnétique, I. Curie et son mari avaient constaté la présence de trajectoires d'électrons rapides atteignant une énergie d'environ 5 MeV en même temps que des trajectoires électroniques courbées en sens inverse, inexplicables par l'hypothèse séduisante de Chadwick. Reprenant alors de nouvelles expériences, ils montrent pour la première fois qu'un rayonnement de photons est capable de provoquer l'apparition de positons, phénomène immédiatement interprété comme une production de paires négaton-positon.

C'est encore au cours de l'étude des transmutations des éléments légers, béryllium, bore et aluminium, par les rayons α du polonium, qu'eut lieu la découverte capitale de la radioactivité artificielle. Si les électrons positifs émis au cours de la transmutation de Be par les rayons α peuvent s'expliquer par le phénomène de production de paire interne, au contraire l'émission de positons par l'aluminium irradié par les α, apparaît à Irène et Frédéric Joliot comme un phénomène tout à fait différent: cette émission, en effet, ne cesse pas immédiatement avec la fin de l'irradiation mais décroît exponentiellement avec une période de 3 min 15 sec. Le même phénomène se retrouve avec le bore et le magnésium, où les périodes de décroissance sont de 10 min et 2 min 30 sec. Des radioéléments, ^{30}P, ^{13}N, ^{27}Si, ont été créés artificiellement. En les séparant et en les identifiant chimiquement, Irène et Frédéric Joliot apportent en outre la première preuve chimique de transmutation. On mesure aujourd'hui les importantes conséquences scientifiques et techniques de cette découverte qui leur valut le prix Nobel.

En 1935, Irène Curie publie avec ses collaborateurs H. Halban et P. Preiswerk, une série de travaux sur les éléments formés lors de l'irradiation du thorium par les neutrons, puis quelques années plus tard, avec P. Savitch, elle fait une observation importante qui devait conduire à la découverte de la fission. Voici comment, dans une notice qu'elle a rédigée, elle rapporte ces expériences: „Nous avons pu extraire de l'uranium irradié par les neutrons

un nouveau radioélément de période environ 3.5 heures. Nous avons tout d'abord pensé que ce corps était un isotope de l'actinium, mais des expériences de fractionnement en présence d'actinium nous ont montré que ce radioélément se séparait aisément de l'actinium et était très analogue au lanthane. A la suite de nos expériences, Hahn et Strassmann, donnant à leurs travaux une orientation nouvelle, observèrent également des radioéléments qu'ils supposèrent d'abord isotopes du radium, mais ils durent constater aussi que ces corps se séparaient du radium et avaient les propriétés du baryum."

Irène Joliot-Curie était avant tout un savant profondément attaché à ses travaux de recherches. Elle n'en a pas moins consacré une partie importante de son activité à des tâches très diverses qui lui incombaient ou qu'elle estimait de son devoir d'accomplir. En 1936, elle est sous-secrétaire d'État à la Recherche Scientifique. Dès la libération, elle participe au côté de son mari à la création du Commissariat à l'Energie Atomique.

C'est aussi depuis 1946 qu'elle a la lourde charge de la direction de l'Institut du Radium et de l'enseignement lié à la chaire de Physique nucléaire à la Faculté des Sciences de Paris. Par son enseignement comme par son exemple, elle contribue à la formation de nombreux jeunes physiciens. L'exemple, elle le donne chaque jour par son travail personnel au laboratoire; M. E. Bauer l'a souligné dans un article qu'il écrivit peu de temps après la mort d'Irène Joliot-Curie: „Jusqu'au jour (10 février) où elle a quitté Paris pour aller se reposer dans les Alpes — d'où on devait la ramener en hâte à l'Hôpital Curie — elle est venue régulièrement chaque matin, chaque après-midi, malgré une santé parfois chancelante, travailler dans son petit laboratoire du rez-de-chaussée de l'Institut du Radium. C'est dans ces deux pièces qu'elle poursuivait ses recherches personnelles, presque solitaire; c'est là qu'elle dirigeait cet institut fondé par sa mère, qu'elle avait développé et où elle avait formé des équipes remarquables; c'est là que ses collaborateurs et ses collègues pouvaient à tout instant la trouver pour discuter avec elle de leurs problèmes." C'est cette simplicité qui fit d'Irène Joliot-Curie au laboratoire un vrai „patron", aimé et respecté par tous les travailleurs.

Mais devant le développement considérable pris par la physique nucléaire, les moyens mis en oeuvre dans les Universités françaises paraissent tout à fait insuffisants. Alors qu'avec la création du Commissariat à l'Energie Atomique, la France peut espérer, dans ce domaine, n'être pas totalement tributaire des autres nations, au contraire le retard pris dans le domaine de la recherche fondamentale en physique nucléaire est considérable. Irène Joliot-Curie insiste à plusieurs reprises sur la nécessité d'un effort important. Les moyens et les locaux dont elle dispose à l'Institut du Radium pour la formation de jeunes physiciens sont en effet hors de proportion avec le but à atteindre; la recherche universitaire dont sont issues tant de décou-

vertes fondamentales ne pourra subsister dans ce domaine que si des appareils modernes sont mis à sa disposition. Après le vote, en 1952, par le Parlement, d'un crédit relatif à l'extension de la Faculté des Sciences de Paris, elle prend une part active à l'élaboration des projets pour les nouveaux laboratoires qui doivent s'édifier à Orsay, et grâce à sa ténacité obtient qu'une première tranche de travaux débute dès 1956. Quelques appareils sont commandés pour l'Institut du Radium: synchrocyclotron de 150 MeV, séparateur d'isotopes, générateurs haute-tension. Mais de grandes difficultés restent à surmonter: pour le personnel, il n'existe pas en effet, dans le cadre de la Faculté, la possibilité d'offrir aux ingénieurs et techniciens hautement spécialisés les salaires nécessaires. De telles difficultés rendent la tâche extrêmement pénible. Ces dernières années, Irène Joliot-Curie, malgré les multiples atteintes de la maladie, y consacrait beaucoup de temps: elle a obtenu les premiers résultats qui permettent de bien augurer de l'avenir.

Malgré l'importance exceptionnelle de ses tâches scientifiques, Irène Joliot-Curie n'est jamais restée indifférente aux problèmes sociaux. Elle avait une haute idée de la mission du savant et n'hésitait pas à prendre position avec netteté pour ce qu'elle pensait être juste et servir la cause de la paix. Elle était en particulier soucieuse des échanges culturels entre les savants de tous les pays. Elle estimait que ceux qui ont donné au monde l'énergie atomique ont une lourde responsabilité et elle lutta contre l'utilisation destructrice qui menace la civilisation. C'est ce même esprit généreux qui la conduisit pendant la guerre de 1914—18, avec sa mère, à s'occuper de la radiographie des blessés et à participer très activement aux côtés de son mari à la résistance, pendant la seconde guerre mondiale. Elle a manifesté tout au long de sa vie et en toutes occasions, le même courage et la même ténacité: les chercheurs de son laboratoire se souviennent qu'avant de partir à l'hôpital où elle devait subir une intervention chirurgicale, elle montrait le même calme et la même attention au problème que venait lui soumettre un travailleur; quelques jours avant sa mort, elle s'inquiétait des progrès des laboratoires d'Orsay.

L'oeuvre d'Irène Joliot-Curie, complétant celle de Marie Curie, est une des plus belles pages de l'histoire des sciences.

Principales fonctions

1934 – Membre de la Commission Internationale de l'Étalon du Radium
1935 – Maître de Recherches à la Caisse Nationale de la Recherche Scientifique
1936 – Sous-Secrétaire d'État à la Recherche Scientifique
1937 – Maître de Conférences à la Faculté des Sciences de Paris

1937 – Professeur sans chaire à la Faculté des Sciences de Paris
1946 – Commissaire à l'Énergie Atomique
1946 – Professeur Titulaire de la Chaire de Physique générale et Radioactivité à la Faculté des Sciences de Paris

Principales distinctions honorifiques

De nombreuses universités et académies étrangères avaient honoré Irène Joliot-Curie. Voici la liste des principales récompenses et distinctions honorifiques qu'elle reçut:

1955 – Prix Nobel de Chimie (en commun avec Frédéric Joliot)
– Chevalier de la Légion d'Honneur
– Membre honoraire de l'Académie des Sciences aux Indes
1936 – Membre correspondant étranger de l'Akademija Nauk Technicznych de Varsovie
1938 – Correspondant étranger de l'Académie Royale de Médecine de Belgique
1939 – Docteur honoris causa de l'Université d'Edinbourg
1940 – Médaille quinquennale Barnard décernée par l'Académie des Sciences des États-Unis (en commun avec F. Joliot)
1946 – Docteur honoris causa de l'Université d'Oslo
1947 – Membre correspondant de l'Académie des Sciences d'U.R.S.S.
1947 – Membre honoraire de l'Edinburgh University Women's Union
1947 – Membre honoraire de l'Institut Grand-Ducal du Luxembourg
1948 – Membre honoraire de l'Indian Chemical Society
1948 – Docteur honoris causa ès-Sciences physiques de l'Université de Sofia
1950 – Docteur honoris causa de l'Université de Delhi (Indes)
– Joykissen Mokerjee Gold Medal (Indes)
– Docteur honoris causa de l'Université de Lublin (Pologne)
– Membre correspondant de l'Académie des Sciences de Berlin
1951 – Docteur honoris causa de l'Université de Cracovie (Pologne)
1953 – Prix Albert 1er de Monaco décerné par l'Académie des Sciences de Paris
1954 – Membre ordinaire de l'Académie Polonaise des Sciences
– Prix de la Ville de Paris, décerné par l'Académie Nationale de Médecine

Liste des principales publications scientifiques

- Recherches sur les rayons α du polonium. Oscillations de parcours, vitesse d'émission, pouvoir ionisant (Thèse de Doctorat, 27 mars 1925). Ann. de Phys. **2** (1925) 403
- Sur la quantité de polonium accumulée dans d'anciennes ampoules de radon et sur la période du radium D. J. Phys. **10** (1929) 305

- Étude du rayonnement absorbable accompagnant les rayons α du polonium (en collaboration avec F. Joliot). J. Phys. **2** (1931) 20
- Préparation des sources de polonium à grande densité d'activité (en collaboration avec F. Joliot). J. Chim. Phys. **28** (1931) 201
- Émission de protons de grande vitesse par les substances hydrogénées sous l'influence des rayons α très pénétrants (en collaboration avec F. Joliot). C. R. **194** (1932) 273
- Projection d'atomes par les rayons très pénétrants excités dans les noyaux légers (en collaboration avec F. Joliot). C. R. **194** (1932) 876
- Sur la nature du rayonnement pénétrant excité dans les noyaux légers par les particules α (en collaboration avec F. Joliot). C. R. **195** (1932) 1229
- Preuves expérimentales de l'existence du neutron (en collaboration avec F. Joliot). J. Phys. **4** (1933) 21
- Contribution à l'étude des électrons positifs (en collaboration avec F. Joliot). C. R. **196** (1933) 1105
- Électrons positifs de transmutation (en collaboration avec F. Joliot). C. R. **196** (1933) 1885
- Électrons de matérialisation et de transmutation (en collaboration avec F. Joliot). J. Phys. **4** (1933) 494
- Un nouveau type de radioactivité (en collaboration avec F. Joliot). C. R. **198** (1934) 254
- Séparation chimique de nouveaux radioéléments émetteurs d'électrons positifs (en collaboration avec F. Joliot). C. R. **198** (1934) 559
- Production artificielle d'éléments radioactifs – Preuve chimique de la transmutation des éléments (en collaboration avec F. Joliot). J. Phys. **5** (1934) 153
- Sur la création artificielle des éléments d'une famille radioactive inconnue, lors de l'irradiation du thorium par les neutrons (en collaboration avec Hans v. Halban et P. Preiswerk). J. Phys. **6** (1935) 361
- Sur les radioéléments formés par l'uranium irradié par les neutrons (en collaboration avec P. Savitch). J. Phys. **8** (1937) 385
- Sur les radioéléments formés dans l'uranium irradié par les neutrons (en collaboration avec P. Savitch). J. Phys. **9** (1938) 355
- Sur la bipartition de l'ionium sous l'action des neutrons (en collaboration avec F. Joliot). Ann. Phys. **10** (1944) 107
- Sur la possibilité d'étudier l'activité des roches par l'observation des trajectoires des rayons α dans l'émulsion photographique. J. Phys. **7** (1946) 313
- Les Radioéléments naturels – Propriétés chimiques – Préparation – Dosage. (Hermann, Paris, 1946)
- Détection et dosage du carbone dans l'acier par l'emploi de la radioactivité artificielle. J. Phys. **11** (1952) 497

Nuclear Physics **4** (1957) 503—528; © *North-Holland Publishing Co., Amsterdam*
Not to be reproduced by photoprint or microfilm without written permission from the publisher

UNE FORMULATION UNIFIÉE DE LA THÉORIE DES RÉACTIONS NUCLÉAIRES

CLAUDE BLOCH

Centre d'Études Nucléaires de Saclay, Gif-sur-Yvette (S. & O.)

Reçu le 13 avril 1957

Abstract: The determination of the scattering matrix in the theory of nuclear reactions is essentially equivalent to the construction of the Green function for the Schrödinger equation in the internal region of the configuration space with proper boundary conditions at the nuclear surface. This Green function can be expressed as the inverse of an operator involving the sum of the Hamiltonian and of a "boundary value operator" which is different from zero only on the nuclear surface where it has a singularity of the same kind as a Dirac function. A general operator expression for the scattering matrix is derived. This expression can be transformed into a matrix expression by introducing an arbitrary basis of orthonormal functions in the internal region. The Wigner-Eisenbud and the Peierls-Kapur formulations are obtained by an appropriate choice of the internal functions. When a large number of resonances contribute to the cross-section, the expansion of the scattering matrix in terms of resonances of the compound system is not useful, and a more appropriate starting point can be obtained from a perturbation expansion of the scattering matrix which is easily derived from the general operator expression. A simple statistical assumption is proposed in order to determine the dominant terms in such an expansion. It leads to the optical model for the elastic scattering and to the direct interactions for the inelastic scattering.

1. Introduction

Les formulations de la théorie des réactions nucléaires connues à l'heure actuelle se classent en deux catégories nettement distinctes:

a) les formulations de Wigner-Eisenbud [1-4]) et de Peierls-Kapur [5]) qui sont particulièrement bien adaptées à l'étude des résonances séparées. Ces théories présentent le défaut de ne pas se prêter facilement à l'étude des cas où le rôle essentiel n'est pas joué par une résonance isolée. Elles font en effet alors intervenir un très grand nombre de paramètres: niveaux d'énergie, largeurs partielles, sur lesquels il est difficile de faire des prédictions. De plus ces paramètres ne sont rattachés aux interactions nucléaires que d'une manière indirecte et compliquée. Ces théories ont de ce fait beaucoup de mal à faire apparaître les interactions directes récemment mises en évidence expérimentalement [6, 7]).

b) les formulations basées sur l'équation intégrale de la diffusion [8]) établissent au contraire une liaison très directe entre les interactions nucléaires et la matrice de collision ou les sections efficaces. Ces formulations se prêtent au calcul des perturbations et conduisent facilement aux interactions

directes. Elles sont valables surtout à haute énergie. Par contre, elle rendent très difficilement compte des résonances se produisant à basse énergie.

Les phénomènes de résonances et d'interactions directes jouent tous les deux un grand rôle dans les réactions nucléaires et il existe même des domaines d'énergie où les deux types de phénomènes coexistent et se superposent. Pour étudier ces cas il est indispensable de disposer d'un formalisme unifié.

La formulation de la théorie des réactions nucléaires présentée ici conserve les notions de *région intérieure* et de *région des voies* dans l'espace de configuration à $3A$ dimensions, caractéristiques des théories du type a). Rappelons que les régions des voies sont les portions de l'espace de configuration où les nucléons sont partagés en deux (ou plusieurs) groupes constituant des particules assez éloignées pour ne plus avoir d'interactions nucléaires entre elles. La région intérieure Ω est celle où tous les nucléons interagissent les uns avec les autres. La surface Σ limitant la région intérieure est constituée par les points de l'espace de configuration où les particules constituant une voie arrivent juste au contact. Cette surface peut être considérée comme généralisant l'idée de surface nucléaire. Il est important de conserver la distinction entre zône intérieure et zône des voies, car dans la zône des voies on peut résoudre exactement l'équation d'onde radiale et calculer avec précision les facteurs de pénétration qui jouent un grand rôle pour des particules chargées de basse énergie.

Dans la région intérieure, le problème consiste à résoudre l'équation de Schrödinger avec des conditions aux limites à la surface nucléaire. Ces conditions sont imposées par les conditions initiales de la collision, c'est-à-dire par la donnée du faisceau incident.

La méthode présentée ici repose sur une résolution formelle de ce problème aux valeurs limites. L'étape essentielle du calcul est la construction de la fonction de Green appropriée au problème de collision nucléaire. Ceci revient à l'inversion d'un opérateur somme de l'Hamiltonien du système et d'un *opérateur de conditions aux limites* défini sur la surface Σ. En choisissant convenablement ce dernier, on peut obtenir par une seule inversion d'opérateur l'expression formelle générale de la matrice de collision.

Cette expression peut servir de point de départ à diverses méthodes d'approximation. On retrouve par exemple les résultats des théories de Wigner et de Peierls-Kapur en introduisant dans la région intérieure des systèmes particuliers de fonctions de base orthonormées.

On peut également mettre l'Hamiltonien du système sous forme de la somme d'un Hamiltonien modèle H_0 et d'un potentiel $\mathscr{V}$ égal à la différence entre les interactions nucléaires véritables et les interactions moyennes introduites dans H_0. L'expression de la matrice de collision peut alors être développée en puissances de $\mathscr{V}$ et on peut regrouper les termes prépondérants.

Ceci donne le principe d'une méthode de calcul des *interactions directes* dans les réactions nucléaires.

2. Exemple Simple

Considérons pour commencer le cas de la diffusion d'une particule d'énergie ε dans un état s par un potentiel central $V(r)$ ayant une portée finie R. Dans la *région intérieure*

$$0 \leqq r \leqq R,$$

la fonction d'onde satisfait à l'équation de Schrödinger

$$(\varepsilon - H)\psi(r) = 0, \tag{1}$$

où l'Hamiltonien s'écrit †

$$H = -\frac{\hbar^2}{2M}\frac{1}{r}\frac{\mathrm{d}^2}{\mathrm{d}r^2}\,r + V(r).$$

Dans la *région extérieure*

$$R \leqq r,$$

la fonction d'onde est une combinaison linéaire d'une fonction d'onde entrante $\psi^{(-)}$ et d'une fonction d'onde sortante $\psi^{(+)}$:

$$\psi(r) = \psi^{(-)}(r) - \psi^{(+)}(r), \tag{2}$$

avec

$$\begin{aligned} \psi^{(-)}(r) &= \frac{1}{r}\,\mathrm{e}^{-ikr}, \\ \psi^{(+)}(r) &= \frac{S}{r}\,\mathrm{e}^{+ikr}. \end{aligned} \tag{3}$$

L'amplitude de l'onde entrante est déterminée par la donnée du faisceau incident. L'amplitude S de l'onde sortante permet le calcul de la section efficace de diffusion; c'est la quantité qu'il faut calculer.

Le problème consiste essentiellement à résoudre l'équation de Schrödinger (1) dans la région intérieure avec comme condition aux limites pour $r = R$ que l'amplitude de l'onde entrante soit égale à l'unité.

L'opérateur H *restreint à la région intérieure* qui va donc jouer un rôle central présente le grave défaut de n'*être pas hermitique*. Si $\psi_1(r)$ et $\psi_2(r)$ sont deux fonctions quelconques on a en effet ††

$$\int_0^R r^2\,\mathrm{d}r\,[\psi_1^*(H\psi_2) - (H\psi_1)^*\psi_2] = -\frac{\hbar^2}{2M}\left[r\psi_1^*\frac{\mathrm{d}(r\psi_2)}{\mathrm{d}r} - \frac{\mathrm{d}(r\psi_1^*)}{\mathrm{d}r}\,r\psi_2\right]_R. \tag{4}$$

† Par $(\mathrm{d}^2/\mathrm{d}r^2)\,r$ on désigne l'opérateur

$$\frac{\mathrm{d}^2}{\mathrm{d}r^2}\,r\psi(r) = \frac{\mathrm{d}^2}{\mathrm{d}r^2}\,[r\psi(r)].$$

†† L'élément de volume s'écrit en réalité $4\pi r^2\mathrm{d}r$. Il faudrait aussi multiplier les expressions (3) par l'harmonique sphérique normalisée $Y_{00} = (4\pi)^{-\frac{1}{2}}$. Tous ces facteurs 4π s'éliminant quand on calcule un élément de matrice on peut les omettre partout sans inconvénient

Cette difficulté bien connue est d'habitude évitée en imposant aux fonctions ψ auxquelles on applique l'opérateur H de satisfaire à certaines conditions aux limites pour $r = R$. Si on impose en effet à toutes les fonctions ψ de s'annuler ou d'avoir une dérivée logarithmique donnée pour $r = R$ on s'assure bien de la nullité de l'expression (4). Cette méthode n'est pas très naturelle dans le cas qui nous intéresse car on ne peut pas connaître à l'avance la valeur pour $r = R$ de la dérivée logarithmique de la fonction $\psi(r)$ solution du problème.

Une façon de rendre H hermitique mieux adaptée au problème considéré consiste à ajouter un *terme de surface* choisi de façon à compenser l'expression (4). Ainsi en posant

$$\mathscr{H} = H + \frac{\hbar^2}{2MR}\,\delta(r-R)\,\frac{\mathrm{d}}{\mathrm{d}r}\,r,$$

on vérifie immédiatement que quelles que soient † ψ_1 et ψ_2 on a

$$\int_0^R r^2\,\mathrm{d}r\,[\psi_1^*(\mathscr{H}\psi_2) - (\mathscr{H}\psi_1)^*\psi_2] = 0. \tag{5}$$

Dans le terme de surface les facteurs $\delta(r-R)$, $\mathrm{d}/\mathrm{d}r$ et r ne commutent pas, mais on vérifiera facilement que seul l'ordre indiqué assure la validité de l'équation (5).

Malgré son caractère singulier l'opérateur $\mathscr{H}$ a des éléments de matrice bien définis entre deux fonctions d'onde quelconques. Ainsi

$$\int_0^R r^2\,\mathrm{d}r\,\psi_1^*\mathscr{H}\psi_2 = \int_0^R r^2\,\mathrm{d}r\,\left[\frac{\hbar^2}{2M}\,\frac{\mathrm{d}(r\psi_1^*)}{\mathrm{d}r}\,\frac{\mathrm{d}(r\psi_2)}{\mathrm{d}r} + \psi_1^* V \psi_2\right].$$

Ceci montre que l'aspect singulier de $\mathscr{H}$ est lié à la représentation $\mathbf{r}$ et qu'il disparaît dans une autre représentation.

Si $\psi(r)$ est une fonction continue et dérivable, $\mathscr{H}\psi(r)$ est continue pour $r < R$, mais peut présenter pour $r = R$ une singularité en fonction de Dirac donnée par

$$\frac{\hbar^2}{2MR}\,\delta(r-R)\left[\frac{\mathrm{d}}{\mathrm{d}r}(r\psi)\right]_R.$$

L'égalité de deux quantités de cette forme, c'est-à-dire se présentant comme les sommes d'une fonction continue dans l'intervalle $(0, R)$ et d'une singularité en fonction de Dirac pour $r = R$:

$$f(r) + A\delta(r-R) = g(r) + B\delta(r-R),$$

implique l'égalité séparée des parties singulières et des parties continues:

$$f(r) = g(r), \qquad A = B.$$

† Nous supposerons toutefois que toutes les fonctions d'onde considérées sont continues ainsi que leur dérivée première et que leur dérivée seconde existe.

Il en résulte que l'équation

$$(\varepsilon - \mathscr{H})\psi(r) = F(r),$$

où le second membre est de la forme

$$F(r) = f(r) + A\delta(r-R), \tag{6}$$

la fonction $f(r)$ étant continue pour $r = R$, *équivaut au système équation différentielle plus condition aux limites*

$$(\varepsilon - H)\psi(r) = f(r) \qquad (r < R),$$

$$-\frac{\hbar^2}{2MR}\left[\frac{\mathrm{d}}{\mathrm{d}r}(r\psi)\right]_R = A \qquad (r = R).$$

La condition aux limites qui apparaît ainsi n'étant pas celle du problème posé nous allons remplacer l'opérateur $\mathscr{H}$ par l'opérateur légèrement différent

$$\mathscr{K} = H + \frac{\hbar^2}{2MR}\delta(r-R)\left(\frac{\mathrm{d}}{\mathrm{d}r} - ik\right)r. \tag{7}$$

En désignant par $\mathscr{L}$ *l'opérateur de conditions aux limites*

$$\mathscr{L} = \frac{\hbar^2}{2MR}\delta(r-R)\left(\frac{\mathrm{d}}{\mathrm{d}r} - ik\right)r, \tag{8}$$

on voit que si $\psi^{(+)}$ est l'onde sortante (3) on a

$$\mathscr{L}\psi^{(+)} = \frac{\hbar^2}{2MR}\delta(r-R)\left(\frac{\mathrm{d}}{\mathrm{d}r} - ik\right) S\mathrm{e}^{ikr} = 0. \tag{9}$$

Cette propriété explique l'importance du rôle que va jouer l'opérateur $\mathscr{L}$. Elle a en effet pour conséquence l'équation

$$(\varepsilon - \mathscr{K})\psi(r) = -\mathscr{L}\psi^{(-)}(r) \tag{10}$$

qui se réduit à l'équation de Schrödinger (1) pour $r < R$ et pour $r = R$ à l'équation

$$\mathscr{L}\psi(r) = \mathscr{L}\psi^{(-)}(r)$$

qui résulte de (9). Dans l'équation (10) le second membre est connu car il ne dépend que de l'onde entrante.

Si l'opérateur $\varepsilon - \mathscr{K}$ a un inverse, ce qui implique en particulier que l'équation

$$(\varepsilon - \mathscr{K})\psi(r) = 0 \tag{11}$$

n'ait pas de solution non identiquement nulle, on peut écrire la solution de (10) sous la forme

$$\psi(r) = -\frac{1}{\varepsilon - \mathscr{K}}\mathscr{L}\psi^{(-)}(r). \tag{12}$$

En utilisant cette expression pour $r = R$ et en introduisant la séparation (2) on obtient immédiatement l'amplitude de l'onde sortante pour $r = R$:

$$\psi^{(+)}(R) = \psi^{(-)}(R) + \left[\frac{1}{\varepsilon - \mathscr{H}} \mathscr{L}\psi^{(-)}\right]_R. \tag{13}$$

Cette expression jointe aux relations (3) permet en principe le calcul de S. Le problème est donc formellement résolu.

Il faut maintenant examiner la validité des opérations formelles effectuées. Ceci est particulièrement facile dans le cas à une dimension.

Considérons une équation avec second membre du type (10):

$$(\varepsilon - \mathscr{H})\psi(r) = F(r), \tag{14}$$

où $F(r)$ est de la forme (6). Le cas qui nous intéressera plus particulièrement sera celui où $f(r) = 0$. Dans le cas opposé où $A = 0$ la résolution de (10) revient à celle du système classique d'une équation différentielle avec second membre et condition aux limites:

$$\begin{aligned} &(\varepsilon - H)\psi(r) = f(r) \qquad (r < R), \\ &\left[\left(\frac{\mathrm{d}}{\mathrm{d}r} - ik\right) r\psi\right]_R = 0. \end{aligned} \tag{15}$$

La solution de ce problème s'exprime par la formule

$$\psi(r) = \int_0^R r'^2 \mathrm{d}r' \, G(r, r') f(r'), \tag{16}$$

où $G(r, r')$ est la *fonction de Green* de l'équation différentielle avec condition aux limites. La construction de cette fonction dans le cas à une dimension est rappelée en Appendice. On y démontre également que la solution de l'équation (14) avec le second membre le plus général de la forme (6), qui équivaut au système

$$\begin{aligned} &(\varepsilon - H)\psi(r) = f(r) \qquad (r < R), \\ &-\frac{\hbar^2}{2MR}\left[\left(\frac{\mathrm{d}}{\mathrm{d}r} - ik\right) r\psi\right]_R = A, \end{aligned} \tag{17}$$

s'exprime au moyen de la même fonction de Green par la formule

$$\psi(r) = \int_0^R r'^2 \mathrm{d}r' \, G(r, r') F(r'). \tag{18}$$

On peut retrouver ce résultat d'une manière heuristique simple en déplaçant la singularité du second membre vers l'intérieur du domaine, c'est-à-dire en remplaçant $F(r)$ par

$$F(r) = f(r) + A\delta(r - R + \eta),$$

où η est infiniment petit positif. La théorie habituelle de la fonction de Green montre alors que (18) donne la solution de

$$(\varepsilon - H)\psi(r) = F(r)$$

avec la condition aux limites (15). Cette équation est identique à l'équation différentielle (15) jusqu'au voisinage de $R-\eta$. Elle montre qu'à ce point la fonction $\psi(r)$ reste continue mais que sa dérivée première effectue un saut dont l'amplitude se calcule immédiatement en intégrant l'équation membre à membre sur l'intervalle infiniment petit $(R-2\eta, R)$, par exemple. Ceci donne

$$\left[\frac{\hbar^2}{2Mr}\frac{\mathrm{d}}{\mathrm{d}r}r\psi\right]_{R-2\delta}^{R} = A.$$

Comme la fonction $\psi(r)$ satisfait à la condition aux limites (15) pour $r = R$, on voit qu'elle satisfait à la condition aux limites (17) au point $R-2\delta$. Il ne reste plus qu'à faire tendre δ vers zéro pour voir que (18) est bien la solution du système (17).

Ces considérations justifient la résolution formelle (12) de l'équation (11). En introduisant les expressions (3) et (8) dans (13) on obtient l'expression de S sous la forme

$$S = \mathrm{e}^{2ikR}\left[1 - \frac{i\hbar^2 kR}{M}G(R, R)\right], \tag{19}$$

et en introduisant dans cette expression la valeur de la fonction de Green indiquée en Appendice on arrive au résultat bien connu

$$S = \mathrm{e}^{2ikR}\frac{\left[\left(\frac{\mathrm{d}}{\mathrm{d}r} + ik\right)r\psi\right]_R}{\left[\left(\frac{\mathrm{d}}{\mathrm{d}r} - ik\right)r\psi\right]_R}, \tag{20}$$

où $\psi(r)$ est la solution de l'équation de Schrödinger qui reste finie pour $r = 0$.

L'expression (13) se prête à des calculs approchés que nous ne discuterons pas dans le cas simplifié à une dimension.

3. Théorie Générale

Nous supposerons dans ce qui suit pour simplifier l'exposé que les seules voies intervenant d'une manière importante sont des voies à deux particules.

Pour spécifier une voie il faut préciser la nature des particules constituant cette voie, les niveaux d'énergie dans lesquels elles se trouvent, le moment orbital relatif des particules et le couplage de leurs spins avec ce moment orbital. Nous désignerons par λ l'ensemble des nombres quantiques caractérisant une voie. Dans la région de l'espace de configuration où les particules constituant les voies λ sont bien séparées, c'est-à-dire lorsque les distances r_λ de leurs centres de masse sont supérieures aux rayons des voies R_λ, la fonction d'onde du système peut être mise sous la forme

$$|\Psi\rangle = \sum_{\lambda} |\lambda) \psi_\lambda(r_\lambda) \qquad (r_\lambda \geqq R_\lambda), \tag{21}$$

où ψ_λ est une fonction d'onde purement radiale et où $|\lambda)$ désigne le produit des fonctions d'onde des deux particules de la voie λ et de la fonction harmonique sphérique décrivant leur mouvement angulaire relatif. Les différentes fonctions $|\lambda)$ sont orthogonales les unes aux autres. Nous les supposerons également normalisées.

Nous utiliserons toujours la notation $|\ \rangle$ pour désigner les fonctions d'onde complètes dépendant de toutes les coordonnées, alors que la notation $|\ )$ sera réservée aux fonctions d'onde incomplètes dépendant de toutes les coordonnées sauf la distance r_λ des centres de masse des deux particules d'une voie. Il sera commode d'utiliser la notion de produit scalaire $(\lambda|\Psi\rangle$ d'une fonction d'onde complète par une fonction d'onde incomplète. Ce produit scalaire se calcule en maintenant la distance r_λ constante et supérieure ou égale à R_λ et en intégrant sur toutes les autres coordonnées y compris les angles fixant la direction du vecteur $\mathbf{r}_\lambda$ joignant les centres de masse. Le produit scalaire ainsi défini est donc une fonction de r_λ et en particulier

$$(\lambda|\Psi\rangle = \psi_\lambda(r_\lambda) \qquad (r_\lambda \geqq R_\lambda). \tag{22}$$

On n'oubliera pas que l'élément de volume dans l'espace $\mathbf{r}_\lambda$ est $r_\lambda^2\, \mathrm{d}r_\lambda\, \mathrm{d}\omega_\lambda$, où $\mathrm{d}\omega_\lambda$ est l'élément différentiel d'angle solide intervenant dans le produit scalaire (22). Par conséquent, lorsqu'on aura à transformer le produit scalaire incomplet (22) en un produit scalaire complet l'élément différentiel à introduire dans l'intégration radiale sera $r_\lambda^2\, \mathrm{d}r_\lambda$.

Pour chaque valeur de l'énergie il existe un certain nombre de voies ouvertes et un certain nombre de voies fermées. Dans les voies ouvertes, les fonctions ψ_λ sont des combinaisons linéaires d'une fonction d'onde entrante et d'une fonction d'onde sortante:

$$\psi_\lambda(r_\lambda) = \psi_\lambda^{(-)}(r_\lambda) - \psi_\lambda^{(+)}(r_\lambda), \tag{23}$$

où

$$\begin{aligned} \psi_\lambda^{(-)}(r_\lambda) &= (\lambda|-)\, \frac{u_\lambda^{(-)}(r_\lambda)}{r_\lambda V_\lambda^{\frac{1}{2}}}, \\ \psi_\lambda^{(+)}(r_\lambda) &= (\lambda|+)\, \frac{u_\lambda^{(+)}(r_\lambda)}{r_\lambda V_\lambda^{\frac{1}{2}}}. \end{aligned} \tag{24}$$

Les fonctions $u_\lambda^{(+)}$ sont les solutions de l'équation d'onde radiale des particules de la voie λ dont le comportement asymptotique pour $r_\lambda \to \infty$ est, lorsque la voie λ comprend un neutron,

$$u_\lambda^{(+)} \to \mathrm{e}^{i(k_\lambda r_\lambda - \frac{1}{2} l_\lambda \pi)},$$

où k_λ et l_λ sont le nombre d'onde et le moment orbital relatif de la voie λ. Si les deux particules de la voie λ ont des charges Z_λ, z_λ on a pour $r_\lambda \to \infty$

$$u_\lambda^{(+)} \to e^{i(k_\lambda r_\lambda - \frac{1}{2}l_\lambda \pi - \gamma_\lambda \log 2k_\lambda r_\lambda)},$$

où

$$\gamma_\lambda = \frac{Z_\lambda z_\lambda e^2}{\hbar V_\lambda}. \tag{25}$$

Dans (24), (25) V_λ désigne la vitesse relative des particules de la voie λ. Les fonctions $u_\lambda^{(-)}$ sont liées aux $u_\lambda^{(+)}$ par

$$u_\lambda^{(-)} = u_\lambda^{(+)*}.$$

Nous aurons besoin par la suite de connaître le comportement des $u_\lambda^{(+)}$ et $u_\lambda^{(-)}$ au voisinage de la surface nucléaire, c'est-à-dire pour $r_\lambda = R_\lambda$. En suivant Blatt et Weisskopf [9]), nous poserons

$$u_\lambda^{(+)}(R_\lambda) = v_\lambda^{-\frac{1}{2}} e^{-i\xi_\lambda},$$
$$\left[\frac{r_\lambda}{u_\lambda^{(+)}} \frac{\partial u_\lambda^{(+)}}{\partial r_\lambda}\right]_{R_\lambda} = \Delta_\lambda + ik_\lambda R_\lambda v_\lambda = L_\lambda^{(+)}, \tag{26}$$

où v_λ est le facteur de pénétration de la voie λ et ξ_λ la phase de diffusion dans la voie λ en supposant que le noyau se comporte comme une sphère impénétrable.

Dans les voies fermées, il existe une seule fonction d'onde radiale restant bornée pour $r_\lambda \to \infty$. Nous la désignerons par $w_\lambda(r_\lambda)$ et nous poserons

$$\left[\frac{r_\lambda}{w_\lambda} \frac{\partial w_\lambda}{\partial r_\lambda}\right]_{R_\lambda} = L_\lambda'. \tag{27}$$

C'est toujours une quantité réelle.

Les nombres complexes $(\lambda|-)$ et $(\lambda|+)$ dans (24) sont les amplitudes des ondes entrantes et sortantes. Les normalisations des $u_\lambda^{(-)}$ et $u_\lambda^{(+)}$ et l'introduction du facteur $V_\lambda^{-\frac{1}{2}}$ ont pour conséquence qu'une amplitude égale à 1 correspond à un flux unité.

Les amplitudes des ondes entrantes $(\lambda|-)$ sont déterminées par la donnée du faisceau incident. L'équation de Schrödinger étant une équation linéaire, les amplitudes des ondes sortantes dépendent linéairement des amplitudes des ondes entrantes. On peut donc écrire

$$(\lambda|+) = \sum_\mu (\lambda|S|\mu)(\mu|-). \tag{28}$$

Cette équation peut être considérée comme définissant la matrice de collision S. La connaissance de S entraîne celle de toutes les quantités physiquement observables.

Pour déterminer S, il faut résoudre dans la région intérieure l'équation de Schrödinger

$$(\varepsilon - H)|\Psi\rangle = 0, \tag{29}$$

où l'Hamiltonien H est donné par

$$H = -\sum_i \frac{\hbar^2}{2M_i} \Delta_i + V. \tag{30}$$

Dans cette expression, M_i désigne la masse du nucléon i, Δ_i le laplacien agissant sur le nucléon i et V l'énergie d'interaction des nucléons.

Ici encore, nous commencerons par remarquer que H n'est pas hermitique dans la région intérieure Ω. Par une application du théorème de Green, on obtient en effet pour deux fonctions quelconques Ψ_1 et Ψ_2

$$\begin{aligned}\int_\Omega [\Psi_1^*(H\Psi_2) - (H\Psi_1)^* \Psi_2] \mathrm{d}\tau \\ = -\int_\Omega \sum_i \frac{\hbar^2}{2M_i} [\Psi_1^*(\Delta_i \Psi_2) - (\Delta_i \Psi_1)^* \Psi_2] \, \mathrm{d}\tau \\ = -\sum_\lambda \frac{\hbar^2}{2M_\lambda} \left[r_\lambda \psi_{1\lambda}^* \frac{\partial}{\partial r_\lambda} (r_\lambda \psi_{2\lambda}) - \frac{\partial}{\partial r_\lambda} (r_\lambda \psi_{1\lambda})^* r_\lambda \psi_{2\lambda} \right]_{R_\lambda},\end{aligned} \tag{31}$$

où M_λ est la masse réduite de la voie, $\psi_{1\lambda}(r_\lambda)$ et $\psi_{2\lambda}(r_\lambda)$ les fonctions radiales de Ψ_1 et Ψ_2 dans la voie λ définies suivant (21) ou (22).

Pour rendre H hermitique, il faut lui ajouter un terme de surface défini sur Σ. Ainsi, l'opérateur

$$\mathscr{H} = H + \sum_\lambda |\lambda) \frac{\hbar^2}{2M_\lambda R_\lambda} \delta(r_\lambda - R_\lambda) \frac{\partial}{\partial r_\lambda} r_\lambda (\lambda| \tag{32}$$

est hermitique. On vérifie en effet facilement que la contribution du terme supplémentaire compense exactement la quantité (31) de sorte que

$$\int_\Omega [\Psi_1^*(\mathscr{H}\Psi_2) - (\mathscr{H}\Psi_1)^* \Psi_2] \, \mathrm{d}\tau = 0. \tag{33}$$

L'opérateur de surface ainsi introduit est nul partout sauf sur Σ. Il a une valeur différente sur la surface nucléaire de chaque voie. Ceci est exprimé par l'opérateur de projection $|\lambda)(\lambda|$ qui a pour effet de sélectionner les différentes portions de Σ.

Pour obtenir une solution formelle de l'équation de Schrödinger dans la région intérieure avec les conditions aux limites d'un problème de collision, c'est-à-dire avec des amplitudes entrantes $(\lambda|-)$ données, nous allons définir un opérateur légèrement différent de $\mathscr{H}$:

$$\mathscr{K} = H + \mathscr{L}, \tag{34}$$

où $\mathscr{L}$ est *l'opérateur de conditions aux limites*

$$\mathscr{L} = \sum_\lambda |\lambda) \frac{\hbar^2}{2M_\lambda R_\lambda} \delta(r_\lambda - R_\lambda) \left(\frac{\partial}{\partial r_\lambda} - \frac{L_\lambda}{r_\lambda} \right) r_\lambda (\lambda| \tag{35}$$

avec

$$\begin{aligned} L_\lambda &= L_\lambda^{(+)} \quad \text{pour les voies ouvertes,} \\ L_\lambda &= L_\lambda' \quad \text{pour les voies fermées,} \end{aligned} \tag{36}$$

conformément aux définitions (26) et (27). Les valeurs de L_λ sont choisies ainsi parce qu'elles entraînent

$$\left[\left(\frac{\partial}{\partial r_\lambda} - \frac{L_\lambda}{r_\lambda}\right) u_\lambda^{(+)}\right]_{R_\lambda} = 0,$$
$$\left[\left(\frac{\partial}{\partial r_\lambda} - \frac{L_\lambda}{r_\lambda}\right) w_\lambda\right]_{R_\lambda} = 0,$$

de sorte que $\mathscr{L}|\Psi\rangle$ ne dépend *que des amplitudes des ondes entrantes*. C'est donc une quantité connue

$$\mathscr{L}|\Psi\rangle = \mathscr{L} \sum_\lambda^\circ |\lambda) \psi_\lambda^{(-)}, \tag{37}$$

où la sommation sur λ est étendue seulement aux voies ouvertes.

Dans la région intérieure Ω nous avons l'équation (29); sur la surface Σ nous avons (37). Nous pouvons donc écrire l'équation

$$(\varepsilon - \mathscr{K})|\Psi\rangle = -\mathscr{L} \sum_\lambda^\circ |\lambda) \psi_\lambda^{(-)} \tag{38}$$

valable dans le domaine $\Omega+\Sigma$. Nous montrerons au paragraphe 5.2 que l'opérateur $\mathscr{K}$ n'a pas de valeur propre réelle, autrement dit que l'équation

$$(\varepsilon - \mathscr{K})|\Psi\rangle = 0 \tag{39}$$

n'a pas de solution non identiquement nulle. Cette propriété, ainsi que l'analogie avec le cas à une dimension traité au paragraphe 2 conduit à admettre que l'opérateur $\varepsilon - \mathscr{K}$ a un inverse bien défini.

Nous pourrons donc écrire la solution de (38) sous la forme

$$|\Psi\rangle = -\frac{1}{\varepsilon - \mathscr{K}} \mathscr{L} \sum_\lambda^\circ |\lambda) \psi_\lambda^{(-)}. \tag{40}$$

Cette expression donne $|\Psi\rangle$ dans tout le domaine $\Omega+\Sigma$. En l'utilisant sur la surface Σ, nous pourrons trouver les amplitudes $\psi_\lambda(R_\lambda)$. D'après (22) on peut écrire

$$\psi_\lambda(R_\lambda) = -\sum_\mu^\circ {}_{R_\lambda}\left(\lambda \left| \frac{1}{\varepsilon - \mathscr{K}} \mathscr{L} \right| \mu\right) \psi_\mu^{(-)}. \tag{41}$$

Ici nous avons utilisé la notation

$${}_{R_\lambda}(\lambda|\Psi\rangle = [(\lambda|\Psi\rangle]_{R_\lambda}, \tag{42}$$

car on se rappellera que les produits scalaires tels que $(\lambda|\Psi\rangle$ sont des fonctions de $r_\lambda \geqq R_\lambda$. La formule (40) ne pouvant pas s'appliquer en dehors du domaine $\Omega+\Sigma$, nous sommes obligés de prendre $r_\lambda = R_\lambda$.

De (23) et (41) on peut enfin tirer les amplitudes des ondes sortantes dans les voies ouvertes: à la surface nucléaire on a

$$\psi_\lambda^{(+)}(R_\lambda) = \psi_\lambda^{(-)}(R_\lambda) + \sum_\mu^{\circ}{}_{R_\lambda}\left(\lambda \left| \frac{1}{\varepsilon - \mathscr{H}} \mathscr{L} \right| \mu\right)\psi_\mu^{(-)}. \tag{43}$$

Cette équation jointe aux relations (24) donne les amplitudes $(\lambda|+)$ en fonction des $(\lambda|-)$, c'est-à-dire qu'elle définit la matrice de collision.

4. Introduction d'une base dans la Région Intérieure

Pour expliciter l'expression (43), nous allons introduire dans la région intérieure une base orthonormale complète

$$|s\rangle, |t\rangle, \ldots$$

qui sera pour l'instant *entièrement arbitraire.*

Cette base nous permettra d'écrire

$$\frac{1}{\varepsilon - \mathscr{H}} = \sum_{s,t} |s\rangle\langle s| \frac{1}{\varepsilon - \mathscr{H}} |t\rangle\langle t|. \tag{44}$$

En reportant cette expression dans (43) on voit apparaître les quantités $(\lambda|s\rangle$ et nous poserons

$$g_s^{(\lambda)} = \left(\frac{\hbar^2 R_\lambda}{2M_\lambda}\right)^{\frac{1}{2}}{}_{R_\lambda}(\lambda|s\rangle. \tag{45}$$

D'une manière équivalente, si les fonctions $|s\rangle$ s'écrivent au voisinage de la surface Σ sous la forme correspondant à (21):

$$|s\rangle = \sum_\lambda |\lambda)\, \varphi_s^{(\lambda)}(r_\lambda), \tag{46}$$

on peut dire que $g_s^{(\lambda)}$ est défini par

$$g_s^{(\lambda)} = \left(\frac{\hbar^2 R_\lambda}{2M_\lambda}\right)^{\frac{1}{2}} \varphi_s^{(\lambda)}(R_\lambda). \tag{47}$$

Ces quantités proportionnelles aux amplitudes des fonctions de base dans les différentes voies à la surface nucléaire sont appelées les *amplitudes réduites* des fonctions de base. Leurs carrés ont la dimension d'une énergie; ce sont les *largeurs réduites* des fonctions de base. Ces quantités visiblement ne dépendent que de la région intérieure et du choix des fonctions de base.

Le calcul de (43) fait également intervenir les quantités †

$$\langle t|\mathscr{L}|\mu)\psi_\mu^{(-)} = \langle t|\mu)\,(\mu|-)\,\frac{\hbar^2 R_\mu}{2M_\mu V_\mu^{\frac{1}{2}}}\left[\left(\frac{\partial}{\partial r_\mu} - \frac{L_\mu^{(+)}}{r_\mu}\right)u_\mu^{(-)}\right]_{R_\mu}.$$

Le crochet se calcule aisément à l'aide des relations (26) et des relations complexes conjuguées. On obtient ainsi

† Ne pas oublier que dans un produit scalaire, l'élément différentiel d'intégration radiale est $r_\lambda^2\, dr_\lambda$.

$$\langle t|\mathscr{L}|\mu)\psi_\mu^{(-)} = \frac{\hbar^{\frac{1}{2}}}{i}(\mu|-)G_t^{(\mu)*}\,e^{i\xi_\mu}, \tag{48}$$

où nous avons posé

$$G_s^{(\lambda)} = g_s^{(\lambda)}(2k_\lambda R_\lambda v_\lambda)^{\frac{1}{2}}. \tag{49}$$

Ces quantités qui contiennent les facteurs de pénétration sont les *amplitudes partielles* des fonctions de base dans les différentes voies. Leurs carrés ont la dimension d'une énergie: ce sont les *largeurs partielles* des fonctions de base.

En reportant dans (43) les expressions (24) (44) et (48) on obtient pour les amplitudes sortantes en fonction des amplitudes entrantes l'expression

$$(\lambda|+) = \sum_\mu{}^{\circ} e^{i\xi_\lambda}\left[\delta_{\lambda\mu} - i\sum_{s,t}\langle s|\frac{1}{\varepsilon-\mathscr{H}}|t\rangle G_s^{(\lambda)}G_t^{(\mu)*}\right]e^{i\xi_\mu}(\mu|-).$$

La matrice S s'en déduit immédiatement. On peut l'écrire sous la forme

$$S = e^{i\xi}\left[1 - i\sum_{s,t}\langle s|\frac{1}{\varepsilon-\mathscr{H}}|t\rangle\,\mathbf{G}_s\times\mathbf{G}_t^*\right]e^{i\xi} \tag{50}$$

où on désigne par $\mathbf{G}_s$ un vecteur d'un *espace symbolique des voies ouvertes* dont les composantes sont les $G_s^{(\lambda)}$, par $\times$ la matrice produit direct de deux vecteurs et par $\exp i\xi$ une matrice diagonale de l'espace des voies ouvertes dont les éléments sont les $\exp(i\xi_\lambda)$. La matrice S est elle-même naturellement une matrice de l'espace des voies ouvertes.

5. Les Réactions Résonantes: Deux Bases Particulières

Pour inverser l'opérateur $\varepsilon-\mathscr{H}$ on peut choisir une base facilitant le calcul. La base la plus naturelle est celle qui diagonalise $\mathscr{H}$: c'est la base utilisée par Peierls et Kapur [5]). Malheureusement la nature de $\mathscr{H}$ introduit certaines difficultés. D'une part $\mathscr{H}$ n'est pas hermitique car les $L_\lambda^{(+)}$ des voies ouvertes figurant dans l'opérateur $\mathscr{L}$ sont des nombres complexes. D'autre part, et ceci est pire encore, les L_λ et par suite l'opérateur $\mathscr{H}$ dépendent de l'énergie ε. Il en résulte que les fonctions de base et par conséquent les amplitudes réduites et les valeurs propres dépendront de l'énergie d'une manière compliquée.

Pour éviter ces difficultés on peut suivant Wigner introduire une base qui diagonalise non pas $\mathscr{H}$ mais l'opérateur

$$\mathscr{H}_W = H + \mathscr{L}(b), \tag{51}$$

où $\mathscr{L}(b)$ est l'opérateur qui se déduit de $\mathscr{L}$ en y remplaçant les L_λ dans toutes les voies, ouvertes ou fermées, par des nombres réels constants arbitraires b_λ. Explicitement on a

$$\mathscr{H}_W = H + \sum_\lambda|\lambda)\frac{\hbar^2}{2M_\lambda R_\lambda}\delta(r_\lambda - R_\lambda)\left(\frac{\partial}{\partial r_\lambda} - \frac{b_\lambda}{r_\lambda}\right)r_\lambda(\lambda|. \tag{52}$$

On définit bien ainsi un problème de valeurs propres indépendant de l'énergie et les amplitudes réduites et les valeurs propres seront des paramètres constants caractéristiques de la région intérieure. Malheureusement dans ce cas l'opérateur à inverser n'est pas complètement diagonalisé et son inversion reste un problème difficile qui ne peut être résolu qu'approximativement.

Les deux méthodes présentent chacune leurs avantages et leurs inconvénients et nous les examinerons successivement.

5.1. LA BASE DE WIGNER

L'opérateur $\mathscr{K}_W$ étant hermitique, ses valeurs propres sont réelles et ses fonctions propres définissent un système orthonormal complet. Nous désignerons par ε_s et $|s\rangle$ les valeurs propres et fonctions propres de $\mathscr{K}_W$:

$$\mathscr{K}_W|s\rangle = \varepsilon_s|s\rangle. \tag{53}$$

Cette équation équivaut au système

$$\begin{aligned} H|s\rangle &= \varepsilon_s|s\rangle, \\ \left[\left(\frac{\partial}{\partial r_\lambda} - \frac{b_\lambda}{r_\lambda}\right) r_\lambda \varphi_s^{(\lambda)}(r_\lambda)\right]_{R_\lambda} &= 0, \end{aligned} \tag{54}$$

où les $\varphi_s^{(\lambda)}$ sont les fonctions d'onde radiales des $|s\rangle$ dans les voies λ dans le développement (46).

En supposant l'Hamiltonien H du système invariant par renversement du temps, on démontre qu'*on peut toujours rendre les amplitudes réduites* $g_s^{(\lambda)}$ *réelles* dans la base de Wigner par un choix approprié des phases des fonctions $|s\rangle$ et $|\lambda)$. Les amplitudes $G_s^{(\lambda)}$ seront alors également des quantités réelles positives ou négatives.

Nous devons ensuite considérer l'opérateur

$$\mathscr{K} = \mathscr{K}_W + [\mathscr{L} - \mathscr{L}(b)], \tag{55}$$

où le dernier terme n'est pas diagonal. D'après (35) on a

$$\mathscr{L} - \mathscr{L}(b) = \sum_\lambda |\lambda) \frac{\hbar^2}{2M_\lambda R_\lambda} \delta(r_\lambda - R_\lambda)(b_\lambda - L_\lambda)(\lambda|, \tag{56}$$

où la sommation est étendue à toutes les voies. En utilisant la définition (45) des amplitudes réduites $g_s^{(\lambda)}$ on obtient

$$\begin{aligned} \langle s|\mathscr{L} - \mathscr{L}(b)|t\rangle &= \sum_\lambda g_s^{(\lambda)}(b_\lambda - L_\lambda) g_t^{(\lambda)} \\ &= \sum_\lambda g_s^{(\lambda)}(b_\lambda - \mathrm{Re}\, L_\lambda) g_t^{(\lambda)} - \frac{i}{2} \sum_\lambda{}^0 G_s^{(\lambda)} G_t^{(\lambda)}, \end{aligned} \tag{57}$$

où la partie réelle de L_λ est égale à L_λ^t dans les voies fermées et à Δ_λ défini par (26) dans les voies ouvertes. Dans le dernier terme, la sommation est étendue aux voies ouvertes seulement. Il est commode de définir des matrices E, ΔE et Γ par les relations

$$\langle s|E|t\rangle = \varepsilon_s \delta_{st},$$
$$\langle s|\Delta E|t\rangle = \sum_\lambda g_s^{(\lambda)}(b_\lambda - \mathrm{Re}\, L_\lambda) g_t^{(\lambda)}, \tag{58}$$
$$\langle s|\Gamma|t\rangle = \sum_\lambda^0 G_s^{(\lambda)} G_t^{(\lambda)}.$$

On a alors

$$\mathscr{K}_W = E, \quad \mathscr{L} - \mathscr{L}(b) = \Delta E - \tfrac{1}{2} i\Gamma. \tag{59}$$

En reportant dans (50) on obtient *l'expression de la matrice S dans la théorie de Wigner* établie par R. G. Thomas [4]):

$$S = e^{i\xi}\left[1 - i \sum_{s,t} \langle s| \frac{1}{\varepsilon - E - \Delta E + \frac{1}{2} i\Gamma} |t\rangle \mathbf{G}_s \times \mathbf{G}_t\right] e^{i\xi}. \tag{60}$$

En négligeant complètement dans (60) les termes non-diagonaux de ΔE et Γ on obtient la *formule de Breit et Wigner à plusieurs niveaux*:

$$S = e^{i\xi}\left[1 - i \sum_s \frac{\mathbf{G}_s \times \mathbf{G}_s}{\varepsilon - \varepsilon_s - \Delta\varepsilon_s + \frac{1}{2} i\Gamma_s}\right] e^{i\xi}, \tag{61}$$

où

$$\Delta\varepsilon_s = \sum_\lambda [g_s^{(\lambda)}]^2 (b_\lambda - \mathrm{Re}\, L_\lambda),$$
$$\Gamma_s = \sum_\lambda^0 [G_s^{(\lambda)}]^2. \tag{62}$$

On pourrait estimer la contribution des termes non-diagonaux de ΔE et Γ en développant S en puissances de ces termes.

Le résultat (60) est démontré dans la théorie de Wigner en plusieurs étapes. On calcule d'abord la matrice dérivée, ce qui revient à inverser l'opérateur $\varepsilon - \mathscr{K}_W$. De la matrice dérivée on passe à la matrice dérivée réduite obtenue en éliminant les voies fermées. Cette nouvelle matrice est liée à l'inversion de l'opérateur

$$\varepsilon - \mathscr{K}_W - \sum_\lambda^f |\lambda) \frac{\hbar^2}{2M_\lambda R_\lambda} \delta(r_\lambda - R_\lambda)(b_\lambda - L_\lambda)(\lambda|,$$

où la sommation est étendue aux voies fermées seulement. Autrement dit on a inclus dans l'opérateur la contribution de $\mathscr{L} - \mathscr{L}(b)$ provenant des voies fermées. Enfin, on passe de la matrice dérivée réduite à la matrice S ce qui revient à inverser finalement l'opérateur complet $\varepsilon - \mathscr{K}$.

5.2. LA BASE DE PEIERLS ET KAPUR; DIAGONALISATION DE $\mathscr{K}$

La base de Peierls et Kapur est constituée par les solutions du problème de valeurs propres

$$\mathscr{K}|s\rangle = E_s|s\rangle \tag{63}$$

dont on suppose qu'elles constituent un *système complet*. Cette équation équivaut au système

$$H|s\rangle = E_s|s\rangle,$$

$$\left[\left(\frac{\partial}{\partial r_\lambda}-\frac{L_\lambda}{r_\lambda}\right) r_\lambda \varphi_s^{(\lambda)}(r_\lambda)\right]_{R_\lambda}=0. \tag{64}$$

L'opérateur $\mathscr{K}$ dépendant de l'énergie par l'intermédiaire des L_λ tout le système de fonctions propres et de valeurs propres est lié à une énergie particulière et change quand cette énergie varie. Ces conditions aux limites reviennent à imposer aux fonctions de base de se raccorder d'une manière continue avec les fonctions $w_\lambda(r_\lambda)$ dans les voies fermées et de comporter des ondes *purement sortantes* dans les voies ouvertes.

Montrons d'abord que *les valeurs propres E_s sont toutes imaginaires* dès qu'il existe au moins une voie ouverte et que les E_s sont dans le plan complexe *en dessous de l'axe réel*. De (63) et de l'équation complexe conjuguée

$$\langle s|\mathscr{K}^+ = \langle s|E_s^*$$

on déduit en effet

$$(E_s-E_s^*)\langle s|s\rangle = \langle s|\mathscr{K}-\mathscr{K}^+|s\rangle = \langle s|\mathscr{L}-\mathscr{L}^+|s\rangle$$

$$= \sum_\lambda{}^{\circ} \frac{\hbar^2 R_\lambda}{2M_\lambda}\,(L_\lambda^{(-)}-L_\lambda^{(+)})\,|(\lambda|s\rangle|^2 = -i\sum_\lambda{}^{\circ}|G_s^{(\lambda)}|^2.$$

Si on pose

$$E_s = \varepsilon_s - \tfrac{1}{2} i\Gamma_s \tag{65}$$

on a par conséquent

$$\Gamma_s = \sum_\lambda{}^{\circ}\,|G_s^{(\lambda)}|^2/\langle s|s\rangle. \tag{66}$$

L'opérateur $\mathscr{K}$ n'est pas hermitique à cause de la présence dans $\mathscr{L}$ des nombres complexes $L_\lambda^{(+)}$. Il possède toutefois la propriété suivante

$$\mathscr{K}^+ = K\mathscr{K}K^{-1}, \tag{67}$$

où K est l'opérateur de renversement du sens du temps [10]). En supposant $\mathscr{H}$ invariant par renversement du temps, on a en effet

$$K\mathscr{H}K^{-1} = \mathscr{H} = \mathscr{H}^+,$$

puisque $\mathscr{H}$ est hermitique. D'autre part, l'opérateur de surface $\mathscr{K}-\mathscr{H}$ satisfait à une relation du type (67). En effet $(\mathscr{K}-\mathscr{H})^+$ et $K(\mathscr{K}-\mathscr{H})K^{-1}$ se déduisent tous les deux de $\mathscr{K}-\mathscr{H}$ par remplacement des $L_\lambda^{(+)}$ par les $L_\lambda^{(-)}$. Ceci démontre la relation (67).

En appliquant l'opérateur K à (63) on obtient, compte tenu de (67) la relation

$$\mathscr{K}^+K|s\rangle = E_s^*K|s\rangle \tag{68}$$

qui montre que $K|s\rangle$ est une fonction propre de $\mathscr{K}^+$ appartenant à la valeur propre E_s^*. Les fonctions propres de $\mathscr{K}^+$ ont dans les voies ouvertes des ondes *purement entrantes*.

Démontrons que si $E_s \neq E_t$, les fonctions $K|s\rangle$ et $|t\rangle$ sont orthogonales. Ecrivons en effet l'équation imaginaire conjuguée de (63) pour $|t\rangle$:

$$\langle t|\mathscr{K}^+ = E_t^*\langle t|.$$

En multipliant cette équation à droite par $K|s\rangle$ et en retranchant (63) multipliée à gauche par $\langle t|$ on obtient

$$(E_t^* - E_s^*)\langle t|(K|s\rangle) = 0;$$

d'où le résultat annoncé.

Les valeurs propres E_s sont le plus souvent dégénérées à cause de l'existence d'un moment angulaire total non nul. Pour simplifier l'exposé, nous admettrons qu'il n'existe aucune autre dégénérescence. Pour mettre en évidence le moment angulaire, nous utiliserons la notation $|sjm\rangle$. Aux fonctions $|sjm\rangle$, nous allons associer les fonctions

$$\widetilde{|sj-m\rangle} = (-)^{m-j}K|sjm\rangle. \tag{69}$$

L'opérateur K renversant les moments angulaires la fonction (69) a bien une composante de moment angulaire égale à $-m$. On voit alors que la fonction $\widetilde{|sjm\rangle}$ est orthogonale à toutes les fonctions $|s'j'm'\rangle$ autres que $|sjm\rangle$ soit parce que $E_s \neq E_{s'}$, soit parce que $m \neq m'$. Si on suppose que le système de base est complet, $\widetilde{|sjm\rangle}$ ne peut être orthogonale à toutes les fonctions. Donc elle ne peut être orthogonale à $|sjm\rangle$. On peut alors en multipliant $|sjm\rangle$ par une constante appropriée s'arranger pour obtenir la normalisation

$$\widetilde{\langle sjm|}s'j'm'\rangle = \delta_{ss'}\delta_{jj'}\delta_{mm'}. \tag{70}$$

Les fonctions $|sjm\rangle$ et $\widetilde{|sjm\rangle}$ forment ce qu'on appelle un *système biorthogonal*.

En reprenant la notation abrégée $|s\rangle$ nous aurons

$$\langle\tilde{s}|s'\rangle = \delta_{ss'}.$$

On notera qu'on a comme pour tout système orthonormal complet

$$\sum_s |s\rangle\langle\tilde{s}| = 1.$$

L'opérateur $\mathscr{K}$ peut être écrit

$$\mathscr{K} = \sum_s |s\rangle E_s\langle\tilde{s}|,$$

et l'inverse de $\varepsilon - \mathscr{K}$ prend la forme

$$\frac{1}{\varepsilon-\mathscr{K}} = \sum_s |s\rangle \frac{1}{\varepsilon - E_s}\langle\tilde{s}|. \tag{71}$$

En reportant cette expression dans (50) on voit apparaître les quantités

$$(\lambda|s\rangle, \qquad \langle\tilde{s}|\lambda).$$

Ces quantités sont égales grâce à la définition (69) des $|\tilde{s}\rangle$ si les phases des $|\lambda)$ ont été choisies en accord avec la convention habituelle de la théorie du renversement du temps; c'est-à-dire telles que

$$K|\lambda jm) = (-)^{m-j}|\lambda j-m).$$

En effet les propriétés de l'opérateur K (antilinéarité et unitarité) entraînent

$$\widetilde{\langle sjm}|\lambda jm) = (\lambda jm|\widetilde{sjm\rangle}^* = (-)^{-m-j}(\lambda jm|(K|sj-m\rangle)^*$$
$$= (-)^{-m-j}\big((\lambda jm|K)|sj-m\rangle = (\lambda j-m|sj-m\rangle = (\lambda jm|sjm\rangle$$

car le produit scalaire obtenu est indépendant de m.

En définissant alors les amplitudes $\mathbf{G}_s$ d'après les relations (45) et (49) et en substituant (71) dans (50), on obtient *la formule de Peierls et Kapur*

$$S = e^{i\xi}\left[1-i\sum_s \frac{\mathbf{G}_s\times\mathbf{G}_s}{\varepsilon-\varepsilon_s+\frac{1}{2}i\,\Gamma_s}\right]e^{i\xi}, \tag{72}$$

où on a utilisé la notation (65). Cette formule qui ressemble beaucoup à la formule de Breit et Wigner à plusieurs niveaux (61) est une expression rigoureuse. Les $G_s^{(\lambda)}$ qui y figurent sont des nombres complexes qui dépendent de l'énergie ε ainsi que les ε_s et les Γ_s d'une manière plus compliquée que les quantités correspondantes de la théorie de Wigner.

Mentionnons enfin que dans le cas de particules sans spin la définition (69) des fonctions associées dans le système de base biorthogonal devient simplement

$$\tilde{\phi}_s = \phi_s^*, \tag{69'}$$

et que la condition d'orthonormalisation (70) prend la forme

$$\int_\Omega \phi_s\,\phi_{s'}\,d\tau = \delta_{ss'}. \tag{70'}$$

6. Le Modèle Optique et les Interactions Directes

Les méthodes basées sur la diagonalisation de $\mathscr{H}$ (ou de $\mathscr{H}_W$) sont très utiles lorsqu'on peut se borner à tenir compte d'un seul ou d'un petit nombre de niveaux du noyau composé que ces théories mettent en évidence. C'est ce qui se produit aux basses énergies lorsque la distance moyenne D des niveaux est très supérieure à leur largeur moyenne Γ.

Considérons dans le plan complexe des énergies le spectre E_s de l'opérateur $\mathscr{H}$ calculé pour une énergie ε. Lorsqu'on se trouve dans le cas d'une énergie telle que ε_1 sur la fig. 1, beaucoup plus proche d'une certaine valeur propre E_s que de toutes les autres, cette valeur propre donnera la contribution principale dans le développement de Wigner ou de Peierls-Kapur de la matrice S. On formera alors essentiellement un niveau bien déterminé du noyau composé et la section efficace présentera l'aspect d'une résonance bien séparée.

Aux énergies élevées, Γ peut devenir supérieur à D. Dans le plan des valeurs propres de $\mathscr{H}$, la situation sera celle du point ε_2 qui se trouve à des distances du même ordre de grandeur d'un grand nombre de valeurs propres E_s. La

section efficace ne montrera plus de résonances: on se trouve dans le domaine du continu.

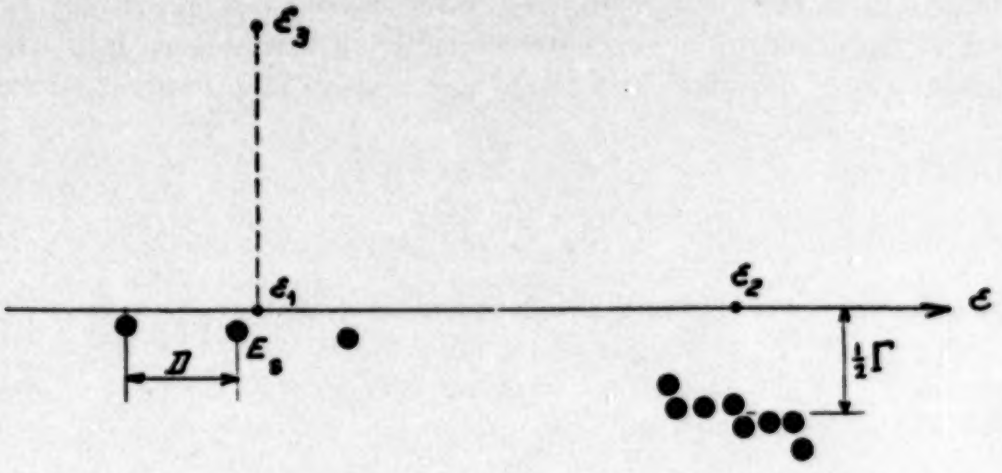

Fig. 1. Les pôles de $(\varepsilon - \mathscr{H})^{-1}$ dans le plan complexe des énergies.

Enfin, aux basses énergies, on peut ne s'intéresser qu'à la section efficace moyenne. Celle-ci peut être mise sous la forme de la somme d'une section efficace „instantanée" et d'une section efficace „retardée" [11, 12]. La section efficace instantanée se calcule à l'aide des valeurs moyennes par rapport à l'énergie des éléments de la matrice de collision. On démontre également [13] que cette valeur moyenne peut être calculée en donnant à l'énergie une composante imaginaire pure qui l'éloigne des pôles d'une distance grande par rapport à D. Ainsi la valeur moyenne de S au voisinage de l'énergie ε_1 (fig. 1) est égale à la valeur de S calculée en un point tel que ε_3.

Nous voyons donc qu'aussi bien dans le domaine du continu qu'en ce qui concerne le calcul des sections efficaces instantanées le problème est de *calculer la matrice de collision en un point situé à une distance de la ligne des valeurs propres de $\mathscr{H}$ grande par rapport à D.*

Les développements de Wigner ou de Peierls et Kapur ne constituent pas alors des points de départ très satisfaisants car on est obligé de faire la sommation d'un grand nombre de termes, c'est-à-dire de tenir compte d'un grand nombre de résonances du noyau composé. Il est possible d'effectuer ces sommations en introduisant des hypothèses statistiques concernant les amplitudes réduites $g_s^{(\lambda)}$, mais il est préférable de renoncer à utiliser les développements très particuliers de Wigner ou de Peierls et Kapur et de rechercher directement une méthode de calcul approchée de $(\varepsilon - \mathscr{H})^{-1}$ adaptée au cas considéré. Le succès du modèle des particules indépendantes suggère la voie à suivre.

Nous allons nous limiter ici à la diffusion élastique et inélastique d'une particule par un noyau. Ecrivons l'Hamiltonien sous la forme:

$$H = H_0 + \mathscr{V}, \tag{73}$$

où H_0 représente l'Hamiltonien du noyau cible et de la particule incidente soumise dans la région intérieure au *potentiel moyen* (réel) créé par le noyau, et où $\mathscr{V}$ désigne la différence entre l'interaction véritable de la particule incidente avec le noyau et l'interaction moyenne introduite dans H_0. Parallèlement, nous écrirons

$$\mathscr{H} = \mathscr{H}_0 + \mathscr{V} \tag{74}$$

où

$$\mathscr{H}_0 = H + \mathscr{L} \tag{75}$$

est l'opérateur qui intervient dans le calcul de la matrice de collision de la particule incidente par le puits de potentiel moyen créé par le noyau cible. Pour une énergie éloignée de la ligne des poles de $(\varepsilon - \mathscr{H}_0)^{-1}$, on peut penser que le développement en puissances de $\mathscr{V}$

$$\frac{1}{\varepsilon-\mathscr{H}} = \frac{1}{\varepsilon-\mathscr{H}_0} + \frac{1}{\varepsilon-\mathscr{H}_0}\mathscr{V}\frac{1}{\varepsilon-\mathscr{H}_0} + \frac{1}{\varepsilon-\mathscr{H}_0}\mathscr{V}\frac{1}{\varepsilon-\mathscr{H}_0}\mathscr{V}\frac{1}{\varepsilon-\mathscr{H}_0} + \frac{1}{\varepsilon-\mathscr{H}_0}\mathscr{V}\frac{1}{\varepsilon-\mathscr{H}_0}\mathscr{V}\frac{1}{\varepsilon-\mathscr{H}_0} + \ldots \tag{76}$$

est suffisamment convergent pour servir de point de départ à un calcul approché de $(\varepsilon - \mathscr{H})^{-1}$.

Nous utiliserons la base de Peierls-Kapur $|a\rangle$, $|b\rangle$ . . . relative à l'opérateur $\mathscr{H}_0$. Les fonctions constituant cette base sont simplement des produits d'une fonction d'onde du noyau cible dans un certain état par une fonction d'onde de la particule incidente dans le puits de potentiel moyen †. Ces fonctions sont naturellement soumises aux conditions aux limites de Peierls et Kapur. Puisque nous considérons ici seulement les voies de diffusion élastique ou inélastique, chaque voie est associée à un niveau du noyau cible et les indices λ peuvent servir à énumérer les niveaux de celui-ci. Si nous désignons par χ un indice servant à énumérer les fonctions d'onde de Peierls et Kapur de la particule incidente dans le puits de potentiel moyen nous pourrons remplacer l'indice a par l'ensemble

$$a = (\lambda, \chi). \tag{77}$$

Les amplitudes $G_a^{(\lambda)}$ s'écriront donc $G_{\mu,\chi}^{(\lambda)}$ et il est clair qu'on aura

$$G_{\mu,\chi}^{(\lambda)} = 0 \qquad \text{si } \lambda \neq \mu. \tag{78}$$

La base de Peierls et Kapur de $\mathscr{H}_0$ permet d'écrire

$$\frac{1}{\varepsilon-\mathscr{H}_0} = \sum_a |a\rangle \frac{1}{\varepsilon - E_a} \langle \tilde{a}|, \tag{79}$$

où $E_a, E_b, \ldots$ désignent les valeurs propres de $\mathscr{H}_0$. En reportant cette expression dans le développement (76) celui-ci prend la forme

† La situation est un peu plus compliquée si on introduit l'antisymétrisation de la fonction d'onde du nucléon incident avec celle des nucléons du noyau cible.

$$\frac{1}{\varepsilon-\mathscr{H}} = \sum_{a} |a\rangle \frac{1}{\varepsilon-E_a} \langle\tilde{a}| + \sum_{a,b} |a\rangle \frac{\langle\tilde{a}|\mathscr{V}|b\rangle}{(\varepsilon-E_a)(\varepsilon-E_b)} \langle\tilde{b}| + \ldots . \quad (80)$$

Il faudrait ici entreprendre une recherche systématique des termes dominants de ce développement et regrouper ceux-ci conformément aux idées de la théorie de Brueckner. Nous allons pour l'instant nous borner à admettre une *hypothèse statistique* très simple concernant les éléments de matrice de $\mathscr{V}$. Celle-ci ne doit pas être considérée comme autre chose qu'une hypothèse de travail dont la validité demande à être établie par une analyse plus détaillée, mais nous allons voir qu'elle conduit très rapidement au modèle optique et à la notion d'interactions directes.

Nous allons dans ce qui suit admettre que les $\langle\tilde{a}|\mathscr{V}|b\rangle$ varient très irrégulièrement quand on passe d'un niveau a ou b à un niveau voisin, et que pour cette raison, les différents éléments de matrice de $\mathscr{V}$ figurant dans le développement (80) peuvent dans une première approximation très grossière être traités comme des *variables aléatoires indépendantes* prenant avec la même probabilité une valeur et la valeur opposée. Les éléments diagonaux $\langle\tilde{a}|\mathscr{V}|a\rangle$ sont nuls car $\mathscr{V}$ est la différence entre l'interaction véritable et l'interaction moyenne.

Cette hypothèse permet [14]) de classer les termes d'un développement tel que (80). Considérons d'abord les éléments *diagonaux* de $(\varepsilon-\mathscr{H})^{-1}$. On peut montrer que les termes dominants d'ordre $2p$ en $\mathscr{V}$ sont ceux qui font intervenir une succession de niveaux intermédiaires telle que

$$a, n_1, a, n_2, a, n_3, \ldots, n_p, a.$$

La somme de ces termes s'écrit

$$\langle\tilde{a}| \frac{1}{\varepsilon-\mathscr{H}} |a\rangle \approx \frac{1}{\varepsilon-E_a} + \frac{W_a}{(\varepsilon-E_a)^2} + \frac{W_a^2}{(\varepsilon-E_a)^3} + \ldots = \frac{1}{\varepsilon-E_a-W_a}, \quad (81)$$

où on a posé

$$W_a = \sum_{n} \frac{\langle\tilde{a}|\mathscr{V}|n\rangle^2}{\varepsilon-E_n} = \langle\tilde{a}|\mathscr{V} \frac{1}{\varepsilon-\mathscr{H}_0} \mathscr{V}|a\rangle, \quad (82)$$

en utilisant la relation

$$\langle\tilde{a}|\mathscr{V}|n\rangle = \langle\tilde{n}|\mathscr{V}|a\rangle$$

qui résulte de l'invariance de $\mathscr{V}$ par renversement du temps. Si on pose

$$W_a = \Delta_a - iV_a, \quad (83)$$

on obtient en première approximation

$$V_a \approx \frac{\pi}{D_\varepsilon} \mathrm{Re}[\langle\tilde{a}|\mathscr{V}|n\rangle^2]_\varepsilon, \quad (84)$$

où D_ε désigne la distance moyenne des niveaux E_n à l'énergie ε et le crochet

la valeur moyenne du carré de l'élément de matrice $\langle\tilde{a}|\mathscr{V}|n\rangle$ prise sur les niveaux d'énergie E_n voisine de ε.

En reportant (81) dans l'expression générale (50) de la matrice de collision on obtient la contribution

$$S^{(0)} = e^{i\xi}\left[1-i\sum_a \frac{G_a\times G_a}{\varepsilon-E_a-W_a}\right]e^{i\xi}. \tag{85}$$

Les conditions (77) et (78) satisfaites par les $G_a^{(\lambda)}$ montrent que la valeur de $S^{(0)}$ donnée par (85) est purement diagonale et ne produit par conséquent que de la *diffusion élastique*. Si dans (85) on fait $W_a = 0$, on obtient simplement la formule de Peierls et Kapur pour la matrice de collision décrivant la diffusion de la particule incidente par le potentiel moyen produit par le noyau cible. La formule (85) montre qu'en présence de l'interaction $\mathscr{V}$ responsable du mélange des configurations du modèle des particules indépendantes, la particule incidente est soumise dans la région intérieure à un *potentiel supplémentaire complexe* W_a. Nous avons donc retrouvé le *modèle optique* de la diffusion élastique.

Dans le cas de la diffusion élastique, on s'intéresse à la seule valeur de λ correspondant à l'état fondamental du noyau cible. La sommation sur a dans (85) porte donc seulement sur les différents états χ de la particule incidente dans le potentiel moyen. A chaque état χ correspond une *résonance géante* dont la largeur est donnée par

$$-\mathrm{Im}\,(E_a+W_a) = \tfrac{1}{2}\Gamma_a+V_a. \tag{86}$$

Considérons maintenant un élément *non diagonal* de $(\varepsilon-\mathscr{H})^{-1}$. Par le même raisonnement on peut montrer que les termes dominants dans le développement (80) dont ceux qui font intervenir une succession de niveaux intermédiaires telle que

$$a, n_1, a, n_2, \ldots, a, n_p, a, b, n_{p+1}, b, \ldots, b, n_{p+q}, b.$$

La somme de ces termes s'écrit avec la notation (82)

$$\langle\tilde{a}|\frac{1}{\varepsilon-\mathscr{H}}|b\rangle \approx \frac{\langle\tilde{a}|\mathscr{V}|b\rangle}{(\varepsilon-E_a)(\varepsilon-E_b)}\sum_{p,q=0}^{\infty}\left(\frac{W_a}{\varepsilon-E_a}\right)^p\left(\frac{W_b}{\varepsilon-E_b}\right)^q$$
$$= \frac{\langle\tilde{a}|\mathscr{V}|b\rangle}{(\varepsilon-E_a-W_a)(\varepsilon-E_b-W_b)}. \tag{87}$$

Ceci donne dans la matrice de collision une nouvelle contribution

$$S^{(1)} = e^{i\xi}\left[-i\sum_{a,b}\frac{\langle\tilde{a}|\mathscr{V}|b\rangle}{(\varepsilon-E_a-W_a)(\varepsilon-E_b-W_b)}G_a\times G_b\right]e^{i\xi} \tag{88}$$

qu'il faut ajouter à $S^{(0)}$.

Nous allons maintenant montrer que $S^{(1)}$ n'est rien d'autre qu'une *interaction directe* proportionnelle à l'élément de matrice de $\mathscr{V}$ calculé entre *deux*

fonctions d'onde du modèle optique décrivant l'état initial et l'état final du système.

Commençons par établir l'expression dans la région intérieure de la fonction d'onde $|\Phi_\alpha\rangle$ du modèle optique pour laquelle les amplitudes entrantes sont nulles partout sauf dans une voie donnée α:

$$\begin{aligned}(\alpha|-) &= 1,\\ (\lambda|-) &= 0, \qquad \text{si } \lambda \neq \alpha.\end{aligned} \tag{89}$$

Les équations (40) et (48) écrites avec la base $|a\rangle$, $|b\rangle$, ... donnent lorsqu'on y introduit l'expression (81) de $(\varepsilon-\mathscr{K})^{-1}$ correspondant au modèle optique:

$$\begin{aligned}|\Phi_\alpha\rangle &= i\hbar^{\frac{1}{2}} \sum_{a,\,b} |a\rangle \langle\tilde{a}| \frac{1}{\varepsilon-\mathscr{K}} |b\rangle G_b^\alpha e^{i\xi^\alpha}\\ &= i\hbar^{\frac{1}{2}} \sum_a |a\rangle \frac{1}{\varepsilon-E_a-W_a} G_a^\alpha e^{i\xi^\alpha}.\end{aligned} \tag{90}$$

Posons par analogie avec (69)

$$\widetilde{|\Phi_\alpha, j, -m\rangle} = (-)^{m-j} K|\Phi_\alpha, j, m\rangle, \tag{91}$$

où nous avons explicité le moment angulaire j, m de $|\Phi_\alpha\rangle$ (c'est-à-dire celui de la voie α).

Les fonctions $\widetilde{|\Phi_\alpha\rangle}$ se déduisant des $|\Phi_\alpha\rangle$ par renversement du temps ont des amplitudes *sortantes* nulles partout sauf dans la voie α et elles correspondent à un potentiel optique changé de signe.

De (90) et (91) on déduit

$$\widetilde{\langle\Phi_\alpha|} = i\hbar^{\frac{1}{2}} \sum_a \langle\tilde{a}| \frac{1}{\varepsilon-E_a-W_a} G_a^{(\alpha)} e_i^{\xi^\alpha}. \tag{92}$$

En effet, le fait de passer de $|\Phi_\alpha\rangle$ à $\widetilde{|\Phi_\alpha\rangle}$ puis de $\widetilde{|\Phi_\alpha\rangle}$ à $\widetilde{\langle\Phi_\alpha|}$ conduit à remplacer deux fois de suite tous les nombres par leurs imaginaires conjugués. Les relations (88), (90) et (92) permettent enfin d'écrire $S^{(1)}$ sous la forme

$$(\lambda|S^{(1)}|\mu) = \frac{i}{\hbar} \widetilde{\langle\Phi_\lambda|} \mathscr{V} |\Phi_\mu\rangle \tag{93}$$

que nous voulions établir.

La forme (88) de la matrice de collision pour l'interaction directe montre qu'on pourra observer des *résonances géantes* aux énergies telles que

$$\varepsilon = \varepsilon_a + \Delta_a \quad \text{ou} \quad \varepsilon = \varepsilon_b + \Delta_b, \tag{94}$$

avec les notations (65) et (83). Dans le premier cas, on a une *résonance de la particule incidente* dans le potentiel complexe créé par le noyau cible. Dans le deuxième cas, au contraire, on a une *résonance de la particule émise* dans le potentiel complexe créé par le noyau résiduel. Dans la mesure où on peut admettre que le potentiel créé par le noyau résiduel dépend peu de l'état d'exci-

tation de celui-ci, les résonances de la particule émise se produiront pour des énergies déterminées de la *particule émise*, et on observera des groupes intenses de particules diffusées inélastiquement dont l'énergie sera pratiquement indépendante de l'énergie de la particule incidente et variera lentement avec le nombre atomique [15, 16]).

L'auteur tient à remercier M. C. De Dominicis pour de nombreuses et très utiles discussions et suggestions.

APPENDICE

Résolution du Cas à une Dimension

En introduisant les notations

$$\psi(r) = \frac{u(r)}{r}, \qquad f(r) = \frac{\varphi(r)}{r}, \qquad A = \frac{a}{R}, \tag{A,1}$$

le système (17) devient

$$\begin{aligned} &\frac{\hbar^2}{2M}\frac{\mathrm{d}^2 u}{\mathrm{d}r^2} + (\varepsilon - V)u = \varphi \qquad (r < R), \\ &-\frac{\hbar^2}{2M}\left(\frac{\mathrm{d}u}{\mathrm{d}r} - iku\right)_R = a, \\ &u(0) = 0. \end{aligned} \tag{A,2}$$

Désignons par $u_1(r)$ et $u_2(r)$ les solutions de l'équation différentielle sans second membre telles que

$$\begin{aligned} &u_1(0) = 0, \qquad \left(\frac{\mathrm{d}u_1}{\mathrm{d}r}\right)_0 = 1, \\ &u_2(R) = 1, \qquad \left(\frac{\mathrm{d}u_2}{\mathrm{d}r}\right)_R = ik. \end{aligned} \tag{A,3}$$

On sait que si $V(r)$ satisfait à certaines conditions de régularité très larges ces solutions existent. Soit W le Wronskien (indépendant de r)

$$W = u_1\frac{\mathrm{d}u_2}{\mathrm{d}r} - u_2\frac{\mathrm{d}u_1}{\mathrm{d}r}. \tag{A,4}$$

Pour $r = R$, en particulier on a

$$W = \left[\left(ik - \frac{\mathrm{d}}{\mathrm{d}r}\right)u_1\right]_R. \tag{A,5}$$

Pour ε réel, W est toujours différent de zéro; autrement dit u_1 et u_2 sont linéairement indépendantes. En effet pour ε réel, la fonction $u_1(r)$ est visiblement réelle quel que soit r. Sa dérivée logarithmique ne pourra pas être égale à

ik pour $r = R$. Ceci montre que le système homogène, c'est-à-dire l'équation (11) n'a pas de solution non identiquement nulle.

Ecrivons maintenant la solution du système avec second membre sous la forme

$$u(r) = c_1(r)u_1(r)+c_2(r)u_2(r). \tag{A,6}$$

D'après la méthode classique de variation des constantes, c_1 et c_2 satisfont aux équations

$$\begin{aligned} c'_1u_1+c'_2u_2 &= 0, \\ \frac{\hbar^2}{2M}(c'_1u'_1+c'_2u'_2) &= \varphi, \end{aligned} \tag{A,7}$$

et aux conditions aux limites

$$\begin{aligned} c_2(0) &= 0, \\ -c_1(R)\frac{\hbar^2}{2M}\left(\frac{\mathrm{d}u_1}{\mathrm{d}r}-iku_1\right)_R &= a. \end{aligned} \tag{A,8}$$

On en tire facilement en utilisant (A,4) et (A,5)

$$\begin{aligned} c_1(r) &= \frac{2M}{\hbar^2W}\left[au_2(R)+\int_r^R u_2(r')\varphi(r')\mathrm{d}r'\right] \\ &= \frac{2M}{\hbar^2W}\int_r^R u_2(r')[\varphi(r')+a\delta(r'-R)]\,\mathrm{d}r', \\ c_2(r) &= \frac{2M}{\hbar^2W}\int_0^r u_1(r')\varphi(r')\mathrm{d}r'. \end{aligned} \tag{A,9}$$

D'où finalement

$$\psi(r) = \int_0^R r'^2\mathrm{d}r'\,G(r,r')F(r'), \tag{A,10}$$

où

$$G(r,r') = \frac{2M}{\hbar W}\frac{u_1(r_<)u_2(r_>)}{rr'}. \tag{A,11}$$

Dans cette expression $r_<$ et $r_>$ sont respectivement la plus petite et la plus grande des quantités r et r'. On remarquera que la formule (A,10) est valable dans l'intervalle $(0, R)$ jusqu'à la limite R comprise. Par contre, les dérivées premières de $G(r, r')$ étant discontinues pour $r = r'$ *on ne peut pas dériver* (A.10) *membre à membre par rapport à r sans précautions spéciales*. Dans tous les calculs faits ici nous n'avons d'ailleurs jamais eu à dériver les formules du type (A,10).

Bibliographie

1) E. P. Wigner, Phys. Rev. **70** (1946) 606; **73** (1948) 1002
2) E. P. Wigner et L. Eisenbud, Phys. Rev. **72** (1947) 29
3) T. Teichman et Wigner, Phys. Rev. **87** (1952) 123

4) R. G. Thomas, Phys. Rev. **97** (1955) 224
5) P. L. Kapur et R. E. Peierls, Proc. Roy. Soc. A **166** (1938) 277
6) A. M. Lane, R. G. Thomas et E. P. Wigner, Phys. Rev. **98** (1955) 693
7) A. M. Lane, communication à la Conférence de Seattle (Sept. 1956)
8) B. A. Lippman et J. Schwinger, Phys. Rev. **79** (1950) 469
9) J. M. Blatt et V. F. Weisskopf, Theoretical Nuclear Physics (Wiley, 1952)
10) E. P. Wigner, Zeitschr. f. Phys. **32** (1932) 546
11) H. Feshbach, C. Porter, V. Weisskopf, Phys. Rev. **96** (1954) 448
12) F. L. Friedman et V. F. Weisskopf, dans Niels Bohr and the Development of Physics (Londres, Pergamon Press, 1955)
13) E. P. Wigner, Ann. Math. **53** (1951) 36; **55** (1952) 7
14) C. Bloch, Nuclear Physics **3** (1957) 137
15) B. L. Cohen, Phys. Rev. (sous presse)
16) P. C. Gugelot, Physica **22** (1956) 1019

Nuclear Physics **4** (1957) 529—531; © *North-Holland Publishing Co., Amsterdam*

Not to be reproduced by photoprint or microfilm without written permission from the publisher

ELECTRIC DIPOLE MOMENT ASSOCIATED WITH OCTUPOLE VIBRATIONS OF A SPHEROIDAL NUCLEUS

AAGE BOHR and BEN R. MOTTELSON

Institute for Theoretical Physics, University of Copenhagen

and

CERN, *Theoretical Study Division, Copenhagen, Denmark*

Received 26 June 1957

Abstract: The electric dipole transition probability associated with collective odd parity transitions is estimated on the basis of the polarization induced by the electric field of the nuclear deformation. The available experimental data are discussed in an attempt to obtain information on the nuclear octupole distortion.

In certain regions of elements, the even nuclei have been found to possess rather low-lying states of odd parity †. The systematic occurrence as well as the low frequency of these levels suggest that they may represent collective oscillations of octupole type [3]).

Some of the properties of such oscillations have been previously discussed, both for the nuclei with spherical equilibrium and for those with non-spherical but axially symmetric shape [4]). In the latter case, the lowest odd parity state is found to be of 1− type and decays by emission of E1 radiation to the ground state and the 2+ first rotational state. The transition probability for this decay (or for Coulomb excitation of the 1− level) depends on the nuclear polarization associated with the vibration, since, for a uniformly charged nucleus, the centre of mass and centre of charge coincide.

The electric field of the nuclear charge distribution provides a force which tends to induce such a polarization ††. The effect is relatively small due to the weakness of the electric forces as compared with the nuclear forces which favour a uniform charge distribution, and the corresponding reduced transition probability, $B(\mathrm{E1})$, is several orders of magnitude smaller than the single-particle unit [4, 6]). Nevertheless, this systematic effect may provide the main contribution to the E1 transition probability, in which case it

† These states have been observed in the α-decay spectrum of the very heavy elements (see especially ref. [1])). More recently, odd parity excitations have also been found in the even nuclei in the rare earth region [2]).

†† Similar polarization effects have been considered in connection with the charge distribution in nuclear fission [5]).

becomes possible, from the observed transition rate, to obtain information on the amplitude of the octupole oscillation.

In order to estimate the polarization effect, we consider a nucleus with a surface deformation

$$R = R_0(1+\beta_2 Y_{20}(\vartheta)+\beta_3 Y_{30}(\vartheta)) \tag{1}$$

containing an octupole deformation (β_3) as well as a quadrupole deformation (β_2). The Coulomb potential, inside the nucleus ($r < R_0$), is given by

$$V(r) = \left(\frac{3}{2} - \frac{1}{2}\left(\frac{r}{R_0}\right)^2 + \frac{3}{5}\left(\frac{r}{R_0}\right)^2 \beta_2 Y_{20}(\vartheta) + \frac{3}{7}\left(\frac{r}{R_0}\right)^3 \beta_3 Y_{30}(\vartheta)\right)\frac{Ze}{R_0} \tag{2}$$

to first order in the deformation parameters †. The resulting polarization is given by

$$\frac{\delta\varrho_p - \delta\varrho_n}{\varrho_0} = -\frac{1}{4C_1} e(V(r)-\bar{V}), \tag{3}$$

where ϱ_0 is the mean total nucleon density assumed to remain constant, while $\delta\varrho_p$ and $\delta\varrho_n$ are the changes produced in the proton and neutron densities, respectively. The mean electrostatic potential is denoted by $\bar{V}$ while the coefficient C_1 is the symmetry energy appearing in the semi-empirical mass formula as

$$E_{sym} = C_1 \frac{(N-Z)^2}{A}. \tag{4}$$

The induced dipole moment is now found to be

$$D = -\frac{81}{8\pi}(35)^{-3/2}\left(\frac{e^2}{R_0}\frac{A}{C_1}\right) Z\beta_2\beta_3 eR_0, \tag{5}$$

leading to an E1 transition probability

$$B(\mathrm{E1};\ I_1 \to I_f) = \frac{3}{4\pi}\langle D^2\rangle_{av} \cdot \langle I_i\, 100 \mid I_1\, 1\, I_f\ 0\rangle^2, \tag{6}$$

where the last factor is the square of a vector addition coefficient. The dipole moment (5) is a static estimate which is justified, since the odd parity excitation energies considered here ($\hbar\omega \lesssim 1$ MeV) are small compared to the main nuclear dipole frequencies ($\hbar\omega_{dip} \approx 15$ MeV).

The transition probability is seen to depend on $\beta_2^2\langle\beta_3^2\rangle_{av}$. It is possible to interpret the observed odd parity states in two somewhat different ways implying different interpretations of the quantity $\langle\beta_3^2\rangle_{av}$. We may have to do either with rotations of a nuclear equilibrium shape possessing a static octupole deformation β_3, or with octupole vibrations about an

† Actually, the surface deformation (1) implies a dipole term in (2) of order $\beta_2\beta_3$, which would be significant for the further calculation. However, this term is a result of the centre of mass shift associated with (1) and vanishes when one adds to (1) the dipole deformation necessary to keep the centre of mass fixed.

equilibrium shape which itself contains no odd parity distortion. The latter situation, which may seem somewhat more probable, would imply the existence of higher excited bands with two or more vibrational quanta. Thus, one would expect a $K = 0+$ band ($I = 0, 2, 4, \ldots +$) with approximately twice the excitation energy of the $K = 0-$ bands. A search for such states would be important in further defining the character of the observed odd parity states.

Some evidence is available on the E1 decay rate of the $I = 3-$ member of the odd parity band in Th^{228} [7]†. If one assumes that the observed 68 keV transition may be identified as the rotational transition from the 3− to the 1− level, and if one further assumes an intrinsic quadrupole moment $Q_0 = 9 \times 10^{-24}$ cm^2 [8], one obtains from the observed branching ratios in the decay of the 3− state, the value $B(\mathrm{E1};\ 3- \rightarrow 2+) = 2.4 \times 10^{-29}\ e^2$ cm^2. From (5) and (6), and taking C_1 to be 18 MeV [9], one may thus estimate $\beta_3 \gtrapprox 0{,}03$ for this transition. This value is somewhat larger than the effective octupole deformation parameter estimated from the fine structure intensities in the α-decay [10]).

For the 960 keV 1− state in Sm^{152}, the reported lifetime [11]) implies $B(\mathrm{E1};\ 1- \rightarrow 0+) = 2 \times 10^{-28}\ e^2$ cm^2. Assuming $\beta_2 \approx 0.25$, one obtains $\beta_3 \approx 0.18$. This value seems considerably larger than would have been expected.

† We are indebted to the authors of this investigation for a discussion of their results.

References

1) Stephens, Asaro, and Perlman, Phys. Rev. **96** (1954) 1568; I. Perlman and J. Rasmussen, to appear in Encyclopedia of Physics
2) H. Kendall and L. Grodzins, Bull. Am. Phys. Soc. **1** (1956) 164; O. Nathan and M. Waggoner, Nuclear Physics **2** (1956) 548
3) R. F. Christy, private communication
4) Alder, Bohr, Huus, Mottelson and Winther, Revs. Modern Physics **28** (1956) 432
5) R. D. Present, Phys. Rev. **72** (1947) 7
6) V. Strutinsky, Physica **22** (1956) 1166
7) S. Bjørnholm, O. Nathan, O. B. Nielsen and R. K. Sheline, Nuclear Physics, **4** (1957) 313
8) Cf., e.g., tables V. 2 and V. 3 of ref. [4])
9) Cf., e.g., J. Blatt and V. F. Weisskopf, Theoretical Nuclear Physics (Wiley and Sons, 1953) p. 229
10) P. O. Fröman, Mat. Fys. Skr. Dan. Vid. Selsk. **1** (1957) no. 3
11) L. Grodzins, Bull. Am. Phys. Soc. **1** (1956) 329; Nuclear Data Cards 57-1-90

Nuclear Physics **4** (1957) 532—563; © *North-Holland Publishing Co., Amsterdam*
Not to be reproduced by photoprint or microfilm without written permission from the publisher

LEE MODEL AND QUANTISATION OF NON LINEAR FIELD EQUATIONS

W. HEISENBERG

Max-Planck-Institut für Physik, Göttingen †

Received 14 July 1957

Abstract: In a model for the theory of elementary particles an unconventional method of quantisation had been applied which makes use of an indefinite metric in Hilbert space. This method is analysed with the help of the Lee model. The constants of the Lee model can be adjusted in such a manner that, after the renormalisation has been carried out, the mathematical structure is in many ways analogous to that of the method of quantisation mentioned above (§ 2). The total Hilbert space can be divided into two parts, the one of which has a positive metric and comprises the physical states of the system, while the other one contains 'dipole-ghosts' and is needed for the commutation relations and the convergence of the theory. The *S*-matrix is unitary for the states of Hilbert space I, since the states of Hilbert space II are separated from those of Hilbert space I in a manner similar to the case of "non-combining term systems" (§§3 and 5). Some general results concerning the Hilbert space of indefinite metric are discussed in § 4. The questions of causality are briefly raised in § 6. The results seem to show that a Hilbert space with indefinite metric can be used for the description of real phenomena.

1. Introduction

Källén and Pauli [1]) have pointed out, in their analysis of the Lee-model [2]), that the renormalisation of the point-source model can only be effected formally by introducing an indefinite metric in Hilbert space ††. In this case a discrete 'ghost-state' appears, the norm of which is negative, and thereby the unitarity of the *S*-matrix in scattering problems is destroyed. An interpretation in terms of quantal probabilities cannot be given.

On the other hand, in some papers on a model for the theory of the elementary particles [4]) a new method of quantisation for a non-linear wave equation has been introduced which also makes use of an indefinite metric in Hilbert space. The total Hilbert space is composed of two parts, the one of which, Hilbert space I, comprises all normal states of the system and has a positive metric. The other part, Hilbert space II, contains states of a different character which, at least partly, can be described as 'dipole-ghosts', i.e. states composed of one normal state and one ghost-state of the

† Essential parts of this paper are the result of an extensive correspondence with W. Pauli to whom the author is indebted for many valuable suggestions. R. Haag has contributed to the sections 2 and 4.

†† An indefinite metric in Hilbert space has first been introduced by Dirac [3]).

same mass. The states of Hilbert space II change the commutator in such a manner that the δ- and δ'-functions on the light-cone disappear, and that actually the wave functions ψ and ψ^+ anti-commute everywhere on the subspace $t = \text{const}$. This behaviour is essential for the convergence of the theory. Arguments have been put forward to show that the S-matrix remains unitary in this method of quantisation, in contrast to the case treated by Källén and Pauli; but a complete analysis of the structure of the theory has not yet been given.

The constants of the Lee-model can be adjusted in such a manner that the energy of the 'ghost-state' becomes equal to the energy of the normal V-particle (subsection 2.3 of the present paper). In this case the process of renormalisation leads to a situation very similar to that in the new method of quantisation mentioned above: The renormalised wave-functions ψ_V and ψ_V^* anti-commute everywhere on the subspace $t = \text{const}$, and the extra states of Hilbert space II are 'dipole-ghosts'. Therefore the analysis of this system seems to provide a clear insight into the structure and the consequences of a method of quantisation along the lines indicated above. The present paper is intended to give this analysis and thereby to decide the question whether an indefinite metric in Hilbert space can be used for the description of real phenomena. In sections 2 and 3 the Lee-model will be discussed in the special case of the 'dipole-ghost'. The more fundamental problems concerning the structure of Hilbert space with indefinite metric will be treated in section 4. The results will be applied to the Lee-model and discussed in sections 5 and 6.

2. The Lee-model; sector N+θ.

2.1. GENERAL DESCRIPTION OF THE LEE-MODEL

The Lee-model introduces three types of particles: V, N and θ. The interaction allows only the transitions

$$V \to N+\theta, \quad N+\theta \to V.$$

If n_V, n_N and n_θ denote the numbers of these particles, the two quantities

$$n_1 = n_V+n_N, \quad n_2 = n_V+n_\theta \tag{1}$$

are constants of motion. Therefore the total ensemble of states of the system can be divided into 'sectors' belonging to fixed values of n_1 and n_2.

The Hamiltonian in momentum space can be written as

$$H = m_V \int \psi_V^*(\mathbf{p})\psi_V(\mathbf{p})\mathrm{d}^3p + m_N \int \psi_N^*(\mathbf{q})\psi_N(\mathbf{q})\mathrm{d}^3q + \int \omega(\mathbf{k})a^*(\mathbf{k})a(\mathbf{k})\mathrm{d}^3k$$
$$-\frac{g_0}{\sqrt{4\pi}}\int \frac{f(\omega)}{\sqrt{2\omega}}\delta(\mathbf{p}-\mathbf{q}-\mathbf{k})[\psi_V^*(\mathbf{p})\psi_N(\mathbf{q})a(\mathbf{k}) + a^*(\mathbf{k})\psi_N^*(\mathbf{q})\psi_V(\mathbf{p})]\mathrm{d}^3p\mathrm{d}^3q\mathrm{d}^3k; \tag{2}$$

$\mathbf{p}$, $\mathbf{q}$ and $\mathbf{k}$ are momentum vectors, $\omega = \sqrt{m_\theta^2+k^2}$; $f(\omega)$ is the cut-off function.

The point-source model is characterised by $f(\omega) = 1$. In this latter case the Hamiltonian can be represented simply in ordinary space. By putting

$$a(\mathbf{x}) = (2\pi)^{-3/2}\int \frac{a(\mathbf{k})}{\sqrt{2\omega}} e^{i\mathbf{k}\cdot\mathbf{x}} d^3k,\ \varphi(\mathbf{x}) = a(\mathbf{x})+a^*(\mathbf{x}),$$

$$\Pi(\mathbf{x}) = \frac{(2\pi)^{-3/2}}{2i}\int \sqrt{2\omega}[a(\mathbf{k})e^{i\mathbf{k}\cdot\mathbf{x}}-a^*(\mathbf{k})e^{-i\mathbf{k}\cdot\mathbf{x}}]d^3k, \tag{3}$$

$$a(\mathbf{x}) = \tfrac{1}{2}[\varphi(\mathbf{x})+i\int \frac{e^{-m_\theta|\mathbf{x}-\mathbf{x}'|}}{|\mathbf{x}-\mathbf{x}'|}\Pi(\mathbf{x}')d^3x'],$$

and neglecting an infinite additive constant in H one obtains

$$\begin{aligned} H = {} & m_V\int \psi_V^*(\mathbf{x})\psi_V(\mathbf{x})d^3x+m_N\int \psi_N^*(\mathbf{x})\psi_N(\mathbf{x})d^3x \\ & +\tfrac{1}{2}\int [\Pi^2(\mathbf{x})+(\operatorname{grad}\varphi)^2+m_\theta^2\varphi^2]d^3x-g_0\pi\sqrt{2}\int [\psi_V^*(\mathbf{x})\psi_N(\mathbf{x})a(\mathbf{x}) \\ & +a^*(\mathbf{x})\psi_N^*(\mathbf{x})\psi_V(\mathbf{x})]d^3x. \end{aligned} \tag{4}$$

It has been assumed in (2) and (4), for simplification, that the energy of the V- and the N-particle does not depend on their momentum. In this respect the Lee-model is very different from the model for a theory of the elementary particles discussed in the introduction and is also rather far from the physical reality.

The commutation relations of the non-renormalized wave-functions are the conventional ones:

$$\begin{aligned} & \{\psi_V^*(\mathbf{p}),\ \psi_V(\mathbf{p}')\} = \{\psi_N^*(\mathbf{p}),\ \psi_N(\mathbf{p}')\} = \delta(\mathbf{p},\ \mathbf{p}'), \\ & \{\psi_V(\mathbf{p}),\ \psi_V(\mathbf{p}')\} = \{\psi_V(\mathbf{p}),\ \psi_N(\mathbf{p}')\} = \ldots = 0, \\ & [a(\mathbf{k}),\ a^*(\mathbf{k}')] = \delta(\mathbf{k},\ \mathbf{k}'), \\ & [a(\mathbf{k}),\ \psi_V(\mathbf{p})] = 0, \\ & \{\psi_V^*(\mathbf{x}),\ \psi_V(\mathbf{x}')\} = \{\psi_N^*(\mathbf{x}),\ \psi_N(\mathbf{x}')\} = \delta(\mathbf{x},\ \mathbf{x}'), \\ & [\Pi(\mathbf{x}),\ \varphi(\mathbf{x}')] = -i\delta(\mathbf{x},\ \mathbf{x}'). \end{aligned} \tag{5}$$

In eqs. (2) and (4) the mass m_N can be put equal to zero without loss of generality, since this constant simply fixes the zero-point of the energy scale in each sector. Therefore we will assume

$$m_N = 0. \tag{6}$$

2.2. SOLUTION OF THE SCHRÖDINGER EQUATION IN THE SECTOR $\binom{N+\theta}{V}$

The simplest non-trivial case in the Lee-model is given by the values $n_1 = n_2 = 1$, which characterise the sector $\binom{N+\theta}{V}$. In this sector a general

state may be defined by

$$\Phi\rangle = (c\psi_V^* + \psi_N^* \int \varphi(\mathbf{k}) a^*(\mathbf{k}) \mathrm{d}^3 k)|\, 0\rangle. \tag{7}$$

Since the kinetic energy of the N- or V-particle is neglected, the position of this particle can be considered as fixed at the origin. The operators ψ_V^* and ψ_N^*, in which the argument is omitted, then refer to the creation of a V- or N-particle at the origin, and we have from (5) $\{\psi_V^*, \psi_V\} = \{\psi_N^*, \psi_N\} = 1$. Eq. (7) may be abbreviated by writing

$$\Phi = \begin{pmatrix} c \\ \varphi(\mathbf{k}) \end{pmatrix}. \tag{8}$$

Applying the Hamiltonian to Φ leads to

$$H\Phi = \Phi' = \begin{pmatrix} c' \\ \varphi'(\mathbf{k}) \end{pmatrix}, \tag{9}$$

where

$$\begin{aligned} c' &= m_V c - \frac{g_0}{\sqrt{4\pi}} \int \frac{f(\omega)}{\sqrt{2\omega}} \varphi(\mathbf{k}) \mathrm{d}^3 k, \\ \varphi'(\mathbf{k}) &= \omega\varphi(\mathbf{k}) - \frac{g_0}{\sqrt{4\pi}} \frac{f(\omega)}{\sqrt{2\omega}} c. \end{aligned} \tag{10}$$

As one sees from (10), the interaction takes place only in the S-states. Confining the calculations to these states one may put $\varphi(\mathbf{k}) = \psi(k)/k\sqrt{4\pi}$. Since we are interested later only in the limit of the point-source, we may omit the cut-off function $f(\omega)$, carry the integrations in $\mathbf{k}$- or ω-space only to an upper limit $\hat{\omega}$ and finally go to $\hat{\omega} \to \infty$. The Schrödinger equation

$$H\Phi = E\Phi \tag{11}$$

gives for the S-states

$$(\omega - E)\psi(k) = \frac{g_0 k}{\sqrt{2\omega}} \cdot c, \tag{12a}$$

$$(m_V - E)c = g_0 \int \frac{k}{\sqrt{2\omega}} \psi(k) \mathrm{d}k. \tag{12b}$$

In the continuous spectrum $E = \sqrt{m_0^2 + k_0^2} \geqq m_0$ we can put, according to (12a),

$$\psi(k) = \delta(k - k_0) - \frac{g_0 k c}{(E - \omega + i\gamma)\sqrt{2\omega}} \qquad (\gamma \to 0), \tag{13}$$

where the additive term $i\gamma$ $(\gamma \to 0)$ in the denominator leads to outgoing waves in the usual manner. Then from (12b)

$$c\left[m_V - E + g_0^2 \int \frac{k^2 \mathrm{d}k}{2\omega(E - \omega + i\gamma)}\right] = \frac{g_0 k_0}{\sqrt{2\omega_0}}. \tag{14}$$

It is convenient to introduce the function $h(z)$ of the complex variable z:

$$h(z) = \frac{z - m_V}{g_0^2} + \int \frac{k^2 \, dk}{2\omega(\omega - z)}. \tag{15}$$

This is a regular analytical function in the z-plane cut along the real axis from $z = m_\theta$ to $+\infty$. Its values on the $(\pm i)$-side of the cut will be called $h^\pm$:

$$h^\pm(E) = \bar{h}(E) \pm \pi i \frac{k_0}{2}; \tag{16}$$

$\bar{h}(E)$ is real. From (14) one gets

$$h^+(E) g_0 c = -\frac{k_0}{\sqrt{2E}} \tag{17}$$

and

$$\psi(k) = \delta(k - k_0) + \frac{k k_0}{2\sqrt{\omega E}\,(E - \omega + i\gamma)\, h^+(E)}. \tag{18}$$

The phase of the scattered wave becomes

$$e^{2i\delta(E)} \equiv S(E) = 1 - \frac{\pi i k_0}{h^+(E)} = 1 - \frac{h^+ - h^-}{h^+} = \frac{h^-}{h^+}, \tag{19}$$

and from (16)

$$\operatorname{tg} \delta(E) = -\pi \frac{k_0}{2\bar{h}(E)}. \tag{20}$$

In the discrete spectrum ($E < m_\theta$) eq. (12a) leads to

$$\psi(k) = \frac{g_0 k}{\sqrt{2\omega}(\omega - E)} \cdot c \tag{21}$$

and

$$h(E) = 0. \tag{22}$$

The discrete eigenstates are defined by the zeros of $h(E)$, the corresponding eigenfunctions are given by (21).

2.3. DISCUSSION OF THE FUNCTION $h(E)$

The integral on the right hand side of (15) diverges linearly in the limit $\omega \to \infty$. Therefore it is convenient to use the relation

$$\frac{1}{\omega - z} = \frac{1}{\omega} + \frac{z}{\omega^2} + \frac{z^2}{\omega^2(\omega - z)} \tag{23}$$

and to put

$$h(z) = a + bz + z^2 G(z), \tag{24}$$

where

$$a = -\frac{m_V}{g_0^2} + \int \frac{k^2 \, dk}{2\omega^2}, \quad b = \frac{1}{g_0^2} + \int \frac{k^2 \, dk}{2\omega^3}, \tag{25}$$

$$G(z) = \int \frac{k^2 \mathrm{d}k}{2\omega^3(\omega - z)}. \tag{26}$$

In $G(z)$ one can at once go to the limit $\hat{\omega} \to \infty$ and one gets, if $\xi = z/m_0$,

$$2m_0\overline{G(z)} = \frac{\pi}{2\xi^2} + \frac{1}{\xi} + \begin{cases} \dfrac{\sqrt{\xi^2-1}}{\xi^2} \ln\left(-\xi + \sqrt{\xi^2-1}\right) & \text{for } \xi \leqq -1, \\ -\dfrac{\sqrt{1-\xi^2}}{\xi^2}\left[\dfrac{\pi}{2} + \arcsin \xi\right] & \text{for } -1 \leqq \xi \leqq 1, \\ -\dfrac{\sqrt{\xi^2-1}}{\xi^2} \ln\left(\xi + \sqrt{\xi^2-1}\right) & \text{for } 1 \leqq \xi. \end{cases} \tag{27}$$

For $\xi > 1$ the principal value of the integral is taken. The integrals in (25) diverge in the limit $\hat{\omega} \to \infty$. Therefore finite values of a and b can only be obtained for negative values of g_0^2, i.e. imaginary values of g_0. From (25) one gets in the limit $\hat{\omega} \to \infty$

$$g_0^2 \sim -\frac{2}{\ln \hat{\omega}}, \quad m_V \sim -\frac{\hat{\omega}}{\ln \hat{\omega}}. \tag{28}$$

Källén and Pauli have shown that imaginary values of g_0 are compatible with the assumption of a self-adjoint or, as we will later say, pseudo-hermitian Hamiltonian only if an indefinite metric is introduced in Hilbert space. The norm of all states with an odd number of V-particles must be counted with the negative sign. In order to make this change and at the same time to preserve the calculations of the subsections 2.2 and 2.3 of the present paper, one has to replace some of the fundamental equations of 2.1 and 2.2 by the following revised version:

$$\{\psi_V^*(\mathbf{p})\psi_V(\mathbf{p}')\} = -\delta(\mathbf{p}\mathbf{p}'), \quad \{\psi_V^*(\mathbf{x})\psi_V(\mathbf{x}')\} = -\delta(\mathbf{x}\mathbf{x}'), \quad \{\psi_V^*\psi_V\} = -1; \tag{5R}$$

$$H = -m_V \int \psi_V^*(\mathbf{p})\psi_V(\mathbf{p})\mathrm{d}^3p + m_N \int \psi_N^*(\mathbf{q})\psi_N(\mathbf{q})\mathrm{d}^3q + \int \omega(\mathbf{k})a^*(\mathbf{k})a(\mathbf{k})\mathrm{d}^3k \tag{2R}$$

$$-\frac{g_0}{\sqrt{4\pi}} \int \frac{f(\omega)}{\sqrt{2\omega}} \delta(\mathbf{p}-\mathbf{q}-\mathbf{k})[-\psi_V^*(\mathbf{p})\psi_N(\mathbf{q})a(\mathbf{k}) + a^*(\mathbf{k})\psi_N^*(\mathbf{q})\psi_V(\mathbf{p})]\mathrm{d}^3p\mathrm{d}^3q\mathrm{d}^3k$$

and correspondingly for (4R) in ordinary space. The pseudo-hermitian character of H is seen at once from (2R). Finally,

$$\Phi\rangle = (-c\psi_V^* + \psi_N^* \int \varphi(\mathbf{k})a^*(\mathbf{k})\mathrm{d}^3k)|\,0\rangle. \tag{7R}$$

After replacing eqs. (2), (5) and (7) by (2 R), (5 R) and (7 R) the equations of 2.2 and 2.3 keep their original form, in spite of g_0 being imaginary. The properties of a Hilbert space with an indefinite metric will be discussed in § 4 of this paper.

For the moment we can be satisfied with discussing the properties of $h(z)$ in the limit $\hat{\omega} \to \infty$. Since $d^2h/dz^2 > 0$ for $z < m_\theta$ and $(dh/dz)(-\infty) = -\infty$, $(dh)/dz)(m_\theta) = +\infty$, the function $h(z)$ has just one minimum between $z = -\infty$ and $z = m_\theta$. Therefore it can have two zeros or no zero on the real axis, and in the limiting case the two zeros combine to one zero, where the curve $h(z)$ touches the real axis: $h(z_0) = h'(z_0) = 0$. If there are no zeros on the real axis, there will be two complex roots of the equation $h(E) = 0$. The existence of complex roots is compatible with the pseudo-hermitian character of the Hamiltonian in an indefinite metric in Hilbert space, as will be pointed out in § 4.

The case of two zeros on the real axis has been discussed by Källén and Pauli [1]) and need not be treated here. The case of two complex roots has some relation to a case treated by Glaser and Källén [5]) and to an earlier paper of Heisenberg [8]), but can probably not be used as a model for real phenomena in nature.

We are here mainly interested in the case of the two coinciding roots on the real axis, which corresponds to the 'dipole-ghost' state discussed in earlier papers [4]). If the location of this double root is given by $\xi_0 = z_0/m_\theta = E_0/m_\theta$, one finds, for $\xi_0 \leqq 1$, $\xi \leqq 1$,

$$h(z) = \frac{m_\theta}{2}\left\{\frac{1-\xi\xi_0}{\sqrt{\xi_0^2-1}} \ln\left(-\xi_0+\sqrt{\xi_0^2-1}\right)\right.$$
$$\left. +\xi-\xi_0+\sqrt{\xi^2-1}\ln\left(-\xi+\sqrt{\xi^2-1}\right)\right\}. \quad (29)$$

Fig. 1 shows the curve $h(z)$ for the special case $\xi_0 = -1$.

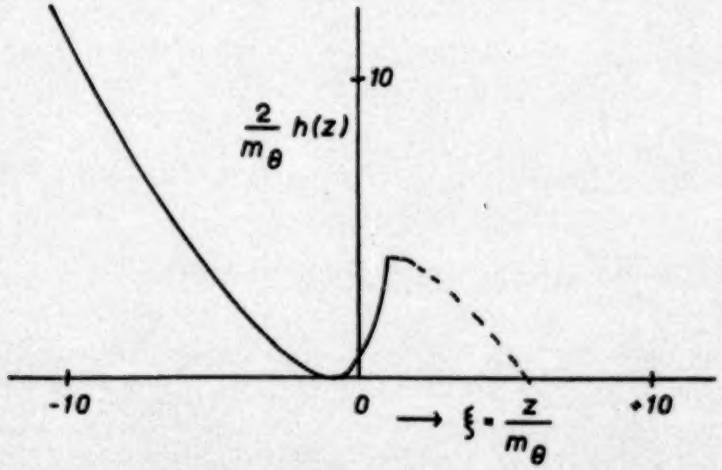

Fig. 1. The function $h(z)$ for $\xi_0 = -1$.

2.4. THE EIGENSTATES IN THE DIPOLE CASE

The situation described by eq. (29) can be considered as a limiting case, which can be obtained from the two real zeros, discussed by Källén and

Pauli, through variation of the constant a in eq. (24). Before one reaches the limit, the root of (22) with the smaller value of ξ belongs to a state with negative norm ('ghost-state'), the other root with the higher value to a normal state. The question arises whether one gets one or two solutions of the Schrödinger equation in the limiting case and what the norm of these states will be. Before one reaches the limit, let the two solutions of the Schrödinger equation be Φ and $\Phi+\Delta\Phi$, the eigenvalues E and $E+\Delta E$. Then one gets

$$H(\Phi+\Delta\Phi) = (E+\Delta E)(\Phi+\Delta\Phi),$$
$$H\Phi = E\Phi, \tag{30}$$

and by subtracting and neglecting terms of higher order

$$H\Delta\Phi = E\Delta\Phi+\Delta E\Phi \tag{31}$$

or

$$H\frac{\Delta\Phi}{\Delta E} = E\frac{\Delta\Phi}{\Delta E}+\Phi. \tag{32}$$

From (30) and (32) one learns that in the case of the double root one has only *one* solution of the Schrödinger equation. But by combining this one solution with the eigenstates of the continuous spectrum one would *not* get the complete Hilbert space of the system. One would for completeness have to add the state characterised by

$$\Phi_{\text{Dip}} = \lim_{\Delta E\to 0}\frac{\Delta\Phi}{\Delta E}, \tag{33}$$

which does not obey the Schrödinger equation but instead eq. (32).

The norm of the discrete solution of (11) is according to (21)

$$\langle\Phi|\Phi\rangle = \left[|g_0^2|\int\frac{k^2\,\mathrm{d}k}{2\omega\,(\omega-E)^2}-1\right]|c^2|, \tag{34}$$

where the -1 in the bracket is due to the component with one V-particle, the norm of which has to be counted with the negative sign according to Källén and Pauli. From (15) and (34) one gets

$$\langle\Phi|\Phi\rangle = |c^2 g_0^2|\frac{\mathrm{d}h(E)}{\mathrm{d}E} = |c^2 g_0^2|h'(E). \tag{35}$$

Since $h'(E) = 0$ at the point of the double root, the state Φ which obeys the Schrödinger equation at this point has the norm 0. (cg_0 is taken as finite even in the limit $\omega\to\infty$.) Therefore we will call this state the zero-state and denote it by Φ_0. Such a state cannot be normalised:

$$\langle\Phi_0|\Phi_0\rangle = 0. \tag{36}$$

Both Φ_0 and Φ_{Dip} are orthogonal to all states of the continuous spectrum, but they are not orthogonal to each other. Besides, Φ_{Dip} is not uniquely

defined by (32) or (33), since a multiplication of Φ by any function of E before going to the limit (33) will generally change Φ_{Dip} by an additive term of the form const. Φ_0. This term cannot be used to make Φ_0 and Φ_{Dip} orthogonal to each other, since the norm of Φ_0 vanishes, but it may be used to make the norm of Φ_{Dip} vanish as well.

Therefore we will add to the definition of Φ_{Dip} the postulate

$$\langle \Phi_{\text{Dip}} | \Phi_{\text{Dip}} \rangle = 0. \tag{37}$$

Instead of the Schrödinger equation, Φ_{Dip} generally obeys the equation

$$H\Phi_{\text{Dip}} = E\Phi_{\text{Dip}} + C \cdot \Phi_0. \tag{38}$$

The two states Φ_0 and Φ_{Dip} are different in character, as one can see when one calculates the expectation value of H in these states. It is of course doubtful whether the mathematical expression which in quantum mechanics gives the expectation value, can find a physical interpretation in a Hilbert space of indefinite metric; still it is interesting to calculate this expression. From (30), (32), (36) and (37) one gets

$$\bar{H}_{\Phi_0} = \frac{\langle \Phi_0 | H | \Phi_0 \rangle}{\langle \Phi_0 | \Phi_0 \rangle} = \frac{\langle \Phi_0 | \Phi_0 \rangle E_0}{\langle \Phi_0 | \Phi_0 \rangle} = \frac{0}{0} (= E_0), \tag{39}$$

$$\bar{H}_{\Phi_{\text{Dip}}} = \frac{\langle \Phi_{\text{Dip}} | H | \Phi_{\text{Dip}} \rangle}{\langle \Phi_{\text{Dip}} | \Phi_{\text{Dip}} \rangle} = \frac{C \langle \Phi_{\text{Dip}} | \Phi_0 \rangle}{\langle \Phi_{\text{Dip}} | \Phi_{\text{Dip}} \rangle} = \infty. \tag{40}$$

The expectation value of the energy in the dipole-state is infinite. If one uses the Schrödinger picture in which the state vector varies as a function of time according to

$$i \frac{\partial \Phi}{\partial t} = H\Phi, \tag{41}$$

one finds from (30) and (38)

$$\Phi_0(t) = \mathrm{e}^{-iE_0 t} \Phi_0(0),$$

but

$$\Phi_{\text{Dip}}(t) = \mathrm{e}^{-iE_0 t} \Phi_{\text{Dip}}(0) - iCt\, \mathrm{e}^{-iE_0 t} \Phi_0(0). \tag{42}$$

The time-dependence of eq. (42) has been discussed in an earlier paper [4]) on the extension of Hilbert space by 'dipole-ghosts' and shows the close analogy between the Lee-model in the case of the double root and the earlier model. A state vector of this type can probably not be used for the description of real phenomena; therefore we shall have to discuss later how this state can be excluded from the mathematical description.

Instead of using the wavefunctions (8) in momentum space one can represent the state vector by wavefunctions in ordinary space:

$$\Phi = \begin{cases} c \\ \varphi(\mathbf{x}) \end{cases}. \tag{43}$$

By Fourier transformation of (21) one finds for Φ_0

$$\varphi(\mathbf{x}) = (2\pi)^{-3/2}\int \frac{\mathrm{d}^3k\, \mathrm{e}^{\mathrm{i}\mathbf{k}\cdot\mathbf{x}} g_0 c}{\sqrt{8\pi\omega}(\omega - E_0)} = \frac{g_0 c}{4\pi \mathrm{i} r}\int_{-\infty}^{+\infty} \frac{\mathrm{e}^{\mathrm{i}kr}\, k\mathrm{d}k}{\sqrt{\omega}(\omega - E_0)}. \tag{44}$$

$\varphi(\mathbf{x})$ is singular at the point $r = 0$:

$$\varphi(\mathbf{x}) \approx \text{const.}\, r^{-3/2} \text{ for } r \to 0. \tag{45}$$

Therefore $\int|\varphi(\mathbf{x})|^2 \mathrm{d}^3x$ diverges logarithmically at $r = 0$. Its contribution to the norm is compensated by the term $-c^2$, which becomes infinite for $\hat{\omega} \to \infty$, $g_0 \to 0$. For large values of r, $\varphi(\mathbf{x})$ decreases exponentially; the exponential term is

$$\mathrm{e}^{-m_\theta r} \text{ for } E_0 \leqq 0,$$
$$\mathrm{e}^{-r\sqrt{m_\theta^2 - E_0^2}} \text{ for } E_0 \geqq 0.$$

If one derives Φ_{Dip} by differentiating (43) and (44) with respect to E and omitting thereby the condition (37), the wavefunction for Φ_{Dip} varies like $r^{-\frac{1}{2}}$ near $r = 0$; the integral $\int|\varphi(\mathbf{x})|^2\mathrm{d}^3x$ converges and gives the norm of this state, since the c-term vanishes after the differentiation. By adding a term const. Φ_0 one can fulfil (37).

2.5. RENORMALISATION AND THE COMMUTATION RULES

The operators ψ_{V}^*, ψ_{V} used in eq. (7R) obey the commutation rule (5R)

$$\{\psi^*_{\mathrm{V}},\ \psi_{\mathrm{V}}\} = -1. \tag{46}$$

The left hand side can be considered as a sum of the contributions of all intermediate states (with some restrictions which will be discussed in subsection 4.1), the discrete states as well as the continuous spectrum. If the eigenfunctions of the states are properly normalised, the coefficient c in each eigenfunction is identical with the matrix element of ψ_{V} belonging to the transition from vacuum to this state. We consider first the case of the two separated roots of $h(E) = 0$. The sum of the absolute squares of these matrix elements should — except for the consequences of the indefinite metric — be equal to unity according to (46), which is just another expression for the Thomas-Kuhn sum rule. If one takes the coefficient c from (35) for the discrete states, and from (17) for the continuous spectrum, eq. (46) can be written as

$$\frac{1}{|g_0^2|}\left[\sum_i \frac{1}{h'(E_i)} + \int_0^\infty \frac{k^2\mathrm{d}k}{2Eh^+(E)h^-(E)}\right] = -1. \tag{47}$$

In the limit $\hat{\omega} \to \infty$ $|g_0^2|$ vanishes. Therefore the sum over the discrete states must in this case compensate the contribution from the continuous spectrum. The influence of the indefinite metric is seen in the fact that the contribution of the state of lowest energy is negative; $h'(E_i)$ is negative for the 'ghost-

state'. The compensation of the two terms in eq. (47) in the case $\hat{\omega} = \infty$, $|g_0^2| = 0$ can be verified by changing the path of integration in (47).

The integral in (47) can be written as

$$g^2 = \int_0^\infty \frac{k^2\,\mathrm{d}k}{2\omega h^+(\omega)h^-(\omega)} = \int_{m_0}^\infty \frac{k\mathrm{d}\omega}{2h^+(\omega)h^-(\omega)} = \int_{m_0}^\infty \frac{\mathrm{d}\omega}{2\pi i}\left(\frac{1}{h^-(\omega)} - \frac{1}{h^+(\omega)}\right)$$
$$= \int_C \frac{\mathrm{d}\omega}{2\pi i h(\omega)} = -\sum_l \frac{1}{h'(E_l)}. \tag{48}$$

The path of integration C starts from $+\infty$ above the cut in the ω-plane, goes to the branching point $\omega = m_0$ and from there below the cut to $+\infty$. Deforming this path to a circle at infinity leaves residual integrals around the poles of $1/h(\omega)$, which give rise to the terms $-1/h'(E_l)$.

In the special case of the double root the situation is essentially the same and we can calculate from (29) the numerical value of the integral (48). By expanding $h(E)$ in powers of $E-E_0$ in the neighbourhood of E_0, one finds ($\xi_0 = E_0/m_0$)

$$g^2 = \lim_{E_1 \to E_2} \sum_l \frac{-1}{h'(E_l)} = \frac{2h'''(E_0)}{3[h''(E_0)]^2}$$
$$= \frac{4[(\xi_0^2-1)^2+3(\xi_0^2-1)+3\xi_0\sqrt{\xi_0^2-1}\,\ln(-\xi_0+\sqrt{\xi_0^2-1})]}{3[\xi_0\sqrt{\xi_0^2-1}+\ln\,(-\xi_0+\sqrt{\xi_0^2-1})]^2}. \tag{49}$$

For large negative values of ξ_0 the integral g^2 tends to the value 4/3; it tends to zero for $\xi_0 \to 1$.

Since all matrix elements c become infinite in the limit $\hat{\omega} \to \infty$, $g_0 \to 0$, it is convenient to renormalise the operator ψ_V by introducing

$$\psi_{Vr} = \frac{g_0}{g}\psi_V, \quad \psi^*_{Vr} = \left(\frac{g_0}{g}\right)^* \psi^*_V = -\frac{g_0}{g}\psi^*_V. \tag{50}$$

Then, in the limit $\hat{\omega} \to \infty$, we have

$$\{\psi^*_{Vr},\ \psi_{Vr}\} = 0. \tag{51}$$

The contributions to the commutator of the normal, continuous states alone, however, are equal to unity as in quantum mechanics; this part is compensated by the contribution of the 'dipole-ghost', just as in the method of quantisation mentioned in the introduction.

If one uses that representation in which the operators are functions of the time t, then the commutator takes the form

$$\{\psi^*_{Vr}(t),\ \psi_{Vr}(t')\} = \frac{1}{g^2}\left[\sum_l \frac{\mathrm{e}^{iE_l(t-t')}}{h'(E_l)} + \int_0^\infty \frac{k^2\,\mathrm{e}^{iE(t-t')}\mathrm{d}k}{2Eh^+(E)h^-(E)}\right]. \tag{52}$$

It vanishes only for $t = t'$ and has generally finite values for $t \neq t'$. Again, this behaviour corresponds very closely to that of the commutator in the method of quantisation mentioned above.

2.6. THE RENORMALISED WAVE EQUATIONS IN ORDINARY SPACE

The operators $\psi_V(\mathbf{x})$ or $\psi_V(\mathbf{p})$ can be renormalised in the same manner as ψ_V. If the wave equations following from eq. (4) are expressed in the renormalised operators $\psi_{V_r}(\mathbf{x})$, the resulting equations do not contain any infinite constants.

The unrenormalised wave equations can be derived from (3) and (4):

$$i\frac{\partial\psi_V(\mathbf{x})}{\partial t} = m_V\psi_V(\mathbf{x}) - g_0\pi\sqrt{2}\,\psi_N(\mathbf{x})a(\mathbf{x}), \tag{53a}$$

$$i\frac{\partial\psi_N(\mathbf{x})}{\partial t} = m_N\psi_N(\mathbf{x}) - g_0\pi\sqrt{2}a^*(\mathbf{x})\psi_V(\mathbf{x}), \tag{53b}$$

$$\frac{\partial\Pi(\mathbf{x})}{\partial t} = \Delta\varphi(\mathbf{x}) - m_0^2\varphi(\mathbf{x}) + \frac{g_0\pi}{\sqrt{2}}[-\psi_V^*(\mathbf{x})\psi_N(\mathbf{x}) + \psi_N^*(\mathbf{x})\psi_V(\mathbf{x})] \tag{53c}$$

$$\frac{\partial\varphi(\mathbf{x})}{\partial t} = \Pi(\mathbf{x}) + \frac{ig_0\pi}{\sqrt{2}}\int \mathrm{d}^3x'\,\frac{\mathrm{e}^{-m_0|\mathbf{x}-\mathbf{x}'|}}{|\mathbf{x}-\mathbf{x}'|}\,[\psi_V^*(\mathbf{x}')\psi_N(\mathbf{x}') + \psi_N^*(\mathbf{x}')\psi_V(\mathbf{x}')]. \tag{53d}$$

The renormalisation of eqs. (53b, c, d) is obvious. For the renormalisation of (53a) it is convenient to integrate (53b) and to express $\psi_N(\mathbf{x})$ in (53a) in terms of $a^*(\mathbf{x})$ and $\psi_V(\mathbf{x})$. Eq. (53b) leads to

$$\psi_N(\mathbf{x}, t) = ig_0\pi\sqrt{2}\,\mathrm{e}^{-im_N t}\int_{-\infty}^{t}\mathrm{d}t'\,\mathrm{e}^{im_N t'}\,a^*(\mathbf{x}, t')\psi_V(\mathbf{x}, t') + \psi_N(\mathbf{x}, -\infty). \tag{54}$$

Instead of (53a) we get (putting again $m_N = 0$):

$$i\frac{\partial\psi_V(\mathbf{x})}{\partial t} = m_V\psi_V(\mathbf{x}) - 2ig_0^2\pi^2\int_{-\infty}^{t} a(\mathbf{x}, t)a^*(\mathbf{x}, t')\psi_V(\mathbf{x}, t')\mathrm{d}t' - g_0\pi\sqrt{2}a^*(\mathbf{x}, t)\psi_N(\mathbf{x}, -\infty). \tag{55}$$

The expression $a(\mathbf{x}, t)a^*(\mathbf{x}, t')$ can be written as

$$a(\mathbf{x}, t)a^*(\mathbf{x}, t') = s(t-t') + [a(\mathbf{x}, t)a^*(\mathbf{x}, t') - s(t-t')], \tag{56}$$

where

$$s(t-t') = \langle 0|a(\mathbf{x}, t)a^*(\mathbf{x}, t')|0\rangle = \frac{1}{4\pi^2}\int_0^\infty \frac{k^2\mathrm{d}k}{\omega}\,\mathrm{e}^{i\omega(t'-t)}. \tag{57}$$

We consider now the expression

$$\frac{1}{g_0^2}\left(i\frac{\partial\psi_V(\mathbf{x})}{\partial t} - m_V\psi_V(\mathbf{x})\right) + 2i\pi^2\int_{-\infty}^{t} s(t-t')\psi_V(\mathbf{x}, t')\,\mathrm{e}^{\gamma t'}\,\mathrm{d}t',\ (\gamma\to 0) \tag{58}$$

[the term $\mathrm{e}^{\gamma t'}$ $(\gamma\to 0)$ has been introduced in order to make it certain that the integral $\int_{-\infty}^{t}$ in (58) converges in every term at $t'\to-\infty$.] If we write

$$\psi_V(\mathbf{x}, t) = \int_{-\infty}^{+\infty}\chi(\mathbf{x}, z)\,\mathrm{e}^{-izt}\,\mathrm{d}z,$$

the Fourier transformation of (58) leads, on account of (3) and (57), to

$$\left\{\frac{z-m_V}{{g_0}^2}+\frac{2i\pi^2}{(2\pi)^3}\int\frac{4\pi k^2\,\mathrm{d}k}{2\omega i(\omega-z-i\gamma)}\right\}\chi(\mathbf{x},z)\,\mathrm{e}^{-izt}=h^+(z)\mathrm{e}^{-izt}\chi(\mathbf{x},z). \quad (59)$$

Hence the operation (58) can be expressed in the form

$$\frac{1}{{g_0}^2}\left(i\frac{\partial\psi_V(\mathbf{x})}{\partial t}-m_V\psi_V(\mathbf{x})\right)+2i\pi^2\int_{-\infty}^{t}s(t-t')\psi_V(\mathbf{x},\,t')\mathrm{d}t'$$
$$=\int_{-\infty}^{+\infty}\chi(t-t')\mathrm{d}t'\,\psi_V(\mathbf{x},\,t'), \quad (60)$$

where

$$\chi(t-t')=\frac{1}{2\pi}\int_{-\infty}^{+\infty}\mathrm{d}z h^+(z)\mathrm{e}^{iz(t'-t)}. \quad (61)$$

By transforming the path of integration one finds

$$\chi(t-t')=0 \text{ for } t'-t>0.$$

Therefore finally the renormalized wave equations are

$$g\int_{-\infty}^{t}\mathrm{d}t'\chi(t-t')\psi_{Vr}(\mathbf{x},t') \quad (62a)$$
$$=-2i\pi^2 g\int_{-\infty}^{t}[a(\mathbf{x},t)a^*(\mathbf{x},t')-s(t-t')]\psi_{Vr}(\mathbf{x},t')\mathrm{d}t'-\pi\sqrt{2}\,a(\mathbf{x},t)\psi_N(\mathbf{x},-\infty),$$

$$i\frac{\partial\psi_N(\mathbf{x})}{\partial t}=-\pi g\sqrt{2}\;a^*(\mathbf{x})\psi_{Vr}(\mathbf{x}), \quad (62b)$$

$$\frac{\partial\Pi(\mathbf{x})}{\partial t}=\Delta\varphi(\mathbf{x})-{m_\theta}^2\varphi(\mathbf{x})+\frac{\pi g}{\sqrt{2}}[\psi_{Vr}^*(\mathbf{x})\psi_N(\mathbf{x})+\psi_N{}^*(\mathbf{x})\psi_{Vr}(\mathbf{x})], \quad (62c)$$

$$\frac{\partial\varphi(\mathbf{x})}{\partial t}=\Pi(\mathbf{x})-\frac{i\pi g}{\sqrt{2}}\int\mathrm{d}^3x'\,\frac{\mathrm{e}^{-m_\theta|\mathbf{x}-\mathbf{x}'|}}{|\mathbf{x}-\mathbf{x}'|}[\psi_{Vr}^*(\mathbf{x}')\psi_N(\mathbf{x}')-\psi_N{}^*(\mathbf{x}')\psi_{Vr}(\mathbf{x}')]. \quad (62d)$$

These wave equations do not contain any infinite constants, and one can forget at this point that they have been obtained by a process of renormalisation. The value of the coupling constant g depends on the position of the 'dipole-ghost' or vice versa. The commutation relations are the conventional ones except for those of the type $\{\psi_{Vr}^*(\mathbf{x},\,t),\;\psi_{Vr}(\mathbf{x}',\,t')\}$ which are zero for $t=t'$ and have been discussed before (§ 2.5). A finite expression for the Hamiltonian in terms of the renormalised wavefunctions at one time t can*not* be given. In fact such an expression cannot exist, since it would commute with ψ_{Vr} or ψ_{Vr}^* at the same time on account of eq. (52)) in contradiction with

$$i\frac{\partial\psi_{Vr}}{\partial t}=[H,\;\psi_{Vr}].$$

The equations (62) contain two non-local operators; the operator

$$\frac{\mathrm{e}^{-m_\theta|\mathbf{x}-\mathbf{x}'|}}{|\mathbf{x}-\mathbf{x}'|}$$

is a direct consequence of the non-local interaction that has been assumed in the Lee-model from the beginning. It should not occur in a relativistic theory of the real elementary particles. The other operator $\chi(t-t')$ is a consequence of the renormalisation procedure; again it should not occur in a realistic theory of matter waves. With respect to this non-local character the Lee-model seems to be rather far from reality.

In the model for a theory of the elementary particles mentioned in the introduction, one has, instead of the rather complicated equations (62a–d), a simple non-linear spinor equation for one wavefunction, the commutator of which corresponds to $\{\psi^*_{\mathrm{Vr}}(\mathbf{x}, t), \psi_{\mathrm{Vr}}(\mathbf{x}', t')\}$. There are no non-local operators, the convergence of the theory is brought about by the unconventional commutator which vanishes at $t = t'$.

3. The sector N+2θ

A theory of the type discussed above can be used for the description of real phenomena only if the S-matrix is unitary and if no states of negative norm can be created in scattering processes. Following the paper of Källén and Pauli we study the behaviour of the S-matrix first in the sector $\mathrm{N}+2\theta$.

3.1. THE WAVE FUNCTIONS IN MOMENTUM SPACE

The state vector in this sector can be represented by two wave functions of one and two variables, respectively,

$$\Phi = \begin{cases} \varphi(\mathbf{k}) \\ \varphi(\mathbf{k}_1, \mathbf{k}_2). \end{cases} \tag{63}$$

By applying the Hamiltonian one gets

$$H\Phi = \Phi' = \begin{cases} \varphi'(\mathbf{k}) \\ \varphi'(\mathbf{k}_1, \mathbf{k}_2), \end{cases} \tag{64}$$

with

$$\varphi'(\mathbf{k}) = (m_{\mathrm{V}}+\omega)\varphi(\mathbf{k}) - \frac{2g_0}{\sqrt{4\pi}}\int \frac{\mathrm{d}^3k'}{\sqrt{2\omega'}}\varphi(\mathbf{k}, \mathbf{k}'), \tag{65a}$$

$$\varphi'(\mathbf{k}_1, \mathbf{k}_2) = (\omega_1+\omega_2)\varphi(\mathbf{k}_1, \mathbf{k}_2) - \frac{g_0}{2\sqrt{4\pi}}\left(\frac{\varphi(\mathbf{k}_2)}{\sqrt{2\omega_1}} + \frac{\varphi(\mathbf{k}_1)}{\sqrt{2\omega_2}}\right). \tag{65b}$$

If the state vector belongs to an energy $E > 2m_\theta$ we get from (11) and (65b)

$$\varphi(\mathbf{k}_1, \mathbf{k}_2) = \varphi_0(\mathbf{k}_1, \mathbf{k}_2) + \frac{g_0}{2\sqrt{4\pi}(\omega_1+\omega_2-E-i\gamma)}\left[\frac{\varphi(\mathbf{k}_2)}{\sqrt{2\omega_1}} + \frac{\varphi(\mathbf{k}_1)}{\sqrt{2\omega_2}}\right], \tag{66}$$

where $\varphi_0(\mathbf{k}_1, \mathbf{k}_2)$ is an arbitrary function of $\mathbf{k}_1$ and $\mathbf{k}_2$ satisfying the condition

$$(\omega_1+\omega_2-E)\varphi_0(\mathbf{k}_1, \mathbf{k}_2) = 0. \tag{67}$$

Inserting this result into eq. (65a) gives

$$h^+(E-\omega)\varphi(\mathbf{k}) = -\frac{1}{8\pi}\int \frac{\mathrm{d}^3k'\,\varphi(\mathbf{k}')}{\sqrt{\omega\omega'}\,(\omega+\omega'-E-i\gamma)} - \varphi_{0i}(\mathbf{k}), \tag{68}$$

where

$$\varphi_{0i}(\mathbf{k}) = \frac{2}{g_0\sqrt{4\pi}}\int \frac{\mathrm{d}^3k'\,\varphi_0(\mathbf{k},\,\mathbf{k}')}{\sqrt{2\omega'}}. \tag{69}$$

We consider only the case of a total angular momentum zero. Then $\varphi(\mathbf{k})$ is a function of the absolute value k only.

Eq. (68) indicates that $\varphi(\mathbf{k})$ as a function of k has a singularity at the point $\omega = \omega_c = E-E_0$, where E_0 is the energy of the 'dipole-ghost'. Since $h^+(E-\omega)$ has a double zero at this point the behaviour of $\varphi(\mathbf{k})$ depends on whether the right hand side of (68) vanishes or does not vanish at the critical point. If the right hand side is different from zero, we get a behaviour for $\varphi(\mathbf{k})$ of the type

$$\varphi(\mathbf{k}) = a\delta(E-E_0-\omega)+b\delta'(E-E_0-\omega)+\frac{\chi(\mathbf{k})}{[E-E_0-\omega]^2}, \tag{70}$$

where we may have to add a term $+i\gamma(\gamma\to 0)$ in the denominator of the last term. Such solutions will certainly exist, but it will be difficult to find any physical interpretation for them. The Fourier-transformation from momentum space to ordinary space shows that a solution of the type (70) does not correspond to incoming and outgoing spherical waves of the form $\mathrm{e}^{\pm ik_c r}/r$; it corresponds to expressions of the type $[(\alpha+\beta r)/r]\mathrm{e}^{\pm ik_c r}$ which can scarcely be interpreted. Therefore the solutions of the type (70) cannot be used for the description of real phenomena. These solutions belong to what is later called Hilbert space II.

A different type of solutions is obtained if the right hand side of (68) vanishes at the critical point. Then we get

$$\varphi(\mathbf{k}) = a\delta(E-E_0-\omega)+\frac{\chi(\mathbf{k})}{E-E_0-\omega+i\gamma}. \tag{71}$$

It is very important to note that the arbitrary factor a of the δ-function in (71) can be used to make the right hand side of (68) vanish at the critical point. Therefore one can actually find a group of solutions of (68) of the behaviour (71), but one cannot choose the constant a arbitrarily.

Inserting (71) into the condition that the right hand side of (68) shall vanish at $\omega = \omega_c = E-E_0$ gives

$$a\frac{k_c}{2(\omega_c-E_0)} = -\frac{1}{8\pi}\int \frac{\mathrm{d}^3k'\,\chi(\mathbf{k}')}{\sqrt{\omega_c\omega'}(\omega_c+\omega'-E-i\gamma)(E-E_0-\omega'+i\gamma)} - \varphi_{0i}(\mathbf{k}_c). \tag{72}$$

The last term $\varphi_{0i}(\mathbf{k}_c)$ vanishes, since $\varphi_{0i}(\mathbf{k})$ according to (67) and (69) can

only be different from zero if $m_\theta \leqq \omega \leqq E-m_\theta$. The resulting integral equation for $\chi(\mathbf{k})$ is

$$\chi(\mathbf{k}) = -\frac{1}{8\pi}\frac{(\omega_c-\omega)^2}{h^+(E-\omega)}\int \frac{d^3k'\,\chi(\mathbf{k}')}{\sqrt{\omega\omega'}\,(\omega+\omega_c-E)(\omega+\omega'-E-i\gamma)\,(\omega_c+\omega'-E-i\gamma)} - \frac{\omega_c-\omega}{h^+(E-\omega)}\varphi_{0i}(\mathbf{k}). \tag{73}$$

The right hand side is automatically regular at the point $\omega = \omega_c$, therefore $\chi(\mathbf{k})$ is regular as well.

The solutions of the type (71) have the same behaviour as ordinary solutions of scattering problems in quantum mechanics. They belong to what is later called Hilbert space I.

3.2. THE INTERPRETATION OF THE WAVE FUNCTIONS IN ORDINARY SPACE

The state vector Φ can be represented in ordinary space by two functions

$$\Phi = \begin{cases} \varphi(\mathbf{x}) \\ \varphi(\mathbf{x}_1,\ \mathbf{x}_2) \end{cases} \tag{74}$$

which can be obtained from (63) by Fourier transformation. Since $\varphi(\mathbf{k})$ and $\varphi(\mathbf{k}_1,\ \mathbf{k}_2)$ have singularities of the type (71) at the point $k = k_c$ or $k_1 = k_c$ or $k_2 = k_c$, the corresponding functions $\varphi(\mathbf{x})$, $\varphi(\mathbf{x}_1,\ \mathbf{x}_2)$ contain parts which behave like in- and outgoing waves of the type $e^{\pm ik_c r}/r$ for large values of r. A comparison of (65a) and (66) with (21) shows that for large values of r — this corresponds to values of k or k_1 or k_2 near $k_c (|k-k_c| \ll k_c)$ in momentum space — these parts of the wave function (74) can be written as product of $e^{\pm ik_c r}/r$ with the wave function of the zero-state Φ_0 of the sector $N + \theta$. Besides these terms, the wave function contains in- and outgoing waves for which the corresponding k-values fulfil the condition $\omega_1+\omega_2=E$, as is seen from the denominator $\omega_1+\omega_2-E-i\gamma$ in (66).

Therefore the wave function (74) allows the following interpretation: There are incoming and scattered waves of two θ-particles hitting one N-particle. The incoming waves can be arbitrarily chosen by taking a suitable function $\varphi_0(\mathbf{k}_1, \mathbf{k}_2)$. Besides, there are incoming and outgoing waves of one θ-particle hitting a V-particle in the zero-state Φ_0. These incoming waves can*not* be arbitrarily chosen, their amplitude is determined by the condition (72).

We will discuss in detail in section 4 what is meant by the statement that the wave function, or part of it, can for large values of r be written as product of a spherical wave in r and an eigenfunction of the sector $N + \theta$. It will be shown that the norm of such a product state is equal to

the product of the norms of the single factors. Therefore a state in which an asymptotic spherical wave is combined with the eigenfunction Φ_0 of the sector $N+\theta$, has the norm zero. It does not contribute to the expectation values of energy or momentum. The other states, in which asymptotically the waves of two separated θ-particles are combined with a single N-particle, have a positive norm, since each factor has a positive norm.

3.3. THE UNITARITY OF THE S-MATRIX

For the general solutions of the type (70) it would be difficult to define a scattering matrix, since these solutions do not represent incoming and outgoing waves, as has been pointed out in § 3.1. If one would try to define the S-matrix by a limiting process — by starting from the case of the two separated zeros of $h(E) = 0$ and going to the limit of the 'dipole-ghost' — this S-matrix would certainly not fulfil the equation $\sum_i |S_{ik}^2| = 1$. Therefore the general solutions of the type (70) cannot be used for the description of real phenomena.

For the solutions of the type (71) however (Hilbert space I) the S-matrix can be defined in the usual way, since such solutions represent incoming and outgoing waves. A detailed calculation concerning the unitarity of this S-matrix will be given in section 5, after the clarification of the general properties of Hilbert space in the case of the 'dipole-ghost'. Therefore it may be sufficient in this section to give a simple proof of the unitarity of the S-matrix which makes use only of the asymptotic behaviour of the wavefunctions.

It should be emphasized at this point that the term 'unitarity' of the S-matrix is ambiguous. If the indefinite metric in Hilbert space is used consistently (cf. section 4). the Hamiltonian is self-adjoint, and the S-matrix, which is connected with e^{iHt} through a limiting process $t \to \infty$, fulfils the equation $S^*S = 1$ and is unitary in this sense, even in the case treated by Källén and Pauli. We will call this property 'pseudo-unitarity' and will reserve the term 'unitarity' for the special case where the equation $S^*S = 1$ is identical with the equation $\Sigma_i |S_{ik}^2| = 1$. It is this equation which is needed for the physical interpretation.

Asymptotically the wave functions (74) are a sum of terms which either mean two separated θ-particles and one N-particle (terms with positive norm) or one θ-particle and a V-particle in the Φ_0-state (terms with zero norm). Asymptotically the state Φ_{Dip} does not occur. The S-matrix transforms from the incoming waves to the outgoing waves. Therefore the S-matrix is a transformation matrix in a Hilbert space of semi-definite metric; states with negative norm do not exist in this space. Hence the S-matrix must be unitary, not only pseudo-unitary. This result will be confirmed later by direct calculation.

From the results of the foregoing sections one can already see that it will be convenient to divide the total Hilbert space into two parts. Hilbert space I comprises all 'normal' solutions of $H\Phi = E\Phi$, i.e. the continuous spectrum in the sector N+θ and the solutions of the type (71). Hilbert space II contains the more general solutions of the type (70) and the state Φ_{Dip} of the sector N+θ. The state Φ_0 may be included in Hilbert space I, but it is a virtual state which does not carry energy or momentum. Within Hilbert space I the S-matrix is unitary; it is only this space which can be used for the description of real phenomena.

3.4. DISCRETE STATES IN THE SECTOR N+2θ

It may be that the Schrödinger equation $H\Phi = E\Phi$ has solutions for $E < 2m_\theta$ or complex values of E. We will distinguish the two possibilities

a) $$E_0+m_\theta \leqq E < 2m_\theta \quad (E \text{ real}) \tag{75a}$$

b) $$E < E_0+m_\theta \text{ and real, or } E \text{ complex.} \tag{75b}$$

In both cases eq. (68) has to be replaced by

$$h^+(E-\omega)\varphi(\mathbf{k}) = -\frac{1}{8\pi}\int \frac{\mathrm{d}^3k'\,\varphi(\mathbf{k}')}{\sqrt{\omega\omega'}(\omega+\omega'-E)}\,. \tag{76}$$

In the first case (75a) the function $\varphi(\mathbf{k})$ again has a singularity at the point $\omega = \omega_c = E-E_0 \geqq m_\theta$. Just as in subsection 3.1 we have to distinguish between the two types of solutions (70) and (71). Again it will not be possible to give a physical interpretation of solutions of the type (70); they will belong to Hilbert space II. Solutions of the type (71), however — if they exist — can be interpreted. At first sight it would seem that these solutions do not describe discrete eigenstates, but radioactive states that can disintegrate into a θ-particle and a V-particle in the state Φ_0. In fact the eigenfunctions do contain a term that means an outgoing (and incoming!) θ-wave multiplied with a Φ_0-eigenfunction. But this wave does not carry energy or momentum, or more simply, it does not carry 'norm' away from the system. Therefore it does not lead to any decay of the state, which hence remains a genuine discrete state. Formally, for large distances from the origin, the eigenfunction behaves like $\Phi_0\, \mathrm{e}^{\pm ikr}/r$. Integrating the absolute square of the wavefunction over the space coordinates would lead to a divergent result, were it not that the norm zero of Φ_0 would cause this contribution from larger distances to vanish. Therefore, if states of this type exist, they have a finite norm-integral and we shall later show that their norm is positive. The eigenfunctions are given by the solutions of the homogeneous equation (73), which can exist only for discrete eigenvalues of E. If such solutions exist, the corresponding states belong to Hilbert space I.

In the second case (75b), the function $\varphi(\mathbf{k})$ has no singularity for real

values of $\mathbf{k}$, since $E-E_0 < m_0$ or E is complex. Therefore $\varphi(\mathbf{k})$ cannot, as in (71), contain a term of the form $a\delta(E-E_0-\omega)$, which would be necessary to make the right hand side in (68) vanish at the point $\omega = \omega_c = E-E_0$ (in the complex plane). Solutions of the type (71) cannot be found in the case (75b). If discrete solutions of $H\Phi = E\Phi$ in the region $E < E_0+m_0$ or complex E exist at all, they belong to Hilbert space II. It will be shown in section 5 that in scattering problems in which one starts from a state in Hilbert space I, only discrete states of the first type (71) can be created; states of the type (70) or of energy values $E < E_0+m_0$ or complex E cannot occur as outgoing waves.

4. General Properties of the Hilbert Space with Indefinite Metric

Since in the foregoing and following calculations we have to make extensive use of the indefinite metric discussed by Källén and Pauli, we shall in this chapter collect some of the most important general formulae concerning this metric.

4.1. REPRESENTATION OF VECTORS AND OPERATORS IN THE INDEFINITE METRIC

If the Hilbert space Ω is constructed by a number of state vectors $\Phi_n\rangle$, any state vector $\Psi\rangle$ in this space can be defined by two sets of components.

We can either write

$$\Psi\rangle = \Phi_l\rangle \cdot \Psi^l, \tag{77}$$

where it is understood that the summation shall be carried out, if the same index occurs as lower and upper index. Then the Ψ^l are called the contravariant components of Ψ. Or one can put

$$\Psi_l = \langle\Phi_l|\Psi\rangle. \tag{78}$$

The Ψ_l are the covariant components of Ψ. The metric is defined by the relation

$$g_{ik} = \langle\Phi_i|\Phi_k\rangle. \tag{79}$$

From (79) we get

$$g_{ik} = g^*_{ki} \tag{80}$$

and from (77), (78) and (79),

$$\Psi_i = g_{ik}\Psi^k. \tag{81}$$

From the $\Phi_n\rangle$ one can generally construct the 'inverse' system of state vectors $\Phi^n\rangle$, defined by

$$\langle\Phi^k|\Phi_i\rangle = \delta_{ki}. \tag{82}$$

From (77) and (82) one gets

$$\Psi^l = \langle\Phi^l|\Psi\rangle. \tag{83}$$

The norm of Ψ can be calculated from the components according to (77)

to (82):

$$\langle\Psi|\Psi\rangle = \langle\Psi|\Phi_l\rangle\Psi^l = \Psi_l^*\Psi^l = \Psi^{*l}\Psi_l = \Psi^{*l}\Psi^k g_{lk} = \Psi_l^*\Psi_k g^{lk}. \quad (84)$$

In a similar way the scalar product is defined as

$$\langle X|\Psi\rangle = X_l^*\Psi^l. \quad (85)$$

The multiplication of matrices representing operators leads to

$$\begin{aligned} {}_k(AB)_l &= \langle\Phi_k|AB|\Phi_l\rangle = \langle\Phi_k|A|\Phi_m\rangle{}^m B_l \\ &= {}_kA_m{}^mB_l = \langle\Phi_k|A|\Phi_m\rangle\langle\Phi^m|B|\Phi_l\rangle \\ &= \langle\Phi_k|A|\Phi_m\rangle g^{mn}\langle\Phi_n|B|\Phi_l\rangle = {}_kA_m g^{mn}{}_nB_l. \end{aligned} \quad (86)$$

Therefore the usual terminology, that in matrix multiplication 'one has to sum over all intermediate states', is to be used with caution. This terminology is correct only in the special case of an orthogonal set of state vectors Φ_n, i.e. if $g^{ik} = \delta_{ik}g^{ii}$. In the Källén-Pauli case the eigensolutions of the Schrödinger equation define a complete orthogonal set of state-vectors. But in the dipole-case this set is not complete; one has to add Φ_{Dip} to get the complete set, but Φ_{Dip} is not orthogonal to Φ_0.

A hermitian or self-adjoint operator is generally defined by

$$\langle\Phi_k|A|\Phi_l\rangle = \langle\Phi_l|A|\Phi_k\rangle^* \text{ or } {}_kA_l = ({}_lA_k)^*. \quad (87)$$

In the indefinite metric we will use the term 'pseudo-hermitian' (or 'self-adjoint') for this property, and reserve the term 'hermitian' for the positive metric — in analogy to the definition of 'pseudo-unitary' and 'unitary' in § 3.3). In this sense the pseudo-hermitian conjugate or adjoint B^* to the operator B is defined by

$$\langle\Phi_k|B^*|\Phi_l\rangle = \langle\Phi_l|B|\Phi_k\rangle^*$$

or

$${}_k(B^*)_l = ({}_lB_k)^*. \quad (87a)$$

The operator B is pseudo-hermitian, if $B^* = B$. The expectation value of a pseudo-hermitian operator is real; but it may be undefined or infinite as in (39) and (40).

4.2. THE EIGENSTATES OF $H\Psi = \Psi E$

Some of the state vectors Φ_n may be eigenstates of the Hamiltonian:

$$H|\Phi_n\rangle = \Phi_m\rangle{}^mH_n = \Phi_m\rangle\delta_n{}^mE_n = \Phi_n\rangle E_n. \quad (88)$$

The eigenvalues E_n, which are the diagonal terms ${}^nH_n$, need not be real, since the pseudo-hermitian character of H leads only to $({}^nH_n)^* = {}_nH^n$. The eigenvalues are generally not identical with the expectation values; they are, however, identical, if the norm of the state n does not vanish. In this case one gets in analogy to (39)

$$\bar{H} = \frac{{}_nH_n}{g_{nn}} = \frac{g_{nm}{}^mH_n}{g_{nn}} = \frac{g_{nn}E_n}{g_{nn}} = E_n. \tag{88a}$$

The pseudo-hermitian conjugate of the equation for Φ_m is

$$\langle\Phi_m|H = E_m{}^*\langle\Phi_m. \tag{89}$$

Multiplying (88) by $\langle\Phi_m$ on the left, (89) by $\Phi_n\rangle$ on the right and substracting, one finds

$$(E_n - E_m{}^*)\langle\Phi_m|\Phi_n\rangle = 0. \tag{90}$$

From (90) one concludes, in the case $n = m$, that the eigenvalue E_n must be real, when the norm of $\Phi_n\rangle$ is different from zero; and that the norm must vanish, when the eigenvalue is complex. For $n \neq m$ eq. (90) gives the orthogonality of $\Phi_n\rangle$ and $\Phi_m\rangle$, if $E_n \neq E_m{}^*$. If $E_n = E_m{}^*$, $\Phi_n\rangle$ and $\Phi_m\rangle$ will generally not be orthogonal.

If the Hilbert space Ω contains the subspace Ω', which is transformed in itself by H, then also the subspace $\Omega'_\perp$, which contains all vectors orthogonal to all vectors of Ω', is transformed in itself by H. This follows from

$$\langle\Psi_2|H\Psi_1\rangle = 0 = \langle\Psi_1|H\Psi_2\rangle^*, \tag{91}$$

if Ψ_1 belongs to Ω', Ψ_2 to $\Omega'_\perp$.

But this does not prove the completeness of $\Omega' + \Omega'_\perp$, because in the indefinite metric Ω' and $\Omega'_\perp$ may have some common elements which have the norm zero. If $\Phi_1\rangle \cdots \Phi_r\rangle$ are the elements of Ω', the condition that $\Psi\rangle$ shall be orthogonal to all vectors $\Phi_i\rangle$ is

$$\Phi_i{}^l\Psi_l = 0 \text{ for } i = 1, 2 \cdots r. \tag{92}$$

If the number of independent vectors in Ω is n, the r equations (92) have $n-r$ independent solutions. Only if they are also independent of $\Phi_1\rangle \cdots \Phi_r\rangle$, then $\Omega' + \Omega'_\perp$ form the complete space Ω:

$$\Omega' + \Omega'_\perp = \Omega. \tag{93}$$

Among the original state vectors of the sector $\binom{N+\theta}{V}$ there is only one state vector of negative norm, that of one V-particle. In this special case any system of independent state vectors can contain only one vector of negative norm. Any vector which is orthogonal to this one, must have a positive norm. Therefore if there are two roots of $h(E) = 0$, the one belonging to the 'ghost-state' of negative norm, no complex roots of this equation can exist. If there are no real roots, the equation must have two — and only two — complex conjugate roots.

4.3. THE NORM OF PRODUCT-STATES

Let $O(\mathrm{R}_1)$ be an operator which creates one or several particles or compound states within the region R_1 of ordinary space. $O(\mathrm{R}_1)$ could for instance be defined by some expression like $\int\varphi(\mathbf{x}_1, \mathbf{x}_2)\psi_N{}^*(\mathbf{x}_1)a^*(\mathbf{x}_2)\mathrm{d}^3x_1\,\mathrm{d}^3x_2$,

where $\varphi(\mathbf{x}_1, \mathbf{x}_2)$ goes sufficiently strongly to zero, when $\mathbf{x}_1$ or $\mathbf{x}_2$ approach the boundary of R_1. Then

$$O(\mathrm{R}_1)|0\rangle \tag{94}$$

defines a state in which the vacuum has not been changed outside of the region R_1. Its norm is given by

$$N_1 = \langle 0|O^*(\mathrm{R}_1)O(\mathrm{R}_1)|0\rangle. \tag{95}$$

$O(\mathrm{R}_2)$ may refer to another region R_2, which is completely outside of R_1. Then $O(\mathrm{R}_2)$ and $O^*(\mathrm{R}_2)$ commute or anticommute with $O(\mathrm{R}_1)$ and $O^*(\mathrm{R}_1)$, since the wavefunctions at distant points in space always commute or anticommute. The state vector

$$O(\mathrm{R}_2) \cdot O(\mathrm{R}_1)|0\rangle \tag{96}$$

describes a state in which the vacuum has not been changed outside of $\mathrm{R}_1+\mathrm{R}_2$. In this state we meet the situation described by $O(\mathrm{R}_1)|0\rangle$ in R_1 and that given by $O(\mathrm{R}_2)|0\rangle$ in R_2.

The norm of this state is given by the product of the norms of the single states:

$$\begin{aligned} N_{12} &= \langle 0|O^*(\mathrm{R}_1)O^*(\mathrm{R}_2)O(\mathrm{R}_2)O(\mathrm{R}_1)|0\rangle \\ &= \langle 0|O^*(\mathrm{R}_1)O(\mathrm{R}_1)O^*(\mathrm{R}_2)O(\mathrm{R}_2)|0\rangle \\ &= \langle 0|O^*(\mathrm{R}_1)O(\mathrm{R}_1)|0\rangle\langle 0|O^*(\mathrm{R}_2)O(\mathrm{R}_2)|0\rangle \\ &= N_1 \cdot N_2. \end{aligned} \tag{97}$$

This result is independent of the type of the metric. In the indefinite metric one of the factors N_1 or N_2 may be zero, and it is important for the calculations in the other sections that then the norm of the product state vanishes as well.

In the practical calculations the operators constructing stationary states or wave packets will not completely vanish outside of a finite region R_1. As a rule they will decrease exponentially outside of these regions. In this case eq. (97) will still be asymptotically correct for large distances between the regions R_1 and R_2. A more careful investigation of the conditions under which eq. (97) holds will be given later by Haag [9]).

4.4. THE ASYMPTOTIC BEHAVIOUR OF THE WAVE FUNCTIONS

The interaction energy in the Hamiltonian (4) vanishes exponentially (according to (3) and (4)) with the distances between the particles concerned. Therefore, at large distance between the particles or compound states the different parts of the total system behave as if the other parts were not present. This leads to the normal quantal behaviour, if asymptotically there are no product states that contain Φ_{Dip} as factor. All other states of the sector $\binom{N+\vartheta}{V}$ including Φ_0 are special solutions of the Schrödinger equation leading to periodical dependence on time of the type $\Phi(t) = \Phi(0)\mathrm{e}^{-iEt}$.

If, however, asymptotically product states occur containing Φ_{Dip} as factor, the behaviour of the system is different. Eq. (42) shows that Φ_{Dip} acts as a source that produces continuously the state Φ_0, and the same is true for a product state containing Φ_{Dip} as factor. Therefore, if the eigenfunction includes parts that asymptotically are product states containing Φ_{Dip} as factor, these parts will lead to a continuous production of product states containing Φ_0 as factor. The result may be a linear increase in time of such product states with Φ_0 as in (42); or, in a stationary solution as in (70), a linear increase with distance from the scattering center, i.e. a contribution of the type

$$\Phi_0 \frac{\alpha+\beta r}{r} e^{\pm ikr}.$$

Therefore the total Hilbert space can be divided into two parts. Hilbert space I comprises all state vectors represented by eigenfunctions that contain asymptotically no product states with Φ_{Dip} as factor. Hilbert space II contains the rest. The eigenfunctions of Hilbert space I behave asymptotically like eigenfunctions in ordinary quantum mechanics; in momentum space these eigenfunctions have only simple poles at the critical points corresponding to discrete stationary states. The eigenfunctions of Hilbert space II can have double poles in momentum space and can asymptotically behave as $\Phi_0[(\alpha+\beta r)/r]\, e^{\pm ikr}$. The asymptotic parts of the eigenfunctions in Hilbert space I can be interpreted in the usual manner and therefore be used for the description of real phenomena. The local behaviour of these eigenfunctions, however, cannot be interpreted, since the contributions from the states $\varphi(\mathbf{k}_1 \cdots)\Phi_{\text{Dip}}$ would eventually lead to negative probabilities which have no meaning. Therefore the theory is essentially an S-matrix theory, in which a local Hamiltonian does not exist and a local description cannot be given.

5. The higher sectors of the Lee-model

5.1. UNITARITY OF THE S-MATRIX IN THE SECTORS $\binom{N+z\theta}{V+(z-1)\theta}$.

The Hilbert space of the sector $\binom{N+z\theta}{V+(z-1)\theta}$ is formed by the state vectors that represent 'product-states', consisting of z θ-particles and one N-particle, or $(z-1)$ θ-particles and one V-particle. Instead of using these state vectors one can define the same Hilbert space by another set of vectors, in which each 'product-state' is formed by one state of the sector $\binom{N+\theta}{V}$ and $(z-1)$ θ-particles. In the following calculations we denote the eigenfunctions of the θ-particles by their momenta $\mathbf{k}_l$, and the state of the $\binom{N+\theta}{V}$-system by $\mathfrak{g}$, where $\mathfrak{g}$ means the momentum of the incident θ-particle in the continuous spectrum, while $\mathfrak{g} = 0$ and $\mathfrak{g} = D$ denotes the states Φ_0 and Φ_{Dip}. Therefore

a general state vector in the sector $\binom{N+z\theta}{V+(z-1)\theta}$ can be characterized by $(\mathbf{k}_l, \mathfrak{g})$ or by any linear combination of such terms. A state $\Phi_{\mathbf{k}_l \mathfrak{g}}$ would be a stationary state of the system, if there were no interactions between the θ-particles and the system $\binom{N+\theta}{V}$. When we try to find a solution of the Schrödinger equation

$$H\Psi = \Psi E \tag{98}$$

that describes the scattering of z θ-particles by an N-particle or of $(z-1)$ θ-particles by a V-particle, we can characterize the state Ψ by the momenta $\mathbf{k}'_l$, $\mathfrak{g}'$ of the incoming particles.

Remembering that, according to section 3, a certain admixture of states $(\mathbf{k}'_l, 0)$ may be necessary to get a scattering state of Hilbert space I, we denote by $(\mathbf{k}'_l, \mathfrak{g}')$ any linear superposition of incident waves. The eigenfunctions of these states shall be expressed in terms of the variables $(\mathbf{k}'', \mathfrak{g}'')$. Therefore we can write the eigenfunction as transformation matrix in the form

$$\Psi_{\mathbf{k}'\mathfrak{g}'}\rangle = \Phi_{\mathbf{k}''\mathfrak{g}''}\rangle \cdot {}^{\mathbf{k}''\mathfrak{g}''}\Psi_{\mathbf{k}'\mathfrak{g}'}. \tag{99}$$

If $\Phi^{\mathbf{k}\mathfrak{g}}$ is the set of state vectors which is inverse to the set $\Phi_{\mathbf{k}\mathfrak{g}}$ i.e. if

$$\langle \Phi^{\mathbf{k}'\mathfrak{g}'} | \Phi_{\mathbf{k}''\mathfrak{g}''}\rangle = \delta(\mathbf{k}'\mathbf{k}'')\delta(\mathfrak{g}'\mathfrak{g}'') = {}^{\mathbf{k}'\mathfrak{g}'}1_{\mathbf{k}''\mathfrak{g}''}, \tag{100}$$

then we have

$${}^{\mathbf{k}''\mathfrak{g}''}\Psi_{\mathbf{k}'\mathfrak{g}'} = \langle \Phi^{\mathbf{k}''\mathfrak{g}''} | \Psi_{\mathbf{k}'\mathfrak{g}'}\rangle. \tag{101}$$

The Schrödinger equation (98) can be written as

$${}^{\mathbf{k}''\mathfrak{g}''}H_{\mathbf{k}'''\mathfrak{g}'''}\,{}^{\mathbf{k}'''\mathfrak{g}'''}\Psi_{\mathbf{k}'\mathfrak{g}'} = {}^{\mathbf{k}''\mathfrak{g}''}\Psi_{\mathbf{k}'\mathfrak{g}'} \cdot E_{\mathbf{k}'\mathfrak{g}'}. \tag{102}$$

The Hamiltonian H can be split into one part U which may be called self-energy of the particles θ and $\binom{N+\theta}{V}$, and another part V called interaction. The first part is characterized mathematically by the fact that it contains the factor $\delta(\mathbf{k}''\mathbf{k}')$:

$$H = U+V; \quad {}^{\mathbf{k}''\mathfrak{g}''}U_{\mathbf{k}'\mathfrak{g}'} = \delta(\mathbf{k}''\mathbf{k}')\,{}^{\mathfrak{g}''}u_{\mathfrak{g}'}. \tag{103}$$

The matrix ${}^{\mathfrak{g}''}u_{\mathfrak{g}'}$ consists mainly of diagonal terms representing the energy of the separated θ-particles and the system $\binom{N+\theta}{V}$. But then there is one term off the diagonal corresponding to the constant C in eq. (38) which is due to the fact that Φ_{Dip} is not a solution of the Schrödinger equation. Finally we get

$${}^{\mathfrak{g}''}u_{\mathfrak{g}'} = \delta(\mathfrak{g}''\mathfrak{g}')(\sum\omega_i'' + E_{\mathfrak{g}''}) + \delta(\mathfrak{g}'', 0) \cdot \delta(\mathfrak{g}', \mathrm{D}) \cdot C. \tag{104}$$

Putting

$$\sum\omega_i + E_{\mathfrak{g}} = E_{\mathbf{k},\mathfrak{g}} \tag{105}$$

the Schrödinger equation takes the form

$$(E_{\mathbf{k}''\mathfrak{g}''} - E_{\mathbf{k}'\mathfrak{g}'})\,{}^{\mathbf{k}''\mathfrak{g}''}\Psi_{\mathbf{k}'\mathfrak{g}'} + \delta(\mathfrak{g}'', 0)\,{}^{\mathbf{k}''\mathrm{D}}\Psi_{\mathbf{k}'\mathfrak{g}'} \cdot C + {}^{\mathbf{k}''\mathfrak{g}''}V_{\mathbf{k}'''\mathfrak{g}'''} \cdot {}^{\mathbf{k}'''\mathfrak{g}'''}\Psi_{\mathbf{k}'\mathfrak{g}'} = 0. \tag{106}$$

It follows from (106) that the matrix elements ${}^{k''g''}\Psi_{k'g'}$ generally have a singularity at the point where $E_{k''g''}-E_{k'g'}=0$. This will be a pole of the first order except in one case: If ${}^{k''D}\Psi_{k'g'}$ has at this point a pole of the first order, then ${}^{k''0}\Psi_{k'g'}$ will, according to (106), have a pole of second order at the same point. If however ${}^{k''D}\Psi_{k'g'}$ is regular at the point $E_{k''D}-E_{k'g'}=0$, then ${}^{k''0}\Psi_{k'g'}$ has again a pole of the first order at this point.

Therefore we can characterize the states of Hilbert space I by the condition that ${}^{k''D}\Psi_{k'g'}$ shall be regular at the critical point. If this condition is fulfilled, the wave function Ψ can in the usual manner be written as

$$ {}^{k''g''}\Psi_{k'g'} = {}^{k''g''}1_{k'g'} + \frac{{}^{k''g''}r_{k'g'}}{2\pi i(E_{k'g'}-E_{k''g''}+i\gamma)} \quad (\gamma \to 0), \tag{107} $$

where

$$ \begin{gathered} r = 2\pi i W \Psi \\ [{}^{k''g''}W_{k'g'} = {}^{k''g''}V_{k'g'} + \delta(g'', 0)\delta(g', D)\cdot C]. \end{gathered} \tag{108} $$

The matrix elements ${}^{k''D}r_{k'g'}$ vanish at $E_{k'g'}-E_{k''D}=0$, because otherwise the elements ${}^{k''D}\Psi_{k'g'}$ could not be regular at this point. The scattering matrix

$$ S = 1+R \tag{109} $$

is defined by

$$ {}^{k''g''}R_{k'g'} = \delta(E_{k'g'}-E_{k''g''})\cdot {}^{k''g''}r_{k'g'}. \tag{110} $$

Therefore

$$ {}^{k''D}R_{k'g'} = 0. \tag{111} $$

(The definitions (109) and (110) for the scattering matrix imply that there are no compound states, consisting of one or several θ-particles and the system $\binom{N+\theta}{V}$. If such states exist, eqs. (109) and (110) do not define the scattering matrix in the usual sense, but a matrix connected with its usual form by a certain transformation which will be discussed in § 5.2.)

We can now follow Møller's [6]) proof for the unitarity of the S-matrix. From (108) and its hermitian conjugate we get

$$ \Psi^* r + r^* \Psi = 0. \tag{112} $$

Multiplying this equation with the δ-function in the initial and final energy and replacing Ψ by (107) gives

$$ R^* + R + R^* R = 1 \tag{113} $$

or

$$ S^* S = 1. \tag{114} $$

This formula so far only proves the pseudo-unitarity of the S-matrix. The unitarity, which is essential for the physical interpretation, follows from (114) in connection with (111). The incident waves of the states in

Hilbert space I do not include the states $(\mathbf{k}', \mathrm{D})$. The same is true about the outgoing waves according to (111). Therefore the matrices R and S operate in a Hilbert space with semi-definite metric, since the initial and final states are linear combinations of states of positive norm $(\mathbf{k}', \mathbf{g}')$ with states of norm zero $(\mathbf{k}', 0)$.

The space of semi-definite metric can be constructed by a set of orthogonal vectors; some of them have the norm zero: $g_{ll} = 0$, the others can be normalized to have the norm unity $g_{ll} = 1$. In this case one can define the most general 'orthogonal' transformation by

$$\Phi'_k\rangle = \Phi_l\rangle {}^l a_k \tag{115}$$

where $\Phi'_k\rangle$ and $\Phi_k\rangle$ form two sets of orthogonal vectors.

The $\Phi'_k\rangle$ must fulfil the condition

$$\langle \Phi'_l | \Phi'_k \rangle = ({}^r a_l)^* \, {}^s a_k \cdot g_{rs} = ({}^r a_l)^* \, {}^s a_k \cdot \delta_{rs} \cdot g_{rr} = g'_{lk} = \delta_{lk} \cdot g'_{ll}. \tag{116}$$

If the 'initial' state l has a finite norm and is normalized to $g'_{ll} = 1$, we get

$$\sum_r |{}^r a_l|^2 = 1, \tag{117}$$

where the sum is to be taken over all states r of positive norm only. Writing (114) in components gives for the orthogonal set in the semi-definite metric:

$$\begin{aligned} \delta_k{}^l = {}^l(S^*)_m \, {}^m S_k = {}^l(S^*)^r \, g_{rm} \cdot {}^m S_k = ({}^r S^l)^* \, g_{rr} \, {}^r S_k \\ = ({}^r S_l)^* \, g^{ll} \cdot g_{rr} \, {}^r S_k, \end{aligned} \tag{118}$$

or

$$\sum_r |{}^r S_l|^2 = 1 \tag{119}$$

in analogy to (117), which means the unitarity of the S-matrix.

5.2. DISCRETE STATIONARY STATES IN THE SECTORS $\binom{N+z\theta}{V+(z-1)\theta}$

The foregoing deductions do not prove that states of Hilbert space I can actually be constructed. We have to repeat the calculations of § 3.1 for the higher sectors in order to show the structure of the eigenfunctions. Employing again the notation of § 3.1 we get for the Schrödinger equation

$$\begin{aligned} \varphi(\mathbf{k}_1 \cdots \mathbf{k}_{z-1})(E - m_V - \sum_1^{z-1} \omega_i) &= -\frac{z g_0}{\sqrt{4\pi}} \int \frac{\mathrm{d}^3 k_z \, \varphi(\mathbf{k}_1 \cdots \mathbf{k}_z)}{\sqrt{2\omega_z}}, \\ \varphi(\mathbf{k}_1 \cdots \mathbf{k}_z)(E - \sum_1^z \omega_i) &= -\frac{g_0}{z\sqrt{4\pi}} \cdot \sum_{i=1}^z \frac{\varphi(\mathbf{k}_1 \cdots \mathbf{k}_{i-1} \, \mathbf{k}_{i+1} \cdots \mathbf{k}_z)}{\sqrt{2\omega_i}}. \end{aligned} \tag{120}$$

If $\varphi_0(\mathbf{k}_1 \cdots \mathbf{k}_z)$ is an arbitrary solution of

$$\varphi_0(\mathbf{k}_1 \cdots \mathbf{k}_z)(E - \sum_1^z \omega_i) = 0 \tag{121}$$

one gets from (120)

$$\varphi(\mathbf{k}_1 \cdots \mathbf{k}_{z-1}) h^+(E - \sum_1^{z-1} \omega_i)$$

$$= \frac{1}{4\pi} \int \frac{\mathrm{d}^3 k_z}{\sqrt{2\omega_z}(E - \sum_1^{z} \omega_i + i\gamma)} \sum_{i=1}^{z-1} \frac{\varphi(\mathbf{k}_1 \cdots \mathbf{k}_{i-1} \mathbf{k}_{i+1} \cdots \mathbf{k}_z)}{\sqrt{2\omega_i}} \tag{122}$$

$$- \varphi_{0i}(\mathbf{k}_1 \cdots \mathbf{k}_{z-1}),$$

where

$$\varphi_{0i}(\mathbf{k}_1 \cdots \mathbf{k}_{z-1}) = \frac{z}{g_0 \sqrt{4\pi}} \int \frac{\mathrm{d}^3 k_z \varphi_0(\mathbf{k}_1 \cdots \mathbf{k}_z)}{\sqrt{2\omega_z}}. \tag{123}$$

For the solutions corresponding to states of Hilbert space I we try in analogy to (71) the assumption

$$\varphi(\mathbf{k}_1 \cdots \mathbf{k}_{z-1}) = a(\mathbf{k}_1 \cdots \mathbf{k}_{z-1}) \delta(E - E_0 - \sum_1^{z-1} \omega_i) + \frac{\chi(\mathbf{k}_1 \cdots \mathbf{k}_{z-1})}{E - E_0 - \sum_1^{z-1} \omega_i + i\gamma}. \tag{124}$$

The coefficient $a(\mathbf{k}_1 \cdots \mathbf{k}_{z-1})$ can be determined by the condition that the right hand side of (122) vanishes at the point $E - E_0 - \sum_1^{z-1} \omega_i = 0$; the symmetry of $\varphi(\mathbf{k}_1 \cdots \mathbf{k}_{z-1})$ and $a(\mathbf{k}_1 \cdots \mathbf{k}_{z-1})$ in the momenta $\mathbf{k}_i$ simplifies the elimination of the $a(\mathbf{k}_1 \cdots \mathbf{k}_{z-1})$.

Using the notation $\omega_{ci} = E - E_0 - \sum_1^{z-1} \omega_l + \omega_i$ one defines the function $a(\mathbf{k}_1 \cdots \mathbf{k}_{z-1})$ by

$$\int \mathrm{d}^3 k_{z-1} a(\mathbf{k}_0 \cdots \mathbf{k}_{z-1}) \delta(E - E_0 - \sum_1^{z-1} \omega_\nu)$$

$$= -(E_0 - \omega_{c,\, z-1}) \sqrt{\omega_{c,\, z-1}} \int \frac{\mathrm{d}^3 k_{z-1} \chi(\mathbf{k}_1 \cdots \mathbf{k}_{z-1})}{\sqrt{\omega_{z-1}}(E_0 - \omega_{z-1} + i\gamma)(\omega_{c,\, z-1} - \omega_{z-1} + i\gamma)}. \tag{125}$$

and gets instead of (73)

$$\chi(\mathbf{k}_1 \cdots \mathbf{k}_{z-1})$$

$$= \frac{(E - E_0 - \sum_1^{z-1} \omega_l)^2}{8\pi h^+(E - \sum_1^{z-1} \omega_l)} \sum_1^{z-1} \int \frac{\mathrm{d}^3 k_z \chi(\mathbf{k}_1 \cdots \mathbf{k}_{i-1} \mathbf{k}_{i-1} \cdots \mathbf{k}_z)}{\sqrt{\omega_i \omega_z}(\omega_i - E_0)(\sum_1^{z} \omega_l - E - i\gamma)(\omega_z - E_0 - i\gamma)} \tag{126}$$

$$- \frac{E - E_0 - \sum_1^{z-1} \omega_l}{h^+(E - \sum_1^{z-1} \omega_l)} \cdot \varphi_{0i}(\mathbf{k}_1 \cdots \mathbf{k}_{z-1}).$$

The right hand side is automatically regular at the point $E - \sum_1^{z-1} \omega_l = E_0$, therefore $\chi(\mathbf{k}_1 \cdots \mathbf{k}_{z-1})$ is regular as well.

The eigenfunctions of Hilbert space I are characterized by the fact that

they fulfil not only the equations (120) but also (124) and (126).

If the homogeneous equation of the type (120) leads to discrete stationary states of the sector $\binom{N+(z-1)\theta}{V+(z-2)\theta}$, these states may possibly occur as final states, together with one outgoing θ-particle, in the scattering problem (120) of the sector $\binom{N+z\theta}{V+(z-1)\theta}$. This could be seen in the eigenfunctions $\varphi(\mathbf{k}_1 \cdots \mathbf{k}_{z-1})$ or $\chi(\mathbf{k}_1 \cdots \mathbf{k}_{z-1})$ by the fact, that they have simple poles at the corresponding values of $\mathbf{k}$ or ω. If the energy of the stationary state would be E_S, the simple poles should be at $\omega_i = E - E_S$. In the neighbourhood of the pole say $\omega_1 = E - E_S$ we can write $(\gamma \to 0)$

$$\chi(\mathbf{k}_1 \cdots \mathbf{k}_{z-1}) = \frac{\psi(\mathbf{k}_1;\ \mathbf{k}_2 \cdots \mathbf{k}_{z-1})}{E - E_S - \omega_1 + i\gamma} + \text{smaller terms.} \tag{127}$$

In ordinary space (127) corresponds to an outgoing wave $e^{ik_1 r_1}/r_1$ multiplied by a function of $\mathbf{x}_2 \cdots \mathbf{x}_{z-1}$ and the angles φ_1, ϑ_1 belonging to $\mathbf{x}_1$. When one inserts $\chi(\mathbf{k}_1 \cdots \mathbf{k}_{z-1})$ from (127) into (126) and goes to the limit $\omega_1 \to E - E_S$, one sees that $\psi(\mathbf{k}_1 \mathbf{k}_z \cdots \mathbf{k}_{z-1})$, considered as function of $\mathbf{k}_2 \cdots \mathbf{k}_{z-1}$, must satisfy the homogeneous equation (126) (without the term φ_{0i}) for the number of variables $z-2$ and the total energy E_S.

This is an important result because it shows that only such discrete stationary states of the sector $\binom{N+(z-1)\theta}{V+(z-2)\theta}$ can occur among the final states, which belong to solutions of eq. (126), i.e. to Hilbert space I. If there are discrete stationary dates defined by solutions of (120) but not of (126), these states cannot be created in scattering problems of the higher sectors, if one starts with a solution belonging to Hilbert space I, i.e. a solution of (126).

When one combines the results of § 5.1 and § 5.2 it seems very plausible that the norm of discrete stationary states in Hilbert space I must be positive. It has been shown in § 5.1 that $\sum_r |{}^r S_l|^2 = 1$, where the summation is to be taken over all states $(\mathbf{k}, \mathfrak{g})$ [$(\mathbf{k}, D)$ does not occur] of the same total energy in a Hilbert space with semi-definite metric. If discrete states exist in the lower sectors, the state vectors of the eigenstates in the lower sectors can be expressed as linear combinations of all state vectors of the form $(\mathbf{k}, \mathfrak{g})$, $(\mathbf{k}, 0)$ *and* $(\mathbf{k}, D)$. The transformation leading from $(\mathbf{k}, \mathfrak{g})$, $(\mathbf{k}, 0)$ and $(\mathbf{k}, D)$ to the eigenstates transforms in the subspace of given total energy from the states r of the matrix elements ${}^r S_l$ to the eigenstates of the same energy, but the states $(\mathbf{k}, D)$ do not take part in this transformation, since ${}^{\mathbf{k}'D}R_{\mathbf{k}'\mathfrak{g}'} = 0$. Therefore the transformation carried out on the states r in ${}^r S_l$ in the subspace of given energy takes place within a Hilbert space of semi-definite metric and belongs to the type discussed in (117). Hence the norm of the discrete states should be positive. It should be emphasized, however, that the validity of this argument depends on certain features concerning the analytic behaviour of the wave functions. The subspace of

given energy requires, in the case of a discrete stationary state, that at least one of the momenta $\mathbf{k}_i$ of the particles must be imaginary or complex. We may assume here that the S-matrix is analytic within this region and that for the calculation of the norm the residua around the poles on the imaginary k-axis should be sufficient in the same way as in the ordinary theory in a Hilbert space of positive metric (cf. Møller [6])); but we have to postpone the proof of this assumption to a later detailed discussion of the discrete stationary states.

So far it is not known whether discrete stationary states of the higher sectors exist in the Lee-model. But in the model defined by the non-linear spinor equation (ref. [4])) the existence of discrete stationary states is very probable since the Tamm-Dancoff approximation does lead to such states in Hilbert space I.

The same method which has been used here for discussing the properties of discrete stationary states, can also be applied to prove the following property of the S-matrix:

$$\mathbf{k}_1''\mathbf{k}_2''\cdots\mathbf{k}_n''\mathfrak{g}''S_{\mathbf{k}_1'\mathbf{k}_2'\cdots\mathbf{k}_n'\mathfrak{g}'} = \delta(\mathbf{k}_1''\mathbf{k}_1')^{\mathbf{k}_2''\cdots\mathbf{k}_n''\mathfrak{g}''}S_{\mathbf{k}_2'\cdots\mathbf{k}_n'\mathfrak{g}'} + \text{terms without the factor } \delta(\mathbf{k}_1''\mathbf{k}_1'). \qquad (128)$$

This formula can be interpreted as stating that one particle can pass at a long distance from the scattering centre without disturbing the scattering of the other particles.

5.3. HILBERT SPACES I AND II IN THE OTHER SECTORS

In the foregoing sections the states of Hilbert space I have been distinguished from those of Hilbert space II by their asymptotic behaviour in ordinary space according to the following scheme: The assumption 'only simple poles in momentum space' implies that the asymptotic behaviour in ordinary space is of the form $e^{\pm ikr}/r$ or $e^{-\varkappa r}/r$, if all other variables except r are kept fixed (for the incident waves of course any combination of plane waves may be possible). When the incoming waves describe product-states consisting of separated states of Hilbert space I only, it is always possible, by adding a suitable 'zero-state' (the term with $a(\mathbf{k}_1\cdots\mathbf{k}_{s-1})$ in (124)), to construct a scattering state in Hilbert space I. On the other hand, the outgoing waves of any scattering state in Hilbert space I contain only discrete bound states that belong to Hilbert space I in the corresponding lower sectors. To that extent the states of Hilbert space I form a 'non-combining term system', in spite of the fact that the expansion of the eigenfunctions in terms of the eigenfunctions of the sector $\binom{N+\vartheta}{V}$ does contain the state Φ_{Dip} that belongs to Hilbert space II. For the description of the local behaviour of the eigenfunctions the whole Hilbert space with indefinite metric is needed; but for the description of the asymptotic behaviour a

Hilbert space with semi-definite metric is sufficient. Therefore a physical interpretation of the local behaviour in terms of probabilities cannot be given.

An extension of this general scheme to sectors with several N- or V-particles meets with the difficulty mentioned in § 2.1, that the kinetic energies of the N- and V-particles have been neglected in (2) and (4), or in other words, that the inertia of these particles has been taken as infinite. One can hope to apply the general scheme only if the N- and V-particles can move, so that they are finally either far apart, or bound together in a stationary state. Hence it would be necessary first to improve the Lee-model in this respect and to assume a finite (possibly very big) inertia of the N- and V-particle, before one can apply the general scheme. Though one cannot see any serious difficulty for developing the theory after the change has been made, we will not follow this line here and will confine the calculations to the Lee-model in its original form.

6. Causality

Since the states of Hilbert space I are intended to describe real phenomena with elementary particles the question arises to what extent this description can be called a causal one. The following sections intend only a short discussion of the problems involved; the proper analysis is postponed to a later paper.

6.1. THE FORMAL CRITERIA OF CAUSALITY

Some recent papers [7]) on the properties of the S-matrix use the following formal criterion of causality: If the S-matrix concerns the asymptotic field operators $A_{\text{in}}(\mathbf{x})$ and $A_{\text{out}}(\mathbf{x})$, this matrix is called 'causal', if $A_{\text{in}}(\mathbf{x})$ and $A_{\text{out}}(\mathbf{x})$ can be interpolated by a field operator $A(\mathbf{x})$ which satisfies $[A(\mathbf{x}), A(\mathbf{x}')] = 0$ for space-like distances $\mathbf{x}-\mathbf{x}'$. This formal criterion cannot be applied properly in the case of the Lee-model, since this model is not relativistic. But it can be checked for the nonlinear spinor equation mentioned in the introduction. Here the field operators actually commute for space-like distances, and the same is true in the Lee-model for the operators at a special time $t = \text{const}$. Therefore formally the criterion is fulfilled. But in the papers quoted above it had been tacitly assumed that the operators $A(\mathbf{x})$ operate on the same Hilbert space of positive metric as $A_{\text{in}}(\mathbf{x})$ and $A_{\text{out}}(\mathbf{x})$. In our case of Hilbert space I, however, the asymptotic operators operate in a Hilbert space of semi-definite metric while the field operators operate on the total Hilbert space of indefinite metric. This difference seems to be unimportant for several deductions, for instance of some results in connection with the dispersion relations; but it may be

relevant for others. We do not attempt here an analysis of the difference between the consequences of the two groups of assumptions.

6.2. THE CONTRIBUTION OF THE Φ_0-PRODUCT STATES

A serious deviation from causality seems at first sight to be produced by the necessity to add to the incoming waves some contributions of Φ_0-product states in order to get a scattering state of Hilbert space I. These incoming Φ_0-product waves cannot be seen in the experiments because they do not contribute to any expectation value on account of $\langle \Phi_0 | \Phi_0 \rangle = 0$. But they should already be established before the experiment begins and seem therefore to require the fulfilment of very special conditions by the foregoing events. On the other hand, if the total system, possibly including the measuring apparatus and the observer, is described by a state vector of Hilbert space I, this is true also for any part of the system that is sufficiently separated from the rest to be treated as independent. Therefore these Φ_0-waves are automatically present to the correct amount if the total system has been in an state of Hilbert space I at the beginning. To that extent one does not see any immediate danger concerning the conventional experimental criteria of causality.

Though the Φ_0-product states cannot be observed directly and should be classified as 'virtual' fields, they belong to the whole mathematical context of the theory and will hence indirectly influence the observable quantities. Especially the fact that every discrete stationary state is surrounded by a spherical zero-wave of the type $\Phi_0 \, e^{ikr}/r$ suggests the possibility of long range forces between the compound systems indirectly produced by the virtual waves. In the case of the non-linear spinor equation the Tamm-Dancoff method has actually led to long range forces of the Coulomb type, to the concept of charge and generally to electrodynamics. Whether similar features can be found in the Lee-model has not yet been analysed.

7. Conclusion

The present discussion of the Lee-model had been undertaken to decide the question whether an indefinite metric in Hilbert space can be used for the description of real phenomena. The results of the calculation have shown that the introduction of the indefinite metric through a 'dipole-ghost' does allow a separation of the total Hilbert space into two parts I and II which in a certain sense can be treated as 'non-combining term systems'. The asymptotic parts of the solutions of Hilbert space I can be interpreted and qualitatively be used for the description of real phenomena.

The present analysis concerns only the Lee-model and it is still an open question to what extent the analysis can be carried over to the non-linear

spinor equation used as model for a theory of elementary particles. This latter model has been treated so far exclusively by the new Tamm-Dancoff method. In order to get the connection between the calculations of the present paper and those of the earlier papers one could try, on the one hand, to derive the solutions in the case of the Lee-model from the renormalized equations (62) by means of the new Tamm-Dancoff method; on the other hand one could try to develop new methods of integration for the spinor model leading to representations more similar to those discussed here for the Lee-model. Only after the connection between the two mathematical schemes has been established will it be possible to give a thorough analysis of the mathematical structure of the spinor model.

The problems of causality should perhaps be discussed best for the spinor model since this model is relativistically invariant and does not show those elements of non-locality that have been mentioned in § 2.6 of the present paper for the Lee-model. To what extent the dispersion relations and similar connections are true for the spinor model remains to be seen. In any case this model seems to provide an interesting example for checking those general properties of the S-matrix that have been studied in many recent papers.

References

1) G. Källén and W. Pauli, Mat. Fys. Medd. Dan. Vid. Selsk. **30** (1955) no. 7
2) T. D. Lee, Phys. Rev. **95** (1954) 1329
3) P. A. M. Dirac, Proc. Roy. Soc. A **180** (1942) 1. Compare also W. Pauli, Rev. of Modern Physics **15** (1943) 175
4) W. Heisenberg, Nachr. Gött. Akad. Wiss. (1953) 111; Zs. f. Naturf. **9a** (1954) 292; W. Heisenberg, F. Kortel u. H. Mitter, Zs. f. Naturf. **10a** (1955) 425; W. Heisenberg, Zs. f. Physik **144** (1956) 1; Nachr. Gött. Akad. Wiss (1956) 27; R. Ascoli u. W. Heisenberg, Zs. f. Naturf. **12a** (1957) 177
5) V. Glaser u. G. Källén, Nuclear Physics **2** (1956) 706
6) Chr. Møller, Mat. Fys. Medd. Dan. Vid. Selsk. **23** (1945) no. 1; **24** (1946) no. 19
7) H. Lehmann, K. Symanzik u. W. Zimmermann, Nuovo Cimento (to be published)
8) W. Heisenberg, Zs. f. Naturf. **6a** (1951) 281
9) R. Haag, lecture at the international conference in Lille (June 1957)

Nuclear Physics **4** (1957) 564—578; © *North-Holland Publishing Co., Amsterdam*
Not to be reproduced by photoprint or microfilm without written permission from the publisher

SOME PROPERTIES OF COMBINED PC-TRANSFORMATION AND ASSOCIATED SELECTION RULES

P. ROMAN
Department of Theoretical Physics, University of Manchester

Received 29 April 1957

Abstract: We derive the transformation rules of the creation and annihilation operators of baryon and lepton fields under a combined charge-conjugation and space-reflection operation, and find eigenstates of the corresponding operator. Also properties of the 'squared' operation are studied, giving a distinction between baryon and lepton fields from which some selection rules are derived. π- and K-meson fields are also studied and some consequences for K-decay are investigated. Then, assuming a universal Fermi interaction, it is proved that the number of baryons is conserved if we demand the invariance of the interaction under a combined charge-conjugation and space-reflection transformation. Some selection rules for allowed processes are also studied.

1. Introduction

As a consequence of some experiments [1, 2]) showing definitely the violation of parity conservation in weak interactions, recently considerable interest has arisen with respect to the less stringent PC-transformation, i.e. a transformation composed of a charge conjugation and a subsequent space inversion (see e.g. ref. [3, 4, 5, 6])). In this paper we develop the formal properties of this transformation in more detail, with a view to deriving selection rules for processes governed by weak interactions. In particular, it can be seen that baryon number conservation in Fermi interactions is a consequence of PC invariance.

2. Fermions

2.1. CHARGE CONJUGATION

The field operator of any fermion can be written as

$$\psi = \sum_{\mathbf{p}} a_{\mathbf{p}} u(\mathbf{p})\, e^{i\mathbf{p}\cdot\mathbf{x}} + b^*_{\mathbf{p}} v(\mathbf{p})\, e^{-i\mathbf{p}\cdot\mathbf{x}} \tag{1}$$

where $a_{\mathbf{p}}$ is the annihilation operator for a particle with momentum $\mathbf{p}$, and $b^*_{\mathbf{p}}$ the creation operator for the corresponding antiparticle. The adjoint field is

$$\bar{\psi} = \sum a^*_{\mathbf{p}} \bar{u}(\mathbf{p})\, e^{-i\mathbf{p}\cdot\mathbf{x}} + b_{\mathbf{p}} \bar{v}(\mathbf{p})\, e^{i\mathbf{p}\cdot\mathbf{x}}. \tag{2}$$

The charge conjugation is defined by

$$\psi^{\mathrm{c}} = C\bar{\psi} \tag{2a}$$

where

$$C^{-1}\gamma_\mu C = -\tilde{\gamma}_\mu, \quad C^{-1} = C^*, \quad \tilde{C} = -C. \tag{2b}$$

Further, it is well known that

$$\begin{aligned} u^c &\equiv C\tilde{\bar{u}} = v \\ v^c &\equiv C\tilde{\bar{v}} = u \end{aligned} \tag{3}$$

and therefore from (2)

$$\psi^c = \sum a_{\mathbf{p}}^* v(\mathbf{p})\, e^{-i\mathbf{p}\cdot\mathbf{x}} + b_{\mathbf{p}} u(\mathbf{p})\, e^{i\mathbf{p}\cdot\mathbf{x}}. \tag{4}$$

2.2. INVERSION: THE TWO CLASSES OF FERMIONS

The striking fact that in any observed process the number of baryons minus antibaryons remains unchanged has raised considerable interest for a long time. The first attempt of an explanation is due to Yang and Tiomno[7]). They ascribed definite space-reflection parities to the different fermions and demanded invariance under space reflection. Their argumentation was refined by Votruba [8]). The strongest objection against this standpoint was raised by Wigner *et al.* [9]) and explained very clearly by Shapiro [10]). It consists in the observation that a system composed of a lepton and a baryon (such as the H-atom) would not form any possible representation of the *extended* Lorentz-group (it would transform under a reflection according to $\phi'_{\mathrm{H}} = i\phi_{\mathrm{H}}$). Later the ideas of Yang were indeed dropped and completely different, in fact rather bold considerations were put forward to explain somehow the stability of baryons (see e.g. Lee and Yang [11]) and Ferretti [12])).

Now, after the beautiful experiments performed by Wu *et al.* (see ref. [1, 2])), proving definitely the violation of space-parity in weak interactions, the situation has changed decisively and the question has to be thoroughly re-investigated. In the first place, it is impossible to demand invariance under reflection, in other words, the *extended* Lorentz group (including inversion) is not a symmetry group of Nature. However, as was shown by several authors (see Landau [3]), Salam [6]), Lee and Yang [4])) it is still possible to impose the condition of invariance under a combined PC transformation, i.e. to demand invariance under a charge conjugation followed by a space-inversion. Therefore we re-adopt the view that baryons belong to the 'real' class and leptons to the 'imaginary' class, i.e. baryons are transformed in case of inversion with $\pm\gamma_4$ whereas leptons are transformed with $\pm i\gamma_4$. It is further well known that *for the real class* u and $u^c = v$ have the opposite space-parity (*one transformation with* $+\gamma_4$ *and the other with* $-\gamma_4$) and *for the imaginary class they have the same relative parity.*

Let us first consider the case of a baryon field.

2.3. BARYONS

Performing on (4) the space-inversion transformation, i.e. going over from a right system to a left system ($\mathbf{x} \to -\mathbf{x}$) and transforming the spinors in the proper way as stated above, we obtain with regard to (3)

$$\psi^{PC} = \sum -a_{\mathbf{p}}^{*}\gamma_4 v(\mathbf{p})\, e^{i\mathbf{p}\cdot\mathbf{x}} + b_{\mathbf{p}}\gamma_4 u(\mathbf{p})\, e^{-i\mathbf{p}\cdot\mathbf{x}}. \tag{5}$$

Now both u and v satisfy the Dirac equation

$$\left(\gamma_i p_i + \gamma_4 \frac{E}{c} + mc\right) \begin{matrix} u(\mathbf{p}) \\ \text{or} \\ v(\mathbf{p}) \end{matrix} = 0. \tag{6}$$

Multiplying with γ_4 one finds

$$\left(-\gamma_i p_i + \gamma_4 \frac{E}{c} + mc\right) \begin{matrix} \gamma_4 u(\mathbf{p}) \\ \text{or} \\ \gamma_4 v(\mathbf{p}) \end{matrix} = 0. \tag{7}$$

Comparing (7) with (6) one sees that

$$\begin{aligned} \gamma_4 u(\mathbf{p}) &= u(-\mathbf{p}) \\ \gamma_4 v(\mathbf{p}) &= v(-\mathbf{p}) \end{aligned} \tag{8}$$

Inserting this into (5)

$$\begin{aligned} \psi^{PC} &= \sum -a_{\mathbf{p}}^{*} v(-\mathbf{p})\, e^{i\mathbf{p}\cdot\mathbf{x}} + b_{\mathbf{p}} u(-\mathbf{p})\, e^{-i\mathbf{p}\cdot\mathbf{x}} \\ &= \sum -a_{-\mathbf{p}}^{*} v(\mathbf{p})\, e^{-i\mathbf{p}\cdot\mathbf{x}} + b_{-\mathbf{p}} u(\mathbf{p})\, e^{i\mathbf{p}\cdot\mathbf{x}}. \end{aligned} \tag{9}$$

Comparing this result (9) with (1) we see that the PC transformation amounts in case of a *baryon field* to the following transformation of the creation and annihilation operators:

$$a_{\mathbf{p}} \to \Omega a_{\mathbf{p}} \Omega^{-1} = b_{-\mathbf{p}}, \quad b_{\mathbf{p}}^{*} \to \Omega b_{\mathbf{p}}^{*} \Omega^{-1} = -a_{-\mathbf{p}}^{*}. \tag{10}$$

In a similar fashion (or directly from (10)) we obtain also

$$a_{\mathbf{p}}^{*} \to \Omega a_{\mathbf{p}}^{*} \Omega^{-1} = b_{-\mathbf{p}}^{*}, \quad b_{\mathbf{p}} \to \Omega b_{\mathbf{p}} \Omega^{-1} = -a_{-\mathbf{p}}. \tag{11}$$

Let us investigate now the corresponding transformation of definite physical states. For instance, a one-baryon state with momentum $\mathbf{p}$

$$\phi_{n(\mathbf{p})} = a_{\mathbf{p}}^{*}\phi^0$$

(where ϕ^0 is the vacuum state) behaves as follows:

$$\phi_{n(\mathbf{p})} \to \Omega\phi_{n(\mathbf{p})} = \Omega a_{\mathbf{p}}^{*}\phi^0 = \Omega a_{\mathbf{p}}^{*}\Omega^{-1}\Omega\phi^0 = b_{-\mathbf{p}}^{*}\phi^0 \equiv \phi_{\bar{n}(-\mathbf{p})},$$

that is, *goes over into a one-antibaryon state with opposite momentum.* Similarly,

$$\phi_{\bar{n}(\mathbf{p})} \to \Omega\phi_{\bar{n}(\mathbf{p})} = -\phi_{n(-\mathbf{p})}.$$

One-particle states are therefore no eigenstates of the PC-operation Ω.

But consider e.g.

$$\alpha = \frac{1}{\sqrt{2}}(a_{\mathbf{p}} a_{-\mathbf{p}} - b_{\mathbf{p}} b_{-\mathbf{p}})$$
$$\beta = \frac{1}{\sqrt{2}}(a_{\mathbf{p}} a_{-\mathbf{p}} + b_{\mathbf{p}} b_{-\mathbf{p}}). \tag{12}$$

By (10) and (11) one finds, taking into account the anticommutation rules

$$\{a_{\mathbf{p}},\ a_{-\mathbf{p}}\} = \{b_{\mathbf{p}},\ b_{-\mathbf{p}}\} = 0,$$

that

$$\alpha \to \Omega\alpha\Omega^{-1} = \alpha$$
$$\beta \to \Omega\beta\Omega^{-1} = -\beta. \tag{13}$$

Therefore the symmetric and antisymmetric states composed of a system containing two baryons and another system containing two antibaryons, the particles in each having opposite momenta, will be antisymmetric or symmetric eigenstates of Ω, respectively:

$$\frac{1}{\sqrt{2}}(\phi_{\mathrm{n}(\mathbf{p})\mathrm{n}(-\mathbf{p})} \pm \phi_{\bar{\mathrm{n}}(\mathbf{p})\bar{\mathrm{n}}(-\mathbf{p})}) \to \mp \frac{1}{\sqrt{2}}(\phi_{\mathrm{n}(\mathbf{p})\mathrm{n}(-\mathbf{p})} \pm \phi_{\bar{\mathrm{n}}(\mathbf{p})\bar{\mathrm{n}}(-\mathbf{p})}). \tag{14}$$

2.4. LEPTONS

Now let us turn to the properties of lepton fields. Equation (4) will of course be unchanged, but when performing the inversion we have to multiply *both* terms with $+i\gamma_4$, and therefore we obtain with (8)

$$\psi^{\mathrm{PC}} = \sum i a^*_{-\mathbf{p}} v(\mathbf{p})\, \mathrm{e}^{-i\mathbf{p}\cdot\mathbf{x}} + i b_{-\mathbf{p}} u(\mathbf{p})\, \mathrm{e}^{i\mathbf{p}\cdot\mathbf{x}}. \tag{15}$$

Comparing this with (1),

$$a_{\mathbf{p}} \to \Omega a_{\mathbf{p}} \Omega^{-1} = i b_{-\mathbf{p}}, \quad b^*_{\mathbf{p}} \to \Omega b^*_{\mathbf{p}} \Omega^{-1} = i a^*_{-\mathbf{p}} \tag{16}$$

and similarly

$$a^*_{\mathbf{p}} \to \Omega a^*_{\mathbf{p}} \Omega^{-1} = -i b^*_{\mathbf{p}}, \ b_{\mathbf{p}} \to \Omega b_{\mathbf{p}} \Omega^{-1} = -i a_{-\mathbf{p}}. \tag{17}$$

One-lepton states are again not eigenstates, e.g.

$$\phi_{\mathrm{l}(\mathbf{p})} \to \Omega\phi_{\mathrm{l}(\mathbf{p})} = -i\phi_{\bar{\mathrm{l}}(-\mathbf{p})}.$$

Here the α and β combinations (12) behave also in an opposite way: one finds indeed

$$\alpha \to \Omega\alpha\Omega^{-1} = -\alpha$$
$$\beta \to \Omega\beta\Omega^{-1} = \beta \tag{18}$$

and therefore

$$\frac{1}{\sqrt{2}}(\phi_{\mathrm{l}(\mathbf{p})\mathrm{l}(-\mathbf{p})} \pm \phi_{\bar{\mathrm{l}}(\mathbf{p})\bar{\mathrm{l}}(-\mathbf{p})}) \to \pm \frac{1}{\sqrt{2}}(\phi_{\mathrm{l}(\mathbf{p})\mathrm{l}(-\mathbf{p})} \pm \phi_{\bar{\mathrm{l}}(\mathbf{p})\bar{\mathrm{l}}(-\mathbf{p})}). \tag{19}$$

One can also investigate 'mixed' composed states and find e.g.

$$\frac{1}{\sqrt{2}}(\phi_{n(\mathbf{p})l(\mathbf{p})} \pm \phi_{\bar{n}(-\mathbf{p})\bar{l}(-\mathbf{p})}) \to \mp i \frac{1}{\sqrt{2}}(\phi_{n(\mathbf{p})l(\mathbf{p})} \pm \phi_{\bar{n}(-\mathbf{p})\bar{l}(-\mathbf{p})}). \tag{20}$$

2.5. SELECTION RULES

More interesting is, however, the investigation of a 'squared' PC-transformation, i.e. the properties of the operator Ω^2. One easily obtains with the aid of eqs. (10, 11) and eqs. (16, 17) respectively, the important fact that *both one-baryon (antibaryon) and one-lepton (antilepton) states are eigenstates of Ω^2, with opposite eigenvalues.* In fact

$$\Omega^2 \phi_n = -\phi_n, \qquad \Omega^2 \phi_{\bar{n}} = -\phi_{\bar{n}} \tag{21}$$

$$\Omega^2 \phi_l = +\phi_l, \qquad \Omega^2 \phi_{\bar{l}} = +\phi_{\bar{l}}. \tag{22}$$

One further finds that also two, three ... baryon, antibaryon, lepton, antilepton and mixed one-baryon — one-lepton etc. states are all eigenstates of Ω^2 alternatingly with eigenvalues ± 1, and one can write for any state

$$\Omega^2 = (-1)^{N+\bar{N}} \tag{23}$$

where N, $\bar{N}$ are the occupation number operators for baryons and antibaryons.

Now we can postulate that all interactions should be invariant under PC-transformation. This imposes by (23) the selection rule

$$N_i + \bar{N}_i = N_f + \bar{N}_f + 2k \tag{23a}$$

where the subscript $_i$ refers to the initial and $_f$ to the final state, and k means any integer. No restrictions follow for the number of leptons involved. This selection rule prohibits a number of processes violating conservation of baryon number, such as

$$\begin{aligned} n &\to l + l + \bar{l} \\ n &\to n + n + \bar{l} \\ n &\to n + \bar{n} + l \\ \bar{n} &\to \bar{n} + n + \bar{l} \end{aligned}$$

but still allows

$$n \to \bar{n} + l + l.$$

For the latter a more detailed discussion is needed (see section 6.1),

3. π-Mesons

The pion field can be written as

$$\begin{aligned} \phi &= \sum p_{\mathbf{p}} e^{i\mathbf{p}\cdot\mathbf{x}} + q^*_{\mathbf{p}} e^{-i\mathbf{p}\cdot\mathbf{x}} \\ \phi^* &= \sum q_{\mathbf{p}} e^{i\mathbf{p}\cdot\mathbf{x}} + p^*_{\mathbf{p}} e^{-i\mathbf{p}\cdot\mathbf{x}} \\ \phi_0 &= \sum s_{\mathbf{p}} e^{i\mathbf{p}\cdot\mathbf{x}} + s^*_{\mathbf{p}} e^{-i\mathbf{p}\cdot\mathbf{x}} \end{aligned} \tag{24}$$

where the operators have the following meaning:

	π^+	π^-	π^0
creation	p^*	q^*	s^*
annihilation	p	q	s

Charge conjugation means

$$\pi^+ \to \pi^-,\ \pi^- \to \pi^+,\ \pi^0 \to \pi^0$$

and can be obtained e.g. by

$$p \to q,\ q \to p,\ s \to s.$$

The charge-conjugate fields of eq. (24) are therefore

$$\begin{aligned} \phi^c &= \sum q_{\mathbf{p}}^{\mathrm{I}} e^{i\mathbf{p}\cdot\mathbf{x}} + p_{\mathbf{p}}^* e^{-i\mathbf{p}\cdot\mathbf{x}} \\ \phi^{*c} &= \sum p_{\mathbf{p}} e^{i\mathbf{p}\cdot\mathbf{x}} + q_{\mathbf{p}}^* e^{-i\mathbf{p}\cdot\mathbf{x}} \\ \phi_0^c &= \sum s_{\mathbf{p}} e^{i\mathbf{p}\cdot\mathbf{x}} + s_{\mathbf{p}}^* e^{-i\mathbf{p}\cdot\mathbf{x}}. \end{aligned} \tag{25}$$

The consecutive inversion is obtained simply by $\mathbf{x} \to -\mathbf{x}$ and by taking into account the pseudoscalar property of π, i.e. by introducing a negative sign. After changing the summation index from p to $-p$, one has finally

$$\begin{aligned} \phi^{PC} &= -\sum q_{-\mathbf{p}} e^{i\mathbf{p}\cdot\mathbf{x}} + p_{-\mathbf{p}}^* e^{-i\mathbf{p}\cdot\mathbf{x}} \\ \phi^{*PC} &= -\sum p_{-\mathbf{p}} e^{i\mathbf{p}\cdot\mathbf{x}} + q_{-\mathbf{p}}^* e^{-i\mathbf{p}\cdot\mathbf{x}} \\ \phi_0^{PC} &= -\sum s_{-\mathbf{p}} e^{i\mathbf{p}\cdot\mathbf{x}} + s_{-\mathbf{p}}^* e^{-i\mathbf{p}\cdot\mathbf{x}}. \end{aligned} \tag{26}$$

Comparing this with eq. (24) we see that for pions the PC-transformation means

$$\begin{aligned} p_{\mathbf{p}} &\to -q_{-\mathbf{p}} & q_{\mathbf{p}}^* &\to -p_{-\mathbf{p}}^* \\ q_{\mathbf{p}} &\to -p_{-\mathbf{p}} & p_{\mathbf{p}}^* &\to -q_{-\mathbf{p}}^* \\ s_{\mathbf{p}} &\to -s_{-\mathbf{p}} & s_{\mathbf{p}}^* &\to -s_{-\mathbf{p}}^*. \end{aligned} \tag{27}$$

One meson states are of course again no eigenstates, e.g.

$$\phi_{\pi^+(\mathbf{p})} \to \Omega\phi_{\pi^+(\mathbf{p})} = -\phi_{\pi^-(-\mathbf{p})}.$$

However, in this case, contrary to the fermions, there are relatively *simple* one-particle eigenstates. So one finds e.g. immediately that

$$\frac{1}{\sqrt{2}}\left(\phi_{\pi^0(\mathbf{p})} \pm \phi_{\pi^0(-\mathbf{p})}\right) \to \mp \frac{1}{\sqrt{2}}\left(\phi_{\pi^0(\mathbf{p})} \pm \phi_{\pi^0(-\mathbf{p})}\right) \tag{28}$$

and

$$\frac{1}{\sqrt{2}}\left(\phi_{\pi^+(\mathbf{p})} \pm \phi_{\pi^-(-\mathbf{p})}\right) \to \mp \frac{1}{\sqrt{2}}\left(\phi_{\pi^+(\mathbf{p})} \pm \phi_{\pi^-(-\mathbf{p})}\right). \tag{29}$$

We mention also that here, of course, we have always

$$\Omega^2 = +1. \tag{30}$$

4. K-Mesons

4.1. TRANSFORMATION PROPERTIES

The K-meson field can be described by

$$\varphi = \sum a_{\mathbf{p}} u\, e^{i\mathbf{p}\cdot\mathbf{x}} + b^*_{\mathbf{p}} v\, e^{-i\mathbf{p}\cdot\mathbf{x}} + c_{\mathbf{p}} v\, e^{i\mathbf{p}\cdot\mathbf{x}} + d^*_{\mathbf{p}} u\, e^{-i\mathbf{p}\cdot\mathbf{x}}$$
$$\varphi^* = \sum a^*_{\mathbf{p}} u^*\, e^{-i\mathbf{p}\cdot\mathbf{x}} + b_{\mathbf{p}} v^*\, e^{i\mathbf{p}\cdot\mathbf{x}} + c^*_{\mathbf{p}} v^*\, e^{-i\mathbf{p}\cdot\mathbf{x}} + d_{\mathbf{p}} u^*\, e^{i\mathbf{p}\cdot\mathbf{x}} \qquad (31)$$

where the meaning of the operators is

	K^+	K^0	K^-	$\overline{K}^0$
creation	a^*	c^*	b^*	d^*
annihilation	a	c	b	d

(K^+, K^0) and $(K^-, \overline{K}^0)$ are understood, as usually, to be distinguishable particles and antiparticles, forming in isobaric space a two-component spinor. The functions u and v in eq. (31) are the corresponding isospinors, depending only on isobaric variables, u referring, say, to isospin $+\frac{1}{2}$ and v to isospin $-\frac{1}{2}$.

Charge conjugation means

$$K^+ \to K^-,\ K^0 \to \overline{K}^0,$$

which is achieved by

$$a \to b,\ c \to d \text{ etc.},$$

and, therefore, from (31),

$$\varphi^c = \sum b_{\mathbf{p}} u\, e^{i\mathbf{p}\cdot\mathbf{x}} + a^*_{\mathbf{p}} v\, e^{-i\mathbf{p}\cdot\mathbf{x}} + d_{\mathbf{p}} v\, e^{i\mathbf{p}\cdot\mathbf{x}} + c^*_{\mathbf{p}} u\, e^{-i\mathbf{p}\cdot\mathbf{x}}$$

and similarly for φ^{*c}.

The subsequent inversion yields, if considering the K to be a pseudoscalar or scalar, respectively,

$$\varphi^{PC} = \mp \sum b_{-\mathbf{p}} u\, e^{i\mathbf{p}\cdot\mathbf{x}} + a^*_{-\mathbf{p}} v\, e^{-i\mathbf{p}\cdot\mathbf{x}} + d_{-\mathbf{p}} v\, e^{i\mathbf{p}\cdot\mathbf{x}} + c^*_{-\mathbf{p}} u\, e^{-i\mathbf{p}\cdot\mathbf{x}} \qquad (32)$$

Comparison with (31) shows that

$$a_{\mathbf{p}} \to \mp b_{-\mathbf{p}}, \quad c_{\mathbf{p}} \to \mp d_{-\mathbf{p}}$$
$$b^*_{\mathbf{p}} \to \mp a^*_{-\mathbf{p}}, \quad d^*_{\mathbf{p}} \to \mp c^*_{-\mathbf{p}} \qquad (33a)$$

and, similarly,

$$a^*_{\mathbf{p}} \to \mp b^*_{-\mathbf{p}}, \quad c^*_{\mathbf{p}} \to \mp d^*_{-\mathbf{p}}$$
$$b_{\mathbf{p}} \to \mp a_{-\mathbf{p}}, \quad d_{\mathbf{p}} \to \mp c_{-\mathbf{p}}. \qquad (33b)$$

An important eigenstate is the linear combination of a K^0 with momentum $\mathbf{p}$ and a $\overline{K}^0$ with opposite momentum. In fact,

$$\frac{1}{\sqrt{2}}(\phi_{K^0(\mathbf{p})} \pm \phi_{\overline{K}^0(-\mathbf{p})}) \to \begin{matrix} P: \mp \\ S: \pm \end{matrix} \frac{1}{\sqrt{2}}(\phi_{K^0(\mathbf{p})} \pm \phi_{\overline{K}^0(-\mathbf{p})}) \qquad (34)$$

and, similarly, for the superposition of $K^+(\mathbf{p})$ with $K^-(-\mathbf{p})$.

4.2. K-DECAY

The decay

$$\theta^0 \to \pi^+ + \pi^- \tag{35}$$

was frequently observed. Now, in the centre-of-mass system, the final state is (for a decay at rest)

$$\phi_{\pi^+(\mathbf{p})\pi^-(-\mathbf{p})} = p^*_{\mathbf{p}} q^*_{-\mathbf{p}} \phi^0.$$

With (27) one finds immediately that this is an eigenstate of Ω with the eigenvalue $+1$. Therefore, assuming conservation of Ω in any process, the initial state has to be also an eigenstate with $\Omega = 1$. The superposition

$$\phi_{\theta_1} \equiv \frac{1}{\sqrt{2}} (\phi_{K^0(\mathbf{p})} - \phi_{\overline{K}^0(-\mathbf{p})}) \tag{36}$$

has just this property (for pseudoscalar K) as seen from (34). Therefore the θ^0 state undergoing the decay (35) is just this superposition.

One can now understand why a *three-particle decay of uncharged K-mesons* never was observed. The final state $\pi^+ + \pi^- + \pi^0$ is (in the rest-system of the π^0, say) of the type

$$\phi_{3\pi} = p^*_{\mathbf{p}} q^*_{-\mathbf{p}} s^*_0 \phi^0.$$

This is also an eigenstate of Ω, *but belonging to the eigenvalue* $\Omega = -1$. Therefore state (36) cannot disintegrate in this fashion. Of course the superposition

$$\phi_{\theta_2} \equiv \frac{1}{\sqrt{2}} (\phi_{K^0(\mathbf{p})} + \phi_{\overline{K}^0(-\mathbf{p})}) \tag{37}$$

can very well undergo a three-pion decay. But, because of the smaller available phase-volume, this has a smaller probability. Further, in an actual experiment, a beam of 'pure' K^0's is produced, which of course can be written as a superposition of θ_1 and θ_2:

$$\phi_{K^0} = \frac{1}{\sqrt{2}} (\phi_{\theta_1} + \phi_{\theta_2}).$$

But from this wave packet first the ϕ_{θ_1} will rapidly decay and one could only observe the 3π-decay when the θ_2-part is predominant. As one has generally only weak beams, this will hardly be detectable, the less so if θ_2 has also an other decay-channel (e.g. into μ^+ and μ^-, which is, as is easily verified, not possible for θ_1).

5. Transformation of Fermi Interaction

In the following sections we will treat the case of four interacting fermion fields in more detail. For this purpose it is more convenient to work in configuration space. We shall denote any baryon field by the field operator

ψ_n and any lepton field by ψ_l. The charge-conjugate field will be, as in general, identified with the corresponding antiparticle field † and thus

$$\psi_{\bar{n}} = \psi_n^c, \ \psi_{\bar{l}} = \psi_l^c, \ \bar{\psi}_{\bar{n}} = \overline{\psi_n^c}, \ \bar{\psi}_{\bar{l}} = \overline{\psi_l^c} \tag{38}$$

where

$$\psi^c = C\bar{\psi}, \ \overline{\psi^c} = \bar{\psi}^c = (C^{-1}\psi)^{\sim}. \tag{38a}$$

Now determine the behaviour of the fields under the combined PC-transformation. Following the suggestions of section 2.2, we obtain the following transformation rules:

$$\begin{aligned} &\psi_n \to \gamma_4 \psi_{\bar{n}} && \bar{\psi}_n \to \bar{\psi}_{\bar{n}} \gamma_4 \\ &\psi_{\bar{n}} \to -\gamma_4 \psi_n && \bar{\psi}_{\bar{n}} \to -\bar{\psi}_n \gamma_4 \\ &\psi_l \to i\gamma_4 \psi_{\bar{l}} && \bar{\psi}_l \to -i\bar{\psi}_{\bar{l}} \gamma_4 \\ &\psi_{\bar{l}} \to i\gamma_4 \psi_l && \bar{\psi}_{\bar{l}} \to -i\bar{\psi}_l \gamma_4 . \end{aligned} \tag{39}$$

(Remember that inversion and charge conjugation as well are interchangeable with adjunction.) Forgetting all we said in the preceding, we could also start from (39), *taking it as the definition of the PC transformation.*

Now the most general Hermitian Fermi interaction between any four Dirac fields has the form

$$L = \bar{\psi}_a \Gamma_r \psi_b \bar{\psi}_c \Gamma_s \psi_d + \psi_d^* \Gamma_s^* \bar{\psi}_c^* \psi_b^* \Gamma_r^* \bar{\psi}_a^* . \tag{40}$$

Here a, b, c, d refer either to particles or to antiparticles and we have chosen the matrices Γ_r in the following way

TABLE 1

Type	r	Γ_r
S	1	1
P	2	γ_5
A	3	$i\gamma_5\gamma_\mu$
V	4	γ_μ
T	5	$1/2i(\gamma_\mu\gamma_\nu - \gamma_\nu\gamma_\mu)$
T′	6	$1/2i(\gamma_\mu\gamma_\nu - \gamma_\nu\gamma_\mu)\gamma_5$

Of course, in (40) summation over the components of Γ_r and Γ_s is understood (tensor product).

The second term in (40) can be rewritten in a more advantageous way:

$$\psi_d^* \Gamma_s^* \bar{\psi}_c^* \psi_b^* \Gamma_r^* \bar{\psi}_a^* = \bar{\psi}_d \gamma_4 \Gamma_s^* \gamma_4 \psi_c \bar{\psi}_b \gamma_4 \Gamma_r^* \gamma_4 \psi_a = \omega_r \omega_s \bar{\psi}_d \Gamma_s \psi_c \bar{\psi}_b \Gamma_r \psi_a$$

where the ω_r are defined by

$$\gamma_4 \Gamma_r^* = \omega_r \Gamma_r \gamma_4 .$$

With help of the definitions and numerical annotation of table 1 one finds immediately for the possible combinations (see below)

$$\omega_r \omega_s = (-1)^{r+s}$$

† We do not adopt the two-component theory of the neutrino.

and therefore eq. (40) can be written

$$L = \bar{\psi}_a \Gamma_r \psi_b \bar{\psi}_c \Gamma_s \psi_d + (-1)^{r+s} \bar{\psi}_d \Gamma_s \psi_c \bar{\psi}_b \Gamma_r \psi_a . \tag{40a}$$

Let us introduce a simplification in notation. Define

$$X^r_{ab} \equiv \bar{\psi}_a \Gamma_r \psi_b \text{ etc.;} \tag{41}$$

we then have

$$L = X^r_{ab} X^s_{cd} + (-1)^{r+s} X^s_{dc} X^r_{ba} . \tag{42}$$

As we did not choose, as is usually done, $r = s$, this interaction will not in general be inversion-invariant and thus we allowed for parity violation. But so as to ensure invariance under the *restricted* Lorentz-group, some restrictions are of course necessary: e.g. one cannot combine a scalar and a vector, etc. Anyway, the eleven possibilities encountered are

Group I	S S	$(r = 1, s = 1)$
	S P	$(r = 1, s = 2)$
	P S	$(r = 2, s = 1)$
	P P	$(r = 2, s = 2)$
Group II	A A	$(r = 3, s = 3)$
	A V	$(r = 3, s = 4)$
	V A	$(r = 4, s = 3)$
	V V	$(r = 4, s = 4)$
Group III	T T	$(r = 5, s = 5)$
	T T′	$(r = 5, s = 6)$
	T′T	$(r = 6, s = 5)$

The interaction (42) is a little ambiguous in so far as the order of the four fermion fields is not fixed. But this can be remedied by making use of Michel's theorem [13]) according to which any permutation of the fields is equivalent with a suitably chosen linear combination of all possible interaction types, the order of the fields taken in a fixed (but arbitrary) manner. (Of course, instead of the 5 possible interactions in the older parity conserving theory we have now to sum over the 11 possibilities listed above.) This will be understood throughout.

Now we are going to calculate the change of the interaction (42) under the combined PC-transformation (39). Using the definitions (41) and those of table 1, one finds immediately for S, A and T-types the transformations listed in table 2, and for P, V and T′ the same changes but with opposite sign. (To save space we have written symbolically simply (ab) instead of X_{ab}, and, similarly for X'_{ab}, the transformed quantity). The values listed are symbolical also in the sense that in the A, V, T-case they refer to the spatial part; the time-components carry an opposite sign, but evidently this will cause no confusion in the following.

TABLE 2

X_{ab}	X'_{ab}	X_{ab}	X'_{ab}
(nn)	$(\bar{n}\bar{n})$	(nl)	$i(\bar{n}\bar{l})$
$(n\bar{n})$	$-(\bar{n}n)$	$(n\bar{l})$	$i(\bar{n}l)$
$(\bar{n}n)$	$-(n\bar{n})$	$(\bar{n}l)$	$-i(n\bar{l})$
$(\bar{n}\bar{n})$	(nn)	$(\bar{n}\bar{l})$	$-i(nl)$
(ll)	$(\bar{l}\bar{l})$	(ln)	$-i(l\bar{n})$
$(l\bar{l})$	$(\bar{l}l)$	$(l\bar{n})$	$i(\bar{l}n)$
$(\bar{l}l)$	$(l\bar{l})$	$(\bar{l}n)$	$-i(l\bar{n})$
$(\bar{l}\bar{l})$	(ll)	$(\bar{l}\bar{n})$	$i(ln)$

Comprising all possibilities into one formula,

$$X'^{r}_{ab} = (-1)^{r-1}\gamma(a, b)X^{r}_{ab} \tag{43}$$

where $\gamma(a, b)$ is ± 1 or $\pm i$, according to table 2.

Now we are prepared to calculate in complete generality the *transformed interaction*. By making repeatedly use of (43) one obtains from (42) by a straightforward calculation

$$L' = \alpha[(-1)^{r+s}X^{r}_{\bar{a}b}X^{s}_{\bar{c}d} + X^{s}_{\bar{d}\bar{c}}X^{r}_{\bar{b}\bar{a}}] \tag{44}$$

with

$$\alpha = \gamma(a, b)\cdot\gamma(c, d) \tag{44a}$$

As we demand invariance under the combined PC-transformation (39), *only those interactions are allowed, for which* (44) *and* (42) *are identical.*

To compare eq. (44) and eq. (42), some more or less familiar connections between X^{r}_{ab} and $X^{r}_{\bar{a}\bar{b}}$ etc. have to be taken into account. For convenience we summarise them here.

As a consequence of eqs (38) and (2*b*) we have

$$\bar{\psi}_a = -\tilde{\psi}_a{}^c C^{-1}, \quad \psi_b = C\bar{\tilde{\psi}}_b{}^c \tag{45}$$

and therefore e.g.

$$\bar{\psi}_a\psi_b = (-\tilde{\psi}_a{}^c C^{-1})(C\bar{\tilde{\psi}}_b{}^c) = -\tilde{\psi}_a{}^c\bar{\tilde{\psi}}_b{}^c = -(\bar{\psi}_b{}^c\psi_a{}^c)\tilde{}\,.$$

Now we may either assume that all fermion fields anticommute, or that *identical fermion fields anticommute, but different fermion fields commute.* In view of the conclusions which will be reached in sections 6.1 and 6.2, we shall only develop in detail the consequences of the latter assumption. We then have

$$-(\bar{\psi}^c_{b_\alpha}\psi^c_{a_\alpha})\tilde{} = \Delta_{ab}(\psi^c_{a_\alpha}\bar{\psi}^c_{b_\alpha}) = \Delta_{ab}\bar{\psi}^c_{b_\alpha}\psi^c_{a_\alpha} = \Delta_{ab}\bar{\psi}_b{}^c\psi_a{}^c$$

where $\Delta_{ab} = +1$ if $a = b$, and $\Delta_{ab} = -1$ if $a \neq b$.

(We have suppressed the (infinite) value of the singular S-function, which amounts, as is well known, to the subtraction of the vacuum value. Thus L has to be understood as the N-product of the operators involved.) So we have obtained (applying the definitions (38))

$$X^{\mathbf{1}}_{\bar{\mathbf{b}}\bar{\mathbf{a}}} \equiv \bar{\psi}_{\bar{\mathbf{b}}}\psi_{\bar{\mathbf{a}}} = \Delta_{\mathbf{ab}}\bar{\psi}_{\mathbf{a}}\psi_{\mathbf{b}} = \Delta_{\mathbf{ab}}X^{\mathbf{1}}_{\mathbf{ab}}.$$

The same applies not only to the S-type now considered but also to P and A; and for V, T and T′ one has a minus sign. Thus, summing up

$$X^{r}_{\bar{\mathbf{b}}\bar{\mathbf{a}}} = \Delta_{\mathbf{ab}}\varepsilon(r)X^{r}_{\mathbf{ab}}, \tag{46}$$

$$\begin{aligned}\varepsilon(r) &= +1 \text{ for } r = 1,\ 2,\ 3\\ \varepsilon(r) &= -1 \text{ for } r = 4,\ 5,\ 6.\end{aligned} \tag{46a}$$

Note carefully that this formula holds only if *both* a and b are particles *or* antiparticles. In the 'mixed' case we have, however, by making use again of Eq. (45) and the anticommutation or commutation law:

$$\begin{aligned}\bar{\psi}_{\mathbf{a}}\psi_{\mathbf{b}^c} &= \bar{\psi}_{\mathbf{a}}C\bar{\bar{\psi}}_{\mathbf{b}} = -\tilde{\psi}_{\mathbf{a}^c}C^{-1}C\bar{\bar{\psi}}_{\mathbf{b}} = -(\bar{\psi}_{\mathbf{b}_\alpha}\psi^{c}_{\mathbf{a}_\alpha})^{\sim}\\ &= \Delta_{\mathbf{ab}}(\psi^{c}_{\mathbf{a}_\alpha}\bar{\psi}_{\mathbf{b}_\alpha})^{\sim} = \Delta_{\mathbf{ab}}\bar{\psi}_{\mathbf{b}_\alpha}\psi^{c}_{\mathbf{a}_\alpha} = \Delta_{\mathbf{ab}}\bar{\psi}_{\mathbf{b}}\psi_{\mathbf{a}^c}\end{aligned}$$

or, in our notation,

$$X^{\mathbf{1}}_{\mathbf{ab}} = \Delta_{\mathbf{ab}}X^{\mathbf{1}}_{\bar{\mathbf{b}}\bar{\mathbf{a}}}.$$

The same holds again for P and A, and with opposite sign for V, T and T′. Therefore

$$X^{r}_{\mathbf{a}\bar{\mathbf{b}}} = \Delta_{\mathbf{ab}}\varepsilon(r)X^{r}_{\bar{\mathbf{b}}\bar{\mathbf{a}}}, \tag{47}$$

where $\varepsilon(r)$ has again the same values as in eq. (46*a*). Note finally that $X_{\mathbf{a}\bar{\mathbf{b}}}$ is 'genuinely' different from (not proportional to) $X_{\bar{\mathbf{a}}\mathbf{b}}$.

Similar formulae hold if we would assume that *all* fermion fields anticommute.

We are now completely prepared to investigate the selection rules associated with the demanded invariance under (39). This we shall do in the next two sections.

6. Selection Rules

6.1. FORBIDDEN PROCESSES

(a) Consider first of all the decay of a baryon into three leptons, e.g.

$$\mathrm{n} \to \mathrm{l}+\mathrm{l}+\bar{\mathrm{l}}. \tag{48}$$

For this process the interaction (42) is

$$L = X^{r}_{\mathrm{ln}}X^{s}_{\mathrm{ll}} + (-1)^{r+s}X^{s}_{\mathrm{ll}}X^{r}_{\mathrm{nl}}. \tag{49}$$

Here we obtain with table 2

$$\gamma(\mathrm{l},\ \mathrm{n}) = -i, \qquad \gamma(\mathrm{l},\ \mathrm{l}) = +1,$$

and therefore, with (44*a*), $\alpha = -i$. We then have, with (44),

$$L' = -i[(-1)^{r+s}X^{r}_{\bar{\mathrm{l}}\mathrm{n}}X^{s}_{\mathrm{ll}} + X^{s}_{\bar{\mathrm{l}}\mathrm{l}}X^{r}_{\mathrm{nl}}],$$

which can be written, with the help of eq. (46),

$$L' = -i\varepsilon(r)\varepsilon(s)\Delta_{nl}(-1)^{r+s}[X^r_{nl}X^s_{ll}+(-1)^{r+s}X^s_{ll}X^r_{ln}]. \tag{50}$$

As the ε-functions defined by eq. (46*a*) are always real, eq. (50) can never be identical with eq. (49) and therefore process (48) is *strictly forbidden.*

(b) Now investigate the more 'dangerous' process

$$n \to \bar{n}+l+l. \tag{51}$$

Here

$$L = X^r_{\bar{n}n}X^s_{l\bar{l}}+(-1)^{r+s}X^s_{\bar{l}l}X^r_{n\bar{n}}. \tag{52}$$

Here we have $\alpha = -1$ and thus by (44)

$$L' = -(X^s_{l\bar{l}}X^r_{\bar{n}n}+(-1)^{r+s}X^r_{n\bar{n}}X^s_{\bar{l}l}) = -L. \tag{53}$$

The process is again *strictly forbidden.*

In a similar fashion one finds that the processes

$$n \to n+\bar{n}+l$$
$$\bar{n} \to \bar{n}+n+\bar{l}$$
$$\bar{n} \to \bar{n}+\bar{n}+l$$

are also prohibited. A few other processes, not treated above, such as $n \to l+l+l$, are already excluded by the more general conservation rule of fermion-number, according to Konopinski [14, 15]).

Summing up we see that *all 'unwanted' processes, in which the number of baryons minus antibaryons would change, are strictly forbidden.* We emphasize that this is a consequence of *only two assumptions*: (i) PC-invariance, (ii) the postulate regarding the baryons and leptons belonging to different classes with respect to inversion. On the other hand, as is easily seen, the forbiddenness of the unwanted processes is *independent* of any assumption concerning the commutability or anticommutability of non-identical fermion fields.

6.2. ALLOWED PROCESSES

Consider first the decay of μ-meson. According to more recent experimental evidence, it is most probable that the μ^- is the 'particle' and μ^+ the anti-particle. Thus, by Konopinski's rule,

$$\mu^- \to e^-+\nu+\bar{\nu}. \tag{54}$$

The interaction reads

$$L = X^r_{e\nu}X^s_{\nu\mu}+(-1)^{r+s}X^s_{\mu\nu}X^r_{\nu e}. \tag{55}$$

Here $\alpha = 1$ and with (44) and also (46)

$$\begin{aligned} L' &= (-1)^{r+s}X^r_{\bar{e}\nu}X^s_{\bar{\nu}\bar{\mu}}+X^s_{\bar{\mu}\nu}X^r_{\bar{\nu}\bar{e}} \\ &= \varepsilon(r)\varepsilon(s)(X^s_{\nu\mu}X^r_{e\nu}+(-1)^{r+s}X^r_{\nu e}X^s_{\mu\nu}). \end{aligned} \tag{56}$$

Comparing this with eq. (55) one finds for the invariance condition

$$\varepsilon(r)\varepsilon(s) = +1. \tag{57}$$

This involves, as one easily finds, that

SS, PP, SP, PS, VV, AA, TT, TT', T'T

are all *possible*, while

VA and AV

are *excluded*.

Now, in fact, the recent experimental results of Lederman *et al.* [2]) show that μ^--decay is exactly described by a parity-violating mixed interaction, and ours are just interactions of that type.

As an other example, let us investigate ordinary β-decay:

$$\mathrm{n} \to \mathrm{p} + \mathrm{e}^- + \bar{\nu}. \tag{58}$$

Here

$$L = X^r_{\mathrm{pn}} X^s_{\mathrm{e}\nu} + (-1)^{r+s} X^s_{\mathrm{e}\nu} X^r_{\mathrm{np}}.$$

We have again $\alpha = 1$ and one obtains finally

$$L' = \varepsilon(r)\varepsilon(s)(X^s_{\mathrm{e}\nu} X^r_{\mathrm{pn}} + (-1)^{r+s} X^r_{\mathrm{np}} X^s_{\mathrm{e}\nu}).$$

Therefore, for invariance

$$\varepsilon(r)\varepsilon(s) = +1$$

is necessary. This again means that

VA and AV

are excluded while

SS, SP, PS, PP, VV, AA, TT, TT', T'T

are all allowed. This corresponds to experimental findings: in Wu's experiment [1]) with Co^{60} (which is a Teller-type β-decay) it turned out that the decay is described by parity-non-conserving tensor interaction (the last three terms). In the case of a Fermi-type β-decay, however, we have at our disposal the S and P interactions, as it should be. Moreover, they can be again constructed in a parity-violating way, as in Salam's theory [6]). Thus we are very much inclined to believe that in principle only parity-violating (but PC-conserving) interactions occur.

In connection with the latter results, we must point out that in contrast to those of section 6.1, they are intimately connected with our assumption made in section 5, namely that *different* fermion fields *commute*. If we made the opposite assumption (different fermion fields anticommute) then we could obtain different selection rules for processes in which two equal particles take part. (An example is given by μ-decay if the factors in the interaction are taken in a certain order.)

Concluding the author wishes to express his gratitude to Professor L. Rosenfeld for granting him the possibility to work in his Department, and also for stimulating interest and criticism in this work.

References

1) C. S. Wu, E. Ambler, R. W. Hayward, D. D. Hoppes and R. P. Hudson, Phys. Rev. **105** (1957) 1413
2) R. L. Garvin, L. Lederman and M. Weinrich, Phys. Rev. **105** (1957) 1415
3) L. Landau, Nuclear Physics **3** (1957) 127
4) T. D. Lee and C. N. Yang, Phys. Rev. **105** (1957) 167
5) T. D. Lee and C. N. Yang, Phys. Rev. **104** (1956) 254
6) A. Salam, Nuovo Cimento **5** (1957) 229
7) C. N. Yang and J. Tiomno, Phys. Rev. **79** (1950) 498
8) V. Votruba, private communication (1954)
9) G. C. Wick, A. S. Wightman and E. P. Wigner, Phys. Rev. **88** (1952) 101
10) N. Shapiro, Uzpekhi Fiz. Nauk (1954) no. 8
11) T. D. Lee and C. N. Yang, Phys. Rev. **98** (1955) 1501
12) B. Ferretti, Nuovo Cimento **4** (1956) 951; **5** (1957) 761
13) L. Michel, Proc. Phys. Soc. A **63** (1950) 514
14) E. J. Konopinski and H. M. Mahmoud, Phys. Rev. **92** (1953) 1045
15) G. Marx, Z. f. Naturf. **9a** (1954) 1051

Nuclear Physics **4** (1957) 579—588; © *North-Holland Publishing Co., Amsterdam*
Not to be reproduced by photoprint or microfilm without written permission from the publisher

DECAY SCHEME OF Pb^{212}

E. M. KRISYOUK, A. G. SERGEYEV, G. D. LATYSHEV and V. D. VOROBYOV
V. N. Obraztsov Institute of Railway Engineering, Department of Physics, Leningrad

Received 29 April 1957

Abstract: The decay scheme of $Pb^{212} \xrightarrow{\beta} Bi^{212}$ is analyzed. It is shown that Bi^{212} has the following levels: 0 keV—1^-, 239 keV—0^-, 300 keV—1^-, 415 keV—0^-. The spin and parity assignments are based on the γ-transition multipolarities and computed log ft values for β-transitions. Configurations which can be ascribed to the levels on basis of the shell model qualitatively explain the γ-transition intensities. The proposed decay scheme implies that the 177 keV transition is an E0-transition; this is compatible with presently available data.

Introduction

In order to determine with greater precision the decay schemes of the nuclei of an active deposit of radiothorium we have investigated their conversion spectra. The spectrum measurements were performed on a magnetic spectrometer of the "caetron" type [1]) possessing improved focusing properties; the apparatus half-width of the lines was 0.25 % and geometrical efficiency 0.3 % of 4π. The electrons were recorded with Geiger-Müller counters. The experimental results have been published in ref. [2, 3, 4]). The aim of the present investigation is to construct with greater precision the decay scheme of $Pb^{212} \xrightarrow{\beta} Bi^{212}$ on basis of our conversion spectrum data and other data cited in the literature.

1. Spacing of Bi^{212} Levels

The position of the Bi^{212} levels which appear in the β-decay of Pb^{212} was established already in the work of Ellis [5]) who explained all the known γ-transitions involved in the decay.

Our internal conversion electron study of radiothorium deposits [2, 3]) confirm this decay scheme. In favour of this scheme one may mention that the energy sum of the 239 and 177 keV γ-lines is equal to that of the 300 and 115 keV γ-lines. A possible explanation of this is the existence of two cascades, each of which starts at the 415 keV level and terminates at the ground state. The difference between the energy sums of these lines is $\approx$ 10 eV which is perceptibly smaller than the experimental errors. The

two energy sums are so nearly equal that it would seem highly improbable to be a casual coincidence. The direct transition from the 415 keV level to the ground state observed by us also confirms this scheme. The time order of the lines in the cascade may be inferred from their intensities. The 239 keV line is much more intense than the 177 keV line and thus

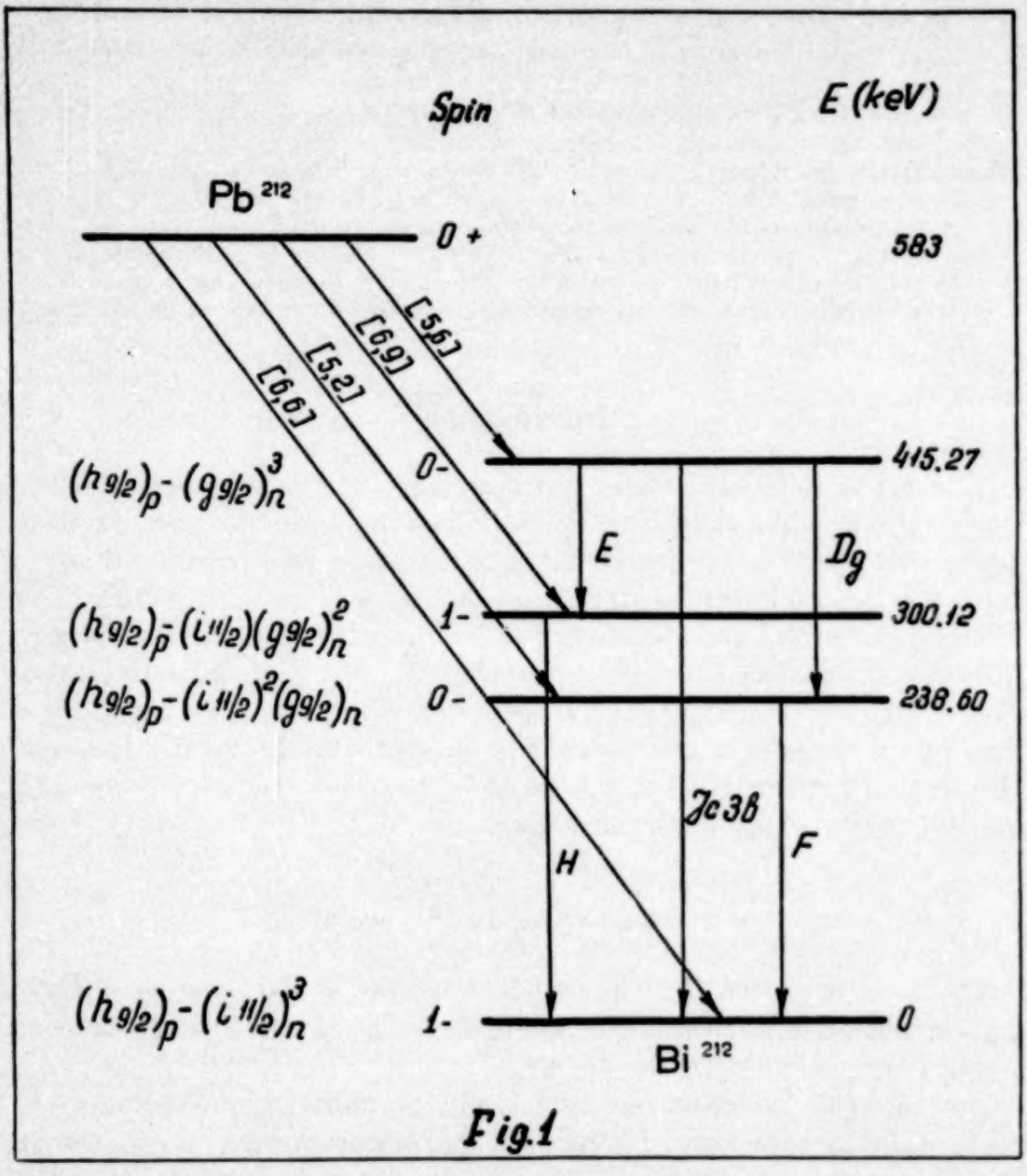

Fig.1

must lie below it. For the same reason the 300 keV line should lie below the 115 keV line. Although in this case the difference is not so significant it nevertheless exceeds the experimental error. In this manner the existence of levels at 239 and 300 keV has been established (fig. 1).

To explain the 250 keV Bi^{212} transition Oppenheimer [6]) suggested that a 250 keV level may exist in Bi^{212}.

The existence of this level is also assumed in all other papers in which the Bi^{212} level scheme is given (e.g. in ref. [7])). This transition has been postulated by Ellis [8]). In the conversion electron spectrum of an active radiothorium deposit investigated by this author by recording the electrons with a photographic plate the intensities of lines Dg and Fa which are produced in the conversion of a 177 keV transition in the K- and L-shells respectively were found to be almost equal. To explain this fact Ellis assumed that the Fa-line is also due to conversion of 250 keV γ-rays in the K-shell. The energy of the corresponding L-line equals that of the intense J-line (from conversion of 239 keV γ-rays in the M-shell) and the aforementioned assumption therefore does not contradict the experiments.

Arnolt [9]) assumed the existence of 164 keV γ-rays due to a transition between 415 and 250 keV levels. In favour of the existence of this line it was pointed out that the energies of conversion lines Df, F and Fa satisfactorily agree with the positions of K, L and M lines for the 164 keV transition. However, an alternative explanation of these lines is possible. The F-line is produced by conversion of 239 keV γ-rays in the K-shell and the Fa-line by conversion of 177 keV γ-rays in the L-shell; finally, the Df-line lies in the Auger electron region. We thus conclude that there is not sufficient ground for assuming the existence of a 164 keV transition which in turn cannot be considered as an argument in favour of the existence of a 250 keV level. The only remaining argument in favour of the existence of such a level is the Dg to Fa-line intensity ratio obtained by Ellis.

Our conversion electron measurements carried out with aïd of G—M counters showed that the ratio between the Dg and Fa-line intensities is in good agreement with the theoretical value of K/L for the 177 keV M1 and E0 transitions and thus there is no need of invoking a 250 keV transition.

The discrepancy between our results and those of Ellis with respect to line intensity can be explained by the difference in electron detection. Photographic registration of electrons applied by Ellis yields larger errors in line intensity determinations due to the necessity of applying corrections to take into account the spectral sensitivity of the photographic plate and the nonlinear dependence of the blackening on irradiation dose.

Thus, at present there are no convincing reasons to assume the existence of a 250 keV level and it therefore has not been included in our level scheme

2. Spins and Parity of Bi^{212} Levels

Contradictory data relating to the spin and parity of the Bi^{212} levels prevailed during a long period of time. Only very recently Horton [10]), who measured the $\alpha-\gamma$ angular correlation in $Bi^{212} \xrightarrow{\alpha} Tl^{208}$ decay and analyzed

the log τf data for the $Bi^{212} \xrightarrow{\beta} Po^{212}$ β-decay, has shown that a spin of 1^- should be assigned to the ground state of Bi^{212}.

In order to ascertain the spins and parities of the excited states we determined the multipolarities of the γ-transitions (see table 1). The multipole order of the 239 keV transition has been previously determined.[11]) It was found to be a pure M1 transition, the E2 admixture being lower than 0.3 %.

TABLE 1

Transition	Conversion line	E_γ keV	I_e %	Multipole order	Transition intensity (I) in %
E	K L_I L_{II} M N O	115.14	2.12 0.47 0.058 0.106 0.033 0.013	MI	3.2
Dg	K L_I	176.67	0.087 0.017	E0	0.1
F	K L_I L_{II} L_{III} M N O	238.60	28.1 4.72 0.032 1.14 0.38	MI	74
H	K L M N	300.12	1.06 0.182 0.041 0.012	MI	4.1
Jc 3b	K	415.2	0.003		0.02

The multipole order of the 115 keV transition was determined from the ratio of the probabilities of conversion in the L-subshells. The experimental value is

$$(L_I : L_{II} : L_{III})_{exp} = 1 : (0.12 \pm 0.01) : < 0.02.$$

The theoretical ratios are

$$(L_I : L_{II} : L_{III})_{M1} = 1 : 0.12 : 0{,}007,$$
$$(L_I : L_{II} : L_{III})_{E2} = 1 : 13 : 9.5.$$

The ratio obtained by us satisfactorily agrees with the theoretical value for a M1 transition; any possible E2 admixture should be very small

(< 0.1 %). The 300 keV transition was also found to be a M1 transition. This can be seen from the ratio of K to L shell conversion:

$$(K/L)_{exp} = 1 : (0.17 \pm 0.01),$$
$$(K/L)_{M1} = 1 : 0.18,$$
$$(K/L)_{E2} = 1 : 0.65.$$

The K/L ratio for the 177 keV transition also agrees with the theoretical value for a M1 transition:

$$(K/L)_{exp} = 1 : (0.18 \pm 0.02),$$
$$(K/L)_{M1} = 1 : 0.18,$$
$$(K/L)_{E2} = 1 : 0.92.$$

The theoretical K-shell internal conversion coefficients (α_K) are taken from Sliv and Band's tables [12]) and the L-subshell conversion coefficients from Rose's tables [13]), the value for α_{LI} being reduced by 27 % to take into account the effect of the finite nuclear dimensions [14]).

From the transition multipolarities established in this way one may determine the parity of the excited levels. Since the transitions are M1 the parity of all levels should be the same as that of the ground state, that is, negative. However transition multipolarity data do not permit one to establish uniquely the spins of the excited levels.

In order to assign spins to the excited levels we computed the absolute transition probabilities (the results are presented in the last column of table 1). The computation was based on the measured absolute intensities of the conversion lines and the theoretical conversion coefficients. The absolute γ-transition probabilities were employed to estimate the probabilities of β-transition to excited levels and these in turn were used for calculation of $\log \tau f$ values. The tables for function f presented in ref. [15]) were used in the calculations. Log τf values of 6.6, 5.2, 6.9 and 5.6 referring respectively to transitions to the ground, first, second and third excited states were obtained. Since the parity of all levels is negative the β-transitions cannot be allowed (as an even-even nucleus Pb^{208} possesses a 0^+ ground state). Transitions to the first and third excited levels, for which $\log \tau f$ is equal to 5.2 and 5.6, may be classified as first forbidden transitions with $\Delta J = 0$; transitions to the ground and second excited level for which $\log \tau f = 6.6$ and 6.9 may be classified as first forbidden transitions with $\Delta J = 1$.

Decrease of $\log \tau f$ for first forbidden transitions in nuclei lying near doubly filled shells has been noted previously [16, 17]). We have attempted to systematize the $\log \tau f$ data near $A = 208$ for first order forbidden transitions by using the new experimental results obtained by us. Available data on $\log \tau f$ for $205 \leqq A \leqq 212$ are tabulated in table 2. Only those transitions have been included for which the values of $\log \tau f$ as well as of

the spins and parities of the mother and daughter nuclei were known. The log τf values for the $Pb^{212} \xrightarrow{\beta} Bi^{212}$ transitions were taken from the present work, for the $Tl^{208} \xrightarrow{\beta} Pb^{208}$ transitions — from our paper [18]) and the remaining values — from ref. [7, 16]).

TABLE 2

Mother nucleus		Daughter nucleus			log τf	ΔJ
Isotope	Spin	Isotope	Spin	Level (keV)		
Hg^{205}	1/2−	Tl^{205}	1/2+	0	5.5	0
Tl^{206}	0−	Pb^{206}	0+	0	5.2	0
Tl^{207}	1/2+	Pb^{207}	1/2−	0	5.2	0
Tl^{208}	5+	Pb^{208}	5−	3198	5.6	0
Tl^{208}	5+	Pb^{208}	5−	3708	5.4	0
Pb^{209}	9/2+	Bi^{209}	9/2−	0	5.5	0
Pb^{210}	0+	Bi^{210}	0−	72	5.4	0
Pb^{212}	0+	Bi^{212}	0−	239	5.2	0
Pb^{212}	0+	Bi^{212}	0−	415	5.4	0
Tl^{207}	1/2+	Pb^{207}	3/2−	569	6.1	1
Tl^{208}	5+	Pb^{208}	4−	3475	5.7	1
Tl^{208}	5+	Pb^{208}	6−	3961	5.9	1
Pb^{212}	0+	Bi^{212}	1−	0	6.6	1
Pb^{212}	0+	Bi^{212}	1−	300	6.9	1
Bi^{212}	1−	Po^{212}	0+	0	7.2	1
Tl^{208}	5+	Pb^{208}	3−	2614	7.6	2

It can be seen from the table that the log τf values for all 9 transitions with $\Delta J = 0$ are very close to each other. The maximal deviation from the mean value, 5.4, is only 0.2. This value for log τf strongly differs from the value 6.5 for log τf of first order forbidden transitions with $\Delta J = 0$ in nuclei located far away from filled shells [16]).

The spread of log τf for transitions with $\Delta J = 1$ is much larger; however, a regularity in the behaviour of log τf can also be noted. Indeed the smallest value of log τf for transitions with $\Delta J = 1$ refer to nuclei with $A = 208$, the daughter nucleus in this case being that with doubly filled shells (Pb^{208}). In either direction from $A = 208$ the log τf values rapidly rise. However, in our opinion the data are not sufficient to permit one to draw a final conclusion concerning the existence of this type of regularity. Only one case of a unique transition ($\Delta J = 2$) in this range of A is known.

Three transitions which are incompatible with this classification of log τf have not been included in table 2. These are the β-decays

$$Pb^{210}\,(RaD) \xrightarrow{\beta} Bi^{210}\,(RaE) \xrightarrow{\beta} Po^{210}\,(RaF).$$

For both of these transitions log $\tau f \approx 8$ although $\Delta J = 1$. The anomalously large value of log τf for the transition $Bi^{210}(RaE) \xrightarrow{\beta} Po^{210}(RaF)$

can be explained by accidental compensation of the transition matrix elements which must be postulated in order to explain the spectrum shape [19]). The anomaly in the case Pb^{210}(RaD) $\xrightarrow{\beta}$ Bi^{210}(RaE) is discussed in ref. [20]).

The case $Tl^{209} \xrightarrow{\beta} Pb^{209*}$ is not clear. The values are $\Delta J = 1$ and $\log \tau f = 5.2$. At present it is difficult to decide whether this case is an exclusive one or the spin assignment for one of the nuclei is wrong.

It can be seen from table 2 that the $\log \tau f$ values for the $Pb^{212} \xrightarrow{\beta} Bi^{212}$ transitions are in good agreement with other first forbidden transitions for $205 \leqq A \leqq 212$.

Thus, analysis of $\log \tau f$ yields the following spin sequence for the Bi^{212} levels: 0 keV-1^-; 239 keV-0^-; 300 keV-1^- and 415 keV-0^-. The ground state spin value agrees with the result of Horton. The transition multipolarities are also consistent with this spin assignment. The spin values for excited levels obtained in this manner indicate that the 239 and 115 keV transitions are pure M1 transitions, a result which agrees well with the experimental data.

This spin sequence, however, leads to difficulties in interpretation of the γ-transition probabilities. Indeed, a direct transition from the 415 keV level to the ground state must be a M1 transition; however its probability is much less than that of the 115 keV transition which is also a M1 transition and in addition it possesses a smaller energy. If the 115 keV transition probability is given by Moszkowski's formula for single-particle transitions[21]), the 415 keV transition would be 2000 times more forbidden than the single-particle one. (This transition was first detected by us [3]) and previously escaped observation because of its low intensity.) The absence of a transition between the second and first excited levels is also inexplicable. It should be of the M1 type and have an energy of 61 keV. The L-line corresponding to it should be situated at a sufficiently large distance from known lines and therefore should be easily detectable. Computations performed on basis of the Moszkowski formula show that the intensity of this transition should be 10 times larger than the upper limit of the measured intensity. The calculations were carried out on the assumption that the 300 keV transition is a single-particle transition.

The small probability of these transitions can be simply explained if configurations are ascribed to the levels.

3. Interpretation of Bi^{212} Levels within the Framework of the Shell Model

We have made an attempt to explain the spins of the ground and excited Bi^{212} states from the standpoint of the shell model.

In odd nuclei the level spins and parities are determined by the

states of the odd neutron and proton. Since odd neutron and proton spins add vectorially a set of levels with spins differing by 1 will correspond to a given proton-neutron configuration.

The state of Bi^{212} should be determined by the spins of the 83rd proton and 129th neutron. The 83rd proton should be in an $h_{9/2}$ state. This can be inferred from data on the spins of the ground states of Bi^{209} and Bi^{207} [7]) (the spins of other odd mass Bi isotopes are unknown). The odd neutron in Pb^{209} and Po^{211} is in the $g_{9/2}$ state [7]). However, the $h_{9/2}-g_{9/2}$ configuration does not explain satisfactorily the spin of the ground state of Bi^{212}. According to ref. [20]) the ground state spin of this configuration should be 0^-. It is natural to assume that the odd neutron in Bi^{212} is in the $i_{11/2}$ state. A confirmation of this is that the odd Bi^{210} neutron is in this state [20]). It is not surprising that the $i_{11/2}$ state is not observed in odd mass nuclei since, according to the shell model, levels with large spins (exceeding 9/2) are filled only by pairs of nucleons. This restriction does not apply to odd nuclei. The $g_{9/2}$ level lies somewhat above the $i_{11/2}$ level and is probably responsible for the formation of excited states.

Thus the $(h_{9/2})_p-(g_{11/2})^3_n$ configuration yields a reasonable explanation of the ground state spin. The lowest energy in this multiplet can be possessed by the spin 1^- level [20]).

For explanation of the excited level spins we assume that the neutrons are successively excited from the $i_{11/2}$ state to the $g_{9/2}$ state. This kind of neutron excitation yields the configuration $(h_{9/2})_p-(i_{11/2})^2(g_{9/2})_n$ for the first excited state. A pair in the $i_{11/2}$ state does not contribute to the nuclear spin and hence the level with a 0^- spin should be the level of minimal energy. Analogously, the spins 1^- and 0^- for the 2nd and 3rd excited levels can be correspondingly explained by the configurations $(h_{9/2})_p-(i_{11/2})(g_{9/2})^2_n$ and $(h_{9/2})_p-(g_{9/2})^3_n$. Thus the configurations yield the spin sequence 1^-, 0^-, 1^- and 0^- which coincides with that which follows from the log τf data obtained by us.

The configurations for the Bi^{212} levels permit one to qualitatively explain the γ-transition probabilities observed experimentally. Thus the direct transition from the 415 keV level to the ground level turns out to be a many-particle transition and should therefore be highly forbidden. The transition between the second and first excited levels is also difficult as it should involve decoupling of a pair of neutrons in the $g_{9/2}$ state with subsequent formation of the pair in the $i_{11/2}$ state.

4. E0-Transition in Bi^{212}

A consequence of the Bi^{212} level scheme proposed by us is that the 177 keV transition should be an E0 transition. This conclusion is in good

agreement with the value of K/L for this transition. Thus the experimental value

$$(K/L) = 1 : (0.18 \pm 0.02)$$

is the same as the theoretical value for an E0-transition [22])

$$K/L = 1 : 0.18$$

although, as can be seen, the theoretical value for a M1 transition

$$K/L = 1 : 0.18$$

is also consistent with the experimental value.

The transition probability was compared with the theoretical value. It was assumed in the calculations that the 115 keV transition is a single particle one (this follows from the proposed level configurations) and that its probability is given by Moszkowski's formula [21])

$$W_{M1} = 2.8 \times 10^{13} E_\gamma^3 \left(\frac{\mu_n}{\mu_p - 0.5}\right) \frac{18}{11} = 4.87 \times 10^{10} \text{sec}^{-1}.$$

Since the 115 keV and 177 keV transitions are competitive the probability of the 177 keV transition will be

$$W_{117} = W_{\gamma 115} \frac{I_{177}}{I_{\gamma 115}} = 4.87 \times 10^{10} \frac{0.087}{0.38} = 1.11 \times 10^{10} \text{ sec}^{-1}.$$

According to ref. [22]) the theoretical value of W/ϱ^2 for the 177 keV transition is

$$\frac{W_{00}}{\varrho^2} = 4.7 \times 10^{11} \text{ sec}^{-1}.$$

Hence the wave function overlap parameter ϱ is

$$\varrho^2 = \frac{1.11 \times 10^{10}}{4.7 \times 10^{11}} = \frac{1}{43}; \quad \varrho = \frac{1}{7}.$$

The value of ϱ thus obtained is in good agreement with the results of direct measurement of the E0-transition times [22, 23]).

Element	ϱ
C^{12}	1/2
O^{16}	1/2
Ge^{72}	1/9
Zr^{90}	1/7

Thus, all presently available experimental data are consistent with the proposed decay scheme and with the assumption that the 177 keV transition is E0. However, in view of the importance of this assertion a direct search for γ-rays corresponding to the 177 keV transition would seem to be desirable.

Our data indicate that if the 177 keV transition is magnetic dipole the intensity of the corresponding γ-line should equal 5×10^{-4} quanta/decay. Absence of γ-rays of even several times smaller intensity would be sufficient proof that the 177 keV transition is E0.

If the level scheme for Bi^{212} suggested here is correct it would signify that we are dealing with the first case of an E0 transition in odd nuclei. All previously known E0 transitions refer to even nuclei and take place between positive-parity levels.

The authors express their appreciation to L. K. Peker for discussion of the results of the present work.

References

1) G. D. Latyshev, A. G. Sergeyev, E. M. Krisyouk, L. A. Ostretsov, Yu. S. Yegorov and N. M. Shirshov, Izv. Akad. Nauk, Ser. Fiz. **20** (1956) 354
2) A. I. Zhernovoy, E. M. Krisyouk, G. D. Latyshev, A. S. Remenny, A. G. Sergeyev and V. I. Fadeyev, JETP (1957) in press
3) V. D. Vorobyov, K. I. Ilyin, T. I. Kolchinskaya, G. D. Latyshev, A. G. Sergeyev, Yu. N. Trofimov and V. I. Fadeyev, Izv. Akad. Nauk SSSR, Ser. Fiz. (1957) in press
4) E. M. Krisyouk, A. D. Vitmen, V. D. Vorobyov, G. D. Latyshev and A. G. Sergeyev, Izv. Akad. Nauk SSSR, Ser. Fiz. **20** (1956) 877
5) C. D. Ellis, International Conference on Physics (London, 1934)
6) F. Oppenheimer, Camb. Phil. Soc. **32** (1936) 328
7) B. S. Dzhelepov and L. K. Peker, Decay Schemes of Radioactive Isotopes (Izdat. Akad. Nauk SSSR, 1956)
8) C. D. Ellis, Proc. Roy. Soc. A **138** (1932) 318
9) R. Arnolt, Ann. Phys. **12** (1939) 241
10) J. W. Horton, Phys. Rev. **101** (1956) 717
11) E. M. Krisyouk, G. D. Latyshev, M. A. Listengarten, L. A. Ostretsov and A. G. Sergeyev, Izv. Akad. Nauk SSSR, Ser. Fiz. **20** (1956) 363
12) A. A. Sliv and I. M. Band, Tables of Gamma Ray Internal Conversion Coefficients (Izdat. Akad. Nauk SSSR, 1956)
13) M. E. Rose in K. Siegbahn, Beta- and Gamma-Ray Spectroscopy (Amsterdam, 1955) p. 905
14) L. A. Sliv and M. A. Listengarten, JETP **22** (1952) 29
15) B. S. Dzhelepov and L. N. Zyryanov, Effect of Atomic Electric Field on Beta Decay, (Izdat. Akad. Nauk SSSR, 1956)
16) R. W. King and D. C. Peaslee, Phys. Rev. **94** (1954) 1284
17) C. S. Wu in K. Siegbahn, Beta- and Gamma-Ray Spectroscopy (Amsterdam, 1955) p. 343
18) E. M. Krisyouk, G. D. Latyshev and A. G. Sergeyev, Report at the VII All-Union Conference on Nuclear Spectroscopy (Leningrad, 1957)
19) E. A. Plassman and L. M. Langer, Phys. Rev. **96** (1954) 1593
20) G. E. Lee-Whiting, Phys. Rev. **97** (1955) 463
21) S. A. Moszkowski in K. Siegbahn, Beta- and Gamma-Ray Spectroscopy (Amsterdam, 1955) p. 373
22) E. L. Church and J. Weneser, Phys. Rev. **103** (1956) 1035
23) M. Deutsch, Nuclear Physics **3** (1957) 83

Nuclear Physics **4** (1957) 589—598; © *North-Holland Publishing Co., Amsterdam*

Not to be reproduced by photoprint or microfilm without written permission from the publisher

PARITY MIXTURES AND DECAY PROCESSES

H. S. GREEN and C. A. HURST
University of Adelaide, S. Australia

Received 18 June 1957

Abstract: This paper examines the hypothesis that the μ-meson as well as the Λ- and Σ-hyperons are parity mixtures, and shows that the facts commonly attributed to parity non-conservation are explained in a unified way by this hypothesis, provided physical theory is invariant with respect to parity conjugation.

A simple theory of parity mixtures is developed in both parity conserving and parity destroying forms, to distinguish those experimental consequences which are incompatible with parity conservation. It is pointed out that the experiments on $\pi-\mu-$e decay do not establish a failure of parity conservation as claimed, and that there is at present no evidence which conclusively verifies the longitudinal neutrino hypothesis. The latter, however, may be regarded as an instance of a more general hypothesis that states of 'left-handed' parity do not occur in nature, in favour of which *prima facie* evidence already exists. The facts concerning the decay modes of the heavy mesons can also be explained readily on this basis.

1. Introduction

The fact that heavy mesons have decay modes of both odd and even parity may be interpreted in two different ways. One may suppose that they are created in both parity states, and that parity is conserved in their decay. Alternatively one may suppose that they are created with a unique parity, but that parity is not conserved in the 'weak' interactions responsible for their decay.

If conservation of parity is not essential, there is no necessity that the neutrino should be an ordinary Dirac particle with both spin states available. A theory in which the spin of the neutrino is uniquely associated with its direction of motion has, in fact, been proposed independently by Landau [1]), Salam [2]), and Lee and Yang [3]).

Lee and Yang [4]) suggested experiments with π- and μ-mesons, and nuclei which suffer β-decay, with the object of discovering failures of parity conservation. These experiments have now been performed, with interesting results.

Experiments with μ-mesons [5, 6, 7]) disclose that the direction of emission of the electrons in decay is correlated with the terminal direction of the mesons, provided these have not suffered depolarizing electromagnetic interactions. This effect is consistent with the hypothesis of the 'screwon', or longitudinal neutrino, and it has been claimed that these experiments demonstrate failure of parity conservation. We shall point out that, ir-

respective of the validity of the hypothesis, such a claim was ill-founded; a different experiment would be required even to show that the μ-mesons emitted in π-decay are uniformly polarized. The experiments so far reported are in fact equally consistent with the parity conserving hypothesis that the μ-meson is a parity doublet.

Other experiments [8, 9]) with oriented Co^{60} nuclei have discovered a correlation between the spin direction of oriented nuclei and the direction of emission in one instance, and the spin in another instance, of the electrons emitted in β-decay. Only one of these experiments furnished *prima facie* evidence of parity non-conservation.

Clearly it is very desirable to have an unambigous way of deciding whether given experimental results are consistent with parity conservation or not, and it is one of the objects of this paper to establish a criterion for this purpose. We wish, however, to examine also the possible validity of a conservation law embracing parity conservation in the 'strong' interactions but also applicable to the 'weak' interactions responsible for μ- and θ-meson decay, and to β-decay. Such a conservation law results from requiring the invariance of physical theory with respect to parity conjugation [10]) instead of reflection. If this requirement is made, fermions of a given type may exist *either* in states of pure parity *or* in states of mixed parity. The transformation properties of their interactions with respect to reflection are then fully determined, though not always what one would expect in a parity conserving theory. The advantages of this scheme are twofold: one can account in a natural way for the conservation of parity in the interactions of the fermions with pure parity states, and predict the precise form of parity nonconservation in interactions involving fermions (including the μ-meson and hyperons as well as the neutrino) with mixed parity states.

To explain our idea in simple terms, it will be necessary to make a distinction between parity mixtures and parity doublets. The Lagrangian density $\mathscr{L}_r$ of a parity mixture is not invariant with respect to space reflections, but transforms to the complementary Lagrangian density $\mathscr{L}_l$. Neither $\mathscr{L}_r$ nor $\mathscr{L}_l$ separately is parity conserving, but $\mathscr{L} = \mathscr{L}_r + \mathscr{L}_l$ is the Lagrangian of a parity doublet and conserves parity. If it is required that $\mathscr{L}_r$ should be invariant with respect to parity conjugation, the decomposition of $\mathscr{L}$ into $\mathscr{L}_r$ and $\mathscr{L}_l$ is unique. Thus, to any parity conserving Lagrangian in our scheme there corresponds a Lagrangian $\mathscr{L}_r$ which need not conserve parity but is invariant with respect to parity conjugation.

For the neutrino field, $\mathscr{L} = i\bar{\psi}\gamma \cdot \nabla\psi$ and $\mathscr{L}_r = \frac{1}{2}i\bar{\psi}(1-\gamma_5)\gamma \cdot \nabla\psi$. The longitudinal neutrino hypothesis may be expressed by asserting that neutrinos with "left-handed" parity do not occur in nature. This, however is clearly a special instance of a more general assertion that *fermions with left-handed parity do not occur in nature*, i.e., that only one of the two parity

states of a parity doublet is actually realized. This hypothesis,we shall show, connects in a simple way the facts concerning the decay modes of the heavy mesons with those concerning $\pi-\mu-$e decay and β-decay.

Although we believe that the hypothesis italicized above is most likely correct and that parity is not universally conserved, we shall first, in the following section, outline a simple theory of parity doublets which is parity conserving. From this the parity non-conserving theory can be derived immediately in the way described above. Comparison of the physical consequences of the two theories will then show clearly which experiments demonstrate a failure of parity conservation and which can be interpreted in alternative ways.

2. Field Theory of Parity Doublets

The field variable of a parity doublet with spin $\frac{1}{2}$ is an 8-component spinor Ψ, which can be resolved into two Dirac spinors: $\Psi=(\psi_1,\ \psi_2)$, where $\psi_e=\psi_1$ and $\psi_o=\gamma_5\psi_2$ have even and odd parity assignments respectively. (Note that $\gamma_5=i\gamma_1\gamma_2\gamma_3\gamma_4$ is hermitean, when $\frac{1}{2}(\gamma_\alpha\gamma_\beta+\gamma_\beta\gamma_\alpha)=g_{\alpha\beta}=(-1,\ -1,\ -1,\ 1)$).

It is convenient to introduce the triad of Pauli matrices defined by

$$\begin{gathered}\varrho_1\Psi=\gamma_5(\psi_2,\ \psi_1),\quad \varrho_2\Psi=i\gamma_5(-\psi_2,\ \psi_1),\\ \varrho_3\Psi=(\psi_1,\ -\psi_2).\end{gathered}\tag{1}$$

Then, in a pure parity state, the eigenvalue of ϱ_3 is $+1$ or -1 according as the parity is even or odd.

The Lagrangian density of the doublet field without interactions is

$$\begin{aligned}\mathscr{L}&=\bar{\Psi}(i\gamma\cdot\nabla-M\varrho_3)\Psi\\ &=\bar{\psi}_1(i\gamma\cdot\nabla-M)\psi_1+\bar{\psi}_2(i\gamma\cdot\nabla+M)\psi_2.\end{aligned}\tag{2}$$

This needs to be supplemented by the statement that both ψ_1 and ψ_2 behave like ordinary Dirac spinors under both proper and improper Lorentz transformations, so that under the particular transformation $T(\mathbf{x}\to T\mathbf{x}=-\mathbf{x})$ symbolizing inversion in the origin of the space co-ordinates one has $\psi_1\to T\psi_1=i\gamma_4\psi_1$ and $\psi_2\to T\psi_2=i\gamma_4\psi_2$. (The transformation T^2 is equivalent to a rotation through an angle 2π, and therefore changes the sign of any spinor.)

The above Lagrangian is reduced to canonical form by substituting

$$\begin{aligned}\psi_r&=2^{-\frac{1}{2}}(\psi_1+\gamma_5\psi_2)\\ \psi_l&=2^{-\frac{1}{2}}(\psi_1-\gamma_5\psi_2),\end{aligned}\tag{3}$$

where ψ_r and ψ_l will be referred to as amplitudes for right and left parity respectively. One has

$$\mathscr{L} = \mathscr{L}_r + \mathscr{L}_l,$$
$$\mathscr{L}_r = \bar{\psi}_r(i\gamma \cdot \nabla - M)\psi_r, \quad \mathscr{L}_l = \bar{\psi}_l(i\gamma \cdot \nabla - M)\psi_l. \tag{4}$$

Since $T\psi_r = i\gamma_4\psi_l$ and $T\psi_l = i\gamma_4\psi_r$, the amplitudes ψ_r and ψ_l are interchanged under spatial reflections, and $\mathscr{L}$ is manifestly parity conserving.

In the canonical form (4), the Lagrangian is ready for quantization. Let

$$\begin{aligned}\psi_r &= \textstyle\sum_{\mathbf{p},s}\{r_-(\mathbf{p}, s)\chi_-(\mathbf{p}, s)e^{-ip\cdot x} + r_+^*(-\mathbf{p}, s)\chi_+(-\mathbf{p}, s)\, e^{ip\cdot x}\},\\ \psi_l &= \textstyle\sum_{\mathbf{p},s}\{l_-(\mathbf{p}, s)\chi_-(\mathbf{p}, s)e^{-ip\cdot x} + l_+^*(-\mathbf{p}, s)\chi_+(-\mathbf{p}, s)\, e^{ip\cdot x}\},\end{aligned} \tag{5}$$

where $\chi_-(\mathbf{p}, s)$ and $\chi_+(\mathbf{p}, s)$ are normalized spinors for particles and anti-particles, respectively, with momentum $\mathbf{p}$ and spin $s(= \pm\frac{1}{2})$ in the direction of motion. Then $r_\pm(\mathbf{p}, s)$ and $l_\pm(\mathbf{p}, s)$ are annihilators for particles of momentum $\mathbf{p}$, spin s, and right and left parity, respectively; they satisfy the usual anti-commutation rules for fermion fields. Since $i\gamma_4\chi_\pm(\mathbf{p}, s) = \chi_\pm(-\mathbf{p}, -s)$, one has $Tr_\pm(\mathbf{p}, s) = l_\pm(-\mathbf{p}, -s)$ and $Tl_\pm(\mathbf{p}, s) = r_\pm(-\mathbf{p}, -s)$.

The above theory degenerates if the mass M of the fermion should vanish. For then the terms involving ψ_1 and ψ_2 in (2) cannot be distinguished from one another, and there is in effect a single spinor field ψ_ν defined by $\psi_\nu = 2^{-\frac{1}{2}}\psi_1 = 2^{-\frac{1}{2}}\psi_2$. Thus (3) becomes

$$\begin{aligned}\psi_r &= \tfrac{1}{2}(1+\gamma_5)\psi_\nu,\\ \psi_l &= \tfrac{1}{2}(1-\gamma_5)\psi_\nu.\end{aligned} \tag{6}$$

So, though the neutrino cannot properly be regarded as a parity doublet, its field theory can be formulated in a similar way. A state of the neutrino with spin $+\frac{1}{2}$ (in a right-handed co-ordinate system) is a state of right parity, in the sense of our definition, and a state with spin $-\frac{1}{2}$ is a state of left parity. For the anti-neutrino, the correspondence between spin and parity is the reverse.

The parity conserving property of the above theory can be expressed in another way. If P_3 is the transformation for which $P_3\psi_1 = \psi_1$ and $P_3\psi_2 = -\psi_2$, P_3 is equivalent to $-i\gamma_4 T$ in its effect on $\psi_e = \psi_1$, $\psi_o = \gamma_5\psi_2$, and hence on ψ_r and ψ_l. The theory is therefore invariant with respect to the transformation P_3.

It is also invariant with respect to parity conjugation, i.e., with respect to the transformation P_1, such that $P_1\psi_1 = \gamma_5\psi_2$ and $P_1\psi_2 = \gamma_5\psi_1$. Finally it is invariant with respect to the transformation $P_2 = iP_1P_3$, and hence with respect to any rotation in parity space, symbolized by an expression of the form $\exp\{i(c_1P_1 + c_2P_2 + c_3P_3)\}$. *We shall require that all interactions of parity doublets exhibit the same invariance.* This requirement makes the various forms of interaction (e.g., scalar, vector, etc., with scalar or gradient coupling) unique.

As a first example of the application of the above requirement, the inter-

action of a parity doublet with the electromagnetic field could not involve a term like $e(\bar{\psi}_2\gamma\cdot A\psi_1+\psi_1\gamma\cdot A\psi_2)$ where A is the electromagnetic 4-vector potential, because, although it is parity conserving, it changes sign under parity conjugation. The only interaction allowed is the one, $e(\bar{\psi}_2\gamma\cdot A\psi_2+\psi_1\gamma\cdot A\psi_1)$, which is also required to preserve gauge invariance. Hence states of right and left parity are not mixed by electromagnetic interactions. This is true more generally of other types of interactions. Thus the only admissible interaction with gradient coupling between a pseudo-scalar field φ and two doublet fields Ψ and Ψ' is proportional to $\bar{\psi}_2(\gamma\cdot\nabla\varphi)\psi'_2-\bar{\psi}_1(\gamma\cdot\nabla\varphi)\psi'_1$. If φ represents the pion field and $\Psi^{(\mu)}$ the (doublet) field of the muon, the interaction leading to the decay of the pion with gradient coupling is

$$\mathscr{L}^{(\pi\mu)}=\tfrac{1}{2}f\{\bar{\psi}_2^{(\mu)}(\gamma\cdot\nabla\varphi)(1+\gamma_5)\psi_\nu+\bar{\psi}_1^{(\mu)}(\gamma\cdot\nabla\varphi)(1-\gamma_5)\psi_\nu \qquad (7)$$
$$+\text{ hermitean conjugate.}$$

The consequences of this interaction will be discussed below.

To conclude this section, we shall outline a way of introducing boson fields with both even and odd intrinsic parity states, based on the obvious analogy between the matrices ϱ_j defined by (1) and the isobaric spin matrices. Let θ_j represent a 3-component vector in parity space with the same transformation properties as $\overline{\Psi}\varrho_j\Psi'$, i.e., such that

$$\begin{aligned}
&P_1\theta_1=+\theta_1 && P_1\theta_2=-\theta_2 && P_1\theta_3=-\theta_3\\
&P_2\theta_1=-\theta_1 && P_2\theta_2=+\theta_2 && P_2\theta_3=-\theta_3\\
&P_3\theta_1=-\theta_1 && P_3\theta_2=-\theta_2 && P_3\theta_3=+\theta_3.
\end{aligned} \qquad (8)$$

Then an interaction of the type $\sum_j(\theta_j\overline{\Psi}\varrho_j\Psi')$ will conserve parity and preserve invariance with respect to parity conjugation, just as the corresponding interaction in the isobaric spin formalism conserves charge and preserves charge independence. The fields $\theta_+=2^{-\frac{1}{2}}(\theta_1+i\theta_2)$ and $\theta_-=2^{-\frac{1}{2}}(\theta_1-i\theta_2)$ are associated with fermion transitions from even to odd and from odd to even parity, respectively, and therefore represent bosons of odd parity, while θ_3 represents bosons of even parity. The application of this theory to the heavy mesons will be considered in § 6 below.

3. Non-Conservation of Parity

The above field theory is formulated as if parity were rigorously conserved, and requires modification if the hypothesis of the longitudinal neutrino is correct. The modification is fortunately very simple to effect. The hypothesis may be stated: with a right-handed system of space coordinates, only states of the neutrino with right parity are found in nature. This hypothesis is not yet experimentally proven, but there is *prima facie* evidence for the more general hypothesis: no states of left parity are found in nature. Parity doublets are then replaced by particles of mixed parity,

represented by a single 4-spinor ψ_1. The above theory is to be modified by omitting expressions involving ψ_1, where they occur, or by setting $\psi_1 = \gamma_5 \psi_2$ elsewhere.

The hypothesis thus adopted violates parity conservation, and if it is correct the invariance of the theory under the transformations T and P_3 no longer holds. On the other hand, the failure of parity conservation cannot occur arbitrarily, and *the invariance of the theory under parity conjugation is retained*. Thus conservation of parity is not simply abandoned, but replaced by another conservation law of wider validity.

4. Production and Decay of the μ-Meson

We shall point out in this section that the experiments we have referred to on $\pi-\mu-$e decay are equally compatible with the theory of § 2 or the modification suggested in § 3. Contrary to claims of the experimenters, they have therefore established neither the failure of parity conservation nor the longitudinal neutrino hypothesis. This is ultimately because the angle involved in the measurements is in fact contained between two polar vectors — the terminal direction of motion of the μ-meson and the direction of emission of the electron; its cosine is therefore a scalar, and not a pseudo-scalar.

The parity conserving interpretation of the experiments is that the μ-meson is a parity doublet. Then, according to (7), the decay of π^--mesons is accompanied by the production of μ^--mesons with right parity, together with anti-neutrinos of spin $+\frac{1}{2}$, and μ^--mesons with left parity, together with anti-neutrinos of spin $-\frac{1}{2}$. As the pion has no spin, the spin of a muon in its direction of motion must be initially the same as that of the anti-neutrino emitted in the reverse direction. On this interpretation, therefore, the decay of π^--mesons results in a symmetrical mixture of 'right-handed' muons with spin $+\frac{1}{2}$, and 'left-handed' muons with spin $-\frac{1}{2}$. Electromagnetic interactions cannot change the parity state, but can reverse the spin; the initial correspondence between spin and parity states will not, therefore, be preserved in the course of depolarizing electromagnetic interactions. Assuming, however, that the muons retain their original state of polarization, the angular distribution of the electrons emitted in decay is independent of the parity state of the decaying mesons. This is easily verified as follows.

The most general form of coupling, without gradient coupling, but consistent with invariance under parity conjugation, leading to the decay of the μ-meson, is

$$\begin{aligned}\mathscr{L}_{\mathrm{r}}^{(\mu e)} &= g_1\bar{\psi}_\nu(1-\gamma_5)\psi_{\mathrm{r}}^{(\mu)}\bar{\psi}_e\psi_\nu\\ &+g_2\bar{\psi}_\nu(1-\gamma_5)\gamma^\alpha\psi_{\mathrm{r}}^{(\mu)}\bar{\psi}_e\gamma_\alpha\psi_\nu\\ &+\tfrac{1}{8}g_3\bar{\psi}_\nu(1-\gamma_5)[\gamma^\alpha,\gamma^\beta]\psi_{\mathrm{r}}^{(\mu)}\bar{\psi}_e[\gamma_\alpha,\gamma_\beta]\psi_\nu\\ &+g_4\bar{\psi}_\nu(1-\gamma_5)\gamma^\alpha\psi_{\mathrm{r}}^{(\mu)}\bar{\psi}_e\gamma_\alpha\gamma_5\psi_\nu\\ &+g_5\bar{\psi}_\nu(1-\gamma_5)\psi_{\mathrm{r}}^{(\mu)}\bar{\psi}_e\gamma_5\psi_\nu\\ &+\text{hermitean conjugate.}\end{aligned} \tag{9}$$

In a parity conserving theory, one would add the parity conjugate $\mathscr{L}_{\mathrm{l}}^{(\mu e)}$ to the above interaction, with $\psi_{\mathrm{l}}^{(\mu)}$ replacing $\psi_{\mathrm{r}}^{(\mu)}$ and $(1+\gamma_5)$ replacing $(1-\gamma_5)$ everywhere. The above Lagrangian still leaves open the question whether the neutrino can have a state of pure parity in its interactions with the electron, or whether the longitudinal neutrino hypothesis is universally true. If the more restrictive hypothesis is made, one must have $g_3 = 0$, $g_2 = g_4$, and $g_1 = g_5$.

The distribution of the decay products resulting from (9) can be written down at once using formulae derived by Michel [11]), if it is noticed that

$$\chi(\mathbf{p},\pm\tfrac{1}{2})\bar{\chi}(\mathbf{p},\pm\tfrac{1}{2}) = \tfrac{1}{4}(1\pm\boldsymbol{\sigma}\cdot\boldsymbol{\gamma}\,\gamma_4\gamma_5)(\gamma\cdot p - M)/p_4,$$

so

$$(1\pm\gamma_5)\chi(\mathbf{p},\tfrac{1}{2})\bar{\chi}(\mathbf{p},\tfrac{1}{2})(1\mp\gamma_5) = \tfrac{1}{2}(1\mp v)(1\pm\gamma_5)(\gamma_4\pm\boldsymbol{\sigma}\cdot\boldsymbol{\gamma}), \tag{10}$$

where $\chi(\mathbf{p}, s)$ is the normalized spinor for a μ^--meson with momentum $\mathbf{p}$ and spin s, $v = |\mathbf{p}|/p_4$ is its velocity, and $\boldsymbol{\sigma} = \mathbf{p}/|\mathbf{p}|$ is its direction of motion. It is now clear that muons with right and left parity will give the same distribution, because although they are associated with different parity projectors $(1\pm\gamma_5)$, their spins are also opposite; moreover, they cannot interfere as they have different creation and annihilation operators. Thus the probability per unit time that a μ^--meson of either type at rest should decay to an electron, a neutrino and an anti-neutrino with 4-vector momenta q, k and l respectively, is

$$\begin{aligned}2(2\pi)^{-5}(k_4 l_4 q_4)^{-1}\ &\{a'\,q\cdot k\sigma'\cdot l + b'\,k\cdot l\sigma'\cdot q\\ &+aq\cdot k\sigma\cdot l + bk\cdot l\sigma\cdot q\\ &+c(q\cdot k\sigma\cdot l - q\cdot l\sigma\cdot k)\}\delta_4(p-q-k-l)\mathrm{d}^3k\mathrm{d}^3l\mathrm{d}^3q\end{aligned} \tag{11}$$

where σ' is the 4-vector $(\sigma, 1)$, σ is the 4-vector $(-\boldsymbol{\sigma}, 1)$, and the constants are given by

$$\begin{gathered}a' = 2(g_2+g_4)^2, \qquad b' = 2(g_2-g_4)^2,\\ a = (g_3+g_1)^2+(g_3-g_5)^2, \qquad b = (g_3-g_1)^2+(g_3+g_5)^2+c,\\ c = 2g_3^2-g_1^2-g_5^2.\end{gathered} \tag{12}$$

Performing [11]) the integrations with respect to k and l, one finds, for the probability per unit time that an electron with momentum $\frac{1}{2}xM$ should

be emitted in a direction making an angle θ with the terminal direction of motion of the muon,

$$\tfrac{1}{2}(4\pi)^{-3}M^5x^2\,dx\,d(\cos\theta)[(a+s')(1-\tfrac{2}{3}x)+(a-a')(\tfrac{1}{3}-\tfrac{1}{3}x)\cos\theta +2(b+b')(1-x)+2(b-b')(1-x)\cos\theta] \quad (13)$$

if the mass of the electron is neglected.

The 'Michel parameter' of this distribution is

$$\varrho=\frac{3}{4}\cdot\frac{(a+a')}{(a+a')+(b+b')} \quad (14)$$

and reduces to the known value 0.75 for the longitudinal neutrino hypothesis, with $b=b'=0$. Recent experimental determinations are perhaps significantly below this value, and may imply that b or b' is different from zero. If so, the longitudinal neutrino interacts directly only with parity mixtures, and another neutrino of pure parity interacts with electrons and nucleons. The correctness of the exclusively longitudinal neutrino hypothesis is not established by present experiments; the $\pi-\mu-$e experiments do not yet even establish a failure of parity conservation.

Failure of parity conservation in $\pi-\mu-$e decay could be established by applying a magnetic field parallel to the direction of motion of the muons, instead of perpendicular to it as in previous experiments [5]); this would decide whether or not both spin states of the muon were present. If both spin states were present, the field would accelerate one and decelerate the other; it would tend to reverse the spins of the latter and thus tend to *destroy* the asymmetry of the observed decay distribution.

The mean angular distribution of the electrons emitted by decay of the μ's is

$$\frac{M^5\,d(\cos\theta)}{12(4\pi)^3}[(a+a')+(b+b')-\{\tfrac{1}{3}(a-a')-(b-b')\cos\theta\}].$$

This is compatible with experiment even if b and b' do not vanish but have suitably related values. The angular distribution does not therefore suffice to establish an exclusively longitudinal neutrino hypothesis. A more exact measurement of the Michel parameter would most easily decide the question.

5. Asymmetric Emission in β-Decay

The asymmetric emission of electrons by polarized Co^{60} nuclei [8]) is of a different character because the angle involved is contained between an axial and a polar vector — the spin of the nucleus and the direction of emission of the electron. The cosine of this angle is a pseudo-scalar, and the observations demonstrate a failure of parity conservation, provided no other pseudo-scalar can affect the decay. As this is, as far as we know, at present

the only unambiguous *prima facie* evidence for parity non-conservation, it is important to examine whether, for example, asymmetries of the crystal lattice which contain the decaying nuclei could not influence the distribution of decay products; we presume that they could not, and therefore that the experiments with β-decay uphold the hypothesis of § 3. They do not distinguish, of course, between the longitudinal neutrino hypothesis and the more general hypothesis of which it may be regarded as a particular instance. For example, the observed asymmetry might be attributed to the virtual production of a parity mixture in the β-decay ($n \to \Lambda + \pi^+ + \theta^0 + \pi^- \to p + e + \nu$). Experiments establishing a correlation between the spin of the nucleus and the polarization of the emitted electron can be explained in this way even without invoking non-conservation of parity.

6. The θ-τ Puzzle

We have not yet considered applications of the assumed invariance with respect to parity conjugation to interactions between a parity doublet, or parity mixture, and particles like electrons or nucleons which are in a pure state of intrinsic parity. Lee and Yang[10]) have reasoned that for such particles that the parity conjugation operator P_1 (C_p in their notation) should commute with the parity operator $-i\gamma_4 T$ (P in Lee-Yang notation), and this is possible only if P_1 has a definite eigenvalue (± 1). We shall take this eigenvalue to be $+1$, i.e., the same as for right-handed parity mixtures, and write down a set of interactions for the production and decay of the strange particles which are invariant with respect to parity conjugation.

In the 8-component spinor formalism, the nucleon field is to be represented by $\Psi_N = (\psi_N, \psi_N)$. The Λ and Σ hyperons will be assumed to be parity mixtures, and the heavy mesons will be represented by a vector θ_j in parity space. (It is assumed here that they have spin 0, though this is not essential.) For the associated production of heavy mesons and γ-particles one has the Lagrangian

$$\mathscr{L}^{(KY)} = \sum_j \theta_j \overline{\Psi}^{(Y)} \varrho_j \Psi_N = \mathscr{L}_r^{(KY)} + \mathscr{L}_l^{(KY)},$$
$$\mathscr{L}_r^{(KY)} = \bar{\psi}_r \{\theta_- + \gamma_5 \theta_+ + 2^{-\frac{1}{2}}(1+\gamma_5)\theta_3\} \psi_N,$$
$$\mathscr{L}_l^{(KY)} = \bar{\psi}_l \{-\theta_- + \gamma_5 \theta_+ + 2^{-\frac{1}{2}}(1-\gamma_5)\theta_3\} \psi_N.$$

If this Lagrangian is correct, since the θ-particles are indistinguishable apart from their parity, one would expect the particles with odd intrinsic parity to be twice as numerous as those with even intrinsic parity. Actually one finds among the 2-body decay schemes of the charged particles that the odd ($\mu\nu$) mode is approximately twice as frequent as the even (2π) mode, and among the less frequent 3-body decay schemes that the odd

(3π) mode is about twice as frequent as the $(\pi\mu\nu)$ and $(\pi e\nu)$ modes together. To this extent, the predictions of the theory are confirmed.

The present interpretation suggests that the occurrence of heavy mesons with both even and odd parity modes of decay is due to the fact that they have different parities rather than any failure of parity conservation in decay. Nevertheless the interactions responsible for all but the (2π) and (3π) modes of decay are probably parity non-conserving. It is, in fact, easy to write down interactions which are invariant with respect to parity conjugation and would lead to the various modes of decay. Here we shall write down only the interaction responsible for the decay of the Λ- and Σ-hyperons:

$$\mathscr{L}_{\mathrm{I}}^{(\mathrm{YN})} = f' \bar{\psi}_{\mathrm{Y}}(\gamma \cdot \nabla\varphi)(1+\gamma_5)\psi_{\mathrm{N}}$$

— assuming that the pion field has gradient coupling. This is also a parity-destroying interaction. If it is correct, the nucleon and pion produced in hyperon decay may be in a state of either odd or even parity. It is hoped that this prediction of the theory will soon be tested.

References

1) L. Landau Nuclear Physics **3** (1957) 127
2) A. Salam, Nuovo Cimento **5** (1957) 299
3) T. D. Lee and C. N. Yang, Phys. Rev. **105** (1957) 1671
4) T. D. Lee and C. N. Yang, Phys. Rev. **104** (1956) 254
5) R. L. Garwin *et al.*, Phys. Rev. **105** (1957) 1415
6) J. I. Friedman and V. L. Telegdi, Phys. Rev. **105** (1957) 1081
7) A. Abashian *et al.*, Phys. Rev. **105** (1957) 1927
8) C. S. Wu *et al.*, Phys. Rev. **105** (1957) 1413
9) H. Frauenfelder *et al.*, Phys. Rev. **106** (1957) 386
10) T. D. Lee and C. N. Yang, Phys. Rev. **102** (1956) 290
11) L. Michel, Proc. Phys. Soc. A **63** (1950) 514

Nuclear Physics **4** (1957) 599—614; © *North-Holland Publishing Co., Amsterdam*
Not to be reproduced by photoprint or microfilm without written permission from the publisher

EXCITED STATES OF N^{16}

JOAN M. FREEMAN and R. C. HANNA
Atomic Energy Research Establishment, Harwell, England

Received 19 June 1957

Abstract: The first four levels of N^{16}, excited by the reaction N^{15}(d, p)N^{16}, have been studied by observing proton groups and gamma radiation, coincidences and angular correlations. The following spins and energies have been assigned to the excited states: 0− at 120 ± 1 keV, 3− at 298 ± 5 keV and 1− at 395 ± 3 keV. The half-life of the 120 keV level is 6.7 ± 0.5 microseconds. The results are in excellent agreement with the shell-model predictions of Elliott and Flowers.

1. Introduction

Intermediate-coupling shell-model calculations have recently been made by Elliott and Flowers [1]) for the odd parity states of O^{16} and N^{16}, formed by raising a particle from the closed 1p shell to the 1d or 2s shells. They have predicted for N^{16} four closely spaced levels with spins 0−, 1−, 2− and 3−, the order being undetermined, followed by another group several MeV higher. A number of other properties of these levels have also been calculated. This work has provided a considerable stimulus to experimental investigations [2, 3, 4]); those to be described here are concerned with the first four levels.

When these experiments were begun the existence of four low-lying levels in N^{16} was already known from the observations of proton groups from N^{15}(d, p)N^{16} by Thirion *et al.* [5]) and of alpha-particle groups from O^{18} (d, α)N^{16} by Pauli [6]). The latter work gave values 116±6, 300±12 and 391±12 keV for the energies of the first, second and third excited states. Observations of gamma-ray transitions between these levels were first reported by Hanna *et al.*[4]); gamma-rays with energies 120, 276 and 400 keV were observed following the bombardment of N^{15} gas with 2.5 MeV deuterons. It was also found that, with a coincidence resolving time of 0.3 microsecond, only $(8\pm5)\times10^{-3}$ of the 120 keV gamma-rays had a 276 keV gamma-ray in coincidence. This result implied either that the observed gamma-rays were all ground-state transitions or that the 120 keV state had a lifetime long compared with 0.3 microsecond. These results have since been confirmed by Wilkinson [3]) who found that the first excited state had a half-life between 1 and 10 microseconds and suggested that the observed 275 keV peak was compounded of two gamma-rays.

Meanwhile Zimmerman [7]) and Warburton and McGruer [8]) reported

measurements on the angular distribution of the protons from the N^{15}(d, p)N^{16} reaction. Interpretation by stripping theory gave assignments of $l_n = 2$ for formation of the ground and second excited states of N^{16}, and $l_n = 0$ for the first and third states.

In the experiments to be described here the same reaction has been used to study proton-gamma as well as gamma-gamma coincidence spectra; more precise values for the level energies and decay scheme of N^{16} and for the lifetime of the first excited state have thus been obtained. The angular correlation of the protons to, and the gamma-rays from, the second excited state have also been measured. These results, taken in conjunction with the stripping data and with β-decay data have allowed spin and parity assignments to be made for all three excited states of N^{16}.

2. Experimental Arrangement

The apparatus was designed to allow coincident observation of the proton groups and gamma-rays from the N^{15}(d, p)N^{16} reaction. A deuteron beam, accelerated by the Harwell Van de Graaff machine, passed through an electrostatic strong-focusing lens to the target which was situated 10 metres from the analysing magnet; a concrete wall one metre thick shielded the detectors from stray radiation produced in the machine and analysing magnet. The target was a gas cell which, for the observation of protons emitted at 0^0 to the bombarding beam, consisted of a straight thin-walled brass tube, closed at each end by a 5 mm diameter window of nickel foil 2.4 μ thick (fig. 1a). These windows were capable of withstanding atmospheric pressure. For observation of protons at 60^0 the straight tube was replaced by a 60° elbow (fig. 1b); N^{15} or other gases of interest could be introduced into the cell or withdrawn to storage reservoirs with a simple gas-handling system. The usual working pressure of N^{15} was about 4 cm of mercury. The deuteron beam and the forward-emitted reaction products from the cell passed through the second nickel window into a xenon-filled chamber 6 cm long; at the end of the chamber there was a 2 mm thick CsI(Tl) crystal, covered with 5μ thick aluminium foil to exclude ionization light, and mounted on an E.M.I. photomultiplier. The pressure of the xenon gas was so chosen that the deuteron beam at the normal working energy (about 2.6 MeV after passing through the first nickel window) was stopped just short of the CsI crystal. The protons from the N^{15}(d, p) reaction then had residual energies from about 1.7 MeV (ground-state group) to 1.1 MeV (3rd excited-state group), on reaching the crystal. Gamma-rays were detected by a 3.7 cm diameter NaI (Tl) crystal, 0.6 cm thick, set up with its front face 2 mm from the wall of the gas target. For gamma-ray coincidence measurements a second 3.7 cm diameter NaI(Tl) crystal of thickness 2.5 cm was put close up on the opposite side of the target. Proton and gamma-

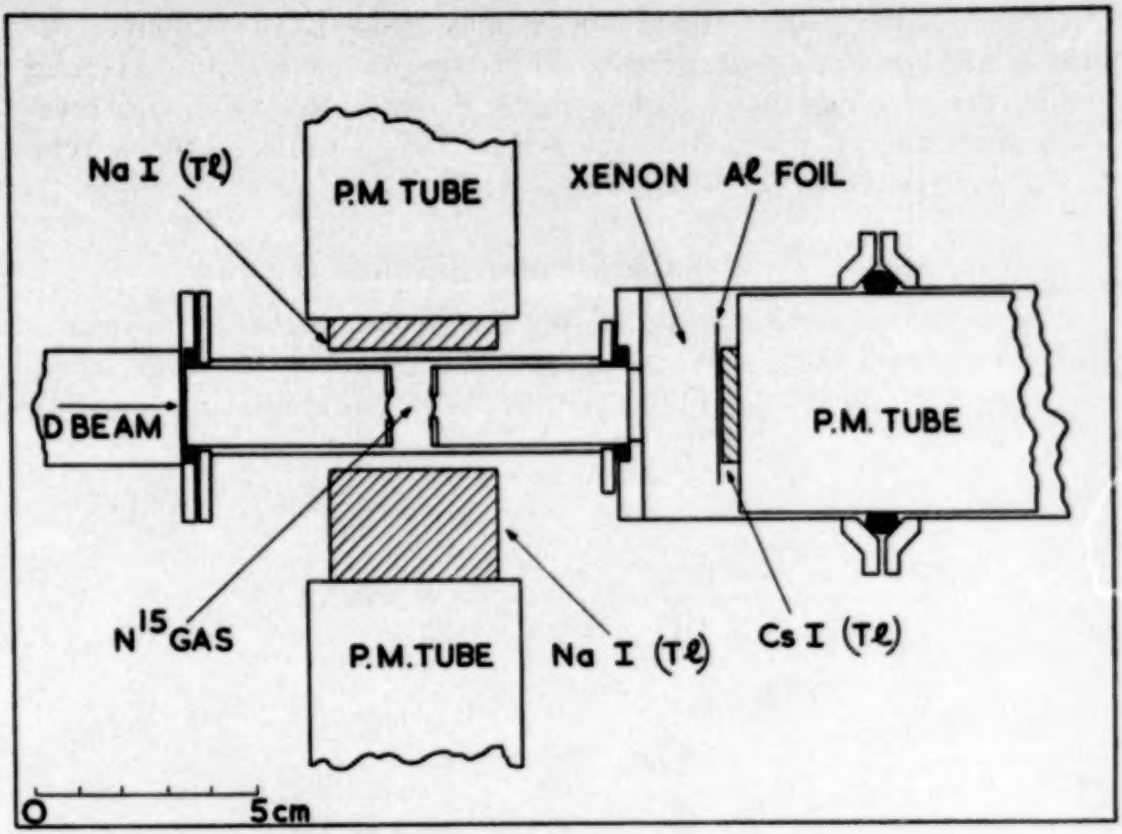

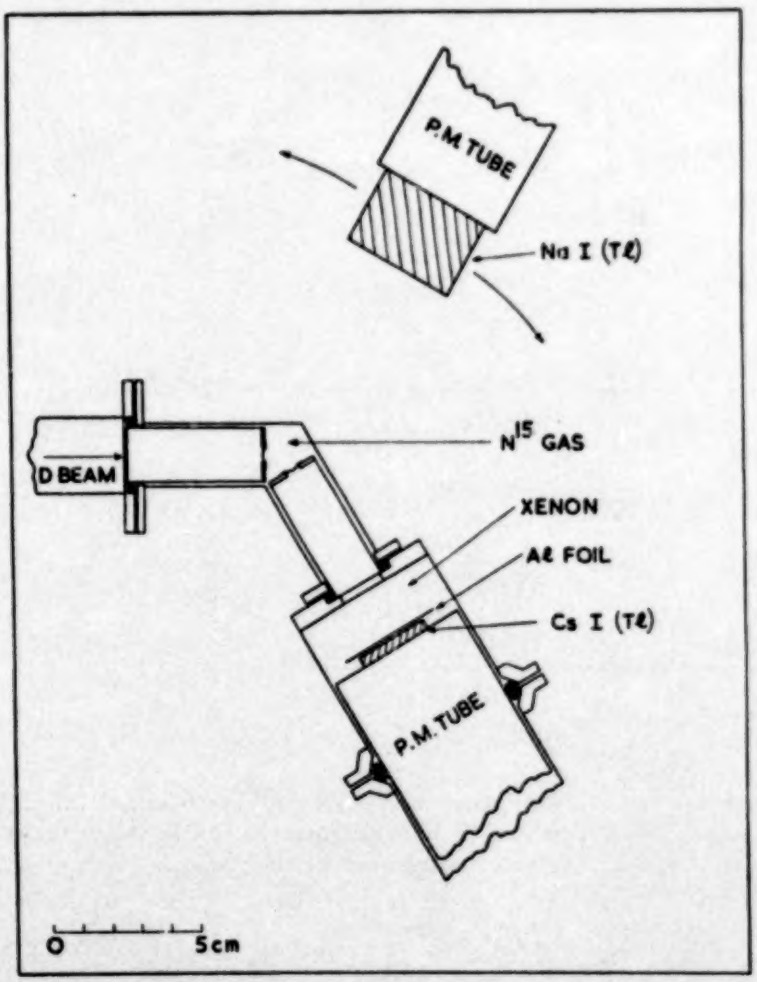

Fig. 1. Schematic diagram of gas target and proton and gamma-ray detectors: (a) for observation of protons emitted at 0° to the direction of the deuteron beam; (b) for observation of protons emitted at 60°, and measurement of (p, γ) angular correlations.

ray spectra were displayed on a 100-channel analyser. The deuteron beam through the gas cell was restricted to about 0.01 microamp for these experiments and monitoring, when required, was achieved by collecting ionization current, produced in the xenon chamber of the proton detector, on a positively charged wire.

3. Experimental Results

The level and decay scheme for the first four states of N^{16}, as deduced from the present work, is shown in fig. 2. The results on which this scheme is based will now be described. For simplicity the ground state and the

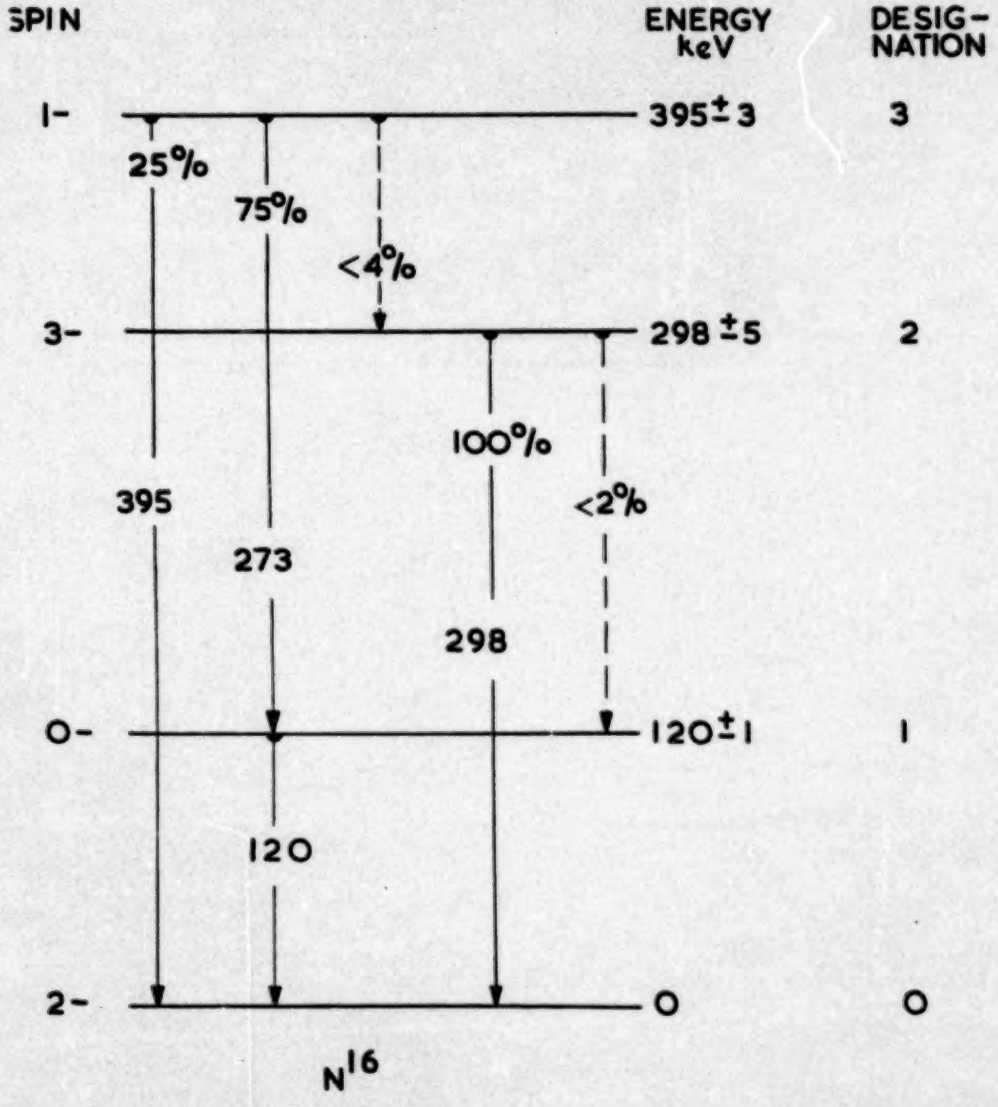

Fig. 2. Level scheme of N^{16}. Gamma-ray transitions are given in keV; percentages refer to the branching ratios of each level. The four numbers on the right are those by which the levels are designated in this paper.

first, second and third excited states will be referred to as levels 0, 1, 2, and 3 respectively and gamma-ray transitions between them as $1 \rightarrow 0$ etc. The corresponding proton groups from the N^{15}(d, p)N^{16} reaction will be denoted by p_0, p_1, p_2, and p_3.

3.1. THE GAMMA-RAY SPECTRUM

The spectrum observed with a 2.5 cm thick NaI crystal is illustrated in fig. 3. It shows peaks at 119 ± 3, 279 ± 3, 399 ± 4, and 511 keV. The 511 keV gamma-rays were ascribed to the annihilation of positons from the decay of unwanted reaction products, chiefly O^{15} from N^{14}(d, n), with possibly

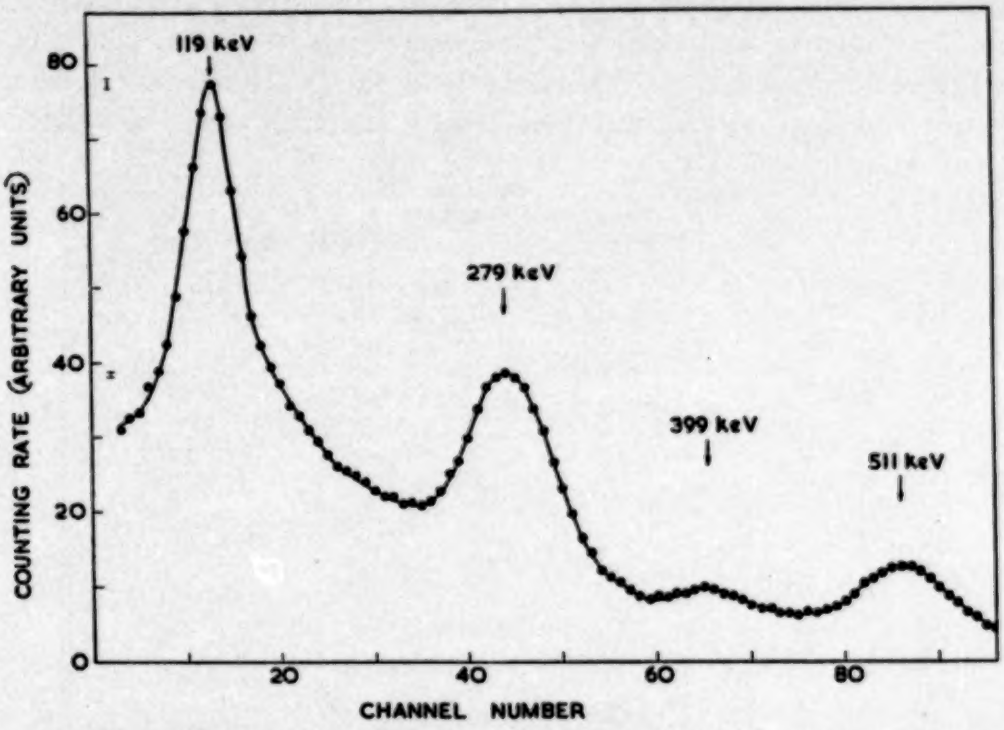

Fig. 3. Spectrum of gamma-rays resulting from the bombardment of N^{15} with 2.6 MeV deuterons.

some N^{13} from C^{12}(d, n), and F^{17} from O^{16}(d, n). The annihilation radiation was used for calibration purposes, along with the following sources of known radiations: Au^{198} (411.8 keV), Hg^{203} (278.3 keV), In^{114} (191.5 keV), and Am^{241} (59.6 keV).

Even with the assumption that the observed gamma-rays in the spectrum of fig. 3 could be attributed to the reaction N^{15}(d, p)N^{16}, the N^{16} level transitions to which they corresponded could not immediately be deduced. The level positions were not known precisely, and the gamma-ray spectrometer had finite resolution; thus the 120 keV peak might have included $3 \rightarrow 2$ transitions as well as $1 \rightarrow 0$. Similarly the 279 keV radiation might have been due to $2 \rightarrow 0$ transitions, or $3 \rightarrow 1$, or both. In some runs a small

gamma-ray group with energy about 170 keV was observed, which could have corresponded to a $2 \rightarrow 1$ transition. However, the spectrum due to annihilation radiation, taken immediately after the deuteron beam was turned off, also showed such a group, due presumably to back-scattered radiation. This offered a reasonable explanation of the 170 keV group and subsequent coincidence measurements (see fig. 4 and section 3.5) have shown that there is very little, if any, such radiation in the spectrum due to N^{16} decay.

3.2. GAMMA-GAMMA COINCIDENCE MEASUREMENTS

As already mentioned, the rate of prompt coincidences between 120 keV gamma-rays and the other gamma-rays in the spectrum was measured and, with a 0.3 microsecond resolving time, was found to be very small. In the next experiment, pulses corresponding to the 120 keV gamma-rays, detected in an 0.6 cm NaI crystal, were selected by a single-channel analyser, and

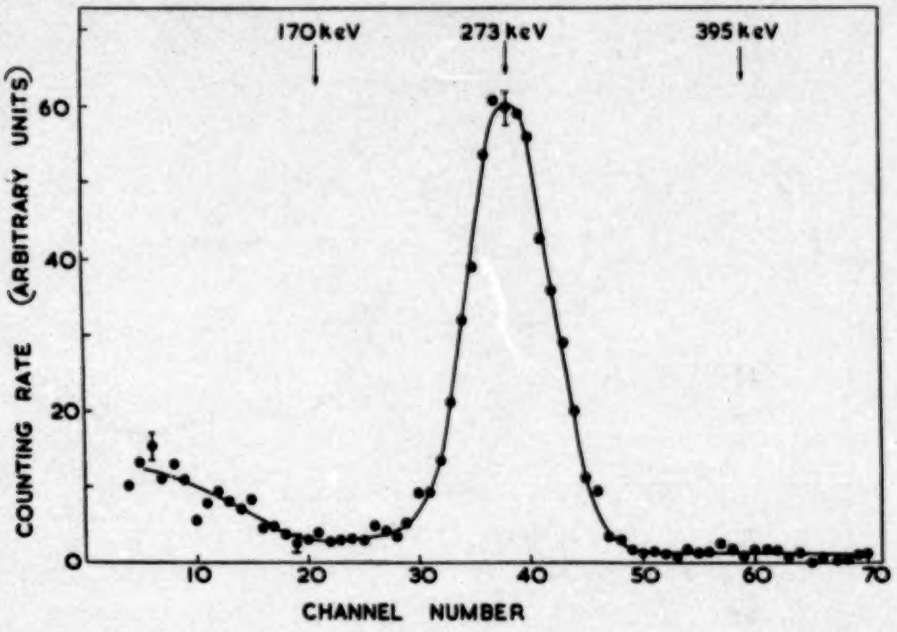

Fig. 4. Spectrum of gamma-rays in coincidence with 120 keV radiation after having been delayed by 3 microseconds.

pulses from a 2.5 cm NaI crystal were fed through a 3 microsecond delay line, as well as to a hundred-channel analyser. Coincidences between these delayed pulses and the single channel analyser pulses were used to open a gate which thus allowed the kicksorter to record the spectrum of delayed gamma-rays in coincidence with 120 keV radiation. A resolving time of 1.1 microseconds was used. The result, after subtraction of the random spectrum, is illustrated in fig. 4. This shows a single gamma-ray with an energy 6 ± 2 keV less than the group appearing at 279 keV in the ungated

spectrum. This experiment proved that the 120 keV state must be long-lived and that a level at about 393 keV (assumed to be level 3) decays to it; moreover the above mentioned 6 keV energy difference suggested that the 279 keV peak in the ungated spectrum might be double, including also a component due to level $2 \rightarrow 0$ transitions. Further inferences from the spectrum of fig. 4 are (i) the absence of 395 keV gamma-rays, which are evident in the ungated spectrum, with the implication that they arise from a ground-state transition from level 3; (ii) absence of the 170 keV peak mentioned in section 3.1. The expected position is indicated; the shape of the 273 keV spectrum agrees within the statistical errors with that for a Hg^{203} (278.3 keV) calibration spectrum and a value of $(-0.1 \pm 0.4)\%$ for the intensity of a 170 keV gamma-ray relative to the 273 keV gamma-ray is deduced.

3.3 LIFETIME OF THE 120 keV LEVEL

Measurements were made of the number of coincident 273 keV gamma-rays, per count in the 120 keV channel, for different values of the delay

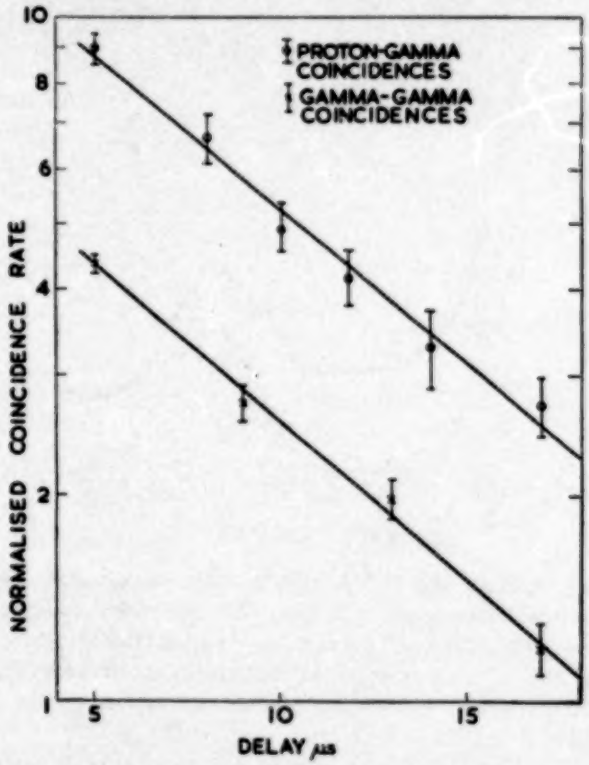

Fig. 5. Lifetime measurements for the 120 keV state. Lower curve: coincidence rate between 120 keV and 273 keV gamma-rays when the latter are delayed by various times. Upper curve: coincidence rate between 120 keV gamma-rays and p_1 and p^3 proton groups when the latter are delayed by various times.

inserted on the 273 keV side of the coincidence circuit. The result is shown by the crosses in fig. 5. A least squares analysis gave a value of 6.67 ± 0.7

microseconds for the half-life of the 120 keV state. The upper curve in the figure is the result of a similar measurement, to be described below, in which coincidences were measured between proton groups p_1 and p_3, and the subsequent 120 keV gamma-radiation; the circles in fig. 5 give the number of coincidences obtained per 120 keV gamma-ray (arbitrary units) when the protons were delayed by various times. This delay curve gives a value of 6.75 ± 0.7 microseconds for the half-life of the 120 keV state; the mean value from the two experiments is thus 6.7 ± 0.5 microseconds.

3.4. THE PROTON SPECTRA AND (p–γ) COINCIDENCES

The proton spectrum obtained with the CsI crystal set at 0° to the direction of the deuteron beam is illustrated by the upper curve in fig. 6,

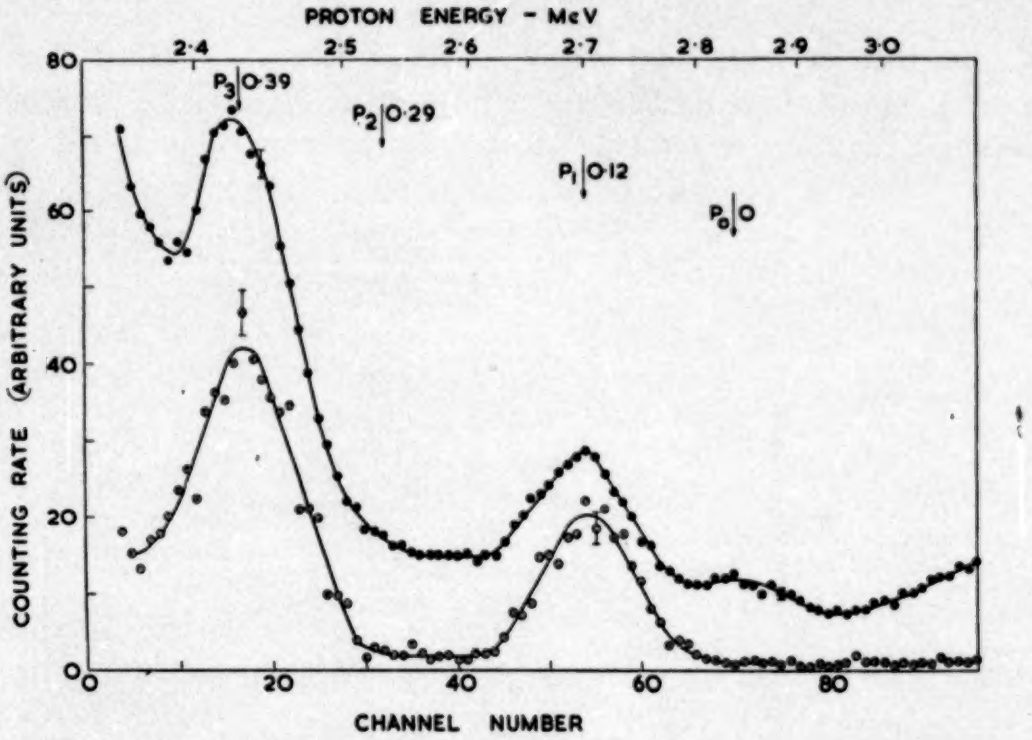

Fig. 6. Spectra of protons from the N^{15}(d, p)N^{16} reaction observed at 0° to the direction of a 2.58 MeV deuteron beam: upper curve is the direct spectrum, lower curve is the spectrum obtained in coincidence with 120 keV gamma-rays when the protons were delayed by 4 microseconds. The upper scale is an energy calibration obtained with Van de Graaff protons; arrows show expected positions of proton groups.

for deuterons of mean energy 2.58 MeV at the centre of the N^{15} gas cell. The proton detector was calibrated by allowing a very minute beam of protons from the Van de Graaff machine to enter the evacuated target cell, and to pass through to the crystal. A number of peaks due to protons of different energies were measured, and the energy scale shown at the top of fig. 6 was derived. (A correction was made for the stopping power of the

nickel entry window.) The arrows indicate the calculated peak positions for the four proton groups from the N^{15}(d, p)N^{16} reaction, the numbers beside the arrows being the energies in MeV assumed for the N^{16} levels. The p_1 and p_3 groups are the most prominent in the 0^0 spectrum, as expected from the stripping data [7]) which show peaks at 0^0 in the angular distribution of these protons, corresponding to $l_n = 0$ transitions. The p_0 and p_2 groups, showing $l_n = 2$ distributions, have minima in the forward direction. The lower curve in fig. 6 gives the proton spectrum obtained in delayed coincidence with pulses in the 120 keV peak of the associated gamma-ray spectrum; a delay of 4 microseconds had been inserted on the proton side of the circuit. The expected contribution of p_3 and p_1 protons is observed. The coincidence rate measured as a function of proton delay, and the half-life of the 120 keV state deduced therefrom, have already been discussed (see fig. 5).

The proton spectra obtained in prompt coincidence with the 279 and with the 395 keV gamma-ray peaks were found to be identical in shape, showing

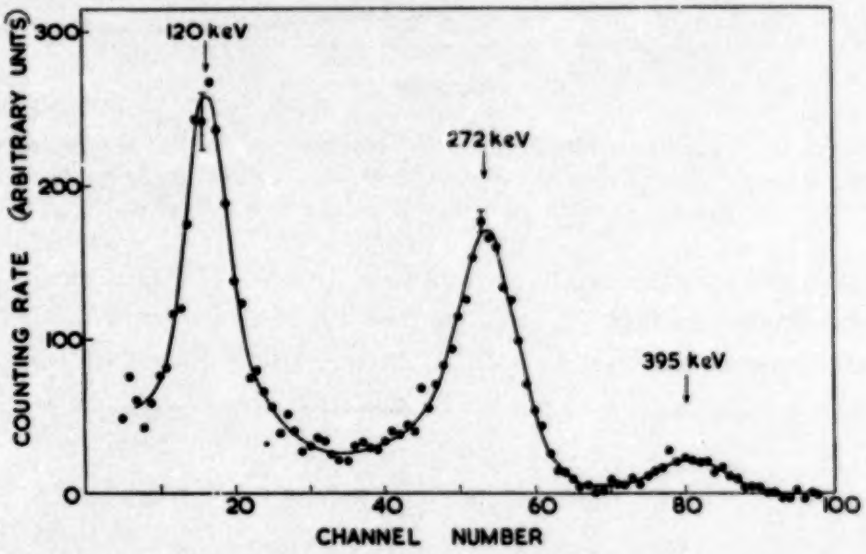

Fig. 7. The spectrum of gamma-rays in coincidence with the protons which excite the 395 keV level of N^{16}; the protons were detected at 0^0 to the deuteron beam.

only the p_3 group. This result confirms that the 395 keV gamma-ray arises from level 3 and implies that either there are no gamma-rays in the 279 keV groups due to level 2 decay or that the p_2 group at 0^0 is negligible compared with the p_3 group. The latter interpretation proves to be correct (see below). It follows that the 0^0 position is a very suitable one for selecting pulses corresponding to the p_3 group and observing the coincident gamma-ray pulses with a hundred-channel analyser. The gamma-ray spectrum obtained in prompt coincidence with p_3 protons is shown in fig. 7, where 120, 272

and 395 keV gamma-ray peaks are in evidence. A mean value of 272 ± 4 keV was obtained for the intermediate energy gamma-ray by comparison with a Hg^{203} (278.3 keV) source; this result again suggests that the cascade gamma-ray from level 3 has an energy slightly less than the mean energy of the peak in the ungated spectrum.

To investigate further the second excited state of N^{16}, the protons were next observed at a laboratory angle of 60°; here all four proton groups appeared with comparable intensities (see fig. 8 upper curve). The proton

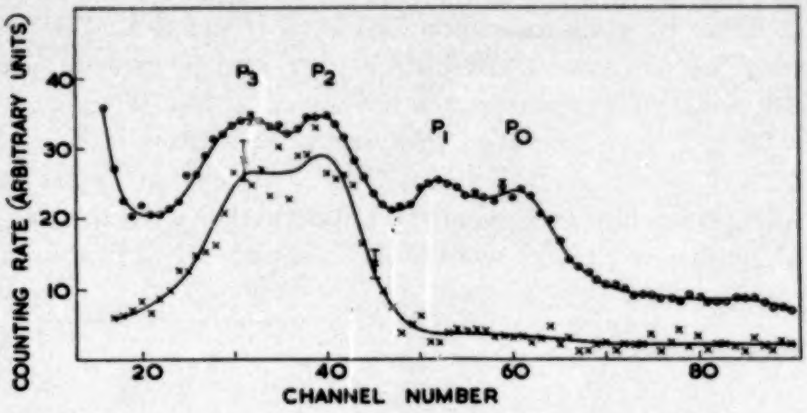

Fig. 8. Spectra of protons from the N^{15}(d, p)N^{16} reaction observed at 60° to the direction of the deuteron beam. Upper curve: the direct spectrum; lower curve: the spectrum obtained in coincidence with gamma-rays in the 279 keV group.

spectrum in coincidence with gamma-rays in the 279 keV peak showed both lower energy groups, p_2 and p_3 (see fig. 8 lower curve).

A single-channel analyser was then used to select pulses at the peak of

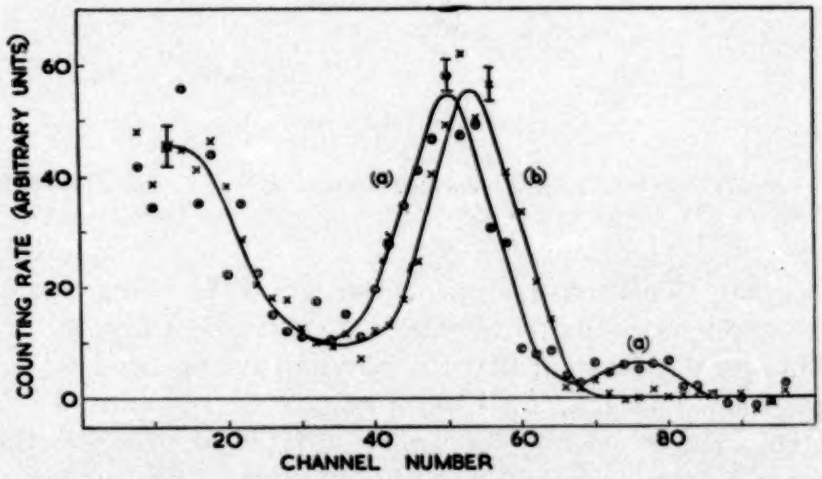

Fig. 9. The spectra of gamma-rays in coincidence with protons which excite the 395 keV level of N^{11} (curve (a)) and the 298 keV level (curve (b)); the protons were detected at 60° to the direction of the deuteron beam.

each of the p_2 and p_3 proton groups in turn, and the gamma-ray spectrum obtained in prompt coincidence was displayed. The result is shown in fig. 9. Curve (a) (circles) is the spectrum in coincidence with the p_3 proton group and curve (b) (crosses) that in coincidence with the p_2 group. The former shows the same peaks as were observed in coincidence with p_3 protons at 0^0 (fig. 7); curve (b) shows a single group corresponding to a ground-state transition from level 2 of N^{16}, and demonstrates that the 279 keV group in the ungated gamma-ray spectrum is indeed double. The energy difference between the two gamma-rays is somewhat greater than appears from the graph because the two proton groups were not completely resolved. After application of a suitable correction for the residual mixing of the gamma-rays, a value of 25 ± 5 keV is deduced for the energy difference. The best value for the lower energy gamma-ray from all our measurements is 273 ± 2 keV, and therefore for the higher energy member of the pair is 298 ± 5 keV. This, then, gives the energy of level 2 of N^{16}. It should be noted that, because of the asymmetrical shapes of the gamma-ray spectra, the mid-point at half-height of the composite 279 keV gamma-ray peak does not correspond to the mean, weighted according to relative intensities, of the corresponding points of the two components.

3.5. BRANCHING RATIOS

An estimate of the relative intensities of 395 and 273 keV gamma-ray emission from level 3 was obtained from p_3-gamma coincidence spectra of the type shown in figs. 7 and 9. This could be assumed to give the branching ratio of level 3 since, for a state formed by capture of $l_n = 0$ neutrons the gamma radiation is expected to be isotropic. Because of the 6.7 microsecond half-life of the 120 keV gamma-ray, the number of pulses appearing in the 395 keV peak due to coincident recording of 120 and 273 keV gamma-rays was negligible. The ratio of 273 keV to 395 keV radiation from level 3 found in this way was 3.0 ± 0.3.

An upper limit to the relative number of transitions from level 3 to level 2 ($\approx$ 100 keV) was found from an analysis of the spectrum in fig. 7. The relative intensities of 120 and 273 keV gamma-rays in this spectrum, when corrected for relative detection efficiencies, are 0.12 : 1. The fraction of 120 keV gamma-rays expected with the assumption of a 6.7 microsecond half-life for the 120 keV state and a resolving time of 1.1 microseconds is 0.11 : 1. The difference is unlikely to be greater than 0.04 : 1. Now any $3 \rightarrow 2$ gamma-ray transitions would contribute to the 120 keV group in the spectrum, being in prompt coincidence with p_3 protons; therefore the probability of such transitions must be not greater than 4 % of the 273 keV decay probability.

An upper limit to the relative intensity of a 178 keV gamma-ray cor-

responding to a level 2 → 1 transition can be obtained from a comparison of the two coincidence spectra of figure 9, for such a transition would be expected in coincidence with p_2 protons, but not with p_3 protons. A comparison of the two spectra, normalized to the same number of counts in each of the "279" keV peaks, after correction for relative absorption and efficiency, leads to the conclusion that (0.5 ± 1.5) per cent of level 2 decays occur via the 120 keV level. Another estimate is obtained as follows: the measurements of section 3.2 give for the intensity of 2 → 1 transitions relative to 3 → 1 transitions a value of (-0.1 ± 0.4) per cent. From Zimmerman's data [7]) the relative populations of levels 3 and 2 are 2 : 1 for the same energy of incident deuterons; allowing for the 25 % branching of 3 → 0 gamma-rays, the intensity of 2 → 0 gamma-rays relative to 3 → 1 gamma-rays is 0.66. Thus the intensity of 2 → 1 relative to 2 → 0 transitions is (-0.15 ± 0.6) per cent, where the errors are due to the statistics of counting. A value of 2 % is taken for the upper limit of this branching ratio.

3.6. PROPORTIONAL COUNTER MEASUREMENTS

The N^{16} gamma-ray spectrum was also examined with a proportional counter filled with xenon to a pressure of 5 atmospheres [9]). This allowed a more precise measurement of gamma-rays due to level 1 → 0 transitions, for which the value 120.4 ± 1 keV was obtained. In the 280 keV region the performance of the counter was impaired by the reduced efficiency and increased wall effects; nevertheless, three small peaks were distinguished. The highest, at 304 ± 5 keV, was interpreted as the full energy peak due to 2 → 0 gamma-rays, and the lowest, at 245 ± 2 keV, as the escape peak (with loss of the 30.4 keV xenon X-ray) due to 3 → 1 gamma-rays; the central peak was then attributed to the overlapping of a main 275 keV peak and the escape peak of the 304 keV gamma-rays.

These results were combined with the crystal measurements to give weighted mean values of 273 ± 2 keV and 298 ± 5 keV for the transitions 3 → 1 and 2 → 0 respectively. The former value plus the 1 → 0 measurements give 393 ± 3 keV for the excitation of level 3 and this combined with the direct measurement of the 3 → 0 gamma-ray leads to a mean of 395 ± 3 keV for the energy of level 3.

Our results for the N^{16} levels are given in table 1 together with the values found by Pauli [6]) and by Wilkinson [3]).

TABLE 1

Excited states of N^{16} in keV

Present Measurements	Pauli	Wilkinson
120 ± 1	116 ± 6	118 ± 3
298 ± 5	300 ± 12	285 ± 8
395 ± 3	391 ± 12	387 ± 5

3.7. MEASUREMENT OF A PROTON-GAMMA ANGULAR CORRELATION

A (d, p) reaction proceeding through the mechanism of stripping can be treated theoretically as a neutron capture process; in particular the interpretation of the angular distribution of gamma-radiation from an excited state of the product nucleus is thereby greatly simplified [13, 14, 15]). The angular momentum brought in by the neutron is determined from the proton angular distribution and a measurement of the angular distribution of gamma-rays relative to the direction of entry of the neutron into the nucleus may, on interpretation, allow a spin to be assigned to the radiating state. The direction of entry of the neutron is that of the recoiling product nucleus and is made unique by observing only those gamma-rays which are in coincidence with protons detected at a chosen angle. The essential assumption that the reaction process is that of stripping is most likely to be correct if the angle of detection of the protons is chosen to correspond to the maximum intensity in the proton angular distribution.

Only for the second excited state of N^{16} can interesting results be expected (levels 1 and 3 are excited by capture of $l = 0$ neutrons). The proton group p_2 exciting level 2 corresponds to absorption of $l = 2$ neutrons and has a maximum intensity at 60° to the direction of incidence of the deuterons of energy 2.8 MeV [7]). The proton detector was therefore set to observe protons emitted at $+60°$ in the horizontal plane. The gamma-detector, a 3.7 cm diameter, 2.5 cm thick sodium-iodide crystal, was mounted 7.5 cm from the centre of the gas target, on a carriage which could rotate about a vertical axis passing through the centre of the target. Pulses from the gamma-detector corresponding to gamma-rays in the energy range 250 to 320 keV were selected with a single-channel analyser. Pulses from the proton detector in prompt coincidence with these gamma pulses were displayed on a hundred-channel analyser. A series of proton spectra were recorded at a selection of angles of the gamma-detector ranging from $-120°$ to $-20°$ relative to the deuteron beam. The spectra showed peaks corresponding to the p_2 and p_3 proton groups. The angular dependence of the p_2-γ coincidence rate could be obtained in two ways: the number of genuine p_2-γ coincidences recorded at a given angle, calculated by summing over the appropriate region of the spectrum, could be normalised by dividing through either by the total number of protons counted or by the corresponding number of p_3-γ coincidences. In so far as the third level is excited by a stripping mechanism with capture of $l = 0$ neutrons, the resultant gamma-rays will be expected to be isotropic; the second method of normalisation then automatically corrects for any instrumental anisotropy due to gamma-ray absorption or misalignment. In practice the two methods of treating the data gave effectively identical results. The normalised coincidence rate is shown plotted against $\cos^2 \theta$ in fig. 10, where θ is the angle between the

observed direction of emission of the gamma-ray and the calculated direction of entry of the neutron into the nucleus. The points are best fitted by

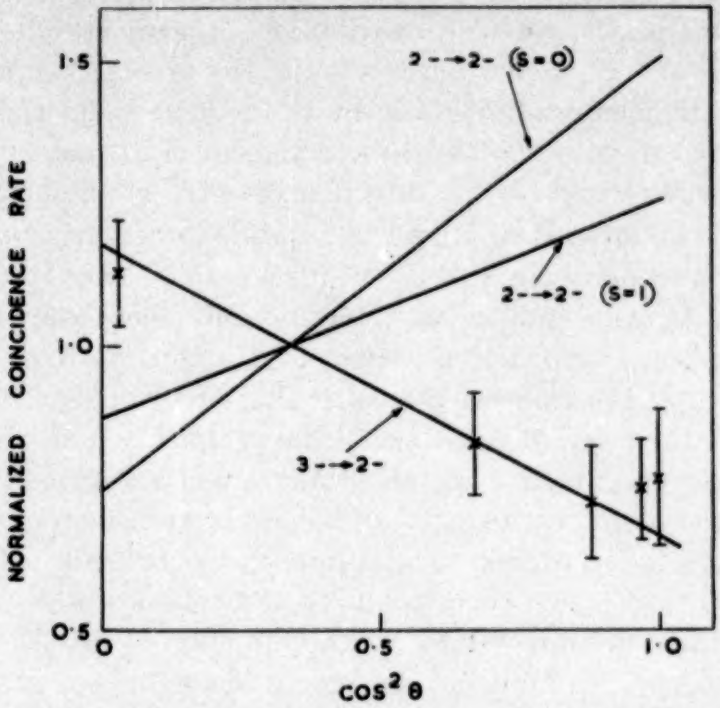

Fig. 10. Angular correlation between the protons which excite the 298 keV level of N^{16}, and the subsequent gamma-rays. The points give the normalised coincidence rate plotted against $(\cos^2\theta)$ where θ is the angle between the observed direction of gamma-ray emission and the calculated direction of entry of the neutron into the nucleus in the stripping process. The lines represent theoretical correlations for the cases of M_1 transitions to a final state 2— from an intermediate state of either 3— or 2—. In the latter case there are two possibilities corresponding to channel spin S of 0 or 1.

the function $k\{1-(0.37\pm0.08)\cos^2\theta\}$. The interpretation of this result will be discussed in the next section.

4. Discussion

The assignment of 2— for the spin and parity of the ground state of N^{16} is fairly certain. Stripping results of Warburton and McGruer [8]) show that the parity is negative and limit the spin to the values 1, 2 or 3. The β-decay proceeds from a single level in N^{16} [2, 4]). Transitions to levels in O^{16} at 6.13, 7.11 and 8.87 MeV are allowed, and to the ground state are first forbidden; the first two levels are 3— and 1— and there is evidence independent of β-decay for believing the level at 8.87 MeV to be 2— [10, 11, 12]). It seems, then, that 2— is the only reasonable assignment for the ground state of N^{16}.

Since the 120 keV level has a half-life of 6.7 microseconds, it is extremely unlikely that it can decay by dipole radiation. If we assume that the

transition is pure E2 then the spin of this level must be 0− or 4−. The latter would be incompatible with the stripping data which demonstrate an $l_n = 0$ distribution, thus requiring a spin of 0− or 1− for this level. Therefore the 120 keV level must be assigned 0−. Now the 395 keV level decays to both 0− and 2− states, with a branching ratio of 3 : 1. Its spin therefore cannot be 0, and the values 1− or 1+ are then the most probable. The stripping results, again showing an $l_n = 0$ distribution, favour 0− or 1−, so that 1− can be made a definite assignment. The spin of the 298 keV level is not so certain from these considerations. The stripping data show an $l_n = 2$ distribution of the protons to this level, making 1−, 2− or 3− the most probable assignments; however 1− is less likely because it could be reached by $l_n = 0$ neutrons. Moreover our observations show that this level decays to the 2− ground state in preference to the 0−120 keV state, again making 1− an unlikely possibility. Hence this level is most probably 2− or 3−. The above conclusions have also been reached by Wilkinson [3]).

Further evidence concerning the spin of the second excited state is afforded by the measurement of the angular distribution of p_2-γ coincidences (subsection 3.7). In the case of the p_2 proton group the neutron is captured with angular momentum 2 into a state with spin which we take to be 3− or 2−. If a 3− state, formed thus from a $\frac{1}{2}$− nucleus, decays by emission of pure M1 radiation to a 2− state, the correlation is given uniquely by $W(\theta) = (1-0.44\cos^2\theta)$; for a 2− intermediate state two channel spins ($S = 0$ or 1) are possible, with corresponding correlation functions $(1+0.6\cos^2\theta)$ and $(1+0.33\cos^2\theta)$. Here θ is the angle between the direction of emission of the gamma-ray and the direction of recoil of the excited N^{16} nucleus. These M1 correlations are shown by the lines in fig. 10, together with the experimental points which are best fitted by a function $[1-(0.37\pm0.08)\cos^2\theta)]$. In the case of a 2− intermediate state an admixture of at least 20 % in intensity of E2 radiation would be required to give a 90°/0° ratio consistent with the experimental value. Such a large contribution of E2 radiation would be very unlikely since the Weisskopf single-particle estimate favours M1 relative to E2 by a factor of nearly 10^5. With the assumption that the radiation from the 298 keV level is predominantly M1 the experimental results strongly favour the assignment 3− to level 2†.

The results are in excellent accord with the calculations of Elliott and Flowers [1]) who predict four low-lying states of N^{16} with the assignments 0−, 1−, 2− and 3− (order undetermined). Our value for the branching ratio of the 395 keV state, namely 3.0 : 1 in favour of the transition to the 120 keV state also agrees well with the theoretical prediction. The observed value of 6.7 ± 0.5 microseconds for the half-life of the 120 keV state is not

† The less likely possibility of 1− for this state is also ruled out by the experimental data since for this case the M1 correlation would be $1-0.07\cos^2\theta$.

far removed from the calculated value of 2.6 ± 1.0 microseconds. The latter includes the effect of collective enchancement, which compensates for the fact that the radiation results from a neutron rather than a proton transition, so that the result is quite close to the Weisskopf single-particle estimate.

It would be interesting to seek the corresponding levels in F^{16}. Recently the cross-section for neutron production when N^{14} is bombarded with 3 MeV He^3 particles has been found by Grace and Hanna [16]) to be about 20 millibarns, and equal to the cross section for production of O^{15}. It may well be that the neutrons are emitted first from a highly excited F^{17} compound nucleus, followed by break-up of proton-unstable F^{16}. A careful study of the neutron spectrum might confirm this mechanism; if the energy release in the decay of F^{16} by proton emission is not too high the lowest states of F^{16} may be sufficiently narrow to give a recognizable structure to the neutron spectrum.

The authors wish to thank J. O. Newton for his participation in the early stages of the experiment, D. West and F. Bradley for the loan of a proportional counter, W. Zimmerman and E. K. Warburton for sending results in advance of publication, and J. P. Elliott, B. H. Flowers and E. B. Paul for helpful discussion.

References

1) J. P. Elliot and B. H. Flowers, Proc. Roy. Soc. (to be published)
2) B. J. Toppel, Phys. Rev. **103** (1956) 141
3) D. H. Wilkinson, Phys. Rev. **105** (1957) 686
4) R. C. Hanna, J. M. Freeman and J. O. Newton, Physica **22** (1956) 1154
5) J. Thirion, R. Cohen and W. Whaling, Phys. Rev. **96** (1954) 850
6) R. T. Pauli, Arkiv. f. Fysik **9** (1955) 571
7) W. Zimmerman, Phys. Rev. **104** (1956) 387
8) E. K. Warburton and J. N. McGruer, Bull. Am. Phys. Soc., **1** (1956) 325
9) D. West, Progress in Nuclear Physics (Pergamon Press) **3** (1953) 18
10) E. Bleuler, P. Scherrer, M. Walter and W. Zunti, Helv. Phys. Acta **20** (1947) 96
11) C. H. Millar, G. A. Bartholomew and B. B. Kinsey, Phys. Rev. **81** (1951) 150
12) D. H. Wilkinson, B. J. Toppel and D. E. Alburger, Phys. Rev. **101** (1956) 673
13) L. C. Biedenharn, K. Boyer and R. A. Charpie, Phys. Rev. **88** (1952) 517
14) G. R. Satchelor and J. A. Spiers, Proc. Phys. Soc. A **65** (1952) 980
15) L. J. Gallaher and W. B. Cheston, Phys. Rev. **88** (1952) 684
16) M. A. Grace and R. C. Hanna (private communication)

Nuclear Physics **4** (1957) 615—624; © *North-Holland Publishing Co., Amsterdam*
Not to be reproduced by photoprint or microfilm without written permission from the publisher

I C REPULSIVE CORE AND NUCLEAR SHELL THEORY

M. BAUER and M. MOSHINSKY

Instituto Nacional de la Investigación Científica e Instituto de Física, Universidad de México, México, D.F.

Received 20 June 1957

Abstract: We discuss the effect on nuclear shell theory of an interaction potential between nucleons containing a repulsive core. We show that a repulsive hard core gives rise to the same interaction energy as a delta function potential of strength $4\pi(\hbar^2 a/m)$, where a is the range of the core and m the mass of the nucleon. The interaction energies for Yukawa potentials with and without repulsive cores, are compared.

1. Introduction

The work of Brueckner [1]), Bethe [2]) and their collaborators, has shown that it is possible to assume for the interactions between nucleons in nuclear matter the same potentials as between free nucleons. The phenomenological nucleon-nucleon potential recently obtained by Gammel, Christian and Thaler [3]) contains a hard core of a range † 0.5*f*, and the presence of this core causes serious difficulties in problems of nuclear structure. The purpose of this paper is to show how one can deal with the problem posed by the repulsive core in nuclear shell theory.

It is quite clear that if one takes a repulsive core of finite range, whose strength goes to ∞, the standard perturbation methods will fail. Yet, if we look at the problem of the bound states in a square well potential with a repulsive core, which can be solved exactly, we see that for a sufficiently narrow core, both energy levels and wave functions do not differ much from the same problem without a hard core. This suggests that a perturbation method should exist for solving this problem, albeit it is not the standard perturbation method. This gives the basic idea for dealing with repulsive cores in nuclear shell theory.

We shall consider first the problem of two nucleons moving in a common potential of the harmonic oscillator form, and interacting only through a hard core. Taking advantage of the form of the common potential [4]), we can pass to relative and centre of mass coordinates for the two nucleons, and reduce the problem to that of a single particle moving in a harmonic oscillator potential with a hard core. The radial equation for this problem can be transformed by a simple translation in such a way that the repulsive

† We denote by *f* the length 10^{-13} cm.

core disappears, and an interaction potential appears, which can be treated by standard perturbation methods. When passing back to the initial coordinate system, we show that the hard core acts to first order as a delta function potential of strength $4\pi(\hbar^2 a/m)$, where a is the range of the core and m the mass of the nucleon.

We next consider an interaction potential between nucleons formed by a hard core plus an attractive central potential of the Yukawa type. The influence of this interaction potential in nuclear shell theory will be analyzed, taking for the parameters of the Yukawa potential the values given by Gammel *et al.* [3])

We shall start our discussion by reviewing some of the results for the two nucleon problem in a harmonic oscillator common potential, that will be useful for the following developments.

2. The Two Nucleon Problem in the Harmonic Oscillator Common Potential

The main advantage in using for the common potential of the nucleons the harmonic oscillator potential discussed by Talmi [4]), Thieberger [5]) and others, is the separability of the problem of two nucleons in an appropriate coordinate system, even in the presence of interactions between nucleons.

Let us write the two nucleon hamiltonian for a harmonic oscillator common potential of frequency ω as

$$H = (2m)^{-1}\mathbf{p}_1^2+(2m)^{-1}\mathbf{p}_2^2+\tfrac{1}{2}m\omega^2\mathbf{r}_1^2+\tfrac{1}{2}m\omega^2\mathbf{r}_2^2+V(|\mathbf{r}_1-\mathbf{r}_2|), \tag{1}$$

where V is the interaction potential which will be assumed central. Introducing the relative and center of mass coordinates

$$\mathbf{r}' = \mathbf{r}_1-\mathbf{r}_2, \quad \mathbf{r}'' = \tfrac{1}{2}(\mathbf{r}_1+\mathbf{r}_2), \tag{2}$$

and their corresponding momenta

$$\mathbf{p}' = \tfrac{1}{2}(\mathbf{p}_1-\mathbf{p}_2), \quad \mathbf{p}'' = \mathbf{p}_1+\mathbf{p}_2, \tag{3}$$

the Hamiltonian becomes

$$H = m^{-1}\mathbf{p}'^2+\tfrac{1}{4}m\omega^2\mathbf{r}'^2+V(r')+(4m)^{-1}\mathbf{p}''^2+m\omega^2\mathbf{r}''^2. \tag{4}$$

The angular momentum associated with the different coordinates is given by $\mathbf{l}_1 = \mathbf{r}_1\times\mathbf{p}_1$ etc., and from (2) and (3) we see that

$$\mathbf{l}_1+\mathbf{l}_2 = \mathbf{l}'+\mathbf{l}'' = \mathbf{L}, \tag{5}$$

where $\mathbf{L}$ denotes now the total angular momentum of the system.

We shall designate the wave functions associated with the different coordinates, without the interaction potential V, by the bracket notation of Dirac in the form

$$|n_1 l_1 m_1\rangle = r_1^{-1}R_{n_1 l_1}(r, r_1)Y_{l_1 m_1}(\theta_1, \varphi_1) \text{ etc.}, \tag{6}$$

where $Y_{l_1 m_1}$ are the spherical harmonics, $R_{n_1 l_1}$ are the radial functions given in the previous references [4,5]), and $\nu = m\omega/\hbar$. For $|n'l'm'\rangle$, ν should be changed [4]) to $\nu' = \frac{1}{2}\nu$, while for $|n''l''m''\rangle$ it should be changed to $\nu'' = 2\nu$.

A wave function with a definite total angular momentum could be formed from (6) and the Clebsch-Gordan coefficient $\langle l_1 l_2 m_1 m_2 | LM\rangle$ to obtain

$$|n_1 l_1,\ n_2 l_2,\ LM\rangle = \sum_{m_1 m_2} |n_1 l_1 m_1\rangle\ |n_2 l_2 m_2\rangle \langle l_1 l_2 m_1 m_2 | LM\rangle. \tag{7}$$

A similar wave function could be formed for the $\mathbf{r}'$, $\mathbf{r}''$ coordinates giving

$$|n'l', n''l'', LM\rangle = \sum_{m' m''} |n'l'm'\rangle\ |n''l''m''\rangle \langle l'l''m'm''|LM\rangle. \tag{8}$$

Because of (5) the transformation brackets taking us from (8) to (7) would contain the same L, so we could write

$$\begin{aligned} |n_1 l_1,\ n_2 l_2,\ LM\rangle = \sum_{n'l',\, n''l''} \{ & |n'l',\ n''l'',\ LM\rangle \\ & \langle n'l',\ n''l'',\ LM|\ n_1 l_1,\ n_2 l_2,\ LM\rangle\}, \end{aligned} \tag{9}$$

where the conservation of energy [4]) restricts $n'l'$, $n''l''$, to the positive integers that satisfy the relation

$$\hbar\omega(2n'+l'+2n''+l''+3) = \hbar\omega(2n_1+l_1+2n_2+l_2+3). \tag{10}$$

From (9) and (10) we see that the interaction energy $E(n_1 l_1, n_2 l_2, L)$ associated with the central potential $V(r')$ will be given by

$$E(n_1 l_1, n_2 l_2, L) = \sum_{n'l',\, n''l''} [\langle n'l', n''l'', LM|\ n_1 l_1, n_2 l_2, LM\rangle]^2 \varepsilon(n'l'), \tag{11}$$

where $\varepsilon(n'l')$ is associated with the interaction energy for the $\mathbf{r}'$ coordinate, and is usually given by

$$\varepsilon(n'l') = \langle n'l'm'|\ V(r')|n'l'm'\rangle. \tag{12}$$

The expression (11) will be our fundamental formula, and in the next section we shall show how to calculate $\varepsilon(n'l')$ for a repulsive hard core potential.

3. The Hard Core Potential

Let us assume for the moment that the interaction potential $V(r')$ of the previous section is a repulsive hard core of range a. To obtain the interaction energy due to this potential, we look at the hamiltonian as given by (4), and notice that it is separable in the coordinates $\mathbf{r}'$, $\mathbf{r}''$, and that the radial function $R_{l'}(r')$ satisfies the equation

$$[-(\hbar^2/m)(\mathrm{d}^2/\mathrm{d}r'^2) + U_{l'}(r')] R_{l'} = E' R_{l'}(r'), \tag{13}$$

where

$$U_{l'}(r') = (\hbar^2/m) l'(l'+1)(r')^{-2} + \tfrac{1}{2} m\omega^2 (r')^2, \tag{14}$$

with r' restricted to $a \leqq r' \leqq \infty$. The radial function satisfies the boundary condition

$$R_{l'}(a) = 0. \tag{15}$$

This problem can be solved exactly [6]), but it is of more interest to devise a perturbation procedure for the solution as we would like to express the interaction energy in the form (11). For that purpose we introduce in (13) the change of variable

$$r' = r + a, \tag{16}$$

so that the equation can be written as

$$\{-(\hbar^2/m)(\mathrm{d}^2/\mathrm{d}r^2) + U_{l'}(r) + [U_{l'}(r+a) - U_{l'}(r)]\} R_{l'} = E' R_{l'}, \tag{17}$$

where r is now restricted to the interval $0 \leqq r \leqq \infty$. From (15), (16) we see that $R_{l'}$ considered as a function of r satisfies now the boundary condition

$$R_{l'}(0) = 0 \tag{18}$$

The eigenvalues E' of the energy for the problems (13), (15) are clearly identical to those of (17), (18), but the advantage of the last form is that for a sufficiently small a, the term in the square brackets in (17) could be considered as a perturbation to which a standard perturbation procedure could be applied.

We expand the square bracket in (17) in powers of a to obtain

$$\begin{aligned} U_{l'}(r+a) - U_{l'}(r) &= a(\mathrm{d}U_{l'}/\mathrm{d}r) \\ + (a^2/2)(\mathrm{d}^2U_{l'}/\mathrm{d}r^2) - a^3(\hbar^2/m)l'(l'+1)(4r+3a)r^{-4}(r+a)^{-2}, \end{aligned} \tag{19}$$

where the last term is the residue of the expansion. From (19) we see that to the first order in a the energy E' would be given by

$$E' = \hbar\omega[2n' + l' + \tfrac{3}{2})] + \varepsilon(n'l'), \tag{20}$$

where $\varepsilon(n'l')$ has the form

$$\varepsilon(n'l') = a\int_0^\infty [R_{n'l'}(\nu', r)]^2 [\mathrm{d}U_{l'}/\mathrm{d}r]\mathrm{d}r, \tag{21}$$

the $R_{n'l'}(\nu', r)$ being the radial functions for the harmonic oscillator potential as in (6).

We can evaluate the matrix element in (21) in a simple fashion by taking the derivative of the unperturbed equation for $R_{n'l'}(\nu', r)$ with respect to r to obtain

$$\begin{aligned} [-(\hbar^2/m)\mathrm{d}^2/\mathrm{d}r^2 + U_{l'}(r) - \hbar\omega(2n' + l' + \tfrac{3}{2})](\mathrm{d}R_{n'l'}/\mathrm{d}r) \\ = -(\mathrm{d}U_{l'}/\mathrm{d}r)R_{n'l'} \end{aligned} \tag{22}$$

Multiplying (22) by $R_{n'l'}$ and integrating with respect to r from 0 to ∞, we see from the boundary condition (18) and the equation satisfied by $R_{n'l'}$ that

$$a\int_0^\infty [R_{n'l'}(\nu', r)]^2 [\mathrm{d}U_{l'}/\mathrm{d}r]\mathrm{d}r = (\hbar^2 a/m)[(\mathrm{d}R_{n'l'}/\mathrm{d}r)_{r=0}]^2. \tag{23}$$

From the explicit form [4,5]) of the $R_{n'l'}(\nu', r)$ radial function we have

$$[\mathrm{d}R_{n'l'}(\nu', r)/\mathrm{d}r]_{r=0} = 0, \quad \text{if} \quad l' \neq 0, \tag{24}$$

so the interaction energy $\varepsilon(n'l')$ is given by

$$\varepsilon(n'l') = (\hbar^2 a/m)[(\mathrm{d}R_{n'0}/\mathrm{d}r)_{r=0}]^2 \delta_{l'0}. \tag{25}$$

We have obtained to first order in a the interaction energy in the $\mathbf{r}'$ coordinate system for a repulsive hard core. The discussion of the second order perturbation effects, and the form of the perturbed wave functions, will be given elsewhere [6]).

Using (25) and (11) we shall show in the next section that to first order in a, the interaction energy for a hard core is the same as that due to a δ function potential of strength $4\pi(\hbar^2 a/m)$.

4. The Interaction Energy for a Hard Core Potential

As $\varepsilon(n'l') \neq 0$ only for $l' = 0$, we have to take the Dirac bracket in (11) with $l' = 0$, and from (8) we see that $l'' = L$, so the interaction energy for a repulsive hard core potential of range a is given by

$$\begin{aligned} &E(n_1 l_1, n_2 l_2, L) \\ &= (\hbar^2 a/m) \textstyle\sum_{n'n''} [\langle n'0, n''L, LM | n_1 l_1, n_2 l_2, LM\rangle]^2 [(\mathrm{d}R_{n'0}/\mathrm{d}r)_{r=0}]^2, \end{aligned} \tag{26}$$

where from (10), n', n'' are positive integers restricted by the relation

$$n'+n'' = (n_1+n_2)+\tfrac{1}{2}(l_1+l_2-L), \tag{27}$$

with l_1+l_2-L being even because of parity considerations [4]).

From (7) and (8) one could evaluate [6]) the Dirac bracket in (26), but it is more interesting to compare the interaction energy with that due to a δ function potential of the form

$$4\pi g \delta(\mathbf{r}_1-\mathbf{r}_2) = 4\pi g \delta(\mathbf{r}'), \tag{28}$$

where g is so far an arbitrary constant. The interaction energy in the $\mathbf{r}'$ coordinate system will be given by (12), and expressing $\delta(\mathbf{r}')$ in polar coordinates [7]) we obtain

$$\begin{aligned} \varepsilon(n'l') = 4\pi g \Big\{ &\int_0^\infty [R_{n'l'}(\nu', r')/r']^2 \delta(r') \mathrm{d}r' \\ &\int_0^\pi \int_0^{2\pi} |Y_{l'm'}(\theta', \varphi')|^2 \delta(\theta') \delta(\varphi') \mathrm{d}\theta' \, \mathrm{d}\varphi' \Big\}. \end{aligned} \tag{29}$$

Taking into account that

$$\lim_{r' \to 0} [R_{n'l'}(\nu', r')/r'] = (\mathrm{d}R_{n'l'}/\mathrm{d}r')_{r'=0} \tag{30}$$

we see from (24) and (30) that the interaction energy for a δ function potential becomes

$$\varepsilon(n'l') = g[(\mathrm{d}R_{n'0}/\mathrm{d}r')_{r'=0}]^2 \delta_{l'0}. \tag{31}$$

Comparing (31) and (25) we see that they are identical if

$$g = \hbar^2 a/m. \tag{32}$$

As the interaction energy for two particles in jj coupling and also the interaction energy for more than two particles, could be obtained [8]) from (26) with the help of $9j$ coefficients or of fractional parentage coefficients, we see that to first order a repulsive hard core potential of range a is equivalent to the δ function potential

$$4\pi(\hbar^2 a/m)\delta(\mathbf{r}_1-\mathbf{r}_2). \tag{33}$$

So far we have considered only a repulsive core potential. As the actual interaction contains an attractive part plus a hard core, we discuss this problem in the next section.

5. The Interaction Energy for an Attractive Yukawa Potential with a Hard Core

We now take for the $V(r')$ in (4) a potential of the form

$$V(r') = \begin{cases} +\infty & \text{if } r' < a \\ -V_0(b/r')\exp[-(r'/b)], & \text{if } a \leqq r' \leqq \infty, \end{cases} \tag{34}$$

where V_0 is the depth and b the range of an attractive Yukawa potential.

The radial equation in r' will also be given by (13), if we introduce in it the attractive part of the potential $V(r')$. As in section 3, we make the change of variable $r' = r+a$ and we see that the perturbation term will now be

$$U_{l'}(r+a)-U_{l'}(r)+V(r+a), \tag{35}$$

where r extends to the interval $0 \leqq r \leqq \infty$. If we again restrict the effect of the hard core to first order in a, we see from (35), (34) and the discussion in the previous section that the equivalent potential will be

$$\begin{aligned} &4\pi(\hbar^2 a/m)\delta(\mathbf{r}_1-\mathbf{r}_2) \\ &-V_0[b/(|\mathbf{r}_1-\mathbf{r}_2|+a)]\exp[-(|\mathbf{r}_1-\mathbf{r}_2|+a)/b]. \end{aligned} \tag{36}$$

To first order perturbation theory the effects of the two terms in (36) are additive, and the contribution of the second term could be discussed with the help of the general methods developed by Talmi [4]) and Thieberger [5]). A particular case of great importance is the one in which both a and b are small compared with the nuclear radius R_0. In that case the second term in (36) could be substituted by an equivalent delta function potential, whose strength $4\pi g'$ would clearly be given by the relation

$$\iiint\{-V_0[b/(r+a)]\exp[-(r+a)/b]\}d\tau = 4\pi g'\iiint\delta(\mathbf{r})d\tau, \tag{37}$$

where $d\tau$ is the volume element. From (37) we see that

$$\begin{aligned} g' &= \int_0^\infty\{-V_0[b/(r+a)]\exp[-(r+a)/b]\}r^2 dr \\ &= -V_0 b^3\{(1-c)\exp(-c)+c^2[-\mathrm{Ei}(-c)]\}, \end{aligned} \tag{38}$$

where $c = a/b$ and [9])

$$-\mathrm{Ei}(-c) = \int_c^\infty x^{-1} \exp(-x)\mathrm{d}x. \tag{39}$$

For a Yukawa potential with a hard core for which both a and b are small compared with the nuclear radius R_0, the interaction energy is the one due to a δ function potential

$$-4\pi G\delta(\mathbf{r}_1-\mathbf{r}_2), \tag{40}$$

where G is given by

$$G = V_0 b^3\{(1-c)\exp(-c)+c^2[-\mathrm{Ei}(-c)]\}-(\hbar^2 a/m). \tag{41}$$

For a Yukawa potential without a repulsive core

$$V(r') = -V_0'(b'/r')\exp(-r'/b'), \text{ with } 0 \leqq r' \leqq \infty, \tag{42}$$

we have for b' small compared with R_0, that it can be substituted by the potential (40) where G is replaced by a G' which by an analysis similar to (37) is given by

$$G' = V_0' b'^3. \tag{43}$$

With the help of (41) and (43) we can compare the effects in nuclear shell theory of the potentials with a repulsive core of Gammel *et al.* [3]), and of the potentials without a repulsive core of Feshbach and Schwinger (as quoted by Blatt and Weisskopf [10])).

For a delta function potential the interaction energy between nucleons in the same shell is different from zero [8]) only for even L. If we restrict ourselves to interactions between identical nucleons, the wave function must be antisymmetric and as L is even, the nucleons must be in the singlet state. Gammel *et al.* [3]) give for the even singlet potential the parameters

$$V_0 = 896.6 \text{ MeV (for the p}-\text{p potential)}, \; a = 0.5f, \; b = 0.588f, \tag{44}$$

so that $c = a/b = 0.85$, and from (41) we obtain

$$G = 28.11 \; f^3 \text{ MeV}. \tag{45}$$

For the singlet potential of Feshbach and Schwinger [10]) we have

$$V_0' = 48.12 \text{ MeV}, \; b' = 1.165f, \tag{46}$$

so that the G' of (43) becomes

$$G' = 76.1 \; f^3 \text{ MeV}. \tag{47}$$

From (45) and (47) we see that the interaction energy between identical nucleons in the same shell and in heavy nuclei for an interaction potential with a repulsive core, is about 37 % of the interaction energy for a potential without a repulsive core.

So far we have not given any numerical values to show whether it is valid to treat the repulsive core and the Yukawa potential with a repulsive core to first order perturbation, for parameters such as those of (44). In

the next section we use some results for the δ interaction potential to discuss these points.

6. Interaction Energy for two and three Particle Configurations

In the previous sections we showed that the interaction energy for a repulsive core would be the same as that due to the δ potential (33). For an attractive Yukawa potential of short range with a repulsive core, the interaction energy can also be obtained from a δ potential as shown in (40). For the two particle configuration in jj coupling, the interaction energy for a δ potential was given by Zeldes [11]) in the form

$$\begin{aligned}\langle (nlj)^2 JM|4\pi g\delta(\mathbf{r}_1-\mathbf{r}_2)|(nlj)^2 JM\rangle \\ = g(2\nu^3/\pi)^{1/2}\ W[(nlj)^2,\ J],\end{aligned} \tag{48}$$

where $\nu = m\omega/\hbar$, and $W[(nlj)^2,\ J]$ is tabulated for several shells and for $J = 0, 2, 4$ in table 3 (where it is written as $W(j^2 J)$) of the paper of Zeldes[11]). For higher values of the total angular momentum J, we could obtain $W[(nlj)^2,\ J]$ by the use of a recurrence relation derived by one of us (M.M.), that has the form [8])

$$\frac{W[(nlj)^2,\ J+2]}{W[(nlj)^2,\ J]} = \left(\frac{J+1}{J+2}\right)^2 \frac{(2j+1)^2-(J+2)^2}{(2j+1)^2-(J+1)^2}. \tag{49}$$

The interaction energy for a three particle configuration will have the form (48), if we replace $W[(nlj)^2,\ J]$ by $W[(nlj)^3,\ J]$ defined as [8])

$$W[(nlj)^3,\ J] = \sum_{J'} 3[\langle (j)^2 J',\ j,\ J|\}(j)^3 \alpha J\rangle]^2 W[(nlj)^2,\ J'], \tag{50}$$

where the term inside the square bracket is the appropriate fractional parentage coefficient, α represents other quantum numbers necessary to define the state, and J' is restricted to even values. From the work of Schwartz and de-Shalit [12]) the fractional parentage coefficients can be given in terms of Racah coefficients, so that evaluating these coefficients [8]) for $j = 5/2,\ 7/2$, we can give in the following tables the values of $W[(nlj)^3,\ J]$ in the $j = 5/2$ and $j = 7/2$ shells.

From table 3 of Zeldes [11]), and from the following tables for the interaction energy in the three particle configuration, we notice that the W's are always smaller than 1, and decrease when J and j increase. An upper bound $E_{\max}$ for the interaction energy would then be given by

$$E_{\max} = g(2\nu^3/\pi)^{1/2} = g(2/\pi)^{1/2}(\hbar\omega/41.36)^{3/2}\ \text{MeV}, \tag{51}$$

where g is given in f^3 MeV and $\hbar\omega$ in MeV.

For a repulsive hard core of range $a = 0.5f$ we see from (33) that $g = 20.68\ f^3$ MeV so that $E_{\max}$ becomes

$$\begin{aligned}E_{\max} &= 0.496\ \text{MeV if } \hbar\omega = 4\text{MeV}, \\ E_{\max} &= 5.55\ \text{MeV if } \hbar\omega = 20\ \text{MeV},\end{aligned} \tag{52}$$

and $E_{\max}$ is small compared with $\hbar\omega$ in both cases.

TABLE 1

The coefficient $W[(nlj)^2, J]$ for the $j = 5/2$ shells.

J \ $(n+1)l_j$	$1d_{5/2}$	$1f_{5/2}$	$2d_{5/2}$	$2f_{5/2}$	$3d_{5/2}$
3/2	0.450	0.328	0.315	0.233	0.256
5/2	0.788	0.575	0.551	0.408	0.448
9/2	0.293	0.213	0.205	0.152	0.167

TABLE 2

The coefficient $W[(nlj)^2, J]$ for the $j = 7/2$ shells.

J \ $(n+1)l_j$	$1f_{7/2}$	$1g_{7/2}$	$2f_{7/2}$	$2g_{7/2}$
3/2	0.328	0.258	0.233	0.185
5/2	0.395	0.311	0.280	0.223
7/2	0.766	0.603	0.544	0.432
9/2	0.264	0.208	0.187	0.149
11/2	0.275	0.217	0.195	0.155
15/2	0.165	0.129	0.117	0.093

For the even singlet Yukawa potential with a repulsive core whose parameters are given in (44), an upper bound for the absolute value of the interaction energy is given by (51) where g takes the value of $28.11/f^3$ MeV, so that

$$\begin{aligned} E_{\max} &= 0.674 \text{ MeV if } \hbar\omega = 4\text{MeV}, \\ E_{\max} &= 7.54 \text{ MeV if } \hbar\omega = 20 \text{ MeV}. \end{aligned} \tag{53}$$

From (53) and the above tables, we see that the interaction energy is small compared with the separation between energy levels in the harmonic oscillator potential, for both values of $\hbar\omega$ that are considered, and therefore restricting the interaction energy to first order seems reasonable.

With the parameter given in (45) we could make an estimate of $\hbar\omega$. The separation [11]) between the levels $J = 0$ and $J = 2$ in Ca^{42} is 1510 keV. Assuming that this separation is due to the difference in interaction energy for two neutrons in the first $f_{7/2}$ shell, when they are in the $J = 0$ and $J = 2$ states, we see from (48) where we take $g = 28.11\ f^3$ MeV, and from (51) and the table 3 of Zeldes [11]), that $\hbar\omega = 9.8$ MeV.

References

1) K. A. Brueckner, Phys. Rev. **97** (1955) 1353
2) H. A. Bethe, Phys. Rev. **103** (1956) 1353
3) J. L. Gammel, R. S. Christian and R. M. Thaler, Phys. Rev. **105** (1957) 311
4) I. Talmi, Helv. Phys. Acta **25** (1952) 185
5) R. Thieberger, Nuclear Physics **2** (1956/57) 533
6) M. Moshinsky, Rev. Mexicana Fis. **6** (1957) to be published
7) Methods of theoretical physics, P. M. Morse and H. Feshbach (McGraw-Hill Book Company, New York, 1953) p. 830
8) M. Moshinsky, Phys. Rev. **106** (1957) 117
9) E. Jahnke and F. Emde, Tables of functions, fourth edition, (Dover Publications, New York, 1945) pp. 1; 7
10) J. M. Blatt and V. F. Weisskopf, Theoretical nuclear physics (John Wiley & Sons, New York, 1952) p. 103
11) N. Zeldes, Nuclear Physics **2** (1956/57) 1
12) C. Schwartz and A. de-Shalit, Phys. Rev. **94** (1954) 1257

Nuclear Physics **4** (1957) 625—631; © *North-Holland Publishing Co., Amsterdam*
Not to be reproduced by photoprint or microfilm without written permission from the publisher

SELECTION RULES FOR BETA AND GAMMA PARTICLE TRANSITIONS IN STRONGLY DEFORMED NUCLEI

G. ALAGA
Institute "Rudjer Bošković" and University of Zagreb, Zagreb

Received 5 June 1957

Abstract: In the present paper we give a complete list of selection rules for beta and gamma particle transitions in strongly deformed nuclei. For the beta decay the list covers all transitions up to the second forbidden ones, while for the gamma decay the selection rules are given for the electric and magnetic dipole, quadrupole, and octupole transitions. This list represents a slight correction and enlargement of the selection rules already given in ref. [5]). References to the papers making use of the selection rules in classifying nuclear states and explaining relative beta and gamma intensities are given at the end of the article.

As a consequence of the interaction of the collective motion and particle motion, the nuclei, especially those between closed shells, have large equilibrium deformations [1]).

The motion of a single particle in a deformed potential and the classification of the nuclear levels have been studied by several authors [2, 3]). We follow the work of S. G. Nilsson [3]) and that of B. R. Mottelson and S. G. Nilsson [2]).

The Hamiltonian used is of the form

$$H = H_0 + C\,\mathbf{l}\cdot\mathbf{s} + D\mathbf{l}^2, \tag{1}$$

$$H_0 = -\frac{\hbar^2}{2M}\Delta + \frac{M}{2}(\omega_x^2 x^2 + \omega_y^2 y^2 + \omega_z^2 z^2); \tag{2}$$

H_0 is the Hamiltonian of an anisotropic harmonic oscillator. The second and the third term in (1) are the spin-orbit and the interpolation terms respectively; C and D are constants properly chosen to reproduce the experimentally known ground state spins of odd-mass nuclei; $\mathbf{l}$ and $\mathbf{s}$ are the orbital and spin angular momenta respectively; M is the nucleon mass. The Hamiltonian (1) is in the body fixed system, i.e. the rotation has already been separated. Assuming equal frequencies in the x and y directions ($\omega_x = \omega_y$) we are faced with a cylindrically symmetrical problem. Beside the total angular momentum, the projection of the particle angular momentum along the z axis $\Omega = \Lambda + \Sigma$ is in that case a good quantum number; Λ and Σ are the projections of the orbital and spin angular momenta along the z axis, respectively.

Using a suitable transformation and representation of an isotropic harmonic oscillator, Nilsson diagonalised the Hamiltonian (1) and evaluated, by means of a machine calculator, the eigenvalues and the eigenfunctions of the Hamiltonian (1) as functions of the deformation.

The wave function belonging to the eigenvalue $E_N^{\Omega}(\alpha)$ is given by

$$\Psi_N^{\Omega}(\alpha) = \sum_{l\Sigma} a_{l,\,\Omega-\Sigma}(\alpha) R_{Nl} Y_l^{\Omega-\Sigma} X_{\frac{1}{2}}^{\Sigma}; \tag{3}$$

R_{Nl} is the normalized radial wave function; $N = n_x+n_y+n_z$ is the oscillator quantum number; $Y_l^{\Omega-\Sigma}$ and $X_{\frac{1}{2}}^{\Sigma}$ are the spherical harmonics and the spin wave functions respectively; $a_{l,\,\Omega-\Sigma}(\alpha)$ are the normalized numerical amplitudes given in the table 1 of S. G. Nilsson's paper [3]).

By using the wave function (3) it is possible to calculate all the quantities connected with particle transitions, as, for instance, beta [3]) and gamma transitions.

Instead of making exact calculations by means of the wave functions (3), which are in some cases rather cumbersome, we may obtain approximate solutions, namely the eigenfunctions of the Hamiltonian (2).

This will correspond physically to the situation when the deformation energy is larger than the spin-orbit coupling and the interpolation term. This approximate solution, in which the particle motion is separated into oscillations along the z axis and those in the plane perpendicular to it is called by S. G. Nilsson the asymptotic solution for very strong deformations. As a consequence of this separation we get n_z and Λ as new constants of the motion. Because of the neglected terms in the Hamiltonian these new constants of the motion are only approximate and the selection rules attached to them will rather "hinder" than forbid the transitions. The neglected terms and the corresponding corrections can be treated by means of perturbation theory.

Solving the separated Hamiltonian (2) first in Cartesian and then in cylindrical coordinates we obtain for the wave functions [4])

$$U(z) = N_z^{-\frac{1}{2}} \exp\left(-\frac{z^2}{2}\right) H_{n_z}(z), \tag{4}$$

$$U(x,\,y) = (N_x N_y)^{-\frac{1}{2}} \exp\left(-\frac{x^2+y^2}{2}\right) H_{n_x} H_{n_y}, \tag{5}$$

$$U(r,\,\phi) = N_n^{-\frac{1}{2}} \varrho^{\frac{1}{2}\alpha} \exp\left(-\tfrac{1}{2}\varrho\right) L_n^{\alpha}(\varrho) \exp\left(i\Lambda\phi\right); \tag{6}$$

H_n are the Hermite polynomials while L_n^{α} are the associated Laguerre polynomials; $\alpha = \Lambda$ and $n = \frac{1}{2}(n_{\perp}-\Lambda)$ are in that way connected with the oscillator quantum numbers $n_{\perp}$ and Λ, respectively. We used also the coordinate transformation $\varrho = (M\omega_{\perp}/\hbar)r^2$; N_z etc. are the normalization factors.

It is possible to establish the correspondence between the approximate

TABLE 1.

Selection rules for beta decay

Type of Transition	Operators	Selection rules			
Allowed	1	$\Delta\Omega = 0$	$\Delta\Lambda = 0$	$\Delta n_z = 0$	$\Delta N = 0$
	$\boldsymbol{\sigma}$	$\Delta\Omega = 0, \pm 1$	$\Delta\Lambda = 0$	$\Delta n_z = 0$	$\Delta N = 0$
First forbidden	$\boldsymbol{\sigma}\cdot\mathbf{r}, \boldsymbol{\sigma}\cdot\nabla$	$\Delta\Omega = 0$ $\Delta\Omega = 0$	$\Delta\Lambda = \pm 1$ $\Delta\Lambda = 0$	$\Delta n_z = 0$ $\Delta n_z =$	$\Delta N = \pm 1, \mp 1$ $\Delta N = \pm 1$
	$\boldsymbol{\sigma}\times\mathbf{r}, \boldsymbol{\sigma}\times\nabla$	$\Delta\Omega = 0, \pm 1$ $\Delta\Omega = \pm 1$	$\Delta\Lambda = \pm 1$ $\Delta\Lambda = 0$	$\Delta n_z = 0$ $\Delta n_z =$	$\Delta N = \pm 1, \mp 1$ $\Delta N = \pm 1, \mp 1$
	$\mathbf{r}, \nabla$	$\Delta\Omega = 0$ $\Delta\Omega =$	$\Delta\Lambda = 0$ $\Delta\Lambda = \pm 1$	$\Delta n_z =$ $\Delta n_z = 0$	$\Delta N = \pm 1$ $\Delta N = \pm 1, \mp 1$
	$T_{21}(\boldsymbol{\sigma}, \mathbf{r})$	$\Delta\Omega = 0, \pm 1, \pm 2$ $\Delta\Omega = 0, \pm 1$	$\Delta\Lambda = \pm 1$ $\Delta\Lambda = 0$	$\Delta n_z = 0$ $\Delta n_z =$	$\Delta N = \pm 1, \mp 1$ $\Delta N = \pm 1, \mp 1$
Second forbidden	$r^2 Y_2$	$\Delta\Omega = \pm 2$		$\Delta n_z = 0$	$\Delta N = 0, \pm 2, \mp 2$
	$T_{22}(\boldsymbol{\sigma}, \mathbf{r})$	$\Delta\Omega = \pm 2$ $\Delta\Omega = \pm 2$	$\Delta\Lambda = \pm 1$ $\Delta\Lambda = \pm 2$	$\Delta n_z = \begin{matrix}\pm 1\\ \mp 1\end{matrix}$ $\Delta n_z = 0$	$\Delta N = \begin{matrix}\pm 2\\ 0\\ \mp 2\end{matrix}$ $\Delta N = 0, \pm 2, \mp 2$
	$T_{21}(\mathbf{r}, \nabla)$	$\Delta\Omega =$	$\Delta\Lambda = \pm 2$	$\Delta n_z = 0$	$\Delta N = 0 \pm 2, \mp 2$
	$T_{21}(\mathbf{r}, \boldsymbol{\sigma}\times\nabla)$	$\Delta\Omega =$ $\Delta\Omega = \pm 2$	$\Delta\Lambda = \pm 2$ $\Delta\Lambda = \pm 1$	$\Delta n_z = 0$ $\Delta n_z = \begin{matrix}\pm 1\\ \mp 1\end{matrix}$	$\Delta N = 0 \pm 2, \mp 2$ $\Delta N = \begin{matrix}\pm 2\\ 0\\ \mp 2\end{matrix}$
	$T_{32}(\boldsymbol{\sigma}, \mathbf{r})$	$\Delta\Omega = \pm 2$ $\Delta\Omega = \pm 2, \pm 3$	$\Delta\Lambda = \pm 1$ $\Delta\Lambda = \pm 2$	$\Delta n_z = \begin{matrix}\pm 1\\ \mp 1\end{matrix}$ $\Delta n_z = 0$	$\Delta N = \begin{matrix}\pm 2\\ 0\\ \mp 2\end{matrix}$ $\Delta N = 0, \pm 2, \mp 2$

TABLE 2

Selection rules for electromagnetic transitions

Multipole	Operator	Selection rules			
E1	rY_1	$\Delta\Omega = 0$	$\Delta\Lambda = 0$	$\Delta n_z =$	$\Delta N = \pm 1$
		$\Delta\Omega =$	$\Delta\Lambda = \pm 1$	$\Delta n_z = 0$	$\Delta N = \pm 1, \mp 1$
E'1	$(\boldsymbol{\sigma} \times \mathbf{r})_1 \approx T_{11}(\boldsymbol{\sigma}, \mathbf{r})$	$\Delta\Omega = 0, \pm 1$	$\Delta\Lambda = \pm 1$	$\Delta n_z = 0$	$\Delta N = \pm 1, \mp 1$
		$\Delta\Omega = \pm 1$	$\Delta\Lambda = 0$	$\Delta n_z =$	$\Delta N = \pm 1, \mp 1$
E2	r^2Y_2	$\Delta\Omega = 0$	$\Delta\Lambda = 0$	$\Delta n_z =$	$\Delta N = \pm 2, \mp 2$
		$\Delta\Omega =$	$\Delta\Lambda = 0, \pm 2$	$\Delta n_z = 0$	$\Delta N = 0, \pm 2, \mp 2$
		$\Delta\Omega =$	$\Delta\Lambda = \pm 1$	$\Delta n_z = \begin{matrix}\pm 1\\ \mp 1\end{matrix}$	$\Delta N = 0 \begin{matrix}\pm 2\\ \mp 2\end{matrix}$
E'2	$T_{22}(\boldsymbol{\sigma}, \mathbf{r})$	$\Delta\Omega = 0, \pm 1, \pm 2$	$\Delta\Lambda = \pm 1$	$\Delta n_z = \begin{matrix}\pm 1\\ \mp 1\end{matrix}$	$\Delta N = 0 \begin{matrix}\pm 2\\ \mp 2\end{matrix}$
		$\Delta\Omega = \pm 1, \pm 2$	$\Delta\Lambda = \pm 2$	$\Delta n_z = 0$	$\Delta N = 0, \pm 2, \mp 2$
		$\Delta\Omega = \pm 1$	$\Delta\Lambda = 0$	$\Delta n_z = \begin{matrix}\pm 2\\ 0\\ \mp 2\end{matrix}$	$\Delta N = \begin{matrix}\pm 2\\ 0\\ \mp 2\end{matrix}, \pm 2, \mp 2$
E3	r^3Y_3	$\Delta\Omega =$	$\Delta\Lambda = \pm 3$	$\Delta n_z = 0$	$\Delta N = \pm 1, \mp 1, \pm 3, \mp 3$
		$\Delta\Omega =$	$\Delta\Lambda = \pm 2$	$\Delta n_z = \begin{matrix}\pm 1\\ \mp 1\end{matrix}$	$\Delta N = \pm 1, \begin{matrix}\pm 3\\ \mp 1\\ \mp 3\end{matrix}$
E'3	$T_{33}(\boldsymbol{\sigma}, \mathbf{r})$	$\Delta\Omega = \pm 2$	$\Delta\Lambda = \pm 1$	$\Delta n_z = 0$	$\Delta N = \pm 1, \mp 1, \pm 3, \mp 3$
		$\Delta\Omega = \pm 2$	$\Delta\Lambda = \pm 1$	$\Delta n_z = \begin{matrix}\pm 2\\ \mp 2\end{matrix}$	$\Delta N = \begin{matrix}\pm 3\\ \pm 1\\ \mp 3\end{matrix}, \mp 1$
		$\Delta\Omega = \pm 2, \pm 3$	$\Delta\Lambda = \pm 2$	$\Delta n_z = \begin{matrix}\pm 1\\ \mp 1\end{matrix}$	$\Delta N = \begin{matrix}\pm 3\\ \pm 1\\ \mp 3\end{matrix}, \mp 1$
		$\Delta\Omega = \pm 2, \pm 3$	$\Delta\Lambda = \pm 3$	$\Delta n_z = 0$	$\Delta N = \pm 1, \mp 1, \pm 3, \mp 3$
	σ_1	$\Delta\Omega = 0, \pm 1$	$\Delta\Lambda = 0$	$\Delta n_z = 0$	$\Delta N = 0$

	σ_1	$\Delta\Omega = 0, \pm 1$	$\Delta\Lambda = 0$	$\Delta n_s = 0$	$\Delta N = 0$
M1	$I_1 \approx T_{11}(\mathbf{r}, \nabla)$	$\Delta\Omega = 0$	$\Delta\Lambda = 0$	$\Delta n_s = 0$	$\Delta N = 0$
		$\Delta\Omega =$	$\Delta\Lambda = \pm 1$	$\Delta n_s = \begin{matrix}\pm 1\\ \mp 1\end{matrix}$	$\Delta N = 0 \begin{matrix}\pm 2\\ \mp 2\end{matrix}$
M2	$T_{21}(\sigma, \mathbf{r})$	$\Delta\Omega = 0, \pm 1, \pm 2$	$\Delta\Lambda = \pm 1$	$\Delta n_s = 0$	$\Delta N = \pm 1, \mp 1$
		$\Delta\Omega = 0, \pm 1$	$\Delta\Lambda = 0$	$\Delta n_s =$	$\Delta N = \pm 1, \mp 1$
	$T_{21}(\mathbf{r}, \mathbf{L})$	$\Delta\Omega =$	$\Delta\Lambda = 0, \pm 2$	$\Delta n_s = \begin{matrix}\pm 1\\ \mp 1\end{matrix}$	$\Delta N = \begin{matrix}\pm 3\\ \pm 1\\ \mp 3\end{matrix}, \mp 1$
		$\Delta\Omega =$	$\Delta\Lambda = \pm 1$	$\Delta n_s = 0$	$\Delta N = \pm 1, \mp 1$
		$\Delta\Omega =$	$\Delta\Lambda = \pm 1$	$\Delta n_s = \begin{matrix}\pm 2\\ \mp 2\end{matrix}$	$\Delta N = \begin{matrix}\pm 3\\ \pm 1\\ \mp 3\end{matrix}, \mp 1$
M3	$T_{32}(\sigma, \mathbf{r})$	$\Delta\Omega = \pm 2$	$\Delta\Lambda = \pm 1$	$\Delta n_s = \begin{matrix}\pm 1\\ \mp 1\end{matrix}$	$\Delta N = \begin{matrix}\pm 2\\ 0\\ \mp 2\end{matrix}$
		$\Delta\Omega = \pm 2, \pm 3$	$\Delta\Lambda = \pm 2$	$\Delta n_s = 0$	$\Delta N = \pm 0, \pm 2, \mp 2$
M3	$T_{32}(\mathbf{r}, \mathbf{L})$	$\Delta\Omega =$	$\Delta\Lambda = \pm 2$	$\Delta n_s = \begin{matrix}\pm 2\\ \mp 2\end{matrix}$	$\Delta N = \begin{matrix}\pm 4\\ 0\\ \pm 4\end{matrix}, \pm 2, \mp 2$
		$\Delta\Omega =$	$\Delta\Lambda = \pm 2$	$\Delta n_s = 0$	$\Delta N = 0, \pm 2, \mp 2$
		$\Delta\Omega =$	$\Delta\Lambda = \pm 3$	$\Delta n_s = \begin{matrix}\pm 1\\ \mp 1\end{matrix}$	$\Delta N = \begin{matrix}\pm 4\\ 0\\ \mp 4\end{matrix}, \pm 2, \mp 2$

and the exact solution. Thus the approximate solution may serve to study qualitatively some of the characteristic features of strongly deformed nuclei.

Writing the beta and gamma operators first in Cartesian and then in cylindrical coordinates and using the known selection rules for Hermite polynomials and their derivatives as well as for the exponential function we get the asymptotic selection rules for the beta [5]) and gamma [6]) decay.

In tables 1 and 2 we give the selection rules for the allowed beta transitions, for first and second forbidden beta transitions† and for the dipole, quadrupole and octupole electric and magnetic transitions.

We give two examples in order to illustrate the use of the tables. The electric quadrupole transition with $\Delta\Omega = \Delta\Lambda = \pm 1$ is consistent with both the upper and lower $\Delta n_z(\frac{\pm 1}{\mp 1})$; so is $\Delta N = 0$, but the upper case $\Delta N = \pm 2$ is consistent only with the corresponding upper change $\Delta n_z = \pm 1$. The same applies to the lower case. If there is besides the upper and lower case also a change of Δn_z in between as in $T_{22}(\boldsymbol{\sigma}, \mathbf{r})$ and $\Delta\Omega = \pm 1$, $\Delta\Lambda = 0$, it should be read that $\Delta n_z = 0$ is consistent with $\Delta N = 0, \pm 2, \mp 2$, but the upper and lower cases of Δn_z are compatible with the corresponding upper and lower case of ΔN.

We confined ourselves to the transitions with $\Delta I = \Delta\Omega$, i.e. we omitted rotational branchings and K-forbidden transitions [7]). It may be seen from tables 1 and 2 that beside the selection rules for I and $\Omega(= K)$ there are also selection rules for other quantum numbers. Those transitions which are permitted with respect to the selection rules for all quantum numbers are called "unhindered" transitions. The transitions permitted by selection rules for I and Ω but forbidden because of the selection rules for other quantum numbers are called "hindered" transitions [5]).

These selection rules, beside the K-selection rules, have proved very useful in the classification of the states, especially in the region of strongly deformed nuclei.

Explanation of some beta and electron capture relative intensities are given in ref. [5]) and [8]). Examples for gamma relative intensities can be found in ref. [6]).

I would like to acknowledge the assistance of I. Šlaus in the calculations.

† Note that the l-forbidden transitions in this case appear as allowed "hindered" transitions.

References

1) A. Bohr, Mat. Fys. Medd. Dan. Vid. Selsk. **26** (1952) no. 14;
A. Bohr, Rotational States in Atomic Nuclei (Ejnar Munksgaard, Copenhagen 1954);
A. Bohr and B. R. Mottelson, Mat. Fys. Medd. Dan. Vid. Selsk. **27** (1953) no. 16; **30** (1955) no. 1;
K. Alder, A. Bohr, T. Hus, B. R. Mottelson and A. Winther, Rev. Mod. Phys. **28** (1956) 432

2) S. Moszkowski, Phys. Rev. **99** (1955) 803;
B. R. Mottelson and S. G. Nilsson, Phys. Rev. **99** (1955) 1615;
K. Gotfried, Phys. Rev. **103** (1956) 1017
3) S. G. Nilsson, Mat. Fys. Medd. Dan. Vid. Selsk. **29** (1955) no. 16;
G. Alaga, Thesis (University of Zagreb, 1955 (unpublished)); Glasnik Matematičko Fizički i Astronomski (in the press)
4) W. H. Shaffer, Rev. Mod. Phys. **16** (1944) 245
5) G. Alaga, Phys. Rev. **100** (1955) 432
6) S. G. Nilsson, On Some Properties of Nuclear States (Berlingska Boktryckeriet, Lund, 1955);
D. Strominger and J. V. Rasmussen, Nuclear Physics **3** (1957) 197;
B. R. Mottelson and S. G. Nilsson, Mat. Fys. Medd. Dan. Vid. Selsk. (to be published)
7) G. Alaga, K. Alder, A. Bohr and B. R. Mottelson, Mat. Fys. Medd. Dan. Vid. Selsk. **29** (1955) no. 9
8) D. M. Chase and L. Wilets, Phys. Rev. **101** (1956) 1038;
W. G. Smith, W. H. Gibson and J. M. Hollander, Phys. Rev. **105** (1957) 1514;
J. M. Hollander, Phys. Rev. **105** (1957) 1518;
E. N. Katch, F. Boehm, P. Marmier and J. W. M. DuMond, Phys. Rev. **104** (1956) 745

Nuclear Physics **4** (1957) 632—633; © *North-Holland Publishing Co., Amsterdam*

Not to be reproduced by photoprint or microfilm without written permission from the publisher

NOTE ON THE ELASTIC SCATTERING OF HIGH-ENERGY PARTICLES

L. I. SCHIFF

Stanford University, Stanford, California †

Received 1 August 1957

In a recent paper in this journal, Khalatnikov [1]) asserted that the large-angle scattering formula derived by the author [2]) is incorrect. This criticism is based on the belief that in the nth term of the Born series, any one of the n regions of stationary phase can be used by itself to approximate the integral. These n regions are characterized by a parameter m which can be chosen equal to $1,2,\ldots n$. Although he does not explicitly say so, Khalatnikov appears to realize that different choices for m lead to different contributions to the scattered amplitude. For example, $m = 1$ yields

$$f_1(\mathbf{k}_f,\ \mathbf{k}_0)=(-4\pi)^{-1}\int\exp(i\mathbf{q}\cdot\mathbf{r})U(\mathbf{r})\exp[(-i/2k)\int_0^\infty U(\mathbf{r}+\hat{\mathbf{k}}_f s)\mathrm{d}s]\mathrm{d}\tau,$$

and $m = n$ yields

$$f_n(\mathbf{k}_f,\ \mathbf{k}_0)=(-4\pi)^{-1}\int\exp(i\mathbf{q}\cdot\mathbf{r})U(\mathbf{r})\exp[(-i/2k)\int_0^\infty U(\mathbf{r}-\hat{\mathbf{k}}_0 s)\mathrm{d}s]\mathrm{d}\tau.$$

It is apparent that f_1 and f_n are not in general equal. Khalatnikov then argues that the average over m, $n^{-1}\sum_{m=1}^{n}$, should be employed, rather than the summation over m, $\sum_{m=1}^{n}$, used in ref. [2]).

We now show that this argument is incorrect, and that the summation rather than the average over m must be used. This is most easily seen in the term $n = 2$, for which the original integral is six-fold. The stationary phase approximation shows that, in the large-angle case, the principal contribution to the integral comes from two distinct regions of the six-dimensional configuration space. One of these, which corresponds to the choice $m = 1$, is that for which the vector $\boldsymbol{\varrho} = \mathbf{r}_2 - \mathbf{r}_1$ is nearly parallel to $\mathbf{k}_f$; the other, corresponding to $m = 2$, is that for which $\boldsymbol{\varrho}$ is nearly parallel to $\mathbf{k}_0$. As pointed out in ref. [2]), the phrase "nearly parallel" means that the angle between the two vectors must be less than or of order $(kR)^{-\frac{1}{2}}$. Since, in the large-angle case, the angle θ between $\mathbf{k}_0$ and $\mathbf{k}_f$ is large in comparison with $(kR)^{-\frac{1}{2}}$, the two regions of the six-dimensional configuration space referred to above are in fact distinct. Thus their contributions must be added. An extension of this argument to general values of n shows that

† Supported in part by the U. S. Air Force through the Office of Scientific Research, Air Research and Development Command.

the contributions from the different values of m must all be added together in the large-angle case.

The analysis of the preceding paragraph shows also that in the small-angle case, for which $\theta \ll (kR)^{-\frac{1}{2}}$, the two regions referred to in the case $n = 2$ are not distinct. In this case either $m = 1$ or $m = 2$ may be used. These two equal contributions are really different ways of expressing the same quantity, and hence must not be added; they come from the same region of six-dimensional configuration space, for which $\boldsymbol{\varrho}$ is nearly parallel to both $\mathbf{k}_0$ and $\mathbf{k}_f$, which are nearly parallel to each other. The explicit calculation of ref. [2]) shows that for general values of n, the contribution is independent of the choice of m, as of course it must be. Thus it is to be expected that the large-angle and small-angle formulas for the scattered amplitude have different structures, and that the former does not go over into the latter as θ decreases.

The principal results of ref. [2]) have recently been rederived and extended in both angular range and accuracy [3]). This work, which is not based on the infinite Born series, confirms the earlier results and error estimates, and also provides a somewhat more complicated formula for the intermediate angle range $\theta \approx (kR)^{-\frac{1}{2}}$.

References

1) I. M. Khalatnikov, Nuclear Physics **3** (1957) 433
2) L. I. Schiff, Phys. Rev. **103** (1956) 443
3) D. S. Saxon and L. I. Schiff, submitted to Nuovo Cimento

Editor's Note: To illustrate the point at issue, it may be useful to give the explicit expressions for the second term of the Born series and the contributions obtained by the stationary phase approximation in the simple case of a Gaussian potential $\exp[-(r^2/2r_0^2)]$. For the wave-number k and the scattering angle 2θ, the integral in question takes the exact form

$$\frac{F(\theta)}{\cos\theta}\left[\Phi\left(2kr_0\cos^2\frac{\theta}{2}\right)-\Phi\left(2kr_0\sin^2\frac{\theta}{2}\right)\right],$$

while the two approximate contributions have the common value

$$-F(\theta)\Phi(kr_0\sin^2\theta);$$

the function $F(\theta)$ is essentially $(i/2k)\exp[-k^2r_0^2\sin^2\theta]$, and

$$\Phi(x)=\left[1+i\frac{2}{\sqrt{\pi}}\int_0^x e^{-u^2}du\right]e^{-x^2}.$$

From these formulae (which have been kindly worked out, at my request, by Mr. R. B. Hall) it is readily seen that the asymptotic value of the integral, for large k, is nearly equal to that of the approximate contribution if θ is small compared with $(kr_0)^{-\frac{1}{2}}$, but to twice the latter expression for finite values of θ.

Nuclear Physics **4** (1957) 634—635; © *North-Holland Publishing Co., Amsterdam*

NEWS ITEMS

COLLOQUIUM ON THE PHYSICS OF ELEMENTARY PARTICLES BALATONVILÁGOS, 5—8 JUNE 1957

A colloquium on the physics of elementary particles has been organized by the Roland Eötvos Society of Physics, Budapest, near the superb lake Balaton (in the western part of Hungary). Its aim was to summarize the work done in this field by Hungarian physicists, to review the topical problems of this branch of research, as well as to give an opportunity of furthering the international scientific relations. The lectures of the first day were dealing with the β-interactions, those of the second and third days considered the problems related to the nucleons and pions and to the strange particles, respectively. The fourth day was devoted to the fundamental questions of the quantum theory of elementary particles.

After the introductory talk of Prof. L. Jánossy in which he recalled the aim of the colloquium, E. Fenyves summarized our experimental knowledge on elementary particles, and D. Berényi gave a review of the present status of the theory of β-decay. G. Csikai then described his cloud chamber investigations concerning the recoil of the daughter nucleus in the He^6 β-decay, as suggested by Prof. S. Szalay, which have been carried out in the Institute for Nuclear Research, Debrecen. On the basis of about 120 photographs, he determined the $\beta-\nu$ angular correlation function in a nice agreement with the theoretical result for a pure tensor transition. A suggestive lecture by G. Marx summarized the recent development of our knowledge concerning the neutrino. J. Mráz gave a report on the polarization and correlation experiments connected with the question of parity non-conservation, now in progress or in course of preparation at the Central Research Institute of Physics, Budapest. According to one of the most interesting ideas put forward the correlation between the transverse polarization and the nuclear recoil can be investigated. If the β-particles are transversally polarized for a given value of the recoil momentum, then if we observe in a cloud chamber the decay and the subsequent Coulomb-scattering of the β-particles in the gas filling the chamber we must observe an asymmetry of the scattered intensity with respect to the decay plane. Prof. M. Danysz (Warsaw) gave a review on the most interesting results announced at the Seventh Rochester Conference, which the Hungarian physicists had no opportunity to attend.

The second day started with the review given by Prof. L. Jánossy on the development and statistical theory of the extended air showers as well as on the G-equation of Jánossy. His aim was to call the attention of young physicists to the open questions of the theory. K. Nagy gave an account of his intermediate coupling calculations on the charge and mass distribution of the nucleons. G. Domokos gave a review of the theories of multiple meson production. G. Györgiy talked on a "maximum likelihood" method for the determination of the energy of a particle scattered in an emulsion, taking into account the noise; this method was worked out following a suggestion of Prof. L. Jánossy. D. Bebel (Berlin-Miersdorf) made some comments on the practical application of the methods of "constant sagittas".

The third day was opened by the review of A. Somogyi on strange particle experiments. G. Marx gave the selection rules of the nucleon-antinucleon annihilation with the emission of $K\overline{K}$ pairs. He pointed out that one gets different selection rules for K particles of one type with definite parity and for parity doublets. This may offer a possibility for the experimental testing of different theoretical ideas. P. Surányi suggested a possible connection between branching ratios of different K-messon decays. G. Domokos considered the charge distribution and magnetic moment of the K-meson cloud surrounding the nucleons. G. Györgyi compared in his lecture the physical consequences of the different possible models for strange particles. In a very graphic lecture Prof. J. Rayski (Toruń) discussed an eigenvalue-equation which

gives the mechanical mass of hyperons. G. Domokos gave an account of some calculations concerning the multiple production of strange particles.

At the beginning of the fourth day F. Karolyházi discussed the possible role of ghost states in quantum electrodynamics. A lecture of Prof. G. Heber (Jena) considered the connection between the measurements of field quantities and space-time coordinates respectively. The considerations of Prof. Rayski concentrated around the possibility of the causal and convergent formulation of field theory. J. Horváth talked on the "anschaulich" geometrical interpretation of the bilocal field theory. Finally P. Szépfalussy pointed out a possible non-linear generalization of the Schrödinger equation and considered some applications of his non-linear equation to nuclear problems.

According to the common opinion of the guests of the colloquium (coming from Poland and Germany) as well as of the Hungarian participants, this well organized meeting showed that besides the experimental work — strongly stimulated by the return of Prof. L. Jánossy to Hungary (in 1950) — the development of the theoretical investigations in Hungary during the last few years is noticeable. The young Hungarian physicists all expressed the wish that similar stimulating colloquiums should be held more frequently in the future, thus giving an opportunity to discuss problems and results with physicists of other countries.

CERN, SECOND ANNUAL REPORT (1956)

The second annual report of CERN, recently published as a 71-page pamphlet, lavishly illustrated with plates of photographs and large-scale drawings of buildings and apparatus, is a document of topical interest and of lasting historical value. It records a phase of impressive growth in one of the greatest international undertakings in the field of physics. It is still mainly concerned with the problems of construction of the big machines, not excluding from this group the double cloud chamber, described and illustrated in the report. However, it is very satisfactory to see that research, which was hitherto confined to the theoretical division, has also made an excellent start in the experimental groups. There is an interesting record of the results achieved by the cosmic ray division, and an outline of the research programme initiated by the synchro-cyclotron division. There is no doubt that the drudgery of the construction period will soon be rewarded by a participation of growing importance and distinction to the common exploration of fascinating phenomena.

L. R.

ERRATUM

O. Nathan, Possible vibrational levels in Dy^{160} (Nuclear Physics 4 (1957)125).
By a deplorable oversight, the date of reception of this paper is erroneously given as 12 May 1957 instead of 12 April 1957

A. Houriet, Méthode des champs adhérents (Nuclear Physics **4** (1957) 408).
The footnote on p. 409 must be cancelled

Nuclear Physics **4** (1957) 636; © *North-Holland Publishing Co., Amsterdam*

BOOK REVIEWS

M. HAÏSSINSKY (Rédacteur,) *Actions chimiques et biologiques des radiations* (2ième série) (Masson et Cie, Paris, 1956. 220 pages. Broché 2800 fr. fr., relié 3400 fr. fr.)

The chief characteristic of post-war radiation chemistry is the uneven state of development in its various branches. For this reason, no textbook offering a unified presentation of the whole subject is at present available; it would be a difficult task for a single author.

The first volume of this series (1955) presented several different aspects of the radiation chemistry of water and aqueous solutions written by different authors. Its successor follows the same plan and contains three long reviews. Professor Mund, a distinguished early pioneer in the field, contributes a highly personal account of the chemical effects of ionisation in gaseous systems. A survey of general principles is followed by a fairly detailed discussion of particular systems and a good but incomplete bibliography. This refreshing account should remind newcomers to the field that its serious study did not commence in 1946. A valuable feature is that it draws attention to the extreme paucity of information on the behaviour of organic vapours.

Professor Ageno's account of "luminescence phenomena provoked by high-energy radiation" is a complete survey of the behaviour of scintillators, written from an experimental viewpoint. It is extremely well documented. Chemists will welcome this summary. The treatment of the mechanism of scintillation is quite inadequate, in view of the still obscure role of excited states in chemical transformations.

The accurate determination of the energy absorbed by condensed phases exposed to ionising radiations is quite vital. Dr. Miller contributes a chapter on radiation dosimetry, which will be of real assistance to new workers. The recent history of the calibration of ferrous sulphate dosimeter should also prove interesting to physicists, since it led to a revision of the energy needed to produce an ion-pair in air, of the energy equivalent of the röntgen, and to the establishment of the "rad" as an international unit of dose. The very clear presentation of the various methods of dosimetry and of the many precautions needed to ensure accuracy is most welcome.

This volume owes a great deal to the excellent work of translators, who have provided a lucid, readable, and accurate text. As in the case of its predecessor, the chemical theory of radiation chemistry does not receive adequate attention. The editor is nevertheless to be congratulated on providing these useful introductions to the literature of a rapidly advancing subject.

W. Wild

C. F. BONILLA (Editor), *Nuclear Engineering* (Mc.Graw-Hill Book Co., New York-Toronto-London 1957. vi-850 pages. $ 12.50)

The enterprising publishers of the primer of nuclear engineering reviewed above are eager to meet the requirements of all classes of readers. At the other end of the scale, they present a bulky collective work, designed not only as a reference volume, but also as an advanced text for engineering students. It will suffice to say that it is a production in the best American style, aiming at accuracy and practical usefulness in the selection and presentation of the material, and that it will admirably serve its twofold purpose.

L. R.

Nuclear Physics **4** (1957) 637—642; © *North-Holland Publishing Co., Amsterdam*

Not to be reproduced by photoprint or microfilm without written permission from the publisher

INELASTIC SCATTERING OF 185 MeV PROTONS ON OXYGEN, CALCIUM AND CARBON

H. TYRÉN and TH. A. J. MARIS

The Gustaf Werner Institute for Nuclear Chemistry, University of Uppsala

Received 8 July 1957

Abstract: The energy spectra at various angles for the inelastic scattering of protons near 180 MeV on oxygen, calcium and carbon have been measured with a magnetic analyser. Maxima corresponding to excited states of the target nuclei have been resolved and some differential and total cross sections are reported.

The measurements of the energy spectra of protons inelastically scattered on light nuclei have been continued with essentially the same technique as used in ref. [1]). The average scattering energy was mostly about 182 MeV, except for the liquid oxygen target where it was 177 MeV. The analyser magnet [2]) had an entrance slit of 1 degree width and the energy resolution corresponded to 1.8 MeV full width at half height. The transmission of the magnet was determined by measuring the areas of the peaks caused by free proton-proton scattering in a polyethylene target at different angles and assuming the p—p cross section to be equal to the average of the two cross sections of ref. [3]), transformed to our energy.

The large angle measurements on oxygen were made with a water target. The considerable width of the p—p peak in the spectra is caused by the finite angular resolution. At small angles a liquid oxygen target was used.

Figures 1, 2 and 3 show the spectra for the indicated elements and angles. The energy scale refers to the excitation energy of the target nucleus. All other quantities are taken in the laboratory system.

The sharp maxima in the spectra are listed in table 1.

TABLE 1

Element	Level
carbon	4.3 ± 0.2 MeV
"	7.6 ± 0.2 "
"	9.6 ± 0.2 "
"	12.6 ± 0.3 "
"	15.0 ± 0.2 "
"	≈ 20 "
oxygen	6.1 ± 0.2 "
"	12.5 ± 0.3 "
"	≈ 20 "
calcium	3.7 ± 0.2 "
"	≈ 7 "
"	≈ 18 "

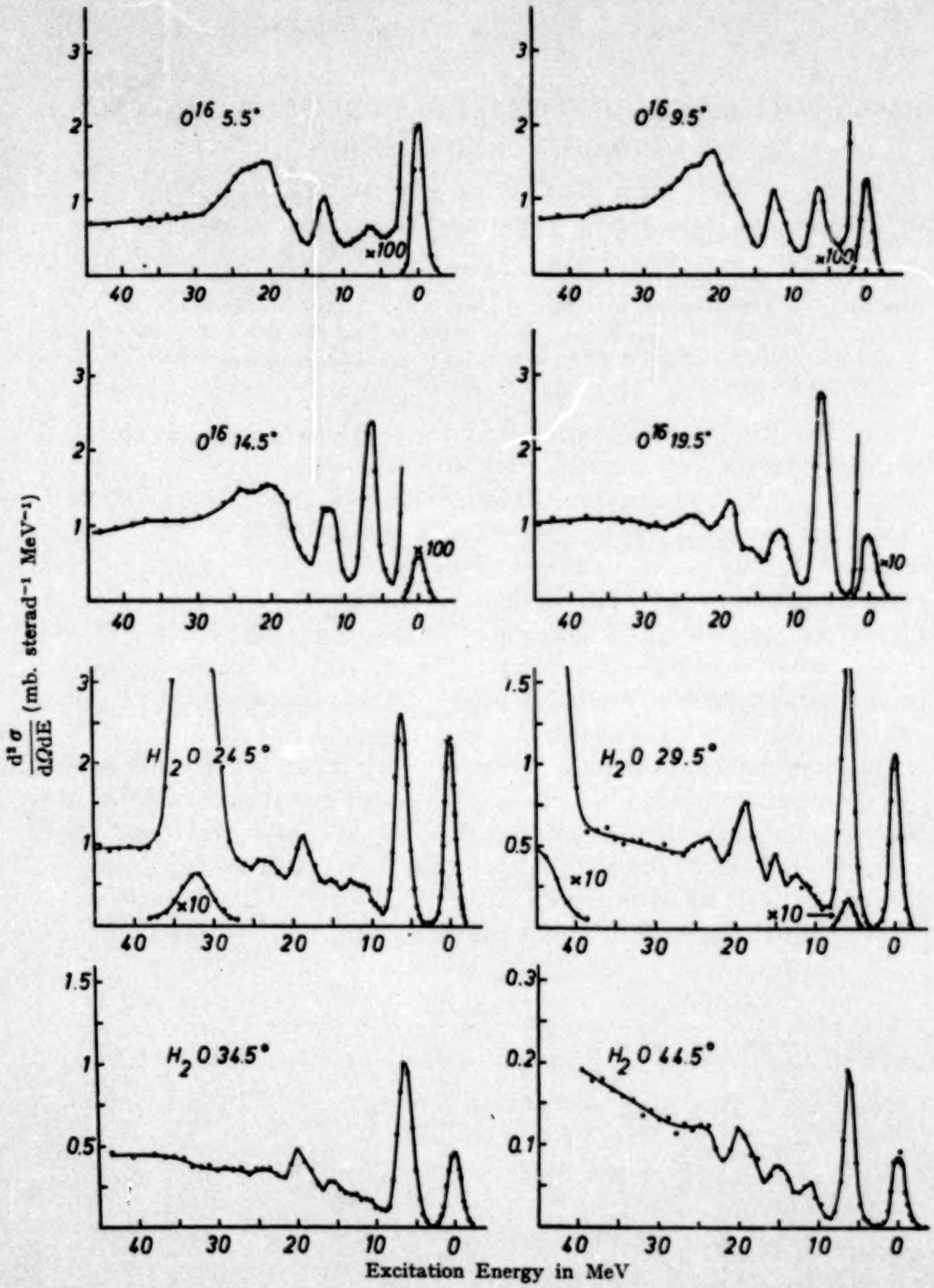

Fig. 1. Energy spectra for inelastic scattering of 181 MeV protons on water and of 177 MeV protons on oxygen. The statistical errors are mostly of the order of the size of the points.

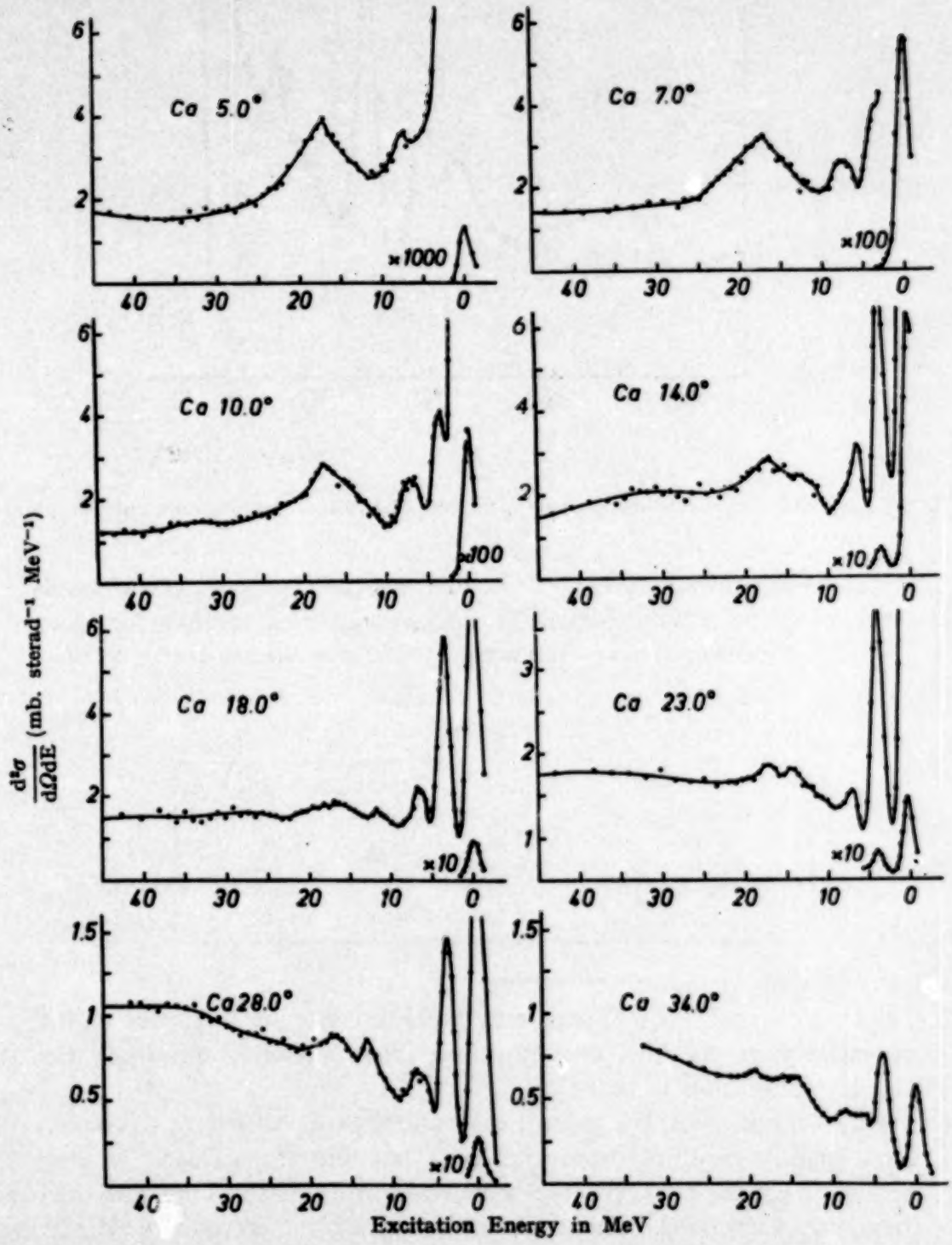

Fig. 2. Energy spectra for inelastic scattering of 182 MeV protons on calcium.

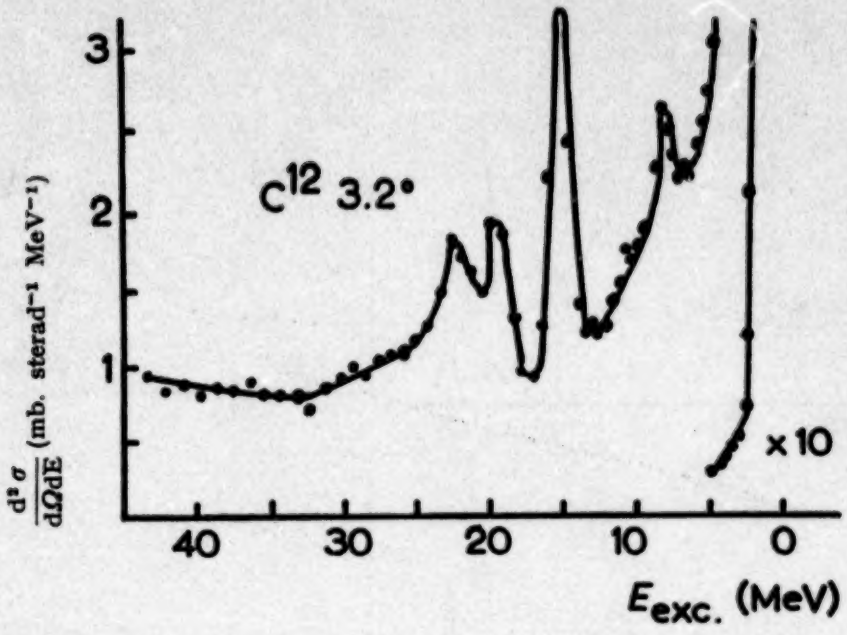

Fig. 3. The energy spectrum for inelastic scattering of 182 MeV protons on carbon at 3.2 degrees.

In fig. 4 † the differential cross sections of some clearly separated levels or level groups have been plotted. The differential cross sections for peaks with a small background have been integrated to give the total cross sections of table 2.

TABLE 2

Element	Level	Cross section ±20 %
carbon	4.3 MeV	5.3 mb
carbon	9.6 MeV	2.4 mb
oxygen	6.1 MeV	5.5 mb
calcium	3.7 MeV	6.4 mb

The following errors are of importance:

1. The absolute cross section scale may have an error of 10 % due to the uncertainty of the free proton-proton cross section [3]) on which the magnet calibration is based.
2. The measurements of the spectra reproduced to about ±5 %, the deviations mainly resulting from the fact that the transmission is very dependent on the beam position which had to be checked and corrected frequently. Compared to this error all other measuring errors in $d^2\sigma/d\Omega dE$ including the statistical one are negligible.
3. The differential cross sections $d\sigma/d\Omega$ have been measured by deter-

† It should be noted that the preliminary cross sections of C^{13} given in our earlier paper [1]) are considerably too large.

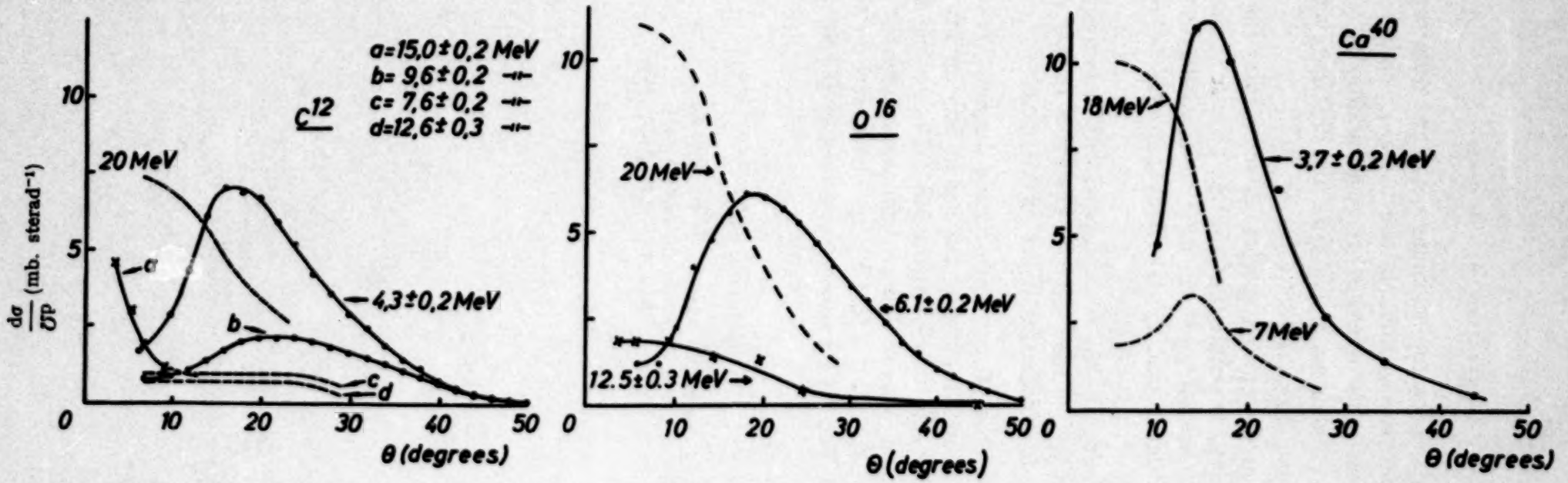

Fig. 4. Differential cross sections for some strongly excited levels in carbon, oxygen and calcium. The errors in the drawn and dotted curves are supposed to be not larger than 20 % and 50 % respectively.

mining the heights of the corresponding peaks and deducing from these the peak areas and cross sections. In the case of a clearly resolved peak without background this procedure gives an additional error of 5 %, and therefore the total errors in $d^2\sigma/d\Omega dE$ and $d\sigma/d\Omega$ are assumed to be less than 15 % and 20 % respectively.

As is evident from the plotted spectra, in some cases the differential cross section for a certain excitation is uncertain because of the large background, which had to be subtracted, consisting of quasi-elastically scattered particles, unresolved levels, and at very small angles the tail of the elastic peak.

The energy determination has been checked with known levels and the error did not exceed 2 % of the excitation energy. A further discussion of the results is given in a following paper of this issue.

We are grateful to Prof. T. Svedberg for his support. We are indebted to Dr. Peter Hillman for stimulating discussions and for his instructions for the building of the cryostat. We thank Mr P. Isacson and Mr B. Smith for technical assistance, Miss I. Widegren for performing the calculations and especially Mr Å. Svanheden and his cyclotron crew for the excellent beam they provided. The work has been supported by the Swedish Atomic Energy Commission.

References

1) H. Tyrén and Th. A. J. Maris, Nuclear Physics **3** (1957) 52
2) A. Lovati and H. Tyrén, Journ. Sci. Instr. **33** (1956) 151
3) O. Chamberlain and J. D. Garrison, Phys. Rev. **103** (1956) 1860

Nuclear Physics **4** (1957) 643—647; © *North-Holland Publishing Co., Amsterdam*
Not to be reproduced by photoprint or microfilm without written permission from the publisher

THE ASYMMETRY OF 155 MeV PROTONS ELASTICALLY SCATTERED FROM IRON, NICKEL AND COPPER

R. ALPHONCE, A. JOHANSSON and G. TIBELL
The Gustaf Werner Institute for Nuclear Chemistry, University of Uppsala

Received 8 July 1957

Abstract: The asymmetry of protons scattered elastically from iron, nickel, and copper has been measured in the angular region 5°—26°. The conventional double scattering technique with range telescopes was used. The angular patterns are quite similar for the three elements and resemble the curves for carbon, oxygen and calcium.

1. Introduction

The results from scattering experiments with beams of high-energy polarized protons [1, 2, 3]) seem to indicate that the variations of the elastic asymmetry with angle are quite similar for different target materials. The dependence of the asymmetry on the target nucleus largely amounts to a contraction of the angular scale by a factor $A^{-1/3}$, where A is the atomic weight of the target material, together with a slow decrease of the first maximum with increasing A.

The present experiment has been an attempt to detect differences in the angular patterns of asymmetry among elements having almost the same A. The three elements studied were iron, nickel, and copper, and differences obtained might be due to different nuclear spins (copper has a ground state spin 3/2, iron and nickel spin zero) or possibly to the closing of a proton shell at nickel ($Z = 28$).

2. Method and Apparatus

The conventional double scattering technique with range telescopes was used. The experimental arrangements have been described earlier [4]). The targets were in most cases 11 MeV thick, resulting in a 1.3° r.m.s. angular resolution most of which was due to multiple Coulomb scattering in the target (1.2° r.m.s.). A few points were taken with targets 5 MeV thick, corresponding to 1.0° r.m.s. angular resolution.

In the study of inelastic scattering from iron, cobalt and copper at this institute [5]) with an energy resolution of about 1.8 MeV full width at half height equivalent the first resolvable group of inelastically scattered protons was found in each case to have an energy about 4 MeV less than the elastically scattered protons. The corresponding cross section seemed to be less than

1/8 of the elastic scattering cross section in the angular region in question. Thus with proper absorbers in the range telescopes the inelastic contribution to the counting rate was made small. It was estimated to be less than 5 % at all angles.

3. Results

The results are given in the table and in fig. 1a-c. The solid circles and

TABLE 1

Asymmetries for protons scattered elastically from iron, nickel and copper

$\vartheta°$	ε_{Fe} %	ε_{Ni} %	ε_{Cu} %
5	6.5±1.4	4.1±0.9	− 4.5±1.0
5			14.8±1.4*
6	23.7±3.3	22.1±1.7	18.6±1.6
6.5	34.4±1.6	31.3±1.4	29.6±1.1
7	41.5±0.7	41.0±0.7	37.7±0.6
7		45.3±2.2*	43.5±1.7*
7.5	45.9±0.6	47.6±0.7	46.0±0.7
8		46.6±1.7*	
9	50.2±0.9	48.1±1.0	49.4±0.9
9		44.2±2.7*	
10	50.4±2.8	51.8±3.2	52.3±2.4
10.5	54.1±1.6	55.6±1.4	53.7±1.6
11	52.0±3.2	54.4±1.9	54.1±1.8
12	60.9±3.5	62.7±3.5	62.3±3.4
14	59.6±4.1	65.6±4.2	68.7±4.3
16	62.9±6.0	58.8±5.6	52.2±5.3
17.9			41.9±4.5*
18	42.7±7.4	26.7±9.0	28.0±6.8
18.4		36.2±5.2*	
19	40.6±7.3	30.1±8.6	47.8±5.9
20	31.7±8.3	44.7±6.5	58.8±6.1
22	51.5±6.5	48.6±6.6	66.3±7.0
24	59.0±7.6	72.3±5.8	78.2±5.9
26	72.8±5.4	74.8±7.6	85.2±4.9

Data marked with asterisk: 1.0° r.m.s. angular resolution; other data: 1.3° r.m.s. angular resolution.

the crosses correspond to measurements with 1.3° and 1.0° r.m.s. angular resolution respectively. The quoted errors are of purely statistical origin. Other errors should be negligible. For comparison between the three elements curves were constructed in the following way. The data were plotted in the same diagram along the horizontal axis $\vartheta A^{1/3}$. The points were fitted by eye as closely as possible by a curve, which was then drawn into the three figures with ϑ as abscissa.

It is seen that the general agreement between the points and the curve is good for all three elements. The only significant deviation appears in the small angle region, where the copper points are below, the nickel points on,

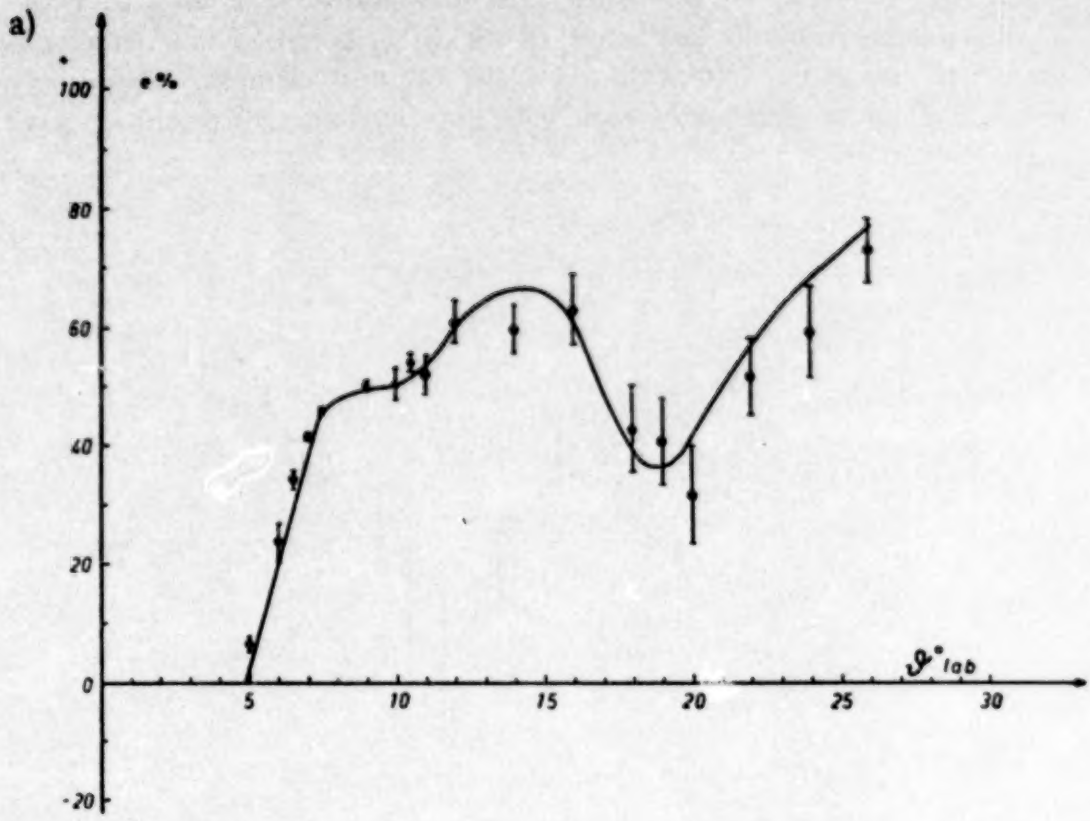
a)
ε %
100
80
60
40
20
0
-20
5
10
15
20
25
30
ϑ° lab

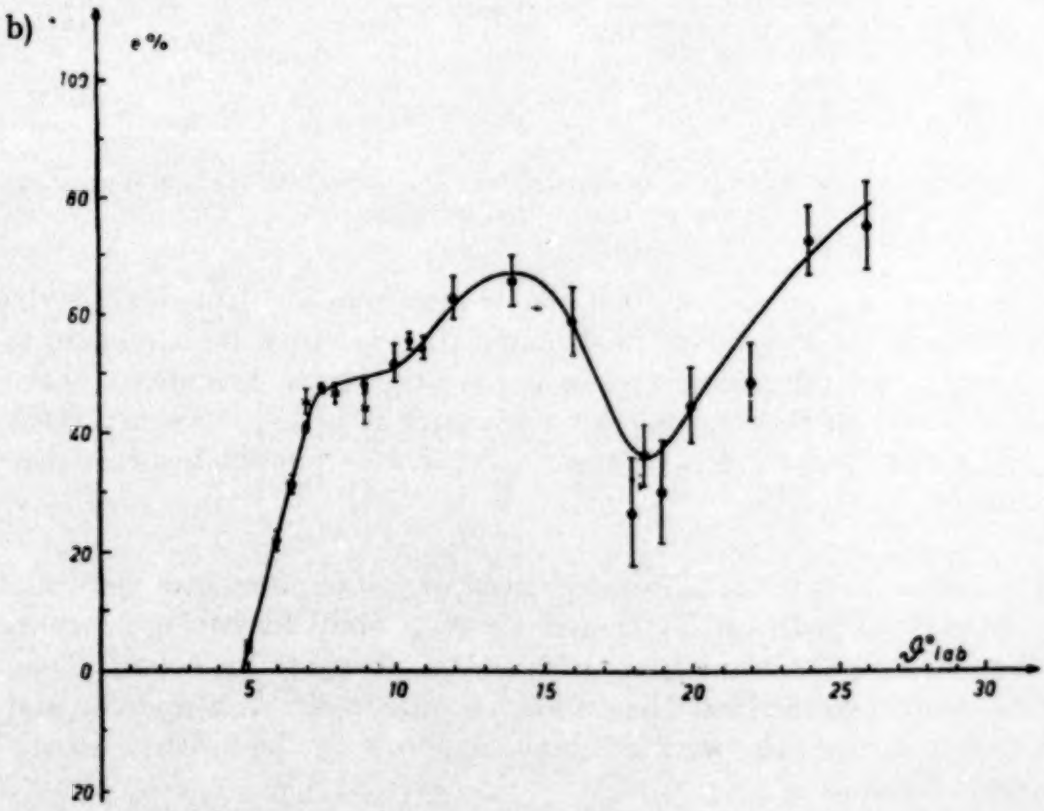
b)
ε %
100
80
60
40
20
0
-20
5
10
15
20
25
30
ϑ° lab

and the iron points above the curve. This effect, however, is most probably due to multiple Coulomb scattering of the direct beam. This scattering is symmetric and is most important for the heaviest element. Accordingly the small angle measurements made with improved angular resolution gave larger asymmetries.

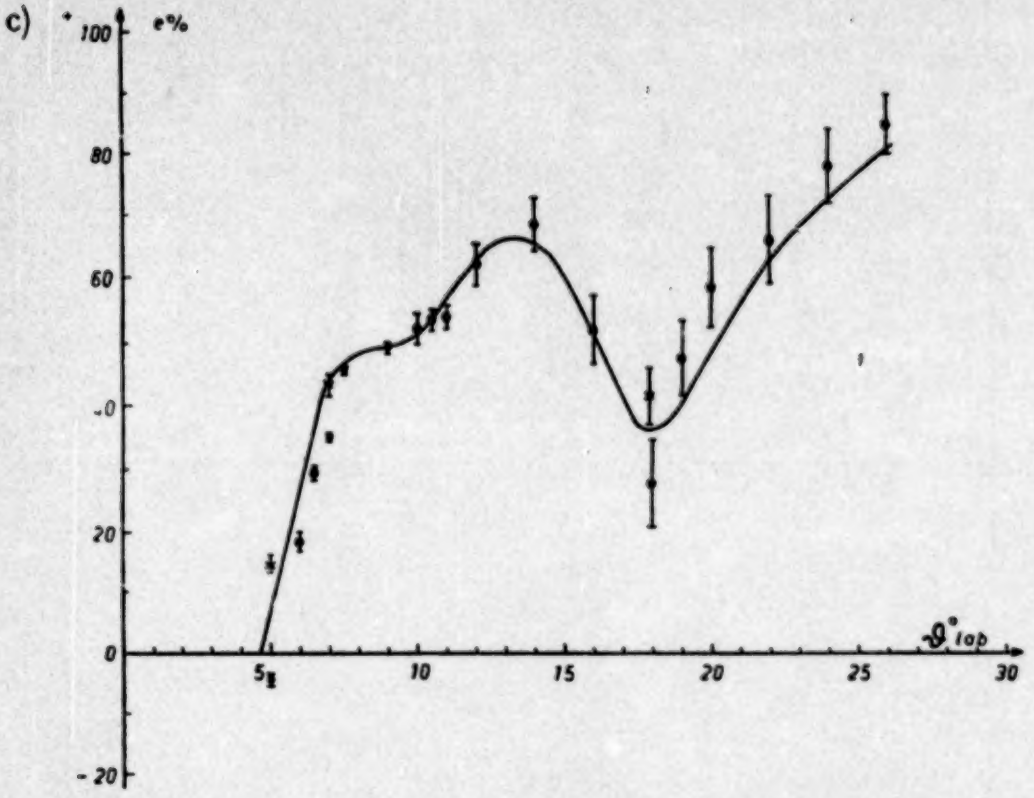

Fig. 1. Elastic asymmetries for protons scattered from a) iron b) nickel c) copper. Curves and symbols are explained in the text.

The only further difference that can be seen from the data concerns the magnitude of the asymmetry in the angular region from the minimum to the second maximum. Copper seems to have the largest asymmetry of the three elements in this region. The asymmetry is perhaps also somewhat larger for nickel than for iron. However, these effects are not quite statistically significant.

The authors wish to thank Professor Svedberg for his interest in this work. We are grateful to Drs. H. Tyrén and Th. A. J. Maris for having informed us about their results before publication and together with Dr. Peter Hillman for stimulating discussions. Thanks are also due to Mr. Å. Svanheden and the cyclotron crew. The work has been supported by the Swedish Atomic Energy Commission.

References

1) J. M. Dickson, B. Rose and D. C. Salter, Proc. Phys. Soc. **68** (1955) 361
2) O. Chamberlain, E. Segré, R. D. Tripp, C. Wiegand and T. Ypsilantis, Phys. Rev. **102** (1956) 1659
3) R. Alphonce, A. Johansson and G. Tibell, Nuclear Physics **4** (1957) 672
4) R. Alphonce, A. Johansson and G. Tibell, Nuclear Physics **3** (1957) 185
5) H. Tyrén and Th. A. J. Maris, private communication

Nuclear Physics **4** (1957) 648—661; © *North-Holland Publishing Co., Amsterdam*
Not to be reproduced by photoprint or microfilm without written permission from the publisher

POLARIZATION OF HIGH ENERGY PROTONS IN ELASTIC AND INELASTIC SCATTERING

PETER HILLMAN †, A. JOHANSSON and H. TYRÉN
The Gustaf Werner Institute for Nuclear Chemistry, University of Uppsala

Received 8 July 1957

Abstract: The polarizations of 173—7 MeV protons inelastically and elastically scattered by carbon, oxygen, and calcium have been measured with an energy resolution of 2—2.5 MeV full-width at half-height equivalent. The polarizations of scattered protons corresponding to the low-lying levels of all three elements are large and show strikingly similar angular patterns. The higher levels are much less polarized. The elastic results differ from measurements of elastic asymmetries in having deeper minima, and have been extended to larger angles.

1. Introduction

Since 1952 considerable experimental and theoretical effort has gone into the study of the elastic scattering of high-energy polarized protons by complex nuclei [1]). Recently it has been shown that at larger angles an appreciable fraction of the scattering is slightly inelastic, i.e. leaves the residual nucleus in a low-lying excited state. With sufficiently good energy resolution, the energy spectra of the scattered protons exhibit peak structures corresponding to selections of the excited levels of the scattering nuclei [2, 3]). The differential cross-sections for these peaks are being measured here [3]) and together with these a knowledge of the spin dependence of the scattering should be useful in determining the nature of the nuclear states involved as well as that of the scattering process itself.

The two spin-dependent parameters measurable in experiments on the double-scattering of spin one-half particles can be chosen to be the polarization P and the asymmetry e. P is the polarization produced in the scattering of an unpolarized beam; e is the ratio of the difference to the sum of the intensities of particles scattered left and right in the plane perpendicular to the direction of polarization of an incident 100 % polarized beam. (The sign of e is positive for spin-up particles scattering more to the left than to the right.)

If parity is conserved it may be shown quite generally that $e = P$ either 1) if the spin of the nucleus is zero before and after the interaction and its

† CERN (European Organisation for Nuclear Research, theoretical study division). On leave of absence from AERE, Harwell, England.

parity unchanged † or 2) for elastic scattering *if* fast interactions are invariant under time-reversal. Since the spin of the three elements here considered is zero, the present measurements on *elastic* polarizations had the sole purpose of complementing and improving previous and accompanying asymmetry measurements, especially in those regions where good energy and angular resolutions are most important, i.e. the diffraction minima, where the angular variations and inelastic contributions are greatest.

For inelastic scattering time-reversibility is no longer applicable, and probably all the levels here investigated have spin different from zero, so differences between the polarizations and asymmetries might in general be expected.

A few measurements of asymmetries in inelastic scattering have been performed by other workers. Those of Chesnut *et al.* [6]) at Rochester on carbon at 220 MeV, and Alphonce *et al.* [7]) here on carbon, oxygen, and calcium at 155 MeV, and preliminary work on carbon at 160 MeV at Harvard [8]), utilized the range method of energy separation. Disadvantages of this method are fairly coarse energy resolution, the inability to measure more than the first prominent excited peaks, and the failure to go to smaller angles or to heavier elements because of the large counting rate from the elastic peak. Recently Dickson and Salter [9]) at Harwell have used a NaI crystal to make measurements on carbon at 135 and 95 MeV of further peaks and the continuum up to large excitation energies, with an energy resolution of 3.4 MeV.

The development of a high-resolution 90° magnetic analyser at this laboratory [10]) together with the extraction of a highly concentrated and monoenergetic external proton beam from the synchrocyclotron [11]) have made possible the investigation described here of the *polarizations* of elastically and inelastically scattered protons over a wide range of angles (2—50°) with a resolution of 2—2.5 MeV full-width at half-height equivalent. The purpose of the experiment was primarily to study the inelastic peaks observed in many light and medium weight elements, paralleling the differential cross section measurements, and also to compare the results with those available from the asymmetry experiments. No other work has been performed on elastic or inelastic polarizations. A preliminary report of this work has already appeared [12]).

We report here on the polarizations of the elastic, 4.4, 9.6, 15, 19, and 21 MeV peaks of carbon; the elastic, 6.1, 12.5, and 20 MeV peaks of oxygen; and the elastic, 3.7, 7, and 18 MeV peaks of calcium.

† There can then be no spin-flip of the scattered nucleon because of angular momentum conservation, implying [4, 5]) $e = P$.

2. Method and Apparatus

If one has available beams of protons of various known polarizations, the apparatus used to determine the polarization P of a beam of unknown polarization can be "calibrated", in other words the (monotonic) relation between the measurable parameter and P can be determined empirically. In this experiment, P is measured by rescattering the protons in a carbon block into two symmetrically placed counters; the observable parameter ε is the ratio of the difference to the sum of their counting rates; and the protons of "known" polarization are the primary unpolarized protons and those scattered elastically from carbon below 20°, for which good published values are available for the asymmetry, which is equal to the polarization for elastic scattering by this spin-zero nucleus.

In principle it would also be possible to *calculate* from such data the relationship between ε and P (since they are nearly proportional, we call their ratio the "analysing power"). However, the energy and angular resolutions of the experiments are determined by a magnetic analyser before the protons reach the carbon block, so that for highest efficiency the block can be made thick and the counter geometry large, making the calculation very difficult.

The apparatus is shown schematically in fig. 1. The primary 185 MeV beam, which is regeneratively extracted from the synchrocyclotron 15 m away, passes through a 2 m thick iron-ore concrete wall into the experimental area. It is concentrated into a spot 4 mm in diameter at the first scattering centre where it has an intensity of 10^{10} protons per second, an angular divergence of $\pm\frac{1}{2}°$, and an energy spread believed less than 1 MeV. The carbon and calcium scatterers are solid blocks 25 and 20 MeV thick respectively. The liquid oxygen is contained in a 32 mm diameter horizontal cylinder of 0.025 mm stainless steel. This is attached to a 4 liter reservoir and is protected by high vacuum and by a radiation shield also attached to the reservoir, to prevent bubbling in the target. The parallel faces of the solid targets and the axis of the cylinder are always turned perpendicular to the line bisecting the scattering angle to give the best energy resolution. The beams enter and leave the scattering chamber, which serves also as the cryostat vacuum jacket, through 0.05 mm Mylar windows, and pass through holes cut in the radiation shield. Almost the entire path to the carbon scatterer is in vacuum, to avoid background, especially at small angles, and to improve energy resolution.

The scattered particles pass into the magnetic analyser through a slit 5 mm high and 15 mm wide 92 cm from the first scatterer. They emerge from the magnet through a 16 mm wide slit, which actually determines the geometrical angular resolution at the first scatterer, about $\pm 0.3°$. The total

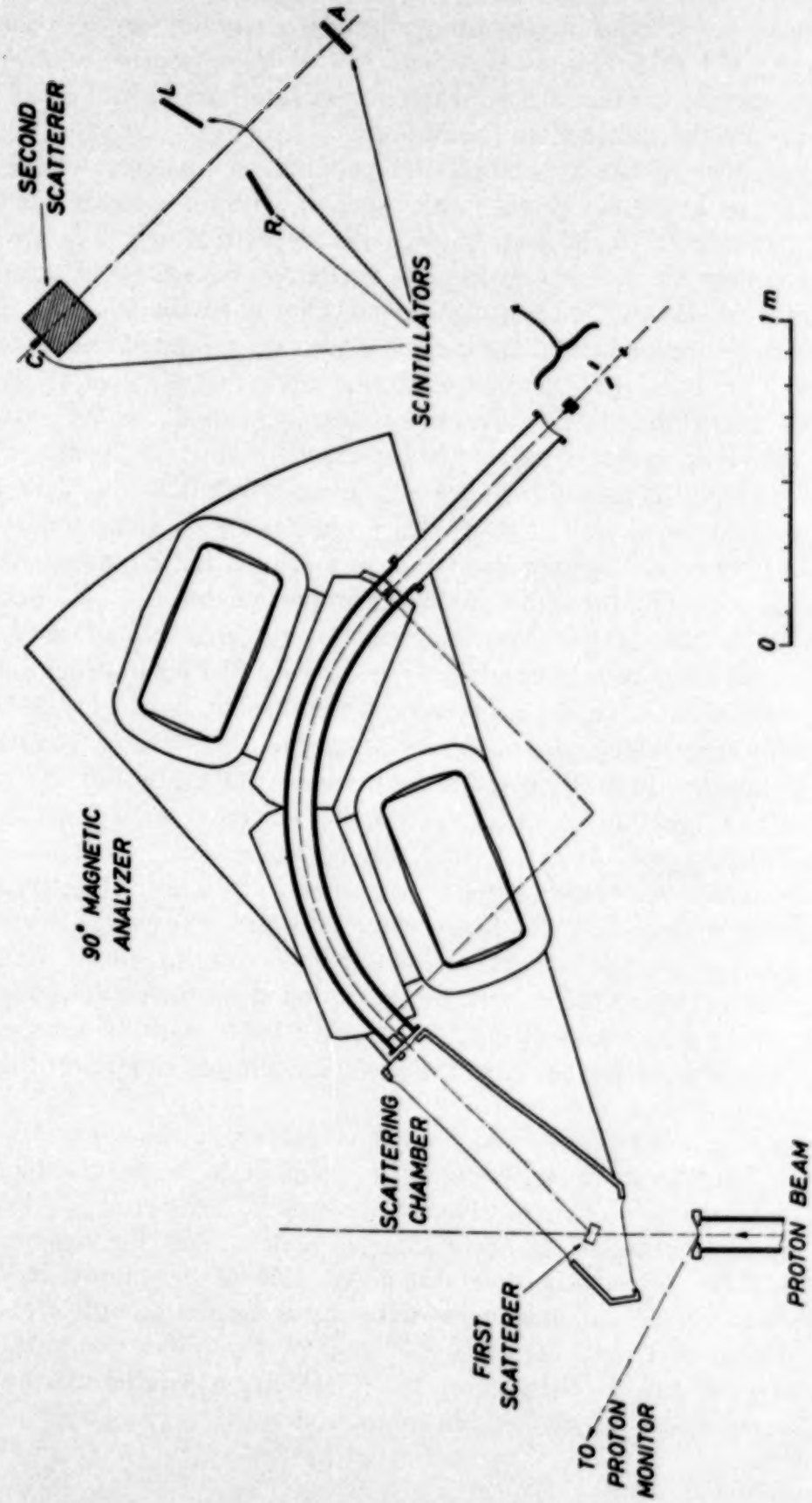

Fig. 1. Schematic diagram of the apparatus.

rms angular resolutions, mostly from multiple scattering, are 0.9° for C and O, and 1.4° for Ca. This last is reduced to 1.0°, by reducing the entrance slit width, for the calcium elastic scattering at small angles and at 19.1°, the bottom of the "diffraction" minimum.

The remainder of the apparatus, the polarization analyser, is shown enlarged in fig. 1. The 5.4 $g \cdot cm^{-2}$ thick carbon scatterer is located at the focus of the magnet 76 cm from the exit slit. A scintillator C 3 mm wide and 25 mm high immediately in front of the carbon defines the geometry. Two scintillators L and R are placed symmetrically to the left and right of the beam centreline behind the carbon. Their size is limited azimuthally (vertically) to about $\pm 45°$ and in scattering angle to the range of about 7° (below which the elastic polarization becomes small) to 20° (above which the scattering cross sections become small). Each is 30 mm wide and 64 mm high and is 16.5 cm from C. Each counts about $\frac{1}{2}$ % of the protons incident on C. An anticoincidence counter 25 cm along the beam centreline from C and 25 mm wide and 35 mm high detects about 82 % of the protons passing through C, reducing proportionately the background of CL and CR accidental coincidences, which is appreciable because of the low ($\approx$ 1/400) duty cycle of the regenerated beam. The pulses from C and A are divided, and $CL\bar{A}$ and $CR\bar{A}$ measured simultaneously in separate 10^{-8} sec resolving time coincidence mixers. ($CL\bar{A}$ means simultaneous counts in C and L but not A.) Intermittent measurements are also made with 38 mμsec delays (= 1 r.f. cycle) in L and R to determine accidental coincidence rates, and with the magnet off to measure real backgrounds.

The whole analyser system is rigidly attached to the exit of the magnet, which can be rotated about the first scattering centre. The energy is varied by changing the magnet current, and is either determined from a magnet calibration curve [3]), or the correct setting is found by direct detection of the appropriate peaks in counting rate in $CL\bar{A}+CR\bar{A}$ or at low intensities CA. The energy resolving power of the system, expressed as a full-width at half-height, is 2—2.5 MeV.

The counting rate for inelastically scattered particles reaches a maximum of 30 counts per minute in each counter ($CL\bar{A}$ and $CR\bar{A}$) corresponding to a first-scattering cross-section of about 7 mb/sterad. The secondary-beam-dependent accidental rate is never more than 5 %, but the magnet-off random and real rates each contribute about $\frac{1}{2}$ count per minute in each counter, limiting the minimum measurable cross section accordingly. For elastically scattered particles below 10° and for the calibration with the unpolarized direct beam, the primary beam intensity is reduced to keep the counting rate below about 500/min in each counter.

2.1. EXPERIMENTAL PROCEDURE

After various standard electronic checks, a typical run begins with calibrations. The parameter $\varepsilon = (\mathrm{CL\bar{A}}-\mathrm{CR\bar{A}})/(\mathrm{CL\bar{A}}+\mathrm{CR\bar{A}})$ is determined with the magnet set at 0.0° and 19.7° (and sometimes some intermediate

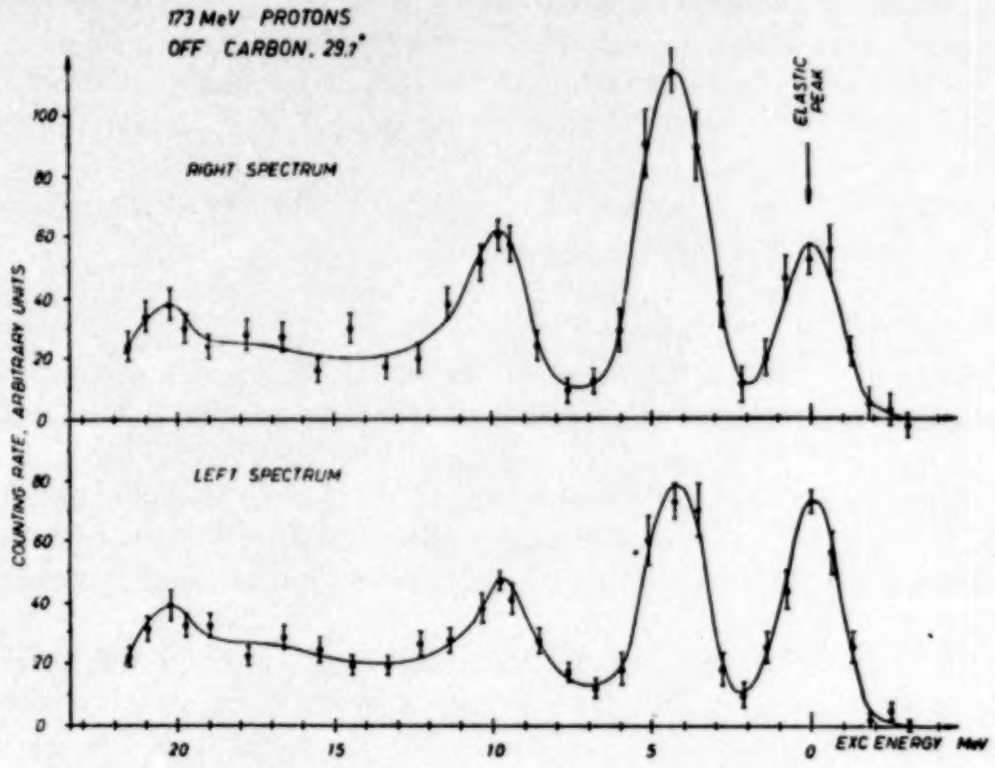

Fig. 2. Typical spectra of "left" and "right" counting rates in the polarization analyser. See text.

angles), a carbon first scatterer, and the energy set for unscattered or elastically scattered protons. (The true magnet angle settings differed from the nominal geometrical angles by 0.3° due to the curvature of the protons in the fringing field of the magnet.) The variation of ε with magnet current is determined by introducing absorbers in front of the magnet or by varying the scatterer thickness. The corresponding polarizations P of the incident beam are 0.0 for the 0° position (direct unpolarized beam) and are determined for all other angles and the appropriate mean scattering energies from the published results available at 135 [9]), 155 [7]), and 220 [6]) MeV for elastic scattering from carbon. After appropriate corrections e.g. for accidental coincidences, a set of calibration curves of ε vs. P for various magnet currents is constructed. The calculated shapes of these, used to interpolate between and extrapolate beyond (to negative polarizations) the few measured points, are not in general straight lines; but if ε is nearly zero at 0°, as is ensured by approximate geometrical symmetry, they are nearly so.

The values of ε are then measured for the various proton groups of

interest from each scatterer, and after similar correction, the corresponding values of their polarization P may be read directly off the calibration curves.

ε is in general determined only for certain proton groups at each angle, but a complete spectrum is sometimes measured, mainly to examine the structureless "continuum". An example is shown in fig. 2, where the corrected counting rates $CL\overline{A}$ and $CR\overline{A}$ are plotted against excitation energy of the residual nucleus (increasing to the left; corresponding to decreasing magnet current) for scattering from carbon at 29.7°. Note the very different ratios ε for the elastic, 4.4, 9.6, and 19—21 MeV peaks. The polarization is about 2.2ε at the upper end of the spectrum and 2.8ε at the lower end (higher excitation energies).

2.2. CHECKS AND SOURCES OF ERROR

Errors may arise in the measurement of the scattered protons from a particular level because of a) contamination by protons from nearby levels and the "continuum", b) *differences* between the conditions of the actual experiment and those of the calibration; c) construction of a calibration curve, including errors in the published polarizations used for the calibration, and in interpolating in energy between them; and d) statistical errors.

a) In most of the cases reported here the energy resolution is sufficient to ensure the clean separation of the proton group in question. In carbon, stray particles contributed more than a few percent only to the 4.4 MeV level at 7.7° and 9.7° (where the elastic peak is tremendous and "spills over" a little); the 9.6 MeV level above 35°; and the 15, 19, and 21 MeV levels at most angles. In oxygen there is uncertainty in the relative contributions of the known 6.05 and 6.13 MeV levels to the observed 6.1 ± 0.2 MeV peak, and the contribution of the 6.9 and 7.0 MeV levels could be as much as 20 %. The 12.5 MeV peak and especially the 20 MeV structure are again superposed on a continuum at all angles. In calcium, the 3.7 MeV peak at 9.7° is contaminated by elastically scattered particles, and above 30° by the continuum to the extent of perhaps 20 %; the 7 MeV point has about a 25 % contamination, and the 18 MeV group at all angles is again not clean. The results for all these cases should therefore be treated with care; the quoted values apply to all protons near the specified energy, not just to those exciting the particular level. In a few cases only, an attempt was made to subtract some of these "stray" particles by measuring the polarizations of the "continuum" on either side of the peak, and interpolating the intensity and polarization, with results presented below; but the process is necessarily somewhat arbitrary.

b) The polarization analysing power is calibrated directly against magnet current, so that magnetic effects on the counters are included. The ex-

perimental situation then can differ from the calibration situation only in the following respects:

1) Electronic drift. This was minimized by checking bias and photomultiplier high voltage plateaux before each run; and by frequently rechecking the calibration points. The error in ε attributable to this cause is therefore generally less than 0.01.

2) Absolute counting rate. The experimental asymmetry was determined to be constant to ± 0.01 over the allowed range of counting rates.

3) Random and background coincidences. These were always measured for each target and at each angle separately, with delays in the L and R counters and with magnet off respectively, and corrected for beam intensity. A proton recoil scintillator telescope was used as a beam monitor.

4) Angle of approach of the protons to the analyser scatterer, i.e. of emergence from the magnet. This varies according to the angular and spatial distributions of protons entering the magnet, and the slope of their energy spectrum (e.g. the side of a peak). The angle of approach to the magnet depends mainly on the thicknesses of target used (up to 35 mm) and the variation in beam position (≈ 2 mm), but on a simple calculation both effects are negligible. The effect of the spatial distribution at the entrance slit due to the angular variation of the first scattering cross-section was checked in two ways: first, a direct measurement of the distribution across the exit slit of counted particles was made by blocking all but a small portion of it at various places, for a peak with cross section sharply falling with angle and another sharply rising. Then the effect on ε is given by a calculation of the shift in the mean angle of approach to the carbon analyser scatterer, together with a direct measurement of the variation of ε against the position of the scatterer and counters. The effect on ε of blocking various portions of the entrance slit was also measured; the results indicate that the largest observed cross-section variation, about 20 % per degree, would give an error in ε of only 0.002.

The effect of a strong energy spectrum slope, which would mean a non-uniform distribution of particles across the exit slit even if uniform over the entrance slit, was checked by measuring ε at various points across a cleanly separated elastic peak. An effect was found, but is small for any likely error in setting on the top of a peak and for all observed continuum slopes.

c) Errors in the construction of calibration curves arise primarily from statistics and from the published values and energy-interpolation between them. A value of 96 ± 4 % for the carbon elastic polarization at 19.7° and 173 MeV was used. This gives an analysing power varying from about 0.50 at 175 MeV to 0.32 at 145 MeV. Since ε for unpolarized protons (magnet 0°) was always less than about 0.04, a straight line was for convenience

always used as a calibration curve, and the error in ε thus introduced, mainly in the region of negative polarization, is calculated to be less than 0.01. Measurements at various positive polarizations (various carbon angles) were not in disagreement with a straight line. The error in interpolating between the measured curves for various magnet currents is generally less than 0.02.

The total calibration error contributes to P about ± 0.05 at $P = 1$, 0.04 at $P = 0$, and 0.07 at $P = -1$; these errors increase somewhat for larger excitation energies. However, they vary smoothly and slowly from point to point.

Thus the most important systematic errors are those arising from contamination by unwanted protons and from the calibration. Since neither is independent from point to point and the former is also very difficult to calculate, the quoted errors are in most cases just statistical mean deviations. Neither the striking trends observed nor the conclusions drawn here or in the following article [5]) should be affected by the systematic errors.

3. Results

The complete results for carbon are shown in fig. 3. Comparisons with the asymmetries measured by other workers, with the angular scales transformed by the square roots of the energy ratios, are shown in figs. 4 and 5 for the 4.4 and 9.6 MeV peaks respectively.

The results for oxygen and calcium are shown in figs. 6 and 7. The triangular points at 19.1° and at small angles for the calcium elastic scattering were measured with improved angular resolution and at a slightly higher energy.

As mentioned above, an attempt was made to check or estimate the contributions of stray particles to the various levels in a few cases. In no case were the results changed appreciably, since the polarization of the contaminating particles never differed strongly from that of the protons in question. The polarizations of those levels into which the elastic peak spilled are clearly slightly too high. The continuum generally was found not to be very strongly polarized, though it was positive, so that the levels with low polarization, the 15 MeV level in carbon, the 12.5 MeV level in oxygen and all the "20" MeV groups, should not be strongly affected, while the 9.6 MeV level in carbon above 35° and the 3.7 MeV level in calcium above 30° have slightly too small (too positive) values of P. It is just possible that the differences between the 4.4 and 9.6 MeV levels in carbon above 35° are accounted for in this way.

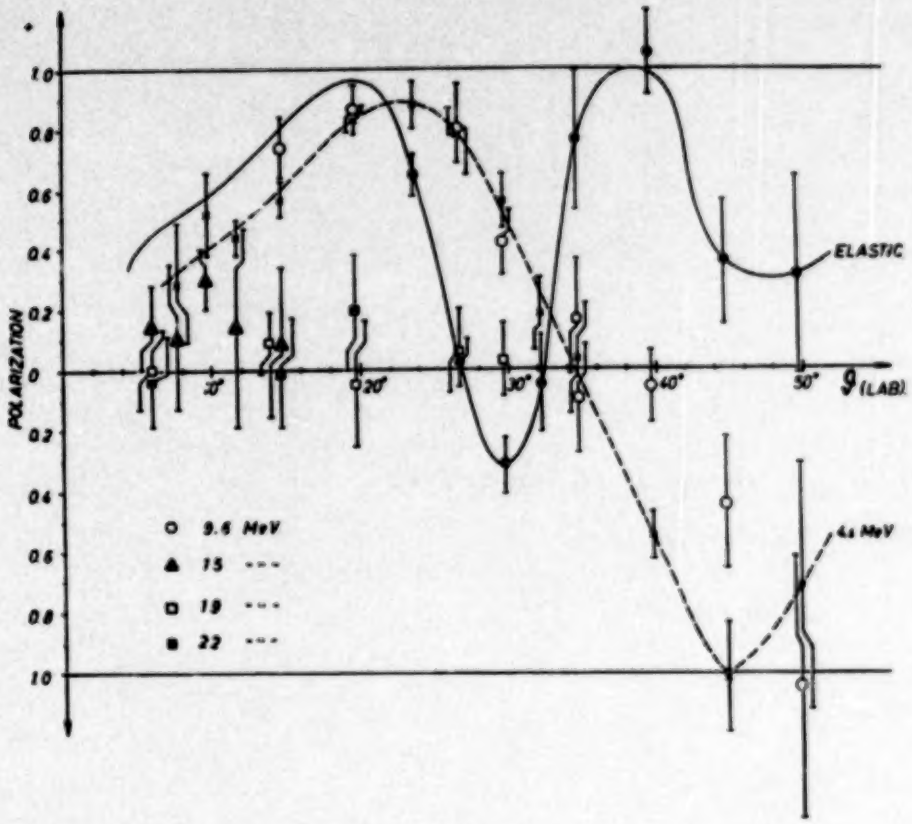

Fig. 3. Polarizations of 173 MeV protons off carbon.

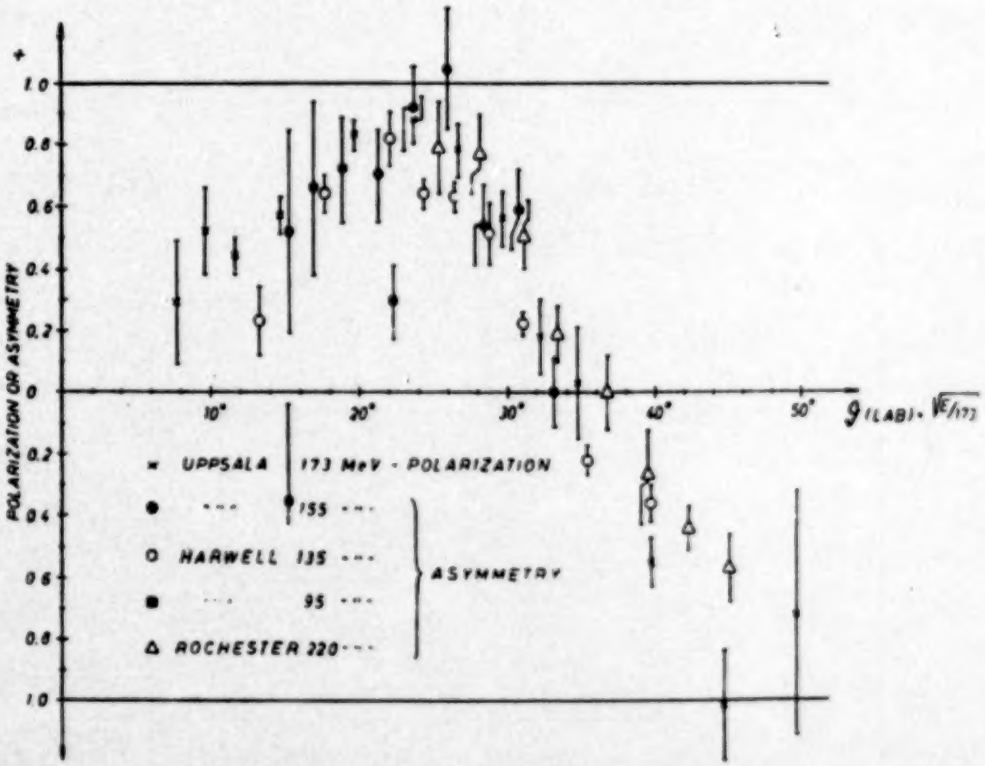

Fig. 4. Polarizations and asymmetries for the carbon 4.4 MeV level.

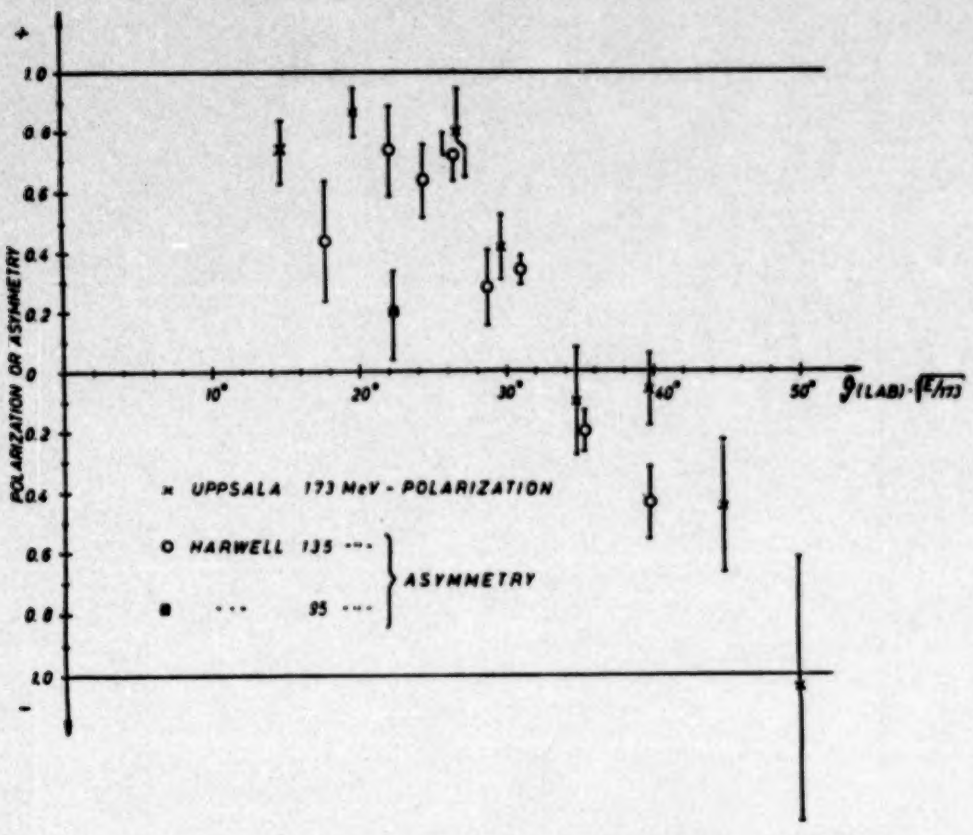

Fig. 5. Polarizations and asymmetries for the carbon 9.6 MeV level.

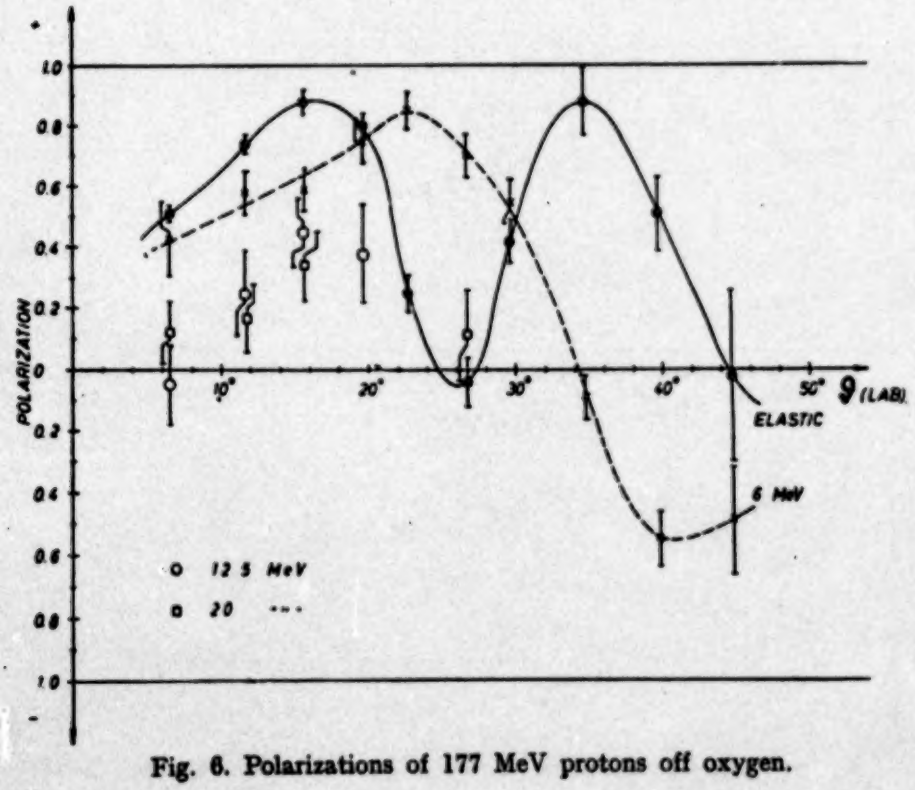

Fig. 6. Polarizations of 177 MeV protons off oxygen.

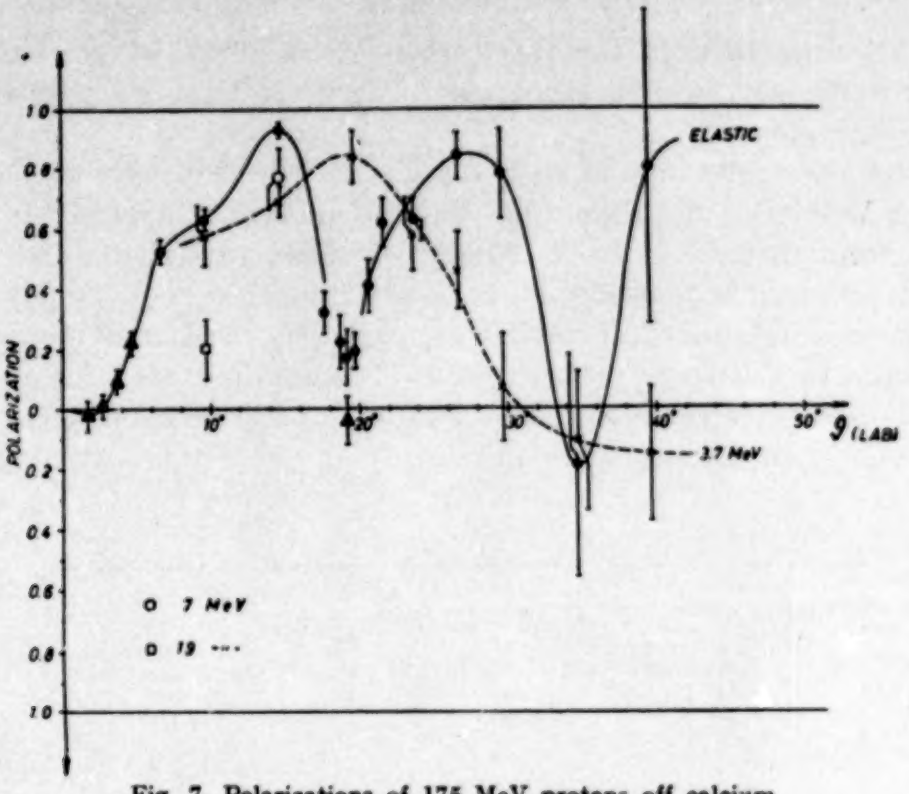

Fig. 7. Polarizations of 175 MeV protons off calcium.

4. Discussion

4.1. ELASTIC POLARIZATIONS

Since carbon, oxygen, and calcium all have spin zero, their elastic asymmetries and polarizations are the same, as mentioned above. In particular we have used previous measurements of the carbon small angle elastic asymmetries directly to give us the polarizations of the protons we use for calibrating our analyser.

Agreement of our results with asymmetry experiments [6, 7, 9]) is good in all three elements. The deeper first "diffraction" minima are due to improved angular resolution and cleaner separation of the inelastic contributions, which are generally large and strongly positively polarized in this region. This elastic feature is in agreement with most theoretical predictions, as is our observation of further diffraction minima and maxima in all three elements at larger angles.

4.2. INELASTIC POLARIZATIONS

The most striking general features of the inelastic polarizations are the very large magnitudes and closely similar patterns of all the low-lying levels (reproduced together in fig. 8) and the much smaller values for the higher levels, especially the persistent "20" MeV structures. As seen in fig. 8, the polarizations of the low-lying levels apparently differ mainly by a slight angular contraction with increasing atomic number, and even that is much less than the contraction observed in the elastic diffraction pattern.

The difference between the two carbon levels above 35° as remarked above is probably real, but does not change the remarkable agreement among the shapes.

In comparing the results with the asymmetries available for the 4.4 and 9.6 MeV levels of carbon, (figs. 4 and 5) one sees no appreciable deviation, except that the Harwell 135 and especially 95 MeV results exhibit what is presumably an energy effect. A real difference would be physically interpretable in terms of the probability of flipping the spin of the incident nucleon in the scattering. Such a process has been proposed, for instance, for "low"-energy stripping [13]). How such a spin-flip probability can enter in may be seen from a consideration of a hypothetical scattering at a

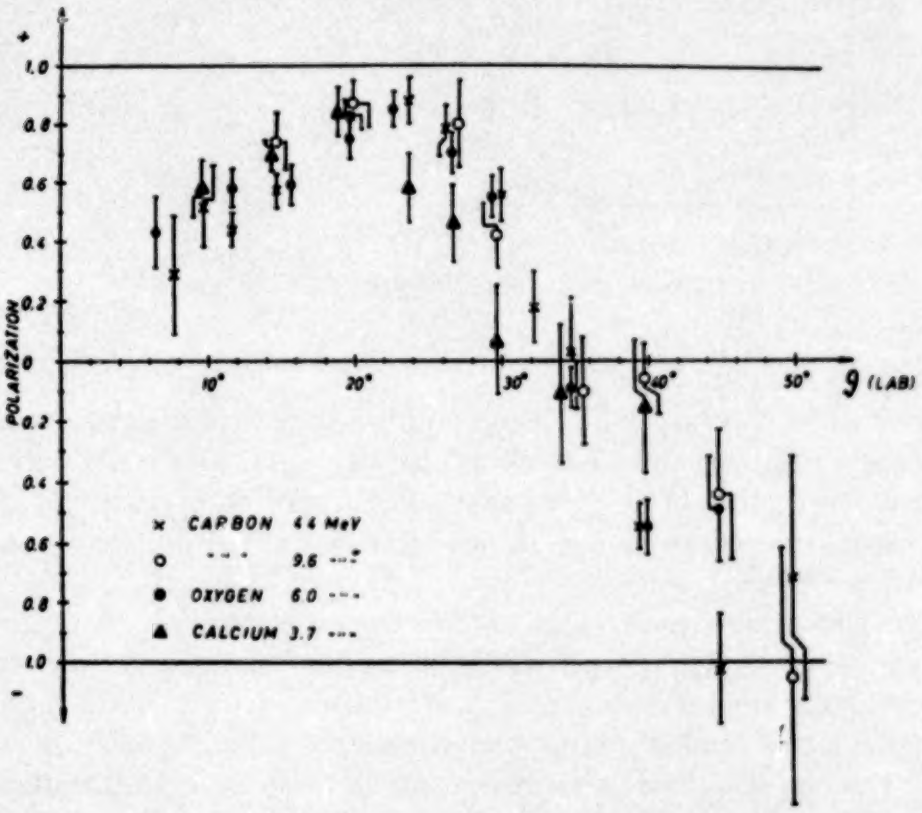

Fig. 8. Polarizations of low-lying levels of carbon, calcium and oxygen.

particular angle for which e is 1, but in which half the scattered particles have their spins flipped. Clearly the particles scattered at the same angle from an unpolarized beam will be unpolarized, i.e. $P = 0 \neq e$.

One can notice that this spin-flip process is not time-reversible, and therefore is not applicable to elastic scattering if time reversal invariance is valid.

A study has been undertaken of possible asymmetry-polarization differences which might be observed, and of the significance of their apparent absence, which is not expected in general, though it is true for collective levels in the first Born approximation [14]).

A further discussion of the relevance of these results to the nature of the scattering and of the nuclear levels is given in the following paper [5]), which also presents these results combined in an interesting manner with the cross sections.

The measurements are continuing on levels in other elements.

We thank Prof. The Svedberg for continued encouragement. We are grateful to Dr. Th. A. J. Maris, who contributed several important suggestions and criticisms, and to Mr Å. Svanheden and the cyclotron and electronic staffs for full cooperation. One of us (P. H.) wishes to thank CERN for its support. The work was supported by the Swedish Atomic Energy Commission.

References

1) Reviewed in L. Wolfenstein, Ann. Rev. of Nuc. Sci. **6** (1956) 43
2) K. Strauch and F. Titus, Phys. Rev. **104** (1956) 191
3) H. Tyrén and Th. A. J. Maris, Nuclear Physics **4** (1957) 637
4) Owen Chamberlain, Emilio Segrè, Robert D. Tripp, Clyde Wiegand and Thomas Ypsilantis, Phys. Rev. **102** (1956) 1659
5) Th. A. J. Maris and H. Tyrén, Nuclear Physics **4** (1957) 662
6) W. G. Chesnut, E. M. Hafner and A. Roberts, Phys. Rev. **104** (1956) 449
7) R. Alphonce, A. Johansson and G. Tibell, Nuclear Physics **4** (1957) 672
8) Private communication
9) J. M. Dickson and D. C. Salter, Nuovo Cimento, in publication
10) A. Lovati and H. Tyrén, Journ. Sci. Instr. **33** (1956) 151
11) Å. Svanheden and H. Tyrén, to be published
12) H. Tyrén, Peter Hillman and A. Johansson, Nuclear Physics **3** (1957) 336
13) D. H. Wilkinson, Phys. Rev. **105** (1957) 666
14) Th. A. J. Maris, Nuclear Physics **3** (1957) 213

Nuclear Physics **4** (1957) 662—669; © *North-Holland Publishing Co., Amsterdam*
Not to be reproduced by photoprint or microfilm without written permission from the publisher

SOME REMARKS CONCERNING MEASUREMENTS ON INELASTIC SCATTERING OF 155-185 MeV PROTONS ON CARBON, OXYGEN AND CALCIUM

TH. A. J. MARIS and H. TYRÉN
The Gustaf Werner Institute for Nuclear Chemistry, University of Uppsala

Received 8 July 1957

Abstract: Semi-quantitative theoretical expectations for the differential cross sections of high energy inelastic proton scattering are summarized and compared with the experimental results for carbon, oxygen and calcium. The general agreement is satisfactory. High energy proton scattering at small angles seems a promising tool for the study of the giant gamma resonances at least in light nuclei.

Some remarks concerning the measured asymmetries and polarizations of the inelastically scattered protons are made.

In this note some measurements done at this laboratory on the cross sections [1, 2]), asymmetries [3]) and polarizations [4]) of 155—185 MeV protons inelastically and elastically scattered on carbon, oxygen and calcium will be discussed on a semi-quantitative basis. In the first part the main conclusions of ref. [5]) concerning the angular distributions in the inelastic scattering of unpolarized protons are summarized, somewhat expanded, and compared with the experimental results. In the second part some features of the observed polarizations and asymmetries of the scattered protons are considered.

On the basis of the Born or impulse approximation it was found that in the inelastic scattering of nucleons of some hundreds of MeV on light nuclei mainly single particle levels will be excited and that the amplitude for the scattering of a bombarding proton from some initial momentum and spin state into another final state, exciting the nucleus into a certain single particle state, is a linear combination of nucleon-nucleon scattering amplitudes each multiplied with a factor dependent on the initial and final nuclear states [6, 5]). These nuclear factors are of the form

$$F_{nmr}(\mathbf{k}_f) = \int \langle \varphi_f | s_n(1) t_r(1) \rangle e^{i(\mathbf{k}_f - \mathbf{k}_i)\cdot \mathbf{r}} \langle s_m(1) t_r(1) | \varphi_i \rangle d\mathbf{r}(1) d(2) \ldots d(A). \quad (1)$$

The symbols have the following meaning:
i and f refer to the initial and final states of the system,
s and t are spin and isobaric spin eigenfunctions,
$\hbar\mathbf{k}$ is the momentum,

$\mathbf{r}$ is the space variable,
φ is the nuclear wave function, antisymmetric in the particles $1 \ldots A$,
$d(2)d \ldots d(A)$ indicates integration and summation over all variables of the particles $2 \ldots A$.

From (1) it follows that for angles for which $\hbar|\mathbf{k}_f - \mathbf{k}_i|$ becomes larger than the sum of the radii of the momentum distributions of the final and initial nuclear states all cross sections become small.

Of special interest is the angular dependence of the cross section at small scattering angles. Using the power series expansion of $\exp[i(\mathbf{k}_f - \mathbf{k}_i) \cdot \mathbf{r}]$ one may write (1) as a sum of terms each of which equals the matrix element of a multipole operator between the initial and final states except for the fact that the summation over the spin and isobaric spin coordinates of one particle has not been performed. Only terms of even or odd order contribute, depending on the parity of the excited state relative to that of the ground state.

At small scattering angles (for light nuclei at about 10 degrees for a bombarding energy of 180 MeV) $|\mathbf{k}_f - \mathbf{k}_i|$ times the nuclear radius becomes of the order 1, and it is small in the forward direction. In this angular region the lowest order non-vanishing multipole term in the expansion of (1) determines the angular dependence of the nuclear factor. Assuming that the nucleon-nucleon scattering amplitudes are smoothly dependent on angle, except for the Coulomb interaction whose matrix element is small for larger angles but proportional to $|\mathbf{k}_f - \mathbf{k}_i|^{-2}$, it follows that:

a. If the monopole and dipole matrix elements vanish, the cross sections will be forward dipped. The contribution due to electromagnetic excitation is negligible for these excitations.

b. If the dipole matrix element is non-zero, but the monopole element vanishes a forward maximum may result from Coulomb-excitation. The matrix element is in this case at very small angles proportional to the one for electric dipole γ-excitation. The excited states are identical to the ones of the giant γ-resonance [7]). For light even nuclei these states have angular momentum 1, odd parity and isobaric spin 1 [8]).

c. If the monopole matrix element does not vanish, for example in the case of an excitation only by a spin flip of a target nucleon, a forward peak is also possible for excitation by nuclear interaction. The parity is not changed and for even nuclei the angular momentum of the excited state is one. If the state is excited by a magnetic interaction the forward peak is sharp.

The possibility of excitation of a collective quadrupole vibration of the nuclear surface has also been considered. The cross sections are forward dipped and for the case of a square well optical potential are of an order of magnitude similar to those for single particle excitations.

The Born and impulse approximations on which this discussion is based are of course not expected to give correctly the detailed features of the cross sections as for example diffraction effects. However, a similar approximation [9]) at an energy almost an order of magnitude lower has proved to be useful in predicting the shapes of the angular distributions. The most serious error we make is probably caused by neglecting the elastic and inelastic scattering before and after the excitation, which may be corrected by taking into account the distortion of the plane ingoing and outgoing waves by a complex optical potential. A rough estimate with a WKB-method shows that at small angles the corrections are considerable for excitations with unchanged parity but indicates that our quantitative conclusions for light nuclei still hold. A closer investigation is however desirable. The bulk of the contribution to the differential cross-section of the distortion by the spin-orbit coupling should average out as long as the scattering of an unpolarized beam is considered.

The conclusions reached will now be compared with the measurements of the cross sections for oxygen, calcium and carbon [1, 2]). At present only strongly excited levels, for which the first order approximation may give correct qualitative results, are considered.

In a closed shell nucleus the space part of the wave function has to be changed by an excitation and on the basis of the foregoing discussion all forward peaked cross sections should in this case be due to the Coulomb excited dipole excitations of the giant γ-resonances. In O^{16} only the 12.5 and 20 MeV level groups have (quite similarly) forward peaked cross sections. The energy of the last one agrees well with that of the giant resonances [7]). The 12.5 MeV level(s) cannot have been observed in those γ-resonance measurements involving detection of the photonucleon, since the energy is below the neutron removal threshold and the Coulomb barrier. The assignment of isobaric spin one is compatible with the dense spectrum of isobaric spin one levels, corresponding to low lying excitations of N^{16}, which are expected in the O^{16} level scheme from 12.5 MeV upwards.

It is interesting to observe that in all three measured elements these forward peaked parts of the energy spectra change their shapes considerably with angle between 15 and 19 degrees. This is in agreement with the interpretation according to which they are at small angles mainly excited by Coulomb interaction and at large angles by nuclear interactions.

The angular distribution of the 20 MeV cross section is much less forward peaked than the one calculated on the basis of the Goldhaber-Teller model of the giant resonance [5]). One reason for this is probably that it is more reasonable to take into the calculation directly the Coulomb potential of the nuclear protons, instead of that of a homogeneously charged sphere. The latter results in a cut off of the cross section already at very small angles.

Furthermore the interference with the nuclear interaction and the distortion of the incoming and scattered waves will tend to broaden the angular distributions.

In Ca^{40} the broad level structure at 18 MeV is forward peaked and again the energy agrees with that of the giant resonance.

In C^{12} the maximum at 20 MeV is quite similar to the one in O^{16} and therefore we assign it also to the giant resonance states. We have already given the arguments [5]) for the assumption that the monopole term in the scattering amplitude expansion is responsible for the excitation of the 15 MeV 1+ isobaric spin one state. Because of its very sharp forward peak and the large, apparently M1, decay rate to the ground state, we suppose that the spin of one nucleon in the nucleus is flipped mainly by magnetic interaction with the bombarding proton, which has about half the velocity of light.

All other strongly excited levels observed are forward dipped. The 4.4 MeV level in C^{12} is a $2+$ state [10]). The 6 MeV peak in O^{16} is caused by the 3^- and/or 0^+ level(s) [10]). On the basis of the single particle model it should mainly be the 3^- state because in a closed shell nucleus a state of positive parity either corresponds to a several particle excitation or to a "jumping over" of a shell, which gives a small nuclear factor. This is in agreement with the fact that we only slightly excite the 7.6 MeV 0^+ level in C^{12}. In the shell model the 7 MeV 1^- level in O^{16} is also a single particle state. An investigation of whether or not the single particle model provides a simple explanation for the difference in the cross sections for the excitation of the 3^- and 1^- levels in O^{16} would be interesting.

In conclusion we may say that the forward peaked angular distributions of the strongly excited levels with high excitation energies qualitatively fit well with their interpretation as mainly electromagnetically excited single particle excitations and that the forward dipped strong excitations are compatible with the assumption of single particle excitations by nuclear interaction. However, it is not excluded that one or more of the forward dipped cross sections may be caused by collective excitations and might be simply understood by using some type of collective interaction between the bombarding nucleon and the nucleus.

The polarizations and asymmetries of elastically and inelastically scattered protons have also been measure in this laboratory [3, 4]). Concerning these results we are at present only able to make a few rather unconnected remarks. To get a simple picture of the relation between asymmetry and polarization we slightly reformulate the treatment of ref. [11]).

Consider the scattering of a proton beam 100 % polarized orthogonal to the scattering plane. For protons scattered with a certain energy at a certain angle to the right and left in the scattering plane we denote by

$R_n(R_t)$ and $L_n(L_t)$ the differential cross sections to the right and left for events in which the spin of the scattered proton has the original direction

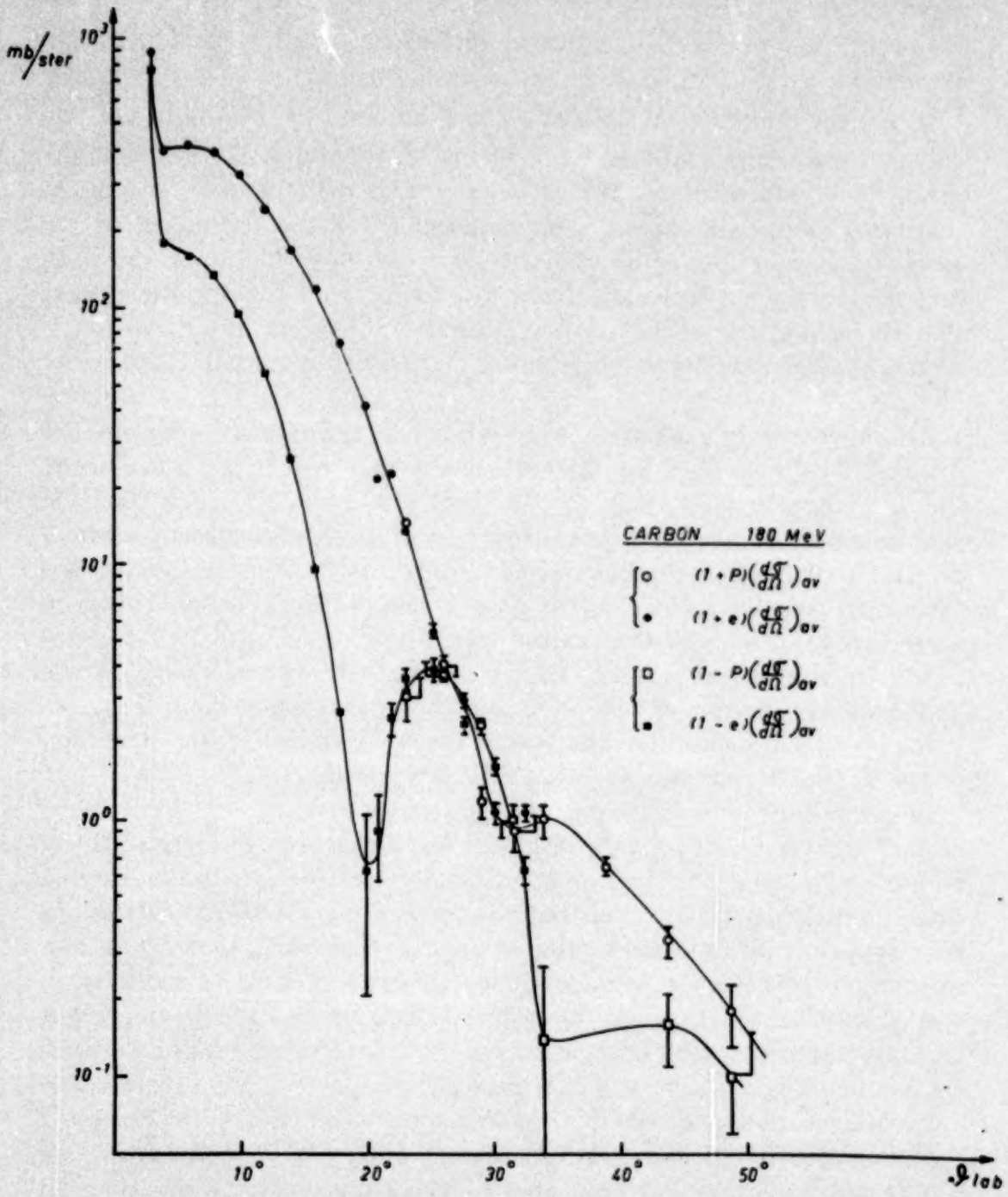

Fig. 1. The left and right hand differential cross sections for the elastic scattering on carbon of a beam 100 % polarized orthogonal to the scattering plane.

(is flipped). We define $R = R_n+R_t$, $L = L_n+L_t$, $e = (R-L)/(R+L)$, $e_n = (R_n-L_n)/(R+L)$ and $e_t = (R_t-L_t)/(R+L)$.

Assuming invariance of the interactions under space inversion and space ro-

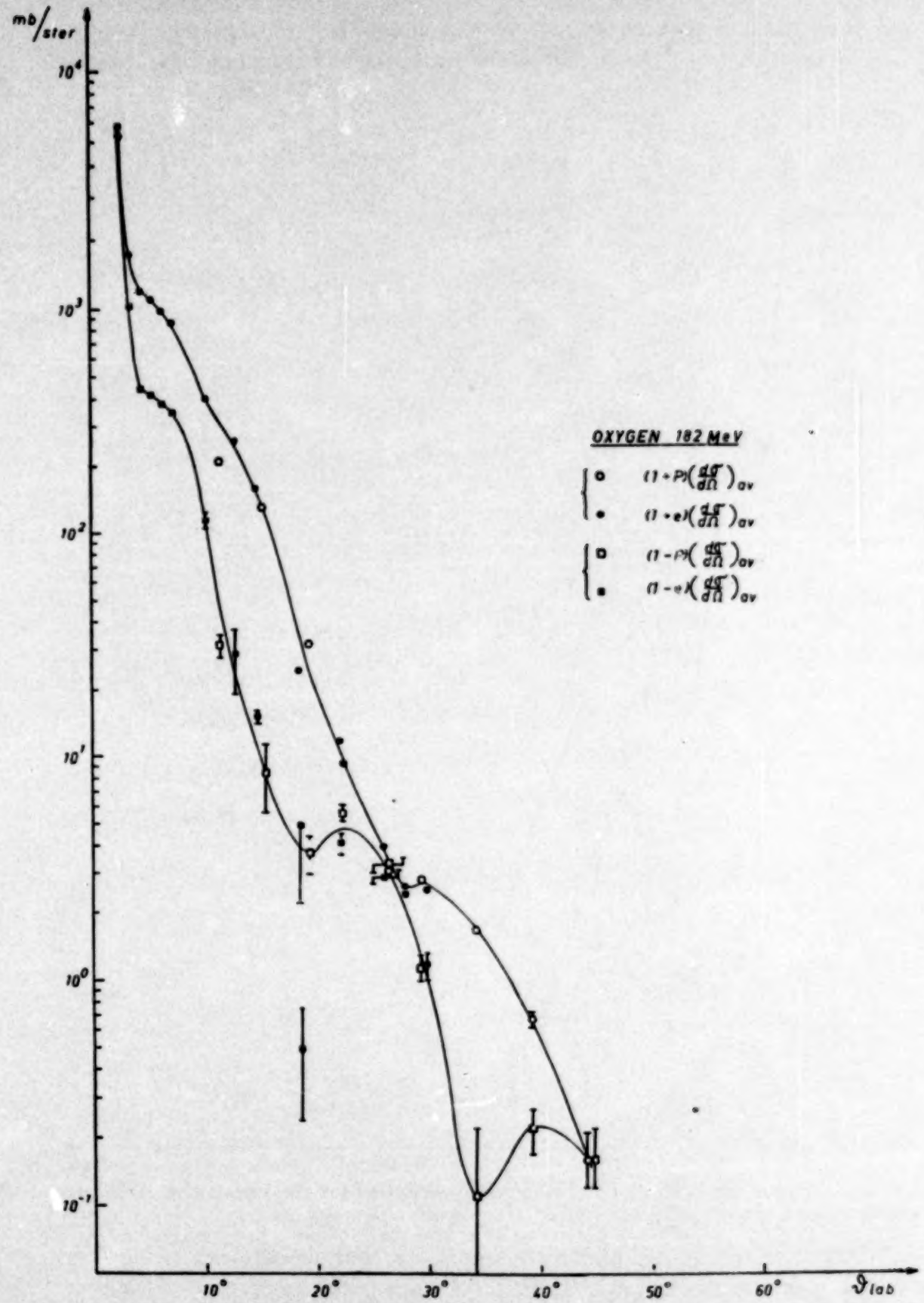

Fig. 1. The left and right hand differential cross sections for the elastic scattering on oxygen of a beam 100 % polarized orthogonal to the scattering plane.

tation one finds that the polarization P equals $e_n - e_t$. From this and $e = e_n + e_t$, it follows that $e - P = 2e_t$. For elastic scattering and assuming time reversal

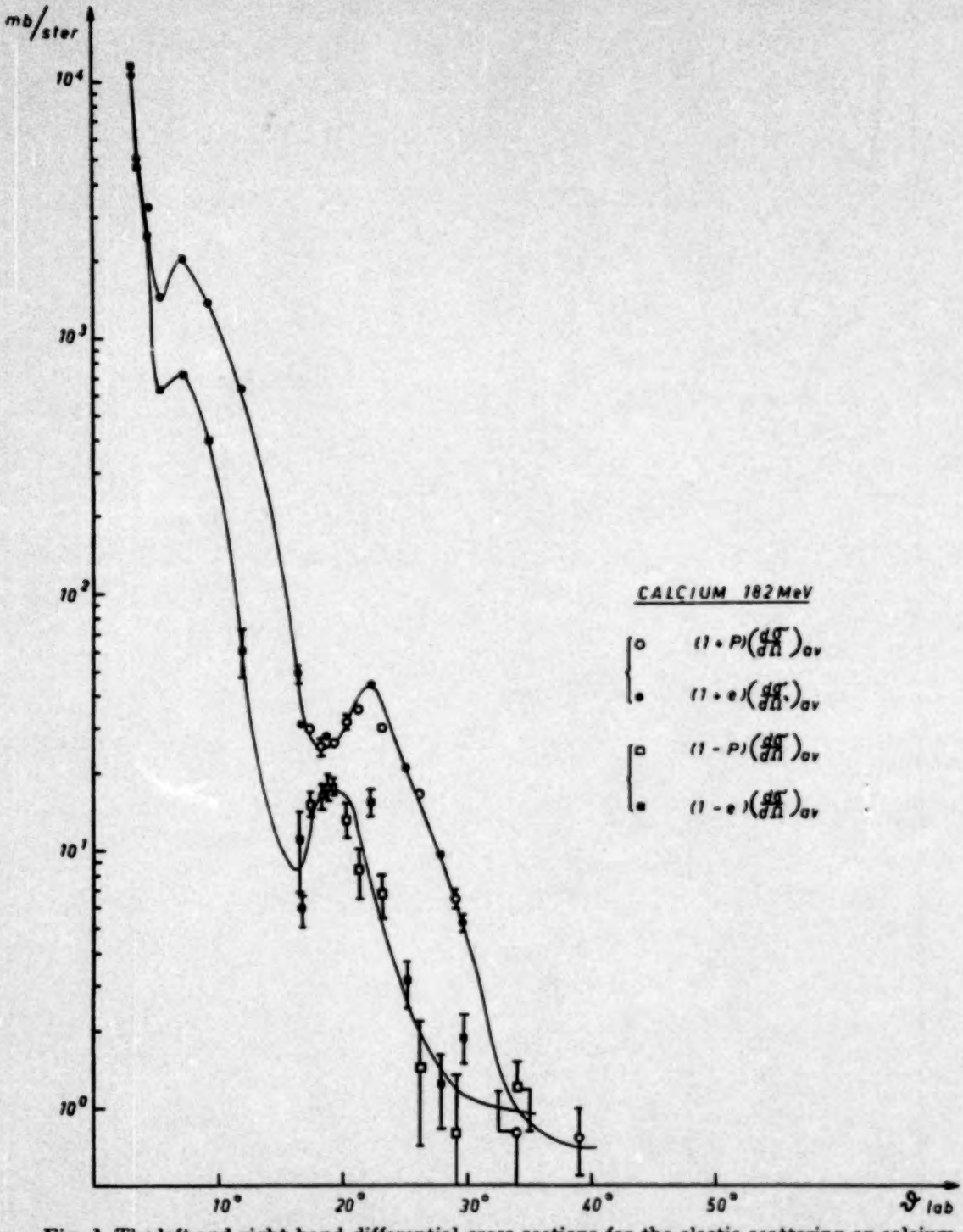

Fig. 1. The left and right hand differential cross sections for the elastic scattering on calcium of a beam 100 % polarized orthogonal to the scattering plane.

invariance, e_t vanishes and therefore $P = e$. For inelastic scattering P is not necessarily equal to e[12]). If, for example, the excitation of a level

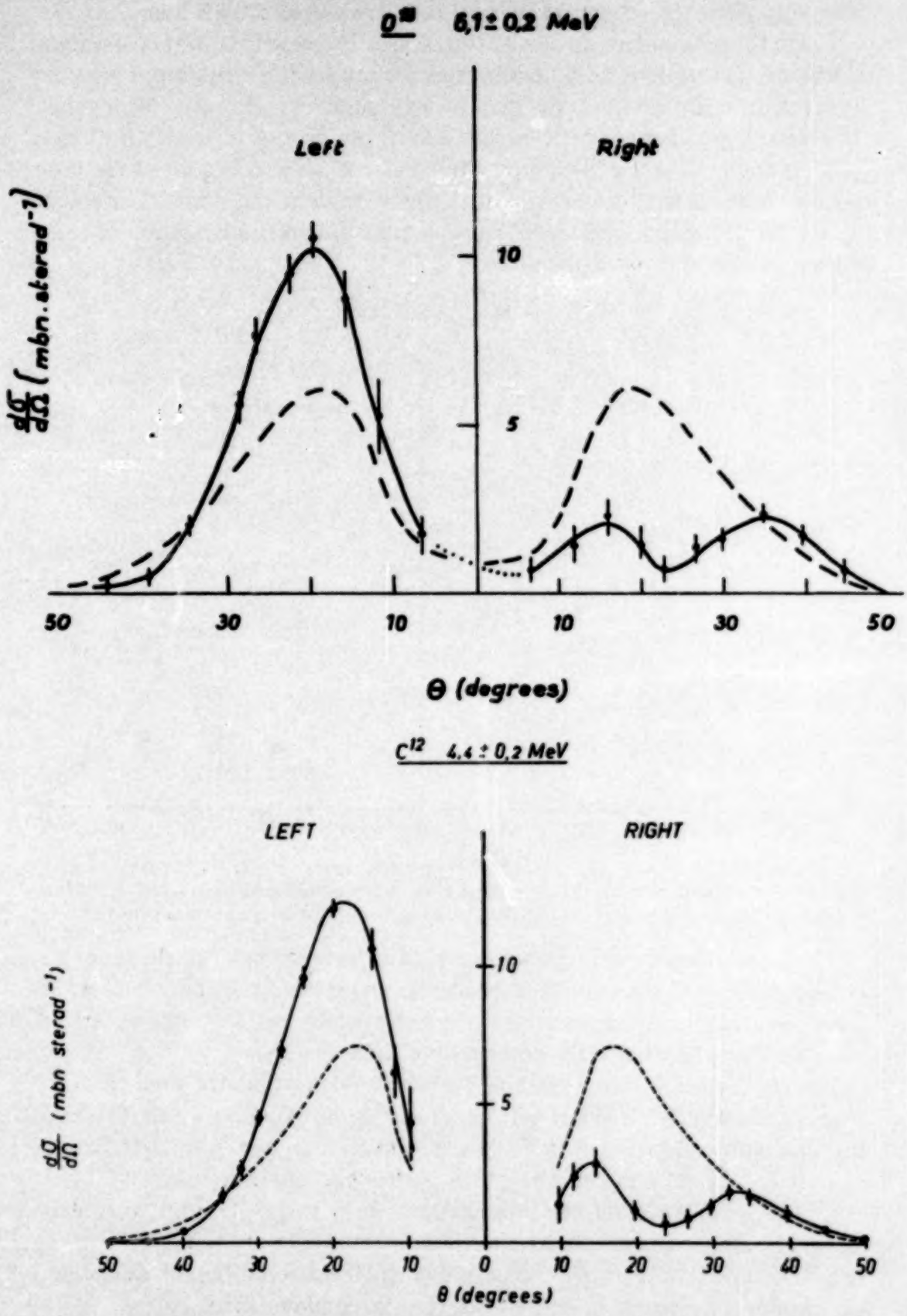

Fig. 2. The left and right hand differential cross sections for inelastics cattering, exciting certain levels in carbon and oxygen, of a beam 100 % polarized orthogonal to the scattering plane.

can only occur by a spin exchange, it follows that $e_n = 0$ and $P = -e$.

Up to the present time in all measured cases $P = e$ within the experimental accuracy. Therefore $e_t \approx 0$, i.e. the cross section for the spin flipped particles is symmetric. In this case it is easy to see that for a certain scattering angle the relative number of particles which have not flipped their spin is at least $|P|$. At angles at which the polarization is large, the major part of the cross section is made up by particles with their spins in the original direction.

For the remaining discussion we shall use the name polarization to mean either polarization or asymmetry.

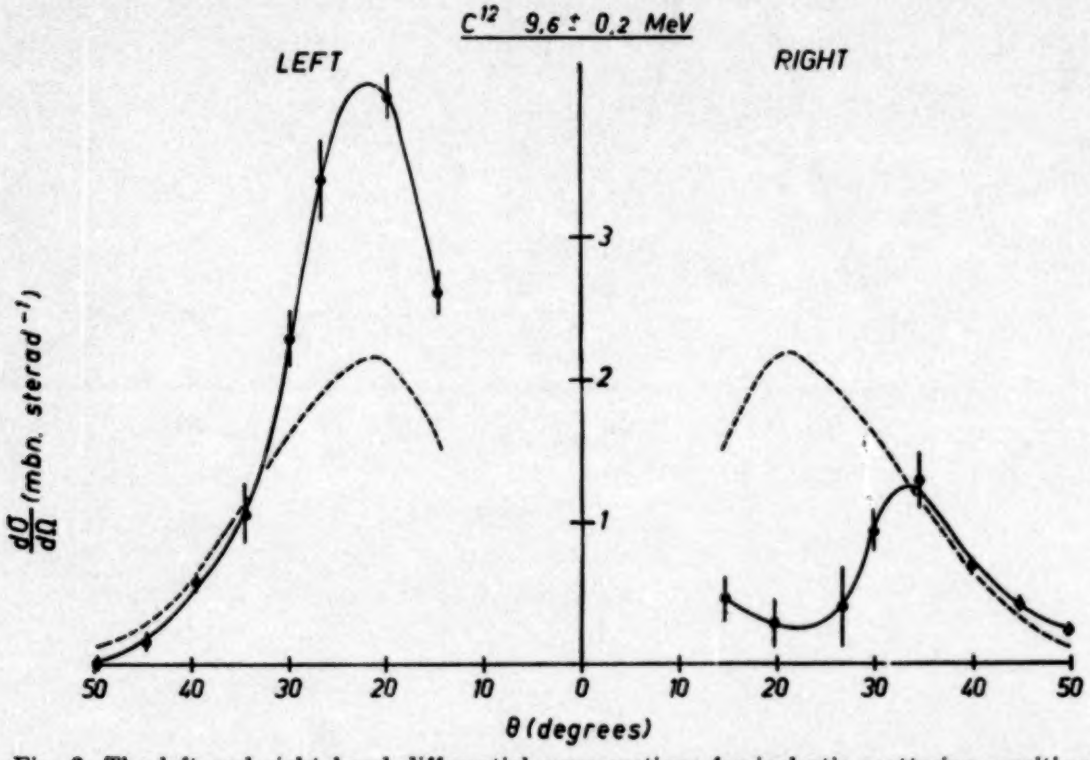

Fig. 2. The left and right hand differential cross sections for inelastic scattering, exciting the 9.6 MeV level in carbon, of a beam 100 % polarized orthogonal to the scattering plane.

The main experimental results are that the protons which have lost considerable energy seem not to be strongly polarized and that those which have excited low-lying, forward dipped, levels are strongly polarized, roughly like the elastically scattered particles.

For the following three reasons it seems unlikely that the high polarizations of the low lying levels will find their explanation by a calculation in impulse approximation which does not take into account modifications caused by the presence of the other nucleons in the nucleus.

a. The magnitudes of the polarizations seem surprisingly large to arise as a rule from the free nucleon-nucleon scattering amplitudes.

b. The uniformity of the polarization patterns for different nuclei and excitations (see fig. 8 of ref. [4])) suggests a common origin.

c. Results obtained at Harwell [13]) for the 4.4 and 9.6 MeV levels of C^{12} at 95 MeV show a radical drop in the polarization with decreasing energy, like the elastic polarization but unlike the free nucleon-nucleon one.

A simple way to understand the results is by assuming that the observed low lying excitations are collective ones [14, 15, 16]). However, a preliminary study of the effect of a complex potential with a spin-orbit term in distorting the wave function has indicated that the collective nuclear potential may still be responsible for the polarization even if the excitation itself occurs by a single particle collision. Another reason may be the failure of the impulse approximation for the case that the struck nucleon is not transferred into a continuum state.

For a few cases in which the measurements are rather complete, the cross section, polarization and asymmetry data have been combined, assuming the polarizations to be equal to the asymmetries. Figure 1 and 2 show some plots of left and right hand cross sections for the scattering of a beam 100 % polarized orthogonal to the scattering plane. For the elastic scattering† these figures bring out the diffraction minima, which in carbon and oxygen are hardly visible in the average cross section; the inelastic cross sections also now show an interesting pattern.

We are thankful to Prof. T. Svedberg for his interest in this work. One of us (T.M.) is grateful for the hospitality he has enjoyed from all members of this institute. Several points of this paper emerged from our frequent discussions with Dr. Peter Hillman. We are indebted to Drs Å. Bohr, Ph Meyer, B. Mottelson and K. Strauch for stimulating remarks. We thank R. Alphonce, A. Johansson and G. Tibell for keeping us continually informed of their experimental results. The work has been supported by the Swedish Atomic Energy Commission.

† The elastic cross sections are preliminary data of Tyrén and Alphonce; final results will be published later.

References

1) H. Tyrén and Th. A. J. Maris, Nuclear Physics **3** (1957) 52
2) H. Tyrén and Th. A. J. Maris, Nuclear Physics **4** (1957) 637
3) R. Alphonce, A. Johansson and G. Tibell, Nuclear Physics **4** (1957) 672
4) P. Hillman, A. Johansson and H. Tyrén, Nuclear Physics **4** (1957) 648
5) Th. A. J. Maris and H. Tyrén, Nuclear Physics **3** (1957) 35
6) G. F. Chew, Phys. Rev. **80** (1950) 196
7) R. Nathans and J. Halpern, Phys. Rev. **93** (1954) 437
8) L. A. Radicati, Phys. Rev. **87** (1952) 521
9) N. Austern, S. T. Butler and H. McManus, Phys. Rev. **92** (1953) 350
10) F. Ajzenberg and T. Lauritsen, Revs. Mod. Phys. **27** (1955) 77
11) O. Chamberlain, E. Segré, C. Wiegand and T. Ypsilantis, Phys. Rev. **102** (1956) 1659
12) L. Wolfenstein, Ann. Rev. Nucl. Sc. **6** (1956) 43
13) J. M. Dickson and D. C. Salter, Nuovo Cimento, in publication
14) M. Ruderman, Phys. Rev. **98** (1955) 267
15) K. Nishimura and M. Ruderman, Phys. Rev. **106** (1957) 558
16) Th. A. J. Maris, Nuclear Physics **3** (1957) 213

Nuclear Physics **4** (1957) 672—676; © *North-Holland Publishing Co., Amsterdam*
Not to be reproduced by photoprint or microfilm without written permission from the publisher

THE ASYMMETRY OF 155 MeV PROTONS ELASTICALLY AND INELASTICALLY SCATTERED FROM CARBON, OXYGEN, AND CALCIUM

R. ALPHONCE, A. JOHANSSON and G. TIBELL
The Gustaf Werner Institute for Nuclear Chemistry, University of Uppsala

Received 8 July 1957

Abstract: The asymmetry of protons scattered elastically and inelastically from oxygen and calcium has been studied with the conventional double scattering technique using range telescopes. Results are given for the asymmetry in scattering from oxygen and calcium together with improved values of previously reported carbon data. The angular distributions of the elastic asymmetry are quite similar for the three elements. For the inelastic asymmetry of oxygen and calcium it has been possible to obtain only qualitative results.

1. Introduction

In the scattering of 185 MeV protons [1]) oxygen and calcium, like carbon, were found to have a low-lying inelastic level (6.1 MeV and 3.7 MeV respectively) rather strongly excited and well separated from other levels. Thus it was possible to determine the purely elastic asymmetries and to obtain at least qualitative information about the inelastic asymmetries by the same range separation technique as was used for carbon [2]).

2. Polarization versus Asymmetry

In double scattering theory one may consider two physical parameters, the polarization P as conventionally defined and the asymmetry e, defined as the difference between the differential cross sections for scattering to the right and to the left divided by their sum in the case that the incoming proton beam is 100 % polarized with spin direction "down".

If the incoming beam has a polarization $P_1(< 1)$ the difference between the cross sections for right and left scattering will be decreased in proportion. In two cases it is true that

$$e = P,$$

namely

a) if the spin of the target nucleus is zero before and after the collision,

b) if the scattering is elastic and the interaction is invariant against time reversal.

In general the connection between the parameters polarization and asym-

metry is related to the probability of spin-flip [3]). Because of the possible difference between P and e in cases where the theorem stated above is no longer applicable it has been preferred here to use the term asymmetry for the data.

3. Experimental Method

The double scattering apparatus used and the method of obtaining inelastic asymmetries have been described earlier [2]). The only change concerned the determination of the ratios between inelastic and elastic scattering cross sections. In the earlier work these ratios were determined for protons scattered from carbon at full energy of the external beam, i.e. 185 MeV. The ratios given in table 1 were obtained with protons that had been slowed down to the energy, 155 MeV, at which the second scattering took place in the main experiment†. In the table the heights of the elastic

TABLE 1

Ratio of cross sections for inelastically to elastically scattered protons from carbon, oxygen, and calcium

$\vartheta°$	Carbon $i(4.43)/e$	Oxygen $i(6.1)/e$	Calcium $i(3.7)/e$
14			0.03
16		0.06	0.14
16.2	0.10		
18	0.15		0.37
20	0.23	0.23	0.40
21	0.37		
22			0.29
24		0.68	0.25
25	0.58		
26			0.29
27.4	0.82		
28		1.07	
30	1.10	1.20	0.55
32.5	1.41		
34			1.13
35	1.71		

and inelastic peaks are denoted by e and i respectively. The figures in brackets, e.g. $i(6.1)$, in the column heads give the excitation energies of the different levels in MeV.

The oxygen asymmetries were determined with a water target. The hydrogen content put a lower limit of 20° on the angle at which the inelastic asymmetry could be measured. For elastic scattering, however, the number of protons coming from the hydrogen was less than 1 % of the total number

† We wish to thank Dr. H. Tyrén for the use of the magnetic analyser [2]) with which the ratios were determined.

of protons counted. This was true for all angles, at large angles due to the energy separation of the telescope, and at small angles due to the smallness of the p—p cross section compared to the oxygen elastic cross section.

4. Results

The degree of polarization of the once scattered beam was recalculated taking account of the fact that the two scatterings occurred at somewhat different energies. In doing so we used the experimentally established dependence of the polarization on energy as reported from different

TABLE 2

Asymmetries for protons scattered elastically and inelastically from carbon, oxygen, and calcium

θ_2°	Carbon		Oxygen		Calcium	
	ε_{el} %	ε_{inel} %	ε_{el} %	ε_{inel} %	ε_{el} %	ε_{inel} %
2	− 4.2±6.6		−6.7±2.0		2.4± 1.4	
2.5	9.2±7.7		−4.3±3.3		1.8± 1.6	
3	− 0.6±4.8		−4.7±1.6		0.8± 2.7	
3.5					−1.4± 4.8	
4	36.7±7.9		15.8±3.0		8.2± 3.6	
5			37.2±3.5		28.3± 1.9	
6	42.8±1.6		44.6±3.7		38.0± 2.1	
7					41.5± 3.0	
8	46.3±2.4		45.6±3.4		48.7± 2.3	
9					54.3± 3.0	
10	51.8±2.5		53.4±4.9		57.6± 2.0	
11	57.0±2.5		56.4±3.4		63.3± 4.5	
12	57.5±3.4				63.6± 5.1	
13	61.9±4.3				69.2± 3.2	
14			71.2±5.8		88.7±15.4	
15	73.1±1.1				84.1± 4.5	
16			83.2±1.1			
16.2	81.1±1.8	52±33			67.9±13.4	
18	87.5±2.8	66±28			68.3± 4.5	31±26
20	94.4±2.0	72±17	96.3±2.2	82±16	27.1± 6.1	93±31
22					43.2± 5.9	16±41
22.5	92.3±3.0	70±15				
24			47.5±5.4	87±12	48.1± 6.1	138±48
25	59.1±4.4	92±14				
27					74.4± 5.5	40±37
27.4	17.5±8.0	105±20				
28			14.5±6.1	47±13		
30	12.0±7.1	54±13	3.2±5.3	80±10	77.2± 7.3	67±26
32			37.1±8.5	44±16	46.8±11.1	24±32
32.5	−20.1±7.9	59±13				
35	25.6±8.9	0±11				

laboratories. The beam was found to be 88.1±0.8 % polarized (previous value 84.3±0.8). The possible systematic error is thought to be less than 2%.

Table 2 and figs. 1—3 give the results of the present experiment. The

quoted errors are of purely statistical origin. The maxima and minima in the angular distribution curves would fall on the same abscissa, if the three graphs were plotted along $\vartheta A^{1/3}$, where ϑ is the scattering angle

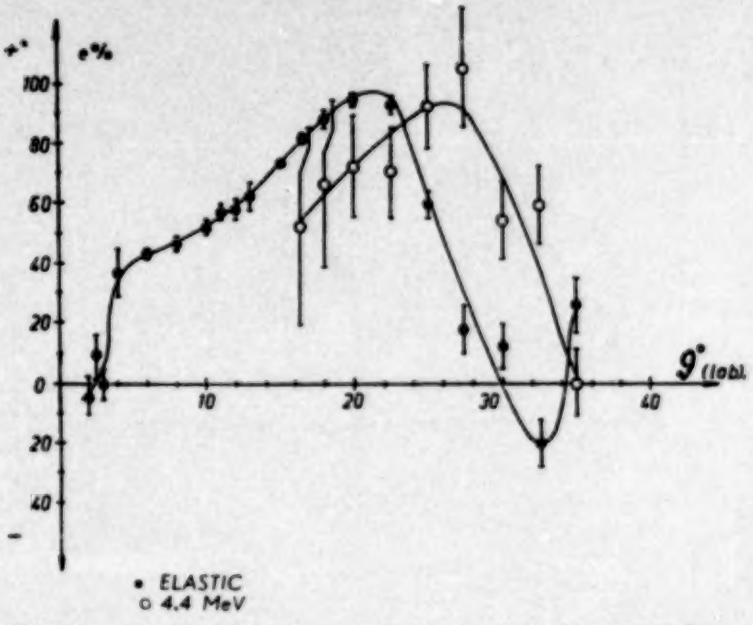

Fig. 1. Elastic and inelastic asymmetries for protons scattered from carbon.

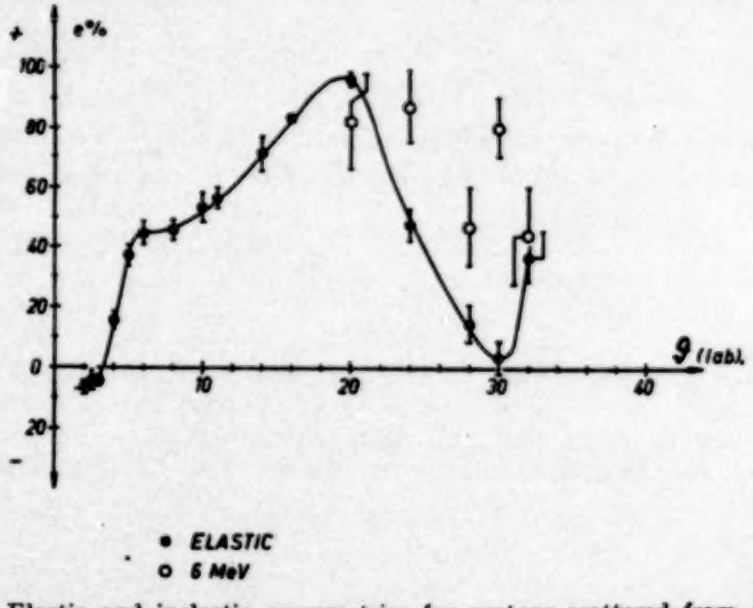

Fig. 2. Elastic and inelastic asymmetries for protons scattered from oxygen.

in the laboratory system and A the mass number. This could be expected from ordinary diffraction theory.

The asymmetries presented here agree well with the polarizations measured at this institute for the same three elements[5]).

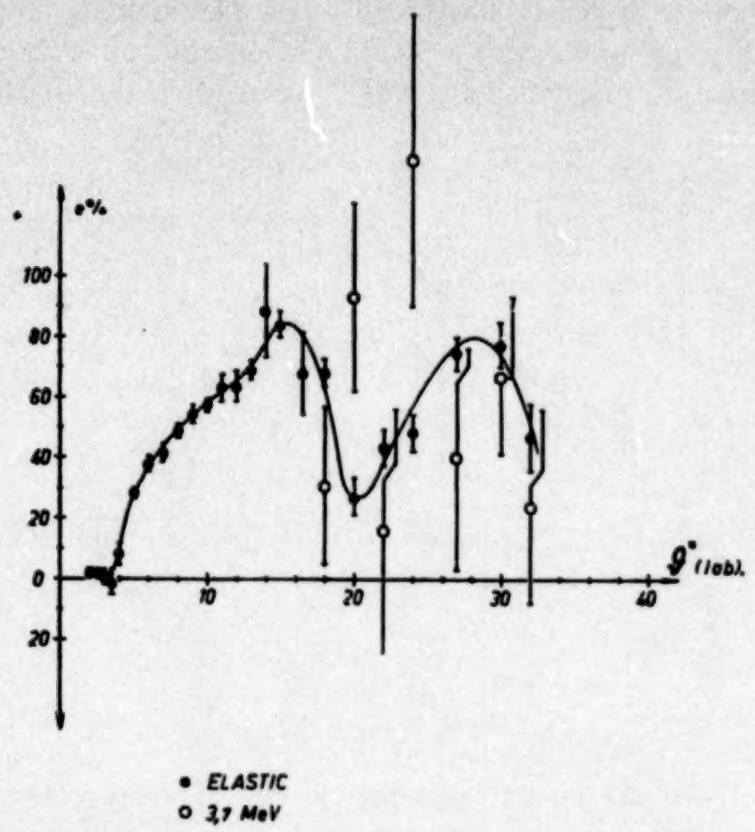

Fig. 3. Elastic and inelastic asymmetries for protons scattered from calcium.

We are grateful to Professor T. Svedberg for his interest in this work. We also wish to thank Drs H. Tyrén, Th. A. J. Maris, and P. Hillman for stimulating discussions. Thanks are due to Mr Å. Svanheden and his cyclotron crew for assistance. The work has been supported by the Swedish Atomic Energy Commission.

References

1) H. Tyrén and Th. A. J. Maris, Nuclear Physics **4** (1957) 637
2) R. Alphonce, A. Johansson and G. Tibell, Nuclear Physics **3** (1957) 185
3) Th. A. J. Maris and H. Tyrén, Nuclear Physics **4** (1957) 662
4) A. Lovati and H. Tyrén, Journ. Sci. Instr. **33** (1956) 151
5) P. Hillman, A. Johansson and H. Tyrén, Nuclear Physics **4** (1957) 648

Nuclear Physics 4 (1957) 677—686; © *North-Holland Publishing Co., Amsterdam*

Not to be reproduced by photoprint or microfilm without written permission from the publisher

SOME REMARKS ON THE INVERSION THEOREMS OF QUANTUM FIELD THEORY

O. KLEIN

Institutet för teoretisk fysik, Stockholm

Received 6 July 1957

Abstract: The new parity situation revealed in experiments on weak interactions suggests the study of the five coordinate inversions of five-dimensional relativity theory. Each of these corresponds to a change of sign of the relevant eight-row Dirac matrix γ_μ ($\mu = 0, 1, 2, 3, 4$). Using this theory as an auxiliary model to a physical theory an eight-component spinor is formed by the combination of a four-component Dirac spinor ψ with its conjugate complex ψ^*. As is then shown the theory is no longer invariant under the old-type space inversion — which would entail a change of sign of γ_0 — but only under the new inversion introduced by Lee and Yang and by Landau, according to which an antiparticle is the mirror image of a particle.

1. Introduction

The following considerations about the new parity situation revealed by recent experiments on weak interactions suggested by Lee and Yang [1]) have for background the writer's tentative generalized field theory, in which the so-called five-dimensional relativity theory is used as a kind of auxiliary model [2]).

In this model, which should thus not be taken literally, there is added to the four components p_1, p_2, p_3, p_4 of the momentum-energy vector of a particle or system, canonically conjugated to the four space-time coordinates x_1, x_2, x_3, x_4, a component p_0 proportional to the electric charge and a coordinate x_0 playing the rôle of the canonical conjugate of p_0. The model theory may be based on an action integral invariant under general transformations of the five coordinates to which belong the five inversions of the coordinate directions.

After some general remarks about the full model theory and its use as an auxiliary to a more realistic theory, we shall in the following mainly consider the simple limiting case which is formally related to quantum electrodynamics including a neutral meson-like Bose-field. As a preparation we shall briefly recapitulate in the first section the well-known inversion theorems of quantum electrodynamics, presenting them, however, in a form suggested by the generalized field theory.

2. The inversion theorems of Quantum Electrodynamics

We consider the following Feynman exponent (i times action integral) η_e for the electrons (to which the Feynman exponent for the pure electromagnetic field has to be added)

$$\eta_e = \frac{i}{2}\int \mathrm{d}^4x(\psi^*\mathscr{L}(e)\psi - \psi\mathscr{L}^{\mathrm{T}}(e)\psi^*), \tag{1}$$

where

$$\begin{aligned}\mathscr{L}(e) &= \gamma_4\gamma_k(p_k+eA_k)+im\gamma_4\\ \mathscr{L}^{\mathrm{T}}(e) &= -(\gamma_4\gamma_k)^{\mathrm{T}}(p_k-eA_k)+im{\gamma_4}^{\mathrm{T}},\end{aligned} \tag{2}$$

ψ and ψ^* being usual spinor field annihilation and creation operators, γ_1, γ_2, γ_3, γ_4 four-row Dirac matrices, of which the first three are assumed to be hermitian and the fourth antihermitian, and A_k the components of the electromagnetic potential vector. The letter e inside $\mathscr{L}(e)$ refers to the elementary electric charge.

Let us now use a Majorana representation for γ_1, γ_2, γ_3, γ_4, so that their elements are all real. Thus it follows that for $k = 1, 2, 3$ ${\gamma_k}^{\mathrm{T}} = \gamma_k$, while ${\gamma_4}^{\mathrm{T}} = -\gamma_4$. This implies that for all four indices

$$(\gamma_4\gamma_k)^{\mathrm{T}} = \gamma_4\gamma_k. \tag{5}$$

Therefore

$$\mathscr{L}^{\mathrm{T}}(e) = -\mathscr{L}(-e),\ \mathscr{L}(e) = -\mathscr{L}^{\mathrm{T}}(-e). \tag{6}$$

Let us now write

$$\chi = \begin{pmatrix}\psi\\ \psi^*\end{pmatrix},\quad \chi^+ = (\psi^*,\ \psi), \tag{7}$$

and thus

$$\eta_e = \frac{i}{2}\int \mathrm{d}^4x\chi^+ L(e)\chi, \tag{8}$$

where

$$L(e) = \begin{pmatrix}\mathscr{L}(e), & 0\\ 0\ , & \mathscr{L}(-e)\end{pmatrix}. \tag{9}$$

For the subsequent considerations it is convenient to give (8) the following form, which follows from (2) and (9):

$$\eta_e = \tfrac{1}{2}\int \mathrm{d}^4x\bar{\chi}(\gamma_k ip_k - m + \alpha\gamma_k ieA_k)\chi, \tag{10}$$

γ_k being now a shorthand notation for $\left(\begin{smallmatrix}1&0\\0&1\end{smallmatrix}\right)\gamma_k$,

$$\bar{\chi} = \chi^+ a,\quad a = \gamma_4 \tag{11}$$

and

$$\alpha = \begin{pmatrix}1 & 0\\ 0 & -1\end{pmatrix}. \tag{12}$$

Now, η_e will maintain its form if we replace any quantity ξ standing

between $\bar{\chi}$ and χ by

$$\xi' = S\xi S^{-1} \tag{13}$$

and at the same time put

$$\chi' = S\chi, \quad \bar{\chi}' = \bar{\chi}S^{-1} \tag{14}$$

and [3])

$$a = S^{+}a'S. \tag{15}$$

After these preparations we consider the following transformation:

$$\chi' = \beta\chi, \quad e' = -e, \quad A'_k = A_k, \tag{16}$$

with

$$\beta = \begin{pmatrix} 0 & 1 \\ 1 & 0 \end{pmatrix}. \tag{17}$$

Since $\chi' = \beta\chi$ is equivalent to

$$\psi' = \psi^*, \quad \psi'^* = \psi, \tag{18}$$

we see that (16) is identical with the particle-antiparticle conjugation C, although usually $e' = e$, $A'_k = -A_k$ is assumed. Since the action integral contains only the product eA_k this change, the reason for which will soon appear, does not influence its invariance under the transformation.

This invariance follows immediately from the fact that the γ_k and p_k commute with β, while α anticommutes with it. Further we see that $a' = a$, when $S = \beta$.

Proceeding now to the five-dimensional viewpoint we assume that $\gamma_0, \gamma_1, \gamma_2, \gamma_3, i\gamma_4$ form a set of five independent hermitian, eight-row Clifford matrices. It follows that their product $\gamma_0, \gamma_1, \gamma_2, \gamma_3, i\gamma_4$ is a hermitian matrix of square 1, which commutes with all five matrices. Putting

$$\alpha = \gamma_0\gamma_1\gamma_2\gamma_3 i\gamma_4, \tag{19}$$

we have thus

$$\gamma_0 = i\alpha\gamma_5, \quad \gamma_5 = \gamma_1\gamma_2\gamma_3\gamma_4, \tag{20}$$

where we shall take for α the quantity defined in (12) and for γ_k the eight-row matrices $\begin{pmatrix} \gamma_k & 0 \\ 0 & \gamma_k \end{pmatrix}$ corresponding to our earlier γ_k. Then the spinor χ will be a solution to the equation

$$[\gamma_k(p_k + \alpha eA_k) + im]\chi = 0, \tag{21}$$

which may be regarded as a simplification of the equation following from the five-dimensional model.

Remembering now the proportionality of p_0 in the five-dimensional model with the electric charge we see that (16) may be characterized as that transformation leaving the action integral invariant, which changes the sign of γ_0 (through α), leaving $\gamma_1, \gamma_2, \gamma_3, \gamma_4$ and $\gamma_0 p_0$ unchanged. We may suitably call (16), which thus corresponds to the inversion $x^0 \to -x^0$ in

the model, *charge inversion*. Since the change of sign in the transition particle-antiparticle of all charges is restored by the change $e \to -e$, it is evident that there should be no change of sign of the potential vector. It should be noted that in the Majorana representation here used β is, so to say, the operator for the transformation $\psi \to \psi^*$, which replaces the transformation $i \to -i$ of the ordinary treatment, replacing thus the transition to the conjugate complex by a linear transformation †.

Let us now consider a transformation which leaves the sign of γ_0 and the γ_k except one (γ_j) unchanged but changes the sign of γ_j and also of p_j. Since an ordinary inversion of x_j includes a change of sign of γ_j it will change the sign of γ_5 and thus of γ_0. To avoid this we include a factor β and have thus the following transformation:

$$\begin{aligned} \chi' &= \gamma_j \gamma_5 \beta \chi \qquad && (j \neq 0), \\ x'_j &= -x_j, && e = e', \\ A'_k &= -A_k && (k \neq j), \\ A'_j &= A_j. \end{aligned} \tag{22}$$

In this transformation a particle-antiparticle transition is included, and, since e is not changed, this implies a change of sign of the electric charges and of all potential components. The exception $A'_j = A_j$ arises from the extra change of sign of this component, due to the inversion of x_j, A_k behaving as the components of an ordinary four-vector when the particle-antiparticle conjugation is not included. According to (13) and (14) every one of the inversions (22) leaves the action integral (10) invariant.

Of the four transformations (22) the first three correspond closely with the considerations of Lee and Yang [1]) and especially of Landau [3]), their product being the PC-transformation. For $j = 4$ the first line of (22) corresponds to the well-known time inversion of Wigner, although there the change of sign of α is replaced by that of i. We see that the similarity between space and time coordinates which was lost in the earlier form of space inversions is restored in the form including the C-transformation in space inversions. From the point of view taken here it would seem more natural to regard the new form as the true space inversion, since it leaves γ_0 invariant. The combination of all four inversions gives

$$\chi' = -\gamma_5 \chi, \tag{23}$$

which is the S.R.-transformation of Schwinger and Pauli [1]).

We may emphasize the similarity between the transformations (16) and (22) still more strongly by replacing the former by

† Professor C. Møller has kindly informed me that he and P. Christensen have recently developed an interesting form of quantum mechanics, where all quantities are real and i is replaced by a matrix which changes sign under inversions.

$$\chi' = \gamma_0\gamma_5\beta\chi \tag{16a}$$

which is equivalent with (16) because $\gamma_0\gamma_5 = -i\alpha$ commutes with what stands between $\bar{\chi}$ and χ in (10) and only produces a phase change (by a factor $-i$) in ψ. Thus the five inversions are similarly related as the components of a five-vector.

3. The Five-dimensional Model and its Modification

In the foregoing section we started from the ordinary representation of quantum-electrodynamics, trying to satisfy certain general requirements concerning inversions taken over from the five-dimensional model. Instead, we shall here begin with the model and try to use the experience gained from the new parity situation for the removal of certain ambiguities in the transition from the model to a more plausible physical theory.

Let us for this purpose consider that part of η_F, the exponent of the Feynman integrand (action integral times i) connected with the spinor field of the five-dimensional model, which may be written

$$\eta_F = \tfrac{1}{2}\int d^5x\bar{\Phi}\gamma^\mu(\partial_\mu - \Gamma_\mu)\Phi. \tag{24}$$

Here γ^μ are five generalized Dirac matrices with real elements, which fulfil the commutation relations

$$\tfrac{1}{2}\{\gamma^\mu, \gamma^\nu\} = \gamma^{\mu\nu}, \tag{25}$$

where $\gamma^{\mu\nu}$ are the contravariant components of the five-dimensional metric tensor and $\partial_\mu = \partial/\partial x^\mu$. The Γ_μ are certain well-known quantities needed in order to make the theory invariant against linear, coordinate-dependent transformations of the eight components of the spinor Φ; they depend on the γ^μ and their first derivatives with respect to the coordinates. Under inversions they behave as the corresponding ∂_μ, which is all we need to know about them in this connection. We have not included any mass term in (24), its presence in a fundamental theory being at least doubtful. In the representation in question Φ may be taken real, an assumption we shall make.

In the transition from the model to a more realistic theory we use an intermediate step, where we assume that the γ^μ and Φ are periodic functions of x^0 with the period $2\pi l_0/e_0$, where $l_0 = \sqrt{2\varkappa}$ ($\varkappa$ = Einstein gravitational constant; $\hbar = c = 1$) is the characteristic length of gravitational quantum field theory ($\approx 10^{-32}$ cm) and e_0 the unrenormalized elementary charge in units $\sqrt{\hbar c}$ †. With this assumption we have the following set of eigenfunctions corresponding to the eigenvalues $0, \pm 1, \pm 2, \ldots$ of $(l_0/e_0)p_0$:

† The assumption $e_0 = 1$ would make the basic equations of the theory particularly simple.

$$u_n(x_0) = \sqrt{\frac{e_0}{2\pi l_0}}\, e^{in\frac{e_0 x_0}{l_0}}, \quad n = 0, \pm 1, \pm 2, \ldots \tag{26}$$

Putting now

$$\Phi(x, x^0) = \sum_n \Phi_n(x) u_n(x^0), \tag{27}$$

where x is short for x^1, x^2, x^3, x^4, η_F will no longer contain x^0 but instead of this a matrix with rows and columns numbered by n, the eigenvalues of $(l_0/e_0)p_0$, the matrix elements being functions of the space-time coordinates and containing, of course, the operators ∂_k, but no longer ∂_0.

Now, a transformation operator representing an infinitesimal coordinate transformation involving x^0, but so as not to upset the periodicity condition, will contain a matrix producing a linear transformation of the $\Phi_n(x)$. The next step is then to put all the Φ_n except the two consecutive ones Φ_0 and Φ_1 equal to zero, whereby only two-row matrices are left in (24) as well as in the formulae expressing the transformation of the $\Phi_n(x)$ in infinitesimal coordinate transformations [2]). This means that we give up the relation between p_0 and ∂_0 and put

$$p_0 = \frac{e_0}{l_0}\begin{pmatrix} 0 & 0 \\ 0 & 1 \end{pmatrix}. \tag{28}$$

To get further we will now return to the model and use the considerations of the foregoing section concerning the inversions, which have so far been left out of consideration. For the sake of simplicity we shall thereby only regard the limiting case where the γ^μ are independent of x^0 and, moreover, neglect gravitation. Then, the γ^1, γ^2, γ^3, γ^4 may be taken equal to the set of ordinary (but eight-row) Dirac matrices, which now we shall call α_1, α_2, α_3, α_4. For γ^0 we have in that case

$$\gamma^0 = \frac{1}{1+\varphi}\alpha_0 - \alpha_k l_0 A_k, \tag{29}$$

where

$$1+\varphi = \sqrt{\gamma_{00}}, \tag{30}$$

φ being a neutral, meson-like field, γ_{00} being normalized to unity at infinity, and where $\alpha_0^2 = 1$, α_0 anticommuting with the four α_k. Thus we have, omitting the Γ_μ,

$$\eta_F = \tfrac{1}{2}\int \mathrm{d}^5 x \bar{\Phi}\left\{\alpha_k(\partial_k - l_0 A_k \partial_0) + \frac{\alpha_0}{\varphi}\partial_0\right\}\Phi. \tag{31}$$

Since there are six independent eight-row Clifford matrices we may complete the set α_0, α_1, α_2, α_3, $i\alpha_4$ by a sixth one, which we denote by $i\alpha_5$ because then we may choose all the α's with real elements. For the comparison of the results of this section with those of the foregoing we shall put

$$\alpha_k = \gamma_k, \quad k = 1, 2, 3, 4,$$
$$\alpha_0 = -\alpha\beta\gamma_5, \quad \alpha_5 = \alpha\gamma_5, \tag{32}$$

which means no new assumption, just a suitable notation.

Coming now to the five inversions which leave (31) invariant, they may be expressed in the following way:

$$\Phi' = R_\mu \Phi,$$
$$R_\mu = \alpha_\mu \alpha_5, \quad \mu = 0, 1, 2, 3, 4, \tag{33}$$

with $\partial'_\mu = -\partial_\mu$, all the A_k changing their sign for $\mu = 0$ but only A_j for $\mu = j$, φ staying invariant under all the transformations.

While in the model the eigenvalues of $-i\partial_0 = p_0$ will be all positive and negative numbers (in the intermediate model e_0/l_0 times all positive and negative whole numbers including zero) we have just seen that according to (28) we have only the two values e_0/l_0 and 0 for p_0 †. On the other hand the theory must, of course, contain both positive and negative charges with the correct symmetry, which means that apart from the expression (28) ∂_0 must also contain a factor which can take both signs. We shall see that the following assumption:

$$\partial_0 \Phi = \varepsilon\alpha\beta p_0 \Phi \tag{34}$$

will conform with the results of the former section. Here ε may be taken as $+1$ in an ordinary space-time frame, but since $\alpha\beta$ changes its sign in any one of the five inversions, while ∂_0 only changes sign in the x_0-inversion we must assume that an odd number of space-time inversions changes the sign of ε, which may thus be regarded as a pseudoscalar ††. We may say that $\varepsilon\alpha\beta$ in (34) replaces the i in the relation $\partial_0 = ip_0$.

Introducing (34) into (31) and performing the transition described from the model to the two-row matrix theory via the intermediate model we get

$$\eta_F = \tfrac{1}{2}\int \mathrm{d}^4x \overline{\Phi}\left\{\gamma_k(\partial_k - \alpha\beta l_0 p_0 A_k) + \frac{\gamma_5}{\varepsilon+\varphi}\, p_0\right\}\Phi. \tag{35}$$

Here we have made a suitable change of notation in that we have absorbed the factor ε in A_k and in φ transforming them thus into a pseudovector and a pseudoscalar respectively.

In order to arrive now at the ordinary representation we perform a unitary transformation

$$\chi = S\Phi, \qquad \chi^+ = \Phi S^+, \qquad SS^+ = 1. \tag{36}$$

† The obvious idea to take care of the two signs of p_0 by a further doubling of the number of spinor components would seem to lead to contradictions with the observed effects of vacuum polarization, as was kindly pointed out to me in a discussion at the Copenhagen Institute for theoretical physics by Drs. A. Bohr, G. Källén and B. Mottelson.

†† We have reason to believe that the theory is also invariant against the simultaneous change of sign of e_0 and γ_0, which will correspond to the C-transformation. See § 4.

With Φ split according to the eigenvalues of α:

$$\Phi = \begin{pmatrix} u \\ v \end{pmatrix}, \tag{37}$$

we put

$$S = \frac{1}{\sqrt{2}} \begin{pmatrix} 1, & i \\ 1, & -i \end{pmatrix}, \tag{38}$$

which gives

$$\chi = \begin{pmatrix} \psi \\ \psi^* \end{pmatrix}, \qquad \psi = u+iv, \qquad \psi^* = u-iv. \tag{39}$$

Since we are not at present studying the two-row matrix theory but just the connection between the new inversion situation and the five-dimensional model we shall replace p_0 in (28) by e_0/l_0 (where we may also let e_0 have the value zero). On account of

$$S\alpha\beta S^+ = -i\alpha \tag{40}$$

we get then

$$\eta_F = \tfrac{1}{2} \int \mathrm{d}^4x \bar{\chi} \left\{ \chi_k(\partial_k + i\alpha e_0 A_k) + \frac{e_0}{l_0} \frac{\gamma_5}{\varepsilon+\varphi} \right\} \chi, \tag{41}$$

or

$$\eta_F = \tfrac{1}{2} \int \mathrm{d}^4x \left\{ \bar{\psi}\gamma_k(\partial_k - e_0 A_k)\psi + \psi\gamma_k{}^{\mathrm{T}}(\partial_k + ie_0 A_k)\bar{\psi} + \frac{e_0}{l_0} \frac{1}{\varepsilon+\varphi} (\bar{\psi}\gamma_5\psi + \psi\gamma_5\bar{\psi}) \right\}. \tag{42}$$

Let us next consider the inversion matrices for χ, which are given by SRS^+. By means of (33) and (38) we get

$$SRS^+ = \gamma_\mu\gamma_5\beta, \quad \mu = 0, 1, 2, 3, 4$$

in conformity with (23) and (16a).

Apart from the last term eqs. (41) or (42) are seen to agree with eqs. (10) and (1) of the preceding section. As to this last term a consideration of the field equation for φ in the model theory shows that this quantity will be very small compared to unity as long as the relevant dimensions are large compared to l_0. In this approximation (42) leads to a pseudoscalar interaction between ψ and φ with a coupling constant of the order of magnitude $e_0\sqrt{\hbar c}$. With $e_0 \approx 1$ this agrees with what is known about the nucleon-π-meson coupling, although we have here only considered the simplified situation of a neutral field, which is a scalar in the isobaric spin space. That this field has no direct physical meaning appears from the fact that it may be removed by means of a unitary transformation when the pseudovector coupling between ψ and φ arising from the Γ_μ, neglected here, is taken into account. We shall expect, however, that the theory sketched above, where

the x_0-dependence of the full model field quantities is replaced by a two-row matrix representation and a doubling of the number of ψ-components, corresponding to charged and neutral particles, will exhibit a still closer and physically significant relationship to the nucleon-π-meson theory. Although the theory in question is not fully formulated as yet and we are still far from being able to see through its physical consequences the results obtained would seem to justify the cautious use of the five- dimensional model in the development of a more realistic physical theory.

4. Concluding Remarks

So far we have mainly considered only electromagnetic interactions where the old inversion theorems are just as valid as the new ones. The background for our considerations is, however, a kind of ideal theory resembling the five-dimensional model with its extended transformation group. Unfortunately this ideal theory is far from being known, although some of its features may be reasonably guessed at by means of the model theory. One such feature is the group of inversions. Thus we have seen that the space-time inversions in this theory take a form corresponding to the combination PC together with the Wigner time inversion T. On the other hand the fifth inversion is analogous to the particle-antiparticle conjugation C, which in combination with PC gives the ordinary space-reflection P. But just at this point already the assumption (28) implies a difference between the model and the theory, which would seem to agree well with the fact that C is no rigorous symmetry of the theory.

On the other hand we shall expect from the foregoing that charge conjugation C coupled to a change of sign of the constant e_0 leaves the theory invariant. Since, however, we do not know where in the complete theory e_0 appears this does not at present help us to make predictions for β-interactions, etc.

Another feature of the model which is probably maintained in the real theory is that the action integral is only bilinear in ψ and $\bar{\psi}$. Thus β-interactions (just as ordinary Coulomb and nuclear forces), where semi-empirical expressions containing four ψ-operators appear in the usual treatment, should from this point of view be expected to represent, so to say, the next approximation after that of non-interacting but renormalized particles,which is in line with the original Yukawa program for the explanation of nuclear forces and β-interactions. We should, therefore, expect that the expressions for β-interactions — although they cannot at present be derived from a basic theory — satisfy the requirement of invariance under the new rather than under the old inversion in agreement with the considerations of Lee and Yang and of Landau. In the actual choice of possible β-interactions

the outcome of this claim of invariance will probably amount to making use of the circumstance that γ_0 in contrast to γ_5 is invariant under the transformations in question.

One further consequence of the above considerations should be pointed out here, namely that the fact that α commutes with the Dirac matrices γ_k and also with γ_0 will make $\int d^3x \chi^+ \alpha \chi$ a good quantum number for the stationary states of the system. This quantum number is in the electrodynamic case equal to the number of particles minus that of antiparticles. Its being a good quantum number in the general case of the five-dimensional model may have something to do with the much discussed conservation laws for baryons and leptons also in weak interactions. We have, however, no theoretical background as yet for the fact that there are these two classes of fermions.

In the preparation of this paper I was very much furthered by numerous discussions with various members and visitors of the Copenhagen Institute for theoretical physics, where, thanks to an invitation from the Theoretical Study Group of CERN, I spent a couple of months in the early part of this year. I wish to express my gratitude to all those who made this stay valuable and agreeable, mentioning in particular Professors C. Møller and W. Pauli. My best thanks are also due to Dr. S. Deser and Professor M. A. Melvin, who took the trouble to read carefully the manuscript, suggesting a number of improvements.

References

1) T. Lee and C. Yang, Phys. Rev. **104** (1956) 254; **105** (1957) 1671
2) O. Klein, Helv. Phys. Acta, Suppl. **4** (1956) 58; see also C. V. Jonsson, Arkiv f. Fysik **3** (1951) 87
3) See V. Bargmann, Berliner Ber. (1932) 347
4) L. Landau, Nuclear Physics **3** (1957) 127; see also A. Salam, Nuovo Cimento **5** (1957) 299
5) See W. Pauli, Niels Bohr and the development of physics (London, 1955) p. 30

Nuclear Physics **5** (1958) 687—689; © *North-Holland Publishing Co., Amsterdam*
Not to be reproduced by photoprint or microfilm without written permission from the publisher

ON THE INTER-RELATION OF SCALAR AND PSEUDOSCALAR THEORIES

ABDUS SALAM
Imperial College of Science and Technology, London

Received 28 June 1957

In this note a general method for transcribing results for charged scalar(s) meson theory into those for pseudoscalar (ps) theory is described. Write the scalar Lagrangian as

$$\mathscr{L} = \mathscr{L}_f(\psi_1)+\mathscr{L}_f(\psi_2)+\mathscr{L}_f(\phi)+\mathscr{L}_{\text{int}} \tag{1}$$

where ψ_1, ψ_2 are the proton and neutron fields, and

$$\mathscr{L}_f(\psi_1) = -\bar{\psi}_1(\gamma\partial+M_1)\psi_1 \tag{2}$$

$$\mathscr{L}_f(\psi_2) = -\bar{\psi}_2(\gamma\partial+M_2)\psi_2 \tag{3}$$

$$\mathscr{L}_f(\phi) = -[(\partial_\mu\phi^*)(\partial_\mu\phi)+m^2\phi^*\phi] \tag{4}$$

$$\mathscr{L}_{\text{int}} = g(\bar{\psi}_1\psi_2\phi+\bar{\psi}_2\psi_1\phi^*). \tag{5}$$

The ps-Lagrangian is obtained from (1) by the substitutions

$$\psi_2 \to i\gamma_5\psi_2, \tag{6}$$

$$M_2 \to -M_2. \tag{7}$$

These substitutions leave the canonical commutation relations unchanged.

To illustrate the results that may be obtained, consider the calculation of self-mass and self-charge. For the scalar case, the self-mass terms are

$$\bar{\psi}_1\psi_1[M_1 f_1(M_1^2, M_2^2)+M_2 f_2(M_1^2, M_2^2)] + \bar{\psi}_2\psi_2[M_2 f_1(M_2^2, M_1^2)+M_1 f_2(M_2^2, M_1^2)]. \tag{8}$$

From dimensions the functions $f(M_1^2, M_2^2)$ have the form $f(M_1^2/M_2^2, m^2/M_1^2)$. For the ps-case the corresponding terms will be

$$\bar{\psi}_1\psi_1[M_1 f_1(M_1^2, M_2^2)-M_2 f_2(M_1^2, M_2^2)] + \bar{\psi}_2\psi_2[M_2 f_1(M_2^2, M_1^2)-M_1 f_2(M_2^2, M_1^2)]. \tag{9}$$

For the self-charge

$$\begin{aligned} \delta g_s &= \frac{M_1}{M_2} F_1(M_1^2/M_2^2, m^2/M_1^2)+\frac{M_2}{M_1} F_2+F_3, \\ \delta g_{ps} &= -\frac{M_1}{M_2} F_1-\frac{M_2}{M_1} F_2+F_3. \end{aligned} \tag{10}$$

Similar results can be obtained for all renormalization constants.

The method can be extended to interrelate general expressions for all Green's functions. As an example consider the one-particle Green's function

$$\langle \mathrm{T}\psi_1^{\mathrm{s}}(x)\bar{\psi}_1^{\mathrm{s}}(x')\rangle_0 = i\int_{-\infty}^{\infty}\int_0^{\infty} \frac{[i\gamma k\varrho_1(K^2)+K\varrho_2(K^2)]\mathrm{d}K^2\, \mathrm{e}^{ik(x-x')}\,\mathrm{d}^4k}{k^2+K^2-i\varepsilon} \tag{11}$$

where

$$K = +\sqrt{K^2}, \quad \varrho = \varrho\left(\frac{K^2}{M_1^2}, \frac{K^2}{M_1M_2}, \frac{m^2}{M_1^2}\right).$$

The same expression holds for $\langle \mathrm{T}\ \psi_1^{\mathrm{ps}}\bar{\psi}_1^{\mathrm{ps}}\rangle_0$ with M_2 changed to $-M_2$, while

$$i\gamma_5\langle \mathrm{T}\ \psi_2^{\mathrm{ps}}(x)\bar{\psi}_2^{\mathrm{ps}}(x')\rangle_0 i\gamma_5 = i\int_{-\infty}^{\infty}\int_0^{\infty} \frac{[i\gamma k\varrho'_1(K'^2)+K'\varrho_2'(K'^2)]\mathrm{d}K'^2\, \mathrm{e}^{ik(x-x')}\,\mathrm{d}^4k}{k^2+K'^2-i\varepsilon} \tag{12}$$

where

$$K' = -\sqrt{K'^2}, \quad \varrho' = \varrho\left(\frac{K^2}{M_2^2}, \frac{-K^2}{M_1M_2}, \frac{m^2}{M_2^2}\right).$$

Note here the reversal of sign for the parameter K'. This is because K' like M_2 is eigenvalue of the mass-operator $\mathscr{M}$, defined by $\mathscr{M} = -i\gamma P$. From (12)

$$\langle \mathrm{T}\ \psi_2^{\mathrm{ps}}\bar{\psi}_2^{\mathrm{ps}}\rangle_0 = i\int_{-\infty}^{\infty}\int_0^{\infty} \frac{i\gamma k\varrho_1'(K^2)+K\varrho_2'(K^2)}{k^2+K^2-i\varepsilon}\, \mathrm{e}^{ik(x-x')}\,\mathrm{d}K^2\mathrm{d}^4k. \tag{13}$$

This is the same expression as for $\langle \mathrm{T}\ \psi_1^{\mathrm{ps}}\bar{\psi}_1^{\mathrm{ps}}\rangle_0$ except that M_1 and M_2 are interchanged.

It does not seem possible to extend the method to the purely neutral meson case, although fully charge-symmetric scalar and pseudoscalar theories can be correlated in the following manner. The results of the usual scalar theory can be obtained by starting with the Lagrangian

$$\mathscr{L}_f(\mathrm{N}_1)+\mathscr{L}_f(\mathrm{N}_2)+\mathscr{L}(\phi)+g(\bar{\mathrm{N}}_1\tau\cdot\phi\mathrm{N}_2+\bar{\mathrm{N}}_2\tau\cdot\phi\mathrm{N}_1) \tag{14}$$

where $\mathrm{N}_1 = \binom{\mathrm{p}_1}{\mathrm{n}_1}$, $\mathrm{N}_2 = \binom{\mathrm{p}_2}{\mathrm{n}_2}$ are two distinct iso-spinor fields with masses M_1 for p_1 and n_1 particles and M_2 for p_2 and n_2 particles, while at the end of the calculation one takes the limit $M_1 \to M_2$. Before the limit is taken, the substitutions $\mathrm{N}_2 \to i\gamma_5\mathrm{N}_2$, $M_2 \to -M_2$ in (14) give the ps-Lagrangian. It must be remembered that for the s-theory any general Green's function, for example $\langle \mathrm{T}\bar{\mathrm{N}}(1)\mathrm{N}(2)\bar{\mathrm{N}}(3)\mathrm{N}(4)\ldots\rangle_0$, equals $\lim_{\mathrm{N}_1\to\mathrm{N}_2}$ of the average of

$$\langle \mathrm{T}\,\bar{\mathrm{N}}_1(1)\mathrm{N}_1(2)\bar{\mathrm{N}}_1(3)\mathrm{N}_1(4)\ldots\rangle_0$$
$$+\langle \mathrm{T}\,\bar{\mathrm{N}}_2(1)\mathrm{N}_1(2)\bar{\mathrm{N}}_2(3)\mathrm{N}_1(4)\cdots\rangle_0+\langle \mathrm{T}\,\bar{\mathrm{N}}_1(1)\mathrm{N}_1(2)\bar{\mathrm{N}}_2(3)\mathrm{N}_2(4)\cdots\rangle_0+\cdots$$

From symmetry

$$\langle T\bar{N}_1(1)N_1(2)\bar{N}_1(3)N_1(4)\cdots\rangle_0 = \langle T\bar{N}_2(1)N_2(2)\bar{N}_2(3)N_2(4)\cdots\rangle_0$$

etc. apart from the interchange of M_1 and M_2. While making the correlation with ps-theory, all N_2 are changed to $i\gamma_5 N_2$ in the manner of eq. (12).

The reason why this method does not work for the purely neutral case is connected with the fact that the trick of introducing two distinct Fermi fields and making these identical at the end of the calculation does not reproduce the conventional neutral scalar theory. The simplest way to see this is to consider the perturbation expansion. All graphs of the neutral theory are reproduced except vacuum polarization graphs with odd number of external meson lines. In a fully charge-symmetric theory these graphs give identically vanishing contributions and there is no difficulty.

I am indebted to Dr. J. C. Taylor for a discussion.

Nuclear Physics **4** (1957) 690—692; © *North-Holland Publishing Co., Amsterdam*
Not to be reproduced by photoprint or microfilm without written permission from the publisher

PARITY VIOLATION IN β-DECAY: CORRELATION OF THE ELECTRON DIRECTION WITH THE POLARISATION OF A SUBSEQUENTLY EMITTED NEUTRON

G. A. JONES and F. MANDL
Atomic Energy Research Establishment, Harwell, Berks.

Received 9 September 1957

Abstract: Parity violation will produce observable effects in the case of delayed neutron emission; the delayed neutron will in general be polarised along the direction of the preceding electron, the degree of polarisation being dependent on the direction of emission of the neutron relative to the electron. In the case considered the polarisation is a maximum for neutrons emitted in a direction perpendicular to that of the electrons and is perpendicular to the direction of motion of the neutron, this being the most convenient for detection. In contrast, emission of γ-radiation following β-decay results only in circular polarisation.

Some details are given concerning a projected experiment to measure the polarisation correlation in the decay of N^{17}.

1. Introduction

Parity violation in β-decay will produce observable effects in the following nuclear decay scheme. A nucleus A (spin, J_1, parity π_1) decays through a β-interaction to a nucleus B (spin J, parity π), which emits a neutron going to a state C (spin J_f, parity π_f). The correlation between the direction of the emitted β-particle and the spin of the neutron depends on the parity violation in the β-decay. In particular, there would be no correlation for an allowed transition if parity were conserved in β-decay; if parity is not conserved there will be a correlation even for allowed transitions, the correlation depending on the degree of the parity violation in the β-interaction.

In order to obtain any *quantitative* information from the above correlation experiment, the decay scheme $A \rightarrow B \rightarrow C$ must be fully known, that is, the spins and parities of these nuclei must be known. In addition, one requires the allowed β-decay $A \rightarrow B$ to be due to only one type of interaction. If several interactions are involved, one can in general not say what the degree of parity violation is for the different interactions. Thus the most convenient decay scheme involves an allowed β-decay with unit spin change ($\pi_1 = \pi$, $|J_1 - J| = 1$.) Lastly, we require that only one level is involved for the intermediate nucleus B or if several levels are involved that they have the same spin and parity assignments. If they have different

assignments we obtain a correlation function which depends on parameters describing the probabilities for the decay to occur via the different intermediate levels. These parameters are not generally known and so we would obtain an indefinite result only.

The nucleus which most nearly meets these reguirements is N^{17}. On the basis of the shell model one expects its spin and parity to be $j_1 = \frac{1}{2}, \pi_1 = -1$. It goes by β-decay to O^{17}, the log ft value being 3.8. This strongly suggests that this is an allowed transition, so that the O^{17} level must have the assignments $\pi = -1$ and $J = \frac{3}{2}$ or $J = \frac{1}{2}$. Unfortunately O^{17} possesses several negative parity levels in the energy region of interest. (For details cf. Ajzenberg and Lauritsen [1].) From the energy spectrum of the neutrons [2] in the above reaction, and the excitation function [3] for the reaction $O^{16}(nn)O^{16}$, it appears that the two $\frac{3}{2}$—levels mainly contribute, the $\frac{1}{2}$— level having the rather high energy of 1.91 MeV, compared with the observed neutron spectrum. This has a maximum at 0.92 ± 0.07 MeV and a half width < 0.5 MeV. As stated above, the question of whether the $\frac{1}{2}$— levels contribute appreciably is very important for the interpretation of the correlation experiment. Incidentally, it might be pointed out that in this case even if the transition $\frac{1}{2}- \to \frac{1}{2}-$ occurs, this could not be by the scalar interaction, since the transition almost certainly involves a change of the isobaric spin. For N^{17}, $T \geqq \frac{3}{2}$, whereas the $\frac{1}{2}-$ level of O^{17} which we consider is almost certainly $T = \frac{1}{2}$, the $T = \frac{3}{2}$ levels corresponding to much higher energies (we are indebted to Dr. J. P. Elliott for this argument).

In the following we shall make the simplifying assumption that the N^{17} goes to O^{17} by an allowed β-transition involving the tensor interaction only. The O^{17} will be assumed to be one pure $\frac{3}{2}-$ level (or several such levels, this does not affect the argument). The O^{17} decays to the ground state of $O^{16}(J_f = 0, \pi_f = +1)$ emitting a $p_{3/2}$ neutron.

2. Electron-Neutron Correlation

One of us (F. Mandl — unpublished note) has derived, using the two component theory, the general expression for the polarisation in the z-direction $\langle \sigma_z \rangle_\theta$ of a neutron emitted in the direction θ following emission of an electron along the z-axis. In the particular case of

$$N^{17}(\tfrac{1}{2}-) \to O^{17}(\tfrac{3}{2}-) \to O^{16}(0+)$$

we have

$$\langle \sigma_z \rangle_\theta = -\beta \cdot \frac{2C_T C'_T}{|C_T|^2 + |C'_T|^2} \cdot \frac{2 - \cos^2\theta}{3}$$

where $\beta = v/c$ for the electron and C_T, C'_T are the strengths of the parity-conserving and parity-violating parts of the tensor interaction.

The maximum asymmetry occurs when $\theta = \pi/2$:

$$\langle \sigma_z \rangle_{\pi/2} = -\frac{2\beta}{3} \cdot \frac{2C_T C'_T}{|C_T + |C_T|^2} .$$

Since $C_T \approx -C_T$ from many recent experiments, of which we quote only the first [4]), the neutrons should show considerable polarisation.

3. Projected Experiment

N^{17} can be produced most conveniently by the reactions $N^{15}(tp)N^{17}$ and $O^{18}(\gamma p)N^{17}$, the former probably requiring tritons of energy 3 MeV or more, the latter a bremsstrahlung spectrum from an electron source of 25—30 MeV. Analysis of the neutron polarisation is possible by scattering through 45° or 135° from carbon †; by utilising carbon in an organic phosphor (quaterphenyl is highly suitable having a very high carbon content, a fast decay and a quantum efficiency not much worse than anthracene) and detecting neutrons scattered through 135° it is hoped to detect carbon recoils in the scatterer and thus employ a triple coincidence technique (β-carbon recoil-scattered neutron)††. This allows of high discrimination against random events, and by removing the need of interposing collimating absorbers between the different detectors, a compact geometry and therefore a high efficiency.

Since the maximum energy of the β-ray spectrum is high (3.7 MeV) it is possible to detect over the greater part of the spectrum with a sensibly constant value of v/c — approximately unity. This makes electron detection extremely simple.

It is hoped to perform this experiment using the A.E.R.E. electron linear accelerator which is scheduled to work in the near future. Equipment to pump the active nitrogen away from the target will therefore be needed. An experiment based on the triton reaction would not require this and would probably be cleaner.

The substance of this note was read at the recent Harwell Conference on Parity Violation, May, 1957, for which no published proceedings are available.

† Neutron scattering from carbon has been performed for neutrons of energy 2.4 to 3.7 MeV by Meier, Scherrer and Trumpy [5]). They obtained almost complete polarisation at 45° at these energies and predict a reduced, but still high degree of polarisation at lower energies e.g. about 2/3 at 1 MeV.

†† Scattering through 135° rather than 45° gives bigger recoil pulses and also ensures that the neutrons cannot be produced by single scattering from the hydrogen in the phosphor. The size of the phosphor is chosen to make a double scattering event unlikely, this being necessary for any method of analysis by scattering.

References

1) F. Ajzenberg and T. Lauritsen, Rev. Mod. Phys. **27** (1955) 77
2) L. W. Alvarez, Phys. Rev. **75** (1949) 1127
3) Bockelman, Miller, Adair and Barschall, Phys. Rev. **84** (1951) 69
4) Wu, Ambler, Hayward, Hoppes and Hudson, Phys. Rev. **105** (1957) 1413
5) Meier, Scherrer and Trumpy, Helv. Phys. Acta **27** (1954) 577

Nuclear Physics **4** (1957) 693; © *North-Holland Publishing Co., Amsterdam*
Not to be reproduced by photoprint or microfilm without written permission from the publisher

POLARIZATION OF μ-MESONS AND ELECTRONS IN K-MESON DECAYS: A CORRECTION

J. WERLE

Institute for Nuclear Research, Warsaw

Received 28 September 1957

The paper with the above title [1]) contains two oversights, which have kindly been pointed out by Dr. J. J. Sakurai and independently by Dr. S. MacDonell.

The use in ref. [1]) of the operator $\frac{1}{2}(1-\gamma_5)$ with respect to an antineutrino is not consistent with the now usual convention of the two-component theory of the neutrino field, which implies that $\frac{1}{2}(1+\gamma_5)$ should be used. The calculations presented in ref. [1]) apply, therefore, to the case when a neutrino, *not* an antineutrino, is emitted with a negative μ-meson or electron. For the case of an antineutrino emission one should just reverse the signs of all those terms in the general expression (20) which are odd in p. Consequently all the polarization curves will have opposite signs if an antineutrino is emitted with a negative μ-meson or electron.

The condition of CI invariance does not imply the relative reality of c_S, c_V, c'_V, c_T, but that of c_S, ic_V, ic'_V, c_T. Therefore, the interference terms which in the expression (20) are proportional to the mass μ do not necessarily vanish in a theory which is invariant under CI transformation. Therefore, in the expression (23) for the longitudinal polarization four additional interference terms appear:

$$a_7 = i(c_S c_V^* - c_S^* c_V), \quad a_8 = i(c_T c_V^* - c_T^* c_V),$$
$$a_9 = i(c_S c_V'^* - c_S^* c'_V), \quad a_{10} = i(c_T c_V'^* - c_T^* c'_V).$$

The corresponding L_i's are as follows:

$$L_7 = -2\mu(W'-E), \quad L_8 = -2\mu(W'-E)\left\{\frac{p}{M} - \frac{W-E}{2(W'-E)}\left(1+\frac{\frac{1}{3}p-E}{M}\right)\right\},$$

$$L_9 = -\mu(M-E+p), \quad L_{10} = -\mu(M-E+p)\left\{\frac{p}{M} - \frac{W-E}{2(W'-E)}\left(1+\frac{\frac{1}{3}p-E}{M}\right)\right\},$$

with the same meaning of the symbols as in ref. [1]).

Reference

1) J. Werle, Nuclear Physics **4** (1957) 171

Editor's Note: In the note (received on 31 August 1957) in which he points out the necessity of the above corrections, Dr. J. J. Sakurai, of Cornell University, Ithaca, N.Y., further observes that the opposite longitudinal polarizations for μ^+ and μ^- follow from the requirement of TCI invariance, whether or not the requirement of CI invariance is satisfied. Dr. Werle, on the other hand, stresses the fact that CI invariance is a sufficient condition for the property in question. The two authors appear to disagree as to which of these invariance requirements is "stronger".

Nuclear Physics **4** (1957) 694—695; © *North-Holland Publishing Co., Amsterdam*

NEWS ITEMS

INTERNATIONAL CONFERENCE ON NUCLEAR STRUCTURE

(Rehovoth, 8-14 September 1957)

This conference, held at the Weizmann Institute of Science at Rehovoth (Israel) under the joint sponsorship of Unesco, the IUPAP, the Israel Atomic Energy Commission and the Weizmann Institute of Science, will rank among the very best in the long list of similar gatherings which are helping nuclear physicists to keep abreast of the rapid growth of their studies. This function was admirably fulfilled by the Rehovoth conference, thanks to a well thought-out program and a perfect organization. By placing the emphasis on extensive reports of a synthetic character, and firmly banning the chaotic succession of 'short communications' which so often taxes the endurance of the audience without bringing it any enlightenment, the Israeli organizers, headed by Prof. A. de Shalit, have set an example for the future. If, as one must hope, the volume containing the proceedings of the conference is published quickly, they will make it hard indeed for the planners of the next conferences to do better.

In the course of four strenuous all-day sessions, the following problems were discussed:

(1) Theories of nuclear structure: the foundations of the shell model on the lines of Brueckner's ideas were reviewed by R. J. Eden, those of the collective model by B. R. Mottelson and R. E. Peierls, and the theory of fission and neutron excitation by L. Wilets.

The Brueckner treatment has hitherto been fully developed only for indefinite nuclear matter: to apply it to a finite nucleus remains a difficult task for the future. The effective interaction between nucleons according to Brueckner's definition is represented, not by a potential, but by an operator of non-local character (the 'non-locality' extending over about 10^{-13} cm): much remains to be done to clarify the relation of this operator to the effective potentials with which the more phenomenological approach of the shell-model operates with such striking success.

The discussion of the collective model was mainly concerned with the problem of accounting for the empirical fact that the collective motions giving rise to a spectrum of excited states with rotational structure are only weakly coupled to the residual motions of the individual nucleons. The peculiar difficulties of the problem were very clearly analysed by Dr. Lipkin, and it was apparent that neither the method outlined by Prof. Peierls, nor the perhaps more promising approach too briefly mentioned by Dr. Mottelson have as yet given us a complete solution.

(2) The nuclear phenomena depending on electromagnetic couplings offer a more satisfactory picture, which was ably sketched by D. Wilkinson and A. de Shalit (radiative transitions), I. Bergström (systematics of energy levels and multipole transitions), M. Rose (effects of finite size), A. H. Wapstra (internal conversion) and P. F. Zweiffel (branching ratios of negaton capture and positon emission).

(3) Parity non-conservation and beta-decay. A most useful and exhaustive survey of the present state of theory and experiment regarding this fashionable topic was provided by a succession of excellent reports, some of them carefully prepared according to plan, by E. J. Konopinski, T. D. Lee, C. S. Wu, L. M. Langer, others brilliantly improvised at the chairman's request by H. Frauenfelder, M. Deutsch and K. Alder.

The most conspicuous weakness of the present situation is the insufficiency of the experimental evidence concerning electron-neutrino correlation; the existing data are even partly contradictory. It is one of the most urgent tasks in this domain to repeat and extend these very difficult experiments, which are of decisive importance for the determination of essential features of the interactions responsible for the processes of β-decay type.

(4) The final session covered various aspects of angular correlation (A. Abragam, H. Frauenfelder, R. M. Steffen) and other experimental methods and instruments (T. R. Gerholm, J. W. M. DuMond), in particular the measurement of very short life-times (S. Devons, F. R. Metzger, S. G. Cohen).

The highest authorities of the State of Israel showed their interest in the conference in the

most graceful and cordial manner: there was a reception by the President of the State at Jerusalem and both the Prime Minister and the Minister of Foreign Affairs attended the inaugural dinner. Extensive and remarkably well-planned tours gave the participants an opportunity of watching, against the background of the alluring sites of ancient history, some of the impressive achievements of the young state of Israel, not least the splendid institutions devoted to science and technology at Jerusalem, Rehovoth and Haifa.

L. R.

ELECTRON MICROSCOPE SOCIETY OF AMERICA

The 1958 Annual Meeting of the Electron Microscope Society of America is to be held on September 4, 5 and 6 in Los Angeles, California. The headquarters for the meeting will be at the Miramar Hotel and the local chairman will be Henry Froula. The program chairman will be Dr. C. M. Schwartz, Battelle Memorial Institute, Columbus, Ohio.

ERRATA

A. H. Wapstra and W. van der Eyck, The decay ^{109}Cd, ^{109}Ag and ^{109}Pd (Nuclear Physics **4** (1957) 325).

The value $x = 33.8 \pm 0.7$ given on page 326 should be $x = 23.8 \pm 0.7$. The authors thank Dr. M. K. Ramaswami for attracting their attention to this printing error.

NOTE ON THE (γ, d) REACTIONS: AN ADDENDUM

J. SAWICKI and W. CZYŻ

Institute of Nuclear Research, Warsaw

Received 30 October 1957

In the note by the authors with this title [1]) the large observed ratios of (γ, d) to (γ, p) cross sections are explained in terms of a two-stage mechanism of the (γ, d) process. The primary photonucleon is assumed to pick-up another nucleon with the right charge and momentum to form an outgoing deuteron. The numerical result for the S^{32} (γ, d) P^{30} reaction near its threshold, at $\hbar\omega = 25$ MeV, was $\sigma(\gamma, \mathrm{d})/\sigma(\gamma, \mathrm{p}) \approx 0.9$. This value seems to be considerably too high (compare e.g. ref. [2])). It was not observed in ref. [1]) that this discrepancy should be mostly due to the fact that the pick-up process matrix elements of ref. [1]) involve integrations over all space. In fact, the mean free path of a deuteron preformed within the nucleus should not be large: most of the deuterons formed in the inner part of the core should dissolve before reaching the nuclear surface. Mathematically, this could be approximated by cutting off the radial integrals of eq. (15)—(16) of ref. [1]) at the lower limit at a certain radius r_0 of the order of the nuclear radius. The limiting case would be to set r_0 exactly equal to the nuclear radius R_0 (Butler approximation). The pick-up process would then be a pure surface mechanism. In other words $V_{np}(r)$ is assumed to be zero within the nucleus (Butler) and eq. (9) of ref. [1]) should be replaced by

$$(\Delta + K^2 - \frac{4M}{\hbar^2} V_{\mathrm{eff}}) D(\mathbf{R}) = \begin{cases} -16\pi \sqrt{\frac{\alpha}{2\pi}} f(\mathbf{R}) w(\mathbf{R}) & \text{for} \quad R \geq R_0 \\ 0 & \text{for} \quad R < R_0. \end{cases} \tag{9'}$$

In this limiting case we obtain $\sigma(\gamma, \mathrm{d})/\sigma(\gamma, \mathrm{p}) \approx 0.1$ for the example considered above. This latter value seems to be realistic.

It is also easier to understand in terms of this surface pick-up mechanism why $\sigma(\gamma, \mathrm{d})$'s are usually smaller than the related $\sigma(\gamma, \mathrm{np})$'s. For instance, for S^{32} at the maximum bremsstrahlung energy 28 MeV, one finds $\sigma(\gamma, \mathrm{d}) = 2.8$ mb while $\sigma(\gamma, \mathrm{np}) = 6$ mb.

References

1) J. Sawicki and W. Czyż, Nuclear Physics **4** (1957) 248
2) B. Forkman, Arkiv f. Fysik **11** (1956) 265

Nuclear Physics **4** (1957) 696; © *North-Holland Publishing Co., Amsterdam*

BOOK REVIEWS

H. C. SCHWENK and R. H. SHANNON, *Nuclear Power Engineering* (McGraw-Hill Book Co., New York-Toronto-London 1957. xvi-319 pages. $ 6.50)

The growth of a new technology calls forth comparisons with similar phenomena in the past. In a recent address, published in *Atom* (No. 6, April 1957), Sir Christopher Hinton has drawn a fascinating parallel between the first steps in the building of industrial reactors and the beginnings of steam engine construction. The book under review has some features curiously reminiscent of the early literature on steam engines: a purely descriptive exposition, avoiding all but the simplest algebraic formulae, an abundance of drawings and diagrams, and above all the 'glossary' at the end, in which the technical jargon is made plain to the unspoilt reader and even the Greek letters in common use are listed with their standard meanings. A sign of the times is perhaps that, in contrast to what happened 120 years ago, it has not been deemed necessary to explain the meaning of the arithmetical symbols of operations. Every other need of the untrained reader seems to have been taken into consideration in the careful preparation of this neatly produced booklet. Each chapter is followed by a list of selected references to more elaborate treatises and a choice of 'review topics' in the form of questions and exercises which may help the reader to test his grasp of the subject. His imagination will receive powerful support from the graphic representations of nuclear structures and what happens to them, especially from the daring vista of an array of uranium nuclei with neutrons flying about them like so many comets, which adorns the book as a frontispiece.

L. R.

C. F. BONILLA (Editor), *Nuclear Engineering* (Mc.Graw-Hill Book Co., New York-Toronto-London 1957. vi-850 pages. $ 12.50)

The enterprising publishers of the primer of nuclear engineering reviewed above are eager to meet the requirements of all classes of readers. At the other end of the scale, they present a bulky collective work, designed not only as a reference volume, but also as an advanced text for engineering students. It will suffice to say that it is a production in the best American style, aiming at accuracy and practical usefulness in the selection and presentation of the material, and that it will admirably serve its twofold purpose.

L. R.

C. FLAMMER, *Spheroidal wave functions* (Stanford University Press, Stanford 1957. ix-86 pages text, 133 pages tables. (68 s.)

This is an excellent monograph, beautifully printed by an English firm, of a family of functions which have already proved useful in numerous problems of mathematical physics, and may still find further application in the study of nuclear deformations.

L. R.

AUTHOR INDEX

ALAGA, G., Selection rules for beta and gamma particle transitions in strongly deformed nuclei 625
ALPHONCE, R., A. JOHANSSON and G. TIBELL, The asymmetry of 155 MeV protons elastically scattered from iron, nickel and copper . 643
ALPHONCE, R., A. JOHANSSON and G. TIBELL, The asymmetry of 155 MeV protons elastically and inelastically scattered from carbon, oxygen and calcium 672
ANDERSEN, S. L., T. HOLTEBEKK, O. LÖNSJÖ and R. TANGEN, Two closely spaced resonances in the reaction Al^{27} (p, γ) Si^{28} . . . 39
ARMBRUSTER, R. *see* Gorodetzky
BAUER, M. and M. MOSHINSKY, Repulsive core and nuclear shell theory 615
BAYUKOV, YU. D., M. S. KOZODAYEV, YU. D. PROKOSHKIN and A. A. TYAPKIN, Production of neutral π-mesons by high energy protons 61
BELL, J. S., Nuclear magnetic moments and the many body problem 295
BHATTACHERJEE, S. K. and SHREE RAMAN, Studies on the long-lived activities of europium. 44
BJØRNHOLM, S., O. NATHAN, O. B. NIELSEN and R. K. SHELINE, Low lying levels in Th^{228} 313
BLOCH, C., Une formulation unifiée de la théorie des réactions nucléaires 503
BLOKHINTSEV, L. D., *see* Shapiro
BOHR, A. and B. R. MOTTELSON, Electric dipole moment associated with octupole vibrations of a spheroidal nucleus. 529
BRENIG, W., Zweiteilchennäherungen des Mehrkörperproblems I. . 363
BRINK, D. M., Individual particle and collective aspects of the nuclear photoeffect. 215
CHERNAVSKY, D. S., *see* Ivanovskaya
CROISSIAUX, M., *see* Gorodetzky
CZYŻ, W., *see* J. Sawicki
DE-SHALIT, A., *see* Thieberger
DOLINSKY, E. I., *see* Shapiro
EBEL, M. E. and G. FELDMAN, Further remarks on Coulomb corrections in allowed beta transitions 213
ERGAKOV, V. A., *see* Vishnevsky
ESTULIN, I. V., L. F. KALINKIN and A. S. MELIORANSKY, Soft γ-rays from the capture of thermal neutrons by nuclei. 91
EIJK, W. VAN DER, *see* Wapstra
FELDMAN, G., *see* Ebel

FREEMAN, JOAN M. and R. C. HANNA, Excited states of N^{16} . . 599
GALLMANN, A., *see* Gorodetzky
GAPONOV, YU. V. and V. S. POPOV, β-γ-correlation for allowed transitions involving non-conservation of parity 453
GOMBÁS, P., P. SZÉPFALUSY und E. MÁGORI, Zur Reichweite der Kernkräfte 488
GORODETZKY, S., A. GALLMANN, M. CROISSIAUX et R. ARMBRUSTER, Distribution angulaire du rayonnement gamma de 8.34 MeV de la réaction $^{14}N(p, \gamma)^{15}O$ 112
GREEN, H. S. and C. A. HURST, Parity mixtures and decay processes 589
GRIGORIEV, V. K., *see* Vishnevsky
HANNA, R. C., *see* Freeman
HEISENBERG, W., Lee model and quantisation of non linear field equations 532
HIGGS, P. W., On four-dimensional isobaric spin formalisms . . . 221
HILLMAN, P., A. JOHANSSON and H. TYRÉN, Polarization of high energy protons in elastic and inelastic scattering 648
HOLTEBEKK, T., *see* Andersen
HOSSAIN, A. and SYEDUZZAMAN, Optical model analysis of proton scattering on some light nuclei 88
HOURIET, A., Méthode des champs adhérents (see also Erratum p. 635) 408
HULTBERG, S. and T. NOVAKOV, The longitudinal angular dependence of the photoelectric effect and its influence on the determination of gamma ray intensities 120
HURST, C. A., *see* Green
IVANOVSKAYA, I. A. and D. S. CHERNAVSKY, Interpretation of cosmic ray jets observed in photographic emulsions 29
JACKSON, J. D., S. B. TREIMAN and H. W. WYLD JR., Coulomb corrections in allowed beta transitions. 206
JOHANSSON, A., *see* Alphonce
JOHANSSON, A., *see* Hillman
JONES, G. A. and E. MANDL, Parity violation in β-decay: correlation of the electron direction with the polarisation of a subsequently emitted neutron. 690
KALINKIN, L. F., *see* Estulin
KEARSLEY, M. J., The energy levels of Pb^{206} 157
KELMAN, V. M., R. YA. METSKHVARISHVILI, V. A. ROMANOV and V. V. TUCHKEVICH, Investigation of conversion lines in the β-spectrum of Ir^{192} 240
KLEIN, O., Some remarks on the inversion theorems of quantum field theory 677
KRISYOUK, E. M., A. G. SERGEYEV, G. D. LATYSHEV and V. D.

VOROBYOV, Decay scheme of Pb^{212} 579
KOZODAYEV, M. S., *see* Bayukov
LAPIDUS, L. I., Time reversal and polarization phenomena in $N+N \rightleftarrows d+\pi$ reactions 145
LATYSHEV, G. D., *see* Krisyouk
LEVINTOV, I. I., On the radius of the alpha-particle 330
LINDQVIST, T. and I. MARKLUND, Mixing ratios of $2^+ \rightarrow 2^+$ transitions in some even nuclei 189
LOGUNOV, A. A., A. N. TAVKHELIDZE and L. D. SOLOVYOV, Photoproduction processes and dispersion relations 427
LÖNSJÖ, O., *see* Andersen
MCCARTHY, I. E., Elastic scattering of antiprotons by nuclei . . . 463
MÁGORI, E., *see* Gombás
MANDL, E., *see* Jones
MARION, J. B., Shell model interpretation of energy levels in Li^7 and Be^7 (see also Erratum p. 492) 282
MARIS, TH. A. J., *see* Tyrén
MARIS, TH. A. J. and H. TYRÉN, Some remarks concerning measurements on inelastic scattering of 155—185 MeV protons on carbon, oxygen and calcium 662
MARKLUND, I., *see* Lindqvist
MELIORANSKY, A. S., *see* Estulin
METSKHVARISHVILI, R. YA., *see* Kelman
MOSHINSKY, M., *see* Bauer
MOTTELSON, B. R., *see* Bohr
MRÁZ, J., A further study of the decay of Ir^{192} 457
NATHAN, O., Possible vibrational levels in Dy^{160} (see also Erratum p. 635) 125
NATHAN, O., *see* Bjørnholm
NIELSEN, O. B., *see* Bjørnholm
NIKITIN, S. J., *see* Vishnevsky
NILSSON, M., *see* Wilhelmsson
NOVAKOV, T., *see* Hultberg
OFER, S., Angular correlations of gamma ray cascades following the decay of Eu^{152} 477
ONEDA, S., A possible test of the primarity of the weak interactions comprising leptons 21
POPOV, V. S., *see* Gaponov
PORTER, C. E., Compound nucleus formation as an irreversible thermodynamical process 472
PROKOSHKIN, YU. D., *see* Bayukov
PUSHKIN, E. V., *see* Vishnevsky

RAKAVY, G., The classification of states of surface vibrations. . . 289
RAKAVY, G., Rotational spectra of nuclei following O^{16} 375
RAMAN, S., *see* Bhattacherjee
RASMUSSEN, J. O., *see* Shirley
ROMAN, P., Some properties of combined PC-transformation and associated selection rules 564
ROMANOV, V. A., *see* Kelman
SALAM, A., On the inter-relation of scalar and pseudoscalar theories 687
SAWICKI, J. and W. CZYŻ, Note on the (γ, d) reactions (see also Erratum p. 695) 248
SCHIFF, L. I., Note on the elastic scattering of high-energy particles 632
SERGEYEV, A. G., *see* Krisyouk
SERPE, J., Remarks on parity conservation and the two-component theory of the neutrino 183
SHAPIRO, I. S., E. I. DOLINSKY and L. D. BLOKHINTSEV, On the interaction between μ-mesons and nucleons 273
SHELINE, R. K., *see* Bjørnholm
SHIRLEY, VIRGINIA S., W. G. SMITH and J. O. RASMUSSEN, Conversion-electron and photon spectra of Gd^{147} and Gd^{149}. 395
SMITH, W. G., *see* Shirley
SOLNTSEFF, N., On the theory of scattering measurements in nuclear emulsion; I. The distribution functions of the coordinate differences 337
SOLOVYOV, L. D., *see* Logunov
SYEDUZZAMAN, *see* Hossain
SZÉPFALUSY, P., *see* Gombás
TANGEN, R., *see* Andersen
TAVKHELIDZE, A. N., *see* Logunov
TEILLAC, J., Irène Joliot-Curie. 497
THIEBERGER, R. and A. DE-SHALIT, The 3^- level in A^{40} 469
TIBELL, G., *see* Tyrén
TIBELL, G., *see* Alphonce
TIDMAN, D. A., The energy loss of fast charged particles, Part III 257
TREBUKHOVSKY, YU. V., *see* Vishnevsky
TREIMAN, S. B., *see* Jackson
TUCHKEVICH, V. V., *see* Kelman
TYAPKIN, A. A., *see* Bayukov
TYRÉN, H., G. TIBELL and TH. A. J. MARIS, The scattering of 181 MeV protons off helium 277
TYRÉN, H. and TH. A. J. MARIS, Inelastic scattering of 185 MeV protons on oxygen, calcium and carbon 637
TYRÉN, H., *see* Hillman
TYRÉN, H., *see* Maris

UMEZAWA ,H. and A. VISCONTI, The isomerism of elementary particles 224
VISCONTI, A., *see* Umezawa
VISHNEVSKY, M. E., V. K. GRIGORIEV, V. A. ERGAKOV, S. J. NIKITIN, E. V. PUSHKIN and YU. V. TREBUKHOVSKY, On the polarization of electrons in β-decay 271
VOROBYOV, V. D., *see* Krisyouk
WAPSTRA, A. H. and W. VAN DER EIJK, The decay of ^{109}Cd, ^{109}Ag and ^{109}Pd (see also Erratum p. 695) 325
WERLE, J., Polarisation of μ-mesons and electrons in K-meson decays 171 (see also Correction p. 693)
WILHELMSSON, H. and M. NILSSON, An alpha-particle model for the nuclear photodisintegration of O^{16} 234
WYLD JR., H. W., *see* Jackson
YVON, J., Une méthode d'étude des corrélations dans les fluides quantiques en équilibre 1

BOOK REVIEWS

BLIN-STOYLE, R. J., Theories of nuclear moments (L. R.) 491
SULLIVAN, W. H., Trilinear chart of nuclides, 2nd ed. (L. R.) . . 491
BONILLA, C. F. (Editor), Nuclear Engineering (L. R.) 696
CERN SYMPOSIUM ON HIGH-ENERGY ACCELERATORS AND PION PHYSICS (Geneva 11—23 June 1956) PROCEEDINGS (L. R.) . . . 188
DAVISON, B., with the collaboration of J. B. SYKES, Neutron transport theory (A. Hassitt) 492
FLAMMER, C., Spheroidal wave functions (L.R.) 696
HAÏSSINSKY, M. (Rédacteur), Actions chimiques et biologique des radiations (W. Wild) 636
MÜNZINGER, F., Atomkraft: Der Bau von Atomkraftwerke und seine Probleme, 2 Aufl. (P. H. Price) 492
SCHWENK, H. C. and R. H. SHANNON, Nuclear Power Engineering (L.R.) 696

SUBJECT INDEX

Beta and Gamma Spectroscopy

Studies on the long-lived activities of europium, S. K. Bhattacherjee and S. Raman 44
The longitudinal angular dependence of the photoelectric effect and its influence on the determination of gamma ray intensities, S. Hultberg and T. Novakov. . 120
Possible vibrational levels in Dy^{160}, O. Nathan (see also Erratum p. 635) 125
Mixing ratios of $2^+ \rightarrow 2^+$ transitions in some even nuclei, T. Lindqvist and I. Marklund 189
Investigation of conversion lines in the β-spectrum of Ir^{193}, V. M. Kelman, R. Ya. Metskhvarishvili, V. A. Romanov and V. V. Tuchkevich 240
Low lying levels in Th^{228}, S. Bjørnholm, O. Nathan, O. B. Nielsen and R. K. Sheline 313
The decay of ^{109}Cd, ^{109}Ag and ^{109}Pd, A. H. Wapstra and W. van der Eijk (see also Erratum p. 695) 325
Conversion-electron and photon spectra of Gd^{147} and Gd^{149}, Virginia S. Shirley, W. G. Smith and J. O. Rasmussen 395
A further study of the decay of Ir^{192}, J. Mráz 457
Angular correlations of gamma ray cascades following the decay of Eu^{152}, S. Ofer 477
Decay scheme of Pb^{212}, E. M. Krisyouk, A. G. Sergeyev, G. D. Latyshev and V. D. Vorobyov 579
Selection rules for beta and gamma particle transitions in strongly deformed nuclei, G. Alaga 625

Cosmic Radiation

Interpretation of cosmic ray jets observed in photographic emulsions, I. A. Ivanovskaya and D. S. Chernavsky 29

Elementary Particles

A possible test of the primarity of the weak interactions comprising leptons, S. Oneda 21
Polarisation of μ-mesons and electrons in K-meson decays, J. Werle 171
Remarks on parity conservation and the two-component theory of the neutrino, J. Serpe 183
Coulomb corrections in allowed beta transitions, J. D. Jackson, S. B. Treiman and H. W. Wyld Jr. 206
Further remarks on Coulomb corrections in allowed beta transitions, M. E. Ebel and G. Feldman 213
On the polarization of electrons in β-decay, M. E. Vishnevsky, V. K. Grigoriev, V. A. Ergakov, S. J. Nikitin, E. V. Pushkin and Yu. V. Trebukhovsky . . . 271
On four-dimensional isobaric spin formalisms, P. W. Higgs 221
The isomerism of elementary particles, H. Umezawa and A. Visconti 224
On the interaction between μ-mesons and nucleons, I. S. Shapiro, E. I. Dolinsky and L. D. Blokhintsev 273
β-γ-correlation for allowed transitions involving non-conservation of parity, Yu. V. Gaponov and V. S. Popov 453
Some properties of combined PC-transformation and associated selection rules, P. Roman 564
Parity mixtures and decay processes, H. S. Green and C. A. Hurst 589
On the inter-relation of scalar and pseudoscalar theories, A. Salam. 687
Parity violation in β-decay: correlation of the electron direction with the polarisation of a subsequently emitted neutron, G. A. Jones and F. Mandl 690

Field Theory

Photoproduction processes and dispersion relations, A. A. Logunov, A. N. Tavkhelidze and L. D. Solovyov 427
Lee model and quantisation of non linear field equations, W. Heisenberg 532

Some remarks on the inversion theorems of quantum field theory, O. Klein . . 677
Méthode des champs adhérents, A. Houriet (see also Erratum p. 635) 408

Methods and Instruments

On the theory of scattering measurements in nuclear emulsion I. The distribution functions of the coordinate differences, N. Solntseff 337

News Items

Northwestern University Conference on liquid scintillation counting (Evanston, 20—22 August 1957) 287
Conference on extra-atmospheric Cosmic Radiation research (Baltimore, March 29, 1957) 288
Electron Microscope Society of America 288, 695
The seventh Rochester Conference (15—19 April 1957) 493
Institute of Nuclear Research of the Polish Academy of Sciences 494
Colloquium on the physics of elementary particles (Balatonvilágos, 5—8 June 1957) 634
CERN, second annual report (1956) 635
International Conference on nuclear structure (Rehovoth, 8—14 September 1957) 694

Nuclear Forces

Zur Reichweite der Kernkräfte, P. Gombás, P. Szépfalusy und E. Mágori . . . 488

Nuclear States

The energy levels of Pb^{206}, M. J. Kearsley 157
Shell model interpretation of energy levels in Li^7 and Be^7, J. B. Marion (see also Erratum p. 492) 282
The classification of states of surface vibrations, G. Rakavy 289
Rotational spectra of nuclei following O^{16}, G. Rakavy 375
The 3^- level in A^{40}, R. Thieberger and A. De-Shalit 469
Electric dipole moment associated with octupole vibrations of a spheroidal nucleus, A. Bohr and B. R. Mottelson 529

Obituary

Irène Joliot-Curie, J. Teillac 497

Passage of Particles through Matter

The energy loss of fast charged particles, Part III, D. A. Tidman 257

Photonuclear Reactions

Individual particle and collective aspects of the nuclear photoeffect, D. M. Brink 215
An alpha-particle model for the nuclear photodisintegration of O^{16}, H. Wilhelmsson and M. Nilsson 234
Note on the (γ, d) reactions, J. Sawicki and W. Czyż (see also Erratum p. 695) . 248

Reactions Induced by Particles

Two closely spaced resonances in the reaction Al^{27} (p, γ) Si^{28}, S. L. Andersen, T. Holtebekk, O. Lönsjö and R. Tangen 39
Production of neutral π-mesons by high energy protons, Yu. D. Bayukov, M. S. Kozodayev, Yu. D. Prokoshkin and A. A. Tyapkin 61
Optical model analysis of proton scattering on some light nuclei, A. Hossain and Syeduzzaman 88
Soft γ-rays from the capture of thermal neutrons by nuclei, I. V. Estulin, L. F. Kalinkin and A. S. Melioransky 91

Distribution angulaire du rayonnement gamma de 8.34 MeV de la réaction $^{14}N(p,\gamma)^{15}O$, S. Gorodetzky, A. Gallmann, M. Croissiaux et R. Armbruster 112
Time reversal and polarization phenomena in $N+N \leftrightarrows d+\pi$ reactions, L. I. Lapidus 145
Compound nucleus formation as an irreversible thermodynamical process, C. E. Porter 472
Une formulation unifiée de la théorie des réactions nucléaires, C. Bloch 503
Excited states of N^{16}, Joan M. Freeman and R. C. Hanna 599

Scattering

The scattering of 181 MeV protons off helium, H. Tyrén, G. Tibell and Th. A. J. Maris 277
On the radius of the alpha-particle, I. I. Levintov 330
Elastic scattering of antiprotons by nuclei, I. E. McCarthy 463
Note on the elastic scattering of high energy particles, L. I. Schiff. 632
Inelastic scattering of 185 MeV protons on oxygen, calcium and carbon, H. Tyrén and Th. A. J. Maris 637
The asymmetry of 155 MeV protons elastically scattered from iron, nickel and copper, R. Alphonce, A. Johansson and G. Tibell 643
Polarization of high energy protons in elastic and inelastic scattering, P. Hillman, A. Johansson and H. Tyrén 648
Some remarks concerning measurements on inelastic scattering of 155—185 MeV protons on carbon, oxygen and calcium, Th. A. J. Maris and H. Tyrén . . . 662
The asymmetry of 155 MeV protons elastically and inelastically scattered from carbon, oxygen and calcium, R. Alphonce, A. Johansson and G. Tibell 672

Structure of Nuclei (Models and Theory)

Une méthode d'étude des corrélations dans les fluides quantiques en équilibre, J. Yvon 1
Nuclear magnetic moments and the many body problem, J. S. Bell 295
Zweiteilchennäherungen des Mehrkörperproblems I, W. Brenig 363
Repulsive core and nuclear shell theory, M. Bauer and M. Moshinsky 615